

TN
1
AS
Vol. 195
N/C

TRANSACTIONS

of the

American Institute of Mining and Metallurgical Engineers

(Incorporated)

*American Institute of Mining, Metallurgical
and Petroleum Engineers*

VOLUME 195

PETROLEUM DEVELOPMENT AND TECHNOLOGY 1952

PETROLEUM BRANCH

PAPERS AND DISCUSSIONS PRESENTED BEFORE THE BRANCH AT MEETINGS HELD
AT NEW ORLEANS, OCTOBER 4-6, 1950; OKLAHOMA CITY, OCTOBER 3-5, 1951;
LOS ANGELES, OCTOBER 25-26, 1951; NEW YORK, FEBRUARY 18-21, 1952;
AND HOUSTON, OCTOBER 1-3, 1952.

PUBLISHED BY THE INSTITUTE
AT THE OFFICE OF THE PETROLEUM BRANCH
800 FIDELITY UNION BUILDING
DALLAS, TEXAS

Headquarters of the Institute are at 29 West 39th Street, New York, N. Y.

COPYRIGHT, 1952, BY THE
AMERICAN INSTITUTE OF MINING AND METALLURGICAL ENGINEERS
(INCORPORATED)

PRINTED IN THE UNITED STATES OF AMERICA

STORM PRINTING COMPANY, DALLAS, TEXAS

FOREWORD

THE YEAR 1952 continued to be a period of growth for the Petroleum Branch of the Institute. It brought no startlingly new concepts of procedure in Branch administration, but rather produced a comfortable consolidation of previous improvements. Perhaps the most striking example of this was the formation of four new Local Sections in the Southwest. These new Sections (the South Plains, West Central Texas, Fort Worth and Lou-Ark) were established upon application of members in the various areas to better serve their interests. Geographically speaking, these new Sections were carved from existing Local Sections, the boundaries being rearranged and separate administrations set up to facilitate the handling of Local Section meetings.

Institute-wise, it was a "Petroleum year." Michael L. Haider, a Petroleum Branch Member, was President of the Institute and, although he served with complete objectivity in regard to the affairs of all three Branches, his familiarity with Petroleum Branch matters strengthened the Petroleum Branch representation on the AIME Board of Directors.

One of the most successful Fall Meetings ever held by the Branch was conducted in Houston. From it came many fine technical papers, some of which appear in this volume. The West Coast Regional Meeting, held annually in Los Angeles, was also highly successful. Both meetings registered record numbers of members, the former attracting more than 1,500 and the latter more than 500. These registration figures give strong indication of the extreme interest of the members in the advancement of the technology of the industry.

Another yardstick of growth within the Branch was the necessitated move of the administrative offices of the Branch in Dallas. In 1951, a move was made to a more spacious location to accommodate an expanding staff. However, in late 1952 it was again necessary to acquire additional space. When this need became apparent, it was decided to locate the office as conveniently to transient members as possible. Consequently, present office space, at 800 Fidelity Union Building, is only three blocks from leading Dallas hotels.

The splendid work of the Technology Committee and Publications Committee of the Petroleum Branch is reflected in the contents of this volume. The authors of the papers contained herein are to be congratulated for their fine contributions. The forty-two technical papers and six technical notes that follow offer adequate testimony to the extreme value to the industry of this, the latest *Transactions* of the Petroleum Branch, American Institute of Mining and Metallurgical Engineers.

PAUL R. TURNBULL, *Chairman*
Petroleum Branch, 1952

Corpus Christi, Texas
January 1, 1953

AIMÉ OFFICERS AND DIRECTORS

For the Year Ending February, 1953

PRESIDENT

MICHAEL L. HAIDER, New York, New York

PAST PRESIDENT

WILLIS MCGERALD PEIRCE, New York, New York

VICE-PRESIDENTS

O. B. J. FRASER
J. L. GILLSON

JAMES B. MORROW
R. W. THOMAS

PRESIDENT-ELECT AND TREASURER

ANDREW FLETCHER, New York, New York

DIRECTORS

C. HARRY BENEDICT
RUSSEL B. CAPLES
T. B. COUNSELMAN
HAROLD DECKER
FRANCIS B. FOLEY
T. L. JOSEPH
CHARLES E. LAWALL

FAY W. LIBBEY
PHILIP KRAFT
D. H. McLAUGHLIN
E. C. MEAGHER
C. V. MILLIKAN
THOMAS C. MOORE

W. S. MORRIS
GAIL F. MOULTON
J. F. MYERS
L. F. REINARTZ
CARL E. REISTLE, JR.
A. C. RUBEL
HOWARD I. YOUNG

DIVISION CHAIRMEN — DIRECTORS EX OFFICIIS

A. LEE BARRETT (Coal)
IAN CAMPBELL (Industrial Minerals)
E. H. CRABTREE (Minerals Beneficiation)
WALTER A. DEAN (Industrial Minerals)
T. D. JONES (Extractive Metallurgy)
EVAN JUST (Mineral Economics)
K. C. McCUTCHEON (Iron and Steel)
HARRY H. POWER (Mineral Industry Education)
PAUL R. TURNBULL (Petroleum)

CONTROLLER

GEORGE I. BRIGDEN

SECRETARY

EDWARD H. ROBIE

ASSISTANT SECRETARIES

JOE B. ALFORD
E. J. KENNEDY, JR.

ROY E. O'BRIEN
E. O. KIRKENDALL

ASSISTANT TO THE SECRETARY

H. NEWELL APPLETON

PUBLICATIONS MANAGER

JOHN V. BEALL

BUSINESS MANAGER

PETER J. APOL

CONTENTS

FOREWORD, by PAUL R. TURNBULL	iii
AIME OFFICERS AND DIRECTORS	iv
PETROLEUM BRANCH OFFICERS AND COMMITTEE CHAIRMEN	viii
PETROLEUM BRANCH PAST CHAIRMEN	ix
THE ANTHONY F. LUCAS FUND AND MEDAL	x
PETROLEUM BRANCH CERTIFICATE OF SERVICE	xi

P A P E R S

PRODUCTION TECHNOLOGY

Method for Determining Wettability of Reservoir Rocks, by R. L. Slobod and H. A. Blum	1
Volumetric Behavior of Condensate and Gas from a Louisiana Field—II, by B. H. Sage and H. H. Reamer	11
Mobility Ratio—Its Influence on Flood Patterns During Water Encroachment, by J. S. Aronofsky	15
A Method for Predicting the Tendency of Oil Field Waters to Deposit Calcium Sulfate, by Henry A. Stiff, Jr., and Lawrence E. Davis	25
Displacement Mechanism in Multi-Well Systems, by Loyd R. Kern	39
Improved Multiphase Flow Studies Employing Radioactive Tracers, by V. A. Josendal, B. B. Sandiford and J. W. Wilson	65
Engineering Study of the Cook Ranch Field, Shackelford County, Texas, by Wallace W. Wilson	77
A Simplified Method for Computing Oil Recovery by Gas or Water Drive, by Henry J. Welge	91
Equilibrium Vaporization Ratios for Nitrogen, Methane, Carbon Dioxide, Ethane and Hydrogen Sulfide in Absorber Oil—Natural Gas and Crude Oil-Natural Gas Systems, by R. H. Jacoby and M. J. Rzasas	99
Correlation of Radioactive Logs of the Lansing and Kansas City Groups in Central Kansas, by John V. Morgan	111
Behavior of Dissolved Oxygen in Oil Field Brine, by George G. Bernard and Glenn A. Marsh	119
The Delta-Log, a Differential Temperature Surveying Method, by R. B. Basham and C. W. Macune	123
Observations from Profile Logs of Water Injection Wells, by H. H. Kaveler and Z. Z. Hunter	129
Prediction of Saturation Pressures for Condensate-Gas and Volatile-Oil Mixtures, by E. I. Organick and B. H. Golding	135
Visual Examinations of Fluid Behavior in Porous Media—Part I, by Alfred Chatenever and John C. Calhoun, Jr.	149
The Resistivity of a Fluid-Filled Porous Body, by J. E. Owen	169
Possibility of Cycling Deep Depleted Oil Reservoirs After Compression to a Single Phase, by Donald L. Katz	175
The Strataflow Process: A Recent Development in Locating Water Entry in Wells, by Ralph E. Hartline and Wilfred Tapper	183
Laboratory Determination of Relative Permeability, by J. G. Richardson, J. K. Kerver, J. A. Hafford and J. S. Osoba	187
Some Properties of Mixed Paraffinic and Olefinic Hydrates, by H. H. Reamer, F. T. Selleck and B. H. Sage	197
Neutron Derived Porosity-Influence of Bore Hole Diameter, by C. B. Scotty and E. F. Egan	203
A Method for Predicting the Tendency of Oil Field Waters to Deposit Calcium Carbonate, by Henry A. Stiff, Jr., and Lawrence E. Davis	213
Electrical Resistivity Measurements on Reservoir Rock Samples by the Two-Electrode and Four-Electrode Methods, by C. F. Rust	217
A High-Pressure Wellhead Lubricator, by Howard E. McKinney	261
X-Ray Shadowgraph Studies of Areal Sweepout Efficiencies, by R. L. Slobod and B. H. Caudle	265
Bubble Formation in Supersaturated Hydrocarbon Mixtures, by Harvey T. Kennedy and Charles R. Olson	271
Surface Area Measurements on Sedimentary Rocks, by C. S. Brooks and W. R. Purcell	289
The Pressure Performance of Five Fields Completed in a Common Aquifer, by W. D. Moore and L. G. Truby, Jr.	297

DRILLING TECHNOLOGY

Radial Filtration of Drilling Mud, by C. L. Prokop	5
The Quantitative Aspects of Electric Log Interpretation, by J. E. Walstrom	47
Lost Circulation Corrective: Time Setting Clay Cement, by J. U. Messenger and J. S. McNiel, Jr.	59
A New Additive for Control of Drilling Mud Filtration, by R. A. Salathiel	85
Drilling Fluid Filter Loss at High Temperatures and Pressures, by F. W. Schremp and V. L. Johnson	157
Experimental Evaluation of Well Perforation Methods as Applied to Hard Limestone, by Henry Lewelling	163
Use of Activated Charcoal in Cement to Combat Effects of Contamination by Drilling Muds, by B. E. Morgan and G. K. Dumbauld	225
A Method of Perforating Casing Below Tubing, by M. P. Lebourg and G. R. Hodgson	303

NATURAL GAS TECHNOLOGY

Efficiency of Gas Displacement from Porous Media by Liquid Flooding, by T. M. Geffen, D. R. Parrish, G. W. Haynes and R. A. Morse	29
Sample Grading Method of Estimating Gas Reserves, by D. L. Katz, C. E. Turner, R. D. Grimm, J. R. Elenbaas and J. A. Vary	207
The Slip Velocity of Gases Rising Through Liquid Columns, by N. Stein, E. B. Elfrink, L. D. Wiener and C. R. Sandberg	233
Natural Gas in the Province of Alberta, Canada, by J. F. Dougherty, Anthony Folger, Howard R. Lowe, Joffre Meyer and E. G. Trostel	241
Phase and Volumetric Behavior of Natural Gases at Low Temperatures, by T. L. Gore, P. C. Davis and F. Kurata	279
Improved Techniques Developed for Acidizing Gas Producing and Injection Wells, by W. H. Justice and Jens P. Nielsen	285
Additional Discussions of Above Papers	311

TECHNICAL NOTES

A Study of the Permanence of Production Increases Due to Hydraulic Fracture Treatments, by C. R. Fast	321
A Note on the X-Ray Absorption Method of Determining Fluid Saturation in Cores, by T. M. Geffen and R. E. Gladfelter	322
Measurement of the Permeability of Set Cement, by B. E. Morgan and G. K. Dumbauld	323
Errors in Calculation of Gas Injection Performance from Laboratory Data, by Forrest F. Craig, Jr.	325
Procedure for Use of Electronic Digital Computers in Calculating Flash Vaporization Hydrocarbon Equilibrium, by H. H. Rachford, Jr., and J. D. Rice	327
Reduction in Permeability with Overburden Pressure, by I. Fatt and D. H. Davis	329
INDEX	331

ERRATA

Vol. 195, 1952

T.P. 3321, "Mobility Ratio — Its Influence on Flood Patterns During Water Encroachment," by J. S. ARONOFSKY.

Page 24, Column 1. Sentence beginning on Line 7 should read: "Specifically, for example, in the case of gas cycling (iso-thermal flow) the voltage should represent P^2 and the current should represent mass gas flow (or volume gas flow under standard conditions)."

T.P. 3309, "A Simplified Method for Computing Oil Recovery by Gas or Water Drive," by HENRY J. WELGE.

Page 92, Column 1. Equation (1) should read as follows:

$$f = \frac{c}{c + h} - \frac{K \Delta D g \sin \theta}{\mu_g v_o} \frac{k_{oil}}{c + h}$$

Note that the small g in the numerator of the second term should not be a subscript but the gravitational constant. This term of the equation, you will note, is clearly given on Page 98 in the table of nomenclature.

On Page 95, the last line of the text at the bottom of Table I should read, "permeability expressed in sq cm" instead of "cu cm."

On Page 97, Column 1. The third line from the top of the page should read "Fig. 7" instead of "Fig. 6."

PETROLEUM BRANCH OFFICERS AND COMMITTEE CHAIRMEN

For the Year Ending February, 1953

CHAIRMAN

PAUL R. TURNBULL
La Gloria Corporation
Corpus Christi, Texas

VICE-CHAIRMEN

JOHN R. McMILLAN
Fullerton Oil Company
Pasadena, California

MORRIS MUSKAT
Gulf Oil Corp.
Pittsburgh, Pennsylvania

EXECUTIVE COMMITTEE

JOHN R. McMILLAN

PAUL R. TURNBULL

MORRIS MUSKAT

R. W. FRENCH
Sohio Petroleum Company
Cleveland, Ohio

JOHN S. BELL
Humble Oil and Refining Company
Los Angeles, California

D. V. CARTER
Magnolia Petroleum Company
Dallas, Texas

R. C. EARLOUGH
Earlougher Engineering
Tulsa, Oklahoma

THOMAS C. FRICK
Atlantic Refining Company
Corpus Christi, Texas

E. N. VAN DUZEE
Shell Oil Co.
New Orleans, Louisiana

G. L. YATES
Amstutz and Yates
Wichita, Kansas

WILLIAM E. STILES, *Treasurer*
Buffalo Oil Company
Dallas, Texas

C. R. DODSON, MIED
Stanley, Stolz and Dodson
Los Angeles, California

LOUIS C. RAYMOND, MED
Ford, Bacon and Davis
New York, New York

MEMBERSHIP COMMITTEE

JACK M. MOORE, *Chairman*
Dowell Incorporated
Midland, Texas

STUDENT ACTIVITIES COMMITTEE

W. S. MORRIS, *Chairman*
East Texas Salt Water Disposal Company
Kilgore, Texas

PUBLICATIONS COMMITTEE

JOHN P. HAMMOND, *Chairman*
Amerada Petroleum Corporation
Tulsa, Oklahoma

R. A. MORSE, *Vice-Chairman*
Stanolind Oil and Gas Company
Tulsa, Oklahoma

ADVERTISING COMMITTEE

BRUCE BARKIS, *Chairman*
B & W, Incorporated
Houston, Texas

ECONOMICS COMMITTEE

KENNETH E. HILL, *Chairman*
Chase National Bank
New York, New York

EDUCATION COMMITTEE

JOHN C. CALHOUN, JR., *Chairman*
Pennsylvania State College
State College, Pennsylvania

PRODUCTION REVIEW COMMITTEE

E. W. BERLIN, *Chairman*
Standard Vacuum Oil Company
New York, New York

R. B. GILMORE, *Domestic*
DeGolyer and MacNaughton
Dallas, Texas

ALEXANDER H. CHAPMAN, *Foreign*
Arabian American Oil Company
Washington, D. C.

TECHNOLOGY COMMITTEE

DOUGLAS RAGLAND, *Chairman*
Humble Oil and Refining Company
New Orleans, Louisiana

Vice-Chairmen

J. H. ABERNATHY, *Drilling*
Big Chief Drilling Company
Oklahoma City, Oklahoma

E. P. HAYES, *Production*
The Texas Company
Houston, Texas

W. H. JUSTICE, *Natural Gas*
La Gloria Corporation
Corpus Christi, Texas

MILTON E. LOY, *for California*
Schlumberger Well Surveying Corporation
Los Angeles, California

STAFF OF THE PETROLEUM BRANCH IN DALLAS

Executive Secretary
JOE B. ALFORD

Editor, Journal of Petroleum Technology
JESS E. ADKINS

PETROLEUM BRANCH, AIME

Established as a Division March 24, 1922

Established as a Branch in 1948

PAST CHAIRMEN

RALPH ARNOLD, 1922
E. DeGOLYER, 1923, 1924
F. JULIUS FOHS, 1925, 1926
JOHN M. LOVEJOY, 1927
A. W. AMBROSE, 1928
JOSEPH B. UMPLEBY, 1929
C. V. MILLIKAN, 1930
C. E. BEECHER, 1931
EARL OLIVER, 1932
W. E. WRATHER, 1933
H. D. WILDE, JR., 1934
HARRY H. POWER, 1935
HALLAN N. MARSH, 1936
M. ALBERTSON, 1937
GEORGE B. CORLESS, 1938
W. H. GEIS, 1939
T. V. MOORE, 1940
EUGENE A. STEPHENSON, 1941
HARRY P. STOLTZ, 1942
C. A. WARNER, 1943
W. S. MORRIS, 1944
M. L. HAIDER, 1945
H. F. BEARDMORE, 1946
HOWARD C. PYLE, 1947
IRWIN W. ALCORN, 1948
LLOYD E. ELKINS, 1949
JOHN E. SHERBORNE, 1950
R. W. FRENCH, 1951
PAUL R. TURNBULL, 1952

THE ANTHONY F. LUCAS FUND AND MEDAL

In 1936 the Institute established the Anthony F. Lucas Gold Medal, to be awarded from time to time "for distinguished achievement in improving the technique and practice of finding and producing petroleum." These awards are sponsored by the Petroleum Branch.

Captain Lucas was a pioneer in the oil industry, one of the early wildcatters and a leading mining and petroleum engineer. He was famous as the discoverer of Spindletop. He became a member of the Institute in 1895 and in 1913 was the first Chairman of the Petroleum and Gas Committee of the Institute, the forerunner of the present Petroleum Branch. He also headed the Committee in 1914, 1917 and 1918.

MEDALS AWARDED

J. EDGAR PEW, 1937
 HENRY L. DOHERTY, 1938
 E. DEGOLYER, 1940
 CONRAD (posthumously) and MARCEL SCHLUMBERGER, 1941
 JOHN ROBERT SUMAN, 1943
 CHARLES VAN ORMER MILLIKAN, 1944
 JAMES OGIER LEWIS, 1946
 WILLIAM NOBLE LACEY, 1947
 WALLACE EVERETTE PRATT, 1948
 WILLIAM EMBRY WRATHER, 1950

COMMITTEE ON AWARDS

FRED M. NELSON, *Chairman*

<i>Until Feb. 1953</i>	<i>Until Feb. 1954</i>	<i>Until Feb. 1955</i>	<i>Until Feb. 1956</i>
J. E. BRANTLY	LLOYD E. ELKINS	R. F. BAKER	I. W. ALCORN
W. E. PRATT	JOHN H. MURRELL	M. L. HAIDER	E. C. GAYLORD
FRED M. NELSON	W. H. GEIS	J. E. SHERBORNE	W. E. WRATHER

Members Ex Officiis

JOHN J. FORBES	FRANK N. PORTER	M. L. HAIDER	MORGAN J. DAVIS
Director, B. of M.	President, API	President, AIME	President, AAPG

PETROLEUM BRANCH CERTIFICATE OF SERVICE

Established in 1948, the Petroleum Branch CERTIFICATE OF SERVICE is awarded to recognize and show appreciation for exceptional services of Members of the Branch.

CERTIFICATES AWARDED

EUGENE A. STEPHENSON, 1948

FRED B. PLUMMER, 1948
(posthumously)

EARL OLIVER, 1948

E. JULIUS FOHS, 1949

JOSEPH B. UMPLEBY, 1949

STUART E. BUCKLEY, 1952

METHOD FOR DETERMINING WETTABILITY OF RESERVOIR ROCKS

R. L. SLOBOD, MEMBER AIME, AND H. A. BLUM, JUNIOR MEMBER AIME, THE ATLANTIC REFINING CO.,
DALLAS, TEX.

ABSTRACT

A semiquantitative method for measuring the wettability of reservoir rocks has been developed. These data are needed for reservoir analysis and for interpretation of laboratory displacement studies. The wettability of a core sample is measured by the contact angle for the system oil-water-solid. These contact angles are calculated from the displacement pressure (threshold pressure) obtained by use of the centrifuge, using first oil-water and second air-oil in the same core sample. This method is based on the assumption that the air-oil and oil-water interfaces occupy similar positions in the porous medium when desaturation of the wetting phase is initiated. The assumption is also made that the contact angle for the air-oil-solid system which is close to zero in value does not change appreciably even when the contact angle for the oil-water-solid system experiences marked changes. "Apparent contact angles" for five different solids ranging from 31° to 82° have been determined, and changes in the "apparent contact angle" of a given sample with laboratory use from 33° to 53° have been observed.

INTRODUCTION

Reservoir rocks vary in their wettability,^{1,2,3,4} some being preferentially water wet while other are apparently preferentially oil wet. The degree of wettability, in theory, is measured quantitatively by the contact angle for the system solid-oil-water, but in practice this quantity is extremely difficult to determine.⁵ The need for obtaining some measure of this quantity has become obvious in recent years as a result of both laboratory and field observations. Several reservoirs such as the Bradford Sand in Pennsylvania and the Wilcox⁷ at Oklahoma City are reported to be oil wet. If these reports correctly reflect the true nature of the surface of the rock in

the ground, then these reservoirs probably will not perform as predicted on the basis of a water wet rock. In the laboratory many core samples have been observed to be oil wet. These samples, while perhaps not correctly representing the reservoir, have markedly different properties from water wet rock. The location of the phases is different (oil is in contact with rock instead of water), and other quantities such as the connate water, the capillary pressure curve, residual oil, relative permeabilities, and the recovery of oil by water flooding are markedly affected by the value of the contact angle. A further complication observed in the laboratory is the changing of the wettability of a rock specimen with use. Such changes mean that repeat runs on the same core are not the duplicate tests desired, but represent new experiments on a more oil wet material. The changes in surface characteristics are sometimes so rapid that by the time an experiment requiring several days is completed, the results may not be representative of the core as originally described.

The rock material itself (silica, carbonates, etc.), when clean and uncontaminated, is water wet. There seems to be little evidence of the presence of oil wet minerals such as heavy metal sulfides. The oil wetness of reservoir samples, therefore, is believed to be caused by the accumulation of an adsorbed film in which the polar group of a large organic molecule is adsorbed on the surface leaving the organic or hydrocarbon part of the molecule projecting out from the solid. Such a surface is much more readily wet by oil than by water.

These considerations indicate the need for a method which will provide some measure of the wettability (contact angle if possible) for reservoir rock samples. The method should be capable of (1) distinguishing between the wettability of different formations, (2) detecting changes in wettability of a core with use, and (3) measuring the changes in wettability which may be accomplished with cleaning operations, such as the use of sodium silicate for increasing water wettability.⁶ A preliminary report on such a method is presented below, not with the idea that this procedure alone will solve the wettability problem, but rather that it may provide encouragement to

¹References given at end of paper.

Manuscript received in the office of the Petroleum Branch, AIME, Aug. 9, 1951. Paper presented at the Fall Meeting of the Petroleum Branch in Oklahoma City, Okla., Oct. 3-5, 1951.

others to initiate critical studies on means for determining wettability and for evaluating its importance in reservoir performance.

DESCRIPTION OF METHOD

The wettability of a rock specimen is determined by carrying out two displacement experiments, the first being the displacement of water by oil, the second the displacement of oil by air. The threshold (initial desaturation) pressures determined from these displacement experiments together with the surface tension and interfacial tension values may then be used to calculate a "wettability number," W , defined by the relationship

$$W = \frac{\cos \theta_{o-w}}{\cos \theta_{a-o}} = \frac{P_{(o-w)T} \gamma_{a-o}}{P_{(a-o)T} \gamma_{o-w}} \quad (1)$$

which is derived in the following section. An "apparent contact angle" the cosine of which is defined by the relation

$$\cos (\theta_{o-w}) \text{ apparent} = \frac{P_{(o-w)T} \gamma_{a-o}}{P_{(a-o)T} \gamma_{o-w}} \quad (2)$$

may also be calculated if the assumption is made that the contact angle is zero in the oil for the air-oil-solid system. This calculation yields the receding contact angle measured in the water phase.

THEORETICAL BASIS OF METHOD

In reservoir problems the question of wettability arises when both water and oil are present to compete for a place on the solid surface. The contact angle at each spot in the system where the three phases are present defines the wettability at that spot. The wettability of the reservoir rock may be defined as some average of these contact angles. A solid is considered to be preferentially water wet if the contact angle measured in the water for the oil-water-solid system lies between 0° and 90° . Similarly solids are designated as preferentially oil wet for contact angles (also measured in the water phase) between 90° and 180° . While systems with contact angles less than 90° are called water wet, it is important to note that considerable variation in core properties due to wettability may be observed in this range. The method of measuring wettability discussed herein is largely concerned with the differentiation of cores exhibiting contact angles in this interval. Measuring all of these individual contact angles does not appear to be practical.

It is possible, however, to calculate a "wettability number" and an "apparent contact angle" of the water phase from displacement pressures, air-oil surface tension, and oil-water interfacial tension data if it is assumed (1) that the relationship between the displacement pressure of the wetting phase and the contact angle for a cylindrical capillary,

$$P_{o-w} = \frac{2\gamma_{o-w} \cos \theta_{o-w}}{r} \quad (3)$$

can be applied to a complex porous system where r is the radius of the capillary, (2) that in a core the same effective radius, r , is applicable in both the air-oil-solid and the oil-water-solid systems at the threshold pressure which represents the condition of initial displacement of the respective wetting phases, and (3) that the apparent contact angle for the air-oil-solid system is close to zero and remains essentially constant with changes in the contact angle for the oil-water-solid system.

The above discussion may be stated in terms of the following equations. For the air-oil-solid system the initial displace-

ment pressure (threshold pressure) is related to the radius, r_1 , and the contact angle, θ_{a-o} by Equation (4)

$$P_{(a-o)T} = \frac{2\gamma_{a-o} \cos \theta_{a-o}}{r_1} \quad (4)$$

Similarly, in the oil-water-solid system the initial or threshold pressure is given by

$$P_{(o-w)T} = \frac{2\gamma_{o-w} \cos \theta_{o-w}}{r_1} \quad (5)$$

on the basis of the assumption that the water and the oil in these two cases are similarly located or that r_1 may be used in both equations. Dividing Equation (4) by Equation (5) eliminates r_1 and gives the ratio

$$\frac{P_{(a-o)T}}{P_{(o-w)T}} = \frac{\gamma_{a-o} \cos \theta_{a-o}}{\gamma_{o-w} \cos \theta_{o-w}} \quad (6)$$

Solving this equation for the ratio of the cosines of the contact angles yields an expression, Equation (7), which is given the name "wettability number," W .

$$W = \frac{\cos \theta_{o-w}}{\cos \theta_{a-o}} = \frac{\gamma_{a-o} P_{(o-w)T}}{\gamma_{o-w} P_{(a-o)T}} \quad (7)$$

This expression may be further simplified by the assumption that $\cos \theta_{a-o}$ is unity. The angle which can be calculated from this assumption, Equation (8), has been named the "apparent contact angle"

$$\cos (\theta_{o-w}) \text{ apparent} = \frac{\gamma_{a-o} P_{(o-w)T}}{\gamma_{o-w} P_{(a-o)T}} \quad (8)$$

Thus, two semi-quantitative terms are available to measure the wettability. The first of these is the "wettability number," W , which is calculable using one assumption which makes possible the elimination of r_1 ; the second is the "apparent contact angle" which is obtained from the wettability number as assuming a zero contact angle for the air-oil system. Since neither of these assumptions is strictly correct, the quantities " W " and "apparent contact angle" are considered to be only semi-quantitative. Future work should establish the validity and limitations of this method.

APPARATUS AND PROCEDURE

The wettability number, W , defined by Equation (7), may be readily calculated by the determination of the threshold pressure for air displacing oil and for oil displacing water. These threshold pressures (pressures at which the displacement of the wetting phase is initiated) have been determined rather conveniently by the use of the centrifuge⁵ using the first portion of the capillary pressure curve to obtain these values accurately. Surface tension and interfacial tensions are measured with the conventional DuNuoy Tensiometer.

The procedure used in handling of the rock sample is very simple. A core plug cut from the reservoir in question is extracted by any of the conventional schemes which may include the use of carbon tetrachloride, chloroform, acetone, pentane, etc. (If desired, the measurements may also be made on the core plug prior to extraction.) The extracted (or unextracted) core is saturated with water or brine, and the threshold pressure for oil displacing water then determined using the centrifuge or any other convenient method. The same core plug is then cleaned, saturated with oil, and using air as the displacing phase the threshold pressure is then determined for this system. The interfacial tension for the oil-water system and the surface tension for the air-oil system are also measured. With these four measured quantities the wettability number, W , may be calculated by use of Equation (7).

The silicate treatment⁶ for increasing the wettability number (making core more water wet) merely involves refluxing

the core in an aqueous solution containing five g per liter of sodium silicate ($\text{Na}_2\text{SiO}_3 \cdot 9\text{H}_2\text{O}$).

The observation of higher displacement pressures on cores flushed with water after the above treatment indicates improved water wettability.

RESULTS

"Wettability numbers" and "apparent contact angles" for a number of cores from five different sources measured by the method described above are shown in Table I. These data show that a wide range in these values is possible. The most water wet material in this series according to these measurements is a Devonian Limestone sample with an apparent contact angle of about 31° and a wettability number of 0.854. The substance most nearly oil wet in this series is a Clearfork Limestone with an apparent contact angle of about 82° and a wettability number of 0.138. All cores included in this table had been extracted with chloroform prior to measurement of the wettability except for the Alundum samples which were fired at $1,400^\circ\text{F}$ prior to testing. Also included in this table are the experimental numbers (threshold pressure, surface tension, and interfacial tension) used to calculate the wettability number (Equation 7) and the apparent contact angle (Equation 8).

Changes in the wettability of a core with use in the laboratory is very clearly shown by the data in Table II. The Devonian Limestone cores when originally measured in the laboratory exhibited an "apparent contact angle" of 33° which increased to about 52° when the core containing connate water and tri-isobutylene as the oil phase was allowed to stand in this oil phase for three weeks. Treatment of these cores with silicate, however, largely restored the core to its original condition since the "apparent contact angle" was decreased by this treatment to about 35° which is essentially equal to the original value. Similarly, the wettability of Alundum cores was also observed to change with use. It is interesting to note, however, that even after firing at $1,400^\circ\text{F}$, the four Alundum cores had appreciably different "apparent contact angles," ranging from about 50° to 70° . These data indicate that Alundum even from the same batch is not a very reproducible material with respect to wettability. After standing in oil, however, this material is remarkably reproducible showing a range in "apparent contact angle" of only 0.6° , the actual values lying between 76.2° and 76.8° .

Table I—Comparison of Wettability Among Core Samples of Different Origins*

Core No.	Description	Initial Desaturation Pressure (Threshold Pressure—psi)		Wettability Number**	Apparent Contact Angle ($^\circ$)
		air-oil	oil-water		
BTL	Devonian	6.5	6.1	0.84	33
BTN	Limestone	6.8	6.2	0.81	36
BTO		6.25	6.0	0.85	31
BTP		6.4	3.9	0.54	57
1588	Yates	0.86	0.32	0.33	71
1589	Sandstone	0.85	0.3	0.31	71
1590		0.85	0.31	0.32	71
1591		1.00	0.4	0.36	69
1542	Alundum	0.70	0.25	0.32	72
1543	(RA 1139)	0.70	0.28	0.36	69
1544		0.68	0.4	0.52	59
1545		0.67	0.28	0.37	68
1592	Synthetic	0.72	0.24	0.30	73
1593	Clearfork	0.54	0.32	0.53	58
1594	Limestone	1.58	0.32	0.18	80
1595		2.90	0.45	0.14	82
1620	Tensleep Sand	0.86	0.21	0.22	78
1621		0.86	0.21	0.22	78
1622		0.63	0.12	0.16	81
1623		0.86	0.27	0.28	74

*Routine Extraction with Chloroform Preceded Wettability Tests Except Alundum Which Had Been Regenerated at 1400°F for Three Hours.
**Air-Oil Surface Tension = 24.9 Dynes/cm. Oil-Water Interfacial Tension = 28.0.

Table II—Changes in Wettability of Cores with Use in Laboratory

Core No.	Core Description	Treatment Prior to Wettability Measurement	Wettability Number	Apparent Contact Angle
BTL	Devonian	Routine Extraction	0.84	33
BTN		with Chloroform	0.81	36
BTO	Limestone		0.85	31
BTP			0.54	57
BTL	Devonian	Cores, at Connate Water, were Stored in Oil for Three Weeks	0.60	53
BTN			0.61	52
BTO	Limestone		—	—
BTP			0.60	53
BTL	Devonian	Cores Refluxed with $\frac{1}{2}\%$ Sodium Silicate ($\text{Na}_2\text{SiO}_3 \cdot 9\text{H}_2\text{O}$) for 24 Hours, Followed by Brine Extraction	0.79	37
BTN			0.76	41
BTO	Limestone		0.89	28
BTP			0.80	37
1542	Alundum	Regenerated at 1400°F	0.32	72
1543	(RA1139)		0.36	69
1544			0.52	59
1545			0.37	68
1542	Alundum	Above Cores — Re-treated by Regeneration at 1400°F	0.76	50
1543	(RA1139)		0.38	71
1544			0.39	67
1545			0.35	70
1542	Alundum	Saturated with and Stored in Oil for 12 Hours Then Dried	0.23	77
1543	(RA1139)		0.23	77
1544			0.24	76
1545			0.24	76

Table III—Comparison of Threshold Pressures for the Air-Oil-Devonian Limestone System Before and After a Series of Laboratory Treatments

Core Number	Threshold Pressures (psi)		
	Before	After	% Change
BTL	6.5	6.6	+ 1.5
BTN	6.3	6.7	- 1.5
BTO	6.25	7.1	+ 13.5
BTP	6.4	6.6	+ 3.2
Avg. = 6.5		Avg. = 6.75	

The uniformity in the wettability of the Alundum samples after exposure to oil, coupled with similar behavior of the Devonian Limestone samples (see Table II) suggests a possible wettability equilibrium condition in the reservoir which is partially oil-wet. Obviously much more extensive studies under carefully controlled conditions must be completed before this possibility can be evaluated reliably.

Results of tests of the basic assumption that the wettability of the air-oil-solid system does not change with core treatment are presented in Table III in which comparison of the air-oil displacement pressures for Devonian Limestone plugs before and after a series of laboratory treatments is made. These data indicate a relatively minor change in the average value of the threshold pressure from 6.5 psi to 6.75 psi, most of this change arising from a large difference in one core. If the results from this core were not considered, the change in the average threshold pressure would have been merely from 6.57 psi to 6.63 psi. Considering the processing to which the cores were subjected (made partially oil wet by storage in oil, dried, saturated with water, oil driven, vacuum distilled, saturated and refluxed with sodium silicate solution, extracted with brine, oil driven, vacuum distilled, saturated with oil, and air driven) these results offer some support for the assumption that the contact angle in the air-oil-solid system is relatively constant.

It is interesting to note that rough tests such as the behavior of oil and water droplets on the surface of the solid are in complete qualitative agreement with the more quantitative results obtained by the method described above. Thus, dry solids with small "apparent contact angles" readily imbibe water droplets as well as oil, while only oil is observed to be readily imbibed by solids which show a large "apparent contact angle." It should be clearly understood, however, that these qualitative tests are unable to differentiate between solids which have appreciable differences in the "apparent contact angle" such as 33° vs 55° . It is in the differentiation

between such materials that the new method offers considerable encouragement. With such precision not only can slight differences between similar cores be distinguished, but changes in a specific specimen can be followed, and the efficiency of methods for modifying the wettability can be measured.

LIST OF NOMENCLATURE

- W = Wettability number — increases toward unity as system becomes more water wet
 θ_{o-w} = Contact angle in water for oil-water-solid system
 θ_{a-o} = Contact angle in oil for air-oil-solid system
 $P_{(o-w)T}$ = Threshold pressure for displacement of water by oil
 $P_{(a-o)T}$ = Threshold pressure for displacement of oil by air
 γ_{a-o} = Surface tension (dynes/cm) for oil-air system
 γ_{o-w} = Interfacial tension (dynes/cm) for oil-water system

ACKNOWLEDGMENT

The authors gratefully acknowledge the able assistance of Mrs. Wesley Marshall, who performed the experimental work reported in this paper.

REFERENCES

1. Kinney, P. T., and Nielson, R. F.: "The Role of Wettability in Oil Recovery," *Producer's Monthly*, (Jan., 1950) 14, 29.
2. Yuster, S. T., and Stahl, C. D.: "Capillary Pressure Studies," *Producer's Monthly*, (Dec., 1948) 13, 24.
3. Calhoun, J. C.: "Criteria for Determining Rock Wettability," *Oil and Gas Jour.*, (May 10, 1951) 50, 151.
4. Stahl, C. D., and Nielson, R. F.: "Residual Water and Residual Oil by Capillary Pressure Techniques," *Producer's Monthly*, (Jan., 1950) 14, 19.
5. Slobod, R. L., Chambers, Adele, and Prehn, W. L., Jr.: "Use of Centrifuge for Determining Connate Water, Residual Oil, and Capillary Pressure Curves of Small Core Samples," *Trans. AIME*, (1951) 192, 127.
6. McCullough, J. J., Albaugh, F. W., and Jones, P. H.: "Determination of the Interstitial Water Content of Oil and Gas Sand by Laboratory Tests of Core Samples," *API Drill. and Prod. Prac.*, (1944), 182.
7. Katz, D. L.: "Possibility of Secondary Recovery for the Oklahoma City Wilcox Sand," *Trans. AIME*, (1942) 146, 28.
8. Benner, F. C., Dodd, C. G., and Bartell, F. E.: "Evaluation of Effective Displacement Pressures for Petroleum Oil-Water Silica Systems," *API Drill. and Prod. Prac.*, (1942) 169.

DISCUSSION

By S. R. Faris, Member AIME, and J. W. Whalen, Magnolia Petroleum Co., Dallas, Tex.

The authors have presented a subject which is of great importance and interest to the industry and this paper should stimulate interest and further work on this subject.

Wetting phenomena are intimately related to the surface of the porous medium and may be expected to vary from point to point on this surface because of the chemical nature of the surface and its physical roughness. Wettability characteristics of chemically homogeneous surfaces have been estimated from displacement pressure measurements by a number of investigators.¹ The nature of the surface forces existing in a reservoir rock material, however, should be described in terms of an average value resulting from consideration of the entire surface. The authors, in utilizing the air-oil and oil-water displacement pressures to calculate a "wettability number," are considering only the largest of capillaries comprising the

porous medium. In addition the "apparent contact angle," in terms of which the "wettability number" is defined, is considered at only one point on the surface of these capillaries. Wettability characteristics based on an infinitesimal fraction of the surface exposed to flow clearly are not representative of the entire porous matrix.

The extension of this method to capillaries of smaller radii by use of the complete air-oil and oil-water capillary pressure curves, at points of equivalent wetting-phase saturation, is severely limited by the assumption of equivalent capillary radii. It would be interesting, however, to compare the "apparent contact angles" obtained in this manner to those obtained at the conditions of initial displacement pressure.

The authors have mentioned the relationship of the "apparent contact angle" to the receding contact angle. Adam² has pointed out that although wetting-phase displacement pressures should indicate receding contact angles and imbibition pressures advancing contact angles, variations shown by different liquids on silica do not indicate that the relationship is a well defined one. The variations noted by Adam may be an additional reason for questioning the assumption of equivalent capillary radii.

Although the authors indicate the semi-quantitative nature of the work described in the paper, and state that the chief utility of their method is to follow apparent changes in the wettability character of the solid surface, it should be emphasized that the concept of wettability as defined by the "apparent contact angle" is a greatly over-simplified one and that the significance of contact angle as applied to reservoir material is poorly, if at all, understood.

The "apparent contact angle" measurements have been obtained for the system under static conditions and from this standpoint their significance may be largely artificial if used to define the wettability characteristics of the rock under dynamic conditions where knowledge of the interfacial character (wetting phase advancing or receding) is necessary. In addition, Adam³ has shown that the geometry of the capillary greatly influences the nature of the interface advance and attendant displacement pressure. It is hoped that the interest created by the static "apparent contact angle" study of the authors will result in the extension of wettability studies to dynamic systems and in better understanding of the complex problems involved in such systems.

REFERENCES

1. Bartell, F. E., and Osterhof, H. J.: *Ind. Eng. Chem.* (1927) 19, 1277.
2. Adam, N. K.: *Physics and Chemistry of Surfaces*, Oxford Press (1938), 191.
3. Adam, N. K.: *Interaction of Water and Porous Materials, A General Discussion of the Faraday Society*, Gurney and Jackson, Edinburgh, (1948), 5. ★ ★ ★

AUTHOR'S REPLY TO MESSRS. FARIS AND WHALEN

The comments of S. R. Faris and J. W. Whalen may be looked on as a continuation of the discussion in the paper. We are in essential agreement with what is said and insofar as the suggested measurement of "apparent contact angles" as a function of saturation, several such determinations were made early in the study and more work is planned. Our intent in presenting this paper was to set forth the method and assumptions clearly and simply. For this reason discussion of complicating factors was deliberately left out of the paper. The above discussion supplies supplementary information which aids in relating the proposed method to other problems within the broad scope of the wettability problem.

RADIAL FILTRATION OF DRILLING MUD

C. L. PROKOP, HUMBLE OIL AND REFINING CO., HOUSTON, TEX., MEMBER AIME

ABSTRACT

A laboratory investigation has been made of the effects of mud hydraulics upon the formation and erosion of mud filter cakes. The tests were conducted to simulate drilling conditions as nearly as possible.

The formation of mud filter cake in a drilling well does not proceed at a uniform and unbroken rate. Instead, the rate of cake accumulation depends upon whether or not the mud is being circulated. If the mud column is quiescent, filter cake formation is a smooth function of the filtration characteristics of the system. If the mud is being circulated filter cake formation depends not only upon the filtration characteristics of the mud but also upon the erosive action of the flowing mud column.

Filter cakes formed during continuous mud circulation were observed to reach an equilibrium thickness after several hours' circulation. Mud circulation was maintained at a constant volumetric rate throughout each experiment. The fluid velocity at equilibrium cake thickness was dependent upon the thickness of the filter cake. Muds having exceptionally high water loss deposited thick filter cakes in spite of very high eroding velocities. The muds having good filtration characteristics deposited thin filter cakes at equilibrium circulating velocities well within the range of those used in a drilling well.

It was observed that filter cakes deposited during stagnant filtration were quite difficult to erode by mud circulation. The rate of erosion computed from the rate of filtrate accumulation after equilibrium cake thickness had been reached was in reasonable agreement with the rate of erosion obtained by direct observation. Continuous mud circulation usually caused the permeability of the filter cake to decrease with time.

INTRODUCTION

Many of the difficulties encountered during the drilling of a well have been attributed to the loss of water from the mud and the attendant deposition of solids upon the walls of the hole. Past experience has shown that a reduction of the filtration rate of the drilling fluid eliminates or greatly reduces these difficulties. Definite filtration requirements, however, are hard to establish for a given set of conditions. This is due, in part, to the fact that the usual filtration test performed upon mud does not simulate well conditions as closely as desirable.

¹References given at end of paper.

Manuscript received in the office of the Petroleum Branch August 9, 1951. Paper presented at the Petroleum Branch Fall Meeting in Oklahoma City, Okla., Oct. 3-5, 1951.

The filtration characteristics of a mud are customarily determined by means of the standard low-pressure API wall-building tester.¹ In this instrument a filter cake is deposited upon a horizontal bed under a pressure differential of 100 psi. The mud is quiescent during the filtration period. In actual practice, mud filtration occurs within a well under quite different conditions. One of the major differences is that mud flows upward across the filter bed as the filter cake forms. This undoubtedly produces a change in the filter cake which cannot be reflected in the results of the API test.

The laboratory work described in this paper had as its primary objective a better understanding of the influence of mud circulation upon the thickness and characteristics of the filter cakes deposited under conditions similar to those existing in a drilling well.

ANALYSIS OF PROBLEM

Once a permeable formation is penetrated by the bit, filtrate from the mud flows into the formation. The mud solids plaster against the walls of the hole, forming a filter cake. If the mud column is stagnant, that is, if it is not being circulated, the filter cake will increase in thickness until the hole is filled. Prior to the time that the hole is filled, the thickness of filter cake existing at any given time will be a function of the filtration characteristics of the mud, the temperature, and the pressure differential. The effects of these variables have been investigated in the past for both flat bed filtration^{2,3} and for radial filtration.⁴

When the mud is circulated in a hole in which a filter cake is being deposited, some of the solids that would ordinarily deposit in the filter cake will be carried away by the eroding action of the mud. This will limit filter cake thickness. Some work has been done to determine the effect of flow upon the filtration rate in a circulating mud system⁴ but little work has been done upon the factors which determine the filter cake thickness existing in a circulating system.

On first sight it would appear that the major factors controlling filter cake formation in a circulating system should be:

1. The rate of deposition of solids from the mud.
2. The erosive force that the flowing mud exerts upon the filter cake.
3. The erodability of the filter cake.
4. Any change in filter cake characteristics attributable to the scouring action of the mud.

The rate at which solids are deposited from the mud will be controlled to a large degree by the filtration characteristics of the mud, the pressure differential, the temperature under

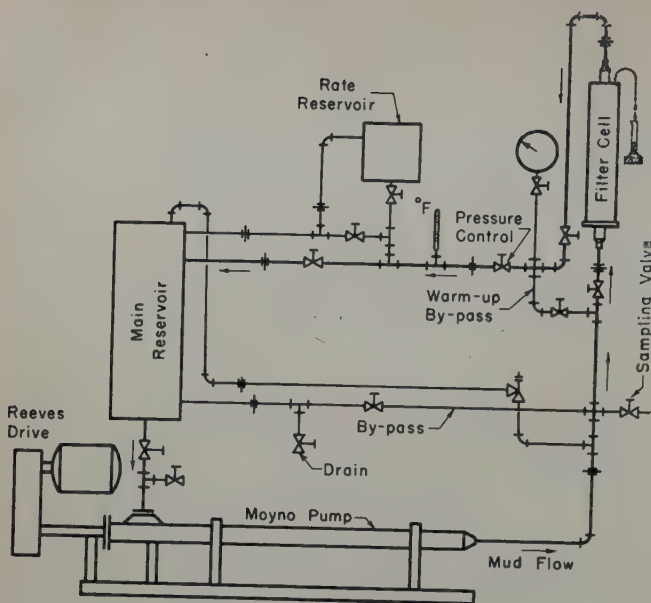


FIG. 1 — DIAGRAM OF RADIAL FILTRATION APPARATUS.

which filtration is taking place, and the thickness of the filter cake already in place.

The erosive action of the circulating fluid should be dependent upon the circulation velocity, the fluid properties, and the type of flow existing in the fluid column, *i.e.*, whether turbulent or viscous.

It seems reasonable to expect some filter cakes to be more difficult to erode than others. Thus, although two muds may have identical filtration rates and filter cake thicknesses as determined by the API test, the filter cakes deposited from the two muds may not offer the same resistance to erosion.

Although the major factors controlling the thickness of a filter cake deposited during circulation should be those mentioned above, the further possibility exists that some classification of the filter cake solids may take place while the cake is being formed. Solids having certain properties may be concentrated in the filter cake. Such an effect might be expected to alter the filter cakes sufficiently to affect their thickness somewhat.

The experimental work described in the following sections was designed to investigate the effects of the foregoing factors on filter cake formation during mud flow.

EXPERIMENTAL PROCEDURE

Apparatus

The laboratory apparatus was designed to simulate as closely as possible the conditions under which filtration occurs in a well. A sketch of the equipment is shown in Fig. 1. The equipment consists essentially of a mud reservoir, a circulating pump, and a radial filter cell. Provisions were made for control of the pressure differential across the filter bed, the circulating volume, and the mud temperature. The filter cell consisted of either (1) a hollow sand cylinder, prepared by consolidation of screened sand with phenol-formaldehyde resin, or (2) a hollow cylinder of permeable sintered brass. The details of the sand filter cell are shown in Fig. 2. The sand column had an inside diameter of 2 in., an outside diameter of 4 in., and was 24 in. in length. The sintered brass filter cell was similar to that using consolidated sand as a filter bed, except that all its dimensions were roughly one-half those of the sand.

Technique

In most of the experiments the pressure differential across the filter cake was kept at 350 psi, and the temperature at about 110°F. It was felt that these conditions were fairly representative of conditions in a well.

Two techniques of investigation were used. These were:

1. Determination of equilibrium thickness of filter cake deposited during continuous mud flow. In the use of this technique mud was circulated through a by-pass until the temperature reached about 110°F. Mud was then allowed to flow through the filter cell at a predetermined volumetric rate, and the by-pass was closed. The thickness of filter cake deposited was measured from time to time. To do this it was necessary to interrupt the run, open the filter cell and gauge the size of the hole open to mud flow. The test was continued until the thickness of the filter cake ceased to increase. A record was kept of the volume of filtrate which had accumulated at various elapsed times.

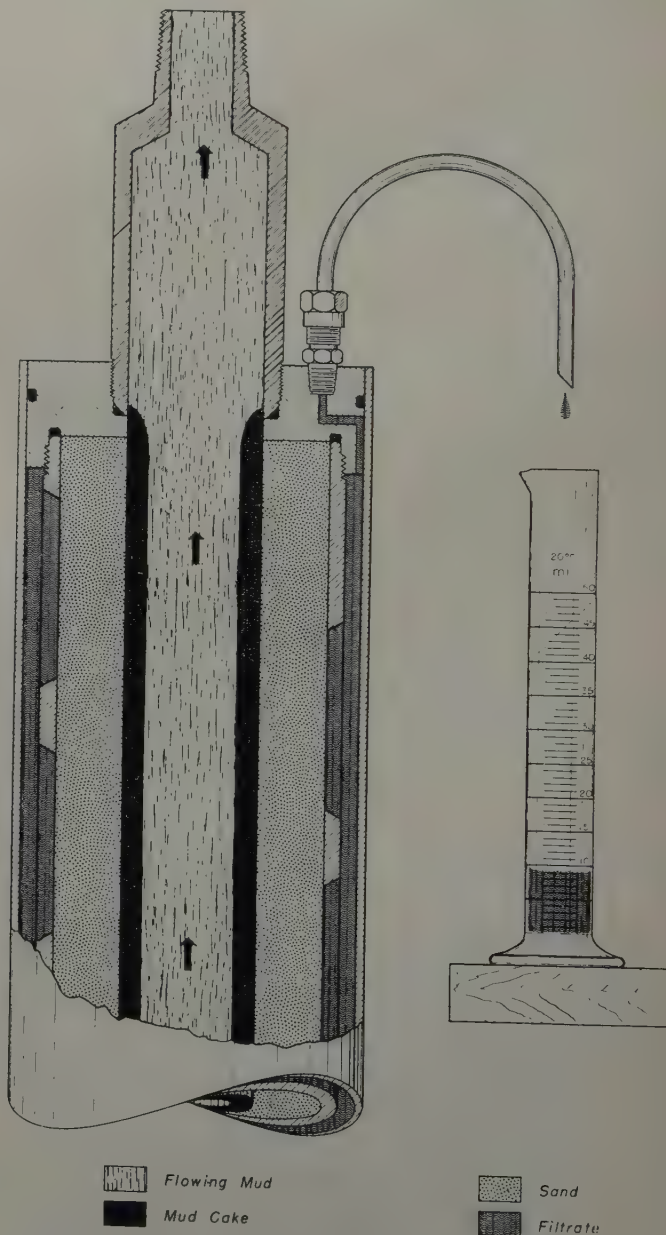


FIG. 2 — RADIAL FILTER CELL.

2. Determination of the thickness of filter cake deposited under static conditions and then eroded by mud flow. In the use of this technique mud was allowed to filter through the filter cell without flowing axially through it. Filtration was allowed to continue at a predetermined pressure and temperature until a very thick filter cake was deposited. Mud was then flowed through the cell at a constant volumetric rate until the filter cake eroded to a constant thickness.

Some auxiliary measurements were made in order to determine the effects of viscosity and velocity upon filter cake erosion. In general, these procedures were similar to those described above.

Muds Used

The muds used in these tests were all prepared in the laboratory. Properties and compositions of the muds are shown in Table I. The muds covered a range of viscosity from 2 to 85 cp (Stormer at 600 RPM) and a filtration range of 7 to 148 cu cm API. The table gives the filtration rates of the muds at both 100 psi and 350 psi. In the discussion to follow the results of the API test (100 psi) will be used as it is a standard test and offers no particular disadvantage to the interpretation of the data.

RESULTS

Effect of Filtration Rate Upon Equilibrium Thickness of Cake

Experiments conducted by depositing a filter cake during continuous mud circulation showed that, in general, the higher the filtration rate of a mud, the thicker was the equilibrium filter cake and the higher was the eroding velocity necessary to stop further formation of filter cake.

Typical results are illustrated in Table II. All of these data were obtained by use of the sand filter cylinder. As shown in Table II, a mud whose API filtration rate was 148 cu cm in 30 minutes caused a filter cake 21/32 in. thick to form before an equilibrium thickness was reached. The velocity required to prevent further formation of filter cake was 530 ft per min. As the API filtration rate was decreased, the filter cake thickness and the velocity required to stop further formation of filter cake decreased, so that for a mud having a filter loss of 19 cu cm in 30 minutes a circulating velocity of 125 ft

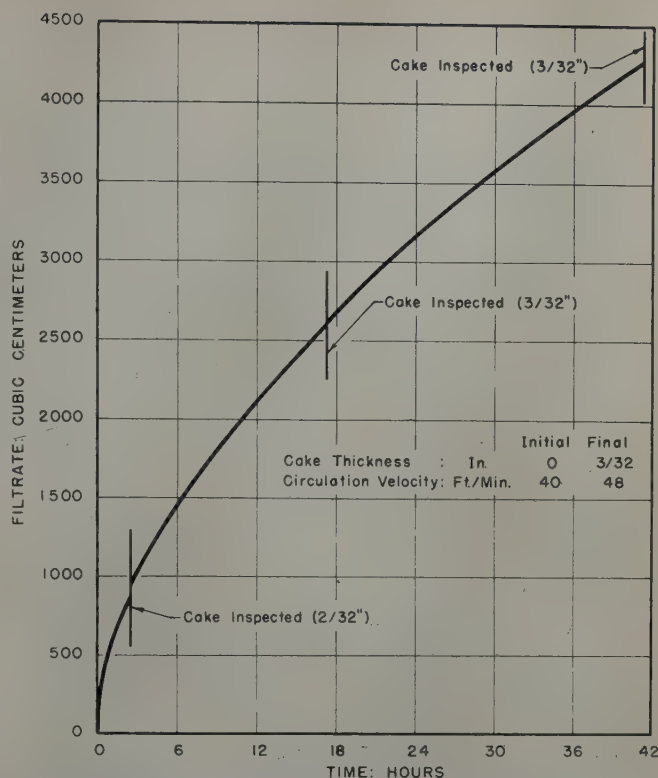


FIG. 3—FILTRATE ACCUMULATION DURING FORMATION OF EQUILIBRIUM FILTER CAKE.

per min permitted only a 1/32 in. cake to form. An 8 cu cm mud formed a cake 3/32 in. thick while exposed to a velocity of only 48 ft per min. The filtration curve for this particular run is shown in Fig. 3. This is a typical curve. The rate of accumulation of filtrate decreased although the filter cake thickness reached a constant value. For this reason the rate of accumulation of filtrate could not be used as an indication of filter cake thickness but actual measurements had to be made.

The filtration rate of a mud had little or no effect on the cake thickness when cakes deposited under static conditions were subjected to several hours' erosion by mud flow. All filter cakes deposited without circulation were extremely difficult to erode by mud flow, and the cake thicknesses determined by this technique were appreciably greater than the equilibrium thicknesses determined by allowing the cakes to build up under continuous mud flow. Table III shows the thickness of each of several filter cakes that were formed in the absence of circulation and then subjected to erosion by mud flow.

The data indicate that a water loss of about 20 cu cm API would be sufficiently low to insure thin filter cakes in a drilling well so long as circulation is continuous. However, during the course of drilling a well mud circulation may be stopped for several reasons, e.g., to run casing, change bits, etc. Once circulation is stopped and a thick filter cake is formed in a hole, the cake will be extremely difficult to erode by circulation alone. Thus, as far as filter cake formation is concerned the lower limits of water loss requirements are probably set by the filter cake that will form when the mud is not being circulated rather than by the filter cake that will form during circulation.

Effect of Viscosity Upon Erosion Rate

Mud viscosity appears to affect erosion only insofar as it controls the type of flow existing in the circulating fluid, i.e., whether it be turbulent or viscous. Experiments undertaken

Table I—Properties of Muds Used in Radial Filtration Experiments

Mud Designation	Filtration Rate, API at 100 psi, cu cm in 30 min	Filtration Rate, API at 350 psi*, cu cm in 30 min	Viscosity Stormer (at 600 RPM) cp	Composition
F	19	21	3	Aquagel, lime, kembreak, caustic, quebracho
G	85	151	2	Zeogel, baroid, lime, kembreak, caustic, quebracho
I	148	217	2	Zeogel, baroid, lime, kembreak, caustic, quebracho
J	35	53	3	Baroco, lime, kembreak, caustic, quebracho
K	10	14	5	El Paso clay, caustic, quebracho
K-a	4.6	—	85	El Paso clay, aquagel, caustic, quebracho
P-a	8	11	2	Baroco, baroid, caustic, quebracho
R	10	14	4	Baroco, lime, caustic, quebracho
S	136	181	2	Zeogel, kaolin, salt, caustic, quebracho
S-a	88	147	70	Zeogel, kaolin, salt, caustic, quebracho
T	49	56	5	Baroco, kaolin, salt, starch
W	7.0	9	3	Baroco, kaolin, caustic, carbonox, lime, diesel oil

*Test at 350 psi run on Baroid HP Tester and results corrected to filter area of LP-API Wall Building Tester.

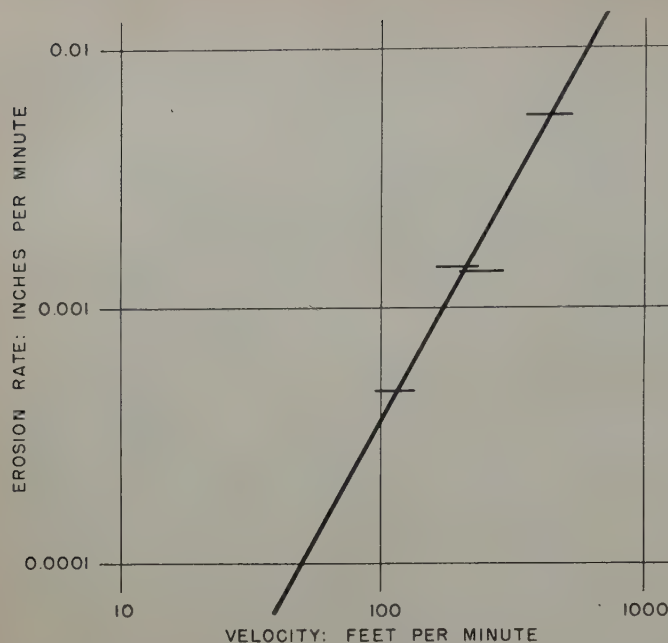


FIG. 4—EFFECT OF CIRCULATION VELOCITY ON EROSION RATE (TURBULENT FLOW).

to determine the effects of very high viscosities upon erosion rate failed to show any significant change in erosion rate except as mentioned. One experiment designed to determine the effect of viscosity upon erosion was conducted by observing the effects of mud circulation upon the erosion of a pre-formed filter cake. To establish a basis for comparison, a low viscosity mud was circulated past the filter cake. The erosion that resulted was observed. This was followed by the same mud but treated to a very high viscosity. The erosion was again observed. Finally a very thin fluid which resembled the mud filtrate in chemical composition was circulated through the filter cylinder. The effect of mud viscosity upon the erosion of pre-formed filter cakes is presented in the upper part of Table IV. The thick, pre-formed filter cake was eroded by the low viscosity mud until the circulation velocity had dropped from 1,200 ft per min to 430 ft per min. Circulation of the very high viscosity mud caused no further change in cake thickness, and the circulation velocity remained at 430 ft per min. Circulation of the thin fluid produced some additional erosion, and the velocity dropped to about 200 ft per min during the run.

In a second series of experiments a low viscosity mud was circulated in turbulent flow until equilibrium had been reached in cake thickness and circulation velocity. The mud viscosity was increased by the addition of clay and the run repeated. This time the mud was circulated in viscous flow. The effects of mud viscosity upon the thickness of filter cakes deposited during mud flow are also presented in Table IV. Of the two muds, the mud of lower viscosity had the higher API filtration rate, but it deposited a thinner filter cake than did the mud of higher viscosity. This difference is further emphasized by the very high flow velocities which existed in the viscous mud at the end of the experiment.

The tests described indicate that a fluid flowing in turbulent flow will be considerably more erosive than will a fluid flowing in viscous flow. This might be expected from a consideration of the difference in the two types of flow. Turbulent flow designates a condition where the flow stream contains many more or less violent eddies. The walls of the flow channel are scoured by currents at oblique angles to the direction

of flow. In contrast viscous or laminar flow denotes a flow condition where the individual fluid particles are all moving in the direction of flow. The walls of the flow channel are exposed to a constant shear stress but to much less scouring.

From the data it appears that changes in mud viscosity will not appreciably affect filter cake erosion rates as long as the changes do not cause a switch between turbulent and viscous flow. It appears that erosion rates are higher and filter cakes are thinner when the filter cakes are exposed to turbulent flow than when they are exposed to viscous flow.

Effect of Velocity Upon Erosion Rate

Some pre-formed filter cakes were eroded by circulating a thin clear fluid past them. The eroding liquid was made to resemble the filtrate from the muds that were used to deposit the filter cakes. Observations were made of the effect of circulation velocity upon erosion rates. This technique allowed direct observation of filter cake erosion in the absence of filter cake deposition. The experiment was conducted at one circulation velocity until significant erosion had occurred. The extent of erosion was measured, and after deposition of a fresh filter cake the run was repeated at another velocity. A pressure differential of 13 psi was held across the filter cake during each erosion test. In all the tests the circulating fluid was flowing in turbulent flow.

It was found that a fluid flowing in turbulent flow would erode a filter cake at a rate proportional to the square of the circulation velocity. These data are illustrated in Fig. 4. Probably the most significant fact illustrated by the data is the slowness with which filter cake erosion occurs. At normal circulation velocities filter cake erosion was in the order of 1/20 in. per hour.

A further check was made upon filter cake erosion by an analysis of the equilibrium data obtained during continuous circulation and filter cake formation. To do this it was assumed that at filter cake equilibrium the rate of deposition of solids was just equal to the rate of erosion of the filter cake. The measured rate of filtrate accumulation and the amount of filter cake deposited per unit volume of filtrate were used to calculate the rate of deposition of solids. The volume of filter cake deposited per volume of filtrate was measured in an auxiliary experiment. The calculated rate of filter cake erosion was plotted against circulation velocity. These data are shown in Fig. 5. The erosion rate increases with circulation velocity, being approximately proportional to the square of the circulation velocity. It can be seen that the erosion rates obtained from the calculations are reasonably close to erosion rates obtained by direct observation. The differences in the erosion rates obtained at any given velocity were probably due to differences in erodability of the various filter cakes.

Erodability

Some muds deposit filter cakes that are harder to erode than others. Direct measurements were made of the erodability of pre-formed filter cakes which were exposed to a circulation velocity of 300 ft per min. The circulating fluid was flowing

Table II—Effect of Filtration Rate on Equilibrium Thickness of Filter Cake

Mud Used	Cake Eroding During Deposition—Turbulent Flow		
	Consolidated sand filter cylinder. Filtration Rate LP-API	Pressure differential—350 psi Filter Cake Thickness in.	Equilibrium Velocity ft/min
P-a	8	3/32	48
R	10	6/32	72
F	19	1/32*	125*
G	85	19/32	220
I	148	21/32	530

*Circulation velocity increased by use of a mandrel.

in turbulent flow and was similar in composition to the filtrate from the muds which formed the cakes. A tenfold difference between the erosion rates was observed for the two muds tested. A caustic-quebracho-clay-barytes mud (API water loss — 8.0 cu cm) deposited a filter cake that would erode at 3×10^{-3} in. per min, whereas a clay-fresh-water mud (API water loss — 52 cu cm) deposited a filter cake that would erode at a rate of only 3×10^{-4} in. per min.

The erosion rates given above are quite low, but it should be noted that once an appreciable filter cake has formed from a mud having a moderate water loss, filter-cake accumulation proceeds at a very low rate. Take, for example, the formation of a filter cake from a mud having a water loss of 10 cu cm API. On the assumption that 0.4 cu cm of filter cake will be deposited for every 1.0 cu cm of filtrate passing through the cake, it was computed that by the time the filter cake has reached a thickness of 4/32 in., the rate of formation of filter cake will be of the order of 1.6×10^{-4} in. per min.

Filter Cake Characteristics

Several investigators⁵ have found that, below a certain critical size, large particles are washed from the bottom of a stream or river with greater ease than are small ones. The critical size has been set near 0.5 mm. That is, for particles below this critical size, larger particles are moved along the bottom of a channel, while the small ones remain in place. With the exception of cuttings, nearly all the material in a drilling mud is below the critical size. This suggests the possibility of a size classification within a filter cake. Several runs were made in the radial filter to check this possibility. It appeared that size classification was the cause of a continual reduction in filter cake permeability during a circulation period.

A filter cake deposited in a quiescent filter cell showed little change in permeability during a long filtration period. Filter cakes deposited during continuous circulation would gradually decrease in permeability as long as the experiment continued. This was evidenced by a continual decrease in filtration rate after the filter cake had reached a constant thickness. During one run, which continued for 3.7 days, the permeability of the filter cake dropped from 6.0×10^{-4} md to 2.0×10^{-4} md.

CONCLUSIONS

1. As far as filter cake thickness is concerned, the lower limits of water loss requirements are probably set by the amount of filter cake that will form during the time the drilling mud is not being circulated rather than by the thickness of filter cake that will form during circulation.
2. In a mud stream that is being circulated continuously, thin filter cakes are formed if the API water loss of the mud is maintained near 20 cu cm or less.
3. A thick filter cake formed during a period of no circulation is very hard to wash away by mud circulation.
4. Much thicker filter cakes are to be expected with the mud flowing in viscous rather than in turbulent flow.

Table III — Filter Cake Thickness After Prolonged Erosion

Mud Used	Cake Deposited, Then Eroded — Turbulent Flow		
	Filtration Rate LP-API cu cm in 30 min	Filter Cake Thickness in.	Final Circulation Velocity ft/min
R	10	23/32	430
J	35	21/32	420
I	143	25/32	920

Table IV — Effect of Viscosity on Filter Cake Erosion

Mud Used	Filtration Rate LP-API cu cm in 30 min	Filter Cake Thickness in.	Cake deposited, then eroded			Type of Flow in Core
			Viscosity Stormer (600 RPM) cp	Equilibrium Velocity ft/min	Pressure differential psi	
Consolidated sand		filter cylinder	—	—	—	350 psi
K	10	23/32*	5	430	—	Turbulent
K-a	46	23/32	85	>430	—	Viscous
**	—	18/32	1	<200	—	Turbulent
Sintered brass		filter cylinder	—	—	—	350 psi
		Cake eroding during deposition				
S	136	4.5/32	2	545	—	Turbulent
S-a	88	7/32	70	1,280	—	Viscous

*Prior to erosion the cake was 27/32-in. thick.

**Caustic-quebracho solution.

3. In turbulent flow, erosion of filter cake increases approximately with the square of the circulation velocity.
6. Continuous mud circulation past a filter cake nearly always decreases the permeability of the filter cake.

REFERENCES

1. *Recommended Practice for Standard Field Procedure for Testing Drilling Fluids* (Tentative), API Code 29, Third Ed., (May, 1950), American Petroleum Institute, Dallas, Tex.
2. Walker, W. H., Lewis, W. K., McAdams, W. K., and Gilliland, E. R.: *Principles of Chemical Engineering*, 3rd Ed., McGraw-Hill Book Co., New York and London, (1937).
3. "Method of Determining the Filtration Characteristics of Drilling Muds," *Drilling Mud*, Baroid Sales, (May, 1948) 6, No. 1.
4. Williams, M.: "Radial Filtration of Drilling Muds," *Trans. AIME*, (1940) 136, 57.
5. Dallavalli, J. M.: *Micromeritics*, Pitman Publishing Corp., New York and Chicago, (1943).

ACKNOWLEDGMENT

The author wishes to thank the Humble Oil and Refining Co. for permission to publish this paper, and to express his appreciation for the help given by his associates in obtaining a large part of the data.

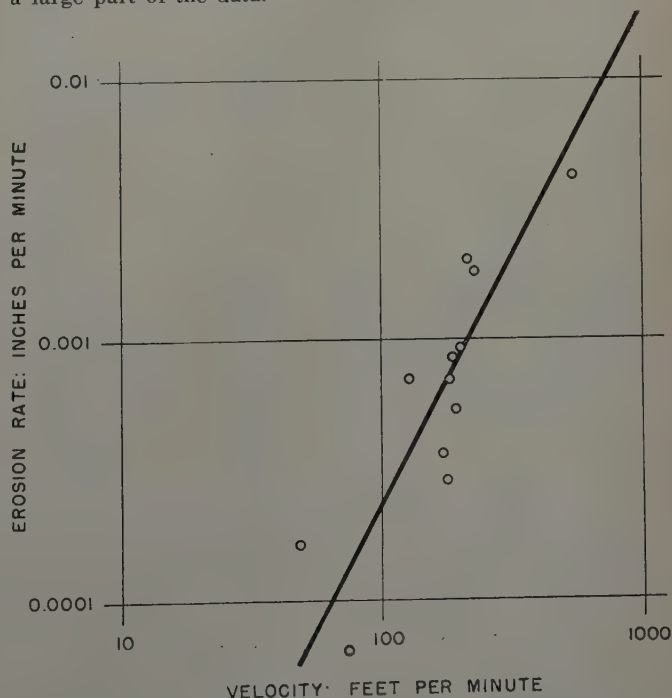


FIG. 5 — EFFECT OF CIRCULATION VELOCITY ON EROSION RATE (TURBULENT FLOW).

DISCUSSION

By O. W. Van Dyke, Magnet Cove Barium Corp., Houston, Tex., Member AIME

Prokop has presented some very interesting facts about mud filtration, cake deposition, and cake erosion by fluid circulation. The radial filtration apparatus and the procedure described indicate some of the complexities of this problem and the large amount of work that is required to study the filtration performance of a mud under laboratory conditions that are designed to simulate hole conditions. The physical properties of the muds used in these experiments do not approximate field drilling fluids as closely as would be desired. It is hoped that Prokop will continue this work and in the future include results obtained using a variety of types of muds taken from drilling wells.

It is evident that there are factors, other than those considered in this paper, which affect filtration and cake deposition in a drilling well, otherwise it would not be possible to work in holes with as much freedom from filter cake trouble as we do. It is probable that the rubbing action of the bit and drill pipe decreases the permeability and thickness of the filter cake deposited on permeable zones in a hole. Prokop observed a continued decrease in the filtration rate after the cake thickness had reached an equilibrium between deposition and erosion. The explanation offered of particle size classification in the filter cake seems very logical. If continued circulation brings about a particle size classification in the filter cake which reduces the permeability, it seems reasonable to expect that the rubbing of the bit and drill pipe may bring about a rearrangement of the particles in a filter cake which influences its permeability.

I would like to suggest that the mechanical action of the bit and drill pipe upon the filter cake be considered in mud filtration studies that are to simulate conditions of a drilling well.

AUTHOR'S REPLY TO MR. VAN DYKE

Van Dyke suggests that the muds used in the experiments did not approximate field muds as closely as desirable. The muds were all laboratory muds designed for stability of properties and made to cover a rather wide range in filtration rates. When an effort was made to use field muds, their properties were observed to change rapidly because of the unusual amount of agitation to which a mud was subjected in the experimental equipment.

The mechanical action of the drill pipe and the bit were not studied. This was because it seemed advisable to find the effects of mud hydraulics upon filter cake formation in a system that was not any more complicated than necessary. No doubt drill pipe rotation and the action of the bit influence filter cake characteristics. But this was considered to be a separate problem.

DISCUSSION

By H. T. Byck and H. C. H. Darley, E. and P. Research Division, Shell Oil Co., Houston, Tex.

We were particularly interested in this paper because it gave experimental evidence on a question in which we have long been interested; namely, how soon does the filter cake on the walls of the hole reach an equilibrium thickness. The point is important because a condition where filtration proceeds without increasing the cake thickness is essentially

different from that prevailing in the API test so that, as Prokop has pointed out, the test will not be a true measure of the performance to be expected in the well. When the cake thickness is constant, the water loss to the formation will be proportional, not to the API test water loss, but to the permeability of the filter cake and the equilibrium thickness it assumes in the well. Fortunately, the former can be calculated approximately from the data of the API test. It can be shown from D'Arcy's Law that the permeability of the cake in millidarcies is equal to the product of the filtrate volume in cubic centimeters, the cake thickness in millimeters and a constant which is equal to 7.18×10^{-5} at 30°C . We would emphasize that cake permeability is not proportional to the test water loss, the difference being that the latter varies with the concentration of solids in the mud, whereas the cake permeability does not.

So two unknowns remain: how soon does the cake reach equilibrium thickness, and what is this equilibrium thickness. Prokop has provided some interesting and valuable data on these points, but we feel that one important factor has been omitted, doubtless because it would be extremely difficult to duplicate in the laboratory; that is, the eccentric rotation of the drill pipe wearing down the cake. There can be no doubt that a long flexible shaft such as the drill pipe must continually sweep the sides of the hole, and in fact we have good evidence of this in the wear on tool joint protectors and the inside of casing strings. This may well be one of the principal factors affecting the equilibrium thickness of the cake, and may upset Prokop's conclusion that the cake laid down under static conditions will retain its thickness after drilling is resumed. Our own feeling on the question of the cake thickness in the well is that this will be determined not so much by the properties of the mud as by the mechanics of drilling, i.e., the circulation rate and other factors mentioned by Prokop, plus the action of the drill pipe, and whether or not the hole has been drilled to gauge, etc. If this is so, then the only significant property of the mud governing water loss to the formation for a condition of constant cake thickness is the permeability of the filter cake.

To sum up, conditions in the hole are so complicated that it appears unlikely that a routine test can be devised to yield data directly proportional to the performance of mud in the well. However, we ought to recognize that two general conditions occur in the well: (1) the filter cake increases as filtration proceeds and (2) the thickness remains constant but water loss continues through it. The API water loss is the best criterion for the former, the cake permeability for the latter.

AUTHOR'S REPLY TO MESSRS. BYCK AND DARLEY

Byck and Darley are correct in emphasizing the influence of cake permeability upon the amount of filtrate that will penetrate a formation once a constant filter cake thickness has been reached. The permeability of a filter cake is, however, a function of several variables. One of the most influential is the pressure differential across the cake. When a single measurement of cake permeability is presented, the pressure at which the measurement was made should be specified. The permeabilities mentioned in the paper were measured while there was a pressure differential of 350 psi across the cake. The formula presented in the discussion appears to be applicable to the standard API test. This test is made at 100 psi.

References 2 and 4 of the paper include a discussion of the effect of filtration pressure upon filter cake permeability.

★ ★ ★

VOLUMETRIC BEHAVIOR OF CONDENSATE AND GAS FROM A LOUISIANA FIELD—II

B. H. SAGE, MEMBER AIME, AND H. H. REAMER, CALIFORNIA INSTITUTE OF TECHNOLOGY, PASADENA, CALIF.

ABSTRACT

The formation volume and the relative volume of the liquid phase of mixtures of condensate and gas from five different parts of a field in the Louisiana area have been established experimentally. These studies included gas-condensate ratios as high as 25,000 cu ft/bbl at pressures up to 5,000 psi. The gravities of the tank condensates were between 53.9° and 63.9° API.

The compositions of the condensate and gas samples investigated are presented in tabular form. The formation volume, the relative volume of the liquid phase, and the specific volume of the mixtures are available. A rough correlation of the formation volume as a function of pressure, temperature, and gas-condensate ratio has been presented. This correlation is considered applicable only to the range of conditions covered in this investigation for systems of similar nature and composition.

INTRODUCTION

Often a knowledge of the influence of temperature, pressure, and relative quantities of condensate and gas upon the volumetric behavior of fluids from a given field has been employed in estimating the conditions existing in the reservoir. The early work of Beecher and Parkhurst¹ and the more recent studies of the Dominguez² and San Joaquin Valley Fields³ are examples of experimental studies of this character. Correlation of the volumetric behavior of naturally occurring hydrocarbon mixtures has proved to be feasible^{4,5} at low gas-condensate ratios for fluids* from a single geographic area. Progress is being made in the prediction of the volumetric behavior of distillate systems at high gas-condensate ratios and pressures. However, the estimation of the retrograde^{6,7} dew-point pressure still remains uncertain and probably can best be established by experiment. For this reason it appears of interest to make available experimental information about the volumetric behavior of mixtures of condensate and gas from five different parts of a single field. This material shows a rough similarity to data for mixtures of condensate and gas from San Joaquin^{3,8} Valley Fields.

In the present paper, no attempt has been made to coordinate the available information on the volumetric behavior of fluids from condensate fields. It appears hopeful that progress can be realized by the utilization of recently developed equations of state.⁹ However, the primary problem in any such correlation is the proper identification of the components and constituents⁹ of naturally occurring systems. Additional experimental information may be required to permit the determination of the values of the constants of the equation of state for

each of the important components and constituents. The extension of experimental work in the region of retrograde phase behavior^{7,10,11} for naturally occurring mixtures appears worthwhile since recent studies¹² indicate the existence of hetero-

Table I—Composition of Trap Samples

Component	Gas		Liquid	
	Mole Fraction	Weight Fraction	Mole Fraction	Weight Fraction
System A				
Methane	0.9032	0.7792	0.0877	0.0136
Ethane	0.0467	0.0755	0.0573	0.0166
Propane	0.0247	0.0586	0.0605	0.0257
Isobutane	0.0094	0.0294	0.0526	0.0295
n-Butane	0.0069	0.0216	0.0500	0.0280
Isopentane	0.0029	0.0113	0.0455	0.0316
n-Pentane	0.0016	0.0062	0.0334	0.0232
Hexanes	0.0016	0.0074	0.0863	0.0717
Heptanes	0.0005	0.0027	0.1073	0.1036
Octanes and heavier	0.0005	0.0034	0.4194	0.6565
Carbon Dioxide	0.0020	0.0047	—	—
System B				
Methane	0.8863	0.73894	0.12716	0.02159
Ethane	0.0457	0.07142	0.03658	0.01164
Propane	0.0344	0.07884	0.07678	0.03583
Isobutane	0.0144	0.04350	0.06663	0.04098
n-Butane	0.0085	0.02563	0.06418	0.03948
Isopentane	0.0040	0.01500	0.06235	0.04761
n-Pentane	0.0014	0.00525	0.03819	0.02916
Hexanes	0.0016	0.00717	0.07831	0.07142
Heptanes	0.0011	0.00573	0.10715	0.11364
Octanes and heavier	0.0006	0.00390	0.34269	0.58865
Carbon Dioxide	0.0020	0.00457	—	—
System C				
Methane	0.8822	0.7283	0.1297	0.0213
Ethane	0.0487	0.0753	0.0368	0.0113
Propane	0.0298	0.0677	0.0619	0.0280
Isobutane	0.0130	0.0388	0.0562	0.0334
n-Butane	0.0094	0.0281	0.0505	0.0301
Isopentane	0.0045	0.0169	0.0552	0.0408
n-Pentane	0.0025	0.0094	0.0343	0.0254
Hexanes	0.0023	0.0103	0.1047	0.0924
Heptanes	0.0022	0.0112	0.1051	0.1079
Octanes and heavier	0.0004	0.0027	0.3656	0.6094
Carbon Dioxide	0.0050	0.0113	—	—
System D				
Methane	0.9102	0.79095	0.13051	0.01969
Ethane	0.0443	0.07216	0.03727	0.01054
Propane	0.0212	0.05064	0.05324	0.02208
Isobutane	0.0087	0.02739	0.03630	0.01985
n-Butane	0.0049	0.01543	0.04666	0.02551
Isopentane	0.0027	0.01055	0.04651	0.03156
n-Pentane	0.0015	0.00586	0.03299	0.02239
Hexanes	0.0015	0.00700	0.08453	0.06852
Heptanes	0.0005	0.00271	0.11860	0.11178
Octanes and heavier	0.0015	0.01016	0.41339	0.66808
Carbon Dioxide	0.0030	0.00715	—	—
System E				
Methane	0.9380	0.8568	0.0779	0.0109
Ethane	0.0322	0.0751	0.0291	0.0076
Propane	0.0139	0.0349	0.0348	0.0134
Isobutane	0.0038	0.0126	0.0262	0.0133
n-Butane	0.0034	0.0113	0.0767	0.0389
Isopentane	0.0019	0.0078	0.0363	0.0229
n-Pentane	0.0005	0.0021	0.0296	0.0186
Hexanes	0.0008	0.0039	0.0908	0.0683
Heptanes	0.0004	0.0023	0.1199	0.1049
Octanes and heavier	0.0001	0.0007	0.4787	0.7012
Carbon Dioxide	0.0050	0.0125	—	—
System F				
Methane	0.9480	0.8929	—	—
Ethane	0.0368	0.0650	—	—
Propane	0.0120	0.0311	—	—
Isobutane	0.0022	0.0075	—	—
n-Butane	0.0009	0.0031	—	—
Pentanes plus	0.0001	0.0004	—	—
n-Pentane	0.0328	0.0543	—	—
Hexanes	0.1804	0.1413	—	—
Heptanes plus	0.7868	0.8044	—	—

*References given at end of paper.

Manuscript received in the office of the Petroleum Branch June 11, 1951.

*For present purposes low gas-condensate ratios will be considered as those below 3,000 cu ft/bbl, and the region of high gas-condensate ratio will be limited to compositions containing more than 5,000 cu ft of gas per bbl of condensate. Mixtures containing between 3,000 and 5,000 cu ft of gas per bbl will be considered of intermediate gas-condensate ratio.

	A	B	System C	D	E
Specific Gravity at 60°F, Atmospheric Pressure	0.7981	0.7881	0.7841	0.7903	0.7971
Average Molecular Weight	162.4	162.3	162.7	171.8	167.8

The terminology used in the discussion of the volumetric and phase behavior of naturally occurring mixtures has become somewhat standardized. In the present instance the terms will correspond to the glossary included in a recent publication⁸ which closely follows earlier discussions. All volumetric quantities unless otherwise specified are considered as measured at 60°F and 14.73 psia. The term "liquid formation volume," which is analogous to "formation volume," refers to the ratio

The procedures, equipment, and methods which have been employed in this investigation already have been described^{8,13,14,15} and no significant modification from the original procedure was necessary in the present study. The composition of the experimentally studied mixtures is available,¹⁶ and a

Vol. 195, 1952

portion of these data constitutes Table IV.* The data have been presented upon a molal and weight basis and were established from a knowledge of the relative weights and the compositions of trap liquid and trap gas used in each of the mixtures.

EXPERIMENTAL RESULTS

The experimental measurements obtained for the several mixtures investigated are recorded¹⁶ for systems A to F. In this tabulation the specific volume, the volume of the liquid phase per unit weight of mixture, formation volume, and the formation volume of the liquid phase³ have been presented at a series of even-valued pressures and temperatures for each of the mixtures. Samples of these tabulations are shown in Tables IV and V.* A sufficient number of illustrative diagrams already is available^{3,8} to make unnecessary the presentation of graphical representation of these data. From a qualitative standpoint, the behavior is similar to that of other naturally occurring condensate hydrocarbon systems.

At present, the prediction of retrograde dew point⁹ is perhaps the most uncertain of the properties to be estimated by existing methods. The experimentally determined retrograde dew-point pressure is recorded in Table VI as a function of even values of the gas-condensate ratios for System F. The relation of the retrograde dew-point pressure and the gas-condensate ratio for this system is shown in Fig. 1. The dew-point pressure reaches a maximum at a gas-condensate ratio of approximately 8,000 cu ft/bbl and decreases rapidly at higher ratios. There was insufficient experimental background to establish with certainty the effect of gas-condensate ratio on the retrograde dew-point pressure for the other systems except within a limited range of conditions. The influence of temperature on the retrograde dew-point pressure for System F is presented in Fig. 2. A maximum in this pressure is encountered for the three gas condensate ratios involved at temperatures between 110° and 130°F. This type of behavior is similar to that occurring in other studies.¹⁷

*In order to conserve publication space only sample portions of Tables IV and V are presented here. For detailed paper order Document 3299 from American Documentation Institute, 1719 N Street, N.W., Washington 6, D. C., remitting \$1.00 for microfilm (images 1 in. high on standard 35 mm. motion picture film) or \$9.90 for photocopies (6 x 8 in.) readable without optical aid.

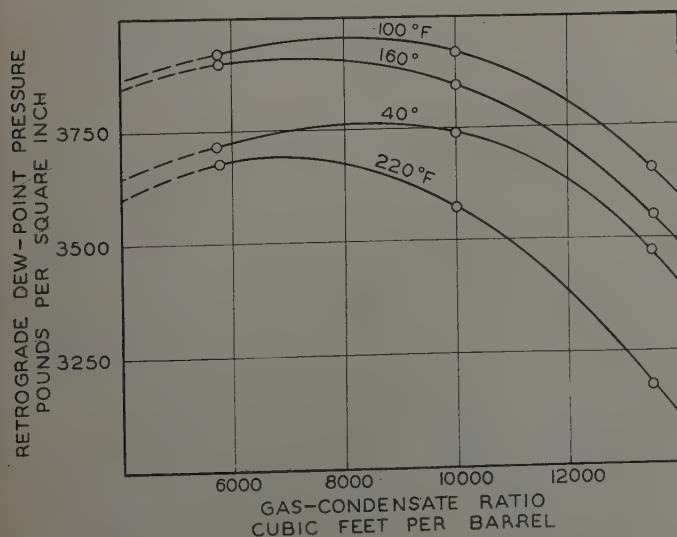


FIG. 1 — RELATION OF RETROGRADE DEW-POINT PRESSURE AND GAS-CONDENSATE RATIO FOR SYSTEM F.

Table IV — Sample of Composition of Experimentally Studied Mixtures

Component	System A		Trap Gas	
	Mole Fraction	Weight Fraction	Mole Fraction	Weight Fraction
Methane	0.6798	0.2601	0.7478	0.3443
Ethane	0.0496	0.0356	0.0487	0.0421
Propane	0.0345	0.0363	0.0315	0.0399
Isobutane	0.0212	0.0294	0.0176	0.0294
n-Butane	0.0187	0.0259	0.0151	0.0252
Isopentane	0.0146	0.0251	0.0110	0.0228
n-Pentane	0.0103	0.0177	0.0077	0.0159
Hexanes	0.0248	0.0510	0.0177	0.0439
Heptanes	0.0297	0.0711	0.0209	0.0600
Carbon Dioxide	0.0015	0.0015	0.0016	0.0020
Octanes and heavier	0.1153	0.4463	0.0804	0.3745
Gas-Condensate Ratio =		3216 ^a		4960
Cu Ft/Bbl		2665 ^b		4031

^aGas-condensate ratio expressed as cu ft/bbl of tank oil.

^bGas-condensate ratio expressed as cu ft/bbl of butanes and heavier hydrocarbons.

Table V — Sample of Volumetric Behavior of Experimentally Studied Mixtures

Pressure, Psia	System A			
	Specific Volume Cu Ft/Lb	Liquid Volume Cu Ft/Lb	Formation Volume	Liquid Formation Volume
	Weight Fraction Trap Gas = 0.3220 Gas-Condensate Ratio = 2,665 cu ft/bbl			
	40°F			
B.P.	(3,630) ^a	0.02987	2.060	2.060
400	0.02987	0.01483	15.199	1.023
600	0.14125	0.01559	9.743	1.075
800	0.10269	0.01627	7.083	1.122
1,000	0.08015	0.01690	5.528	1.166
1,250	0.06272	0.01763	4.326	1.216
1,500	0.05180	0.01837	3.573	1.267
1,750	0.04463	0.01911	3.078	1.318
2,000	0.03980	0.01997	2.745	1.377
2,250	0.03651	0.02087	2.518	1.440
2,500	0.03426	0.02193	2.363	1.513
2,750	0.03274	0.02320	2.258	1.600
3,000	0.03168	0.02470	2.185	1.704
3,250	0.03086	0.02641	2.128	1.822
3,500	0.03020	0.02855	2.083	1.969

^aFigure in parentheses represents bubble-point pressure expressed in pounds per square inch absolute.

Table VI — Retrograde Dew-Point Pressure

Temperature °F	System F Gas-Condensate Ratio cu ft/bbl				
	6,000	8,000	10,000	12,000	14,000
40	3,694 ^a	3,758	3,740	3,628	3,408
70	3,850	3,890	3,863	3,754	3,549
100	3,928	3,956	3,920	3,808	3,599
130	3,943	3,960	3,911	3,790	3,581
160	3,904	3,904	3,845	3,712	3,487
190	3,825	3,804	3,731	3,576	3,329
220	3,714	3,676	3,576	3,388	3,100

^aRetrograde dew-point pressure expressed in pounds per square inch absolute.

It has been found^{3,5,6,8} that there exists a nearly linear variation in the formation volume with the gas-condensate ratio under isobaric-isothermal conditions. In the case of distillate fields the following expression³ describes the volumetric behavior in the heterogeneous region with reasonable accuracy:

$$v = \frac{ArT}{P} \quad (1)$$

The coefficient A of Equation (1) has been considered as a function only of pressure and temperature. The data recorded in Table VII represent average values of this coefficient for each of the mixtures investigated. There was an average deviation of 3.4 per cent of the individual values of this coefficient at a particular pressure and temperature from the quantities

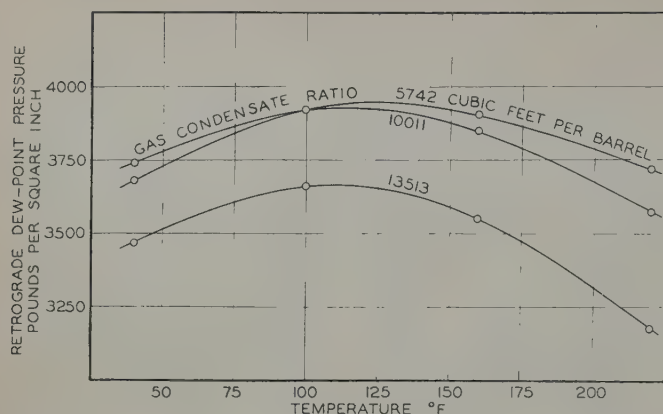


FIG. 2 — INFLUENCE OF TEMPERATURE UPON THE RETROGRADE DEW-POINT PRESSURE FOR SYSTEM F.

recorded in Table VII. This deviation was much larger than that encountered in two other investigations of gas-condensate fields.^{3,17*} A comparison was made of the formation volumes computed from the coefficients in Table VII with experimentally determined values. The average deviation of the predicted and experimental formation volumes at 18 states chosen at random was 3.8 per cent. Table VIII presents a comparison of the coefficients which were obtained at several temperatures and pressures from the present studies and from measurements of the volumetric behavior of mixtures of condensate and gas from fields in the San Joaquin Valley³ and Louisiana.¹⁷ There appears to be a larger variation in this coefficient from one field to another than is experienced with the changes in gravity of the tank condensate from one zone to another in a particular field. It is expected that the coefficient of Equation (1) will be primarily a function of the relative quantity of the lighter hydrocarbons present rather than those of intermediate molecular weight. For this reason it is not surprising that minor changes in the gravity of the tank condensate did not influence the coefficients greatly.

*The legend of Fig. 1 of Reference 17 is in error and should read, "Pressure Specific Volume Product for System C Containing 0.8928 Weight Fraction Trap Gas." The discussion of Fig. 1 should be modified to "... 0.8928 weight fraction trap gas."

Table VII — Values of Coefficient A
 $A \times 10^3$

Pressure, Psia	40°F	100°F	160°F	220°F
600	4.39	4.65	4.85	5.01
800	4.22	4.54	4.77	4.95
1,000	4.07	4.44	4.70	4.90
1,250	3.91	4.35	4.63	4.84
1,500	3.79	4.27	4.58	4.81
1,750	3.72	4.22	4.55	4.79
2,000	3.70	4.19	4.54	4.78
2,250	3.70	4.20	4.54	4.78
2,500	3.73	4.23	4.57	4.80
2,750	3.83	4.29	4.61	4.83
3,000	3.98	4.38	4.67	4.87

Table VIII — Comparison of Volumetric Behavior of
Fluids from Several Fields
Coefficient $A \times 10^3$

Pres- sure, Psia	100°F			160°F			220°F		
	San Joa- quin	Louis- iana 1	Louis- iana 2	San Joa- quin	Louis- iana 1	Louis- iana 2	San Joa- quin	Louis- iana 1	Louis- iana 2
600	4.58	4.45	4.65	4.75	4.90	4.85	4.89	5.03	5.01
1,000	4.35	4.07	4.44	4.59	4.74	4.70	4.77	4.93	4.90
1,500	4.09	3.75	4.27	4.41	4.59	4.58	4.66	4.84	4.81
2,000	3.99	3.59	4.19	4.29	4.51	4.54	4.59	4.80	4.78
3,000	3.92	3.70	4.29	4.29	4.52	4.67	4.61	4.81	4.87

NOMENCLATURE

- A Dimensional coefficient
 P Pressure, psia
 r Gas-condensate ratio, cu ft/bbl
 T Absolute temperature, °R
 v Formation volume

ACKNOWLEDGMENT

This investigation was made possible by the financial support, cooperation and interest of the Texaco Development Corp. which also provided the samples for this experimental study. The Texas Co. carried out the analyses of the trap samples reported. R. H. Olds and Betty Kendall assisted with the preparation of experimental measurements in a form suitable for publication.

REFERENCES

- Beecher, C. E., and Parkhurst, I. P.: "Effect of Dissolved Gas Upon the Viscosity and Surface Tension of Crude Oil," *Trans. AIME*, (1926), 51.
- Sage, B. H., and Lacey, W. N.: "Formation Volume and Viscosity Studies for Dominguez Field," *API Drill. and Prod. Prac.*, (1935), 141; *The Oil Weekly*, (1935) 77, 10.
- Sage, B. H., and Olds, R. H.: "Volumetric Behavior of Oil and Gas from Several San Joaquin Valley Fields," *Trans. AIME*, (1947) 170, 156.
- Standing, M. B., and Katz, D. L.: "Density of Crude Oils Saturated with Natural Gas," *Trans. AIME*, (1942) 146, 159.
- Sage, B. H., and Lacey, W. N.: "The Prediction of the Properties of Hydrocarbons at Elevated Pressures," *API Drill. and Prod. Prac.*, (1941), 308.
- Sage, B. H., and Lacey, W. N.: *Volumetric and Phase Behavior of Hydrocarbons*, Stanford Univ. Press, (1939), 183.
- Kuenen, J. P.: *Theorie der Verdampfung und Verflüssigung von Gemischen und der Fraktionierten Destillation*, J. A. Barth, Leipzig, (1906).
- Olds, R. H., Sage, B. H., and Lacey, W. N.: "Volumetric and Phase Behavior of Oil and Gas from Paloma Field," *Trans. AIME*, (1945) 160, 77.
- Benedict, M., Webb, G. B., and Rubin, L. C.: "An Empirical Equation for Thermodynamic Properties of Light Hydrocarbons and Their Mixtures," *Jour. Chem. Phys.*, (1940) 8 (4), 334.
- Kurata, F., and Katz, D. L.: "Critical Properties of Volatile Hydrocarbon Mixtures," *Trans. AICHE*, (1942) 38, 995.
- Standing, M. B., and Katz, D. L.: "Density of Natural Gases," *Trans. AIME*, (1942) 146, 140.
- Rzasa, M. J., and Katz, D. L.: "The Coexistence of Liquid and Vapor Phases at Pressures Above 10,000 PSI," *Trans. AIME*, (1950) 189, 119.
- Sage, B. H., Webster, D. C., and Lacey, W. N.: "Phase Equilibria in Hydrocarbon Systems. Thermodynamic Properties of Ethane," *Ind. and Eng. Chem.*, (1937) 29, 658.
- Sage, B. H., and Lacey, W. N.: "Apparatus for Study of Pressure-Volume-Temperature Relations of Liquids and Gases," *Trans. AIME*, (1940) 136, 136.
- Sage, B. H., and Lacey, W. N.: "Apparatus for Determination of Volumetric Behavior of Fluids," *Trans. AIME*, (1948) 174, 102.
- Sage, B. H., and Reamer, H. H.: American Documentation Institute, Doc. No. 3299, Washington, D. C., (1951).
- Reamer, H. H., and Sage, B. H.: "Volumetric Behavior of Oil and Gas from a Louisiana Field — I," *Trans. AIME* (1950) 189, 261.

★ ★ ★

MOBILITY RATIO—ITS INFLUENCE ON FLOOD PATTERNS DURING WATER ENCROACHMENT

J. S. ARONOFSKY, MAGNOLIA PETROLEUM CO., DALLAS, TEX.

ABSTRACT

The results of potentiometric model studies and numerical computations are described. The purpose of these studies was to determine the influence of the mobility ratio on flooding efficiencies during water encroachment in petroleum reservoirs, in systems of regular well geometry.

The direct line drive well pattern having relative spacing distances of one and one-half to one was investigated for water to oil mobility ratios of 10, 1, and 0.1. The results of these studies indicate that the pattern sweep efficiency is very dependent upon the mobility ratio.

INTRODUCTION

The almost universal occurrence of water in the immediate neighborhood of oil-bearing sands lends considerable emphasis to the desirability of having a rational analysis of water encroachment into petroleum reservoirs. This problem has become increasingly important with the accelerated use of water injection for secondary recovery operations.

The water encroachment problem has been studied from both the theoretical and experimental viewpoints by Muskat.¹ He has formulated, in a precise manner, differential equations to express flow in a water encroachment system, and rigorous analytical solutions have been developed for the linear, radial, and spherical cases.² However, it becomes exceedingly difficult to solve the encroachment problem rigorously for any general two-dimensional system in which the shape of the two-fluid interface is not immediately evident from the geometry of the system. The difficulty lies in the fact that a rigorous analytical

solution requires that the shape of the two-fluid interface be known simultaneously with its instantaneous position and with the pressure distribution on both sides of the interface.

Although this paper concerns the study of the two-fluid system of oil and water, the methods described in the paper are generally applicable to other systems of incompressible and immiscible fluids in which the displacing fluid sweeps the displaced fluid down to a residual value. In each region it is assumed there is only one mobile fluid and its mobility is constant throughout the region. The same procedure, with minor alterations, is applicable for gas injection systems provided the assumption can be made that both the displaced and displacing gases can be described by steady state formulas.

For the particular two-fluid problem considered in this paper, there is a relative permeability, K , and a viscosity, μ , associated with the water zone, and a different permeability and viscosity associated with the oil zone. The K/μ (mobility) value associated with a particular volume element of the porous medium, at any instant of time, will depend upon whether the element is ahead of, or behind the advancing interface. It is assumed that all volume elements ahead of the interface are characterized by the K/μ value for oil, while all the elements behind the interface are characterized by the K/μ value for water. That is, the K/μ value in the oil zone is constant throughout the oil zone, and the K/μ value in the water zone is also constant but different from the value in the oil zone. The symbols are defined at the end of the paper. The well pattern chosen for initial study is the direct line drive; the swept-out area at breakthrough was determined by two different methods which are described in the section on theory. These are:

1. Potentiometric analyzer
2. Numerical computation

The use of the potentiometric analyzer for studying water flooding problems is adequately described in the literature, particularly for cases where the mobility in the water zone is assumed equal to the mobility in the oil zone.^{3,4,5}

¹References given at end of paper.

Manuscript received in the Petroleum Branch, AIME, office, Aug. 7, 1951. Paper presented at the Fall Meeting of the Petroleum Branch in Oklahoma City, Okla., Oct. 3-5, 1951.

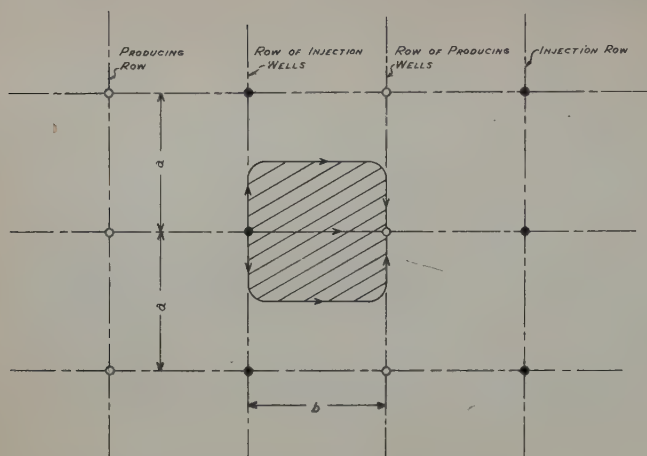


FIG. 1 — DIRECT LINE DRIVE WELL SPACING.

In the last 20 years, considerable interest has developed in the general use of numerical approximation methods for solving difficult mathematical problems when rigorous analytical methods proved impractical. To our knowledge, these numerical methods have not previously been applied to water encroachment problems,* although the numerical methods have been used by Southwell and co-workers in England to describe water flow under a coffer dam.⁶

Two specific examples are worked out in detail in this paper. The well pattern in both is the direct line drive consisting of alternate rows of injection and producing wells:

1. For the first example, the ratio of mobility values, water to oil $\frac{(K/\mu)_w}{(K/\mu)_o}$, is equal to 10. This problem was worked out by both methods described above.
2. The second example assumes a mobility ratio of 0.1; i.e., the mobility for water is equal to 0.1 the mobility for oil. This second problem was examined only by the potentiometric analyzer method.

Results obtained using a mobility ratio of one to one were used as a reference in interpreting the effects of variations in mobility ratio on sweep efficiency.

DISCUSSION

Method

The geometry of the direct line drive well pattern used in this problem is illustrated in Fig. 1. This well geometry consists of alternate rows of injection and producing wells. The spacing of the direct line drive network may be altered by changing the b/a ratio of Fig. 1, where b represents the distance from a row of injection to a row of producing wells, and a is the distance between neighboring producing or injection wells. Since the sweep efficiency is dependent upon the b/a ratio, this ratio has been arbitrarily fixed at 1.5 for all investigations described in this paper. From the geometrical symmetry of the pattern, it is clear that the whole network may be represented by the rectangular section shown in Fig.

*It has been called to our attention that a paper entitled "Numerical Methods for Cycling and Flooding Problems," by C. H. Fay and M. Prats was presented at the World Petroleum Congress, June, 1951, at The Hague, Netherlands. They used a numerical method to study the flooding efficiency of a conventional five-spot well pattern for a mobility pattern of four to one.

1 or 2. This rectangular section is used throughout this presentation to represent the line drive pattern.

A convenient yardstick for measuring the relative success of a flooding operation is the amount of oil displaced by the encroaching water. Though also dependent on a number of other considerations, the quantity of oil displaced is proportional to the area swept out by the water phase, since both the oil and water phases are assumed to be incompressible and immiscible. Techniques for determining the swept-out area or sweep efficiency for various well spacings are recorded in the literature. However, in all of these solutions the assumption is made that the K/μ (permeability to viscosity) ratio in the water zone is the same as the K/μ ratio in the oil zone. Based on laboratory information, it is believed that the mobility ratio $\frac{(K/\mu)_w}{(K/\mu)_o}$ may vary over a minimum range between 20 and 0.05, so it is desirable that this parameter be considered in determining sweep efficiencies.

This two-dimensional encroachment problem has not been solved rigorously for the case of mobility values differing on the two sides of a liquid-liquid boundary.² In this report an approximate solution to this problem is worked out by making use of the method of successive corrections.^{6,7,8} This method is applied in the following manner:

1. Determine by numerical or analogue means the potential (pressure) distribution Φ_o in the oil zone and Φ_w in the water zone for an initial assumed position and shape of the interface.
2. Compute velocity vectors $\frac{(K \nabla \Phi)}{\mu}$ at a selected number of well-distributed points on the interface.
3. Advance the selected points on the interface to a new position corresponding to some increment of time Δt .
4. Compute new values for the potential (pressure) distribution of the interface. The $(K/\mu)_w$ ratio is assumed to be constant in the new water zone. Similarly the $(K/\mu)_o$ ratio is constant throughout the new oil zone, but $(K/\mu)_w \neq (K/\mu)_o$.
5. Compute new velocity vectors; the whole step-wise process is then repeated until "breakthrough" occurs.

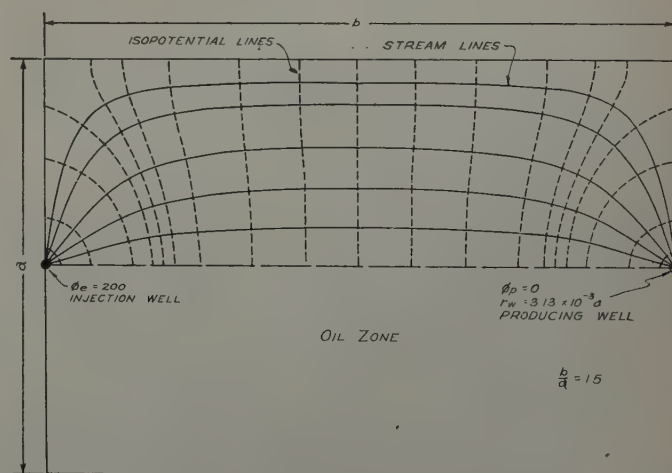


FIG. 2 — STREAMLINE AND POTENTIAL DISTRIBUTION FOR TYPICAL SECTION OF LINE DRIVE SPACING.

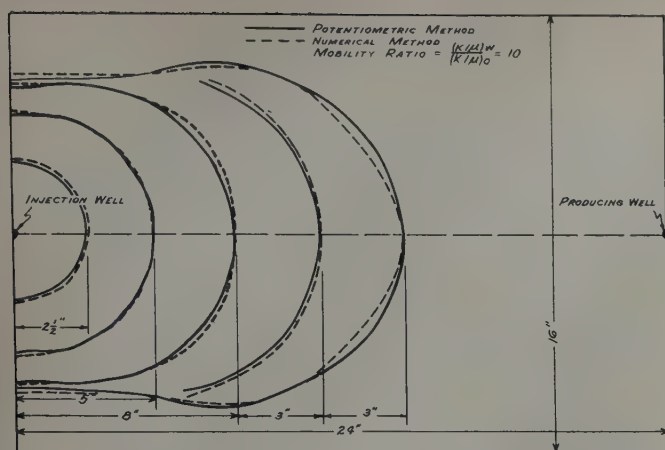


FIG. 3 — INSTANTANEOUS POSITIONS OF OIL-WATER INTERFACE FOR $M = 10$.

Mobility Ratio of 10

The above procedure can best be illustrated by examining the following problem:

Consider the two-well problem of the dimensions given in Fig. 2. This corresponds to a line drive "well spacing" of one and one-half to one as explained previously. Let $(K/\mu)_w = 10$ in the water zone and $(K/\mu)_o = 1$ in the oil zone. The permeability, K , may be measured in darcys and the viscosity, μ , in centipoises. We thus have a mobility ratio $M = \frac{(K/\mu)_w}{(K/\mu)_o} = 10$ for this problem.* Let us assume also that the injection well pressure is maintained at a constant value of $\Phi_e = 200$ atmospheres gauge throughout the investigation and similarly the producing well pressure is maintained at a constant value of $\Phi_p = 0$ atmospheres gauge.

Following Step 1 above, the pressure distribution and the streamline distribution are determined at that instant when injection commences (see Fig. 2). The exact manner in which the potential distribution may be calculated will be described in the section on Theory. The water-oil interface is now advanced to a new position as shown in Fig. 3 (drawn to represent the dimensions of an actual potentiometric model employed) which corresponds to some increment of time, Δt , that the water was injected. This interface position is designated $2\frac{1}{2}$ in. since the nose of the interface was advanced arbitrarily $2\frac{1}{2}$ in. out of 24 in. between wells of the model. Next, the pressure and streamline distributions on either side of the new interface position must be determined, based on the concept that the $(K/\mu)_w = 10$ throughout the now larger water-invaded zone and that $(K/\mu)_o = 1$, as before, in the remaining uninvaded region. Following this procedure the nose of the interface was advanced at specific increments of $2\frac{1}{2}$ in., 5 in., 8 in., 11 in., 14 in., 17 in., 20 in., 22 in. out of a total distance of 24 in. between wells. Figs. 3 and 4 illustrate the positions of all the interfaces except that at 22 in. The increments of time, Δt , were allowed to change for each stage of advancement. The distance of nose advance was specified

instead of the time increment in order to compare the swept areas for different mobility ratios.

The sweep efficiency then is determined from graphical integration of the flooded area at breakthrough as shown on Fig. 4. The percentile sweep efficiency is defined to be $\frac{\text{area of water zone at breakthrough}}{\text{total network area}} \times 100$. The sweep

efficiency for the mobility ratio of 10 was 59.1 per cent as determined by the numerical method and 62.9 per cent as determined by the potentiometric method, or an average of 61.5 per cent.

Mobility Ratio of 1.0

It is of interest to compute the sweep efficiency by both the numeric and potentiometric techniques for the case of $M = 1$, particularly since such a solution has been described in the literature.⁹ The flooded areas for $M = 1$ are shown in Fig. 5. The sweep efficiency determined by the numeric and potentiometric methods are 70.0 per cent and 71.6 per cent respectively. This is an average value of 70.8 per cent which is very close to the 70.74 per cent computed from Muskat's analytical solution. Such a close agreement with the theoretical solution is gratifying as a check on both the numeric and potentiometric methods.

Mobility Ratio of 0.1

Based on the analysis presented above, a comparison of 61.5 per cent sweep efficiency for $M = 10$ and 70.8 per cent efficiency for $M = 1$ indicates that approximately 10 per cent of the oil in place *could not* be swept out at breakthrough for $M = 10$ that was swept out for $M = 1$. This interesting result indicated that a flooding experiment should be run for the case where the mobility ratio $M = 0.1$. This problem was run off on the potentiometric analyzer following the steps described above. The details of operating the potentiometer analyzer will be discussed later. The successive advances of the interface are given in Fig. 6; the sweep efficiency is 86.6 per cent.

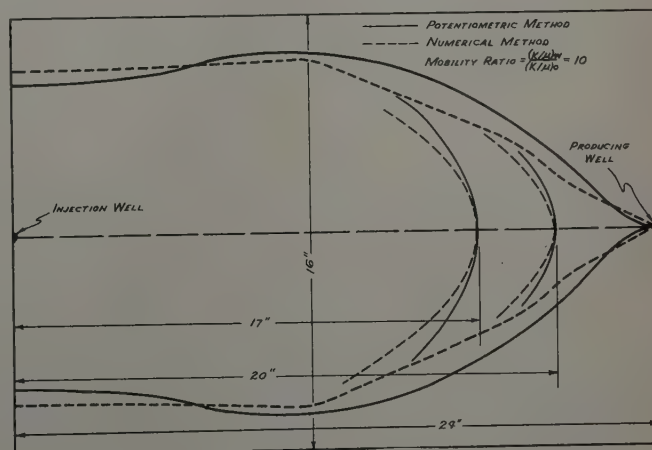


FIG. 4 — VARIOUS INTERFACE POSITIONS FOR $M = 10$.

*It should be understood that in a specific field problem the mobility ratio would have to be determined from auxiliary laboratory experiments and, of course, may have values different from 10.

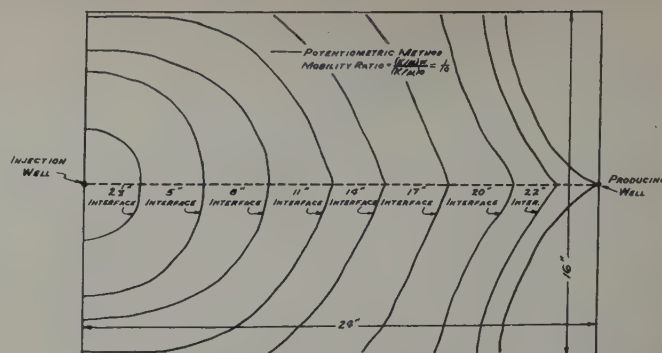
COMPARISON OF FLOODED AREAS FOR THE
VARIOUS MOBILITY RATIOS

A comparison is made between the flooded areas for the line drive pattern with mobility ratios $M = \frac{(K/\mu)_w}{(K/\mu)_o} = 10$, 1, and 0.1. The interfaces at breakthrough are shown in Fig. 7 where the curves are labeled "A," "B" and "C" for ratios of 10, 1, and 0.1 respectively. Curves "A" and "B" are average curves based on results of the two methods (potentiometric and numeric) of advancing the interface. Curve "C" was determined by the potentiometric method only.

The most significant fact is that the sweep efficiency is very much dependent upon the mobility ratio $M = \frac{(K/\mu)_w}{(K/\mu)_o}$, these efficiencies being 61.5 per cent, 70.8 per cent, and 86.6 per cent for ratios of 10, 1, and 0.1 as quoted previously. Such large changes in efficiency indicate that the effects of mobility ratio variations should be considered in practical field problems where careful economic studies must be made. The production rates also would be considerably different in the above three cases, although production rates have not been considered in this study.

A further interesting factor in this analysis is the shape of the interface itself at breakthrough for the three cases considered. All three curves of Fig. 7 have the typical "fingering" or "cusping" that must occur near the producing well. Because of the complexity of the problem, it would be impossible to predict a priori what the shape of the interface should look like for $M = 10$ based upon the shape of the interface curve for $M = 1$.

Muskat predicted the effect of the difference in viscosity between the fluids on the two sides of the interface (see page 478, *Flow of Homogeneous Fluids*:⁹ "The effect on the encroachment of the water into the oil of higher viscosity will be an accentuation of the distortion and the sharpening of the 'fingering' or 'cusping'—for the single-fluid system. For the replacement of the higher viscosity oil by the encroaching water will evidently decrease the total resistance of the system and hence increase the average fluid velocities. The increase of the velocities, however, will be maximal along the main axis of the fingering where more of the oil has already been displaced by the water. This differential increase in the fluid velocities will, therefore, accentuate the distortion in such a

FIG. 6 — INTERFACE POSITIONS FOR $M = 0.1$.

way as to make the fingering more pronounced, although the effect will not become large until the interface approaches the vicinity of the output wells . . ."

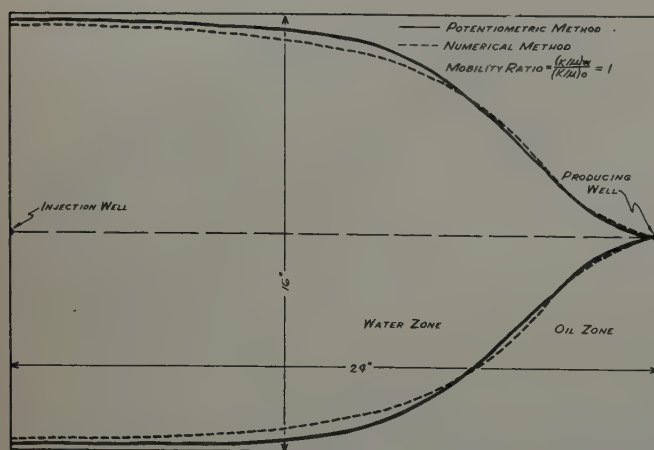
In the above quotation, Muskat was interested in viscosity differences; the same argument applies to differences in K/μ ratios. Consider that the relative permeability in the water zone

is the same as oil permeability. Then the mobility ratio $M = \frac{\mu_o}{\mu_w}$.

Also let $\mu_o = 10 \mu_w$ and assume that the oil is of higher viscosity than water as in the case that Muskat discussed. He predicted that the "fingering" would be more pronounced for this case ($M = 10$) than for the single-fluid system ($M = 1$). A comparison of these two cases is given in Fig. 7. Notice that the fingering for curve "A" ($M = 10$) is more pronounced than curve "B" ($M = 1$), and the flooded area is smaller for curve "A." The modification of curve "B" ($M = 1$) is just reversed when the mobility ratio $M = 0.1$. In the latter case, as indicated by curve "C," the flooded area is larger than for $M = 1$. No explanation is offered as to why curves "A" and "B" of Fig. 7 intersect near the producing well.

In a more recent article,¹⁰ Muskat studied the effect of mobility ratios on water-drive systems producing from formations containing horizontal permeability stratifications and having zero vertical permeability. The general result is that when the mobility ratio of water to oil is larger than unity the channelling tendency, resulting from permeability stratification, becomes aggravated as the higher permeability zones become flooded out. Conversely, for mobility ratios less than unity, the flooding of the high-permeability zones will lead to a retarding and choking effect. It is interesting to note that the results described in the present paper confirm the concept that the "fingering" is aggravated for mobility ratios larger than unity and retarded for mobility ratios less than unity.

Still another instance may be cited where the "fingering" is aggravated for mobility ratios larger than unity and retarded for mobility ratios less than unity. Chatenever and Calhoun¹¹ have described the use of photomicrographic techniques for investigating water encroachment into a cell of spheres saturated with a high-viscosity oil. For this case where the so-called mobility ratio is less than unity, they observed that the flood front pattern had a stringy appearance as the water fingered through the flow bed. The condition of mobility ratio less than unity was represented by flooding the high-viscosity oil into a water-saturated cell. The flood front for this case appeared to advance with piston-like action, showing little tendency toward fingering and by-passing.

FIG. 5 — SWEEP PATTERN AT BREAKTHROUGH FOR $M = 1$.

EFFECT OF MAGNITUDE OF INCREMENTAL NOSE ADVANCE ON SWEEP EFFICIENCY DETERMINATION

In the actual case of water flooding, it is clear that the potential distributions in both the oil and water zones must vary continuously with time as the interface advances. The assumption is made that the history of these flow systems can be described in terms of a continuous succession of steady states, although the system is actually in an unsteady state of flow. In this investigation the nose of the interface was advanced in nine steps to the final (24 in.) position of breakthrough. At each successive advance of the interface, new streamline and/or potential fields were computed on a steady-state basis.

As shown in Fig. 3, the nose of the interface was advanced from 11 in. to 14 in., representing a three-in. increment. In order to compare the effect of increment size on the solution obtained it was thus desirable to advance the interface by smaller increments than three in. A comparison is made in Fig. 8 of interface advances from 11 in. to 14 in. by one-in. and three-in. increments. The comparison of Fig. 8, which is from potentiometric studies, shows that the area for the 14 in. interface by one-in. increments is about one per cent smaller than the swept area for three-in. increment advance of the nose. This indicates that the swept area at 14 in. nose position would be even smaller if smaller increments than one in. were taken; such effects are believed to be of secondary importance. This same procedure of advancing the interface nose from 11 in. to 14 in. by one-in. increments was computed numerically, and the results are similar to the potentiometric results given in Fig. 8.

THEORY

Potentiometric Models

One of the methods of analysis discussed in a preceding paragraph is the use of potentiometric models to solve water encroachment problems. The basic theory of such models will be explained briefly here. There are excellent papers available on this subject by Muskat,³ Lee,⁴ and others.

These model studies are generally based on a two-dimensional idealization of the porous medium flow system by current flow in an electrolytic medium. The equation of continuity for the porous system is*

*List of Nomenclature given at end of paper. The symbol Δ is used to represent the "del" operator because conventional symbol was not available.

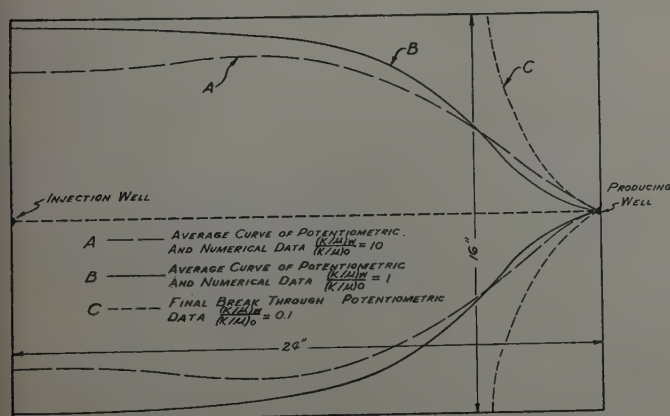


FIG. 7 — COMPARISON OF FLOODED AREAS FOR $M = 10, 1$ AND 0.1

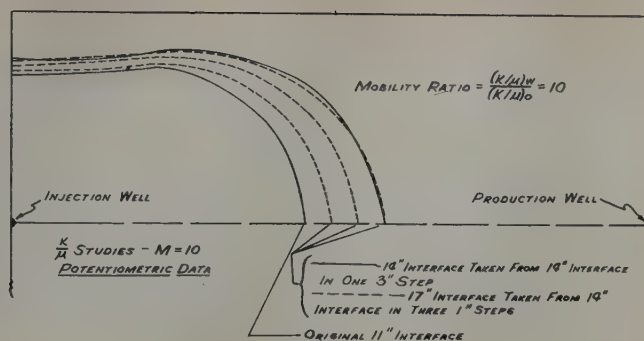


FIG. 8 — COMPARISON OF INTERFACE ADVANCES FROM 11 IN. TO 14 IN. BY ONE AND THREE-IN. INCREMENTS.

$$\Delta \cdot v = 0 \quad (1)$$

where v represents the macroscopic velocity vector.

The analogous continuity equation for the electrical system is

$$\Delta \cdot i = 0 \quad (2)$$

where i is the vector current density. The generalized Darcy's law may be written as

$$v = -\frac{K}{\mu} \Delta P \quad (3)$$

for two-dimensional flow where gravity forces are neglected.

Ohm's law becomes

$$i = \sigma \Delta V \quad (4)$$

where

σ = equivalent electrical conductivity

V = voltage

K = permeability

μ = viscosity

h = thickness of porous medium.

The continuity equation can now be rewritten by using Ohm's and Darcy's laws.

$$\Delta \cdot \sigma \Delta V = \Delta \cdot \frac{Kh}{\mu} \Delta P = 0 \quad (5)$$

In order to build an electrolytic tank model to have geometric similarity with a fluid in a porous medium, Equation (3) must be equivalent to Equation (4). This indicates that the electrical conductivity, σ , must be proportional everywhere

to $\frac{Kh}{\mu}$ even though K , μ , and h may vary from point to point

in the x, y , plane. The effective electrical conductivity, σ , may be varied by changing the depth, h_e , of the electrolyte layer so that

$$\sigma = \sigma_e h_e \quad (6)$$

where

σ_e = specific conductivity of the electrolyte

h_e = depth of electrolyte layer

we find then that

$$h_e = C \frac{Kh}{\mu} \quad (7)$$

where C is a model scale factor.

Equation (7) can be simplified further for the water encroachment problem since it can be assumed that the sand thickness remains constant, or

$$h_e \propto \frac{K}{\mu} \quad (8)$$

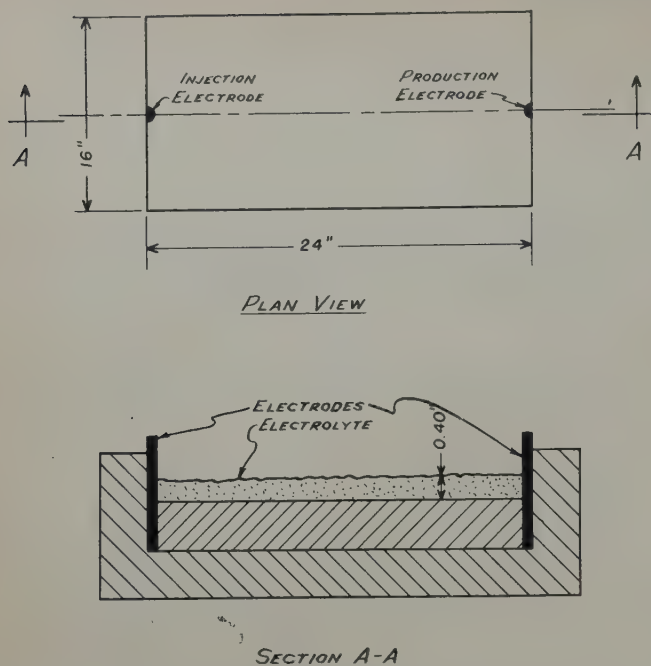


FIG. 9 — INITIAL POTENTIOMETRIC MODEL.

The requirement of geometrical similarity of voltage and pressure distribution will be insured if the electrolyte depth, h_e , is everywhere proportional to $\frac{K}{\mu}$. This concept can now be applied to the specific water drive problem where the mobility ratio $M = \frac{(K/\mu)_w}{(K/\mu)_o} = 10$. The electrolytic model initially has a uniform electrolyte depth of say 0.40 in. as shown in Fig. 9. The initial streamline and potential fields must be determined for this set-up and the interface advanced by standard procedures to the position illustrated in Fig. 10. The interface was advanced to this position by integrating time, t , along each streamline such that

$$\Delta t \cong \frac{(\Delta S)^2}{\Delta V} \quad \dots \quad (9)$$

The incremental time, Δt , representing the time for a particle of fluid to travel a short distance ΔS . Each particle on the oil-water interface can then be advanced a short distance ΔS for some fixed time unit, Δt .

The interface for the first advance is shown in Fig. 10. Before advancing the interface again the condition $(K/\mu)_w = 10(K/\mu)_o$ must be approximated, which means $(h_e)_w = 10(h_e)_o$. This condition is shown in Fig. 10 where the electrolyte depth $(h_e)_o$ for the oil zone is 0.40 in. and the depth $(h_e)_w$ for the water zone is 4.0. This same process is repeated to get the successive advances of the interface that are illustrated in Figs. 3 and 4.

This technique of integrating time along a streamline for a short distance ahead of the interface is slightly different from the method involving successive corrections; however, the net result will be the same if the interface is advanced by very small increments.

Methods of Numerical Calculations

The most difficult step in calculating solutions of the type described earlier in this paper is to determine the potential

or pressure distribution and/or streamline distribution for each successive advance of the interface. Some powerful numerical methods have been developed for finding solutions of Laplace's equation, $\nabla^2 P = 0$. The elegance of such numerical schemes is that the desired solutions are obtained in the form of numerical values of the function at a preassigned network of points covering the entire field where the differential equation is valid. Considerable progress has been made in recent years in applying numerical methods to practical problems. An extensive volume has been written by Southwell on this subject.⁶ The specific method of interest involves replacement of the partial differential equation $\nabla^2 P = 0$ by a corresponding difference equation, followed by numerical treatment of the difference equation.

Consider a potential field that is divided into a rectangular network, as in Fig. 11.

The Laplacian equation $\frac{\partial^2 \Phi}{\partial x^2} + \frac{\partial^2 \Phi}{\partial y^2} = 0$ can be approximated by finite difference equations:

$$\left(\frac{\partial \Phi}{\partial x} \right)_m \cong \frac{\Phi_{m+1} - \Phi_{m-1}}{2(\Delta x)} \quad \dots \quad (10)$$

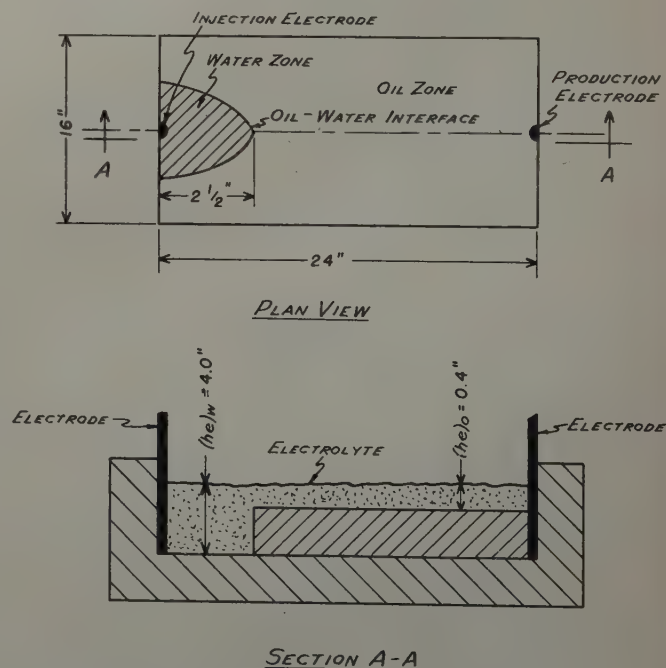
$$\left(\frac{\partial^2 \Phi}{\partial x^2} \right)_m \cong \frac{\Phi_{m+1} + \Phi_{m-1} - 2\Phi_{m,n}}{(\Delta x)^2} \quad \dots \quad (11)$$

Similarly,

$$\left(\frac{\partial^2 \Phi}{\partial y^2} \right)_n \cong \frac{\Phi_{n+1} + \Phi_{n-1} - 2\Phi_{m,n}}{(\Delta y)^2} \quad \dots \quad (12)$$

Δx and Δy must be small for good approximation. For simplicity consider a square grid spacing where $\Delta x = \Delta y$.

$$\text{MOBILITY RATIO} = \frac{(K/\mu)_w}{(K/\mu)_o} = \frac{(h_e)_w}{(h_e)_o} = \frac{4''}{0.4''} = 10$$



$(h_e)_o$ — DEPTH OF ELECTROLYTE IN OIL ZONE
 $(h_e)_w$ — DEPTH OF ELECTROLYTE IN WATER ZONE

FIG. 10—POTENTIOMETRIC MODEL ALTERED FOR CHANGING OIL ZONE.

The finite difference approximation of $\Delta^2\Phi = 0$ at the typical point, m, n in the x, y , plane will be

$$0 = (\Delta^2\Phi)_{m,n} = \left(\frac{\partial^2\Phi}{\partial x^2} \right)_{m,n} + \left(\frac{\partial^2\Phi}{\partial y^2} \right)_{m,n} \\ = \frac{\Phi_{m+1} + \Phi_{m-1} + \Phi_{n+1} + \Phi_{n-1} - 4\Phi_{m,n}}{(\Delta x)^2} \dots (13)$$

The finite difference approximation of La Place's equation must be

$$\Phi_{m+1} + \Phi_{m-1} + \Phi_{n+1} + \Phi_{n-1} - 4\Phi_{m,n} = 0 \dots (14)$$

$$\text{Or } \Phi_0 = \frac{\Phi_1 + \Phi_2 + \Phi_3 + \Phi_4}{4} \dots (15)$$

A simple physical interpretation would be that the value of Φ_0 is approximated as being the arithmetic mean of its four nearest neighbors as shown in Fig. 11.

To solve for Φ_0 , one must write out Equation (15) for each mesh point in the x, y plane. There will be obtained a set of l linear algebraic equations for the l mesh points from which Φ is to be determined. This set of l equations may be evaluated by the usual rules of algebra. In a practical case where there necessarily must be a large number of mesh points, the direct solution of Equation (15) would be tedious and laborious for practical use, so approximation methods have been developed for obtaining the desired result without treating Equation (15) explicitly as a difference equation.

Perhaps the most convenient of these approximation techniques is the so-called "iteration method."^{7,8} The advantage of this method for solutions of $\Delta^2\Phi = 0$ is that it is simple to carry out regardless of the shape of the boundary. Also, it has been proved that the iteration process will always converge to the solution of the differential equation for very small increments.¹² This method will always work provided values of the function, Φ , or its normal gradient, $\frac{\partial\Phi}{\partial n}$, is specified at every point on the boundary.

The numerical results given in Figs. 4 through 9 were determined by this iterative process; however, the bulk of the computations were performed on IBM punch card machines. The chief advantages claimed for the punched card method are the speed with which the results can be obtained and the fully automatic procedure.

No rigorous attempt is made to justify the approximations introduced for both the potentiometric and numeric methods. First of all there are the approximations that are common to both methods or any other method that follows the basic procedure outlined above in this paper. Then, there are some approximations introduced that are associated only with the potentiometric method, and others that are associated only with the numeric method.

For instance, the potentiometric results are somewhat in error because of contact resistance, "three dimensional effect" at the abrupt change in electrolyte depth, and others. A different set of errors is introduced into the numerical calculations. The main difficulty in numerical work is the impracticability of greatly reducing the network spacing. Yet, small network spacing in the neighborhood of the interface is mandatory for accurate results.

It is pertinent to emphasize the manner in which the numerical and model solutions in this paper are tied to a known solution for the purpose of comparison. First, the numerical and model solutions were both checked against the analytical solution known for the mobility ratio of one to one. Then, both numerical and model methods were used for the ratio 10

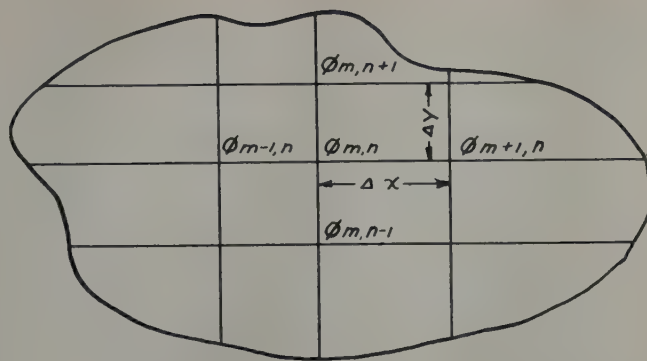


FIG. 11 — POTENTIAL FIELD DIVIDED INTO RECTANGULAR NETWORK. with reasonably good comparison. It was then deemed safe

to use the model alone for the ratio 0.1.

One source of error that is common to both potentiometric and numeric studies is that in all studies the interface was advanced to breakthrough in nine steps. It is possible that a considerably larger number of steps should be taken.

More model work of this nature is in progress and will be presented at some later date.

CONCLUSIONS

The results described in this paper clearly indicate that the sweep efficiency is very much dependent upon the mobility ratio $M = \frac{(K/\mu)_w}{(K/\mu)_o}$. These efficiencies are 61.0 per cent, 70.8 per cent, and 86.6 per cent for mobility ratios of 10, 1, and 0.1 respectively for the systems studied. This illustrates that the value of sweep efficiency can vary by 25 per cent for the change in mobility ratio from 10 to 0.1. Stated in other terms, the amount of oil recovered at breakthrough by water displacement is about 42 per cent greater where the mobility ratio is 0.1 as compared to the case where it is 10.

Such large changes in pattern sweep efficiencies indicate that the effects of mobility ratio variations should be considered in future reservoir analyses where careful economic studies are desired.

Emphasis is placed on the fact that the values of sweep efficiency reported here are not necessarily those to be obtained in practice, but are indicative only of the relative effects of the mobility ratio on an idealized system. In these studies no evaluation of the influence of variations of horizontal and vertical permeability upon sweep efficiencies was made, and only one well-spacing arrangement has been considered. When the effects of such variables as these are known and included in the determination of recovery efficiencies, substantially different values for over-all recovery efficiencies may result.

ACKNOWLEDGMENT

Acknowledgment is made to the management of the Field Research Laboratories, Magnolia Petroleum Co., for permission to publish this investigation. The writer is grateful to Paul Reichertz for suggesting the problem and for his active interest. H. W. Ballew and W. Wahl assisted in carrying out the potentiometric and numeric studies. Acknowledgment is

also due A. C. Buchanan of the Magnolia Petroleum Co.'s Comptroller's Department for his effective help in the punch card operations.

DISCUSSION

By M. Prats, Shell Oil Co., Houston, Tex.

NOMENCLATURE

K	permeability in darcys
μ	viscosity in centipoises
$\frac{(K/\mu)_w}{(K/\mu)_o}$	mobility ratio of water to oil
b	distance from a row of injection to a row of producing wells (inches, in the potentiometric studies)
a	distance between neighboring producing or injection wells (inches, in the potentiometric studies)
t	time in seconds
S_o	
S_p	closed surfaces
v	macroscopic velocity vector
Φ	velocity potential
i	vector current density
σ	electrical conductivity
h	sand thickness
C	model scale factor
V	electrical voltage
\blacktriangle Nabla	$\blacktriangle = \frac{\partial}{\partial x} + \frac{\partial}{\partial y}$

REFERENCES

1. Muskat, M.: "Two Fluid Systems in Porous Media Encroachment of Water into an Oil Sand," *Physics*, (1934) 5, 250.
2. Muskat, M.: "A Note on a Problem in Potential Theory," *Jour. of App. Physics*, (1937) 8, 434.
3. Muskat, M.: "Theory of Potentiometric Models," *Trans. AIME*, (1949) 179, 216.
4. Lee, B. D.: "Potentiometric Model Studies of Fluid Flow in Petroleum Reservoirs," *Trans. AIME*, (1948) 174, 41.
5. Wyckoff, R. D., Botset, H. G., and Muskat, M.: "Mechanics of Porous Flow Applied to Water Flooding Problems," *Trans. AIME*, (1933) 103, 219.
6. Southwell, R. V.: *Relaxation Methods in Theoretical Physics*, Oxford Clarendon Press.
7. Grinter, L.: *Numerical Methods of Analysis in Engineering*, MacMillan Co., New York.
8. Frocht, M.: *Photoelasticity*, McGraw-Hill Co.
9. Muskat, M.: *Flow of Homogeneous Fluids in Porous Media*, J. Edwards, Inc., Ann Arbor, Mich.
10. Muskat, M.: "The Effect of Permeability Stratification in Complete Water-Drive Systems," *Trans. AIME*, (1950) 189, 349.
11. Chatenever, A., and Calhoun, J. C.: "Visual Examinations of Fluid Behavior in Porous Media," presented at Petroleum Branch AIME Fall Meeting at Oklahoma City, Okla., Oct. 3-5, 1951.
12. Courant, R., Friedrichs, K., Levy: *Math. Ann.* (1928) 100.

Aronofsky uses the close agreement between sweep efficiencies for the single fluid case obtained by numerical and potentiometric methods and the sweep efficiency obtained from Muskat's analytical solution "as a check on the numeric and potentiometric methods." This, in effect, is a check on one point of the production history, while the shape of the swept-out areas at water breakthrough do not indicate close agreement of production histories at later times, especially for the case where the mobility ratio is 10.

Although the following is (to some extent) a matter of opinion, I believe that, for a method of advancing fronts not involving successive corrections, the size of the steps taken is too large. The results of the study of the effect of the magnitude of size of steps on sweep efficiency determination may be highly misleading, since this study was carried out in the region where such effects would be small. If the study had been done in the neighborhood of the producing well, the results might have been startling.

The last remark arises from my experience doing similar work. Using a mobility ratio of 10 and a total electrolyte depth of one in., I found (from graphical measurements) that the refraction condition failed to be satisfied by ± 20 per cent. I would expect that for a total electrolyte depth of four in. the effects of the third dimension would be even more pronounced. How well was the refraction condition met at the interfaces?

There is always room for improvements in any method based on approximations. Regardless of this, Aronofsky has well succeeded in simply and effectively showing the importance of the mobility ratio on flooding efficiencies.

DISCUSSION

By A. B. Dyes, The Atlantic Refining Co., Dallas, Tex., Member AIME

The importance of the effect of mobility of the phases on flood pattern efficiency and the consideration which must be given this factor in planning an injection operation cannot be overemphasized. We feel that the author has done a fine job, but should not do himself an injustice by limiting his subject to water encroachment. The analytical and experimental procedures which are used in studying the influence of the mobility of the phases on sweepout pattern efficiency apply equally well to gas injection operations. During the past year, some of us in The Atlantic Refining Co. have been involved in an investigation into the effect of this variable on the pattern efficiency of a five-spot flood. This study has not been completed and consequently the procedures employed and the final results will not be reported on until a later time. However, we would like to make a preliminary report of the results that have been obtained on a five-spot flood to supplement that reported by Aronofsky on the line drive.

In analyzing the results of this study, the mobility of the phases ahead of the displacing front to that behind the front has been called the mobility ratio. This is the definition used by Muskat in a previous publication. The selection of the mobility to be used as numerator and denominator in this ratio is arbitrary and this ratio could just as well be defined as the ratio of the mobility behind the displacing front to that ahead of the displacing front as used by the author of the preceding paper. We would like to urge the adoption of some

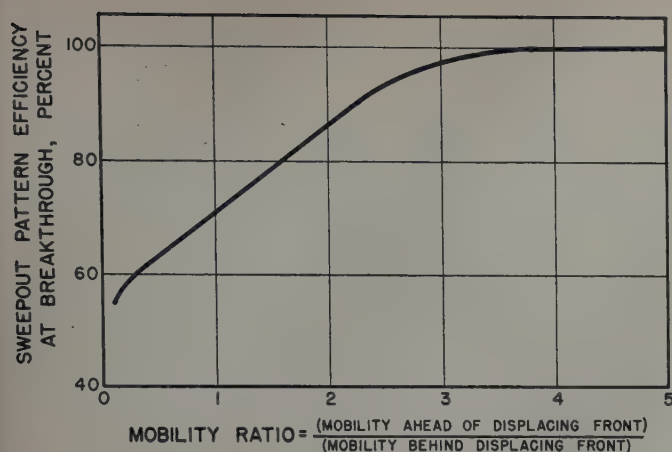


FIG. 1-A — EFFECT OF MOBILITY RATIO ON SWEEPOUT EFFICIENCY OF FIVE-SPOT FLOOD.

standard definition of this mobility ratio as related to flood pattern efficiency. Our preference is for the definition as used by Muskat and which has previously appeared in the literature.

In a given reservoir the mobility of the system must necessarily involve the mobility of each phase flowing. In a system of multiphase flow the mobility would be represented by the summation of the relative permeability-viscosity ratio of each phase. It is desirable to show the mobility ratio in a form applicable to multiphase flow problems. The reason for this is that the application of relative permeability data to the displacement of oil by water or gas indicates that in general two phases will be flowing in a portion of the reservoir behind the front, and in flooding operations of a reservoir depleted by solution gas drive two phases will be flowing in some portions ahead of the injected front.

The results which we have obtained showing the effect of the mobility ratio on flood pattern efficiency of a five-spot, considering that the specific permeability is constant throughout the system and that lengths on all sides of the five-spot are equal, are presented in Fig. 1-A. This figure shows that a mobility ratio equal to one yields a pattern efficiency of 71 per cent. This is in agreement with the values reported by Muskat, 71 per cent by calculation and about 73 per cent for potentiometric studies. As we increase the mobility ahead of the injected front with respect to that behind the front, we find that the flood pattern efficiency at breakthrough increases and approaches 100 per cent at a mobility ratio of four. For higher mobility ratios, the pattern efficiency is considered to be essentially 100 per cent. Conventional water flooding would generally fall in the region of 70 per cent to 100 per cent pattern efficiency at breakthrough for the system considered here. On the other hand, conventional gas injection would generally result in mobility ratios less than 1.0 and lower sweep-out efficiencies of only 55 to 70 per cent are indicated. At present the lower section of this curve below a mobility ratio of 1.0 has been defined by only one point. Consequently this section may be subject to some revision as this point is checked and other points obtained.

Comparison of the results obtained by Aronofsky for the line drive to these for a five-spot shows that changes in the mobility ratio result in a smaller change in the percentage

sweepout efficiency at breakthrough for the line drive than for a five-spot. This might be expected from the difference in the geometry of the two systems. For the mobility ahead of the displacing front to that behind the front of 0.1, the line drive gives 61 per cent compared to 54 for the five-spot; each yields 71 per cent efficiency at a mobility ratio of one. At a ratio of 10 the line drive attains 87 per cent compared to 100 for the five-spot.

We must emphasize that the sweepout efficiencies reported are those at first breakthrough of the injected fluid. The possibility that we can exercise some control on the mobility ratio to change breakthrough recovery, points to a need for an accurate determination of the performance of a reservoir in the period after breakthrough whenever the sweep efficiency is less than 100 per cent. A thorough economic analysis of both phases of production will be required in justifying the additional expense that may be necessary to bring about changes in the mobility ratio.

AUTHOR'S REPLY TO MESSRS. PRATS AND DYES

Prats mentions that he did not have success in conducting a similar model experiment for mobility ratio of 10. He used a total electrolyte depth of one in. which means that the shallow depth was 0.1 in. Prats states that the refraction condition failed to be satisfied by ± 20 per cent in his experiment. Our own experience with this problem is that the shallow depth of electrolyte should be larger than at least one quarter in. in order to get reliable results. The inaccuracies in constructing the model and non-uniformity of the electrolyte layer becomes critical for shallow depths in the range of 0.1 in. and this could account for a large portion of his ± 20 per cent error. Certainly Prats is aware that the distortion of streamlines in the third dimension depends almost entirely on the ratio of depths of electrolyte and not on absolute magnitude, so there is some question as to the exact nature of the errors he is referring to.

Of course it is recognized that there must be some errors introduced by distortion of streamlines in the third dimension due to the abrupt change in electrolyte depth which represents the interface. Nevertheless these slightly distorted streamlines must still approximately obey the refraction condition, so it is possible to obtain useful information by making comparative studies of model experiments. There are several experimental techniques available that one could use to minimize the so-called "three dimensional effect" but such second order errors were neglected in this initial study.

Prats points out that it would be better if the interface was advanced by a larger number of steps in order to decrease the size of each step. The author would like to emphasize the importance of this observation. Perhaps, after more experience is gained, we will be able to correlate some relationship between errors in sweep efficiency and size of incremental advances of the interface.

Although Dyes is correct in pointing out that the procedures described in this paper for water-flooding are also valid for gas injection operations, the actual results presented in the text may or may not be applicable. There is some question whether Dyes is referring to displacement of liquid by gas, or displacement of gas by gas. It should be remembered, however, that one of the fundamental assumptions involved in the calculations presented in the paper is that a discrete interface exists which is characterized by a discontinuity in the mobility ratio. If this assumption is valid for both of the above dis-

placement mechanisms (and we question the assumptions for at least the first mechanism) then the basic method described in this paper would be applicable with certain modifications. Such modifications are required by the fact that the voltage and current in the electrical system represent different properties in the gas injection case than in the water-flood case. Specifically, for example, in the case of gas cycling (isothermal flow) the voltage should represent mass gas flow (or volume gas flow under standard conditions). In the other case of liquid displacement by injected gas, still further complications arise which make it difficult to represent the system by a suitable model.

It does seem desirable that the term mobility ratio be standardized. Admittedly Muskat previously used the term mobility ratio to be the mobility of the fluid ahead of the dis-

placing front to that behind the front; whereas in this paper the term mobility ratio is defined as the reciprocal to that defined by Muskat.

The author will not attempt to discuss the results of the five-spot tests presented by Dyes since it would be preferable to wait until the method is disclosed by which these results were obtained. The author has also studied the five-spot pattern by the potentiometric model method and these results will be presented at some later date.

The comments by Prats and Dyes are certainly appreciated. It is most gratifying to find out that other workers are concentrating on these problems. As more information becomes available perhaps the answers to the questions suggested by the discussers will be forthcoming.

★ ★ ★

A METHOD FOR PREDICTING THE TENDENCY OF OIL FIELD WATERS TO DEPOSIT CALCIUM SULFATE

HENRY A. STIFF, JR., MEMBER AIME, AND LAWRENCE E. DAVIS, THE ATLANTIC REFINING CO., DALLAS, TEX.

ABSTRACT

A graphic method was developed which can be used to predict the tendency of oil field waters to precipitate calcium sulfate under a variety of conditions. Application of this method is made to the prediction of sulfate scale formation in heater treaters, boilers, oil wells, cooling systems and water injection wells.

INTRODUCTION

A solution may be said to be in equilibrium with respect to a given salt when the concentration of that salt is equal to its solubility. If for any reason the concentration of the salt is increased or its solubility decreased, the equilibrium is upset and precipitation of the salt takes place. Thus, if the concentration of a salt in a particular solution is known and its solubility can be calculated for a given set of conditions, the tendency of this salt to form a precipitate under these conditions can be predicted. Based on these principles a method has been developed for determining the tendency of oil field waters to form calcium sulfate precipitates under various conditions.

THE SOLUBILITY DIAGRAM

Calcium sulfate precipitation most frequently occurs when two waters are mixed; one containing calcium ions, and the other sulfate ions. As one of these waters is added to the other a point may be reached where the concentration of calcium sulfate is greater than its solubility, thus causing the

formation of a precipitate. The solubility diagram is a graphic device for determining the location of such points, thereby making possible a prediction of the tendency of such a system to deposit sulfate scale. A similar diagram can be used to solve many other problems involving the precipitation of calcium sulfate.

Fig. 1 shows a solubility diagram representing the mixing of two waters. Water "A" contains a high concentration of sodium, magnesium, and sulfate ions together with a small amount of calcium. Water "B" contains a high concentration of calcium ions together with sodium, magnesium and a small amount of sulfate ions. The percentage mixture of these waters is plotted along the abscissa of a system of rectangular coordi-

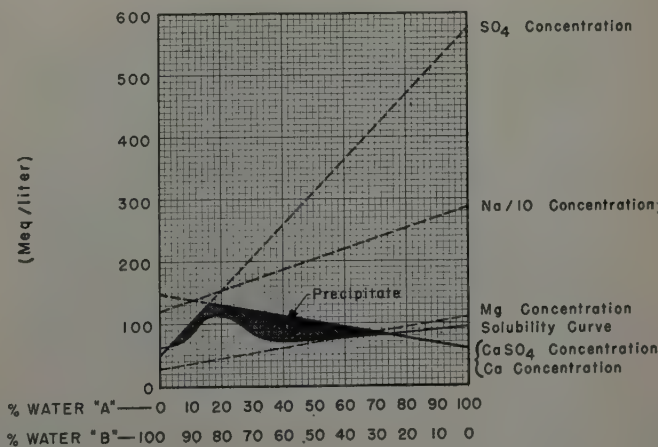


FIG. 1 — SOLUBILITY DIAGRAM, CALCIUM SULFATE DEPOSIT FORMATION WHEN TWO WATERS ARE MIXED.

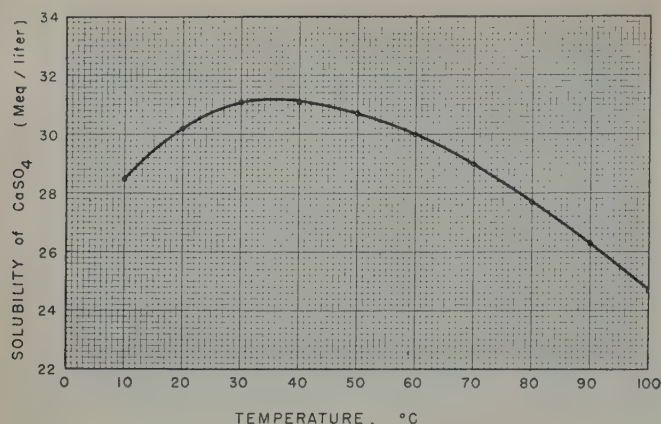


FIG. 2 — SOLUBILITY OF CALCIUM SULFATE IN DISTILLED WATER AT VARIOUS TEMPERATURES (S_T).

nates, while the concentration of the individual ions (in meq. per liter) is shown on the ordinate. The analysis of water "A" is plotted at 100 per cent "A," while the analysis of "B" appears at 100 per cent "B." Straight lines connecting the points representing the same ion then give the concentration of this ion at any percentage mixture of the two waters. The concentration of calcium sulfate is limited up to a certain point by the amount of calcium present. Above this point the amount of sulfate becomes the limiting factor. Thus the concentration of calcium sulfate at any percentage mixture of the two waters can be determined.

The solubility of calcium sulfate at any point is determined from the equation

$$S = S_T \times F_1 \times F_2 \times F_3$$

where:

S = The solubility of calcium sulfate under a given set of conditions.

S_T = The solubility of calcium sulfate in distilled water at the temperature T , as shown in Fig. 2.

F_1 = The common ion factor, or the solubility of calcium sulfate in the presence of an excess of calcium or sulfate ion, as given in Fig. 3.

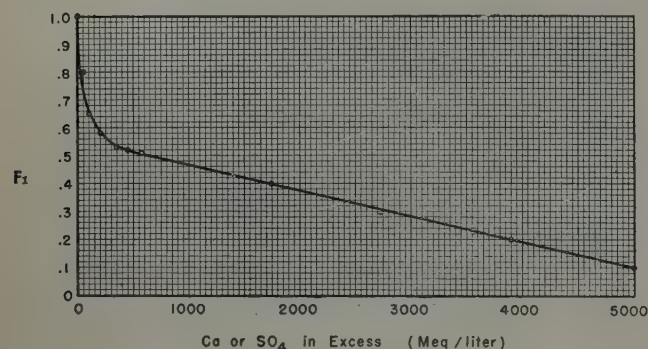


FIG. 3 — THE COMMON ION FACTOR, OR THE SOLUBILITY OF CALCIUM SULFATE IN THE PRESENCE OF AN EXCESS OF CALCIUM OR SULFATE ION.

$$F_1 = \frac{\text{Solubility of CaSO}_4 \text{ in presence of common ion}}{\text{Solubility of CaSO}_4 \text{ in distilled water}}$$

F_2 = The sodium ion factor, or the solubility of calcium sulfate in the presence of sodium ion, as shown in Fig. 4.

F_3 = The magnesium ion factor, or the solubility of calcium sulfate in the presence of magnesium ion, as in Fig. 5.

When the solubility of calcium sulfate at several points has been calculated, a solubility curve can be plotted as shown in Fig. 1. Then at the percentage mixtures of the two waters where the concentration exceeds the solubility, as shown in the shaded areas, precipitation of calcium sulfate will take place.

Precipitation of calcium sulfate can be caused by evaporation of the solvent to the point where the concentration of the salt exceeds its solubility. This case can be treated by the diagram shown in Fig. 6. The ionic content of the water under consideration is plotted along the ordinate at one extreme of the abscissa. The abscissa itself is then marked off in percentage volume concentration of the solvent. At some convenient percentage volume concentration, (50 per cent or 75 per cent) the ionic content is recalculated and plotted. Straight lines connecting the points representing the individual ions are then drawn as before. The calcium sulfate concentration and solubility curves can then be plotted and the areas of precipitation shaded.

Decreases in solubility brought about by changes in temperature can be handled by the solubility diagram shown in Fig. 7. Temperature is laid off along the abscissa. Ionic concentrations are plotted on the ordinates intersecting at the extremes of temperature being studied. The points representing the same ions are connected as before, the concentration and solubility curves drawn, and the areas of precipitation shaded.

EXPERIMENTAL PROCEDURE

The evolution of the calcium sulfate solubility formula was based upon a series of preliminary experiments which led to the conclusion that the solubility of calcium sulfate in oil field brines in the pH range from 6.0 to 8.0 can be closely approximated by consideration of the four factors shown; and further that these factors seem to function independently of each other. Data from which the graphs were originally plotted were obtained from the International Critical Tables.¹ From this data several series of solubility diagrams were pre-

¹References given at end of paper.

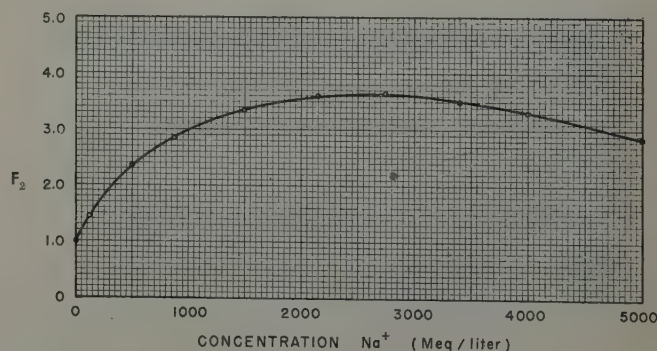


FIG. 4 — THE SODIUM ION FACTOR, OR THE SOLUBILITY OF CALCIUM SULFATE IN THE PRESENCE OF SODIUM ION.

$$F_2 = \frac{\text{Solubility of CaSO}_4 \text{ in presence of Na}^+}{\text{Solubility of CaSO}_4 \text{ in distilled water}}$$

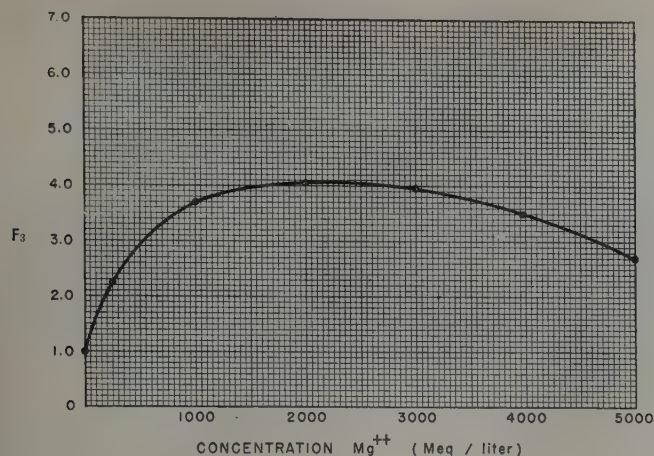


FIG. 5 — THE MAGNESIUM ION FACTOR, OR THE SOLUBILITY OF CALCIUM SULFATE IN THE PRESENCE OF MAGNESIUM ION.

$$F_3 = \frac{\text{Solubility of CaSO}_4 \text{ in presence of Mg}^{++}}{\text{Solubility of CaSO}_4 \text{ in distilled water}}$$

pared similar to Fig. 1, in which one water contained calcium ion and the other sulfate. One of the other ions (sodium, magnesium and either calcium or sulfate) was made to vary in each series while the rest were held constant. Actual samples of the waters represented were then made up and mixed in various proportions. After equilibrium had been reached at a given temperature, the precipitated calcium sulfate was filtered off, ignited and weighed. On the basis of these data a new solubility curve was plotted and the curve for the corresponding factor corrected. The final curves were verified by mixing both prepared solutions and actual oil field waters. Data from these experiments also confirmed our conclusions that the factors affecting the solubility of calcium sulfate are mutually independent.

APPLICATION

The solubility diagram allows a prediction of the tendency of a water to form deposits of calcium sulfate under a given set of conditions. A few applications of this system are shown:

Scale Deposits in Heater Treaters, Boilers, Etc.

Calcium sulfate scale may be deposited in heater treaters, boilers, etc., because the increase in temperature brings about a decrease in the solubility of the salt. The tendency of a particular water to deposit this type of scale can be shown by a solubility diagram such as is given in Fig. 7. The intersection of the solubility and the concentration curves indicates the point at which calcium sulfate will begin to precipitate.

Scale Formation Due to Casing Leaks

If the analyses of the formation water and that of the strata from which the extraneous water is coming are available, a solubility diagram of the type shown in Fig. 1 can be constructed to show scaling tendencies. Conversely, the formation of calcium sulfate scale in excessive amounts in a well may

indicate a casing leak, provided such scale can be shown to form as the result of the mixture of the formation water with water from an extraneous source.

Recirculating Cooling Water Systems

In some cases it may become necessary to use water containing considerable amounts of dissolved salts for cooling purposes in recirculating systems. In one such system water flows through heat exchange equipment where it is raised to a certain temperature. It is then passed through a spray pond or cooling tower in order to dissipate the heat. This water in passing through the tower is concentrated to a certain extent due to evaporation. By the use of a solubility diagram of the type shown in Fig. 6 the concentration at which calcium sulfate precipitates out can be calculated.

In the construction of such a diagram it should be remembered that the calculations are made at the temperature of the heat exchanger, rather than at the temperature of the spray pond.

Water Injection

Water injection problems are handled by diagrams similar to that shown in Fig. 1. In this case the graph may be considered as a cross section of the formation itself. Water "B" is being injected into a formation containing water "A." Along the length of the capillaries various percentage mixtures of the two waters will occur. If a deposit forms in any of these mixtures there will be considerable danger of plugging the capillaries with subsequent decrease in the permeability of the formation. Thus the solubility diagram can be used to forecast any tendency of two waters to form precipitates at any percentage mixture.

CONCLUSIONS

A method is presented by which the tendency of an oil field water to form calcium sulfate scale can be predicted from its analysis. Several applications of the method to the solution of typical production problems are given.

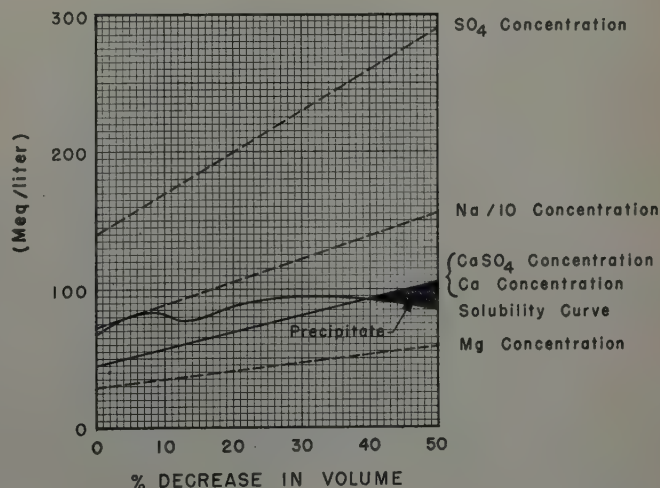


FIG. 6 — SOLUBILITY DIAGRAM, CALCIUM SULFATE DEPOSIT FORMATION WHEN SOLUTION IS CONCENTRATED.

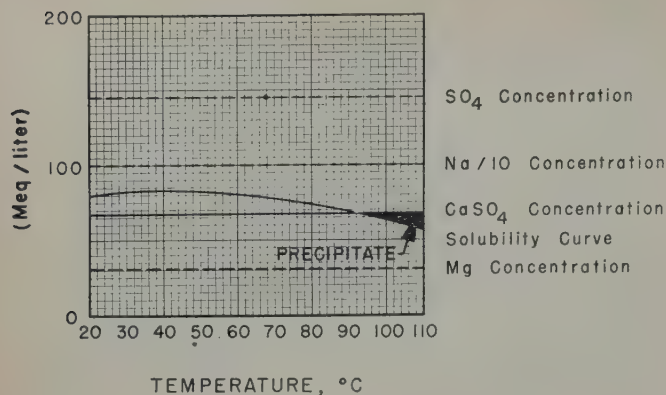


FIG. 7—SOLUBILITY DIAGRAM, CALCIUM SULFATE DEPOSIT FORMATION WITH CHANGE IN TEMPERATURE.

ACKNOWLEDGMENTS

The authors wish to thank The Atlantic Refining Co. for permission to publish this paper, and to acknowledge the valuable assistance and cooperation of the staff of the Chemical Engineering Group of this organization. Illustrations were prepared by Gene Nigh.

REFERENCES

1. International Critical Tables, 1st Edition, Vol. IV, pp. 287-290.

DISCUSSION

By J. D. Sudbury, Continental Oil Co., Ponca City, Okla.

The authors are to be congratulated on their presentation of this timely paper. Its greatest importance lies in the prediction of the chemical compatibility of a water being injected into a formation containing a different water. Such systems include water injection systems for water flood projects and for disposal.

The prediction tool as described is purely mechanical and is quite simple to use, provided reliable analyses of the waters in question are available. Proof that the various factors affecting the solubility of calcium sulfate are mutually independent is very significant. This allows the determination of the various factors individually in the laboratory as they have done for the common ion effect, sodium effect, and magnesium effect.

By determining curves for only these three factors, it is feared that the authors have oversimplified the complex nature of many oil field brines. For example, strontium, barium, potassium, and lithium have also been found in most of the waters which we have analyzed. Strontium has been found in quantities as high as 2,200 ppm, barium up to 500 ppm, potassium up to 1,400 ppm, and lithium up to 100 ppm. In many cases, the strontium and barium contents are about as great as the magnesium content of the water. The solubilities of barium sulfate and strontium sulfate are 1/500,000 and 1/200 that of calcium sulfate. Thus, in many cases where concentrations of barium and strontium are appreciable, we would expect to get precipitation of their sulfates before

getting any calcium sulfate deposition. Cases have been found where the deposition products are largely salts of barium or strontium. Even if they are not present in sufficient concentration to be precipitated ahead of calcium sulfate, factors should be determined for all of these ions in the same manner as was done for the sodium and magnesium. To illustrate the importance of this: the factor for 2,200 ppm strontium (49 meq per liter) is 1.35, and the factor for 1,400 ppm potassium (34 meq per liter) is 1.15; neglecting these factors would result in errors of 26 and 13 per cent in a calculated calcium sulfate solubility. These calculations assume that strontium follows the curve for magnesium (Fig. 5) and potassium follows the curve for sodium (Fig. 4).

Another factor which should be determined is the effect of *pH* on the solubility of the calcium sulfate. The solubility of calcium sulfate increases considerably with a decrease in *pH*. This effect is especially pronounced at temperatures near the boiling point of water. The *pH*'s of oil field brines have been found to vary in the range from three to nine. The presence of acid gases and organic fatty acids especially affect the *pH*.

It should be pointed out that the correction curves for sodium and magnesium were determined at one temperature and can be accurately used only at this temperature unless it is proved that the temperature effect is negligible. The only readily available calcium sulfate solubility data at various temperatures are for hydrochloric acid, ammonium sulfate, and sucrose. However, for these three the correction factor curves vary markedly with temperature.

Since the work of the authors showed all the factors affecting solubility to be mutually independent, it should be relatively simple to extend this paper by determining these additional correction factors. This would greatly broaden the applicability of their prediction method.

We have had considerably more trouble due to the deposition of calcium carbonate than of calcium sulfate. For this reason, I would like to ask the authors if they plan to extend this method to a study of the solubility of calcium carbonate? More specifically, have they determined whether or not the various factors affecting the solubility of calcium carbonate are mutually independent as was the case for calcium sulfate?

AUTHORS' REPLY TO MR. SUDBURY

The authors wish to thank the reviewer for his interesting and comprehensive discussion of this paper. We have, of course, given a great deal of thought to the matter of simplification and we agree that there are probably cases where our approach may be oversimplified.

The object of this study was to devise a workable technique for predicting the formation of calcium sulfate scale. Our most difficult problem was to determine the extent to which we could simplify the method. If too many factors are required, the solution of a problem would be too complex for practical use. If too few factors are taken into account accuracy would be sacrificed. We believe we have reached a satisfactory compromise. In the majority of cases the method will give good results. In some instances, however, the factors pointed out by Sudbury should, no doubt, be given more consideration.

Our studies were limited to brines within the *pH* range of from 6.0 to 8.0. We are sorry that this fact was inadvertently omitted from the preprint furnished the reviewer.

The authors are happy to announce that they also have a method for predicting the formation of calcium carbonate scale. We expect this paper to be available in the near future.

★ ★ ★

EFFICIENCY OF GAS DISPLACEMENT FROM POROUS MEDIA BY LIQUID FLOODING

T. M. GEFFEN, JUNIOR MEMBER AIME, D. R. PARRISH, G. W. HAYNES, MEMBER AIME, AND R. A. MORSE, JUNIOR MEMBER AIME, STANOLIND OIL AND GAS CO., TULSA, OKLA.

ABSTRACT

Flow tests on small core plugs have indicated that a large amount of gas is trapped and not recovered by water flooding a gas sand. Instead of 1 to 15 per cent pore space, as is usually assumed, the residual gas saturation is 15 to 50 per cent pore space, and is thus of the same magnitude as residual oil after water flooding oil sands.

A thorough investigation was made to ascertain that large amounts of residual gas actually remain in reservoirs after a water flood and that this condition is not merely a laboratory phenomenon. In field experiments, the amount of gas left in a watered-out gas sand was measured by use of a pressure core barrel and the residual gas saturation of two watered-out gas sands was determined by electric log evaluation. In the laboratory, an investigation was made of factors that could possibly cause the value of residual gas saturation as measured on small core plugs to differ from that in the reservoir, and the effect of these factors on the amount of residual gas saturation was studied. The factors studied include flooding rate, static pressure, temperature, sample size and saturation conditions before flooding. All evidence established that a relatively high gas saturation is trapped in water flooded gas sands and that this residual gas saturation can be measured in the laboratory by tests on small core plugs.

INTRODUCTION

There has been general agreement among engineers that very high recovery of gas could be obtained from natural reservoirs by water displacement. Gas recoveries of 80 to 95 per cent of the original gas in place have become the normal expectation in water drive fields. The assumption of high recovery has been based on:

1. low density and viscosity of gas compared with water;
2. the erroneous assumption that the flow relationships in a gas-liquid system where gas is the displaced phase will be the same as when it is the displacing phase.

It has long been recognized that gas can flow at very low gas saturations (in the range of 1 to 15 per cent pore space) in systems where liquid is being displaced by gas. By assuming the reversibility of this process, the conclusion was reached that the residual gas saturation following water flooding of a gas reservoir would be the same (1 to 15 per cent) as that

at which gas first flowed continuously as a displacing phase. Recent laboratory relative permeability studies^{1,2,3} have demonstrated that the flow characteristics are very different in gas-liquid systems, depending on whether gas is displacing or being displaced by, a liquid. Also, it has been shown that there is no difference between the flow characteristics of oil and water or gas and water in water wet porous rocks. The residual gas saturation that can be expected following water flooding of a gas reservoir then would be in the same range as the residual oil saturation normally expected after water flooding an oil reservoir, *i.e.*, in the range of 15 to 50 per cent pore space, depending on the rock characteristics.

Obviously, such a difference in residual gas saturation means very important differences in recoverable gas reserves from water drive reservoirs. For example, if the original gas saturation in a field were 70 per cent, and the residual gas following flooding were 35 per cent, only half of the gas in place could be recovered by complete water drive, compared to the previously expected 80 to 95 per cent. This is a situation in which complete pressure maintenance could result in very greatly reduced recovery, since straight pressure depletion recoveries from gas reservoirs can approach 80 to 90 per cent. Such a change in thinking must be based on more complete information than a series of small core tests. Hence the work reported herein was undertaken with the objective of determining whether or not residual gas saturations indicated from small core relative permeability tests at atmospheric pressure and room temperature are representative of the residual gas saturations which could be expected after water flood of natural reservoirs. A study was made both through laboratory and fields tests to determine any differences in residual saturation which might be occasioned by differences in pressure, temperature, rate of flooding, and original saturation conditions.

Four separate types of laboratory experiments and two field measurements were made in this investigation. The apparatus and testing methods of each will be discussed individually.

LABORATORY EXPERIMENTS, APPARATUS AND PROCEDURE

Relative Permeability Tests

Steady state flow experiments were conducted using the Penn State type apparatus. The equipment used has been described in a previous publication.¹ "Irreducible" water saturation was established in the core by imposing a capillary pressure of 45 psi before simultaneous flow of air and water

¹References given at end of paper.
Manuscript received in the office of the Petroleum Branch Sept. 18, 1951.
Paper presented at the Fall Meeting of the Petroleum Branch in Oklahoma City, Okla., Oct. 3-5, 1951.

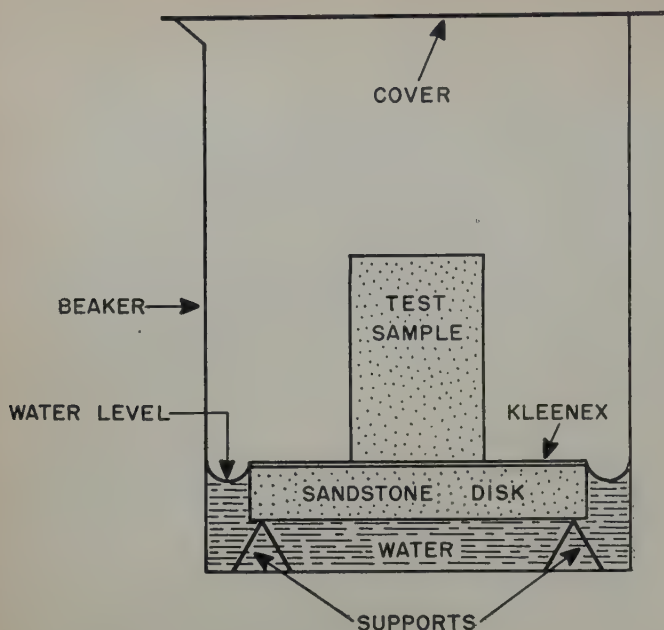


FIG. 1 — SCHEMATIC DIAGRAM OF WATER IMBIBITION TEST.

was started. The air and water were injected so that each succeeding equilibrium run had a higher water/gas ratio. Saturations were determined by electrical conductivity and gravimetric measurements.

Gas Displacement by Water in One-Foot Cores

Nellie Bly sandstone cores were used in this study. Cylindrical cores one and one-half in. in diameter and approximately one ft long were cut parallel to the bedding planes. Copper wire rings were placed at intervals along the length of the core and brass screen wires were placed against each end of the cores. Cores used in tests conducted at room temperature were encased in Lucite plastic sheaths, whereas those used for tests at 250°F were sealed in either phenol formaldehyde plastic or 3-M rubber sealing compound.

The cores were completely saturated with water, and then gas was injected into each end alternately to remove all but a near "irreducible" water saturation. After this, a desired gas pressure was established under a suitable back pressure and the cores were placed in a vertical position in a constant temperature bath. Flood water was supplied to the bottom of the cores in two ways. In those tests which were conducted at atmospheric pressure, water was injected at constant rates utilizing positive displacement pumps. In other tests, in which the gas pressure was 5,000 psi, a leveling bottle supplied the flood water under a head of a few inches of water.

Electrical conductivity measurements were made during the flooding operations. These values were converted to water saturations by means of an appropriate calibration curve. After flood-out, several pore volumes of water were passed through the cores.

Water Flood of a Simulated Gas Reservoir

A 16-ft column of Torpedo sandstone was made by butting together two cores which were cut parallel to the bedding planes. Bronze screen wire was placed across both ends of

the two-in. diameter column and copper ring electrodes placed at two-in. intervals along its length. This entire assembly was sealed in a Lucite plastic sheath.

The core column was placed vertically in a constant temperature (80°F) cabinet. The core was completely saturated with brine and then allowed to drain to capillary equilibrium, at which time only the lower one-half foot remained fully water saturated. Above this, the water saturation covered the range from 100 to 30 per cent pore space.

After water drainage stopped, the top of the core was pressured with 96 psig nitrogen pressure and water injection was started. A pump was used to inject water into the bottom of the core at constant rates. Several injection rates were used until flood-out. After flood-out, testing continued with alternate periods during which water was injected and periods during which no water was supplied to the core.

Gas Displacement from Dry Core Plugs By Water Imbibition

Cleaned dry core plugs of the type usually used for core analysis were placed so that one end contacted a source of water, as shown in Fig. 1. Weight measurements were made at time intervals as the core imbibed water. Residual gas saturation was determined as the break in the curve of average water saturation *vs* the imbibition time.

FIELD EXPERIMENTS, APPARATUS AND PROCEDURE

Physical Measurement of Gas Saturation in a Watered-Out Gas Sand

The Carter Oil Co.'s pressure core barrel was used in measuring the gas saturation in cores cut from a watered-out gas sand. Operation and design features of the pressure core barrel have been adequately described in other publications.^{4,5}

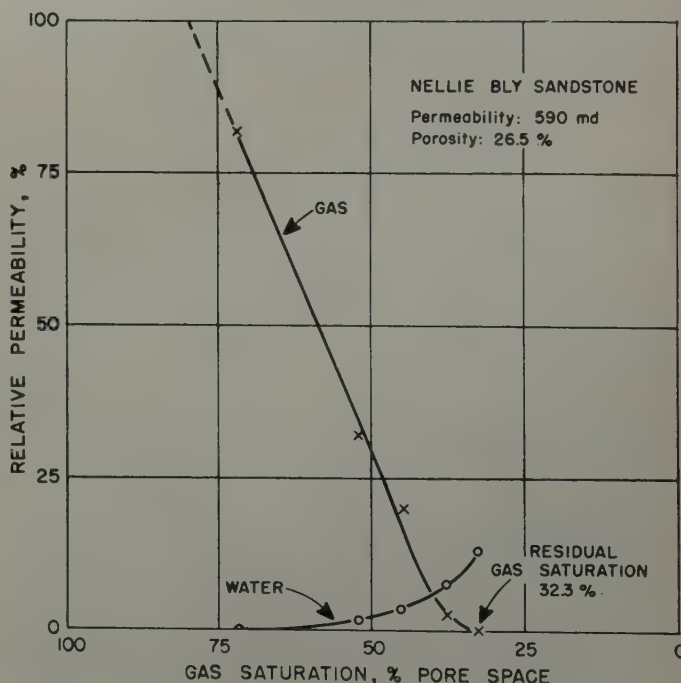


FIG. 2 — RELATIVE PERMEABILITY FOR DISPLACEMENT OF GAS BY WATER IN NELLIE BLY SANDSTONE.

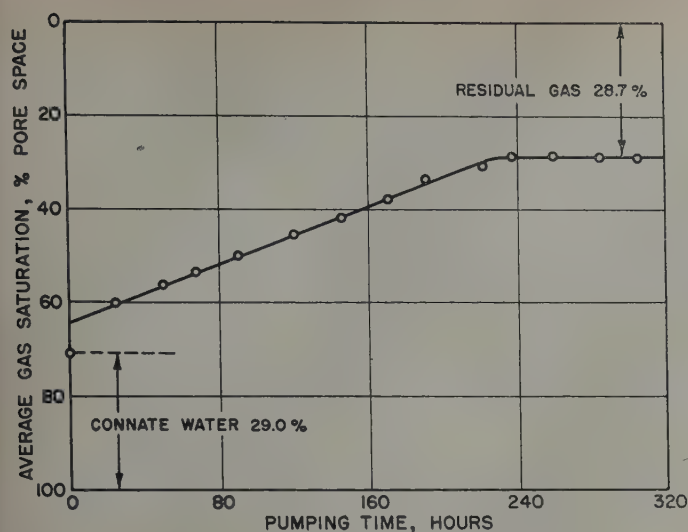


FIG. 3 — SATURATION HISTORY OF SLOW FLOOD (THEORETICAL RATE OF WATER RISE OF APPROXIMATELY ONE IN. PER DAY), NELLIE BLY SANDSTONE.

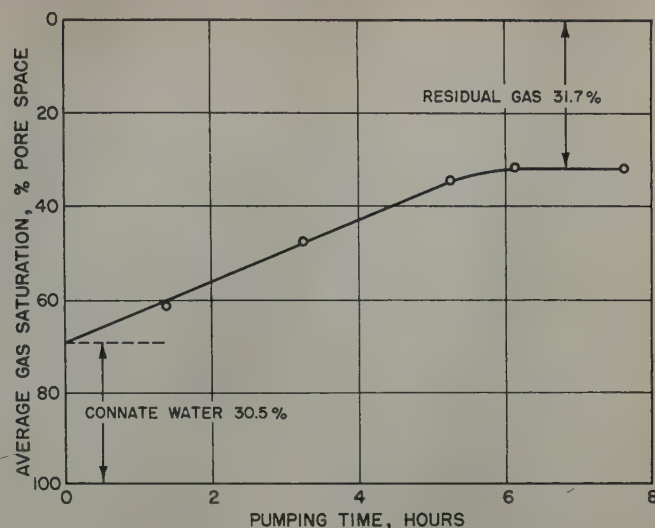


FIG. 4 — SATURATION HISTORY OF FAST FLOOD (THEORETICAL RATE OF WATER RISE OF APPROXIMATELY 54 IN. PER DAY), NELLIE BLY SANDSTONE.

The tool affords a means of coring subsurface strata and retrieving the cores at the surface under the same pressure that existed in the ground. Facilities are provided for making physical measurements on the core and the fluids it contains.

The entire section of the 4,500-ft gas sand of the West Beaumont Field, Tex., was cored with the pressure core barrel in four- and five-ft intervals. After pulling each core, all necessary measurements on the contents of the barrel were made. In addition to the physical measurement of gas saturation of the recovered cores, electrical logs were run and the gas saturation of the cored section calculated using the usual methods.⁶ The residual gas saturation of a partially watered-out reservoir, Siphonina Davisi sand, Lakeside Field, Louisiana, was calculated using electric log data.

Results of each of the four laboratory tests and the two field studies are discussed separately below:

RESULTS AND DISCUSSION OF LABORATORY STUDIES

Relative Permeability Tests

The flow sequence in gas-water relative permeability tests on small core plugs simulates conditions of saturation changes that occur in gas sands that are undergoing a water flood. Provided there are no effects present in reservoirs which are not present in laboratory tests, the value of residual gas should be the same for a specific piece of rock regardless of its location. Residual gas referred to herein is the saturation at which gas ceases to be recoverable by water displacement.

Gas-water steady state relative permeability characteristics for a sample of the Nellie Bly sandstone are given in Fig. 2. Maximum water saturation attained on this core plug was 67.7 per cent at flood out. This is equivalent to a residual gas saturation of 32.3 per cent pore space and will be compared to results of other laboratory flood tests conducted under simulated reservoir conditions.

Gas Displacement by Water in a One-Foot Core

The purpose of these tests was to evaluate the effect on residual gas saturation of: (a) rate of water advance, (b) static pressure, and (c) temperature.

A summary of results of the flood tests and relative permeability test on a small core plug is given in Table I. Agreement between all tests on order of magnitude of residual gas saturation after water flooding is good considering that several different cores of the same porous material were used in the studies. There is a small apparent effect of rate from a comparison of results of tests conducted on the same core with all conditions being the same except rate. This will be discussed further under a more thorough evaluation of each factor studied.

Effect of Rate of Water Advance

The histories of the two floods in which the rates of water advance were 1 and 54 in. per day are shown in Figs. 3 and 4, respectively. In both floods, a constant rate of average saturation change occurred until flood-out, then no change occurred with continued water injection.

The same core was used in these tests, yet the lower flooding rate resulted in a three per cent pore space lower residual gas saturation. This difference can partly, but not entirely, be attributed to experimental accuracy. It is recognized that

Table I — Vertical Flooding of Gas by Water
Nellie Bly Sandstone
Summary of Results

Rate of Water Advance In. Per Day Avg. (Approximate)	Pressure Static psig	Temp. °F	Residual Gas Saturation Per Cent Pore Space
100*	Atmospheric	80	32.3
1	Atmospheric	80	28.7
54	Atmospheric	80	31.7
4	5,000 psi	80	32.8
4	5,000 psi	250	33 - 36.5
(Three Cores)			

*Reference run: relative permeability test on core plug.

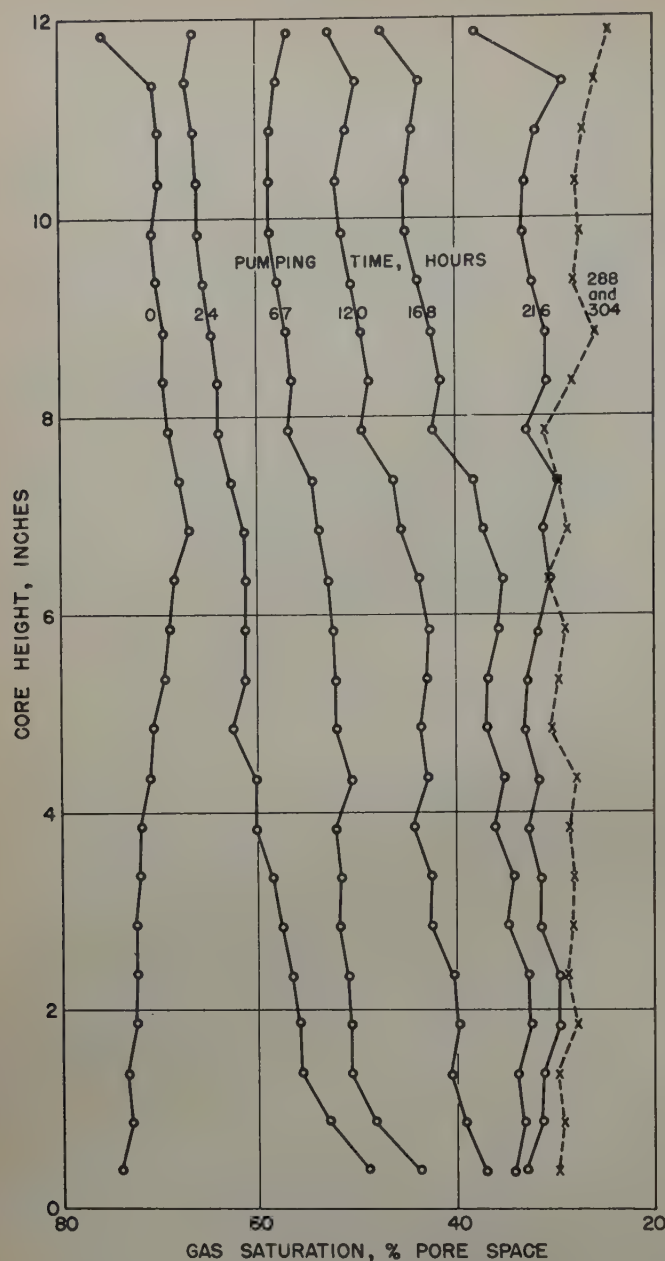


FIG. 5 — SATURATION PROFILES DURING SLOW FLOOD, NELLIE BLY SANDSTONE.

gas displacement by water does not result in a stable system. Trapped gas bubbles tend to leave the system by diffusion in order to establish thermodynamic equilibrium. A portion of the difference in residual gas saturation on the two tests in question can be considered a result of diffusion. The important question arises from this as to what the rate of diffusion would be in terms of saturation units at reservoir conditions of temperature and pressure. Gilliland⁷ has developed from the kinetic theory of gases an expression for diffusivity which permits a reasonable evaluation of the problem. From this it was determined that for reservoir conditions of 250°F and 5,000 psi, the change in gas saturation by diffusion is 1/220 of the rate at 80°F and atmospheric pressure. Therefore, three per cent pore space gas that was removed from the one-ft core by diffusion during the laboratory tests at a rate

of water advance of one ft in ten days would, in the reservoir, necessitate a rate of one ft in approximately six years. This rate is much less than usually occurs in producing reservoirs; therefore, it appears that gas diffusion could influence the results of laboratory tests at low pressures but is of little importance in the recovery of gas from reservoirs.

Following the fast rate flood, the core was left in contact with a source of water for 21 days, with no significant change in saturation taking place. This is attributed to an extremely low gas diffusion rate which resulted from the length of diffusion path. In this case, the average path was one-half the core length, or approximately six in. During the slow flood diffusion of gas was appreciably faster, since gas diffusion paths were small — in the order of sand grain diameters — in the saturation transition zone or flood front.

The data of the two floods show interesting results when analyzing the saturation distribution during the flooding periods. Figs. 5 and 6 show saturation profiles during the slow and fast floods, respectively. It is significant to note that in the slow flood the entire core saturation progressively changed while in the fast flood a typical flood front moved up the core. If only capillary (imbibition) forces are available to move water into the core, the profiles would assume a shape equivalent to the static capillary pressure curve of the system. In the slow flood the profile is elongated such that the total range of saturations between initial and flood-out conditions covers a length greater than the length of the core. In the fast flood the flood front is compressed to such a degree that the entire range of saturation exists within the core. Thus, the shapes of the saturation profiles of the two floods under discussion indicate that the low rate flood operated at a rate less than the imbibition rate and the other test at greater than imbibition rate.

It is concluded from the above discussion, that at reservoir conditions of temperature and pressure and reasonable flood rates, the effect of water flood rate on the efficiency of gas displacement is negligible.

Effects of Static Pressure

Flood history of an experiment in which methane at 5,000 psi static pressure was displaced by water is shown in Fig. 7. The driving force on the water in this experiment was capillary suction plus a few inches of water head. This produced a declining rate of water advance in the core. At flood-out the average residual gas saturation was 32.8 per cent pore space and was not changed by flowing enough water to replace the water in the core more than three times.

As in the preceding floods, the temperature of this test was maintained at 80°F. The value of residual gas saturation measured under pressure conditions of this test agree with those measured at atmospheric pressure.

Effects of Temperature and Pressure

Floods were performed at 5,000 psi static pressure and 250°F to simulate high pressure gas reservoir conditions. Recent research⁸ has indicated that in certain systems a wettability change takes place at these conditions. Such an occurrence could change the displacement efficiency of gas by water from that at lower temperatures and pressures. Although the cited work investigated a system in which the solid phase was steel and not rock material, it was thought advisable to investigate the possibility of wettability changes in rocks at high temperatures and pressures.

Three separate Nellie Bly cores were flooded starting with approximately 27 per cent connate water. Flood histories for these tests are shown in Fig. 8. Residual gas saturations for

these were 34.0, 36.5, and 33.0 per cent pore space. Precision of measuring saturation was not as good in these tests as those conducted at 80°F because of difficulties in obtaining good electrical insulation at the high temperature. Regardless of this, the magnitude of residual gas saturation agrees with values measured at lower temperatures. The erratic flood histories of the three tests are a result of restricting the flow of water into the cores by regulating needle valves. It is significant to note that in each case after flood-out no additional gas was recovered regardless of the previous flood histories.

Saturation profiles at various times during the flood on core 2 are presented in Fig. 9. The driving force for the water in

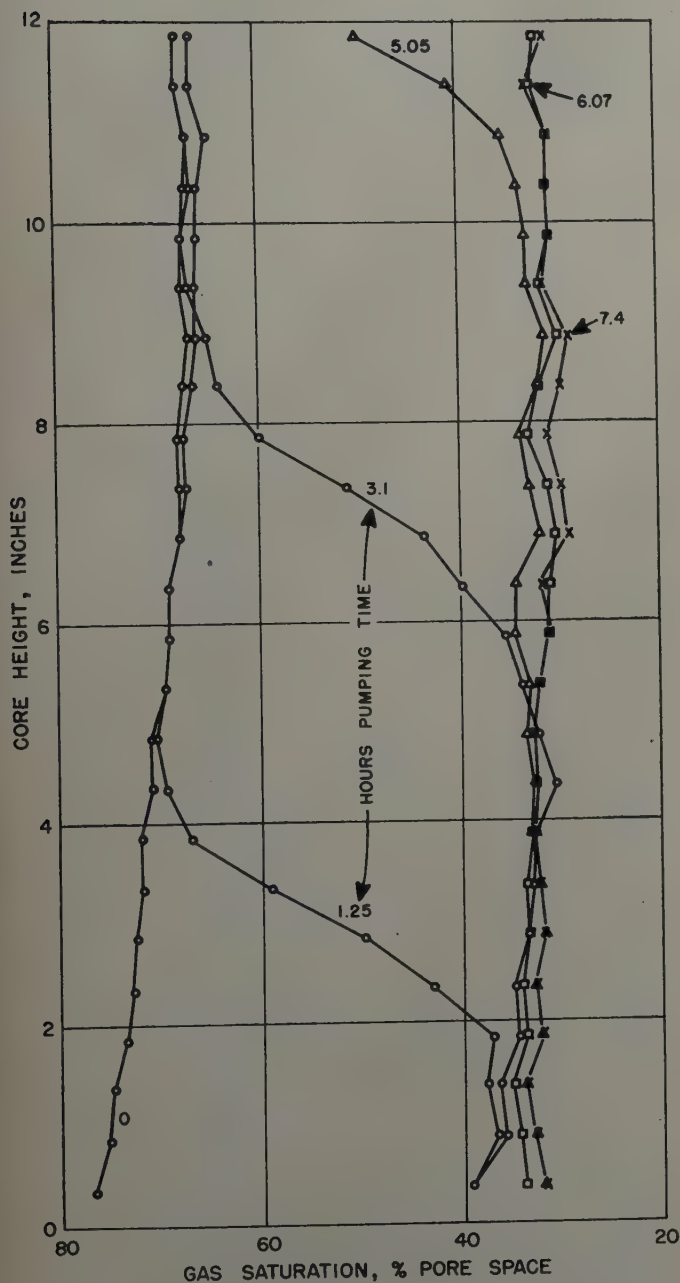


FIG. 6—SATURATION PROFILES DURING FAST FLOOD, NELLIE BLY SANDSTONE.

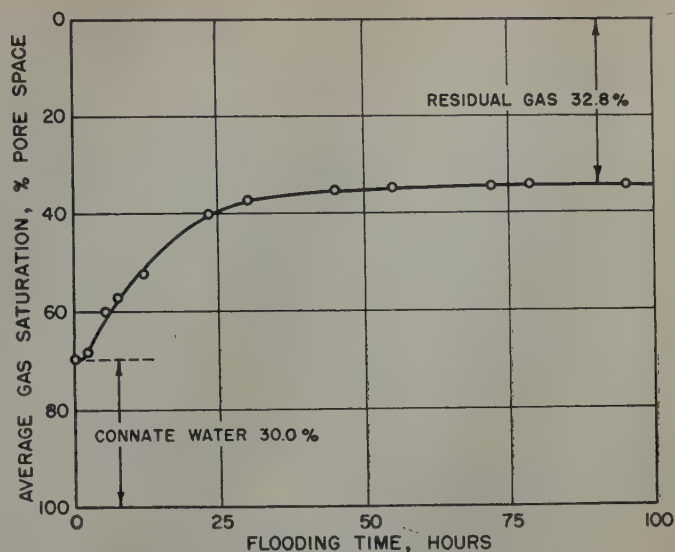


FIG. 7—SATURATION HISTORY OF UPDIP WATER FLOOD WITH STATIC PRESSURE AT 5,000 PSI AND TEMPERATURE OF 80°F, NELLIE BLY SANDSTONE.

this case was capillary suction. The fact that the core imbibed water is sufficient to establish that the water was the wetting phase as it was in the floods at atmospheric conditions.

Water Flood on a Simulated Gas Reservoir

In a gas sand at the time of discovery, the vertical distribution of gas and water is in equilibrium with the capillary forces of the sand. Gas saturation starts from zero, low in the structure, and increases progressively upward. The flood tests already discussed were performed with the entire core at a high gas saturation before the flood. A flood experiment on a 16-ft column of Torpedo sandstone (an outcrop formation) was made with the gas saturation before the flood in equilibrium with the capillary forces to find out if this factor had an influence on the amount of residual gas remaining after a water flood. Results of this experiment are given in Fig. 10, in which the vertical distribution of gas in the core is shown at various times during the water flood.

Connate water saturation in the core before the flood ranged from 30 per cent in the uppermost portion, gradually increasing to 100 per cent pore space in the lower one-half ft. It should be noted that at about nine and one-half ft up from the bottom of the core the continuity of the connate water saturation profile is broken. This is at the location of the joint plane between the two cores in the column. The discontinuity means the cores were not in complete capillary contact and a saturation gradient due to end effect resulted when the core was drained. During the water flood the discontinuity had no disturbing effect on the saturations as a non-wetting fluid was displaced by a wetting fluid.

Flood-out occurred after 24 days of continuous water injection. The residual gas saturation remaining in the core varied in the same manner as the original gas saturation. A maximum residual gas saturation of 34 per cent pore space was measured in the uppermost portion of the column. Relative permeability tests on several Torpedo sandstone core plugs resulted in residual gas saturations covering the range of 34 to 37 per cent pore space when the connate water saturation before flooding was in the same range as in this portion of the long

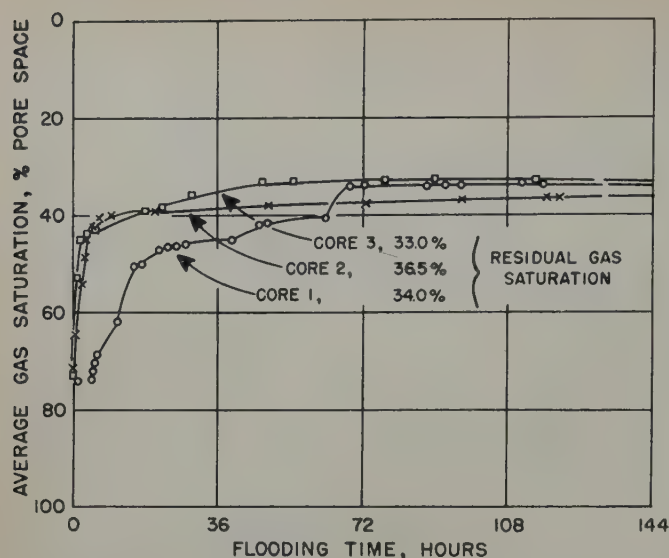


FIG. 8 — SATURATION HISTORIES OF THREE WATER FLOOD TESTS ON NELLIE BLY SANDSTONE CORES AT 5,000 PSI AND 250°F.

core column. Small core flow tests¹ have been shown to give the same variation in residual gas saturation as measured in the lower portions of the column when starting with comparable water saturation. After flood-out, an amount of water sufficient to flood out an additional 100 ft of sand was pumped through the core over a three-month period. During this time the gas saturation in the lower portion of the core gradually diminished. In the following two and one-half months period, during which no water was pumped into the system, the saturation at every position in the core remained stable. It is concluded that the small reduction in gas saturation in the lower portion of the core after flood-out was caused by solution effects. Considering the amount of water required to remove gas by solution, this method of gas recovery is not thought to be of practical importance in reservoirs.

In Fig. 10 the effect of rate of the displacement process can be seen. During the first 67 hours of the flood, the water was injected at a rate resulting in a water advance of approximately 20 in. per day. For the next 438 hours (67-505 hours total) the rate was reduced to approximately 10 in. per day. It can be seen that a twofold decrease in rate of water injection caused a twofold increase (from 3 to 6 ft) in the length

of transition zone or flood front. This is the only apparent effect rate had on the displacement process; the magnitude of residual gas saturation was not affected.

Gas Displacement from Dry Core Plugs By Water Imbibition

In all preceding experiments described, the cores contained connate water before being water flooded. The question arose as to the amount of residual gas saturation that would remain after water flooding cores which were not initially subjected to the restored state technique. This involved water flooding a completely gas saturated core.

Capillary forces will cause spontaneous imbibition of water into porous materials that are wet by water in preference to air. Water thus imbibed into the core will displace air to zero air permeability in the same manner that it would if it were pumped into the core. This flooding-out of a core by water imbibition will progress until the vertical height flooded is equivalent to the displacement pressure of the rock sample.

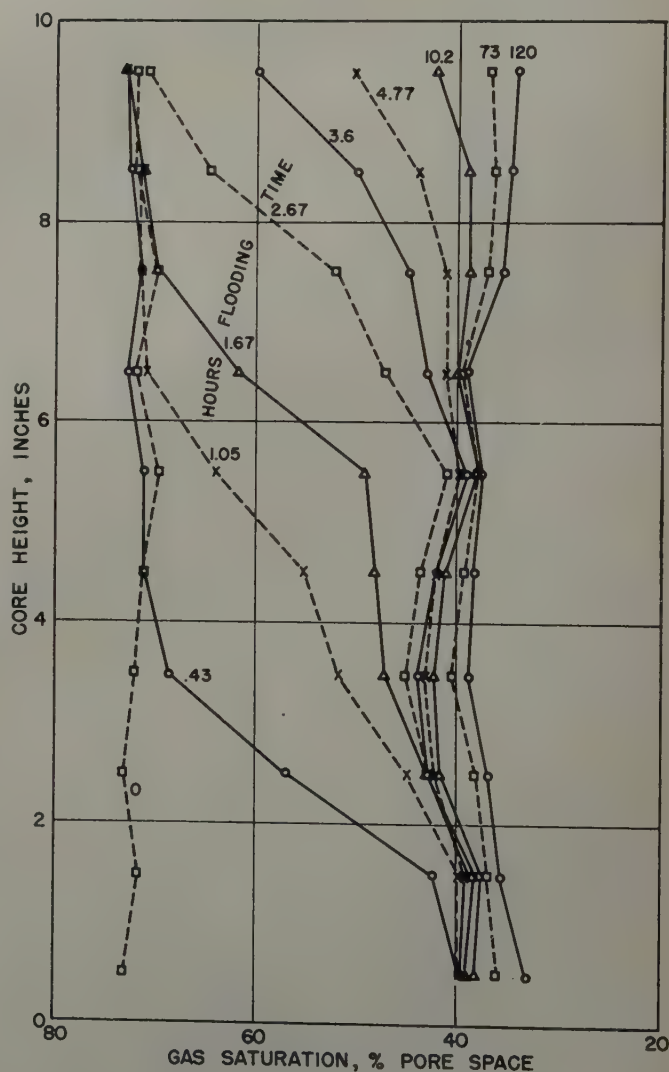


FIG. 9—SATURATION PROFILES DURING UPDIP WATER FLOOD AT 5,000 PSI AND 250°F, NELLIE BLY SANDSTONE (CORE NO. 2 OF FIG. 8).

Table II—Reproducibility of Determination of Residual Gas Saturation by Imbibition (1½-in. Diameter Samples)

Sandstone	Sample No.	Residual Gas Saturation, % Pore Space		
		Test 1	Test 2	Test 3
Torpedo	1*	34.5	—	—
Torpedo	2*	34.0	—	—
Torpedo	3*	34.2	33.6	34.3**
Torpedo	4*	35.1	—	—
Torpedo	5*	35.5	35.0	35.1**
	Avg.	34.7		
Nellie Bly		31.8	32.1	

*Cut from same block in order of number.

**Curved surface plastic coated.

Table III — Reproducibility of Residual Gas by Imbibition Tests (Different Size Samples)

Sandstone	Diameter, In.	Residual Gas Saturation % Pore Space	
		Test 1	Test 2
Nellie Bly	1½	31.8	32.1
Nellie Bly	¾	31.8	—

Above this height only a partial flood will take place. Displacement pressures of the type porous materials of interest are greater than one in. of water; therefore, natural sand core plugs in the order of one in. in length can be completely flooded by water imbibition.

In these experiments water was imbibed from the lower face of the core with the remainder of the core in the atmosphere. It was found that completely submerging the cores had the disadvantage of mechanically trapping gas in the central portion of the core as water invaded from all directions, thus complicating interpretation of the data.

Cores used in these experiments were outcrop sandstones, reservoir cores, and synthetic porous materials. Typical data of a water imbibition test are shown in Fig. 11. Each set of data points is for the same core. The significant feature is the reproducibility of the residual gas saturation. Difference in measured values is in the order of precision that saturations can be determined by weighing the core. Before flood-out, and after the same amount of time, the amount of water imbibed in each test was different. This was entirely due to differences in the resistance offered by the supporting porous disks to the flow of water.

Repeat tests on the same cores were found to be reproducible within 0.6 per cent pore space. This is shown in Table II. The five Torpedo sandstone cores were cut from the same piece of rock and three tests were conducted on each of two cores. Sample diameter had no effect on the results as shown by data in Table III. Similar agreements of results were found between tests using core plugs whose curved surfaces were covered with an impervious plastic and tests before plastic was molded onto the core.

Table IV lists comparative results of imbibition tests on two cores performed with and without connate water saturation in the sample before imbibing water. The agreement is within acceptable limits. Table V gives comparative results of residual gas saturations measured on the same cores by flow experiments (relative permeability tests) and by water imbibition into dry cores. Again the agreement is acceptable, as the average of the five cores tested by the two methods differs only by one per cent pore space.

Oil was used for the imbibed fluid in other tests and results for cores in which both water and oil imbibition tests were conducted are shown in Table VI. The agreement is exceptionally good. These results indicate that over the range investigated, viscosity, density, and interfacial tension of the fluids

Table IV — Comparison of Residual Gas by Imbibition Tests on Cores When Dry and When Containing Connate Water

Sandstone	Residual Gas Saturation, % Pore Space	
	Originally Containing Irreducible Water	Originally Dry
Nellie Bly	34.7	33.0
Nellie Bly	34.5	32.3

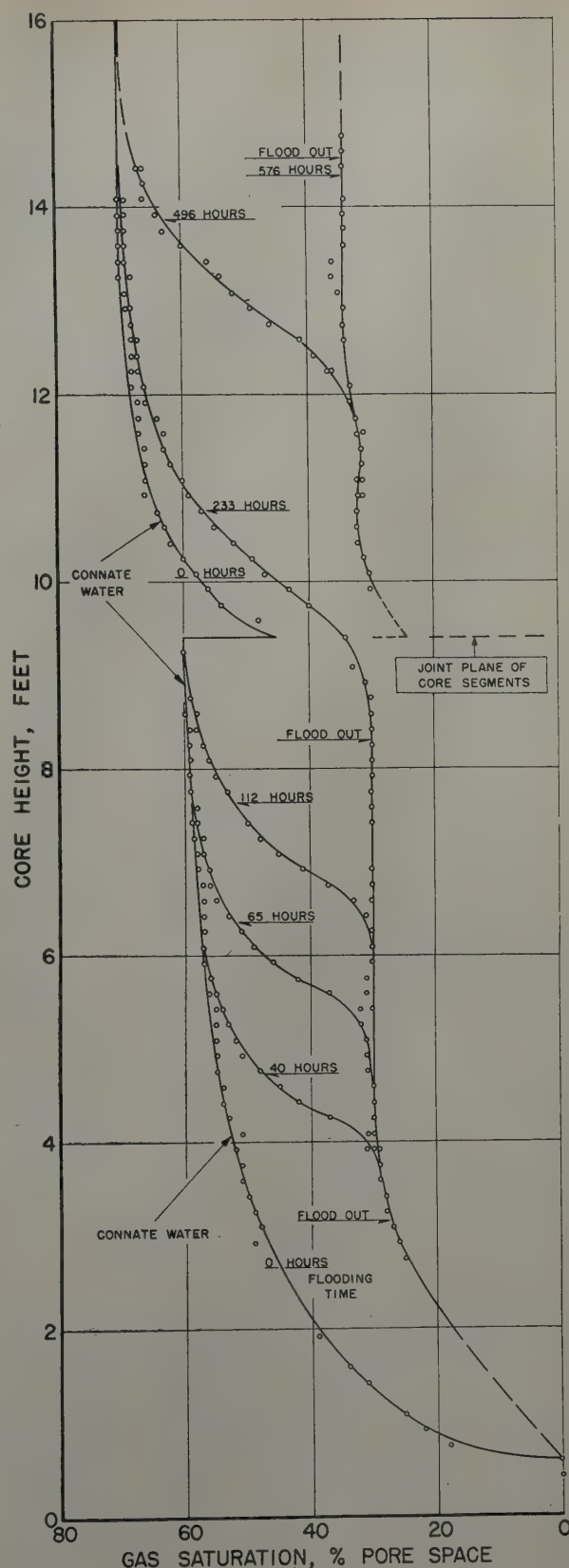


FIG. 10 — SATURATION PROFILES DURING UPDIP FLOODING OF GAS BY WATER, TORPEDO SANDSTONE.

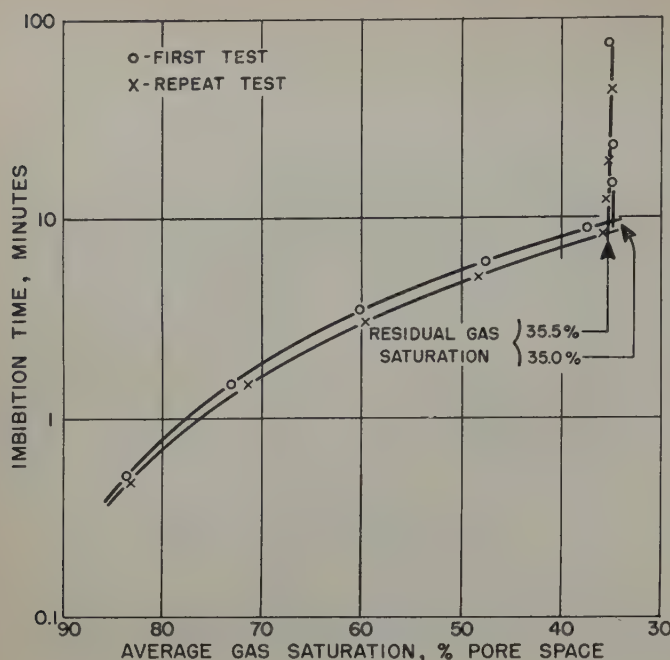


FIG. 11—TYPICAL WATER IMBIBITION TEST DATA SHOWING REPRODUCIBILITY OF RESULTS, TORPEDO SANDSTONE. (PERMEABILITY 425 MD, POROSITY 26.5 PER CENT).

have no effect on residual gas saturation provided the flooding liquids wet the rock to the same extent.

It is concluded from the preceding data, that residual gas saturations measured on dry cores by water imbibition are essentially the same as those values measured by flow tests starting with connate water in the core.

Incidental to the main subject under discussion, a significant observation was made in these imbibition tests. All cores tested imbibed oil, but some of them would not imbibe water. These cores which were repellent to water were identified by other laboratory tests as being preferentially oil wet. Thus the imbibition test can be used to indicate wettability characteristics of rocks.

Many types of porous materials were investigated in the laboratory to evaluate the range of residual gas saturations that can be expected in reservoirs. A listing of the results of

Table VI—Oil Imbibition vs Water Imbibition

Sample	Residual Gas Saturation, % Pore Space	
	By Oil Imbibition	By Water Imbibition
Selas Porcelain	16.3	17.5
Torpedo Sand	35.4	34.5
Frio Sand	34.0	34.2
Frio Sand	33.4	33.6
Frio Sand	29.8	30.2
Frio Sand	29.8	29.6

these tests is given in Table VII. The significant feature of these data is that residual gas saturations after water flooding reservoir rocks range from 16 to 50 per cent pore space, which is the same range of values for residual oil saturation obtained in the laboratory when water flooding "oil sands." Craze and Buckley⁹ have determined from field data that residual oil saturations in water drive oil reservoirs are within this same range of values.

MEASUREMENT OF RESIDUAL GAS SATURATION IN WATER FLOODED GAS RESERVOIRS

Field data were reviewed to find out if residual gas saturation in watered-out gas sands could be evaluated by a material balance calculation as Craze and Buckley⁹ did for residual oil in water drive oil sands. No suitable field data were located, due primarily to the fact that at this time very few water drive gas sands have been completely flooded. Also, the usual wide well spacing in gas fields makes difficult the precise determination of field areal extent, which is an important factor in the calculation of residual gas saturation. In the absence of field performance data, other means of evaluating residual gas saturation in watered-out portions of gas reservoirs were used, namely, physical measurements of gas content of cores and calculation of gas saturation using electric log data.

West Beaumont Field, Tex.

Production history and recent drilling have established that the 4,500-ft gas sand of the West Beaumont Field, Jefferson County, Tex., has been partly flooded out due to a rise in the water level as a result of production. Seeking deeper pay, a well was recently drilled in a portion of the field in which the 4,500-ft gas sand had been flooded out by water for approximately five years. The original elevation of the gas-water contact was accurately determined from the electric logs of an original gas well located 170 ft from the new well.

The 4,500-ft gas sand was cored with Carter Oil Co.'s pressure core barrel. Ten cores were cut making a total of 43 ft cored. In three of these runs the equipment operated completely satisfactorily, recovering core at the surface under bottom hole pressure. Gas volumes bled from the cores at the surface were converted to reservoir volumes, taking into account an experimentally determined compressibility factor of 0.85. Results of the tests are given in Table VIII.

Porosity values are averages of several samples from each core. These values may not reflect the true porosities that existed in the reservoir because the soft nature of the rock as the core was removed from the core barrel made it evident that it was reworked during cutting operations. This being the

Table V—Comparison of Residual Gas Saturation Obtained by Relative Permeability and Brine Imbibition Tests

Sandstone	Residual Gas Saturation, % Pore Space	
	By Rel Perm Tests	By Imbibition
Frio	34.5	32.5
Frio	35.0	34.7
Frio	33.7	37.0
Frio	34.7	35.3
Frio	34.1	37.0
	Avg - 34.4	35.3
Nellie Bly	32.3*	30-36**
Torpedo	37.0*	34.7***

*One sample only.

**Range for 12 cores.

***Average five other samples (See Table II).

Table VII—Summary of Results, Residual Gas Saturation After Water Flood as Measured on Core Plugs in Laboratory

Porous Material	Formation	Residual-Gas Saturation % Pore Space	
		16	(13-ft Column)
Unconsolidated Sand	—	21	(1 Core)
Slightly Consolidated Sand (Synthetic)	—	21	(1 Core)
Synthetic Consolidated Materials	Selas Porcelain	17	(1 Core)
	Norton Alundum	24	(1 Core)
	Wilcox	25	(3 Cores)
	Frio	30	(1 Core)
	Nellie Bly	30-36	(12 Cores)
	Frontier	31-34	(3 Cores)
	Springer	33	(3 Cores)
	Frio	30-38	(14 Cores)
		(Average 34.6)	
	Torpedo	34-37	(6 Cores)
	Tensleep	40-50	(4 Cores)
Limestone	Canyon Reef	50	(2 Cores)

situation, residual gas saturations calculated are minimum values, due not only to use of too large porosity values, but also to the possibility of gas bubbles escaping from the cut rock before recovery at the surface. Considering these possibilities, it is estimated that the residual gas saturation is more probably in the order of 22 per cent pore space.

It is significant to note that the higher measured value of residual gas was found in the core which was closer to the original gas-water contact which, of course, had been flooded out the greater length of time. Therefore, based on these results, it is indicated that diffusion has not been an effective means of gas removal in this sand. The core taken from below the original gas-water contact contained no gas, although it was under bottom hole pressure when retrieved at the surface.

In addition to the physical measurements, an electric log analysis was made on the watered-out gas sand. In Table VIII are values of residual gas for the three cored sections using the Archie formula⁶ for calculating saturations. There are uncertainties in the electric log interpretation since the cores recovered were of such a nature that no basic electrical measurements could be made on them. The results reported are those calculated using the most reasonable values for factors involved. It was found that by varying porosity over a range of 25 to 35 per cent; cementation factor, 1.4 to 1.6; and true reservoir resistivity at 100 per cent water saturation, 0.65 to 0.85 ohm-meter; the value of residual gas for the first core reported in Table VIII ranged from 22.7 to 40.0 per cent pore space. Results from the electric log cover a wide range of values; but even by using the most extreme conditions, the residual gas saturation is of the order measured in the laboratory on cores.

The friable nature of the sand did not permit laboratory measurement of residual gas saturations by flow tests. But on similar types of material, unconsolidated to slightly consoli-

Table VIII—Gas Saturations Measured on Cores Cut With Pressure Core Barrel

Depth Interval	Porosity	Gas Saturation Physical Measurement	Gas Saturation Electric Log Calculation
4,564	Top of Sand	—	—
4,573-77	32.9	16.7	37
4,589-93	31.0	18.5	19.4
4,600	ORIGINAL GAS - WATER CONTACT	—	—
4,601-06	8.1	0	0

dated sand, values from 16 to 21 per cent pore space have been measured which agree in magnitude with the physical measurements of residual gas in the West Beaumont cores.

Lakeside Field, Louisiana

A well drilled in 1950 near the west edge of the Lakeside Field, Cameron Parish, Louisiana, penetrated the Siphonina Davisi sand. This reservoir had produced gas and distillate starting in 1941. Field data indicate that the reservoir has an active water drive and that the water-gas contact has moved up approximately 30 ft as a result of production. The sand logged in this new well included both the water flooded and unflooded portions of the pay. In Table IX are given calculated gas saturations using the Archie formula,⁶ as well as other pertinent information concerning the well.

The calculation of gas saturations was based on a 30 per cent porosity measured on a core and the most reasonable values for other factors involved in the determination, so the numbers are subject to the usual limitation on quantitative electric log data. The drill stem test confirmed that the lower portion of the sand was flooded out, and calculations indicated that 21.8 per cent gas saturation still remained. This value is of the same order of magnitude as residual gas saturation measured in the laboratory on friable type sand samples (see Table VI).

Table IX—Analysis of Siphonina Davisi Sand Lakeside Field, Louisiana

Depth	Calc. Gas Saturation From Electric Log Data	General Data
9,978	68	—
9,974-90	—	Completion; produced gas and distillate with no water
9,998	60.9	—
10,010	—	Top of flooded-out zone at time of completion of this well (calculated from field performance data)
10,018	21.8	—
10,020-30	—	Drill stem test; recovered salt water
10,040	—	Original water-gas contact

CONCLUSIONS

1. Laboratory and field evidence both substantiate the conclusion that residual gas saturations as determined in the laboratory on core plugs are, within practical limits, the same as will occur in a gas sand under a water flood.
2. Residual gas saturations vary from 15 per cent to 50 per cent pore space for different sands, which is the same range of variations for residual oil saturations after water flooding oil sands.

ACKNOWLEDGMENTS

The authors wish to acknowledge the cooperation of the Research Department of the Carter Oil Co. in the pressure coring operation at West Beaumont and the helpful suggestions and cooperation of many individuals in the Producing

Department of Stanolind who contributed greatly to the entire investigation. Also, appreciation is expressed to the Stanolind Oil and Gas Co. for permission to present this paper.

REFERENCES

1. Geffen, T. M., Owens, W. W., Parrish, D. R., and Morse, R. A.: "Experimental Investigation of Factors Affecting Laboratory Relative Permeability Measurements," *Trans. AIME*, (1951) **192**, 99.
2. Osoba, J. S., Richardson, J. G., Kerver, J. K., Hafford, J. A., and Blair, P. M.: "Laboratory Measurements of Relative Permeability," *Trans. AIME*, (1951) **192**, 47.
3. Caudle, B. H., Slobod, R. L., and Brownscombe, E. R.: "Further Developments in the Laboratory Determination of Relative Permeability," *Trans. AIME*, (1951) **192**, 145.
4. Sewell, Ben W.: "The Carter Pressure Core Barrel," *API Drill. and Prod. Prac.*, (1939), 69.
5. Mullane, J. J.: "Pressure Core Analyses," *API Drill. and Prod. Prac.*, (1941), 163.
6. Archie, G. E.: "The Electrical Resistivity Log as an Aid in Determining Some Reservoir Characteristics," *Trans. AIME*, (1942) **146**, 54.
7. Gilliland, E. R.: *Ind. Eng. Chem.*, (1934) **26**, 681.
8. Hough, E. W., Rzasa, M. J., and Wood, B. B.: "Interfacial Tensions at Reservoir Pressures and Temperatures; Apparatus and the Water-Methane System," *Trans. AIME*, (1951) **192**, 57.
9. Craze, R. C., and Buckley, S. E.: "A Factual Analysis of the Effect of Well Spacing on Oil Recovery," *API Drill. and Prod. Prac.*, (1945) 144.

DISCUSSION

By J. G. Richardson, Junior Member AIME, and J. S. Osoba, Humble Oil and Refining Co., Houston, Tex.

The authors are to be commended for their pioneering efforts in studying the magnitude and significance of residual gas saturations obtained when gas-filled porous media are liquid flooded. The laboratory experiments described represent a major undertaking both from a standpoint of the complexity of apparatus required and also the diversity of the experiments performed. The critical issue involved in this paper is whether the imbibition distribution of saturation noted in laboratory experiments is sufficiently stable to apply to reservoir conditions of pressure, temperature and rate of water advance, and to permit a determination of the efficiency of water floods in reservoirs from laboratory data. Therefore, on such an important issue as reserves left in the ground,

a critical examination of the evidence presented by the authors should be made.

No anomalous results due to boundary discontinuities can be noted in these experiments. Theoretically, boundary effects should not influence results at the residual gas saturation where the gas permeability goes to zero and the flat saturation profile shown in Figs. 5, 6, and 9 as the outflow end is approached verifies this. The good agreement obtained among the residual gas saturations in flooding experiments over a wide range of pressure and temperature with those obtained by imbibition experiments on small core samples indicates that the fast and simple imbibition experiments duplicate the laboratory flooding results. This agreement has been found in our laboratories also among results from water and oil floods at laboratory temperature and low pressures and those of immersion experiments.

Deemed particularly significant is the apparent lowering of the residual gas saturation by diffusion, Figs. 3 and 5. It should be pointed out that the relation developed by Gilliland referred to applies only to gases diffusing in gases and cannot be applied to gases diffusing in liquids, which system is involved in this case.

While the effect of temperature upon the diffusivity coefficient in Fick's Law can be approximated by the Stokes-Einstein

equation $D \propto \frac{T}{\mu}$, the effect of pressure upon the diffusivity

coefficient is not readily obtainable. Therefore, additional study will be required before this diffusional effect can be interpreted in terms of rate of water advance at reservoir pressure and temperature.

AUTHORS' REPLY TO MESSRS. RICHARDSON AND OSOBA

Richardson and Osoba have brought up an important point concerning the applicability of the Gilliland equation for estimating the effects of temperature and pressure on the rate of diffusion of gas. The authors fully realize that the relation was not derived for diffusion of a gas through a liquid. Unfortunately, no information is available which can be used to evaluate precisely this problem. Although Gilliland's equation cannot be used to evaluate the absolute value of the diffusivity coefficient, the upper limit of the effect of temperature and pressure on diffusion rate can be reasonably estimated. Qualitatively, the conclusion that gas diffusion in terms of saturation is of minor significance, considering the length of the producing life of a reservoir, is substantiated by the fact that residual gas saturations measured on cores cut with a pressure core barrel in the West Beaumont Field were in the range of values expected, based on other measurements made on cores in the laboratory.

★ ★ ★

DISPLACEMENT MECHANISM IN MULTI-WELL SYSTEMS

LOYD R. KERN, THE ATLANTIC REFINING CO., DALLAS, TEX.

ABSTRACT

A procedure for determining the behavior of a reservoir under a gas or water injection program was reported by Buckley and Leverett in 1942.¹ This method, which allowed the calculation of the phase saturation distribution behind the front of a displacing fluid, has been extended to apply to a more general situation.

The reservoir may initially contain flowing quantities of the displacing fluid, or the fluid in the reservoir may be above saturation pressure so that solution effects are present. Production may occur behind the front as in the case of a well which is produced after breakthrough of the displacing fluid. The calculating procedure is simplified in that the graphical integration necessary to determine breakthrough saturation is eliminated by performing a direct integration and the graphical differentiation necessary to determine saturation distribution is eliminated by representing the displacing phase fraction of the flowing stream by an empirical equation. This representation results in simple expressions for the producing gas or water/oil ratio and cumulative production.

INTRODUCTION

A method for the calculation of the saturation distribution behind the front (interface between the displaced and displacing phases in a gas injection or water flooding operation) was reported by Buckley and Leverett in 1942. The method leads to a curve for the saturation distribution which is double-valued; consequently, part of the curve was interpreted to be physically meaningless. That part of the curve which has physical significance was determined by a graphical integration (material balance).

¹References given at end of paper.

Manuscript received in the office of the Petroleum Branch Aug. 9, 1951. Paper presented at the Fall Meeting of the Petroleum Branch in Oklahoma City, Okla., Oct. 3-5, 1951.

In this paper it is shown that the integration may be performed analytically with a resulting equation for the saturation of the displacing phase at the front. The case in which the displacing fluid is initially flowing and the case in which the reservoir is initially above the saturation pressure so that some injected gas goes into solution are included in the integration. The calculations are considerably simplified by representing the fraction of the flowing stream which is oil by an exponential function of saturation.

The method is extended to apply approximately to reservoirs in which wells located between the injection well and the front are produced. An illustrative example utilizing the methods presented is included.

RESERVOIR BELOW SATURATION PRESSURE

In the case of a water flooding operation or in the case of a gas injection operation in which no gas goes into solution in the displaced oil, the equation for saturation in a linear flow system as a function of time and position as given by Buckley and Leverett is

$$\left(\frac{dx}{dt}\right)_{\rho_d} = \frac{5.61q}{fA} \Psi'_d \quad \dots \quad (1)$$

where*

q = total reservoir volume flow rate, rvb/day

A = cross sectional area of system, sq ft

f = porosity of formation

x = distance from injection point, ft

t = time, days

ρ_d = saturation of the displacing phase

$$\left(\frac{dx}{dt}\right)_{\rho_d} = \text{velocity of planes of constant saturation, ft/day}$$

*The nomenclature used here is not the same as that used by Buckley and Leverett. A complete nomenclature is given in Appendix A.

Ψ_d = fraction of flowing stream which is the displacing phase =

$$\frac{1}{1 + \frac{k_o}{k_d} \frac{\mu_d}{\mu_o}}$$

$\Psi_d' = \frac{d\Psi_d}{d\rho_d}$, the change of the fraction of the flowing stream with saturation (displacing phase)

k_o = relative permeability to oil

k_d = relative permeability to the displacing phase,

$\frac{\mu_d}{\mu_o}$ = ratio of the viscosity of the displacing phase to the viscosity of the displaced oil.

Equation (1) and the developments presented here apply to linear flow systems. Application to actual reservoirs may be achieved approximately by considering the product fAx to be the pore volume enclosed by a surface of fixed saturation and approximately determining the shape of these surfaces by independent means. If $V = \frac{fAx}{5.61}$ is the pore volume in barrels enclosed by the surface of saturation ρ_d , Equation (1) may be written as

$$\left(\frac{dV}{dQ} \right)_{\rho_d} = \Psi_d' \quad (2)$$

where $Q = \int_0^t q(t) dt$ is the total number of barrels of injected fluid (measured at reservoir conditions)

and $\left(\frac{dV}{dQ} \right)_{\rho_d}$ is the change in the pore volume enclosed by the surface of saturation ρ_d per unit volume of injected fluid.

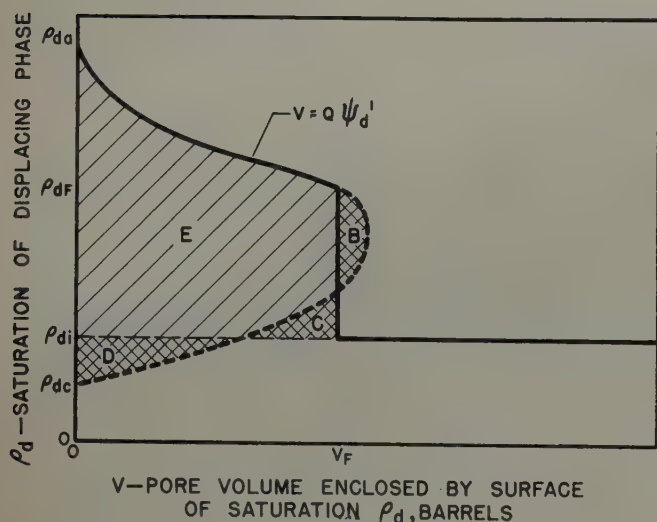


FIG. 1 — SATURATION DISTRIBUTION IN A GAS INJECTION OR WATER FLOODING OPERATION.

ρ_{dc} = Saturation at which permeability to the displacing phase goes to zero. ρ_{d1} = Initial saturation of displacing phase. ρ_{dF} = Saturation of displacing phase at the front. V_F = Pore volume swept out by the front. ρ_{da} = Saturation at which permeability to the displaced phase goes to zero.

If the saturation does not vary with position before injection occurs, Equation (2) may be integrated directly:

$$V = Q \Psi_d' \quad (3)$$

Saturation plotted vs V from Equation (3) for a particular Q appears as shown by the curve in Fig. 1. The dotted portion of the curve is taken to be imaginary and is determined by material balance methods.

The area enclosed by the curve and the axis $V = 0$ is equal to the volume of displacing fluid which has been injected. It can be shown (Appendix B) that the area D is equal to the volume of displacing fluid initially present which has flowed out of the volume occupied by the front; and therefore the saturation at the front is determined by making the area B equal to the area C . If the initial saturation is equal to or less than ρ_{dc} (the saturation at which permeability to the displacing phase goes to zero) the area D is zero. If the initial saturation is equal to or greater than the saturation at which the maximum occurs in the $\frac{d\Psi_d}{d\rho_d}$ curve, areas B and C are zero and the saturation at the front is equal to the initial saturation (there is no discontinuity at the front).

From the condition that area B equal area C an expression is obtained for the saturation existing at the front:

$$\rho_{dF} - \rho_{d1} = \frac{\Psi_{dF} - \Psi_{d1}}{\Psi_{dF}'} \quad (4)$$

where

ρ_{dF} = saturation of the displacing phase at the front

ρ_{d1} = initial saturation of the displacing phase,

Ψ_{dF} = value of Ψ_d at $\rho_d = \rho_{dF}$

Ψ_{d1} = value of Ψ_d at $\rho_d = \rho_{d1}$

Ψ_{dF}' = value of $\frac{d\Psi_d}{d\rho_d}$ at $\rho_d = \rho_{dF}$

Equation (4) expresses the value of the saturation at the front in terms of known quantities; the initial saturation of the displacing phase (assumed constant with position) may have any value. If the initial saturation of the displacing phase is equal to or greater than the saturation at which the maximum occurs in the $\frac{d\Psi_d}{d\rho_d}$ curve, the correct solution of Equation (4) is: $\rho_{dF} = \rho_{d1}$. If the initial saturation is less than the saturation at which the maximum occurs but greater than the saturation at which the permeability to the displacing phase goes to zero, there are two solutions, $\rho_{dF} = \rho_{d1}$ again being a solution but the incorrect one in this case (the saturation at the front cannot be less than the saturation at which the maximum in the $\frac{d\Psi_d}{d\rho_d}$ curve occurs). If the initial saturation is less than the saturation at which the permeability goes to zero, there is only one solution.

RESERVOIR ABOVE SATURATION PRESSURE

If it is assumed that the reservoir fluid is instantaneously saturated at the front by the solution of gas with no further solution effects behind the front, Equations (2) and (3) may be applied to the case in which the reservoir is above the saturation pressure.

In this case the initial saturation of the displacing phase is zero and the area D of Fig. 1 is zero. To satisfy material balance considerations the area B of Fig. 1 must equal area C .

plus the volume of free gas which has disappeared by going into solution. This condition is expressed as

$$\rho_{gF} = \frac{\Psi_{gF} + \frac{S - S_1}{\gamma\beta - S + S_1}}{\Psi_{gF}} - (1 - \rho_w) \frac{S - S_1}{\gamma\beta - S + S_1} \quad (5)$$

where the subscript g refers to the displacing gas phase and S = gas solubility of the saturated oil behind the front, SCF/STB

S_1 = gas solubility of the original reservoir oil, SCF/STB

γ = gas conversion factor, SCF/rvb

β = formation volume factor of the saturated oil behind the front, rvb/STB

ρ_w = connate water saturation

Equation (5) (derived in Appendix C) relates the saturation of the displacing gas at the front to quantities which are known or may be measured. The viscosity of the displaced fluid which appears in Ψ_g is taken in this case to be the viscosity of the saturated oil behind the front.

Since some of the gas is going into solution at the front and since in general the solution of a given volume of gas in oil does not increase the volume of oil by that amount, the total volume flow rate ahead of the front differs from that behind the front. That is to say, in the case of a reservoir above saturation pressure the volume production rate is less than the volume injection rate even though pressure gradients are negligible. The ratio of the production rate to the injection rate is given by

$$\Gamma = \frac{\gamma\beta_1}{\gamma\beta - S + S_1} + (1 - \rho_w) \left[1 + \frac{\gamma\beta_1}{\gamma\beta - S + S_1} \right] \Psi_{gF}' \quad (6)$$

where β_1 is the formation volume factor of the displaced fluid (rvb/STB) ahead of the front and Γ is the desired ratio (see Appendix E).

PRODUCTION BEHIND THE FRONT

Consider a reservoir in which gas or water is injected through a single well and production occurs from several wells in the field (some of the wells may continue production after the front of the displacing phase has passed them). The method of Buckley and Leverett may be applied approximately in this case if it be assumed that the sweepout pattern is known and that the surfaces coincident with the front as it progresses through the reservoir will later coincide with surfaces of fixed saturation. Let V_1 be the pore volume enclosed by the frontal surface when the front reaches the first well or group of wells, V_2 the pore volume enclosed by the frontal surface when the front reaches the second group of wells, and so on for V_3, V_4, \dots

The preceding analysis applies for the zone $0 < V < V_1$. However, in the second zone ($V_1 < V < V_2$) and other zones after the front has entered those zones Equation (3) may not be applied because both the displacing phase and the displaced phase are entering the zone. (In the first zone only the displacing phase is injected). Furthermore, the total volume flow rate in each zone is decreased by production from wells behind the front.

If these factors are taken into account, the saturation distribution in the second zone is given by

$$V - V_1 = \Psi_d' \int_{Q_1}^Q (1 - q_1) dQ \quad (7)$$

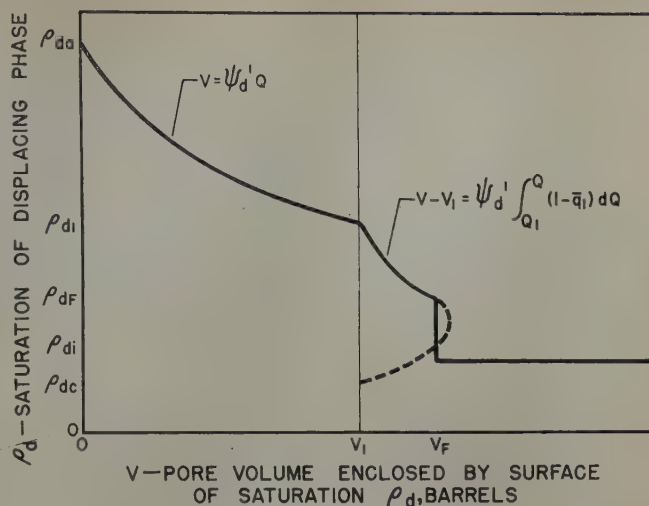


FIG. 2 — SATURATION DISTRIBUTION IN A TWO-ZONE RESERVOIR. V_1 = Pore volume of first zone. V_F = Pore volume enclosed by the front. ρ_{d1} = Saturation of the displacing phase at $V = V_1$. Saturation distribution shown by solid line.

where

q_1 = fraction of total volume flow which is being voided at the first group of wells (assumed to be known)

Q_1 = volume of displacing fluid which has been injected when the surface of saturation ρ_d passes the surface $V = V_1$

The factor Q_1 may be evaluated in terms of the saturation by setting $V = V_1$ in Equation (3):

$$Q_1 = \frac{V_1}{\Psi_d'} \quad (8)$$

Equation (7) states that the volume enclosed by the surface V of saturation ρ_d is equal to the volume of the first zone plus a factor proportional to the total volume of gas and oil which has entered the second zone since the surface passed the boundary of the first zone.

The saturation distribution for a two-zone reservoir is shown in Fig. 2. There is a group of producing wells at $V = V_1$ and production has continued after the front has entered the second zone. The saturation distribution in the first zone was obtained from Equation (3) and the saturation distribution in the second zone was obtained from Equation (7). The dotted portion of the curve (between ρ_{dc} and ρ_{dF}) as plotted from Equation (7) is the same as that which would have been obtained had the total volume entering the zone been gas rather than gas plus oil. The dotted portion of the curve is taken to be imaginary since the saturation at the front remains the same in the second zone as in the first (see Appendix D).

For the n th zone ($V_{n-1} < V < V_n$) the saturation distribution is given by

$$V - V_{n-1} = \Psi_d' \int_{Q_{n-1}}^Q (1 - q_1 - q_2 - \dots - q_{n-1}) dQ \quad (9)$$

where q_k is the fractional voidage rate at the k th group of wells and Q_{n-1} is the volume of displacing fluid which has been injected when the surface V of saturation ρ_d passes the $(n-1)$ th group of wells.

The Q_2 which would appear in the limit of the integral if Equation (9) were applied to the third zone could be evalu-

ated in terms of saturation by setting $V = V_2$ in Equation (7). Thus by considering succeeding zones, the saturation distribution could be uniquely determined as a function of V and Q .

This procedure, however, is unwieldy unless the q_k 's are constants or simple integrable functions of Q . If the integrals

$\int_0^Q (1 - q_1 - q_2 - \dots - q_{n-1}) dQ$ cannot be evaluated directly,

the variation of ρ_d with Q at each group of wells may be determined by a simple graphical procedure (it is necessary to know only the variation in saturation at each producing well in order to specify producing gas or water/oil ratio and cumulative oil production histories).

Equation (9) may be written for $V = V_n$ as

$$\frac{V_n - V_{n-1}}{\Psi_d} + \int_0^{Q_{n-1}} (1 - q_1 - q_2 - \dots - q_{n-1}) dQ = \int_0^{Q_n} (1 - q_1 - q_2 - \dots - q_{n-1}) dQ \quad (10)$$

where Q_n is the total volume of displacing fluid which has been injected when the surface of saturation ρ_d reaches the n^{th} group of wells.

If saturation is known at the $(n-1)^{\text{st}}$ group of wells as a function of the volume of gas or water injected, saturation at the n^{th} group of wells as a function of the volume injected may be determined from Equation (10) by plotting the integral

$\int_0^Q (1 - q_1 - q_2 - \dots - q_{n-1}) dQ$ vs Q . For any given saturation

the first term on the left hand side of Equation (10) may be directly calculated; the second term may be evaluated by

referring to the plot of the integral $\int_0^Q (1 - q_1 - q_2 - \dots - q_{n-1}) dQ$

vs Q (saturation at the $(n-1)$ group of wells is known as a function of Q); the value of Q_n which will make the integral on the right side of Equation (10) equal to the left side may then be determined by referring to the plot of the integral. By considering successive zones in this manner the saturation at each group of wells as a function of the volume of gas or water injected may be readily determined and with this it is a simple matter to determine the gas/oil or water/oil ratio and production history of each well in the field.

EMPIRICAL METHODS

The calculations encountered in the application of these methods to practical uses are greatly simplified by representing the Ψ_d function by an analytical function of saturation.

Since breakthrough saturation is specified by Equation (4) or (5) and since gas or water/oil ratio and cumulative oil production at the well can be determined from the saturation existing at the well, accurate results may be obtained from any analytical representation which fits the data in the saturation range from breakthrough to abandonment saturation regardless of the fit outside this range.

A representation which greatly facilitates the calculations necessary in the type of problems under consideration here is an exponential. In all of a number of cases which have been studied it has been possible to choose a factor λ such that a plot of $\log (\Psi_o + \lambda)$ vs ρ_d is a straight line over the

range of interest (between breakthrough and abandonment saturations). That is, Ψ_d may be represented by

$$\Psi_d = 1 - \Psi_o = 1 + \lambda - \exp \left\{ \frac{\theta - \rho_d}{\omega} \right\} \quad (11)$$

where ω and θ are constants and are determined by the slope and intercept of the straight portion of the $\log (\Psi_o + \lambda)$ vs ρ_d plot.

With this representation it is only a matter of a few minutes to calculate the breakthrough saturation and the entire gas or water/oil ratio and production history once Ψ_d or Ψ_o vs ρ_d has been plotted.

For a water injection operation or a gas injection operation in which the reservoir initially is at or below saturation pressure, the equation for the saturation at the front becomes:

$$x = C_1 e^x \quad (12)$$

where $x = 1 + \frac{\rho_{dF} - \rho_{d1}}{\omega}$

$$\text{and } C_1 = (1 + \lambda - \Psi_{d1}) \exp \left\{ \frac{\rho_{d1} - \theta}{\omega} - 1 \right\}$$

Equation (12) may be readily solved by trial or graphical means for the factor x from which breakthrough saturation may be obtained.

In the case of a reservoir which is above the saturation pressure, the equation for the saturation at the front is:

$$y = C_2 e^y \quad (13)$$

where $y = 1 + \frac{\rho_{dF} + (1 - \rho_w) \frac{S + S_1}{\gamma\beta - S + S_1}}{\omega}$

$$C_2 = \left(1 + \lambda + \frac{S - S_1}{\gamma\beta - S + S_1} \right) \exp \left\{ -\frac{1}{\omega} \left[\omega + \theta + (1 - \rho_w) \frac{S - S_1}{\gamma\beta - S + S_1} \right] \right\}$$

Equation (13) may be solved by trial for the factor y from which the value of the breakthrough saturation may be obtained.

With the exponential representation simple expressions are obtained for gas or water/oil ratio and cumulative production

at the producing well since Ψ_d varies linearly with Ψ_d' and hence the fraction of the flowing stream which is oil at any well may be determined easily as a function of Q .

For example, the cumulative oil production at the first group of wells is given by

$$N = N_b + \frac{1}{\beta} \int_{Q_b}^Q q_1 \Psi_o(\rho_{d1}) dQ = N_b + \frac{1}{\beta} \int_{Q_b}^Q q_1 \left(\frac{\omega V_1}{Q} - \lambda \right) dQ \quad (14)$$

where N = cumulative oil production, STB

N_b = cumulative oil production at breakthrough, STB

Q_b = volume of displacing fluid which has been injected when breakthrough occurs, rvl.

Since q_1 is known as a function of Q , Equation (14) expressly defines the cumulative oil production at the first group of wells as a function of the amount of displacing fluid which has been injected.

As another example, the gas/oil ratio at the first group of wells after breakthrough in a gas injection operation is given by

$$R = \frac{\Psi_g}{\Psi_o} \gamma\beta + S = \frac{\gamma\beta Q}{V_1 \omega - \lambda Q} - \gamma\beta + S \quad (15)$$

where R is the gas/oil ratio, SCF/STB.

ILLUSTRATIVE EXAMPLE

Since this paper is intended primarily for the use of practical engineers, a numerical example illustrating the use of the methods proposed here will be given in detail. The case to be considered is a reservoir initially above saturation pressure with production occurring behind the front. The constants of the system are listed below:

Fluid Properties

	Initial	Flooded Volume
oil viscosity μ_o	0.93 cp	0.60 cp
gas viscosity μ_g		0.022 cp
gas solubility S	400 $\frac{\text{SCF}}{\text{STB}}$	600 $\frac{\text{SCF}}{\text{STB}}$
formation volume factor β	1.20 $\frac{\text{rvb}}{\text{STB}}$	1.32 $\frac{\text{rvb}}{\text{STB}}$
gas conversion factor γ		1160 $\frac{\text{SCF}}{\text{rvb}}$

The values shown are obtained by measurements on the initial under-saturated oil and on oil just brought to the saturation point by the addition of gas.

Reservoir Properties

$V_1 = 29 \times 10^6$ bbl = Pore volume swept by front when injected gas breaks through the first group of producing wells.

$V_2 = 66 \times 10^6$ bbl = Pore volume swept by front when injected gas breaks through second group of producing wells.

$q_1 = \frac{2}{3}$ before breakthrough.

$= \frac{1}{3}$ after breakthrough.

= total production rate of first group of producing wells relative to gas injection rate (measured on reservoir volume basis).

$\rho_w = 0.40$ = connate water saturation.

Relative Permeability

ρ_g	0.15	0.20	0.25	0.30	0.35
k_g/k_o	0.043	0.208	0.796	3.30	31.6
Ψ_o	0.460	0.150	0.044	0.011	0.0016

The curve marked $\lambda = 0$ in Fig. 3 is the plot of gas saturation vs log Ψ_o . The curve marked $\lambda = 0.0039$ is a plot of gas saturation vs log $(\Psi_o + 0.0039)$; since this curve is straight over a large range, λ is taken to be equal to 0.0039 for this example.

The constant θ is given by the intercept of the straight portion of the curve and the ordinate $\Psi_o + \lambda = 1$; here $\theta = 0.12$. The constant ω is given by the negative of the slope of the straight portion; in this example $\omega = 0.0426$.

The fraction of the flowing stream which is oil is then represented by

$$\Psi_o = e^{\frac{0.12 - \rho_g}{0.0426} - 0.0039}$$

Breakthrough saturation is calculated from Equation (13). The constant C_2 in Equation (13) has the value 0.00305. The value of γ which satisfies Equation (13) in this case is 7.87. Then

$$1 + \frac{\rho_{gp} + (1 - 0.40) \frac{600 - 400}{(1160)(1.32) - 600 + 400}}{0.0426} = 7.87$$

$$\text{or } \rho_{gp} = 0.203$$

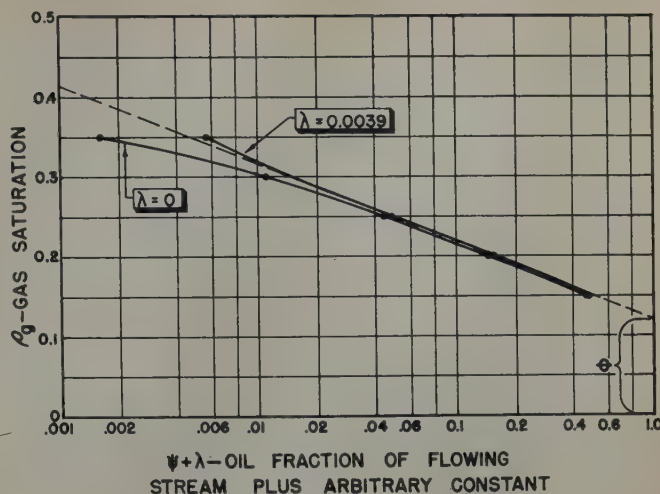


FIG. 3 — GAS SATURATION PLOTTED AGAINST LOG $(\Psi_o + \lambda)$ FOR ILLUSTRATIVE EXAMPLE.

With $\lambda = 0.0039$, curve is practically straight over a wide range. The constant θ is determined by the value of saturation when $\Psi_o + \lambda = 1$.

$$\text{and } \Psi_{gp} = \frac{1}{\omega} e^{\frac{\theta - \rho_{gp}}{\omega}} = 3.36$$

The amount of gas which has been injected when breakthrough occurs at the first group of wells is obtained from Equation (3):

$$Q_{1b} = \frac{V_1}{\Psi_{gp}} = \frac{29 \times 10^6}{3.36} = 8.65 \times 10^6 \text{ rvb} = 10.0 \times 10^6 \text{ SCF gas.}$$

The gas/oil ratio at the first group of wells after breakthrough is given by Equation (15).

$$R_1 = \frac{1530 Q}{1.235 \times 10^6 + 0.0039 Q} - 930 \frac{\text{SCF}}{\text{STB}}$$

The wells in this field are abandoned at a gas/oil ratio of $30,000 \frac{\text{SCF}}{\text{STB}}$; the amount of gas which has been injected when the first group of wells is abandoned is determined by setting $R_1 = 30,000$:

$$Q_{1a} = 23.2 \times 10^6 \text{ rvb} = 26.9 \times 10^6 \text{ SCF gas.}$$

The cumulative oil production of the first group of wells at breakthrough is

$$N_{1b} = \frac{(q_1)(Q_{1b})}{\beta_1} = \frac{(2/3)(8.65 \times 10^6)}{1.20} = 4.80 \times 10^6 \text{ STB oil.}$$

After breakthrough the cumulative oil production of the first group of wells is given by Equation (14):

$$N_1 = 4.80 \times 10^6 + \frac{1}{1.32} \int_{Q_{1b}}^Q \frac{1}{8.65 \times 10^6} \left[\frac{(0.0426)(29 \times 10^6)}{Q} - 0.0039 \right] dQ$$

$$= 4.89 \times 10^6 + (0.312 \times 10^6) \log \frac{Q}{8.65 \times 10^6} - 9.85 \times 10^{-4} Q \text{ STB}$$

At abandonment ($Q = 23.2 \times 10^6$ rvb) cumulative production is

$$N_{1a} = 5.17 \times 10^6 \text{ STB oil}$$

The saturation distribution in the reservoir zone between the first and second group of wells after the first group of wells has been abandoned is determined from Equation (7):

$$\begin{aligned} V - V_1 &= \Psi_g' \left\{ \int_{Q_1}^{Q_{1a}} (1 - 1/3) dQ + \int_{Q_{1a}}^Q (1 - 0) dQ \right\} \\ &= \Psi_g' \left\{ \int_{Q_1}^{Q_{1a}} 2/3 dQ + \int_{Q_{1a}}^Q dQ \right\} \\ &\quad \Psi_g' \end{aligned}$$

$$\text{or } V - \frac{1}{3} V_1 = \Psi_g' \left(Q - \frac{1}{3} Q_{1a} \right)$$

for saturation less than abandonment saturation.

The amount of gas which has been injected when breakthrough occurs at the second group of wells is obtained by setting $V = V_2$:

$$Q_{2b} = 24.5 \times 10^6 \text{ rvb} = 28.4 \times 10^6 \text{ SCF gas}$$

[Note: If breakthrough at the second group of wells had occurred before abandonment of the first group of wells, it would be necessary to determine the saturation distribution existing in the second zone before abandonment of the first group of wells.]

The gas/oil ratio (constant before breakthrough) at the second group of wells after breakthrough is given by:

$$\begin{aligned} R_2 &= \frac{\Psi_g'}{\Psi_o} \gamma\beta + S = \frac{\gamma\beta}{\omega\Psi_g' - \lambda} - \gamma\beta + S \\ &= \frac{\gamma\beta}{\omega \left(\frac{V_2 - 1/3 V_1}{Q - 1/3 Q_{1a}} \right) - \lambda} - \gamma\beta + S \\ &= \frac{1530 (Q - 7.33 \times 10^6)}{2.43 \times 10^6 - 0.0039 Q} - 930 \end{aligned}$$

The amount of gas injected when the gas/oil ratio is 30,000 SCF is:

$$Q_{2a} = 52.4 \times 10^6 \text{ rvb} = 60.7 \times 10^6 \text{ SCF gas}$$

The ratio of the total volume flow rate head of the front to that behind the front is obtained from Equation (6):

$$\begin{aligned} \Gamma &= \frac{(1160)(1.20)}{(1160)(1.32) - 600 + 400} + (1 - 0.40) \\ &\quad \left[1 - \frac{(1160)(1.20)}{(1160)(1.32) - 600 + 400} \right] (3.36) = 0.952 \end{aligned}$$

At breakthrough in the first group of wells 8.65×10^6 rvb of gas had been injected but only $(0.952)(8.65 \times 10^6) = 8.24 \times 10^6$ rvb of oil had been produced. Since $2/3(8.65 \times 10^6)$ rvb were produced at the first group of wells, the production at the second group of wells was 2.47×10^6 rvb or 2.06×10^6 STB oil.

At abandonment of the first group of wells 23.2×10^6 rvb of gas had been injected or 14.6×10^6 rvb since breakthrough. One third of this volume was voided at the first group of wells in the form of both gas and oil with $2/3$ or 9.73×10^6 rvb entering the second zone. Hence, the production from the second group of wells during this phase is $(0.952)(9.73 \times 10^6) = 9.26 \times 10^6$ rvb or 7.72×10^6 STB oil. During the phase of production between abandonment of the first group and breakthrough at the second group of wells a total of 1.3×10^6 rvb of gas was injected which corresponds to $(0.952)(1.3 \times 10^6) = 1.24 \times 10^6$ rvb or 1.03×10^6 STB of oil production.

The total cumulative production of the second group of wells at breakthrough is then $(2.06 + 7.72 + 1.03) \times 10^6 = 10.81 \times 10^6$ STB of oil.

After breakthrough, the cumulative oil production is given by

$$\begin{aligned} N_2 &= 10.81 \times 10^6 + \frac{1}{\beta} \int_{24.5 \times 10^6}^Q \Psi_o dQ \\ &= 10.81 \times 10^6 + \frac{1}{1.32} \int_{24.5 \times 10^6}^Q \left[\frac{\omega(V - 1/3 V_1)}{Q - 1/3 Q_{1a}} - \lambda \right] dQ \\ &= 10.88 \times 10^6 - 0.00296 Q + 1.82 \times 10^6 \log \frac{Q - 7.73 \times 10^6}{16.8 \times 10^6} \end{aligned}$$

The cumulative production at abandonment is obtained by setting $Q = 52.4 \times 10^6$:

$$N_{2a} = 12.51 \times 10^6 \text{ STB}$$

The total production for the field is $12.51 \times 10^6 + 5.17 \times 10^6 = 17.68 \times 10^6$ STB oil.

ACKNOWLEDGMENTS

The author wishes to express his gratitude to W. W. Schriever, C. A. Hutchinson, Jr. and F. A. Collins for valuable contributions to this paper.

REFERENCES

1. Buckley, S. E., and Leverett, M. C.: "Mechanism of Fluid Displacement in Sands," *Trans. AIME*, (1942) 146, 107.

APPENDIX A — NOMENCLATURE

A	Cross sectional area, sq ft
f	Porosity
k	Relative permeability, md/md
N	Cumulative oil production, STB
q	Total reservoir volume flow or injection rate, rvb/day
q_n	Total reservoir volume production rate of the n^{th} group of wells relative to injection rate $\frac{\text{rvb/day}}{\text{rvb/day}}$
Q	Total volume of fluid injected, rvb
R	Gas/oil ratio, SCF/STB
S	Gas solubility factor, SCF/STB
t	Time, days
V	Pore volume enclosed by surface of fixed saturation, rvb
x	Distance from injection point, ft
β	Formation volume factor, rvb/STB
γ	Gas conversion factor, SCF/rvb
Γ	Ratio of flow rate ahead of front to flow rate behind front
θ	Constant
λ	Constant
μ_a/μ_o	Viscosity ratio of displacing phase to displaced phase, cp/cp
ρ	Saturation
Ψ	Fractional flowing stream
ω	Constant

Subscripts

<i>b</i>	Breakthrough
<i>d</i>	Displacing phase
<i>g</i>	Gas
<i>i</i>	Initial
<i>m</i>	Mean
<i>n</i>	Number
<i>o</i>	Oil
<i>w</i>	Water

APPENDIX B — BREAKTHROUGH SATURATION — RESERVOIR BELOW SATURATION PRESSURE

Referring to Fig. 1, the area enclosed by the curve and the axis $V = 0$ is

$$\int_{\rho_{dc}}^{\rho_{da}} Q \Psi'_d d\rho_d = Q = E + B + D$$

The area D is

$$D = \int_{\rho_{dc}}^{\rho_{d1}} Q \Psi'_d d\rho_d = Q \Psi_{d1}$$

= volume of displacing fluid which has flowed out of the volume V_F .

The area E plus C must equal the volume of injected fluid less the volume of displacing fluid which has flowed out of the volume V_F or $Q - D$.

Therefore area B must equal area C . The condition that area C equal area B is

$$\begin{aligned} E + B &= Q - D = E + C \\ &= V_F(\rho_{dF} - \rho_{d1}) + \int_{\rho_{dF}}^{\rho_{da}} Q \Psi'_d d\rho_d \\ &= Q \Psi_{dF}(\rho_{dF} - \rho_{d1}) + Q(1 - \Psi_{dF}) \end{aligned}$$

from which

$$\rho_{dF} = \rho_{d1} + \frac{\Psi_{dF} - \Psi_{d1}}{\Psi'_{dF}}$$

APPENDIX C — BREAKTHROUGH SATURATION — RESERVOIR ABOVE SATURATION PRESSURE

Referring to Fig. 1, area D is zero for this case and area E plus C must equal the volume of gas which has been injected less the volume of gas which has gone into solution. Therefore, area B must equal area C plus the volume of gas which has gone into solution.

The volume of gas which has gone into solution may be determined by considering the quantity of oil left behind the front. The volume of oil left behind the front is

$$V_F \rho_{om} = \Psi'_{gF} Q(1 - \rho_w - \rho_{gm})$$

where ρ_{om} is the mean oil saturation behind the front and ρ_{gm} is the mean free gas saturation behind the front. Now,

$$\rho_{gm} = \rho_{gF} + \frac{1}{V_F} \int_{\rho_{dF}}^{\rho_{da}} Q \Psi'_{gF} d\rho_g = \rho_{gF} - \frac{1 - \Psi_{gF}}{\Psi'_{gF}}$$

Then, the volume of oil left behind the front is

$$\Psi'_{gF} Q \left(1 - \rho_w - \rho_{gF} - \frac{1 - \Psi_{gF}}{\Psi'_{gF}} \right)$$

The amount of gas originally in solution in this volume of oil is $\Psi'_{gF} Q \rho_{om} \frac{S_1}{\beta}$ SCF. The amount of gas in solution in this

volume of oil after it is saturated is $\Psi'_{gF} Q \rho_{om} \frac{S}{\beta}$ SCF. The

volume of gas which has gone into solution in this volume of oil is the difference of these divided by the gas conversion

factor: $\Psi'_{gF} Q \rho_{om} \frac{S - S_1}{\gamma \beta}$ rvb.

Then area B must equal area C plus the factor

$$\Psi'_{gF} Q \left(1 - \rho_w - \rho_{gF} - \frac{1 - \Psi_{gF}}{\Psi'_{gF}} \right) \frac{S - S_1}{\gamma \beta}$$

or,

$$Q \Psi'_{gF} \rho_{gF} + Q(1 - \Psi_{gF}) + Q \Psi'_{gF} \left(1 - \rho_w - \rho_{gF} - \frac{1 - \Psi_{gF}}{\Psi'_{gF}} \right) \frac{S - S_1}{\gamma \beta}$$

= Q

from which

$$\rho_{gF} = \frac{\Psi_{gF} + \frac{S - S_1}{\gamma \beta - S + S_1}}{\Psi'_{gF}} - (1 - \rho_w) \frac{S - S_1}{\gamma \beta - S + S_1}$$

APPENDIX D — BREAKTHROUGH SATURATION — PRODUCTION BEHIND THE FRONT

The solution as given by Equation (7) for the saturation distribution in the second zone is equivalent to the solution for a one-zone reservoir in which both gas or water and oil are injected so that the saturation of the displacing phase at the injection point varies from ρ_{dF} to ρ_{da} in a known manner with time. That is, Equation (7) may be written as

$$V - V_1 = \Psi'_d [P(Q) - \phi_d(\rho_d)]$$

where

$$P(Q) = \int_{Q_b}^Q (1 - q_1) dQ$$

= total volume of both gas or water and oil which has entered the zone since breakthrough

$$\text{and } \phi_d(\rho_d) = \int_{Q_b}^{Q_1} (1 - q_1) dQ.$$

ϕ_d is a function of ρ_d such that it describes the variation of the saturation at the boundary of the two zones with quantity injected when V equals V_1 .

The area enclosed by the curve and the line $V = V_1$ in Fig. 2 is

$$\begin{aligned} \text{Area} &= \int_{\rho_{dc}}^{\rho_{dF}} \Psi_d' P d\rho_d + \int_{\rho_{dF}}^{\rho_{d1}} \Psi_d' (P - \phi_d) d\rho_d \\ &= \Psi_d P \Big]_{\rho_{dc}}^{\rho_{dF}} + \Psi_d (P - \phi_d) \Big]_{\rho_{dF}}^{\rho_{d1}} + \int_{\rho_{dF}}^{\rho_{d1}} \Psi_d \frac{d\phi_d}{d\rho_d} d\rho_d \\ &= \int_{Q_b}^Q \Psi_d \frac{dP}{dQ} dQ \\ &= \int_{Q_b}^Q \Psi_d (\rho_{d1}) (1 - q_1) dQ \\ &= \text{total volume of the displacing phase which has entered the zone.} \end{aligned}$$

Since the area enclosed by the curve is equal to the total volume of the displacing phase which has entered the zone and since the dotted portion of the curve is a multiple of the curve obtained for the first zone, the same relation must hold here for the areas identified as *B* and *C* in Fig. 1 and therefore the saturation at the front is the same in the second zone as in the first.

In a similar manner it may be shown that the saturation at the front does not change as the front progresses through the remaining zones.

APPENDIX E—RATIO OF FLOW RATES AHEAD OF AND BEHIND THE FRONT

Consider a small fixed section containing the front. The difference in the rates at which gas enters and leaves this section must be equal to the rate of accumulation of gas in the section; i.e.,

$$\gamma \Psi_{gF} q + \frac{S}{\beta} \Psi_{oF} q - \frac{S_1}{\beta_1} \Gamma q = \left[\gamma \rho_{gF} + \frac{S}{\beta} \rho_{oF} - \frac{S_1}{\beta_1} (1 - \rho_w) \right] \frac{fA}{5.61} \frac{dx_F}{dt}$$

$$\text{or } \left(\gamma - \frac{S}{\beta} \right) \Psi_{gF} + \left(\frac{S}{\beta} - \Gamma \frac{S_1}{\beta_1} \right) =$$

$$\left[\left(\gamma - \frac{S}{\beta} \right) \rho_{gF} + (1 - \rho_w) \left(\frac{S}{\beta} - \frac{S_1}{\beta_1} \right) \right] \Psi_{gF}'$$

This equation must lead to the same expression for ρ_{gF} as that given by Equation (5); a comparison shows that Γ must be equal to the expression given by Equation (6). ★ ★ ★

THE QUANTITATIVE ASPECTS OF ELECTRIC LOG INTERPRETATION

J. E. WALSTROM, STANDARD OIL CO. OF CALIFORNIA, SAN FRANCISCO, CALIF.

ABSTRACT

While intensive research continues to promote a more complete understanding of the potential and resistivity measurements that comprise the electric log, it is believed that consideration should also be given to translating these numerous and often widely separated findings into a coordinated and readable body of fundamental facts designed specifically for the petroleum engineer and geologist. Although provision is made through publication for a ready exchange of new theoretical concepts, it is also desirable to provide reviews and appraisals of the more established techniques and methods from the operating standpoint so that an economic and practical application may be realized concurrently with the theoretical progress. With these basic premises as a guide the author reviews the present state of electric log interpretation.

The paper is directed not so much to the logging or research specialist as to the petroleum engineer and geologist to whom the electric log is only one of the many tools which he employs. Frequently, these persons do not have the time to follow in detail the many specialized contributions that appear and, as a consequence, are not in a position to place these contributions in proper relation to each other, or to the art as a whole.

The paper reviews the basic steps in making quantitative determinations from the electric log of the amount of oil or gas present in subsurface formations and also discusses the degree of reliability of these determinations under various conditions. The paper also indicates the trend of future developments in electric logging systems and methods of interpretation.

INTRODUCTION

The electric log has been used about 20 years as a means for studying the formations penetrated by a well bore. The first half of this period is characterized by the development of suitable logging techniques and equipment. Although progress in this direction is continuing at a satisfactory rate, the last ten years are characterized more by an increasing interest in methods of electric log interpretation. During this period, a large number of fundamental papers have been published, expounding various logging techniques and particular phases

of the interpretation problem. Many of these papers represent important contributions, and a few are classic.

This paper is an effort to outline as concisely as possible and in simple terms the main course of progress in electric log interpretation. More specifically, it is the purpose of the paper to review the necessary elements and basic steps used in making quantitative determinations of water saturation from the electric log; and to point out the degree of reliability of these determinations under different conditions.

It is strongly advised that the operating staffs of the drilling and exploration departments of oil companies cooperate wholeheartedly with both the electric logging service companies and research organizations in the testing and development of new logging systems and interpretation methods. One purpose of the paper is, however, to indicate the degree of caution which must be exercised in placing confidence in new techniques and interpretation methods that have not been thoroughly tested in the field. It is entirely possible to be cooperative in trying new methods and yet reluctant to believe in the results until the methods are firmly established.

It is important to define the meaning of quantitative electric log interpretation. In the most general sense, an interpretation of the log has been made when the electrical characteristics of the formations, as portrayed on the log, have been translated into terms describing the formation geometry, rock type, or any other physical characteristics of the formations. The determination that the top of a sand is at a certain depth is an interpretation of the log. Structural determinations made by correlating electric logs from a given area are also interpretations of the logs. The term quantitative interpretation, however, will be used in this paper in the restricted sense to indicate the determination of the water saturation of a formation. This determination defines the fluid content of an oil and gas productive formation only if the porosity is known, and it assumes that the remainder of the pore space contains hydrocarbons. This assumption is believed to be true for most oil and gas productive formations. The quantitative electric log interpretation may be said to be a determination of the fluid content only to the extent which the water saturation, under the conditions given above, defines it.

THE BASIC STEPS

The fundamental steps in calculating water saturation from the electric log are:

1. Determination of the true resistivity of the formations from the apparent resistivities as recorded on the electric log.

¹References given at end of paper.
Manuscript received in the office of the Petroleum Branch Oct. 15, 1951. Paper presented at the Fall Meeting of the Petroleum Branch in Los Angeles, Calif., Oct. 25-26, 1951.

2. Determination of the water saturation of the formations from the true resistivities.

Having taken these steps, and having considered the results in conjunction with other available data, it then becomes possible to:

3. Predict the type and possibly the amount of fluid production from the formations, or;
4. Utilize the determination of water saturation in calculating reserves, planning remedial operations, or making a stratigraphic or structural analysis.

Steps 1 and 2 comprise the determination of water saturation; steps 3 and 4 comprise the practical application of this determination. Although the quantitative interpretation has several uses, some of which are outlined in step 4, this paper is more specifically concerned with steps 1 and 2 and with the practical application of the quantitative determination of water saturation as indicated in step 3. The results of step 3 are of considerable value when deciding what zones to include in the production when completing a development well and when evaluating the formations exposed in an exploratory well.

In all of the steps indicated above, information obtained by other logging and testing methods is almost invariably used to supplement the electric log information. This is particularly true of steps 3 and 4. This coordinated use of the several sampling, testing and logging methods, in order to obtain the most efficient evaluation of the production possibilities of formations, has been previously reviewed.¹ Therefore, "interpreting" the electric log usually implies using all of the information that is available.

The dynamic characteristics of a reservoir, as evidenced by its ability to produce fluid, are not well resolved by means of the electric log. Adequate formation pressure, for instance, is necessary for a reasonable production of fluid but is not evaluated by the electric log. Expressed simply; what is in a sand, and what will come out of it are often two different matters. The electric log pertains chiefly to the former.

DETAILS OF STEP 1 — TRUE RESISTIVITY

Determination of true resistivity from apparent resistivity, as noted above, is the first step in calculating water saturation from the electric log. There are three factors which cause the resistivity, as indicated on any of the resistivity curves, to differ from the true electrical resistivity of the formations. These factors are:

1. Hole effect: the effect of the presence of a conductive column of drilling fluid.
2. Invasion effect: the effect of the presence of an invaded zone of formation around the well bore. This zone, which may vary in extent from a few inches to several feet, is invaded with drilling fluid filtrate. Its electrical resistivity is ordinarily different from that of the uninvaded formation.
3. Bed thickness effect: the effect of the presence of neighboring strata. Since the electrical measuring system used has a finite length, and since the thicknesses of the subsurface strata may or may not be large in comparison to that length, the measurement that is made is often affected by more than one stratum. In this case, the apparent resistivity is characteristic not of one stratum but of several.

These three effects must generally be considered. Since they are interdependent they must be corrected for simultaneously. In many instances one or more of these perturbing effects may be of minor importance, in which case consideration need be given only the remaining factors. Part of the art of electric

log interpretation lies in knowing which of these effects are important for any given conditions. Thus:

1. Hole effect, in noninvaded formations, is not pronounced for the 10 and 20 ft three-electrode systems, provided the formation resistivity is not greater than about ten times the drilling fluid resistivity. This implies a conventional water base drilling fluid and hole size.
2. Invaded zone effect is not pronounced when the invaded zone resistivity is nearly equal to the true resistivity. It is also not important when the depth of invasion of the filtrate is very small.
3. Bed thickness effects decrease in importance as the thickness of the stratum increases beyond several times the length of the electrode system employed, and are usually of less importance in low resistivity media than in high resistivity media.

Hole Effect — The Effect of the Conductive Column of Drilling Fluid

When considering the effect of the mud column, it is necessary to know the diameter of the hole and the resistivity of the drilling fluid opposite the formation being studied. When dealing with fairly well consolidated sandstone formations, or other formations that do not cave, the diameter of the drill bit may be used as an approximation of the diameter of the hole. It is believed that the error introduced in this manner is usually not serious. If any doubt exists concerning the validity of this approximation, it may be removed by running a hole caliper device. The error introduced into the determination of true resistivity from the long spacing three-electrode curves, due to a ten per cent error in the diameter of the hole, will probably be small in comparison to errors introduced from other sources. The running of a caliper device is probably warranted in exploratory drilling, where the nature of the formations is unknown, and where the caliper curve may assist in other ways than that mentioned above.

The resistivity of the drilling fluid opposite the formation is obtained from the resistivity of a drilling fluid sample as measured at the surface, and the bottom hole temperature as recorded by a maximum reading thermometer when running the electric log survey. If the formation lies some distance above the bottom of the hole, it is desirable to calculate a reduced temperature, subtracting the appropriate amount from the bottom hole temperature. Charts are provided that readily convert the drilling fluid resistivity from the surface temperature to the temperature opposite the formation.

Invasion Effect — Effect of the Invaded Zone

If the resistivity of the invaded zone differs considerably from that of the uninvaded formation, there will usually be a corresponding difference between the apparent resistivity as recorded by a very short spacing system, and that recorded by a long spacing system which reflects more nearly the true resistivity of the uninvaded formation. This is important from the standpoint that invasion implies permeability and shows at least one reason why it is desirable to record more than one resistivity curve.

The parameters that describe the invaded zone cannot be determined accurately. The extent of invasion, for instance, depends upon:

1. The density and type of the drilling fluid,
2. The rate of drilling,
3. The duration of the exposure of the formations to the drilling fluid,
4. The permeability and porosity of the formations.

Although the nature of the invaded zone has been studied² much remains to be learned. The mixing of the drilling fluid

filtrate and formation water and the displacement of oil in the invaded zone must be taken into account. Attempts have been made to utilize quantitatively invaded zone measurements,³ but these have not been established on a firm basis and cannot be depended on in the general case. This does not condemn the use of such special methods under those particular conditions in which they are known to give fairly good results.

The short spacing two-electrode curve (usually 10 in. or 16 in.) is ordinarily used to indicate the nature of the invaded zone, and consequently can be used to show the absence or presence of permeability. It can also be used to detect the presence of oil in the invaded zone. Furthermore, since its spacing is small, it is less affected by bed thickness effects and thus gives a more correct picture of the geometry of the sedimentation than the longer spacing systems.

The true resistivity of the uninvaded formation is best determined by employing a sufficiently long spacing to minimize the influence of the well bore and the invaded zone. This is possible under certain conditions and provided the formation is much thicker than the electrode spacing employed. This will be discussed more fully in a following section.

Bed Thickness Effect — Effect of Neighboring Strata

The influence of neighboring strata is a very complicated effect, since their thicknesses and resistivities all enter into the problem. In fact, even the simplest case; that of a single sand of finite thickness lying in an infinite shale and penetrated by a well bore of uniform diameter and resistivity, has not lent itself to accurate calculation by analytical methods. Approximate methods of calculation and model experiments have nevertheless resulted in demonstrating bed thickness effects for this simple case for two-electrode systems.⁴ Unfortunately, the relationships that have been published up to the present time do not apply to the long spacing three-electrode systems that are commonly employed.

If the length of an electrode system is small in comparison to the thickness of a formation, the apparent resistivity recorded opposite that formation will be determined by the true formation resistivity, the invaded zone effect, and the hole effect. If, however, the thickness of the formation is less than two or three times the length of the spacing, neighboring formations affect the reading of apparent resistivity.

Bed thickness effects probably introduce the most serious error in the calculation of true resistivity. This is particularly true for beds less than 30 or 40 ft in thickness. Much progress will probably be made in the next few years toward improving our knowledge of bed thickness effects and designing electric logging systems that are less susceptible to these effects. The latter has to some extent already been accomplished by developing systems of electric logging that tend to confine the current distribution to a horizontal segment of formation.^{5,6}

As far as bed thickness effects are concerned, it is desirable to use an electrode spacing small in comparison to the thickness of the average stratum. From the standpoint of determining true resistivity, however, it is desirable to use a long electrode spacing so that the region of the investigation is composed primarily of uninvaded formation. These two requirements are opposed to each other and may be said to be the dilemma of electric logging systems. This condition of diametrically opposed requirements again demonstrates the desirability of recording more than one apparent resistivity curve. The small spacing curve provides a means for studying the hole and invasion effects and the long spacing curves are primarily used for determining the true resistivity. If the bed is sufficiently thick, it is desirable to use the longest spacing for the true resistivity determination and the inter-

mediate length spacing as a check. In beds of somewhat restricted thickness, one must frequently depend upon the intermediate spacing curve for the true resistivity determination. The two long spacing curves thus supplement each other in their findings.

In thin beds, of much less than 30 or 40 ft in thickness, it is at present often impossible to determine the true resistivity with a satisfactory degree of accuracy.

The Departure Curves

Departure curves permit the determination of true resistivity for various values of electrode spacing, apparent resistivity, invaded zone resistivity, drilling fluid resistivity, bed thickness, and hole diameter. Separate curves are provided for various values of the diameter of the zone of invasion. Departure curves for infinitely thick beds are available for both two-electrode and three-electrode systems. Unfortunately, curves that apply to a finite thickness of stratum are for the most part available only for two-electrode systems. This is a particular disadvantage in California where both of the long spacing electrode systems are of the three-electrode type. When using the departure curves referred to above, it is particularly important to read the limitations that are imposed on their application, as outlined at the beginning of the publication.

One factor that limits the successful application of departure curves is the difficulty of being able to choose proper values for the effective diameter of the invaded zone and its effective resistivity. The properties of the invaded zone are not uniform throughout its cross-section and therefore effective values must be chosen which most accurately represent the true conditions. Another limitation, and one of a more general nature, results as a consequence of the large number of parameters describing the problem, some of which are not known accurately. Consequently, the application of departure curves to the determination of true resistivity sometimes causes a feeling of doubt concerning the accuracy of the results. This is particularly true if one must determine resistivity from three-electrode curves since, in this case, there are only those curves for infinitely thick beds.

In order to gain a good understanding of the relative magnitude of invasion and bed thickness effects, it is suggested that the engineer or geologist study carefully the departure curves. He may, for instance, by choosing several values for the diameter of the invaded zone, determine the effect of various amounts of invasion on the electric log. By solving many examples of this sort it is possible to learn much about the effect on apparent resistivity due to the presence of the mud column, invaded zone, and neighboring strata. Knowledge gained in this manner is of value in determining when these effects are of a serious nature, and when they may be safely neglected.

A person well acquainted with the fundamental behavior of electric logging systems might, in a particular case, decide to formation test knowing that an electric log interpretation would in any case be unreliable. This fact alone can be of considerable economic significance. It is not only important to know what the electric log can do, but is equally important to know its limitations. Disregard of these limitations may be as serious, if not more so, than an ignorance concerning the basic fundamentals.

DETAILS OF STEP 2 — DETERMINING WATER SATURATION

Once the value of true formation resistivity has been determined as closely as possible, it is used in obtaining the water saturation.

The relationship between the electrical resistivity and water saturation of rocks has been studied extensively. Electrical conduction in rocks is electrolytic in nature and takes place in the water channels. The resistivity of a clean sand, free of argillaceous material, is determined by the amount of interstitial water per unit volume of sand, the electrical resistivity of the interstitial water, and the manner of distribution of the water channels in the sand. It has been shown⁷ that the resistivity of such a sand saturated 100 per cent with a brine solution is proportional to the resistivity of the brine solution and may be expressed by:

$$R_o = FR_w \quad (1)$$

where R_o represents the electrical resistivity of the brine saturated sand, R_w represents the resistivity of the brine solution, and F is a formation resistivity factor; or, more briefly, formation factor. The relationship has been verified over a considerable range of porosities and salinities.

As would be expected from the above considerations, the formation factor depends upon the porosity of the sand and the manner in which the void space is distributed throughout the sand. The formation factor is a unique parameter which assists in describing the physical nature of the sand. It is dimensionless and may, for a clay free sand, be defined as the ratio of the resistivity of the fully saturated sand to the resistivity of the brine solution filling its pores. It is by taking the ratio of these resistivities, as determined experimentally in the laboratory, that the formation factor of such a sand is determined.

By displacing various amounts of the water in the interstices of a fully wet clay-free sand with a nonconducting fluid such as oil, it has been demonstrated⁷ that the true resistivity and water saturation may be empirically related by the following equation:

$$R_t = R_o S^n \quad (2)$$

where S represents the water saturation, and n is called the saturation exponent. A value of 1.9 or 2.0 is often chosen for this exponent.⁸ If a value of 2.0 is used, the water saturation becomes equal to the square root of the ratio of the resistivity of the 100 per cent wet sand to the true resistivity of the sand. This may be expressed as follows:

$$S = (R_o/R_t)^{1/2} \quad (3)$$

This relationship has two important applications:

1. If the true resistivity of a particular sand can be determined from an electric log, and if the resistivity of this sand when it is 100 per cent wet can be determined from another log in the area, the water saturation of the sand shown on the first log may be calculated by taking the square root of the ratio indicated above. This method is subject to the following assumptions which are not always justified:
 - (a) It is assumed that the physical characteristics of the sand and its interstitial water are the same at the two locations;
 - (b) It is assumed that the exponent 2.0 applies and that the sand is free of argillaceous material.
2. If the resistivity in the top portion of a very thick sand is high, and the resistivity in the bottom portion is low, the water saturation in the top portion may be obtained by taking the square root of the ratio of these two resistivities. This method is subject to the following assumptions which are not always justified:
 - (a) It is assumed that the true resistivities may be determined from the electric log.
 - (b) It is assumed that the resistivity in the bottom portion of the sand represents the resistivity at 100 per cent water saturation.

- (c) It is assumed that the physical characteristics of the sand and its interstitial water are the same in the upper and lower portions of the sand.
- (d) It is assumed that the exponent 2.0 applies and that the sand is free of argillaceous material.

In making decisions on a basis of electric log calculations it is important to know the assumptions that have been made and be prepared to judge their probable degree of applicability. The assumption 1(a) and 2(c), noted above, imply that the physical characteristics of the sand are the same at two different positions. From Equation (1), it is apparent that this condition will be fulfilled to the extent necessary for these calculations, if the formation factor is the same at the two positions. This in turn will ordinarily be true if the porosity of the sand is the same at the two positions, since formation factor is primarily a function of porosity.

The resistivity of the 100 per cent water saturated clean sand, R_o , is by Equation (1) equal to the product FR_w . Substituting this value for R_o in Equations (2) and (3) they become:

$$R_t = FR_w S^n \quad (2a)$$

$$S = (FR_w/R_t)^{1/2} \quad (3a)$$

Equation (3a) is applicable in those instances in which both F and R_w are known and in which R_o may or may not be directly obtainable from the electric log.

The value of F may be determined from laboratory measurements on cores obtained in the sand under consideration. The value of the interstitial water resistivity may be determined from water obtained in a drill stem test provided the amount of water recovered is sufficient to be representative of the uncontaminated formation water. Representative interstitial water samples may also be obtained from wells that are producing exclusively from one zone and which yield some water.

Equation (2a) is fundamental and indicates that a high value of true resistivity may be due to three basic causes:

- (1) High F factor — (low porosity - "tight" formations)
- (2) High value of R_w — (fresh water)
- (3) Low value of S — (presence of oil or gas)

It is very important to understand this thoroughly and to be aware of these three factors when evaluating highly resistive intervals on the electric log.

Equation (2), expressing the resistivity of a clay-free sand in terms of its 100 per cent water saturated resistivity and the water saturation, demonstrates a convenient rule of thumb. A productive oil sand that produces little or no interstitial water usually has a water saturation of less than 50 per cent. Equation (2), with $n = 2$, indicates that such a sand has a resistivity of more than four times its resistivity when 100 per cent water saturated. The rule of thumb is consequently that an oil sand usually has four times or more the resistivity of the same sand fully saturated with the same interstitial water. A 25 per cent water saturation would of course result in 16 times the resistivity. It is important to emphasize that the above rule of thumb applies to sands that are free of clay and for which the saturation exponent value of two applies.

The preceding discussion concerning the relationship between water saturation and resistivity indicates the great necessity of obtaining as much data as possible on the nature of the interstitial water and the value of the formation factor of individual sands in oil productive horizons. A knowledge of the values of R_w and F is of great importance to electric log interpretation.

The Exponent n in the Resistivity-Water Saturation Equation

No relationship has yet been found between the water saturation exponent n and porosity or permeability. Equation

(2) is empirical and, as previously stated, it has been found that a value of 1.9 or 2 for n will often give a good relationship between water saturation and resistivity. There are, however, a few observers who have found that the value of n may differ appreciably from the value of two.⁹ There is even some evidence that a value as high as 4.3 may apply.¹⁰

The following demonstrates the error that may be introduced into a calculation of the water saturation due to an incorrect value of n :

Saturation Exponent	Water Saturation
n	S
1.5	22%
2.0	32%
2.5	40%
3.0	46%

For: $R_o = 2.0$ ohm-m
and, $R_t = 20.0$ ohm-m

The rather discouraging aspects of obtaining an answer that may vary to the extent indicated in the above tabulation is at once apparent and makes it desirable to consider what exactly should be expected of the electric log. For instance, if it could be determined with a reliable degree of accuracy that a particular 100-ft sand body, as revealed on the electric log of an exploratory well, had a water saturation of between 20 and 50 per cent, it would readily be admitted that the electric log had performed a useful function. The sand would obviously be formation tested and, if necessary, casing would be set to make the evaluation. This again shows that a properly coordinated use of all of the testing and logging methods is necessary. The electric log is often used in exploratory drilling as a means either to justify, or not justify, the cost of further and more diagnostic testing.

It is important to point out that in development drilling there is little excuse for discrepancies such as indicated above. Cores taken in the producing horizon may be analyzed and values of the water saturation exponent determined. Furthermore, resistivity values as obtained from electric logs may be compared with capillary pressure water saturation data obtained in the laboratory.

One of the problems that remains to be solved is the nature of the dependency of the water saturation exponent n on the physical characteristics of the sand. It is even possible that the empirical relationships between resistivity and water saturation that have been established may not be in the best possible form. An analytical, rather than an empirical, development of a relationship between resistivity and water saturation is highly desirable but has not been obtained. Investigation in this direction offers a fertile field for the theoretically inclined researcher.

The Effect of Clay in Sands

It has been demonstrated experimentally that sand which contains an appreciable quantity of clay shows a different electrical behavior than the same sand when free of such material and that the total conductivity of a clayey sand is comprised of the conductivity due to the interstitial water together with the conductivity due to the presence of wetted clay.¹¹ It is further demonstrated that the definition of formation factor previously given is valid only for sands that are relatively free of clay. For the general case, in which a sand may or may not contain such conductive material, it is necessary to define the formation factor as the ratio of the resistivity that a sand would have when fully saturated with a brine solution to the resistivity of the brine solution were none of

the solid material conductive. The conductivity of a sand saturated 100 per cent with a brine solution may thus be written:

$$C_o = C_c + C_w$$

where C_o = total conductivity of the 100 per cent saturated sand

C_c = conductivity due to the wetted clay

C_w = conductivity due to interstitial water not associated with clay

In terms of resistivity, which is the reciprocal of conductivity, this becomes:

$$1/R_o = 1/R_c + 1/FR_w \quad \dots \quad (4)$$

It is apparent that if the wetted clay is assumed to be non-conductive (i.e.: R_c infinite) this relationship reduces to Equation (1) which is applicable to clean sands that are free of argillaceous material.

The recognition of the new term R_c complicates to some extent the laboratory measurement of formation factor since two unknown quantities must be found rather than one. It is possible, however, by saturating a core sample with a very concentrated brine solution, to make the conductivity due to the interstitial water considerably larger than the conductivity due to the presence of clay. In such an instance, the first term on the right-hand side of Equation (4) becomes insignificant with respect to the second term. The formation factor can then be obtained simply by dividing R_o by R_w .

Much remains to be learned concerning the effect of clay on the electrical behavior of fully and partially water saturated sands. The following points are offered as a practical guide to assist in understanding these effects until more quantitative information is available:

1. The electrical resistivity of an oil sand is considerably reduced when argillaceous material is present.
2. The rule of thumb, previously referred to, and which states that the resistivity of an oil sand is four or more times greater than the resistivity of the same sand when fully wet, must be modified when considering clayey sands. Clayey sands may show an increase of only two or three times the resistivity of the fully wet sand.
3. A decreased value of self-potential on the electric log opposite a sand may be due to the presence of clay. Although the presence of clay may sometimes be detected in this manner, it is only a qualitative indication since reduced self potential may also indicate a change in the formation interstitial water salinity.
4. A decreased value of the apparent resistivity as indicated by the short spacing two-electrode curve opposite a salt water sand will sometimes be indicative of the presence of such a sand.
5. The calculation of the water saturation may suffer an appreciable error unless it is known that the sand does not contain clay, or unless a satisfactory method is employed to correct for the presence of the clay.
6. A rather "poor looking" sand on the electric log should not be overlooked on the premise that it is wet due to its low resistivity. It may be a productive oil or gas sand that contains an appreciable quantity of clay. All possible clues which might reveal the presence of clay should be noted.
7. Although the relative occurrence of clay in oil producing sands is not known with any degree of accuracy, it appears that this effect must be taken into account in a considerable number of instances.

Interstitial Water Saturation of Oil Sands

It may be demonstrated experimentally that as oil is gradually caused to replace the interstitial water from a sand originally 100 per cent water saturated, the water saturation will gradually diminish until it reaches a low value beyond which

it is not significantly reduced, even though the pressure on the displacing fluid is increased considerably. Comparison of these minimum water saturation values with water saturations determined from cores taken in oil base fluid, indicates that a somewhat similar displacing mechanism has probably been effective in the accumulation of oil in subsurface formations. When a reservoir with such a minimum water saturation is produced, little or no water will flow since the easily removable water has previously been displaced.

The water that remains in an oil sand, and is so strongly attached to it, adheres to the surface of the grains and in the small interstices by capillary attraction. The amount of water retained in an oil sand depends to a large extent upon the permeability of the sand. A high permeability sand retains much less water than a low permeability sand. The water retained in commercially productive oil sands will vary from approximately 10 to about 60 per cent.

The dependency of the amount of retained water on the permeability of the sand may be qualitatively understood when it is considered that the specific surface ordinarily increases with decreasing average particle size. Since the latter implies decreasing permeability, it becomes apparent that more water will be retained on the increased surface of low permeability sands.

The conclusion to be reached from the above considerations is that high permeability oil sands will show higher electrical resistivity than low permeability oil sands because the high permeability sand will contain less water and more oil. For a given porosity the higher permeability will result in greater reserves, due to the lower water saturation. In this way it becomes apparent how electric logs are useful in estimating reserves.

That permeability is very important in determining the resistivity of an oil sand, becomes clear when one considers that the resistivity of a clay-free sand is inversely proportional to a power of the water saturation. High permeability oil sands are consequently more easily detected on the electric log than low permeability oil sands since they have considerably greater resistivities, other factors remaining the same.

The resistivity of 100 per cent water saturated sands, commonly called "wet" sands, does not depend to any great extent on permeability because the resistivity of such a sand is given by the product $\bar{F}R_w$ in which F is primarily a function of porosity and is to a much lesser degree influenced by the permeability. Since the porosity of a sand varies less than the permeability, water sands will usually give a flatter appearing resistivity curve than oil sands.

The quantitative determination of permeability from electric log data has been considered¹² and it is indicated that it may be possible to estimate a lower limit to the average formation permeability from the connate water saturation and formation factor as computed from the electric log data. In development drilling, however, formation factor is determined from cores taken in the producing sand in which case permeability can also be directly measured. Consequently, there is little need for attempting to determine permeability from the electric log when cores must be used to make this interpretation. If no other information is available except an electric log, such as is sometimes the case in exploratory drilling, it is not believed that the formation factor can be determined from the log with sufficient accuracy to warrant its further use in attempting to calculate a minimum permeability.

THE POTENTIAL CURVE OF THE ELECTRIC LOG

The potential curve or SP curve, as it is often called, has universally been used to distinguish sand from shale. In the

light of newer concepts, it is more correct to say that it distinguishes shale from nonshale formations. The idea that SP was primarily an indicator of permeability grew in popularity as a consequence of the fact that many geologic sections are composed almost solely of sands and shales. In such a geologic section the nonshale formations are all sands and all relatively permeable; hence, the potential curve indirectly became correlatable with permeability. The older premises still find general application and are of considerable value provided it is understood that exceptions to such reasoning may frequently occur.

It has been established that electric currents exist in the mud column in the vicinity of sand-shale contacts. The potentials produced in the drilling fluid by these spontaneous currents may be measured by suitable devices. The potential variations recorded in this manner comprise the potential curve of the electric log. Such a curve shows that at a sand-shale contact the drilling fluid opposite the sand is negative with respect to the drilling fluid opposite the shale. It is thus deduced that in the vicinity of the sand-shale contact electric current flows in the mud column from the shale towards the sand. The total current flowing in the mud column at the sand-shale contact is often of the order of a few thousandths of one ampere.

Consider a sand lying between two very thick shales. The electric current in the mud column, at the top of the sand, is in a downward direction. At the bottom of the sand the current is also in shale-to-sand direction so is upward in direction. Thus as the logging electrode enters the sand from the top, it attains a negative potential at the boundary due to the drop in electric potential encountered there. Nothing alters this situation until the electrode leaves the sand at the lower boundary where it encounters an oppositely directed electric potential drop in the drilling fluid. Since the conditions there are equal but reversed, the potential curve returns to its shale line on the log. Since only changes of potential are indicated on the curve, there is no zero line for this recording. The shale line is usually conveniently situated a short distance from the edge of the recording tract.

It was indicated at an early date¹³ that the potential difference measured in the drilling fluid, when moving the measuring electrode across a sand-shale boundary, is to a great extent a result of the contrast in the ion content of the formation water and the drilling fluid. Opposite shallow fresh water horizons, where little difference exists between the drilling fluid resistivity and the formation water resistivity, a very flat curve is obtained. This verifies the hypothesis that differences in the electrical characteristics of the formation water and drilling fluid have a great deal to do with establishing the spontaneous potentials observed in a well bore.

Much research has recently been devoted to obtaining a more exact explanation of the nature and origin of the electromotive forces that are responsible for the potential phenomenon.^{14,15} Considerable effort has also been expended in establishing sound principles of interpretation of the potential curve of the electric log.¹⁶ It is believed that the results of these studies have increased considerably the ability of the engineer or geologist to use the potential curve of the electric log to better advantage. Although both porosity and permeability are indirectly involved in the potential phenomenon, it is realized that the relationship is not simple and involves many other factors.

The presence of appreciable quantities of shale or clay in sands causes a reduction in the magnitude of the potential curve. Silty sands thus have a smaller SP development than clean silt-free sands. This behavior has recently been discussed in some detail.¹⁷ It was indicated above that the potential

curve may qualitatively be considered to differentiate between shale formations and non-shale formations. The reduced development opposite clayey sands and sandy shales conforms to this concept since a shaley sand is less in contrast to a shale than a clean shale-free sand. Since shaley sands are generally less permeable than clean shale-free sands, it is once again apparent why a relationship between permeability and potential was both natural and easy to imply.

If a thick sand is oil or gas bearing in its top portion and fully water saturated in its bottom portion, it will often be noticed that the SP curve is slightly less developed opposite the upper part of the sand than opposite the lower portion. This reduced value of potential opposite part of a sand is frequently used to assist in establishing the possible presence of hydrocarbons in a formation. This effect is noticed primarily in formations containing quite saline interstitial water, and is believed to occur chiefly in formations that contain an appreciable amount of shaley material.¹⁷ The presence of such a reduction of SP, however, does not furnish proof that a sand is hydrocarbon bearing.

It was stated above that electric currents have been detected in the drilling fluid in the immediate vicinity of sand-shale boundaries, and that these currents usually flow in a direction toward the sand. Consider a shale overlying a sand. Upon entering the portion of the mud column opposite the sand, the electric current diverges outward and flows into the sand; then upward and across the sand-shale interface into the body of the shale. It then flows toward the mud column and enters it above the sand-shale contact to begin again its downward descent in the mud column toward the sand. The electric currents thus form a circulating vortex type of distribution in the neighborhood of the shale-sand contact. The path of current flow thus includes as constituent parts (1) drilling fluid, (2) filter cake on sand face, (3) water in the invaded zone, (4) formation water in the sand, (5) shale, and (6) drilling fluid. The SP current distribution is shown in Fig. 1.

In order for electric current to flow in the ground, as described above, it is necessary that electromotive forces exist at one or more points along the path. This is analogous to the statement that the flow of fluid in a porous medium is a

result of forces that act to produce a pressure differential in the medium.

There is good reason to believe that three sources of electromotive force exist in the system under consideration. They are:

- (1) The liquid boundary potential
- (2) The shale potential
- (3) The streaming potential

These three sources of potential give rise to the electric currents that are detected in the mud column and formations in the vicinity of sand-shale contacts. The nature of these potential sources will now be discussed.

Liquid Boundary Potential

Theory has established that an electromotive force exists at the contact of two solutions differing in their electrochemical characteristics. Such a contact exists between the drilling fluid filtrate in the invaded zone and the interstitial formation water. Since this contact is represented by phases (3) - (4) of the current circuit described above, it is logical to assume that this electromotive force will contribute in establishing current flow. The potential so established is called the liquid boundary potential and is, with certain provisions, proportional to the logarithm of the ratio of the electrical resistivities of the two solutions.¹⁴

Shale Potential

It has been demonstrated experimentally that if a piece of solid shale be interposed between two solutions differing in their electrochemical properties, the potential difference between the two solutions is often greater in magnitude than the liquid boundary potential that would occur between the two solutions in the absence of the shale barrier. Such a series of phases occurs in the current path considered above and is represented by the elements (4), (5), (6), i.e., formation interstitial water, shale and drilling fluid. The potential that is established in this manner may, for simplicity, be called the shale potential. It is presently believed that the shale potential is ordinarily responsible for a large portion of the total SP effect. Like the liquid boundary potential, the shale potential has been shown, with certain provisions, to be proportional to the logarithm of the ratio of the electrical resistivities of the two solutions that are in contact with the shale.¹⁴

Streaming Potential

If drilling fluid filtrate, or other similar electrochemical solution, is caused to flow under pressure through a semipermeable membrane, such as a drilling fluid filter cake, an electric potential difference becomes established across the membrane. In this case only a single solution is involved in contrast to the liquid boundary and shale potentials in which two solutions are involved; the other being the formation interstitial water. The potential developed in this manner may be called streaming potential since it is produced by the streaming of a fluid through a semipermeable membrane. Since a considerable pressure differential normally exists across the filter cake opposite a sand, a significant streaming potential will be developed in this manner in the well bore. Since the filter cake constitutes phase (2) of the current circuit previously discussed, the streaming potential contributes to the total SP effect. A quantitative laboratory study of streaming potential phenomena has recently been made, with the result that an empirical relationship has been derived for this effect.¹⁶

Quantitative Use of the Potential Curve

It was indicated previously that in order to be able to make the best possible interpretation of the electric log, it is neces-

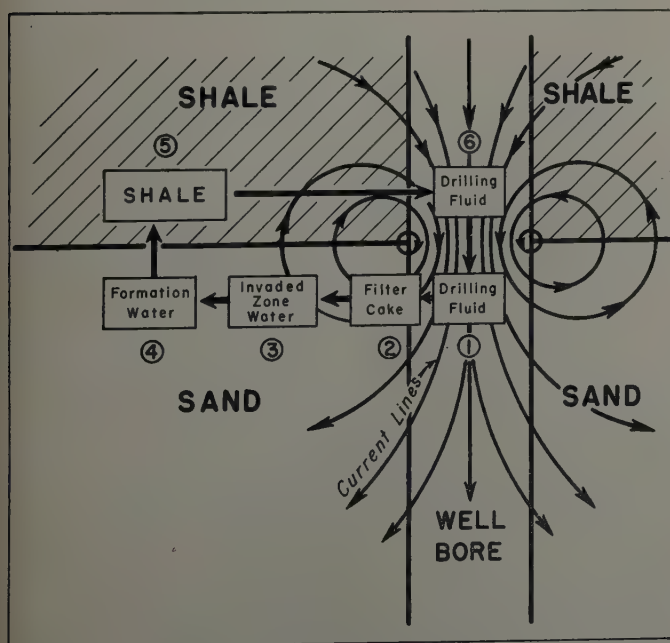


FIG. 1 — THE SP CURRENT DISTRIBUTION AT A SAND SHALE CONTACT.

sary to know the resistivity of the formation interstitial water. Much of the research concerned with well bore potentials has been initiated with the primary object of finding a way to determine this quantity from the potential curve. Although it is possible in some instances to determine the resistivity of the formation water, it is not believed advisable, at the present state of development, to place any marked degree of confidence in the preciseness of this determination in the general case. The accurate calculation of formation water resistivity from the potential curve depends upon the degree of validity of several assumptions. Some of these assumptions are:

1. It is assumed that the streaming potential can be made either inconsequential or can be determined so that its effect can be subtracted from the total SP, leaving that portion of the total potential from which the formation water resistivity is calculated.
2. Certain assumptions concerning the electrochemical nature of the drilling fluid and interstitial water must be made in order that the theoretically derived equations may apply.
3. It is assumed that the electric potential drops occurring in the formations are small in comparison to the ohmic potential drop occurring in the mud column. The total electromotive force of the SP phenomena is then closely determined by measurements made in the well bore.
4. It is assumed that the effect of clay in sands can be taken into account when determining formation water resistivity from the SP curve.
5. It is assumed that the sand is sufficiently thick to allow the SP curve to attain its maximum development.

It has been suggested that the resistivity of the drilling fluid be lowered, by the addition of salt, to approximately the value of resistivity of the interstitial water in the more interesting group of formations. It is claimed that this would minimize the value of streaming potential so that a more accurate determination of interstitial water resistivity could be obtained. There are, however, several undesirable features of such a practice. They are:

1. Highly conductive drilling fluid results in poor resistivity curves.
2. The addition of appreciable quantities of sodium chloride to the drilling fluid is in most instances undesirable.
3. A highly conductive drilling fluid column would result in a redistribution of the ohmic potential drops in the sand-shale-mud column system. Such a redistribution would be in a direction to increase the percentage of the total ohmic drop taking place in the formations.

There is little doubt that the precision of quantitative SP methods, for the determination of formation water resistivity, will increase with further development and research. A word of caution is advisable, however, against the tendency to develop a sense of security and confidence in the results of theoretical relationships that have not had a chance to prove themselves fully dependable in field application.

THE POSSIBILITY OF DETERMINING WATER SATURATION USING ONLY THE POTENTIAL AND RESISTIVITY CURVES

From what has preceded it is apparent that three factors are generally essential to making a determination of water saturation from the electric log. These factors are (1) Knowledge of the resistivity of the interstitial water, (2) knowledge of the formation factor, (3) Knowledge of the clay characteristics of the sand.

Factors (2) and (3) are ordinarily determined from cores, and factor (1) is determined by measuring the resistivity of a sample of formation water. Lacking these data the quanti-

tative interpretation of the log usually becomes qualitative in nature. It is, however, interesting to consider what can be done with only the electric log, and with no information concerning formation factor, water resistivity or clay characteristics.

There is little question concerning the desirability of determining water saturation from electric log data alone. A great advantage would be obtained, particularly in exploratory drilling, where interesting horizons that were not cored frequently show up on the electric log. For many years an avenue of approach to such a goal has been apparent. The reasoning involved is briefly:

1. Determine the formation water resistivity from the potential curve.
2. Determine the formation factor from a measurement of the invaded zone resistivity. (This will be discussed more fully.)
3. From (1) and (2) determine the resistivity of the fully wet sand (*i.e.*, $R_o = FR_w$).
4. Using this value of R_o in Equation (2), calculate the water saturation of the formation from the value of true resistivity as determined from the electric log.

Step (2) involves determining the resistivity of the drilling fluid filtrate and the resistivity of the invaded zone. If then, the invaded zone could be assumed to be 100 per cent saturated with drilling fluid filtrate, the formation factor would be given by the ratio of invaded zone resistivity to the drilling fluid filtrate resistivity. Unfortunately, there are several reasons why such a simple method cannot be used, at least at the present time, for the determination of formation factor. Some of these reasons are:

1. If the formation contains oil, the invaded zone will not be 100 per cent saturated with drilling fluid filtrate.
2. No accurate means is presently available for determining the resistivity of the invaded zone. There is, however, good reason to believe that such techniques may be developed.
3. If the formation is impermeable, there is no invaded zone. Proceeding on the basis that one exists would give an erroneous answer.
4. There is the possibility, in at least some instances, of the mixing of interstitial water and drilling fluid filtrate, by ionic diffusion or otherwise, to produce a fluid in the invaded zone different than drilling fluid filtrate.

Aside from these obstacles there are certain questions which arise concerning the overall method. Some of these questions are:

1. How accurately can the true resistivity be determined from the electric log?
2. How accurately can the interstitial water resistivity be calculated from the potential curve?
3. Can the effect of clay on the determination of true resistivity, formation water resistivity, and invaded zone resistivity be adequately taken into account?
4. How accurately can the interstitial water saturation be determined from Equation (2)? What is the value of the saturation exponent n ?

On a basis of the present state of knowledge of the petrophysical behavior of rocks and electric log interpretation in general, it may be said that the answers to these questions indicate that the calculation of water saturation from strictly electric log data alone is subject to so many assumptions that it is at best only a qualitative evaluation which, however, may still be of great value from the practical viewpoint.

The Electric Log and Exploratory Drilling

The determination of water saturation from strictly electric log data alone, as discussed above, becomes necessary when

little is known concerning the nature of the formation interstitial water, porosity, formation factor, and clay characteristics of the various horizons. This is frequently the case in exploratory drilling. Fortunately, however, in this case even a qualitative evaluation of water saturation is of considerable value. As mentioned previously, if it could be determined that a particular 100 ft thick sand, as revealed on the log of an exploratory well, had a water saturation of between 20 and 50 per cent, it would ordinarily be considered entirely economic to set casing if this were necessary to test the sand adequately.

In exploratory drilling we are hunting for new oil and gas fields. The stakes involved are so great that it is entirely undesirable and unwise to attempt to place all of our confidence in any one formation evaluation tool. It is only through a coordinated use of coring, testing, and logging methods that economic exploratory drilling may be achieved.¹ The purpose of the electric log in exploratory drilling is to single out those more promising appearing formations for further evaluation. In this respect it fulfills a tremendously important need. As the quantitative methods improve in accuracy, it will be possible to single out more efficiently those formations exposed in an exploratory well that are most likely to yield oil or gas.

Over the course of years as electric log interpretation methods become more quantitative and less qualitative, more confidence will be instilled in those who apply them. As this occurs, exploratory drilling will require less coring and testing. This process, however, is slow and it is important that overconfidence is not placed in new techniques until their degree of reliability has been established.

The Electric Log in Development Drilling

Once an oil producing horizon has been found, and the probable extent of production estimated, a program for the development of the field is designed. This program should include coring of the productive horizons in a selected number of strategically situated wells. If a particular horizon is a sand or sandstone, the following core analysis measurements should be made: (1) porosity; (2) permeability; (3) formation factor; (4) clay analysis; (5) capillary pressure water saturation (experimentally determined so that it approximates the saturation in a virgin oil or gas reservoir sand); (6) residual water saturation (saturation in a core as recovered from the well bore); and (7) residual oil saturation (saturation in a core as recovered from the well bore).

If any water is obtained during a drill stem test, or along with produced oil, it should be analyzed immediately for ion content and electrical resistivity. Such tests should be made in every instance possible, and the values of water resistivity catalogued for each of the producing horizons. Information concerning formation water characteristics is not only valuable in electric log interpretation but also in tracing the origin of waters produced from the well.

When a few wells have been cored and analyzed in the manner described above, the electric logs can then be used in a quantitative fashion in completing the remaining wells in the field. In this manner the full advantage of the quantitative technique may be obtained. In a sense, the core analysis and water data are used to calibrate the electric log readings.

Cores from the producing sand horizons may be sent to the laboratory and the relationship of resistivity and water saturation determined. This eliminates the errors that may otherwise be introduced by clay effects or improper choice of water saturation exponent.

It should be noted, however, that even in this optimum condition for the use of electric logs in a quantitative manner an evaluation of hole effect, invasion effect, and bed thickness effect must be made in order to obtain the true resistivity. This

implies that best accuracy will be obtained in thick beds in which invasion is not too deep.

Fractured Formations

Certain formations having a nongranular type of porosity have been found to be oil and gas productive. Typical of this class are fractured shales, cherts, limestones, and vuggy limestones. Combinations of vuggy, fractured and intercrystalline limestone may also occur.

Electric logs lose much of their diagnostic value in formations of this sort. When analyzing an electric log made in an exploratory well, the first question to be answered is: What type of formations are represented on this electric log? It is partly in order to answer this question that coring, sidewall sampling, and drilling fluid analysis are employed.

When the drill bit encounters a highly fractured formation in which the oil and gas exist only in the fractures, it is entirely possible to have very serious and deep invasion of the drilling fluid into the formation fissures. This has a tendency to drive the oil and gas back into the formations making them very difficult to detect by any means whatsoever. In this case, the fluorescence of the drill cuttings may be the only evidence of hydrocarbons that is obtained.

REVIEWING AN ELECTRIC LOG

When an electric log has been obtained, there is a strong tendency to examine the curves immediately and then proceed to make decisions concerning the fluid content of the various horizons depicted on the log. Although this may in some instances be excusable, a much better procedure is to consider in detail other factors related to the log before examining the curves. The more important of these factors are indicated by means of the following questions:

1. What is the resistivity of the drilling fluid and the diameter of the hole? A qualitative estimation should be made of the effect of the drilling fluid on the resistivity curves and on the SP curve.
2. What type of drilling fluid has been used in drilling and logging the hole? Some types of drilling fluid affect the SP curve adversely, and some types affect the resistivity curves adversely. This matter should be clarified before examining the curves. Low water loss fluids will often result in a smaller invaded region. This is frequently reflected in the reading of the small spacing resistivity curve.
3. What scales have been employed in recording the resistivity curves and the SP curve? The absolute value of the resistivity is related to porosity and water saturation. It is necessary to know the ohm-meters of resistivity in order to properly evaluate the formations. It is advisable to check that there are no scale changes between the end of the log and the portion being examined. The value of the SP deflection above the shale line is related to the type of formation water.
4. How did the depth measurements made by the logging service company check the depth measurements made by the drilling crew?

When these factors have been considered, a more effective examination of the curves will result.

When examining the electric log curves recorded opposite a particular horizon, it is necessary to consider the length of time that the formation has been exposed to the action of drilling fluid. It is also necessary to take into consideration all available data pertaining to the physical and chemical nature of the formation and its fluid content. Such additional data is furnished by drilling fluid analysis logging, sidewall samples, cores, or formation tests.

When comparing electric logs, it is necessary to compare the conditions under which the logs were made. This implies a comparison of the spacings employed, mud resistivities, scales, and types of drilling fluid. If an electric log is very old, it is necessary to consider the changes in the reservoir conditions that may have occurred due to subsequent depletion. In this regard it is interesting to note that since the high resistivity portions of an oil sand are often the most permeable, it is possible that these portions will yield water first as edge-water encroaches.

SUMMARY

1. In development drilling, a quantitative determination of the water saturation of sands and sandstones may be made from the electric log. This requires, however, that the formation factor and the formation water resistivity are known. A knowledge of the clay content and its effect on the electrical behavior of the sand is also necessary. The determination of water saturation becomes unreliable in thinly interbedded sand-shale sections. Coring of the productive sand in selected wells is desirable in order to determine formation factor and clay characteristics.
2. In exploratory drilling the electric log assists in singling out those formations that show evidence of containing oil or gas. These formations can then be evaluated by the more diagnostic formation testing methods. When examining exploratory well logs, great caution should be exercised in order not to miss any possibly productive horizons of a fractured nature. Under exploratory drilling conditions, the electric log interpretation often becomes quite qualitative in nature, but is still of considerable value in the overall formation evaluation program.
3. Past and present research and development have improved our ability to make a good electric log interpretation. It appears that further research in the field of petrophysics and further development of electric logging systems will increase the accuracy of the quantitative methods. It is probable that improved logging methods will make possible a more accurate determination of formation factor from invaded zone measurements. Further research may provide a more precise method of determining formation interstitial water resistivity from the potential curve. It is important that the results of research be adequately and thoroughly tested in the field before placing too much confidence in them.

ACKNOWLEDGMENT

The author expresses his appreciation to the management of Standard Oil Co. of California for permission to publish this paper.

REFERENCES

1. Walstrom, J. E.: "Optimum Use of Various Testing Methods in Exploratory Wells," *API Drill. and Prod. Prac.*, (1950) 79.
2. De Witte, L.: "Resistivity and Saturation Distribution in Invaded Zones of Porous Formations," *Oil and Gas Jour.*, (July 27, 1950) 49, 246.
3. Tixier, M. P.: "Electric Log Analysis in the Rocky Mountains," *Oil and Gas Jour.*, (1949) 48, 143.
4. "Resistivity Departure Curves," Schlumberger Document No. 3, (1949).
5. Keller, G. V.: "An Improved Electrode System for Use in Electric Logging," *Producers Monthly*, (Aug. 1949).
6. Doll, H. G.: "The Laterolog: A New Resistivity Logging Method with Electrodes Using an Automatic Focusing System," *Trans. AIME*, (1951) 192, 305.

7. Archie, G. E.: "The Electrical Resistivity Log as an Aid in Determining Some Reservoir Characteristics," *Trans. AIME*, (1942) 146, 54.
8. Archie, G. E.: "Introduction to Petrophysics of Reservoir Rocks," *AAPG Bull.*, (May 1950), 956.
9. Dunlap, H. F., Bilhartz, H. L., Shuler, E., and Bailey, C. R.: "The Relation Between Electrical Resistivity and Brine Saturation in Reservoir Rocks," *Trans. AIME*, (1949) 186, 259.
10. Guyod, H.: "Electric Logging Developments in the U.S.S.R.," *World Oil*, (Aug. 1948), 120.
11. Patnode, H. W., and Wyllie, M. R. J.: "The Presence of Conductive Solids in Reservoir Rocks as a Factor in Electric Log Interpretation," *Trans. AIME*, (1950) 189, 47.
12. Wyllie, M. R. J.: "Theoretical Considerations Involved in the Determination of Petroleum Reservoir Parameters from Electric Log Data," Third World Petroleum Congress, The Hague, Netherlands, May 28-June 6, 1951, Section II, Preprint 3.
13. Schlumberger, C. and M., and Leonardon, E. G.: "A New Contribution to Subsurface Studies by Means of Electrical Measurements in Drill Holes," *Trans. AIME*, (1934) 110, 273.
14. Wyllie, M. R. J.: "A Quantitative Analysis of the Electrochemical Component of the SP Curve," *Trans. AIME*, (1949) 186, 17.
15. Wyllie, M. R. J.: "An Investigation of the Electrokinetic Component of the Self Potential Curve," *Trans. AIME*, (1951) 192, 1.
16. Doll, H. G.: "The SP Log: Theoretical Analysis and Principles of Interpretation," *Trans. AIME*, (1949) 179, 146.
17. Doll, H. G.: "The SP Log in Shaley Sands," *Trans. AIME*, (1950) 189, 205.

DISCUSSION

By M. E. Loy, Schlumberger Well Surveying Corp., Los Angeles, Calif., Member AIME

The interpretation of well logs is a skill which can be developed only with practice. The established interpretative techniques discussed by the author, as well as the refinements now in the progress of development, are subject to the effects of several variable formation characteristics. Very often, assumptions must be made as to the exact degree of these effects on each individual case, and the computed results weighed in the light of the probable accuracy of the necessary assumptions. This process of assuming and weighing can be highly successful, but practice and experience are necessary. Quite often it will be found that even though assumptions have to be made, the conclusions will be quite definite.

The complex nature of the factors governing the relations between well logs and the petrophysical behavior of rocks suggests that this study is a full-time job. Many organizations are developing well logging specialists within their ranks. This is proving to be successful, but these specialists cannot be everywhere at once; consequently, they are valuable as consultants and final review authorities for the exploration geologists, development engineers, production engineers, reservoir engineers, etc. It still remains that every individual who can benefit by the use of well log information should be capable of analyzing these logs.

We urge you, then, to attempt to use all the interpretative methods and to determine for yourselves the range of reliability for the various methods under all conditions. This is necessary in order that you may develop, with practice, the experience needed to be best guided by a full use of the data available from well logs.

DISCUSSION

By C. C. Liedholm, *Signal Oil and Gas Co., Los Angeles, Calif., Member AIME*

The field engineer, or geologist, must be able to interpret the results of the many methods now available for evaluating the fluid content of a formation. Consequently, he cannot always devote the time and study required to keep abreast of the latest evaluation techniques for electric logs. Most development engineers have recognized the factors which influence the resistivity values recorded by the electric log and have by comparison evaluated zonal saturation in a purely qualitative manner. The quantitative methods introduced in the last few years for evaluating saturation may have sometimes been confusing, particularly when the answer conflicted with the engineer's intuitive determination. Walstrom's paper shows that there can be a meeting ground between the two outlooks — that a quantitative approach can be used to supplement the purely qualitative outlook. Conversely, the limitations on a quantitative determination due to uncertainty in some of the variables used can be examined to advantage by qualitative methods. Walstrom's careful use of approximate limiting values makes the transition from one approach to the other natural and reasonable.

Walstrom states that the electric log is primarily intended to determine the fluids in a formation and not what will come out of a formation. If we are concerned only with conventionally spaced resistivity curves, this is true in most cases. However, the use of short spacing resistivity measurements to detect the presence or absence of mud cake has proved to be of considerable value in determining the ability of a formation to conduct fluid. In areas with high resistivity pay, these short spaced curves make it easier to determine whether or not something will come out of the zone than to evaluate what is in the zone. In development drilling the approximate zone pressure is generally known, and in exploratory drilling pressure can be assumed to be near the original. Consequently, assuming that the zone is not filled with immovable tar, an approximation of a formation's ability to give up fluid can be made with presently available electrical logging equipment. I would like to ask Walstrom why the use of these short spaced curves were omitted from his paper.

DISCUSSION

By Loy M. Charter, *Shell Oil Co., Los Angeles, Calif.*

Electric log interpretation, either quantitative or qualitative, truly is a combination of an art and a science. As stressed by Walstrom, all petrophysical data obtainable must be utilized, not only to supplement the electric log interpretation, but in the actual interpretation of the electric log itself. Needless to say, the more supplemental data available, the better will be the interpretation, but there always is an economic optimum. We have found that adequate electric logs, including special devices such as MicroLogs, focusing system logs, etc., together with interval cores, sidewall samples, and possibly formation tests, and continuous ditch samples, cutting analyses if representative, drilling speeds, etc., usually are sufficient to allow quite reliable evaluations of the fluid saturations of most possible reservoir formations. The instances of formations that are not evaluable from such data usually are determinable, and additional means such as additional sidewall samples or testing can be resorted to if economically justified.

As pointed out by the author, the determination of precise formation resistivities often is difficult and sometimes impossible because of bore hole, invasion, and adjacent bed effects.

A quantitative approach even under the more difficult conditions usually will result, however, in at least a valid qualitative evaluation. As discussed by Walstrom, mud filtrate invasion and adjacent beds are the primary perturbing effects that make determinations of true resistivities often difficult and sometimes impossible. Their effects often can be minimized, however, by logging at frequent intervals. Their effects also can be evaluated by comparing overlapped portions of logs and rerunning questionable intervals. In very high resistivity intervals such as limestones where bore hole, invasion and adjacent bed effects have been a real bugaboo, our limited experience to date indicates that the newer focusing logging systems are a tremendous improvement over conventional logging systems under these conditions. It might be well to stress here that the conventional, self-potential and resistivities are only three forms of numerous systems now available, and it would be to the benefit of the industry to build up an experience as rapidly as possible with other applicable forms of electric logs, term them what you will.

We grant that formation factors are not always determinable from electric logs, but we have found that with a reasonable amount of supplemental data they can be determined rather reliably in most cases. If the various resistivity curves indicate different resistivities after correction for bore hole and adjacent bed, but not invasion effects, the resistivity of the invaded zone usually can be approximated if some supplemental data for calibration is available and adjacent bed effects are not too severe. We have found that the MicroLog often assists in making this approximation. From this invaded zone resistivity the formation factor usually can be approximated, by assuming if necessary a residual hydrocarbon saturation in the invaded zone. If, however, there is a possibility of very viscous oils, this technique breaks down since estimations of residual oil effects then are not reliable. In this case, though, ditch samples and/or sidewall samples should show the presence of the viscous oil.

It is pointed out that the determination of the fluid saturations is dependent on the values of the saturation exponent "n" which has been reported to vary appreciably. This is a problem that is perennial. In extensive laboratory work we have found that the value of the exponent "n" does vary from sample to sample, even within a sand body and with samples of comparable porosity and permeability. The average, though, when sufficient data are available, is very close to two, as reported by Archie in 1942. Since the responses of the electric log, particularly those of the longer spacings, are necessarily averages from appreciable formation volumes, it is the average value of "n" which appears rather constant, and not individual values, with which we should be concerned.

AUTHOR'S REPLY TO MESSRS. LOY, LIEDHOLM
AND CHARTER

In the formal comments published above and in some of those received more informally, three criticisms of the paper are made which deserve a closer analysis and a specific rebuttal. These criticisms may be summarized as follows:

1. The conclusions which may be inferred from the paper could create the impression that the ability of electric logging in its present state is more limited than it actually is.
2. The possibility of forthcoming improvements in the response of the electric log is not apparent enough in the paper.
3. Most of the discussion is centered around the determination of water saturation and nothing constructive is said about the determination of porosity and permeability.

Careful examination of these criticisms indicates that they are basically not a question of correctness or incorrectness,

but concern the manner in which the author has judged the relative merits and demerits of electric log interpretation. In other words, the comments indicate dissatisfaction with the slightly conservative tinge that the author had injected into the paper. The author wishes it to be understood that every word in the paper, and every possible implication that might be made from the phrasing, were carefully considered. His reply to these criticisms is summarized in the following paragraphs.

For the last five years, the author has been associated exclusively with an oil producing organization. In this time he has not only had the opportunity of studying electric log interpretation in detail, but has had the opportunity of appraising the relationship of the electric log to the overall economics of discovering and producing oil. A primary function of an oil producing company is to find oil and to produce it economically. Electric logging, although an important phase of this work, is only a small part of it.

Although it is desirable to get as much information as possible from the electric log, this information must be correct. The stakes involved are too great to be concerned with seeing how far one can stretch an electric log interpretation and probably be correct. There are other tools of evaluation that may be used to complement the electric log findings when there is any doubt. A very real problem concerning the electric log interpretation, however, is to know when there is doubt and when there is not. If there is any chance of doubt, one should then use every other possible means to evaluate the particular formation correctly.

When drilling an exploratory well, one is greatly concerned with the security of the investment and the success of the venture. For this reason there is a tendency to be very careful in all steps of the operation. In particular, one must be cautious in reaching conclusions on the basis of the evidence provided by the various logging and testing methods. It is perhaps better that a petroleum engineer be over cautious and make an unnecessary drill stem test, than over confident of his ability to interpret an electric log and miss an oil field.

It must be remembered that the author stated at the beginning of the paper that it was "directed not so much to the logging or research specialist, as to the petroleum engineer and geologist." A reasonably conservative philosophy has been employed in the paper because it is considered best.

The second of the above three criticisms indicates that the author has not emphasized sufficiently the possibilities of forthcoming improvements in the response of electric logs. We must bear in mind that the principal purpose of the paper was to point out the utility which the engineer or geologist can derive from the log delivered to him today. This course of presentation was decided upon since the petroleum engineer or geologist is more interested in what can be done with his present logs than what may be possibly done with them in the future. This latter is a responsibility that rests more directly with the electric logging service companies.

In order to indicate something of the developments that tomorrow may bring, the author does discuss the determination of F -factor from wall resistivity measurements and the determination of formation water characteristics from the SP curve. This is emphasized in part (3) of the summary of the paper.

Thus, contrary to what some may believe, the author's opinion is that he has placed sufficient emphasis on what may come in the future—at least he has indicated the possible direction that such developments may take. It is best not to be

over-optimistic in what these improvements will do for us until they have proven themselves. We have been mistaken before.

The author purposely avoided any emphasis on the quantitative use of electric logs in limestone formations—particularly in exploratory drilling. Generally speaking, the electric log loses much of its diagnostic value in this type of rock and other means of formation evaluation should also be employed. For a more detailed discussion of this phase of exploration, the author refers to his paper entitled "Optimum Use of Various Testing Methods in Exploratory Wells," which appears in the 1950 edition of the *API Drilling and Production Practice*.

The author's experience with MicroLogs indicates that although the MicroLog may show the presence of porosity, the porosity may not be sufficient for commercial production. On the other hand, vuggy porosity or fractured porosity in limestone or similar rocks—sufficient for commercial production—may not be evident from the MicroLog. Thus, although a useful tool, one must interpret the MicroLog with caution. It is best to depend on the fluorescence of drill cuttings and upon drill stem testing in exploratory wells penetrating limestone formations. This is a practical and straightforward approach to the problem. In a secondary degree one may place confidence in the neutron and MicroLog techniques.

The author is familiar with the special and experimental techniques that are being developed for the determination of porosity and permeability from electric log data alone. He also believes, however, that these techniques are not yet reliable—particularly as they apply to exploratory operations. In development operations, opportunity is ordinarily afforded to determine porosity and permeability in a reliable manner from cores taken in a selected number of development wells strategically situated throughout the field. For these reasons, the author decided against placing more emphasis on these techniques than he has already done in his paper.

In exploratory operations the determination of the oil and gas saturation of the various formations is of most importance. This is indirectly determined from the electric log by determining the water saturation and subtracting it from unity. For this reason emphasis was placed on the determination of water saturation. If in an exploratory well a good oil saturation is determined from the electric log for a particular horizon, the formation is ordinarily tested exhaustively to determine its productive ability, despite any speculation concerning the porosity and permeability.

It is well to mention that what the author has incorporated into his paper is partly the result of the study of a tremendous amount of core analysis data and careful watching of production results and drill stem test data. In addition, the results of a very considerable amount of basic research on electric log interpretation have, although not referred to directly, influenced the manner in which the author has appraised the present state of electric log interpretation.

The author believes that his appraisal of electric log interpretation methods is neither pessimistic nor over-optimistic. He believes it is reasonable.

In conclusion, the author again states that the criticisms of his paper primarily concern the degree of reliability with which he describes the present state of electric log interpretation. The author's approach is the more cautious. The opinions of those commenting upon the paper are of interest to the author and he hopes that his thoughts may be stimulating to them.

★ ★ ★

LOST CIRCULATION CORRECTIVE: TIME-SETTING CLAY CEMENT

J. U. MESSENGER AND J. S. McNIEL, JR., MAGNOLIA PETROLEUM CO., DALLAS, TEX.

ABSTRACT

In the drilling of oil wells the control and prevention of lost circulation of the drilling fluid is a problem which is frequently encountered; in many cases existing materials and methods for alleviating this condition have not been adequate. For severe cases of lost circulation in which the simpler methods, such as application of various bridging materials to the mud system, have proven unsatisfactory, a new material and method for applying to the loss zones have been developed which appear to be superior to existing techniques in many respects.

The material, called a clay cement, is capable of being handled as a drilling fluid after initial mixing of the solid ingredients with water and may be pumped down the drill pipe and squeezed into loss zones. After a short period, the material develops a very high gel strength which seals off the zone against further losses of the drilling fluid.

In field tests, the process has been demonstrated to be a very effective method for combatting lost circulation.

INTRODUCTION

Methods of treating lost circulation in rotary-drilled wells by the addition of special materials to drilling fluids have long been in the process of development and are continuing to improve.¹ However, the annual drilling costs which can be traced directly to lost circulation difficulties still run into the millions of dollars. The loss of mud materials into highly

permeable zones may range up to \$50,000 per well in some areas. In addition to mud costs, excessive requirements of casing, cement, rig time, and the attendant blowout hazards further emphasize the importance of the need for improved methods of combatting lost circulation. The shortcomings of presently-used materials and methods have led to the development of a new lost returns material in the form of a time-setting clay cement. In field tests this material has proven very successful in plugging off loss zones, which other more conventional materials had failed to do.

REVIEW OF PRESENT CORRECTIVE MEASURES

The proper control of such operating factors as pump pressure, clearance between pipe and hole, and speed of running pipe in a hole² is of primary importance in preventing and minimizing lost circulation problems. These factors, however, concern matters of drilling technique and do not directly involve lost circulation materials. Aside from setting casing past loss zones, three principal methods are generally employed for the purpose of avoiding or combatting lost circulation: (1) adjustment in properties (principally density) of the drilling fluid, (2) addition of fibrous, flaky, granular or other types of bridging materials to the mud system, and (3) the application of cements to the loss zones. The latter method is usually employed only after the first two have proven unsuccessful. In Table I are listed some advantages and disadvantages of the common corrective measures. Frequently, a combination of bridging material and cementing material is used.³ This combination is based on the premise that a bridge will

¹References given at end of paper.

Manuscript received in the office of the Petroleum Branch Aug. 7, 1951. Paper presented at the Fall Meeting of the Petroleum Branch in Oklahoma City, Okla., Oct. 3-5, 1951.

Table I—Methods of Correcting Lost Returns

	(1) Adjustment of mud properties (density and gel strength)	(2) Addition of bridging plastering agents to mud system.	(3) Use of cementing materials.
Types of Materials Used	1. Water 2. Clay 3. Weighting materials 4. Viscosity-reducing additives	1. Fibrous or flaky material 2. Size-graded granular solids	1. Gel cement 2. Quick-setting cement 3. Neat cement
Advantages	1. Economical 2. Requires no special materials	1. Tends to offer protection as soon as bridgeable loss zones are encountered in drilling 2. Treatment does not involve extensive loss of rig time	1. In some cases will protect against most severe types of loss 2. Will tolerate high pressure surges
Disadvantages	1. Applicable only to mild loss, usually at shallow depths 2. Correction requires close control and is often temporary	1. Will not protect against more severe types of losses where crevices and cavities exist 2. Will not withstand appreciable back-pressure surges 3. Loss of effectiveness while circulating often requires constant addition of new material	1. Loss of rig time because of: a. Placement time b. WOC time c. Time required to drill plug 2. Danger of sticking pipe 3. Possible deviation of hole while drilling plug 4. Adverse effects on mud properties by contamination with cement 5. Anticipatory treatment not possible

be built up within the loss zone at some distance from the well bore, affording a base against which a solid plug of cement might be formed.

Perhaps the most dependable method of overcoming lost circulation troubles is by method 3, the use of cementing materials. The expense and difficulties of this method are such however, that cementing materials generally are used in loss zones only where bridging and plastering materials have been proved ineffective. The use of gel cement and quick-set cement is common practice; however, neat cement is sometimes used in areas where gel cement is not available or in deep hot wells in which the mud weight is high. Shorter WOC times with quick-setting cement and a more easily drilled plug with gel cement has saved some rig time, but the danger of sticking pipe has made operators reluctant to "squeeze" in open hole.

Thermosetting plastics have been used for correcting lost returns and have shown some promise. While their applicability may involve less loss of rig time than do cements, they usually have no gel strength or bridging ability, and are diffi-

cult to apply, particularly in deep hot holes. Because of their limited applicability, of the fact that they are only partially effective, and of their high cost, they are not in wide use for this purpose.

Sodium silicate mixed with a clay slurry opposite the loss zones (by displacing one material down the pipe and the other down the annulus) has also been successfully applied to lost returns problems. However, the method of applying sodium silicate muds is difficult, requiring simultaneous control of pumping rates in pipe and annulus.

For the purpose of combatting lost circulation in cases where the simpler and more expedient methods have proven unsuccessful, a time-setting clay cement and technique of application have been developed which do not suffer many of the limitations of other materials and methods.

PROPERTIES OF TIME-SETTING CLAY CEMENT

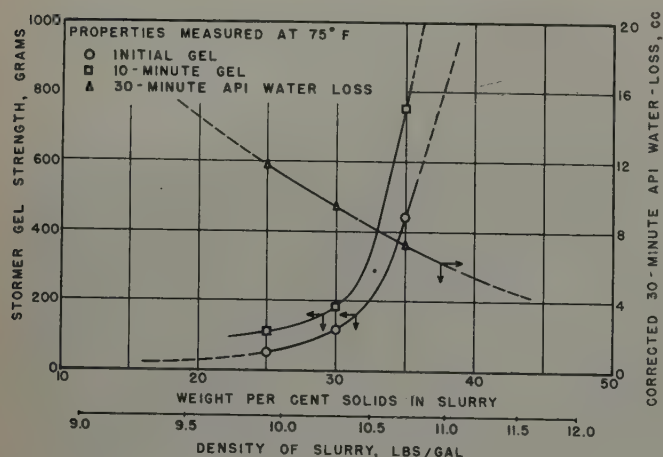


FIG. 1—EFFECT OF SOLIDS CONCENTRATION OF TIME-SETTING CLAY CEMENTS ON INITIAL AND 10-MINUTE STORMER GEL STRENGTH, AND CORRECTED API 30-MINUTE WATER LOSS.

Time-setting clay cement, as referred to herein, consists of an aqueous slurry of an especially selected clay, a smaller amount of an aluminum silicate to increase the strength of the set clay cement, and a retarder for increasing the pumping time of the slurry during application. The properties of the slurry immediately after mixing are such that it may first be pumped down a well to a highly permeable zone responsible for lost circulation and then squeezed into such a zone. After a relatively short period, the gel strength of the slurry increases to a very high level and becomes a plastic-like material with sufficient strength, in most cases, to seal off the zone against mud losses during subsequent drilling operations.

The physical properties of the slurry immediately after mixing closely resemble those of a highly thixotropic drilling mud. In the following table are given the properties of a typical time-setting clay cement slurry. In Fig. 1 are shown the Stormer initial and 10-minute gel strengths and API 30-minute water loss values of freshly mixed clay slurries as a function of the concentration of clay cement solids. The relatively low water loss level and high gel strength of the slurry immediately after mixing constitute added benefits for the application to which the clay cement has been designed. The

low water loss of the slurry makes possible squeezing opposite a highly permeable zone without danger of a flash set and the attendant hazard of stuck drill pipe, whereas the high gel strength aids in obtaining efficient displacement of formation fluids or drilling mud present in the loss zone. This latter property is essential in obtaining effective plugging of the loss zone.

Properties of a Typical Time-Setting Clay Slurry

Total Solids	35 wt per cent
Density of Slurry	10.7 lb/gal
Initial Stormer properties:	
600-rpm viscosity	250 cp
Initial gel	400 g
10-minute gel	800 g
Water-loss (30-minute API, corr.)	7 cu cm
24-hour equivalent Stormer gel (aged at 160°F)	40,000 g

Fig. 3 shows data on the effect of clay cement solids concentration on the strength or hardness of the clay cement after static aging for 24 hours at 170°F. The strength of the clay cement is expressed in terms of depth of penetration obtained with an ASTM penetrometer in which a cone with an apex angle of 50° was substituted for the conventionally employed needle. Use of this type instrument became necessary inasmuch as the clay cements containing as much as 35 weight per cent solids had strengths far in excess of the limits of the previously used gel strength measuring equipment. As might be anticipated, the higher solids concentration gave considerable lower penetration values, indicating greater strengths of the clay cement.

TECHNIQUE OF PLACEMENT

Time-setting clay slurries have been applied thus far only to loss zones against which plastering and bridging materials have proved to be relatively ineffective. The method of application closely resembles a cementing operation.

The time-setting clay slurry is preferably placed in a well by using conventional cementing equipment wherein the clay

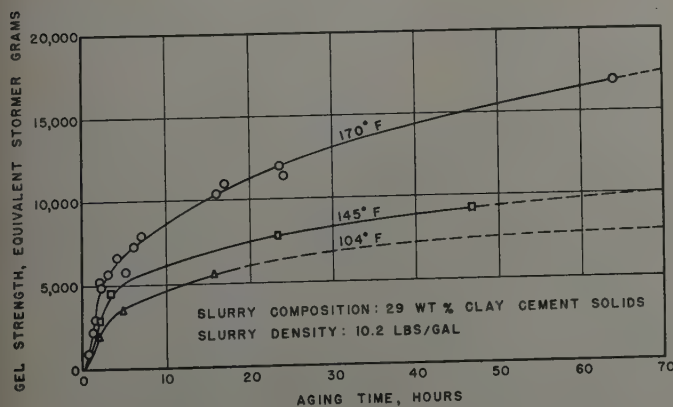


FIG. 2—EFFECT OF AGING TIME AND TEMPERATURE ON GEL STRENGTH OF TIME-SETTING CLAY CEMENT.

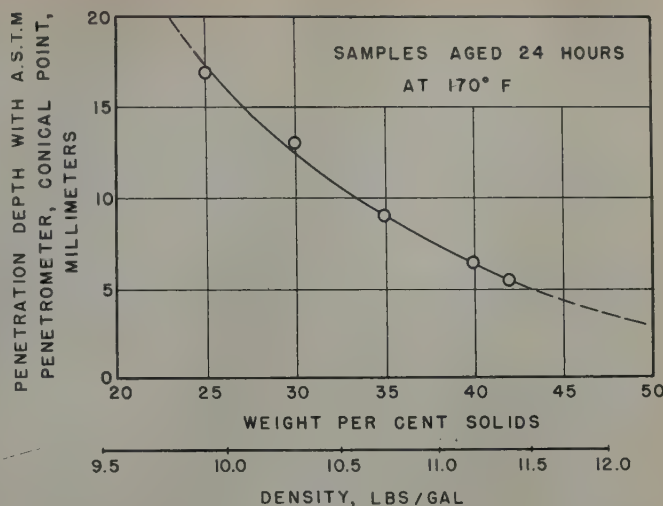


FIG. 3—EFFECT OF TIME-SETTING CLAY CEMENT SOLIDS CONCENTRATION ON STRENGTH OF CLAY CEMENT.

cement solids and mixing water are jet-hopper mixed and then pumped directly into the drill pipe. In certain areas, particularly in application to shallow loss zones, it should be feasible to utilize regular mud pumps and eliminate the need for cementing equipment.

On the basis of field experiences with these slurries, the following general procedure of placement has been developed.

1. Drill pipe is run, preferably open-end, to a point opposite or slightly below the loss zones.
2. An attempt should be made to establish at least partial circulation, using the cementing pumps, for the purpose of clearing the hole in the vicinity of loss zones of other materials which may have accumulated from former operations.
3. The time-setting clay cement slurry is "spotted" against the loss zones by being displaced down the pipe with the drilling fluid available at the well.
4. The slurry should be pumped into the hole until mud returns are obtained and then the blowout preventers closed. If the amount of clay cement placed is sufficient to plug the loss zone and if the fluid level is so far down the hole that returns cannot be established by forcing clay cement up around the drill pipe, the hole should be filled with drilling fluid through the fill-up line after one-third to one-half of the clay cement has been displaced against the loss zone, and if the hole then stands full or flows, the blowout preventers should be closed. This technique has been used and is satisfactory where the loss zone is below or within a short distance above the end of the drill pipe.
5. An attempt should be made to obtain a positive squeeze pressure (annulus pressure) sufficient to withstand the differential pressure which the loss zone is expected to withstand during further drilling operations. In order to allow more of the slurry to penetrate into the loss zones without exceeding squeeze pressures which may cause the formation to be fractured at other weak points, the pumping rate may be reduced toward the completion of the squeeze.
6. After all of the slurry has been displaced from the pipe, pressure should be maintained on the closed system for the

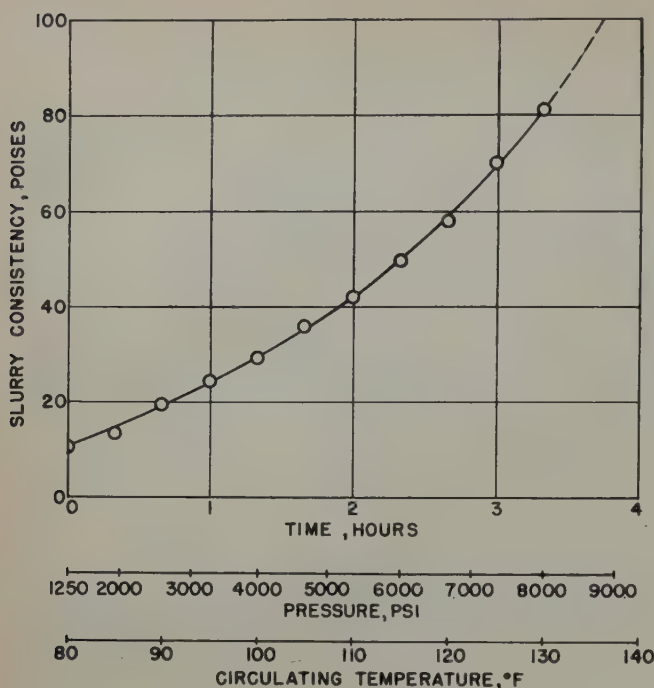


FIG. 4 — PUMPING CONSISTENCY OF CLAY CEMENT AS AFFECTED BY SIMULATED WELL CONDITIONS DURING PLACEMENT.

- duration of the setting period or for whatever period is considered safe under the specific conditions. Undesirable swabbing effects due to the withdrawal of the pipe from the plug are largely eliminated by having the drill pipe placed so that a minimum of clay cement gets up around the pipe. Under conditions where clay cement was thought to have been up around the drill pipe, swabbing effects resulting from the withdrawal of the pipe have not caused any perceptible damage to the plug applied to the loss zone.
- After removing the pipe from the hole, a wire line may be run to establish the location of the top of the clay cement. From this information, the amount of clay cement squeezed into the formation may be estimated.
 - If the formation temperature is above 150°F, the clay cement plug may be drilled after only a short waiting period of one to three hours. For lower temperatures, a waiting period up to ten hours should be allowed.
 - In drilling out the clay cement in the hole, the bit is lowered to the top of the plug and drilled through at a rate no greater than ten feet per minute.

PERFORMANCE OF TIME-SETTING CLAY CEMENT IN FIELD APPLICATIONS

Lost returns zones in 12 wells located in six fields have been treated with time-setting clay cement. A summary of these applications is given in Table II. In all these wells, the loss zones are considered to have been relatively severe, and the application of clay cement was made only after attempts to seal off the zones by other means (bridging materials, and in

some cases, portland cement were employed). It is to be noted that, in most instances, returns were regained after application of the clay cement. In the two cases where circulation was not regained, drilling proceeded with partial to complete loss of circulation until casing was set past the loss zone.

Several of the applications have been in relatively deep wells. To illustrate the pumpability of time-setting clay cement, the material was tested in a high pressure, high-temperature cement consistometer. In Fig. 4, the consistency-pumping time characteristics of a clay cement slurry containing 38 weight per cent solids are shown. The pressure and temperature schedule employed is also shown. These data indicate that pumping periods of satisfactory length are realizable with clay cements providing, in many instances, a greater flexibility in placement operations than is available by other methods.

Attention should be called to the shape of the pumping curves for clay cement and conventional cements. While the pressures at which clay cement can be safely pumped are generally higher than those for conventional cement, its setting curve shows that it does not exhibit a rapid set near the limit of its pumpability. In deep hot holes, it is recommended that the drill pipe not be filled with clay cement because of its high gel strength. However, pumpable batches of from 15 to 30 bbl have been applied easily and found very effective in restoring circulation under relatively high temperature conditions.

CONCLUSIONS

As a result of the field trials conducted with this material, the following advantages of time-setting clay cement over other materials and techniques for combatting lost circulation have become apparent.

- Because of its low water loss, a time-setting clay cement slurry can be safely squeezed in open hole and up around the drill pipe. There is no danger of sticking the drill pipe as a result of flash-setting of the clay cement.
- Because of its high gel strength, a time-setting clay cement slurry is resistant to dilution by formation waters and the drilling fluid, and can be used to fill large cavities and crevices.
- Longer loss zones can be treated at one time than is practical using conventional cementing materials, and because of the low density and high gel strength of clay cement, the likelihood of success is enhanced.
- Because of the much lower final strength of clay cement as compared to conventional cements, plugs may be drilled more rapidly and with much less danger of deviating the hole.
- No tools have to be set to keep the slurries from coming up around the drill pipe inasmuch as the pipe may be withdrawn from the clay cement surrounding it after placement.
- Unlike cements, time-setting clay slurries will not impair the physical properties of a mud to any appreciable degree.
- Time-setting clay slurries cost less to use than common cement because they require less WOC time and less time to drill.
- Because of the low water loss of clay cements, the possibility of further damage and weakening of formations resulting from filtrate effects is largely eliminated.

In its present stage of development, the application of time-setting clay cements has limitations in certain cases. For example, because of the cements' lower strengths, large quan-

Table II—Summary of Field Applications of Time-Setting Clay Cement

Case No.	No of Jobs	Loss Zones Treated			Clay Cement Application Data				
		Estimated Depth ft	Formation Temperature °F	Type of Loss Zone	Mud Loss, Bbl/Hr		Amount Placed bbl	Calculated Amt. Squeezed into Formation bbl	Slurry Density lb/gal
					Before Treatment	After Treatment			
1	2	6,520-6,760	100-120	Fractures	25	None	125	32	10.8
		5,970-6,480		Fractures	25	None		38	
2	5	5,500-6,650	100-120	Fractures	Complete	None	522	372	11.1
3	6	6,650-6,660	100-120	Fractures	Complete	Complete	467	320	11.0
4	2	4,295	100	Solution Channels	Complete	Partial	426	399	10.8
		4,340				Complete			Containing expanded perlite
5	1	400-685	60-80	Fractures in Salt	Complete	None	225	171	11.3
									Containing expanded perlite
6	1	4,864-4,899	180-220	Broken Limestone	25	None	184	95	11.0
7	4	4,230	180-220	Broken Limestone	Complete	None	177	96	11.0-11.4
		4,290			20	None			
		4,320			60	None			
		4,524			25	None			
8	1	5,655	180-220	Broken Limestone	Complete	None	34	11	10.9
9	1	1,091	100-140	Broken Limestone	Complete	None	21	*	11.2
10	1	11,343	200-230	Fractures	Complete	None	14	*	11.0
11	1	11,439-11,709	200-230	Fractures	Complete	None	23	*	11.0
12	2	10,600-11,000	200-220	Fractures	Complete	None	112	76	11.0-11.2

*Measurement of top of plug after squeezing not made.

ties are sometimes necessary to seal severe loss zones, especially where formation temperatures are low. This has been caused partially by the necessity for sacrificing some strength in the final set materials in order to retain other advantages previously discussed. While the material is not yet a cure-all for lost circulation problems, it has thoroughly demonstrated decisive advantages over other materials and techniques for curing a number of very serious types of lost circulation. The application of time-setting cements has thus become a valuable method for combatting these problems.

The authors wish to express their appreciation to the petroleum engineering and producing departments of Magnolia Petroleum Co. for their arranging and assisting in the field applications. Appreciation is also extended to B. F. Taylor for assistance and cooperation in conducting much of the experimental work. Acknowledgment is made to the management of Magnolia Petroleum Co. for permission to publish this paper.

REFERENCES

1. Anon.: *Principles of Drilling Mud Control, Eighth Edition*, Div. of Extension, The University of Texas and American Association Oilwell Drilling Cont., Austin, Texas, (1951).
2. Goins, W. C., Jr., Weichert, J. P., Burba, J. L., Jr., Dawson, D. D., Jr., and Teplitz, A. J.: "Down-the-Hole Pressure Surges and Their Effect on Lost Circulation," presented at API Southwest District Meeting, 1951. (Also, in *Oil and Gas Jour.*, April 12, 1951, 86.)
3. Carlson, R. F.: "Lost Circulation Materials and Mud Additives," *Oil and Gas Jour.*, (Dec. 28, 1950).

DISCUSSION

By W. C. Goins, Jr., Gulf Oil Corp., Houston, Tex.

The authors are to be complimented for making a fine contribution to an important phase of the lost circulation problem.

It is often found that the use of the common sealing materials such as mica, wood fibres, cellophane strips, etc., fail to seal off a loss. This makes the use of cement or highly viscous squeezing mixtures necessary, but their application is frequently attended with difficulties.

Gel-cement is probably the best material that can be used for losses at or near a casing seat, but complications arise if it is used in open hole, particularly where it is desired to squeeze the cement into a loss zone in a long open hole section. It must be squeezed from the casing through the long open hole section, or a packer must be set in the open hole. This latter measure is usually difficult, if not impossible. If the squeeze is made in soft formations there is danger of side-tracking the hole when the cement is drilled out. Also, chunks of cement may fall into the hole during later drilling and stick the pipe.

The sodium silicate squeeze mentioned by the authors has frequently been used successfully, but usually requires pumping in both the annular space and drill pipe to accomplish effective below-bit mixing of the silicate and fresh water mud. Two cementing trucks are usually necessary, and if the annular space does not stand full during the squeeze there can be no certainty that the squeeze mixture is going down the hole to the point of loss. It may turn up around the end of the bit and tend to stick the pipe.

The method presented in the paper would require only one cementing truck and would be simpler in general to apply. Since no annular space pumping is required, a packer could

be set at the casing seat for those jobs where the annular space does not remain full.

In the Gulf Coast area circulation can usually be regained through the use of the common bridging and plastering agents, but squeezes of the type described here become necessary in "pressure conditioning" formations. This is the problem which arises when the well loses circulation with a mud of a given density, and it is anticipated that a higher mud density will be required before casing is set. This makes it not only necessary to regain circulation but also to strengthen the loss zone to the point where it will circulate the anticipated high mud

density. If there is considerable drilling to be done before the high pressure zone is to be penetrated then it is possible to gamble on the loss zone strengthening with time; but before the high pressure is encountered the well should be pressure tested to determine whether the higher density mud can be circulated. Frequently it cannot be circulated, and additional sealing measures are required, even though the well is experiencing no loss of circulation with the mud in use. Repeated squeezes with cement or other squeeze mixtures are often necessary before the well withstands the required pressure. It will be very interesting to follow the use of the authors' clay cement in this application.

★ ★ ★

IMPROVED MULTIPHASE FLOW STUDIES EMPLOYING RADIOACTIVE TRACERS

V. A. JOSENDAL, JUNIOR MEMBER AIME, B. B. SANDIFORD AND J. W. WILSON, MEMBER AIME, UNION OIL CO. OF CALIFORNIA, BREA, CALIF.

ABSTRACT

Two radioactive tracers have been tested as a means of determining core saturation in multiphase flow studies. Cesium¹³⁴chloride was tried as a water-phase tracer, but complications in its use in low permeability cores resulted from sorption of cesium by the core or water-wet pads. Iodo¹³¹benzene proved very satisfactory as an oil-phase tracer. The synthesis of iodobenzene from the sodium iodide as received from Oak Ridge is simple and direct. The tracer is insoluble in water and there was no evidence of sorption by any of the core materials used.

Use of the method to determine saturation profiles during capillary and dynamic desaturations and relative permeability measurements on oil-water and oil-gas systems is described. Comparisons of the dynamic and capillary methods of relative permeability determination were made using the tracer to check core saturation and saturation distribution. Other experiments are also described in which mobility of the oil phase at various saturations was measured by displacing labeled oil by flowing inactive oil. Similar experiments were made using water labeled with cesium 134.

INTRODUCTION

To be fundamentally sound, any laboratory method of determining relative permeability must meet, among others, the following requirements: (1) the core saturation between the pressure taps must be uniform, and (2) there must be uniform pressure difference between the phases in the region between the pressure taps. In practice it may eventually be shown that appreciable departure from either or both of these conditions may be permitted without introducing sensible error, but the magnitude of such error remains to be established. There is need then for methods of saturation determina-

tion which will determine the saturation profile in a core as well as the overall average saturation given by the gravimetric or material balance methods usually employed.

Methods which have received consideration include resistivity, X-ray absorption, gamma ray absorption, neutron diffraction, and radioactive tracers. The resistivity method has use in the determination of profile, but needs checking by independent means.¹ The X-ray method has been used successfully, but requires elaborate equipment and calibration.^{2,3,4} At present gamma ray absorption is practical only for very large cores.⁵ The neutron method⁶ does not appear adaptable to measurement of saturation variations in short cores since it is a scattering method. Russell, Morgan and Muskat⁷ employed radiovanadium in a study of the mobility of interstitial water. Coomber and Tiratsoo⁸ used radioiodine as an oil-phase tracer and measured profiles in unconsolidated sand packs.

ADVANTAGES OF RADIOACTIVITY METHOD

A thorough discussion of the theory of radioactive tracers and the technique of using them to study the movement of fluids in sands is given by Coomber and Tiratsoo⁸ and need not be detailed here. The method requires less equipment than the X-ray method; the counting problem is similar, but the generation and regulation of the radiation, which is a major problem in the X-ray method, is not required in the radioactivity method. In the X-ray method it is customary to add up to 20 per cent of absorber, usually an iodine compound, to the phase to be labeled, while in the radioactivity method a mere trace is sufficient. A possible disadvantage of the radioactivity method is that a disproportionate amount of the activity comes from the portion of the core nearest the counter, whereas the X-ray gives a true average saturation in the region traversed by the beam. On the other hand, this characteristic of the radioactivity method renders it peculiarly adaptable to study of certain types of radial variations in saturation.

As with the X-ray method, a tracer may be added to either the oil or water-phase. An oil-phase tracer is more generally useful, however, since it permits work on oil and gas in the

¹References given at end of paper.
Manuscript received in the office of the Petroleum Branch Sept. 25, 1951. Paper presented at the Petroleum Branch Fall Meeting in Los Angeles, Calif., Oct. 25-26, 1951.

presence of interstitial water as well as on oil-water systems. There are a number of available radioactive metals which can be considered for use as water-phase tracers, the only probable difficulties being sorption or ion-exchange on clays. However, except for oil-soluble, water-insoluble compounds that might be prepared from these metals, the selection of suitable oil-phase tracers is quite limited. Iodine 131 is a natural choice since it is readily available, relatively inexpensive, and has an acceptable half-life (eight days). A half-life somewhat longer than eight days would be desirable; however, this period allows experiments of three to four weeks duration, and there is the definite advantage that contaminated articles need merely be set aside for several weeks, after which they will be perfectly safe.

Coomber and Tiratsoo⁸ used free iodine as an oil-phase tracer, which was feasible in their work since they found the distribution coefficient of iodine between oil and water to be about 2,500. However, the presence of reducing substances, such as hydrogen sulfide in either the oil or water, or the presence in the water of complexing agents would rule out the use of free iodine.

MATERIALS AND COUNTING EQUIPMENT

In the initial experiments cesium 134 in the form of cesium chloride was used as a water-phase tracer. Cesium 134 has a half-life of 2.3 years, and the energies of the principal gamma components of the radiation are 0.568, 0.602 and 0.794 mev. Six-tenths of a gram of cesium carbonate obtained from the Atomic Energy Commission having an activity of about 40 millicuries at the time of use was dissolved in three per cent aqueous sodium chloride solution containing a slight excess of hydrochloric acid to convert it to cesium chloride. For each experiment a 10 ml portion of this solution was added to 140 ml of three per cent sodium chloride solution, stirred under vacuum to mix and de-gas, and adjusted to a pH of five with sodium hydroxide.

In later experiments iodine 131 in the form of iodobenzene was used as an oil-phase tracer. Iodine 131 has a half-life of eight days and the energies of the principal components of the gamma radiation are 0.638 and 0.364 mev. Heptyl iodide had been prepared in this laboratory by exchange for use as a tracer.⁹ However, the aryl halides are known to be more stable, and since the preparation of iodobenzene is simple, direct, and gives excellent yields, it was chosen for this work. Details of the preparation as carried out in this laboratory are given in Appendix A. No activity is removed from the labeled oil when shaken with concentrated hydrochloric acid, concentrated sodium hydroxide, or sodium bisulfite solution. A quantity of 25 or 50 millicuries of iodine 131 in 100 to 200 ml of oil was generally employed. The concentration of iodobenzene was 0.02 to 0.04 per cent.

The counting apparatus consisted of the following units:

- Geiger-Mueller end window counting tube, Tracerlab TGC-1 or TGC-2 or Radiation Counter Laboratories Mark I-Model 13.
- Predetermining count scaler, range of two to 8,192 counts, custom-built by Technical Associates, Glendale, Calif.
- Printing interval timer, Tracerlab SC-5A.

A special shield providing two in. of lead around the counting tube was built and is shown in Fig. 1. Plug A is removable so that different sized openings can be provided. In most of the work a slit in front of the G-M tube one-fourth in. wide by one in. high was used. With a shield two in. thick and a half-inch sheath of Lucite around the core, the length of the core in view of the counter averaged about one-half in. when the counter was operated as close to the core as possible. Two in. of lead was desirable in the work with cesium. This thickness was also employed for the iodine, but further investigation might show that thicknesses of the order of one in. may be adequate. For better definition a narrower slit can be used, but it must be remembered that as the slit width is reduced, the amount of activity passing through the lead from the remainder of the core may become appreciable compared to the quantity passing through the slit, thus tending to de-

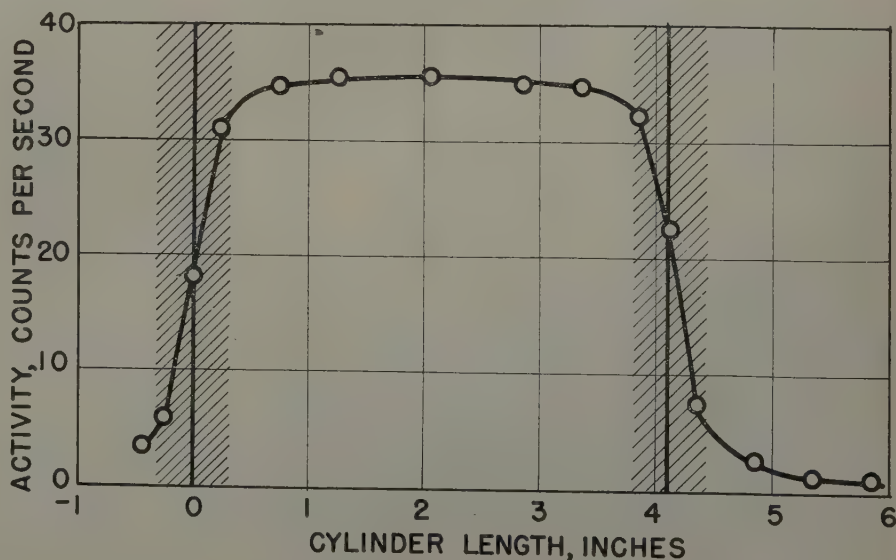
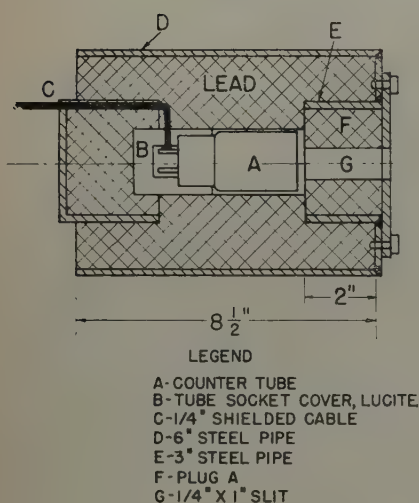


FIG. 1 — DETAIL OF COUNTING TUBE SHIELD.

FIG. 2 — ACTIVITY PROFILE OF KEROSENE FILLED HOLLOW CYLINDER.

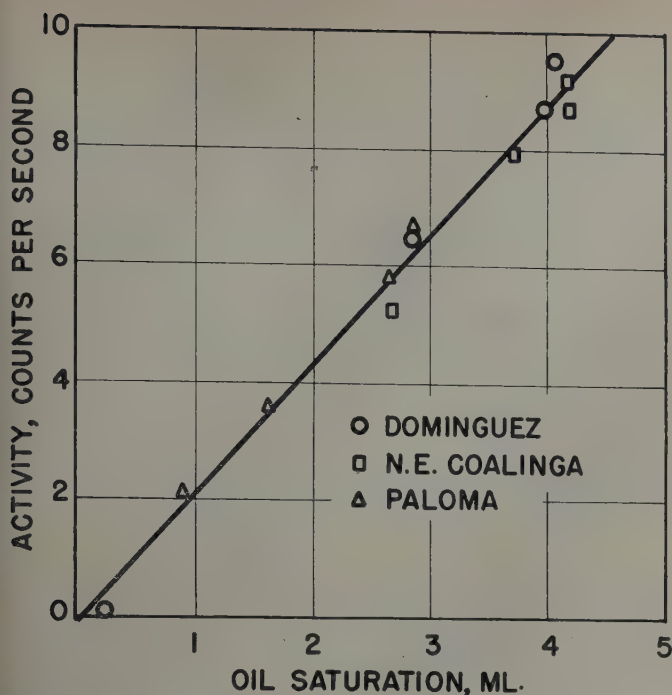


FIG. 3—CORRELATION OF ACTIVITY IN NATURAL CORES WITH OIL SATURATION.

crease definition. The counter shield was clamped in the vise of a milling attachment to permit horizontal movement of the counter along the length of the core, which was held in a frame in front of the counter. The position was read to 0.01 in. on an attached scale. Originally, the counter was moved by turning the screw by hand, but later was motor driven to permit automatic counting.

CORRELATION BETWEEN ACTIVITY AND SATURATION

To check the definition obtained in this work, a Lucite cylinder two in. in diameter and with a hollow space one in. in diameter by about four in. long was filled with kerosene labeled with iodine 131 and scanned in the usual manner. The results are shown in Fig. 2. Geometric consideration and experimental results show that the activity can be expected to decrease over a distance of travel of about five-eighths in. as the field of view of the counter moves past the ends of the cylinder. This region is shaded on the graph. Over the remainder of the active region the profile is very flat.

To determine the applicability of iodobenzene as a tracer in natural cores containing clay, three samples representing widely varying clay types were selected.¹⁰ Properties of these samples are listed in Table I.

Table I—Properties of Natural Cores

Field	Predominant Clay Type	Length in.	Diameter in.	Pore Volume ml	K _w md
Dominguez	Kaolin, Montmorillinite	1.85	0.985	5.82	70
Paloma	Montmorillinite	1.83	0.985	4.23	18
N.E. Coalina	Kaolin	1.92	0.985	4.60	925

The cores were mounted in Lucite¹¹ and saturated with three per cent sodium chloride solution. They were clamped vertically side by side in front of the G-M tube carriage, with a one-quarter by one and one-half in. vertical slit in front of the counter tube so that in each case nearly an entire core was in view of the tube. The cores were then subjected to capillary desaturation employing iso-octane labeled with iodo¹³¹benzene. The activities within each core were measured at intervals during the desaturation for comparison with the oil contents as measured by the volumes of brine expelled. The results are given in Fig. 3. The relation appears to be linear, and there is fair agreement among the different cores in spite of the varying compositions and pore volumes and the fact that no special effort was made to obtain exactly the same distances between cores and counter tube. It would be desirable to check linearity by a method permitting greater accuracy of volume readings. Coomer and Tiratsoo,⁸ by measurements in brass cells of varying thicknesses, found a non-linear relation between oil volume and activity, and stated that this was attributable to self-absorption. It is probable, however, that the non-linearity which they describe is principally the result of the distance effect (details are not given, but it appears that each increment of oil was farther from the counter). The distance effect does not apply in measurements on a core, where, if the saturation is uniform radially, the average distance between the counter and the core does not vary with saturation. There would be a slight non-linearity because the absorption by water differs from that by oil, and in the case of oil and gas the variation would probably be detectable (rough calculations indicate an error of not over two or three per cent).

After desaturation the cores were flooded to residual oil with brine and the activities measured. At a later date after

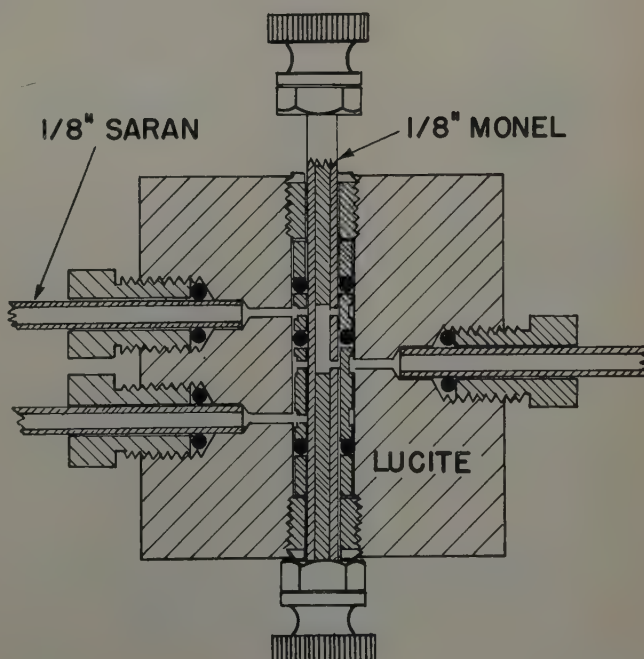
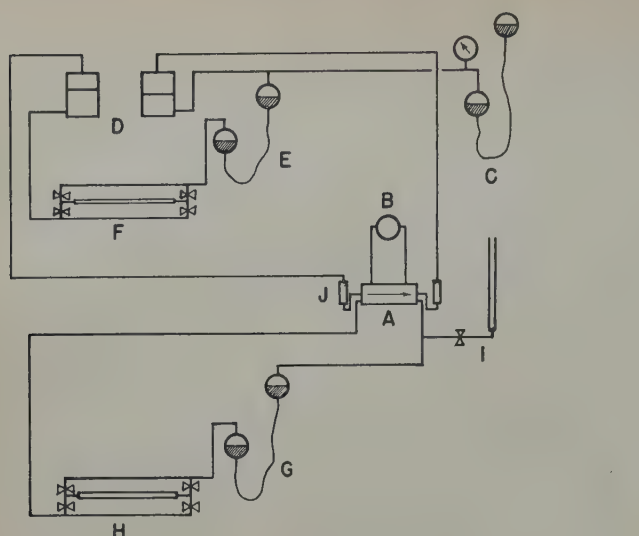


FIG. 4—ZERO VOLUME DISPLACEMENT "O" RING VALVE.



LEGEND

- | | |
|-----------------------------|--------------------------------|
| A — CORE | F — OIL FLOW METER |
| B — GAGE | G — WATER PUMP |
| C — CAPILLARY PRESSURE HEAD | H — WATER FLOW METER |
| D — ACTIVE OIL RESERVOIRS | I — WATER RESERVOIR |
| E — OIL PUMP | J — ACTIVITY CALIBRATION CELLS |

FIG. 5—FLOW DIAGRAM OF CAPILLARY METHOD RELATIVE PERMEABILITY APPARATUS.

the activity had decayed to a safe value, the cores were subjected to a vacuum distillation to determine the true residual oil contents (Table II).

It is apparent that there was no significant sorption of activity by any of the cores. It should be pointed out that these cores were all water-wet and were initially saturated with water. Sorption might be more likely in dry or oil-wet cores.

USE OF RADIOACTIVITY METHOD IN FLOW WORK

The radioactivity method of measuring saturation as described above was used to measure saturation profiles during capillary and dynamic desaturation, to determine the mobility of oil and water in cores, and to compare the measurement of relative permeability by different methods.

It is believed that the methods of relative permeability determination in use can be classified as capillary and dynamic, the principal distinction being the method of bringing about saturation changes. The capillary pressure method¹² of relative permeability measurement has been described by many in the literature and is characterized mainly by the fact that the

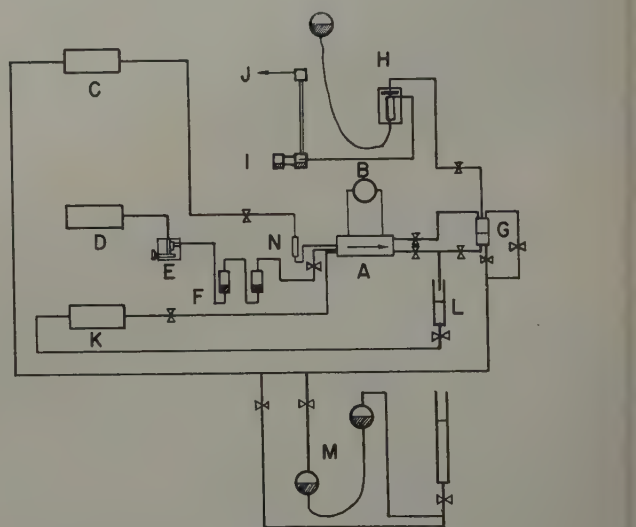
saturation is changed by applying capillary pressure across the non-wetting phase ports and the wetting phase semi-permeable membranes. In the dynamic displacement method¹³ the phases are flowed simultaneously until no further saturation change is detectable.

DESCRIPTION OF FLOW APPARATUS

It is essential in working with radioactive fluids to maintain a high degree of reliability in the fluid system. Glass stopcocks and tubing were considered inadequate. Accordingly, zero volume displacement "O" ring valves, one-eighth in. diameter Saran tubing, and Lucite vessels were used. The Saran tubing was connected to the core, valves, and Lucite reservoirs by "O" ring fittings. Construction of the valves and fittings is shown in Fig. 4.

Capillary Pressure Method

The apparatus described herein differs from the usual set-up mainly in the fact that the pressure is measured through taps on the side of the core rather than at the ends. Also, the liquids are forced through the core by mercury head pumps rather than air pressure. The closed liquid flow systems prevent any change in the average core saturation during flow. Liquid flow rates were measured by movement of an air bubble



LEGEND

- | | |
|--------------------|---------------------------------------|
| A — CORE | H — GAS PHASE BACK PRESSURE REGULATOR |
| B — GAGE | I — GAS FLOW METER |
| C — OIL PUMP | J — VENT |
| D — GAS SUPPLY | K — WATER PUMP |
| E — FLOW REGULATOR | L — WATER BURET |
| F — GAS SATURATOR | M — OIL PHASE BACK PRESSURE REGULATOR |
| G — SEPARATOR | N — CALIBRATION CELL |

FIG. 6—FLOW DIAGRAM OF DYNAMIC METHOD RELATIVE PERMEABILITY APPARATUS.

Table II—Correlation of Residual Oil Saturation With Saturation Indicated by Activity

Core	Residual Oil Saturation, ml	
	Indicated by Activity	Found by Distillation
Dominguez	1.2	1.2
N.E. Coalinga	1.4	1.5
Paloma	1.2	1.4

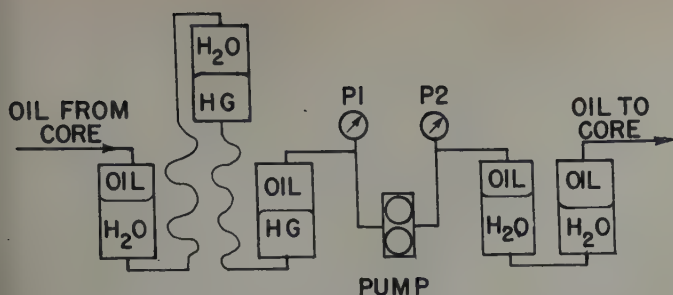


FIG. 7 — USE OF ZENITH PUMP AT LOW FLOW RATES.

in a precision bore tube. By means of the zero volume displacement valves the bubble could be moved in either direction or the tube by-passed. The capillary method apparatus for the oil-water system is shown in Fig. 5. A similar apparatus was used for oil-gas runs. The oil system in these runs was the same as shown in Fig. 5 except that a burette was added to measure the volume of oil desaturated from the core. The gas system was similar to that shown for the dynamic method in Fig. 6. However, the gas was introduced to the gas saturator at a constant pressure, the capillary pressure. A manometer was also added to measure the pressure head across the entire core. To start gas flow, the pressure at the outlet end of the core was reduced by lowering the mercury head on the back pressure regulator.

Dynamic Displacement Method

Referring again to Fig. 6, it will be seen that constant rate metering pumps were used in the dynamic flow experiments. Zenith* model 1/2B gear pumps (0.297 ml/rev) were found satisfactory when used in an arrangement as diagrammed in Fig. 7. A viscous oil (about 2,500 cp at 75°F) was metered by the pump, and by means of the mercury leveling bulb the pump suction pressure was maintained approximately the same as the discharge pressure. In this way, slippage in the pump was practically eliminated.

Pressure Measurement

Pressures were measured through the side taps by means of low volume displacement type gauges in both the dynamic and capillary method runs. Two types of differential pressure gauges were employed, an Aerojet** gauge with interchangeable diaphragms and a 0-20 psi Wiancko† gauge. Pressure drops as low as 0.12 psi were measured with suitable accuracy. The volume displacement of the Aerojet gauge with a 0.005 in. diaphragm is 7 cu mm per psi applied pressure while the Wiancko displaces 2.5 cu mm per psi. Both gauges operate on the principle of changing magnetic reluctance. Gauge outputs were recorded on a Foxboro Dynalog Recorder used in conjunction with simple bridge circuits.

With the Wiancko gauge, it was possible to measure the absolute pressures in the core directly. With the Aerojet gauge, it was necessary to match the core pressure with an applied pressure measured by a manometer.

Core Mounting

The Alundum and natural cores with end diaphragms and pressure taps were mounted in Lucite. Pressure taps were mounted only on the sides of the cores at a sufficient distance from the ends to minimize flow distortion. In those positions where unimpeded flow into the core was desired a plate of high permeability Aloxite was placed against the core. To make connections with the fluid lines, holes were drilled through the Lucite sheathing to the Aloxite plates against the core and backing the diaphragms. Fig. 8 illustrates a core mounted for a relative permeability study, comparing the dynamic and capillary methods in the oil-water system. Water-wet diaphragms and open ports were provided at the ends of the core for flow and along the side for pressure measurement.

Johns-Manville Snow Floss was the material usually used for water-wet semi-permeable membranes. It is an unconsolidated diatomaceous earth having a particle size of 1-2 microns. An oil pressure of 30 psi was required to displace water from

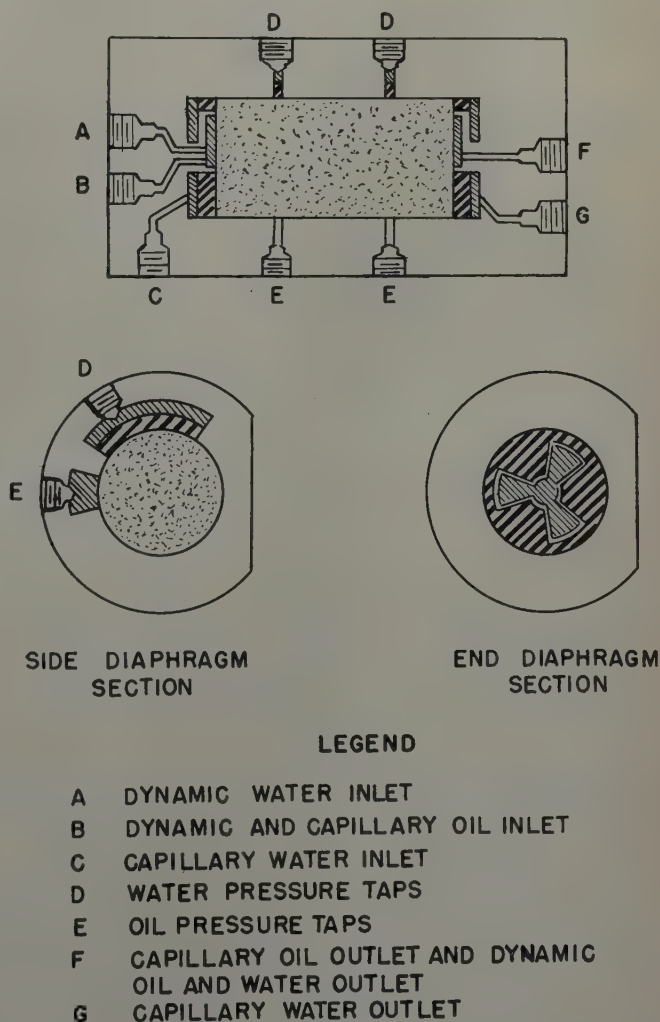


FIG. 8 — MOUNTED CORE FOR OIL-WATER RELATIVE PERMEABILITY MEASUREMENTS BY CAPILLARY AND DYNAMIC METHODS.

*Zenith Products Co., West Newton, Mass.

**Aerojet Engineering Corp., Azusa, Calif.

†Wiancko Engineering Corp., Altadena, Calif.

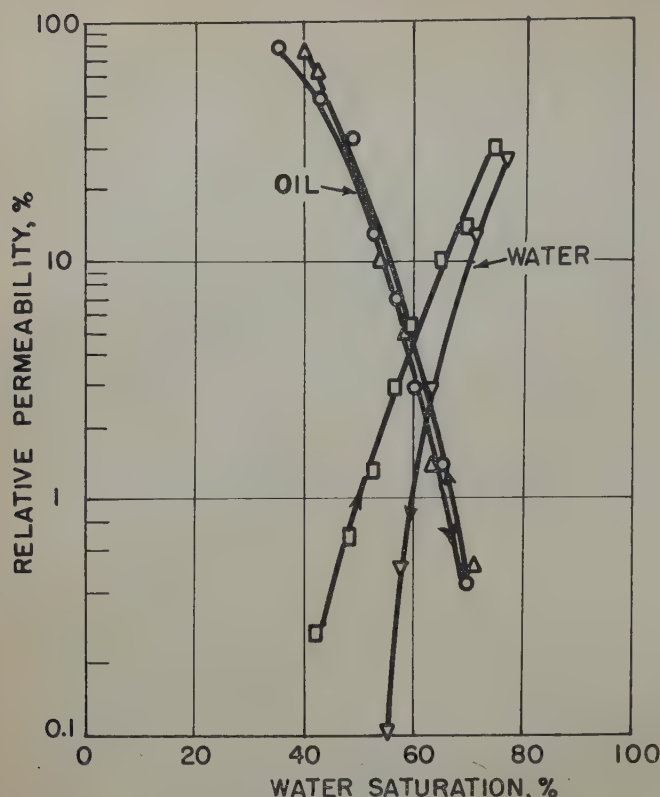


FIG. 9—EFFECT OF THE DIRECTION OF SATURATION CHANGE ON RELATIVE PERMEABILITY, CORE A.

the material after it had been compressed by the mounting procedure. For oil-wet diaphragm material Coors No. 740 porcelain was treated with Dri-Film.

In order to mount the core, a number of Lucite sections were machined in such a manner that they could be fitted together to enclose the core and diaphragms. Snow Floss was pressed into the grooves in the partially assembled sections prior to insertion of the core. The sections were then cemented

together and the assembly subjected to external pressure and heat.¹¹ The mounting was completed by drilling and tapping the Lucite for flow connections.

EXPERIMENTAL PROCEDURES

The cores were cut to the dimensions given in Table III.

The natural cores were cleaned in a Soxhlet extractor first with toluene and then with dioxane and dried at 220°F for about three hours. The Alundum cores were extracted in the same manner with constant boiling hydrochloric acid, successively extracted with water, methanol, toluene, and dioxane, and dried at 220°F. Pore volumes were then determined by weighing the cores saturated with kerosene. The kerosene was removed by another extraction with toluene and dioxane, followed by the usual drying. Following this, the cores were mounted as described above with diaphragms as indicated in Table III. Air permeabilities corrected for Klinkenberg effect were next determined. Cores A, B, and C were saturated with appropriate synthetic formation water and D, E, F, and G with three per cent sodium chloride solution. Brine permeabilities are indicated in the table. Cores A, B, and C were desaturated by the capillary pressure method using a close-cut redistilled kerosene (B.P. 420-500°F, viscosity 2.15 cp). Cores E, F, and G were similarly desaturated, but with iso-octane. The maximum capillary pressure employed was 15 psi.

In the studies of Core A, the kerosene used for desaturation was tagged with iodo¹³¹benzene. The activities at five points along the core were measured, and from the values determined at interstitial water saturation the activity vs saturation calibration was established on the basis of a linear relation as found above. It was assumed that the core saturation was uniform at interstitial water; a better basis of calibration would be measurements taken when the core was 100 per cent saturated with the labeled fluid. Capillary pressure was increased in increments and oil and water effective permeabilities were measured after attaining equilibrium following each step. Activities were measured at the five points along the core to check uniformity and determine saturation. After the minimum brine saturation had been attained, the capillary pressure was

Table III—Summary of Core Properties

Core No.	Type	Diam. in.	Length in.	Pore Vol. ml	Porosity %	K _{air} md	K _w md	I.W.* %	M o u n t i n g **		
									Inlet	Outlet	Side Taps
A	Natural	0.993	4.13	8.97	17.6	546	415	34.8	2-OH 1-SF	2-OH 1-SF	2-OH 2-SF
B	Natural	0.998	2.035	5.52	21.7	72.6	39.2	35.8	1-OH 1-SF	1-OH 1-SF	2-OH 2-SF
C	Natural	0.965	1.94	5.12	23.0	79.5	23.2	39.4	1-OH 1-OWC	1-OH 1-OWC	2-OH 2-OWC 1-SF
D	Alundum	1.047	3.98	14.4	26	80	—	—	1-OH	1-OH	none
E	Alundum	1.00	3.57	12.5	27.3	26.5	35	28.0	1-OH 1-SF	1-OH 1-SF	5-OH 5-SF
F	Alundum	1.00	3.545	11.17	24.4	21	22.9	28.0	1-OH	1-OH 1-SF	2-OH
G	Natural	0.985	1.85	5.82	25.0	—	70	34.0	1-OH	1-OH 1-SF	2-OH

*Residual water after application of 15 psi oil capillary pressure.

**OH = Open Hole, SF = Snow Floss, OWC = Oil-Wet Coors.

reduced to nearly zero, and the core permitted to imbibe brine. During the imbibition process relative permeability measurements were taken at only one saturation because the imbibition was extremely slow. Therefore, the core was flooded with brine to residual oil saturation, and another series of capillary method relative permeability measurements made during a second desaturation. Following this, the kerosene was flushed out with inactive kerosene since the activity had decayed to a low value. The core was transferred to the dynamic displacement method apparatus, and new labeled kerosene flowed until the inactive kerosene had been replaced. Oil was then flowed at 16.8 ml/hr and brine at 0.23 ml/hr. This resulted in an increase in brine saturation from 35 per cent to 43 per cent. The brine to oil flow rate ratio was then increased in steps to give additional points on the relative permeability curves, and finally only brine was flowed. With brine flow maintained at a high rate, oil flow was commenced at a low rate, and finally the oil to brine rate ratio was progressively increased to give relative permeability curves in the direction of increasing oil saturation.

Core B was treated in a similar manner.

A third core, C, was used for studying relative permeability of oil and gas in the presence of a constant amount of interstitial water. With the core in the restored state condition, desaturation was commenced using nitrogen, and the capillary pressure was increased in steps, with relative permeability measurements being taken at each point after equilibrium was attained. During this process, activity was measured at four positions along the core. Unfortunately, because of end diaphragm failure, only two oil relative permeability values could be obtained. After measurements at a capillary pressure of 4.5 psi, the nitrogen pressure was decreased to zero, oil was flowed through the core, and essentially all gas was removed by alternately increasing and decreasing the absolute pressure on the system. Dynamic studies were then begun by continuing oil flow at a high rate and starting gas flow at a low rate. Fine adjustment was obtained by means of a gas flow regulator.¹⁴ After equilibrium was attained and pressure and gas flow rate measurements were taken, the oil rate was reduced, which resulted in an increase in gas rate and a decrease in oil saturation. The time required to come to equilibrium after changing rates varied from one to five hours. Finally, gas only was flowed at an increased rate (242 ml/hr), and after equilibrium was attained, the oil flow rate was increased in increments, and relative permeability data were taken in the direction of increasing oil saturation.

In order to evaluate brine mobility, Alundum cores D and E, in which radioactive cesium was employed as a brine phase tracer, were flooded with active brine to minimum oil, and then were swept with inactive brine.

Alundum core F and natural core G were employed in oil-gas (in the presence of interstitial water) dynamic flow studies similar to those described for Core C. Oil-phase mobility observations are reported herein.

RESULTS AND DISCUSSION

Saturation History

It has been recognized that the nature and sequence of changes in fluid saturation in porous media play an important part in fluid flow behavior, and these changes, which have conveniently been described by previous workers¹⁵ as saturation history, should be considered when planning studies of

such phenomena. In such work it is desirable to duplicate as nearly as possible the reservoir saturation conditions before initiating fluid flow studies. In relative permeability experiments designed to simulate conditions attending oil production, the core saturation should be brought to the restored state condition.¹⁶ The correct saturation history permits the distribution of gas, oil and water in pores of the proper sizes. The distribution of the fluids within the pores appears to affect directly the relative permeability results, the pressure differences between the phases, the mobility of the fluids, the time necessary to reach equilibrium, and the quantity of oil which will remain in the residual state. To illustrate some of these effects, typical data are presented from relative permeability studies in which the radioactivity technique was employed to check saturation uniformity. These data rule out the possibility that the hysteresis effects could be attributed solely to non-uniformity in saturation.

The effects of the direction of the saturation change upon the dynamic displacement relative permeability curves obtained in studies of cores A and C are shown in Fig. 9 and 10. There is little difference in the oil relative permeabilities taken in the two directions in this example (Fig. 9), but there is a pronounced difference in the case of water. These results appear to be in agreement with those of Geffen, Owens, Parrish and Morse.¹⁵ Water is normally the wetting phase, which fact causes it to be held more tightly by the reservoir sands. It

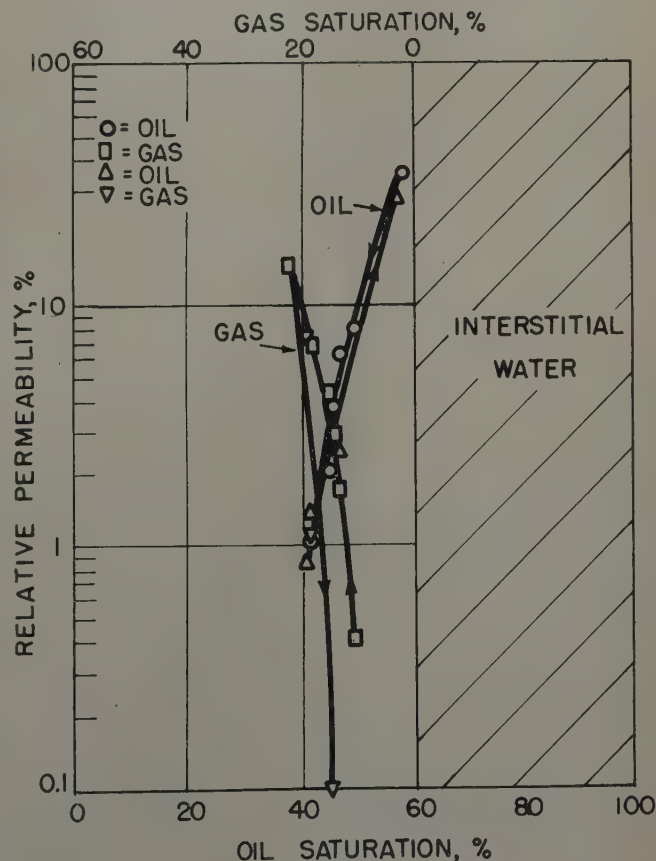


FIG. 10 — EFFECT OF THE DIRECTION OF SATURATION CHANGE ON RELATIVE PERMEABILITY, CORE C.

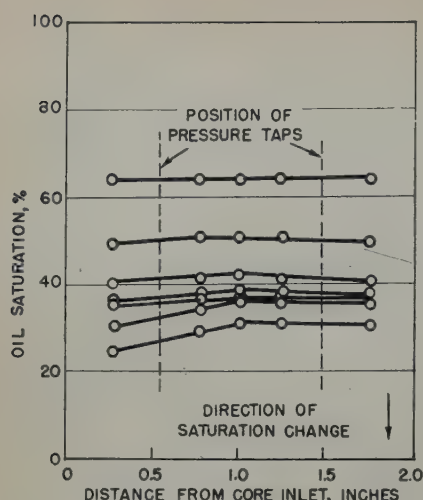


FIG. 11 — OIL SATURATION DISTRIBUTION DURING DYNAMIC TWO-PHASE FLOW OF OIL AND WATER IN CORE B.

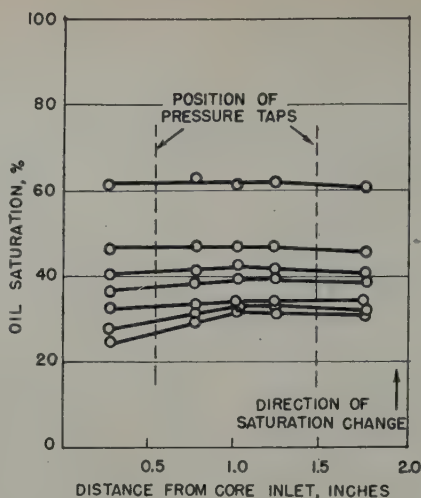


FIG. 12 — OIL SATURATION DISTRIBUTION DURING DYNAMIC TWO-PHASE FLOW OF OIL AND WATER IN CORE B.

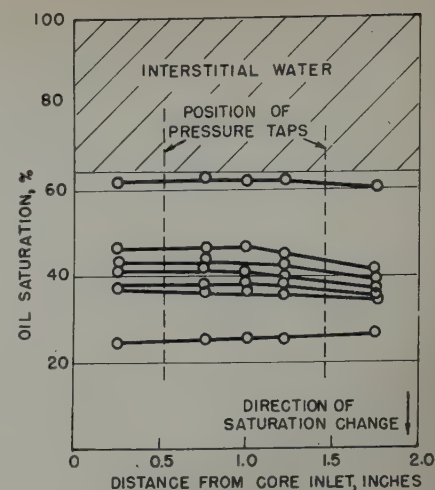


FIG. 13 — OIL SATURATION DISTRIBUTION DURING DYNAMIC TWO-PHASE FLOW OF OIL AND GAS IN CORE B.

was observed in water-wet sands that it was not possible after a certain saturation was reached by flowing oil and water at a given set of rates to duplicate the results by flowing at the same rates but in an opposite direction of saturation change. For example, in Fig. 9, a given set of oil and water rates resulted in a water saturation of 52.5 per cent during the direction of saturation change which represented oil production. The same oil and water rates resulted in a water saturation of 58.5 per cent when changing saturation in the opposite direction.

From Fig. 10 it can be seen that the effect of the direction of saturation change during gas and oil flow at interstitial water is quite pronounced. The relative permeability curve for gas during gas desaturation sharply approaches zero, probably because the gas phase becomes discontinuous.

From these observations the importance of changing the saturation in the proper direction according to reservoir conditions can be readily appreciated.

Saturation Distribution — Dynamic

In order to measure accurately effective permeabilities during multiphase flow studies it is necessary to attain uniformity of saturation throughout the test section of the core sample. It has been widely believed that the saturation distribution would not be uniform during dynamic two-phase flow of oil and water because of end effects. These effects may be very pronounced during brine desaturation, but as pointed out by Caudle, Slobod and Brownscombe,¹⁷ when oil is displaced by water the end effect is small in the dynamic method. The results of saturation distribution flow studies on core B are shown in Figs. 11 and 12. The greatest variation in saturation between the two pressure taps was four per cent, and this variation occurred at residual oil. It is probably more difficult to attain uniformity in saturation at or close to residual oil because the oil phase tends to lose continuity. The results show that there was no appreciable accumulation of water at the exit end of the core as might have been predicted from the fact that oil and water were emerging at the same outlet pressure. It should be noted that brine desaturation was started from residual oil (Fig. 12), and in our experience the end effect is not as pronounced as when desaturation is started from 100 per cent brine. After completing the saturation cycle from maximum oil to residual oil and back to maximum oil during two-phase flow of oil and water, two-phase flow of oil and gas at constant interstitial water was studied from maximum oil to residual oil. The saturation distributions during these flow studies are presented in Fig. 13. The greatest varia-

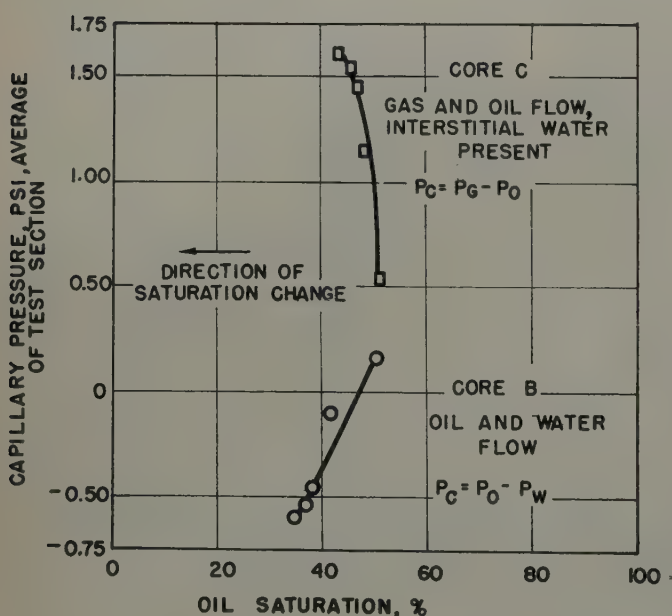


FIG. 14 — DYNAMIC CAPILLARY PRESSURE CURVES.

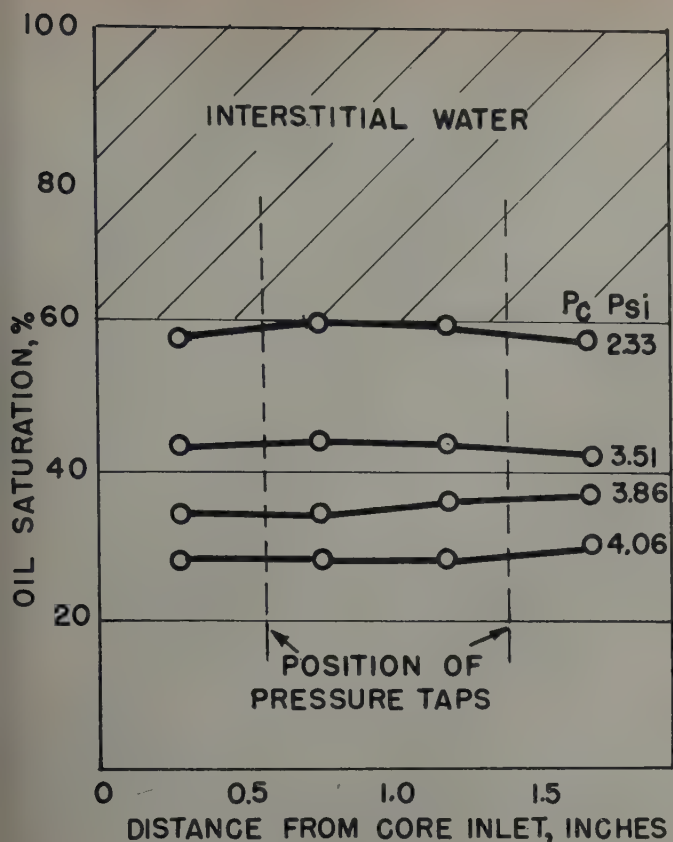


FIG. 15—SATURATION PROFILES DURING CAPILLARY DESATURATION WITH GAS OF CORE C.

tion in saturation in the test section during oil and gas flow was three per cent, which may have resulted from a slight accumulation of water at the outlet end of the core. Thus it can be seen that it is possible to attain fairly uniform saturation distributions during dynamic flow studies.

Any variation in the saturation distribution directly affects the pressure drops in the flowing phases. In most of the oil

and water flow studies reported herein, pressures and pressure drops were measured in each phase separately by means of water-wet diaphragms and open holes. If the saturation distribution were completely uniform throughout the core, the pressure drops in each phase should be identical. In all of the oil and water flow studies in which the pressure drops were measured separately in each phase only a slight variation in the measured readings was obtained at any steady state of flow. Core C was mounted with oil-wet side diaphragms and open holes as pressure taps to permit the measurement of pressure drops in the gas and oil phases separately. Again only a slight difference was found in the measured readings in the two flowing phases, which could be attributed to some variation in the saturation distribution. End effects are less important in dynamic flow systems than might be expected from static capillary pressure curves because the pressure differences between the flowing phases are small. In Fig. 14, dynamic capillary pressure curves for cores B and C are shown. In the first core the pressure difference between oil and water was determined during the saturation change from maximum oil to residual oil, and in this example the oil is, in effect, the wetting phase since it exists at a lower pressure than the water. This phenomenon may be related to hysteresis of the contact angle, and does not necessarily mean that the core material has changed in wettability properties. For core C, Fig. 14, the pressure difference between gas and oil at interstitial water was also determined in the direction of oil production. In this example the gas as expected performed as the non-wetting phase and existed at a slightly higher pressure than did the oil phase. The data support the conclusion that it is possible to attain uniformity of saturation during dynamic multiphase flow studies when the determinations are made across a test section in the center of the core.

Saturation Distribution — Capillary

Measurement of the saturation profile was advantageous in the capillary method in determining when the cores had come to capillary equilibrium. The saturation profiles were found to be quite uniform during desaturation, as was previously

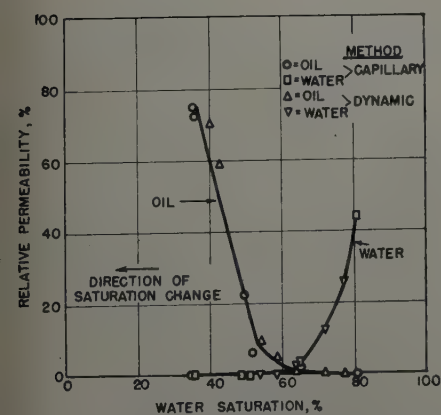


FIG. 16—COMPARISON BETWEEN CAPILLARY AND DYNAMIC RELATIVE PERMEABILITY METHODS, CORE A.

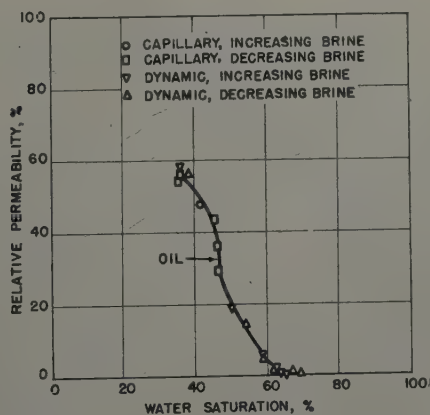


FIG. 17—RELATIVE PERMEABILITY TO OIL BY DYNAMIC AND CAPILLARY METHODS, CORE B.

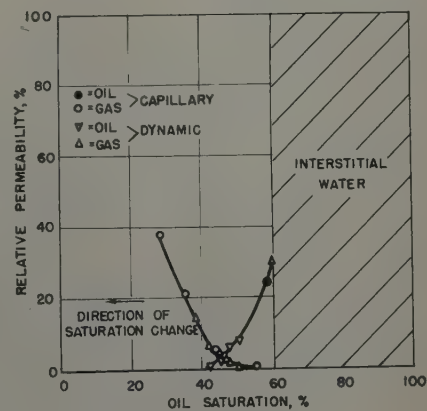


FIG. 18—COMPARISON BETWEEN CAPILLARY AND DYNAMIC RELATIVE PERMEABILITY METHODS, CORE C.

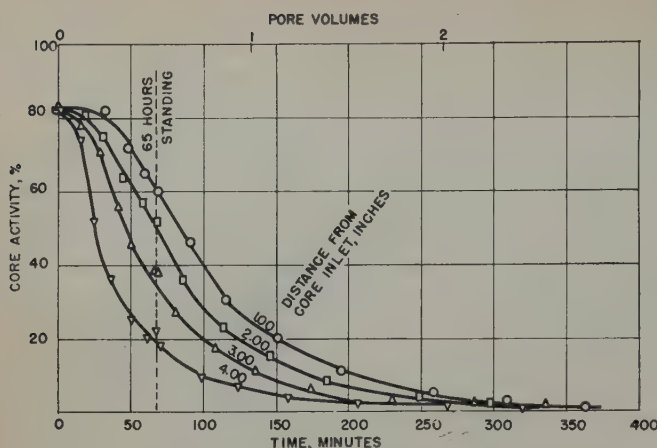


FIG. 19 — DECREASE IN ACTIVITY ON FLUSHING OF CORE D WITH INACTIVE BRINE.

shown by Morgan, McDowell and Doty⁴ for the oil-water system. Repeated desaturations of flooded cores starting from residual oil resulted in uniform profiles. In Fig. 15 data are presented for core C showing that saturation uniformity is also readily achieved during capillary desaturation of oil with gas.

Imbibition of water by cores which had been placed in the restored state was found in many cases to be exceedingly slow. In addition, the brine saturation was usually highest in the region near the core entrance. It is conceivable that if sufficient time were allowed, however, uniform saturation profiles might be obtained. It was concluded that because of the excessive time required, use of the capillary method is generally not practical for the oil-water system in the direction of increasing water saturations, although oil-water data need to be taken in that direction to reproduce reservoir conditions. It appears that data taken during a first desaturation from 100 per cent brine to interstitial water would not be pertinent.

Comparison Between the Dynamic and Capillary Methods

Osoba, Richardson, Kerver, Hafford and Blair¹⁸ made a comprehensive comparison of methods of relative permeability determination and found general agreement. However, it seemed desirable to supplement their work with a few experiments in which saturation and saturation uniformity were checked in the course of the measurements. An attempt was made to keep the method of saturation change the only variable.

Figs. 16, 17 and 18 show relative permeability curves obtained on each of three cores (A, B, and C) by both the dynamic and capillary methods. In each case the capillary method curves were obtained first, reducing the core to the restored state condition as the final step. Dynamic method curves were then obtained by introducing both phases to the inlet Aloxite distribution plate. Typical saturation profiles observed in this study have already been presented (Figs. 11, 12, 13 and 15). Oil-water relative permeability data are shown

in Fig. 16 for the direction of increasing oil saturation only. The capillary method was impractical in this case for measuring permeabilities in the direction of increasing brine, because imbibition did not occur at an acceptable rate. Therefore, it was water flooded to residual oil, and capillary method data were taken during a second brine desaturation. It seemed appropriate to compare these data with data taken by the dynamic method during a similar cycle. Results of the dynamic method studies for both directions of saturation changes have already been given (Fig. 9). It was noted that during dynamic displacement in the direction of increasing water saturation, the pressure in the water-phase exceeded that in the oil-phase. The fact that relative permeability curves can be measured rapidly by the dynamic method but not by the capillary method in the direction of increasing water saturation can be explained by these pressure differences. In other words, the saturation change is forced when the dynamic method is used.

Comparisons made with a short core (core B) are presented in Fig. 17. Data are shown for both directions of saturation change; however, only one point was obtained by the capillary method in the direction of increasing brine saturation. The effective brine permeabilities of this core were too low to permit any valid comparison.

Oil and gas relative permeability data determined by the dynamic and capillary methods (core C) are compared in Fig. 18.

Data obtained by the two methods are in substantial agreement. Because of a diaphragm failure on core C it was not possible to obtain, by the capillary method, as many points on the oil curve as would have been desired; a comparison of the data obtained by these two methods is of particular interest since it represents the only discrepancy for different methods reported by Osoba, Richardson, Kerver, Hafford and Blair.¹⁸

Mobility of Brine

Russell, Morgan and Muskat⁷ reported experiments indicating a high degree of mobility of interstitial water, but it was pointed out that diffusion might have played a part. Data

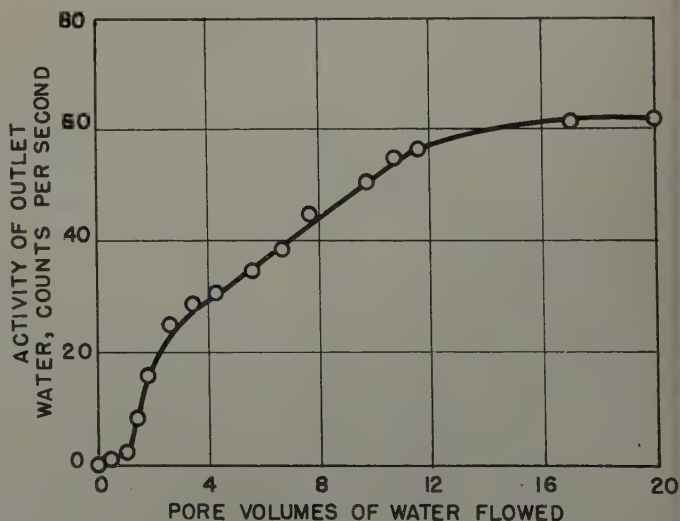


FIG. 20 — SORPTION OF RADIOACTIVE CESIUM FROM WATER FLOWED THROUGH SNOW FLOSS DIAPHRAGM.

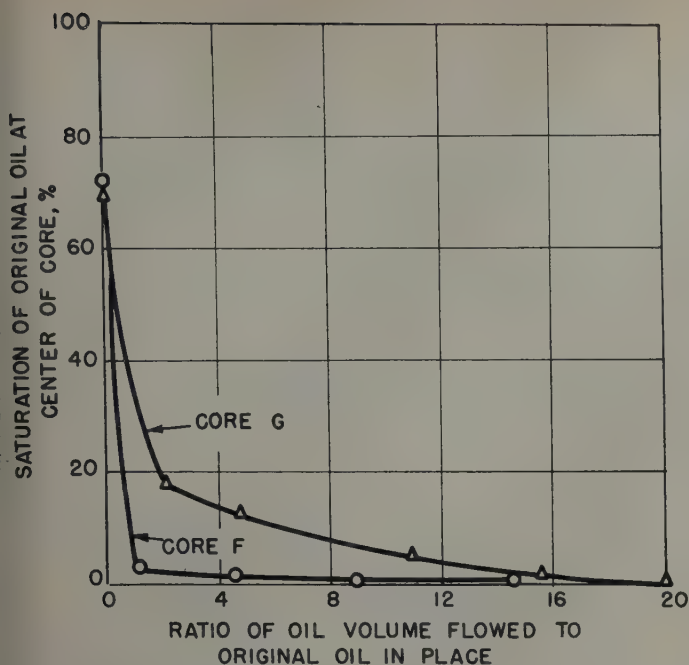


FIG. 21.—REPLACEMENT OF OIL BY FRESH OIL IN RESTORED STATE CORES F AND G.

on an Alundum core (core D) are presented in Fig. 19 confirming these results and indicating that diffusion played no significant part. In these tests core D, containing radioactive cesium in the brine phase was flooded with inactive brine. The decrease in activity at four key positions symmetrically placed along the core is shown. After flow of less than three pore volumes the activity was less than one per cent of the 100 per cent brine saturation value. After 68 minutes of flow, the core was allowed to stand 65 hours. On resumption of flow the activity-time curves continued without break. Diffusion would proceed during standing as well as during flow, and had any appreciable diffusion taken place resumption of flow should have caused a sudden drop in activity.

In the mobility test on Alundum core E, difficulty was encountered in flushing out the cesium 134. Even after 30 pore volumes of inactive brine had been flowed, the activity of the core remained 32 per cent of the original value, varying from 22 per cent at the inlet to 42 per cent at the outlet. This core had Snow Floss diaphragms at both ends; however, flushing through the open holes was also ineffective. Accordingly, a supplementary test was conducted in which a three per cent sodium chloride solution containing a tracer amount of cesium chloride was flowed through two Snow Floss diaphragms which were mounted in Lucite with an Aloxite disk between them. The brine which flowed out of the Snow Floss diaphragms passed through a counting cell, and the radioactivities of various portions were determined until the activity of the outgoing brine equaled the activity of the original brine solution. These results are plotted in Fig. 20, and they show that the radioactivity of the outgoing brine solution continued to increase until about 17 pore volumes had been flowed through the diaphragms. This study definitely demonstrates that Snow Floss diaphragms do not allow passage of cesium ions until a certain quantity has been sorbed in the Snow Floss. Distilled

water was then flowed in the opposite direction through the diaphragms until the radioactivity of the effluent was zero. It was necessary to flow about 30 pore volumes before reaching zero activity, and even then the activity of the mounted diaphragms remained quite high. Investigators should be alert to the possibility that sorption of ions in diaphragms might complicate flow studies in cores in which diaphragms are incorporated as part of the system.

Mobility of the Oil Phase

In some of the experiments reported herein, cores in the restored state were saturated with labeled oil by flowing the oil until it had completely replaced the unlabeled oil. The quantities of fresh oil necessary to remove the oil in place in an Alundum core (F) and in a natural core (G) are shown in Fig. 21. The difference in the required volumes of fresh oil in the two cores is probably directly related to the size distribution of the pores occupied by oil. The experimental results show that it takes about twice as much fresh oil to remove the oil in place in core G as compared to that for core F at maximum oil saturations. The effect of pore size distribution on the efficiency of replacement of oil can be more clearly noted in Fig. 22. In this example the oil saturation of core G was reduced to residual oil by flowing gas. It may be inferred that at this saturation the size distribution of the pores occupied by oil was probably much narrower than in the previous example at maximum oil and interstitial water saturation because the gas had displaced the oil from the larger pores. Fig. 22 shows that it was possible to remove all of the oil in place by flowing only about one-twentieth as large a volume of oil as required at maximum oil. The mech-

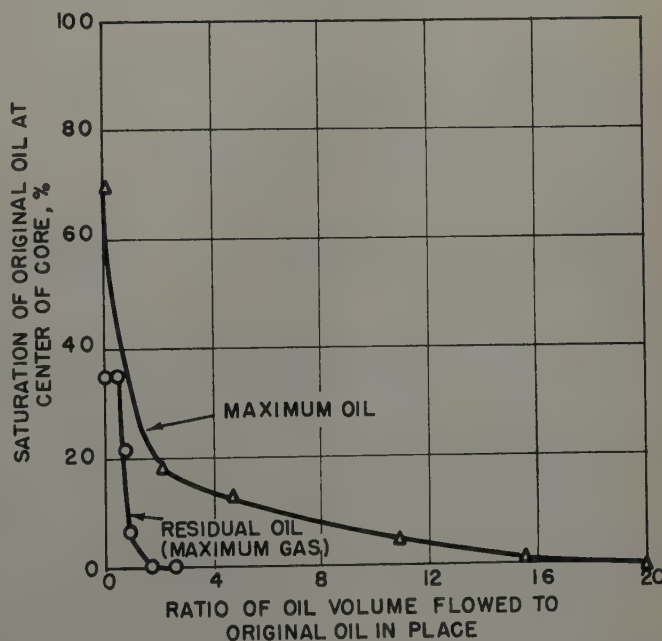


FIG. 22.—REPLACEMENT OF OIL BY FRESH OIL IN CORE G AT TWO SATURATIONS.

anism of displacement of fluids in pores is very important and deserves careful consideration in flow studies. The results obtained indicate that all of the oil in an oil sand is mobile, but that the degree of mobility depends on the size distribution of the pores occupied by oil, which in turn is dependent on the previous history.

CONCLUSIONS

1. An improved method of determining core saturation by means of radioactivity has been developed.

2. Iodo¹³¹benzene was demonstrated to be a suitable oil phase tracer.

3. That the radioactive tracer method is well adapted to the study of the mobility of the fluid phases has been established. Oil phase mobility has been found to vary greatly. This is believed to depend on the size distribution of pores occupied by the oil.

4. The dynamic displacement method, as employed in this work, has been shown to be a suitable method of relative permeability determination, giving uniform saturation and uniform pressure drops in the separate phases. The dynamic displacement method is to be preferred over the capillary method for the oil-water system since uniform profiles can be more easily attained as the water saturation is increased from the restored state condition. The greater rapidity and simplicity of the method are attractive.

ACKNOWLEDGMENTS

The authors wish to thank the management of the Union Oil Co. of California for permission to publish this report and the many members of the Research Department who aided in the experimental work.

REFERENCES

- Henderson, J. H., and Yuster, S. T.: "Relative Permeability Studies," *Prod. Monthly*, (Jan., 1948) 12, 13.
- Boyer, R. L., Morgan, F., and Muskat, M.: "A New Method for Measurement of Oil Saturation in Cores," *Trans. AIME*, (1947) 170, 15.
- Laird, A. D. K., and Putnam, J. A.: "Fluid Saturation in Porous Media by X-Ray Technique," *Trans. AIME*, (1951) 192, 275.
- Morgan, F., McDowell, J. M., and Doty, E. C.: "Improvements in the X-Ray Saturation Technique of Studying Fluid Flow," *Trans. AIME*, (1950) 189, 183.
- Holmgren, C. R.: "Some Results of Gas and Water Drives on a Long Core," *Trans. AIME*, (1949) 179, 103.
- Brunner, E., and Mardock, E. S.: "A Neutron Method for Measuring Saturations in Laboratory Flow Experiments," *Trans. AIME*, (1946) 165, 133.
- Russell, R. G., Morgan, F., and Muskat, M.: "Some Experiments on the Mobility of Interstitial Waters," *Trans. AIME*, (1947) 170, 51.
- Coomber, S. T., and Tiratsoo, E. N.: "The Application of Radioactive Tracer Techniques to the Study of the Movement of Oil in Sands," *Jour. Inst. Pet.*, (1950) 36, 543.

9. Albaugh, F. W.: Unpublished work.

10. Nahin, P. G., Merrill, W. C., Grenall, A., and Crog, R. S.: "Mineralogical Studies of California Oil-Bearing Formations, I—Identification of Clays," *Trans. AIME*, (1951) 192, 151.

11. Showalter, W. E.: "Mounting Core Analysis Specimens in Thermoplastic," *Jour. Pet. Tech.*, (Dec., 1950) 2, No. 12, 8.

12. Hassler, G. L.: "Method and Apparatus for Permeability Measurements," U. S. Patent 2,345,935.

13. Morse, R. A., Terwilliger, P. L., and Yuster, S. T.: "Relative Permeability Measurements on Small Core Samples," *Prod. Monthly*, (Aug., 1947) 11, No. 10, 19.

14. Rose, Walter: "Packless Valve Flow Regulator," *Rev. Sci. Inst.*, (1950) 21, 772.

15. Geffen, T. M., Owens, W. W., Parrish, D. R., and Morse, R. A.: "Experimental Investigation of Factors Affecting Laboratory Relative Permeability Measurements," *Trans. AIME*, (1951) 192, 99.

16. Welge, H. J.: "Displacement of Oil from Porous Media by Water or Gas," *Trans. AIME*, (1949) 179, 133.

17. Caudle, B. H., Slobod, R. L., and Brownscombe, E. R.: "Further Developments in the Laboratory Determination of Relative Permeability," *Trans. AIME*, (1951) 192, 145.

18. Osoba, J. S., Richardson, J. G., Kerver, J. K., Hafford, J. A., and Blair, P. M.: "Laboratory Measurements of Relative Permeability," *Trans. AIME*, (1951) 192, 47.

19. Lucas, H. J., and Kennedy, E. R.: *Organic Syntheses*, Collective Volume II, 351.

APPENDIX A

Preparation of Iodo¹³¹benzene

Benzenediazonium chloride solution was prepared according to the procedure of Lucas and Kennedy¹⁹ in a 200 ml three-necked flask using 1/50 of all given quantities. One hundred ml of solution was obtained and stored at 0°F for use as needed.

The sodium iodide was received from Oak Ridge in a concentration of about 20 millicuries/ml. A quantity of 25 or 50 millicuries was generally employed. The iodine was carrier free and the calculated weight was less than one-millionth of a gram; about 30 mg of solid potassium iodide was added as carrier. A volume of concentrated hydrochloric acid equal to one-fourth the volume of active solution was added, the reaction being carried out in the bottle received. One ml of the benzenediazonium chloride solution was added, the mixture agitated gently, and let stand overnight. The diazo solution was kept cold, but it was found unnecessary to cool the iodide solution, at least not when the volume was less than two ml.

The iodobenzene was extracted with the oil to be labeled. It does not dissolve as readily as might be expected. The contents of the small shipping bottle were rinsed into an eight-oz. bottle with four 5-ml portions of oil and one 5-ml portion of water, and then the large bottle was rolled for one hour. The water layer was separated, and free iodine removed by washing the oil solution with 10 ml of five per cent sodium bisulfite solution, agitating until all purple color was removed from the oil. The sulfite solution was drawn off and the oil diluted to the desired volume. Nearly always over 90 per cent of the activity received was found to be in the oil phase. ★ ★ ★

ENGINEERING STUDY OF THE COOK RANCH FIELD, SHACKELFORD COUNTY, TEXAS

WALLACE W. WILSON, CONTINENTAL OIL CO., PONCA CITY, OKLA., MEMBER AIME

ABSTRACT

The Cook Ranch Field produces from a very permeable lens of Cook Sand of lower Permian or upper Pennsylvanian age, occurring at an average depth of 1,300 ft. The field was discovered in 1926, and has been operated with low pressure gas injection since July, 1927, one of the first such projects in Texas. Cumulative recovery to Dec. 31, 1950, was 14,701,131 bbl of crude oil, an average of 1,013 bbl per acre-ft of oil section, and 72.5 per cent of the oil originally in place. Analysis of the reservoir performance indicates that gravity drainage has been an important factor in the producing mechanism. The high permeability and uniformity of the reservoir were extremely favorable for this type of operation.

Pendleton, Inc., and Continental Oil Co., and has been operated by Roeser and Pendleton, Inc., since it was discovered. This study has been made possible through the cooperation of Roeser and Pendleton, Inc., in making available a remarkably complete set of records covering all phases of their operations. The purpose of this paper is to present a summary of the history of the operations through Dec. 31, 1950, and to analyze some of the factors which appear to be responsible for the success of the project. Information concerning the physical plant and the early gas injection history has been presented in an earlier paper.¹

RESERVOIR CHARACTERISTICS

Production in the Cook Ranch Field is from a large lens of Cook Sand, of lower Permian or upper Pennsylvanian age, occurring at an average depth of 1,300 ft. The average dip of the sand body, as shown in Fig. 1, is only about 50 ft per mile to the northwest. The reservoir has an area of 950 acres and contains 15,512 acre-ft of sand, consisting of about 14,512 acre-ft of productive oil zone, and an estimated 1,000 acre-ft of primary gas-cap. The isopachous map (Fig. 2) was prepared from drillers' logs. Recent coring in the

field has proven these logs to be quite accurate. The productive limits of the field are defined by shale on all sides but the southwest where a small zone of edgewater was encountered. This water does not appear to have encroached into the reservoir, and water production has been small. A smaller producing area to the south of the Cook Ranch Field also produces from the Cook Sand, but is separated from the reservoir under consideration by a band of shale.

The sand consists of well sorted, coarse grained, rounded and subangular quartz fragments, very poorly cemented. The analysis of 46 chip-core samples from two recently completed test wells indicates a range of porosity values between 12.5 and 28.2 per cent, with an arithmetic average of 24.0 per cent. Air permeability values range between 50 and 2,300 md, with an arithmetic average of 1,200 md. The reservoir where cored is a solid sand body, with no discernible major shale breaks or impermeable streaks. Vertical permeability appears to be of the same magnitude as the horizontal permeability. A core of the Cook Sand was cut in the smaller field to the south, using lubricating oil as drilling fluid. The connate water content of the sand in this core was found to average about ten per cent, and the porosity and permeability were comparable with the values reported above.

No analysis was made of subsurface or recombined hydrocarbon samples,

INTRODUCTION

The Cook Ranch Field is the largest of a number of relatively small, shallow producing areas near Albany, in Shackelford County, Texas. This field is one of the first to be operated by gas injection in Texas, and probably is the most successful low pressure gas injection project ever attempted. The field is owned entirely by Roeser and

¹References given at end of paper.

Manuscript received in the Petroleum Branch office Aug. 18, 1951. Paper presented at the Petroleum Branch Fall Meetings in Oklahoma City, Okla., Oct. 3-5, 1951, and in Los Angeles, Calif., Oct. 25-26, 1951.

and no bottom-hole pressure measurements were made. The original API gravity of the produced oil averaged about 39°, and currently is about 37°. The early production records suggest a solution GOR of about 400 cu ft per bbl. The cumulative net produced GOR on Dec. 31, 1950, was 396 cu ft per bbl. The original formation volume factor is assumed to have been about 1.20, and now is approximately 1.05. The initial stock-tank oil content of the reservoir is

calculated to have been 20,273,264 bbl, or 1,397 bbl per acre-ft.

HISTORY OF DEVELOPMENT

The field was discovered Feb. 19, 1926, with the completion of the Roeser and Pendleton, Inc.-Marland Oil Co. W. I. Cook "A" No. 1, in Section 85. This well was completed at a total depth of 1,242 ft for an initial flowing

production of 1,000 B/D of 39° API oil, after penetrating only one ft of the Cook Sand. The development of the field was rapid, and by the end of 1929, 213 wells had been completed. The peak oil production was reached in December, 1926, when the total monthly oil production was 264,785 bbl from 112 wells. A natural gasoline plant of the absorption type was installed and placed in operation in September, 1926, to serve the Cook Ranch Field and sev-

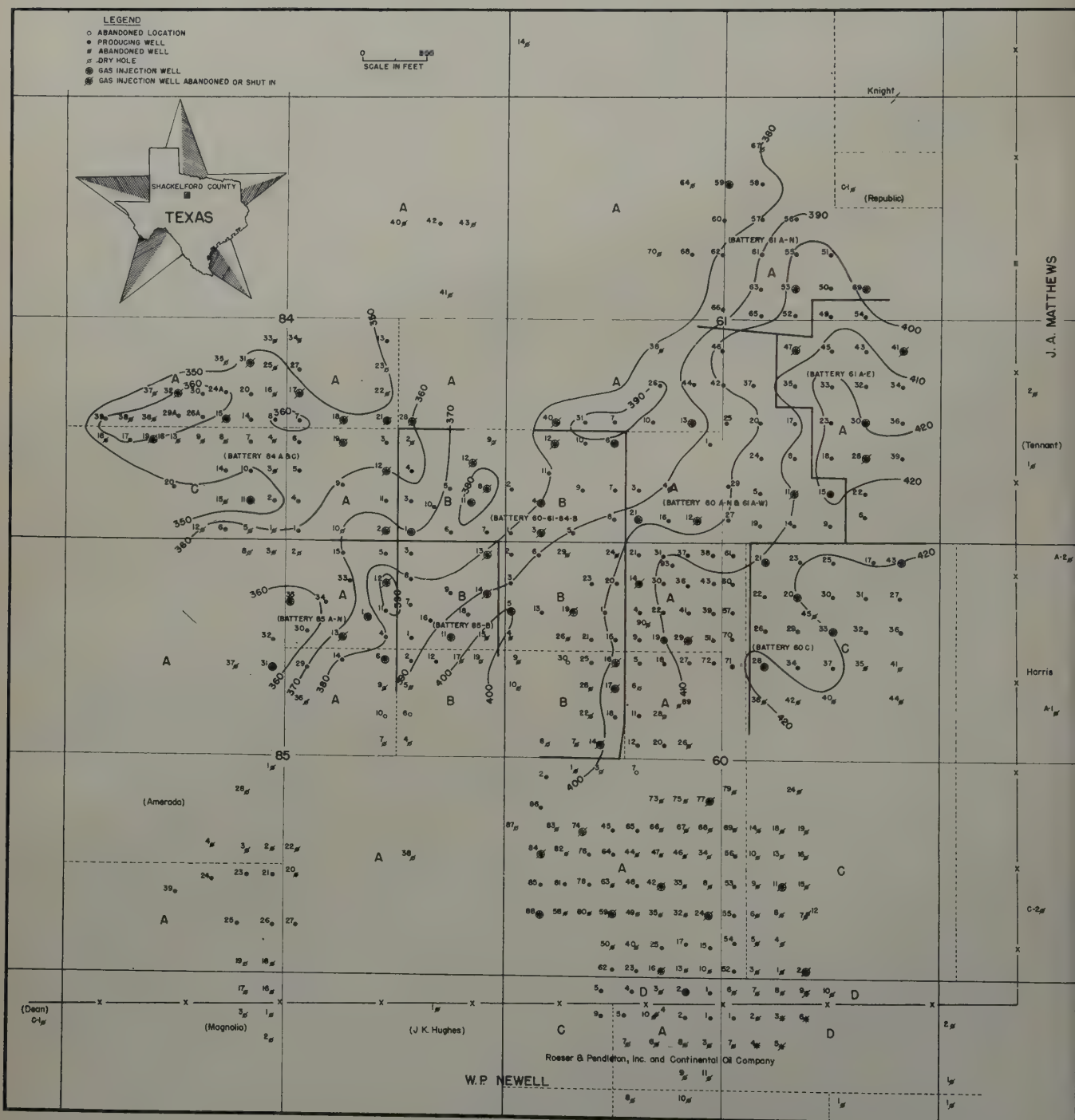


FIG. 1 — STRUCTURAL CONTOUR MAP OF TOP OF COOK SAND.

eral smaller nearby fields. After successful experiments with a portable compressor, facilities were installed in the gasoline plant for compressing fractionator vapors and residue gas at pressures up to 400 psi, and gas injection was started July 15, 1927.

The operators realized the importance to the success of the project of maintaining a complete set of records on all phases of the operation, and set

up special gauging and metering facilities for this purpose. As originally developed, the field was divided into 12 tank battery areas, numbered according to lease ownership and location. Each battery area was provided with equipment to measure continuously the produced gas and oil from the area. A small test tank and trap also were installed in each area to enable frequent periodic tests to be made of each well.

A system of well test files and production graphs was set up in order to use the information in observing the reservoir performance.² Several of the batteries have been combined from time to time for economical operation; eight batteries were in operation on Dec. 31, 1950.

The unit type of operation of the field has permitted more flexible operating conditions than otherwise could be

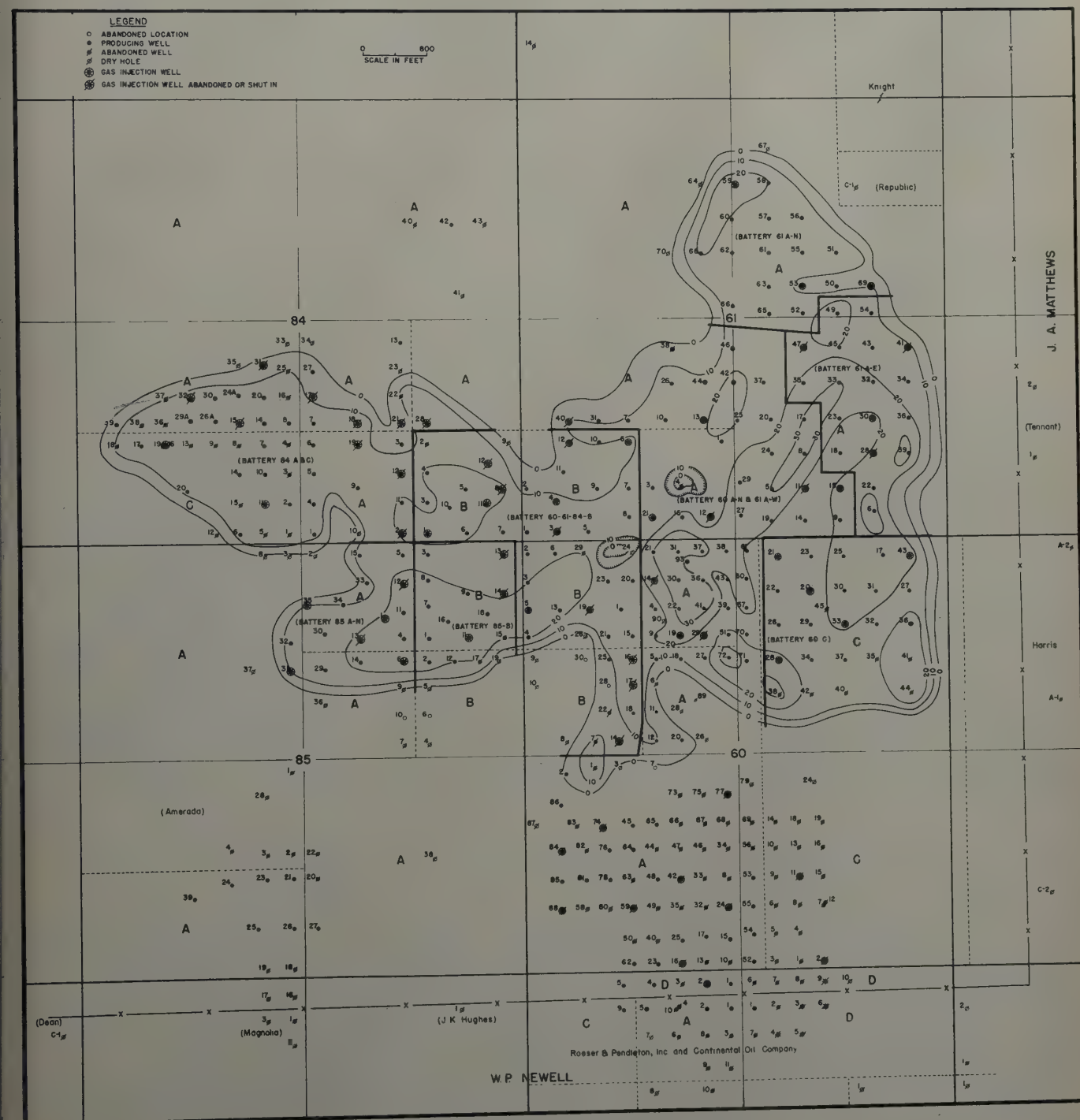


FIG. 2 — ISOPACHOUS MAP OF COOK SAND.
PETROLEUM TRANSACTIONS, AIME

achieved. The operator thereby was enabled to inject gas at the most advantageous locations, and to effect a substantial control of producing gas/oil ratios by shutting in wells where desired. The number and location of gas injection wells have changed from time to time, as dictated by well performance and gas supply. A total of 56 wells have been used for injection, not over 29 of which were operated simultaneously. Cumulative injection volumes for individual wells range from one million to 1.4 billion cu ft of gas. Wellhead injection pressures are not available; pressures at the plant have been maintained at between 250 and 375 psi.

RESERVOIR PERFORMANCE

Table I is a summary of the production and gas injection statistics through Dec. 31, 1950. The cumulative oil production is 14,701,131 bbl, an average of 15,475 bbl per acre or 1,013 bbl per acre-ft of productive oil section. A total of 46,558,446 gal of natural gasoline has been recovered from the produced gas, making a total liquid product recovery of 15,809,665 bbl. The cumulative volume of injected gas is 27,481,295 Mcf, averaging 1,772 Mcf per acre-ft of gross sand.

The performance of the entire reservoir is shown graphically in Fig. 3. With unrestricted production and a rapid development program under way, the oil production increased rapidly during 1926 to a peak of nearly 265,000 bbl for December of that year. In the early part of 1927, unsettled market conditions prevailed which necessitated a short period of voluntary proration between May and November, 1927. No wells were completed during that time, although a number of wells were drilled to the top of the sand and were allowed to remain uncompleted until the latter

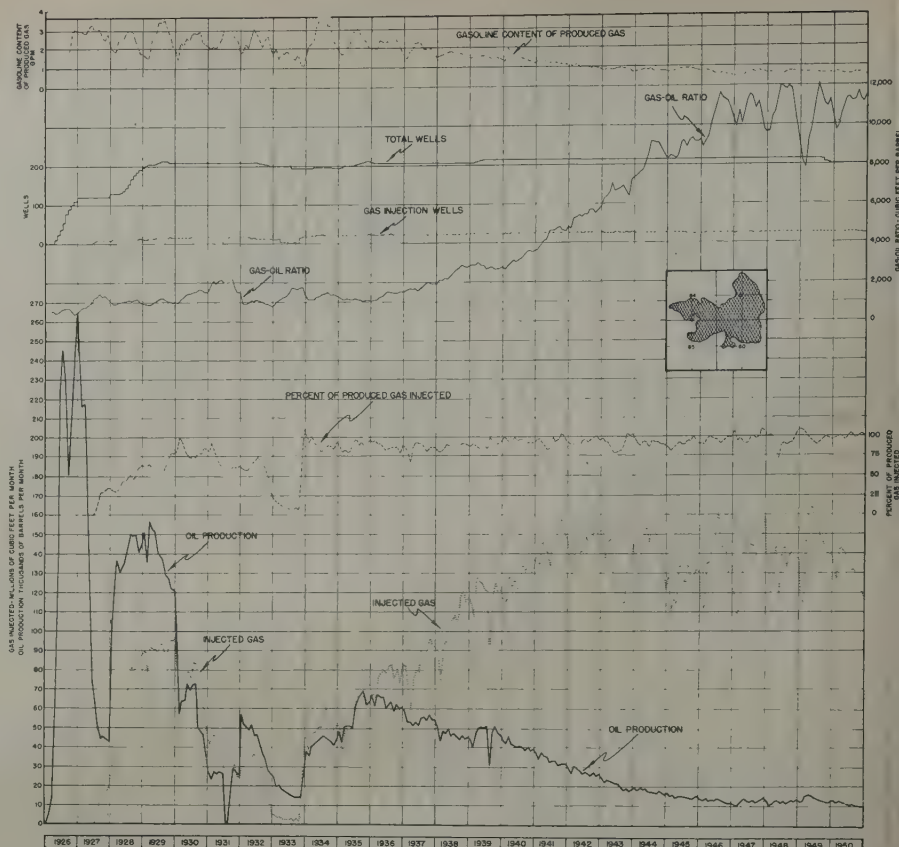


FIG. 3 — RESERVOIR PERFORMANCE, COOK RANCH FIELD.

part of 1928. The rapid decline during most of 1927 evidently was not all due to proration, however, as a decline was evidenced before proration began. Gas/oil ratios exceeded 5,000 cu ft per bbl during the latter half of 1927 at Battery 85B (Fig. 11) and Battery 85A-N (Fig. 10). Gas injection was started July 15, 1927. During the latter part of 1927 and throughout 1928 and 1929, an average of less than half of the produced gas was injected, and 90 new wells were completed. As a result of these factors, the oil production exceeded 157,000 bbl in March, 1927,

after which a high decline rate again was established. A second period of proration began Jan. 23, 1930, and continued through 1931. It is difficult to estimate the effect of the injected gas on the oil production rate during 1928 and 1929, but it is significant that the shapes of the oil production and injected gas curves are very similar. It seems probable that the injection of only a relatively small volume of gas during the early productive life of this highly permeable reservoir stimulated the production rate substantially. Throughout 1930 and 1931, the volume

Table I — Summary of Operations to December 31, 1950

Battery	Productive Area Acres	Reservoir Volume Acre-Ft.	Cumulative Production			Oil Recovery Bbl./Acre	Oil Recovery Bbl./Acre-Ft. Gas Injected (Oil Zone)	Gas Injected Mcf	Gas Injected Mcf/Acre-Ft.	Cumulative Produced Gas-Oil Ratio	Cumulative Net Produced Gas-Oil Ratio	Cumulative Produced Gas Injected Per Cent	
			Gas Mcf	Oil Barrels	Natural Gasoline Gallons								
60A-N and 61A-W	232.7	4,112.1	7,129,399	3,722,464		15,997		5,452,260	1,326		1,915		76.5
60C-N	107.2	2,102.3	2,630,551	696,617		6,498		2,770,358	1,318		3,776		105.3
60-61-84B	154.8	2,286.1	6,075,689	2,372,559		14,215		5,146,891	2,251		2,561		84.7
61A-N	87.9	1,213.3	4,673,908	1,474,376		16,773		3,017,302	2,487		3,170		64.6
61A-E	90.0	1,717.0	3,285,660	1,757,834		19,531		3,471,071	2,022		1,869		105.6
84A and C	168.5	2,123.2	3,185,757	1,826,546		11,679		2,678,762	1,262		1,744		84.1
85A-N	59.8	939.6	3,327,615	1,447,265		24,202		3,525,036	3,752		2,299		105.9
85B	49.1	1,018.4	2,990,470	1,403,470		25,584		1,419,615	1,394		2,131		47.5
Total Field	950.0	15,512.0*	33,299,049	14,701,131	46,558,446	15,475	1,013	27,481,295	1,772	2,265	396		82.5
*Oil Section: 14,512 Gas Cap: 1,000													

*Oil Section: 14,512
Gas Cap: 1,000

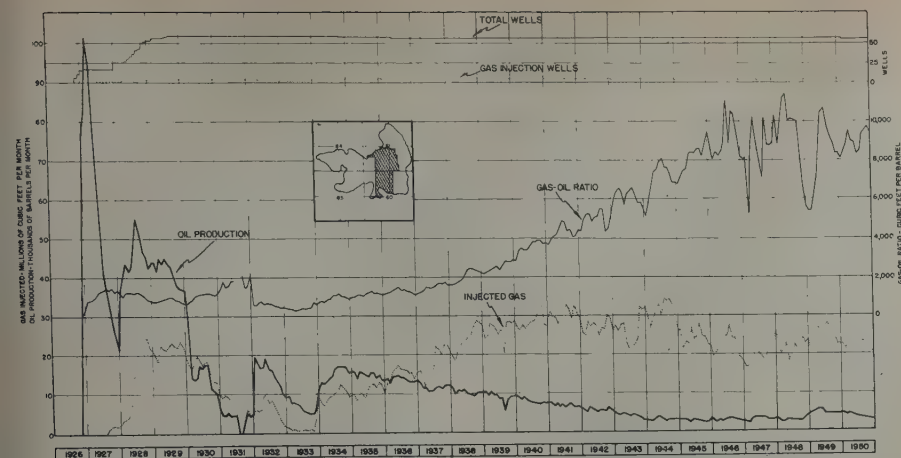


FIG. 4 — RESERVOIR PERFORMANCE, BATTERY 60A-N AND 61A-W.

of gas injected decreased as successive cuts were made in the allowable production, but a higher percentage of the produced gas was being returned to the reservoir. The shapes of the oil production and injected gas curves are remarkably similar during this period. Following the complete shutdown during July and August, 1931, gas injection again was started, and the oil production rate was increased after proration was terminated in January, 1932. During the latter part of 1932, the supply of residue gas available for injection decreased rapidly, and the oil production rate declined at about the same rate. In November, 1933, arrangements were made to purchase dry gas from another area, and the injection rate was stepped up greatly. The similarity between the oil production and injection rate was decreased, and the is striking, and it is believed that substantially all of the oil production after this date is attributable to the gas injection operations. Following this date the volume of gas injected has been maintained approximately equal to the volume produced.

It is interesting to note that the produced GOR increased gradually during the first half of 1927 as the oil production declined rapidly, which would be expected of solution gas-drive depletions. Following the injection of gas, however, the produced GOR declined and remained at about 1,000 cu ft per bbl until 1930 and 1931, when the gas injection rate was decreased, and the GOR increased to about 2,000. This cycle was repeated between 1932 and 1933, when gas injection was curtailed because of a diminishing gas supply. In the early part of 1936, however, the produced GOR started to increase again,

and the upward trend has been consistent since that time.

The produced gas enrichment curve shows the characteristic seasonal variations through 1935, but the average enrichment declined perceptibly during 1936 and continued to decrease steadily to about 0.5 GPM in 1950, as increasingly large quantities of dry gas were cycled through the reservoir.

Battery 60A-N and 61A-W is the largest of the eight producing areas in the field, and was formed by combining two batteries in 1935. The southern half of the area was developed largely in 1926 and early in 1928; the northern half was developed in the latter part of 1928 and during 1929. The difference in the magnitude of flush production of each area is readily apparent in Fig. 4. The average initial potential of wells in the southern half was 387 B/D; in

the northern half the average initial potential was 94 B/D, which may indicate poorer sand conditions or significant drainage from that area before it was drilled. The oil production curve shown closely parallels the injected gas curve, especially from 1930 on. No explanation is suggested for the increase in oil production and the corresponding decrease in GOR in 1948 and 1949.

Battery 60C-N (Fig. 5) is located structurally in the highest part of the field, and the reservoir in this area contained a primary gas-cap which appears to have occupied about half of the reservoir volume served by this battery. The initial potentials of the wells in this area were generally lower than in the offsetting batteries, and the gas/oil ratios were higher. Nine of the wells, drilled in September and October, 1928, were shut in before the end of the year because of low oil production and gas/oil ratios in excess of 3,000 cu ft per bbl. The cumulative oil recovery from this battery to December 31, 1950, was only 6,498 bbl per acre. This low recovery is largely attributable to the presence of only a thin oil section in this battery, but also may have been partially the result of drainage before the area was drilled.

Battery 60-61-84B was formed by the successive combination of three of the original batteries during 1929 and 1950. The performance curves of this area (Fig. 6) are similar in most respects to those of the entire field shown in Fig. 3. The GOR of this battery also was affected favorably by the gas injection prior to the time of major gas breakthrough in 1936. After 1936, however, the GOR increased rapidly to the current average of about 30,000 cu ft per

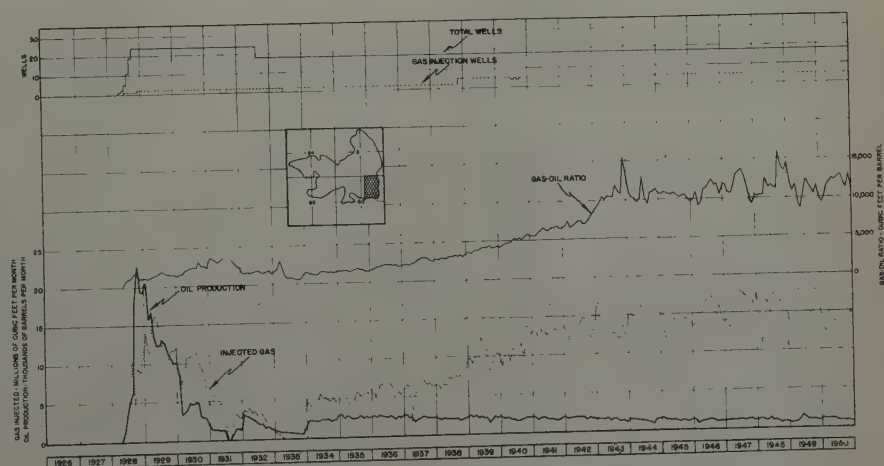


FIG. 5 — RESERVOIR PERFORMANCE, BATTERY 60C-N.

bbl, the highest values for any battery in the field. The portion of this battery lying in Section 60 has produced over 60 per cent of the total oil recovered, and contains about 40 per cent of the total area of the battery.

Battery 61A-N (Fig. 7) was developed during the latter part of 1935, nine years after the field was discovered. This 107.2-acre area has produced 1,474,376 bbl of oil, which indicates that substantial drainage from the area did not occur. Two former gas injection wells, located near the southern edge of this battery, were in operation early in 1930. A cumulative volume of over 260,000 Mcf of gas was injected through those wells between 1930 and the time development started in 1935, which probably minimized the drainage from the Battery 61A-N area. Some of the first wells completed in this area produced initially at very low gas/oil ratios, in the order of 50 cu ft per bbl, but the initial produced GOR of the entire area was not much lower than the other batteries which were developed in 1926 and 1927. Gas injection was started in the battery in 1936, and the oil production rate after the middle of 1936 appears to have been affected materially by the injection operations.

The production histories of Batteries 61A-E (Fig. 8) and 84A&C (Fig. 9) illustrate the effect of reducing the gas injection rate after substantial gas breakthrough has occurred. The injection rates in both areas were reduced when the produced GOR reached about 10,000 cu ft per bbl, with little, if any, apparent effect on the oil production rate. In Battery 61A-E, the average injection rate was reduced only about one-third, with little effect on the GOR trend. In Battery 84A&C, the injection rate was reduced by about two-thirds, which resulted in a substantial immediate reduction in GOR followed by a more gradual rate of increase during the last ten years of operation.

Battery 85A-N (Fig. 10) is the area in which the discovery well of the field is located. This battery was one of the first to be developed, and the peak oil production of 63,712 bbl during June, 1926, was followed by a rapid decline. The produced GOR increased rapidly in July and August, 1927, to a peak value of 5,547 cu ft per bbl, but declined to an average of about 1,100 cu ft per bbl as the rate of gas injection was increased. The oil production rate appears to have been controlled by the injection rate almost as soon as gas injection was started, until 1939. Nine new producing wells were drilled in a westward extension of the field during

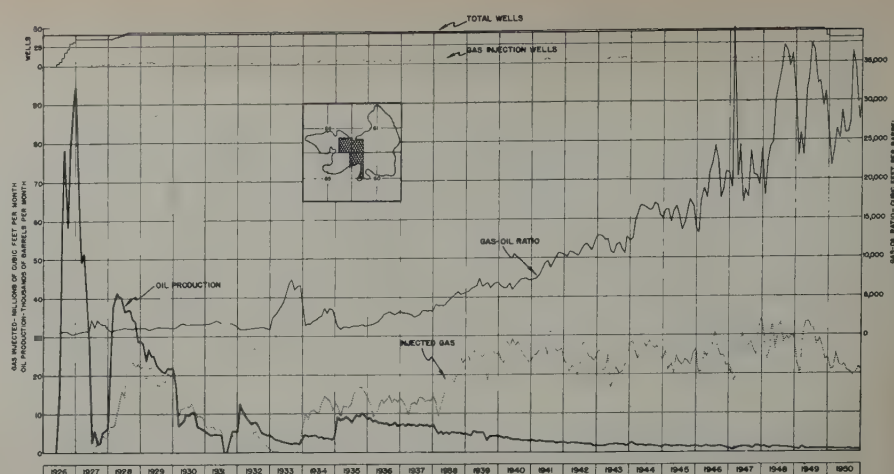


FIG. 6 — RESERVOIR PERFORMANCE, BATTERY 60-61-84B.

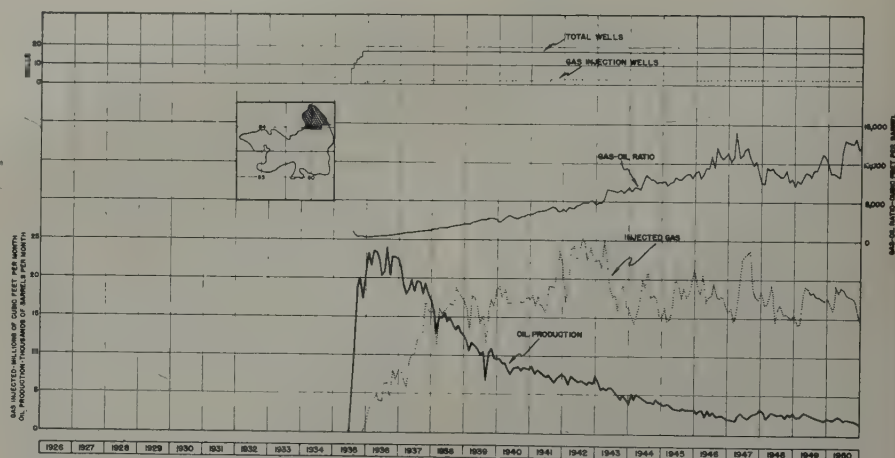


FIG. 7 — RESERVOIR PERFORMANCE, BATTERY 61A-N.

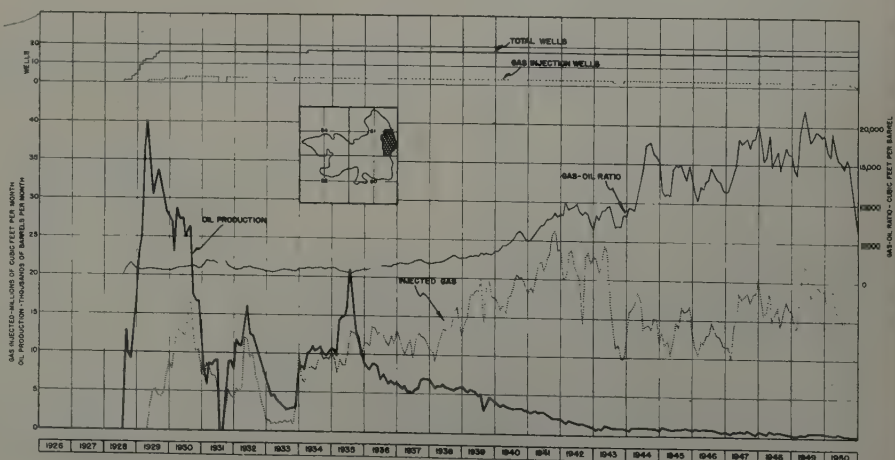


FIG. 8 — RESERVOIR PERFORMANCE, BATTERY 61A-E.

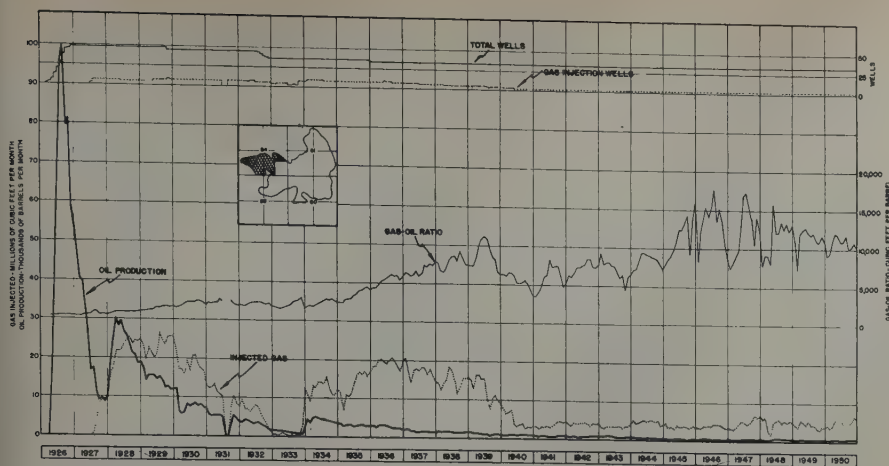


FIG. 9 — RESERVOIR PERFORMANCE, BATTERY 84A AND C.

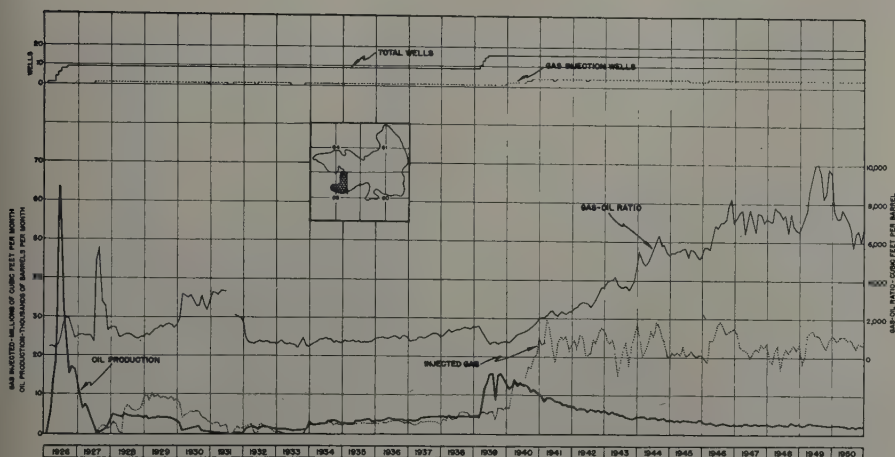


FIG. 10 — RESERVOIR PERFORMANCE, BATTERY 85A-N.

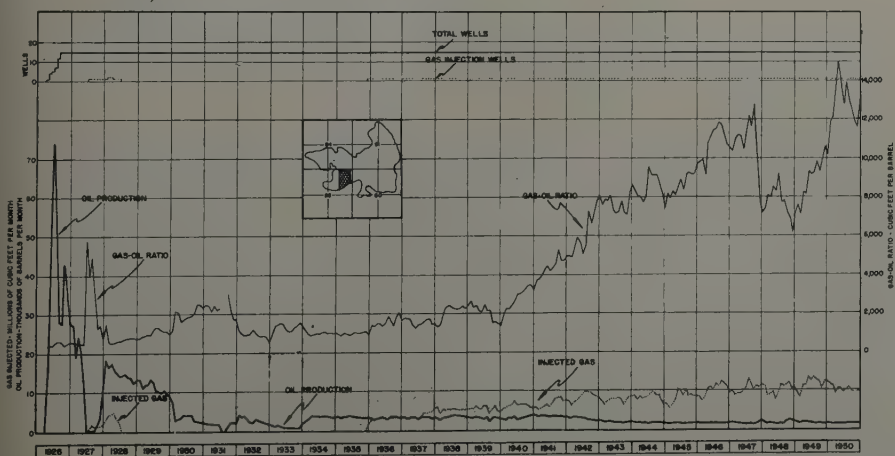


FIG. 11 — RESERVOIR PERFORMANCE, BATTERY 85B.

1939, which caused an immediate increase in oil production. During 1940, the gas injection rate was stepped up and the GOR began to increase rapidly. The effect of the increased gas injection rate on the oil production rate is difficult to determine, and may not have been significant.

Battery 85B (Fig. 11) was developed about the same time as 85A-N, and also sustained an early peak production followed by a rapid decline. The produced GOR increased sharply in June, 1927, and remained above 4,000 cu ft per bbl for three months. Only one well in this area was used for gas injection initially, and the volumes injected were small. Three other nearby wells in offsetting battery areas were used for gas injection beginning in 1927 and 1928, and the operation of these wells undoubtedly contributed to the greatly increased oil production rate early in 1928 and the slow decline rate after gas injection within the battery was stopped. This appears to be confirmed by the increase in production which occurred in early 1934 when supplies of outside gas became available to augment the injection rate. When the injection of gas within the battery was resumed during 1936, two of the three nearby injection wells were shut in, and the sustained oil production rate appears to have been the result of renewed injection within the area.

EVALUATION OF RESULTS

Five test wells have been drilled during the last three years to assist in evaluating the results of the gas injection operations. Well No. 93, in Battery 60A-N and 61A-W, was drilled midway between four old producing wells in November, 1948, and was completed with an initial potential of 23.8 B/D. Well No. 45, in Battery 60C-N, also was drilled between four older wells, and was completed and abandoned in December, 1948, as a dry hole, with an estimated gas potential of 150 Mcf/D. Neither of these wells was cored. Two additional test wells were drilled during August and September, 1951, and one was being drilled as this paper was prepared. The chip-core³ analysis results from well No. 91 in the southern part of Battery 60A-N and 61A-W, are shown in Table II. It will be noted that the bottom five feet of sand at this well has an average oil saturation of 40 per cent while the upper 27 feet has an average oil saturation of only 18 per cent. This well at last report was pro-

ducing 20 B/D at an average GOR of 5,300 cu ft per bbl. The other test well, in Battery 60-61-84B, was cored through substantially dry sand and was plugged as a dry hole.

An analysis of the reservoir performance curves and the core analysis results indicates that gravity drainage across the bedding plane of the sand body has been a very important factor in the oil recovery mechanism, and is in part responsible for the present high recovery of 72.5 per cent of the oil originally in place. Initially, the movement of the oil displaced by the injected gas probably was substantially horizontal, which would account for the relatively low produced GOR during the first few years of operation. Following the major gas breakthrough, the producing mechanism probably was comparable with the development of a secondary gas cap, with vertical movement of the oil toward the bottom of the section. Some movement of oil down-structure also may have occurred, which could account in part for the higher per acre recovery of Batteries 85A-N and 85B.

Fortunately, the permeability of the reservoir and the uniformity of the sand section permitted great freedom of fluid movement within the reservoir, which enabled the low pressure injection operation to perform so efficiently. It may

be concluded that reservoir conditions were extremely favorable for this type of operation.

ACKNOWLEDGMENTS

The author wishes to express his appreciation to the management of Roeser and Pendleton, Inc., for permission to utilize their records in preparing this paper, and in particular to G. P. Crutchfield and V. H. Moore for their kind assistance in analyzing the data. He desires also to acknowledge the capable assistance provided by the Reservoir Engineering Section of Continental Oil Co. The author wishes to thank the managements of Roeser and Pendleton, Inc., and Continental Oil Co. for permission to publish this paper.

★ ★ ★

REFERENCES

1. Crutchfield, G. P.: "Methods and Effects of Unit Repressuring in the Cook Pool," *Trans. AIME*, (1931) 138.
2. Wilson, G. M.: "Record System Aids Repressuring Efficiency," *Oil Weekly* (June 15, 1942) 106, No. 2, 16.
3. May, D. T.: "Chip Coring Technique," *Prod. Monthly*, (Aug. 1948) 12, No. 10, 30.

★ ★ ★

Table II—Chip-Core Data, W. I. Cook Ranch Estate, Well No. 60A-91

Depth Ft	Porosity Per Cent	Air Permeability Md	Core Oil Saturation Per Cent
1,256.1	23.5	420	9
1,257.1	22.5	180	13
1,258.1	21.5	160	20
1,259.0	27.0	710	15
1,260.0	23.9	550	13
1,261.1	23.7	400	35
1,262.2	23.1	740	30
1,263.0	22.9	570	24
1,263.9	15.6	50	39
1,265.0	23.0	1,100	13
1,266.1	24.9	1,650	23
1,267.4	24.9	1,600	25
1,268.6	24.5	1,250	13
1,269.6	24.7	1,400	10
1,270.8	27.1	2,300	14
1,272.0	26.3	1,600	11
1,273.4	25.6	1,900	15
1,274.6	24.0	1,350	11
1,276.3	27.6	1,200	21
1,277.5	24.8	1,100	17
1,278.7	24.8	1,050	19
1,280.0	22.7	650	18
1,281.2	24.6	1,250	13
1,282.5	24.1	1,150	29
1,283.7	24.2	900	32
1,285.0	26.2	1,950	44
1,286.2	27.0	1,100	40
1,287.6	28.1	2,200	44
1,288.7	2.9	0	3

A NEW ADDITIVE FOR CONTROL OF DRILLING MUD FILTRATION

R. A. SALATHIEL, HUMBLE OIL AND REFINING CO., HOUSTON, TEX., MEMBER AIME

ABSTRACT

A new synthetic material has been developed which is highly effective in treating drilling muds to reduce filtration rate. The material is the soluble salt of a very high molecular weight condensation product of sulfonated phenol and formaldehyde (SPIF). Laboratory tests show that SPIF is effective in muds of all salinities varying from fresh water to saturated salt water. Alkaline materials, such as soda ash or caustic and quebracho, may be used in combination with SPIF to advantage, and are essential in muds containing saturated salt water. In a field test where the water used in the mud had a salinity of about one-half that of sea water, SPIF in combination with caustic and quebracho made a very satisfactory mud. SPIF does not ferment, but due probably to additional polymerization a slight decrease in effectiveness is found when it is subjected to high pH and high temperature for a long time.

INTRODUCTION

Drilling mud is essential in rotary drilling. The influence of variations in the different properties of a mud on its ability to perform the various functions in drilling of wells is thoroughly understood in some cases and poorly understood in others. For instance, the function of mud density in restraining high pressure fluids is simple and well known. On the other hand, while the value of low filtration is widely recognized, it is seldom possible to determine precisely what filtration rate is required for the mud to perform its functions properly. Filtration rate is important because it influences the ease of

moving tools in or out of the hole. Filtration rate also affects the stability of the bore hole walls, which are subject to softening and degradation by aqueous filtrate. Difficulties in rotary drilling are often avoided by using low-filtration muds.

Treatment of fresh-water muds to provide moderately low filtration rates usually consists of adding chemicals to improve the dispersion of the clays. To provide very low filtration rates, organic colloidal materials are added. Among the materials that are used in this way are starch, natural gums, and altered celluloses. In muds that contain large amounts of salt or calcium or magnesium ions, the clays are coagulated and, as a consequence, the filtration rate is undesirably high. In such muds organic colloids are of great importance.

LIMITATIONS OF PRESENT FILTRATION ADDITIVES

Starch and water-soluble gums are widely used as filtration control agents. Starch is the most important material of this kind being used. It has the advantage of relatively low cost. It is effective in promoting low filtration rates, not only in fresh water muds, but also in muds containing large amounts of salts. However, both starch and natural gums are subject to fermentation and must be preserved from damage caused by microbiologic attack. Also, both starch and natural gums tend to increase the mud viscosity undesirably. Furthermore, the quantity of material required may be quite large. This is especially true when substantial amounts of salts are present. In such a case small additions of starch may increase rather than reduce the filtration rate of the mud.

Carboxy-methyl-cellulose, a chemically altered form of cellulose, has some advantages over starch. It is effective in smaller concentrations and does not increase the viscosity as much as

Manuscript received in the office of the Petroleum Branch Aug. 20, 1951. Paper presented at the Petroleum Branch Fall Meeting in Oklahoma City, Okla., Oct. 3-5, 1951.

does starch. However, it is much more expensive than starch and like starch requires a preservative for long, continuous use, although it is subject to microbiological attack somewhat less readily than starch.

Soaps are also used to a considerable extent, usually in combination with oil in emulsion muds. Soap in combination with oil may promote low filtration rates. The addition of soap, however, may increase the mud viscosity greatly, and such soap-emulsion systems are as sensitive to contamination as the clay-water system from which they are prepared.

None of the currently used materials has all the properties desired of a treating agent for control of filtration rate in drilling muds.

NEW SYNTHETIC MUD-TREATING AGENT

In order to develop a material which would have all of the properties desired, a laboratory investigation was initiated. A number of materials were investigated as additives for drilling muds with the objective of discovering a material highly effective at low concentration in reducing filtration rate, especially in salt-water muds, and which would not require preservative and not increase the viscosity greatly. One of the most promising of the materials investigated was a water-soluble, very high

molecular weight condensation product of partially sulfonated phenol and formaldehyde. This material has been called SPIF for convenience.

SPIF is a synthetic product made by partially sulfonating phenol with concentrated sulfuric acid and reacting the product with slightly less than an equal molar amount of formaldehyde. The reaction is stopped by neutralization with an alkali when viscosity measurements show that gel formation is about to take place. High molecular weight is necessary for SPIF to be effective; low molecular weight products are useless. The molecular weight is indicated by the viscosity of the solution. A desirable molecular weight is obtained in a viscosity range from 100 to 300 cp at 25°C for solutions containing 30 per cent crude SPIF. The product after neutralization can be dried and powdered for ease of handling. The yield of the crude SPIF is 300 per cent based on the weight of phenol used, and is composed of about 40 per cent active ingredient, 40 per cent salts resulting from neutralization, and 20 per cent low molecular weight polymers.

It is not known just what the cost of manufacturing SPIF in commercial quantities will be. However, the raw material cost is moderate, and the manufacturing steps are simple. It is anticipated that a favorable cost figure will develop. Procedures for preparing SPIF were developed in Humble Oil and Refining Co. laboratories, and manufacture of a quantity sufficient for a field trial was carried out by Monsanto Chemical Co.

ACTION OF ORGANIC COLLOIDS IN MUD

One theory presumes that organic additives reduce the filtration rate of a mud by plugging the small openings between mineral particles in the filter cake. Any treatment of a mud which diminishes the size of the openings to be plugged, as, for instance, dispersion of clay by chemicals, permits reduction of filtration rates with smaller concentration of organic colloids. Thus, it appears that any of the organic treating agents would be effective in fresh water mud at low concentration because the pores of the filter cake are very small at the beginning of the treatment. However, when substantial amounts of salt or calcium and magnesium ion are present in the mud the clays are coagulated and the pore sizes in the filter cake are much larger. In such muds larger concentrations of the organic colloid are required to give a low filtration rate. In addition, when starch or carboxy-methyl-cellulose is used in such muds the first addition of the agent usually results in higher filtration rates. It is only after the addition of substantial quantities that a desirably low filtration rate is obtained. The absence of a favorable effect from initial additions of starch or CMC is considered to be a result of adsorption of the organic colloid by the mineral solids. There is no evidence that SPIF is adsorbed by mineral solids in either fresh or saline muds since SPIF at low concentrations causes substantial reduction of the filtration rate.

LABORATORY TESTS OF SPIF

The effectiveness of SPIF in synthetic muds of various salt concentrations was tested in the laboratory. Starch, at present the most widely used filtration-control agent, was used as the

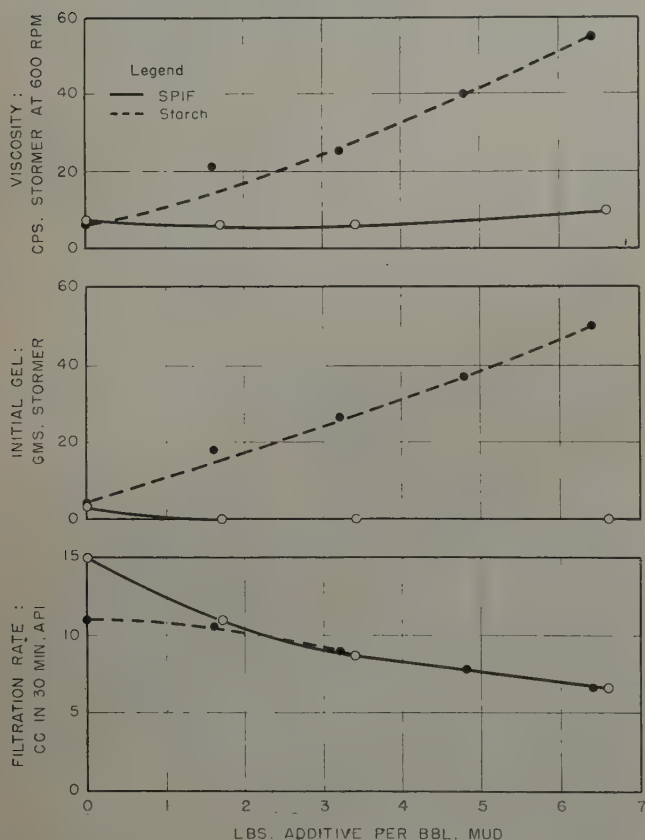


FIG. 1 — EFFECT OF SPIF ON FRESH WATER MUD.

basis on which to compare SPIF. The fluid phase of the muds was varied from fresh water to saturated salt water. The following discussions illustrate the results obtained.

Effect of SPIF in Fresh-Water Muds

Fig. 1 shows the effect of the addition of SPIF to a neutral mud composed of 1.6 per cent Bentonite clay, 18 per cent medium-yield clay, and 80.4 per cent fresh water. Included on the chart are comparative data for starch. The effect on viscosity, on initial gel strength, and on the filtration rate is shown for each additive. It is of interest to note that the addition of 6.6 lb/bbl of SPIF decreased the filtration rate from 15 cu cm to 6.6 cu cm API. In comparison, starch in a concentration of 6.4 lb/bbl lowered the filtration rate from 11 cu cm to 6.6 cu cm API. Thus, in a neutral fresh-water mud SPIF is as effective as starch, pound for pound of material, in decreasing the filtration rate. The contrast in the effect of starch and SPIF on the viscosity and initial gel strength of the mud is striking. Addition of starch increased drastically both the viscosity and the initial gel strength, whereas SPIF was almost without influence on these properties.

It should be pointed out that SPIF may be prepared as either the sodium or calcium salt, both forms being water soluble and effective as filtration control agents. It is well known that clays adsorb by base exchange the polyvalent ions such as calcium and at the same time release sodium ions to the solution. As contrasted with clay, SPIF in solution is a completely-ionized salt and as such shows no preference for any particular ion. As a consequence, SPIF cannot be expected to remove ions harmful to the mud but, instead, if added as the calcium salt would increase the concentration of the calcium ion in the mud. Thus it is preferable to use the sodium salt of SPIF, especially in fresh-water muds.

Effect of SPIF in Sea-Water Muds

The effect of SPIF on the filtration rate, viscosity, and gel strength of a neutral sea-water mud composed of five per cent Bentonite clay, 30.1 per cent shale from South Louisiana and 64.9 per cent sea water is shown in Fig. 2. Included on this chart are similar data for starch in a neutral sea-water mud and starch added as a 10 per cent paste in one per cent caustic solution.

In sea-water mud SPIF affected the viscosity and gel strength but little, and reduced the water loss from 52 cu cm to 6.8 cu cm API at a concentration of six lb/bbl of mud. The addition of 7.4 lb/bbl of starch reduced the filtration rate from 49 cu cm to 29 cu cm API, and at the same time the viscosity and gel strength were increased from 32 to 194 cp Stormer at 600 rpm and from 50 to 120 g Stormer, respectively.

It was recognized that the addition of dry starch to a neutral sea-water mud did not entirely simulate well conditions, where higher pH, normally used in conjunction with starch treatment, and heat would aid in the hydration of the starch and render it more effective. Accordingly, the starch was pasted as a 10 per cent slurry in one per cent caustic solution for addition to the mud. The results of the addition of the pasted starch are also shown in Fig. 2. It may be noted that both viscosity and

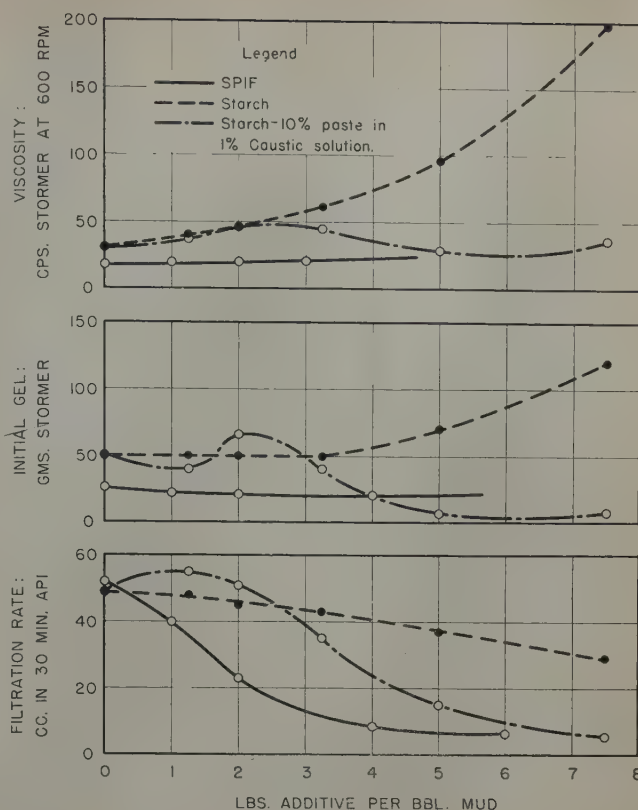


FIG. 2 — EFFECT OF SPIF ON SEA WATER MUDS.

gel strength first increased, passed through a maximum, and then decreased to values well below the original. This decrease of the viscosity and gel strength was caused by dilution by addition of rather large quantities of water with the starch as a 10 per cent paste, and not by any viscosity or gel-treating ability that might be ascribed to the alkaline starch paste. Pasting the starch made it more effective as a filtration-reducing agent. The filtration rate first increased, passed through a maximum, and finally was reduced from the original 49 cu cm to 5.5 cu cm API after addition of 7.4 lb of starch (74 lb of the starch paste) per bbl of mud.

Effect of SPIF in Five Per Cent Salt-Water Mud

A comparison of the influence of SPIF and starch on the properties of a mud in which the fluid phase was composed of five per cent salt water is shown in Fig. 3. In this mud starch caused an increase of the viscosity and gel strength, while SPIF affected these properties but slightly. SPIF proved to be very effective in reducing the filtration rate of this mud in that the water loss was decreased from 30 cu cm to 6.3 cu cm API on addition of 6.4 lb/bbl. When the quantity of SPIF was increased to 13 lb/bbl, the water loss was decreased to four cu cm API. In contrast, starch, on addition of the first four lb/bbl, caused the filtration rate to increase from 33 cu

cm to a maximum of 37 cu cm and then decrease to 34 cu cm API. Further additions of starch caused the filtration rate to decrease so that the water loss was 7.8 cu cm API after the addition of 10 lb/bbl.

Effect of SPIF in Saturated Salt-Water Mud

SPIF in a neutral mud in which the liquid phase was saturated salt water did not cause a significant decrease of the filtration rate and did not affect greatly the viscosity or the gel strength of the mud. In comparison, the first 3.4 lb of starch per bbl mud caused the filtration rate to increase from 54 cu cm to 118 cu cm API. When the starch concentration was increased to 7.4 lb/bbl, the filtration rate was decreased to 17.5 cu cm and on further increase to 11.1 lb/bbl, the water loss was decreased to 5.3 cu cm API. Addition of starch caused viscosity of the saturated salt-water mud to increase in a somewhat erratic manner, increasing from 25 to 175 cp, then decreasing to 122 cp and finally increasing to 162 cp as 11.1 lb of starch per bbl was added. The gel strength was increased

from 48 to 75 g Stormer and then decreased to six g, which value did not change further as more starch was added. These data are illustrated in Fig. 4.

It was found that by increasing the alkalinity of the saturated salt-water mud with soda ash or caustic SPIF became effective as a filtration reducer. Illustrated in Fig. 4 is the manner in which SPIF reduced the water loss of a saturated salt-water mud containing four lb of soda ash per bbl. It may be seen that the filtration rate was reduced from 150 cu cm to 27 cu cm, then to 13 cu cm and finally to 6.5 cu cm API, respectively, on addition of four, six, and eight lb of SPIF per bbl of mud. SPIF did not cause any significant change in the viscosity when these additions were made. Thus, if the alkalinity of the mud is increased, SPIF becomes effective as a filtration-control agent in saturated salt-water muds.

Stability of SPIF

One of the principal difficulties in the use of starch or carboxy-methyl-cellulose for filtration control is their susceptibility to fermentation, which makes necessary the use of a preservative. The use of a preservative in many cases adds considerably to the mud treating costs. SPIF, by virtue of its composition, is immune to microbiological attack. With SPIF there does exist a possibility of certain chemical reactions that could lead to a loss of effectiveness. First, continued polymerization could occur, which might increase the molecular weight to a point where the SPIF is no longer completely soluble. Second, there exists a possibility that a reaction similar to hydrolysis might take place and cause a decreased molecular weight and a decreased efficacy. Other than the reduction of the effect on filtration rate, no products formed would be deleterious to the mud properties.

To test the rate at which SPIF decreases in efficacy with time, a mud was made with sea water and shale taken from a well drilled in South Louisiana. This mud, which had a water loss of 90 cu cm API, was treated with six lb/bbl SPIF to decrease the water loss to 6.8 cu cm API. The treated mud was divided into four aliquots, two of which were adjusted to pH 12.1 with caustic and quebracho solution, and the other two left at pH 8.3. One sample each of pH 8.3 and pH 12.1 was aged at 75°F, and the other samples were aged at 190°F. The results of these tests are summarized in Table I. These data show very little effect on the filtration rate of the mud aged 50 days at pH 8.3 and at 75°F; the water loss increased from 6.8 cu cm to 9.6 cu cm API during this time. When the pH was increased to 12.1 at 75°F or the temperature at either pH was increased to 190°F, the deterioration was increased, the filtration rate increasing from 6.8 cu cm to 23.8 cu cm API in 50 days at pH 12.1 at 75°F. It is of interest to note that both viscosity and gel strength changed but slightly, and in most cases both decreased.

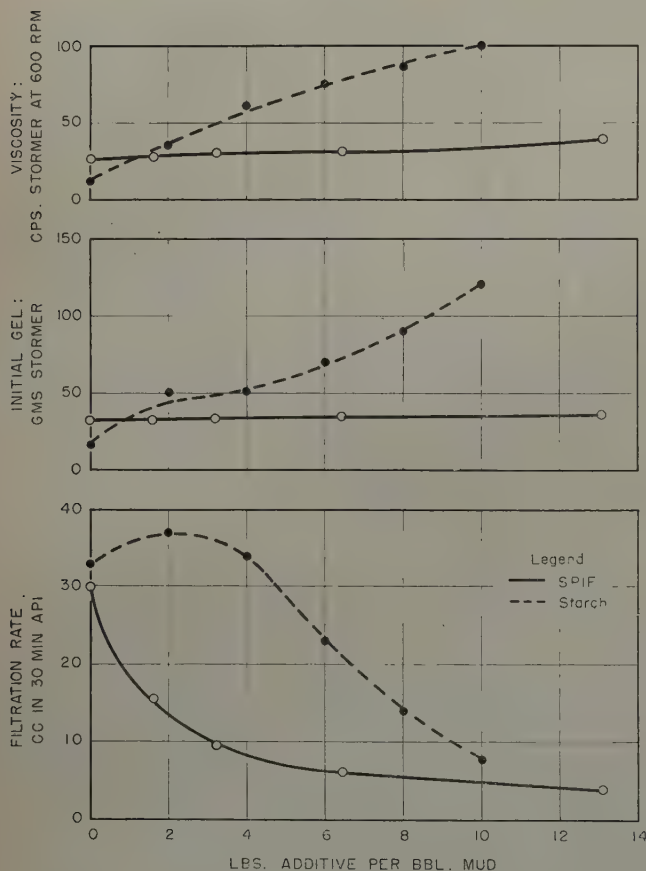


FIG. 3 — EFFECT OF SPIF ON FIVE PER CENT SALT WATER MUDS.

FIELD TEST OF SPIF

To provide a supply of SPIF for a field test in a well, Monsanto Chemical Co. cooperated in the preparation of 22,000 lb of the material. The details for the manufacture were worked out jointly.

The well chosen for the test of SPIF was a 14,000-ft test to be drilled in Lake Raccourci, Louisiana, designated as State Lease 1449, Well 1. This well was chosen for several reasons. First, the location made it advantageous that the relatively salty water, 11,600 ppm chloride, of the Lake Raccourci embayment be used for the mud in order to save tug and barge costs incurred in hauling fresh water. The diesel-electric rig did not require fresh water. Second, the well was to be a deep test and would give an extended time for the test. Third, several other wells had been drilled in the area using the salty water for the mud and standard filtration control materials to reduce water loss which could serve as a basis for comparison of the cost and efficacy of SPIF.

The well was spudded in April 22, 1951, using a mud made from bentonite, lime, and the salt water of the lake. Conductor pipe was set at 228 ft and 13³/₈-in. surface pipe was set at 1,817 ft. Chemical treatment was started at 7,030 ft with the addition of caustic quebracho solution. The drill pipe was twisted off at 7,484 ft while drilling in 12¹/₄-in. hole, resulting in a five-day fishing job to recover the drill collars and bit. The first addition of SPIF was made on April 30, 1951, while the fishing operations were in progress. The material was added as a dry powder through a mechanical mud mixer. The addition and mixing were accomplished with no difficulty and after addition of 9,350 lb of SPIF, about 4.7 lb/bbl of mud based on an estimated mud volume of 2,000 bbl, the water loss was reduced from 52 cu cm to 12 cu cm API. Sufficient water had been added to reduce the mud weight from 10.7 to 10.1 lb/gal and the viscosity increased with clay to 37 sec Marsh funnel. The alkalinity was 0.01 per cent and the chloride content was 11,400 ppm.

Table I—Aging Tests of SPIF in Sea-Water Mud*

Time, days	pH	Temp., °F.	Stormer Viscosity cp	Stormer Initial Gel, g	Filtration cu cm, API
0	8.3	75	6.	2	6.8
0.75			6.	2	7.0
4			5.	3	7.5
11			5.	2	6.5
22			4.5	1	7.5
50			4.5	0	9.6
0	12.1	75	4.5	2	6.4
0.75			5.	0	6.0
4			4.5	0	6.0
11			4.5	0	9.6
22			4.5	0	10.6
50			4.5	0	23.8
0	8.3	190	6.	2	6.8
0.75			4.5	1	6.8
4			4.5	1	7.8
11			4.5	1	8.6
22			4.5	1	11.0
50	Sample lost during aging period				
0	12.1	190	4.5	2	6.4
0.75			4.5	0	6.6
4			4.5	0	9.2
11			4.5	0	10.5
22			4.5	0	15.5
50			6.5	0	18.6

*Mud prepared by stirring shale from a well in South Louisiana into sea water. Initial filtration of 90 cu cm API reduced to 6.8 by treatment with 6 lb/bbl of SPIF. The pH was adjusted in two aliquots from 8.3 to 12.1 using caustic and quebracho solution. pH adjustment decreased filtration rate from 6.8 to 6.4 cu cm API.

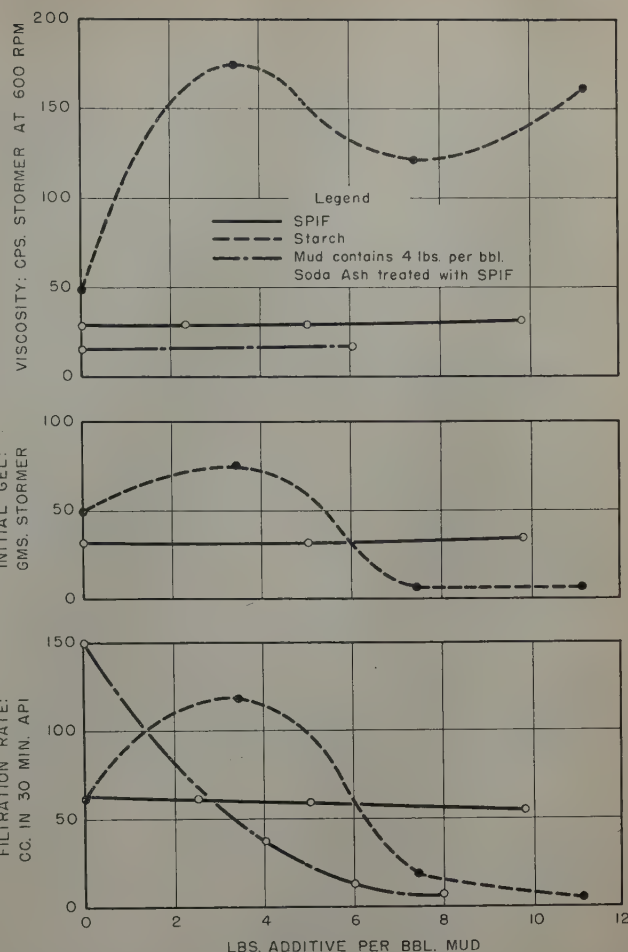


FIG. 4—EFFECT OF SPIF ON SATURATED SALT WATER MUD.

After the fish was removed on May 4, 1951, the hole size was reduced to 9⁷/₈ in. and drilling was continued to 9,180 ft. The average mud properties maintained while drilling the 1,700 ft in this interval were: weight, 10.4 lb/gal; viscosity, 37 sec Marsh funnel; chloride, 12,500 ppm; alkalinity, 0.07 per cent; filtration rate, 11.0 cu cm API. Maintenance of the mud in this interval required 3,740 lb of SPIF. Caustic quebracho and caustic lignite solutions were used for viscosity control.

The mud was converted at 9,180 ft to an oil emulsion by addition of diesel oil. After emulsification was complete, the mud weighed 10.4 lb per gal, the viscosity was 51 sec Marsh funnel, chloride content was 13,000 ppm, the alkalinity 0.09 per cent, oil content 14 per cent, and the filtration rate was eight cu cm API.

The 9⁷/₈-in. hole was drilled to 10,450 ft, at which depth drilling was halted, the hole was reamed to 12¹/₄ in. from 7,492 to 8,600 ft, and 9⁵/₈-in. casing was set and cemented at 8,594 ft on May 13, 1951. The average mud properties while drilling the 1,300 ft of hole and reaming were: weight, 10.4 lb/gal; viscosity, 42 sec Marsh funnel; chloride, 14,000 ppm; alka-

linity, 0.09 per cent; oil content, 12 per cent; filtration rate, 8.6 cu cm API. The SPIF required to maintain the filtration rate during this 1,300 ft interval was 1,320 lb.

On May 13, 1951, the cement was drilled from the casing, which caused a slight contamination from the cement. The mud was converted at 10,500 ft to a SPIF-emulsion-lime mud. The filtration rate increase to 23 cu cm API after addition of 2,100 lb of lime. It required 4,620 lb SPIF to lower the water loss to 10 cu cm API. The well was drilled from 10,500 to 12,900 ft, during which time lime was added to the mud, along with caustic quebracho and caustic lignite solutions for viscosity control. The SPIF requirement for this 1,400 ft of hole was 2,530 lb to maintain an average filtration rate of eight cu cm API. The alkalinity was maintained at about 0.25 per cent, and the other properties remained as previously carried.

The supply of SPIF was exhausted at 12,900 ft, making necessary the use of starch for filtration control below this depth. The conversion to starch was made with no difficulty other than an increased viscosity normally experienced when starch is added to a mud.

There were no special treatments required at any time during the SPIF test. The material was easy to handle and to mix with the mud. There was no evidence of deterioration of the SPIF during the 27 days over which the test was conducted.

The maintenance cost, once the initial SPIF treatment had been made, was comparable with the average of three other wells drilled in Lake Raccourci using the lake water for the

mud. Although the total mud cost on this job was somewhat more than the average of the three comparison wells, the difference was due to the relatively high cost of the experimental quantity of SPIF. A lower price for the polymer may be anticipated with commercial manufacture, and more experience with SPIF mud treatments should make its use competitive with the filtration control agents now in use.

CONCLUSIONS

The results obtained from laboratory studies and field use of a sulfonated phenol formaldehyde polymer for control of filtration rate of drilling muds have led to the following conclusions:

1. A new synthetic material, SPIF, has been made that will control water loss from drilling mud;
2. The material is suitable for treatment of muds made from fresh water or water that contains salt in concentrations up to saturation;
3. SPIF is not subject to fermentation;
4. SPIF does not increase the viscosity or gel strength of a mud to an undesirable degree;
5. The new filtration control agent requires no special mud treating techniques.

★ ★ ★

A SIMPLIFIED METHOD FOR COMPUTING OIL RECOVERY BY GAS OR WATER DRIVE

HENRY J. WELGE, THE CARTER OIL CO., TULSA, OKLA., MEMBER AIME

ABSTRACT

The approximate methods which are now in use for calculating oil displacement from reservoirs by gas-cycling or gravity-drainage at constant gas pressure, or by water flooding, make use of fundamental relationships derived by Leverett¹ and Buckley and Leverett.² The mathematical equations needed are derived by applying Darcy's law to the flowing phases, and by material balance considerations. In general, any treatment of this type gives, for any particular exploitation time considered, a plot of oil saturation against distance in the reservoir. The oil recovery must then be obtained by integrating in some manner the area under the plot.

A useful analytical method has been derived for computing the average saturation, and hence the oil recovery. Use of this method simplifies the calculations because it makes unnecessary any numerical integrations, and even the saturation distribution plots are not needed. A further advantage of the method is that knowledge of the relative permeabilities is required only for a limited and intermediate saturation range.

In both the Buckley and Leverett method and the method discussed here, a linear sand section is assumed, and in the case of gas drive the gas pressure is assumed sufficiently constant both with respect to reservoir position and time so that changes in gas density, solubility, or reservoir volume factor are negligible. Thus, the exploitation contemplates oil displacement as by an immiscible phase. Examples are given to illustrate how the new method can be used.

INTRODUCTION AND THEORETICAL BACKGROUND

This paper treats a simplified method for computing oil recovery when the oil is displaced from the reservoir sand by a fluid which, within the limits of accuracy desired, can be assumed to be incompressible and immiscible with the oil. The method makes use of two basic relations originally developed for the case of water displacing oil. However, the case of gas displacing oil saturated with gas at a constant (or nearly constant) pressure may also be considered a displacement by an immiscible fluid. This is possible for the reason that the concentration of the gas in the oil never changes if the pressure is fixed. Consequently, any additional free gas must remain undissolved in the oil, and so must act essentially as an immiscible phase. For convenience, the case of gas drive will be considered first.

Both of the two basic relations needed refer to a linear reservoir, or one which may be somewhat idealized so that a constant cross-section is exposed to fluid flow. Further, the displacing phase is injected at one end, or face, of the reservoir, while the produced fluids are understood to emerge at one point only, which is the opposite face of the reservoir. As indicated in Fig. 1, the reservoir may be inclined by some angle θ .

The first of the required equations may be derived by applying Darcy's law to both displacing and displaced phases, and subtracting the two equations. The result for water drive has been given previously, as Equation (13) of the reference by

¹References given at end of paper.
²Manuscript received in the office of the Petroleum Branch Sept. 25, 1951. Paper presented at the Petroleum Branch Fall Meeting in Oklahoma City, Okla., Oct. 3-5, 1951.

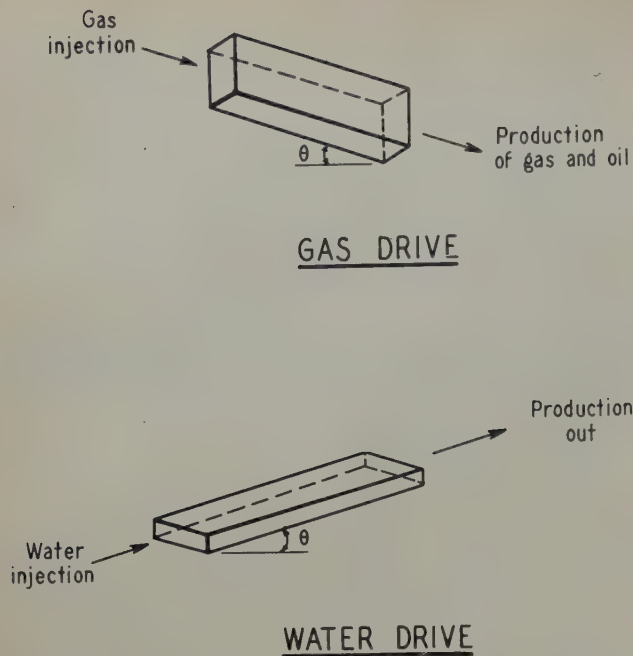


FIG. 1

Leverett¹ cited above. The result for the case of gas drive, derived in completely analogous manner, may be written:

$$f = \frac{c}{c+h} - \frac{K \Delta D_g \sin \theta}{\mu_g v_o} \frac{k_{o11}}{c+h} \dots \dots (1)^*$$

The term comprising the capillary pressure gradient has been dropped from Equation (1). This procedure is usual practice in reservoir calculations, and justification will be given later in this paper. Equation (1) may equally well be expressed in terms of f_{o11} which is $1-f$ to give:

$$f_{o11} = \frac{h}{c+h} + H \frac{k_{o11}}{c+h} \dots \dots (1a)$$

The second basic relation required appears as Equation (1) on page 109 of the reference by Buckley and Leverett² cited above. It expresses a material balance over a thin section of the reservoir. In terms of gas drive it may be written in the form:

$$v \frac{\partial f}{\partial x} + \frac{\partial S}{\partial t} = 0 \dots \dots (2)$$

Since f by Equation (1) is a function of S only (through k_{o11} and h), we may write for the first derivative in Equation (2),

$$\frac{\partial f}{\partial x} = \frac{df}{dS} \cdot \frac{\partial S}{\partial x} \dots \dots (3)$$

in which the total derivative df/dS is obtainable from Equation (1). After substituting (3) into (2), Equation (2) can be rearranged and partially solved by standard methods to give the relation:

$$\left(\frac{\Delta x}{\Delta t} \right)_S = \left(\frac{dx}{dt} \right)_S = - \frac{\frac{\partial S}{\partial t}}{\frac{\partial S}{\partial x}} = v \frac{df}{dS} = v f' \dots (4)$$

The value of df/dS , hereinafter denoted by f' , for any given saturation, S , must be obtained by plotting f as calculated from Equation (1) and taking slopes from the plot (see Fig. 2).

Equation (4) gives the distance traveled by the various gas saturations in any given time, Δt . The distance traveled, Δx , is proportional to the f' function, the constant of proportionality being $v\Delta t$. Thus, a plot of S against f' , such as the one in Fig. 2, gives also the gas saturation as a function of distance. It is necessary only to multiply the f' scale by the value of $v\Delta t$ corresponding to the time at which the saturation distribution is desired. Thus the curve describing saturation as a function of position in a core or reservoir at any time during the exploitation remains always similar except for horizontal "stretching," or multiplying of all abscissae by a constant factor.

In a system which is being held at constant pressure the oil recovery can be directly related to the change in volume of free gas, i.e., to the average gas saturation. In general, in order to find the average gas saturation from any plot of S vs x , it has in the past been necessary to integrate in some manner the area under the plot. The operation of plotting and integrating must be performed as often as recovery evaluations are desired. It is well realized by anyone who has had to carry through the entire process of evaluation that it is a tedious and time-consuming job.

In the event the velocity of the front of farthest gas penetration and the gas saturation at break-through are desired, the f' curve must be cut off as indicated in Fig. 2, in such a manner that the areas lying beneath and to the left of the original and the amended curves are equal in accordance with the suggestion made by Buckley and Leverett.² This construction was recently shown to be mathematically valid by von Neumann* and, somewhat later, by Brinkman.³ It is equivalent to making equal in size the two areas shown shaded in Fig. 2.

*Private consultation. John von Neumann also originated the more convenient method for determining the point at which the f' curve must be cut off that is presented in the next paragraphs.

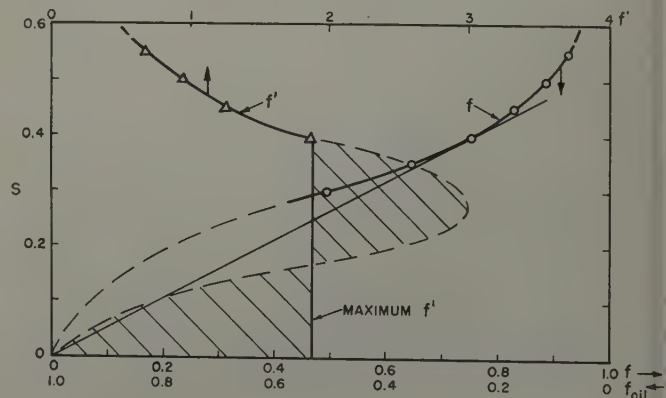


FIG. 2 - FLOWING GAS FRACTION IN TERMS OF GAS SATURATION MILE SIX POOL, PERU.

*A complete table of nomenclature is given at the end of this paper.

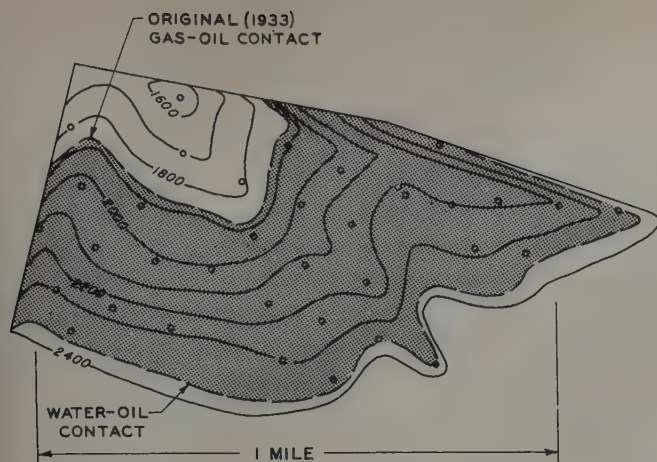


FIG. 3 — MILE SIX POOL, PERU.

The cut-off construction applied to the f' curve is analytically equivalent to the use of an average f' value covering the gas saturation range from zero to the cut-off gas saturation. It will be noted further that the required average value of f' (see Fig. 2) is the slope of a line drawn through the origin and tangent to the originally constructed f curve. This is true because of the requirement, developed in analytic geometry, that the slope of a secant intersecting a curve in two points is the average slope of the curve. Since the tangent intersects the f curve at the origin and at the point of tangency, it fulfills the above requirement.

The slope, then (with reference to the S axis), of the tangent shown in Fig. 2 represents the maximum value of f' , or f'_{\max} . This maximum slope corresponds to the highest velocity with which any gas saturation moves, and therefore can be used in conjunction with Equation (4) to obtain the time of gas break-through at the producing wells.

The construction of a tangent line like that shown in Fig. 2 indicates the lower limit of saturation below which the plot of the f curve is not required; hence relative permeability information is also unnecessary below this saturation. In particular, it should be noted that knowledge of the so-called equilibrium gas saturation, or lowest gas saturation at which gas can flow, is not required in this method of evaluating performance by gas drive. Relative permeabilities are difficult to measure in the region of low gas saturation, and considerable experimental time can be saved if they are not needed. It will be shown later that relative permeabilities are likewise usually not needed in the region of very high gas saturations. The regions in which the f function is not required are shown by dashed lines in Fig. 2; they are inserted there only for the purpose of illustrating the foregoing discussion.

The error resulting from dropping the term containing the capillary pressure gradient in arriving at Equation (1) may now be briefly discussed. As described above, the S vs f' curve in Fig. 2 will give the saturation distribution with respect to distance along a rock sample or a reservoir at any instant during the progress of the exploitation. Consider the instant at which gas is first produced; the abscissal position f'_{\max} will then represent the outflow point of the rock system receiving flow, or the field position of the producing wells. As the

length of the system considered increases, the distance corresponding to the abscissa length from zero to f'_{\max} increases. That is, a distance scale laid off along the f' axis must be compressed more and more. When this is done, the saturation gradient or slope of the S vs x curve proportionately decreases as the system length encompassed in the distance from zero to f'_{\max} increases. The capillary pressure depends solely on the saturation,¹ so the capillary pressure gradient also will become of smaller importance as longer systems are considered. Test calculations have been made in which the capillary term was retained in Equation (1) for the purpose of comparing its magnitude with the size of the other terms. These calculations showed that the term frequently could not be dropped if the systems were only a few inches long, as in the case of cores intended for core analysis; but that it became negligible in systems having the dimensions of reservoirs.

A similar line of reasoning may be applied to any later stage in the gas drive after the instant of gas break-through. In this case the saturation and capillary pressure gradients will be smaller still than they were before, and hence of still less consequence.

DERIVATION OF PROPOSED METHOD OF CALCULATION

Consider the nature of the f function at a point near the inlet to the linear sand body. If the first section or slice, δx thick, of the sand body is very thin compared to the maximum distance penetrated by the injected gas front, it is evident that the slice has experienced a great many of its pore volumes of gas throughput. Accordingly, the flow of oil must have all but ceased in the slice, which means that $f = 1$ and $f' = 0$ at $x = 0$.

A further convenient relationship may be derived from Equation (4) by applying it to the situation near the outlet face of the linear sand body, where $x = L$, the reservoir length. Here

$$\frac{1}{f'} = \frac{1}{f'(S)} = \frac{v \Delta t}{L} = Q_1,$$

where Q_1 is the cumulative injection in pore volumes at the time the saturation, S , reaches the outflow face.

With the aid of the considerations noted in the preceding paragraphs, the desired average gas saturation in the sand, S_{av} , can be evaluated:

$$S_{av} = \frac{\int_1^2 S dx}{x_2} \dots \dots \dots (5)$$

where the limits 1 and 2 refer to the inlet and outlet of the sand. Equation (4) shows that the distance, x , attained in the sand by a given saturation is proportional to the f' function; consequently this function may be used instead of x in the numerator and denominator of Equation (5) for the purpose of averaging:

$$S_{av} = \frac{\int_1^2 S df'}{f'_2} \dots \dots \dots (6)$$

since f' denotes df/dS , it is possible to integrate Equation (6) by parts,

$$S_{av} = \frac{S_2 f'_2 - \int_1^2 f' dS}{f'_2} = S_2 - \frac{\int_1^2 df}{f'_2} = S_2 - \frac{f_2 - 1}{f'_2}$$

$$\text{or } S_{av} - S_2 = (f_{oil})_2 Q_1 \dots \dots \dots (7)$$

Equation (7) readily gives the difference between the average and terminal gas saturation, so that only one saturation, the one near the outlet of the sand, need be evaluated for the purpose of calculating oil recovery by gas cycling or gas cap drive at constant gas pressure.

It should be particularly noted that the product $(f_{oil})_2 Q_1$ always gives the saturation increment between the average gas saturation and the terminal gas saturation obtaining near the outflow face of the sand. Evaluation of this product for any stage in the exploitation whatever readily permits calculation of S_{av} , which is the total fractional recovery of oil from the reservoir.

ILLUSTRATIVE EXAMPLE

To illustrate the use of the average gas saturation, recovery calculations made for the Mile Six Pool in Peru⁴ were selected, because the results of the calculations can be compared directly with the actual known behavior of this pool over most of its producing life. A contour map of this field is shown in

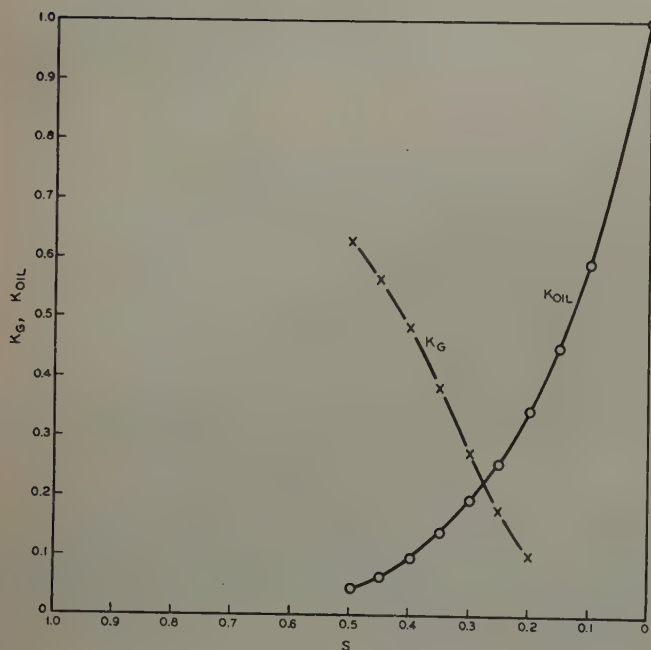


FIG. 4—RELATIVE PERMEABILITIES AS FUNCTIONS OF GAS SATURATION EXPRESSED AS A FRACTION OF HYDROCARBON-OCCUPIED PORE SPACE.

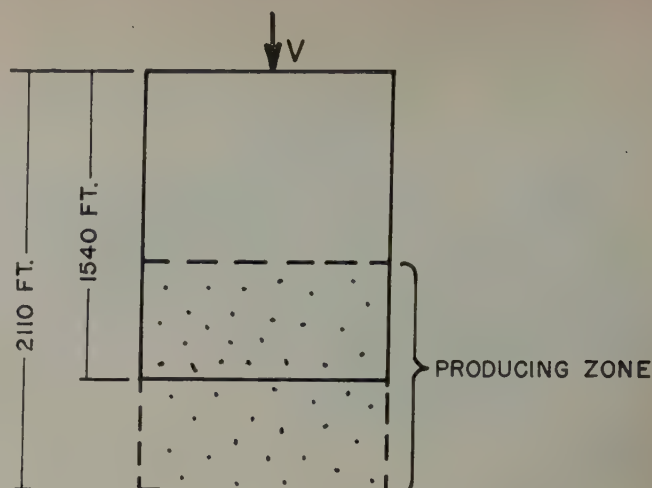


FIG. 5—IDEALIZED REPRESENTATION, MILE SIX POOL, PERU.

Fig. 3. The average dip is 17.5° , the average permeability was taken to be 300 md, and the average hydrocarbon occupied porosity* was 0.1625. The viscosity of the reservoir oil and gas were estimated to be 1.32 and 0.0134 cp, respectively, and their densities were taken at 0.78 and 0.08 g/cu cm, respectively.

The relative permeability functions used are shown in Fig. 4. It should be remembered that the relative permeabilities as measured on laboratory core samples should be corrected for the effects of stratification before being used in field calculations. This factor was considered in arriving at the curves given in Fig. 4. An alternate procedure that can be used whenever adequate core analysis information is available is to make separate reservoir behavior calculations for each layer.

Since the calculation of reservoir behavior can be applied only to flow in one direction, as illustrated in Fig. 1, some geometric adjustment is needed to produce even an approximate answer in a problem of this type. Essentially the actual irregularly shaped field is replaced by an assumed parallelepiped in which the dimensions are chosen to give the closest representation possible. The plan view of the idealized field is shown in Fig. 5. The overall length of 2,110 ft shown is obtained from Fig. 3 and is the estimated average distance (parallel to the formation) from the original gas-oil contact to the oil-water contact. The length of 1,540 ft, also scaled from Fig. 3, represents the distance along the dip from the original gas-oil contact to the average withdrawal point. The latter point or level is taken midway between the producing wells so that as many wells lie upstructure from it as downstructure. The distance of 1,540 ft will be taken as the average length of the idealized linear reservoir.

The average fluid velocity in the hydrocarbon-occupied pore space v is obtained in the following manner. The average cross-section exposed to flow may first be obtained by dividing the volume of original reservoir oil-in-place, 55×10^6 bbl or 309×10^6 cu ft, by 1,540 ft; the result is 201,000 sq ft. The average withdrawal rate, in terms of reservoir volume, of oil and free gas during the interval 1933-1946 was 23.5×10^6 cu ft

*Total porosity multiplied by the factor, $(1 - \text{fraction of connate water})$.

per year. Division of this withdrawal rate by the average cross-sectional area yields a pore velocity v of 116.8 ft per year (1.13×10^{-4} cm/sec).

In Table I are shown the calculations carried out in accordance with the relations developed above. It will be observed that the terminal gas saturation is treated as the independent variable in constructing the table. Next the function h is evaluated for each saturation chosen, and entered in column (2). This function is then used in calculating the values appearing in columns (3) and (5), the sum of which gives the value for f_{o11} which appears in column (6). The quantity f_{o11} is plotted against S as in Fig. 6, which is a copy of Fig. 2 from which the portion of the construction has been deleted that is not needed in the usual reservoir evaluation. The slope of the f (or f_{o11}) curve in Fig. 6 (with reference to the S axis) is measured with a straight edge for each value of S taken originally, and entered in column (7).

It will be observed in Table I that the oil recoveries are in reasonable agreement with the field data. The differences observed are in part due to the fact that the exploitation velocities were somewhat lower than the average assumed in the calculations for the first eight years of the gas injection program, and somewhat higher for the next four years. The calculated gas/oil ratios differ more widely from the field data. It has been observed, in general, that the flowing gas/oil ratio is a more sensitive function of the assumed conditions, such as gas velocity, permeability, or geometrical complexities, than is the oil recovery. It may be of interest to mention that

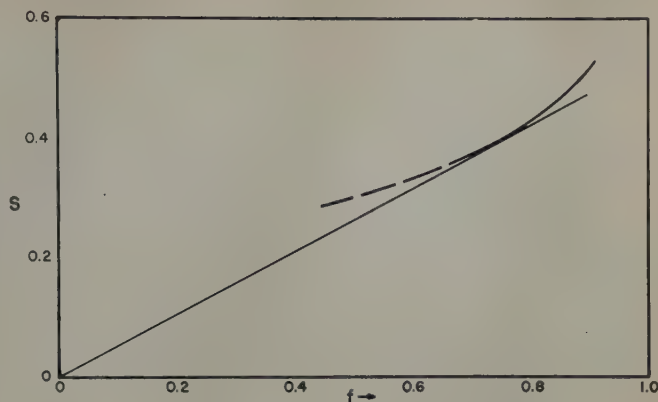


FIG. 6—FLOWING GAS FRACTION IN TERMS OF GAS SATURATION, MILE SIX POOL, PERU.

the calculation time for the above example was about a man-day; this time is contrasted with an estimated man-week if the conventional integration technique is used.

It is unnecessary to plot a curve showing the saturation distribution with distance in the reservoir (such as the f' vs S curve), since the average gas saturation suffices to determine

Table I—Typical Calculations of Gas Cap Drive Performance

(1)	(2)	(3)	(4)	(5)	(6)	(7)	(8)	(9)	(10)	(11)	(12)	(13)
Gas Saturation Near Outlet S_2	$h = \frac{K_g}{k_{o11}}$ (Fig. 4)	$\frac{h}{c+h}$	$\frac{k_{o11}}{c+h}$ (Fig. 4)	$\frac{Hk_{o11}}{c+h}$	$(f_{o11})_2 = \frac{1}{(3) + (5)}$	$\left(\frac{df}{dS}\right)_2 = \frac{1}{Q_1}$	$\frac{t}{1,540 \text{ ft}} = \frac{116.8 \text{ ft/yr}}{Q_1}$	$S_{av} - S_2 = f_{o11} Q_1$	$S_{av} = \frac{S_{av} - S_2}{(1) + (9)}$	Fraction of Oil in Place Recovered (Cumulative)	Actual Field Data	Flowing GOR (cu ft/bbl)
0.30	0.715	0.00725	0.197	0.497	0.504							
0.35	0.364	0.0037	0.140	0.354	0.358							
0.395*	0.210	0.00214	0.102	0.2585	0.261	1.875	7.05	0.139	0.534	0.535	1,800	800
0.40	0.200	0.00204	0.097	0.243	0.245	1.81	7.1	0.135	0.535	0.543	1,930	700
0.45	0.118	0.00120	0.0667	0.169	0.170	1.25	10.6	0.136	0.586	0.614	2,820	2,300
0.50	0.0715	0.00073	0.045	0.114	0.115	0.94	14.1	0.122	0.622	0.675	4,220	2,100

Dimensionless ratios required:

$$c = \frac{\mu_{o11}}{\mu_g} = 98$$

$$H = \frac{K \Delta D g \sin \theta}{\mu_g v_o} = 248.5^{**}$$

Reservoir oil volume factor = 1.25

Super compressibility factor for reservoir gas (Z factor) = 0.74

$$\frac{\text{Volume Surface Gas Per Volume Stock Tank Oil}}{\text{Volume Reservoir Gas Per Volume Reservoir Oil}} = \frac{850 \text{ psi}}{14.7 \text{ psi}} \times 1.25 \times \frac{(60^\circ\text{F} + 460)}{(114^\circ\text{F} + 460)} \times \frac{1}{0.74} = 88.6$$

*Oil "bank", or shock front, occurs at this saturation (see Fig. 2). For all earlier stages in the gas injection program, $S_2 = 0$, and oil recovery = $S_{av} = Q_1$. The values shown for f and f_{o11} (column (6) above) for saturations less than the "bank" saturation of 0.395 are not required after the position of the bank is determined, and they should not be used further.

**c.g.s. units will be found convenient for expressing the non-dimensional number H . The c.g.s. unit for permeability is sq cm; darcies $\times .987 \times 10^{-8}$ = permeability expressed in cu cm. $V_o = V\pi = 1.13 \times 10^{-4}$ cm/sec $\times 0.1625 = 0.184 \times 10^{-4}$ cm/sec.

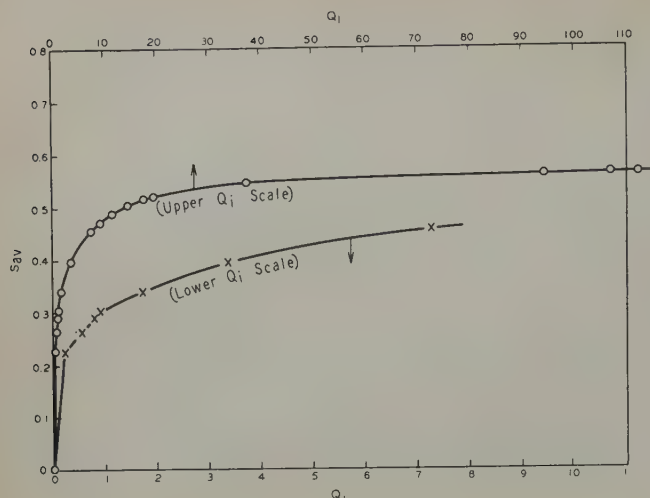


FIG. 7—RESULTS OF A GAS DRIVE EXPERIMENT ON A CORE OF BARTLESVILLE SANDSTONE.

the recovery, while the terminal saturation near the outflow face (the independent variable first assumed in column 1) fixes f , and hence the flowing gas/oil ratio at any desired time during the exploitation. It will also be noted that the maximum value of S for which relative permeabilities are needed is the value (column 1) corresponding to the greatest exploitation time (column 8) in which one is interested.

It is realized that the geometric and other approximations required in the illustrative example used are more severe than they would be in many other cases. Frequently the field geometry and the disposition of the wells are more amenable to simulation by a linear reservoir.

SUGGESTED TREATMENT FOR THE CASE INVOLVING AN INITIAL PERIOD OF DECLINING PRESSURE

Frequently a field has been exploited by dissolved gas drive for a time before a gas injection and pressure maintenance program is begun. In this event the calculations are made as before, except that at the end of the computations the time scale must be aligned in relation to calendar time. This is done as follows: In general, the stock tank oil that has been recovered by primary depletion up to the start of the gas injection program will be known; this oil recovery should be expressed as a fraction of the original oil in place and subtracted from unity. The so obtained fraction representing the residual oil, if multiplied by the ratio of the later to the initial formation volume factors, gives the residual oil saturation at the start of gas injection. The complement of this number gives the average gas saturation at the start of injection. The time at which this particular saturation is reached, computed by the method shown in Table I, is then identified with the date of the start of gas injection.

The average gas saturation at later times will not, in this case, be equal to the fractional oil recovery as before. Instead,

the latter must be calculated by a process which uses the formation volume factors in a precisely inverse manner to that described above.

A calculation made as outlined above for the case including a period of primary production with pressure decline will be subject to some error, for the reason that the distribution of gas in the reservoir arising from dissolved gas drive will not be identical with the distribution caused by gas injection at constant pressure. The accuracy to be expected from this type of calculation has, however, been tested for the case just discussed. The test consisted of a comparison between results obtained by the method described in this paper and by a much more comprehensive treatment in which most of the simplifying assumptions with regard to reservoir linearity, constancy of pressure, etc., were removed. The latter exhaustive computation gave a result for oil recovery after 30 years' gas cycling of 31.5 per cent; the former simple treatment, 29.8 per cent. The reasonably good agreement between these two figures suggests that the accuracy obtainable by the approximate method will be satisfactory for engineering purposes, particularly if gas throughputs in excess of about one pore volume are considered.

The work described in this paper represents part of a continuing program relating to mathematical and physical aids for carrying out pool studies and the associated reservoir engineering. The method of calculation described above has been used by a number of reservoir engineers in a semi-routine manner and has given results upon which economic evaluations have been based.

CALCULATION OF RELATIVE PERMEABILITY RATIO FROM LABORATORY GAS DRIVE DATA

The above relations are also useful when it is desired to make a calculation of relative permeability ratio from laboratory displacement data. The information required consists of (1) cumulative gas injection volumes at average core pressure and (2) the corresponding average gas saturations in the core. If the core is initially completely liquid-saturated, the average gas saturation at any time will be equal to the cumulative

Table II

$c = \frac{\mu_{o11}}{\mu_{N2}} = \frac{0.82}{0.018} = 45.6$					
(1)	(2)	(3)	(4)	(5)	(6)
		$f_{o11} =$	$S_{av} - S_2$	S_2	
		$\frac{dQ_1}{dS_{av}}$	$=$	$\frac{k_g}{k_{o11}}$	$\frac{1 - f_{o11}}{45.6 f_{o11}}$
S_{av}	Q_1	(Fig. 6)	$f_{o11} Q_1$	(1)-(4)	
0.225	0.251	0.1127	0.028	0.197	0.1723
0.30	0.90	0.0525	0.047	0.253	0.396
0.35	2.02	0.038	0.077	0.273	0.555
0.40	3.63	0.025	0.091	0.309	0.855
0.45	7.2	0.0112	0.081	0.369	1.933
0.475	9.8	0.00778	0.076	0.399	2.79
0.50	13.8	0.0048	0.066	0.434	4.54
0.525	22	0.00214	0.047	0.478	10.22
0.55	55	0.000333	0.018	0.532	65.9
0.56	107	0		0.56	∞

liquid discharged, expressed in pore volumes. For purpose of illustration, a typical set of such data is shown plotted in Fig. 6. The data were obtained by displacing n-decane from a core of Bartlesville sandstone by nitrogen gas, using a pressure drop sufficiently high so that the end effect, or abnormal capillary retention of liquid near the downstream core face, was restricted to negligible importance in comparison with the total amount of liquid in the core.

A typical calculation of liquid-gas relative permeability ratio from the data in Fig. 7 and using the relations developed previously, is given in Table II. Here columns (1) and (2) represent the starting experimental data plotted in Fig. 7. The loss of oil with reference to total input (or outflow) will be equal to f_{o11} and is given by the slope of the curve in Fig. 7; it is entered in column (3). The k_G/k_{o11} ratio obtained is shown plotted in Fig. 8.

If independent information on one or the other relative permeability, k_G or k_{o11} , is available, the other may obviously be obtained from the ratio. For example, it has been previously shown⁵ that k_{o11} may be estimated by computation from the nature of the capillary pressure *vs* saturation curve^{6,7} obtained on a porous material. The separate relative permeabilities may thus be measured, if desired, through the use of two relatively inexpensive and routine laboratory procedures: (1) a simple gas-oil displacement experiment, and (2) a capillary pressure experiment.¹

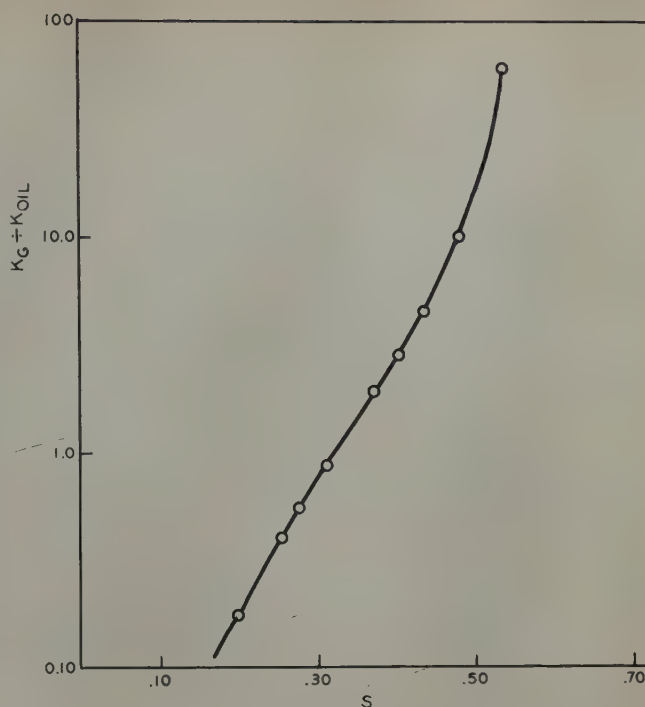


FIG. 8—RELATIVE PERMEABILITY RATIO FOR A BARTLESVILLE SANDSTONE CORE.

APPLICATION TO WATER FLOODING OR WATER DRIVE

The method described in this paper can be applied equally well to the evaluation of oil recovery by linear water flooding or water drive. In fact, as mentioned previously, it is of historical interest that the two basic relations employed by the author were first derived by Buckley and Leverett^{1,2} in connection with water-oil displacement. In general, all of the basic principles derived by them are equally applicable to the cases of displacement of oil by gas or by water.

In the case of water flooding, however, it is frequently found that the last term in Equation (1), containing the contribution of gravity, is of negligible importance unless the angle of dip is comparatively large or the flow velocity relatively small, or both. This is true because the viscosity of water as the driving fluid replaces the smaller gas viscosity in the denominator of the non-dimensional coefficient H . The change in the value of ΔD , the density difference between water and oil, further operates to reduce the importance of the gravitation term.

If the gravity term is found to be negligible, there will theoretically be no advantage resulting from injecting all of the water at the base of the structure. In this event the calculations may be taken to suggest that the flooding may as well be more quickly completed by employing a pattern of injection wells such as the 5-spot, for example. One possible way of calculating oil recovery in such a flooding program is to base the computations on a unit area served by one injection and one producing well. The distance between these two wells may be taken as L , the sand length, and the average breadth of the sand section is taken such that its product with L is equal to the area of the unit considered. In other words, the actual pattern unit is considered replaced by a linear sand section of equal length and of the same average breadth.

In the case of water flooding or water drive, there is present in the reservoir an initial saturation of the driving fluid (the connate water). The presence of this saturation alters the construction in Fig. 2 in two ways. First, it is more convenient now to consider the entire pore space as receiving the fluid flow, rather than only the hydrocarbon occupied space as before. Second, because of the initial saturation (connate water) of the driving liquid, the considerations described in connection with the tangent construction in Fig. 2 now require that the tangent be drawn from a point on the f curve lying at the height of the original water saturation, rather than from the origin. In general, this point will also lie on the saturation axis, since the connate water is usually immobile. The height of the point of tangency to the f curve now gives the water saturation at the outflow face just after the time of water break-through, and the slope of the tangent can be used to give the flowing water/oil ratio just after break-through. After break-through, the calculations are based primarily on the f curve above the point of tangency, and are made in the same manner as those illustrated in Tables I or II.

ACKNOWLEDGMENTS

The author wishes to thank the management of The Carter Oil Co. for permission to publish this paper. Charles D. Russell, D. R. Shreve, K. H. Andreson, L. W. Welch and W. A. Bain have assisted with suggestions and calculations.

NOMENCLATURE

c	= Viscosity of reservoir oil \div viscosity of reservoir gas
D_g	= Gas density
D_{oil}	= Oil density
ΔD	= Oil density less gas density, or water density less oil density
f	= Fraction of gas in flowing stream
f_{oil}	= Fraction of oil in flowing stream
g	= Gravitational constant
h	= k_{oil}/k_g
H	= $\frac{K \Delta D g \sin \theta}{\mu_g V_o}$ (dimensionless)
k_g	= Relative permeability to gas with connate water in place
k_{oil}	= Relative permeability to oil with connate water in place
K	= Total permeability to oil with connate water in place
L	= Total length of idealized sand section or reservoir
Q_1	= Cumulative gas injection in pore volumes
π	= Fractional hydrocarbon occupied porosity
S	= Gas saturation, fraction of hydrocarbon occupied space
S_{av}	= Average gas saturation in reservoir
t	= Time

v_o	= Velocity of gas approach to sand face = velocity of gas and oil stream after leaving outlet sand face
v	= v_o/π
x	= Distance from inlet face of system
θ	= Average angle of stratum dip
μ_g	= Gas viscosity
μ_{oil}	= Oil viscosity

REFERENCES

1. Leverett, M. C.: "Capillary Behavior in Porous Solids," *Trans. AIME*, (1941) **142**, 152.
2. Buckley, S. E., and Leverett, M. C.: "Mechanism of Fluid Displacement in Sands," *Trans. AIME*, (1942) **146**, 107.
3. Brinkman, H. C.: "Calculations on the Flow of Heterogeneous Mixtures Through Porous Media," *App. Sci. Res.*, Netherlands, (1949) **A1** (No. 5-6), 333.
4. Muskat, M.: *Physical Principles of Oil Production*, (1949) 496.
5. Rapoport, L. A., and Leas, W. J.: "Relative Permeability to Liquid in Liquid—Gas Systems," *Trans. AIME*, (1951) **192**, 83.
6. Welge, H. J.: "Displacement of Oil from Porous Media by Water or Gas," *Trans. AIME*, (1949) **179**, 133.
7. Rose, W. D., and Bruce, W. A.: "Evaluation of Capillary Character in Petroleum Reservoir Rock," *Trans. AIME*, (1949) **186**, 127.

★ ★ ★

EQUILIBRIUM VAPORIZATION RATIOS FOR NITROGEN, METHANE, CARBON DIOXIDE, ETHANE AND HYDROGEN SULFIDE IN ABSORBER OIL—NATURAL GAS AND CRUDE OIL—NATURAL GAS SYSTEMS

R. H. JACOBY AND M. J. RZASA, MEMBER AIME, STANOLIND OIL AND GAS CO., TULSA, OKLA.

ABSTRACT

Experimental equilibrium vaporization ratios (K values) were obtained for nitrogen, methane, carbon dioxide, ethane and hydrogen sulfide in two natural gas-absorber oil mixtures and in two natural gas-Elk Basin crude oil mixtures. For each mixture of constant over-all composition, data were obtained at 100°, 150° and 200°F and at various pressures in the range 200 to 5,000 psia. Some effects of composition on the K values were obtained to serve as a guide in choosing K 's for engineering calculations on other mixtures.

The pressure cell used to obtain the data is a new type and is described here for the first time.

INTRODUCTION

The phase equilibria of complex hydrocarbon mixtures such as natural gases, crude oils and their mixtures have been studied previously for the purpose of finding equilibrium vaporization ratios for the hydrocarbon constituents. In a few cases, such non-hydrocarbons as nitrogen, carbon dioxide, and hydrogen sulfide were included in the mixtures studied because they occur in the fluids obtained from petroleum reservoirs.

The increasing occurrence of these non-hydrocarbons and their growing economic importance, make it necessary to account for them more accurately in engineering calculations than is now possible using the meager published data.

The available data for non-hydrocarbons may be classified into two groups; namely, binary mixtures of a hydrocarbon and a non-hydrocarbon, and mixtures containing three or more components, only one of which is a non-hydrocarbon. Among the former, phase analyses are available for two nitrogen- HC

mixtures, five carbon dioxide- HC mixtures and three hydrogen sulfide- HC mixtures. Data for more complex mixtures are available as follows: Nitrogen-Methane-Pentane¹; Nitrogen-Methane-Hexane²; Nitrogen-Methane-Heptane²; Carbon dioxide-Natural Gas-Natural Gasoline⁴; Carbon dioxide-Natural Gas-Crude Oil⁶.

These data have been used generally for engineering calculations, often with little regard for their precise applicability because data for the non-hydrocarbons in the complex mixtures being dealt with were not available. The use of K values from binary data for calculations involving complex mixtures is open to criticism because such K 's are not a function of composition and very often show large differences from the K 's for the same components in a complex mixture.

Thus the effects of composition must be evaluated when obtaining K 's for components in complex mixtures. Poettmann and Katz^{4,5} varied the carbon dioxide content of their mixtures from about five to ten mol per cent and found substantially no effect on the K values due to this change. This was not surprising since one might expect that changing a minor component by \pm three mol per cent would have little effect. It is more important to find the composition changes which have the largest effect on the K values. For example, varying the methane or heptanes—plus compositions over a wide range may have a large effect on the K 's of all components in the mixture. Interesting data to this effect were obtained by Eilerts and Smith.⁶

It was toward these problems that the experimental data presented here were directed.

EQUIPMENT

The pressure cell used to obtain the data is somewhat different from those which have been described in the past. Photographs of the equipment are shown in Figs. 1 and 2. Fig. 1 shows the front panel; from a seated position at the right the

¹References given at end of paper.

Manuscript received in the Petroleum Branch office Aug. 25, 1951. Paper presented at the Fall Meeting of the Petroleum Branch in Oklahoma City, Okla., Oct. 3-5, 1951.

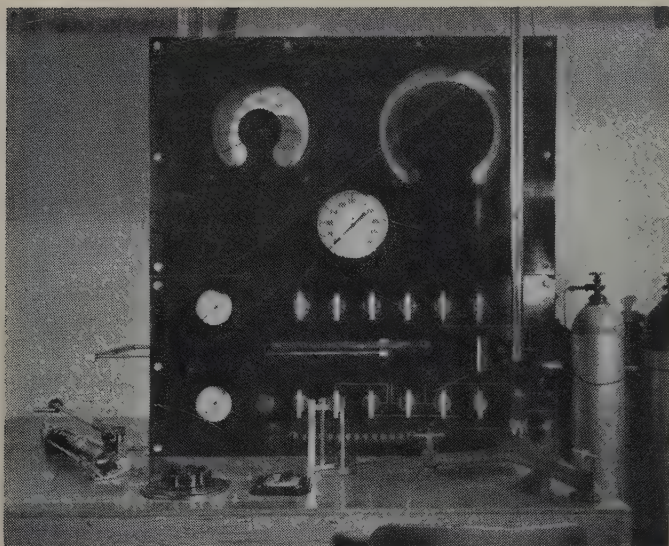


FIG. 1 — FRONT VIEW OF EQUIPMENT SHOWING ALL CONTROLS.

operator has access to all controls necessary to operate the cell. A schematic flow sheet of the equipment is shown in Fig. 3.

The cell itself consists of a hollow stainless steel (AISI Type 316) cylinder fitted with a piston and placed in a horizontal position. The end of the cylinder through which the piston rod projects is sealed by a steel plug having a tool-joint thread; pressure seals are an unsupported area type at the cylinder wall and V-rings around the piston rod. The head end of the cylinder is fitted with a glass window sealed with O-rings, a steel back-up plate, and a steel plug with a tool-joint thread. Fig. 2 shows the assembly of these parts and the head end of the cell. The space between the piston head and the glass window is used to contain the mixtures being investigated. The metal parts of the head assembly are provided with a slit so that the cell contents can be seen through the glass window. The principal auxiliaries are a pressure intensifier, injector cell, hot air bath, cathetometer, vacuum pump and magnetic pump for circulating the fluid mixture in the cell.

The cell volume may be varied from 40 to 1,200 cc and steel parts of the cell were designed to make it operable at 25,000 psia and 500°F. In its present state, however, certain pressure seals employing rubber or Teflon limit use of the cell to temperatures nearer 300°F.

EXPERIMENTAL PROCEDURE

Experimental runs were made as follows: a mixture of appropriate composition was made up by charging the components to the cell one at a time. First, hydrogen sulfide was measured directly into the windowed cell after flushing the cell several times. Other gaseous components were then charged with the injector cell. For each gas, the evacuated injector was filled with gas from a cylinder and measured volumes of this gas were then displaced into the windowed

cell at a known pressure. The liquid component of the mixture was the last one to be charged. From measurements of volume, pressure and temperature and molar volume data on the components, the amounts charged were calculated.

A mixture so charged was then heated and pressured to desired conditions and the cell liquid circulated with the magnetic pump until no further changes in pressure could be observed at constant volume and temperature. When equilibrium was thus attained the pump was shut off and samples of the liquid and vapor phases displaced into 100 cc sample bombs while holding the equilibrium pressure on the cell contents. The amounts of the phases drawn off for sample were proportional to the amounts existing in the cell at equilibrium conditions. In this way the overall composition remaining in the cell after sampling both phases was substantially the same as the original mixture charged to the cell. Thus by changing to another set of equilibrium conditions (change of pressure only in most cases) additional sets of phase samples could be obtained without recharging the cell. Calculations made from the charging measurements showed that the compositions given in Table II were consistently reproduced within ± 0.5 mol per cent of any component.

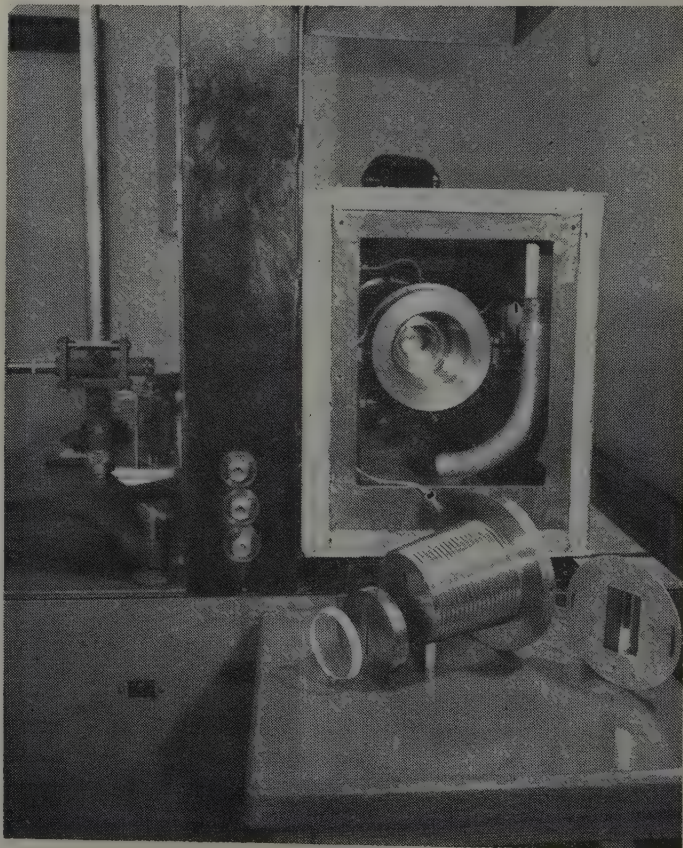


FIG. 2 — END VIEW OF CELL SHOWING THE GLASS WINDOW AND HEAD END ASSEMBLY.

Analysis of Samples

Vapor samples were analyzed directly by the mass spectrometer. In a number of runs, the sample bombs were not filled at the pressure of operation and the bomb was outside the air bath at room temperature. It was thus possible to en-

counter dew point conditions for the vapor being sampled. After a portion of the vapor sample was taken for analysis by mass spectrometer, the remainder was flashed away to the atmosphere and the bombs examined for dew-point liquid.

For many of the absorber oil vapor samples above 2,000 psia operating pressure the inside surface of the bombs was wet with a film of liquid; the greatest amount of liquid thus

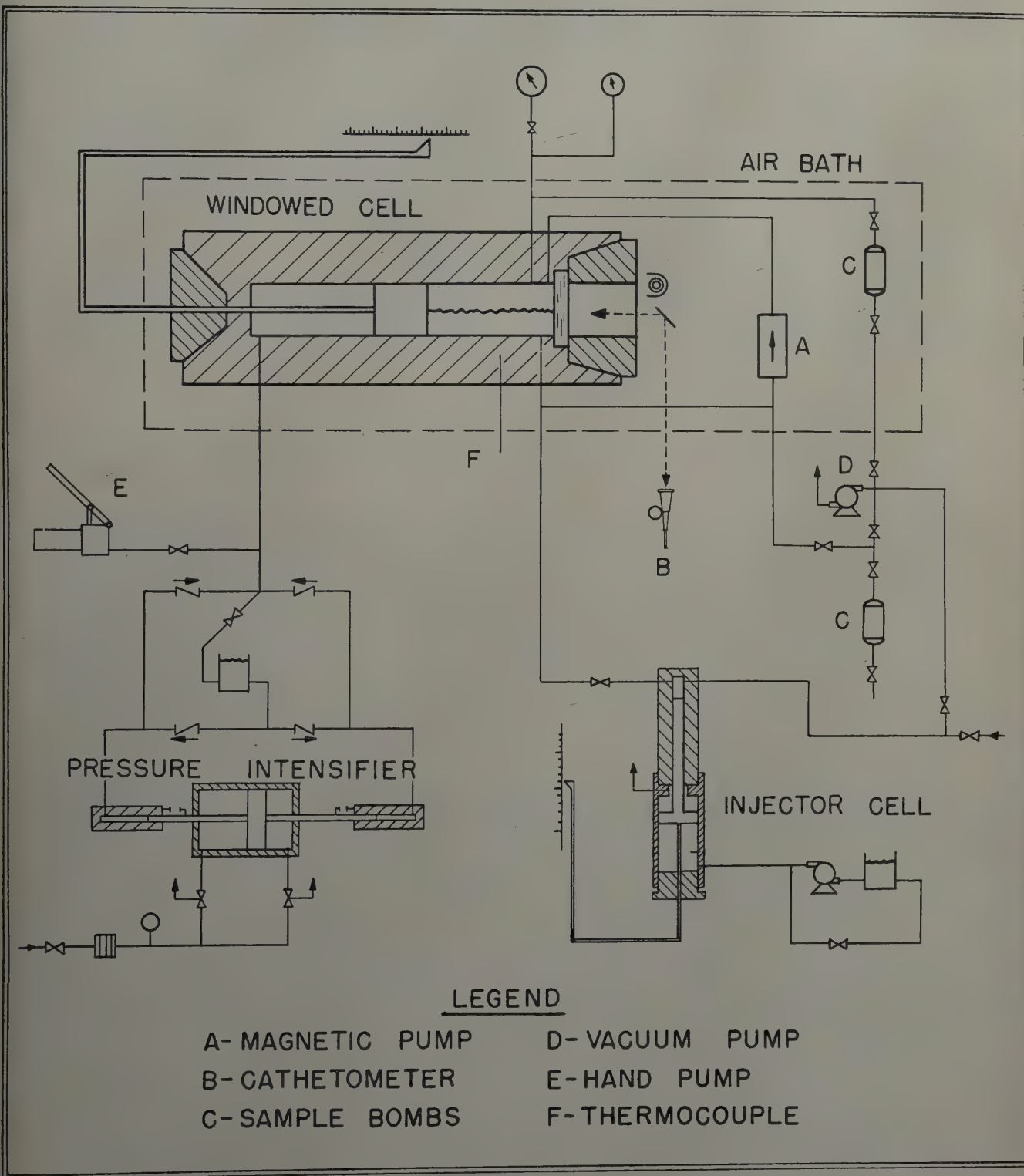


FIG. 3 — SCHEMATIC FLOW SHEET OF CELL AND ASSOCIATED EQUIPMENT.

Table I — Analyses of Materials Used to Make Up the Mixtures Shown in Table II

	Natural Gas	Absorber Oil	Crude Oil
Nitrogen	2.28 mol %		
Methane	95.78		
Ethane	1.74		
Propane	0.20		
Isobutane			0.09 mol %
n-Butane			0.67
Isopentane			2.68
n-Pentane			2.52
Hexanes			2.44
Heptanes - plus			91.60
MW C_7+			227
Sp. Gr. 60/60 C_7+			0.894
Mol. Wt.		1.77	224
Sp. Gr. 60/60		0.835	0.882

observed appeared to be about 0.5 cc and could not be recovered for measurement. The mass spectrometer analysis was then considered as the vapor analysis. Estimates were made of the C_7+ content of the vapor and they varied from 0.4 mol per cent at 2,000 psia and 100°F to 5 mol per cent at

5,000 psia and 100°F. These estimates are a measure of the error to be encountered if all the C_7+ had been omitted from the reported analyses as a result of the sampling procedure used.

Similar observations were made on vapor samples from the crude oil mixtures and in no case were any traces of liquid found in the bombs. The mass spectrometer analyses thus represent the actual vapor compositions to the limits of accuracy of the spectrometer.

The liquid samples were analyzed by charging to a low temperature Podbielniak column which flashed off the C_1 - and lighter components essentially as a fraction. The volume of this fraction was measured on the Pod column and it was then analyzed by mass spectrometer. The remainder of the liquid samples heavier-than- C_4 was then fractionated through hexanes, and specific gravity and cryoscopic molecular weight of the C_7+ fraction were measured. From these data the liquid analyses were computed.

Materials

The components used to make up the mixtures were: Matheson pre-purified nitrogen, natural gas (Matheson 96 per cent methane), Matheson bone-dry carbon dioxide, Matheson hydro-

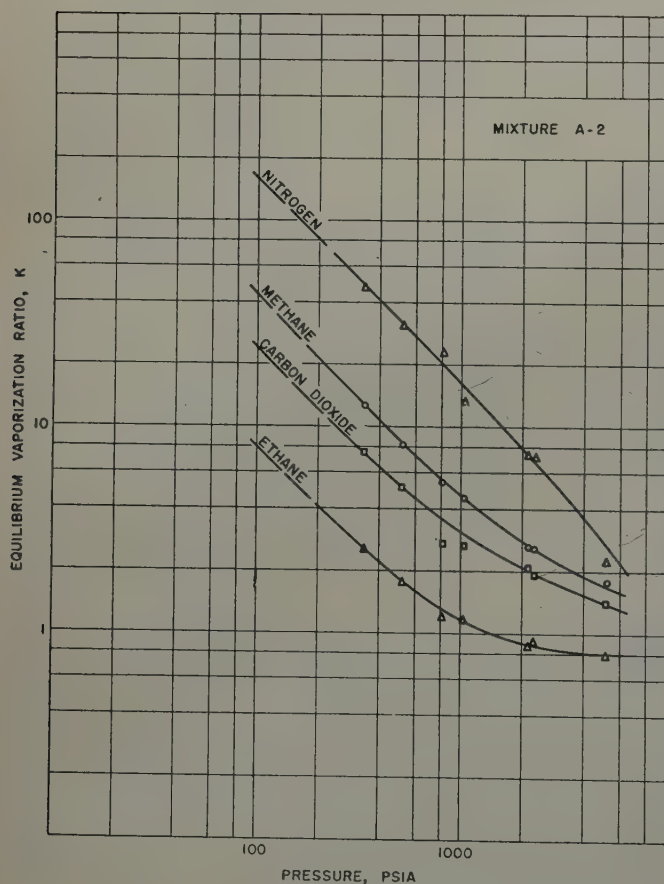


FIG. 4 — K VALUES IN ABSORBER OIL MIXTURE A-2 AT 100°F.

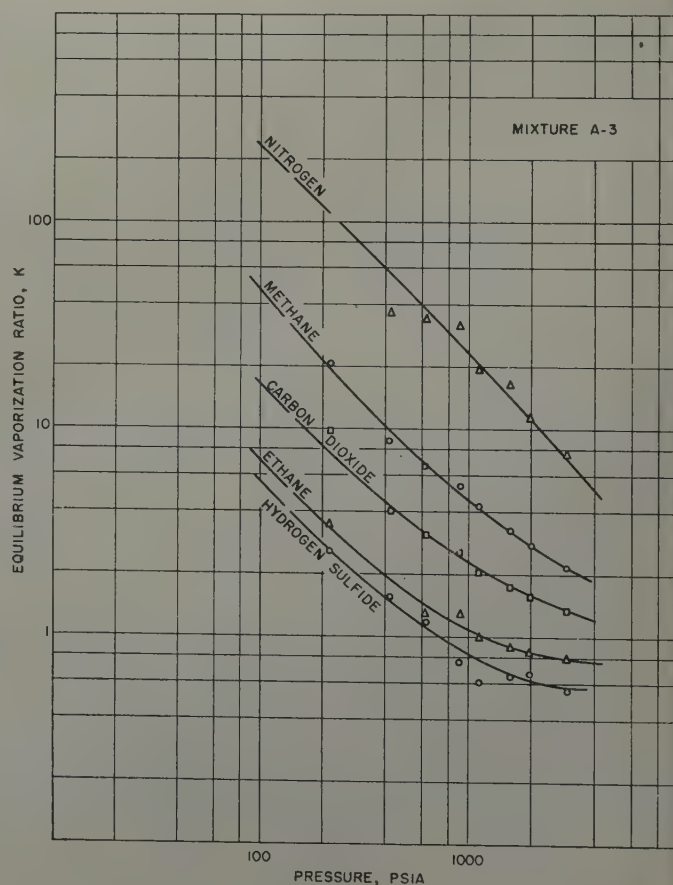


FIG. 5 — K VALUES IN ABSORBER OIL MIXTURE A-3 AT 100°F.

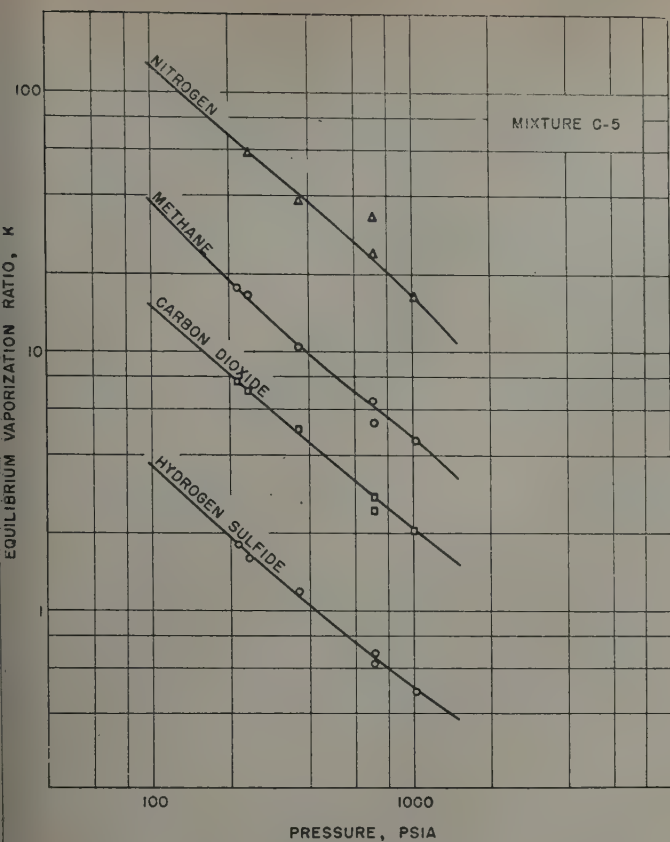


FIG. 6 — K VALUES IN CRUDE OIL MIXTURE C-5 AT 100°F.

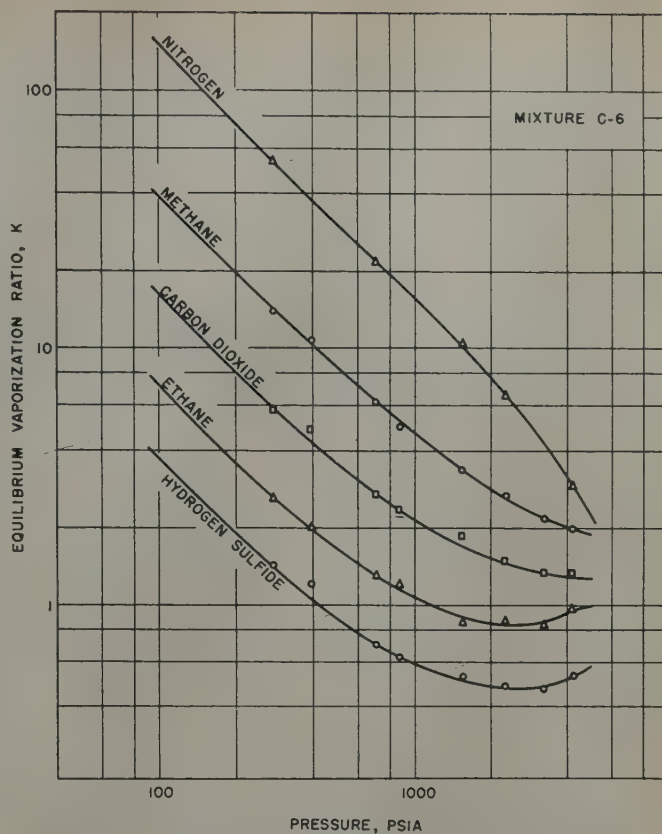


FIG. 7 — K VALUES IN CRUDE OIL MIXTURE C-6 AT 100°F.

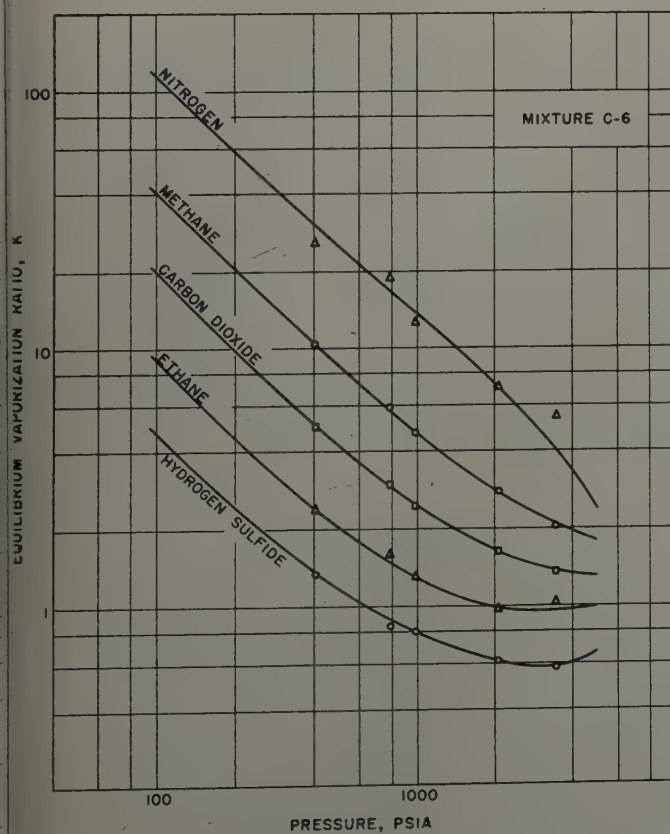


FIG. 8 — K VALUES IN CRUDE OIL MIXTURE C-6 AT 150°F.

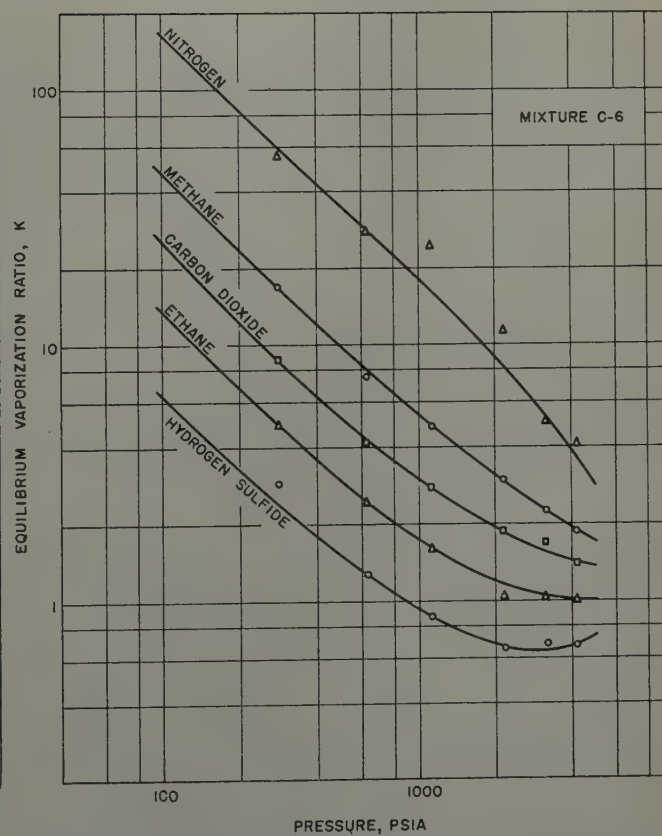


FIG. 9 — K VALUES IN CRUDE OIL MIXTURE C-6 AT 200°F.

gen sulfide, lean absorber oil from Stanolind's Hastings gasoline plant, and crude oil from the Tensleep formation in Elk Basin, Wyoming. Samples of the nitrogen, carbon dioxide, and hydrogen sulfide were checked for purity by mass spectrometer and found to be essentially 99.9 per cent pure. Analyses of the other materials are shown in Table I.

RESULTS

The mixtures studied in this work were natural gas-absorber oil and natural gas-crude oil, to each of which small amounts of nitrogen, carbon dioxide and hydrogen sulfide were added. Two different absorber oil mixtures and two crude oil mixtures

Table II — Overall Compositions of Mixtures Studied

Component	Absorber Oil		Crude Oil	
	A-2	A-3	C-5	C-6
Nitrogen	10.0 mol %	10.0 mol %	5.0 mol %	5.0 mol %
Natural Gas	65.0	40.0	10.0	40.0
Carbon Dioxide	5.0	5.0	5.0	5.0
Hydrogen Sulfide		5.0	5.0	5.0
Absorber or Crude Oil	20.0	40.0	75.0	45.0

Table III — Equilibrium Flash Vaporization Data

Pressure psia	A-2 Mixture		A-3 Mixture		C-5 Mixture		C-6 Mixture	
	100°F	200°F	100°F	200°F	100°F	200°F	100°F	200°F
	VOLUME PER CENT LIQUID							
200	3.5	2.5	7.9	6.4	37.2	31.1	16.3	10.1
500	9.0	6.7	20.0	17.2	68.8	62.0	26.2	22.2
1,000	14.8	13.1	37.2	33.2	92.8	86.8	45.0	40.1
1,500	22.5	20.1	51.5	46.2			62.0	54.1
2,000	29.6	26.8	62.0	56.6			75.7	65.1
2,500	35.7	32.6	70.8	64.8			84.2	74.1
3,000	41.0	37.6	77.7	72.0			89.3	82.1
3,500	45.6	42.2					93.3	88.1
4,000	50.0	46.2					96.7	94.1

were used; the overall compositions of these are shown in Table II. For each of the four mixtures, phase analyses were obtained over a range of pressures at 100°F, 150°F and 200°F.

The experimental phase analyses and the K values calculated from them are given in Tables IV and V. K values were calculated for nitrogen, methane, carbon dioxide, ethane and hydrogen sulfide. The hydrocarbons from propane through hexane were present to such a small extent that reliable analyses for them in both phases were not obtained, and hence K 's were not calculated for them. In Table IV, "trace com

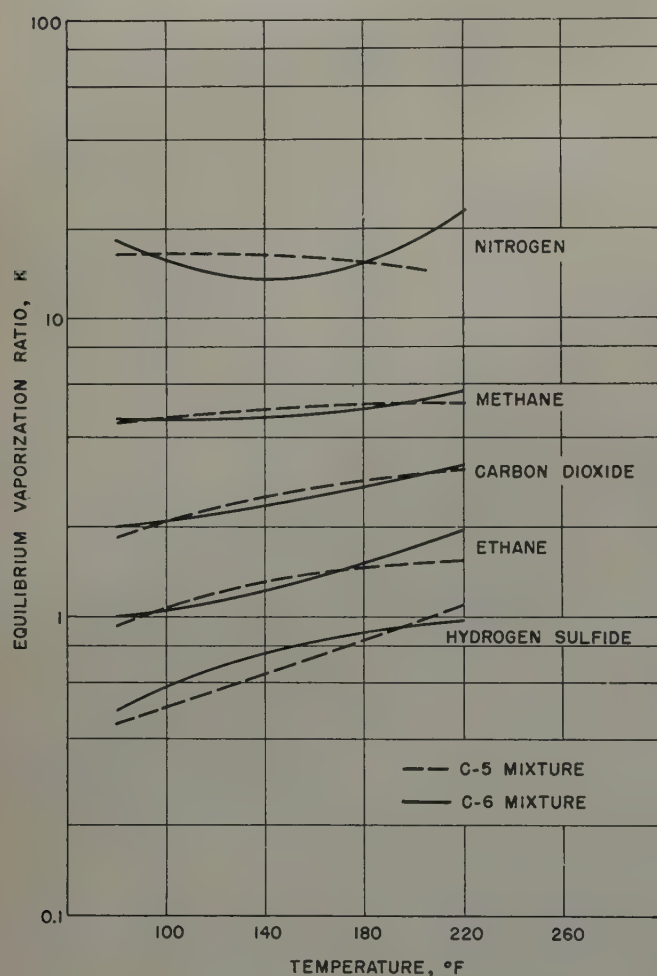


FIG. 10 — COMPARISON OF K 'S IN CRUDE OIL MIXTURES C-5 AND C-6 AT 1,000 PSIA.

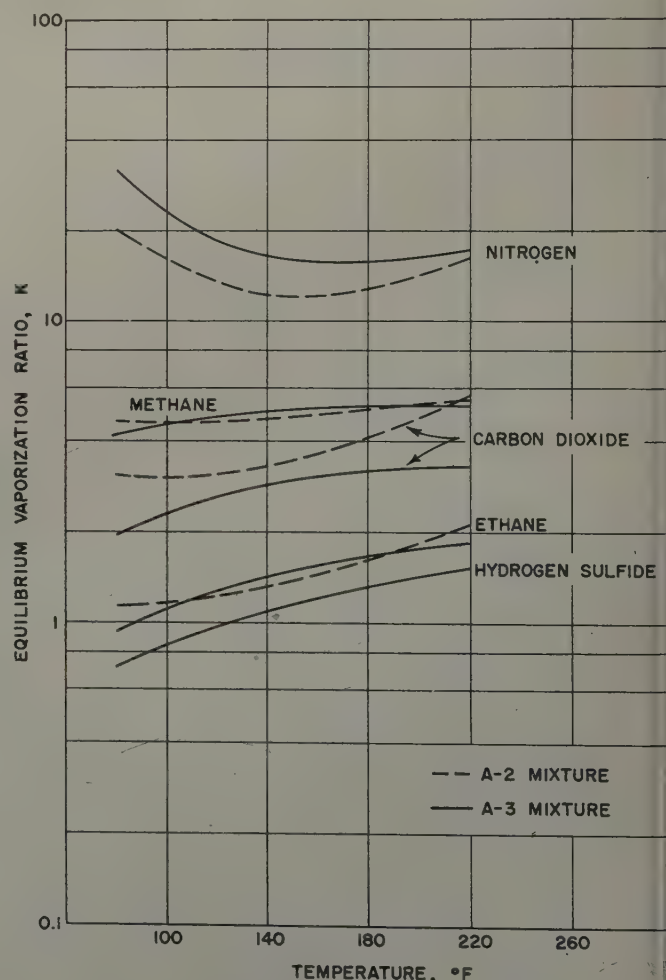


FIG. 11 — COMPARISON OF K 'S IN ABSORBER OIL MIXTURES A-2 AND A-3 AT 1,000 PSIA.

Table IV — Experimental Data for Absorber Oil Mixtures

Table IV — Experimental Data for Absorber Oil Mixtures																	
Run No.	Temp. °F	Pres. psia	Nitrogen		K	Methane		Carbon Dioxide		Ethane		Hydrogen Sulfide		Trace Comp.		Heptanes-plus Sp. Gr. 60/60 MW	
			x	y		x	y	K	x	y	K	x	y	x	y		
A-2 MIXTURE																	
84	98.2	336	.0032	.1517	47.4	.0608	.7559	12.43	.0097	.0723	7.45	.0051	.0129	2.53	.0052	.9160	.838
82	99.2	519	.0048	.1468	30.6	.0933	.7631	8.18	.0144	.0724	5.03	.0072	.0126	1.75	.0127	.8676	.839
90	99.4	813	.0065	.1483	22.8	.1425	.7661	5.376	.0269	.0733	2.72	.0086	.0103	1.20	.0036	.8119	.839
80	100.1	1029	.0102	.1329	13.03	.1725	.7755	4.496	.0270	.0718	2.66	.0106	.0123	1.16	.0189	.7608	.837
81	97.4	2121	.0222	.1612	7.26	.2825	.7470	2.644	.0311	.0649	2.09	.0125	.0109	0.872	.0094	.6423	.838
83	100.2	2275	.0249	.1783	7.16	.2871	.7267	2.531	.0412	.0786	1.91	.0116	.0106	0.914	.0152	.6200	.838
89	99.4	5119	.0524	.1166	2.23	.4492	.7994	1.780	.0516	.0721	1.40	.0117	.0093	0.79	.0083	.4268	.839
171	151.3	309	.0055	.1921	34.9	.0469	.7192	15.33	.0065	.0727	11.2	.0029	.0113	3.90	.0031	.9351	.837
169	150.6	609	.0098	.1775	18.1	.0979	.7309	7.47	.0136	.0761	5.60	.0058	.0109	1.88	.0053	.8676	.838
167	150.2	970	.0130	.1602	12.3	.1494	.7445	4.983	.0141	.0639	4.53	.0070	.0110	1.57	.0113	.8052	.838
166	149.8	2237	.0276	.1683	6.10	.2770	.7427	2.68	.0339	.0625	1.84	.0095	.0099	1.04	.0063	.6457	.838
170	150.6	5069	.0765	.2229	2.91	.4079	.7047	1.728	.0482	.0620	1.29	.0082	.0079	0.96	.0124	.4468	.838
87	200.7	535	.0053	.1588	30.0	.0848	.7493	8.84	.0076	.0721	9.49	.0042	.0140	3.33	.0072	.8909	.835
92	202.2	794	.0067	.1410	21.0	.1184	.7734	6.532	.0149	.0722	4.85	.0054	.0112	2.07	.0047	.8499	.838
85	200.0	1111	.0127	.1581	12.4	.1542	.7452	4.833	.0169	.0742	4.39	.0065	.0113	1.74	.0080	.8017	.838
86	201.0	2070	.0260	.1653	6.36	.2577	.7424	2.881	.0234	.0676	2.89	.0107	.0126	1.18	.0173	.6649	.838
91	198.9	4914	.0441	.1562	3.54	.4599	.7661	1.666	.0386	.0669	1.73	.0096	.0095	0.99	.0088	.4390	.838
A-3 MIXTURE																	
110	100.6	218	.0005	.18240309	.6325	20.5	.0093	.0916	9.85	.0025	.0087	3.5	.0017	.9205	.838
98	99.4	425	.0045	.1649	36.6	.0739	.6543	8.85	.0238	.0971	4.08	.0045	.00250059	.8563	.838
100	100.6	630	.0063	.2161	34.3	.0963	.6388	6.63	.0295	.0923	3.13	.0050	.0063	1.3	.0115	.8146	.838
94*	99.3	792	.0084	.1985	23.6	.1295	.7066	5.456	.0251	.0784	3.12	.0058	.0080	1.38	.0016	.8296	.837
109	101.9	917	.0068	.2164	31.8	.1204	.6485	5.386	.0329	.0849	2.58	.0050	.0065	1.3	.0039	.7779	.838
95	100.7	1108	.0094	.1821	19.4	.1678	.7189	4.284	.0326	.0667	2.05	.0068	.0068	1.0	.0016	.7424	.838
97	99.5	1591	.0134	.2209	16.5	.2031	.6688	3.293	.0464	.0812	1.75	.0062	.0056	0.90	.0014	.6852	.838
96	100.2	1977	.0211	.2430	11.5	.2317	.6451	2.78	.0495	.0783	1.58	.0063	.0054	0.86	.0040	.6484	.838
93*	100.8	2000	.0233	.2115	9.08	.2505	.7092	2.831	.0400	.0712	1.78	.0070	.0059	0.84	.0015	.6777	.838
99	100.6	2979	.0371	.2829	7.63	.2837	.6128	2.160	.0559	.0750	1.34	.0063	.0050	0.79	.0058	.5725	.838
114	150.3	303	.0041	.1902	46.4	.0389	.6016	15.5	.0121	.0984	8.13	.0023	.0082	3.6	.0044	.9036	.837
107	151.3	611	.0099	.2084	21.1	.0803	.6258	7.79	.0223	.1010	4.53	.0040	.0075	1.88	.0102	.8421	.838
111	151.8	960	.0105	.2008	19.1	.1242	.6505	5.24	.0316	.0939	2.97	.0046	.0070	1.5	.0056	.7804	.838
106	151.4	1092	.0162	.2244	13.9	.1358	.6286	4.629	.0294	.0956	3.25	.0051	.0069	1.4	.0098	.7745	.838
113	150.8	1556	.0224	.2350	10.5	.1712	.6111	3.570	.0438	.0868	1.98	.0052	.0060	1.2	.0102	.6795	.837
108	150.8	2171	.0343	.2614	7.62	.2177	.6152	2.83	.0478	.0833	1.74	.0065	.0055	0.85	.0045	.6413	.838
118	200.2	206	.0024	.1961	81.7	.0258	.6059	23.5	.0076	.0969	12.8	.0017	.0102	6.0	.0038	.9410	.838
103	201.4	377	.0020	.1556	77.8	.0497	.6432	12.9	.0131	.0991	7.56	.0025	.0089	3.6	.0128	.8903	.838
117	199.6	516	.0061	.2073	34.0	.0646	.6179	9.57	.0169	.0938	5.55	.0037	.0091	2.5	.0042	.8746	.838
115	201.7	884	.0121	.2325	19.2	.1063	.6137	5.77	.0283	.0957	3.38	.0045	.0083	1.8	.0055	.8088	.837
102	200.5	1000	.0145	.1830	12.7	.1247	.6681	5.358	.0268	.0927	3.46	.0045	.0079	1.8	.0139	.7873	.838
116	199.3	1604	.0240	.2432	10.1	.1607	.6169	3.84	.0366	.0872	2.38	.0055	.0076	1.4	.0077	.7279	.838
101	201.2	2057	.0318	.2062	6.48	.2033	.6582	3.238	.0424	.0861	2.03	.0054	.0071	1.31	.0069	.6739	.838
105	200.3	2993	.0384	.2652	6.91	.2068	.5988	2.896	.0467	.0819	1.75	.0049	.0062	1.3	.0036	.6521	.838

*The mixtures used in these runs contained no hydrogen sulfide.

Table V — Experimental Data for Crude Oil Mixtures

Run No.	Temp. °F	Pres. psia	Nitrogen		Methane		Carbon Dioxide		Ethane		Hydrogen Sulfide		C ₃ -C ₆		Heptanes-plus*							
			x	y	K	x	y	K	x	y	K	x	y	x	y	x	y	Sp. Gr. 60/60	MW			
C-5 MIXTURE																						
139	99.4	214	.0000	.2544	.0256	.4532	17.7	.0270	.2068	7.66	.0012	.0032	2.67	.0399	.0718	1.80	.1061	.0106	.8002	...	0.895	252
165	100.7	236	.0046	.2710	.0269	.4469	16.6	.0284	.2010	7.08	.0011	.0031	2.8	.0437	.0701	1.60	.1024	.0079	.7929	...	0.897	250
133	101.5	369	.0086	.3302	.0433	.4517	10.4	.0324	.1625	5.02	.0014	.0035	2.5	.0388	.0461	1.19	.0976	.0060	.7779	...	0.899	255
140	99.7	713	.0167	.3986	.0792	.4247	5.36	.0561	.1375	2.45	.0018	.0014	0.78	.0509	.0320	0.629	.0809	.0058	.7144	...	0.896	252
124	100.0	713	.0117	.3889	.0704	.4525	6.43	.0449	.1236	2.75	.0015	.0021	1.4	.0414	.0282	0.681	.0674	.0047	.7627	...	0.894	(247)
134	100.5	1019	.0296	.4767	.0854	.3873	4.54	.0512	.1052	2.05	.0001	.00150493	.0240	0.487	.0852	.0053	.6992	...	0.896	256
128	150.0	230	.0038	.2437	.0266	.4417	16.6	.0202	.1960	9.70	.0010	.0038	3.8	.0386	.0912	2.36	.0661	.0236	.8437	...	0.886	(243)
141	150.0	416	.0072	.3081	.0075	.4612	9.71	.0328	.1632	4.98	.0015	.0035	2.33	.0378	.0521	1.38	.0665	.0119	.8067	...	0.894	251
127	149.4	514	.0082	.3057	.0555	.4625	8.33	.0395	.1658	4.20	.0015	.0014	0.93	.0432	.0521	1.21	.0681	.0125	.7840	...	0.886	(242)
125	149.6	813	.0154	.3928	.0626	.4307	6.88	.0422	.1331	3.15	.0014	.0011	0.78	.0452	.0356	0.788	.0442	.0067	.7890	...	0.890	(243)
136	150.5	963	.0248	.3888	.0849	.4422	5.21	.0461	.1247	2.70	.0016	.0022	1.38	.0483	.0340	0.704	.0771	.0081	.7172	...	0.895	250
129	150.3	1062	.0280	.4332	.0834	.3942	4.73	.0513	.1227	2.39	.0015	.0026	1.73	.0451	.0337	0.747	.0769	.0136	.6889	...	0.888	(243)
163	150.3	1285	.0362	.4811	.0904	.3574	3.95	.0557	.1198	2.15	.0015	.0018	1.2	.0449	.0281	0.626	.0824	.0118	.6898	...	0.896	250
137	201.7	229	.0033	.2127	.0196	.4511	23.0	.0151	.1977	13.1	.0008	.0041	5.1	.0272	.1066	3.92	.0925	.0278	.8415	...	0.896	252
130	200.6	514	.0104	.2750	.0461	.4575	9.92	.0317	.1797	5.67	.0013	.0038	2.9	.0359	.0690	1.92	.0908	.0150	.7838	...	0.895	250
132	201.5	793	.0188	.3321	.0734	.4591	6.25	.0394	.1380	3.50	.0016	.0032	2.0	.0472	.0529	1.12	.0832	.0147	.7364	...	0.896	251
131	202.0	1034	.0255	.3656	.0885	.4528	5.12	.0429	.1249	2.91	.0018	.0025	1.4	.0456	.0434	0.952	.0801	.0108	.7156	...	0.895	250
138	201.8	1351	.0399	.3964	.1072	.4242	3.957	.0512	.1251	2.44	.0018	.0018	1.0	.0366	.0403	1.10	.0483	.0122	.7150	...	0.896	252
C-6 MIXTURE																						
159	99.5	279	.0018	.0970	.0523	.7284	13.9	.0183	.1054	5.76	.0037	.0098	2.6	.0352	.0501	1.42	.0752	.0093	.8135	...	0.898	250
145	100.2	392	.0010	.1069	.0707	.7464	10.6	.0175	.0840	4.80	.0043	.0084	2.0	.0385	.0461	1.20	.1051	.0082	.7629	...	0.897	255
160	99.9	701	.0049	.1064	.1244	.7603	6.112	.0321	.0864	2.69	.0062	.0080	1.3	.0501	.0350	0.699	.0833	.0039	.6990	...	0.897	250
143	100.9	867	.0015	.1127	.1556	.7634	4.906	.0298	.0696	2.34	.0065	.0076	1.2	.0512	.0316	0.617	.0721	.0151	.6833	...	0.894	250
144	98.7	1548	.0127	.1318	.2285	.7636	3.342	.0349	.0646	1.85	.0075	.0064	0.85	.0052	.0261	0.518	.0901	.0066	.5742	...	0.894	252
146	100.6	2277	.0184	.1196	.2884	.7693	2.667	.0473	.0697	1.47	.0074	.0064	0.86	.0052	.0261	0.473	.0641	.0089	.5192	...	0.895	251
147	99.1	3228	.0248	.1702	.3399	.7298	2.147	.0470	.0619	1.32	.0075	.0062	0.83	.0470	.0218	0.464	.0590	.0101	.4748	...	0.895	250
148	99.2	4166	.0578	.1676	.3683	.7306	1.984	.0459	.0605	1.32	.0070	.0067	0.96	.0404	.0212	0.525	.0524	.0134	.4282	...	0.895	252
158	149.8	406	.0035	.0906	.25.9	.7329	10.4	.0213	.1060	4.98	.0039	.0095	2.4	.0365	.0490	1.34	.0822	.0120	.7823	...	0.894	250
157	150.3	783	.0053	.0996	18.8	.7412	5.864	.0341	.1009	2.96	.0054	.0087	1.6	.0456	.0383	0.840	.0583	.0113	.7249	...	0.896	251
154	149.3	982	.0097	.1228	12.7	.7279	4.690	.0398	.0974	2.45	.0064	.0081	1.3	.0445	.0351	0.789	.0827	.0087	.6617	...	0.899	250
155	149.4	2068	.0200	.1404	7.02	.7279	2.777	.0545	.0880	1.61	.0069	.0067	0.97	.0450	.0273	0.607	.0725	.0097	.5390	...	0.899	250
156	151.1	3453	.0287	.1554	5.41	.7216	2.011	.0608	.0826	1.36	.0067	.0070	1.04	.0388	.0223	0.575	.0595	.0111	.4467	...	0.899	255
162	200.0	283	.0017	.0945	55.6	.7084	16.99	.0112	.0982	8.77	.0022	.0108	4.91	.0240	.0691	2.88	.0778	.0190	.8414	...	0.898	251
152	199.6	625	.0039	.1090	27.9	.7222	7.50	.0267	.1113	4.17	.0011	.0100	2.44	.0317	.0403	1.27	.0755	.0072	.7618	...	0.894	250
149	198.4	1112	.0041	.1005	24.5	.7345	4.788	.0400	.1104	2.76	.0057	.0092	1.6	.0414	.0359	0.867	.0626	.0095	.6728	...	0.897	255
150	199.3	2166	.0113	.1260	11.2	.7334	2.967	.0513	.0959	1.87	.0069	.0072	1.04	.0418	.0271	0.648	.0648	.0164	.5767	...	0.894	251
151	199.3	3177	.0276	.1380	5.00	.7269	2.22	.0578	.0913	1.58	.0068	.0070	1.03	.0365	.0245	0.671	.0586	.0123	.4860	...	0.895	250
153	198.4	4194	.0406	.1659	4.09	.7034	1.851	.0641	.0888	1.39	.0065	.0064	1.0	.0360	.0239	0.664	.0544	.0116	.4183	...	0.895	251

ponents" is listed as a component of the phase analyses. This was necessary in order to compact the information from the mass spectrometer analyses. Those analyses reported trace amounts of hydrocarbons between ethane and hexane as well as small amounts of hydrogen, carbon monoxide and sulfur dioxide. It would be dubious to report these individually since the amounts were generally below the limits of good accuracy of the spectrometer. The fractions of these compounds were summed and reported as "trace components."

The pressures and temperatures reported in Tables IV and V are believed accurate within ± 10 psia and $\pm 2^\circ\text{F}$.

The 100°F data for A-2, A-3 and C-5 mixtures are plotted on graphs of $\log K$ vs \log pressure in Figs. 4, 5 and 6. All three isotherms are plotted for C-6 mixture in Figs. 7, 8 and 9. In order to facilitate use of the C-6 data, the $\log K$ vs \log pressure graphs were cross-plotted to obtain $\log K$ vs temperature graphs for nitrogen, methane, carbon dioxide, ethane and hydrogen sulfide; these are shown in Figs. 12 to 16.

Some equilibrium flash data were obtained from the observations of volume per cent liquid in the cell at equilibrium con-

ditions previous to sampling. These data were plotted as isotherms on a graph of pressure vs volume per cent liquid. Readings from these smoothed curves are given in Table III.

DISCUSSION

In addition to finding the variation of the K values with pressure and temperature, it was intended to evaluate composition effects which might be important.

The composition variables discussed in this work refer to overall mixture compositions, z . These were preferred over liquid and vapor compositions (x and y) even though it is necessary to specify one more independent variable than the phase rule requires to completely identify a particular equilibrium of components.

The composition variations made were of two main types, (A) use of both absorber oil and crude oil for the heptanes plus component, and (B) varying the proportions of natural

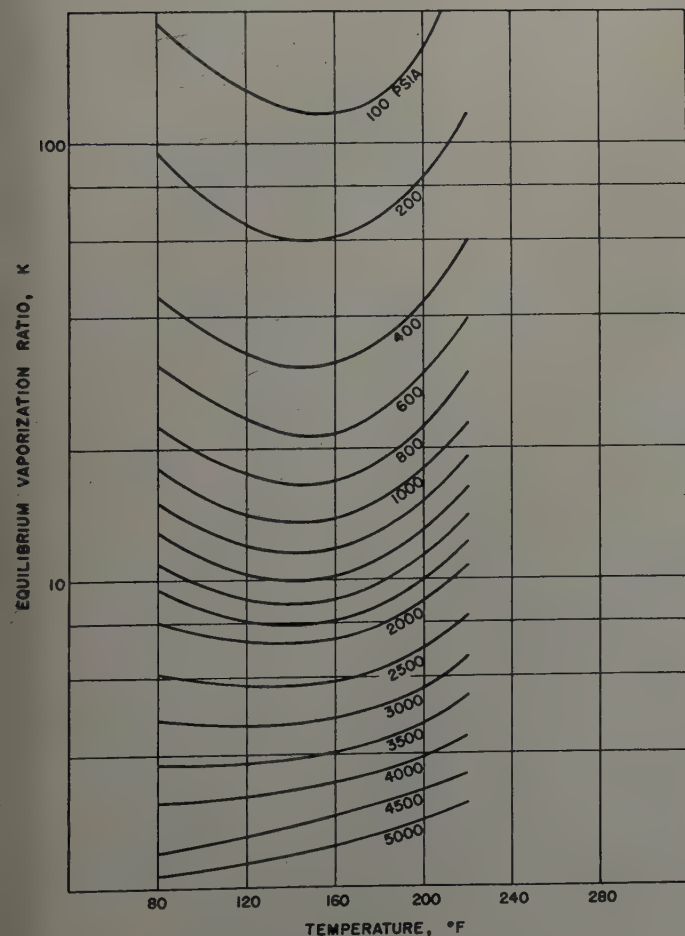


FIG. 12 — NITROGEN K 'S IN CRUDE OIL MIXTURE C-6 AS A FUNCTION OF TEMPERATURE AND PRESSURE.

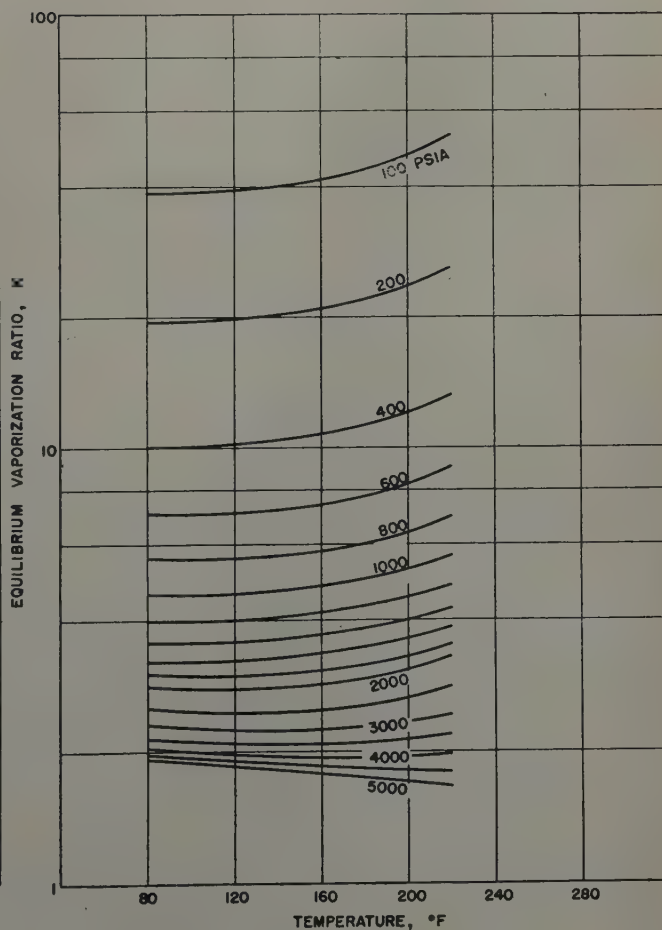


FIG. 13 — METHANE K 'S IN CRUDE OIL MIXTURE C-6 AS A FUNCTION OF TEMPERATURE AND PRESSURE.

gas to heptanes plus. The latter was essentially a variation of the gas/oil ratio. An additional variation was introduced in the work on absorber oil mixtures by eliminating hydrogen sulfide from some of the mixtures, i.e., all A-2 mixtures and runs 93 and 94 of A-3 mixture at 100°F. In the composite used in runs 93 and 94, the 5 mol per cent of hydrogen sulfide was replaced with natural gas. This variation was made to provide data for gasoline plant absorbers where the feed gas is free of hydrogen sulfide but many contain nitrogen and carbon dioxide.

The primary graphs of the data are the $\log K$ vs \log pressure curves at constant temperature and composition. Such graphs are not shown for all temperatures and compositions because of the number of them; examples of all compositions are given at 100°F and all temperatures are given for the C-6 composition. These graphs are the best means of showing the data points since the experiments were conducted at constant temperature and composition. On these graphs the convergence effect is shown most by the mixtures of higher bubble point pressure (BPP) at 100°F. Fig. 6 brings out clearly the fact that these curves become discontinuous at the single phase pressure and do not necessarily converge toward $K = 1$ except

at the critical temperature of the mixture. Convergence is shown more readily by mixtures of higher BPP at higher pressures where the properties of the phases become more nearly alike and the components show less preference for one phase or the other. The K 's thus approach unity.

The effects of composition are more clearly observed on graphs of $\log K$ vs temperature as in Fig. 10. At 1,000 psia

the curve for nitrogen in C-5 was such that $\frac{\partial K}{\partial t}$ became less

positive with increase in temperature (concave down; $\frac{\partial^2 K}{\partial t^2}$

is negative) while for C-6 mixture $\frac{\partial K}{\partial t}$ became more positive

with increase in temperature (concave up; $\frac{\partial^2 K}{\partial t^2}$ is positive).

For nitrogen in the two crude oil mixtures this was true over the pressure range investigated, but in general, the sign of $\frac{\partial^2 K}{\partial t^2}$ depended on the pressure also. Thus the effects of com-

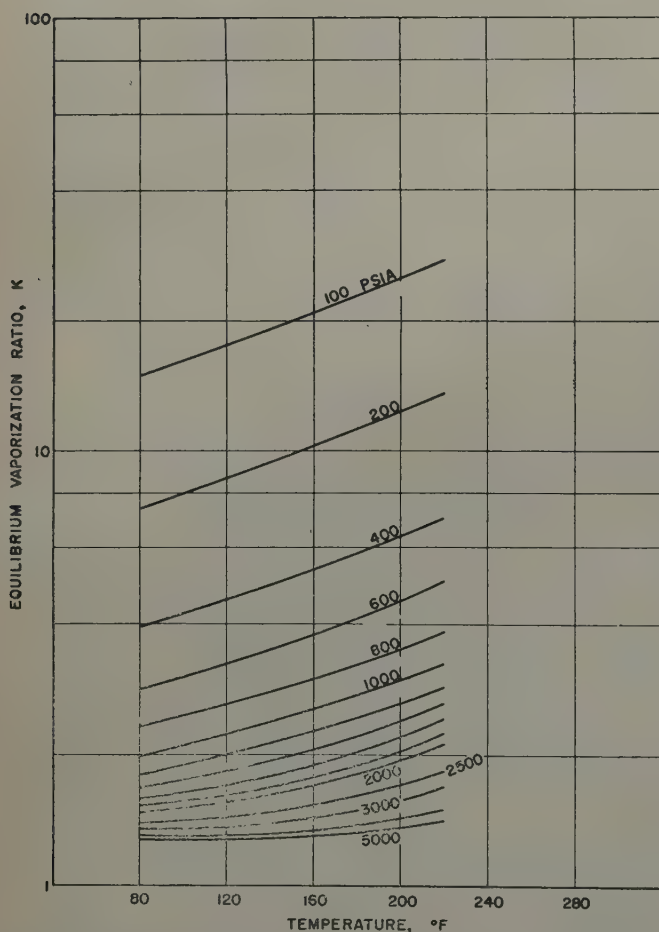


FIG. 14 — CARBON DIOXIDE K 'S IN CRUDE OIL MIXTURE C-6 AS A FUNCTION OF TEMPERATURE AND PRESSURE.

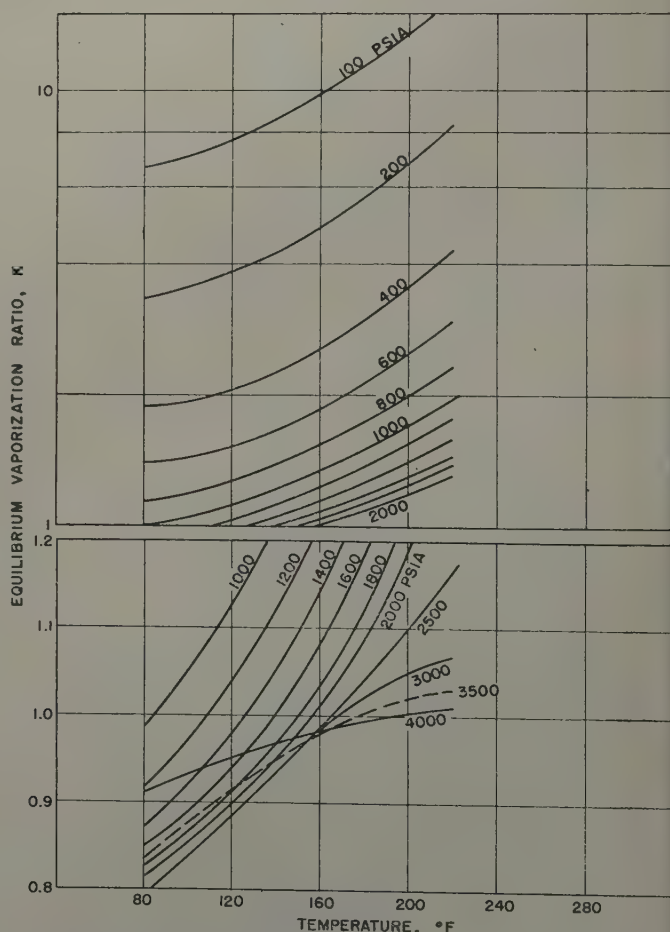


FIG. 15 — ETHANE K 'S IN CRUDE OIL MIXTURE C-6 AS A FUNCTION OF TEMPERATURE AND PRESSURE.

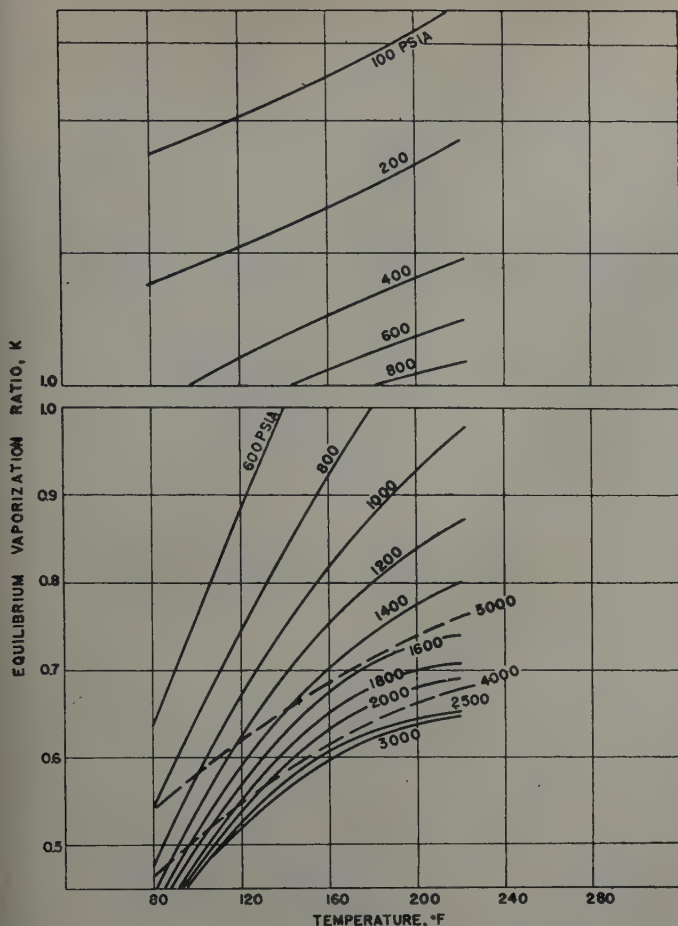


FIG. 16 — HYDROGEN SULFIDE K 'S IN CRUDE OIL MIXTURE C-6 AS A FUNCTION OF TEMPERATURE AND PRESSURE.

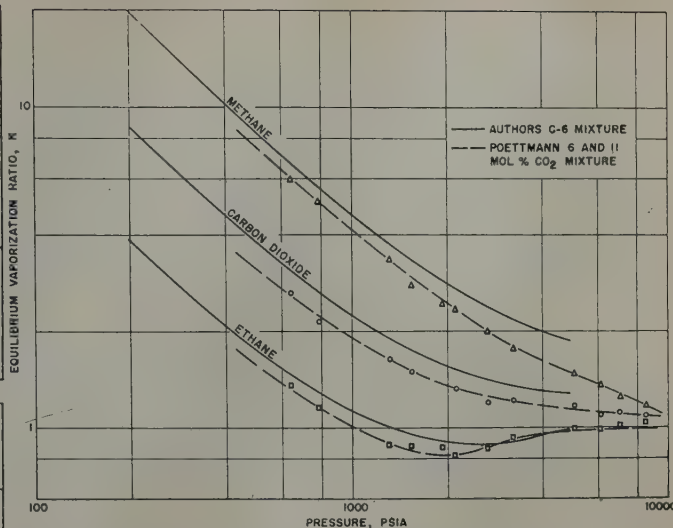


FIG. 18 — COMPARISON OF K 'S IN CRUDE OIL MIXTURE C-6 WITH POETTMANN'S DATA AT 120°F.

position are evident but are mingled with pressure effects to the extent that it is difficult to make simple statements regarding the effect of composition on the K 's of any component. For example, from Fig. 10 it may be seen that nitrogen K 's at 1,000 psia in C-5 mixture are lower than those in C-6 at 80°F, higher from 94 to 182°F and lower again at 200°F. Fig. 11 compares the K values from the two absorber oil mixtures at 1,000 psia. The greatest numerical differences are in the non-hydrocarbon K 's although the hydrocarbon K 's show the qualitative composition effects described above.

The most interesting effect of temperature was the actual decrease in nitrogen K 's with increasing temperature in certain temperature ranges. This was shown by no other components except methane over a very narrow range of temperature and pressure in the A-2 and C-6 mixtures. Such behavior of the nitrogen K 's was not unexpected since other experimental data have shown the same.^{1,2,3,7}

Comparisons of the data obtained by the authors with similar data in the literature are made in Figs. 17 and 18. In Fig. 17, methane and ethane K 's from Webber's⁸ data for absorber oil mixtures at 100°F are compared with data from A-2 mixture at 100°F. The scattering of Webber's data points is characteristic of data obtained from mixtures of varying overall composition. Poettmann's⁹ data from a carbon dioxide-natural gas-crude oil mixture at 120°F are compared with C-6 data interpolated at 120°F in Fig. 18. The C-6 K 's for methane, carbon dioxide and ethane are 10-30 per cent higher over the entire range of temperature and pressure. The difference may be attributed to the large difference in overall composition of the two mixtures. It is believed that the presence of nitrogen and hydrogen sulfide in C-6 mixture is less the cause of this than the large difference in the methane to heptanes-plus ratio between the two mixtures.

CONCLUSIONS

Equilibrium vaporization ratios were obtained for the non-hydrocarbons nitrogen, carbon dioxide, and hydrogen sulfide and for the hydrocarbons methane and ethane in two types of mixtures which are important in petroleum producing and

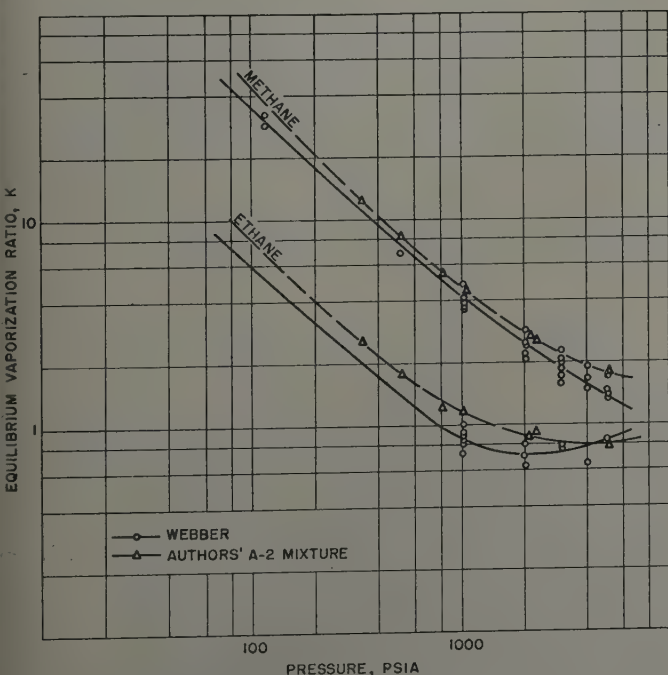


FIG. 17 — COMPARISON OF K 'S IN ABSORBER OIL MIXTURE A-2 WITH WEBBER'S DATA AT 100°F.

natural gasoline refining operations. Some effects of varying the overall mixture composition were obtained to serve as a guide in the application of these K values to other mixture compositions not specifically investigated. In making a choice as to which data to use it is recommended that overall compositions be matched as closely as practicable. It is believed that these data will apply with little error to mixtures having concentrations of the non-hydrocarbons within 5 mol per cent of those in the experimental mixtures.

ACKNOWLEDGMENT

The authors wish to express appreciation to the management of the Stanolind Oil and Gas Co. for permission to publish this paper; to J. B. Opfell for his assistance in designing and constructing equipment; to J. A. White who helped obtain the data; and to H. Thompson and L. Green for obtaining analyses.

REFERENCES

1. Boomer, E. H., Johnson, C. A., and Piercey, A. G. A.: "Equilibria in Two-Phase, Gas-Liquid Hydrocarbon Systems. II. Methane and Pentane," *Can. J. Research*, (1938) **16B**, 319.
2. Boomer, E. H., Johnson, C. A., and Piercey, A. G. A.: "Equilibria in Two-Phase, Gas-Liquid Hydrocarbon Systems. IV. Methane and Heptane," *Can. J. Research*, (1938) **16B**, 396.
3. Boomer, E. H., and Johnson, C. A.: "Equilibria in Two-Phase, Gas-Liquid Hydrocarbon Systems. III. Methane and Hexane," *Can. J. Research*, (1938) **16B**, 328.
4. Poettmann, F. H., and Katz, D. L.: "Carbon Dioxide in a Natural Gas-Condensate System," *Ind. Eng. Chem.*, (1946) **38**, 530.
5. Poettmann, F. H.: "Vaporization Characteristics of Carbon Dioxide in a Natural Gas-Crude Oil System," *Trans. AIME*, (1951) **192**, 141.
6. Eilerts, K., and Smith, R. V.: "Specific Volumes and Phase-Boundary Properties of Separator-Gas and Liquid-Hydrocarbon Mixtures," U. S. Bureau of Mines, R.I. 3642 (April, 1942).
7. Miller, P., and Dodge, B. F.: "The System Benzene-Nitrogen," *Ind. Eng. Chem.*, (1940) **32**, 434.
8. Webber, C. E.: "Equilibrium Constants for Hydrocarbons in Absorption Oil," *Trans. AIME*, (1941) **142**, 192.

DISCUSSION

By Fred H. Poettmann, Phillips Petroleum Co., Bartlesville, Okla., Member AIME

The authors of this paper are to be complimented for their thorough manner of studying the equilibrium vaporization ratios of the non-hydrocarbons which commonly occur in reservoir fluids. The data presented will go far in satisfying a long standing demand of the natural gasoline, refining and production phases of the oil industry for information on the vapor-liquid equilibrium conditions of these non-hydrocarbons.

The comments made here will be confined to the authors' carbon dioxide equilibrium vaporization ratios in the natural gas-crude oil systems. The following table shows the variation of methane and C_7+ composition on four reservoir fluid mixtures for which carbon dioxide K data have now been determined.

	Natural Gas Billings Crude	Mole Per Cent Natural Gas Erath Condensate	Jacoby-Rzasa C-5	C-6
C_1	70 - 80	60 - 65	9.58	38.3
C_7+	8 - 10	25 - 26	68.7	41.2

The variation of the authors' carbon dioxide K values due to variation of the methane and C_7+ concentration is very small, almost negligible. As stated by the authors, the K data for carbon dioxide in the natural gas-crude oil system containing only 8-10 per cent C_7+ had carbon dioxide K 's 10-30 per cent lower than the authors' K 's in a system containing from 41.2 to 68.7 per cent C_7+ . The authors failed to make one comparison, that of the carbon dioxide K 's in a natural gas-condensate system. In the region removed from the convergence pressure, the authors' K 's agree almost exactly with the K 's in the natural gas-condensate system although the C_7+ concentration was only 25-26 per cent and the character of the C_7+ fraction was considerably different. Neglecting for a moment the character of the C_7+ fraction, it would seem that it takes a considerable variation in C_7+ concentration to cause only a minor variation in the carbon dioxide K values (C_7+ from 68.7 to 25 per cent with no change in K). On the other hand the agreement of the authors' carbon dioxide K 's with those in the natural gas-condensate system may be purely coincidental, the effect of the C_7+ concentration on the K values being offset by the difference in character of the C_7+ fractions.

★ ★ ★

CORRELATION OF RADIOACTIVE LOGS OF THE LANSING AND KANSAS CITY GROUPS IN CENTRAL KANSAS

JOHN V. MORGAN, STANOLIND OIL AND GAS CO., TULSA, OKLA., JUNIOR MEMBER AIME

ABSTRACT

Although the Lansing-Kansas City groups constitute one of the more important producing horizons of Central Kansas, exploitation has been hindered by inability to consistently identify and correlate the various productive intervals. A study of gamma ray-neutron logs and core data indicates that definite zones exist which are related to production and which may be generally correlated over an appreciable portion of Central Kansas. A suggested system of zoning and nomenclature is developed and illustrated, along with examples of its specific application in overall evaluation and in development of zonal production characteristics. General adoption of the suggested system should aid appreciably in the future development of commercial Lansing-Kansas City production in Central Kansas. It is probable that similar systems might be developed for other regions where production is obtained from various uncorrelated and unnamed zones in thick pay intervals.

GENERALIZED GEOLOGY OF CENTRAL KANSAS

The most important large subsurface feature in Central Kansas regarding oil production is the Barton Arch, which is part of the Central Kansas uplift. The Barton Arch is a buried ridge of Pre-Cambrian granite running northwest-southeast, near which the majority of Central Kansas oil fields have been found. To the northeast of this arch, the granite dips sharply into the Salina Basin and similar basin areas to the west and south are termed the Hugoton Embayment and Anadarko

Basin, respectively. This report deals primarily with the region of the Central Kansas Uplift and its southwestern flank. Fig. 1 indicates the general location of subsurface structural features along with the oil and gas fields of Central Kansas.

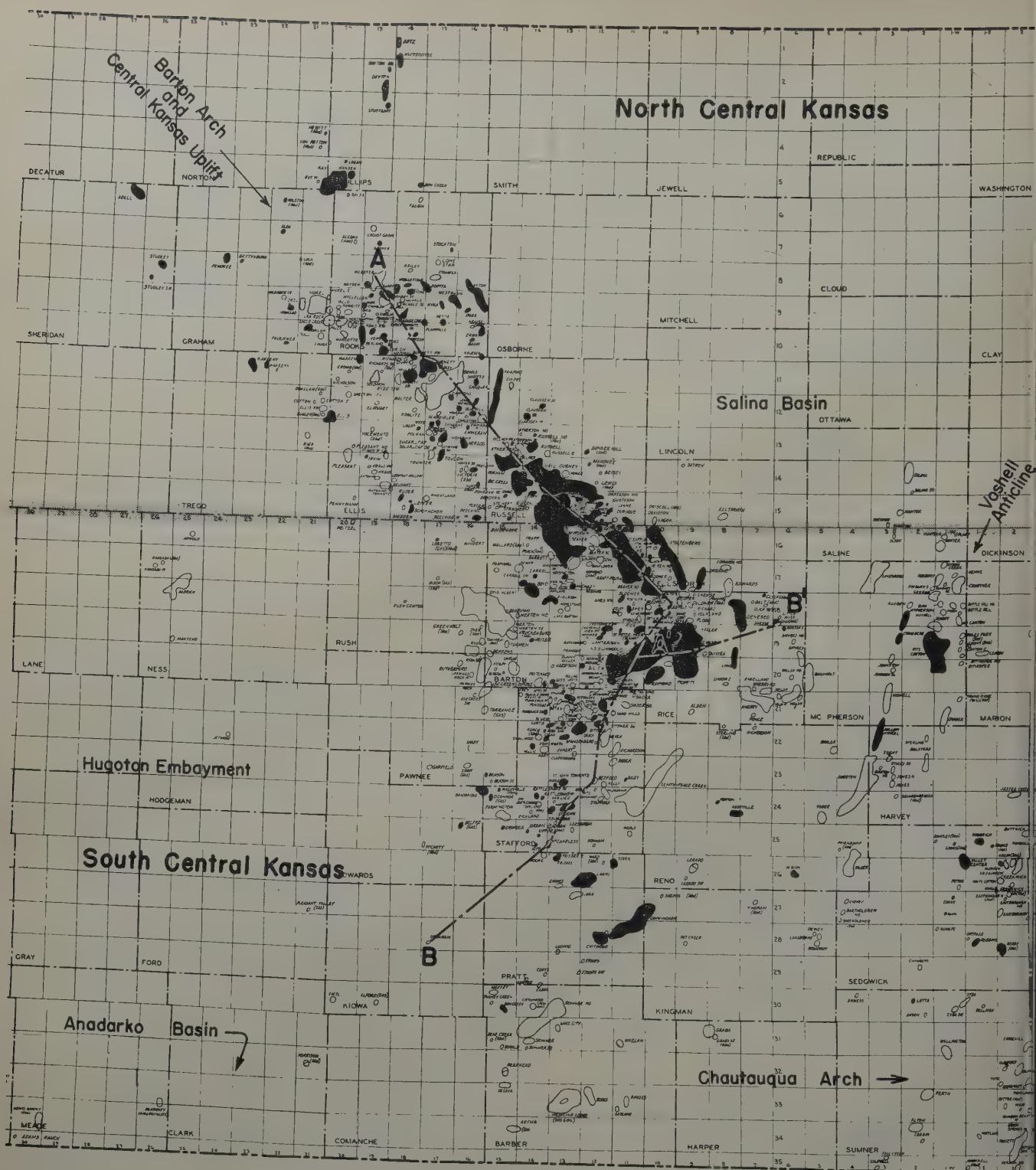
Above basal granite lies the Cambro-Ordovician Arbuckle Dolomite which is the principal oil producing zone in Central Kansas. This formation, as well as those higher in the section, reflects the general underlying granite structure; however, the Arbuckle top is an erosional surface and most oil producing structures are probably topographic hills. Formations above the Arbuckle in ascending order may include those of the Ordovician, Silurian, Devonian, Mississippian, Pennsylvanian, and Permian periods as well as certain recent sediments. As the Barton Arch is approached, those formations below the Pennsylvanian and above the Arbuckle tend to pinch out until Pennsylvanian rocks, which include the Lansing-Kansas City groups, rest directly upon the Arbuckle. The Arbuckle itself is also completely eroded away at points on the Arch, but is up to 600 ft thick only 20 to 30 miles down dip.

Formations of the Pennsylvanian system vary considerably in thickness but probably average about 1,000 ft as an overall total. The more commonly known oil productive zones are the Tarkio, Topeka, Toronto (Dodge), Lansing-Kansas City and Marmaton. Of these, the Lansing-Kansas City, which varies from about 200 ft to 400 ft in thickness, is the most important, since its areal frequency of oil production is exceeded only by that of the Arbuckle.

Most Pennsylvanian rocks in Central Kansas were deposited in shallow seas which alternately covered, then retreated from the land. This resulted in recurring cycles of thin beds which cover relatively large areas. Small surface deformations during the period of deposition also caused variations in the type material deposited and its thickness. The local structures of Pennsylvanian time probably influenced the accumulation of

¹References given at end of paper.

Manuscript received in the Petroleum Branch office Sept. 14, 1951. Paper presented at the Fall Meeting of the Petroleum Branch in Oklahoma City, Okla., Oct. 3-5, 1951.



LEGEND
FIELDS WITH LANSING-KANSAS CITY PRODUCTION
OTHER FIELDS

FIG. 1 — OIL AND GAS FIELDS OF CENTRAL KANSAS.

oil so that today our primary interest in these series is at points where maximum sedimentary variations may be expected.

THE LANSING-KANSAS CITY GROUPS

The Lansing-Kansas City groups are a series of limestones and shales over the majority of Central Kansas but shale intervals increase and sand members are observed near the Oklahoma border. These groups are exposed at the surface near the eastern border of Kansas but are found at depths of 3,000-4,000 ft in the central part of the state. Overlying formations, which are ordinarily easily identified by gamma ray-neutron logs include, in ascending order, the Iatan lime, Douglas shale, Toronto lime, and Heebner shale. The Heebner shale is a valuable marker since it is highly radioactive and produces large gamma ray curve deflections. The Heebner-Lansing interval decreases to the northwest on the Barton Arch until the Toronto lime immediately overlies the Lansing.

Oil production of the Lansing-Kansas City groups is found in porous streaks of various limes within the section. Identification and correlation of these limes by formational samples has not been generally possible over wide areas and identification on the basis of penetration from a Lansing-Kansas City top has been used in some localities. This method is not satisfactory due to the considerable variations in thickness of the lime and shale zones. It is also difficult to pick a uniform Lansing-Kansas City top from samples and drilling time since the "top" is usually a gradational change. Accurate lithological interpretation and identification of important zones can be performed by use of gamma ray-neutron logs.

Lithological Characteristics and Zoning of the Lansing-Kansas City Groups

Fig. 2 is the gamma ray-neutron log of one of the first wells in Kansas where the Lansing-Kansas City was diamond cored, and oil shows and lithology, as indicated by cores, are shown thereon. The correlation of limes and shales with the log is apparent. Identification of the various zones is necessary, since only one or two zones will usually be found commercially productive in any field and changes in zonal thickness and lateral lithology may be important factors in the accumulation of oil. A standardized zonal nomenclature must also be used to permit accumulation of data regarding each zone's possible characteristics on a field or areal basis.

This and similar data at other wells prompted initial attempts to apply correct geologic names to the various Lansing-Kansas City intervals or zones. It was not found feasible to assign geologic names, as applied at Eastern Kansas outcrops and, therefore, letters have been used to define those arbitrary zones selected. The log of Fig. 2 is typical of recent good quality logs and shows all selected units or zones except zone M which, it was later discovered, is missing at this specific location. It is also speculative as to whether zone G' is present since this zone was not specifically observed until later at other locations.

The arbitrary zonal boundaries generally coincide with various gamma ray (shale) peaks which, of course, do not necessarily represent shale mid-points, nor top of a succeeding lime. It is advisable to examine the neutron curve to confirm shale

interpretations and, at certain locations, the neutron curve must be used almost exclusively to determine the real, or apparent, zonal boundary. The foregoing method is believed the easiest approach for initially separating the various primary lime sequences which are of major importance. Since the shales are of little interest, the top of the included lime in each zone is the data that should be reported and analyzed on an individual well basis.

Correlation of Lansing-Kansas City Zones

The Lansing-Kansas City groups are sufficiently uniform in Central Kansas generally to allow correlation of the arbitrarily selected zones over an appreciable distance. Such correlation is presented on Fig. 3 where cross section AA' proceeds for a distance of about 100 miles northwest-southeast generally atop the Barton Arch, while cross section BB' is of a similar length but approximately at right angles to cross section AA'. Cross section BB' begins on the western flank of the Barton Arch, then proceeds up and over the Arch and into the Salina Basin. The specific location of these cross sections is shown on Fig. 1.

It should be noted that the indicated upper boundary line for zone A is above the true lithological or gamma ray-neutron Lansing-Kansas City top which would be near the mid-point

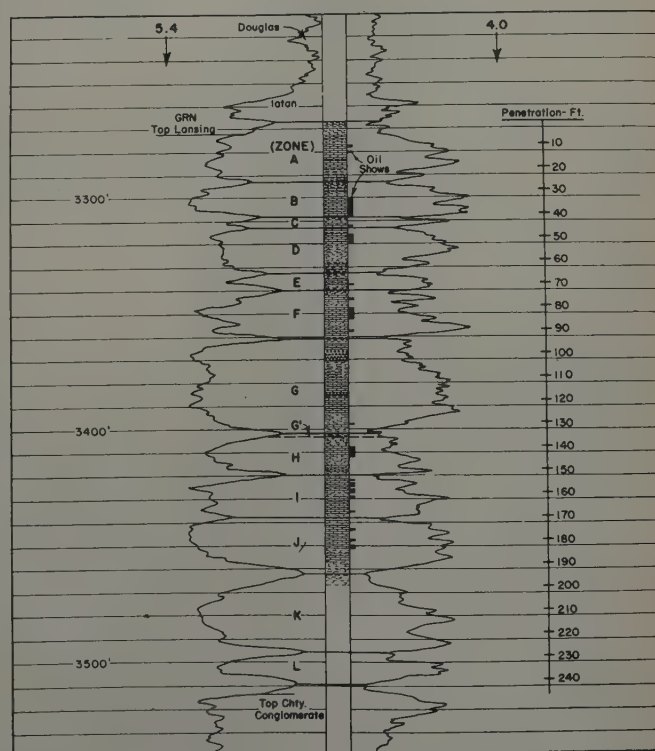


FIG. 2 — GAMMA RAY-NEUTRON LOG, STANOLIND E. SIEFKES "B" NO 11, SEC. 3-22S-12W, STAFFORD COUNTY, KANSAS.

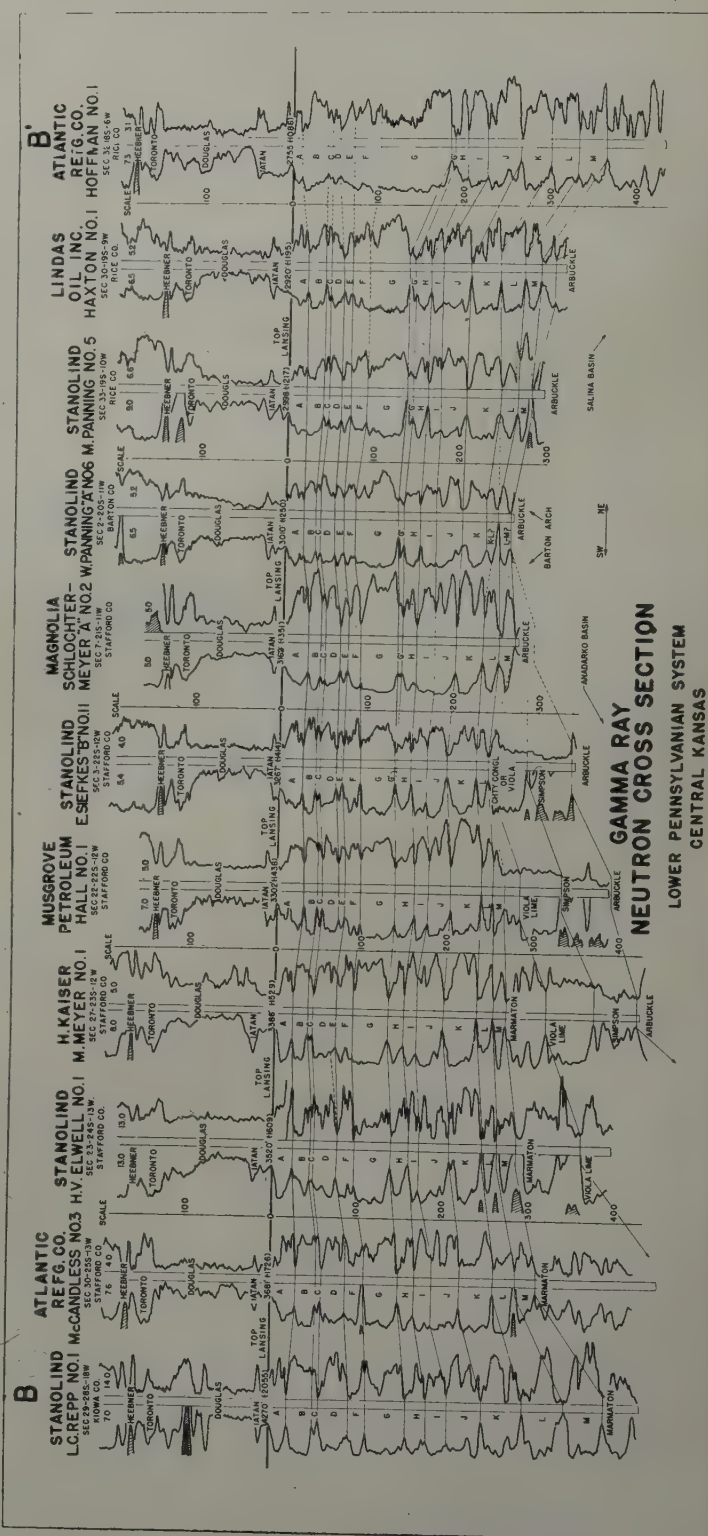
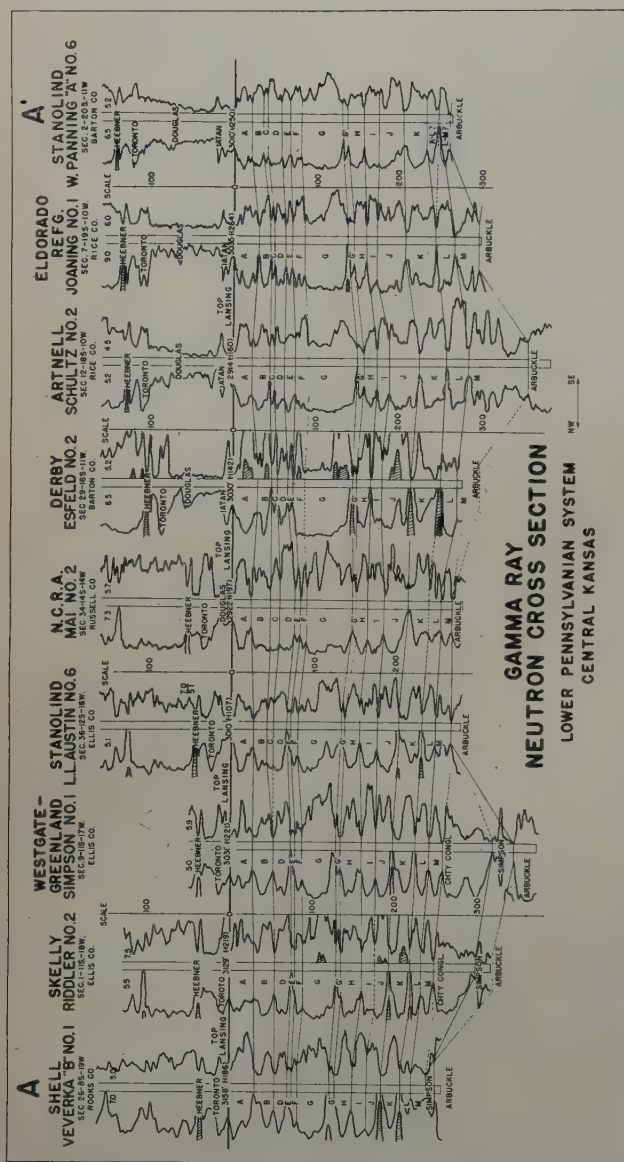


FIG. 3—GAMMA RAY-NEUTRON CROSS SECTIONS, LOWER PENNSYLVANIAN SYSTEM, CENTRAL KANSAS.

of the gamma ray curve shift. Also, the cross sections do not fully illustrate subsurface structure since logs are plotted flat on the Lansing-Kansas City top. Data show that cross section AA' is relatively flat on the Lansing-Kansas City structurally with only 157 ft maximum variation in true subsea elevation while the Lansing-Kansas City top similarly varies almost 1,000 ft on cross section BB'.

Variations in zonal thickness are immediately apparent, and it is obvious that identification on the basis of penetration is impractical over any appreciable area. Also, some zones disappear in certain areas as does zone C on cross section AA' and also zones E and G' on cross section BB'. It has been further noted that the logs of wells in a single field will often show as much variation in certain zones as is indicated for them over the entire cross section AA'. Nevertheless, correlation of the selected zones is generally definite and consistent over the large area involved.

PRODUCING CHARACTERISTICS AND METHODS OF EVALUATION

The Lansing-Kansas City (LKC) is desirable to produce since it usually contains sweet crude with considerable volumes of gas. In no place has it been found to have a wholly effective water drive, and control is usually assumed to be completely volumetric even though recoveries in some cases approach 250 bbl per acre ft of net pay. Some limited water production is found (usually greater in zone G); however, it often appears to be relatively constant, or to decline in quantity along with the oil. The zones respond to acid treatment readily and should be treated during any test except in the event of good natural productivity. It is being gas driven at the Cunningham Field and water flood success is indicated in the more porous zones at certain accidental floods. Its erratic permeability development at many fields may prevent extensive future water flood programs although such programs should be considered.

It appears that formation sample analysis and drilling time correlation are not always sufficient for location of the probable productive zones. This arises from several factors, some of which are:

(1) Recent diamond cores have at times logged up to 40 separate oil shows over the LKC interval. In these wells many shows were of insignificant extent, but do illustrate that an oil show in samples could be carried practically all through the section.

(2) The upper portion (about 100 ft) often drills quite rapidly with rotary tools so that "breaks" are not observed. Also, certain dolomitic shales often break and drill at the rate of one-half min. per ft. When samples are poor these zones have been erroneously drill stem tested, as revealed by subsequent gamma ray-neutron (GRN) logs.

Cores, both diamond and conventional, are not the complete answer for accurate evaluation during initial rotary drilling. This arises since drill stem test of zones indicated to be oil bearing by cores have at times given only 10-30 ft mud with zero shut-in bottom hole pressure (BHP) recorded. It is not positively known whether this means that there is actually little or no pressure in the zone, or if an almost complete lack of inherent permeability prevents formational pressure from being recorded by the tool. It appears, however, that such lack of BHP indication has been regarded as positive con-

demnation by most operators, since no record could be found showing further tests of any such LKC zone.

Since the LKC is quite susceptible to acid treatment, the presence of low core permeability may not be serious if other factors are favorable. This is illustrated by a well which cored a very soft zone (K) that was oil bearing with 21.3 per cent average porosity but permeability was all less than .05 md. The log appeared favorable for this interval and, after 9,000 gal acid, the zone (8-ft thick) flowed 50 bbl oil per hour.

Lansing-Kansas City evaluation in a small area may often be made by use of gamma ray-neutron logs and diamond cores at certain wells, while drill stem tests with samples and drilling time in conjunction with logs are used at the remainder. This allows zones of oil saturation, as positively revealed by diamond core, to be checked by drill stem test at other nearby wells. Any drill stem test taken should allow 15 to 30 minutes for a closed in pressure reading since this may be as important data as actual fluid recovery.

It has been noticed that LKC structure, as revealed by its top, is usually not the primary factor controlling zonal productivity at any individual well. This structure generally reflects to some degree that of the underlying Arbuckle, although closure is normally not so extreme. Realizing the variations in zonal thickness which may occur within the LKC, it appears that the local structure of individual zones may not fully coincide with structure of the LKC top. It is therefore advisable to examine the structure of the lime zones of interest, along with the LKC top, in any field where such is possible.

It is probable that local or areal changes in lateral lithology within any zone were a factor in the accumulation of oil. It has been noted that porous zones in the limes as shown by GRN sometimes tend to become somewhat shale filled at other locations. In the presence of some slight regional or local dip these conditions would appear to fulfill those of a stratigraphic trap.

The cross sections of Fig. 3 show that shale breaks between certain zones, particularly those above G, tend to be somewhat erratic in occurrence. Concurrently with this, thick porous limes are usually present in the overall interval and such are often oil productive if other conditions are favorable. The occurrence of zonal thickening and/or absence of correlatable shale breaks should therefore be regarded as favorable for localized zonal productivity.

Characteristics of Individual Zones

It has been found that certain zonal characteristics may be observed by examining well and log data where positive Lansing-Kansas City tests have been made. A positive test is deemed to be the actual production test of a zone, a definite drill stem test, or positive fill-up when the zone was penetrated with cable tools. Lack of electric or GRN logs at many wells makes their inclusion impracticable; however, in fields where relatively uniform thickness of all zones is indicated, the producing zone (A through M) may at times be selected by correlation with logs of nearby wells.

The statistical results of a study of this type, which included 471 positive tests at 174 wells, are shown on Fig. 4, with division made for North Central and South Central Kansas as indicated by Fig. 1. When viewed in regard to the total area involved, the number of tests analyzed is obviously quite low and indicated characteristics should be regarded as preliminary in nature. The use of standardized zonal nomenclature

by all operators should allow any inherent zonal characteristics to be further observed and interpreted.

It is emphasized that the percentages of success indicated for the various zones do not mean that such commercially productive frequency can be expected in every field or well. Obviously the major portion of the tests to which the percentage success figures each apply would not have been made if all factors available for analysis had not indicated good chances for success. Even after all possible prior analysis, the overall success frequencies are quite low and it is hoped that use of zonal nomenclature will ultimately allow improvement in this respect.

It is noted that over $3\frac{1}{2}$ times more tests are shown for North Central Kansas than for the South Central portion. It is probable that this total number of tests is a function of the frequency of oil occurrence with North Central Kansas being the more favorable area. This is not wholly true, however, since LKC production off the Barton Arch has sometimes been disregarded in the past. The upper zones are indicated generally the most favorable in North Central Kansas where they are somewhat difficult to correlate, while the lower zones are generally better in the South Central part. The lower zones have also produced considerable oil in the northern area.

Zone A is the uppermost zone and commonly shows a gradational upper contact with lime gradually replacing shale as the zone is penetrated. It is normally productive only in Russell County and immediately adjacent areas, although one well was noted in Zone A at Chindberg Field of McPherson County. Porous intervals in the lime are usually about four to six ft in thickness and many logs show one porous interval near the top and one at the bottom of the zone.

Zone B is primarily productive in the general vicinity of Russell, Rooks and Phillips Counties where it is called the 30-ft zone and usually attains its maximum thickness. More tests are recorded in this zone than for any other in North Central Kansas and the 85 per cent success frequency is one of the highest shown. Production from B in South Central Kansas is believed less likely, but, when such is found, recoveries are good, as at Cunningham Field in Pratt County where

B is probably the producing zone. No wells from Cunningham Field were included in the present statistical study.

Zone C is a very thin unit originally selected primarily for aid in correlation. It is usually readily correlated off the Barton Arch and at many places on the Arch; however, its presence is not apparent north of Ellis County. In Russell and Ellis counties, it often tends to merge with zone B as the separating shale break becomes less distinct. It is highly productive in this locality and has the highest success frequency of any zone in North Central Kansas. Zones B and C are good examples of production being obtained from an interval which has thickened or where shale breaks tend to disappear.

Zone D like other upper zones is good in North Central Kansas, and at times its upper portion tends to merge with zone C. It is probably the equivalent at most places of the so-termed 60-ft zone and also has a very high success frequency in South Central Kansas, where it is probably the best upper zone. It tends to produce more gas than any other upper zones.

Zone E was originally named primarily for correlation purposes, as it rarely attains sufficient thickness to be commercially productive even if oil bearing. Zone F is of near equal significance in both areas since it has generally given good recoveries. It tends to disappear or become part of G at some locations when the intervening shale break is not distinct. Like D, it is usually somewhat more gas productive than other upper zones.

Zone G is the thickest lime sequence selected for correlation and is usually the one most readily identified in preliminary correlation work. It is often characterized by a weathered chert section at the top and porosity-permeability conditions are generally good. It has given good recoveries at certain locations in both areas, but available data show no successful tests south of Barton County. Initial productivities are usually high and it normally has a considerable amount of water present.

Production from G is usually obtained in the upper portion or probable 90-ft zone and oil is not commonly produced from the lower part unless a localized shale streak develops such as shown on the log of Stanolind's L. L. Austin No. 6. This lower part may then be termed the 120-ft zone in Russell County, but it has no readily observed counterpart in other areas. The thickness and good porosity-permeability of G indicate it to be the most feasible zone for salt water disposal usage in the Lansing-Kansas City.

Zone G' is a very small zone which was discovered correlatable after having selected the zonal letters on the Siefkes "B" No. 11 log. It has no production at any place and serves only to make interpretation of zone H more difficult. This arises since where G' is not obviously present, a slight neutron curve reversal in the top on Zone H may be a shale tendency rather than porosity. Of course, if this shale is of any extent it should be revealed by the gamma ray; however, on old logs this is not always the case.

Zone H is one of the most disappointing zones since it nearly always has favorable log characteristics and oil saturation is not infrequently encountered. Unfortunately, tests of this zone often produce water only and zero BHP is also apparently common. The shale tendency due to G' as discussed above has also been an unfavorable factor; nevertheless, recoveries of 70,000-80,000 bbl of oil per well may be had in the event the zone is productive.

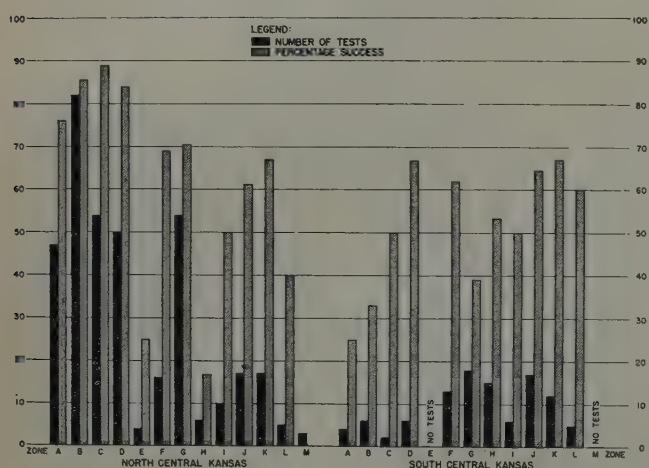


FIG. 4 — GRAPHICAL SUMMARY OF LANSING-KANSAS CITY TESTS.

Zone I is an average zone with 50 per cent success frequency but oil occurrence is apparently somewhat rare since number of total tests is quite low. Porosity of a high degree is not often indicated and little consideration is indicated for I unless it can be correlated with offset production.

Zone J is one of the most favorable zones in the Lansing-Kansas City and gives excellent recoveries when productive. The GRN log usually shows a large porous interval in this zone, however, due to its depth within the LKC, zone J has probably been often overlooked in the past, even though it has produced over 100,000 bbl per well in certain instances.

Zone K has probably also been overlooked at times in the past but it does have a very high success percentage in both areas and is usually quite commercial when productive. Very few tests have been made in zone L and it is assumed that oil occurrence is infrequent since only moderate success has been obtained when it was tested. No ultimately successful tests were found for zone M but it is noted that the zone pinches out at places and, for example, it is not present on cross section BB' at the E. Siefkes "B" No. 11 log.

CONCLUSIONS

1. The Lansing-Kansas City groups can be zoned and correlated in most of Central Kansas by use of gamma ray-neutron logs.
2. Identification of the various zones will permit correlation of test results and should increase the possibility of obtaining commercial production.
3. A standardized nomenclature among the various operators will permit accumulation of experience and information regarding possibilities of the various intervals and help in exploitation of the section.
4. The technique of zonation and correlation on the basis of gamma ray-neutron logs should be helpful in exploitation of other producing horizons where pay is scattered throughout a thick, generally undifferentiated interval.

ACKNOWLEDGMENTS

Acknowledgment is made to Stanolind Oil and Gas Co. for permission to publish this material and to various Stanolind engineering and geological personnel for their suggestions.

REFERENCES

Portions of the below listed publications were helpful in developing background material on the general geologic conditions of Central Kansas. The publication by VerWiebe also provided the primary data for showing Central Kansas fields which have Lansing-Kansas City production.

1. Moore, Raymond C.: "Divisions of the Pennsylvanian System in Kansas," State Geol. Survey of Kansas, *Bulletin 83*, (1949).
2. Moore, Raymond C., Frye, John C., and Jewett, John Mark: "Tabular Description of Outcropping Rocks in Kansas," State Geol. Survey of Kansas, *Bulletin 52*, (1944).

3. Lee, Wallace, Leatherock, Constance, and Botinelly, Theodore: "The Stratigraphy and Structural Development of the Salina Basin of Kansas," State Geol. Survey of Kansas, *Bulletin 74*, (1948).
4. VerWiebe, W. A., et al: "Oil and Gas Developments in Kansas During 1949," State Geol. Survey of Kansas, *Bulletin 87*, (1950).

DISCUSSION

By Kenneth L. Smith, Champlin Refining Co., Enid, Okla.,
Member AIME

Morgan is to be complimented upon his system of zoning and nomenclature as it has been developed. He has shown the logic and feasibility of such a correlation which should be a most valuable aid to the oil operator in Central Kansas. This study should be expanded further to show how it can be applied to other types of logs in the same area.

The prime objective of this paper is the correlation of the various productive zones in the Lansing-Kansas City groups throughout Central Kansas by a study and comparison of gamma ray-neutron logs and core data. The identification of these zones by alphabetical nomenclature appears to be an excellent method for identifying the various members of the Lansing-Kansas City groups which are often found to be productive in the Central Kansas areas outlined in Fig. 1 of this paper. As pointed out, the presently used method of identifying these zones by depth from the top of the Lansing has led to considerable misunderstanding due to the change in thickness of the zones. If the oil operator in this section of Kansas is provided with a means to correlate accurately, not only the productive Lansing-Kansas City zones within the same field, but from one field to another it should be a considerable aid in the efficient exploitation of the Lansing-Kansas City production.

The various productive zones in the Lansing-Kansas City have been designated from A through M, with a zone G' shown on a considerable number of logs in Fig. 3. On most of the logs it appears that the zone G' could very easily be incorporated into the zone H, which would tend to simplify the method of zoning. It is stated in the paper that G' is a very small zone with no record of individual production; therefore, elimination of this additional breakdown, and placing it into zone H should tend to simplify the classification procedure. No mention is made as to whether zone G' could be the top of the Kansas City group; if this is the case, it could account for the irregularities in this portion on most of the logs presented.

Fig. 4 of this paper graphically illustrates the percentage of success for the completion of oil in all zones A through M. It is doubtful if this information is of sufficient accuracy to make such a tabulation for each individual zone. This would be particularly true for those tests which were made by perforating casing after it has been set through any group of particular zones. Field experience has shown that the cement bond behind casing is very poor throughout the Lansing-Kansas City section whenever there are oil shows present and it is not unusual to encounter communication between zones which might be 40 to 50 ft removed from the zone being tested. The possibility of communication up and down the well bore is almost assured if the well is acidized through

the perforations. With the previous facts in mind, it is suggested that Fig. 4 should only be used as a relative guide as to what group of zones have experienced the highest percentage of success.

It is suggested to the industry to use the nomenclature of the Lansing-Kansas City zones as set forth in this paper and that some type of study group be organized in an attempt to collect all available data from operators throughout the Central Kansas area. This should include the following: number of attempted completions, percentage of success, initial production, estimated recoverable oil per acre, type of reservoir

control, and any other pertinent data which might be useful. If these data are collected, properly assembled and correlated, it is probable that the percentage of success in the Lansing-Kansas City completion attempts would be increased. Further, such a study might evolve certain prerequisite characteristics on the gamma ray-neutron logs before any particular zone could carry oil in commercial quantities. If this study does not refine itself to such a point, it might at least show what zones in any particular area would have the best chance for a successful completion, provided that their logs meet certain qualifications.

★ ★ ★

BEHAVIOR OF DISSOLVED OXYGEN IN OIL FIELD BRINE*

GEORGE G. BERNARD AND GLENN A. MARSH, THE PURE OIL CO., CRYSTAL LAKE, ILL.

ABSTRACT

It is often assumed that aerated oil field brines which are to be injected underground contain dissolved oxygen in amounts which will cause appreciable corrosion. Through the use of a new portable dissolved oxygen meter, accurate determinations were made at three brine conditioning plants. At two older plants, dissolved oxygen concentration in the final treated brine was found to be almost zero in spite of aeration during the conditioning process. At a new plant, dissolved oxygen was initially present but disappeared soon after the brine was "inoculated" with oxygen-free brine from one of the other plants. Corrosion tests at the two older plants have substantiated predictions that the brines would not be corrosive. These results show that mechanical deaeration may not always be required in brine treating plants.

INTRODUCTION

The present work was undertaken to add to our knowledge of aeration and deaeration of oil field brines in brine conditioning plants. It is commonly assumed that brines which are exposed to the air soon become more or less saturated with dissolved oxygen. Since oxygen-containing brines are known to be corrosive, precautions are often taken to keep air out of

brine through the use of closed systems or mechanical deaeration.

The study of oxygen in brine has been seriously hampered in the past because of the lack of a suitable analytical tool. The standard Winkler method for the determination of dissolved oxygen is satisfactory for use in fresh water, but not in many oil field brines. Corrections have to be made for a number of reducing substances such as ferrous iron and hydrogen sulfide which are commonly present in natural brines. Very often the correction factors are much greater in magnitude than the amounts of oxygen which are to be determined, and consequently erroneous results are obtained. Also, erratic Winkler data are obtained when appreciable concentrations of calcium and magnesium salts are present.

The first step in carrying out a systematic study involved designing a portable dissolved oxygen apparatus which would operate in natural brines. Subsequently, this apparatus was used in three brine conditioning plants. Dissolved oxygen data obtained here, and certain corrosion rate data, illustrate the interesting behavior of oxygen in these oil field brines.

APPARATUS

A portable dissolved oxygen meter described in detail elsewhere,⁴ was developed specifically for use with oil field brines. It is a polarographic apparatus employing a small rotating platinum electrode (cathode) and calomel reference electrode (anode). A potential of 0.7 volts is applied across the electrodes while they are immersed in the brine to be tested.

⁴References given at end of paper.

Manuscript received in the Petroleum Branch office Aug. 15, 1951.
*This paper is Part 3 of the paper entitled "Behavior of Dissolved Oxygen in Brine" which was presented at the Fall Meeting of the Petroleum Branch in Oklahoma City, Okla., Oct. 3-5, 1951. Part 1, "Portable Dissolved Oxygen Meter for Use with Oil Field Brines," was published by *Analytical Chemistry* (Ref. 4 of this paper). Part 2, "Reaction Between Ferrous Iron and Dissolved Oxygen in Brine," is in publication by *Industrial and Engineering Chemistry* (Ref. 2 of this paper).

Table I—Composition of Brine at Oklahoma Plants

Constituent	ppm Present at		
	Plant "A" near Delaware	Plant "B" near Delaware	Plant near Madill
Hydrogen sulfide	150	150	0
Calcium	5,650	3,142	12,360
Magnesium	1,352	840	1,790
Sodium	37,688	18,238	31,600
Iron	0	0	0.5
Bicarbonate	282	260	114
Chloride	71,889	35,700	75,483
Sulfate	330	1,186	469
Dissolved Solids	116,861	68,500	125,550
pH	6.5	7.0	6.4
Sp.G. (60°)	1.080	1.042	1.098

Current through the electrodes, at a given temperature, is a linear function of dissolved oxygen concentration, and is measured on a microammeter.

The instrument, being portable and direct reading, is simple to operate and requires only 30 seconds to make a determination. The results are reproducible within 0.05 mg of dissolved oxygen per liter of brine, with an accuracy of about ± 5 per cent.

The accuracy of the dissolved oxygen meter is not affected by the presence of a number of common substances, which include ferrous, ferric, sulfide, calcium and magnesium ions, and various organic compounds. This interference-free operation has permitted a study of the reaction between ferrous iron and oxygen in brine over the pH range from five to nine,² as well as the study of oxygen in natural brines described here.

PROCEDURE

Determining Dissolved Oxygen in Three Brine Conditioning Plants

The first step in the procedure was the determination of dissolved oxygen concentration at various points in three brine conditioning plants. These plants are located in Oklahoma, two near the town of Delaware (designated as Plants "A" and "B"), and the other near Madill. The dissolved oxygen meter was used here, because it had been found that these brines yielded uncertain results with the Winkler method. The compositions of the brines are given in Table I. The dissolved oxygen data are given in Tables II, III, and IV.

Determining Corrosion Rates of Steel in Oil Field Brines

Corrosion tests were carried out at both Delaware "A" and Madill, subsequent to the dissolved oxygen determinations. Clean pipe nipples were weighed before and after seven to eight months of service to establish the corrosion rate. The nipples were also inspected for tuberculation and pitting. Results of these tests are given in Tables V and VI.

RESULTS

Results of Dissolved Oxygen Determination in Three Brine Conditioning Plants

Tables II and IV show that at two of the plants where dissolved oxygen determinations were made, namely Delaware "A" and Madill, the oxygen concentration in the plant effluent was very low in spite of the fact that no mechanical deaeration was used. The oxygen concentration increased with forced aeration, of course, but decreased rapidly on standing, even in the presence of air.

Table III shows that at the third plant (Delaware "B") the dissolved oxygen concentration was initially high when the plant started up. The brine in this plant was then inoculated with oxygen-free brine from Delaware "A", two weeks after startup. One week after inoculation another determination showed no oxygen in the Delaware "B" brine. This absence of oxygen has been confirmed in subsequent tests.

In all cases where little or no oxygen was found in brine, the operation of the meter could be checked by blowing air through the brine sample. After a short period of such aeration, the sample would yield a reading of one or two mg of dissolved oxygen per liter.

Results of Corrosion Tests at Delaware "A" and at Madill

Corrosion rates as determined on test nipples which have been in service for seven to eight months were reasonably low (Tables V and VI). At Delaware "A", the average rate

Table II—Analysis of Brine for Oxygen at Plant "A" Near Delaware, Okla.

Description of Sample	Mg Dissolved Oxygen per liter of Brine
Brine from supply well	0.4
Brine after third aeration	2.3
Filtered brine with no mechanical deaeration	0.1

Table III—Analysis of Brine for Oxygen at Plant "B" Near Delaware, Okla.

Description of Sample	Mg Dissolved Oxygen per liter of Brine
Brine in pond at startup of plant	2.4
Filtered brine at startup	1.8 - 2.4
Filtered brine one week after inoculation with brine from Delaware "A" plant (No mechanical deaeration)	0.0

Table IV—Analysis of Brine for Oxygen at Plant Near Madill, Okla.

Description of Sample	Mg Dissolved Oxygen per liter of Brine
Brine before aeration	0.7
Brine after first aeration	1.5
Brine after second aeration	2.6
Brine in flocculation reactor	0.9
Brine after filtration with no mechanical deaeration	0.3

was about 0.005 in. penetration per year, and at Madill 0.003 in. per year. Nipples removed from service after seven to eight months showed no tuberculation or pitting, although they were coated with a thin layer of rust.

DISCUSSION

Oil field brines which are exposed to the air are commonly assumed to contain considerable amounts of dissolved oxygen. Thus Voss and Nordell⁶ state "Aerated waters (brines) obviously are practically saturated with dissolved oxygen while waters which have been exposed to the atmosphere in open tanks or while flowing through troughs contain varying amounts (of dissolved oxygen)." The corrosiveness of brines containing dissolved oxygen is well recognized,^{1,3} and for this reason brines are sometimes deaerated by means of vacuum or they are handled in closed systems to avoid contact with air.

The dissolved oxygen data obtained here indicate that such precautions may be unwarranted. At Delaware "A", for example, brine is pumped from a well into a pond where it is retained 6 to 12 hours. Next, the brine is (1) passed through a forced draft aerator, (2) kept in a tank while air is bubbled through it, (3) passed through another forced draft aerator, (4) treated in a sludge contact reactor, and (5) filtered. In spite of repeated, intimate and thorough aeration, the filtered brine is found to be substantially free of oxygen (Table II).

In the second case, Delaware "B", the plant was started up several years after Delaware "A". Brine is lifted from a well, passed through an aeration tower to remove H_2S , then passed through an open trough to a pond where it is retained about one day. Then the brine is passed through a sludge reactor and is filtered.

When this plant was placed in operation, dissolved oxygen determinations revealed as high as 2.4 mg of oxygen per liter in the final treated brine (Table III). The presence of oxygen was surprising because the plants at both Delaware "A" and "B" take brine from the same limestone formation and are only a few miles apart. After the discovery of oxygen at Delaware "B", it was decided to try to "seed" the Delaware "B" brine with a little of the oxygen-free brine of Delaware "A". This was done with the possibility in mind that the oxygen at Delaware "A" is consumed by biochemical action. Two weeks after the startup of the Delaware "B" plant, a truckload of 12 bbl of Delaware "A" brine was dumped into the pond of Delaware "B". Dissolved oxygen determinations, made one week after this "inoculation," showed that the oxygen concentration in final treated brine had dropped to zero.

In the third case, at Madill, the brine is aerated and kept in an open tank for three days. Here, after this long exposure to air, the brine is found to be almost free of oxygen (Table IV). Corrosion tests here and at Delaware "A" show that the oxygen concentration in the plant effluents has been reduced to a low figure.

While sufficient work has not yet been done to tell what happens to the oxygen at these plants, certain information is known. The disappearance cannot be attributed to reduction by ferrous iron or by hydrogen sulfide. Iron is low or absent in the injection brines before aeration, as shown in Table I. Hydrogen sulfide is removed very easily in all plants by aeration. After aeration, hydrogen sulfide is absent but dissolved oxygen is present, at first in appreciable concentrations, and

Table V — Results of Corrosion Tests in Brine Effluent From Plant "A" Near Delaware, Okla.

Test Nipple No.*	Penetration Rate, In. per Year, During 8-Month Period
1	0.0045
2	0.0057
3	0.0056
4	0.0043
5	0.0057
6	0.0045
7	0.0050
8	0.0059
9	0.0038
Average	0.0045

*Test nipples were distributed throughout brine injection system.

Table VI — Results of Corrosion Tests in Brine Effluent From Plant Near Madill, Okla.

Test Nipple No.*	Penetration Rate, In. per Year, During 8-Month Period
1	0.0015
2	0.0013
3	0.0023
4	0.0022
5	0.0037
6	0.0017
7	0.0036
8	0.0025
Average	0.0028

*Nipples were distributed throughout brine disposal system.

eventually in practically zero concentrations. It is likely that the observed decrease in dissolved oxygen concentration is caused by biochemical action. For example, methane-containing waters have been known to consume oxygen through the action of *bacterium methanomonas*. The reaction is supposed to proceed in the following manner:⁵



This or a similar biochemical mechanism would account for the interesting decrease in dissolved oxygen at Delaware "B" plant within one week after inoculation with oxygen-free water from Delaware "A."

Regardless of the mechanism of oxygen consumption in the brines, the fact remains that mechanical deaeration may not always be necessary in order to insure low corrosion rates. From the work described here, the need for careful dissolved oxygen analysis in each brine treating plant is apparent.

ACKNOWLEDGMENT

It is a pleasure to acknowledge the assistance and cooperation of the Pure Oil Co. field engineers who helped to make this study possible.

REFERENCES

1. Anderson, K. H., and Gardner, F. T.: "Requirements of Subsurface Injection Water in Oil Production," *Oil and Gas Jour.*, (Sept. 7, 1950) 49, 72.
2. Bond, D. C., and Bernard, G. G.: "Reaction Between Ferrous Iron and Dissolved Oxygen in Brine," *Ind. and Eng. Chem.* (in press).

3. Breston, J. N.: "Conditioning Water for Secondary Oil Recovery in Appalachian Fields," *Oil and Gas Jour.*, (Aug. 24, 1950) 49, 159.
4. Marsh, G. A.: "Portable Dissolved Oxygen Meter for Use with Oil Field Brines," *Analytical Chem.*, (1951) 23, 1427.
5. Pape, Carl H. V. (Denmark): U. S. Patent 2,527,444, Oct. 24, 1950.
6. Voss, N. A., and Nordell, Eskel: "Water Conditioning for Oil Field Flooding Operations," *Oil and Gas Jour.*, (Nov. 9, 1950) 48, 174.

DISCUSSION

By Paul G. Carpenter, Phillips Petroleum Co., Bartlesville, Okla., Member AIME

The authors have contributed a very urgently needed analytical technique which should aid materially in the successful operation of water floods.

We have had considerable experience with a modified instrument of this type during the past year and find that it performs in general as is described in the paper.

Analyses contained in Tables I and IV show that brine from the supply well at Plant "A" contains both hydrogen

sulfide and oxygen. Have the authors made any study of the reaction rate between hydrogen sulfide and oxygen?

We would like to thank the authors and the Pure Oil Co. for making available to the industry this valuable analytical tool.

DISCUSSION

By L. C. Case, Gulf Oil Corp., Tulsa, Okla.

The observations relative to the permanence of oxygen in brines are of especial interest and significance. As a result of these findings it might be concluded that much existing equipment, for the purpose of preventing air entry into brine disposal systems, will shortly be found unnecessary. It should be kept in mind, however, that in many cases air exclusion is necessary from the standpoint of scale prevention.

A great many previous conclusions concerning the existence of oxygen in brines and its effects on equipment may now be open to question. For example, I recall a field experiment wherein oxygenated fresh water was added to a well annulus and the well effluent tested for oxygen. When no oxygen was found at the wellhead, it was concluded, perhaps erroneously, that it disappeared via the corrosion process. The authors have given us promise of early solution to similar problems where corrosion, although not definitely known, must be assumed at considerable cost in preventive measures. ★ ★ ★

THE DELTA-LOG, A DIFFERENTIAL TEMPERATURE SURVEYING METHOD

R. B. BASHAM AND C. W. MACUNE, WESTRONICS, INC., FORT WORTH, TEX.

ABSTRACT

Very small anomalies in oil well temperatures are detected and measured by recording the difference in temperature existing between two thermally sensitive elements which are spaced several feet apart on a small diameter carrier and lowered into the bore hole. The elements operate in a balanced electrical circuit, sending only a reference signal to the surface as long as normal gradient temperatures are encountered. When either element enters a temperature disturbance, the circuit is unbalanced and produces large recorder deflections for minute anomalies. The system is highly sensitive to small changes in thermal gradients caused by gas or fluid movements and to the boundaries between beds of different thermal conductivities. Typical logs show successful applications of the process to locating gas and water leaks in casing, gas entry, and gas-oil contact.

INTRODUCTION

Temperature measurements in oil wells have been made for many years in the search for additional sub-surface data. It has been generally agreed that many conditions in the bore hole cause temperature anomalies which, if located and measured, could yield useful information. But it has been recognized also that many of the irregularities, such as those produced by small water and gas leaks in casing, might be very small and therefore difficult to detect with certainty.¹ Although temperature measurements have been made which show anomalies of less than one degree deviation from normal gradient temperatures, the results are usually uncertain and unconvincing. The general practice, therefore, has been to apply temperature

surveys only to well conditions known to produce appreciable disturbances, such as large gas movements and cement hydration.

The recent demand for additional data has focused attention on the problem of making dependable temperature measurements in the many instances when anomalies are small but none the less significant. It was for the purpose of detecting these minute irregularities in bore hole temperature that the program described in the following text was undertaken.

It is emphasized that this presentation is not offered as a complete study, for the process is still partially experimental. But it is believed that the results obtained thus far will be of interest to the industry and will indicate some of the system's potential usefulness.

DIFFERENTIAL MEASUREMENT

The chief value of differential measurement lies in the fact that a difference between two factors can be measured with a scale of values best suited to that difference, a scale that might be cumbersome or impractical if applied to the factors themselves. When it is known that all factors will be nearly equal in value, and therefore the differences consistently small, it is possible to select a scale which will permit very accurate measurement of the differences.

This advantage is in contrast to the difficulty of measuring small increments of a single variable, where the increment must be measured by a large scale which is suitable for measuring the entire factor. Gradient temperatures are usually measured under this latter condition where temperature measuring apparatus must have a scale extending over the range of expected temperatures, say 50° to 250°F, and it becomes almost impossible to detect small irregularities of less than one degree. The use of large strip chart recorders and divided multiple ranges tend to amplify the small anomaly and make it more pronounced. But the instability of instruments, both

¹References given at end of paper.

Manuscript received in the office of the Petroleum Branch Sept. 10, 1951. Paper presented at the Petroleum Branch Fall Meeting in Oklahoma City, Okla., Oct. 3-5, 1951.

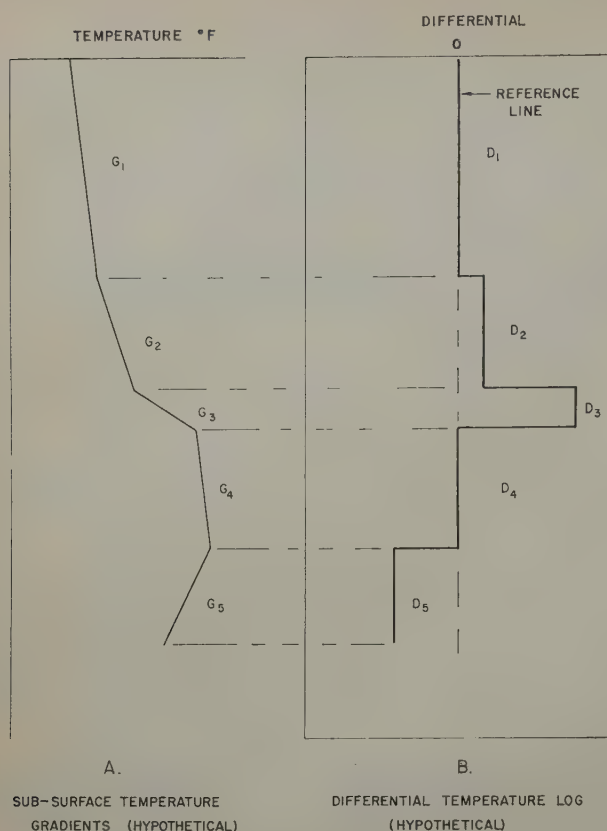


FIG. 1 — APPLICATION OF DIFFERENTIAL MEASUREMENT TO SUB-SURFACE TEMPERATURE GRADIENTS.

electrical and mechanical, limits the efforts in this direction and much of the disadvantage of measuring the increment in terms of the total range remains.

Another important characteristic of the differential system is its tendency to respond only passively to normal conditions encountered in the measuring process, such as when the factors being compared are all equal in value, but to respond actively to the abnormal or unequalized condition, thus emphasizing the abnormal in its measurements.

DIFFERENTIAL TEMPERATURE MEASUREMENT IN THE BORE HOLE

Since the chief interest in temperature surveys usually centers on the irregularities and deviations from the normal gradient temperatures, it appeared that the differential type of measurement would be useful in spotlighting those points of interest. Some of the considerations in the application of this system to bore hole temperatures are reviewed in the following section.

Two thermometers spaced several feet apart in the bore hole will read essentially the same temperature; but since the geothermal gradient produces an increase of approximately one degree for each 60 ft of traverse downward, the lower thermometer will be slightly warmer than the upper.² If the

thermometers are spaced six ft apart, the lower one will be 0.1° warmer. As the two thermometers move slowly downward, they will both increase in temperature as determined by the depth, but will maintain the 0.1° difference as long as the gradient is constant. For each value of gradient there is a fixed difference in the readings of the two thermometers. And it is evident that a record of this difference on a strip chart will be a straight vertical line for each value of the gradient, as shown in Fig. 1-B, with displacement from a reference line being proportional to the value of the gradient at any given depth.

This reference line can be established at the "zero" gradient level, the condition where both thermometers are at the same temperature when placed side by side just below the surface. However, it is more practical to take the gradient measured by the spaced thermometers at some point approximately 100 ft below the surface as a prime reference to which all other gradients below or above will be compared.

It should be noted that the recorded difference in thermometer readings is essentially a mathematical first derivative of the geothermal gradient curve. The derivative of a straight line function having the slope G_2 in Fig. 1-A is a constant, and it is represented numerically by the displacement of the recorded line D_2 from the reference line in Fig. 1-B. Since the differential recording has the character of a first derivative, it will change value abruptly at points where the temperature gradient changes slope; and the recorded line will be displaced abruptly the full amount corresponding to the new gradient.

This characteristic enables the differential measuring system to detect and magnify the small disturbances and irregularities in bore hole temperatures. When the lower thermometer enters an area cooled locally by gas escaping from a casing leak, it

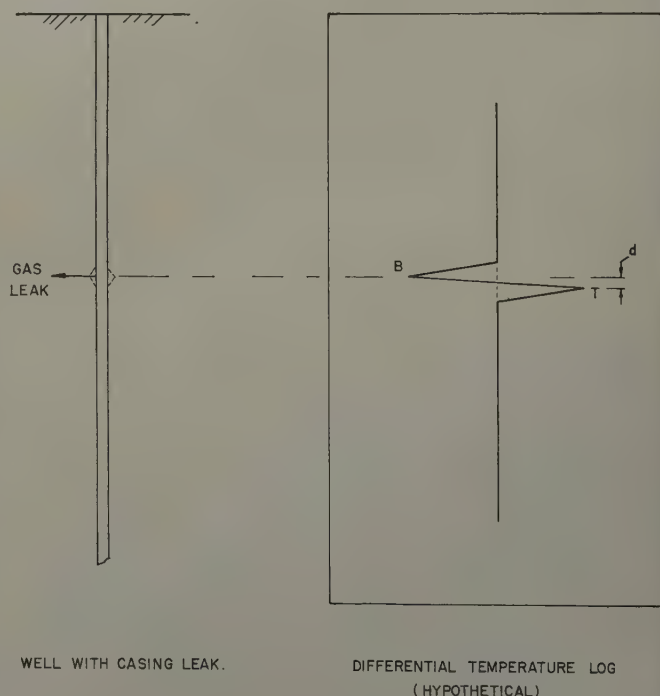
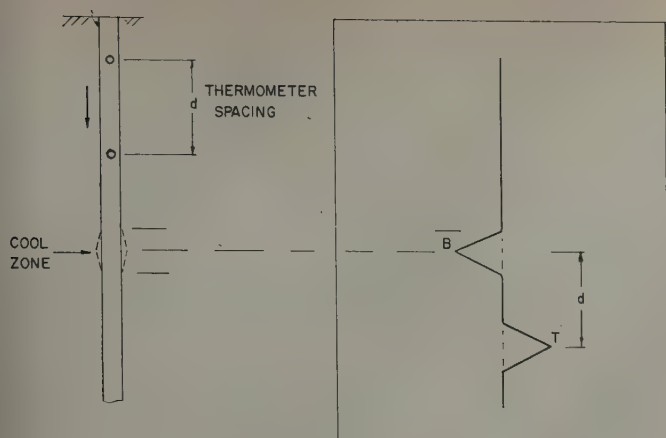
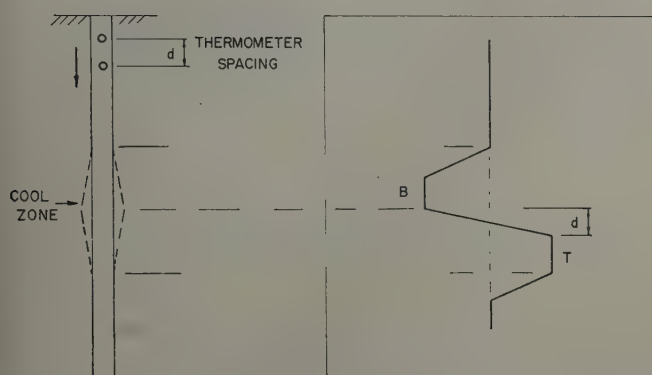


FIG. 2 — THEORETICAL APPLICATION OF DIFFERENTIAL TEMPERATURE SURVEY TO LOCATION OF CASING LEAK.



A. THERMOMETER SPACING LARGE WITH RESPECT TO COOL ZONE.



B. THERMOMETER SPACING SMALL WITH RESPECT TO COOL ZONE.

FIG. 3 — INFLUENCE OF THERMOMETER SPACING ON APPEARANCE OF DIFFERENTIAL TEMPERATURE LOG.

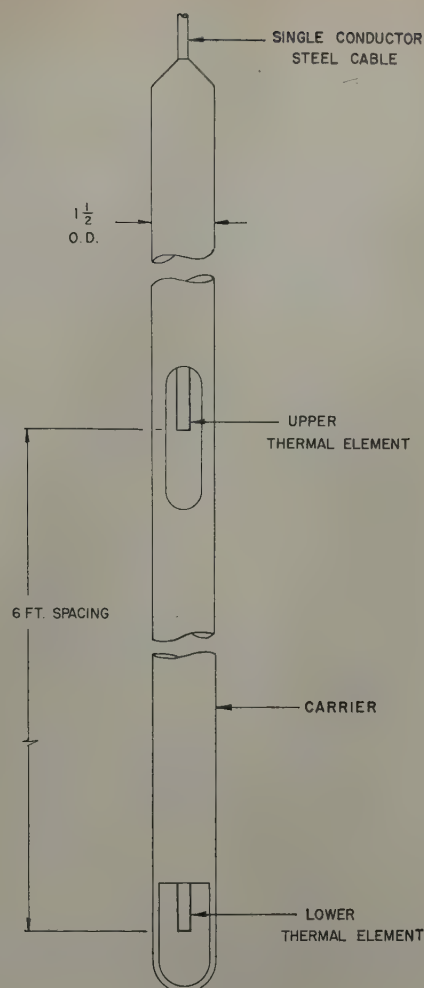


FIG. 4 — CARRIER AND THERMAL ELEMENTS USED IN DELTA-LOG TEMPERATURE SURVEY.

establishes a negative differential with respect to the reference, and the recorded trace moves abruptly to the negative side of the reference line, as shown in Fig. 2. Point *B* represents the maximum differential measured as the lower thermometer passes the leak point. Having passed the point of maximum cooling, the lower thermometer moves into warmer fluid and therefore the negative differential diminishes until it returns to the reference line, at which point the thermometers are straddling the leak point. Continuing the traverse downward, the lower thermometer has returned to fluids of normal temperature as the upper thermometer enters the cooled area. Then the lower thermometer, though at normal temperature, appears to be relatively much warmer than the upper, and a positive differential is recorded, peaking at Point *T* when the upper thermometer passes the leak point. The interval *d* is the thermometer spacing.

The spacing between thermometers has considerable influence on the form of the differential recording. When the separation is large with respect to the cooled area, the peak *B* and *T* are widely spaced, as in Fig. 3-A; and with the spacing small in comparison to the cooled zone these peaks become flattened plateaus, as in Fig. 3-B.

EQUIPMENT

Differential temperature surveys have been run for the past year using equipment which functions in the manner just described. Recordings of temperature anomalies agree essentially with the results which could be predicted from a straightforward analysis of the two thermometer action.

The thermometers used are a special type of thermally sensitive elements of the electrical resistance type developed specifically for this application. Each element is enclosed in a slender steel tube to prevent contamination from well fluids and the two elements are spaced six ft apart on a carrier tube $1\frac{1}{2}$ in. in diameter, with the lower element caged at the bottom end and the upper element housed in a slotted chamber in the body of the tube. Fig. 4 illustrates this arrangement. Simplicity of the electrical circuit requires that very few electrical components be included in the sub-surface equipment. As a result, the carrier tube serves principally to support and space the thermal elements and to provide weight when the tube is lowered into the well.

Electrical equipment on the surface consists of voltage regulated power supplies both AC and DC, precision resistance

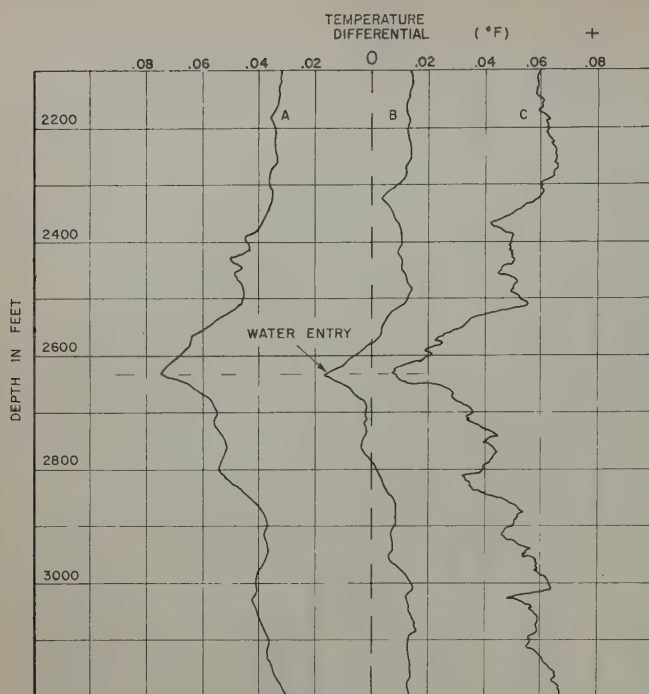


FIG. 5—SAMPLE DELTA-LOG SHOWING LOCATION OF WATER LEAK IN CASING.

bridge circuits, balancing and sensitivity controls, and an electronic strip chart recorder. When simultaneous logs of both gradient and differential temperatures are run, it is necessary to use a dual recorder.

Hoisting equipment installed in the instrument truck provides speeds of 15 to 500 ft/min in the single conductor steel armored cable supporting the sub-surface equipment.

Since the differential survey is made with the carrier and elements in continuous rather than in point to point movement, it is necessary to reduce thermal lag in the sensing elements to a minimum. This is accomplished by (1) using very small thermal elements having little mass, (2) separating the elements from well fluids by a thin, highly conductive window for maximum heat transfer, and (3) isolating the elements thermally from the conducted heat of the carrier body.

High sensitivity and stability in the system are largely a result of the characteristics of the thermal elements and associated circuits. The electrical circuits make a null-type measurement in which a potential between the thermal elements is balanced automatically by a potential in the surface equipment, with little current flow involved; therefore changes in line resistance have no effect on the measurements.

PROCEDURE

In general the procedure in conducting a differential temperature survey follows the familiar pattern of other well logging operations.

The first step in all cases requires that a prime reference gradient be determined by holding the sub-surface tool at approximately 100 ft below the surface for 15 minutes if in

fluid and longer if above fluid. Temperatures at that level are considered to be free of diurnal and annual variations.³ Observations of the electrical instruments will determine when thermal equilibrium is attained, and the recorder pen is set at center scale on the strip chart for that condition. When points of interest are located, it is common practice to detail those limited areas by establishing a new reference gradient at center scale immediately above the area and then operating the equipment at higher sensitivity.

Logging is usually performed on the downward traverse so that the well fluids are encountered in their state without being previously disturbed by passage of the carrier and wire line.

Logging speeds generally fall in the range of 50 to 100 ft/min. It has been determined by field test that logs made at slower speeds produce little more detail of significance, whereas logs made at speeds greater than 100 ft/min begin to suffer some loss of detail and amplitude in the recorded anomalies.

On the initial logging run, the selection of a proper sensitivity setting which will keep the recorder on scale and avoid resets is a matter of estimate. The usual practice is to select a low sensitivity setting for an exploratory log which will locate the major anomalies and serve as a guide for succeeding runs at higher sensitivities.

TEMPERATURE SENSITIVITY

Differences in temperature between the two thermal elements are recorded on a scale of $.02^\circ$ per in., and therefore differences of $.001^\circ$ can be detected. It is this high sensitivity which opens up a new range of bore hole temperature measurements which might be described as "microscopic." Field examples shown in the following section were logged at this sensitivity, and examination of the logs (Figs. 5, 6 and 7) will show that full scale recorder deflection from the center reference line is produced by a difference of only 0.1° between the thermal elements. Therefore, small anomalies which are not perceptible to conventional sub-surface thermometers can produce full scale deflections on the differential temperature log.

It should be recognized that the amplitude of an anomaly as recorded on the differential temperature log does not necessarily represent quantitatively the total change in local temperatures occurring at the point of the anomaly. The differential log is a record only of the difference in temperature existing between the two thermal elements at any point in the bore hole.

FIELD EXAMPLES

Some representative logs made in the Permian Basin of West Texas are offered to illustrate the application of the differential survey to well conditions which are known to create temperature anomalies. The principles of interpretation are by no means complete on this process and no effort will be made to analyze all portions of the curves shown. It is believed, however, that the basic principle of the differential measurement is well demonstrated by the examples, and the conditions which brought about the surveys are conspicuously prominent in each case.

In the reproduction of the logs having several curves from successive logging runs, the curves were arbitrarily offset from the reference line for the sake of clarity.

Location of Water Leak in Casing

The three curves *A*, *B* and *C* in Fig. 5 are successive runs made to locate the point of water entry into casing. A few bailer runs lowered the fluid level slightly prior to the survey to upset pressure equilibrium and accelerate water entry through the casing leak, and during two hours between runs *A* and *C* the fluid top rose 70 ft in the seven-in. diameter casing. Runs *A* and *B* were made under similar conditions and both indicate water entry at the depth where the differential curve changed from increasingly negative values on the downward traverse to increasingly positive values. With an average water flow of approximately one gal/min the anomaly was small and therefore the sensitivity necessary to make it appear on the log also amplified other temperature variations in proportion, some of which are in the same order of magnitude as the leak anomaly. Although the negative slope down to the leak and the positive slope below it served to locate the leak point, it was further substantiated by the correlation of the breaks at 2,637 ft on three successive curves and the lack of correlation among the other temperature variations. Curves *A* and *B* were logged at 100 ft/min, and *C* was run at a slower rate of 50 ft/min, with a resulting increase in detail or showing of minor anomalies. A casing caliper survey later verified this indicated leak point by finding a 20-in. casing split at 2,637 ft.

Locating Gas Leaks in Casing

The expansion of gas at a casing leak produces much greater temperature anomalies in general than water entry and makes the gas leak more simple to locate. Fig. 6 shows the correlation of two prominent kicks on successive runs made two hours apart, with curve *B* logged at lower sensitivity than *A*. Gas from the leak was allowed to accumulate between the oil casing string and the salt string for 24 hours before the survey; then it was bled off and allowed to flow during the survey in order to create maximum gas movement through the leak. The sub-surface equipment was lowered into the tubing which was shut off under 700 lb pressure. The sharpness and amplitude of the breaks in the log at 1,275 ft make the location of the leak at that point fairly definite, and squeeze cementing at that level later shut off the flow of gas into the salt string and put the well back in production.

Location of Gas Producing Zone

Similarly the expansion of gas emerging from a producing formation into the bore hole creates a relatively cool zone. Fig. 7 shows a determination of such a zone in a well producing at a gas/oil ratio of 5,000. After a 24-hour shut-in period the well was allowed to flow for three hours from the seven-in. casing at 400 lb pressure. Casing was set at 3,147 ft and tubing at 3,265 ft. The gas entry anomaly was detected at 3,185 ft by the carrier and elements lowered in the tubing. Curve *A* was run at full sensitivity and *B* and *C* were made at a lower sensitivity, as indicated by their reduced ampli-

tudes. However, the correlation of the sharp breaks on the three successive logs at the same depth is strong evidence that gas entry was occurring at that point.

It appears likely that the sharp break to the right side of the log immediately below the gas entry indicates the top of the oil producing zone, but no verification has been made to date in support of this theory.

In this instance the reference gradient was established at 3,000 ft rather than near the surface, because the approximate location of the producing zone was known; and starting the log at center scale near the anomaly permitted surveying the area at a higher sensitivity than might have been possible otherwise.

Prior to the differential log a self-contained recording thermometer of the conventional type was run in the well to locate this gas zone, and it failed to indicate any anomaly.

OTHER APPLICATIONS

Full appreciation of the temperature sensitivity offered by the differential survey and analysis of the results obtained in the field examples presented suggest other uses for the system, and several investigations are currently in progress to explore its potential. Some of the additional applications are:

1. Old Cement. General practice requires that the top of cement be located by conventional temperature gradient measurements within 72 hours after a cementing operation is completed, for most of the heat released by the exothermic reaction of hardening cement will be dissipated in that period. But the reaction continues at a reduced rate over an extensive

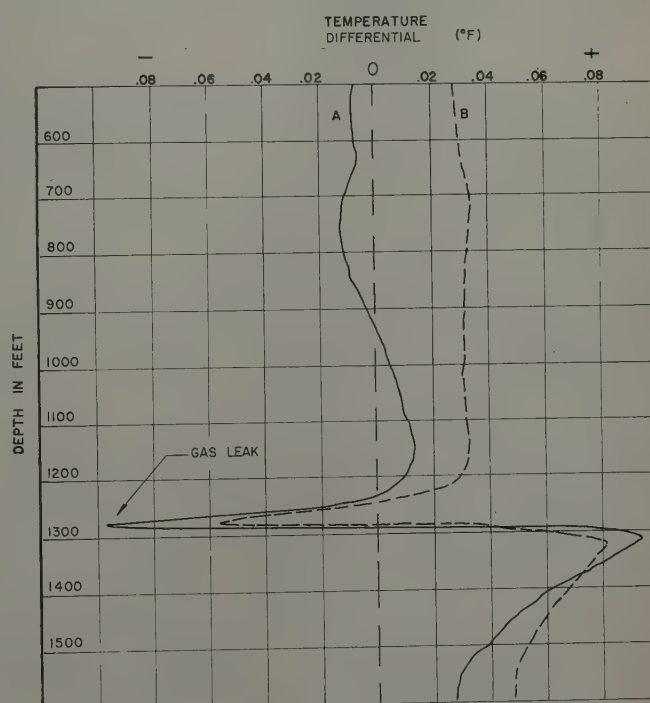


FIG. 6—SAMPLE DELTA-LOG SHOWING LOCATION OF GAS LEAK IN CASING.

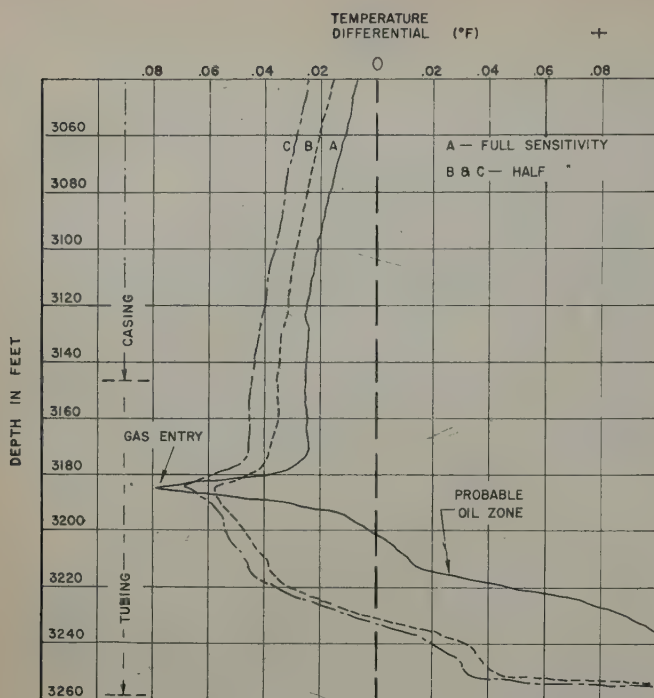


FIG. 7—SAMPLE DELTA-LOG SHOWING LOCATION OF GAS-PRODUCING ZONE AND PROBABLE OIL ZONE.

period, and it is possible that current field tests will determine that the sensitive differential measurements are capable of detecting residual heat in cement several weeks after the initial set.

2. Permeable Zones. Formations capable of absorbing fluid pumped down the bore hole can be located by the relative disturbance of normal temperature gradients above and below a permeable zone. The fluid, being at surface temperature and somewhat cooler than the formations it traverses, lowers the normal temperatures down to the point where it enters the formation. Below this point the gradient remains more nearly normal, and the boundary is clearly marked by a difference in temperature which is proportional to the per cent of the total fluid flow absorbed by the formation. Recent test well results showed that the system is sensitive to a flow of a small fraction of a gallon per minute leaving the fluid column.

3. Lost Circulation. Operating on the same principle used in detecting permeable zones, the system should be useful in locating points at which circulation of drilling fluid is lost.

The quantity of fluids moving into the thief zones and the relative temperature between the fluid and formations are widely varying factors, but it is reasonable to suppose that an anomaly large enough to be detected will usually exist when sufficient circulation is lost to be considered a problem.

4. Formation Logging. Correlation of differential temperature logs with electric logs indicates that the former will record anomalies characteristic of the various formations, their heat capacities and conductivities in particular. It is generally recognized and previous measurements have shown that the heat conductivities of the various sedimentary beds differ widely, and it is this difference between beds which alters the flow of heat from the earth's center toward the surface. Each formation transmits heat at a particular rate and has a characteristic geothermal gradient which is determined by its composition, compaction, and fluid content.³ In view of the high sensitivity discussed in previous sections, it is possible that the differential survey will offer significant results in the identification of formations.

CONCLUSIONS

The differential temperature logging system, because of its high sensitivity to small temperature changes, opens up a new phase in the search for sub-surface information. Numerous well conditions which are known to cause temperature disturbances too small to be measured by conventional means can now be explored thermally. Field examples demonstrate the system to be effective, and the results are consistent with theory. Experience in interpretation of the logs and continued exploration of its potential applications will determine the full extent of its usefulness.

ACKNOWLEDGMENTS

The authors wish to thank Westronics, Inc., for permission to write this article and Worth Well Surveys, Inc., for the data supplied from test and field operations. The cooperation and interest of many friends in Welex Jet Services, Inc., and the Chemical Process Co. are also greatly appreciated.

REFERENCES

1. Van Orstrand, C. E.: "Description of Apparatus for Measurement of Temperature in Deep Wells," API Bulletin 205 (1930) 8.
2. Uren, L. C.: *Petroleum Production Engineering — Oil Field Development*, (1941) 3rd Ed., 655.
3. Guyod, H.: "Temperature Well Logging — Part 1, Heat Conduction," *The Oil Weekly*, (Oct. 21, 1946). ★ ★ ★

OBSERVATIONS FROM PROFILE LOGS OF WATER INJECTION WELLS

H. H. KAVELER, MEMBER AIME, AND Z. Z. HUNTER, PHILLIPS PETROLEUM CO., BARTLESVILLE, OKLA.

ABSTRACT

Variation of the horizontal permeability (parallel to the bedding plane) in the vertical section of reservoir rocks has long been observed as a characteristic of a normally heterogeneous system which reservoir rock represent.

The use of a recently developed water injection profile device offered opportunity to measure with a high degree of reliability the rate of inflow of water into Burbank sandstone in wells previously cored. Water injection profiles were not correlative with core permeability profiles in such wells. Apparently the vertical permeability substantially influences the flow between strata in a formation in a manner as to void the usual conclusions that have been drawn from consideration of the horizontal permeability measurements alone. The results obtained in comparing water injection profiles with horizontal permeability profiles suggest that many of the usual production operations based upon "selective" behavior or treatment of rock exposed in well bores need to be re-evaluated and re-examined.

INTRODUCTION

Petroleum reservoir rock are heterogeneous systems. Heterogeneity exists in respect to lithologic character insofar as such rock are composed of distinguishable solid phases. Heterogeneity also exists in respect to certain properties, such as porosity and permeability, that vary due to variation of the physical structure of the rock. Except in exceptional cases, both the horizontal permeability (measured parallel to the bedding planes) and the vertical permeability (measured perpendicularly to the bedding planes) exhibit significant variation in any common source of supply. The variation in horizontal permeability, as reflected by core analyses, has drawn the greatest attention of petroleum technologists probably out

of the general notion that the mass movement of fluids in a reservoir is predominantly in the horizontal direction. Furthermore, in the usual case, the rock permeability measured in the horizontal direction is greater than that in the vertical.

The variation of horizontal permeability of reservoir rock has been the basis for developing a number of operating practices and procedures intended to improve the petroleum production operation. Many such procedures are referred to as "selective" in the sense that the practice is intended to control the flow to a more, or less, permeable interval within the common source of supply. It is often said that such practices are "tailored" to the permeability profile. The practices referred to involve, among others, the following: selective perforation of casing; selective shooting, acidizing and plugging; plugging back to intervals of low permeability; and, regulation of flow to prevent coning of water or gas, or irregular encroachment of water or gas. Certain expressed notions involving a concept of "by-passing," or "trapping," that are held to be particularly harmful in causing the avoidable loss of recoverable petroleum have grown from observed variations in the horizontal permeability. Oftentimes estimates of the reserve of a common source of supply are tempered by conclusions relating variation in horizontal permeability to recoverability of the oil-in-place.

Certain conclusions attributed to the significance of the variation of the horizontal permeability often extend to the design and operation of pressure-maintenance projects involving both water flooding and gas-injection. Many advocate increasing the number of injection wells, advocate maintaining uniform and equidistant input-output well patterns, or advocate so-called "dispersed" gas-drive techniques rather than gas-cap injection because the permeability profile of cored wells is supposed to indicate that "by-passing" or "trapping" would otherwise exist.

It is important, therefore, to have an opportunity to test whether the variation in the horizontal permeability found through core analyses of a typical reservoir rock is sufficient to establish the paths of fluid flow in a reservoir. It is particularly important to have an opportunity to determine whether flow at the sand face of a well conforms to the permeability profile as established by core analyses. In that manner, the merit of certain so-called "selective" operating procedures and other notions may be evaluated. The purpose of this paper is to compare horizontal permeability profiles of wells in the Bartlesville (Burbank) sandstone with water injection profiles, for the purpose of showing that there is no correlation between the horizontal permeability of a core and the water intake characteristics of a typical sandstone.

GENERAL CHARACTERISTICS OF BARTLESVILLE (BURBANK) SANDSTONE

The Bartlesville sandstones of Northeastern Oklahoma are off-shore bar deposits.¹ Although other reservoirs had different processes associated with their deposition or with the formation of their porous, permeable structure, the Bartlesville sandstones on which these field tests were made are, in every respect, typical petroleum reservoir rock. The permeability of the Bartlesville sandstones shows a typical variation in both the horizontal and vertical direction. Furthermore, the permeability profile logs of wells in any pool are not correlative, even as between wells as close as 660 ft and 330 ft apart.^{2,3} The same condition exists in such sandstones as the Jones Sand at Shuler⁴ and is the ordinary and usual characteristic of reservoir rock.

THE FIELD DATA

The data reported herein are those obtained from coring of nine wells on the center of ten-acre locations for the purpose of providing water-injection wells in the Bartlesville (Burbank)

¹References given at end of paper.
Manuscript received in the Petroleum Branch office Aug. 20, 1951. Paper presented at the Petroleum Branch Fall Meeting in Oklahoma City, Okla., Oct. 3-5, 1951.

sand of the North Burbank Field in Osage County, Oklahoma. Eight of the wells were cored by diamond bit and recovery was 100 per cent. The usual core analyses were made, including a permeability measurement on a plug taken from each foot of the 4½-in. diameter core. A typical core analysis reflecting porosity, permeability, oil saturation, water saturation and salinity is shown in Fig. 1. The cores were taken with a low-water-loss water-base mud.

Recently a flow profile device was developed⁵ and used to obtain water-injection profiles of the nine wells. The profiling device was of such design as to provide measurements of more than ordinary reliability. The water-injection profiles were determined by repeated traverses carried on during a period of six hours, over which period of the time the measurements were found to be reproducible. The hydrostatic head at the sand face was determined by the use of a float. The water injected into the well during the course of the experiment was measured by means of a surface meter. All measurements were carried on under stabilized conditions. Filtered water, treated to prevent growth of bacteria and algae, is injected into these wells and, for that reason, plugging action arising from suspended solids could not account for any of the intake characteristics here reported.

Figs. 2 to 10, inclusive, are a comparison of the horizontal permeability profile of each of the nine wells with the water-injection profile. In some instances the change in injection profile over a period of one year is also shown.

Generally, the water was found entering the reservoir rock at points that were not correlative with the measured horizontal permeability of the sandstone.

The injection profile shown for Well 127-W-1 in Fig. 2, for example, at the rates of injection indicated, shows the water entering the rock mainly in the interval 2,933-2,937 ft. The core analyses showed permeability in this section of less than one millidarcy, but examination of the core itself showed evidence of vertical fracturing in the interval 2,935-2,940 ft. Later injection profiles indicated the water entering the formation above the fractured zone at 2,926-2,934 ft.

Fig. 3 shows the injectivity profile for Well 127-W-2. The most permeable section in this well is 2,917-2,922 ft. Permeabilities were measured as high as 288 md at the top of this interval. The profile made in April, 1950, after

25,000 bbl of water had been injected showed the main flow to be in sections above and below this point and, more particularly, in the next most permeable interval, 2,883-2,892 ft. In January, 1951, a second profile was run when the cumulated water injection was approxi-

mately 252,000 bbl. The principal in flow was observed to be in the interval 2,930-2,936 ft, which was taking 495 bbl of the 605 bbl being injected per day. In March, 1951, another profile was run after approximately 46,000 bbl of additional water had been injected

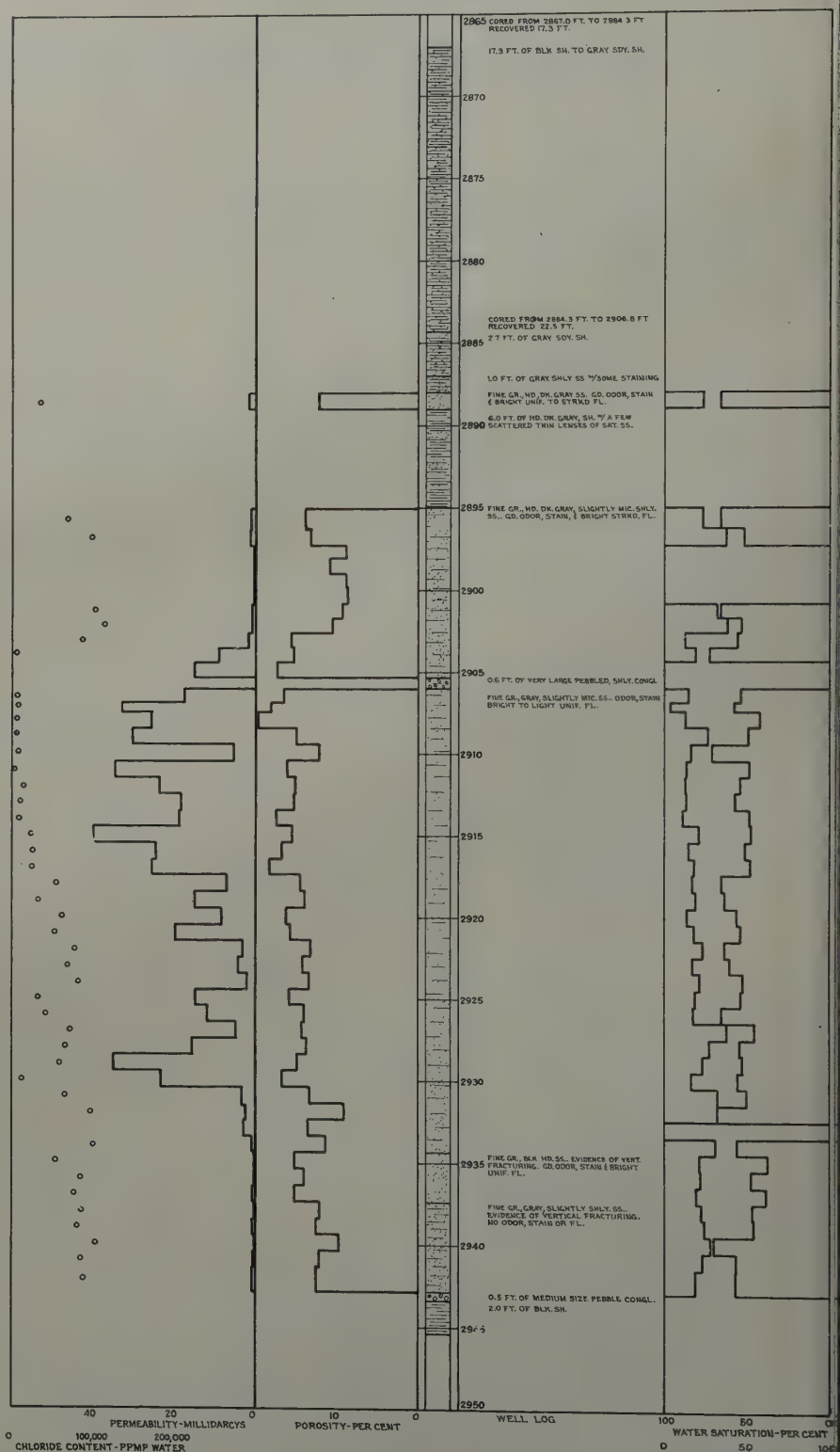


FIG. 1—ANALYSIS OF CORE FROM NORTH BURBANK UNIT 127-W1 SW/4 SEC. 16-26N-6E OSAGE COUNTY, OKLA.

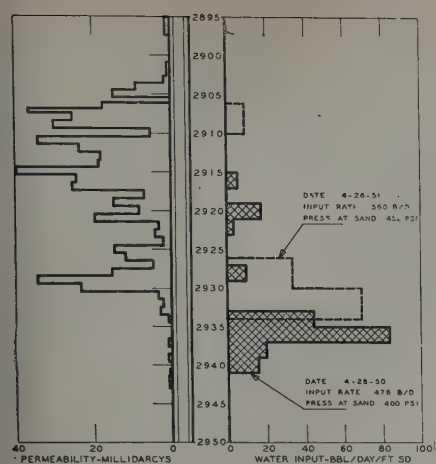


FIG. 2 — PERMEABILITY AND WATER INJECTIVITY LOGS, NBU 127-W-1.

and the interval 2,930-2,938 ft was found to continue to be taking disproportionately large quantities of water. The core description from this well revealed a tight section of sand and conglomerate with vertical fractures from 2,937-2,941 ft, and the conclusion was that the fractured conglomerate section was a "thief" horizon. Accordingly, a cement plug was set on March 22, 1951, with a top at 2,934 ft. In April, 1951, a profile log was run as shown in Fig. 3, with a high rate of influx indicated for the interval 2,925-2,928 ft. The intake capacity of the well was not decreased as a result of setting the cement plug in the zone of fracturing, nor was the injection profile of the well substantially altered. Undoubtedly, the flow into the fractured zone still continues.

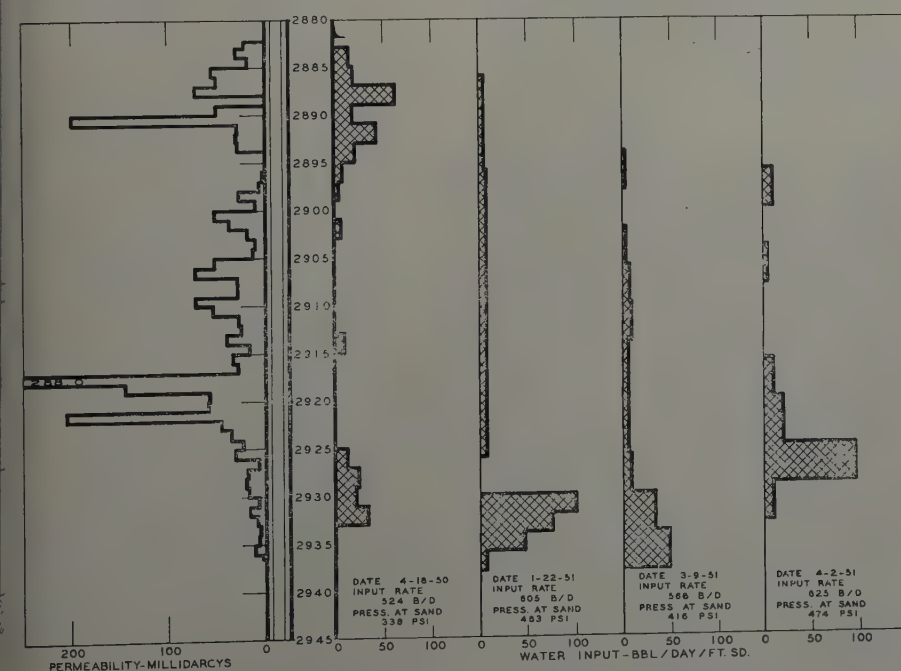


FIG. 3 — PERMEABILITY AND WATER INJECTIVITY LOGS, NBU 127-W-2.

Fig. 4 shows that the intake capacity of the sandstone in Well 127-W-3 was quite uniform over the entire section in April, 1950, in spite of wide variation in horizontal permeability; but the log taken in January, 1951, shows one section of the sand to be substantially increased in daily rate of intake. Fig. 5 for Well 127-W-4 shows on the first survey in August, 1950, a relatively uniform distribution of intake through the section, but in March, 1951, after approximately 314,000 bbl of water had been injected, a significant change in profile characteristics had occurred with the lower section taking a relatively large percentage of the total input. The core showed no fracturing or unusual conditions in the interval 2,970-2,975 ft.

Fig. 6 for Well 127-W-5 is of particular interest because the water inflow is almost entirely into those sections shown by the core analyses to be less permeable and because the section from 2,989-2,994 ft was shown by core inspection to contain vertical fractures. In this instance, there was no inflow into a fractured section.

In Figs. 7 and 8 for Wells 127-W-6 and 127-W-7 there was again no consistent relationship between intake capacity and horizontal permeability, and in the instance of Fig. 9, even though Well 127-W-8 was found to have a fractured conglomerate at the base of the Burbank Sand from 2,990-2,991 ft., this section was found to have no intake capacity. Finally, in Fig. 10, even though the interval 2,967-2,979 ft in Well 127-W-9 exhibited on the basis of

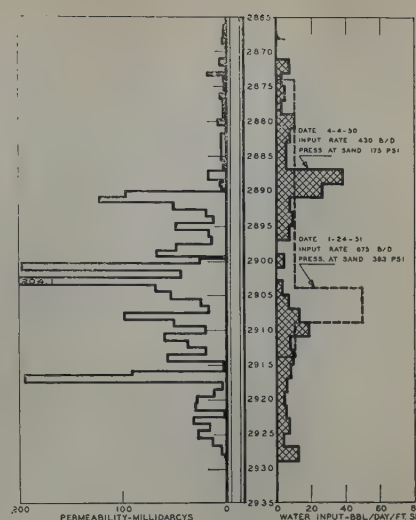


FIG. 4 — PERMEABILITY AND WATER INJECTIVITY LOGS, NBU 127-W-3.

core data the large fraction of the millidarcy-feet capacity, the water influx was comparatively uniform throughout the section.

A GENERAL CONCLUSION

The lack of correlation between permeability and flow at the sand face of wells is not due to conditions peculiar to this reservoir. What has been observed in this instance is likely to be found in all other reservoir rock with few exceptions. It may be concluded, therefore, that the core permeability measurements for any well will not serve as the basis for predicting the fluid flow characteristics of any particular interval in a productive section. The change in injection profile with time further indicates that flow changes within the body of the rock are occurring so that the permeability profile or the water-injection profile do not reflect even approximately the flow through any stratum of the entire reservoir. The lack of correlation between the profiles is of such magnitude as to require explanation by consideration of other than effective permeability relationships arising from variation in fluid saturation of the rock.

THE IMPORTANCE OF VERTICAL PERMEABILITY

If flow in a reservoir were strictly in the horizontal direction parallel to the bedding planes, flow would be through "series conductors" of varying permeability. This is readily confirmed by such observations as were made on the 4½-in. cores taken from the Bartlesville

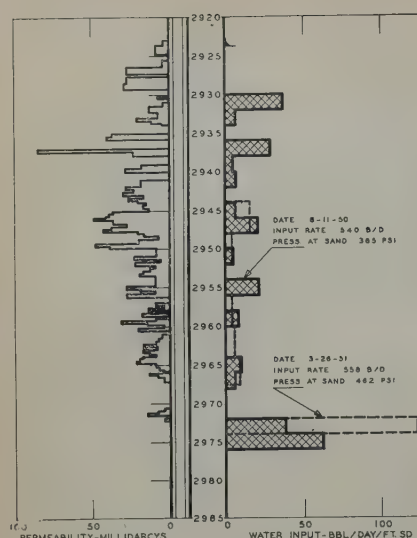


FIG. 5 — PERMEABILITY AND WATER INJECTION LOGS, NBU 127-W-4.

(Burbank) sandstone. A permeability plug was cut parallel to bedding planes and broken into three pieces of equal length, and permeabilities were run on each piece. The horizontal permeability showed variation of as much as 300 per cent between adjacent pieces with no regularity in value between the pieces taken from the center of the core or from either side. Over distances as short as $4\frac{1}{2}$ in. there is marked variation in horizontal permeability. This alone would account for the lack of correlation between the horizontal permeability profile and the water-injection pro-

file of a well and might substantially account for the variation of the injection profile with time as the reservoir fills up and the water moves through horizontal strata into sections of higher or lower permeability.

But, in addition, the vertical permeability must influence the path of flow of fluids through the rock and have its effect also in establishing intake capacity different from that expected from the horizontal permeability profile established by core analyses. The Burbank sands are typical in respect to the fact that the vertical permeability has values as high as 50 per cent of the horizontal permeability and show wide variation. Nevertheless, the fact that the area through which vertical flow may

meability as the sole criterion of flow at the face of the sand and, for that reason, one would not expect flow at the sand face to be correlative with the horizontal permeability. One of the interesting investigations that might be carried out, using a proper analog, would be to study the composite permeability of a network of conductors arranged so as to represent various combinations of horizontal and vertical permeability components. Such a study, even though carried on under idealized conditions, would serve to interpret the significance of the permeabilities measured on cores in the horizontal direction.

CONCLUSIONS APPLYING TO PRODUCTION PRACTICE

The principle conclusion that comes from the studies herein reported is that most of the practices employing the principle of "selective" control of the flow of fluids at the face of the sand in a well need to be re-examined. It appears doubtful that the operations tailored after the horizontal permeability profile have a sound basis. The horizontal permeability of cores does not measure relatively the flow at the sand face of a productive section. In a similar fashion the concept of "by-passing" based upon observed variations in horizontal permeability needs to be re-examined, particularly in connection with pressure maintenance operations. Eliminating obviously "thief" horizons lying within or immediately adjacent to a common source of supply, and eliminat-

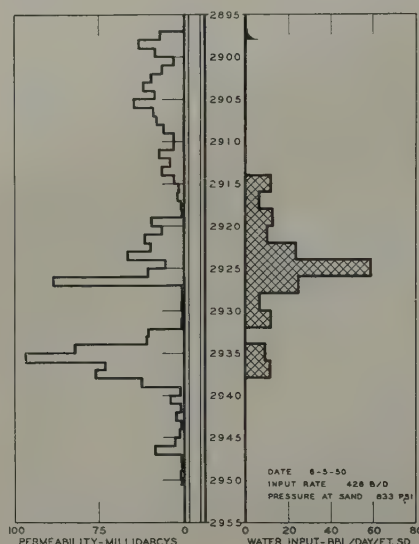


FIG. 7 — PERMEABILITY AND WATER INJECTION LOGS, NBU 127-W-6.

occur in a reservoir increases as the square of the radius outward from the injection well (or producing well) results in a condition whereby a substantial part of the fluid passing the sand face in the well-bore could move through vertical paths even though the permeability in that direction is relatively low. As a consequence, flow through the bulk of the reservoir rock must be a meandering flow such as would be expected in a radial system. Actually, the potential field and the corresponding lines of flow constitute a complex of meandering paths defined by the "composite" permeability arising from the existing values of the horizontal and vertical components from point to point. The influence of vertical permeability would be to remove the horizontal per-

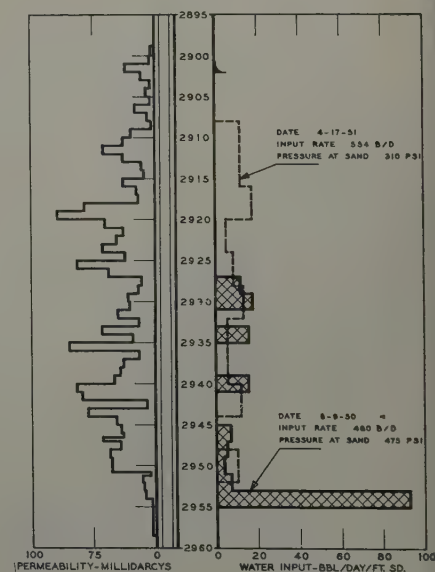


FIG. 8 — PERMEABILITY AND WATER INJECTION LOGS, NBU 127-W-7.

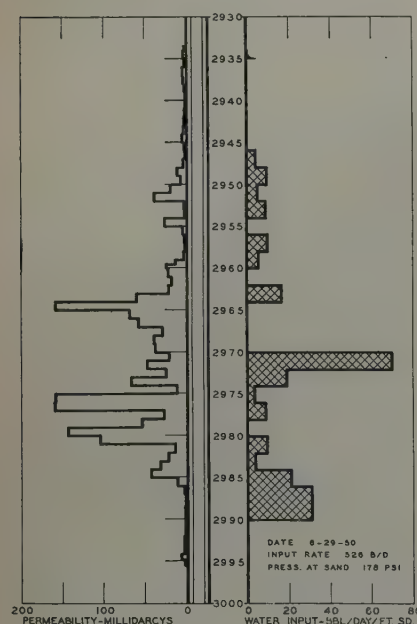


FIG. 6 — PERMEABILITY AND WATER INJECTION LOGS, NBU 127-W-5.

ing recognizable instances of earth cleavage, the conclusions of this paper would indicate that the measured permeability of cores is not a basis for predicting that fluid will pass through only a part of the permeable productive section. In fact, experience in water-flooding operations indicates that the "fill-up," which is the volume of water that needs to be injected before first response is had from offset producing wells, is more often than not quite close to the computed fill-up. This fact indicates that in spite of variation in horizontal permeability, water permeates to and fills the entire body of sand. "By-passing," in the sense the phrase is usually used, is absent. This confirms the conclusions reached by profile measurements on wells.

REFERENCES

1. Bass, Leatherrock, Dillard and Kennedy: "Origin and Distribution of Bartlesville and Burbank Shoestring Oil Sands in Parts of Oklahoma and Kansas." *AAPG Bull.*, (1937) 21, 30.
2. McClain, Halbert: "Some Practical Aspects of Water Flooding," *Petr. Engr.*, (April, 1947) 18, (7) 128.
3. McCaslin, L. S., Jr.: "Water Flood Increases Production," *Oil and Gas Jour.*, (Feb. 26, 1948) 46, (43) 108.
4. Kaveler, H. H.: "Engineering Features of the Shuler Field and Unit Operation," *Trans. AIME*, (1944) 155, 58.

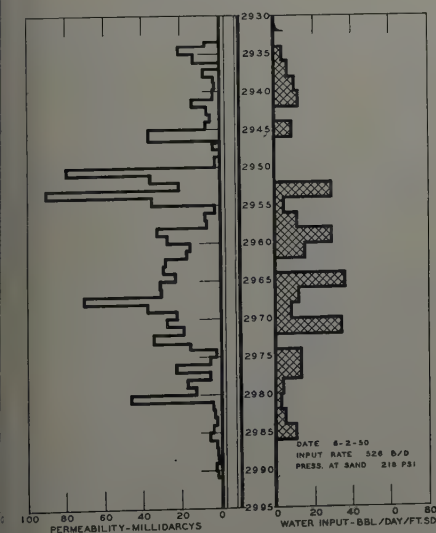


FIG. 9 — PERMEABILITY AND WATER INJECTIVITY LOGS, NBU 127-W-8.

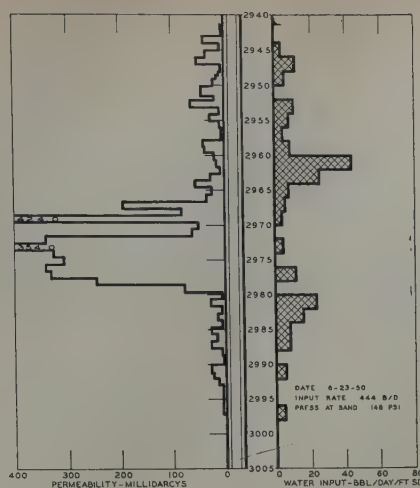


FIG. 10 — PERMEABILITY AND WATER INJECTIVITY LOGS, NBU 127-W-9.

5. Piety, R. G.: "Flow Meter for Water Injectivity Profiling," *World Oil* (May, 1952).

DISCUSSION

By E. T. Heck, Minard Run Oil Co., Bradford, Pa., Member AIME

Kaveler and Hunter should be complimented on calling attention to the fact that some have erred in over emphasizing the supposed uniformity of actual conditions in oil reservoirs. Their introduction is well worded and appropriate. It appears, however, that these gentlemen have made an even more serious error and assumed that the nine wells they describe are typical of all intake wells, not only in the Burbank sandstone, but everywhere. This writer is familiar with several thousand intake wells and knows of none that take comparable volumes of water at comparable sand face pressures. This fact alone would seem to refute Kaveler and Hunter's basic assumption.

The paper states "the permeability profile logs of wells in any pool are not correlative, even between wells as close as 660 ft and 330 ft apart." In the Bradford-Allegheny fields (well over 100,000 acres of net productive territory) there are literally thousands of cores and electric logs that testify to the existence of a reasonable degree of correlation. Hundreds of acres have been cored and/or electric logged on a density of one well per acre. While remarkable variations in detail are

known, overall correlation of the permeability profiles does exist over distances much greater than the figures quoted above. Of course, it is necessary that the profiles be properly matched.*

Very little information is given in the paper on the procedures followed in well completions. Eight of the nine wells were cored with a diamond bit using a "low-water-loss water-base mud." The fact that Fig. 1 shows the core to be flushed (more or less in proportion to the permeability profile as shown by core analysis) indicates that the pressure in the mud column was greater than the reservoir pressure. This fact raises the question of how the sand face was cleaned and prepared for the intake of water. The more permeable layers were probably pretty well plugged during the coring process and unless some positive, effective, action was taken to clean the sand face, all of the observations reported may be readily explained on this basis alone.

The following statement appears to be entirely too sweeping, "Filtered water, treated to prevent growth of bacteria and algae, is injected into these wells and, for that reason, plugging action arising from suspended solids could not account for any of the intake characteristics here reported." This discussor has investigated a number of intake systems and has first-hand knowledge of many others. In no case was the intake system sterile. In the absence of specific tests, it is safe to assume that organic growths are present in the wells in question. Such growths are not so apt to plug cracks as they are the small pores of the sand.

The presence of fractured zones is mentioned in several places in the paper. In fact, it is stated that a large part of the water is entering the fracture system instead of the sand proper. If these fractures cross the bedding planes, there is no reason to expect the intake to be distributed according to the permeabilities shown by the core analyses. On the other hand, if the fracture system does not cross the bedding planes of a major part of the reservoir, there should still be a reflection of the permeability profile, provided

*This fact is very important. The top or bottom of the sand is rarely the correct correlating base. The usual core description can rarely be used and the standard multiple point electric log is little better. Proper correlations require detail inspection of the cores or, even better, detailed electric logs such as those given by the Keller system developed at Pennsylvania State College under the sponsorship of the Penn Grade Crude Oil Association — research program in 1948-49. The "Laterolog" and "Guarded Electrode" systems are apparently analogous. Frequently, an electrical marker can be found, just above or below the sand proper, that will greatly aid in making correct correlations.

ing that the measurements of water inflow are sufficiently accurate.

For example — in well NBU 127-W-1, the 40 md sand should take less than 2 bbl per day per foot of sand. The 5 md sand should take less than 0.5 bbl per day per foot of sand. Due to the large amount of water entering the fracture zone, the metering instrument must have an accuracy considerably better than one per cent. This writer knows of no well metering device of such accuracy. Furthermore, it would be impossible to plot values of this magnitude using the scale shown in Fig. 2.

The following statement is found under the section "A General Conclusion." "It may be concluded, therefore, that the core permeability measurements for any well will not serve as a basis for predicting the fluid flow characteristics of any particular interval in a productive section." As pointed out in this discussion, there are good reasons to doubt that this conclusion is valid even for the wells described in the paper. There is a wealth of information, (some of it, undoubtedly, available to Kaveler and Hunter) on other areas that proves the opposite. Numerous cores drilled in old water floods during reworking operations, demonstrate without question that the flood has progressed in direct ratio to the permeability of the various sections of the sand.

In the section "Conclusions Applying to Production," the authors not only assume that the area discussed in this paper is identical with all other areas, but they reverse the process and cite "fill-up" behavior in other areas as though it is identical with the area under discussion. This piling of assumption upon assumption is never wise and in this case should have been unnecessary. Production data for the surrounding oil wells should have been included in the paper. It would then have been possible for the reader to judge whether or not this flood was behaving in the expected manner.

In conclusion, it may be stated that Kaveler and Hunter have described a problem area that is not at all typical of the vast majority of presently operating water floods. It is probable that many of the problems have been introduced, or at least aggravated by the methods used in well completion and/or operation. This last statement cannot be confirmed on the basis of the information supplied in paper and additional data, particularly complete rate curves on both intakes and producers, is greatly to be desired.

AUTHORS' REPLY TO MR. HECK

The authors appreciate the discussion offered by Heck. All viewpoints must be weighed in arriving at any conclusion and, in addition, discussion will encourage further investigation of the thesis raised, to the benefit of further development of fact. An effort will be made to reply briefly in respect to the points that Heck appears to raise in his discussion.

1. There are wells that take greater volumes of water at lower sand face pressures than do the wells in the North Burbank Sand, and many will be found in the Burbank Sand Area that have intake capacities such as those at North Burbank.

2. The correlation of permeability referred to in the paper was such correlation as to reflect whether or not stratigraphic intervals of the sand ran continuously in a sheet from well to well over a large portion of the reservoir, whereas Heck deals with the existence of "a reasonable degree of correlation" which is an indefinite reference. Furthermore, we have found no means to use electric logs as a means for anything more than just generalized correlations of sand characteristics.

We have been impressed by the observation of Danielson and Martin in Technical Paper No. 181 of the Mineral Industries Experiment Station, Pennsylvania State College, titled "Selective Plugging in the Bradford Field" wherein it is stated: "Oil reservoirs, including those of the Bradford Field, are made up of many sand strata possessing wide variations in permeability. *These strata are separated by impermeable shales which make them independent conductors of fluids.*" The North Burbank reservoir is definitely one common source of supply and is not separated into multiple common sources of supply by strata of shale, which is a fact that is important to bear in mind if experience in one area of the country is compared to experience in the Burbank Sands.

3. In respect to the method of input well completions: The wells were cored with a diamond bit and were not shot. Caliper surveys in each of the wells under test showed a remarkably uniform well bore. When mud was bailed from the wells after drilling was complete, oil and gas came into the well bore. The wells were swabbed and in some cases were acidized with mud acid and in other cases a mechanical scratcher was used to further clean the sand face.

4. Heck overlooks the statement in the paper that permeability plugs cut in the horizontal direction through the core and then broken into three pieces of equal length showed variation in the horizontal permeability over the short distance of four and one-half in. of the core — variation as much as 300 per cent between adjacent pieces with no regularity in variation in respect to location of the piece of core in the diameter. On the face of it, there is substantial variation in horizontal permeability within the reservoir rock. If it occurs within the core, it must undoubtedly occur throughout the body of the sand. Further, in respect to the plugging of wells by either drilling practice or by plugging material in the injected water, we may say that the intake characteristics or the injectivity of the wells were consistent in a general way with the permeability feet of the section. And further, one might observe that whether partial plugging occurred or other effects referred to by Heck were present, the fact still stands that the relative capacity of any interval to take water was not reflected by the core analyses.

5. The profile log showed excessive intake of water in fractured areas in some instances, and in other instances where fracturing appeared in the core the section of sand showed a lower than normal intake capacity; and in that instance, again, the core analyses could not be relied upon to predict intake capacity of any interval, no matter what circumstances might otherwise prevail.

6. A number of cores have been taken in sands following waterflood operations or in sands that were water-invaded in the area of the Burbank Sands, and the residual oil saturation has been found to bear no relation to the specific permeability of the core, and there is no reason, except in the case of parallel common sources of supply separately subject to the action of a waterflood, that the core taken from the sand after waterflooding should show flood progress in direct ratio to the permeability of the various sections of the sand.

7. The "fill-up" in the North Burbank Field where the profile study was carried on was found to be surprisingly close to calculated fill-up, which is the experience that is generally had after the net productive sand thickness is known in waterflooding operations in the area of the Burbank Sands generally.

8. In respect to Heck's final point, we only inquire of how many instances that a reliable profile of fluid flow at the face of the sand has been found to be correlative with the permeability of the core taken in the well. ★ ★ ★

PREDICTION OF SATURATION PRESSURES FOR CONDENSATE-GAS AND VOLATILE-OIL MIXTURES

E. I. ORGANICK AND B. H. GOLDING, UNITED GAS CORP., SHREVEPORT, LA., JUNIOR MEMBERS AIME

ABSTRACT

A simple correlation is presented for the prediction of saturation pressures in condensate-gas and volatile-oil mixtures. Saturation pressure is related directly to the composition of the mixture with the aid of two generalized composition characteristics, \bar{B} , the molal average boiling point, and \bar{W}_m , the modified weight average equivalent molecular weight. The need for hydrocarbon equilibrium constants is entirely eliminated. Only the values of the two composition parameters need be obtained, and these are calculated in a simple and reproducible manner from the stream analysis of the mixture and the ASTM distillation for the heavy ends.

The correlation is given in the form of a set of 14 working charts in which saturation pressures, either retrograde dew points or bubble points, are plotted *vs* temperature, forming partial phase envelopes for mixtures having discrete values of the composition parameters, \bar{B} and \bar{W}_m . A locus of critical states on each chart intersects the partial phase envelopes, distinguishing retrograde dew point pressures from bubble pressures.

A comparison between experimental and predicted saturation pressures reveals that: the probable error of the predicted values, when considering the data as a whole (214 experimental points), is five per cent; for high gas/oil ratio condensate fluids (approximately 40,000 or more cu ft/bbl) the probable error is about 8 per cent. In either case, however, the probable error is comparable with the overall uncertainty of the data from which the correlation is derived.

INTRODUCTION

There is a present need for a simplified, yet reasonably accurate method for predicting upper phase boundaries of reservoir fluids. In the case of high gas/oil ratio fluids, namely

the so-called highly volatile oils and the condensate gases, no simple method, accurate within 5 to 10 per cent, is now available by which bubble point and retrograde dew point pressures may be predicted.

In order to calculate the upper phase boundary of a volatile reservoir fluid, using correlations now available, it is necessary to find and employ the proper K -values (equilibrium volatility ratios of the hydrocarbons in that fluid). This process of finding the proper K -values usually involves a double trial and error computation. Since the K -values are in themselves dependent upon the composition of the fluid, their use in the calculation of a saturation pressure actually represents an unnecessary complication.

The correlation described in this paper relates saturation pressure directly to the stream composition, entirely eliminating the need for K -values. The only data required to calculate the stream composition are obtained from the customary low temperature fractional analyses of separator gas and liquid, and from the ASTM distillation of the C_7+ fraction of the separator liquid. A considerable simplification in the procedure for predicting saturation pressures is thereby effected without significant loss in accuracy.

BASIS FOR A CORRELATION

Empirical relationships between the saturation pressure and the composition of the fluid in question have already been partially explored by one of the authors.⁶ In particular, a relationship between the critical pressure for a hydrocarbon mixture and its composition was developed. The critical pressure is in reality a saturation pressure, as it represents a limiting case either of a dew point or of a bubble point pressure for any given mixture.

It was found that the critical pressure may be correlated as a function of two generalized composition characteristics or variables. One characteristic expressed a molal average property, the other a weight average property of the mixture. Specifically, the molal average boiling point (MABP, or \bar{B} as it

⁶References given at end of paper.

Manuscript received in the Petroleum Branch office Aug. 17, 1951. Paper presented at the Petroleum Branch Fall Meetings in Oklahoma City, Okla., Oct. 3-5, 1951, and in Los Angeles, Calif., Oct. 25-26, 1951.

will be called in this paper) and the weight average equivalent molecular weight \bar{W} , defined below, were used to obtain critical pressure directly from a convenient, empirically derived working chart. As will be shown, the values of the parameters \bar{B} and \bar{W} may be readily computed from the analysis of the mixture. Deviations between observed critical pressures and values predicted from this chart averaged about five per cent, or roughly, a deviation comparable to the uncertainty of the experimental values themselves.

Since critical pressures can be correlated with composition in such a simple manner, it is logical to expect that other saturation pressures along the upper phase boundary may be correlated using similar techniques. This expectation led to the correlation developed and presented below.

TREATMENT OF EXPERIMENTAL DATA

All available experimental dew point and bubble point data for complex hydrocarbon mixtures were collected, and each mixture was analyzed for the purpose of calculating values of \bar{B} and \bar{W}_m , the proposed correlating parameters. The definition of these parameters and an outline of the actual techniques used to calculate their numerical values follow.

The molal average boiling point, \bar{B} , is defined as the sum of the products of the mol fractions and the boiling points of the individual components,

$$\bar{B} = \sum_i (\text{mol fraction})_i \cdot (\text{boiling point})_i$$

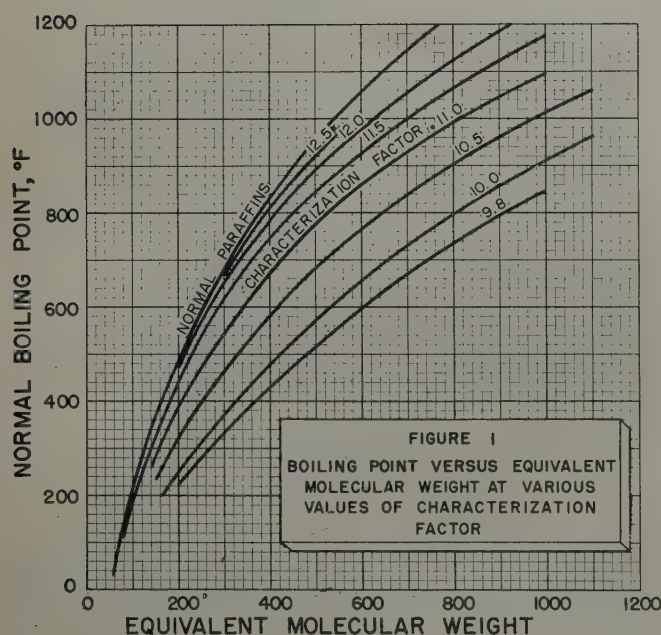


TABLE OF EQUIVALENT MOLECULAR WEIGHTS FOR NATURAL GAS CONSTITUENTS:

Methane	16.0	n-Pentane	72.2
Ethane	30.1	Hexanes	85.0
Propane	44.1	Ethylene	26.2
iso-Butane	54.5	Nitrogen	28.0
n-Butane	58.1	Carbon Dioxide	44.0
iso-Pentane	69.0		

FIG. 1

In this paper \bar{B} is always computed in degrees Rankine.

The modified weight average equivalent molecular weight, \bar{W}_m , is a somewhat more complex function. It is defined as a practical approximation to \bar{W} , the weight average equivalent molecular weight. The latter has been previously defined⁶ as the sum of the products of the weight fractions and the equivalent molecular weights of the individual components:

$$\bar{W} = \sum_i (\text{weight fraction})_i \cdot (\text{equivalent molecular weight})_i$$

The equivalent molecular weight is an empirically derived function designed to account for differences in chemical structure of the various hydrocarbon components in a mixture.⁶ For a n-paraffin the equivalent molecular weight is the actual molecular weight. For iso-paraffins and for olefin compounds, however, the equivalent molecular weight is defined as the molecular weight that a n-paraffin would have if it boiled at the same temperature as the iso-paraffin or olefin in question. For other hydrocarbons, such as the naphthenic and aromatic types, the equivalent molecular weight is defined in Fig. 1 as a function of the normal-boiling point and also of the Watson or U.O.P. characterization factor.¹¹

Unfortunately, the experimental information normally available on naturally occurring mixtures is not sufficient to permit an accurate calculation of \bar{W} for these mixtures. The usual type of analysis available on complex hydrocarbon mixtures, particularly on volatile crude oils and on gas-condensate mixtures, is a low temperature fractionation analysis through pentanes or hexanes combined with an ASTM distillation of the heavy ends. The ASTM distillation is far from being an accurate fractionation and is frequently incomplete because the cracking temperature is reached before the end of the distillation. The heavier the stock, the less complete is the distillation information.

The estimation of the weight average equivalent molecular weight for the C_7+ fraction of these naturally occurring mixtures is thus subject to considerable uncertainty. Furthermore, the calculated numerical values of the weight average equivalent molecular weight for naturally occurring mixtures are generally quite dependent on the value of the weight average equivalent molecular weight assigned to the C_7+ fraction.

For this reason an arbitrary but systematic and reproducible technique has been adopted for estimating the weight average equivalent molecular weight of the C_7+ fraction. The experimental information required consists of an ASTM distillation of the C_7+ and, when feasible, specific gravities of the individual cuts. \bar{W}_m of a mixture or of a portion of a mixture (such as the heavy ends) is defined in this paper as that weight average equivalent molecular weight which is obtained when the weight average equivalent molecular weight of the C_7+ fraction is estimated by the following technique:

Calculation of \bar{W}_m for the Heavy Ends

1. The ASTM distillation, when incomplete because of cracking, is extrapolated in the following manner. The ASTM boiling points of the C_7+ fraction are plotted on a graph whose coordinates are log boiling point (in degrees absolute) and cumulative weight per cent of the entire mixture from which the C_7+ material is derived. A best straight line is drawn through the plotted points on this graph and extended to the intersection of the line representing 100 cumulative per cent. Boiling point for any portion of the "residue" may then be read directly from the extrapolated portion of this straight line.
2. The heavy ends are broken up into an arbitrary number of cuts each of known average ASTM boiling point and of known or estimated characterization factor.

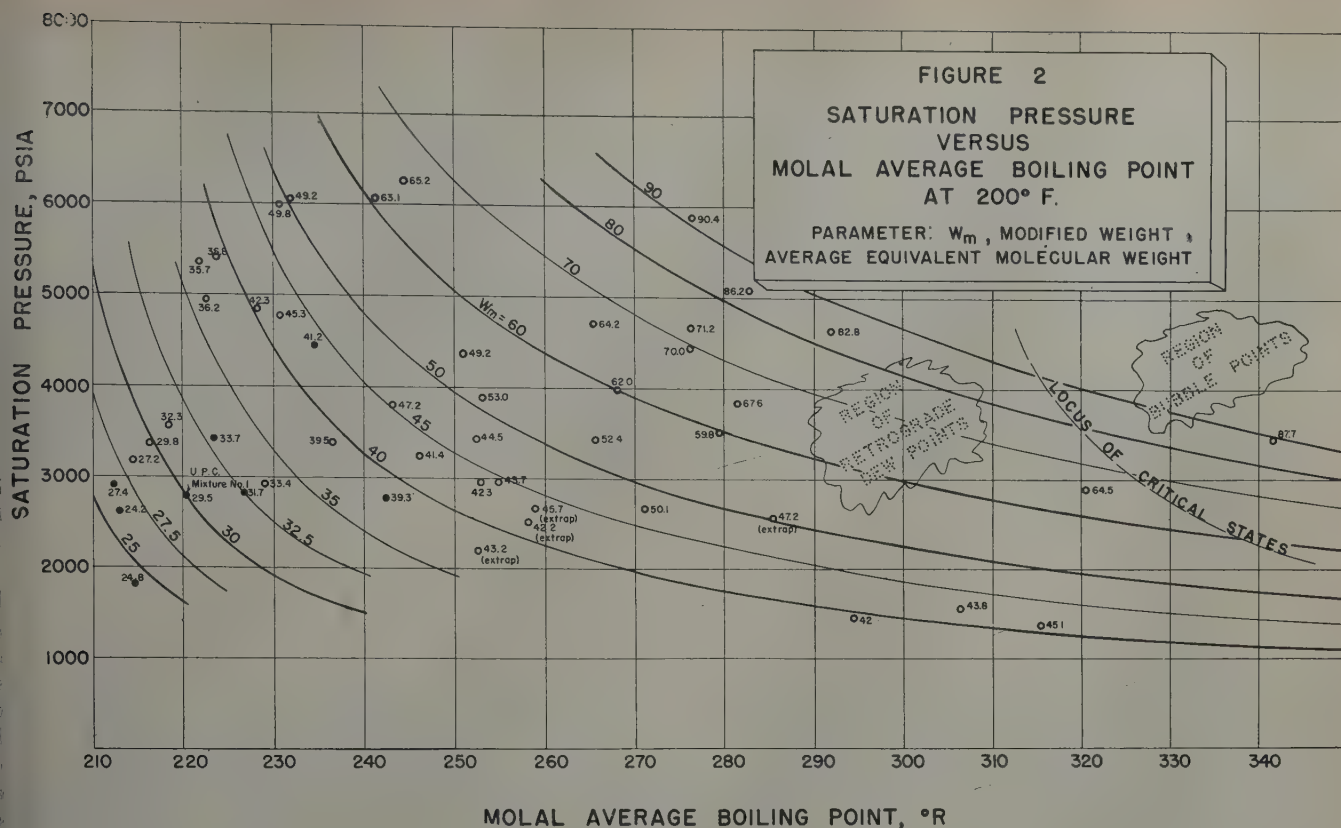


FIG. 2

- The equivalent molecular weight for each cut of the C_7+ fraction is defined in terms of the ASTM boiling point (rather than true boiling point) and characterization factor of that cut. Fig. 1 is used to obtain the equivalent molecular weights of the cuts.
- The terms $[(\text{weight fraction})_i \cdot (\text{equivalent molecular weight})_i]$ for each cut are summed to obtain the value of \bar{W}_m .

An illustrative problem, given in a later section, describes in detail the calculations for \bar{W}_m . Short-cut procedures for computing \bar{W}_m and \bar{B} for C_7+ fractions are also described.

DISTINCTION BETWEEN SIMPLE AND COMPLEX MIXTURES

The value of \bar{W}_m of a naturally occurring hydrocarbon mixture calculated by the above procedure is usually less than the value of \bar{W} for the same mixture. This means that pure components and simple mixtures of pure components (e.g., binary and ternary mixtures) cannot always be treated satisfactorily by the correlation presented in this paper. The value of \bar{W} for a mixture of methane and normal decane, for example, cannot be compared with the value of \bar{W}_m for a mixture of methane and a distillate material whose average volatility characteristic is the same as that of normal decane. Since no empirical relationship has been worked out between \bar{W} and \bar{W}_m , available data on binary and ternary mixtures of pure components were not included in the preparation of the empirical correlation described below. If this correlation is used to predict the saturation pressure of a simple mixture of pure components, the predicted saturation pressure will generally be somewhat high. It may, however, be possible to develop a similar correlation in terms of \bar{W} (rather than \bar{W}_m) and \bar{B} for direct prediction of the saturation pressures of these simple mixtures of pure components.

THE CORRELATION

Saturation pressures at any given temperature may be correlated as a function of the composition parameters, \bar{B} and \bar{W}_m . A plot of the data at 200°F is shown in Fig. 2. This graph shows the first step in the preparation of the final working charts and illustrates several important aspects and limitations of this correlation.

Typical Isothermal Plot of the Data

The saturation pressure for each mixture is plotted *vs* the molal average boiling point, with the value of \bar{W}_m corresponding to that mixture indicated numerically beside the plotted point. It is apparent that a family of curves representing constant values of \bar{W}_m may be faired through the points in such a way that each experimental point lies close to the curve corresponding to the \bar{W}_m value of that point. If the curves define "predicted" values of saturation pressure, the average deviation between predicted and observed pressure for all points in Fig. 2 is about 6 per cent; the maximum deviation is roughly 15 per cent.

Distinction Between Dew Points and Bubble Points

The saturation pressures defined in Fig. 2 may be either retrograde dew points or bubble points. For any given temperature the more volatile the mixture, i.e., the lower the \bar{B} and \bar{W}_m , the more likely will it exhibit retrograde dew point behavior rather than bubble point behavior. Conversely, heavier mixtures (higher boiling point and higher molecular weight) will more likely exhibit bubble point behavior for any specified temperature. Some mixtures will be at their critical temperatures; consequently, the saturation pressures exhibited for these mixtures will be neither dew points nor bubble points, but critical pressures. These mixtures are defined at each temperature by a locus of critical states as shown in Fig. 2. The region to the left of the critical locus,

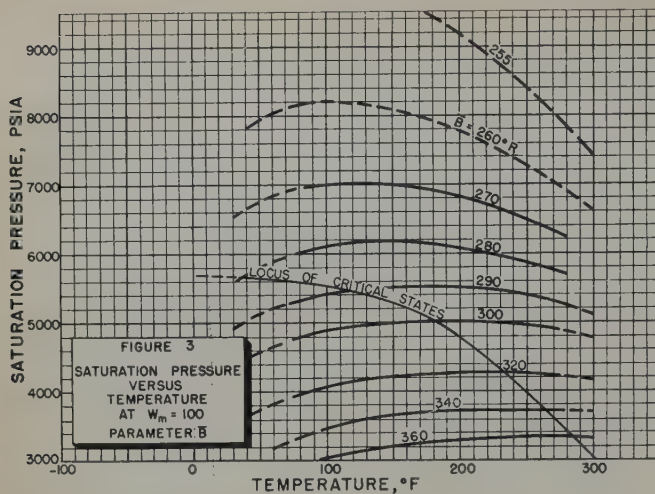


FIG. 3

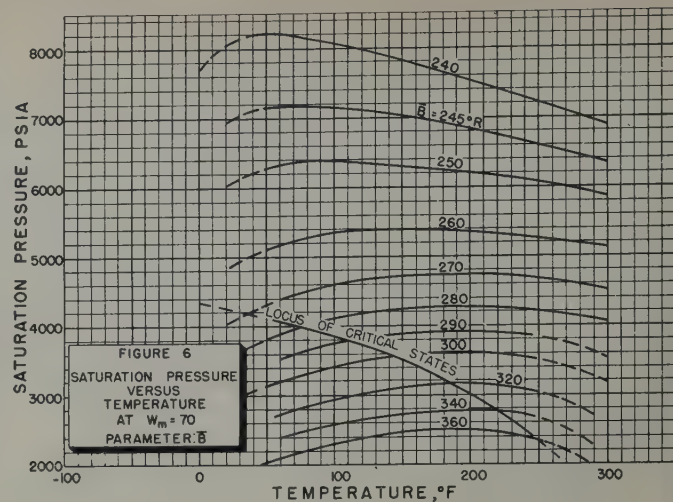


FIG. 6

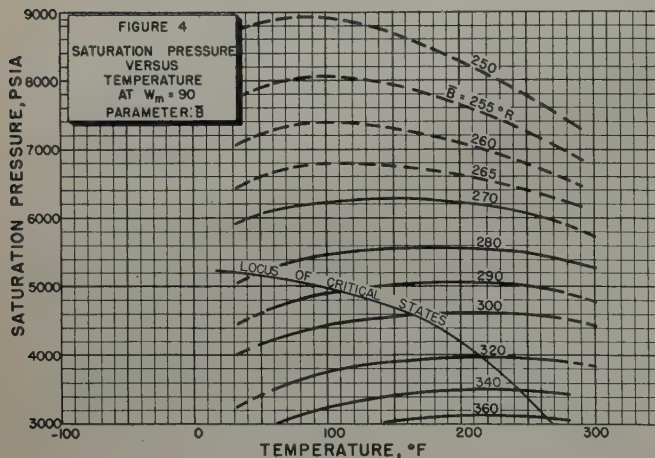


FIG. 4

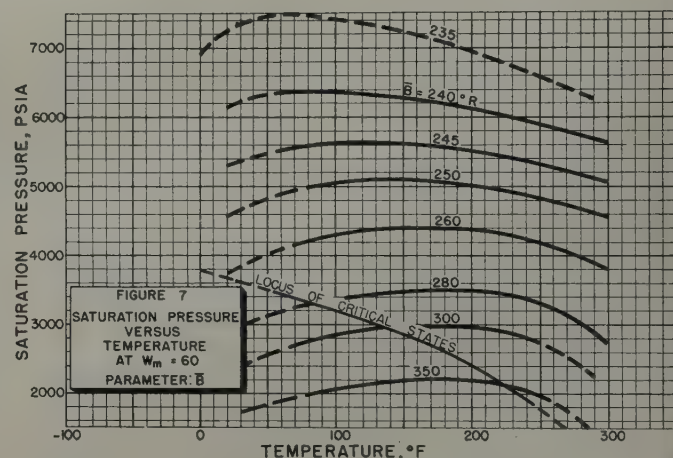


FIG. 7

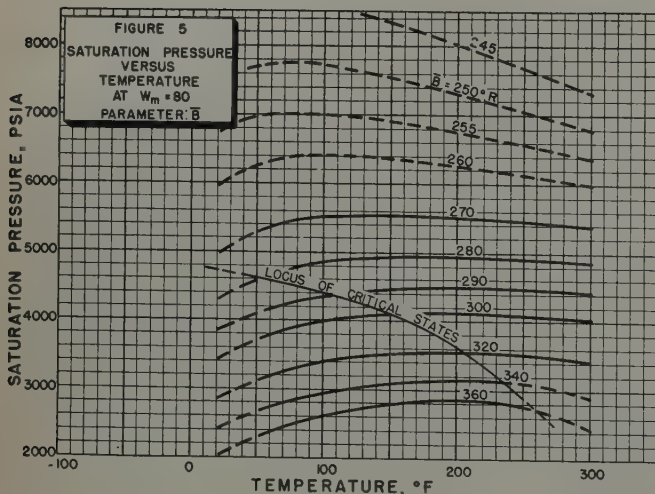


FIG. 5

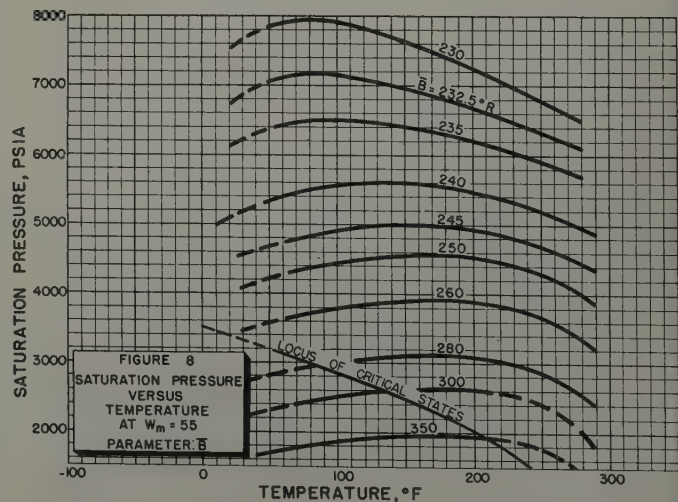


FIG. 8

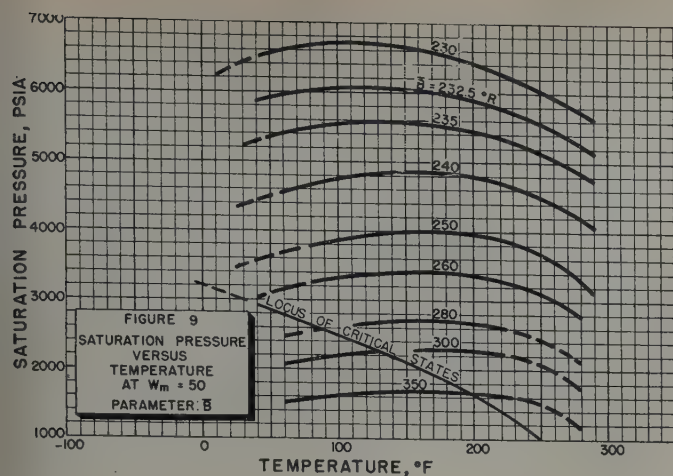


FIG. 9

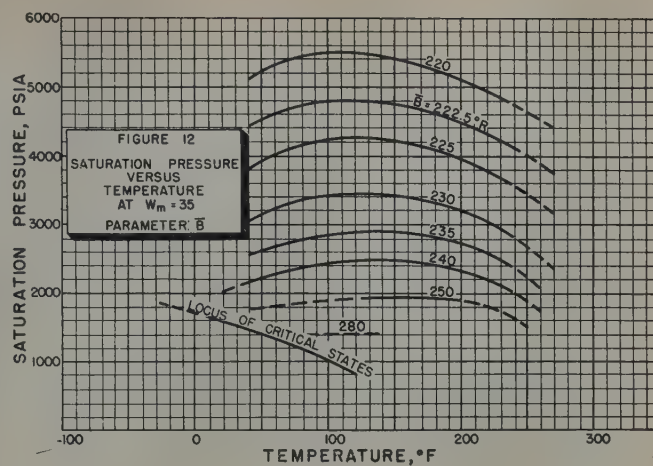


FIG. 12

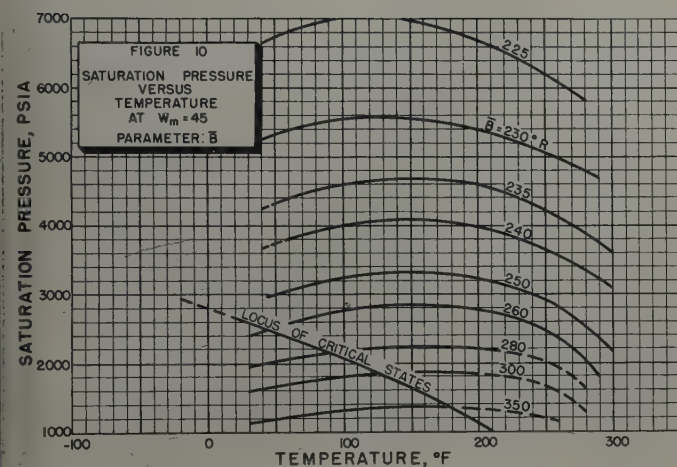


FIG. 10

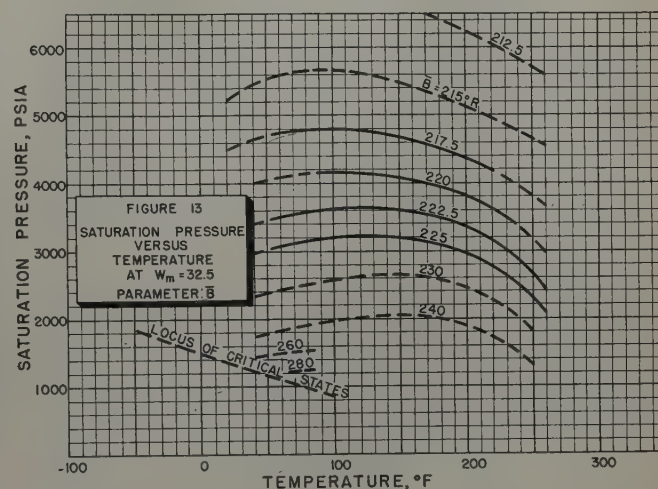


FIG. 13

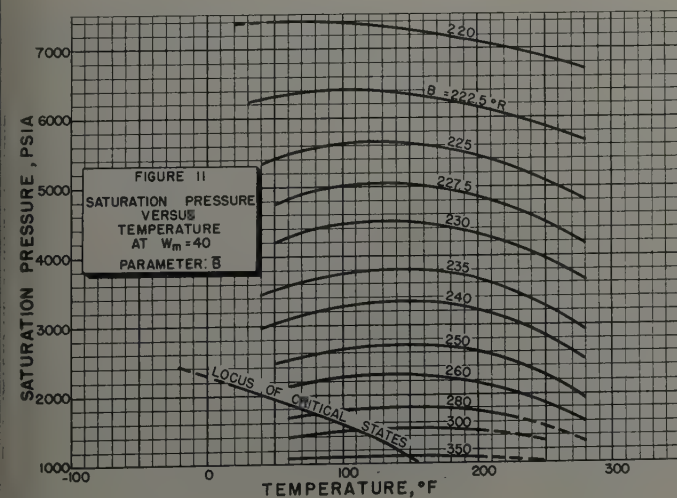


FIG. 11

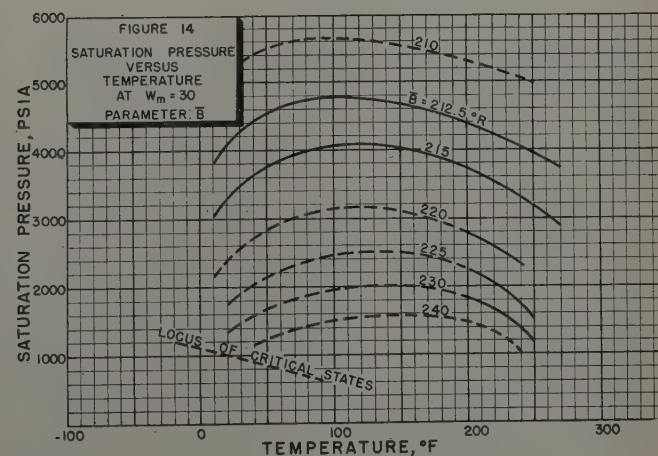


FIG. 14

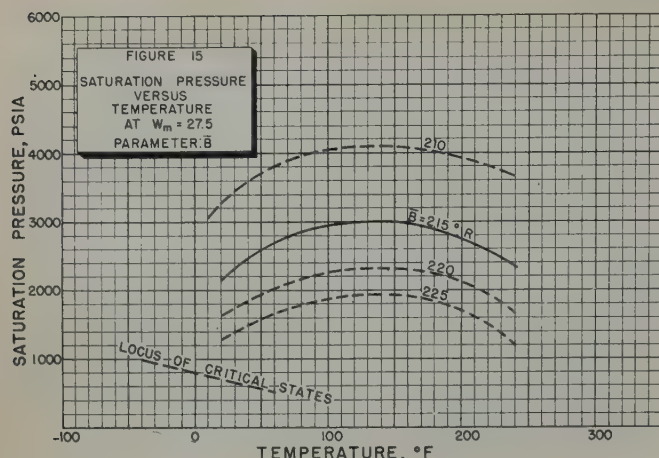


FIG. 15

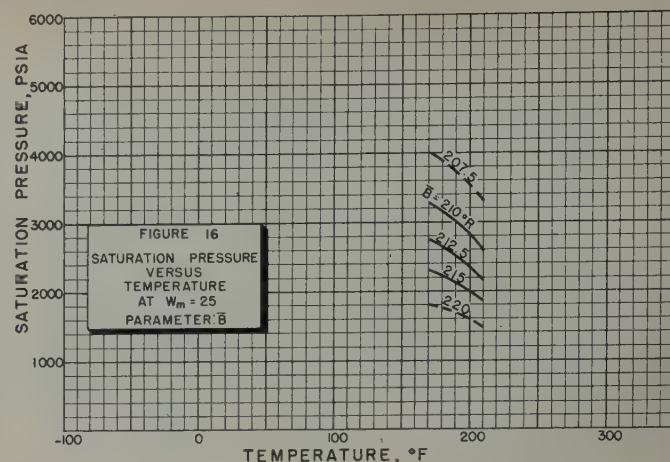


FIG. 16

therefore, denotes retrograde dew point saturation pressures, while the region to the right of this curve represents bubble point saturation pressures. It should be noted also that there is no discontinuity in the transition from mixtures which behave as bubble point liquids to mixtures which behave as condensate gases. In Fig. 2, plotted experimental points are divided into two categories. Open circles refer to data published in the literature and summarized in Tables II through VII. Solid circles refer to unpublished data from files of the United Gas Corp. on Union Producing Co. wells, Table VIII. The latter data represent gas depletion runs on high gas/oil ratio condensate fluids which were observed in an equilibrium windowed cell.

Final Set of Working Charts

The isothermal plots of saturation pressure *vs* molal average boiling point, such as Fig. 2, were cross-plotted and smoothed several ways, once with respect to W_m and once with respect to temperature, yielding as the result a set of 14 working charts, Figs. 3 through 16. Each chart contains a

family of partial phase envelopes, or upper phase boundaries, plotted on pressure *vs* temperature coordinates. Each curve in the family represents a hydrocarbon mixture having a different value of \bar{B} . Values of W_m are held constant for any one chart. Loci of critical states which intersect the partial phase envelopes separate regions of bubble point and of retrograde dew point behavior on each chart. The determination of the critical states for these complex mixtures is described in another paper.⁵ The ranges of \bar{B} and W_m covered in these charts are 210° to 380°R , and 27.5 to 100 respectively. These ranges cover nearly all condensate and highly volatile oil mixtures. The dashed portions of the curves on these plots represent smoothed extrapolations of the correlation into regions in which experimental data are lacking.

Agreement Between the Correlation and Experimental Data

In order to evaluate the accuracy of the recommended working charts, a comparison was made between predicted and observed saturation pressures for all experimental mixtures

Table I—Deviation of Predicted Saturation Pressures from Experimental Values
Part One: Distribution of Deviations According to Source of Data

Source of Data Author Reference	Distribution of Expt'l Points Among Various Per Cent Deviations										Total Number of Expt'l Points	Arithmetic Mean Deviation %	Standard Deviation %
	-25% to -20%	-20% to -15%	-15% to -10%	-10% to -5%	-5% to 0%	0% to 5%	5% to 10%	10% to 15%	15% to 20%				
Eilerts and Smith ²	0	0	0	0	3	11	10	0	0	24	+ 4	3.1	
Hanson and Brown ³	0	0	0	1	2	3	1	3	0	10	+ 3.6	7.5	
Kurata and Katz ⁴	0	0	6	12	14	17	8	1	0	58	- 1.3	6.2	
Olds, Sage and Lacey ⁷	1	0	1	1	6	6	0	0	0	15	- 3.6	6.3	
Reamer and Sage ⁹	0	1	5	7	7	15	7	9	0	51	+ 1.3	8.4	
Sage and Olds ^{10,8}	0	0	6	7	11	7	4	0	0	35	- 3.2	6.3	
Union Producing Co. ¹²	0	0	3	3	3	6	5	1	0	21	0.0	8.2	
Total Points (or frequency)	1	1	21	31	46	65	35	14	0	214	- 0.19	7.0	

Part Two: Distribution of Deviations According to Temperature Range

Temperature Range, °F	< 100	100-150	151-200	201-250	> 250	Entire Range
Number of Points	25	71	58	56	4	214
Maximum Deviation						
Positive	+13.3%	+13.6%	+13.4%	+15.0%	+6.9	+15.0%
Negative	-14.4%	-15.5%	-11.7%	-21.8%	-10.1	-21.8
Arithmetic Mean Deviation	-1.9%	-0.64%	+1.38%	-0.1%	+0.5%	-0.19%
Standard Deviation	8.0%	6.7%	6.7%	7.5%		7.0%
95% Confidence Limit for the Arithmetic Mean Deviation	+3.3%	±1.56%	±1.76%	±2.0%		±0.93%

the ranges covered by the charts. At the computed values of \bar{B} and W_m for each mixture, values of saturation pressure were read directly from the working charts or interpolated usually without further crossplotting.

A total of 214 experimental points are listed in Tables II through VIII. Each table represents a different collection of data, and lists computed values of \bar{B} and W_m for each mixture, the experimental and predicted saturation pressures at the observed temperature, and the per cent deviation of the predicted saturation pressure from the observed value. These per cent deviations are summarized for statistical analysis in

Table II—Comparison of Predicted and Observed Saturation Pressures, Data of Eilerts and Smith²

Weight Per Cent Trap Gas	W_m	\bar{B} °R	Temp. °F	Sat'n Press. psia		Per Cent Deviation Pred. from Obs.
				Obs.	Pred.	
28.88	87.9	342.0	70	3005	3050	+ 1.5
			100	3178	3200	+ 0.7
			160	3389	3350	- 1.2
			228	3411	3390	- 0.6
			250	3370	3390	+ 0.6
29.16	87.7	341.5	228	3430	3390	- 1.2
			70	3620	3780	+ 4.4
			100	3775	3900	+ 3.3
			160	3870	4100	+ 5.9
			228	3750	4040	+ 7.7
50.01	67.6	281.5	250	3685	4030	+ 9.4
			280	3575	3820	+ 6.9
			70	3690	3810	+ 3.3
			100	3852	3950	+ 2.5
			160	3929	4100	+ 4.4
66.41	53.0	252.4	228	3775	3980	+ 5.4
			250	3665	3840	+ 4.8
			280	3485	3540	+ 1.6
			70	3720	3920	+ 5.4
			100	3850	4080	+ 5.6
73.59	47.2	243.1	160	3880	4200	+ 7.6
			228	3678	3950	+ 7.4
			250	3555	3800	+ 6.9
			280	3330	3460	+ 3.9

Table III—Comparison of Predicted and Observed Saturation Pressures, Data of Hanson and Brown³
Natural Gas Type Mixtures

Mixture	W_m	\bar{B} °R	Temp. °F	Sat'n Press. psia		Per Cent
				Obs.	Pred.	Deviation Pred. from Obs.
A	44.0	285.5	100	1990	2000	+ 0.5
			160	1990	2030	+ 2.0
B	43.0	281.8	100	1980	1960	- 1.0
			160	1900	2030	+ 7.0
*A _v	34.0	252.7	100	1822	1790	- 1.8
			100	1639	1490	- 9.0
B _v	32.2	243.2	100	1736	1770	+ 2.0
			100	1822	2030	+ 11.4
A _L	52.8	324.7	100	1822	2030	+ 11.4
			100	1639	1860	+ 13.6
B _L	53.4	339.7	100	1736	1930	+ 11.1
*A _v	Equilibrium vapor phases from mixture A					
B _v	Equilibrium vapor phases from mixture B					
A _L	Equilibrium liquid phases from mixture A					
B _L	Equilibrium liquid phases from mixture B					

Table I. Deviations in saturation pressure are expressed as per cents of the observed pressures rather than as absolute pressure differences in order to give equal weight to deviations representing equal *percentage* differences regardless of the absolute value of the observed pressures about which the deviations are recorded.

Part One of Table I shows the frequency of deviations listed in Tables II through VIII according to the source of the data and according to the magnitude of the deviations. The frequency of the deviations for all 214 observations is given in the last row. These deviations are seen, for all practical pur-

Table IV—Comparison of Predicted and Observed Saturation Pressures, Data of Kurata and Katz⁴
Natural Gas-Natural Gasoline Mixtures

Mixture	W_m	\bar{B} °R	Temp. °F	Sat'n Press. psia		Per Cent Deviation Pred. from Obs.
				Obs.	Pred.	
B-1	39.0	278.6	60*	1803	1600	- 11.3
			80	1830	1640	- 10.9
			100	1840	1680	- 8.6
			120	1823	1730	- 5.1
			60*	1776	1600	- 9.8
B-2	42.0	294.5	100*	1821	1680	- 7.8
			120	1790	1700	- 5.0
			140	1745	1700	- 2.6
			160	1682	1680	- 0.2
			60*	1630	1580	- 3.1
B-3	43.8	306.5	100*	1748	1660	- 4.9
			120*	1754	1700	- 3.0
			140*	1731	1680	- 3.0
			160*	1695	1690	- 0.2
			180	1645	1680	+ 2.1
B-4	45.1	315.6	60*	1635	1540	- 5.8
			100*	1770	1660	- 6.2
			120*	1775	1670	- 5.9
			140*	1739	1680	- 3.4
			160	1670	1680	+ 0.7
T-1	43.2	252.6	180	1560	1660	+ 6.3
			60	2651	2620	- 1.2
			80	2728	2760	+ 1.1
			100	2740	2860	+ 4.2
			120	2721	2875	+ 5.4
T-3	45.7	258.9	140	2672	2890	+ 8.1
			160	2570	2910	+ 13.2
			60*	2650	2720	+ 2.8
			100	2800	2930	+ 4.7
			140	2859	2990	+ 4.7
T-4	50.1	271.1	160	2850	3000	+ 5.2
			180	2785	3000	+ 7.7
			60*	2620	2720	+ 3.9
			80*	2680	2800	+ 4.5
			100	2760	2880	+ 4.2
T-5	64.5	320.5	120	2790	2910	+ 4.2
			140	2820	2950	+ 4.5
			160	2800	2960	+ 5.8
			180	2730	2960	+ 8.4
			190	2700	2930	+ 8.7
S-2	42.2	258.3	80*	2794	2600	- 6.8
			120*	2928	2740	- 6.5
			160*	2942	2780	- 5.5
			180*	2920	2820	- 3.5
			190	2901	2850	- 1.8
S-3	47.2	285.5	60	2417	2350	- 2.6
			80	2496	2500	+ 0.2
			100	2563	2550	- 0.6
			120	2604	2610	+ 0.2
			140	2613	2620	+ 0.3
S-3	47.2	285.5	160	2603	2610	+ 0.3
			180	2580	2600	+ 0.8
			60	2353	2120	- 9.9
			100	2549	2240	- 12.1
			120	2594	2290	- 11.6
S-3	47.2	285.5	140	2615	2330	- 10.8
			160	2610	2330	- 9.6
			180	2590	2310	- 10.7

*Indicates bubble point pressures. Remainder of points represent retrograde dew point pressures.

Table V—Comparison of Predicted and Observed
Saturation Pressures, Data of Olds, Sage and Lacey⁷
Paloma Field, California

Weight Fraction Trap Gas	W_m	$\bar{B}^{\circ}R$	Temp. $^{\circ}F$	Sat'n Press. psia		Per Cent Deviation Pred. from Obs.
				Obs.	Pred.	
0.5335	82.8	293.0	100	4490	4440	-1.1
			190	4590	4550	-0.9
			250	4630	4520	-2.4
0.6292	71.2	276.4	100	4560	4470	-2.0
			190	4730	4620	-2.1
			250	4780	4540	-5.1
0.8111	49.2	251.1	100	3835	3670	-4.3
			190	4305	3760	-12.8
			250	4440	3470	-21.8
1st mod.	86.2	282.8	100	4967	5070	+2.0
			190	5077	5180	+2.0
			250	5022	5100	+1.5
2nd mod.	90.4	276.5	100	5910	5950	+0.8
			190	5815	5870	+0.8
			250	5644	5750	+1.9

Table VI—Comparison of Predicted and Observed
Saturation Pressures, Data of Reamer and Sage⁹
Louisiana Fields

Mixture	W_m	$\bar{B}^{\circ}R$	Temp. $^{\circ}F$	Sat'n Press. psia		Per Cent Deviation Pred. from Obs.
				Obs.	Pred.	
A-1	45.3	230.8	40	4494	5090	+13.3
			100	4810	5400	+12.3
			160	4858	5420	+11.6
			200	4758	5320	+11.8
A-2	42.3	228.2	40	4630	5090	+9.9
			100	4914	5370	+9.9
			160	4943	5310	+7.4
			200	4830	5200	+7.7
A-3	36.2	222.7	40	4850	5200	+3.1
			100	5115	5450	+6.5
			160	5106	5370	+4.9
			200	4943	5180	+4.8
C-1	65.3	244.5	100	6650	6450	-3.0
			160	6440	6370	-1.1
			220	6145	6160	-0.2
			250	5930	5980	+0.8
C-2	49.2	232.0	100	6400	5900	-7.8
			160	6190	5910	-4.5
			220	5900	5690	-3.6
			250	5700	5450	-4.4
C-3	36.9	223.6	100	5750	5350	-7.0
			160	5550	5050	-9.0
			220	5280	4730	-10.4
			250	5090	4450	-12.4
D-1	63.1	241.4	100	6400	6700	+4.7
			160	6220	6520	+4.8
			220	5940	6350	+6.9
			250	5740	6150	+7.2
D-2	49.8	230.7	100	6380	6450	+1.1
			160	6170	6360	+3.1
			220	5870	6120	+4.3
			250	5660	5850	+3.2
D-3	35.7	221.8	100	5780	5400	-6.6
			160	5580	5330	-4.5
			220	5230	4950	-5.3
			250	5010	4700	-6.2
E-1	32.2	218.3	100	4020	4450	+10.7
			130	3935	4450	+13.2
			160	3825	4300	+12.2
			190	3658	4150	+13.4
E-2	29.8	216.4	220	3345	3850	+15.0
			100	3815	3760	+1.4
			130	3729	3780	+1.3
			160	3605	3650	+1.2
E-3	27.3	214.5	190	3445	3480	+1.0
			220	3145	3200	+1.8
			100	3612	3050	-15.5
			130	3520	3070	-12.7
			160	3405	3100	-8.9
			190	3265	2880	-11.7
			220	2990	2680	-10.4

Table VII—Comparison of Predicted and Observed
Saturation Pressures
San Joaquin Valley Field, California

Mixture	W_m	$\bar{B}^{\circ}R$	Temp. $^{\circ}F$	Sat'n Press. psia		Per Cent
				Obs.	Pred.	Deviation Pred. from Obs.
Data of Sage and Olds ¹⁰						
A-1	44.5	252.5	40	3095	2650	-14.4
			100	3394	3040	-10.7
			160	3480	3100	-10.9
			220	3295	2990	-9.3
A-2	41.4	246.0	40	3010	2720	-9.6
			100	3245	3120	-3.9
			160	3294	3130	-5.0
			220	3073	2940	-4.3
B-1	62.0	270.0	100	3900	3980	+2.1
			190	3850	4120	+7.0
			250	3655	3910	+7.0
B-2	39.5	236.5	100	3600	3450	-4.2
			160	3288	3450	+4.9
B-3	33.4	229.0	100	3010	3100	+3.0
			160	2960	3160	+6.8
C-1	43.7	253.7	40	2820	2480	-12.0
			100	3080	2880	-6.5
			160	3090	2900	-6.2
			220	2795	2760	-1.3
C-2	42.3	252.8	40	2810	2410	-14.2
			100	3065	2790	-9.0
			160	3075	2850	-7.3
			220	2780	2860	+2.9
D-1	70.0	276.2	100	4060	4340	+6.9
			190	4388	4490	+2.3
			250	4420	4410	-0.2
D-2	64.2	268.4	100	4344	4240	-2.4
			190	4677	4430	-5.3
			250	4705	4200	-10.7
Data of Olds, Sage and Lacey ⁸						
1	59.8	279.5	100	3300	3360	+1.8
			190	3494	3510	+0.5
			250	3385	3320	-1.9
2	52.4	265.6	100	3325	3260	-2.0
			190	3420	3330	-2.6
			250	3220	3140	-2.5

Table VIII—Comparison of Predicted and Observed
Saturation Pressures, Data of Union Producing Co.³
Mid-Continent and Gulf Coast Fields

Mixture	W_m	$\bar{B}^{\circ}R$	Temp. $^{\circ}F$	Sat'n Press. psia		Per Cent Deviation Pred. from Obs.
				Obs.	Pred.	
1	29.5	220.1	199	2760	2650	-4.0
2	39.3	242.2	202	2740	2860	+4.4
3	54.0	270.0	230	3200	3240	+1.3
4	31.1	227.8	219	2380	2160	-9.2
5	36.0	233.3	229	3020	2950	-2.3
6	34.6	232.1	233	2500	2610	+4.4
7	33.3	229.3	233	2650	2700	+1.9
8	35.8	232.3	230	2820	2930	+3.9
9	35.8	231.9	233	2740	2970	+8.4
10	36.4	234.6	235	2800	3000	+7.1
11	33.9	229.5	217	3120	3030	-2.9
12	33.5	229.3	213	2620	2980	+13.7
13	31.7	226.6	206	2750	2530	-8.0
14	72.8	268.5	280	5560	5000	-10.1
15	45.2	239.2	240	4560	3880	-14.9
16	33.6	223.3	199	3400	3700	+8.8
17	41.2	233.9	211	4587	3980	-13.2
18	45.3	256.0	238	3050	2880	-5.6
19	27.4	212.3	196	2950	3150	+6.8
20	34.2	231.2	215	2520	2770	+9.9
21	32.2	228.1	215	2375	2390	+0.6

poses, to be normally distributed about 0 per cent deviation. The overall arithmetic mean deviation is in fact -0.19 per cent, or substantially zero, while the standard deviation about this mean is 7.0 per cent.

Part Two of Table I describes the distribution of the same per cent deviation according to temperature range. The number of experimental points falling in each range and the maximum positive and negative deviations found in each range of temperature are given in the first two rows, respectively. No significant trend is noticeable in the value of the arithmetic mean deviations over the five temperature ranges chosen, as may be seen in row three, indicating thereby that the saturation pressure curves are drawn with approximately the same degree of fit to the experimental points in all ranges of temperature. The standard deviation about each of the five mean deviations (row four) are all of the same order of magnitude as that for the entire group. Ninety-five per cent confidence limits for these arithmetic mean deviations are given in the last line.

Probable Accuracy of the Correlation

The probable error for the data taken as a whole is about five per cent, or approximately the same as the overall uncertainty for most of the data from which the correlation is derived. It should be noted, however, that the data for condensate mixtures having high gas/oil ratios (greater than about 40,000 cu ft/bbl) have a somewhat greater uncertainty than five per cent. Examples of these mixtures are found in references 9 and 12. The increased uncertainty for these mixtures is due to at least two factors: (1) The difficulty in measuring accurately the exact ratio of separator gas to separator liquid charged to the experimental cell in the recombination study. (2) The difficulty in measuring accurately the proportionately smaller quantities of condensed liquid obtained in the retrograde region. As more accurate dew point data for these mixtures become available, it may be possible to improve considerably the correlation in this region.

ILLUSTRATIVE PROBLEM

In order to clarify the procedure to be followed when applying the correlation to an actual problem, an illustrative example is given here.

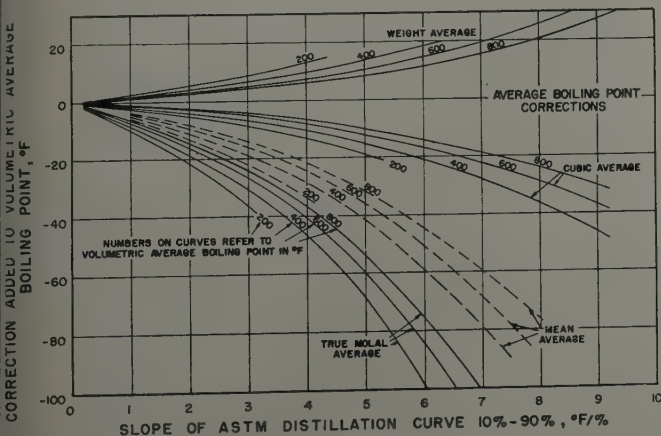


FIG. 17—CORRECTION TO VOLUMETRIC AVERAGE BOILING POINTS.

Problem

To predict the dew point pressure at 199°F for a well effluent having the following composition (Mixture No. 1, Table VIII):

Well Stream Composition

Component	Molecular Weight	Separator Gas Wt. Fraction	Separator Liquid Wt. Fraction	Well Stream Weight Fraction	Well Stream Mol Fraction
CO ₂	44	.0145	-----	.0134	.0059
N ₂	28	.0334	-----	.0316	.0218
C ₁	16.04	.7910	.0155	.7313	.8860
C ₂	30.07	.0762	.0096	.0713	.0460
C ₃	44.09	.0317	.0164	.0306	.0134
i-C ₄	58.12	.0137	.0114	.0135	.0045
n-C ₄	58.12	.0137	.0217	.0144	.0048
i-C ₅	72.15	.0075	.0348	.0097	.0026
n-C ₅	72.15	.0068	.0221	.0078	.0021
C ₆ +	86.17	.0090	.1078	.0164	.0037
C ₇ +*	114	.0025	-----	.0018	.0003
C ₇ **	139	-----	.7607	.0582	.0081

*Separator Gas
**Separator Liquid

ASTM Distillation of C₇+ from Separator Liquid

Gravity: 56.3° API; 0.7535 g/ml

Distillation

I.B.P.	216°F
10%	232
20%	245
30%	260
40%	289
50%	313
60%	349
70%	383
80%	416
90%	497
95%	-----
End Point	-----

Remarks: 10-90 Slope = 3.31

Volumetric Average B. Pt. = 337°F

Solution

Step 1. Calculation of Molal and Weight Average Properties of the Heavy Ends.

In order to compute \bar{B} and \bar{W}_m for the well stream composition, it is desirable first to determine these properties for the C₇+ fractions in the separator gas and separator liquid streams. The C₇+ fraction from the separator gas may be assumed to have the properties of normal octane: $\bar{B} = 718^\circ\text{R}$ and $\bar{W}_m = 114$. Two methods are recommended for computing \bar{B} and \bar{W}_m for the C₇+ in the separator liquid. The first method is a short-cut procedure designed for quick estimates of these properties. For more accurate calculation of \bar{B} and \bar{W}_m the second, somewhat more involved method, is recommended.

The first method, the short-cut procedure, assumes that \bar{B} is approximately equal to the mean average boiling point and that \bar{W}_m for a C₇+ fraction may be obtained directly from the ASTM slope and the average characterization factor.

The mean average boiling point as obtained from Fig. 17¹¹ is 316°F, or 776°R.

\bar{W}_m is obtained from the ASTM slope and the average characterization factor. The latter may be read from Fig. 18¹ from a knowledge of the density and the cubic average boiling point. Fig. 17 is also used to obtain the cubic average boiling point which is 328°F. From Fig. 18, the average characterization is 12.3. \bar{W}_m may now be read directly from Fig. 19, which is a plot of \bar{W}_m vs ASTM slope with lines of constant characterization factor. From this chart, $\bar{W}_m = 142$.

The second method is a more precise calculation because the heavy ends are broken up into a number of arbitrarily

selected cuts. The properties of each cut are ascertained and summed to obtain the property of the entire fraction. Table IX summarizes this calculation. Columns 3 and 4 list the mid-boiling points of 10 selected cuts as read from the ASTM distillation curve plotted in Fig. 20. This curve is obtained from the data given in the statement of the problem. If it is assumed that the characterization factor is identical for all cuts (12.3), Fig. 18 may be used to obtain the densities and weights of each cut listed in columns 5 and 6. For a 100 ml sample, assuming no losses, the total weight of the 10 cuts should be 75.35 g since the density was given as 0.7535 g/ml. The weight of each cut, therefore, may be expressed as a weight fraction of the entire separator liquid (column 7) by multiplying the weight of each cut by the ratio $0.7607/75.35$, the ratio of the weight fraction of the C_7+ to the total weight of C_7+ . These weight fractions are expressed as cumulative weight fractions of the separator liquid (column 9).

A plot of log absolute mid-boiling point *vs* average cumulative weight per cent is constructed (Fig. 21). A best straight line through all points in Fig. 21 is extrapolated to 100 cumulative per cent and the average boiling point of the residue (cut No. 10) is obtained from the extrapolated portion of the line. This value, 940°R , or 480°F , is used to determine the density and thus the weight of the cut (7.97 g).

Two parenthetical remarks are in order here: (1) The fact that the total weight of the C_7+ fraction (75.20 g), as obtained from column 6, checks fairly closely with the actual weight (75.35 g) serves as a check on the original assumption that the characterization factors for the various cuts were substantially the same; (2) the technique used for extrapolating the distillation curve to 100 per cent is probably more elaborate than is necessary in this instance. Any reasonable extrapolation from 90 per cent to 100 per cent, such as the one shown in Fig. 20, would be satisfactory. Extrapolating on log absolute boiling point *vs* cumulative weight per cent coordinates is recommended primarily when treating higher boiling mixtures,

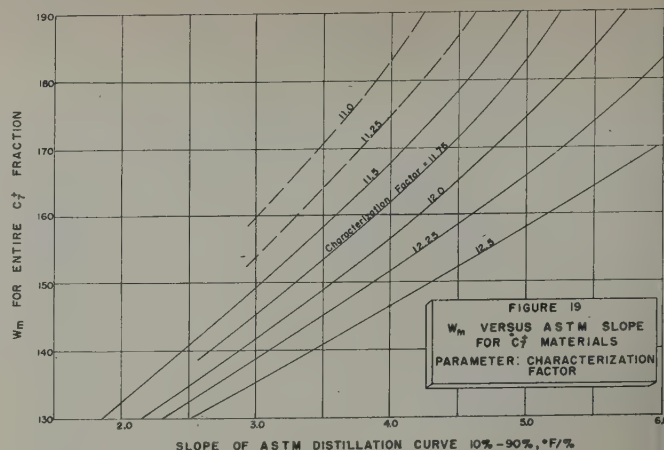


FIG. 19

where the extrapolation is more extended. It is used here principally for illustrative purposes.

The equivalent molecular weight fraction of each cut (column 10) is a function of the average boiling point and the characterization factor and may be read from Fig. 1. The weight average equivalent molecular weight for the entire C_7+ fraction is then computed to be 142.8, the summation in column 11 divided by the total weight of sample, found in column 6. The molal average boiling point for the C_7+ fraction is shown as the summation of column 14 divided by the summation of column 13, the total mols of sample, and is 778°R . The mols are computed in column 13 by using the actual molecular weights as read from Fig. 18 from a knowledge of the boiling point and characterization factor or density for each individual cut.

The close agreement between the values of \bar{B} and \bar{W}_m for the C_7+ fraction as computed by the long method and by the short-cut procedure indicates that the short-cut procedure would have been entirely adequate in this case:

	$\bar{B}(C_7+)$	$\bar{W}_m(C_7+)$
Accurate method	778°R	142.8
Short-cut method	776°R	142

Step 2. Calculation of \bar{B} and \bar{W}_m for the Well Stream Composition.

Once the properties of the C_7+ materials have been determined, it is possible to compute the values of \bar{B} and \bar{W}_m for the well stream composition, as shown in Table X.

Columns 1 and 4 are merely a restatement of the original well stream composition. Columns 2 and 5 represent boiling points and equivalent molecular weights of the hydrocarbons including the lumped values for the C_7+ fraction as computed in Table IX. In computing \bar{B} , the molecular weight of the C_7+ fraction which is used is that obtained from Table IX (or that obtained from Fig. 18 if the short-cut method were used). \bar{B} for the well stream is the summation in column 3, or 219.8°R . \bar{W}_m is the summation in column 6, or 29.4.

Step 3. Reading the Saturation Pressure from the Working Charts.

The values of \bar{B} and \bar{W}_m just computed define somewhere in Figs. 3-16 a unique saturation pressure at any given temperature. In the present case the saturation pressure is interpolated between Figs. 15 and 14. At a temperature of 199°F and at \bar{B} equal 219.8°R , the saturation pressure read from Fig. 15 ($\bar{W}_m = 27.5$) is 2,150 psia, while from Fig. 14 ($\bar{W}_m = 30$) it is 2,860 psia. The interpolated value for $\bar{W}_m = 29.4$, therefore, is about 2,690 psia. This saturation pressure is clearly a retrograde dew point pressure since it lies to the right of the critical loci indicated in Figs. 15 and 14.

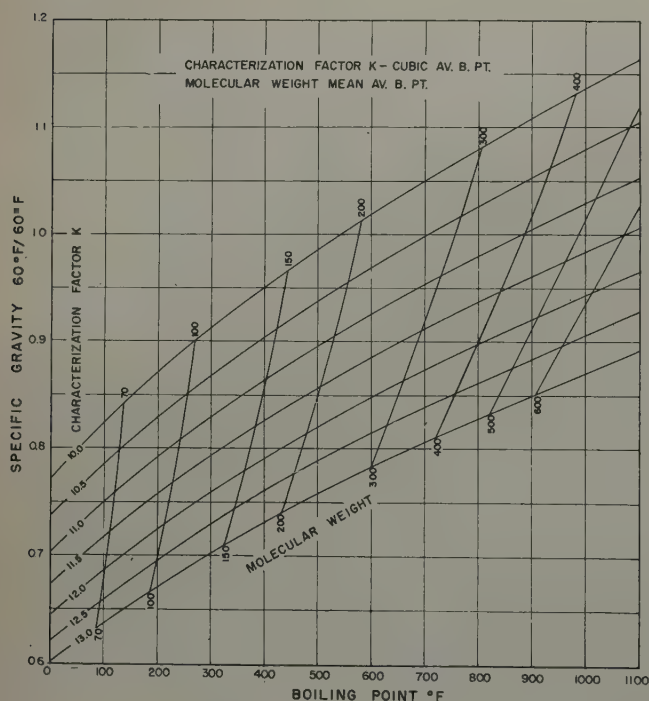


FIG. 18 — RELATIONSHIPS BETWEEN MOLECULAR WEIGHT, CHARACTERIZATION FACTOR, DENSITY, AND BOILING POINTS.

Table IX — Calculation of Molal and Weight Average Properties of the Heptanes and Heavier Fraction of the Separator Liquid

Cut. No.	ml	Mid-boiling Pt., °F	Mid-boiling Pt., °R	Density, g/ml	Wt, g	Wt. Fraction of Separator Liquid, g x .7607	Cumulative Wt. Fraction of Separator Liquid	Avg. Cumulative Wt. Fraction of Separator Liquid	Equivalent Molecular Wt.	g x Equivalent Molecular Wt.	Actual Molecular Wt.	mols = g	mols x Boiling Pt., °R
1	2	3	4	5	6	7	8	9	10	11	12	13	14
1	10	223	683	.716	7.16	.0723	.2393	.3116	.2755	103	737	.0675	46.1
2	10	239	699	.721	7.21	.0728	.3844	.3480	.109	786	110	.0655	45.8
3	10	255	715	.727	7.27	.0734	.4578	.4211	.112	814	115	.0632	45.2
4	10	275	735	.734	7.34	.0741	.5319	.4949	.119	873	122	.0602	44.2
5	10	300	760	.743	7.43	.0750	.6069	.5694	.127	944	131	.0567	43.1
6	10	330	790	.752	7.52	.0759	.6828	.6449	.137	1030	141	.0533	42.1
7	10	366	836	.764	7.64	.0771	.7599	.7214	.150	1146	155	.0493	41.2
8	10	406	866	.776	7.76	.0783	.8382	.7991	.168	1304	172	.0451	39.1
9	10	458	918	.790	7.90	.0798	.9180	.8781	.191	1509	195	.0405	37.2
10 (res)	10	(480)*	(940)*	(.797)	(7.97)	.0805	.9985	.9583	.200	1594	207	.0385	36.2
Total					75.20					10737		.5398	420.2

$$W_m = \frac{10737}{75.20} = 142.8$$

$$\text{Mol Wt} = \frac{75.20}{.5398} = 139.3$$

$$\bar{B} = \frac{420.2}{.5398} = 778^\circ\text{R}$$

*Extrapolated values read from Fig. 21.

It may be noted that the predicted dew point pressure of 2,690 psia compares well with the experimental value, which is 2,760 psia.

THEORETICAL CONSIDERATIONS

Speculation as to the reason for the effectiveness of the two composition parameters, \bar{B} and W_m , in correlating saturation pressures is worthwhile in that it may point the way for future investigations. It is well known that only two composition parameters are necessary to define adequately the composition of a ternary mixture. From this it follows that by employing a two-parameter correlation for complex mixtures, each mixture is treated as if it were a "restricted" multicomponent mixture having many of the characteristics of a ternary mixture. It cannot, of course, be concluded, prior to an actual

investigation, that the mere restriction of the degrees of freedom of the composition to two for all mixtures permits a correlation with sufficient accuracy. Nor is it likely that any two composition parameters when used in combination will be as effective as any other two, even if it turns out that only two properly chosen parameters are sufficient. The discussion which follows is, therefore, an attempt to explain, after-the-fact, the effectiveness of the particular parameters, \bar{B} and W_m .

To begin with certain generalizations concerning the composition of naturally occurring mixtures are in order.

Distribution Among Components of a Mixture

Any naturally occurring mixture may be viewed statistically with regard to the number of molecules of each component contained in that mixture. The incidence, or frequency of any one component is, in addition to being a function of the temperature and pressure, directly related to the relative volatility of that component and, consequently, also related to any other property (such as the molecular weight) of which

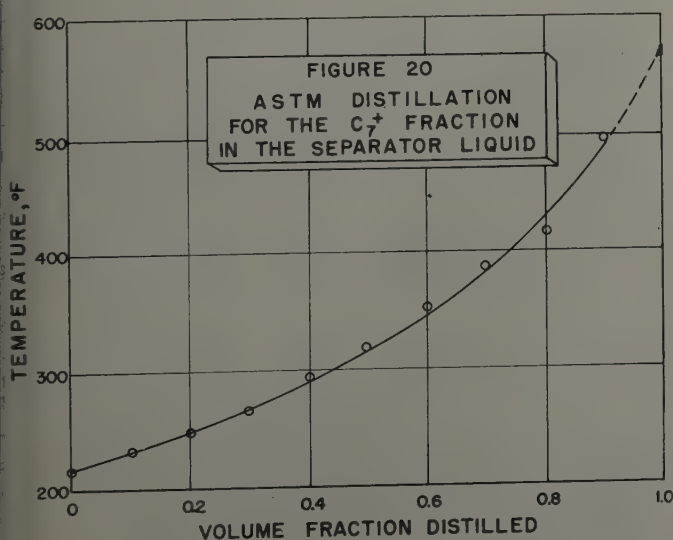


FIG. 20

Table X — Calculation of \bar{B} and W_m for the Well Stream Analysis

Component	1 Mol Fraction	2 Boiling Point, °R	3 Mol Frac. x Boiling Point, °R	4 Weight Fraction	5 Equiv. Mol. Wt.	6 Wt. Frac. x Equiv. Mol. Wt.
CO ₂	.0059	350	2.06	.0134	44	.59
N ₂	.0218	139	3.03	.0316	28	.88
C ₁	.8860	201	178.09	.7313	16.04	11.73
C ₂	.0460	332	15.27	.0713	30.1	2.15
C ₃	.0134	416	5.57	.0306	44.1	1.35
iC ₄	.0045	471	2.12	.0135	54.5	.74
nC ₄	.0048	491	2.36	.0144	58.1	.84
iC ₅	.0026	542	1.41	.0097	69	.67
nC ₅	.0021	557	1.17	.0078	72.2	.56
C ₆ S	.0037	600	2.22	.0164	85	1.39
C ₇ + Sep. gas.	.0003	718	.22	.0018	114	.21
C ₇ + Sep. liq.	.0081	778*	6.30	.0582	142.8*	8.31

$$\bar{B} = 219.8^\circ\text{R}$$

$$W_m = 29.4$$

*Computed in Table IX.

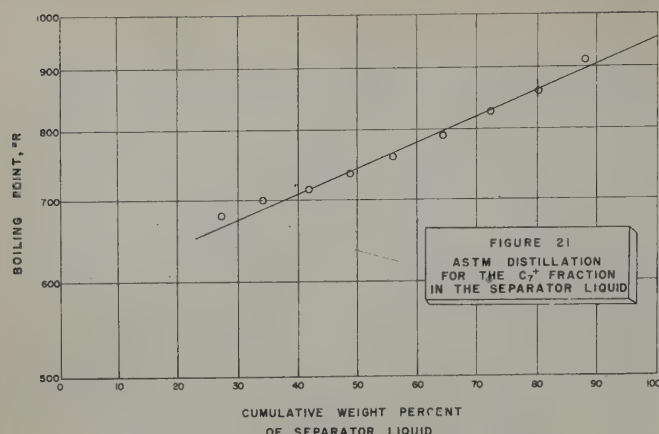


FIG. 21

the volatility is a function. For example, a typical natural gas existing at its dew point has a distribution of components characterized by the presence of progressively smaller and smaller amounts of the high boiling components which are characteristically non-gaseous at the existing temperature. Similarly, a typical naturally occurring crude oil existing at its bubble point contains progressively smaller and smaller amounts of the low boiling components which are characteristically non-liquid at the existing temperature. To go one step further, a saturated condensate liquid, obtained from a natural gas cap over a crude oil reservoir, has a distribution of components which is characterized by having progressively smaller and smaller quantities of both heavy and light ends (methane excepted) about some central or average boiling component.

Relationship Between the Distribution of Components and Selected Composition Parameters

It may be possible with a set of selected composition parameters, to describe statistically the composition of a mixture in terms of the mean value and in terms of the distribution about the mean value, of any property of the components in that mixture. The boiling point, for example, may be used as the characterizing property to describe the composition of a naturally occurring mixture.

The molal average boiling point may be selected as the parameter which describes the mean boiling point for the mixture. This parameter as defined in Table XI is the first moment of the boiling point. The second moment, defined in Table XI, may also be selected as a composition parameter. This second moment provides information concerning the distribution of components about that component which has a boiling point equal to the mean value.

Higher moments about the mean value provide still more definition of the distribution of components about the mean. In general, each succeeding moment, when used as a composition parameter, adds less information than the preceding one. Consequently, for any particular correlation in which compositions of mixtures are to be described by these parameters, there is always a practical limit to the number of such parameters which may be used effectively. Furthermore, if the composition parameters are used to describe mixtures whose distributions of components about any given mean value are roughly similar, as is the case for naturally occurring mixtures, it is reasonable that relatively few of these parameters are required.

It has been shown mathematically that \bar{W}_m is in fact related to the second moment of the boiling point,⁵ so that the parameters \bar{B} and \bar{W}_m , when used in combination, describe a complex mixture by referring its composition to a component of mean volatility and to the distribution of the actual components about that component of mean volatility. Since saturation pressure at any given temperature is a function only of the composition, it is possible to account in this way for the effectiveness of these parameters in correlating saturation pressures.

FUTURE INVESTIGATIONS

The foregoing analysis carries with it the implication that the correlating technique described here is a general one and may be used for predicting other physical properties of complex naturally occurring mixtures, such as saturated densities and viscosities of mixtures along the upper phase envelope. Perhaps, in addition to properties in the single phase, the technique may prove useful for predicting two-phase conditions such as the relative quantity of liquid and gas within the phase envelope as a function of pressure and temperature. If this latter proves feasible, it may eventually be possible to construct a nearly complete phase diagram from a set of generalized composition coordinates for the mixture in question. It is hoped that further work along these lines may be reported soon.

CONCLUSIONS

An empirical correlation has been developed for predicting saturation pressures in natural gas-condensate and volatile oil mixtures. Saturation pressure is related directly to the composition of the mixture with the aid of two generalized composition characteristics: \bar{B} , the molal average boiling point, and \bar{W}_m , defined as the modified weight average equivalent molecular weight. Each composition parameter may be calculated in a simple and reproducible manner from the stream analysis of the mixture and an ASTM distillation of the C_7+ fraction. It is preferable, although not essential, to know also the specific gravity of several cuts from the ASTM distillation in order to determine more precisely the characterization factor of these cuts.

The correlation is presented in the form of a set of 14 working charts in which saturation pressures (retrograde dew point or bubble points) are plotted *vs* temperature, forming partial phase envelopes for mixtures having discrete values of the composition parameters, \bar{B} and \bar{W}_m . The intervals between the plotted values of \bar{B} and \bar{W}_m are sufficiently small to permit visual interpolation.

Table XI—Definition of the Mean Value* and Its Moments

First Moment (= Mean Value)	$= \sum_i \text{mol fraction}_i \cdot B_i$
Second Moment	$= \sum_i \text{mol fraction}_i \cdot B_i^2$
Third Moment	$= \sum_i \text{mol fraction}_i \cdot B_i^3$
nth Moment	$= \sum_i \text{mol fraction}_i \cdot B_i^{n+1}$

*Arbitrarily selected to be the molal average boiling point in this case

A comparison between experimental saturation pressures and those predicted from the working charts of this correlation reveals that:

1. The probable error when considering the data as a whole (214 experimental points) is about five per cent, or approximately the same as the overall uncertainty of the data from which the correlation is derived.

2. For high gas/oil ratio condensate fluids, approximately 40,000 or more cu ft/bbl, the probable error is about eight per cent, perhaps because of the greater uncertainty of the available experimental data for mixtures of this type.

Other empirical techniques may exist for predicting saturation pressures of condensate and volatile oil mixtures to the same degree of accuracy. The technique presented in this report, however, eliminates completely the use of the hydrocarbon K-values. It is believed, therefore, that an important simplification of the problem has been effected, providing the engineer with a quick yet accurate method for predicting saturation pressures.

ACKNOWLEDGMENT

The authors wish to thank W. M. Dow for his constructive suggestions. The authors also wish to express their appreciation to the United Gas Corp. for permission to prepare and publish this paper.

REFERENCES

1. Brown, Katz, Oberfell and Alden: *Natural Gasoline and the Volatile Hydrocarbons*, (Section One). Natural Gasoline Association of America, Tulsa, (1948) 79.
2. Eilerts, C. K., and Smith, R. V.: "Specific Volumes and Phase-Boundary Properties of Separator-Gas and Liquid-Hydrocarbon Mixtures," U. S. Bureau of Mines, Report of Investigation 3642, (1942).
3. Hanson, G. H., and Brown, G. G.: "Vapor-Liquid Equilibria in Mixtures of Volatile Paraffins," *Ind. and Eng. Chem.*, (1945) 37, (4), 821.
4. Kurata, F., and Katz, D. L.: "Critical Properties of Volatile Hydrocarbon Mixtures," *Trans. AICHE*, (1942) 38, (6), 995.
5. Organick, E. I.: "Prediction of Critical Temperatures and Critical Pressures of Complex Hydrocarbon Mixtures," Paper presented at AICHE meeting, Dec., 1951, Atlantic City.
6. Organick, E. I.: "Prediction of Hydrocarbon Vapor-Liquid Equilibria," PhD Thesis, University of Michigan, 1950. Also, Organick, E. I., and Brown, G. G.: AICHE Phase Equilibria Symposium to be published.
7. Olds, R. H., Sage, B. H., and Lacey, W. N.: "Volumetric and Phase Behavior of Oil and Gas from Paloma Field," *Trans.*, AIME, (1945) 160, 77.
8. Olds, R. H., Sage, B. H., and Lacey, W. N.: "Volumetric and Viscosity Studies of Oil and Gas from a San Joaquin Valley Field," *Trans. AIME*, (1949) 179, 287.
9. Reamer, H. H., and Sage, B. H.: "Volumetric Behavior of Oil and Gas from a Louisiana Field," *Trans. AIME*, (1950) 189, 261.
10. Sage, B. H., and Olds, R. H.: "Volumetric Behavior of Oil and Gas from Several San Joaquin Valley Fields," *Trans. AIME*, (1947) 170, 156.
11. Smith, R. L., and Watson, K. M.: "Boiling Points and Critical Properties of Hydrocarbon Mixtures," *Ind. and Eng. Chem.*, (1937) 29, (12), 1408.
12. Union Producing Co. data, United Gas Corp., Research Department Files.

DISCUSSION

By C. Kenneth Eilerts, U. S. Bureau of Mines, Bartlesville, Okla., Member AIME

We have used the correlations of Organick and Golding to estimate the dew points at reservoir temperature of two gas-condensate fluids on which measured dew points are available, with results indicating agreement to within 50 psi in one case and less than 500 psi in the other. One of these fluids was well above and the other well below average in liquid/gas ratio, and both fluids have been found difficult to correlate on any basis. The test made of the authors' diagrams for estimating phase-boundary pressure is probably a severe one, and it seems likely that lower differences between measured and computed pressures would be experienced on fluids with liquid/gas ratios in the proximity of 1.0 gal per Mcf of gas.

The authors are to be commended for developing a correlation method that can be applied to multicomponent hydrocarbon mixtures on a statistical basis. Computation of "molal average boiling points," "weight average equivalent molecular weight," and similar functions seems to be a logical step in estimating the properties of a complex hydrocarbon mixture from the properties and concentrations of its components.

We have found, however, that a further step is desirable in predicting some phase boundary properties of gas-condensate fluids, such as the critical temperature and the cricondenbar pressure or maximum pressure for coexistence of gas and liquid phases. The first step may consist of use of functions of the type,

$$T_{ce} = \frac{N_1 B_1 T_{c1} + N_2 B_2 T_{c2} + \dots}{N_1 B_1 + N_2 B_2 + \dots} \quad (1)$$

where

T_{ce} = a particular property of a mixture that is to be computed.

T_{c1}, T_{c2}, \dots = values of the corresponding property of the respective components in the mixture,

N_1, N_2, \dots = mole fraction of components 1, 2, ... in the mixture, and

B_1, B_2, \dots = a suitable property of components 1, 2, ... for altering their relative effects in the summation. The value of B may be unity in all terms.

This function, however, does not provide for values of T_{ce} that may be more or less than the value of the corresponding property for any component in the mixture. For example, the cricondenbar pressure and the critical pressure of a gas-condensate fluid can be and usually are greater than the critical pressure of any component in the fluid. We have shown* that the critical temperature of a gas-condensate fluid can be lower than the critical temperature of either the separator gas or liquid of the fluid.

Equation (1) above is not suited for indicating maximum or minimum values of the dependent variable T_{ce} . If the mixture property to be described passes through maximum or minimum values as the proportions of the components are systematically varied—adding a mixture of hydrocarbon liquid components to natural gas is an example—then a second correlation step usually will be necessary. In addition to an equation like that shown above, use must be made of an equation or of a graphic treatment that will provide for maximum or minimum effects as required.

*"Phase Relations of a Gas-Condensate Fluid at Low Temperature Including the Critical State," by C. K. Eilerts, V. L. Barr, N. B. Mullens and Betty Hanna, *Pet. Engr.*, (Feb., 1948) pp. 154-180, Fig. 11.

It is possible that the authors' correlations can be made to show maximum phase-boundary pressure effects by consideration of additional fluids of lower molal average boiling point. Their Figs. 3 to 16 inclusive in the boiling-point range presently shown indicate that, for given values of "weight average equivalent molecular weight," \bar{W}_m , the saturation pressure increases continuously as the "molal average boiling point," \bar{B} , decreases. If gas were added to fluid without limit to provide mixtures with successively lower molal average boiling points, then, at some boiling point not much lower than the lowest shown in the figures, the curves of saturation pressure should begin to indicate lower and lower pressures as the boiling point was lowered. At the limit, when the mixture is essentially of the composition of the added gas, the saturation pressures indicated may be lower than 2,000 psia.

This result could be obtained whether or not the experiment was conducted in such way as to maintain \bar{W}_m constant. It follows, moreover, that, for a given value of the property T_{ce} , as given by Equation (1) above, there may be two restricted compositions and two molal average boiling points.

It is entirely possible that the dew point pressure of gas-condensate fluids of average composition may equal reservoir pressure. The results* of Bureau of Mines tests made at flowing wells show for seven reservoir fluids that the reservoir pressure exceeded the dew point pressure at reservoir temperatures by an average of only 152 psi and in no case by more than 300 psi. The dew-point pressures measured ranged from 2,946 to 4,900 psia and are estimated to be accurate to ± 25 psi. Reservoir temperatures ranged from 191° to 251°F. It does not seem likely that this close agreement between reservoir and fluid dew point pressure for seven reservoirs is only coincidental. The original pressure of a gas-condensate reservoir depends on factors associated with the origin, accumulation, and retention of petroleum hydrocarbons, but the reason for the agreement between dew point and reservoir pressures must be latent in substances associated with dew point phenomena; the presence of a liquid phase in the reservoir would be an explanation. Twenty to 30 per cent of the volume of the reservoir pore space could be filled with liquid without appreciable entry of liquid into the well bore during fluid flow, and part of this liquid can be a mixture of hydrocarbons in equilibrium with the reservoir-gas phase. It would, therefore, be expected that the flowing fluid would be the reservoir-gas phase, with a dew point equal to reservoir pressure at reservoir temperature.

GOLDING'S REPLY TO MR. EILERTS

As Eilerts points out, the use of functions of the type (Eilerts' nomenclature)

$$T_{ce} = \frac{N_1 B_1 T_{c1} + N_2 B_2 T_{c2} + \dots}{N_1 B_1 + N_2 B_2 + \dots}$$

for direct computation of phase boundary properties is generally unsuitable. These functions may often, however, be used satisfactorily as correlating parameters to help systematize the observed behavior of hydrocarbon systems. Thus, although the functions used in this paper would not serve for direct calculation of maximum or minimum values of phase boundary properties, the combination of these functions as

empirical correlating parameters does serve to correlate such properties. The critical loci presented in this paper, for instance, were taken in their final smoothed form from another paper by one of the authors (reference 5 of text) in which the correlation techniques described in the present paper are extended to the direct correlation of the critical temperatures and pressures of complex hydrocarbon mixtures ranging from condensate gases to refinery mixtures. Though no cricondenba loci are presented in the present paper, the authors feel that visual inspection of Figs. 3 to 16 will reveal the approximate location of such loci with as much accuracy as the presently available experimental information permits.

The present correlation indicates that, at a given temperature and pressure, a single restricted composition (that is only one set of parameter values) represents all possible saturated fluids. Eilerts speculates that in some cases two restricted compositions may be possible at the same temperature and pressure. If such behavior is indeed found, it would result in an interesting addition to the present correlation. The curve of constant \bar{W}_m , as shown in Fig. 2 of the paper would then reach a maximum at some point of lower \bar{B} than their present termination, and turn downwards to lower saturation pressure at still lower values of \bar{B} . Extension of the correlation into such regions will, at any rate, have to wait upon publication of additional experimental data.

Eilerts suggests that "if gas were added to fluid without limit . . . then at some boiling point not much lower than the lowest shown in the figures, the curves of saturation pressure should begin to indicate lower and lower pressures . . ." This behavior can actually be followed on the correlation charts in a gas which is itself within the range of the correlation is used. As gas is added to the initial liquid, both \bar{B} and \bar{W}_m decrease, the initial decrease in \bar{B} being relatively the greatest. The corresponding saturation pressures will normally increase initially, reach a maximum pressure, and eventually decrease to the saturation pressure of the gas itself.

Eilerts also suggests that the dew point pressure of gas condensate fields of average composition may be equal to reservoir pressure. It is worth emphasizing that those condensate fields which are not in two phase equilibrium upon discovery are often of especial engineering interest. In particular, condensate reservoirs in which the initial reservoir pressure is above the dewpoint pressure may offer the possibility of increasing the expected economic yield through cycling above the dew point thus reducing the amount of heavier hydrocarbons lost through retrograde condensation in the reservoir.

The correlation presented in this paper allows an engineer to tell quickly from the well stream analysis and the reservoir temperature and pressure whether a new field is possibly in two phase equilibrium or whether it is definitely a single phase reservoir. It is furthermore often possible to predict the general production behavior of a given reservoir from the relationship between the reservoir temperature and the indicated critical temperature of the particular reservoir material. An estimation of the probable retrograde condensation in gas condensate fields can often be made from this temperature relationship, for instance. Even more important in some cases is the knowledge of whether a field will produce as a volatile oil reservoir or as a rich condensate reservoir. The sum of this information is often sufficient in itself to permit an engineer to decide whether a given reservoir should be produced by routine techniques or whether further experimental study and economic analysis is warranted.

*"Gas Condensate Reservoir Engineering" by C. Kenneth Eilerts, Oil and Gas Jour., (Feb. 8, 1947) pp 63-68.

VISUAL EXAMINATIONS OF FLUID BEHAVIOR IN POROUS MEDIA—PART I

ALFRED CHATENEVER, UNIVERSITY OF OKLAHOMA, NORMAN, OKLA.; AND JOHN C. CALHOUN, JR.,
PENNSYLVANIA STATE COLLEGE, STATE COLLEGE, PA., MEMBER AIME

ABSTRACT

An exploratory study was made to examine the possibilities of a visual approach in investigations into microscopic mechanisms of fluid behavior in porous media. Appropriate apparatus and techniques were developed so that microscopic phenomena could be recorded on color movie film as well as be observed visually. The observation flow cells in which the fluid behavior studies were made were essentially single-layered matrices of spheres between plates, sometimes all-glass, sometimes all-Lucite and sometimes a combination of the two. The fluids were limited to water and a filtered crude oil.

Two flow regimes were observed during the flow of the immiscible liquids: channel flow and slug flow. In the former, transport was effected through stable networks of interconnecting channels; and in the latter, part of the movement took place in the form of slugs. Under certain conditions, flood-front patterns were found to be different depending upon which liquids were the displacing and displaced phases and not depending upon whether the matrix was water-wet glass or oil-wet Lucite. Residual formations of oil and water were observed and are described. Some of the ramifications and significance of the observed phenomena are discussed.

INTRODUCTION

In recent years considerations of microscopic mechanisms of fluid flow in porous media have taken on greater significance. Much needs to be learned before the fundamentals of petroleum technology are completely established. For example, many unanswered questions exist in connection with relative

permeability, displacement phenomena, residual fluid formations, flow structure, etc.; and further analytical mathematical formulations are seriously indicated. It is hoped that systematic investigations into the microscopic mechanisms connected with the behavior of fluids in porous media will shed some light on some of the problems extant.

Until recently microscopic mechanisms have been considered almost exclusively as speculative hypotheses. Within the past few years, however, the problem has been submitted to a limited number of experimental investigations. Nuss and Whiting¹ made some studies on the pore-space geometry of sandstones and limestones by impregnating cores with an inert plastic and leaching the solid matrices to leave behind plastic models of the pore spaces. Schaefer² traced pore spaces microscopically through lengths of limestone cores by cutting away thin sections from the exposed faces normal to the line of view.

In 1949 two projects were organized in which dynamic flow phenomena were examined microscopically to uncover microscopic mechanisms. One was set up at the Pennsylvania State College where Lowman³ observed heterogeneous fluid flow phenomena in capillaries. The second was the American Petroleum Institute Research Project 47B at the University of Oklahoma where microscopic studies of dynamic fluid phenomena in synthetic porous matrices have been made by visual observation and cinephotomicrography.⁴ It is with the latter that this paper is concerned, treating the techniques involved and the observations made.

TECHNIQUES

Observation Flow Cells

The observation flow cells formed a focal point in the techniques employed. Essentially, these were matrices composed of a single layer of spheres sandwiched between two flat plates. This design was arrived at after a series of pre-

¹References given at end of paper.
²Manuscript received in the office of the Petroleum Branch, AIME, May 21, 1951. Paper presented at the Petroleum Branch Fall Meeting in Oklahoma City, Okla., Oct. 3-5, 1951.
³The movie film which records studies reported in this paper is available from the offices of Elmer O. Mattocks, American Petroleum Institute, 50 West 50th St., New York, 20, N. Y.

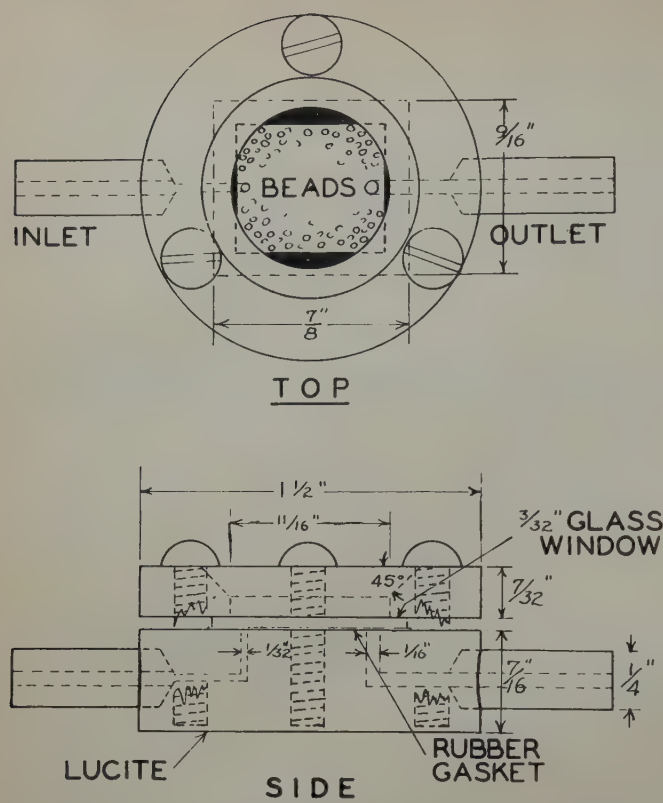


FIG. 1 — TYPE "B" CELL.

liminary investigations. It has been found that in multi-layered cells it was extremely difficult to differentiate one phase from another and the observations of flow phenomena were almost hopelessly complicated. For matrices that were opaque, it was impossible to carry out continuous microscopic observations through the depth of the beds. Thus a single-layered matrix, composed of glass spheres where possible, was decided upon as the structure most likely to produce easily observed flow phenomena despite its highly ideal nature. Flow phenomena established in this way would then provide a basis for further studies in more natural systems.

Two types of flow cells have been used. The first of these is the Type B cell of which a typical example is diagrammed in Fig. 1. The four principal parts of this cell are the base, the compression cover, the observation window and the gasket. The diagram is explicit with regard to the functions of the different components.

The base in all cells of this type was either wholly or principally Lucite. It was prepared from a Lucite cylinder (1 1/2-in. diam. and 7/16 in. height) that was molded from molding powder at 140°C and 3,000 psig. The dimensions and shape, which in turn determined the dimensions and shape of the rest of the cell, were dictated primarily by the more ready availability of the molding equipment involved. In the diagram two ports are shown. These could be changed in number and position at will. Tubing connections were either cemented in as shown or threaded in. In those cases where it was desired to make an all-glass matrix composed of a glass top, glass spheres and a glass base, a glass plate was molded into the Lucite base in a press. This was done by pouring the requisite amount of molding powder over the glass plate in a cylindrical mold and

molding in an hydraulic press at 140°C and 3,000 psig. With the ports drilled in by means of a carbide milling cutter type burr, this plate served as the base for the all-glass cell.

The compression ring, by means of which force was brought to bear against the sealing gasket through the observation window, was made of Lucite as diagrammed or aluminum. The Lucite rings were cut from molded Lucite discs. The aluminum rings were machined and could be prepared slightly thinner. The observation window served as the top wall of the matrix and provided a means for observing the phenomena. It was limited in thickness by the working distance of the microscope objective under which it was to be used. In general, the thicker glass windows were less liable to breakage and buckling than were the thinner ones. For all-Lucite matrices requiring a Lucite top wall, a thin Lucite disc was used backed up by a glass window. In this way the undesirable optical properties of the Lucite were reduced to a minimum and the necessary rigidity was maintained. The gasket was usually cut from rubber commonly found in toy balloons.

Before assembling any of the cells all but one port were first plugged up with 150-mesh screens to keep the spheres from flowing out. Then the gasket was placed in its proper position and covered by the observation window and compression ring. With the components in place, the compression screws were turned down evenly until the cell bed was of the desired depth (0.0075 in.). The spheres used to fill the flow beds were carefully screened so as to be uniform in size (0.007 in.). They were introduced through the free port and packed into place by the use of an air stream, tapping and vibration. In this way single-layered cells closely approximating a rhombic pattern of packing were attained.

The second cell design that found wide use was the Type C cell of which a typical example is shown in Fig. 2. The component parts are quite similar to the corresponding parts in

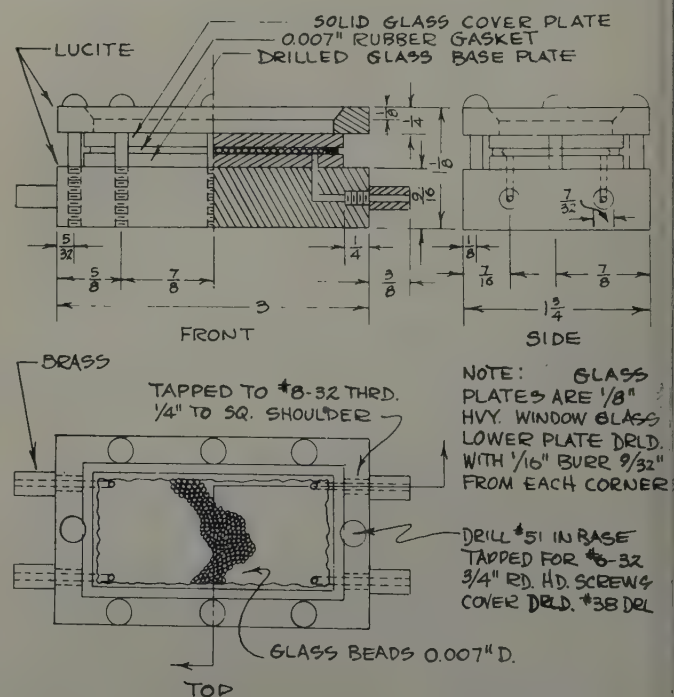


FIG. 2 — TYPE "C" CELL.

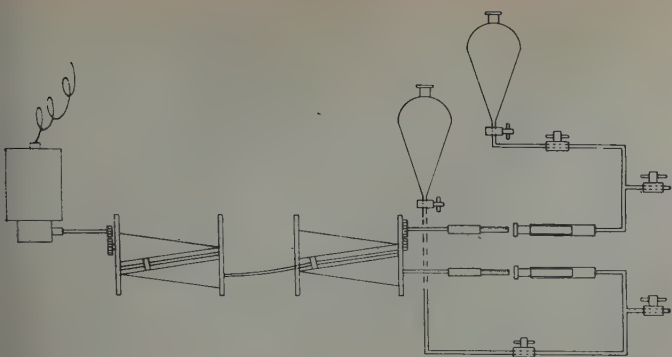


FIG. 3 — PUMPING APPARATUS.

the Type B cell except for shape and size. The greatest difference lay in the structure of the base. In most instances, the base was made in two pieces as indicated in Fig. 2. For all-glass cells aluminum was most often used for the framework holding the inlets and outlets. The other material that found some use was Lucite. With aluminum it was necessary to cut a window to permit the use of transmitted light for the examinations. The Lucite framework could be used in its solid form. For an all-glass cell, the lower plate of the flow bed was simply a plate of glass with holes drilled through it to match those of the inlets and outlets in the framework. Where a sealing aid was required to prevent leakage between the plate and the framework an inert lacquer was used. In those cells requiring a Lucite plate on the bottom of the flow bed, a one-piece solid Lucite base was used.

The gaskets, upper plates and compression frame were functionally the same as with the Type B cell. In addition to rubber, lead foil was used for gaskets in these designs. The cells were assembled and filled with the same spheres and in the same manner as were the Type B cells. The principal advantage offered by this design was a much larger observable flow bed.

Positive displacement pumps provided the means of moving the fluids through the cells. One pumping system was constructed as diagrammed in Fig. 3. With this apparatus, two liquids could be pumped through hypodermic syringes which were activated by micrometer heads. Each micrometer head was rotated by the shaft of one of two cones placed base-to-apex and driven by a common friction pulley. By positioning this pulley along the length between the cones, different flow ratios could be established between the two fluids. The pulley in turn was driven by a motor at the various desired speeds. A second system was composed of Zenith gear pumps, one for each fluid, driven through Revco variable speed reducers.

Since the flow beds were packed with uniformly dimensioned spheres, the cross-sectional pore area available for fluid flow was fairly uniform down the length of the bed. Basing calculations upon this cross sectional area and volume flows, it was estimated that the range of flow velocity lay between 1.5 and 2,000 ft per day.

Cinephotomicrography

Color cinephotomicrography proved itself to be an indispensable tool for studying as well as recording dynamic flow phenomena. A phenomenon on film could be examined in much greater detail than is possible in a single viewing through

the microscope at experimental rates. The apparatus involved consisted of an appropriate microscope and accessories, a 16-mm movie camera, a beam splitter, an arc illuminator and an exposure meter.

The microscope used was a research type microscope with a substage condenser and mechanical stage. The mechanical stage was fitted so as to accommodate the observation flow cells. Objectives with magnifications up to 10X were used in conjunction with eye-pieces of 10X magnification. The stage was kept in a horizontal position and the illumination was reflected by a mirror up through the flow bed lying parallel to the plane of the stage. The techniques for properly aligning the optical illuminating systems for even lighting and undistorted image reproductions may be found in treatises on photomicrography.⁵

A camera that was found adaptable to this work was of the Bell and Howell G.S.A.P. type. This was motor-driven and accommodated a 50-ft, 16-mm film magazine. It was capable of taking pictures at a rate as high as 64 frames per second, but only speeds of 16 and 32 frames per second were employed. The camera was used with and without its lens. A special viewer was built so that the image in the focal plane of the camera could be observed for purposes of synchronization. This was simply an empty magazine fitted with a clear or ground glass in the film aperture, a magnifying glass to enlarge the image and a viewing aperture at the other end. When it was inserted into the magazine chamber with the camera shutter open, the image in the focal plane could be easily seen. The film used was Kodachrome, daylight type.

With this apparatus it was necessary to use a high-intensity source of illumination. A Bausch and Lomb 4.5-amp. a-c carbon arc illuminator was found to be practicable for this purpose. It produced sufficient illumination to take pictures at a speed of 32 frames per second and produced a picture on Kodachrome, daylight type film, free of chromatic aberrations and with good color fidelity. An undesirable feature of this instrument lay in its tendency to flicker and drift despite the spring-wound clockwork used on the carbon-feed mechanism.

A light meter was essential for the estimation of proper light intensities. One based on that of Clemens and Brar⁶ using a phototube in an electronic circuit was employed. The circuit is given in Fig. 4. The phototube was covered with a light shield and fitted with a small window and adapter so that it could be used on the eyepiece of the beam splitter. This instrument is of the balanced circuit type operating on

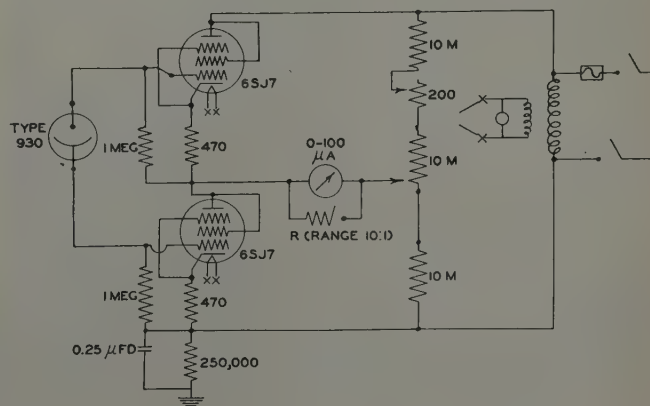


FIG. 4 — WIRING DIAGRAM FOR PHOTOTUBE EXPOSURE METER.

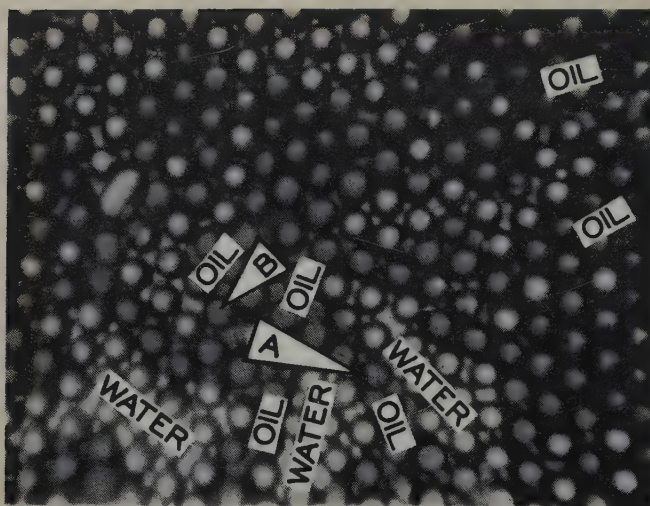


FIG. 5

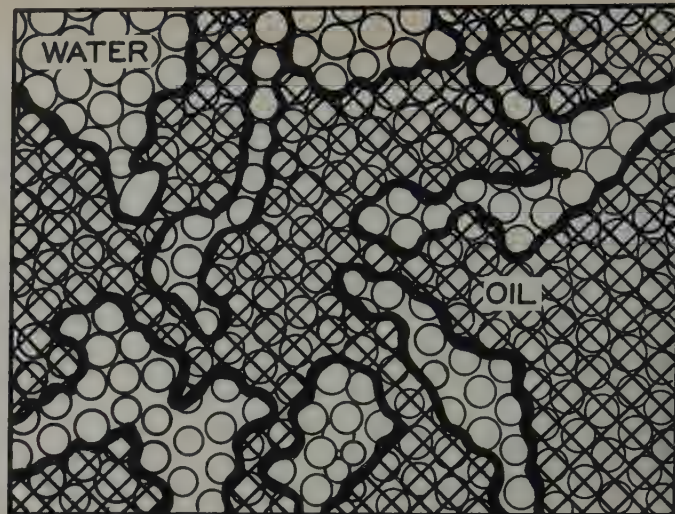


FIG. 5A

a 110-volt, 60-cycle line. The zero point is set by means of the variable resistance and potentiometer. The response follows from the disturbance in the balance caused by the phototube current. Calibration using a G.E. photo light meter as a standard showed the response to be linear with the intensity for a given source of illumination. For use in cinephotomicrography, the exposure meter was calibrated directly against film exposures.

OBSERVATIONS

Channel Flow

Channel flow is the name given to one of the flow regimes observed to prevail under certain conditions of simultaneous two-liquid flow. When water and crude oil (viscosity: 14 cp, specific gravity: 0.9, interfacial tension with water: six dynes/cm) were pumped through the observation flow cells at total velocities up to 1,000 ft per day, they were observed to move in channel flow.

This regime has several characteristics by which it may be described. Each fluid effects transport through its own network of interconnecting channels. The channels might vary in diameter from about one grain diameter to many. They are bound by liquid-liquid interfaces as well as liquid-solid surfaces and meander tortuously through the flow bed. It is probable that with the flow cells described above, each of the two flowing systems was transported through a single continuous network of channels.

For steady flow conditions, the channels maintained fixed geometries and positions throughout the flow bed. No movement was observed at the liquid-liquid interfaces at magnifications as high as 100X. With a change in saturation, the geometries of the channels were altered. An increase in oil saturation with a simultaneous decrease in water saturation was accompanied by a general growth in the diameters of the oil channels and a reduction in those of the water channels. There was a tendency for the channels to hold their posi-

tions in the flow bed. In the case of temporary flow disturbances the flow channels exhibited an elasticity whereby they tended to resume almost their exact starting configurations with the reestablishment of the original steady conditions.

By observing the movement of particles suspended in the flowing fluids, it was seen that the flow within any channel was essentially streamlined in nature. The moving particles delineated smooth lines of flow devoid of eddy currents despite the tortuosities of the channels. This was the type of behavior that was also observed in the flow of homogeneous fluids.

A photomicrograph showing a portion of the channel flow structure established in an observation flow cell is given in Fig. 5.* The oil and water channels are indicated in the photographs. They are distinguishable from each other by a difference in the darknesses occurring on either side of the

*A diagrammatic tracing of the photograph in Fig. 5 is given in Fig. 5A.

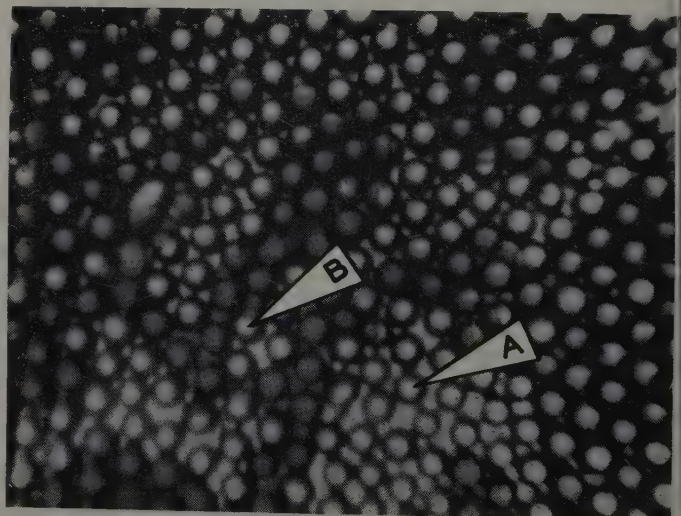


FIG. 6



FIG. 7

oil-water interfaces. This is only that small portion of the flow bed included in the microscopic field. The matrix is an all-glass cell of a single layer of spheres (0.007 in. diam.) and the simultaneously flowing fluids are water and crude oil. The flow velocity of each of the fluids is about 350 ft per day. This phenomenon has been observed in other matrices including all-Lucite cells, glass-Lucite cells, and double-layered cells, as well as with other fluid systems including refined oils and brines with flow velocities ranging from 1.5 to 1,000 ft per day and flow ratios from 1:3 to 3:1.

Slug Flow

With a system composed of an all-glass observation flow cell flowing oil and water at less than 1,000 ft per day as noted above, a channel flow regime prevailed. However, increasing

the total flow rate while keeping the flow ratio constant resulted in a change at some velocity less than 2,000 ft per day to a new flow regime in which slug flow was in evidence. By this it is meant that some of the transport was effected in the form of separate, isolated slugs or globules.

In an all-glass matrix, the oil phase formed the slugs while the water phase remained continuous. Fig. 6 is a photomicrograph of a system under slug flow. This is the same system and the same field shown in Fig. 5. The fluids, however, are flowing at a velocity of about 1,500 ft per day at a 1:1 ratio. To indicate differences in the flow structure two spheres have been labeled A and B respectively in the two figures. It is to be noted that in each case the sphere is under oil in Fig. 5 but not in Fig. 6, indicating that those parts of the oil flow structure have moved or disappeared during the existence of the slug flow regime. This phenomenon has been observed over ratios ranging from 1:3 to 3:1 and in cells of more than one layer of spheres. With an increase in total velocity past the point of slug flow genesis the frequency of slug formation and the number of slugs in the flow bed increased. Characteristic of these systems is the ease with which an oil globule or slug coalesces with another body of oil upon collision.

Flowing the same liquids under the same conditions in all-Lucite matrices, the oil appears as the continuous phase and the water as the slug-forming phase. If water slugs or globules are introduced into an oil stream, they will persist in slug flow resisting coalescence throughout their transport across the flow bed even upon strong collision with other water bodies. A photomicrograph of such a system is given in Fig. 7. The solid matrix is an all-Lucite one composed of a single layer of Lucite spheres (0.007 in. diam.) between two Lucite plates. Arrows indicate moving water globules.

Flooding Phenomena

"Flooding," here, is the term used to describe those systems in which only one fluid is being pumped into the observation flow cell. In an all-glass cell having an arbitrary initial water saturation with oil filling the remainder of the pore volume,

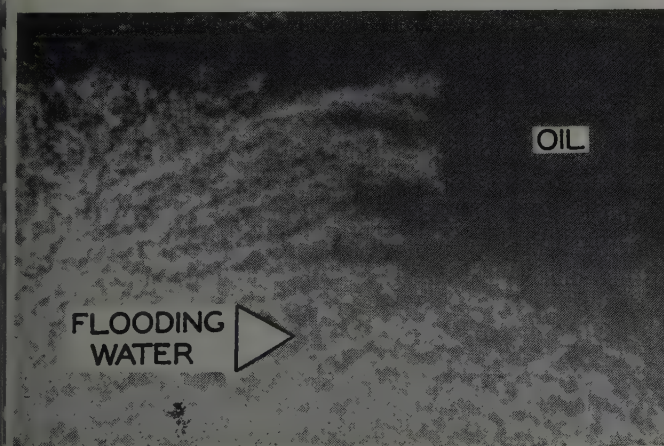


FIG. 8

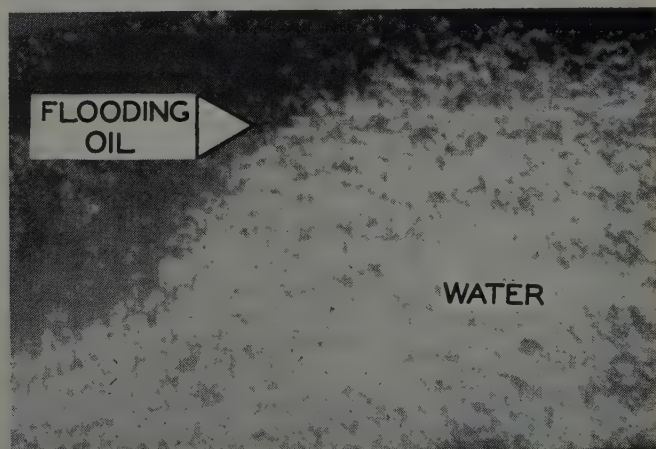


FIG. 9

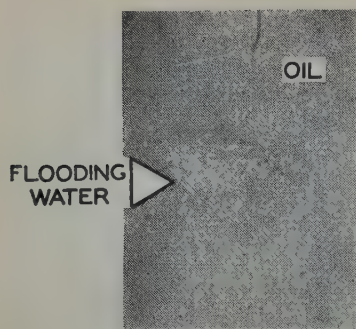


FIG. 10

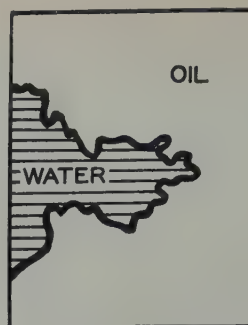


FIG. 10A

flooding with water results in a certain flood-front pattern. A stringy appearance is created by the water as it fingers through the flow bed, by-passing a considerable amount of oil. There is also a tendency for these fingers to branch out in dendritic patterns again by-passing oil.

A flood-front of this sort is shown in Fig. 8. This is a macroscopic view of an all-glass observation flow cell of a single layer. The velocity of water flow is about 1,500 ft per day. The dark areas are those occupied by oil while the light ones are those occupied by the flooding water. An arrow indicates the general direction of flood. The oil involved is the same as that whose properties are given above.

When a water-saturated cell is flooded with oil, a new type of flood-front pattern develops. In this case, the flood-front appears to be a circumferential band around the inlet port. This is seen in Fig. 9 where the system described in Fig. 8 is undergoing a flood by the oil at a velocity of about 1,500 ft per day. In a flood of this type the displacement mechanism appears to be more of a piston-like action with little tendency toward fingering and gross by-passing. It would be expected that this would result in more efficient displacements.

Floods were carried out with the same liquids in all-Lucite flow cells. These were of the same dimensions as the all-glass cells but presented a solid matrix or different surface proper-

ties, the Lucite being preferentially wet by the oil and the glass by the water under the conditions of the experimentation. Despite this difference, similar flood-front patterns developed as with the all-glass flow beds. Figs. 10* and 11 are photographs of a water flood and oil flood respectively in an all-Lucite matrix, both at velocities of about 1,500 ft per day. In all of these floods the transport of fluids took place through continuous phases without any formation of slugs.

Residual Formations

"Residual Formations" refer to those fluid formations left behind a flood front in the matrix of an observation flow cell. In water floods, the most apparent residual oil formations were those large volumes by-passed by the water. Depending upon conditions of flooding and the physical characteristics of the fluid system and porous matrix, these varied from very small to very large portions of the total void volume. They were continuous over many sphere diameters and sometimes over the length of the whole cell.

Almost always, smaller residual oil formations were also found in the flow bed. One form that these took is shown in Fig. 12. In this case the oil formation covering a few spheres has been left behind in flooding an all-glass matrix with water. Apparently held in place by capillary forces, these formations are not displaced by flooding rates as high as 10,000 ft per day. The liquids were the same in properties as those described above.

Another form of residual oil is shown in Fig. 13. This is a free spherical globule, usually no larger than a sphere of the matrix, occupying an insular region between the spheres. One of the interesting characteristics of these is that they are subject to rotation in place during water flooding. Such rotation has been observed in globules that were not entirely free but attached to some solid surface in the matrix. For a given globule, the rotation was always in the same direction even

*A diagrammatic tracing of the photograph in Fig. 10 is given in Fig. 10A.

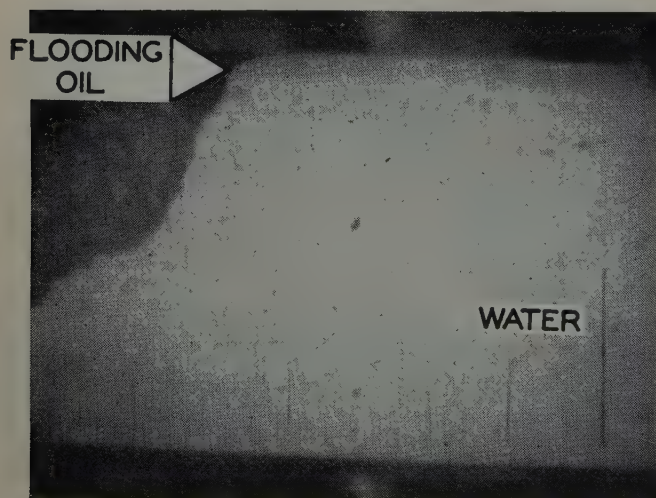


FIG. 11

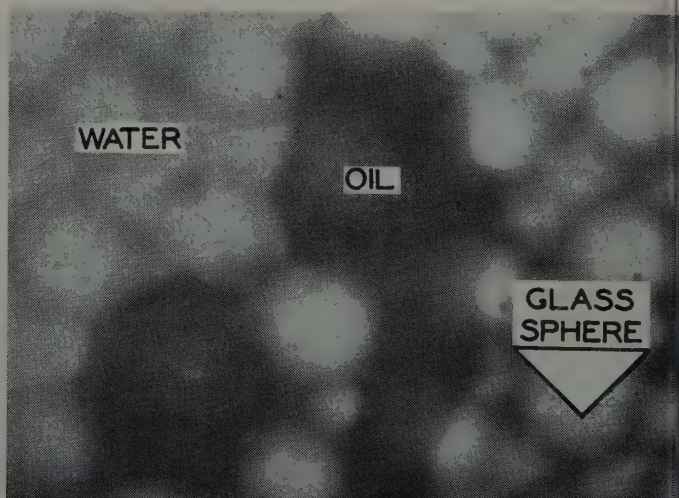


FIG. 12

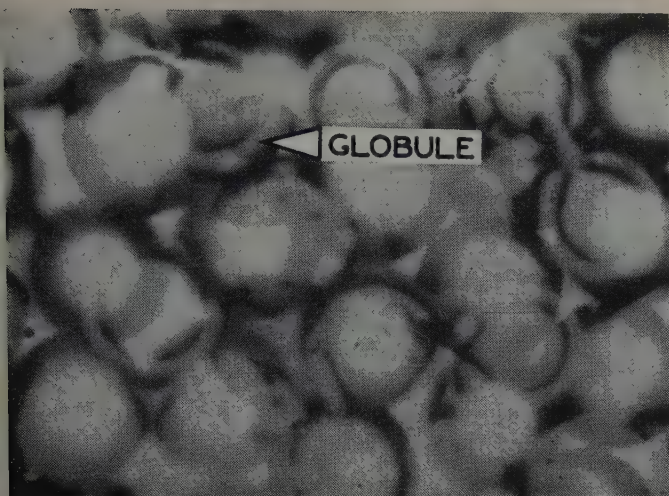


FIG. 13

with intermittent water flooding. While a larger flooding velocity produced a higher speed of rotation, the velocity of the rotating globule appeared to be somewhat smaller than that of the flooding water. Some of the residual oil also remained behind in similar globules, smaller than the spheres of the matrix, which were attached to surfaces in the funicular regions and in which rotational movement was not observed.

In all-glass flow cells accommodating oil and water as described above, the predominating formation for the residual water was that of pendular rings. Most clearly observed were those that formed between the horizontal plates and the spheres of the flow matrix. However, they were found to form in a perpendicular plane between the spheres as well. Fig. 14 shows the intermediate step in the form of a "figure 8" as well as the final pendular rings formed during an oil flood. By suspending fine oil globules in the water phase, rotational movement has been observed in these pendular formations during flooding by oil.

In displacing water by oil in an all-Lucite flow cell, residual water remained behind as globules in the funicular regions rather than as pendular rings. Fig. 15 is a photograph of such formations in a single-layered Lucite matrix. These residual water formations were similar to some of the residual oil formations in all-glass cells during water floods.

DISCUSSION

These studies were, for the greatest part, exploratory in examining the possibilities of the visual approach in the investigation of microscopic mechanisms for fluid behavior in porous media. It is evident that with the development of the necessary techniques this approach is applicable to experimental systems which are somewhat idealized. Within such systems, as against more natural systems, some phenomena can be examined with considerable clarity and thoroughness leading to the eventual establishment of flow mechanisms for these particular systems. The most obvious idealizations are the single (or double) layer, the regular and uniform solid

matrix, the use of flat plates in the flow bed and the use of processed fluids. Thereby, probable mechanisms are arrived at for natural systems which will grow in significance with the extension of investigations into systems more truly representative of petroleum reservoirs. Studies such as those described in this paper indicate a direction for such experimentation and further simplify the problem in providing definite phenomena to look for.

Channel flow as observed in the observation flow cells is consistent with developments in other directions. Rapoport and Leas⁷ arrived at mathematical expressions defining the limits of liquid relative permeability in a liquid-gas system based on the postulation that the flow regime is that of channel flow or "parallel flow" as they term it. Comparing experimental data with theory they find satisfactory agreement.

In a paper by Geffen, Owens, Parrish and Morse⁸ two points are of interest in this connection. Their saturation profiles for any one oil-water flowing ratio are different for different pressure gradients. However, the shapes of the profiles for all the pressure gradients are generally similar for the one flowing ratio. The second point involves the effect of saturation history upon relative permeabilities. They find that at a given saturation of brine, for example in an oil-brine system, the oil relative permeability curve is reversible with higher brine saturations. Upon reducing the brine to some lower value a new curve is arrived at which again is reversible but different from the previous curve. This hysteresis effect and the saturation profile variations may both be explained on the basis of a channel flow regime.

Wilson, Calhoun, and Chatenever⁹ have found visual evidences of channel flow in synthetic cores. Flowing glycerine and melted paraffin through consolidated salt cores, and solidifying the wax, they found a flow structure composed of a network of interconnecting channels.

It is difficult to evaluate the significance of slug flow without additional data. The important factor in the genesis of slug flow is probably capillary pressure rather than velocity of flow. Further work is required in order to be able to estimate that portion of total flow that might be in the form of slug flow. It is indicated that in phases that tend to coalesce easily the slug flow regime will be less prevalent than in those where

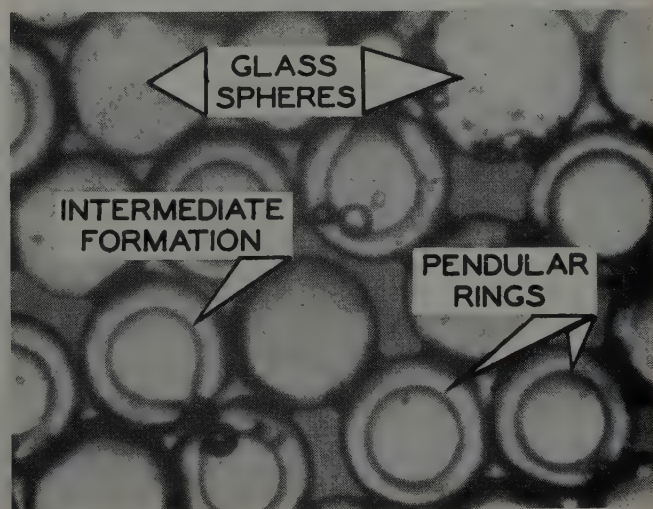


FIG. 14

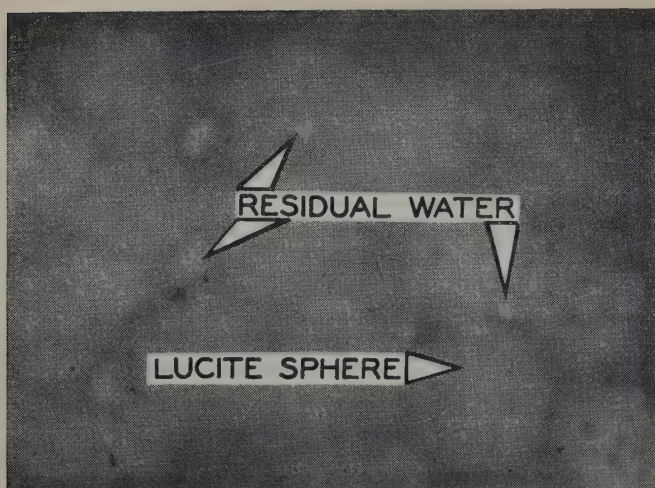


FIG. 15

there is a strong tendency not to coalesce. It is possible that this mode of fluid transport might have a bearing upon displacement phenomena as well as flow behavior. Thus, where by-passing is usually thought of in terms of sidetracking, a mechanism is introduced here in which a fluid may be by-passed by another flowing through it in globules or bubbles.

Of the flood-front patterns noticed in the flooding experiments, it would be expected that floods subject to the fingering mechanism would not be as efficient as those with regular linear fronts. It would be expected, too, that ultimate recoveries in the former case would be less although the relationships here are more subtle. As a consequence of the similarity of flooding behavior in glass and Lucite systems, preferably wet by water and oil respectively, it appears on the basis of these limited investigations that the wettability properties of the solid matrix may have relatively little effect upon the flood-front pattern. As a consequence of this, surface tension effects on flooding behavior might be relegated to a minor role. One relationship that suggests itself strongly in this connection is the ratio between the viscosities of the displaced and the displacing fluids. It is pertinent that flood-front characteristics have been studied here only over the length of a small observation cell; and it is possible that further ramifications may develop in cells of larger dimensions.

Most of the interest in residual oil formations derives from a desire to avoid them or, having formed them, to displace them. Again, it is as yet difficult to determine on the basis of these studies the relative importance of the various formations discussed. However, there are suggestions that any process that would favor the establishment of more numerous channels of flooding water would also favor smaller residual oil formations. It appears as if those that are given to rotation are probably the most difficult to displace by purely physical means. For those that are held in place primarily because of capillary forces, it would be expected that surface tension lowering agents would be efficacious in aiding displacement. Unlike the conditions attending flood-front phenomena, the wettability of the solid matrix is of definite consequence in

residual formations. Thus in an all-glass water-wet cell none of the residual oil finds itself in the pendular regions. On the other hand, pendular rings are the most prevalent residual water formations in a matrix of this sort. This would be expected on the basis of Leverett's¹⁰ work on capillary behavior. The movements within the pendular rings are noteworthy, as are those of the rotating oil globules in that they might have some bearing upon the dissipation of reservoir energies.

It is important to realize that the observations under discussion have been carried out in only a limited number of artificial systems. It is necessary, therefore, that the conclusions arrived at be confirmed by more extensive investigations before they are applied to natural petroleum reservoirs. One particular point that requires clarification, for example, is the apparent importance of surface tension in residual formations and the apparent lack of significance of this property in flood-front patterns. Current researches have already indicated significant possibilities and it is hoped that more work in this connection will be forthcoming.

ACKNOWLEDGMENT

The authors are grateful to the American Petroleum Institute for the support making this work possible and permission for its publication.

REFERENCES

1. Nuss, W. F., and Whiting, R. L.: "Technique for Reproducing Rock Pore Space," *AAPG Bulletin*, Nov., 1947.
2. Schaefer, W.: "Limestone Pore Space Study," a movie produced by the laboratories of Stanolind Oil and Gas Co., presented before Petroleum Division, AIME, Dallas, Tex., October, 1948.
3. Lowman, Q.: "Microscopic Studies of Capillary Flow," a film produced by the Petroleum and Natural Gas Department, The Pennsylvania State College, August, 1950.
4. Calhoun, J. C., and Chatenever, A.: "Microscopic Behavior of Heterogeneous Fluids in Porous Media," a series of films presented before annual American Petroleum Institute Meetings in Chicago, Ill., November, 1949; and Los Angeles, Calif., November, 1950.
5. "Photomicrography," Eastman Kodak Co., Rochester, N. Y., (1944).
6. Clemens and Brar: "Exposure Meter for Photography," A.E.D.D.-2271, Technical Information Branch, Oak Ridge, Tenn., AEC, Oak Ridge, Tenn., (1948).
7. Rapoport, L. A., and Leas, W. J.: "Relative Permeability to Liquid in Liquid-Gas Systems," *Trans. AIME*, (1951) 192, 83.
8. Geffen, T. M., Owens, W. W., Parrish, J. R., and Morse, R. A.: "Experimental Investigation of Factors Affecting Laboratory Relative Permeability Measurements," *Trans. AIME*, (1951) 192, 99.
9. Wilson, D. A., Calhoun, J. C., and Chatenever, A.: "A Visual Examination of Fluid Saturations in a Porous Medium," to be published.
10. Leverett, M. C.: "Capillary Behavior in Porous Solids," *Trans. AIME*, (1941) 142, 152.

★ ★ ★

DRILLING FLUID FILTER LOSS AT HIGH TEMPERATURES AND PRESSURES

F. W. SCHREMP AND V. L. JOHNSON, CALIFORNIA RESEARCH CORP., LA HABRA, CALIF.

ABSTRACT

This paper discusses the results obtained from high temperature, high pressure filter loss studies in which field samples of clay-water, emulsion, and oil base fluids were used. High temperature, high pressure tests of some premium priced emulsion and oil base drilling fluids show filter loss peculiarities that are not predicted by standard API tests. It is recommended that high temperature, high pressure filter loss tests be used to evaluate the performance of such fluids.

Apparatus is described which proved to be satisfactory for evaluating filter loss behavior over a wide range of temperatures and pressures.

INTRODUCTION

The petroleum industry spends large sums of money each year on chemical treating agents for lowering filter loss and on premium-priced low filter loss drilling fluids.

While it is an accepted fact that low filter loss is advantageous during drilling operations, it is questionable whether the present standard method of determining filter loss gives a reliable indication of the loss to be expected under bottom hole conditions. The purpose of this paper is to show that high temperature, high pressure filter loss tests should be used to evaluate filter loss behavior of fluids for deep drilling.

Concern over possible effects of filter loss on oil well drilling and well productivity dates back to the early 1920's. During the years 1922 to 1924, filtration studies were reported by Knapp,¹ Anderson² and Kirwan.³ These studies were the first to be reported in the literature on this subject. No further information was published on the subject until 1932 when Rubel⁴ presented a paper in which he discussed the effect of drilling fluids on oil well productivity.

In 1935, Jones and Babson⁵ constructed the first laboratory tester designed to study the effects of temperature and pressure on the filter loss behavior of clay-water drilling fluids. In a discussion of their investigations, Jones and Babson⁵ stated, "Performance characteristics of a mud can be evaluated with considerable reliability by a single test at 2,000 psi and 200°F. Exact correlation between the results of performance tests made under these conditions and the behavior of muds in actual drilling operations is of course impossible." Jones and Babson apparently were well aware that at best laboratory tests can give only qualitative answers to the question of what is the actual behavior of a drilling fluid when subjected to deep drilling conditions. Jones⁶ presented a paper in 1937 in which he described a static filter loss tester to be used for

routine filter loss tests. This instrument subsequently was adopted as the standard API filter loss tester.

In 1938, Larsen⁷ developed a relationship between filtrate volume and filtrate time that is in general acceptance today. Larsen was cognizant of the danger of estimating bottom hole behavior from filter loss measurements at room temperature. He tried to predict the effect of temperature on filter loss by relating temperature effects through the temperature dependence of filtrate viscosity. This was undoubtedly an oversimplification of the temperature dependence of drilling fluid filter loss.

In 1940, Byck⁸ published a summary of experimental results of filter loss tests made on six representative California clay-water drilling fluids. He concluded that "no existing method will permit even an approximate determination of the filtration rate at high temperature from data at room temperature. It is necessary to measure filtration at the temperature actually anticipated in the well, or to make a sufficient number of tests at various lower temperatures so that a small extrapolation of these data to the anticipated well temperature may be applied."

Byck's findings were presumably well accepted and recognized by drilling fluid technologists, and yet, they did not lead to wide adoption of high temperature drilling fluid filtration equipment. This is evidenced by the fact that no additional information has appeared in print on the subject since 1940.

Study of Byck's data shows that there was a useful consistency in them. The fluids did not show predictable losses at high temperatures, but they did line up at high temperatures in approximately the same order that they lined up at low temperatures. That is, if a fluid appeared to be a good fluid with relatively low loss at low temperatures, it would also be a good fluid with relatively low loss at high temperatures.

In the last decade, the above situation has changed. The drilling fluid art is markedly different from what it was. The outstanding change, as far as the present discussion is concerned, has been the adoption of wholly new types of drilling fluids. Oil base and emulsion drilling fluids have come into wide use. It is, therefore, necessary to re-examine previously satisfactory generalizations to see if they are still valid.

It turns out, as might have been expected, that Byck's explicit generalization, already quoted, is still true. Filter losses at high temperatures cannot be predicted from filter losses at low temperatures. However, no further generalizations are valid now. Fluids of different chemical types show different general behaviors. No longer do the fluids line up approximately the same at high temperatures as they do at low temperatures. They may line up entirely differently. Special fluids exhibiting very low loss at low temperatures may have losses as high as those of ordinary clay-water fluids at high temperatures. This fact is highly significant, because premium prices are being paid for the special fluids.

¹References given at end of paper.

Manuscript received in the Petroleum Branch office Oct. 4, 1951. Paper presented at the Fall Meeting of the Petroleum Branch in Los Angeles, Calif., Oct. 25-26, 1951.

The new types of fluids have invalidated the old generalizations, and it now seems time to urge (or urge again) that high temperature, high pressure filter testing methods be adopted throughout the drilling industry.

It is perhaps still true that the standard API filter test constitutes a good method for control of a single fluid in the field. As far as we know, it is still good practice to assume that when the surface-measured filter loss is going up, the bottom-hole loss is going up, and when chemical treatment lowers the surface-measured loss, the bottom-hole loss is lowered.

The thesis of this paper is that conventional filter tests are not satisfactory for comparisons of *different* fluids, particularly, if those fluids are of different types. The following sections describe apparatus and methods used to obtain high temperature, high pressure filter loss data. Experimental data are given from 141 tests of 18 different fluids.

APPARATUS

Apparatus used for determination of high temperature, high pressure filter loss behavior is pictured in Fig. 1. The apparatus consists of two identical filter units, each unit being a

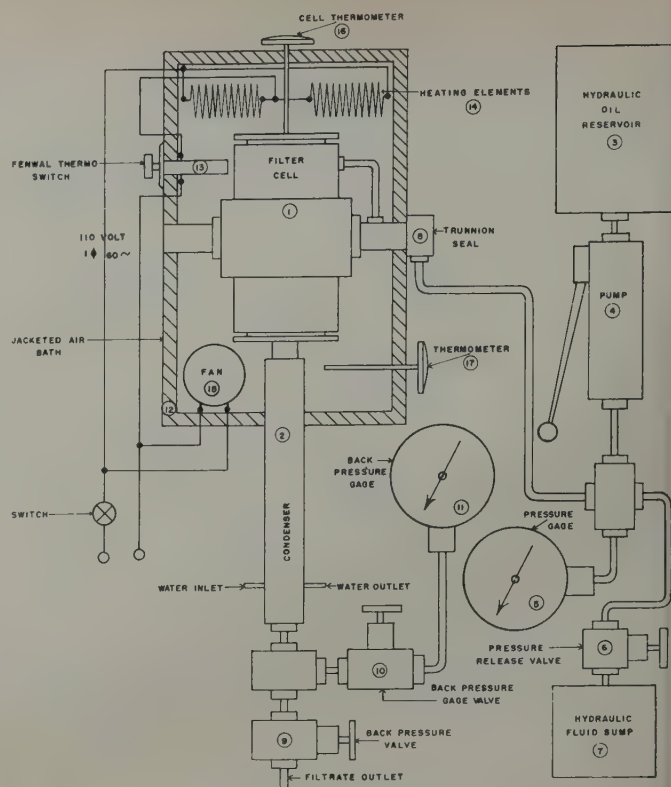


FIG. 2 — SCHEMATIC DIAGRAM OF HIGH TEMPERATURE, HIGH PRESSURE FILTER LOSS UNIT.

complete test instrument with individual temperature and pressure controls. Fig. 2 is a schematic diagram showing the essential features of one of the units.

The filter cell (1) shown in Fig. 2 consists of a cylindrical shell pivoted on trunnions in such a fashion that either end of the shell is accessible for attachment of other parts and for cleaning. Each end of the shell is threaded so that top and bottom plate assemblies may be fastened to the shell. The bottom plate, which is the filter plate assembly* is held in position inside the cylindrical shell by a threaded clamp ring. The top plate is held in position inside the cylindrical shell by a threaded clamp ring which is an integral part of the top plate. Both the filter plate and the top plate are fitted with O-rings that act as pressure seals.

A removable condenser (2) is attached to the bottom side of the filter plate assembly. The condenser is necessary to prevent filtrate vaporization when tests are made at high temperatures.

The pressure system consists of a hydraulic fluid reservoir (3), a hand-operated hydraulic pump (4), a pressure gauge (5), a pressure release valve (6), and a hydraulic fluid sump (7). These items are connected by pressure tubing as shown.

In normal operations, hydraulic fluid (white oil) is pumped from the reservoir (3) through a trunnion seal (8) into the filter cell (1). Fluid enters the filter cell through the wall of the cylindrical shell at a point directly below the top plate assembly. Pressure is indicated by pressure gauge (5). Pressure may be released by opening valve (6), which allows the pressured hydraulic fluid to escape into the fluid sump (7). Pressures up to 5,000 psi can be maintained in routine tests.

Associated with the hydraulic system is the back pressure system, which is attached to the bottom end of the condenser

*Patent applied for, licensed to Oil Base, Inc., Compton, Calif.

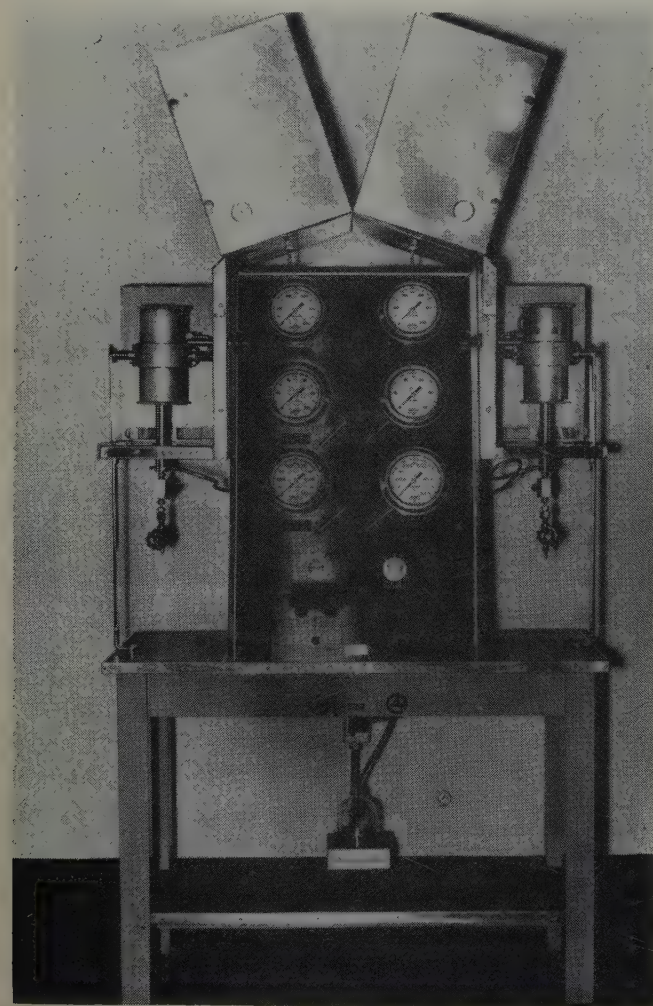


FIG. 1 — APPARATUS FOR DETERMINING HIGH TEMPERATURE, HIGH PRESSURE FILTER LOSS BEHAVIOR.

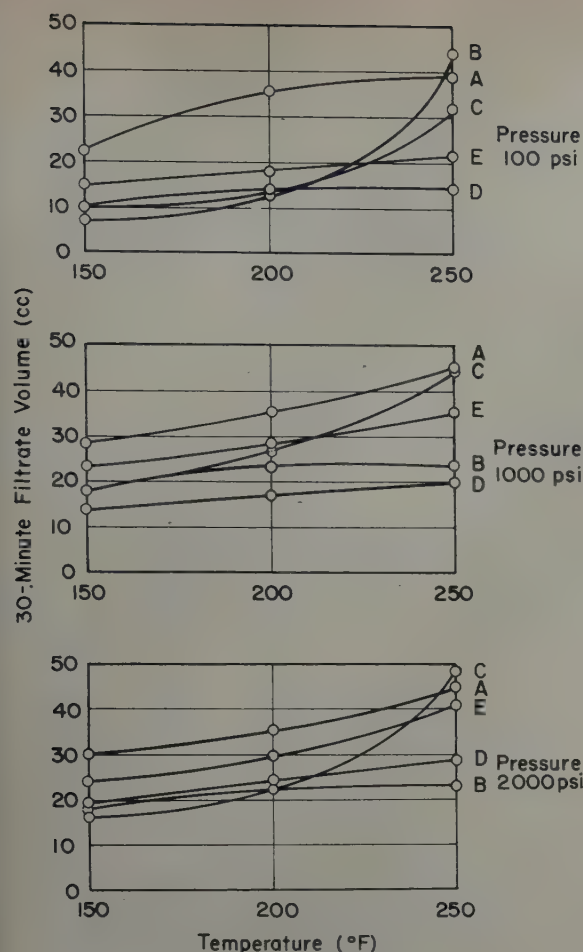


FIG. 3 — EFFECT OF TEMPERATURE ON FILTER LOSS OF CLAY-WATER FLUIDS.

(2). The back pressure system consists of a back pressure valve (9), a back pressure gauge valve (10), and a back pressure gauge (11), all of which are connected by pressure tubing as shown. Back pressure is regulated by operation of valve (9).

The filter cell (1) and the upper end of the condenser (2) are enclosed in an insulated, thermostatic air bath (12). Temperature is controlled by a Fenwal thermostatic switch (13), fin-type electric heating elements (14) and a circulating fan (15). Filter cell and thermostat temperatures are measured with Weston dial thermometers (16) and (17) respectively. Temperature may be controlled from room temperature to 350°F.

EXPERIMENTAL METHOD

Prior to using the cell for test purposes, the bottom plate assembly, consisting of the filter plate and condenser, is flooded with liquid to make filtrate hold-up negligible. As a result, filtrate errors never exceed 1 cu cm. Water is used to flood the assembly for clay-water and emulsion fluid tests, and oil is used for oil base fluid tests. Flooding is accomplished by attaching a fluid reservoir to the lower end of the condenser. Once the assembly is filled, the back pressure valve (9) is closed and the fluid reservoir is disconnected from the end of the condenser. Excess fluid is wiped from the filter plate surface. Two sheets of fluid-saturated Whatman No. 50 filter paper are placed on top of the filter plate and are held in place by a clamp ring. After the bottom plate assembly is

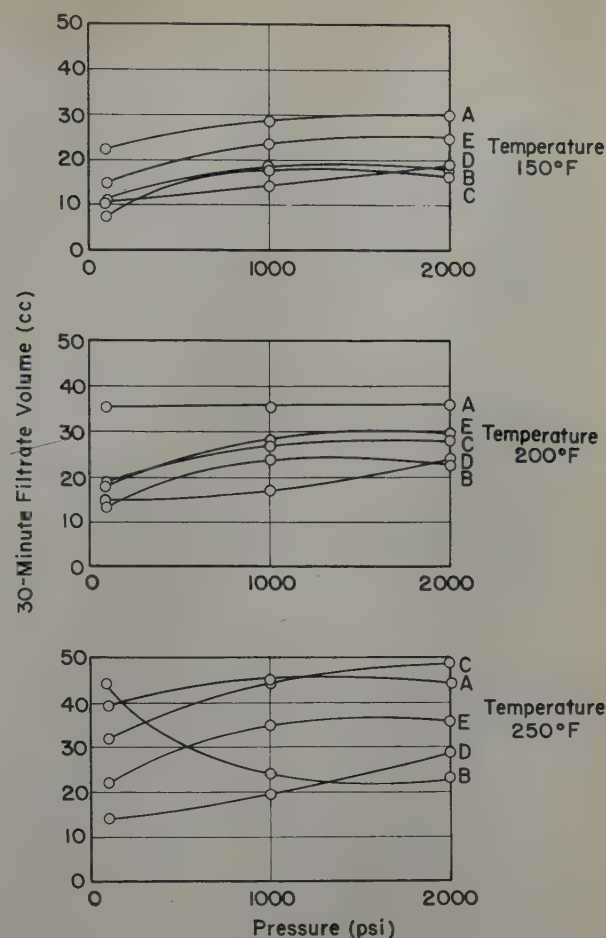


FIG. 4 — EFFECT OF PRESSURE ON FILTER LOSS OF CLAY-WATER FLUIDS.

flooded and the filter paper is clamped to the upper surface of the filter plate, the assembly is locked in position inside the filter cell cylindrical shell by the lower clamp ring. Drilling fluid now may be poured into the cell.

After the drilling fluid sample is mixed for 30 minutes, approximately 425 cu cm of the sample are poured into the filter cell. The remaining free space above the sample is filled with hydraulic fluid (white oil) and the cell is closed. The air thermostat (12) is closed and thermometers (16) and (17) are inserted in their proper locations. Pressure is applied to the cell by use of hydraulic pump (4) until the desired pressure is reached. Fenwal thermostatic switch (13) is set to the desired temperature and heating elements (14) are turned on. A rotary selector switch (not shown) controls the rate of heating by selecting the proper combination of heating elements. Pressure is maintained constant during the heating interval. Water is circulated through the condenser jacket. Once the desired temperature is reached, the back pressure valve (9) is opened sufficiently to develop the desired differential pressure across the filter cake. Filtrate is collected in a graduated cylinder which has been placed beneath the end of the condenser. Filtration time is recorded from the instant the back pressure valve (9) is opened. Pressure is maintained constant throughout the test. When the test is completed, pressure release valve (6) is opened and heating elements (14) are shut off. The filter cell is allowed to cool before it is opened for filter cake inspection and cleaning.

Filter loss is determined by the quantity of filtrate collected in 30 minutes. Occasionally the 30-minute reading is incorrect

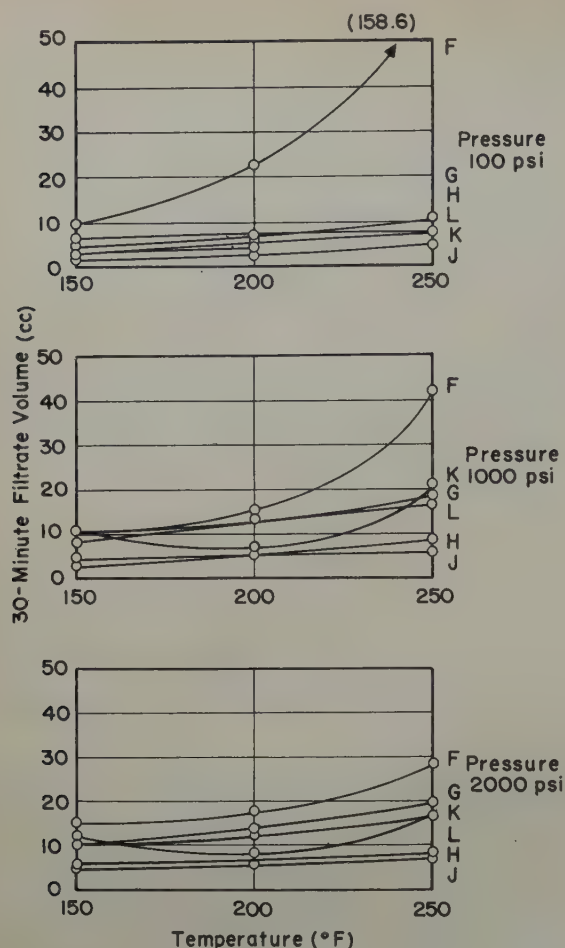


FIG. 5—EFFECT OF TEMPERATURE ON FILTER LOSS OF EMULSION FLUIDS.

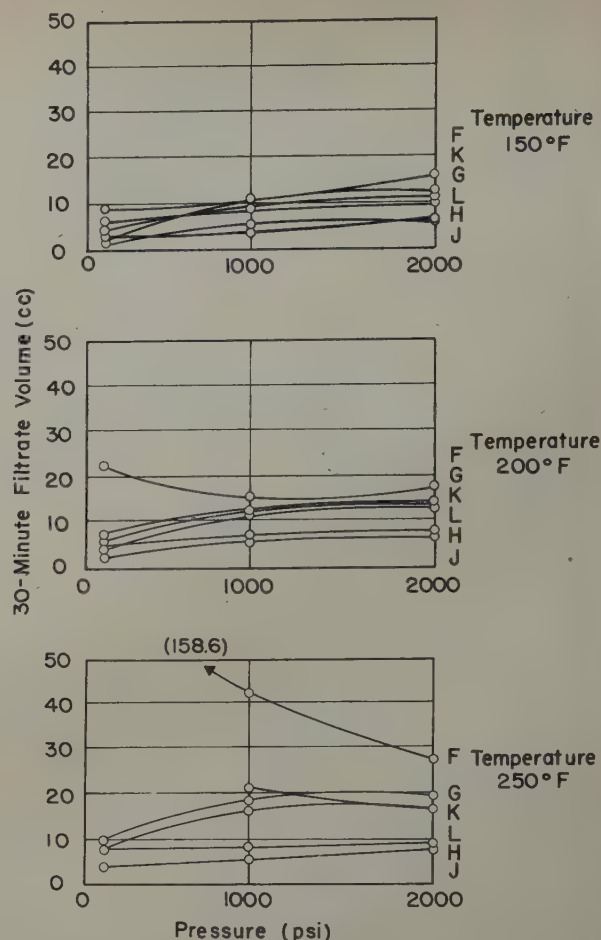


FIG. 6—EFFECT OF PRESSURE ON FILTER LOSS OF EMULSION FLUIDS.

because of minor variations in flooding the bottom plate assembly. The magnitude of the error may be determined by extrapolating the filtrate-volume-*vs*-square-root-of-time curve to zero time. The intercept on the filtrate volume coordinate is a measure of the correction which must be applied to the 30-minute reading. This correction is never greater than 1 cu cm.

EXPERIMENTAL RESULTS

Filtration behavior of drilling fluids is influenced largely by the kind, concentration, and particle size of solids present in the fluids. Filtration rates are influenced by the dispersion of particles in the fluids, the hydration of the particles, the presence or absence of hydrated colloidal materials, and the presence or absence of dispersing or agglomerating chemicals.

Two steps involved in the process of filtration are (1) bridging of openings in the filter medium and (2) filtering of fluid through the filter cake that develops on the filter medium as filtration takes place. Drilling fluids which do not contain finely divided minerals will be unable to bridge the openings in filter media and will have poor filter loss properties. Of the three kinds of drilling fluids, clay-water, emulsion, and oil base; oil base drilling fluids are most likely to show poor filter loss behavior unless they have been used in a drilling well for sufficient time to acquire mineral fines. All drilling fluid samples used in this investigation were taken from drilling wells that had been drilling for considerable time.

Filter loss tests were made at 150, 200, and 250°F, and at differential pressures of 100, 1,000, and 2,000 psi. Differential

pressures were used because independent tests showed that drilling fluid filter loss behavior is dependent more on differential pressure than on total pressure.

Clay-Water Drilling Fluids

Five different clay-water drilling fluids were tested. Table I presents the filter loss data obtained for each fluid. The data are plotted as filtrate volume *vs* temperature curves in Fig. 3 and as filtrate volume *vs* pressure curves in Fig. 4.

Examination of Fig. 3 shows that, at constant pressure, filter loss increases with increasing temperature. The change in filter loss with increasing temperature is non-linear and, in general, is different for each fluid tested. Fig. 4 shows that the effect of pressure on filter loss is unpredictable. At 150

Table I—Filter Loss Behavior of Clay-Water Drilling Fluids

Temp. °F	Pressure psi	30-Minute Filtrate Volume (cu cm)				
		A	B	C	D	E
150	100	22.6	7.5	11.6	10.8	15.0
	1,000	28.4	18.2	17.8	14.2	23.4
	2,000	30.0	18.2	17.0	19.0	24.4
200	100	35.6	13.0	18.8	14.0	18.0
	1,000	35.6	23.6	27.4	16.8	28.4
	2,000	35.6	22.6	28.0	23.6	29.2
250	100	39.0	44.4	32.2	14.0	22.0
	1,000	45.0	23.6	44.6	19.8	35.2
	2,000	44.6	23.0	48.4	28.6	35.6

Table II—Filter Loss Behavior of Emulsion Drilling Fluids

Temp. °F	Pressure psi	30-Minute Filtrate Volume (cu cm)					
		F	G	H	J	K	L
150	100	9.3	4.4	4.0	2.0	2.5	6.2
	1,000	11.2	10.2	4.2	4.8	11.0	8.4
	2,000	15.6	10.4	5.8	5.4	12.6	9.8
200	100	22.8	6.0	5.0	2.8	4.2	7.2
	1,000	15.2	13.2	6.8	5.6	7.4	12.8
	2,000	17.6	13.8	7.4	6.4	7.8	12.6
250	100	158.6	10.2	8.2	4.0	—	7.7
	1,000	42.0	18.4	8.4	6.2	20.8	16.4
	2,000	27.8	19.4	8.6	7.6	16.6	16.6

Table III—Filter Loss Behavior of Oil Base Drilling Fluids

Temp. °F	Pressure psi	30-Minute Filtrate Volume (cu cm)						
		M	N	O	P	Q	R	S
150	100	8.6	0.4	0.5	1.0	1.4	0.0	0.0
	1,000	8.0	0.9	0.7	—	—	—	—
	2,000	7.6	1.0	1.0	—	—	—	—
200	100	16.4	0.9	0.6	—	—	—	—
	1,000	14.8	2.2	0.8	—	—	—	—
	2,000	28.2	2.4	1.3	—	—	—	—
250	100	43.2	1.2	4.4	—	—	—	—
	1,000	125.6	2.5	1.8	—	—	—	—
	2,000	175.4	2.7	1.6	—	—	—	—
300	2,425	—	—	—	1.7	4.6	8.6	232.0

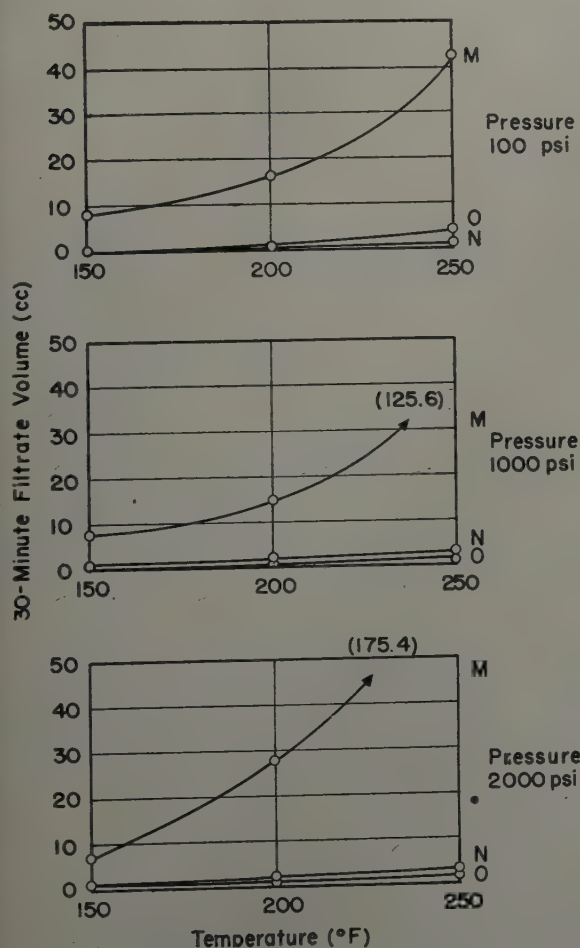


FIG. 7—EFFECT OF TEMPERATURE ON FILTER LOSS OF OIL BASE FLUIDS.

and 200°F there is a tendency for filter loss to increase with increasing pressure, but at 250°F both increases and decreases in filter loss can be observed with increasing pressure.

Emulsion Drilling Fluids

Six emulsion drilling fluids were tested. Experimental data are presented in Table II. The data are plotted as filtrate volume *vs* temperature curves in Fig. 5 and as filtrate volume *vs* pressure curves in Fig. 6.

Examination of Fig. 5 shows that filter loss, measured at constant pressure, increases with increasing temperature. Fig. 6 shows that pressure effect on filter loss behavior is unpredictable.

Comparison of the filter loss behavior of clay-water and emulsion fluids shows that in many instances emulsion fluids break down at high temperatures and pressures. They then exhibit filter loss properties that are no better than those of ordinary clay-water fluids. This comparison shows the need for more complete testing of premium priced fluids. Apparently filter loss behavior cannot be predicted from a single low temperature, low pressure filter loss measurement.

Oil Base Drilling Fluids

Three oil base drilling fluids were tested at 100, 1,000, and 2,000 psi, and 150, 200, and 250°F. Four additional samples were tested at 100 and 2,425 psi, and 150 and 300°F. Experimental data are presented in Table III. The data obtained from tests of the first three samples are plotted as filtrate volume *vs* temperature curves in Fig. 7, and as filtrate volume

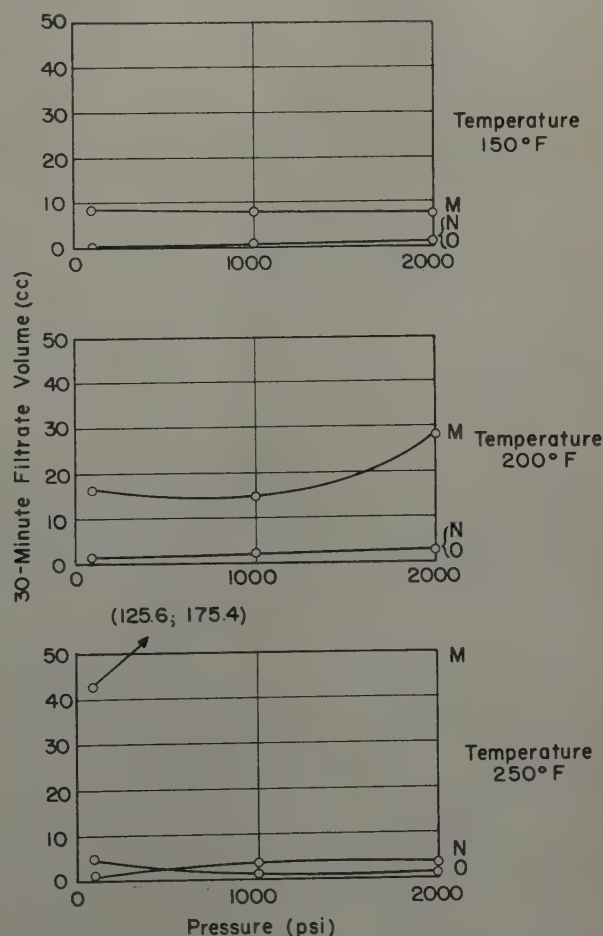


FIG. 8—EFFECT OF PRESSURE ON FILTER LOSS OF OIL BASE FLUIDS.

vs pressure curves in Fig. 8. Data obtained from tests of the four additional field samples are plotted as filtrate volume vs temperature curves in Fig. 9.

Examination of Fig. 7 shows that filter loss increases with increasing temperature at constant pressure. Fig. 8 shows that pressure effects on filter loss behavior are unpredictable. Fig. 9 compares the filter loss behavior of four fluids tested at 100 and 2,425 psi, and 150 and 300°F. The curves show that filter loss increases with increasing temperature. The curves also show that fluid S, a premium-priced fluid, apparently has unusually low filter loss in standard tests and that it breaks down completely at high temperature and pressure; in fact, the filter loss of fluid S at high temperature and pressure is greater than that of the poorest clay-water fluid examined in these tests.

Comparison is made in Fig. 10 between the filter loss behaviors of an ordinary clay-water drilling fluid, as represented by fluid D, and of selected emulsion fluids. Examination of Fig. 10 shows that two emulsion fluids, F and K, exhibit filter losses at high temperatures and pressures which are as great or greater than the filter loss shown by the clay-water fluid, D. The behavior of a satisfactory emulsion fluid is shown for comparison.

Failure of some premium priced emulsion and oil base drilling fluids to maintain satisfactory filter loss values at high temperatures and pressures demonstrates clearly the necessity for making filter loss tests under conditions which simulate those actually encountered in deep drilling.

CONCLUSIONS

1. Bottom-hole filter loss behavior cannot be predicted from measurements at surface temperatures in the standard API tester.

2. The standard test may serve well to control the behavior of a single fluid in the field. It may be assumed that when the standard API filter loss is lowered, the bottom hole filter loss is lowered. But confident comparisons between different fluids cannot be made.

3. Some premium-priced fluids, which in the standard test appear to have unusually low filter losses, actually have as high losses as ordinary clay-water fluids under bottom-hole conditions.

4. Comparisons between the filter losses of different drilling fluids should be made at temperature and pressures approximating those under which the fluids will be used.

REFERENCES

1. Knapp, A.: "Action of Mud-laden Fluids in Wells," *Trans. AIME*, (1923) 1076. (Also *Mining and Metallurgy*, Dec. 1922.)

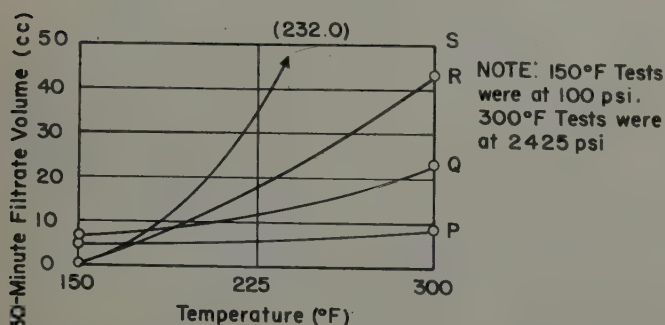


FIG. 9—EFFECT OF TEMPERATURE ON FILTER LOSS OF OIL BASE FLUIDS.

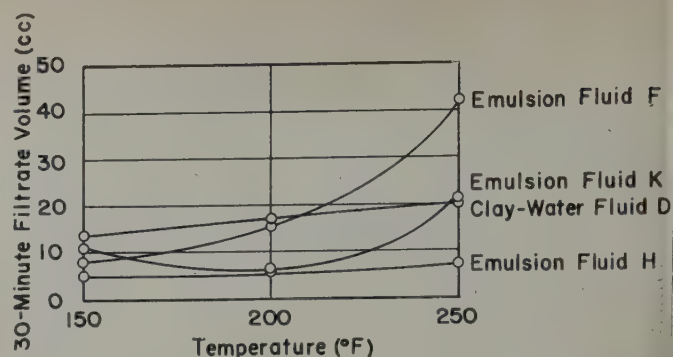


FIG. 10—FILTER LOSS BEHAVIOR OF CLAY-WATER AND EMULSION DRILLING FLUIDS AT 1,000 PSI.

2. Anderson, H. H., in Burrell, L., Gaylord, E. G., Wagye, E. W., Case, J. B., Barnes, R. M., and Parsons, B. E.: "Committee Report to State Oil and Gas Supervisor, Summary of Operations, California Oil Fields," (1923) 8, (7) 60. Cf. ref. 4, 34.
3. Kirwan, M. J.: "Mud Fluid in Drilling and Production of Wells," *Oil Weekly*, (July 5, 1924).
4. Rubel, A. C.: "Effect of Drilling Mud on Production in California," *API Prod. Bull.*, (1932) 34, 60.
5. Jones, P. H., and Babson, E. C.: "Evaluation of Rotary Drilling Muds," *API Drill. and Prod. Prac.*, (1935) 22.
6. Jones, P. H.: "Field Control of Drilling Mud," *API Drill. and Prod. Prac.*, (1937) 24.
7. Larsen, D. H.: "Methods of Determining the Filtration Characteristics of Drilling Muds," *Petr. Engineer*, (Sept. Nov., 1938). Also *Drilling Mud*, Baroid Sales Division National Lead Co., (May, 1938).
8. Byck, H. T.: "Effect of Temperature on Plastering Properties and Viscosity of Rotary Drilling Muds," *Trans. AIME*, (1940) 136, 165.

DISCUSSION

By J. M. Bugbee, Shell Oil Co., Houston, Tex., Member AIME

The authors are to be congratulated for a timely and useful contribution. Some additional remarks as to the bridging and filtration phenomena they mention may be helpful. Common filtration embodies two phenomena, the initial, generally minor one of the bridging of mud particles on the filter bed openings (the pre-bridging penetration of fines has been called the mud loss or mud spurt), and the major one of filtration. No one has yet derived a formulation which includes the two, although William and Cannon¹ attempted it. Larsen (Ref. 7 of text) sensed that the bridging could be, practically, neglected and his expression is for filtration alone. This is the reason that in making a Larsen-plot of filtration values for a test even where every precaution has been observed to properly flood the base plate assembly that a 0-intercept is rarely secured. A 0-intercept would indicate that bridging and the initiation of filtration occurred simultaneously. This is worthy of emphasis for fine-particle bentonite, starch and oil-base muds prepared in the laboratory lack the coarse particle range necessary for bridging on coarser filter media such as actual sands. As the authors state, however, a short period of use in a well generally supplies coarser mineral particles for bridging and the mud loss then becomes minor.

REFERENCE

1. Williams, M., and Cannon, G. E.: "Evaluation of Filtration Properties of Drilling Muds," *API Drill. and Prod. Prac.* (1938) 13.

★ ★ ★

EXPERIMENTAL EVALUATION OF WELL PERFORATION METHODS AS APPLIED TO HARD LIMESTONE

HENRY LEWELLING, THE ATLANTIC REFINING CO., DALLAS, TEX., MEMBER AIME

ABSTRACT

An experimental investigation of the relative effectiveness of standard bullets and "shaped charges" in perforating dense, hard formations is reported. A method is described which simulates the conditions under which a shot is normally fired. Results are evaluated on the basis of depth of penetration, extent of fracturing, extent and nature of formation damage, and other physical characteristics.

INTRODUCTION

A study was made of the relative merits of bullets and "shaped charges" as applied to well completions in hard, dense formations such as those encountered in the Permian Basin. The planning of the laboratory program stipulated that core samples should be prepared and mounted in such a way that perforation shots of either kind** could be fired into them, keeping the factors pertinent to good shooting practice similar to what they would be in a well.

The shooting was done in a buried tank, with the sample and shooting equipment covered with water. The depth of water was calculated to be sufficient to simulate the inertial effects of well fluids for the duration of an explosion (a few micro-seconds).

Flow measurements were attempted on the specimens after perforation. Due to the lack of uniformity of the limestone, shale breaks, etc., these measurements proved to be of little value to the study. The mounting materials were removed, so that the character of the penetration, fracturing, etc., could be observed.

METHOD

Laboratory samples were selected from the hard, dolomitic sand and cores from Block 31 Field. Core pieces having a $3\frac{3}{4}$ in. diameter and a useful length of 10 to 12 in. were used. Selection was aimed at those pieces having a minimum of shale streaks and other irregularities. The ends were cut off square

with the diamond saw. Prior to being mounted, the cores were soaked in water to prevent them from absorbing water out of the wet concrete, thus weakening it.

A set of steel capsules was fabricated for holding the core samples. Seven-in. casing was cut in two-ft lengths, of which one end was closed by "orange-peeling" and welding, and the other was threaded to accept a standard bull plug. The bull plugs were fitted with copper tube connections so that pressure could be applied when the capsules were made up.

The cores were mounted in the capsules by means of wire centralizers whose function was to hold the core in proper position while concrete was poured and set. A special aggregate was prepared using a graded sand and gravel mixture

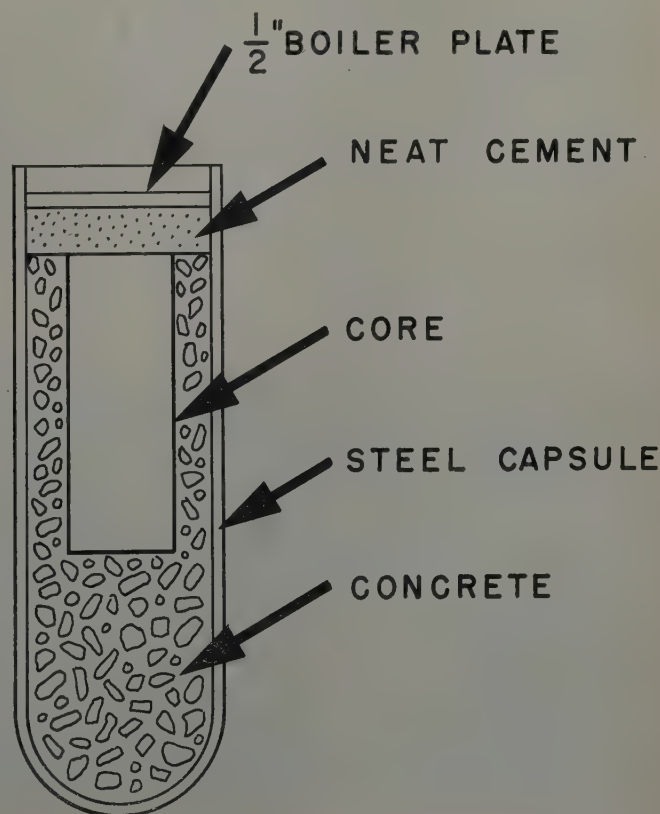


FIG. 1

Manuscript received in the Petroleum Branch office June 28, 1951. Paper presented at the Petroleum Branch Fall Meeting in Oklahoma City, Okla., Oct. 3-5, 1951.

**"Shaped charge" and "jet" are used interchangeably in this report. **The equipment used for these tests was that offered by the Lane-Wells Co. in early 1949 when the study was made. Equipment has since become available for bullet perforating which is capable of superior penetration to that reported here.

designed to leave a minimum of voids in the slurry. With the capsules held in a vertical position, the concrete was poured and tamped around the wet cores. The capsules were made up and 50 atmospheres of nitrogen pressure applied for three days to reduce any voids to a minimum size. This elaborate mounting procedure was adopted with the purpose of giving the cores an extremely dense, firm mounting, so that they could react to the shots as if they were still integral with the reservoir.

In certain instances, cracks appeared in the concrete during the setting process. This was undesirable because of the importance attached to having mountings of maximum solidity. The extent of the cracks was explored by drilling with a standard seven-eighths in. core bit. It was found that the cracks were shallow and superficial. All the cracked areas were drilled out, and the resulting holes were packed with neat cement.

Ten samples were mounted vertically, so that the shots would enter them in a direction perpendicular to the bedding plane. Four additional samples were prepared by sawing sections from a core, and mounting them side by side sandwich-wise so that the shots would enter in a direction parallel to the bedding plane. Each sample was covered with a layer of neat cement 1.4 in. thick. All the samples, except four of the vertically mounted ones, had a disc of one-half in. thick boiler plate placed against the wet neat cement layer. The 1.4 in. neat cement, plus the boiler plate were intended to correspond to the cement and casing in a standard completion. The samples with no boiler plate were intended to simulate open-hole completions.

Gun holders were fabricated from eight-in. pipe by notching and fitting with set screws. It was necessary to cut excess metal out of the holder in the part nearest the gun in order to allow a relatively free path for expanding gas. Fig. 2 shows a cut out gun holder in place on a capsule. Fig. 3 shows one not so prepared, and Fig. 4 shows the rupture caused by a single shot.

The gun shown in Fig. 3 was the one used for conventional bullet shots. The muzzle is centered over the core sample. The small pipe extending up is a conduit to prevent wetting the detonating wires. The shaped-charge gun was similar in appearance, but was sealed against water by the use of end plates held in place by shear pins.

The bullet equipment used for these tests was called the "type A" gun, which fired $1\frac{1}{8} \times 15/32$ -in. bullets propelled

by 150 grains of powder. Target distance was one in. The standard 28 g shaped-charge was used with a one-in. target distance in all jet shots except two, which were made with the 21 g jet, and a target distance of $1\frac{7}{8}$ in.

A simple wooden crate was prepared to support the sample and gun assembly in a vertical position. The assembly, as in Fig. 3, was submerged in water for firing the shot. Most of the water was blown out of the tank with each shot. Some idea of the difference in intensity of the respective explosions may be obtained by comparing Fig. 5 with Fig. 6. Both photographs were taken at approximately the maximum height of the water column. Fig. 5 shows the effect of a bullet charge, while Fig. 6 is from a shaped-charge.

The tank in which the shooting was done was prepared by welding together two oil drums and cutting off part of one. It was buried with only a small part extending out of the ground, and was tightly packed in place with rocks and earth. The tank was deformed to the extent of splitting before the testing was completed, in spite of the top being open. Fig. 7 shows the extent of stretching. Note that the "V-crimp" lines of the complete drum are almost invisible.

Flow test results are presented in Table I. These were made by drilling into the sample capsules (after firing the shots) perpendicular to sample axis, with a small core drill. The distance from the hole to the top of the core was held constant and as great as the shortest sample would allow. A small packer was seated in the hole to prevent air flow going directly into the mounting concrete. An air pressure at 50 psig was imposed, and the flow rate of all air coming from the top of the capsule was measured. This number is expressed below as "flow-rate." Additionally, permeabilities were measured on the plugs cut from the concrete and from the formation sample.

OBSERVATIONS

There is a significant difference between bullet and jet perforations in depth of penetration and in extent of fracturing. A comparison of the two in regard to depth of penetration is given in the tabulations (Table I). The column called, "Net Penetration," contains a set of data giving the amount (depth) of open perforation hole in the core left by the shots. The data were obtained by subtracting from the total penetration

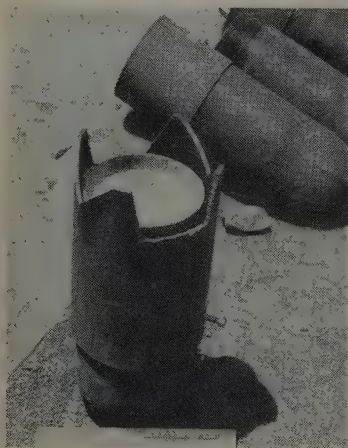


FIG. 2

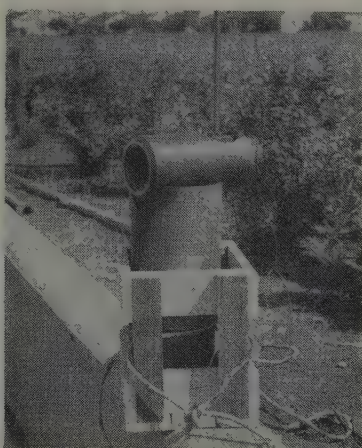


FIG. 3



FIG. 4

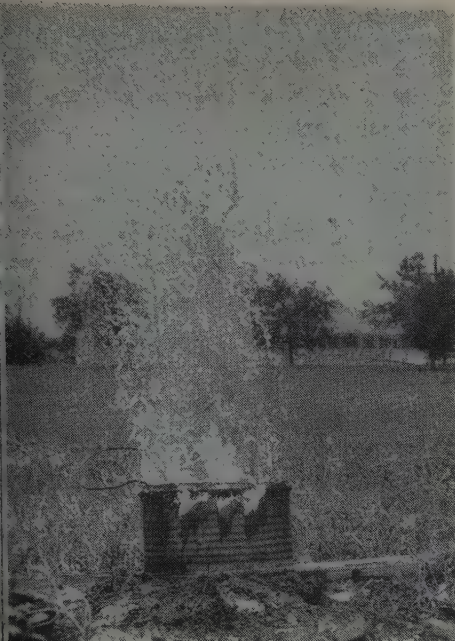


FIG. 5



FIG. 6

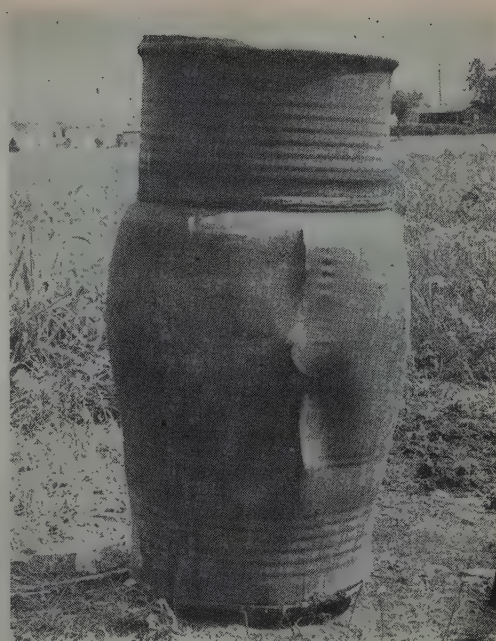


FIG. 7

the thickness of steel plate and/or neat cement traveled through. Total penetration in bullet holes was measured to the base of the bullets. On this basis of penetration alone, and assuming for the moment no fracturing, compacting, or other side effects, there is a substantial advantage in using jet shots. The average net jet penetration is 3.0 in., while the average for bullets is 0.2 in.

It would be expected that other effects than penetration should be evaluated. These would include fracturing, compaction, etc. The extent of fracturing that occurs in a hard, tight formation is important in its contribution of surface area from which oil may flow. A study of the photographs will show that in every case, bullet or jet shot, there was considerable fracturing. It will be observed that the fractures are more extensive in those samples shot with the shaped-charge. A significant fact that is not evident in the photographs is that a large number of fractures occurred in each case which did not open up enough to be visible. In the vicinity of the shot and throughout

the zone of penetration of the core, the rock can be broken up into gravel sized pieces with the hands. This is true of every sample, bullet or jet, and the effect seems to extend some distance radially from the shot-path.

A study of Table I shows that there is no correlation from these experiments between flow results and type of perforation. While the samples were selected for their uniformity, it would hardly be expected that they should be sufficiently uniform to allow tests to vary directly with penetration. A slight shale break through a core would upset the flow tests, as would any other variation in permeability. Probably a greater cause of error in the flow data is the fact that the cores were not isolated from the concrete mounting material. It is possible that air, entering the core under pressure, traveled immediately to the cement, and thence out at the low pressure end, giving essentially a measure of the cement permeability.

In the immediate vicinity of the jet shots, and extending into the formation a distance of one-eighth in. to one-fourth in. the

Table I—Summary
Shot Record with Resultant Measurements

Sample No.	Core Orientation	Cover ¹	Type Shot	Depth of Penetration, ² in.	Net Penetration, ³ in.	Air Permeability, md.		Flow Rate ⁴ cu cm/min
						Core Plug	Cement Plug	
1	Vertical	None	Jet	5-3/4	4.4	1.2	0.10	333
3	Vertical	None	Jet	4-1/2	3.1	0.25	0.07	105
4	Vertical	None	Bullet	1-5/8	.2	0.08
5	Vertical	Plate	Jet	4-5/8	2.7	0.60	312
6	Vertical	None	Bullet	2-1/4	.8	0.05	0.25	109
10	Vertical	Plate	Bullet	1-7/8	-.3	0.05	0.02
12	Vertical	Plate	Small Jet	1-3/8	.5	3.0	0.30	250
16	Vertical	Plate	Small Jet	3-3/16	1.2	0.17	0.50	38
18	Vertical	Plate	Bullet	1-7-8	.0	1.3	0.07	172
20	Vertical	Plate	Jet	6-1/4	4.4	1.0
A	Horizontal	Plate	Bullet	2-5/8	.7	1.58	0.22
B	Horizontal	Plate	Jet	5-5-16	3.4	0.10	0.20	10
C	Horizontal	Plate	Jet	5-1/8	4.2	5.04	0.32	136
D	Horizontal	Plate	Bullet	1-5/8	.0	0.43	0.29

¹No cover simulated open-hole; cover plate simulated casing.
²Open hole to base of bullet and to bottom of jet shot.

³Length of open perforation hole in core.
⁴cu cm/min at 50 psig differential.

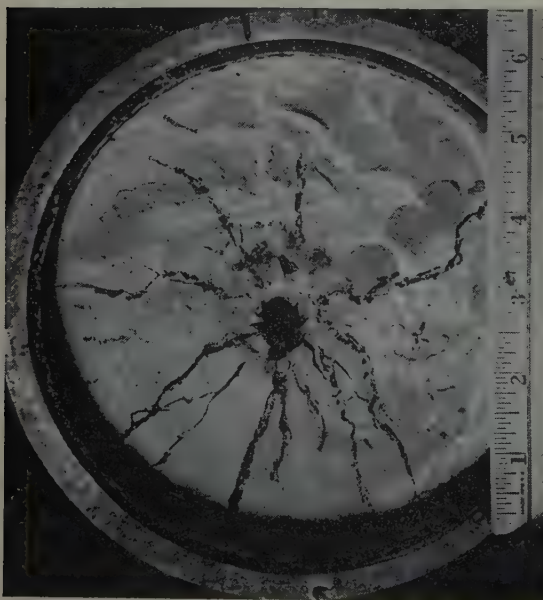


FIG. 8—BULLET SHOT NO. 6 WITH NO COVER PLATE. FRACTURE LINES IN NEAT CEMENT WERE DARKENED.



FIG. 9—BULLET SHOT SAMPLE NO. 6 AFTER REMOVING MOUNT. LARGE PIECES FRACTURED OFF EXTENDING ABOUT 2 IN. AHEAD OF BULLET NOSE.

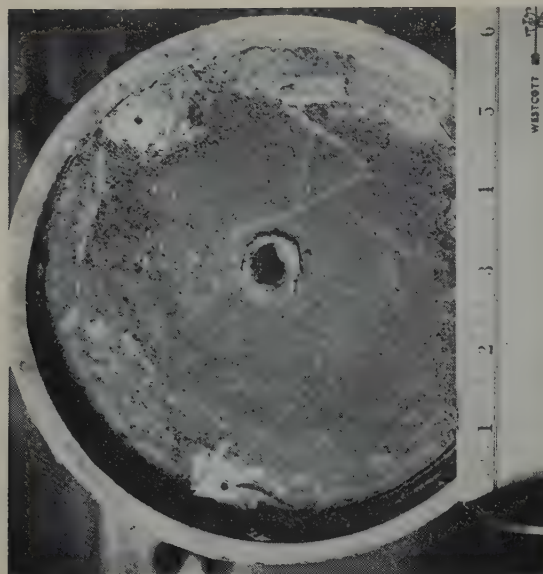


FIG. 10—BULLET SHOT NO. 10 WITH COVER PLATE. NOTE BURR AROUND BULLET HOLE.



FIG. 11—BULLET SAMPLE NO. 10 AFTER REMOVING COVER PLATE AND NEAT CEMENT. BULLET DID NOT COMPLETELY ENTER CORE. NOTE ABSENCE OF FRACTURES IN

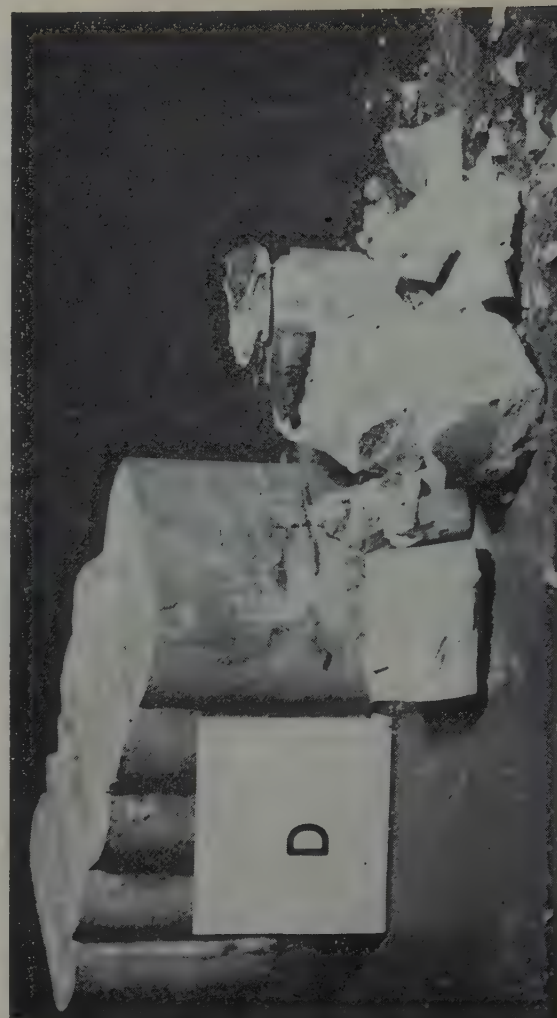


FIG. 12—BULLET SAMPLE D, MOUNTED FOR HORIZONTAL PENETRATION. FRACTURE PENETRATED ONLY FIRST LAYER.

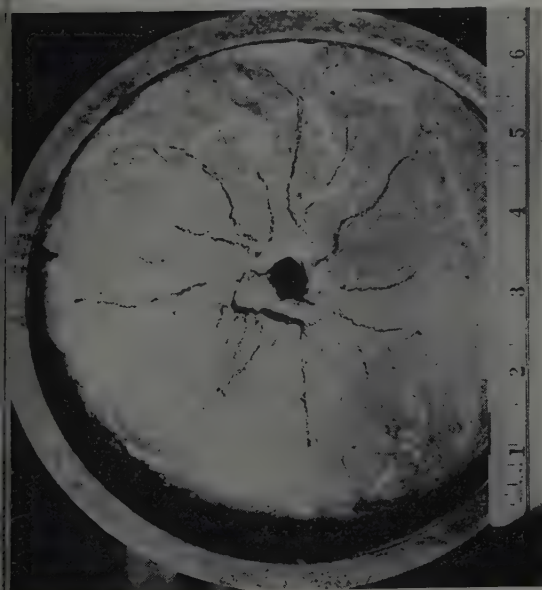


FIG. 13 — JET SAMPLE NO. 3 WITH NO COVER PLATE. FRACTURE LINES WERE DARKENED AS IN FIG. 8.

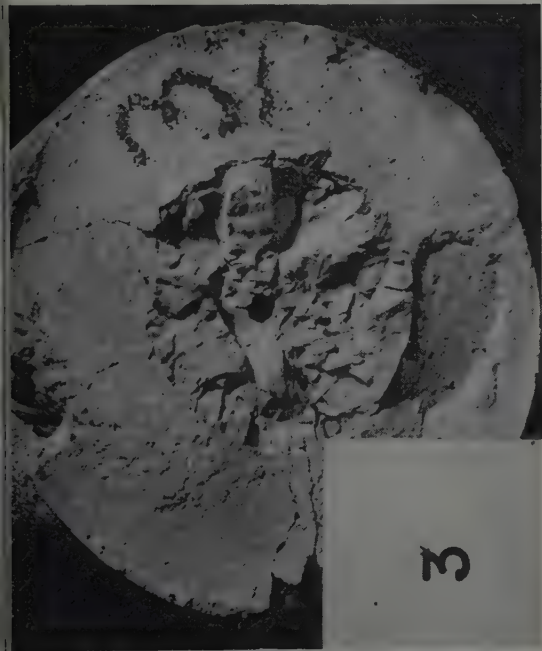


FIG. 14 — JET SAMPLE NO. 3 AFTER REMOVAL OF NEAT CEMENT AND CAPSULE. COMPARE FRACTURING WITH BULLET SHOT, FIG. 11.



FIG. 15 — JET SAMPLE WITH COVER PLATE. NOTE ABSENCE OF BURR. VISIBLE PARTICLE IN HOLE IS BRASS "CARROT."

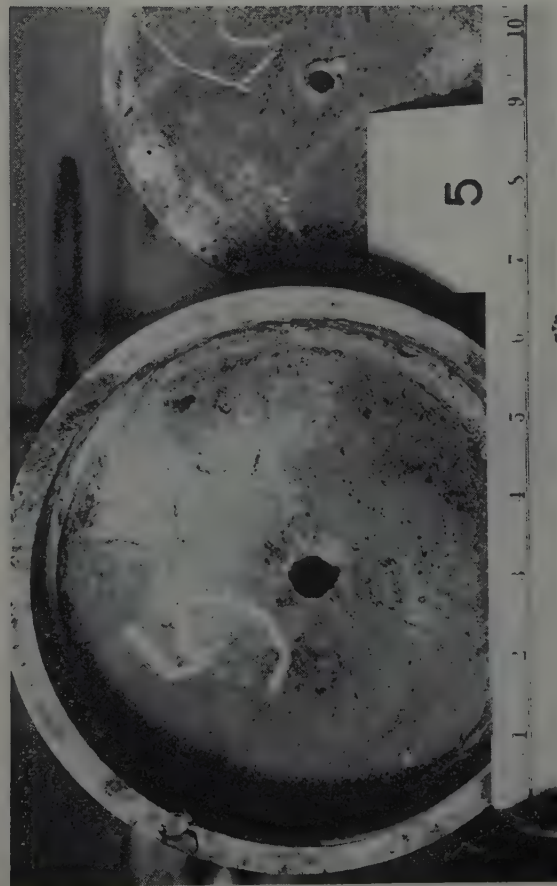


FIG. 16 — JET SAMPLE NO. 5. COVER PLATE WAS BLOWN OFF BY EXPLOSION. NOTE DIFFERENCE IN DIAMETER OF ENTERING HOLE IN PLATE AND IN NEAT CEMENT. ALSO, NOTE FRACTURES ARE MINOR IN NEAT CEMENT.

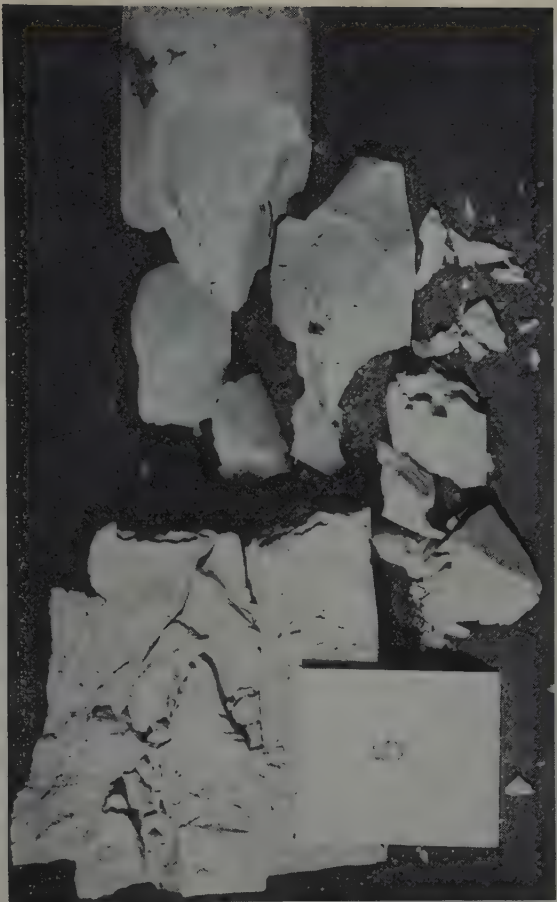


FIG. 17 — JET SAMPLE NO. 5 AFTER REMOVAL OF MOUNTING MATERIAL. PENETRATION OF ONLY 4% IN., BUT WITH SEVERE FRACTURING AND WITH CRACKS AHEAD OF PENETRATION 4 TO 5 IN.

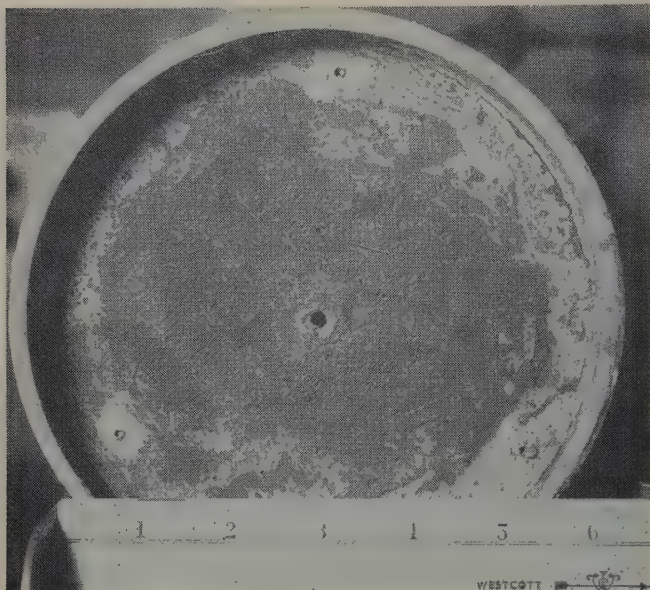


FIG. 18 — SMALL JET SAMPLE WITH COVER PLATE. COMPARE HOLE SIZE WITH FIGS. 15 AND 16.



FIG. 19 — SMALL JET SAMPLE AFTER REMOVAL OF MOUNTING MATERIAL. FRACTURED PIECES HELD TOGETHER WITH TAPE TO ILLUSTRATE GEOMETRY OF FRACTURE.

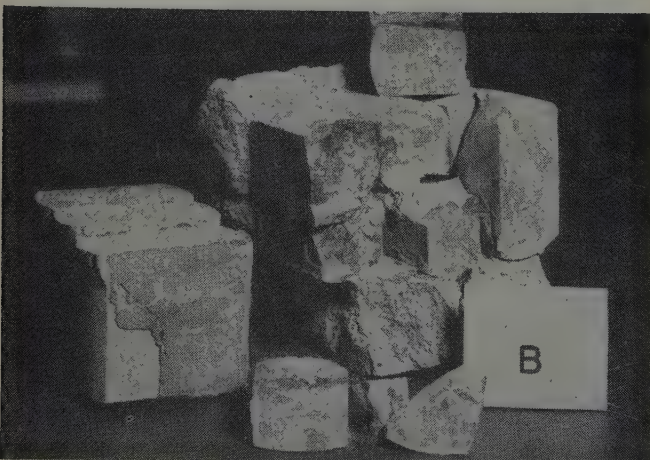


FIG. 20 — JET SHOT FIRED INTO HORIZONTALLY MOUNTED SAMPLE. PENETRATION AND FRACTURING IN THREE LAYERS, BUT FRACTURING NOT SO SEVERE AS IN VERTICALLY MOUNTED SAMPLES.

rock is practically powdered. It is believed that this effect rather than restricting flow, will possibly assist by opening up a larger effective hole than the actual diameter of the perforation.

INDIVIDUAL SAMPLES

Table I provides a summary of the conditions under which each test shot was fired. Figs. 8 through 20 are photographs of representative samples at various stages of the study. Included are examples of each type perforation on each type target, and of fracturing caused by each. The captions are intended to be self-explanatory.

CONCLUSIONS

1. Insofar as the application of perforation methods to hard dense limestone formations is concerned, the shaped-charge shows superiority over the conventional bullet both in depth of penetration and in extent of fracturing.
2. The formation sustained no apparent damage from perforating with shaped-charges due to fusion, compaction or similar effects that might interfere with the flow of fluids.
3. On simulated open hole completions, the neat cement layers seemed to be fractured as badly by one method as the other.
4. Based on limited data, it seems that when perforating through casing the shaped-charge causes less fracturing of the neat cement layer than does the bullet.
5. The extent of "preceding" cracks, coning ahead of the perforation, is thought to be significant, and is superior for the shaped-charge.
6. The data obtained from these experiments should not be used indiscriminately on formations of different characteristics from the one studied. Evaluation of perforation methods on different type formations can either come from additional laboratory work, from field experience, or both.

ACKNOWLEDGMENT

The writer wishes to express his appreciation to the Lane Wells Co. for providing the special equipment and personnel necessary to make these tests. Appreciation is also expressed for the able assistance offered by P. B. Morris of The Atlantic Refining Co.

DISCUSSION

By George C. Howard, Stanolind Oil and Gas Co., Tulsa, Oklahoma
Member AIME

The problem of accurately evaluating the performance of a bullet and jet perforators under simulated well conditions is very difficult, particularly if the results are to be extrapolated or applied to field use. Lewelling has presented a suggested method of accomplishing this objective that should furnish a fairly accurate indication of the relative ability of bullets and jet perforators to penetrate the cores tested. There is some question, however, on whether or not the extent of fracturing, indicated in Lewelling's work, is representative of what actually takes place in a well. Similar tests conducted to evaluate this point have shown a wide variation in the amount of fracturing caused by both bullets and jets when fired in massive sandstone outcrops when compared to similar shots fired in substantially backed sandstone cores. ★ ★ ★

THE RESISTIVITY OF A FLUID-FILLED POROUS BODY

J. E. OWEN, GEOPHYSICAL RESEARCH CORP., TULSA, OKLA.

ABSTRACT

A model of a porous body is presented in which the pore space consists of a system of voids and interconnecting tubes. Relationships between porosity and resistivity formation factor are determined partly by calculation, partly by experiment. Constriction effects characteristic of the model are shown to be sufficient to account for high formation factors. It is shown that constriction may be combined with moderate amounts of tortuosity to give model pore systems exhibiting to a first approximation porosity and resistivity properties similar to those of natural porous bodies.

INTRODUCTION

The relationship between the electric resistivity of a fluid-filled porous body and the geometry of its pore space is so complex that the calculation of the resistivity of a natural porous rock is a practical impossibility. Both the resistivity of a body and its porosity are measurable quantities, however, and previous successes at relating them have been reached by an empirical approach. Efforts at obtaining theoretically derived formulae relating them have generally been unsatisfactory. One of the reasons for this may lie in the pore geometry that has been assumed.

THE TORTUOSITY CONCEPT

A parameter called the formation factor is useful in discussing the resistivity of a fluid-filled porous body. This parameter is the ratio of the resistivity of a fluid saturated porous body to the resistivity of the saturating fluid. Formation factors are often available from measurements on cores or from electric logs, and many attempts have been made to correlate formation factors and porosities of geological formations. Whenever a successful correlation is found, the engineer working with electrical logs has a useful tool for the determination of porosities of pay sections. One of the more successful formulae applicable to these correlations is the familiar equation empirically obtained by Archie.¹

$$F = \phi^{-m} \quad (1)$$

in which F is the formation factor, ϕ is the porosity, and m is an exponent called the cementation factor. When the for-

mula applies, the cementation factor usually is found to be between 1.3 and 2.2.

The values for formation factors experimentally obtained are often higher than simple pore geometry would lead one to expect. In an effort to account for such high values certain formulae have been derived based on a so-called "tortuosity concept." In deriving these formulae a synthetic porous body is usually assumed in which the solid material is an electrical non-conductor, and in which the pore system consists of three sets of fluid-filled tubes of uniform diameter connecting opposite faces of the body which, for convenience, is considered to be cubical in shape. The three sets of tubes account for the whole of the effective porosity of the body, and usually, it is specified that they do not interconnect. By considering that the pore tubes are not straight but tortuous, their resistance to the flow of electric currents can be made as high as needed to explain high formation factors. Such an explanation has some basis in fact, but it appears that the tortuosity concept is often incorrectly applied when other factors are largely responsible for observed high resistivities. Recently, Wyllie and Spangler have recognized that tortuosity as calculated by conventional formulae has little if any physical significance.²

RESISTIVITY AND THE CONSTRICTION CONCEPT

Any explanation of high formation factors which depends solely on tortuosity of uniform pore paths necessarily ignores the effect that variations in the cross-sectional area of the conducting paths have on the resistivity of a body. Although, as previously pointed out, the calculation of such paths for an actual body is impossible, it will be shown that a synthetic pore network can be devised which will yield to analysis, and lead to results in agreement with the experimental data represented by Equation (1).

The porous body to be considered is assumed to be homogeneous and isotropic or, for present purposes, identical in its characteristics in the three directions parallel to its coordinate axes. It will be assumed to be built of identical unit cubes, each of which contains a single pore network connecting all faces of the unit cube. A unit of such a pore network is shown

¹References given at end of paper.

Manuscript received in the Petroleum Branch office Jan. 22, 1952.

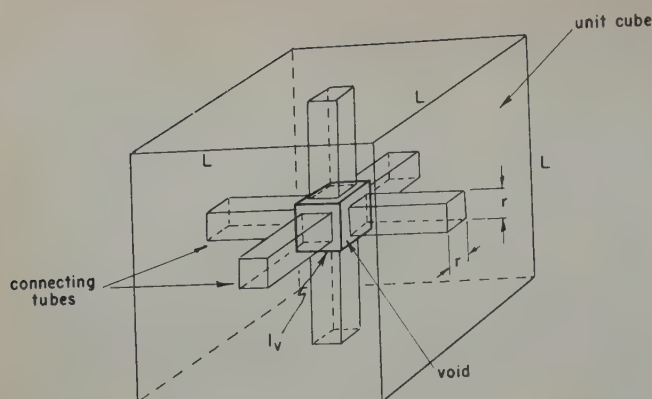


FIG. 1 — UNIT CUBE OF SYNTHETIC POROUS BODY.

in Fig. 1. The solid portion of this unit cube is electrically non-conducting. Within the unit cube is a cubical void centrally located, with faces parallel to corresponding faces of the unit cube. The connecting tubes are square in cross section normal to the axis of the tube. In Fig. 1 these connecting tubes are shown with their axes normal to the faces of the unit cube. A more general case, however, is that of Fig. 2. In this figure a cross section of a portion of a synthetic porous body is shown in which the connecting tubes make an angle θ with the normal faces of the unit cube. Such a porous body exhibits both constriction and tortuosity.

The electric resistance between two of the opposite faces of a unit cube is the sum of the resistances through the tubes connecting the void with those faces, and the resistance through the void cube measured from the contacts made with the void faces by the two tubes directly in the path of current flow. This resistance is somewhat greater than would be the case if each contact were made with the entire face of the void cube. The effect of the four side tubes is to lower the resistance of the void. Calculations of these two effects would be difficult to carry out, and their determination was therefore made experimentally. A series of simple experiments was carried out in which a bakelite box cubical in shape was used as a model for the void. Square metallic electrodes were placed at the midpoints of two of the opposite faces of the cube which was then filled with a saline solution. The resistance between the electrodes was measured for a number of electrodes of different areas. The results are given in Fig. 3 in which the value plotted as the ordinate is the ratio of the resistances measured through the cube as the size of the electrode was varied, to the resistance measured when the electrode covered the entire face of the cube. This resistance ratio is plotted as a function of the term C which will be called the constriction factor. It is defined as

$$C = \frac{l_v}{r} \quad (2)$$

In Fig. 1 this is seen to be the ratio of an edge of the void cube to a side of the square which is the cross section of a connecting tube. C , in the experimental work, is the ratio of the lengths of one edge of the void cube and one edge of the electrode.

The influence of the side tubes on the resistance through the void was determined by measurements on a model for the limiting case in which the void has become merely the intersection of the connecting tubes. This is obviously the case for which the shunting effect of the side tubes is the greatest, and is the case for which $C = 1.0$. For this case it was found

that the ratio of the resistances of a void cube with and without the four side tubes is 0.5. The shunting effect of the side tubes decreases quite rapidly with increasing values of C , and for values of $C > 3$ this effect is negligible. By combining the data from the model experiments, the curve of Fig. 4 was prepared. In this figure the factor f represents the correction factor to be applied to the resistance shown by the void of Fig. 1 in which the resistance of the void is first calculated as though contact were made with the entire face of the void cube. This correction factor may be shown to be slightly in error when $C < 1.4$ and simultaneously $\phi > 0.3$, but this combination of conditions is not of particular interest in this paper.

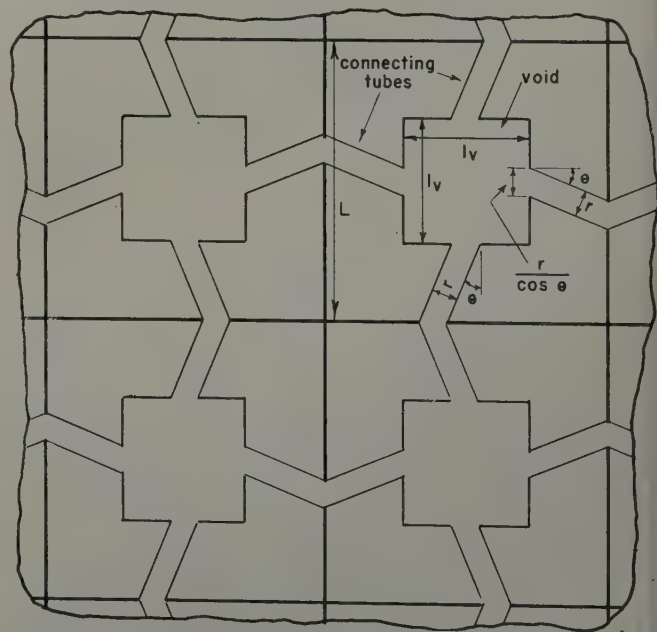
Let each connecting tube connect the void and face of the cube as shown in Fig. 2. The tube makes an angle θ with the normal to the face of the cube to which it connects. The intersection of the tube with the face of the void or the face of the cube, is a rectangle $r \cdot r / \cos \theta$. The resistance through the void from the rectangular intersection is to a sufficiently close approximation the same as the resistance from squares of the same equivalent area. The corresponding value for the side r' of the equivalent square contact is

$$r' = \frac{r}{\sqrt{\cos \theta}} \quad (3)$$

The curve of Fig. 4 applies to a pore network in which the angle $\theta = 0$. Hence the constriction factor to use in determining f for the case in which $\theta \neq 0$ is a value of C' , corresponding to the value r' , or

$$C' = \frac{l_v}{r'} = \frac{l_v \sqrt{\cos \theta}}{r} = C \sqrt{\cos \theta} \quad (4)$$

The resistance R from one face of a unit cube to the opposite face is the sum of the resistance R_v through the void and

FIG. 2 — CROSS SECTION THROUGH FOUR UNIT CUBES OF SYNTHETIC POROUS BODY WITH TORTUOUS CONNECTING TUBES. VALUES USED: $C = 5.0$, $\theta = 22.5^\circ$ or $r^{1/2} = 1.08$, $\phi = 0.10$.

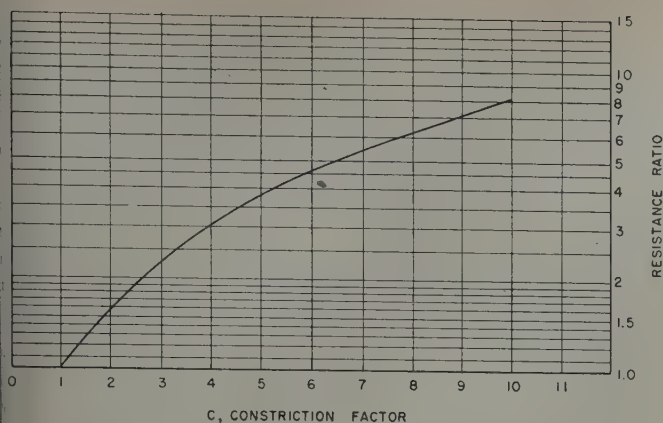


FIG. 3 — EXPERIMENTAL VOID CUBE RESISTANCE DATA.

the resistance R_t through the tubes connecting the void and these faces.

$$R_v = \rho_w \frac{f}{l_v} \quad (5)$$

and,

$$R_t = \frac{\rho_w (L - l_v)}{r^2 \cos \theta} \quad (6)$$

In these equations ρ_w is the specific resistivity of the fluid filling the pore space. The factor f is obtained from Fig. 4 in any particular case for the value of C being considered.

$$R = R_v + R_t = \rho_w \left(\frac{f}{l_v} + \frac{L - l_v}{r^2 \cos \theta} \right) \quad (7)$$

The resistivity ρ of the porous body is

$$\rho = RL = \rho_w L \left(\frac{f}{l_v} + \frac{L - l_v}{r^2 \cos \theta} \right) \quad (8)$$

The formation factor F is defined as

$$F = \frac{\rho}{\rho_w} = L \left(\frac{f}{l_v} + \frac{L - l_v}{r^2 \cos \theta} \right) \quad (9)$$

The porosity ϕ of the body is given by

$$\phi = \frac{l_v^3 + \frac{3(L - l_v)r^2}{\cos \theta}}{L^3} \quad (10)$$

From (9) and (10)

$$F = L \left(\frac{f}{l_v} + \frac{3(L - l_v)^2}{(L^3 \phi - l_v^3) \cos \theta} \right) \quad (11)$$

The term for tortuosity may now be introduced and is defined as $T^{1/2} = \frac{1}{\cos \theta}$. For convenience, also, let $a = \frac{r}{L}$ and

$b = \frac{l_v}{L}$. Since $C = \frac{L - l_v}{r}$, it follows that $C = \frac{b}{a}$. The porosity of

body, from Equation (10), can be expressed

$$\phi = b^3 + 3(1 - b)a^2 T^{1/2} \quad (12)$$

Equation (11) reduces to

$$F = \frac{f}{b} + \frac{3(1 - b)^2 T}{\phi - b^3} \quad (13)$$

This may also be expressed in the form

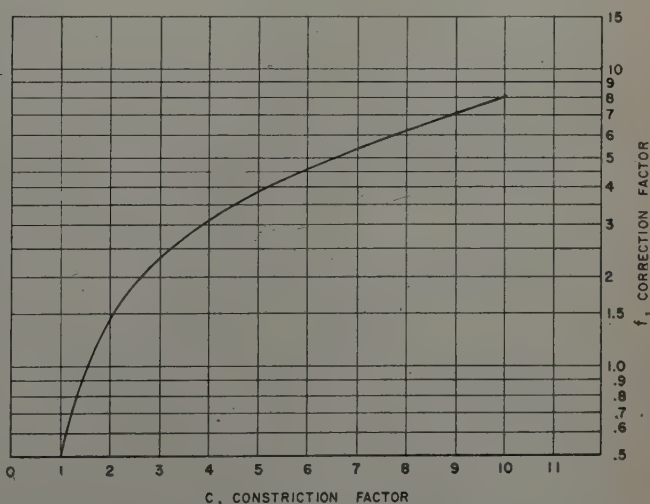
$$F = \frac{f}{b} + \frac{(1 - b)T^{1/2}}{a^2} \quad (14)$$

APPLICATION OF FORMULAE

From the formulae that have been developed, the curves of Fig. 5 have been prepared. Here are given calculated formation factors of synthetic porous bodies for four values of porosity, and corresponding to each of these, three values of tortuosity. It is interesting to note that for any chosen porosity and tortuosity, the formation factor is nearly independent of the constriction factor for values of C less than two. For higher values of C , however, F increases rapidly with increasing constriction. High values of formation factor that are observed in actual porous bodies can thus be accounted for by combinations of tortuosity and constriction effects or, if desired, by constriction alone. For example, a porous body with a porosity of 0.2 and a formation factor of 50 may be said to be equivalent to a synthetic porous body of the same porosity and with any of the following combinations of constriction and tortuosity:

$$\begin{array}{ll} T^{1/2} = 1.0 \quad (\theta = 0^\circ), & C = 5.75; \\ T^{1/2} = 1.08 \quad (\theta = 22\frac{1}{2}^\circ), & C = 5.6; \\ T^{1/2} = 1.41 \quad (\theta = 45^\circ), & C = 4.8 \end{array}$$

Any of these values or other that can be interpolated from the curves of Fig. 5 are geometrically reasonable, whereas the extremely high angles of tortuosity required by previously derived formulae based solely on tortuosity concept are difficult to accept as being representative of conditions in a porous body. This is illustrated by the example chosen here, assuming no constriction, one-third of the total porosity in each set of non-interconnecting tortuous tubes corresponding to the three coordinate axes of the body, and using formulae previously given in the literature.³ The average or effective angle of tortuosity is approximately 72° . Based on the conventional tortuosity concept, values of tortuosity as high as 200 have been reported.⁴ Such a value of tortuosity as defined in this reference corresponds to a flow path at an angle of 86° to the general direction of current flow through the body. It is hardly conceivable that the true direction of current flow through a porous body is so nearly perpendicular to the direction in which resistivity measurements are made.

FIG. 4 — f , CURRENT DISTRIBUTION CORRECTION FACTOR vs C , CONSTRICTION FACTOR, $T^{1/2} = 1$.

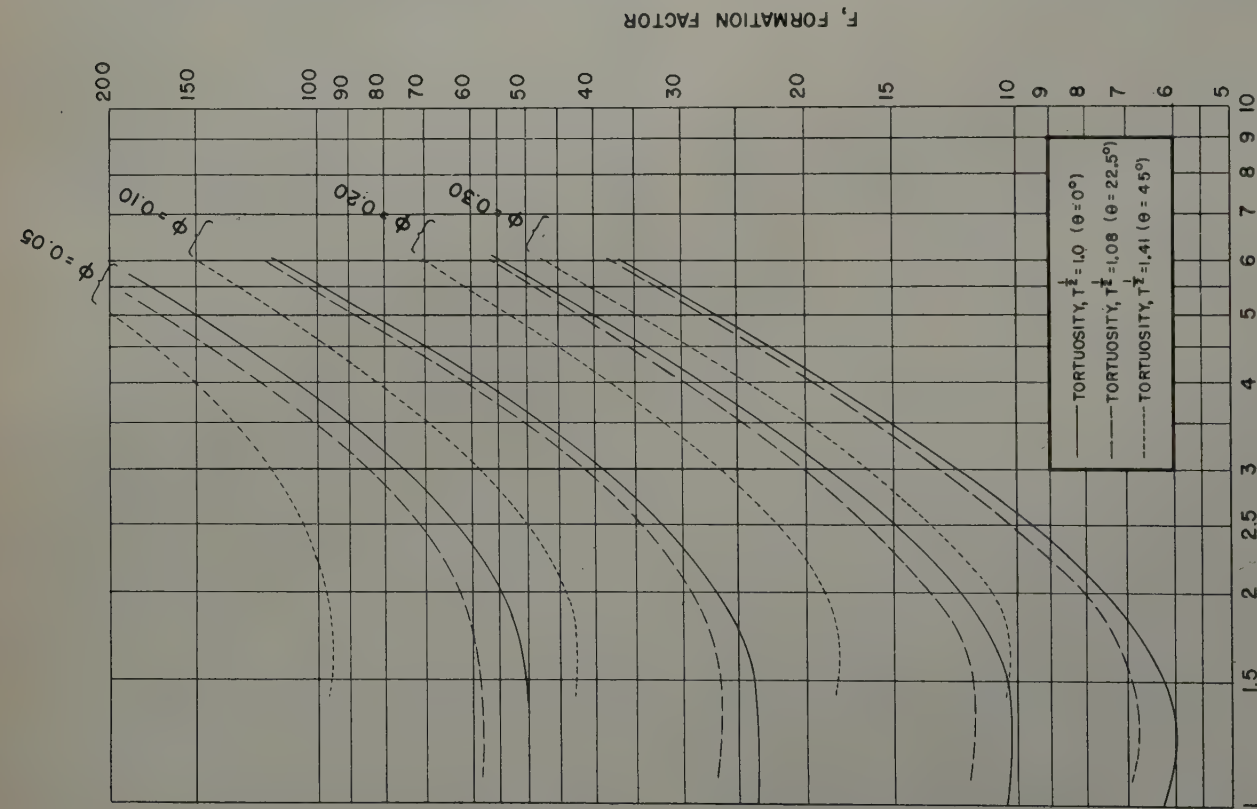


FIG. 5 — RELATION BETWEEN FORMATION FACTOR F AND CONSTRICTION FACTOR C OF VOID-TUBE NETWORK. ϕ = FRACTIONAL POROSITY, T = TORTUOSITY, T^2 = TORTUOSITY SQUARED, θ = ANGLE OF CONSTRUCTION.

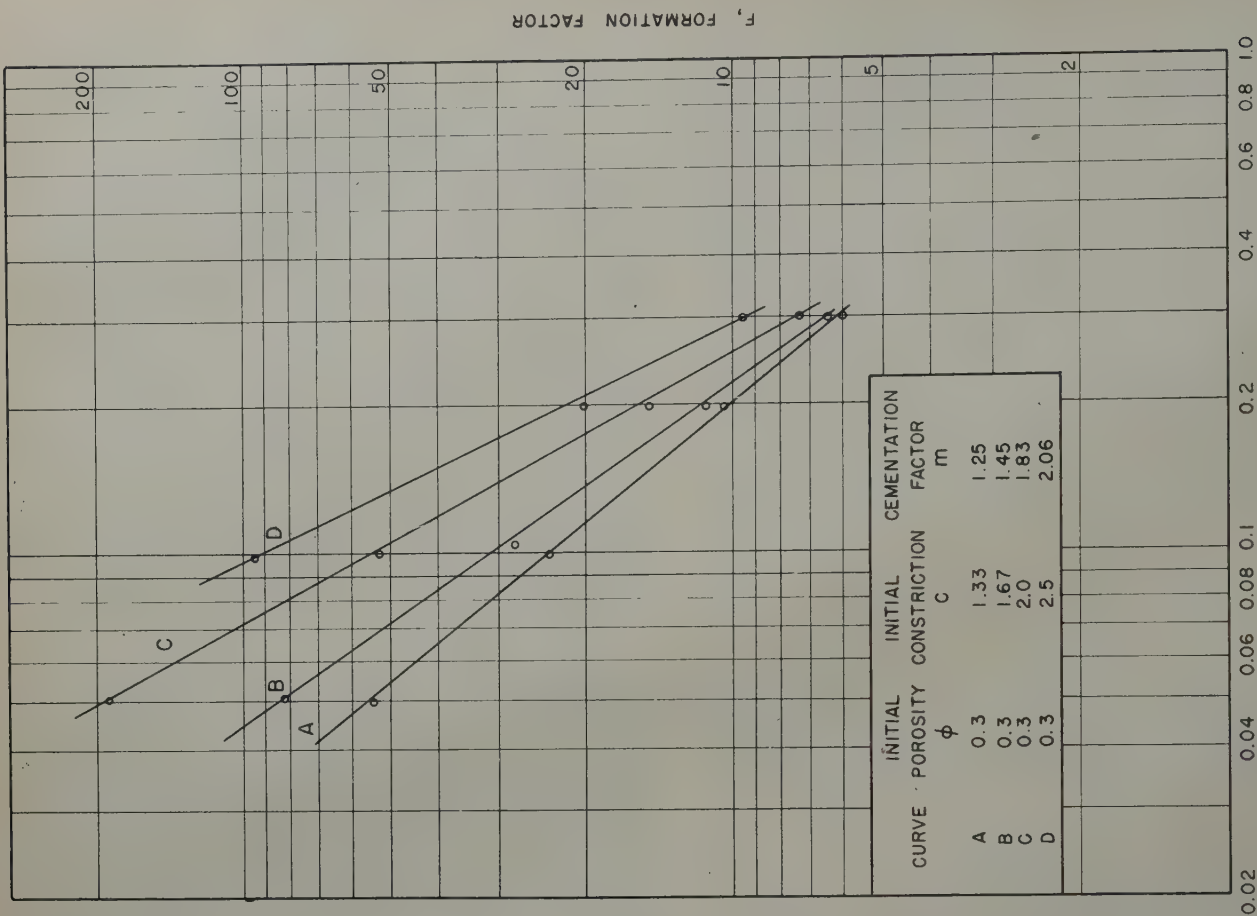


FIG. 6 — RELATION BETWEEN FORMATION FACTOR F AND POROSITY ϕ FOR VOID-TUBE NETWORK WITH PROGRESSING CEMENTATION, $T^{1/2} = 1$.

the formulae used in obtaining the curves of Fig. 5 are based on voids cubical in shape, and connecting tubes square cross section, and the discussion thus far has been limited to voids and tubes having these shapes. It is obvious, however, that uniform tubes of any shape having the same cross-sectional area will exhibit the same electric resistance as square tubes. A spherical void of the same volume can also be substituted for a cubical one with approximately the same results. Thus the particular shape of the voids and connecting tubes used in this analysis is not essential to the friction concept or to its use in explaining high formation factors. The pore network to which this discussion and the derived formulae may be applied, then, consists of any regular array of voids and connecting tubes similar to the one investigated here. The particular pore network described was chosen for convenience in experimentation but no objection can be made to the acceptance of such a network as a synthetic porous body in terms of which constriction and tortuosity of natural porous bodies may be expressed. This analysis can be extended to include anisotropic bodies by using in the calculations directions through the body connecting tubes of different lengths and with different tortuosities.

CEMENTATION AND THE CONSTRICTION FACTOR

Earlier in this paper it was pointed out that empirical correlations have been established by various investigators relating porosities and formation factors, and that one of the best is the one expressed by Equation (1). It is of interest to consider the effect of cementation upon the pore network of Fig. 1 when certain assumptions are made regarding initial conditions and the manner in which cementation takes place. Consider, for example, a case in which samples taken from a particular porous body vary widely in porosity solely because of differences in the amount of cementing material deposited. Before the deposition of the cementing material these body samples are considered to have been identical in general nature of their pore spaces, and corresponding to an initial condition, the equivalent pore network of the type of Fig. 1 (no tortuosity) will be considered as having had a uniform porosity of 0.3 and a constriction factor of 1.33. In other words, the pore body before cementation was characterized by voids and connecting tubes of a size giving a porosity of 0.3 and with the connecting tubes nearly as large as the voids themselves. Conditions which controlled the deposition of cementing material in the pore space, however, varied from sample to sample and thus the final porosities differed. According to the actual case of cementation it will be assumed that in the equivalent pore network of Fig. 1 a uniform deposition of cementing material has taken place on the walls of the voids and the walls of the connecting tubes. For a given amount of deposition it is possible, then, to calculate the porosity of the body and the resulting formation factor from the formulae developed here. In this manner the data for line *A* of Fig. 6 was obtained from an initial condition of 0.3 and $C = 1.33$, by assuming that the cementation consisted of a uniform layer of material on the walls of the voids and connecting tubes. The slope of line *A* is calculated to be 1.25.

Similarly, with initial porosities of 0.3 and initial values of 1.67, 2.0, and 2.5 the porosities and formation factors progressing cementation plot in Fig. 6 quite close to the data for lines *B*, *C*, and *D*, respectively, and with slopes that can be calculated as cementation factors from their correspondence to the exponent of Equation (1). Throughout a rather wide range of porosities the value of m under a progressing cement-

ation process is thus approximately constant, and is a function of the values of ϕ and C at its beginning. Obviously, if the calculated porosities and formation factors were related precisely as described by Equation (1), lines *A*, *B*, *C*, and *D*, if extended, would pass through the point (1, 1). This they will not do if extended as drawn, and hence the data are somewhat better represented by an equation of the form $F = a\phi^{-m}$.

Experimental work reported by Archie,¹ indicates that unconsolidated sands obey the relation given by Equation (1) in which m is approximately 1.3. It may be assumed that these unconsolidated sands were composed of grains of fairly uniform size when the porosities that he observed were as great as 0.3. A sand of this type has a low constriction factor, as it does not contain large voids with small connecting tubes. On the other hand, it is likely that the low porosity unconsolidated sands that Archie used were mixtures of grains of different sizes, or were silty. Fine materials would be expected to clog a part of the smaller passageways through a sand as well as to fill a portion of the voids. It makes little difference, whether, from an initial condition of high porosity, low porosity is obtained in a sand by reducing the somewhat smaller passageways with loose, relatively fine material, or by a cementation process of the kind previously described. The high porosity conditions for unconsolidated sand, then, correspond to the initial conditions for Curve *A* of Fig. 6, and the calculated value of m that is observed with changes in porosity is seen to be approximately the same as that observed experimentally.

Archie also found that highly cemented sandstones are characterized by a high value of m . Sandstones that are highly cemented and yet have good porosity must have been highly porous before cementation and hence necessarily contained large voids. The process of cementation, then, resulted in a relatively high value for C even at a porosity of 0.3. Curves such as *C* or *D* of Fig. 6 may therefore be expected to apply to such sandstones as cementation proceeds from the condition described. It will be seen that the values of m for curves *C* and *D* correspond to the values observed by Archie for highly cemented sandstones.

CONCLUSIONS

The void and tube network described in this paper appears to meet many of the requirements for a synthetic porous body which may be used as an equivalent of a natural porous body. The equations for the flow of electric current through this network have been derived. These equations show how constriction effects can cause porous bodies to exhibit high formation factors. Such a void and tube network is suggested, therefore, as being more nearly analogous to conditions within a natural porous body than is a uniform diameter tube system which requires high tortuosity values to explain large formation factors.

The work in this paper is not sufficiently complete to enable the full determination of the geometry of a synthetic porous body in all ways equivalent to a natural porous body. In an example that was chosen it was found that for a body with a porosity of 0.2 an infinite number of combinations of tortuosity and constriction factors may be chosen to give a formation factor of 50. For moderate values of tortuosity, however, the constriction factors lie within a narrow range. The actual size of the unit cube for the synthetic porous body does not enter into the calculations, but it is obvious that the size of the unit cube must be related to the grain size or the pore size of the body. The size of the unit cube and the chosen combination of tortuosity and constriction factor will together determine the permeability of a synthetic porous body. A dis-

cussion of the relationships between grain size, permeability, tortuosity and constriction factor, however, is beyond the scope of this paper.

ACKNOWLEDGMENT

The author wishes to thank the Amerada Petroleum Corp. and the Geophysical Research Corp. for permission to publish this paper, and E. E. Finklea for his assistance in obtaining and arranging the data that were used.

REFERENCES

1. Archie, G. E.: "The Electrical Resistivity Log as an Aid in Determining Some Reservoir Characteristics," *Trans. AIME*, (1942) 146, 54.
2. Wyllie, M. R. J., and Spangler, M. B.: "Application of Electrical Resistivity Measurements to Problem of Fluid Flow in Porous Media," *AAPG Bull.*, (1952) 36 (2), 359.
3. Wyllie, M. R. J., and Rose, W. D.: "Some Theoretical Considerations Related to the Quantitative Evaluation of the Physical Characteristics of Reservoir Rock from Electrical Log Data," *Trans. AIME*, (1950) 189, 105.
4. Rose, W. D., and Bruce, W. A.: "Evaluation of Capillary Character in Petroleum Reservoir Rock," *Trans. AIME*, (1949) 186, 127.

DISCUSSION

By M. R. J. Wyllie, Gulf Research and Development Co., Pittsburgh, Pa., Member AIME.

This is a most interesting paper. It will undoubtedly be found particularly useful by those who are repelled by the purely mathematical definition of tortuosity offered in References 2 and 3 of the author. Personally, I believe that the constriction and tortuosity effects proposed by the writer to account for formation factor variations are essentially correct. It would be unfair, however, if I did not point out that Winsauer, Shearin, Masson and Williams¹ put forward last year a basically similar proposal. Fig. 1 of their paper should be compared with Fig. 1 of the writer's.

While I concur with the general conclusions of the writer, I am on principle unhappy about his use of the pore system of Fig. 2 to compute even semi-quantitative data. The system of Fig. 2 is basically anisotropic. Thus, while the resistivity across cube faces is always the same, that measured across cube diagonals, for example, will be different. A porous medium in which the pores are truly randomly disposed is electrically isotropic.

The writer, like all others before him, has failed to resolve the fundamental difficulty: to separate the measurable quantity, formation factor, into independently measurable components. It would seem that this can only be done on the basis of certain assumptions. If the free area of the medium is assumed constant, it is possible from the measured formation factor and porosity to calculate a fictitious average path length (tortuosity). This is the method of Wyllie and Rose and its object is to permit the Kozeny equation to be extended. If the average path length in the direction of current flow is considered to be equal to the overall length of the medium, a fictitious average porosity, less than the true porosity, can be calculated. This method was used for convenience by Garrels, Dreyer and Howland² when solving diffusion equations. In the present paper by making use of the measured formation factor and porosity, Owen can assume a tortuosity and find a constriction factor or vice versa. But he cannot independently measure either. It is true that Winsauer *et al.*¹ have claimed to measure tortuosity independently, but a more detailed analysis of their method will reveal that actually theirs is an

ingenious method to measure formation factor. In this section, a comparison of their method with that used discussed by Schofield and Dakshinamurti³ will be found to be helpful.

REFERENCES

1. Winsauer, W. O., Shearin, H. M., Jr., Masson, P. H., Williams, M.: *Bull. AAPG*, (1952) 36, 253.
2. Garrels, R. M., Dreyer, R. M., and Howland, A. L.: *Geol. Soc. Am.*, (1949) 60, 1809.
3. Schofield, R. K., and Dakshinamurti, C.: *Discussions, day Soc.*, (1948), No. 3, 56.

AUTHOR'S REPLY TO MR. WYLLIE

Wyllie's comments on this paper are greatly appreciated and certainly a synthetic pore system isotropic in all sections is to be desired. However, the writer feels that in choosing a single pore system identical, when desired, in its characteristics in the directions of its three coordinate axes, a system sufficiently close for present purposes to a truly isotropic system has been achieved. The purpose of this system, of course, is to represent to a first approximation, simply in a systematic manner, the random pore system of actual porous bodies. The effects of constriction such as are obviously present in varying degrees in natural porous bodies are easily determinable for the chosen synthetic system, and shown that the magnitude of such effects can be large. The writer recognizes, of course, that new cube faces cut normal to the diagonals of the assumed unit cubes will not have resistivities identical with those in the directions chosen. He insists that this, however, is a matter of no particular importance, as the axes of the synthetic body can always be chosen to align with those of the natural porous body it is intended to represent.

In regard to the paper by Winsauer, Shearin, Masson and Williams, the writer feels that here the concept of constriction as an important factor in porous body resistivity was emphasized and not missed. In Fig. 1 in the Winsauer, *et al.*, paper the apparent purpose is to show that there is some degree of tortuosity in the pore space between sand grains. The value of constriction involved in the figure is probably two or three, and it can be seen that by making the upper sand grains in the figure approach the lower ones the value of constriction can be increased enormously without appreciably modifying the tortuosity. That such a change in constriction will lead to a large increase in the resistivity of the porous body was not considered. The writer's present paper was given by personal communication in essentially its present form to Winsauer, Shearin, and Williams in August, 1950. The fact that Winsauer, *et al.*, made no reference to the concept of constriction as given them by the writer through this personal communication 18 months before publication of their paper may be taken to mean that they did not recognize the constriction effect as herein presented to be of importance in resistivity calculations. In the writer's judgment Winsauer, *et al.*, have truly measured tortuosity in the experiments they have described.

Wyllie points out that the present paper does not describe methods of measurement by which effects of tortuosity and constriction in an actual porous body can be independently determined. This is correct. However, it was shown that the assumptions are made limiting tortuosity to reasonable values and that constriction in any actual case will be bracketed within narrow limits. The writer feels that the information obtained justifies the present attempt to represent actual porous bodies with a synthetic pore system of the type described. ★

POSSIBILITY OF CYCLING DEEP DEPLETED OIL RESERVOIRS AFTER COMPRESSION TO A SINGLE PHASE

DONALD L. KATZ, UNIVERSITY OF MICHIGAN, ANN ARBOR, MICH., MEMBER AIME

ABSTRACT

The compressing of gas into a partially depleted gas drive reservoir to bring the contents to a single phase miscible with gas is proposed as a process worthy of serious study. The compressed gas and vaporized oil would be recovered by cycling. This paper explores the possibility of recovering oil from reservoirs of 6,000 ft or more by this method.

INTRODUCTION

Many new methods for increasing the recovery of oil from reservoirs are under consideration in the various research laboratories. One method which should be considered for recovering oil from partially depleted gas drive fields is to compress gas into the reservoir until the contents become a single phase miscible with more gas. Natural gas then may be cycled through the reservoir to recover the oil. This procedure ideally will eliminate the capillary effects of the liquid in the porous media and should permit recoveries similar to those obtained in cycling operations, probably of the order of 80 per cent. This paper explores the information now available for the prediction of the performance of such a process and discusses the problems likely to be encountered in recovering oil by cycling.

For many years dry natural gas has been passed through oil reservoirs to recover natural gasoline which would vaporize from the oil. Recently a process of recovering more of the high boiling hydrocarbons has been described by employing high pressures at which the heavier hydrocarbons have a higher volatility.¹⁶ Nevertheless, this reported method does not eliminate the differential nature of the vaporization process and capillary forces are still present in the reservoir. The process under discussion in this paper would minimize differential vaporization and would remove capillary forces which are responsible for low oil recoveries. Higher gas pressures are required to accomplish this removal of the meniscus, but it does not follow that more gas is required for oil recovery. The process is limited to reservoirs deep enough to permit the use of the required pressure—probably 6,000 ft and deeper.

DESCRIPTION OF THE PROCESS

Briefly, the process is to compress natural gas into an oil reservoir which is partially depleted so that it has an oil saturation in the range of 40 to 60 per cent of the hydrocarbon pore space. The injected gas will pass through the channels formerly carrying gas to the wells to build up the pressure and dissolve in the oil phase. This injection will continue without production from the field until the reservoir reaches a single phase. If one were to select unique conditions such that the gas composition, the reservoir oil composition and the per cent saturation would bring the mixture in the reservoir to the critical temperature and pressure simultaneously the phase behavior accompanying injection is shown by Fig. 1.⁶ The oil-gas mixture in the depleted reservoir has a critical temperature at C_1 . Addition of natural gas to the mixture will give a new critical temperature for each addition. Mixture No. 3 is shown to have its critical temperature at the reservoir temperature and reservoir pressure at P_3 , the critical pressure. Under ideal behavior, the entire reservoir would be at its critical temperature and pressure and the entire hydrocarbon content would be at a single phase.

If the reservoir content were a binary system of methane and a heavy constituent, it would be miscible with more methane. However, for complex mixtures the critical locus does not confine the two phase region, and the dew point curves of Fig. 1 occur above the critical locus. If fluid which was injected into the reservoir at the critical point were of the

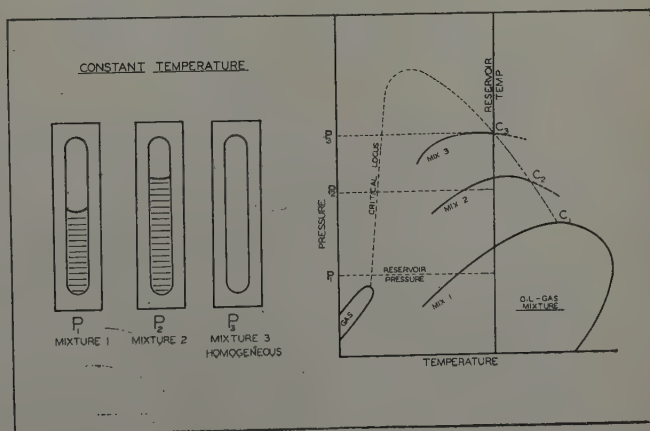


FIG. 1 — EFFECT OF ADDING GAS TO PARTIALLY DEPLETED CONSTANT VOLUME OIL RESERVOIR.

¹⁶References given at end of paper.
Manuscript received in the Petroleum Branch office Aug. 20, 1951.
Paper presented at the Fall Meeting of the Petroleum Branch in Oklahoma City, Okla., Oct. 8-5, 1951.

same composition as the reservoir fluid, obviously these fluids would be miscible. It is believed that injected fluid containing the more volatile and intermediate constituents without the less volatile constituents would also be miscible at the increased pressure resulting from injection of such gas. The injection of relatively pure methane could require considerably higher pressures before one reached a condition of complete miscibility.

In case only dry gas were available for injection and some liquid did precipitate at the front between the reservoir fluid and the displacing gas at pressures above the critical locus, it is quite possible that such liquid would revaporize in a differential manner and not seriously interfere with the displacing process. Such a process is more nearly like the differential process described¹⁰ excepting that only a relatively small fraction of the reservoir fluid at the displacing front is involved.

The usual reservoir and gas mixture when compressed will likely cause the reservoir to become liquid full at single phase, Fig. 2A. Under this condition, the single phase liquid could be produced much as a virgin reservoir. This second production could be halted as gas/oil ratios increased and a gas phase was created which could be used as channels for a subsequent repressuring to a higher pressure at which a single phase miscible with gas could be attained.

Some reservoirs would reach a dew point upon injection of natural gas, Fig. 2B. This dew point mixture is miscible with natural gas at a slightly increased pressure and could be cycled.

Cycling of reservoirs which have been brought to a single phase by gas injection would be generally similar to current practice, except that penalties for allowing the reservoir pressure to drop would be more severe.

The process depends upon the ability to vaporize mixtures by compression of natural gas over crude oils. The phase relations of oil-gas mixtures will be considered to find the necessary pressures.

PHASE RELATIONS FOR COMPRESSION OF GAS OVER CRUDE OILS

Over 10 years have passed since the writer observed that a condensate from a vapor phase at 9,300 psi and 120°F has most of the properties of a crude oil, except the presence of asphalt.¹⁴ In the school year 1941-42, students designed a plant to separate lubricating oil from asphaltic crude oils by

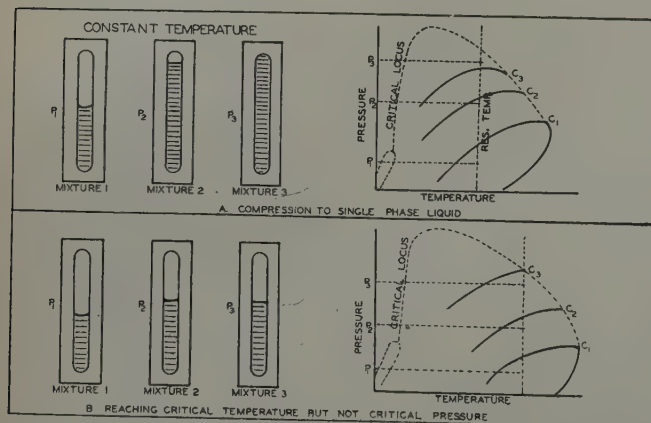


FIG. 2 — ALTERNATE POSSIBILITIES UPON GAS INJECTION.

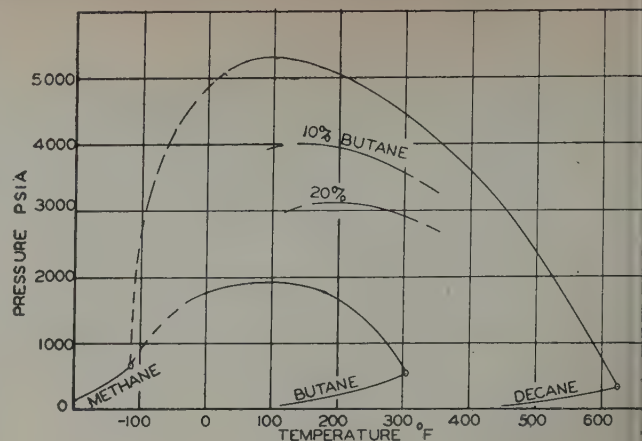


FIG. 3 — CRITICAL LOCUS FOR METHANE-BUTANE-DECANE SYSTEM

fractional retrograde condensation from gas phases at moderate temperatures and pressures around 8,000-10,000 psia. It was evident that the pressure required for vaporization of heavy oils was related to the total composition of the mixture or in particular to the concentration of ethane, propane, butane, etc.

Several crude oil-natural gas systems have been investigated to indicate the pressures required to bring mixtures to a single phase miscible with gas. However, it is worthwhile to consider a simpler ternary system to develop the principles involved.

THE METHANE-BUTANE-DECANE SYSTEM

Sage, Lacey and co-workers^{11,12,13} have studied the methane-butane-decane ternary system. Fig. 3 indicates the nature of the critical locus for the binary mixtures and the nature of the locus for some ternary mixtures. It may be seen that mixtures composed only of methane and decane may require compression to 5,000 psia to bring them to the critical pressure while the addition of butane to the mixture will lower the pressure for reaching the critical condition. Fig. 4 shows the lowering of the critical pressure by butane addition.

At any given pressure, the vaporization characteristics depend upon the degree of approach to the critical pressure which in turn depends on the mixture composition. Fig. 5 shows the effect of butane concentration upon the ability of the vapor to carry decane. It may be seen that the effect of butane on the decane carrying capacity of methane is increasing with increased pressure.

Consider the compression at 280°F of a system composed of 14.3 mol per cent decane and 85.7 per cent methane. It would be in the two phase region until the pressure reaches 4,600 psia, the critical pressure, and above that pressure, it would be in the single phase region. If a mixture of 10 per cent decane, 20 per cent butane, and 70 per cent methane were compressed at 280°F, it would become a single phase at 3,000 psia. The addition of butane, or any intermediate constituent, lowers the critical pressure and the dew point pressure for the mixture.

Suppose the methane-decane mixture were present in porous media at 4,000 psia and 280°F. It would be in the two phase region and capillary forces would be present. The addition of natural gas to displace the mixture from the porous media would bring relative permeabilities into play, with gas flowing preferentially to the liquid. If the mixture had been com-

pressed to a pressure greater than 4,600 psia in the media prior to the injection of the displacing gas, capillary forces would be absent and the displacing gas could completely displace the methane-decane mixture from the media.

If the methane-butane (70-20-10) mixture had been in the media, it could have been displaced as a vapor at pressures just above 3,000 psia.

Information on the miscibility of natural gas with a crude oil-natural gas mixture which has been brought to the critical condition, such as in Fig. 1, may be gained from the ternary system. Fig. 5a taken from Reamer, Sage and Lacey¹³ may be used to illustrate the problem and give a solution for the three component system. Consider a reservoir liquid at 1,000 psia of the composition indicated by point *A* (20 mol per cent methane, 36 per cent butane, and 44 per cent decane) to which is added gas of composition *B* (85 per cent methane, 15 per cent butane) with increasing pressure. At point *C* (70 per cent methane, 20 per cent butane, and 10 per cent decane) the total mixture would be at its critical point if the pressure were at 3,000 psia and could correspond to point *C* on Fig. 1. If more gas of composition *B* were added to the critical mixture, it would be miscible with the gas. However, should pure methane (point *D*) be added to this critical mixture *C* at 3,000 psia, the mixture would be in the two phase region along line *CD* until point *E* was reached. It may be seen that if the addition of methane to the critical mixture at *C* should have been accompanied by a pressure rise to around 3,250 psia, the new mixtures would not be in the two-phase region.

PHASE DIAGRAMS FOR COMPLEX MIXTURES

The author became convinced some 10 years ago that phase diagrams should be measured for complex hydrocarbon systems upon which vapor-liquid equilibria data were obtained. To that end phase diagrams were estimated for the systems

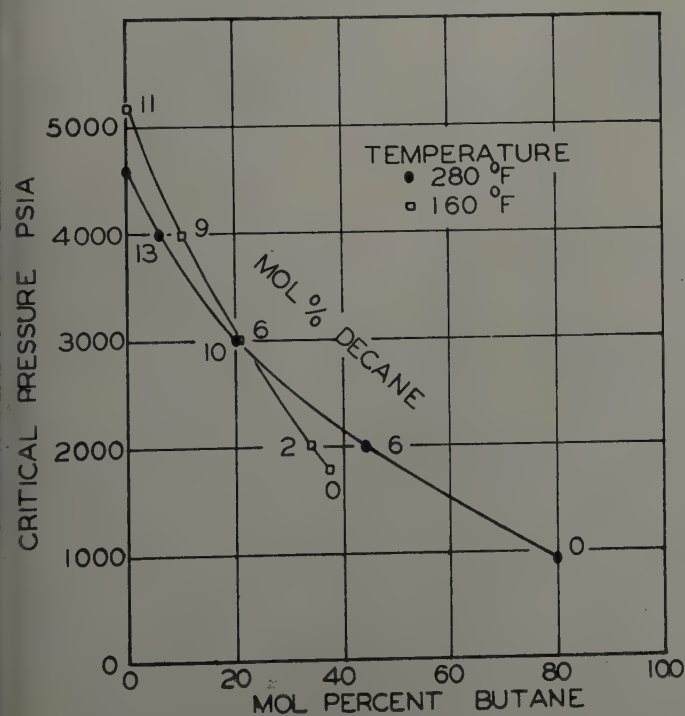


FIG. 4—CRITICAL PRESSURES FOR METHANE-BUTANE-DECANE SYSTEM.

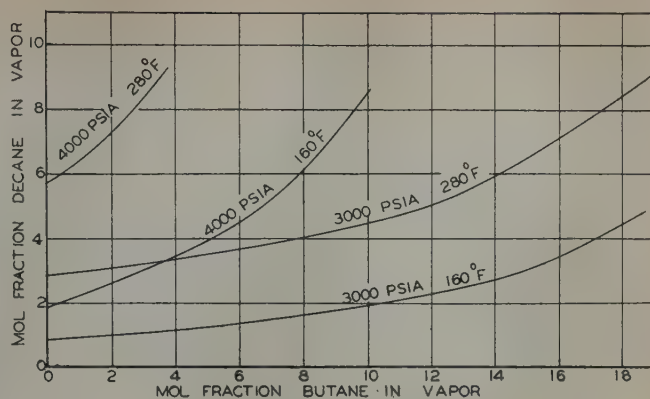


FIG. 5—EFFECT OF BUTANE CONCENTRATION ON DECANE VAPORIZATION.

studied by Standing¹⁵ and Roland.¹⁴ The natural gas-crude oil mixtures employed are given on Table I along with the estimated pressures at which they become single phases. The phase behavior of many condensate systems has been determined. A few condensate systems are included in Table I.

The pressure at which a given mixture of natural gas and crude oil will reach a single phase is of prime importance in the proposed process. This pressure may be computed from equilibrium constants¹⁰ by calculations which are rather involved and which require a careful analysis of the higher boiling constituents. The pressure may be determined experimentally in the laboratory. To give some idea of the single phase pressures and the influence of intermediate constituents, Fig. 6 has been prepared. The ratio of the methane concentration, mol fraction, to the combined concentration of ethane, propane and butane is plotted as a function of the single phase (dew point) pressure. It is known that the total composition of the system must be considered but this simplification may be some guide to the influence of the concentration of intermediate constituents.

Examination of the compositions in Table I is worthwhile from the standpoint of what causes a 9,300 psia dew point pressure for the crude oil-gas mixture¹⁴ while the rich condensate *A* is at its dew point at 4,000 psia. There is a minor difference in the molecular weight of the heptanes and heavier constituents, 198 as compared to 172, but the major difference is in the concentration of constituents ethane through hexane. It seems quite likely that if the ethane through hexane concentrations or ratio to methane had been as high for the crude oil as for condensate *A*, the crude oil-gas mixture would have become a single phase below 5,000 psia.

EFFECT OF ASPHALT ON DEW POINTS

One of the problems to be faced when compressing natural gas over crude oils containing asphaltic constituents is whether these asphaltic constituents will vaporize. If they do not vaporize continuously with the other high boiling constituents, they will form a plastic solid phase in equilibrium with the gaseous phase. Thus, some of the pores in the porous media may be filled with this plastic solid.

Some indication of unusual dew point phenomena has been found by the writer when discussing the experiences of different laboratories. Generally the dew point is sharp, or slight

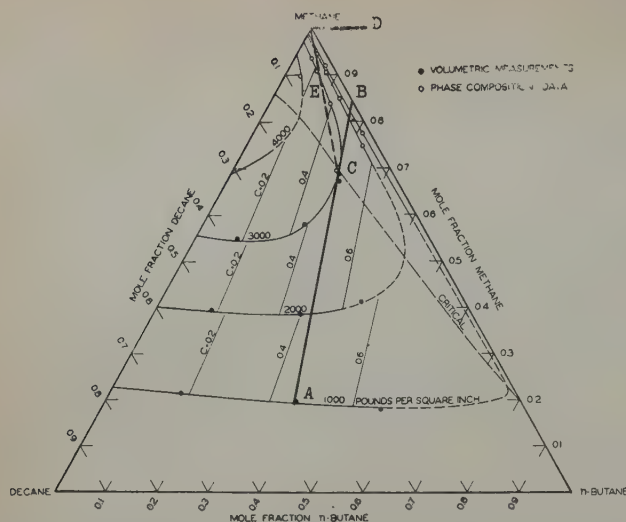


FIG. 5a — COMPOSITION OF COEXISTING PHASES IN METHANE-BUTANE-DECANE SYSTEM AT 280°F AFTER REAMER, SAGE AND LACEY¹³ USED TO ILLUSTRATE MISCIBILITY OF GASES WITH CRITICAL MIXTURES.

decreases in pressure cause large quantities of liquid to form by retrograde condensation as shown on Fig. 7 for condensate A. However, for some mixtures containing small amounts of high boiling constituents, the first unit of liquid formation requires a relatively large pressure drop as shown by curve B, Fig. 7. The presence of asphaltic constituents which would resist vaporizations would cause a similar behavior near the dew point since the dew point no longer would exist as a definite point capable of determination. Curve C represents the author's concept of the effect of asphalt in the absence of any data. Some asphaltic constituents may vaporize, but the "pseudo dew point," point D for mixture C on Fig. 7, should be considered as the top pressure for compression of a reservoir containing crude oil with an asphalt content which would give a condensation curve similar to curve C.

RESERVOIR PROBLEMS

There are many problems of phase behavior and fluid flow which must be considered for the compression of natural gas into a partially depleted crude oil reservoir to bring it to a single phase. The pressures required may be considerably higher than those originally present in the reservoir. How high a pressure can be used in a reservoir? The best answer known by the writer is that pressure just below the well pressure which parts or fractures the formation. No accurate figure for various areas is available, but it is likely to be from 0.8 to 1.2 psi per foot of depth. Thus, a 6,000 ft reservoir would likely stand 4,800 psi pressure and this pressure could be sufficient to vaporize some crude oils if a gas rich in intermediate constituents were used. The process should be considered for reservoirs at depths of about 6,000 ft and more. Reservoirs at 10,000 ft would give a high degree of latitude in safety and ability to vaporize crude oils.

One of the main problems is to introduce the gas so that it will go into solution throughout the reservoir. For a partially depleted reservoir with high producing gas/oil ratios, the injected gas should pass through the porous media without displacing much liquid except near the injection well. With pressure increases in the reservoir, the liquid will swell in

Table I — Compositions of Complex Mixtures
Mol Per Cent

	Crude oil-gas ¹⁴	Crude oil-gas ¹⁵	Paloma Condensate ⁵	Condensate A ⁹	Condensate B ⁹	Condensate C ⁹
carbon dioxide		0.42	0.77	0.45		
methane	81.11	75.86	71.92	64.38	80.68	73.81
ethane	3.91	3.46	8.28	7.36	5.73	6.37
propane	1.96	1.48	5.23	5.93	3.41	5.10
butanes	1.63	1.62	3.27	5.71	2.11	3.38
pentanes	1.11	5.22	1.62	3.09	0.95	2.25
hexanes	1.20	3.96	8.91	2.48	0.62	1.40
heptanes	9.08	7.98		10.60	6.50	7.69
sp. gr. C ₇	.8268	.850	.798	.806	.823	.801
mol wt C ₇	198.	199.	137.	172.	175.	137.
dew point pressure psia	9,300.	8,500.	4,650.	4,000.	8,000.	4,250.
temperature °F	200	170	235	260	220	210
ratio C ₂ C ₃ C ₄	10.8	11.5	4.28	3.39	7.2	4.97
gas/oil ratio	4,700	3,660	6,777	3,340	8,520	6,280

volume and decrease the gas permeability. If the liquid percentage reaches some 90 per cent, no more gas may travel through the porous media. If subsequent compression does not bring the mixture to a single phase miscible with natural gas, it will be necessary to produce some of the liquid from the reservoir to give more room for the gas. A second injection would permit the entire reservoir to be raised to a critical pressure or a dew point.

At this point, it is interesting to note that the increase in pressure toward a critical pressure does not necessarily mean the liquid phase is swelling. For a constant composition system at its critical temperature, compression to the critical pressure will not increase the percentage liquid beyond some 50-55 per cent by volume. With changing composition at constant volume, there is no reason to expect high liquid saturations before reaching a critical pressure. This means that gas movement may continue throughout the reservoir as the critical pressure or dew point is approached. The amount of oil still in a reservoir and injection gas composition can become very important factors in the percentage gas phase in the reservoir and hence on gas movement throughout the reservoir.

There will be strata in the reservoir which will contain a higher saturation with oil than others. These strata will not

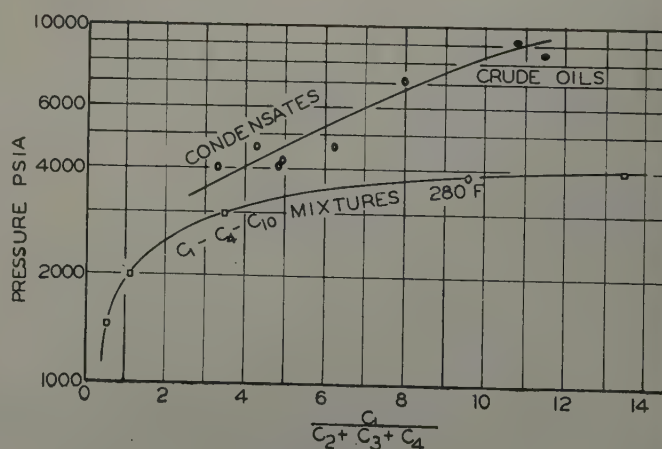


FIG. 6 — EFFECT OF INTERMEDIATE CONSTITUENTS ON PRESSURE FOR SINGLE PHASE.

like as much gas, and hence they will not be completely vaporized upon compression even though the oil in other zones might be completely vaporized.

Diffusion time for the gas to go into solution in oil with which it is in contact will be no problem for uniform porous media into which gas is flowing, but if it is expected that gas will travel either horizontally or vertically through liquid filled sand, diffusion will take far too long a time to put gas to solution.

To the extent that these items interfere with the ideal compression of the entire contents of a reservoir to a single phase, there will likely be differential processes which will increase the amount of gas injection required to recover the oil.

When reservoir pressures are employed which are considerably in excess of those originally in the reservoir, the competition of wells and corrosion of casing or fittings become of concern. Any abandoned wells in the reservoir should be plugged in a manner to make certain that leaks will not occur.

APPLICATION OF METHOD TO A FIELD BY STUDENTS

Students in petroleum production engineering at the University of Michigan^{2,7} were given the problem of designing a plant and making a cost estimate for compressing gas into a field followed by cycling to recover the crude oil. The characteristics of the oil and general data for the field correspond to the North Lindsay Reservoir, McClain County, Oklahoma.^{1,3,4} Since much of the data on the geology of the reservoir and other details were not available, assumptions were made. Thus, the field will be described as Field "A" as the formation is in part hypothetical and the results should not be considered as applying to a particular field. The results of the study are presented as a basis for discussion of the problem and decisions to be made on such a project.

Both groups assumed that they could purchase high pressure gas of the following composition—methane 86.1 mol per cent, ethane 7.5, propane 4.2, butanes 1.26 and pentanes plus

Table II — Summary of Data and Results for Student Design Problems: Data on Field A

	Group I*	Group II**
Depth, ft	10,700	10,700
Discovery pressure, psia	4,600	4,925
Reservoir Temp. °F	189	189
Initial Formation Volume Factor	2.2	3.073
Initial Solubility, cu ft/bbl	2,180	3,694
Reservoir Volume, MM bbl	24.	24.
Production, MM bbl	2.4	2.4
Gas Production, billion cu ft	10.0	10.0
Current Producing GOR cu ft/bbl	18,000	18,000

CALCULATED RESULTS

Current Equalized	1,440.	2,400.
Reservoir Pressure, psia		
Black Tank Crude Oil still in Reservoir, MM bbl	8.7	5.48
Minimum Pressure for Single Phase in Reservoir, psi	5,300	4,800
Pressure during Cycling, psi	6,000	5,300
Gas Required, billion cu ft	27.5	21.
Time to Inject Gas, years	1	1.5
Time to Cycle Field, years	3.25	9.5
Plant Capacity, MMcf/D	47.	17.
Production in Process, MM bbl	7.0	4.4
Gas Purchased per bbl oil recovered cu ft/bbl	3,950	4,800

*Based on analysis of reservoir fluid in Reference 1.
 **Based on analysis of reservoir fluid in Reference 3.

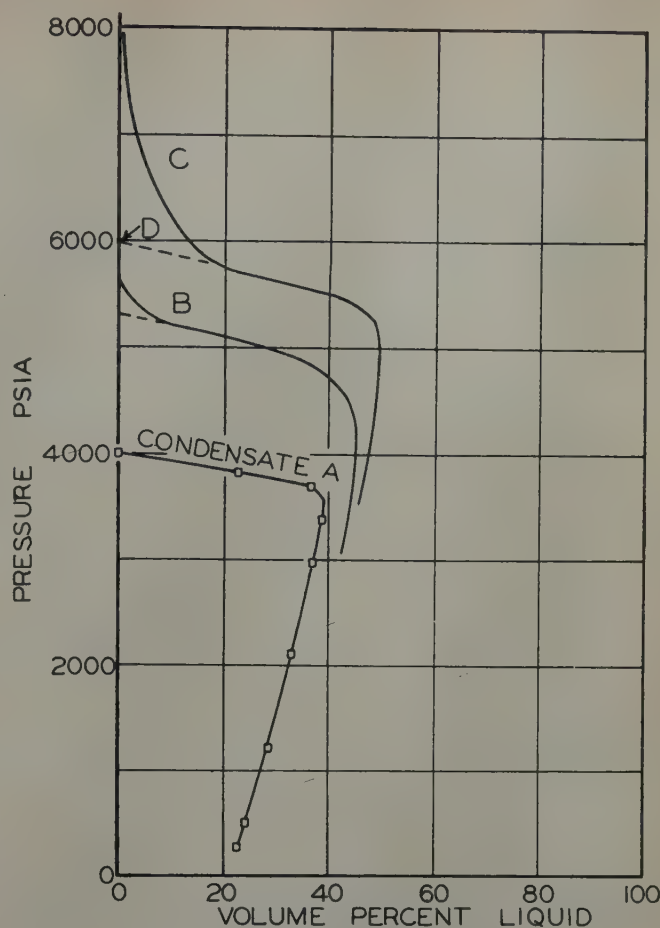


FIG. 7 — EFFECT OF ASPHALT ON DEW POINT.

0.94. A three stage operation is proposed. The first stage consists of gas injection without production from the field. The second stage consists of cycling at substantially constant pressure to recover the crude oil. The third stage is the production of gas for pipe line sale. The two groups of students made independent studies based on different compositions for the reservoir fluid and using different types of plants. Some of the results of these calculations are given in Table II.

Group I

This group based their calculations on the published data of crude oil behavior for the discovery well.¹ They computed that the reservoir would become single phase at 5,300 psi and be below its critical temperature at 189°F. At 6,000 psi they estimated that the displacing gas would become miscible with the reservoir fluid.

During the period of crude oil production, oil-gas separators, cooling equipment and compressors comprised the plant, since the wet gas was returned to the reservoir. Separators at 3,000, 1,000, 330, 100 and 30 psi were used, with 2,750 gas compression horsepower.

After substantially all the oil had been recovered, the wet gas in the field was produced for pipe line sale through 1,000 psi absorption equipment. The total plant cost was estimated as under three million dollars.

Group II

This group used the well fluid analysis published by engineers of the U. S. Bureau of Mines.⁸ They estimated that gas compression would bring the reservoir to a dew point at 4,800

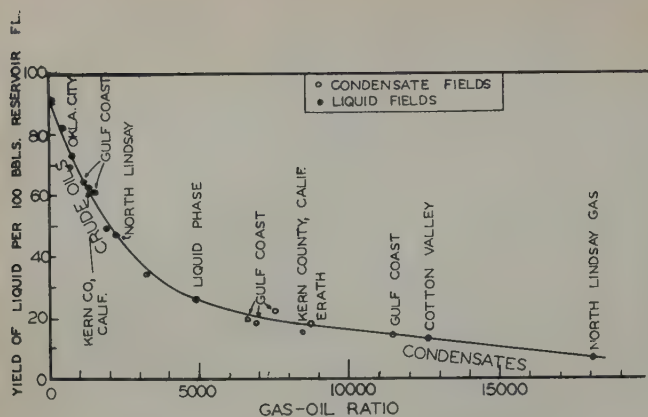


FIG. 8 — COMPARISON OF YIELDS.

psi and cycled at 5,300 psi. They recovered the natural gasoline and LPG during a normal cycling operation with absorbers operating at 2,800, 1,400, 800, 300 and 75 psi. The reservoir was full of dry gas at the end of the cycling. The plant cost for this operation was calculated to be around two million dollars.

Insufficient information was available to make studies of the effect of varying permeabilities on lack of reservoir equilibrium or premature break-through of cycling gas over the displaced fluid.

Needless to say, the costs of production in these idealistic calculations are low, but they constituted only one-fourth to one-half of the total income from product sales.

GAS REQUIREMENTS AND VALUE OF LPG CONSTITUENTS

A mixture which is at its critical temperature and at or above its critical pressure contains the greatest amount of crude oil per unit of gas in a state miscible with a gas phase. Fig. 8 shows the gas/oil ratio from separator operation at 200-500 psi for crude oils and condensates as a function of the yield of liquid per 100 bbl of reservoir fluid. Those mixtures between 3,000 and 5,000 cu ft/bbl are close to the critical temperature and represent the richest condensates. Crude oils may be brought to this state by injection of the proper composition gas. Added gas is required during cycling to maintain the reservoir pressure, and some gas will mix with the crude oil not recovered, bringing the total gas to 6,000-10,000 cu ft/bbl of oil recovered. This gas is available for reuse or resale at the end of the project, except for plant fuel requirements.

No study has been made of the value of LPG in reducing the maximum pressure required to vaporize a given oil. In some cases the enriching of injection gas may be necessary to obtain a single phase within the pressure range permissible in the reservoir. In other cases, it may be cheaper to use less enriched gas because of the lower pressure required. Consider the use of an enriched gas for vaporizing crude oil studied by Roland¹⁴ in place of the gas employed. The ratio of the volume of ethane through hexane fractions to the heptanes plus is 0.4 for the single phase mixture. In other words,

there is about 0.4 bbl of LPG and light natural gas per bbl of crude oil in the vaporized mixture at 9,500 psi. On the other hand, consider condensate A. This mixture contains one bbl of ethane through hexane per bbl of heptanes plus for the vapor at 4,000 psi. It is estimated that if the crude oil mixture would have had one bbl of intermediate constituents ethane through hexane per bbl of crude oil, it would have become a single phase at around 5,000 psi instead of at 9,500 psi. The 0.6 bbl of intermediate constituents per bbl of crude oil no doubt would reduce the pressure required bringing the reservoir to a single phase to around one-third the previous value.

Following these concepts, it would seem that a stockpile of natural gas and intermediate hydrocarbons ethane through butane or pentane might be accumulated and used in succeeding reservoirs over and over again. The investment per bbl of oil recovered in such a program requiring a very rich gas might be as follows:

8,000 cu ft gas @ 6 cents	= \$.48
0.6 bbl LPG @ \$1.68	= 1.01
	<hr/>
	\$1.49

If the investment were recovered in six years on the average, the cost at four per cent per year would be 38 cents per bbl of oil recovered for the use of the compression fluid.

CONCLUSIONS

Further study of the proposed process is recommended. Laboratory measurements should be made of the pressure required to bring given crude oils and various enriched gases to a single phase miscible with natural gas. At the present time, the author concludes that:

1. The proposed process is feasible for reservoirs of 6,000 psi and deeper which have characteristics which would permit cycling for condensate recovery.
2. It is possible to bring most crude oils of 35° API and higher to a single phase by the use of natural gas enriched with LPG. The asphaltic constituents present may not vaporize but become a plastic solid.
3. The compression of gas over oil to bring it to a single phase miscible with gas requires less gas circulation through the reservoir to recover a barrel of oil and should give higher recoveries than differential vaporization processes.
4. Problems of contacting the gas with the oil to realize ideal phase behavior in the reservoir may be serious.
5. Details economic studies on deep reservoirs are likely to show the process to be the most economical secondary recovery process for some of these reservoirs.

REFERENCES

1. Barnes, K.: *Oil and Gas Jour.*, No. 31, 76, (1946) 44.
2. Constan, G. L., Cornell, D., and Ebner, E. E.: Report Course C.M. 355, Group II, U. of Mich., (June, 1951)
3. Cook, A. B., et al.: *Petr. Eng.*, (1948) 19, 158.
4. Hatfield, J. R.: Private communication, Cities Service Oil Co.

5. Huber, T. A.: Private communication, Humble Oil & Refining Co.
6. Katz, D. L., and Williams, B.: AAPG Meeting, (April, 1951).
7. McNeese, C. R., Scott, J. O., and Stinson, D. L.: Report in Course C.M. 355, Group I, U. of Mich., (June, 1951).
8. Olds, R. H., Sage, B. H., and Lacey, W. N.: *Trans. AIME*, (1945), 160, 77.
9. Organick, E. I.: Private communication, United Gas Corp.
10. Organick, E. I., and Brown, G. G.: *Chem. Eng. Prog., Symposium Series, No. 2*, (1952) 48, 97.
11. Reamer, H. H., Olds, R. N., Sage, B. H., and Lacey, W. N.: *Ind. Eng. Chem.*, (1942) 34, 1526.
12. Reamer, H. H., Fiskin, J. M., and Sage, B. H.: *Ind. Eng. Chem.*, (1949) 41, 2871.
13. Reamer, H. H., Sage, B. H., and Lacey, W. N.: *Ind. Eng. Chem.*, (1951) 43, 1436.
14. Roland, C. H.: *Ind. Eng. Chem.*, (1945) 37, 930.
15. Standing, M. B., and Katz, D. L.: *Trans. AIME*, (1944) 155, 232.
16. Whorton, L. P., and Kieschnick, W. F.: *Oil and Gas Jour.*, (1950) 48, (48), 78.

DISCUSSION

By C. S. Matthews and J. G. Roof, Shell Oil Co., Houston, Tex., Members AIME.

Some of the confusion which has arisen concerning the concepts in this paper might have been avoided if, since the systems under consideration are essentially isothermal, the discussion had been referred to pressure-composition diagrams rather than the pressure-temperature diagrams shown in Figs. 1 and 2. Although a pertinent pressure-composition diagram was published at least as early as 1945 (Reference 8 of the paper), Allen¹ recently presented more detailed diagrams, one of which serves as the basis of Fig. A. From this diagram it is readily seen that the reservoir pressure must be increased to p_A to insure miscibility of reservoir fluid with separator gas during displacement by that gas. If the injected gas is rich in intermediate components, it is probable that the difference between p_A and the critical pressure will be reduced from that shown in Fig. A. However, the important idea is that from a diagram of this type, obtained for the crude oil and the proposed injection gas, one can readily recognize the minimum pressure required for miscibility.

That Katz is aware of this fact is indicated by his second paragraph under "Description of the Process." However, confusion arises when in a subsequent section the statement is made: "The pressure at which a given mixture of natural gas

and crude oil will reach a single phase is of prime importance in the proposed process." It is easily seen from Fig. A that the single-phase pressure for any given composition is of no importance. It is the position of the cricondenbar, p_A , which is of importance generally. In another section Katz makes the general statement, "This dew-point mixture is miscible with natural gas at a slightly increased pressure and could be cycled." The data of Allen¹ show that "slightly increased pressure" may mean thousands of pounds per square inch.

It is clear that there is the need for a study of the significance of pressure-composition diagrams for given systems. Consider a partially depleted constant volume reservoir into which gas is injected until a dew point is reached. This dew-point gas is not necessarily miscible with additional gas during subsequent cycling at constant pressure. It is the cricondenbar rather than the dew-point pressure which determines the minimum pressure for achieving complete miscibility. Therefore, it is questioned whether the data in Fig. 6 and Table I have any bearing on the problem. The dew point pressure so reported tells nothing about the pressure required for miscibility. The data presented by Allen¹ give significant informa-

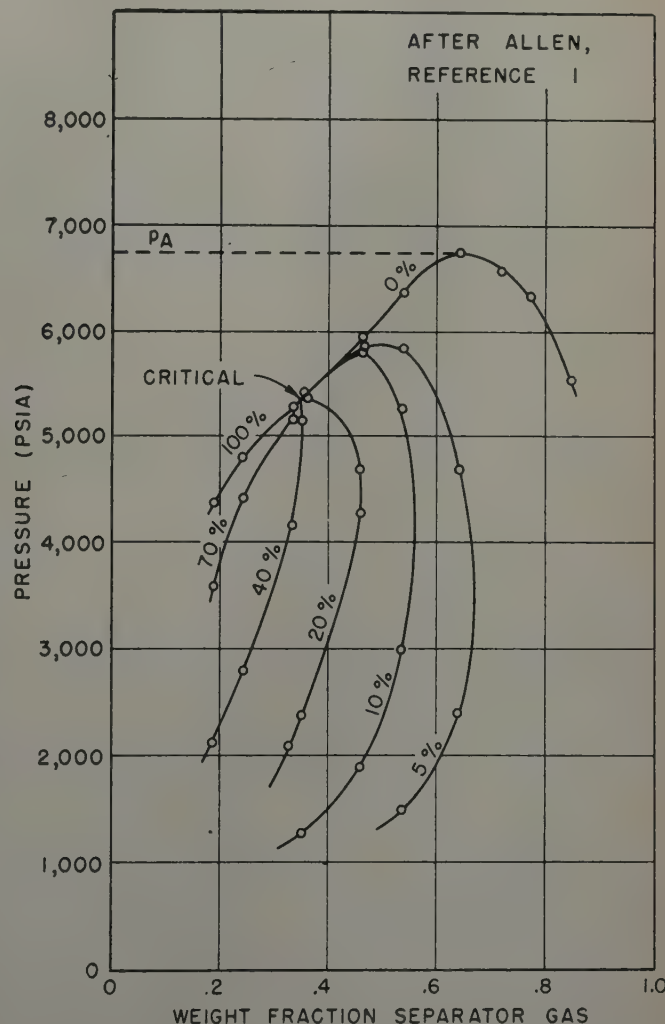


FIG. A — PRESSURE-COMPOSITION DIAGRAM AT 251°F, GULF COAST CONDENSATE FIELD.

tion in this regard. Allen's data indicate that the cricondenbar (or minimum pressure for miscibility) will generally be not lower than 7,000 psi for mixtures of high-gravity black oil and separator gas. Only for condensate liquids (as illustrated in Fig. A) is the difference between the cricondenbar and the critical pressure of a low order of magnitude.

The operation proposed in this paper differs from that discussed by Whorton and Kieschnick in 1951 (Reference 16) only in that it is now proposed to operate at all times in the one-phase region which, for the type of systems under consideration, means operating at or above the cricondenbar, p_A .

REFERENCE

1. Allen, J. C.: "Factors Affecting the Classification of Oil and Gas Wells" paper presented at the Spring Meeting of the Southwestern District, Division of Production, API, Shreveport, La., March 5, 6, 7, 1952.

AUTHOR'S REPLY TO MESSRS. MATTHEWS AND ROOF

The author agrees heartily that the paper by Allen is most helpful in presenting data which answer questions raised in the paper. Allen's paper was not available until some six months after the paper under discussion was prepared and presented. It should be pointed out that Allen presented other systems in figures similar to Fig. A, two of which show the dew points rising only about 200 and 500 psi respectively above the critical pressure while two other systems have rises greater than that shown in Fig. A.

Matthews and Roof apparently did not understand the main point to the paper, *i.e.*, the value of bringing the entire reservoir to a single phase *before* displacing the contents of the reservoir. Their point that the pressure at which the returned

gas is miscible with such a single phase may be considerably higher than the single phase pressure is well taken. If they had data similar to that published by Allen, presentation of the facts at the time this paper was presented would seem to have constituted a more informative discussion. Granted that complete miscibility of returned gas with a single phase reservoir fluid may require too high a pressure to be practical for some reservoirs, there may be many for which the pressures are not above practical limits. In those cases, the reduction in gas requirement for high oil recovery is a factor of two or three less than passing gas through the reservoir at a pressure some 80 per cent of that required to bring the reservoir to a single phase.

Consider the case of a reservoir brought to a single phase at 6,500 psi but with a pressure requirement of 8,500 psi for complete miscibility of the reservoir contents with the returned gas. Consider further that it is not practical to cycle at pressures above 7,000 psi and so cycling is started at this mean reservoir pressure. Only at the interface between the single phase reservoir fluid and the returned gas will precipitation occur. The gas at this interface would likely attain a composition such that further precipitation would be minimized as cycling progresses. The condensate formed would then be recovered by the returned gas to the extent that the differential process described in Reference 16 is sufficient for such recovery.

It should be mentioned that this paper and discussion has the same significance for cycling rich condensate reservoirs as for recovery of crude oils. Matthews and Roof are saying that it may be necessary to cycle such a reservoir at a 1,000 psi or more above the dew point. The emphasis of my paper is something generally recognized for condensate reservoirs, *i.e.*, it is a much more efficient operation to cycle at or above the dew point pressure than at some 80 per cent of the dew point (single phase) pressure.

★ ★ ★

THE STRATAFLOW PROCESS: A RECENT DEVELOPMENT IN LOCATING WATER ENTRY IN WELLS

RALPH E. HARTLINE, STANOLIND OIL AND GAS CO., TULSA, OKLA., AND WILFRED TAPPER, HALLIBURTON OIL WELL CEMENTING CO., DUNCAN, OKLA., MEMBER AIME

ABSTRACT

The Strataflow process for locating water entry in producing wells is now available. This method as now practiced utilizes the fact that fluids of different salinities have different electrical resistivities. By introducing into the well a fluid of a markedly different salinity than that of the fluid being produced, a pronounced resistivity change will occur at the point of entry. By running a Strataflow survey the points of major and minor water entry may be interpreted from changes in the resistivity of fluid in the hole.

Strataflow results are obtained with the well operating under almost normal producing conditions, and are a logical primary step in any workover program, having as its purpose shutting off of the water.

INTRODUCTION

Water production is a serious problem in many producing oil wells. It certainly increases lifting costs and in some cases presents a disposal problem. It often aggravates corrosion problems and can even endanger oil production. With accurate information to guide an effective workover program, many marginal wells could be restored to profitable production.

The shortcomings of previous meth-

ods of water entry location were recognized. The Strataflow process is the result of several years of development and field testing directed toward overcoming these limitations. It represents the continued development of a process reported by Silverman and Brown.¹ The earlier work established the basic soundness of fresh-to-salt water resistivity contrast in delineating zones of water entry, but its application was limited by the difficulty of maintaining static balance of the well during preparation for the test. A more serious deterrent to its use, however, was its unadaptability to existing well logging service equipment and field operating methods.

STRATAFLOW PRINCIPLE

The general principle of the new method involves, first, conditioning the well by displacing the fluid in the bore of the well adjacent to the zone to be tested by a conditioning fluid which is miscible with the formation fluid. This displacement is carried out without interruption of the well production. The conditioning fluid must have some measurable physical, chemical, nuclear, or electrical property which is distinctive from that of the formation fluid. As the well continues to produce, formation liquid entering the well bore dilutes the conditioning fluid so that

zones of entry may be determined by making a log of the property undergoing change. This general principle may be applied to indicate zones of either water or oil entry by suitable selection of conditioning fluid and proper logging equipment.

The Strataflow process, as it is currently practiced for water entry location, uses fresh water as the conditioning fluid and depends for its operation upon the marked difference of electrical resistivity between this fresh water and the salty water produced by the formations. If possible, any necessary modifications of the well equipment are made a week or so before the test. The well is then returned to normal production. On the day the test is to be carried out, the conditioning water is landed at the bottom of the well and the test is made without interrupting production except for a brief period required for the conditioning water to consolidate into a continuous column extending to a point well above the test section. With this general description of the process in mind, a more detailed step-by-step description of the process will be clearer.

PRELIMINARY PREPARATION OF WELL

The Strataflow survey, as it is currently practiced for water entry location, is applicable only to pumping wells. Since the required electrical measurements are made by a special

¹References given at end of paper.
Manuscript received in the office of the Petroleum Branch Feb. 8, 1952. Paper presented at the Annual Meeting of the AIME in New York City, Feb. 18-21, 1952.

fluid resistivity measuring electrode lowered down the well annulus, the tubing head is removed and the tubing string hung on a clamp in order to make the annulus accessible, unless the well is already equipped with an offset tubing head, particularly designed to admit an instrument into the annulus. Such an offset head is required on any well that might occasionally flow.

The electrode is one inch in diameter and can be run in any well in which the inside diameter of the casing exceeds the diameter of the tubing collar by at least one and one-half in. This means that in wells with 5½-in. casing and 2½-in. EUE tubing, it is necessary to change to a 2-in. tubing string prior to the test. Since the operation of the process is such that zones of water entry can be established only in sections of the well in which the conditioning water can be landed, it is desirable to set the pump inlet as low as possible. This sometimes makes it necessary to pull the tubing and replace the mud or gas anchor with a short perforated nipple. Below the pump inlet only aggregate production of water can be determined. This is done in a separate step in the testing procedure.

A careful check for tubing leaks should be made and any leaks detected should be corrected during the well preparation. This is necessary since the method would detect salt water entering the annulus from a tubing leak equally as well as that entering from the formation. The well is then returned to production and, if possible, operated continuously up to the time of the test. Several days' or a week's operation is desirable to insure that all formations are producing their normal fluids.

PURGING AND CONDITIONING

A supply of fresh water adequate for the test is provided by the well operator. A portable stock tank is used for storage if water is not available on location. A 100-bbl tank is adequate for most well testing. It is desirable to have a resistivity contrast between the conditioning water and that produced by the formation of at least four to one. In the case of wells producing brackish or comparatively fresh water, satisfactory Strataflow tests have been made using a conditioning water of lower resistance than that of the formation water. This can be prepared by adding salt to the water produced by the well.

On the day preceding the test a stream of fresh water is started into the

casing at the well head and continued until the time of the actual test. The rate of injection is adjusted at approximately one-half the rate of total oil and water production of the well. This rate, however, is not critical, and supervision is not required to maintain it constant.

The circulation of water in this manner through the well annulus serves to purge the casing and standing oil column of water-soluble electrolytes and insures that the water landing at the bottom just prior to the test will have the maximum possible electrical resistance. The water continuously in transit through the oil column serves as a reservoir to supply the conditioning water required for the test.

On the day of the test service equipment is set up on the well, which is continued on pump until the fluid resistivity measuring electrode is run down the annulus to the bottom of the hole. The location of the pump inlet should be checked by observation of the sharp resistivity contrast at the oil-water interface, which always stabilizes at the pump inlet.

The injection of fresh water is then stopped, and the well is shut in temporarily to permit conditioning water, after falling through the oil, to consolidate in the annulus and form a continuous column from the pump inlet upward and beyond. The time required for this waiting period is difficult to estimate, but the progress of the water accumulation may be followed by scanning the well bore with the logging electrode. Twenty to thirty minutes is a typical example. During this interval the formation continues to produce so that the lower section of the column is progressively contaminated by salt water from the formation. A preliminary log of the fluid resistivity in the hole is made prior to the test to ascertain the resistance and the quantity of fresh water standing above the zone to be surveyed.

THE STRATAFLOW TEST

As soon as fresh water has accumulated to a point well above the top of the zone of interest, the "drawdown" step of the test is started by returning the well to production. Fresh water injection may also be resumed, as the input rate of fresh water into the annulus serves as an effective means of controlling the rate of production from the formation. For example, if fresh water is admitted at 30 per cent of the total production rate, the well will stabilize

with 70 per cent of the fluid delivered to the surface being produced by the formation. By adjusting the rate of fresh-water input, the operator has a positive and convenient means of controlling the formation production. The injected water also replenishes the conditioning water in the standing column and prolongs the period over which the well test can be run.

Additional water injection may be omitted if control of formation producing rate is not necessary, and if the supply of water in the consolidated water column is large enough to carry out the test.

As the well is produced, the resistivity electrode is run in the annulus to produce a log of the resistivity of the fluid mixture in the zone under test. Successive records are made at frequent intervals so the operator can study the resistivity pattern as it develops. The logging speed is not critical, and experience has shown that there is a little tendency toward distortion of the pattern due to movement of the electrode.

Since the pump inlet is near the bottom of the hole, the movement of all water in the fluid column is downward. The high-resistance conditioning water, in passing formations producing salt water, has its resistance lowered. As the well production stabilizes, the downward flow of the column of fresh water and the flow of formation water into the column, both approach stable values. The change in resistivity across any producing horizon therefore reaches a value dependent upon the rate of formation production. In contrast, the fluid resistivity in the liquid column remains unchanged through sections of the bore hole where no salt water production occurs. This resistivity pattern is characteristic of the water productivity of the well formations.

When the characteristic resistivity pattern has developed, it is stable and can be repeated as long as production is continued and a supply of fresh water is available in the standing column above the zone of test. The way in which this pattern develops from the initial fluid-resistivity record varies with the method of well treatment but more specifically with the water-producing capabilities of the formations. In wells having a high productivity index, the preliminary log of this resistivity run just prior to the drawdown often shows all of the significant features of the final water productivity profile, and the fully stable pattern is developed in a few minutes of testing.

In most other wells, significant features, particularly in the upper sections

the hole, may be indicated in the first few minutes of testing, but 15 to 30 minutes are required to develop a reliable pattern. The test should be extended considerably beyond this time to ensure that each stratum has reached producing equilibrium.

The water resistivity pattern developed by this drawdown step is capable of showing water-entry zones only down to the pump inlet. Wells having bottom water usually show a sharp resistivity drop at the pump inlet but this alone is not a diagnostic feature. Bottom water can be more positively indicated in an additional step of the test procedure, the "buildup." Water injection is stopped, and pumping is discontinued. All fluids produced now move up the well. Bottom water is indicated by an upward movement of the sharp resistivity change originally occurring at the pump inlet. The initial rate of this movement permits an estimate of the rate of bottom water production.

It is advisable to make several draw-down and buildup tests during the course of each Strataflow survey. A brief buildup should be made early, perhaps before the final resistivity pattern is fully developed. Knowledge of bottom water from such a buildup is helpful in planning the remainder of the test.

STRATAFLOW RESULTS

The Strataflow method of water-entry location has recently been made available to the industry as a commercial well service. A workover done on Continental Oil Co. No. 4 B. B. Ainsworth in the Genesee Field, Rice County, Kansas, is of particular interest since it was done in such a way as to test the accuracy of the interpretation of a Strataflow survey for water entry. The daily production of the well prior to the survey was about 60 bbl of oil and 200 bbl of water.

Table I

Zone	Strataflow Interpretation
Above 3,136	No water entry
3,136 - 3,141	Water entry
3,141 - 3,153	Minor entry
3,153 - 3,157	Major water entry
3,157 - TD	No entry

The Strataflow survey was made in the manner that has been described. Several of the resistivity profiles obtained during the testing procedure are shown in Fig. 1. Individual profiles have been offset on the resistivity scale for the sake of clarity of presentation. Keeping in mind that zones in which no water is produced show a constant fluid resistivity and that sections showing changes of resistivity are indicative of zones of water entry, the interpretation shown in Table I becomes clearly evident.

The entry at 3,153-3,157 ft is considered more prolific than that at 3,130-3,141, since a proportionately greater amount of salt is required to make a given change in fluid resistivity at high salt concentration than at lower concentrations.

In testing the accuracy of the above interpretation, the well was cemented to the casing seat and then progressively redrilled through the producing horizon with periodic production tests made by swabbing. The results of these tests are shown in Table II. It is evident that no water is produced above 3,125. The water produced during four hours of swabbing at 3,131 was progressively decreasing and it appears that any water produced at this level was minor. The top of the water indicated by the Strataflow survey was 3,136.

The hole was then plugged back a second time with 30 sacks of cement. Hole was made to 3,095 ft when 300 ft of oil stood in the hole. At 3,112 ft oil was swabbed at 17 bbl per hour with no water. This substantiated the first plugback test at 3,111 ft, and the well was completed at this total depth. A 24-hour production on pump gave 336 B/D of oil with no water.

STRATAFLOW ADVANTAGES

An important advantage of the Strat-flow method is that the record is made with the well operating under conditions almost identical to those which exist in normal production of the well. In the case of wells having a moderate

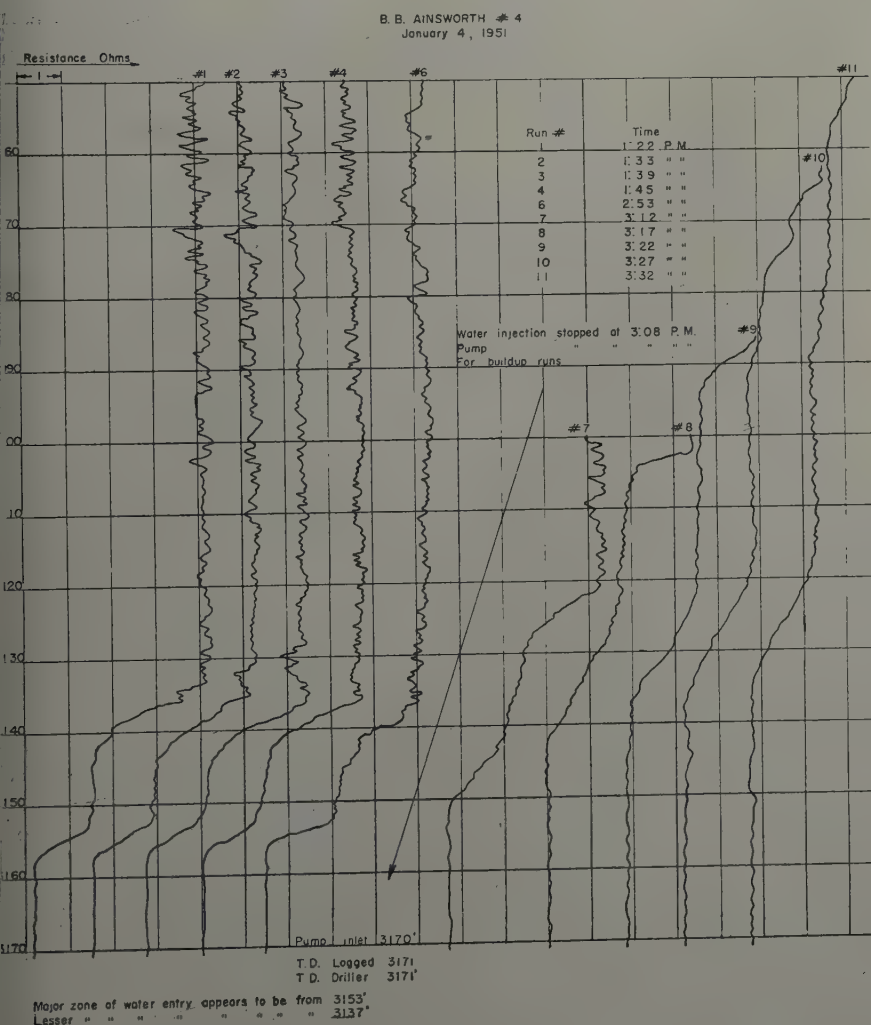


FIG. 1 — STRATAFLOW TEST, CONTINENTAL OIL CO. B. B. AINSWORTH NO. 4, JAN. 4, 1951.

to low productivity index, it is doubtful if other fluid-entry methods produce the well to an extent sufficient to develop the characteristic production of each formation. In the Strataflow procedure, except for the temporary shut-down for water consolidation, the well is produced continuously prior to and during the test, and at no time is the well likely to approach static equilibrium. There is, therefore, little danger of low pressure formations being flooded by foreign fluids. Each formation, whether water- or oil-producing, produces its normal fluid prior to and throughout the full test period.

The Strataflow method of water-entry location is dependable, easy to interpret, widely applicable and economically practical. This is borne out by the following features, many of which are unique among methods of water-entry location.

The survey provides a continuous log which clearly indicates those zones from which water is entering the bore hole. Quantitative interpretation of the log is possible by reference to the per cent salt calibration of the electrode.

The method can be applied to any ordinary type of pumping well, regardless of the total production rate and the per cent water production. This includes wells producing hydrogen sulfide and those completed in limestone or dolomitic formations.

Operation of the electrode in the annulus yields a saving in cost. This is based on the fact that in wells where no mud anchor is normally used, and in which the tubing is of a size small enough to afford adequate electrode clearance in the annulus, there is no need to pull and rerun the tubing and rod strings. In these cases all that is required is to remove the normal well-head seal and lower the tubing string sufficiently to set the pump inlet close to bottom.

It is not necessary to have a pulling unit stand by during the survey. Conducting of the actual well test is carried out with the use of Strataflow equipment only, and the only pulling unit time required is that necessary to prepare for the test and to return the well to its normal condition after the test. The survey can usually be conducted in a period of 24 hours with about eight to ten hours working time.

In conclusion, it may be said that the Strataflow survey is a logical investigative step to be taken on any well upon which a workover to shut off the water is contemplated. By combining water-entry location service with oil well cementing facilities, it is pos-

Table II

Depth Drilled	Fluid Swabbed in BBL per Hour			
	First Plugback		Second Plugback	
	Oil	Water	Oil	Water
3,100	6	---		
3,105	12	---	6	---
3,111	17	---		
3,112			17 ^e	
3,115	17	---		
3,120	17	1/4 ^a		
3,125 ^b				
3,131	{ 18 ^c 18 ^c	11		7 ^d
3,137	20	26		
3,145	12	21		

a. Water disappeared after 16 hours of swabbing.

b. At 3,125 ft, 2,200 ft of fluid stood in the hole. No water was recovered from bailer run to bottom.

c. Results of two separate 2-hour swab tests.

d. Hourly water production rate decreased during the test.

e. New plugback TD.

sible to undertake the broad problem of finding and shutting off the water.

ACKNOWLEDGMENT

The authors wish to express their appreciation to the Continental Oil Co. for granting permission to publish results of their testing during the workover of the B. B. Ainsworth well.

REFERENCES

1. Silverman, D., and Brown, A. R.: "Location of Points of Water Entry in Oil Wells," *Trans. AIME*, (1948) 174, 286.

DISCUSSION

By J. T. Gary, *Continental Oil Co., Wichita, Kans., Member AIME.*

The Strataflow process for locating water entry in wells appears to be an improvement over previous methods and may develop into a tool of extreme importance, especially for use in Kansas where the control of water production is of vital concern. The authors' paper should be considered as a progress report as much remains to be done in further developing the process and it is felt that additional uses for the tool will be developed. The authors have presented an accurate account of the results of the survey run of the B. B. Ainsworth well No. 4.

One limitation to the Strataflow process, which the authors did not mention, was found when a survey was run, on another well in the Genesco Field. In this particular well, the hole was deepened in the Arbuckle below a former plug back depth for the express purpose of determining whether any water-free oil zones existed below an upper water zone which had been plugged

off. The Strataflow survey did not pick up any zone of water entry except the high volume zone at the bottom. Since tests made while deepening and also electric log interpretation indicated the presence of minor water zones, it is thought that the high volume flow from the bottom zone restricted the flow from these minor zones to the extent that the instrument was unable to locate them. Possibly these minor zones could have been located had several Strataflow surveys been run as the hole was deepened, or at least one survey made before the bottom zone was penetrated.

AUTHORS' REPLY TO MR. GARY

As a general rule Strataflow surveys are particularly indicative of water entry from upper zones. However, there are several possible explanations for this well's failing to show water above the initial plugback depth after being deepened.

1. The water production could have been leakage around the plug.
2. The reservoir may have vertical permeability through fissures or more particularly, in limestone through solution cavities. A shortened path, opened by the deepening of the well would completely bypass the water flow to the upper zone.
3. It is possible that the upper zone had formation pressure which was abnormally low compared to that of the lower horizon. In this case there would be a tendency for the upper zone to "take" rather than produce water until the hydraulic head associated with the lower horizon was drawn down to a low value. Since this was one condition that was anticipated, clues indicating its occurrence were looked for in the experimental and developmental work on the process. The first 30 wells surveyed were examined in considerable detail with many of the surveys repeated under varying hydraulic conditions. In this work there was no evidence of "low pressure horizons."
4. It is possible that a mistake could have been made in the well conditioning. For example, if the fresh conditioning water flow were set in excess of the production, on a weight basis, the well would become overbalanced with the excess fresh water being taken by the formations. On the actual test the well might not be produced sufficiently to initiate formation water production from the less productive zones.

★ ★ ★

LABORATORY DETERMINATION OF RELATIVE PERMEABILITY

G. RICHARDSON, J. K. KERVER, JUNIOR MEMBERS AIME, J. A. HAFFORD AND J. S. OSOBA, HUMBLE OIL AND REFINING CO., HOUSTON, TEX.

ABSTRACT

A detailed study of a number of methods of relative permeability measurement has been made in a search for the technique most suited to routine analysis of cores taken from reservoir rock. It has been found from tests run on the same samples of core material by a number of techniques that the Penn State, Hassler, Hafford, and dispersed feed techniques yield results which are felt to be reliable. Conditions under which the faster single core dynamic technique may be used are described. Further work on the calculation of relative permeabilities to oil from data obtained by the gas drive method is needed before this latter rapid method can be utilized.

Correlations between theoretical studies and experimental results have been obtained in studies of the boundary effect, pressure distribution in two-phase flow, and gas expansion effects. Previous conclusions that the effects of the outflow boundary could be made negligibly small have been substantiated. Results of experimentally determined oil and gas pressure distributions along a core sample during flow are presented. Further studies of the effects of rate of flow in the measurement of relative permeability-saturation relations have shown that results are independent of the rate of flow as long as the flow rate is below the point where inertial effects commence. An analysis of the effects of a severalfold expansion of gas along the flow path indicates that while saturation gradients are induced in the test sample, the errors caused by this phenomenon in relative permeability measurements are small.

INTRODUCTION

Many pages of literature have been devoted to pointing out the need for relative permeability-saturation relations in reservoir engineering. One of the most attractive ways of obtaining this information is by the analysis of samples of core material taken from the formation in question, and again literature has described many methods for obtaining these data. It is the purpose of this paper to present the work that has been done in the study of some of these published methods together with some other methods that have been recently developed in this laboratory. Also, a study of some of the factors that influence the laboratory determination of relative permeability-saturation relations is presented.

References given at end of paper.

Manuscript received in the Petroleum Branch office March 24, 1952.

FACTORS WHICH AFFECT LABORATORY STUDY OF FLUID FLOW THROUGH RESERVOIR ROCK

To determine relative permeability-saturation relations of samples of reservoir rock in the laboratory, it is important to know what factors affect these measurements in order that the magnitude of these effects can be ascertained and steps then can be taken to eliminate or, in some cases, to minimize them. The factors that have been investigated are the boundary effect, the effect of gas expansion, and the rate effect.

Boundary Effect

In laboratory experiments in which two immiscible fluids are flowed through a porous medium, there exists a discontinuity of capillary properties at the outflow face. This discontinuity exists because the fluids pass from a region of finite capillary pressure in the sample to a region of zero capillary pressure in an open receiving vessel. The capillary forces existing in the core cause the rock to tend to retain

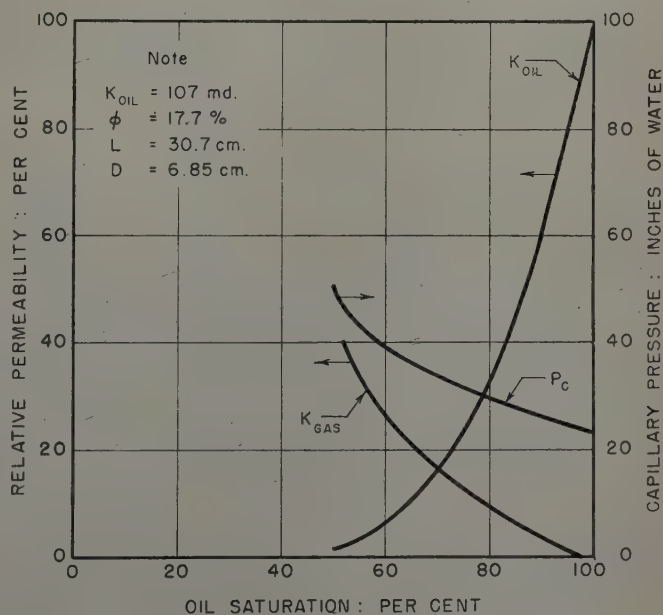


FIG. 1 — RELATIVE PERMEABILITY AND CAPILLARY PRESSURE SATURATION RELATIONS FOR BEREA OUTCROP SAND.

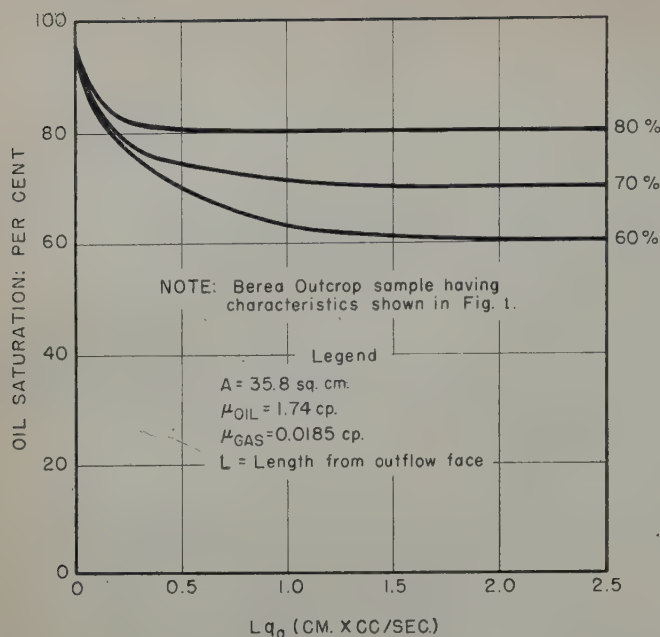


FIG. 2—CALCULATED SATURATION GRADIENTS DUE TO BOUNDARY EFFECTS.

the wetting fluid, which results in the saturation of the wetting face being maintained at a higher level near the outflow end of the core than throughout the remainder of the core. This phenomenon is called the boundary effect. In a recent publication, Caudle, Slobod and Brownscombe¹ pointed out that the predicted influence of the boundary effect was larger than was determined experimentally. Since the influence of the boundary effect must be reckoned with in nearly all laboratory investigations dealing with multi-fluid flow, it is important to know exactly the role played by the boundary effect in these investigations.

Theory

When two immiscible fluids flow horizontally through a porous medium, they obey the three differential equations listed below:

$$-dP_w = \frac{q_w \mu_w dL}{K_w A} \quad (1)$$

$$-dP_{nw} = \frac{q_{nw} \mu_{nw} dL}{K_{nw} A} \quad (2)$$

$$dP_c = dP_{nw} - dP_w \quad (3)$$

Equation (1) is Darcy's Law applied to the wetting fluid and Equation (2) is Darcy's Law applied to the non-wetting fluid. Equation (3) expresses in differential form the capillary pressure relating the pressures in the two fluids. By substituting Equations (1) and (2) in Equation (3), the following differential equation can be developed:

$$\frac{dS_w}{dL} = \left(\frac{q_w \mu_w}{K_w} - \frac{q_{nw} \mu_{nw}}{K_{nw}} \right) \frac{1}{A} \cdot \frac{1}{dP_c} \quad (4)$$

One condition for which a solution of Equation (4) is desired is the condition that the fluids move through the porous medium in such a manner that the wetting fluid saturation is always decreasing from 100 per cent saturation. This type of behavior has been termed drainage. To solve Equation (4) for drainage conditions, a knowledge of the

drainage flow characteristics of the porous medium is required. The boundary condition imposed on the solution of Equation (4) is that the saturation at the outflow face be the equilibrium non-wetting fluid saturation, which is the saturation at which the permeability to the non-wetting fluid becomes greater than zero. Experimental evidence has shown that this saturation exists at the outflow face.

For a sample of sandstone from a Berea outcrop, the saturation distribution of the wetting fluid that would exist was calculated for various ratios of non-wetting to wetting fluid flow rates. The drainage capillary pressure and relative permeability-saturation relations for the Berea outcrop are shown in Fig. 1. Inasmuch as the calculations of the saturation distribution required a solution of Equation (4), the first step in the solution was to select arbitrarily the rates of flow of the two fluids. This fixed the saturation of the wetting fluid within the sample at an infinite distance from the outflow end. Next, about ten saturations in incremental steps were chosen between the saturation at infinite distance from the outflow end and the saturation of the wetting fluid accompanying the equilibrium non-wetting fluid saturation. At each saturation the quantity dS_w/dL was determined from Equation (4). Then, the reciprocal, dL/dS_w , was plotted as a function of saturation and by graphical integration of this relation the plot of the saturation as a function of the distance from the outflow end was obtained. By repeating this calculation for a number of fluid flow rates, a set of curves relating saturation and distance from the outflow end was obtained. These curves representing the saturation gradient due to the end effect at various rates of flow are shown in Fig. 2.

Experimental Results—Long Core Cut into Sections

A study was made to determine experimentally the saturation distribution in a sample of porous material due to the boundary effect when two fluids were flowing simultaneously through the material. For this investigation, a Berea outcrop sandstone was cut in a cylindrical shape with the axis of the cylinder parallel to the bedding plane. The sample, 30 cm long and 6.85 cm in diameter, was cut into eight sections with the slices made perpendicular to the axis of the sample; the faces of the sections were machined flat. The sections were then placed in the fluid flow apparatus end to end with porous tissue between the faces. A drawing of this apparatus is shown in Fig. 3. A strong spring was used to force the sections together to insure capillary contact between the sections.

The study of saturation gradients within the sample was made using various rates of flow. For each determination the

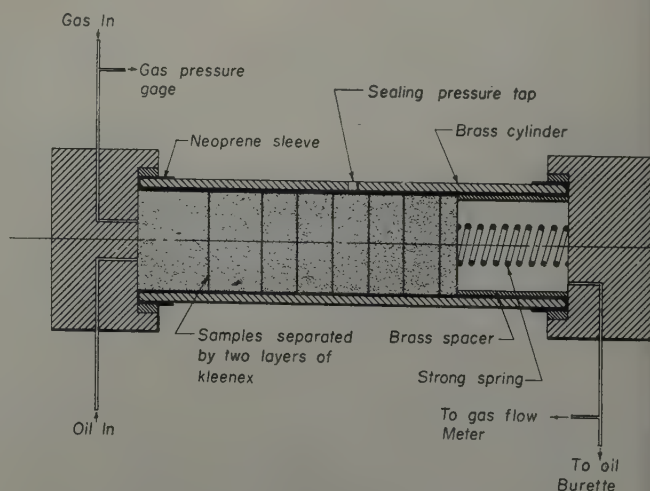


FIG. 3—APPARATUS UTILIZING LARGE CORE SECTIONS

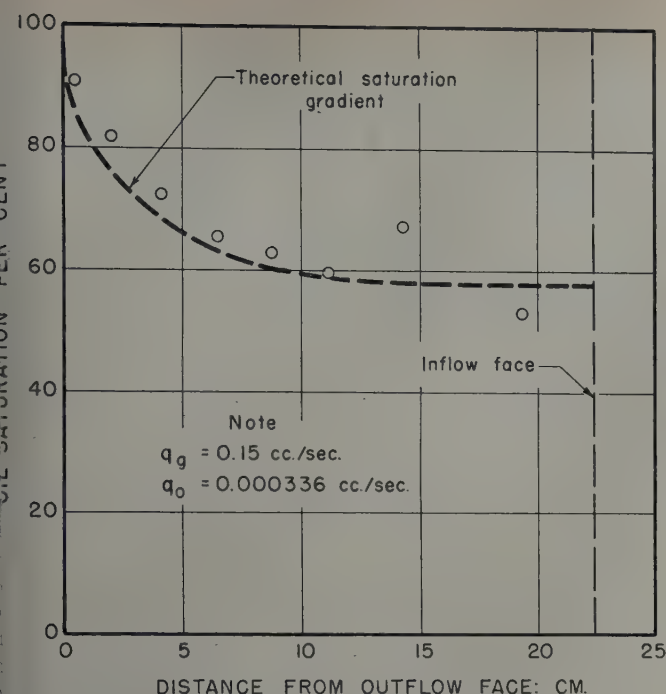


FIG. 4—COMPARISON OF EXPERIMENTAL AND THEORETICAL SATURATION GRADIENTS DUE TO BOUNDARY EFFECT.

sections were first completely saturated with the wetting fluid (kerosene) which was then flowed through the sample. Next, the non-wetting fluid (helium) was introduced and flowed along with the oil through the sample at a rate giving the desired pressure gradient until both flow rates and pressures were no longer changing. The flow was then stopped and the oil saturation of each section was determined by weighing. The resulting saturations of the sections for three runs are shown in Figs. 4, 5, and 6. Also shown in these figures for comparison are the saturation distributions that were predicted by the solutions of Equation (4) for the Berea sample.

Experimental Results — Flowing Pressure Studies

In an effort to obtain information about the pressures existing in the wetting and in the non-wetting fluids while two fluids were flowing through porous material, a special long core apparatus was constructed whereby the pressure in the wetting and non-wetting fluids could be measured at several points along the length of a sample of porous material. Of particular interest was the behavior of these pressures near the outflow end where the boundary effect influenced the pressures.

The porous material used for this investigation was a piece of Berea sandstone outcrop. A cylindrical sample was cut with its axis parallel to the bedding plane. The sample was 30.7 cm long and 6.85 cm in diameter. Three cylindrical semi-permeable porcelain discs (oil pressure pads), 1 cm in diameter and 0.6 cm thick, were cemented into the samples at distances at 2.91, 15.35, and 27.79 cm from the inflow end to measure the pressures in the wetting fluid. These discs were connected to Moore Products pressure gauges by passing a probe through the rubber sleeve and sealing the probe to the semi-permeable discs with O-rings. The rubber sleeve had embedded piezometric rings to measure the pressures in the non-wetting fluid. A drawing of the apparatus is shown in Fig. 7.

With this apparatus, the pressures in the wetting fluid at three points along the sample length were measured and the

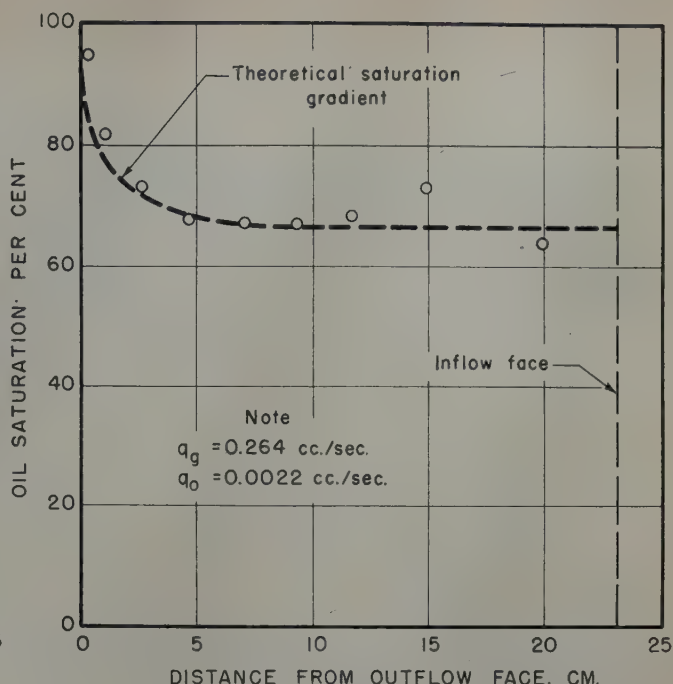


FIG. 5—COMPARISON OF EXPERIMENTAL AND THEORETICAL SATURATION GRADIENTS DUE TO BOUNDARY EFFECT.

pressures in the non-wetting fluid were measured at seven points. A number of runs were made flowing oil and gas through the sample at various rates. In each run the sample was initially saturated with oil to insure that true drainage conditions existed. The pressure distributions in the oil and in the gas within the sample for two typical runs are shown in Figs. 8 and 9.

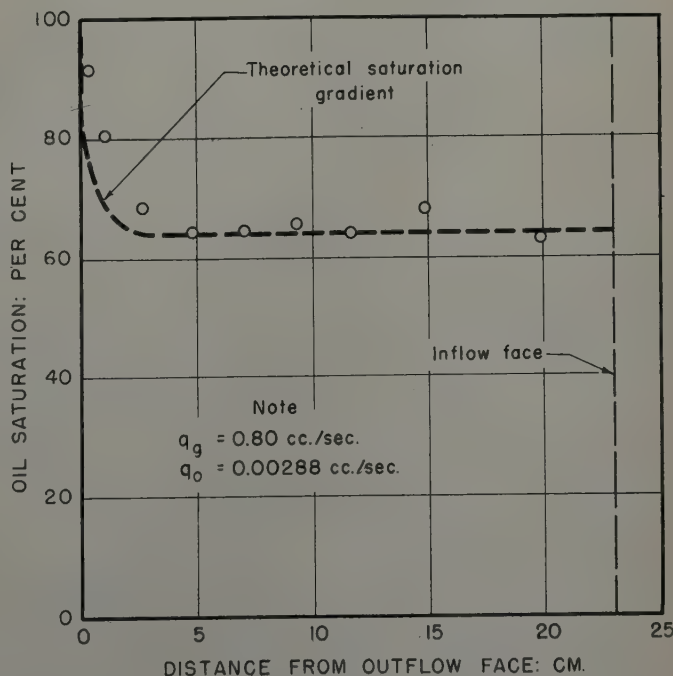


FIG. 6—COMPARISON OF EXPERIMENTAL AND THEORETICAL SATURATION GRADIENTS DUE TO BOUNDARY EFFECT.

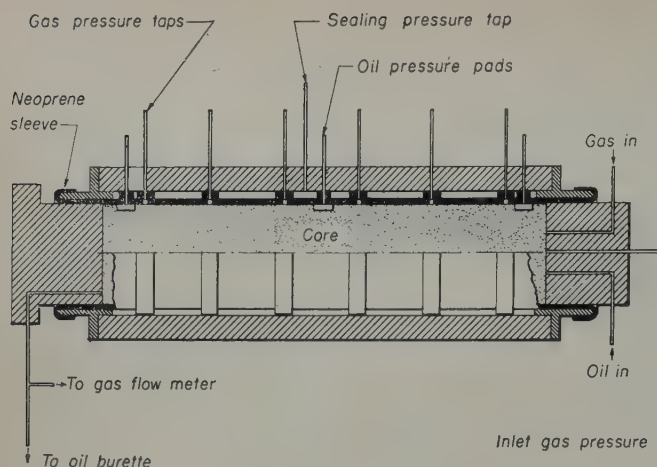


FIG. 7 — LONG CORE APPARATUS

In Fig. 8 the curvature caused by the boundary effect in the oil-pressure and in the gas-pressure distribution curves can be seen to extend a considerable distance into the core. These measurements were made at low rates of flow. The pressure distribution curves shown in Fig. 9 were obtained at high rates of flow and show that the curvatures in the pressure distribution curves caused by the boundary effect were confined to only a small part of the sample. The saturation gradients caused by the boundary effect extended into the sample for about 15 per cent of the length for the run shown in Fig. 8 and for about 3 per cent of the length for the run shown in Fig. 9.

It can be noted that at the outflow end all pressure distribution curves for gas were extrapolated to a value corresponding to the capillary pressure of the sample at the equilibrium gas saturation.

Interpretation of Results

The results obtained in these laboratory studies indicate that the influence of the boundary effect can be predicted by the fundamental equations of fluid flow and the relative permeability- and capillary pressure-saturation relations of the porous medium. A number of calculations made to determine the average permeability to gas and to oil that a sample would have if the saturation distribution were that shown in Fig. 8 revealed that the relative permeability to gas is the only one appreciably affected by the saturation gradient caused by the boundary effect. The errors in gas permeability measurements become negligible as the rate of flow is increased. At low rate of flow the error in the measurements of relative permeability is due primarily to the inability to determine the correct pressure gradients simply by measuring terminal pressure and sample length.

When a wetting and a non-wetting fluid flow through porous media the pressure difference between the two fluids at every point is equal to the capillary pressure corresponding to the saturation at that point. As the wetting fluid saturation increases near the outflow boundary as a result of the boundary effect the pressure difference between the two fluids decreases accordingly. Also, it was found that the wetting fluid pressure is continuous across the outflow boundary whereas the non-wetting fluid pressure is discontinuous at the outflow boundary. The magnitude of the discontinuity is equal to the capillary pressure at the equilibrium non-wetting fluid saturation.

Flow of Compressible and Non-Compressible Fluid Through Reservoir Rock

The use of a gas in studies of multiphase flow in the laboratory introduces a complication not encountered when two non-compressible fluids are flowing. The fact that the volume of gas flowing increases as the pressure on the gas decreases causes the gas-to-wetting fluid ratio to increase along the direction of flow. This increase in gas-to-wetting fluid ratio causes a saturation gradient along the flow path.

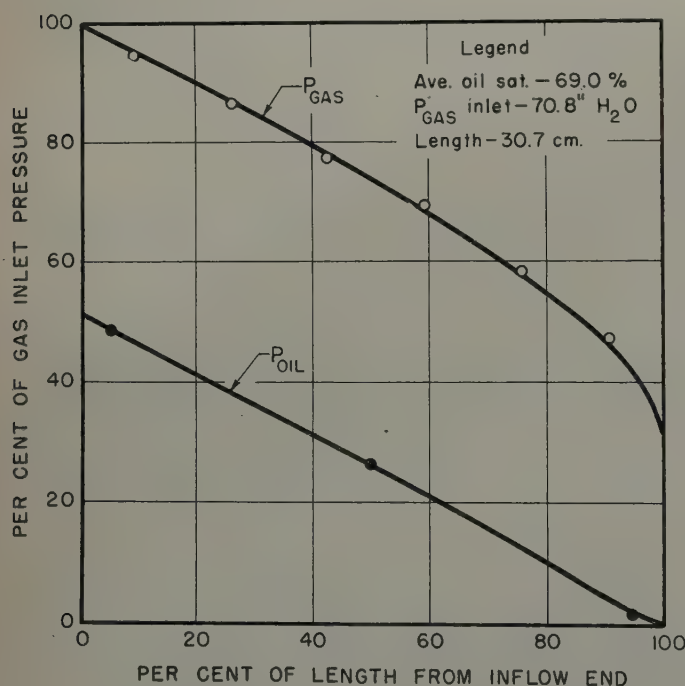


FIG. 8 — FLOWING PRESSURE-LENGTH RELATION FOR GAS AND OIL IN STEADY STATE FLOW.

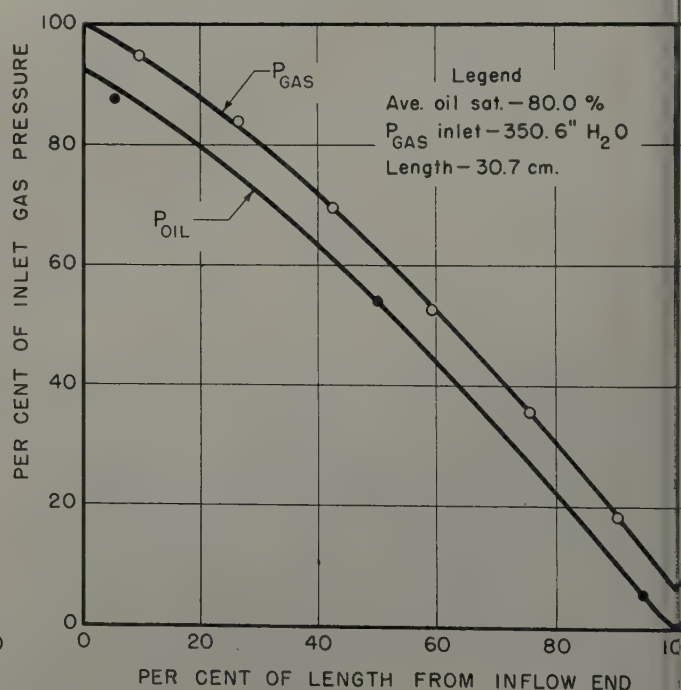


FIG. 9 — FLOWING PRESSURE-LENGTH RELATION FOR GAS AND OIL IN STEADY STATE FLOW.

has been pointed out by several investigators.^{2,3} The magnitude of the saturation gradient and the magnitude of the errors incurred in relative permeability measurements under conditions where the volume of gas flowing in a test sample increases severalfold along the length of the sample has been the subject of some conjecture in the literature. An attempt is made in the following discussion to describe mathematically the nature of the saturation gradient caused by gas expansion and the amount of error introduced thereby into relative permeabilities measured under these conditions. Also, experimental results are presented as a corollary to the theoretical study.

Theory

The equation governing the simultaneous flow of two fluids through porous media is Equation (4). For the study of the effect of gas expansion, this equation can be rearranged into the more convenient form shown in Equation (5).

$$\frac{q_g}{q_o} = \frac{K_{g\mu_o}}{K_{o\mu_g}} \frac{K_g A}{q_o \mu_g} \cdot \frac{dP_o}{dS_o} \cdot \frac{dS_o}{dL} \quad (5)$$

where subscript *g* refers to the gas phase and subscript *o* refers to the oil phase. From this equation and Darcy's Law for each phase, the gas/oil ratio at any point in the medium may be obtained as a function of the saturation and the saturation gradient at the point. A solution of Equation (5) was obtained for the specific set of conditions of flow using a Berea outcrop sample for which the relative permeability and capillary pressure-saturation relations are shown in Fig. 1. Calculations were made to determine the saturation distribution that would exist in a sample 22.4 cm long and 6.85 cm in diameter with gas and kerosene flowing at a high rate through the sample. For the calculation, three conditions were arbitrarily fixed for the flowing system. These were a pressure in the gas of 3.069 atmos. at the inflow face, a pressure in the oil of 2.996 atmos. at the inflow face, and an oil flow rate of 0.733 cu cm/sec. The gas flow rate, the pressures of the gas and oil along the length, and the saturation along the length

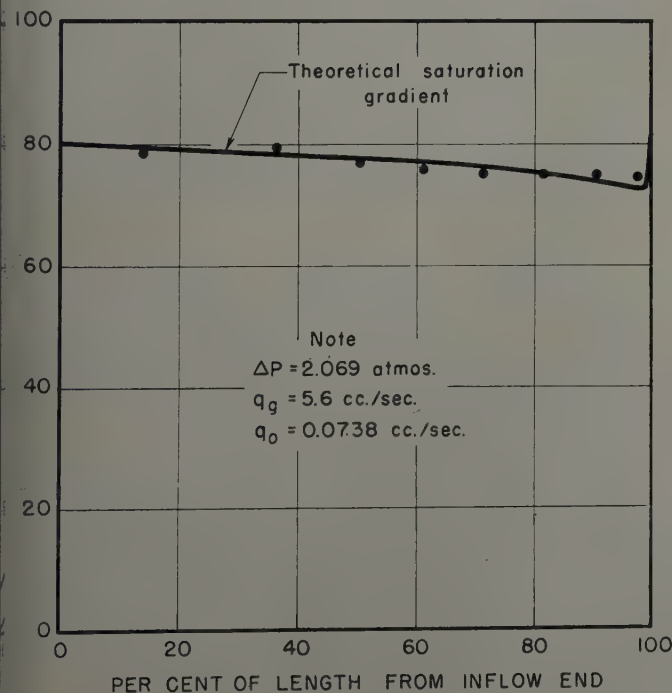


FIG. 10—COMPARISON OF EXPERIMENTAL AND THEORETICAL SATURATION GRADIENTS DUE TO GAS EXPANSION.

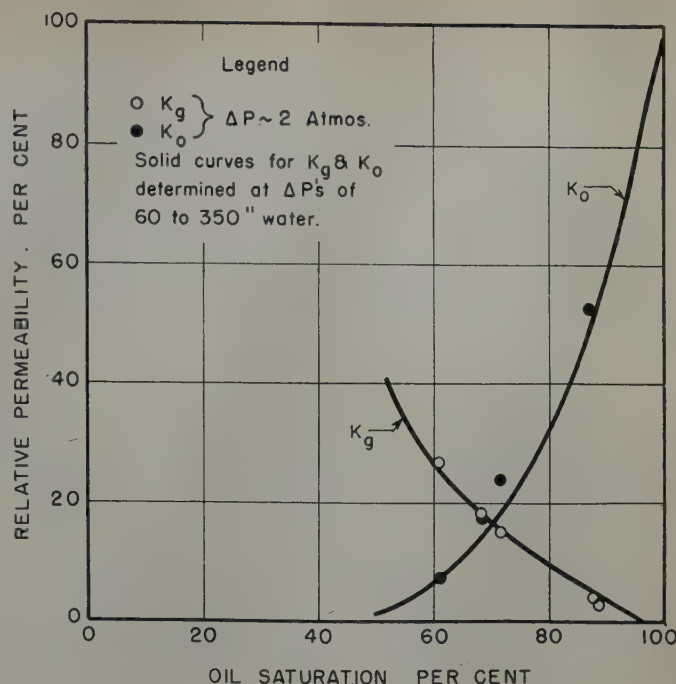


FIG. 11—EFFECT OF GAS EXPANSION ON THE RELATIVE PERMEABILITY-SATURATION RELATION.

were computed. Using the computed saturation-length relations, the average saturation of the sample was calculated to be 77 per cent by an integration process. The relative permeabilities to oil and gas were computed using the inlet gas pressure and the appropriate flow rates as would be done in laboratory flow tests. The relative permeability to oil was calculated to be 12.4 per cent and the relative permeability to gas was calculated to be 27.2 per cent. The relative permeabilities to oil and gas at 77 per cent saturation obtained from Fig. 1 are 12.0 per cent and 27.8 per cent respectively. Thus the error in oil relative permeability measurement was 0.4 per cent in 12 per cent and the error in gas relative permeability was 0.6 per cent in 27.8 per cent, which are less than experimental errors in most flow tests.

Experimental Results

A set of experimental investigations was conducted to determine the effect of gas expansion on the flow of two fluids through porous material. In particular, one of the investigations was directed toward determining the saturation vs length relation for a sample of porous material through which gas and oil were flowing at high rates. The Berea outcrop sample cut into eight sections previously described and the apparatus described in Fig. 3 were used to study this saturation distribution.

Several experiments were performed in which gas and oil were flowed through the sections of Berea outcrop at high rates to obtain large pressure differences between the ends of the sample. The pressure difference was such that the volume of gas flowing through the sample changed severalfold along the length of the core because of the expansion of the gas as the pressure decreased. The apparatus was then broken apart and each of the sections was weighed to determine its saturation. A plot of the saturation of each of the sections as a function of its position within the sample is shown in Fig. 10. Also shown in Fig. 10 is the theoretical saturation distribution calculated from Equation (5).

In addition to determining the saturation distribution within the sample, the relative permeability-saturation relations were determined at high rates of flow of oil and gas with the long solid Berea sample previously described. These steady-state runs were made at sufficiently high pressure drops that the volume of gas flowing in the core changed severalfold as the gas expanded with the decreasing pressure along the length of the sample. In Fig. 11 the results of these runs are shown as points for comparison with the relative permeability-saturation relations obtained at much lower rates of flow shown as solid lines where there was a relatively small change in gas flow rate due to gas expansion.

Interpretation of Results

The agreement between the theoretically predicted saturation gradient for a particular set of conditions, as shown in Fig. 10, indicates Equation (5) correctly describes the flow conditions.

It has been determined theoretically that the relative permeability-saturation relations obtained with gas and oil are not appreciably affected by the fact that the gas flow rate increases along the length of the sample as the pressure declines. From the data plotted in Fig. 11 no apparent difference can be noted in the relative permeability-saturation relations obtained at pressure drops from 0.15 to 2 atmos. across the sample. Thus, it may be concluded that gas expansion effects have no important bearing on relative permeability measurements where the gas expands severalfold along the flow path. This analysis is not compatible with a mathematical analysis by Rose² of the simultaneous flow of gas and a liquid through porous media. His analysis contains a simplifying assumption which invalidates his results. Implicit in his treatment is the assumption that the permeability to gas and oil throughout the core sample is constant; whereas in the actual case, the permeabilities vary along the length of the core with changes in saturation caused by the increasing gas/oil ratio along the flow path.

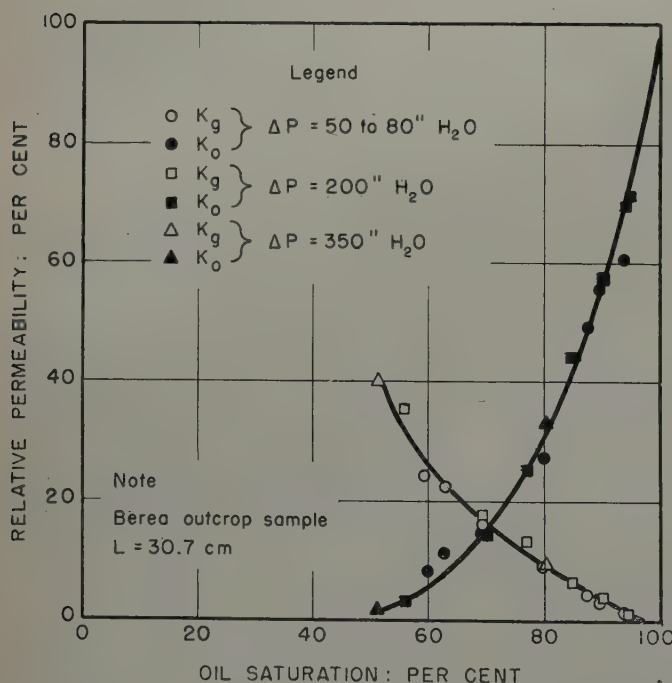


FIG. 12—EFFECT OF FLOW RATE ON THE RELATIVE PERMEABILITY-SATURATION RELATION (DRAINAGE CONDITIONS).

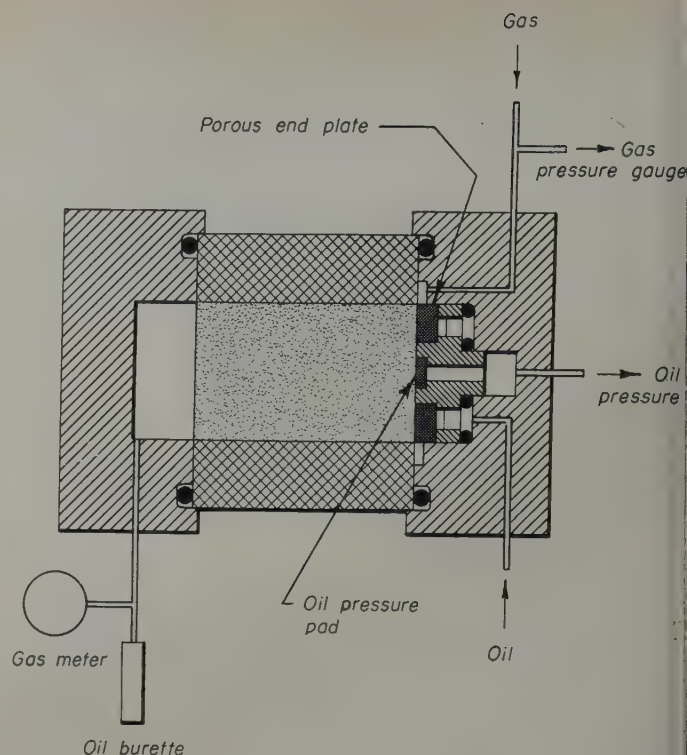


FIG. 13 — HAFFORD APPARATUS.

Rate of Flow

The laboratory determination of relative permeability-saturation relations of reservoir rock can be made more rapidly if the rate of flow through the sample is increased above reservoir flow rates. However, before the results of measurements of relative permeability made at high rates of flow on a routine basis can be accepted, it must be ascertained that the relative permeability-saturation relations are independent of the rate of flow.

It is known that the permeability of a porous medium to a single liquid is independent of the rate of flow through that medium provided the flow rate is not so high that inertial effects become important. Therefore, the investigations of the effects of rate of flow on the relative permeability were conducted at rates lower than those at which inertial effects became important.

Experimental Results — Long Core

With a large Berea sandstone core, it was possible to measure both the pressure in the gas and in the oil at various points along the sample length. By knowing both the pressure distribution in the oil and in the gas, studies of the effect of rate of flow on relative permeability could be made without the troublesome influence of the boundary effect.

To determine the relative permeability to oil or gas, the portion of the pressure distribution curve that was not influenced by the boundary effect was used to obtain the pressure gradient, see Figs. 8 and 9. The rate of flow was determined by measuring the throughput of each fluid for a known length of time, and the average saturation of the sample was determined by weighing. The drainage relative permeability-saturation relations obtained at pressure gradients varying from 2 to 11 in. of water per cm are shown in Fig. 12.

If instead of using the straight line portion of the pressure distribution curve to determine the pressure gradient, the dif-

ference between the inlet pressure and atmospheric pressure and the sample length were used, the calculated relative permeability to each of the fluids at the particular saturation would be lower than the correct relative permeability of the reservoir rock at that saturation. The difference between the two methods would be very small at high rates of flow, but at low rates the difference becomes large.

The results of these tests show that changing the pressure gradient or rate of flow (in the viscous flow range) did not change the drainage relative permeability-saturation relations.

MEASUREMENT OF DRAINAGE RELATIVE PERMEABILITY-SATURATION RELATIONS FOR SHORT CORE SAMPLES

The relative permeability characteristics of a great many core samples will be run at considerable expense in the laboratories of the oil industry. It is important, therefore, that the techniques utilized in any one laboratory yield reliable results and that these techniques permit measurement on as many samples as possible in a given time. Also, the tests in all the laboratories should yield the correct results, as operation of many reservoirs requires joint agreement of the participating companies. In the following discussion, a series of experiments is described in which six of the methods of relative permeability measurement that might be utilized in the industry were each used to obtain the flow characteristics of a single sample of sandstone. Comparisons between the methods are

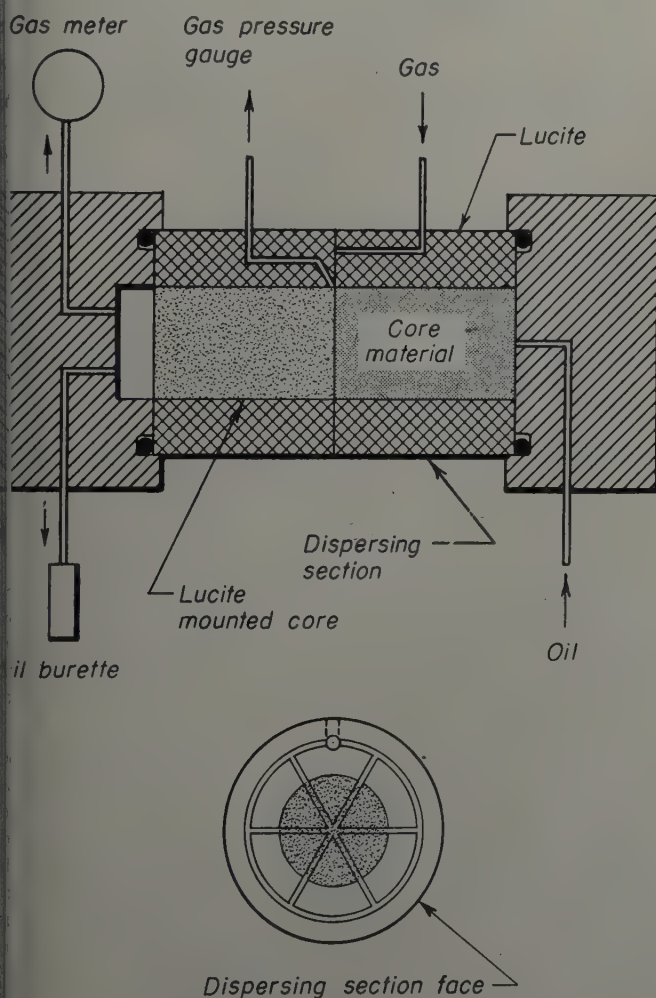


FIG. 14 — DISPERSED FEED APPARATUS.

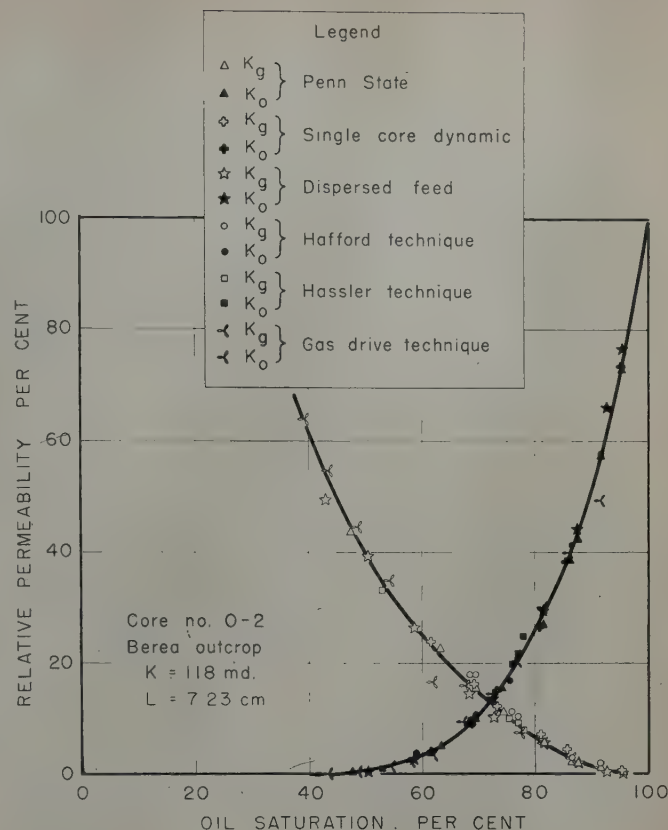


FIG. 15 — RELATIVE PERMEABILITY — SIX METHODS. LONG SECTION.

made as to the reliability of results and the rapidity with which results may be obtained. The six methods used were the Penn State, Hassler, single core dynamic, gas drive, Hafford, and the dispersed feed. The Penn State, Hassler, single core dynamic, and the gas drive techniques were described in a previous paper⁴ and will not be discussed here. The two more recently investigated methods, the Hafford and the dispersed feed techniques, are described in the following:

Hafford Technique

Many of the earlier laboratory apparatus to measure relative permeability-saturation relations of reservoir rock were designed primarily to eliminate errors due to the boundary effect. When it was demonstrated that this error could be made insignificant if high rates of flow were used, attention was shifted from the outflow end of the sample to the inflow end of the test sample.

In the Hafford technique the non-wetting fluid is fed directly into the sample and the wetting fluid is fed into the sample through a semi-permeable disc that allows only the wetting fluid to pass. A drawing of the apparatus is shown in Fig. 13. The central portion of the semi-permeable disc is isolated from the remainder of the disc by a small metal sleeve. The central portion is used to measure the pressure in the wetting fluid at the input end of the core. The pressure in the non-wetting fluid is measured through the standard pressure tap machined into the Lucite surrounding the core. The pressure difference between the wetting and the non-wetting fluid is a measure of the capillary pressure of the sample at the inflow end.

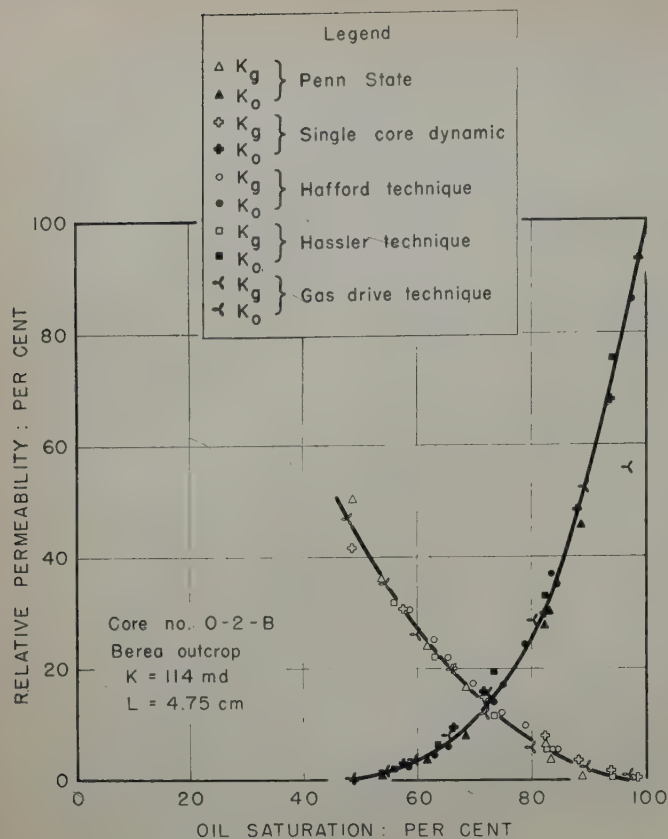


FIG. 16 — RELATIVE PERMEABILITY — FIVE METHODS, INTERMEDIATE SECTION (DRAINAGE CONDITIONS).

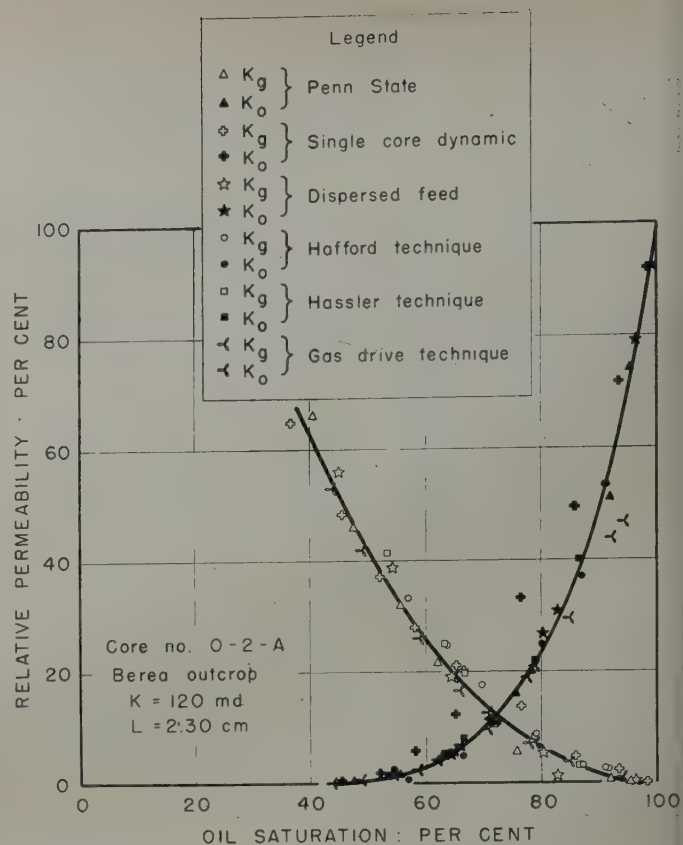


FIG. 17 — RELATIVE PERMEABILITY — SIX METHODS, SHORT SECTION (DRAINAGE CONDITIONS).

To measure drainage relative permeability-saturation relations the sample is first saturated with oil. The sample is then placed in the apparatus and oil is allowed to enter the core through the semi-permeable disc. The oil was previously subjected to vacuum to remove any dissolved gases. The oil flow rate is adjusted to give the desired pressure in the oil at the inflow end of the core. Gas is then allowed to enter and flow through the core at very low rates. When the pressure gauges read constant values, indicating that equilibrium has been reached in the sample, the pressures in the oil and gas at the inflow end of the sample, together with the flow rates of the oil and gas, are measured. The apparatus is broken apart and the sample removed to determine the saturation by weighing. The sample is then returned to the apparatus and oil and gas are again allowed to flow through the sample at the previous rates. The oil rate is then reduced and the gas rate is increased slightly to maintain essentially the same pressure in the gas at the inflow end. When equilibrium is again reached, the above procedure is repeated until complete relative permeability-saturation relations are obtained.

Dispersed Feed Method

The dispersed feed method is similar to the Hafford and single core dynamic methods. In this method the wetting fluid enters the test sample by first passing through a dispersing section. This dispersing section is made of porous material similar to the test sample, but it does not contain a device for measuring the pressure in the wetting fluid at the inflow end of the test sample as does the Hafford method. This porous

material, which in some cases has been made from the same core material as the test sample, serves to disperse the wetting fluid so that the wetting fluid enters the test sample more or less uniformly over the inflow face.

Radial grooves are machined into the outflow face of the dispersing section. Gas is introduced to the test section through these radial grooves at the junction between the two cores. A drawing of the apparatus is shown in Fig. 14.

In measuring relative permeability-saturation relations by this method, the same procedure is employed as is used for the single core dynamic technique described in a previous paper.⁴ Errors due to the boundary effect are made insignificant by using high rates of flow. During several initial runs employing the dispersed feed method, the dispersing section was weighed after each relative permeability determination to determine its average oil saturation. This section remained essentially 100 per cent saturated with the wetting fluid even though the saturation of the test sample had been reduced to about 60 per cent saturation.

Saturation Determinations

The standard method of determining fluid saturations in the flow experiments described in this paper was by gravimetric means. A simple ratio of the weight of oil in the sample after any one run to the weight of oil held in the saturated sample was used to calculate saturations. The use of this method, particularly where one of the fluid phases is a gas, has been criticized in the literature because there is a tendency for the gas to expand from the sample as the flow is

interrupted and the apparatus is broken apart, the expanding gas carrying oil from the sample with it.

A series of tests was conducted on a sample mounted in Lucite to determine quantitatively the amount of saturation error which would be incurred by gas forcing oil from a sample after a run had been completed. The test procedure involved placing an 8-cm-long sample having a known initial oil saturation in a cylindrical pressure chamber. Then the gas pressure in the cylinder was set at 100 psi. When sufficient time had been allowed to build up the pressure in the sample, the pressure was quickly reduced, the faces of the sample were wiped free of oil, and the sample was weighed to determine the saturation change. This procedure was repeated for various initial saturations. The maximum change in saturation incurred at a pressure reduction from 100 psi to atmospheric pressure was 2.3 per cent for a sample originally at 8 per cent oil saturation, the change being much less at all other saturations. When the chamber pressure was built up to only 10 psi, the maximum change in saturation was one per cent at 83 per cent oil saturation, being less at all other saturations.

The results of this investigation show that when a sample is removed from an apparatus after a flow experiment the change in saturation caused by the expulsion of oil by the expanding gas is quite small at the pressures normally used in these laboratory tests.

Comparison of Drainage Relative Permeability-Saturation Relations by the Six Methods

To compare the drainage relative permeability-saturation relations obtained by six methods, a small uniform sample

of Berea sandstone outcrop was used. The sample was 7.23 cm long and 1.85 cm in diameter and was mounted in Lucite. The drainage relative permeability-saturation relations that were obtained are shown in Fig. 15.

The 7.23 cm sample was then cut into two sections; one section, 0-2-B, was 4.75 cm long and the other section, 0-2-A, was 2.30 cm long. Relative permeability determinations were made on sample 0-2-B by five methods and on sample 0-2-A by six methods. The results of these determinations are shown in Figs. 16 and 17. Sample 0-2-B was then cut into two sections; 0-2-BC was 2.24 cm long and 0-2-D was 2.29 cm long. These short sections were tested in the gas drive, Penn State, dispersed feed, and single core dynamic apparatus. The results obtained by these four methods on the two short sections, 0-2-BC and 0-2-D, are plotted in Figs. 18 and 19.

Interpretation of Results

The results indicate that determinations of relative permeability-saturations by the Penn State, the Hassler, the Hafford, and the dispersed feed systems all yield essentially the same drainage relative permeability-saturation relations for all sample lengths. The results indicate that the correct relative permeability-saturation relations can be obtained by these methods on samples that are as short as those taken from wire-line cores.

Since the measurements of relative permeability by the Hafford and the dispersed feed methods are made with the saturation gradient due to the boundary effect present in the test sample and in the Hassler and Penn State methods the saturation gradient is not present, it can be concluded that correct relative permeability-saturation relations can be made

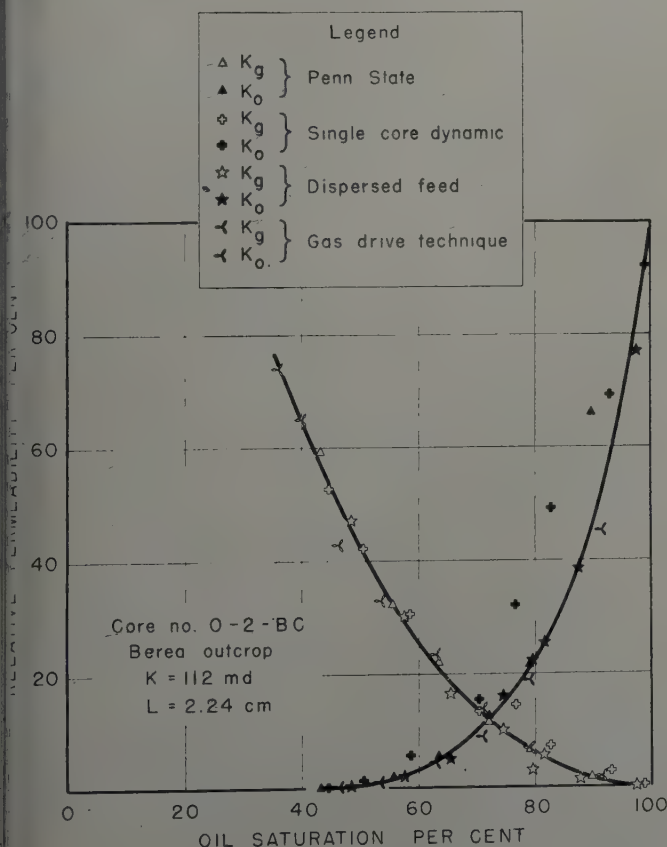


FIG. 18 — RELATIVE PERMEABILITY — FOUR METHODS, SHORT SECTION (DRAINAGE CONDITIONS).

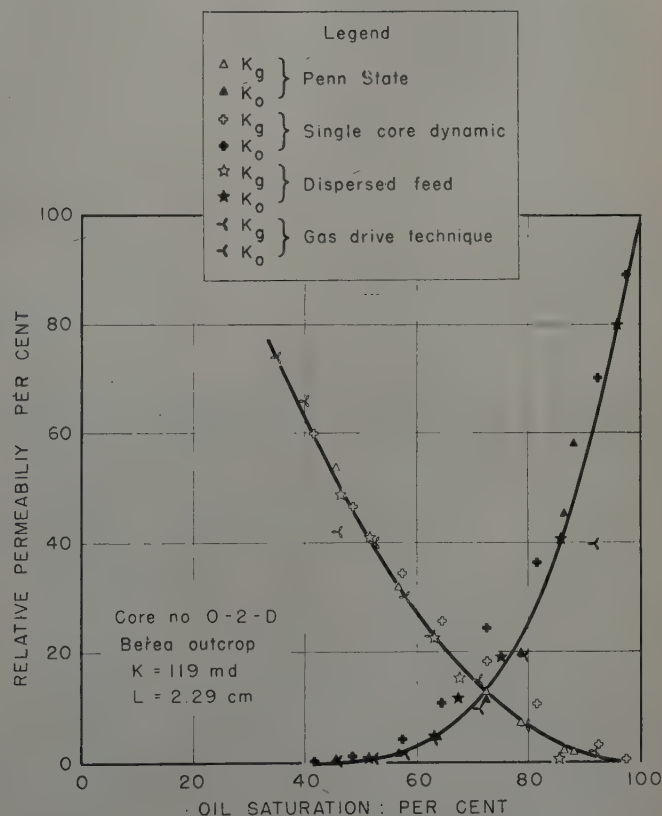


FIG. 19 — RELATIVE PERMEABILITY — FOUR METHODS, SHORT SECTION (DRAINAGE CONDITIONS).

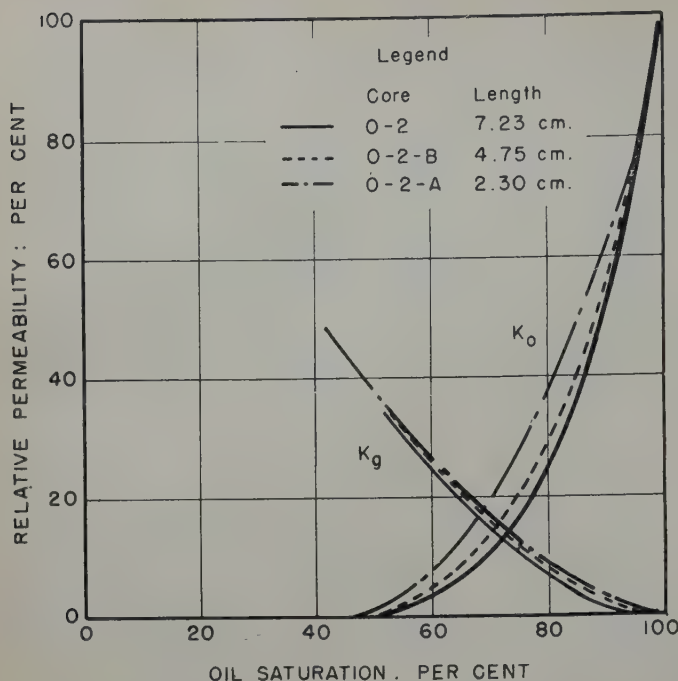


FIG. 20 — EFFECT OF CORE LENGTH ON SINGLE CORE DYNAMIC RELATIVE PERMEABILITY (DRAINAGE CONDITIONS).

with the saturation gradient from the boundary effect present within the test sample if high rates of fluid flow are used.

The measurement of relative permeability by the Hassler, Penn State, Hafford, and dispersed feed methods are made when the saturation at every point within the sample is not changing with time. Measurement of relative permeability by the gas drive technique is made when the saturation in the sample is changing at every point within the sample. However, the relative permeability-saturation relations were calculated in the same manner for the gas drive technique as for the other methods; that is, the rates at which the fluids flowed through the test sample were determined, the pressure at the inflow end of the sample was measured, and the average saturation in the sample was determined by weighing. The oil flow rate used in the calculation of oil permeabilities from gas drive data was the effluent oil flow divided by two. The oil pressure drop used in the calculation of the relative permeability to oil was the inlet gas pressure minus the capillary pressure at the average saturation of the sample. Comparison of the data obtained from gas drive experiments with those from steady state tests has indicated that the factor of one-half brings the data into agreement in many cases. It has been found experimentally that the oil flow rate increases almost linearly with the length, so one-half the effluent rate is approximately the average rate. The effluent oil flow rate was calculated from the weight loss of the sample during the run, the density of the oil, and the time period over which the run was made. From these data, the relative permeability-saturation relations were then obtained.

The results of the investigation on the Berea outcrop samples showed that the oil relative permeability-saturation relations determined by the gas drive technique agreed with those by the Penn State, Hassler, Hafford, and dispersed feed methods for samples O-2 and O-2B but was slightly lower than the other methods for O-2-A, O-2-BC, and O-2-D. Comparisons using other samples indicated that the oil relative permeability determined by the gas drive technique was not always in agreement with those of other methods. A reason for this

disagreement is the lack of ability to compute the permeability to oil from gas drive data in the correct manner.

The results, also, indicated that the relative permeability-saturation relations measured by the single core dynamic method were affected by sample length. This effect is illustrated in Fig. 20. As shown in Fig. 15, the relative permeabilities measured on the long sample by the single core dynamic method agreed with those measured by the Penn State and dispersed feed methods. On short samples the relative permeability-saturation relations determined by the single core dynamic method, particularly the oil relative permeabilities were incorrect and were higher than those obtained by the Hassler, Penn State, Hafford, and dispersed feed methods. The inaccurate measurements by the single core dynamic method on short core samples may be attributable to the point-feed system which does not allow uniform dispersion of the two fluids within the short sample length.

Of the methods of relative permeability described, the Hassler technique is the slowest, requiring one week for the determination of a complete set of results on one sample. Data can be obtained by the Penn State, single core dynamic, Hafford, and dispersed feed methods at a rate of one relative permeability curve per day on samples having more than 100 md permeability. The gas drive method yields results at the greatest rate with the least chance for operator errors. About two hours is required to run one sample by this method.

CONCLUSIONS

From the investigations of the factors that influence the flow of fluids through porous material, the following conclusions can be drawn:

1. The influence of the boundary effect can be predicted from equations of fluid flow.
2. In laboratory measurements, errors caused by the boundary effect can be eliminated or made insignificant in many cases.
3. When gas and a liquid are used to determine the relative permeability-saturation relations, the effect of a several-fold gas expansion along the flow path has no important bearing on the laboratory measurements.
4. The drainage relative permeability-saturation relations are independent of the rate of fluid flow as long as the flow rates are below the point where inertial effects are important.
5. The Hafford, Penn State, Hassler, and dispersed feed methods measure the correct relative permeabilities to oil and gas.
6. Present techniques of calculating oil permeabilities from gas drive data are not adequate. Further work on the calculation methods is needed before this rapid technique can be utilized in routine testing.
7. On short core samples, the relative permeability to oil determined by the single core dynamic method is too high, while the relative permeability to gas is slightly high.

REFERENCES

1. Caudle, B. H., Slobod, R. L., and Brownscombe, E. R. "Further Developments in the Laboratory Determination of Relative Permeability," *Trans. AIME*, (1951) 192, 145.
2. Rose, Walter: Technical Note—"Fluid Distributions Characterizing Gas-Liquid Flow," *Trans. AIME*, (1951) 192, 372.
3. Geffen, T. M., Owens, W. W., Parrish, D. R., and Morse, R. A.: "Experimental Investigation of Factors Affecting Laboratory Relative Permeability Measurements," *Trans. AIME* (1951) 192, 99.
4. Osoba, J. S., Richardson, J. G., Kerver, J. K., Hafford, J. A., Blair, P. M.: "Laboratory Measurements of Relative Permeability," *Trans. AIME*, (1951) 192, 47. ★ ★

SOME PROPERTIES OF MIXED PARAFFINIC AND OLEFINIC HYDRATES

H. H. REAMER, F. T. SELLECK AND B. H. SAGE, MEMBER AIME, CALIFORNIA INSTITUTE OF TECHNOLOGY, PASADENA, CALIF.

ABSTRACT

An experimental investigation was made of the effect of temperature upon the three-phase pressure associated with the propane-water and propene-water systems when hydrates were present. In addition, the characteristics of the propane-propene-ether system were established over a limited range of temperatures under conditions such that hydrate was formed. The hydrate phase for this system may be a solid solution and the distribution of propane and propene in it is similar to that found in the coexisting hydrocarbon liquid phase.

INTRODUCTION

A knowledge of the characteristics of hydrates of the hydrocarbons encountered in industrial practice is of importance in connection with the design of process equipment. Villard^{1,2} carried out early studies of hydrates, and de Forcrand³ considered the more probable compositions of the hydrates of hydrocarbons. Hammerschmidt⁴ presented information about the propane-water and the isobutane-water systems. Scheffer⁵ studied the hydrate of hydrogen sulfide in detail, and de Forcrand reported on the hydrates of krypton, argon, and xenon.^{6,7} Roberts and co-workers^{8,9} determined the nature of the hydrates formed in the methane-water and ethane-water systems. Carson and Katz¹⁰ studied the methane-propane-water, ethane-pentane-water, and the methane-hexane-water systems in the four-phase region. The results of this rather extensive investigation indicated that the paraffinic hydrates formed solid solutions. The experimental evidence now available does not support the existence of hydrates of the pentanes-and-heavier hydrocarbons but it cannot be stated with certainty that such hydrates are not formed. Stackelberg^{11,12,13} made extensive studies of the crystal structure of paraffinic hydrates by means of x-ray techniques and found that hydrates possess definite structure and composition. The existence of such a structure does not preclude the formation of solid solutions of hydrates in aqueous systems containing two or more hydrocarbons.

Wilcox, Carson and Katz¹⁴ reviewed the information on the hydrates of importance in the processing of natural gas and presented data concerning their formation from natural gas. Kobayashi and Katz¹⁵ made studies at high pressure of the hydrate of methane, and Unruh and Katz¹⁶ investigated hydrates in mixtures of carbon dioxide and methane.

Frost and Deaton^{17,18,19,20,21} contributed to the knowledge of the composition of the paraffinic hydrates. The irregularities in the experimental results were several times the expected certainties. This experience confirms the behavior encountered by other investigators indicating that hydrates tend to include water during their formation, thus rendering difficult the direct measurement of their composition. Miller and

Strong²² investigated a number of paraffinic hydrates from the standpoint of their possible application to the industrial storage of gas. Powell²³ studied the effect of solutes upon the decomposition temperature of paraffin hydrates. Marked lowering of the decomposition temperature at a given pressure may be obtained by the use of such additive agents as ethylene glycol, urea, and sodium chloride.

APPARATUS AND METHODS

Two methods were here employed to study the behavior of hydrates. The first involved a glass capillary within which the hydrocarbons and water were confined over mercury. The second made use of a double-ended weighing bomb technique.²⁴ The glass capillary equipment has been described elsewhere.²⁵ A schematic drawing of it is presented in Fig. 1, where the arrangement of the agitator and mercury reservoir is shown in some detail. The lower part of the glass capillary, *D*, was enlarged to afford space within which the fluids used in the investigation could be stored at low pressures after their introduction through the valve, *G*. The temperature of the capillary was controlled by the circulation of a hydrocarbon oil of low viscosity from the agitated bath, *B*, through the vacuum jacketed column, *C*. The pump, *A*, was employed for the circulation of this oil. A relatively clear view of the capillary tube, *D*, was obtained through the vacuum jacket. Mercury was introduced into the lower part of the vessel, *E*, from

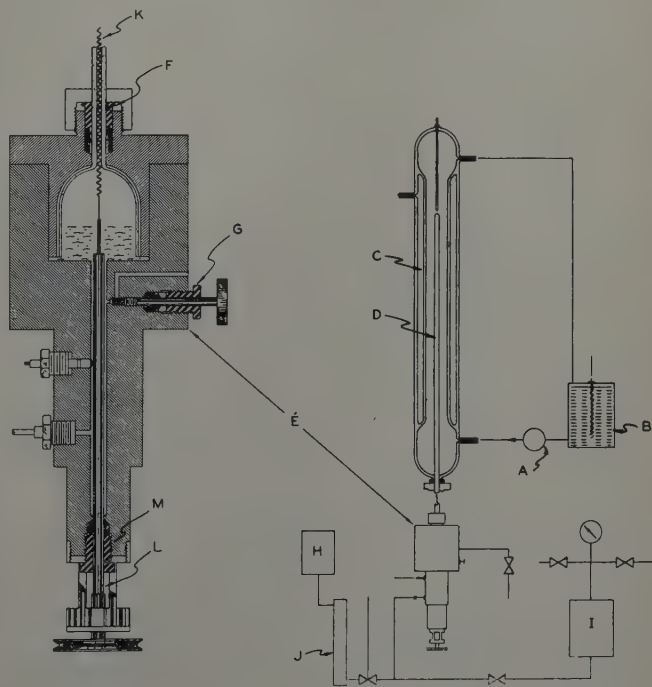


FIG. 1 — SCHEMATIC VIEW OF ARRANGEMENT OF GLASS CAPILLARY.

References given at end of paper.

Manuscript received in the Petroleum Branch office March 31, 1952.

For material supplementary to this article order Document 3809 from American Documentation Institute, 1719 N Street N.W., Washington 6, D.C., remitting \$1.00 for microfilm (images one in. high on standard 35 mm motion picture film) or \$1.00 for photocopies (six by eight in.) readable without optical aid.

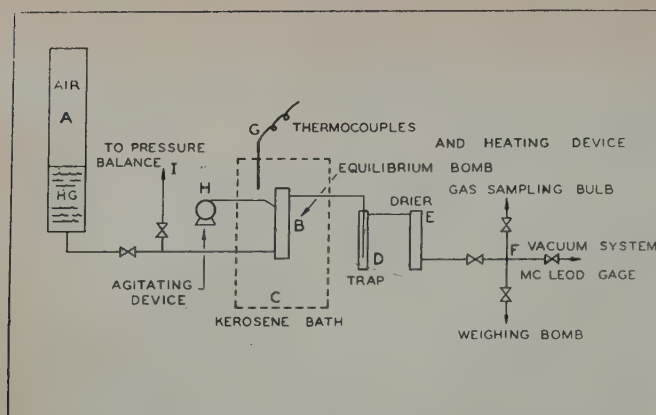


FIG. 2 — ARRANGEMENT OF EQUILIBRIUM BOMB EQUIPMENT.

the chamber, *I*, and the pressure within the system was determined by means of the balance, *H*.²⁴ The latter instrument was used in conjunction with the steel U-tube, *J*, which was arranged so as to permit elevation control of the mercury-oil interface in one of the arms of the U-tube. The uncertainty in the measurement of pressure was estimated to be 0.2 psi or 0.1 per cent, whichever was larger. Agitation within the capillary was provided by means of a stainless steel spiral, *K*, which was driven by the shaft, *L*, through the packing gland, *M*. The glass capillary was introduced into the vessel, *E*, through the packing gland, *F*.

The temperatures of the observations were determined by means of copper-constantan thermocouples used in conjunction with a double potentiometer of the White type having a range of 10,000 microvolts. The thermocouples were calibrated by means of a strain-free platinum resistance thermometer, the characteristics of which had been established by the National Bureau of Standards. The temperature of the exterior surface of the capillary tube was known within 0.2°F relative to the international platinum scale. The total effective volume of the capillary was determined from the elevation of the mercury interface relative to the closed end of the tube, which had been previously calibrated by weighing quantities of mercury withdrawn from the filled tube. The total volume of the system was believed known within one per cent except in the condensed regions when the volumes were so small that the uncertainties may have been as large as three per cent. The elevation of the mercury interface relative to the closed end of the glass capillary was determined by means of a cathetometer.

The desired amounts of the hydrocarbons to be investigated were introduced gravimetrically as has been described.²⁴ The quantity was checked by volumetric measurements under conditions at which the specific volumes of the hydrocarbons in question were known.²⁶ The proper quantity of water was then added and the amount established from the change in the total volume of the system. A small uncertainty resulted from the mutual solubility of water and the hydrocarbons. Appropriate corrections were made for such solubilities and uncertainties greater than one per cent were not experienced in determining the quantity of water and hydrocarbon employed.

The temperature then was reduced below that at which hydrates were formed. It was subsequently brought to the value chosen for the investigation of the isothermal change in total volume with pressure. The phenomenon of partial melting and the decomposition of the last trace of the hydrate phase were followed in some detail by such isothermal investigations. Similar studies were made under isobaric conditions. However, it was found that as a result of the longer time

required to obtain thermal equilibrium, the isobaric studies were much less effective than those made at a constant temperature. The majority of the results presented here have been obtained from isothermal investigations.

The equipment employed to determine the composition of the coexisting phases in the propane-propene-water system is shown schematically in Fig. 2. It involved the equilibrium bomb, *B*; the agitator, *H*; a means of introducing or withdrawing mercury from the vessel, *A*; and a sample withdrawal system shown at *D*, *E*, and *F*. A photograph of the double ended equilibrium vessel used in these investigations is presented in Fig. 3. The details of the design of this equipment are already available.²⁴ Desired quantities of hydrocarbon and water were introduced into the equilibrium bomb, *B*, of Fig. 2 and the whole was brought to temperature equilibrium. Agitation was accomplished by oscillation of the equilibrium vessel about an axis symmetrical with and normal to it. After hydrate had been formed, the pressure was raised by the introduction of mercury from the chamber, *A*, and agitation continued until there was no further change in pressure with time at a constant temperature. The pressure and temperature measurements were carried out in a similar manner and were of comparable accuracy to those described for the glass capillary equipment.

After equilibrium had been obtained, the liquid phases were displaced from the equilibrium vessel, *B*, by further introduction of mercury, the temperature and pressure within being held constant. A small internal filter was located in one end of the bomb, *B*, to prevent removal of the hydrates. After the liquid phases had been displaced from the equipment, the mercury was withdrawn in part and the temperature was raised sufficiently to decompose the hydrates. The displaced hydrocarbons were dried and the gain in weight of the drier, *E*, was considered to be the water associated with the hydrocarbons. The change in weight of the weighing bomb or of the gas sampling bulb was treated as hydrocarbon. The excess mercury displaced through the vessel, *B*, of Fig. 2, was collected in the trap, *D*. After displacement this trap was weighed, evacuated, and reweighed. Any loss in weight was considered to result from the presence of water and this weight was added to that collected in the drier, *E*.

After the hydrate had been decomposed, mercury was again introduced into the vessel, *B*, from *A* and the hydrocarbon and water were collected in the gas sampling bulb attached at *F*, and the drier, *E*, respectively. These procedures permitted the total quantity of hydrocarbons and of water to be accounted for with an uncertainty of not more than one per cent. The distribution of the propane and propene in the hydrocarbons withdrawn was determined by catalytic hydro-

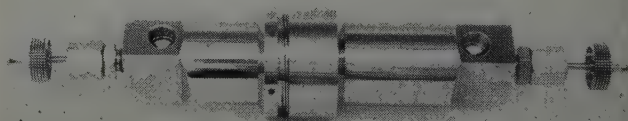


FIG. 3 — PHOTOGRAPH OF EQUILIBRIUM BOMB.

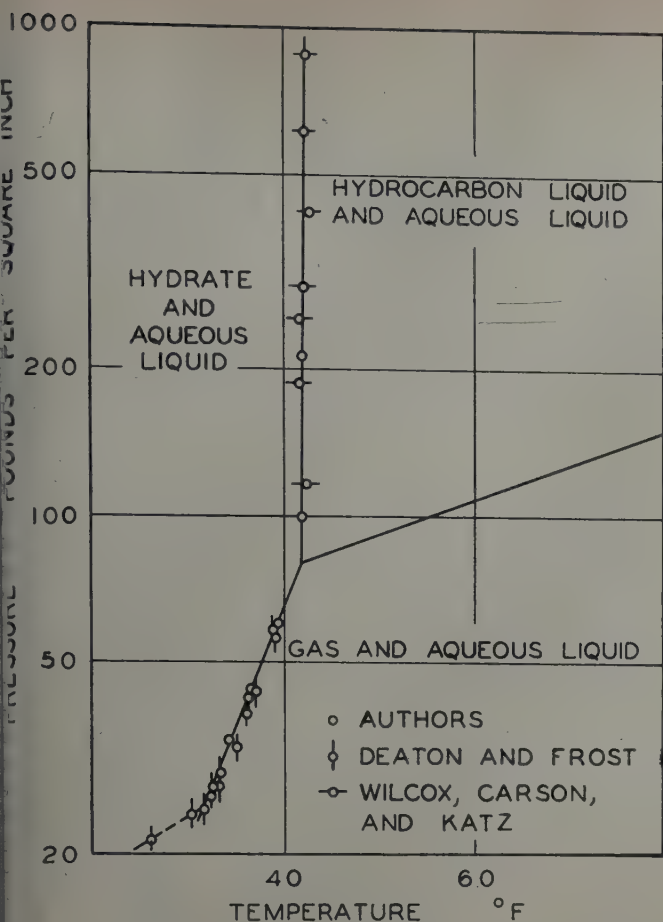


FIG. 4 — LOCUS OF THREE-PHASE STATES FOR PROPANE-WATER SYSTEM.

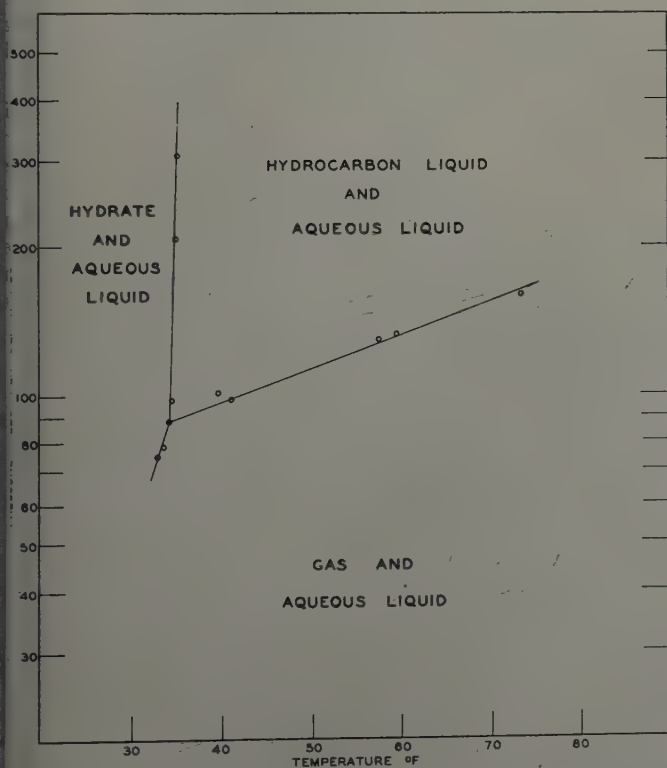


FIG. 5 — LOCUS OF THREE-PHASE STATES FOR PROPENE-WATER SYSTEM.

Table I — Three-Phase States for Propane-Water System

Pressure, psia	Temperature, °F	Phases Present
296.8	42.1	Hydrate, aqueous liquid, and hydrocarbon liquid
214.2	41.9	Hydrate, aqueous liquid, and hydrocarbon liquid
99.2	41.8	Hydrate, aqueous liquid, and hydrocarbon liquid
60.0	39.3	Hydrate, aqueous liquid, and gas
44.2	36.6	Hydrate, aqueous liquid, and gas
34.9	34.1	Hydrate, aqueous liquid, and gas

Table II — Three-Phase States for Propene-Water System

Pressure, psia	Temperature, °F	Phases Present
74.9	32.9	Hydrate, aqueous liquid, and gas
78.6	33.4	Hydrate, aqueous liquid, and gas
88.5	34.1	Hydrate, aqueous liquid, and gas
98.6	41.0	Gas, aqueous liquid, and hydrocarbon liquid
100.9	39.6	Gas, aqueous liquid, and hydrocarbon liquid
129.0	57.4	Gas, aqueous liquid, and hydrocarbon liquid
132.6	59.4	Gas, aqueous liquid, and hydrocarbon liquid
159.8	73.4	Gas, aqueous liquid, and hydrocarbon liquid
98.2	34.5	Hydrate, aqueous liquid, and hydrocarbon liquid
207.7	34.9	Hydrate, aqueous liquid, and hydrocarbon liquid
308.3	35.2	Hydrate, aqueous liquid, and hydrocarbon liquid

Table III — Three-Phase States* for Ethane-Water System

Isobaric Measurements

Pressure, psia	Temperature, °F
141.0	44.1
241.7	49.4
308.8	52.7
478.4	57.6

*Hydrate, gas, and aqueous liquid

Table IV — Three-Phase States* for Ethene-Water System

Pressure, psia	Temperature, °F	Pressure, psia	Temperature, °F
Isobaric Measurements			
143.6	34.7	322.2	47.4
168.3	41.4	349.5	49.3
179.9	41.3	362.6	49.5
203.6	42.0	385.7	51.0
257.3	43.0	427.7	50.5
280.9	45.1	454.0	52.7
302.4	43.7	474.9	53.7
		513.3	55.3
Isothermal Measurements			
82.2	29.9	258.6	46.3
91.0	32.0	302.6	47.9
99.3	34.6	335.3	50.4
127.0	39.0	402.3	52.6
171.5	41.3	440.2	54.7
226.4	43.7		

*Gas, aqueous liquid, and hydrate

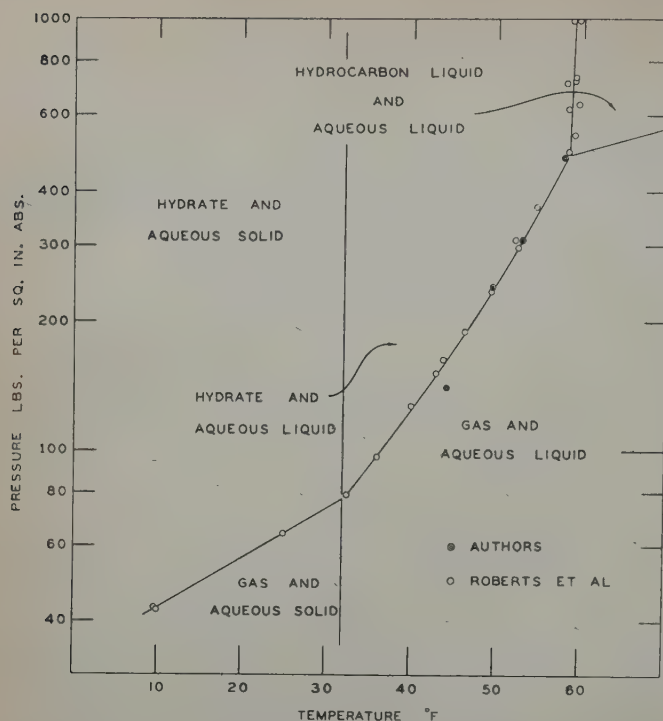


FIG. 6 — LOCUS OF THREE-PHASE STATES FOR ETHANE-WATER SYSTEM.

genation of the unsaturated hydrocarbons.²⁷ The relative quantity of propane and propene was established within 0.003 mole fraction.

MATERIALS

The ethane used in these studies was obtained from the Carbide and Carbon Chemicals Corp. and was purified by repeated fractionation in a glass column packed with small helices. The purified material contained enough impurities to yield approximately two lb change in vapor pressure at 70°F as a result of a change in quality from 0.2 to 0.9. The ethane was prepared by catalytic dehydration of purified ethyl alcohol by contact with aluminum oxide at approximately 840°F and atmospheric pressure. The crude ethene was purified by fractionation in the same column used for the purification of ethane. The refined material showed less than 0.6 psi change in pressure from dew point to bubble point. These samples were stored in stainless steel weighing bombs before use.

The propane and propene were obtained from the Phillips Petroleum Co. An analysis submitted by the company indicated that the propane contained less than one per cent of impurities. However, the olefin sample may have had as much as one per cent of material other than propene. The propene was purified by fractionation in the column previously described and was believed to contain not more than 0.002 mole fraction material other than propene. It was found that the decomposition temperatures for propene hydrate prepared from the crude and from the purified propene agreed within 0.1°F.

The water employed was obtained from laboratory distilled stocks which were fractionated once before use in order to remove dissolved gases.

EXPERIMENTAL RESULTS

The experimental results for the propane-water and the propene-water systems at three-phase states are recorded in Tables I and II and in Figs. 4 and 5. The data of Deaton and

Frost²⁰ and Wilcox, Carson and Katz¹⁴ have been included in Fig. 4. The present measurements for the propane-water system are in good agreement with those of the other investigators. The four-phase pressure of the propene-water system was approximately 10 psi higher and occurred at a temperature 7°F lower than the propane-water system.

Information concerning the ethane-water and ethene-water systems is recorded in Tables III and IV respectively. The data have been segregated into isobaric and isothermal measurements as was described earlier. The data of Roberts Brownscombe and Howe⁸ have been included in Fig. 6 along with the present data for the ethane-water system. Two four-phase states are presented in this diagram. No experimental data are available for the three-phase equilibrium involving hydrate, ice, and aqueous liquid or for the three-phase equilibrium involving gas, ice, and aqueous liquid; however, these latter states may be established with but small uncertainty from the behavior of water. The results of the investigation of the ethene-water system under isothermal conditions are presented in Fig. 7. These data represent the three-phase equilibria involving gas, hydrate, and aqueous liquid. The measurements made at constant pressure with a change in temperature gave slightly lower values of the decomposition temperature of the hydrate than were obtained from the studies involving a change in pressure at constant temperature.

A limited series of measurements was made of the propane-propene-water system. In these studies the ratio of the mole fraction of propane to propene was maintained at a fixed value as has been done for other ternary systems.^{20,28} In this instance the composition parameter C may be defined in the following way:

$$C = \frac{n_3}{n_3 + n_{III}} = \frac{X_3}{X_3 + X_{III}} \quad \dots \quad (1)$$

In this equation n is the mole fraction in the system and X the mole fraction in the liquid phase whereas the subscripts 3 and III refer, respectively, to propane and propene. The

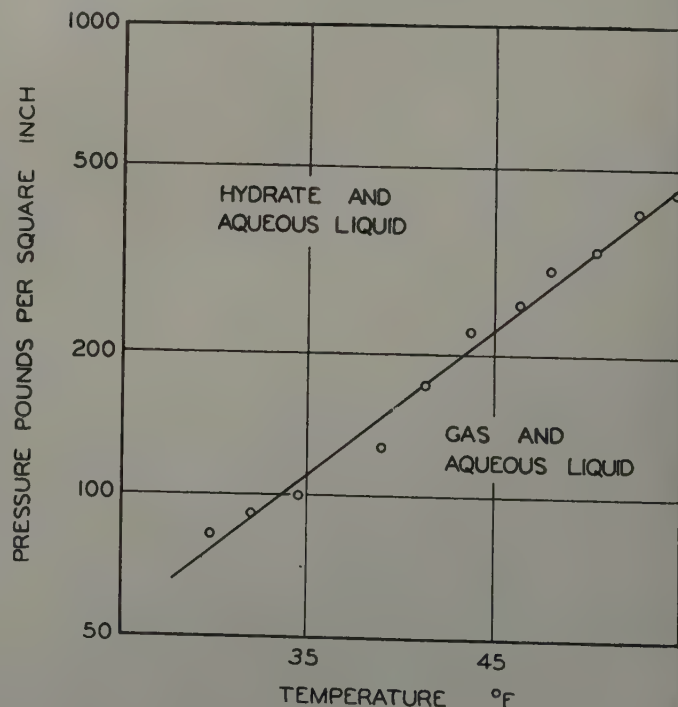


FIG. 7 — LOCUS OF THREE-PHASE STATES INVOLVING HYDRATE, GAS, AND AQUEOUS LIQUID FOR ETHENE-WATER SYSTEM.

experimental techniques were similar to those used in the propane-water and the propene-water systems. The hydrate was made up of translucent crystals which became substantially transparent upon partial melting. The experimental work indicated that the mixed hydrates decomposed over a range of temperatures at a given pressure. The first traces of hydrate decomposition under isobaric conditions occurred at a temperature between that corresponding to the decomposition of pure propane hydrate and of pure propene hydrate. In Table V are reported corresponding values of pressure and temperature at which hydrate initially decomposed for two different mixtures of the restricted ternary system. As indicated by the phase rule for a three-component system, a three-phase locus possesses two degrees of freedom and the four-phase state is univariant.

The behavior of the two mixtures investigated is shown graphically in Fig. 8. At a given pressure the temperature at which the hydrate begins to melt is a function of the parameter C . Such behavior appears to occur both for the ternary equilibrium involving hydrate, aqueous liquid, and hydrocarbon liquid and for the equilibrium including hydrate, aqueous liquid, and gas. The mixtures behave essentially as binary two-phase systems because of the very limited solubility of hydrocarbon in the aqueous phase and the small amount of water present in the gas phase. From the smoothed data for the equilibrium behavior of hydrate, aqueous liquid, and gas, together with the assumption of no intersolubility of the

Table VI—Comparison of Experimental and Calculated Three-Phase Pressures for the Propane-Propene-Water System

Composition ^a parameter C	Pressure ^b		Pressure ^b	
	Experimental	Calculated	Experimental	Calculated
	40°F		70°F	
0.3148	92.0	92.0	145.6	145.8
0.3711	91.4	91.1	144.2	144.5
0.5246	88.3	88.5	140.3	140.8
0.7589	84.3	84.2	133.7	133.9

^aDefined in Equation (1).

^bPressures expressed as psia.

water and hydrocarbons in liquid phases and of an ideal solution in the gas phase, it is possible to compute the corresponding values of equilibrium pressure and temperature for chosen values of the parameter C . By utilizing recently available data²⁰ such calculations were made for temperatures of 40° and 70°F and were used as the basis for the series of curves in that temperature range in Fig. 8. It appears from the correspondence between the experimental points and the curves and from the comparison shown in Table VI that the behavior of the propane-propene-water system at low pressures and temperatures may be predicted with reasonable accuracy as long as hydrate is not formed.

By means of the weighing bomb techniques which have been described earlier in this discussion 14 measurements were made to determine the composition of the coexisting hydrocarbon and hydrate phases in the three-phase equilibria in-

Table V—Three-Phase States for a Restricted Propane-Propene-Water System

Pressure, psia	Tempera- ture, °F	Phases Present
$C = 0.5246$		
43.6	33.0	Hydrate, aqueous liquid, and gas
51.3	34.3	Hydrate, aqueous liquid, and gas
53.7	34.1	Hydrate, aqueous liquid, and gas
53.8	34.2	Hydrate, aqueous liquid, and gas
57.7	34.6	Hydrate, aqueous liquid, and gas
62.8	35.6	Hydrate, aqueous liquid, and gas
65.4	35.3	Hydrate, aqueous liquid, and gas
66.5	35.3	Hydrate, aqueous liquid, and gas
72.4	37.4	Hydrate, aqueous liquid, and gas
72.7	37.0	Hydrate, aqueous liquid, and gas
72.8	36.4	Hydrate, aqueous liquid, and gas
73.2	37.3	Hydrate, aqueous liquid, and gas
88.7	39.2	Aqueous liquid, hydrocarbon liquid, and gas
90.3	41.3	Aqueous liquid, hydrocarbon liquid, and gas
93.2	45.5	Aqueous liquid, hydrocarbon liquid, and gas
105.5	52.3	Aqueous liquid, hydrocarbon liquid, and gas
120.6	59.5	Aqueous liquid, hydrocarbon liquid, and gas
138.3	71.2	Aqueous liquid, hydrocarbon liquid, and gas
98.3	38.3	Aqueous liquid, hydrocarbon liquid, and hydrate
116.7	38.3	Aqueous liquid, hydrocarbon liquid, and hydrate
126.9	38.3	Aqueous liquid, hydrocarbon liquid, and hydrate
137.8	38.4	Aqueous liquid, hydrocarbon liquid, and hydrate
183.2	38.4	Aqueous liquid, hydrocarbon liquid, and hydrate
264.4	38.8	Aqueous liquid, hydrocarbon liquid, and hydrate
277.0	38.8	Aqueous liquid, hydrocarbon liquid, and hydrate
288.2	38.8	Aqueous liquid, hydrocarbon liquid, and hydrate
396.8	38.9	Aqueous liquid, hydrocarbon liquid, and hydrate
$C = 0.3148$		
57.1	33.2	Hydrate, aqueous liquid, and gas
64.6	34.4	Hydrate, aqueous liquid, and gas
72.1	35.4	Hydrate, aqueous liquid, and gas
74.9	35.6	Hydrate, aqueous liquid, and gas
77.5	35.7	Hydrate, aqueous liquid, and gas
94.0	41.7	Aqueous liquid, hydrocarbon liquid, and gas
113.3	53.6	Aqueous liquid, hydrocarbon liquid, and gas
131.9	63.9	Aqueous liquid, hydrocarbon liquid, and gas
107.5	36.9	Aqueous liquid, hydrocarbon liquid, and hydrate
194.9	37.0	Aqueous liquid, hydrocarbon liquid, and hydrate
278.3	37.1	Aqueous liquid, hydrocarbon liquid, and hydrate

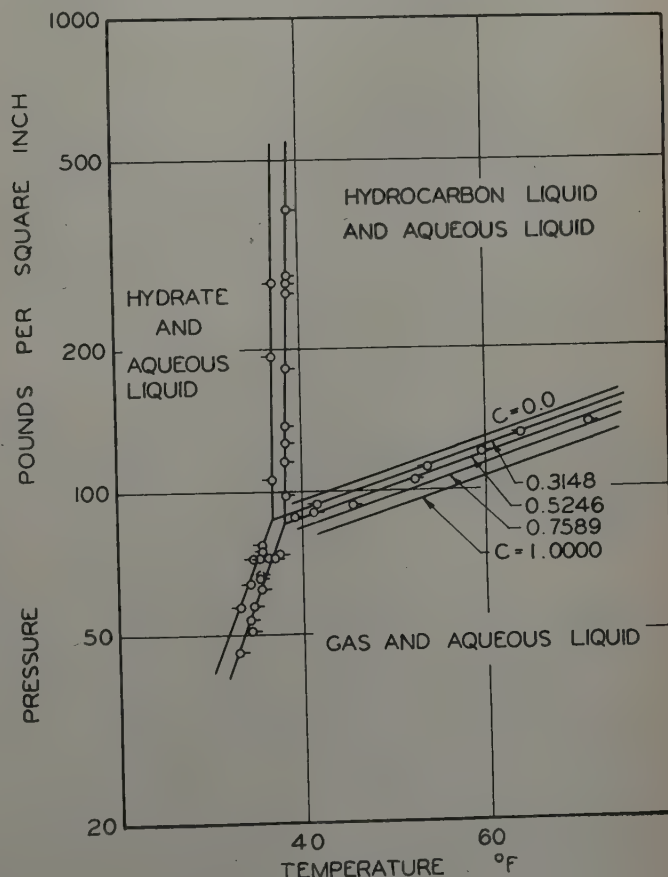


FIG. 8—PRESSURE-TEMPERATURE DIAGRAM FOR RESTRICTED MIXTURES FOR PROPANE, PROPENE, AND WATER.

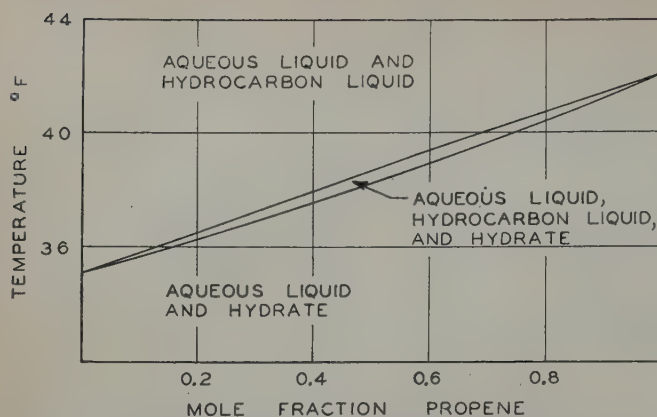


FIG. 9 — PRESSURE-TEMPERATURE DIAGRAM FOR RESTRICTED PROPANE-PROPENE SYSTEM AT 400 PSI.

volving hydrate. The results of these measurements are available elsewhere.³⁰ All measurements were made at a pressure of 400 psi and at temperatures between 32° and 39°F. The values of the equilibrium ratios for the components in the hydrocarbon liquid and hydrate phases were near unity. It was necessary to carry out a relatively large number of measurements in order to make sure that the results obtained were trustworthy. The standard deviation of five measurements for which complete data were obtained was 0.011. One measurement was discarded because of an excessive deviation, and no hydrate was formed in the remaining eight measurements. It appears that the hydrates may form a solid solution. The composition of the solid hydrate phase or phases follows closely that of the coexisting hydrocarbon liquid phase.

By combining the data obtained from the direct measurements of the composition of the coexisting phases and those shown in Fig. 8, it is possible to construct a temperature-composition diagram for the hydrocarbon phases. It should be realized that this diagram corresponds to a restricted ternary system in which there exists an excess of the aqueous liquid at all compositions. Fig. 9 is such a temperature-composition diagram for a pressure of 400 psi. Data regarding the compositions of the coexisting phases were employed to aid in establishing the aqueous liquid, hydrocarbon-liquid boundary curves and they involve somewhat more uncertainty than does the aqueous liquid-hydrate boundary which also is presented in Fig. 9.

ACKNOWLEDGMENT

This program of investigation was made possible by support from the Texaco Development Corp. Virginia Berry and Olga Strandvold aided in the assembly of the data and in the preparation of the manuscript, which was reviewed by W. N. Lacey.

REFERENCES

- Villard, P.: "Sur Quelques Nouveaux Hydrates de Gaz," *Compt. rend.*, (1888) 106, 1602.
- Villard, P.: "Sur les Hydrates de Méthane et de éthylène," *Compt. rend.*, (1888) 107, 395.
- de Forcrand, R.: "Sur la Composition des Hydrates de Gaz," *Compt. rend.*, (1902) 135, 959.
- Hammerschmidt, E. G.: "Formation of Gas Hydrates in Natural Gas Transmission Lines," *Ind. and Eng. Chem.*, (1934) 26, 851.
- Scheffer, F. E. C.: "Das System, Schwefelwasserstoff-Wasser," *Zeit. f. phys. Chem.*, (1913) 84, 713.
- de Forcrand, R.: "Sure les Hydrates de Krypton et d'Argon," *Compt. rend.*, (1925) 176, 355.
- de Forcrand, R.: "L'Hydrate de Xénon," *Compt. rend.* (1925) 181, 15.
- Roberts, O. L., Brownscombe, E. R., and Howe, L. S.: "Constitution Diagrams and Compositions of Methane and Ethane Hydrates," *Oil and Gas Jour.*, (1940) 391, 30.
- Roberts, O. L., Brownscombe, E. R., Howe, L. S., and Ramser, H.: "Phase Diagrams of Methane and Ethane Hydrates," *Petr. Eng.*, (1941) 12, [6] 56.
- Carson, D. B., and Katz, D. L.: "Natural Gas Hydrates," *Trans. AIME*, (1942) 146, 150.
- von Stackelberg, M.: "Struktur und Formel der Gashydrate," *Fortschr. der Mineralogie*, (1947) 26, 122.
- von Stackelberg, M.: "Feste Gashydrate," *Naturwiss.* (1949) 36, No. 11, 327.
- von Stackelberg, M.: "Feste Gashydrate," *Naturwiss.* (1949) 36, No. 12, 359.
- Wilcox, W. I., Carson, D. B., and Katz, D. L.: "Natural Gas Hydrates," *Ind. and Eng. Chem.*, (1941) 33, 662.
- Kobayashi, R., and Katz, D. L.: "Methane Hydrate at High Pressure," *Trans. AIME*, (1949) 186, 66.
- Unruh, C. H., and Katz, D. L.: "Gas Hydrates of Carbon Dioxide-Methane Mixtures," *Trans. AIME*, (1949) 186, 83.
- Frost, E. M., Jr., and Deaton, W. M.: "Gas Hydrate Formation and Equilibrium Data," *Oil and Gas Jour.*, (1946) 15, [12] 170.
- Deaton, W. M., and Frost, E. M., Jr.: "Gas Hydrates in Natural Gas Pipe Lines," *Amer. Gas Assoc. Monthly*, (1937) 19, 219; *Oil and Gas Jour.*, (1937) 36, 75; *Amer. Gas Jour.*, (1937) 146, 17; *Gas Age*, (1937) 80, 37.
- Deaton, W. M., and Frost, E. M., Jr.: "Gas Hydrates," *Proc. Amer. Gas Assoc.*, (1938) 112.
- Deaton, W. M., and Frost, E. M., Jr.: "Gas Hydrates and Their Relation to the Operation of Natural-Gas Pipe Lines," Bureau of Mines Monograph, (1946) 8.
- Deaton, W. M., and Frost, E. M., Jr.: "Gas Hydrates," *Gas Age*, (1938) 81, [11] 33.
- Miller, B., and Strong, E. R., Jr.: "Hydrate Storage of Natural Gas," *Amer. Gas Assoc. Monthly*, (1946) 28, 63.
- Powell, J. S., Jr.: "Lowering Decomposition Temperature of Natural Gas Hydrates by Solutes in Aqueous Solutions," *Proc. Pacific Gas Assoc.*, (1939) 30, 52; *Gas*, (1939) 15, 39.
- Sage, B. H., and Lacey, W. N.: "Apparatus for Study of Pressure-Volume-Temperature Relations of Liquids and Gases," *Trans. AIME*, (1940) 136, 136.
- Nysegander, C. N., Sage, B. H., and Lacey, W. N.: "Phase Equilibria in Hydrocarbon Systems. The Propane-n-Butane System in the Critical Region," *Ind. and Eng. Chem.*, (1940) 32, 118.
- Sage, B. H., and Lacey, W. N.: *Thermodynamic Properties of the Lighter Hydrocarbons and Nitrogen*, API, New York, 1950.
- McMillan, W. A., Cole, H. A., and Ritchie, A. V.: "Determination of Gaseous Olefins or Hydrogen by Catalytic Hydrogenation," *Ind. and Eng. Chem. Anal. Ed.*, (1936) 8, 105.
- Carter, R. T., Sage, B. H., and Lacey, W. N.: "Phase Behavior in the Methane-Propane-n-Pentane System," *Trans. AIME*, (1941) 142, 170.
- McKay, R. A., Reamer, H. H., and Sage, B. H.: "Volumetric and Phase Behavior in the Propene-Propane System," *Ind. and Eng. Chem.*, (1951) 43, 1628.
- Reamer, H. H., Selleck, F. T., and Sage, B. H.: "Composition of the Coexisting Hydrocarbon and Hydrate Phases in the Propane-Propene-Water System," American Documentation Institute, Washington, D. C., Document No. 3609, (1952).

★ ★ ★

NEUTRON DERIVED POROSITY-INFLUENCE OF BORE HOLE DIAMETER

C. B. SCOTTY AND E. F. EGAN, MEMBER AIME, THE TEXAS CO., BELLAIRE, TEX.

INTRODUCTION

The neutron-gamma log has been used for stratigraphic correlation by the oil industry for a number of years. In the past few years, the quantitative application of the log to provide information with respect to porosity has received considerable attention. The basic concept of quantitative interpretation has been pointed out in the literature.^{1,2,3} It shall be the purpose of this paper to develop by empirical means a method whereby the relationship of porosity to neutron-gamma deflection may be predicted for various bore hole diameters. This relationship is applicable to the present commercially available neutron-gamma log run in open hole. Data available at present are insufficient to establish similar correlations for cased holes. Through the development of such a correlation, the importance of the various factors which influence the log become evident.

NEUTRON-GAMMA CURVE

The logging tool consists of a source of neutrons and a means of detecting and measuring gamma rays, the detector being shielded from the direct emission from the source. The gamma rays reaching the detector have three sources of origin: 1) the natural gamma radiation emitted by the formations; 2) induced gamma radiation resulting from neutron bombardment; (3) gamma rays emitted by the source and scattered by the formation.

It has been found that a neutron derived porosity correlation is best for shale-free formations. Under this condition the natural gamma ray radiation is quite low, and therefore, will be neglected in this work.

The induced gamma ray radiation resulting from neutron bombardment is predominantly a function of the hydrogen atom concentration of the substance penetrated. Due to the geometry of the presently used system, the neutron-gamma curve indicates low radioactivity opposite high hydrogen concentration and high radioactivity opposite low hydrogen concentration (Figs. 1 and 2). Having a curve which measures hydrogen atom concentration, it follows that if the matrix of the formation penetrated consists only of atoms other than hydrogen, and if the fluid filling the pores is either oil or water, the curve should be an indication of porosity (both oil and water have practically the same number of hydrogen atoms per unit volume). The above criteria for a porosity correlation are fulfilled in clean sandstones and limestones in which the pore volume is completely filled with liquids (oil or water), but not in formations containing either free gas or shale or both.

Free gas, even under pressure, contains considerably less hydrogen per unit volume than oil and water; therefore, a variation in response on the curve would be expected. Camp-

bell and Winter,⁴ indicate that this difference in hydrogen concentration is sufficient to distinguish between sands containing water or oil and those containing dry gas.

Shale is a mineral that contains hydrogen in its molecular structure in addition to the hydrogen which is present in the water of hydration. Thus, in formations containing variable amounts of shale, the hydrogen concentration indicated by the curve is not a direct indication of porosity. Bush and Mardock¹ have indicated that a correction may be made by use of the gamma ray curve to provide a porosity correlation.

Since the induced gamma rays are predominantly a function of hydrogen concentration, it would be anticipated that the fluid filled bore hole would materially influence the logs. It has been pointed out that the neutron-gamma curve response decreases with increase in hydrogen concentration, therefore, the response due to the induced gamma ray component decreases with increase in fluid filled bore hole diameter.

The scattered gamma ray component of the log increases with increase in bore hole diameter. Although there is an

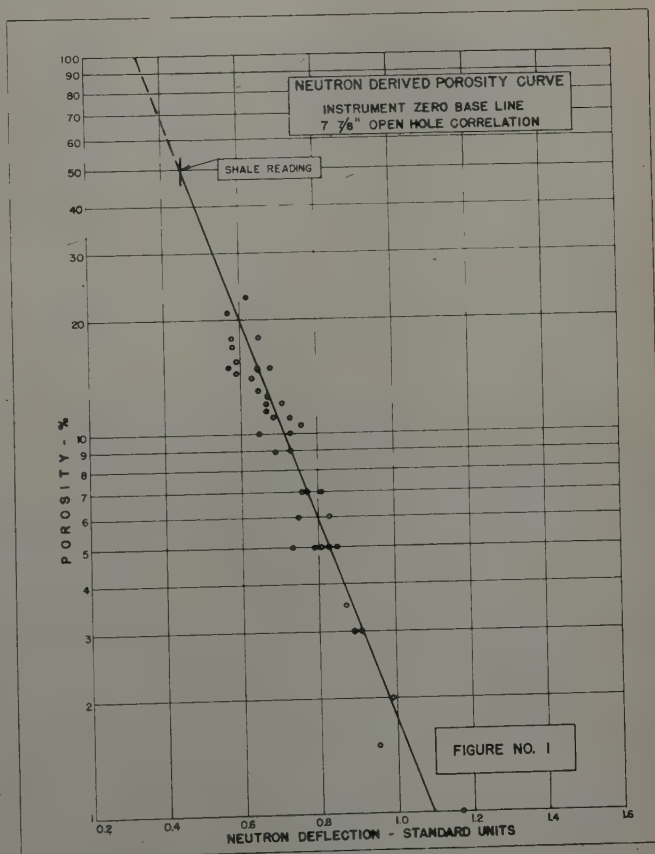


FIG. 1 — NEUTRON DERIVED POROSITY CURVE.

¹References given at end of paper.
²Manuscript received in the office of the Petroleum Branch April 18, 1952.

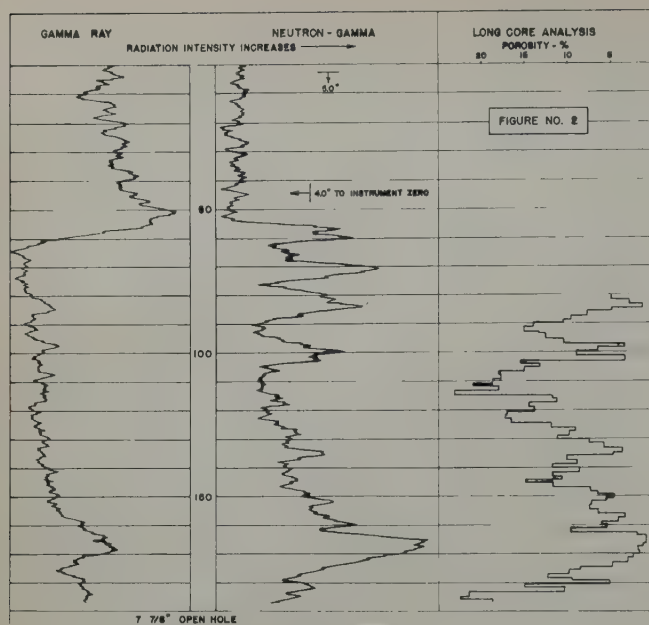


FIG. 2

influence due to the density of the formation, with the present commercially available instrumentation the scattered gamma ray component is essentially constant for a given bore hole diameter. This means that the scattered gamma ray component causes a shift of a fixed amount on the neutron-gamma log response for various bore hole diameters.

POROSITY CORRELATION

It has been shown that the neutron-gamma log responds logarithmically to liquid filled porosity.^{1,2,3} Such a correlation is established empirically by plotting the neutron-gamma deflection from a convenient base line (instrument zero or shale base) as the abscissa and the porosity as the ordinate on semi-log graph paper and drawing a straight line through the points. An example of such a correlation is shown in Fig. 1. Fig. 2 is a reproduction of a neutron-gamma log from the Canyon Reef of West Texas and the corresponding core analysis from which the above correlation was developed. It will be noted from Fig. 1 that the neutron-gamma deflection is plotted in "standard units." The "standard unit" represents the neutron-gamma curve deflection from the base line of correlation measured in inches divided by the sensitivity of the log. This nomenclature supplies a quantity which is applicable to any log irrespective of sensitivity. Such a correlation may be established using any convenient base line; instrument zero or shale base line. However, it should be pointed out that the use of instrument zero would provide a correlation which is applicable in any area; whereas the application of the shale reference correlation is limited to an area in which it can be ascertained that the hydrogen content of the shale is constant.

Empirical porosity correlations such as that shown in Fig. 1 have been developed for five bore hole diameters. These open hole correlations were developed from core analysis data obtained in the Canyon Reef of West Texas. An analysis of these correlations has provided a basis for the development of relationships necessary to predict the neutron derived porosity correlation for various bore hole diameters.

INFLUENCE OF BORE HOLE

In order to determine the influence of bore hole diameter on the neutron-gamma porosity correlation, the factors controlling the slope and intercept of the curves must be analyzed. The induced gamma ray component of the log determines the slope of the curve, whereas the intercept is dependent upon both the induced and scattered gamma ray components.

The variation in intercept with hole size may be removed by selecting a base line on the log. In the past it has been found convenient to use the shale as a reference. However, it was not possible in every case to establish a shale base line; therefore, the equivalent porosity of the shale of 50 per cent was selected as the base line (see Fig. 1). Such a correlation is readily developed by transposing the proper slope of the porosity correlations developed wherein the curve intersect 50 per cent porosity at zero deflection. In essence, this produces a neutron derived porosity correlation with a shale base line. This correlation for the various bore hole diameters in the Canyon Reef is shown in Fig. 3.

Having developed a series of porosity correlations with a common intercept, it is now possible to relate the influence of bore hole diameter to the slope of curve. Since it has been shown that the neutron-gamma log responds logarithmically to liquid filled porosity, it may be anticipated that the volume of the fluid in the bore hole may influence the induced gamma ray component of the log in a like manner. This may be shown by a plot of the equivalent bore hole area vs neutron deflection from the shale base line for any given value of porosity. Fig. 4 represents such a plot on semi-log graph

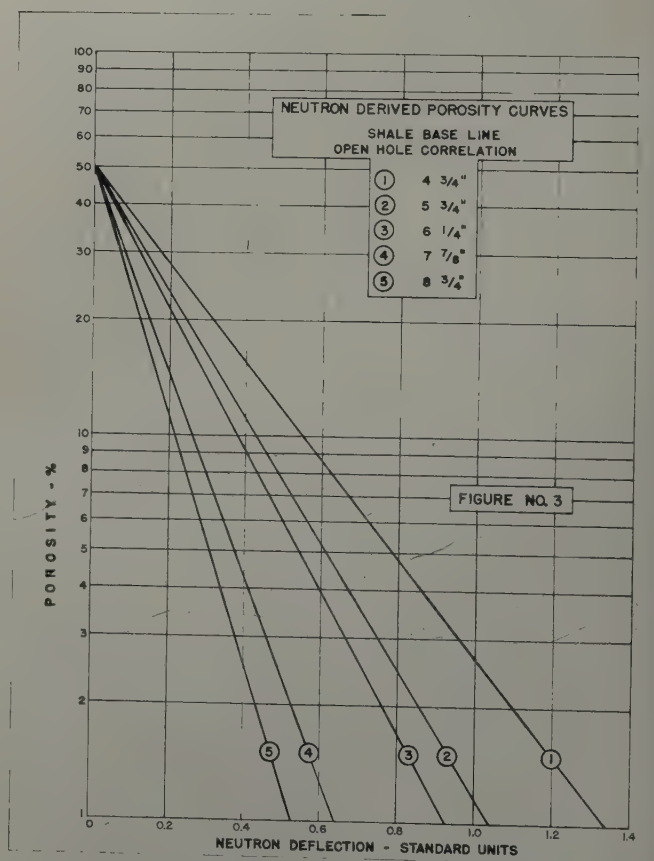


FIG. 3 — NEUTRON DERIVED POROSITY CURVES.

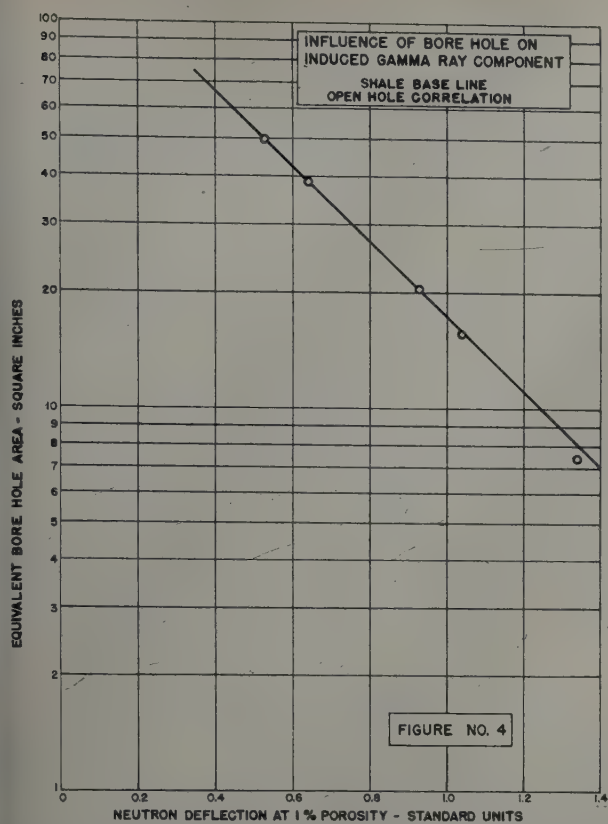


FIG. 4 — INFLUENCE OF BORE HOLE ON INDUCED GAMMA RAY COMPONENT.

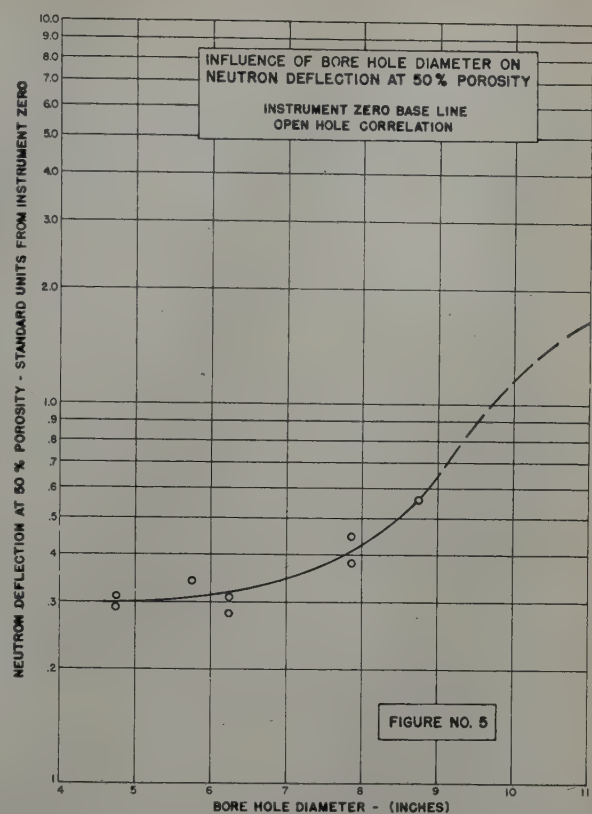


FIG. 5 — INFLUENCE OF BORE HOLE DIAMETER ON NEUTRON DEFLECTION AT 50 PER CENT POROSITY.

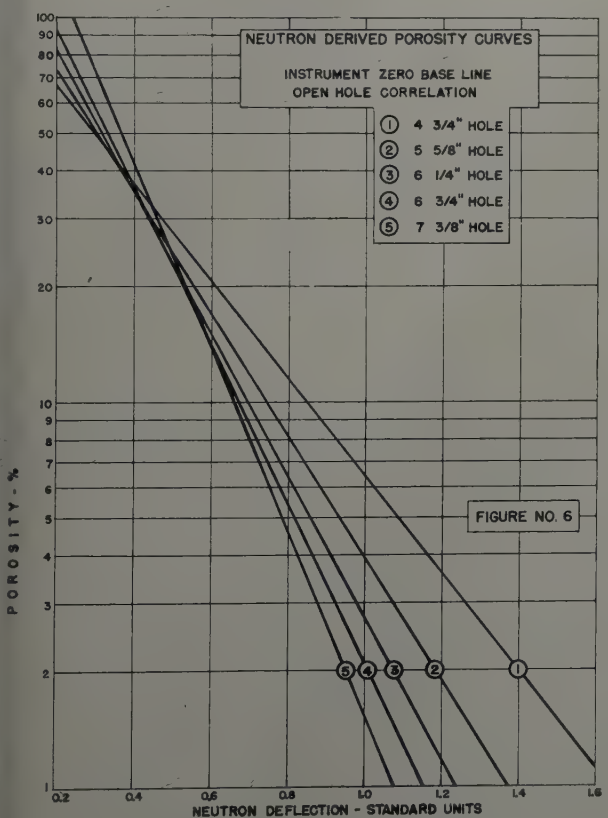


FIG. 6 — NEUTRON DERIVED POROSITY CURVES.

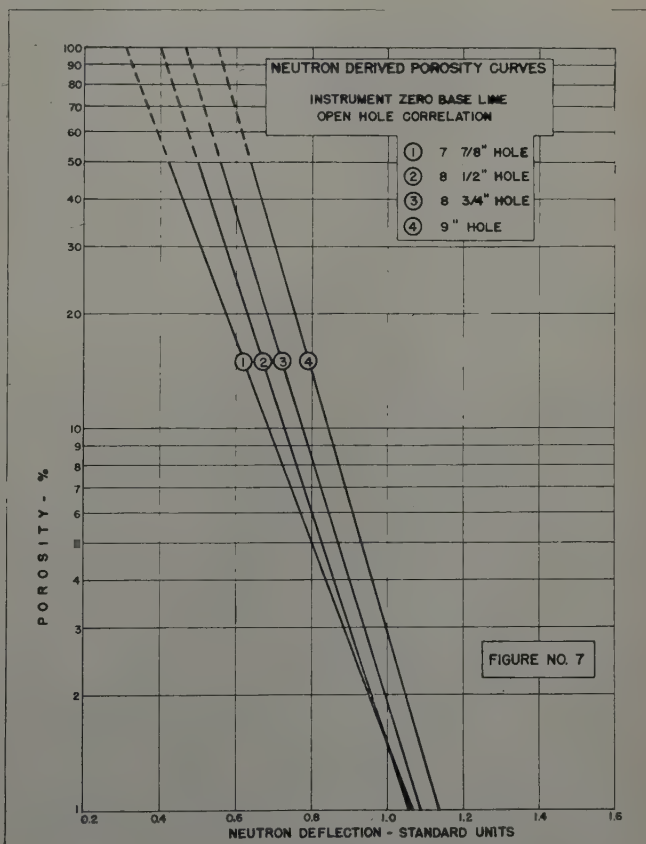


FIG. 7 — NEUTRON DERIVED POROSITY CURVES.

paper wherein the neutron deflection was obtained from Fig. 3 at one per cent porosity. The equivalent bore hole area is the area of the bore hole minus the area of the logging sonde ($3\frac{5}{8}$ -in. diameter).

The variation in intercept with hole size may be readily demonstrated by a plot of neutron-gamma deflection from instrument zero for a fixed porosity vs bore hole diameter. Fig. 5 is a plot of the neutron-gamma curve deflection from instrument zero to the shale base line (50 per cent equivalent porosity) vs bore hole diameter. As stated previously the intercept is dependent upon both the induced and scattered gamma ray components. Whereas the two components cannot be separated with the data available, it may be stated that the induced gamma ray component is the predominant factor in small holes; that is, six in. or less. The scattered gamma ray component becomes predominant in larger sized holes. The dotted portion of the curve indicates the anticipated trend of the scattered gamma ray component with further increase in bore hole diameter.

It will be noted from Fig. 5 that there is considerable scatter of data. This scatter is attributed to non-productivity of instrument zero since the two data points for $7\frac{7}{8}$ -in. hole were obtained from repeat runs in the same hole.

CALCULATED NEUTRON - GAMMA DERIVED POROSITY CORRELATIONS FOR OPEN HOLE OF VARIOUS DIAMETERS

Having established the influence of bore hole diameter on the induced gamma ray and scattered gamma ray components, it is now possible to calculate liquid filled neutron-gamma porosity correlations for shale-free formations. Figs. 6 and 7 show open hole porosity correlations for the more common bore hole sizes as calculated from Figs. 4 and 5.

An examination of these curves reveals several critical factors which influence the quantitative interpretation of neutron-gamma logs. The sensitivity of the neutron-gamma curve to changes in porosity decreases with increase in bore hole diameter. This requires an accurate determination of instrument zero if reasonable estimates of porosity are to be obtained in large holes. Of even more importance is the large influence of small changes in bore hole diameter on the log when run in large holes. This becomes evident when curves three and four of Fig. 7 are compared. A change in bore hole diameter of one quarter of an inch ($8\frac{3}{4}$ in. to 9 in.) corresponds to a large change in the neutron derived porosity. The scattered gamma ray component is primarily responsible for this shift.

STATISTICAL ERROR AND REPRODUCIBILITY OF THE NEUTRON-GAMMA LOG

In order to determine the reproducibility of the log and the magnitude of statistical error, repeat logs were obtained in the same hole at two different sensitivities. Fig. 8 is a cross plot of the neutron-gamma deflections of the two logs.

SUMMARY AND CONCLUSIONS

Empirical correlations are presented whereby neutron-gamma porosity correlations for open hole conditions may be calculated for various fluid filled bore hole diameters. Although the correlations were developed from the Canyon Reef of West Texas, they are applicable to other liquid filled formations substantially free of shale. The correlations developed are only valid for the commercially available neutron-gamma instrumentation as run at present.

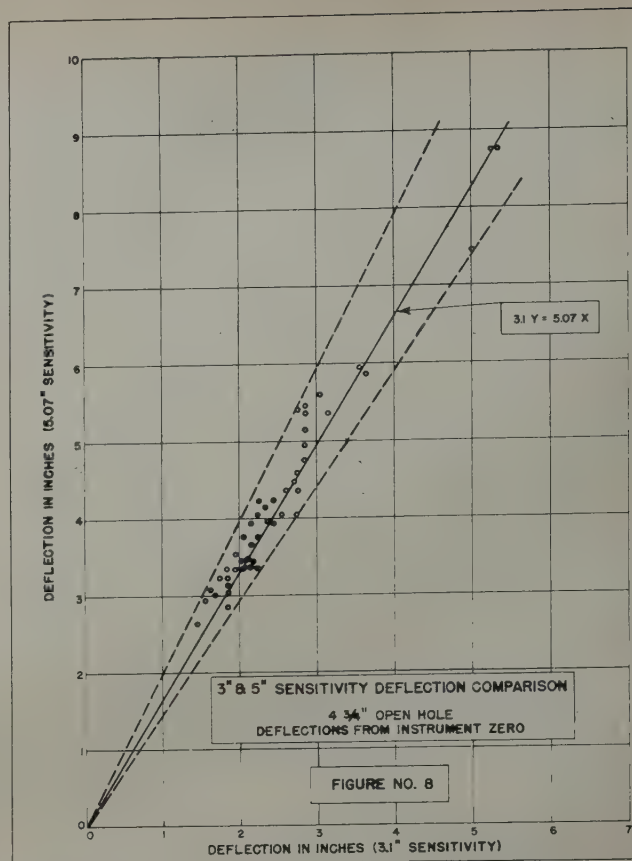


FIG. 8 — THREE AND FIVE IN. SENSITIVITY DEFLECTION COMPARISON

The application of these neutron gamma porosity correlations should provide a good means of estimating porosity in wildcat wells wherein the bore hole diameter is less than eight in. In large holes, the influence of small changes in bore diameter materially influence the log; therefore, an accurate knowledge of hole diameter is required. Porosity interpretation in large bore holes is further hampered due to decrease in the neutron-gamma log response to changes in porosity with increase in bore hole diameter. This factor can be minimized by a more accurate determination of instrument zero.

ACKNOWLEDGMENTS

The authors acknowledge helpful discussion of the subject by G. Herzog, K. C. ten Brink and A. S. McKay. They thank the management of The Texas Co. Producing Department for the permission to publish this paper.

REFERENCES

1. Bush, R. E., and Mardock, E. S.: "Some Preliminary Investigations of Quantitative Interpretations of Radioactivity Logs," *Trans. AIME*, (1950) 189, 19.
2. Scotty, C. B.: "Quantitative Log Interpretation of the San Andres Dolomite," *World Oil*, (1951) 133, (1), 166.
3. Bush, R. E., and Mardock, E. S.: "The Quantitative Application of Radioactivity Logs," *Trans. AIME*, (1951) 192, 191.
4. Campbell, J. L. P., and Winter, A. B.: "Dry Gas Sand. Tomorrow's Tools Today, Lane-Wells Co., (1947). ★ ★

SAMPLE GRADING METHOD OF ESTIMATING GAS RESERVES

L. KATZ, UNIVERSITY OF MICHIGAN, ANN ARBOR, MICH., MEMBER AIME; C. E. TURNER, MEMBER AIME, AND D. GRIMM, PHILLIPS PETROLEUM CO., BARTLESVILLE, OKLA.; AND J. R. ELENBAAS, JUNIOR MEMBER AIME, AND J. A. VARY, MEMBER AIME, MICHIGAN CONSOLIDATED GAS CO., GRAND RAPIDS, MICH.

ABSTRACT

A technique is presented by which well samples and core plugs of dolomite formations are classified by microscopic examination into seven different porosity grades. Quantitative values of porosity and permeability are determined for each grade by a statistical correlation of the core plug test data with the porosity grading system. These quantitative values are applied directly to the grades exhibited in the well samples for the purpose of estimating the reservoir void space in wells that were not cored.

The procedure is described for estimating the gas reserves per unit area for the South Hugoton gas field, but a reserve estimate for the field is not given.

INTRODUCTION

The microscopic examination of well samples and the graphic recording of their lithologic qualities and other distinguishing characteristics of various geologic formations is both a science and an art of long standing and wide application. Usually the primary objective of a geologist who "looks on the well" and examines the samples are: to identify the formation being drilled, determine the total depth, casing point, and completion interval. In most cases the porosity is described, if done at all, in general terms, such as: trace, scattered, fine, poor, fair, medium, good, excellent, or in some other relative terms. In fields where various geologists have examined samples and recorded observations on many wells considerable variations in lithologic terms and porosity descriptions occur unless there is primary effort to establish uniformity of logging observations and standards of recording observable porosity.

When an estimate of the pore volume of a reservoir is made a geologic concept of the processes that control the magnitudes of porosity and permeability is developed by microscopic examination of well samples. The characteristics and appearances are then mentally related to rather general quantitative units of porosity based on physical core data from the same reservoir or on such data or experience in other reservoirs that have similar qualities. The reliability of such estimates depends largely on the variations of the lithology of the formations, the geometric properties of its void system, the extent of comparisons of sample appearances with porosity data, as well as the uniform recording of all relevant characteristics. This statement is particularly significant for dolomitized limestone formations of substantial thicknesses and heterogeneity such as the Permian Dolomites of the Hugoton field. In this field, as well as in most of the Permian dolomite fields, the producing formations are of relatively great thicknesses in which the porosity and permeability of the reservoir varies substantially in all directions, depending on the crystalline structure, degree and kind of impurities, kind of fossils and cementation thereof, degree of dissolution,

and fracturing. The variations of the lithologic texture of the dolomites and post deposition alterations have resulted in porosities and permeabilities of such magnitudes that only a part of the gross thickness can be counted as "pay." At the time of this study insufficient gas production had been experienced to apply the pressure decline production method in the South Hugoton Field and the electric logs are not definitive enough. The problem of estimating gas reserves in the south part of the Hugoton Field is primarily one of determining the pay thickness and porosity from well samples and core data. The area studied embraced all that part of the field lying south of an east-west line through Guymon, Okla., and containing approximately 1,000,000 acres.

This paper describes a technique of correlation of physical core data with well samples so that quantitative values of pay thickness, porosity, permeability, and connate water may be assigned to well samples that are representative of a given interval, and thereby permitting the estimation of gas reserves for a given unit area. The procedure was developed by a uniform microscopic qualitative porosity grading of the dolomite core plugs, and relating these grades to the respective physical core data on a statistical basis. The well samples were also graded in a similar manner in order that the quantitative values established for the core plugs could be applied to the well samples for wells that were not cored.

GRADING OF DOLOMITE

A group of experienced geologists was given the assignment of examining the samples on all wells in South Hugoton in order that they could log their observations in a uniform and standardized manner and grade the observed porosity so that it could be related quantitatively to the core data.

The group initiated the study on chips from cores which had been tested for porosity and permeability. This study continued until all of the geologists developed a common knowledge of lithologic terms and of the characteristic appearances of the samples and their relations to measured porosity. The characteristic appearances of the dolomite samples under twelve-power magnification as related to their qualitative porosities afforded a classification of the dolomite into seven grades of porosity, ranging from dolomite of no-visible porosity under twelve-power magnification to dolomite of excellent porosity. The assigned grade for a specific 10-ft interval is a weighted average of all visible grades of porosity exhibited by the cuttings representing that interval. The porosity characteristics were recorded by a color graph adjacent to the lithology column in conjunction with a numerical system for further definition of relative porosity as shown in Fig. 1. The three vertical lines to the right of the lithology column each represent $33\frac{1}{3}$ per cent, which lines were used to record the percentage of the samples, for any particular interval, that showed porosity under the microscope. The colors were used to denote actual pore size, i.e., orange, blue and red for pore diameter of one-fourth or less, one-fourth to one-half, and greater than one-half millimeter, respectively. The area colored by one or more colors represents the percentages of the samples exhibiting pores of the respective size or sizes. The numerals from one to six inclusive shown on the log in

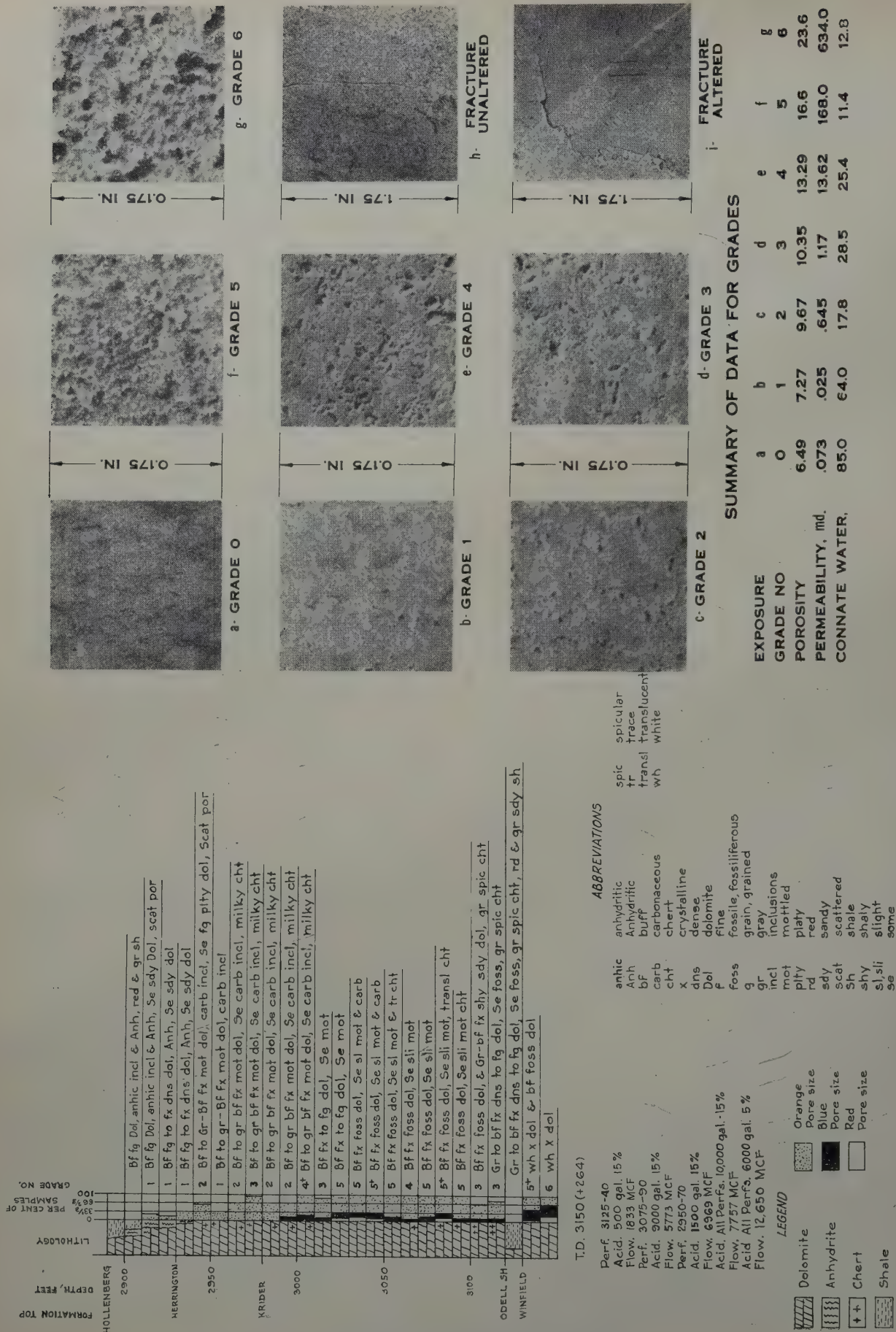


FIG. 1 — EXAMPLE WELL, SAMPLE LOG, HUGOTON FIELD, SHERMAN COUNTY, TEXAS.

FIG. 2 — PHOTOGRAPHS OF DOLOMITE.

g. 1 were established as grades in order of increasing visible porosity. The percentage of samples of no visible porosity, called grade 0, was not recorded on the "per cent of samples" graph of the log. The geologic group followed this procedure and worked without interruption in the relogging of the samples for 762 wells. It was found that grades were controlled primarily by the crystalline structure, frequency and size of secondary porosity, *e.g.*, pin-point solution tubes, and percentages of associated impurities such as anhydrite and chert. The assignment of porosity grades to the samples involved more judgment than any other element of the logging.

At this point it was necessary to determine the quantitative porosity corresponding to each grade in order to make mathematical application of the grading system. The most feasible means of relating porosity and permeability to the grade classifications was to grade the core plugs in the same manner as the well samples, including the recording of the percentage of the weighted average grade present. In order to avoid the possibility that observations of the smooth surfaces of the core plugs would result in basic differences in grading from that of the well samples, the plugs were chipped or broken for thorough examination and comparison. The results were found to be no different on smooth surfaces, chipped surfaces, or core chips. The core plugs were graded without reference to their measured values of porosity and permeability. The grading of the core plugs showed that not only the dolomite vary within 10-ft intervals, but also that in some plugs it varied within the size range of the core plug. Each is 0.75 in. in diameter and approximately 1.25 in. long. Each plug was given a grade number and a percentage value, called per cent-of-grade, in units of five, which represented a portion of the plug of the assigned grade. The remainder of the plug was grade zero, impurities or both. A lithologic description of the plugs was also recorded. The geologic group thus classified 2,077 core plugs of the producing formation. The photographs in Fig. 2, Parts "a" through "g" show polished surfaces of core plugs having grades zero through six. Because of the heterogeneity of the dolomite, the photographs are not typical of the different grades but portray the general appearance of the various dolomite lithologies.

POROSITY AND PERMEABILITY

At the time of this study, 3,434 ft of formation had been cored in 23 wells, including three core holes, from which 3,059 core plugs were tested for porosity and permeability. Of the 3,434 ft of core formation, 2,722 ft were from 20 wells from which 2,519 core plugs were tested. The number of core plugs available for examination at the time of grading was 2,077 from these 20 wells. The plugs from three wells were not available.

The porosity measurements were by the grain density and Washburn-Bunting methods. All values of permeability were determined by air flow and at dry conditions. Reliable values of dry permeabilities were determined to as low as 0.001 md. A plot of the porosity and permeability values of 2,547 specimens shown on Fig. 3 disclosed a relationship similar to that found by Bulnes and Fitting¹ for dolomitic limestone.

The porosity and permeability data derived from the 2,077 core plugs which were graded by the geologic group were arranged by the plug grades, zero through six and by the per cent-of-grade, and plotted in chart form in order to facilitate the evaluation of the grading system. For convenience of charting and statistical reasons the core data were arranged within grades in percentage groups for the plugs 0 to 20, 21 to 40, 41 to 60, 61 to 80, and 81 to 100 per cent-of-grade: Fig. 4-a shows porosity distributions by grades for the plugs 81 to 100 per cent-of-grade and Fig. 4-b shows similar charts except that the porosity data for the core plugs having permeability of 0.03 md and less were deleted.

The distribution charts just described show that the geologists were able to identify quite accurately the various qualities of porosity in the dolomite. This is best seen in Figs. 4-a and 4-b, where the numerical average porosity increases gradually and orderly with the increase of grade numerals. While there is considerable porosity-range in the distribution, the limits are relatively narrow for the great majority of the plugs. The average permeability also increases with the increase of grade number as would be expected when cognizance is given to the relationship shown in Fig. 3. When plotted by grades, the permeability distribution is similar to the porosity distribution shown in Figs. 4-a and 4-b.

¹References given at end of paper.

Fig. 3 POROSITY-PERMEABILITY RELATIONSHIP FOR PERMIAN DOLOMITE AT SOUTH HUGOTON
X-CORE PLUGS (179) USED IN CAPILLARY PRESSURE STUDY.

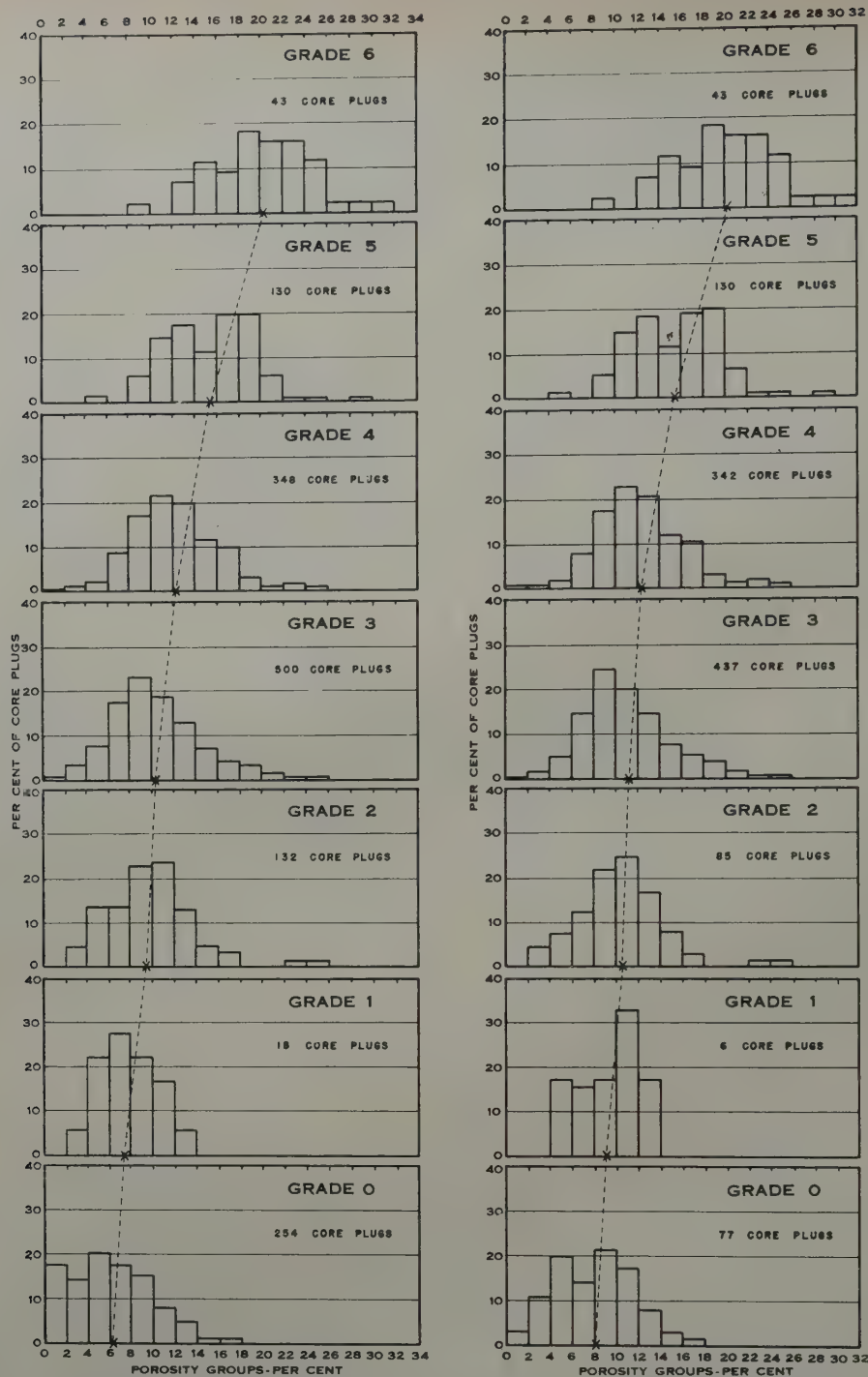


FIG. 4 — (A) POROSITY DISTRIBUTION BY GRADES. ALL CORE PLUGS CLASSIFIED 81 TO 100 PER CENT OF THE GRADE.

(B) POROSITY DISTRIBUTION BY GRADES. ALL CORE PLUGS GREATER THAN 0.03 MD PERMEABILITY AND 81 TO 100 PER CENT OF THE GRADE.

X — NUMERICAL AVERAGE POROSITY.

Not only does the numerical average porosity increase with increasing grade but it also increases with the increase of per cent-of-grade within the different grades. Specifically, the average porosity of the core plugs 81 to 100 per cent-of-grade is higher for each grade than that for the core plugs of 61 to 80 per cent-of-grade and so on for the lower ranges of per cent-of-grade. This is evidence of the validity of dividing the core plugs into per cent-of-grade groups.

At this point, the question arose as to what per cent-of-grade corresponded to the grade assigned to the samples for a given

interval of a well sample log. Since the samples were divided into dolomite of a given grade, above grade zero, and dolomite of no-visible porosity, the core plugs which correspond to the grade of the samples is 100 per cent-of-grade. The 81 to 100 per cent-of-grade group for all grades was selected to represent the characteristics of the different grades since there were insufficient plugs of 100 per cent-of-grade to provide a satisfactory statistical base. The use of this group resulted in slightly lower porosities and permeabilities than would have been the case for plugs of 100 per cent-of-grade.

CONNATE WATER

The connate water was estimated from the results of capillary pressure experiments on 179 core plugs that were selected so that the full range of permeability would be evaluated. The plugs were saturated with distilled water and placed on a porous ceramic plate in an air-pressured chamber. Most of the plugs were tested for saturation after having set in the air chamber for 5 to 14 days at a pressure of 40 psig. The water saturations and the corresponding permeability data were plotted on Fig. 5 and a curve drawn for the estimation of connate water values for the various grades.

CALCULATIONS OF FACTORS FOR DETERMINATION OF RECOVERABLE GAS

The core data for the plugs of permeability of 0.03 md and less were deleted because it was judged after extensive study that dolomite of this character would contain only very small quantities of gas due to relatively low porosity and high connate water and that this dolomite would not yield its gas to the well bore in a reasonable period of time. This deletion, therefore, required the determination of the percentage of the total dolomite that may be called "pay." This percentage is termed "effective-fraction-of-grade" and is simply the ratio of the number of core plugs of 81 to 100 per cent-of-grade with a permeability greater than 0.03 md to the total plugs of 81 to 100 per cent-of-grade. For example, the "effective-fraction-of-grade" factor for Grade 3 is the number of plugs shown on Fig. 4-b (437) divided by the number of plugs shown on Fig. 4-a (500) or 0.874. Also, this deletion required a re-determination of the average permeability of the respective grades. Such values are numerical averages. The results of these calculations are summarized in Table I.

The statistical base afforded by the large number of core plugs available permits the application of this "effective-fraction-of-grade" to the well samples of given grades to determine at portion of the dolomite interval that has permeability greater than 0.03 md and, therefore, may be counted as "pay."

These factors are applied to the well sample logs by 10-ft intervals in order to arrive at the effective-grade-feet which is the footage for a given interval of known grade that has permeability greater than 0.03 md.

The gross porosity for the geologic grades was the numerical average porosity of the core plugs more than 81 per cent of that grade and having a permeability greater than 0.03 md (shown on Fig. 4-b and tabulated on Table I). The above core plugs in each geologic grade were divided into permeability groups and the numerical average permeability and gross porosity of the plugs in each group was determined. From Fig. 5 the connate water corresponding to the numerical average permeability in each permeability group was read. From the gross porosity and connate water figures, the effective porosity (porosity containing gas) was calculated for each permeability group within each grade. These values were weighted by the fraction of core plugs in each permeability group to obtain the effective porosity for each grade shown on Table I.

The ultimate gas recovery for each per cent of effective porosity in one acre-ft of reservoir was computed by the gas laws to be 12,069 cu ft at 14,735 psia pressure base and 60°F temperature base. The computation was based on the following discovery and abandonment conditions.

- (1) Initial reservoir pressure, psia 485.0
- (2) Abandonment reservoir pressure, psia 84.0
- (3) Reservoir temperature, °F 90.0
- (4) Compressibility factor at original pressure 0.939
- (5) Compressibility factor at abandonment pressure 0.991

Table I summarizes the above reserve factors.

APPLICATION OF RESERVE FACTORS TO GEOLOGIC SAMPLE LOGS

Before an example application of the reserve factors shown in Table I is given, it is important to examine the credibility of the more significant elements of the technique developed herein. This credibility is dependent upon:

- (1) The uniformity and thoroughness of porosity grading of

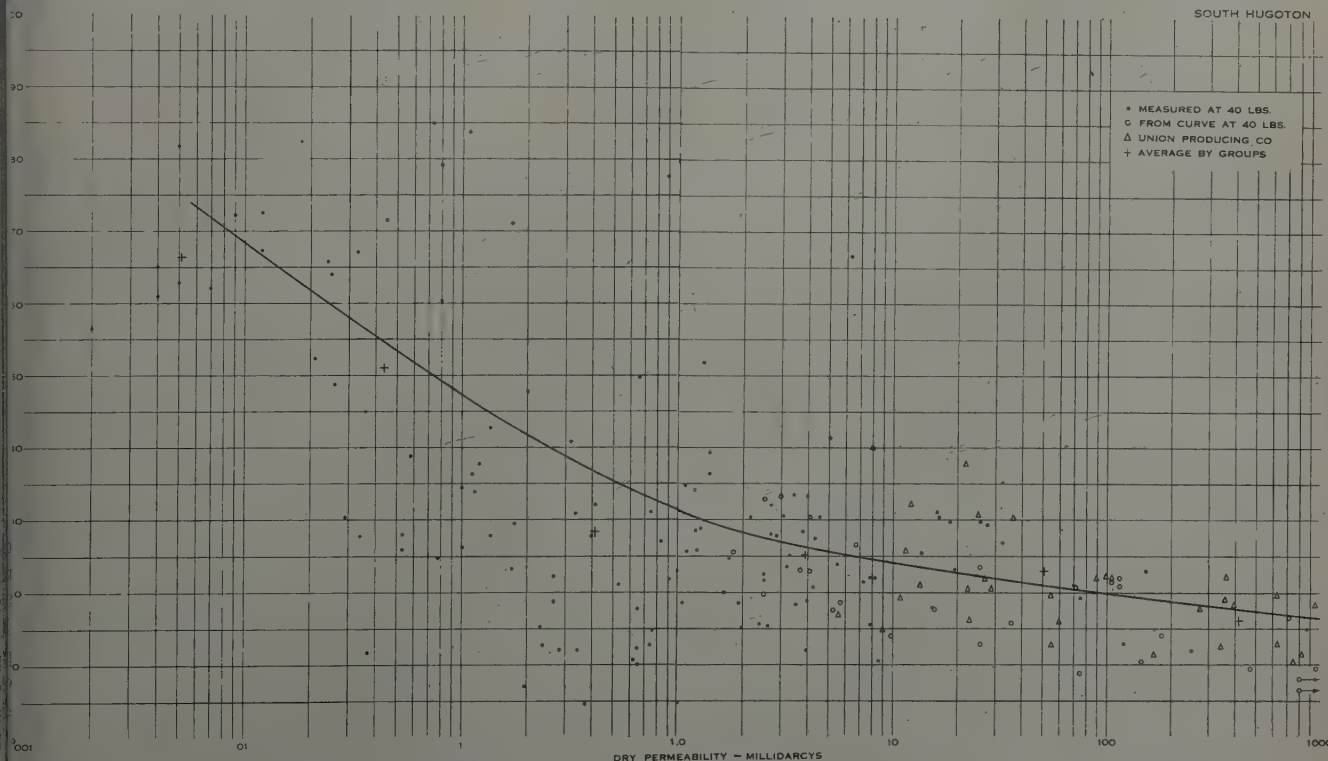


FIG. 5 — PERMEABILITY VS. CONNATE WATER FOR SOUTH HUGOTON.

Table I—Summary of Data and Factors for Estimating Recoverable Gas by Grades

Grade No.	All Core Plugs of 81 to 100 Per Cent-of-Grade		Core Plugs of 81 to 100 Per Cent-of-Grade and Greater than 0.03 Md Permeability		Connate Water, Per Cent ¹	Effective Porosity Per Cent ¹	Recoverable Gas Content Cu Ft of Gas Per Acre-Ft ²	Effective Fraction of Grade
	Permeability Md	Gross Porosity Per Cent	Permeability Md	Gross Porosity Per Cent				
0	0.13	6.1	0.37	7.97	46.7	4.25	51,300	0.303
1	0.71	7.8	2.01	9.14	43.1	5.20	62,800	0.351
2	2.16	9.6	3.32	10.47	41.3	6.15	74,200	0.644
3	3.46	10.4	3.96	10.95	34.1	7.22	87,200	0.874
4	12.43	12.3	12.64	12.41	28.0	8.93	107,800	1.000
5	77.02	15.3	77.02	15.32	23.0	11.79	142,300	1.000
6	277.90	20.2	277.9	20.16	19.4	16.25	196,100	1.000

¹Computed for Core Plugs of 81 to 100 per cent-of-grade and greater than 0.03 md permeability.²Computed at 14.735 psia and 60°F.

the core plugs and well samples.

- (2) The availability of a sufficient number of porosity and permeability measurements to establish reliable average values for the different grades of dolomite.
- (3) The reliability of laboratory tests.
- (4) The degree to which the porosity occurring in the samples and cores is representative of the porosity occurring in the reservoir.

The first three of these elements are validated by the data and related information. The fourth and most important deserves further attention because the credibility of the technique depends to a great extent on the degree of representation of the in situ porosity by the cores and well samples. The study of 230,000 ft of samples of the formation from 762 wells, 2,722 ft of core from 20 wells, and the performance of the wells during completion discloses that the void space is primarily in the form of intercrystalline porosity and, for that reason, the well samples and the core data accurately reflect the porosity characteristics of the dolomite. Secondary porosity is present to some degree by dissolution and fracturing. Most of the solution porosity is in the form of small diameter tubes, small vugs and a few small solution cavities. Figs. 2-h and 2-i show photographs of polished surfaces of two cores which demonstrate the general nature of the great majority of the fractures. Fig. 2-h shows the unaltered type and Fig. 2-i shows the alterations caused by dissolution and secondary deposition. The secondary porosity of microscopic size and a large portion of that of megascopic size is defined in the examination of the dolomite and therefore is evaluated by this procedure.

The plot of gross porosity as a function of dry permeability (Fig. 3) exhibits a pattern of points of definite shape and size which is characteristic of porous media having intercrystalline void geometry of normal sandstones.¹ Other evidence of the intercrystalline nature of the void system is exhibited in the porosity and permeability distribution charts such as Fig. 4. It is notable that all such charts, including one that was prepared for all plugs tested, show normal distribution of both porosity and permeability throughout the

range of values, which is characteristic of intercrystalline media. This would also be the case for solution type porosity when its shape and size approximate that of intercrystalline porosity.

The sample log shown in Fig. 1 is used to show the application of the reserve factors. For the sake of brevity only the interval from 3,100 to 3,110 is described. It is noted on the log that this interval is recorded as Grade 3 for two-thirds of the samples and the other one-third as no visible porosity, or Grade 0, therefore, the interval is divided into 6.7 ft, called grade-ft, as Grade 3, and 3.3 ft as Grade 0. This procedure is followed by 10-ft intervals throughout the log and the footages totaled by grades. The grade-ft totals and application of reserve factors are given in Table II.

CONCLUSIONS

The procedure presented herein for estimating the net reservoir void space by sample grading can be applied to all dolomitized limestone formations in which the geometry of its internal-void space is primarily determined by intercrystalline type porosity. In reservoirs for which this procedure is valid the variations of porosity and permeability can be evaluated from representative well samples with an accuracy approaching that for cored wells. It is not purported that this technique gives sufficiently accurate results to supplant core data but provides a reliable basis for augmenting and extending the use of such data over greater areas of the reservoir and to other similar reservoirs.

ACKNOWLEDGMENTS

This paper is primarily based on the study made for the preparation of a report submitted in evidence by D. L. Katz as Exhibit 78 before the Federal Power Commission in Docket G-1302. The authors especially acknowledge the essential contributions made by the geologic group which was supervised by the late M. N. Harlin. The persons in the group were Dean Chaddock, E. C. Gimlet, J. F. Healy, W. E. Lumb, D. F. Miller, H. H. Platt and M. F. Robitshek. Special acknowledgment is also made of the able assistance of W. B. Barry, C. W. Binckley, P. G. Carpenter, H. O. Dixon, G. H. Hannum, G. L. Knight, R. W. Miller, W. S. Walls, and many others who assisted in the calculations and assembling of data. Grateful acknowledgment is also made for contributions by Max W. Ball, Ralph E. Davis and J. M. Wege, consulting geologists and reserves engineers, who participated in the study and independently employed the technique developed herein for estimating the gas reserves of South Hugoton.

The authors are grateful to the Michigan-Wisconsin Pipe Line Co., Michigan Consolidated Gas Co., and Phillips Petroleum Co. for permission to publish this paper.

REFERENCES

1. Bulnes, A. D., and Fitting, R. U.: "An Introductory Discussion of the Reservoir Performance of Limestone Formations," *Trans. AIME*, (1945) 160, 179. ★ ★ ★

Table II—Application of Reserve Factors to the Total Grade-Ft of Example Sample Log

Geologic Grades	Total Grade-Ft	Effective Fraction of Grade	Effective Grade-Ft	Gas Recovery Mcf per Acre-Ft	Gas Reserve Mcf per Acre
0	38.6	0.303	11.7	51.3	600.0
1	10.1	0.351	3.5	62.8	219.8
2	30.6	0.644	19.7	74.2	1,461.7
3	30.7	0.874	26.8	87.2	2,336.9
4	20.0	1.000	20.0	107.8	2,156.0
5	80.0	1.000	80.0	142.3	11,384.0
6	10.0	1.000	10.0	196.1	1,961.0
Totals	220.0		171.7		20,119.4

A METHOD FOR PREDICTING THE TENDENCY OF OIL FIELD WATERS TO DEPOSIT CALCIUM CARBONATE

HENRY A. STIFF, JR., MEMBER AIME, AND LAWRENCE E. DAVIS, THE ATLANTIC REFINING CO., DALLAS, TEX.

ABSTRACT

The authors previously presented a method for predicting the tendency of oil field waters to deposit calcium sulfate. The present paper gives a similar method for calcium carbonate.

Methods for predicting calcium carbonate scaling tendencies in fresh waters have been available for some time, but these could not be used for brines. By experimentally deriving the value of the K term in the Langelier equation, a method has been developed which applies to waters of high salt content. A statistical study is included which shows that the experimentally derived values of K are in good agreement with actual conditions. Several applications of the final equation to production practice are given.

INTRODUCTION

The authors previously presented a method for predicting the formation of calcium sulfate scale in oil field waters.¹ Although calcium sulfate deposition is important in production operations, the majority of scale problems involve calcium carbonate. The present communication discusses a method by which the formation of this type of scale in oil field waters can be predicted.

Calcium carbonate precipitation is caused by a shift toward carbonate in the carbonate-bicarbonate-carbon dioxide equilibrium. When equilibrium shifts in the other direction, the precipitate goes back into solution. Since there is usually considerable delay between the establishment of an equilibrium and the precipitation or solution of calcium carbonate, unstable conditions exist in which a water will precipitate or dissolve calcium carbonate on standing.

Tillmans,² who did a major part of the early work on carbonate scaling, pointed out that the condition of equilibrium not only indicates the tendency of a water to scale but also an indication of its corrosive properties. Previously precipitated calcium carbonate combines with iron to form a dense rust which inhibits corrosion. If the water tends to dissolve

carbonate, the scale becomes porous, and electrolytic corrosion takes place. Tillmans' work was extended by several investigators until in 1934 Langelier³ developed an equation setting forth the conditions of carbonate equilibrium. By the use of this equation the pH of a water at equilibrium can be calculated. If the actual pH is higher than the calculated pH , the water has a tendency to form scale. If it is lower, the water has a tendency to be corrosive.

Langelier's equation can be expressed in a simple form as follows:

$$SI = pH - pCa - pAlk - K$$

where:

SI is the stability index. A positive index indicates scale formation. A negative index indicates corrosion.

pH is the pH of the water sample, as actually determined.

pCa is the negative logarithm of the calcium concentration.

$pAlk$ is the negative logarithm of the total alkalinity.

K is a constant, the value of which depends on the total salt concentration and the temperature.

This equation has been shown to apply to waters with total solid concentrations as high as 4,000 ppm. In fact, control of fresh water treatment by means of this equation has been standard text-book practice for a number of years. Nomographs have been worked out⁴ so that the stability index of a fresh water sample can be determined in a matter of minutes. Most oil field waters, however, contain well over 4,000 ppm of salts and for this reason the usual application of Langelier's equation can not be made.

By an empirical method we have extended the application of the Langelier equation to waters of high salt concentration. By the use of this equation the tendency of oil field waters to deposit calcium carbonate can be predicted.

THEORETICAL

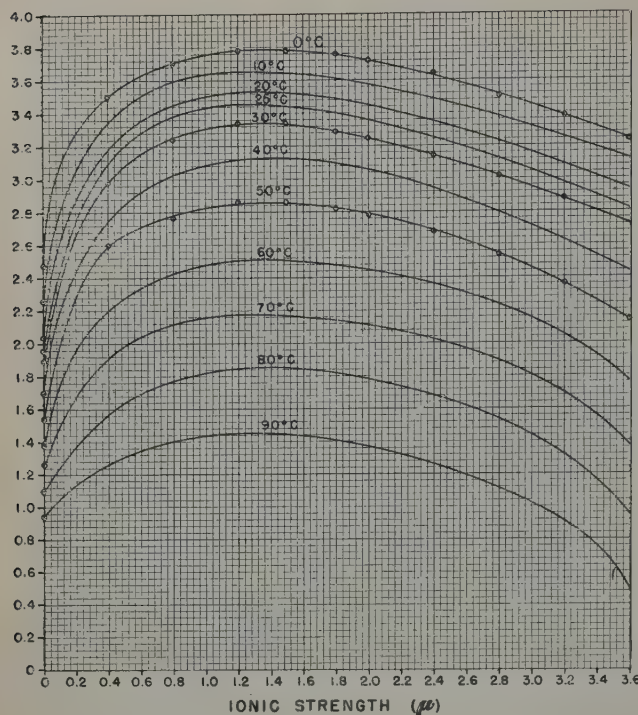
When a water is in equilibrium the stability index is zero. The Langelier equation then becomes:

$$0 = pH - pCa - pAlk - K$$

and,

$$K = pH - pCa - pAlk$$

¹References given at end of paper.
²Manuscript received in the Petroleum Branch office March 18, 1952.
³Paper presented at the Houston meeting Oct. 1-3, 1952.

FIG. 1 — VALUES OF K AT VARIOUS IONIC STRENGTHS.

The value of K depends on the temperature and total salt concentration of the water. If a water is allowed to come to equilibrium with calcium carbonate the value of K for that particular water can be found by determining the pH , calcium and alkalinity, and substituting in the above equation. By making such determinations on waters of varying salt content in equilibrium at different temperatures, data can be obtained from which values of K at any salt content or temperature can be taken.

Different salts influence the value of K to different extents. In fresh waters this effect is negligible, but in salt water it must be taken into account. Corrections are obtained by substituting ionic strength for total salt concentration by the usual methods. Ionic strength can be calculated as follows:⁵

$$\mu = .5 (C_1 V_1^2 + C_2 V_2^2 + \dots + C_n V_n^2)$$

where:

C is the concentration of each ion expressed as gram ions per 1,000 gms of solvent.

V is the valence of that ion.

EXPERIMENTAL

To various concentrations of sodium chloride ranging from 0 per cent to 20 per cent were added solutions of calcium chloride and sodium carbonate of such strength that calcium carbonate would precipitate out and leave an excess of calcium chloride. A few drops of hydrochloric acid were added to form bicarbonate and the solutions brought to equilibrium by shaking at constant temperature for 24 hours. The solutions were then filtered and the concentration of carbonate, bicarbonate, chloride, and calcium determined by actual analysis. Temperatures employed were 0°, 30°, and 50°C.

Analytical determinations insofar as possible were carried out at the equilibrium temperature. Standard procedures of analysis were used. All titrations, with the exception of chloride, were performed on the Beckman Automatic Titrator.

RESULTS

Fig. 1 shows curves giving the values of K at various ionic strengths. Curves at 0°, 30°, and 50°C were plotted from experimental data, while the curves at all other temperatures were extrapolated.

The stability indices of 100 salt water samples taken at random from our files were calculated. The frequency distribution curve is shown in Fig. 2. It will be noted that the curve is of typical shape and that the maximum frequency is at a point where the stability index is close to zero. Since it is probable that the stability indices of brines, as well as those of fresh waters have normal distribution, we believe that Fig. 2 indicates that the values of K are probably valid.

APPLICATION

To facilitate calculation of the stability indices of various oil field waters, we have included in the report Table I, which gives the factors used to obtain the ionic strength from the results of a standard water analysis. The individual ion is simply multiplied by the appropriate factor. The sum of these products gives the ionic strength.

Also included is a graph (Fig. 3), from Langelier, by which the values of $pAlk$ and pCa can be obtained.

From the ionic strength, calculated as above, the value of K can be taken from Fig. 1.

The values of these terms when substituted in the following equation will give the stability index.

$$SI = pH - K - pCa - pAlk$$

Stability index calculation on oil field brines can furnish valuable information in petroleum production operations where

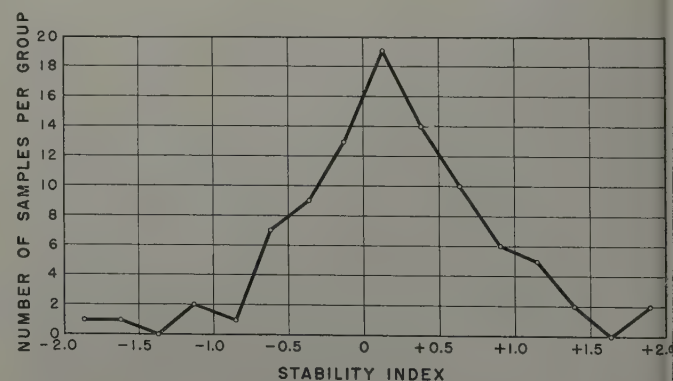


FIG. 2 — DISTRIBUTION CURVE—STABILITY INDEX OF 100 WATER SAMPLES COLLECTED AT RANDOM.

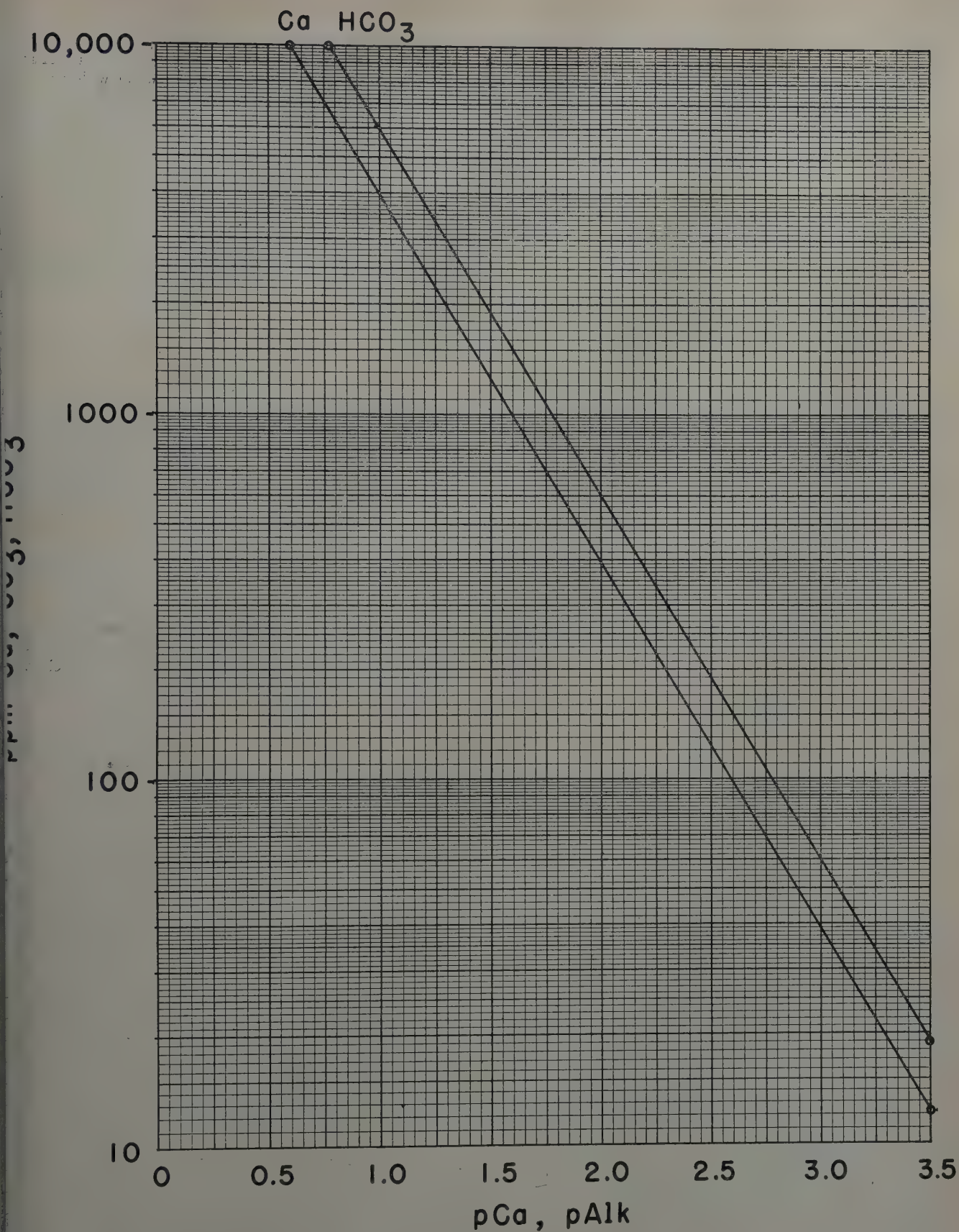


FIG. 3 — GRAPH FOR CONVERTING PARTS PER MILLION OF CALCIUM AND ALKALINITY INTO pCa AND $pAlk$.

Table I—Factors for Converting the Results of a Water Flood and Water Disposal Water Analysis to Ionic Strength

(The total ionic strength is the sum of the ionic strengths of the individual ions)

Ion	Factor, ppm	Factor, meq/liter
Na	2.2×10^{-5}	5×10^{-4}
Ca	5.0×10^{-5}	1×10^{-3}
Mg	8.2×10^{-5}	1×10^{-3}
Cl	1.4×10^{-5}	5×10^{-4}
HCO ₃	$.8 \times 10^{-5}$	5×10^{-4}
SO ₄	2.1×10^{-5}	1×10^{-3}

carbonate scaling and certain types of corrosion are involved. Following are a few examples of the application of the stability index

Scale Deposits in Heater Treaters

A consideration of Fig. 1 shows that the value of K diminishes as the temperature of the water increases. This results in a more positive index which in turn indicates an increase in scaling tendencies. Thus, a brine which is stable at the wellhead is often scale forming at the higher temperature of the heater. The calculation of stability index for the first time makes possible the quantitative calculations of scaling tendencies of oil field waters under these conditions. It is believed that the judicious use of this tool in study of scaling condition in heater treaters will not only clarify the mechanism of these problems but also will be of considerable aid in prescribing treatment.

Scale Deposits in Producing Wells

Calcium carbonate deposits in producing oil wells is a serious problem because of loss of production and possible damage to in-hole equipment. Fundamentally, such deposits appear to be due to pressure drops which allow the escape of carbon dioxide. The resulting shift in equilibrium causes the calcium carbonate to precipitate. Usually equilibrium is not completely reached so that wellhead water samples often give an indication of the tendency for scale to form in the well.

It should be pointed out, however, that while the stability index foretells the future behavior of a water, it does not necessarily indicate its past. Actually there may be several equilibrium states in the water between the formation and the wellhead, a condition which could lead to corrosion at one point and scale at another. Studies are now in progress which we hope will clarify this situation and considerably extend the application of the stability index to the problems of scaling and corrosion in producing wells.

Water Flood and Water Disposal

The importance of injecting stable water into the formation has long been recognized, and a considerable amount of money has been spent in achieving this end. If water with a tendency to scale is injected, calcium carbonate deposits soon plug the formation. In the case of a fresh water flood the standard Langelier formulas can be used to control treatment and make sure that a stable water is being injected, but when salt water is used these equations do not apply. In such water flood operations the new stability index has found extensive application.

Disposal projects almost always involve water of high salt content. Here the injection of stable water is just as necessary as in water flooding. In this project the new stability index has proved valuable.

CONCLUSIONS

Experimental values were developed for the K term in the Langelier equation. By the use of these values the stability index of oil field waters can be calculated. A statistical evaluation of these values was made and several applications of the stability index to production problems are given.

ACKNOWLEDGMENT

The authors wish to thank The Atlantic Refining Co. for permission to publish this paper, and to acknowledge the valuable assistance and cooperation of the staff of the Chemical Engineering Group of this organization. Illustrations were prepared by Gene Nigh.

REFERENCES

1. Stiff, H. A., Jr., and Davis, L. E.: "A Method for Predicting the Tendency of Oil Field Waters to Deposit Calcium Sulfate," *Trans. AIME*, (1952) 195, 25. (*Jour. Pet. Tech.* April, 1952.)
2. Tillmans, J.: *Die Chemische Untersuchung von Wassen und Abwassen*, 2nd Ed. Wilhelm Knap Halle (Saale) (1932)
3. Langelier, W. F.: *Jour. Am. Water Works Assn.*, (1934) 28, 1,500.
4. Ryan, William J.: *Water Treatment and Purification*, McGraw-Hill Book Co., New York, (1946) 78.
5. Lewis and Randall: *Thermodynamics and the Free Energy of Chemical Substances*, McGraw-Hill Book Co., New York (1923) 373.

★ ★

ELECTRICAL RESISTIVITY MEASUREMENTS ON RESERVOIR ROCK SAMPLES BY THE TWO-ELECTRODE AND FOUR-ELECTRODE METHODS

C. F. RUST, MAGNOLIA PETROLEUM CO., DALLAS, TEX.

ABSTRACT

Experimental evidence is presented showing that reproducible formation resistivity factor measurements and resistivity index determinations on reservoir core samples may be made utilizing either the two- or four-electrode methods. Equipment is described which permits the application of either technique to the core specimen without loss of time and with a minimum amount of effort. Since electrical resistivity measurements on reservoir rocks are important not only in electric log interpretations, but also in the study of fundamental rock parameters, it was considered desirable to compare the applicability of both techniques of resistivity measurement.

INTRODUCTION

The techniques employed in the measurement of electrical resistivity on reservoir rocks, as practiced in the petroleum industry, may be reduced to two fundamental methods: one utilizing two electrodes only, usually referred to as the two-electrode method; the other using two additional electrodes and commonly known as the four-electrode method. In the former, the core sample whose resistivity is to be measured is mounted between two electrodes, usually metal discs, which serve to pass a current of known magnitude through the sample. The potential drop across the sample, measured between the same two electrodes, and the core dimensions furnish the necessary data to compute the resistivity of the sample. In the four-electrode technique the end plates, again usually metal, still serve as current electrodes. Additional probes or electrodes dispersed along the sample are utilized to measure the potential drop. Both methods are used in practice^{1,2} and it is the purpose of this paper to compare the two techniques as applied to the determination of formation resistivity factors and the resistivity index exponent n , in Archie's³ empirical equation $I = \rho / \rho_o = S_w^{-n}$. To evaluate the two techniques it is desirable to point out the experimental precautions which must be taken to insure reliable results. It is evident from the electrode arrangements of the two- and four-electrode methods that, for a given sample, the volume of sample included by the four-electrode method is less than the volume included by the two-electrode method. One of the prime difficulties associated with the two-electrode method is the possible occurrence of an abnormally high

resistance between the electrodes and the brine-saturated sample, which results in erroneous resistivity values for the core sample itself. Attempts to alleviate this difficulty meet varying degrees of success. Methods used in the past employ such absorbent materials as brine-saturated Kleenex, chamois, or felt. A technique described by Morgan, Wyllie, and Fulton,² appears to be more satisfactory. Their method consists of spraying or painting the end areas of a core sample with conductive silver paint. This technique reduces contact resistances between the porous medium and the electrodes to a value which is generally negligible as compared to the resistance of the sample itself.

In the four-electrode method these requirements are not as stringent since separate probes are used to measure the potential difference across a portion of the sample. In this case, contact resistance occurring at the current electrodes are of no consequence, and those appearing at the potential

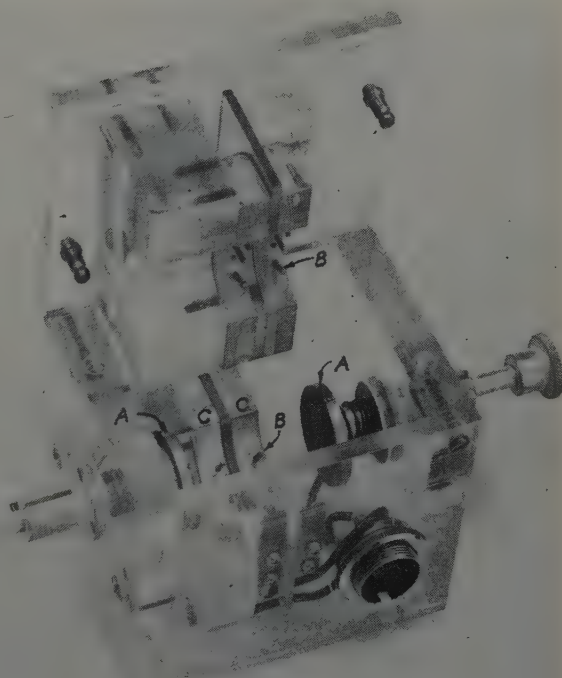


FIG. 1 — CORE SAMPLE RESISTIVITY CELL.

References given at end of paper.
Manuscript received in the Petroleum Branch office June 20, 1952.
Paper presented at Houston meeting, Oct. 1-3, 1952.

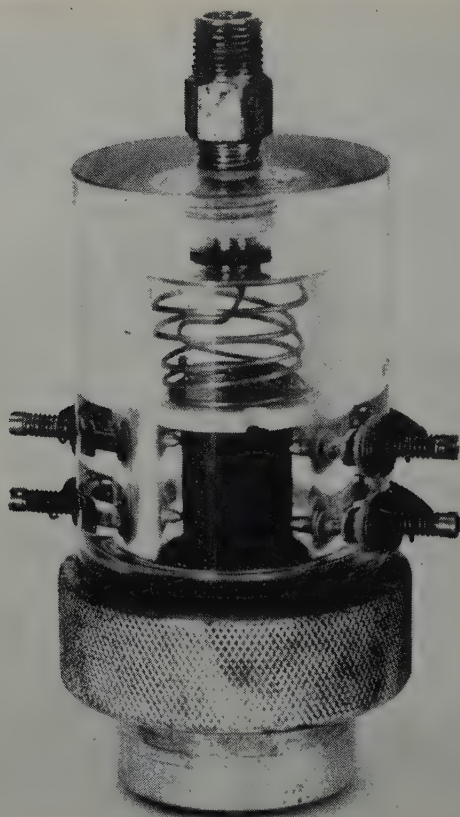


FIG. 2 — COMBINED INTERSTITIAL WATER AND RESISTIVITY CELL.

probes are easily detected by a method to be described below. However, for the measurements presented in this paper, techniques were used which reduced contact resistances at the current and potential electrodes to a minimum.

EQUIPMENT

The resistivity cell developed by Magnolia Petroleum Co.'s Field Research Laboratories and used for the determination of formation resistivity factors presented in this report is shown in Fig. 1. It is designed to permit either a two- or four-electrode measurement to be made without disturbing the core sample once it is placed in the cell. The electrode system is enclosed in a Lucite housing which is partially filled with brine to reduce evaporation of water from the core sample during the measurement. The metal disc current electrodes are seated in a ball-and-socket joint. Two sets of six solid-silver potential probes *B*, also under spring tension, are distributed along the core circumference and seated in each of two electrically insulated metal blocks *C*. The electrical wiring of the cell is permanent, and connections to the measuring circuit are made through a Cannon plug. The end areas of the core samples measured in this cell may be coated with conducting silver paint,* if the cell is used for two electrode measurements. For four-electrode measurements refined techniques, to eliminate contact resistances between the current electrodes and the core sample, are not necessary, since they do not affect the resistance measurements of the sample. This

resistivity cell accommodates samples having a maximum diameter of 1 in.; the limiting lengths are between 0.7 and 1.5 in.

A combined interstitial water and resistivity cell is used for electrical resistivity determinations during the process of capillary desaturation. It is shown in Fig. 2. In this technique the brine-saturated core sample is placed in contact with porous diaphragm, permeable to brine but impermeable to isooctane, the medium used to displace the brine. Pressure is applied in steps to the displacing medium, forcing the brine through the diaphragm into a graduated pipette, which permits the amount of expelled brine and thus the sample brine saturation to be determined volumetrically. Resistivity measurements are made, using an electrode system similar to the one described above, except that the brine-saturated porous diaphragm replaces one of the metal disc current electrodes. The cell is mounted in a constant-temperature box to minimize effects of temperature fluctuations during the process of measurement.

PROCEDURE

A schematic wiring diagram of the electrical measuring circuit, used in conjunction with either resistivity cell, is shown in Fig. 3. With the core sample mounted in the cell, the desired current through the sample is obtained by adjustment of the potential drop across a 100-ohm wire-wound precision resistor. Manipulation of selector switches I and II permits potential-drop measurements to be made, either across the entire core sample (two-electrode method), or across a portion of the sample (four-electrode method). Any appreciable contact resistance introduced in the measurement is detected by inserting a resistor in series with the vacuum tube voltmeter. The value of this resistor is chosen to be equal to the input impedance of the measuring instrument. If the contact resistance is zero, the potential drop across the sample is one-half of that measured without the resistor in the circuit. This is a well-established procedure in electrical measurements and was first reported in petroleum literature by Dunlap *et al*. With this circuit it is possible to make reliable resistivity measurements in rapid succession, using either the two- or four-electrode methods.

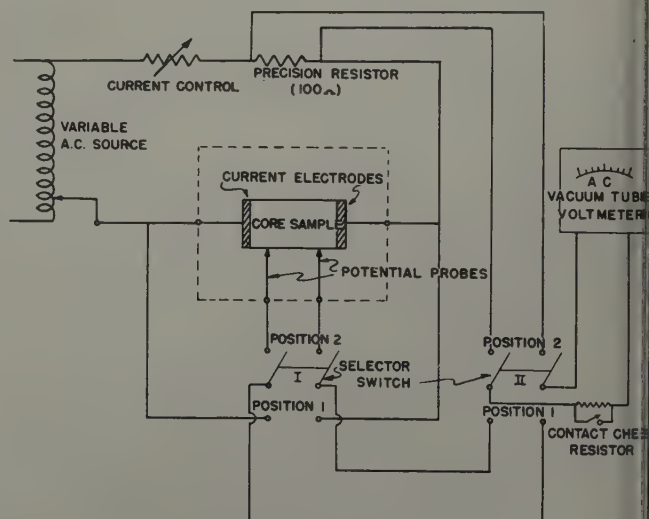


FIG. 3 — CIRCUIT DIAGRAM FOR RESISTIVITY MEASUREMENTS ON RESERVOIR ROCKS.

*Type S.C. 11 Microcircuits Co., New Buffalo, Mich.

Table I—Two- and Four-Electrode Resistivity Measurements on Saturated Core Samples

Sample Number	Formation	Effective Porosity %	Nitrogen Permeability md	Resistivity, Ohm-Meters		Per Cent Brine Saturation	Salinity of Saturating Brine ppm NaCl
				Two-Electrode Method	Four-Electrode Method		
58	Aux Vases SS	25.6	307	1.66	1.42	98.1	50,000
59A	Aux Vases SS	21.6	80.8	6.86	6.76	100	10,000
51	Aux Vases SS	21.7	122	2.04	1.81	99.2	50,000
52	Aux Vases SS	20.7	56.8	7.31	7.45	95.7	10,000
53	Aux Vases SS	23.3	129	6.46	6.16	99.1	10,000
56	Aux Vases SS	23.2	170	6.46	6.60	98.0	10,000
58	Aux Vases SS	25.6	307	0.86	0.82	98.0	100,000
51	Aux Vases SS	21.7	122	1.10	1.04	99.0	100,000
59	Aux Vases SS	21.0	80.0	7.52	7.39	100	10,000
52*	Aux Vases SS	20.7	56.8	7.13	7.24	100	10,000
53	Aux Vases SS	23.3	129	1.99	1.83	95.2	50,000
56	Aux Vases SS	23.2	170	1.87	1.68	96.1	50,000
4	Stevens SS*	20.2	24.1	0.26	0.25	99.7	50,000
1	Stevens SS*	19.0	43.6	8.29	8.47	99.6	1,000
2	Stevens SS*	19.3	39.7	5.08	5.12	99.2	20,000
59	Edwards LS	38.2	82.5	1.88	1.89	91.4	50,000
1	Alundum	20.0	818	5.25	5.10	98.0	10,000
20	Annona Chalk	23.9	0.5	2.15	2.10	93.0	50,000
21	Annona Chalk	33.0	1.4	1.35	1.36	93.2	50,000
22	Annona Chalk	31.0	1.7	1.33	1.20	94.7	50,000
23	Annona Chalk	27.7	1.7	1.60	1.52	95.0	50,000
28	Annona Chalk	25.0	1.4	2.00	2.25	93.0	50,000
31	Annona Chalk	29.3	0.9	1.64	1.61	96.0	50,000
33	Annona Chalk	28.9	1.0	1.51	1.56	95.4	50,000
35	Annona Chalk	28.5	1.1	1.62	1.72	95.7	50,000
44	Annona Chalk	24.4	0.8	1.99	2.10	96.0	50,000
48	Annona Chalk	23.1	0.9	2.08	2.24	97.2	50,000
51	Annona Chalk	31.5	1.1	1.47	1.57	96.8	50,000
20	Bearhead SS*	24.4	278	0.60	0.50	98.0	50,000
9	Cotton Valley SS*	10.0	0.5	5.06	5.30	95.0	100,000
19	Cotton Valley SS*	9.9	0.4	4.72	4.77	93.8	100,000
22	Cotton Valley SS*	7.3	0.6	4.99	5.00	96.0	100,000
26	Cotton Valley SS*	8.4	0.5	8.65	8.70	96.2	100,000
27	Cotton Valley SS*	11.2	0.4	3.88	4.21	96.4	100,000
54	Aux Vases SS*	22.3	121	53.0	55.5	98.0	500
51	Aux Vases SS*	21.7	122	27.1	28.8	99.0	1,000
54	Aux Vases SS*	22.3	121	26.5	27.8	100	1,000
58	Aux Vases SS*	25.6	307	24.5	25.1	99.7	1,000
19A	Stevens SS	20.0	92.5	20.6	20.1	98.4	1,000
19C	Stevens SS	19.4	52.0	20.0	18.9	99.0	1,000
19H	Stevens SS	19.5	85.3	24.5	23.7	98.2	1,000
19J	Stevens SS	18.7	67.0	21.2	19.1	99.5	1,000
19K	Stevens SS	18.7	71.0	22.1	20.9	99.8	1,000
19L	Stevens SS	19.1	75.8	22.7	22.6	99.7	1,000
21C	Madison LS	9.5	0.1	9.19	9.44	97.9	75,000
22I	Madison LS	5.5	0.1	16.9	16.7	95.5	75,000
23C	Madison LS	5.3	0.1	27.5	29.8	96.8	75,000
23S	Madison LS	5.2	0.1	23.0	22.6	97.4	75,000
24B	Madison LS	7.5	0.1	14.1	14.8	94.7	75,000
24F	Madison LS	6.7	0.1	13.8	13.4	94.1	75,000
24L	Madison LS	7.8	0.1	13.7	14.0	94.2	75,000
25B	Madison LS	9.4	0.1	12.0	11.0	95.8	75,000
25C	Madison LS	11.1	22.0	6.58	6.78	92.9	75,000
25D	Madison LS	10.9	24.5	6.92	6.98	98.3	75,000
25H	Madison LS	10.2	0.6	7.44	6.98	100	75,000
26E	Madison LS	12.2	0.1	6.02	5.16	93.7	75,000
27E	Madison LS	6.6	0.1	9.93	9.88	95.2	75,000
27H	Madison LS	5.2	0.1	13.1	12.7	99.4	75,000
25D	Madison LS	10.9	24.5	32.8	32.8	98.0	7,000
25I	Madison LS	10.4	4.5	32.7	31.3	99.1	1,000

*Painted Core Samples

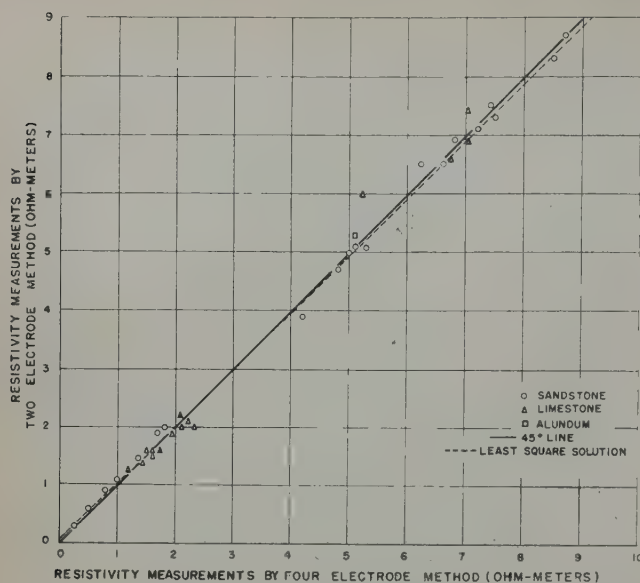


FIG. 4 — RESISTIVITY MEASUREMENTS. TWO- VS FOUR-ELECTRODE TECHNIQUES. RANGE 1-10 OHM METERS.

DISCUSSION

The electrical resistivities of 60 core samples were measured utilizing both the two-electrode and four-electrode systems. These samples, nominally three-fourths in. in diameter and one in. in length, were selected from typical sandstone and limestone formations. The brine saturations were determined in the following manner: the core samples were cleaned, dried in an oven, and weighed. The pore volumes were then measured with a Kobe gas-compression porosimeter.⁴ Following this measurement, the samples were placed in a bell jar, evacuated, and flushed several times with carbon dioxide. The brine was then admitted to the evacuated chamber and the weight of the saturated samples subsequently was determined. From these data the degree of saturation was computed as a fraction of the measured pore volume. The range of saturations so obtained varied between 91.4 and 100 per cent.

Resistivity measurements were made on the above samples using both techniques. The results of these determinations are summarized in Table I and plotted in Figs. 4 and 5. Fig. 4 covers the resistivity range from 0 to approximately 10 ohm-meters; Fig. 5 includes the results ranging from 6 to 36 ohm-meters. It is evident that the data points fall closely on a line whose slope is unity. A least-square solution⁵ of the data for the resistivity range from 0 to 10 ohm-meters (Fig. 4) shows that the equation of the line of best fit is of the form $y = ax + b$, in which a is the slope of the line, and b the intercept with the y -axis. The values of these constants are $a = 0.988$ and $b = 0.039$. For the data in Fig. 5, covering a range from 6 to 36 ohm-meters, $a = 0.952$ and $b = 0.978$. The dotted lines represent the lines of best fit, obtained by the method of least squares.

The agreement between the two methods depends among other things on the nature of the sample. For homogeneous samples the agreement is invariably excellent, as would be anticipated for situations in which the contact resistance is negligible. On the other hand, for heterogeneous samples, small deviations, such as are observed in these data, are in-

evitably observed. A practical illustration of the agreement of resistivity measurements made with both techniques on samples from a single formation, the Annona Chalk, is shown in Fig. 6. Formation resistivity factors, representing the ratio of the resistivity of a sample to the resistivity of the saturating brine, are plotted vs the porosity fractions on log-log paper. The open circles represent data points obtained from resistivity measurements with the four-electrode technique, and the solid circles represent the data obtained from the two-electrode measurements. This type of plot is commonly used to determine the "cementation factor," m , in Archie's³ relation $F = \phi^{-m}$; it shows that the scattering is somewhat larger for the two-electrode data. However, the effect on the determination of the cementation factor m is small.

Measurements on core samples during the process of desaturation are complicated by the fact that not only is the resistivity measurement itself involved, but reliable determinations of the volume of expelled brine, and hence of the brine saturation of the sample, are required. For these measurements the combined interstitial water and resistivity cell, shown in Fig. 2, is used. This cell permits the obtention of data for the capillary pressure curve as well as the necessary information for Archie's³ empirical saturation equation $I = \rho/\rho_o = S_w^{-n}$. In these capillary pressure experiments as the pressure is increased the saturation decreases and in time, becomes substantially constant at a given capillary pressure. This constant value of saturation is the equilibrium saturation obtained at the applied capillary pressure. In a like manner the resistivities change continuously as the saturation decreases in a capillary pressure experiment and therefore the resistivities may be plotted against both equilibrium and non-equilibrium saturations.

Fig. 7 is a plot of the resistivity index vs brine saturation for a "clean" sandstone core sample from the Planulina sand of the miocene. The designation "clean" implies that the

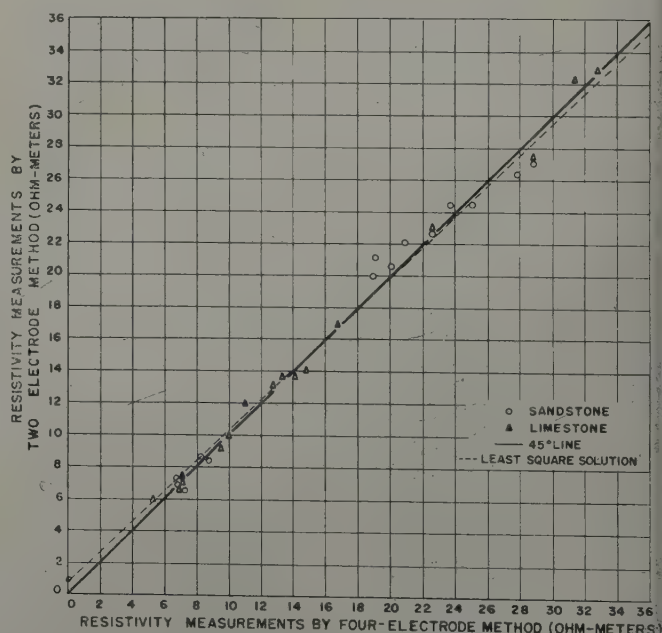


FIG. 5 — RESISTIVITY MEASUREMENTS. TWO- VS FOUR-ELECTRODE TECHNIQUES. RANGE 6-36 OHM METERS.

Table II — Resistivity Index as a Function of Brine Saturation, Planulina Sand of Miocene
Permeability 112 md
Effective Porosity 19.3%

Capillary Pressure psi	Run 1 Two-Electrode Method		Capillary Pressure psi	Run 1 Four-Electrode Method		Capillary Pressure psi	Run 2 Four-Electrode Method	
	Brine Saturation Per Cent of Pore Volume	Resistivity Index $I = \rho/\rho_o$		Brine Saturation Per Cent of Pore Volume	Resistivity Index $I = \rho/\rho_o$		Brine Saturation Per Cent of Pore Volume	Resistivity Index $I = \rho/\rho_o$
0	100	1.00	0	100	1.00	0	100	1.00
0	96.4	1.10	0	96.4	1.04	4*	35.2	6.21
2	45.0	3.84	2	45.0	4.13	8*	29.4	8.46
2*	43.1	4.45	2*	43.1	4.32	12*	26.2	9.51
4	37.7	5.60	4	37.7	5.39	20*	21.5	13.3
4*	36.5	5.71	4*	36.5	5.87			
8	32.5	7.00	8	32.8	6.48			
8	31.8	7.18	8	31.8	7.32			
8*	30.6	8.10	8*	30.6	7.67			
12*	27.4	9.71	12*	27.4	9.41			
16*	26.2	10.4	16*	26.2	10.1			
20*	22.2	14.0	20*	22.2	12.6			

*Equilibrium saturation values

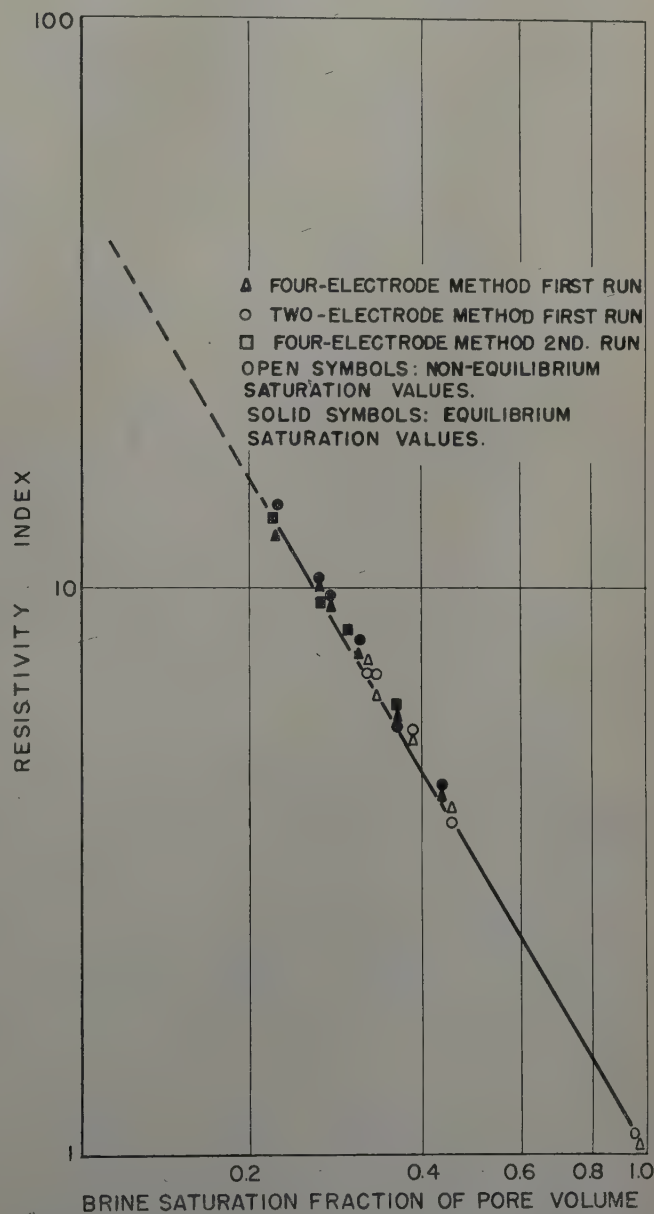
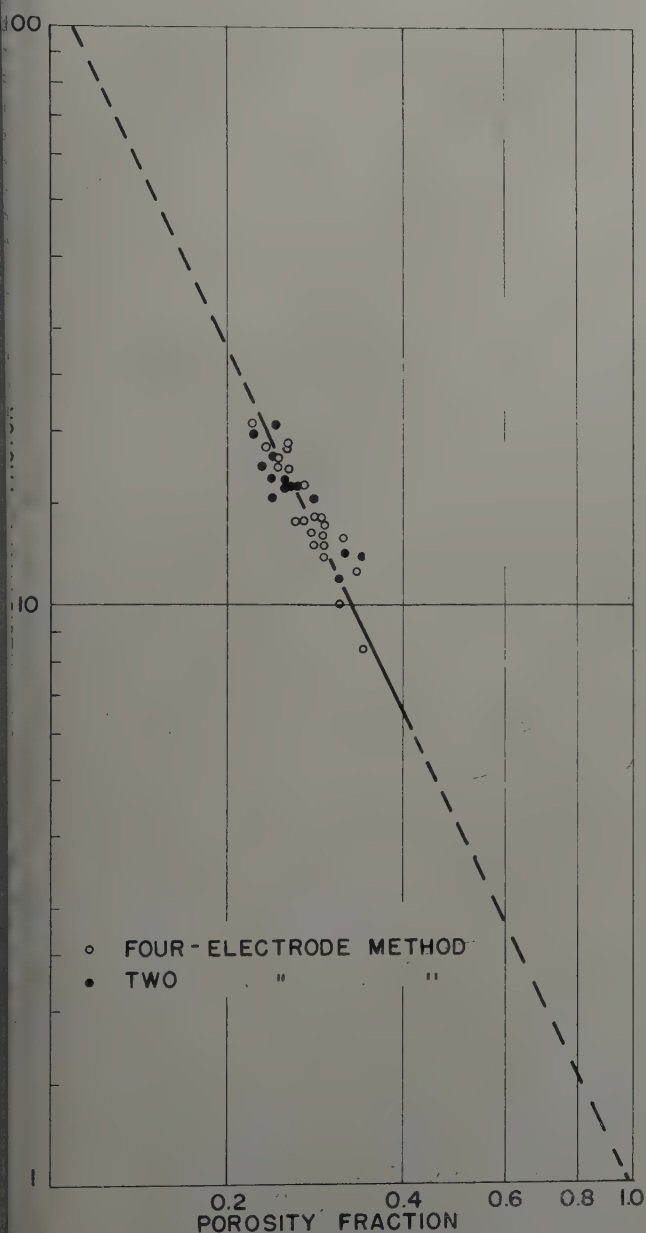


FIG. 6 — FORMATION RESISTIVITY FACTOR VS POROSITY FRACTION. NONA CHALK FORMATION.

FIG. 7 — RESISTIVITY INDEX VS BRINE SATURATION. PLANULINA SAND. GAS PERMEABILITY 112 md. EFFECTIVE POROSITY 19.3%.

Table III — Resistivity Index as a Function of Brine Saturation, Clear Fork Sandstone

Sample 2796A: Permeability 357 md; Effective Porosity 23.6%

Sample 2796B: Permeability 377 md; Effective Porosity 23.6%

Sample 2796A Four-Electrode Method			Sample 2796A Two-Electrode Method			Sample 2796B Four-Electrode Method		
Capillary Pressure psi	Brine Saturation Per Cent of Pore Volume	Resistivity Index $I = \rho/\rho_o$	Capillary Pressure psi	Brine Saturation Per Cent of Pore Volume	Resistivity Index $I = \rho/\rho_o$	Capillary Pressure psi	Brine Saturation Per Cent of Pore Volume	Resistivity Index $I = \rho/\rho_o$
	100	1.00		100	1.00		100	1.00
2	88.1	1.39	2	88.1	1.65	8	34.8	20.0
2	50.2	6.50	2	50.2	7.04	8*	30.5	29.9
2*	45.0	8.44	2*	45.0	10.5	16*	25.5	43.0
4	36.8	17.5	4	—	—	20	17.4	59.1
4*	33.9	24.4	4*	—	—	20*	13.1	63.9
8*	31.2	31.6	8*	31.2	33.0			
12	24.5	49.0	12	—	—			
12*	21.4	52.5	12*	—	—			
16*	19.1	55.0	16*	—	—			
20*	17.0	56.4	20*	17.0	53.5			

*Equilibrium saturation values

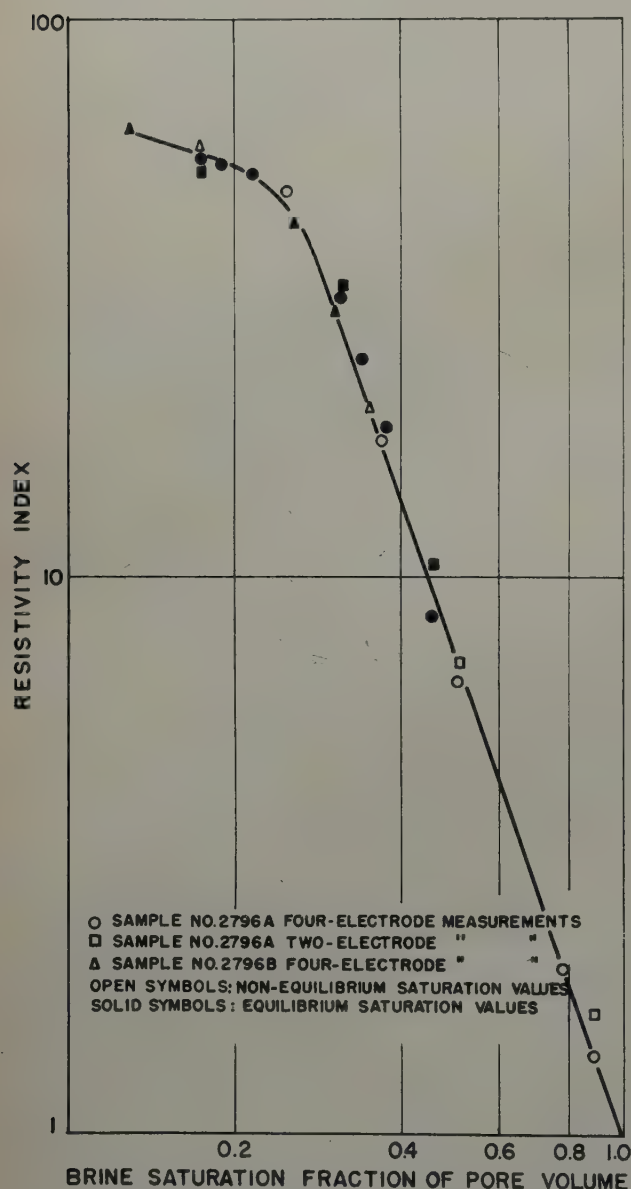


FIG. 8 — RESISTIVITY INDEX VS BRINE SATURATION. CLEAR FORK SANDSTONE. SAMPLE NO. 2796A: PERMEABILITY 357 md; EFFECTIVE POROSITY 23.6%. SAMPLE NO. 2796B: PERMEABILITY 377 md; EFFECTIVE POROSITY 23.6%.

sample is not contaminated by the presence of clays or other argillaceous matter, thereby complicating the measurement. The data (Table II) represent two independent runs on the same sample. During the first run both two- and four-electrode measurements were made. The open symbols represent non-equilibrium data points; the equilibrium data points are shown by solid symbols. It is evident that the reproducibility of the four-electrode data is good and that the four-electrode results agree well with those obtained by the two-electrode method. The sample is obviously one for which the saturation exponent is independent of saturation.

Another type of reproducibility test based on the data listed in Table III is illustrated in Fig. 8. Two adjacent plugs were drilled from a shaly sandstone. The values of the permeability and effective porosity for these two adjacent samples are nearly identical. Resistivity index determinations made for each sample with the four-electrode method show good agreement. Good agreement also exists between the four-electrode measurements and the two-electrode data taken on one of the samples. It appears that for both samples the saturation exponent is independent of saturation at the higher brine saturations. At the lower saturations, however, Archie's equation is no longer applicable. This lack of applicability may be attributed to the fact that, at the lower saturations, the resistance of the core matrix itself may be important. This effect has been noted by other investigators⁶ and may be explained on the basis of conductive solids, such as shales, clays, and other colloidal matter capable of conducting electric current.

In order to extend these tests to the study of core samples longer than one inch, a combined interstitial water and resistivity cell similar to that shown in Fig. 2, was constructed and provided with four pairs of potential electrodes along the longitudinal axis of the cell. In this new form the resistivity cell accommodates a core sample three in. long. A schematic diagram of the electrode arrangement is shown in Fig. 9. Consecutive resistivity measurements were made on a "clean" sample with the four-electrode technique, using six different combinations of the potential electrodes. These electrode combinations are numbered, the spacing being 0.5 in. for combinations 1 through 4, and 1 in. for combinations 5 and 6. A two-electrode measurement across the total length of the core was also made. These data are listed in Table IV. Fig. 10 represents the computed resistivity indices plotted against saturation. The results for the two-electrode method are shown in Fig. 11. Both techniques yield essentially the same saturation exponent. Two other interesting observations may be made with regard to this experiment, the first being that the data

presented in Figs. 10 and 11 include indices computed both for equilibrium and non-equilibrium saturations.

This indicates that, for the samples investigated, during resistivity index measurements it was not necessary to attain saturation equilibrium unless a plot of the capillary pressure saturation curve was desired at the same time. This observation is consistent with numerous results obtained during routine measurements but not reported herein. Another point of interest is that, for this sample at least, the brine saturation distribution within the sample during the desaturation process remains essentially uniform, as indicated by the resistivity measurements made on various portions of the core sample. The two observations, while coincidental in these experiments, are of sufficient interest to deserve mention.

CONCLUSIONS

It is concluded, from the foregoing comparison of the two- and four-electrode methods as applied to formation resistivity factor and resistivity index determinations on the 60 core samples investigated:

1. That, provided proper techniques are employed either the two-electrode or four-electrode method will yield reliable resistivity values. Because of the different volumes of samples associated with each of the two methods of measurement, it is possible to measure, on any one sample, two equally reliable

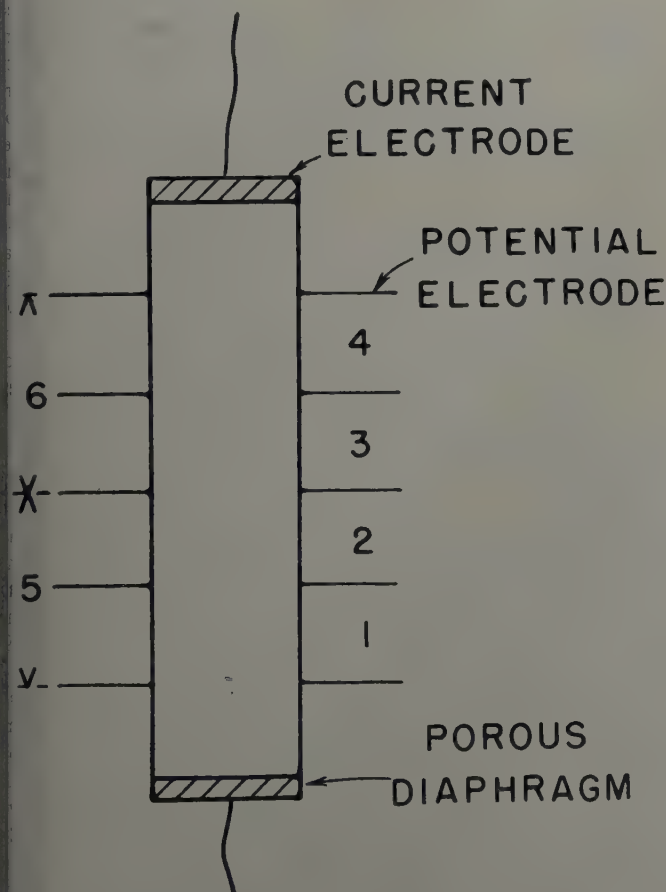


FIG. 9 — ELECTRODE ARRANGEMENT. LARGE CORE SAMPLE RESISTIVITY CELL.

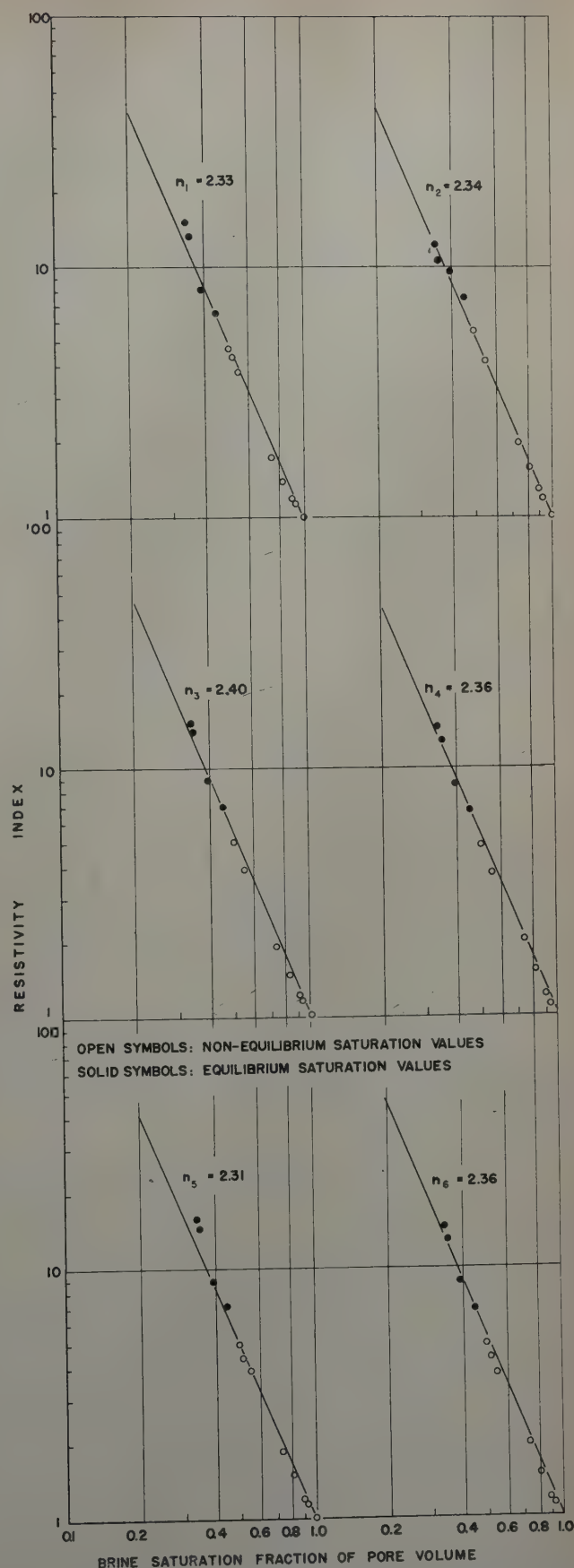


FIG. 10 — RESISTIVITY INDEX VS BRINE SATURATION. FOUR-ELECTRODE METHOD. WOODBINE OUTCROP. GAS PERMEABILITY 1130 md; EFFECTIVE POROSITY 38.8%.

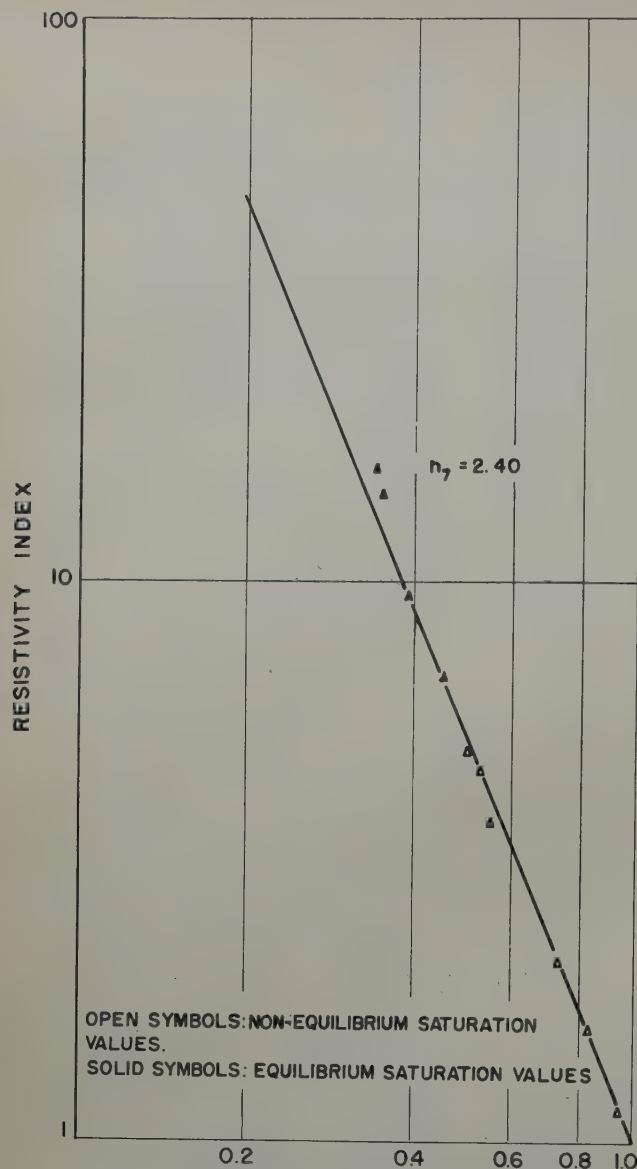


FIG. 11 — RESISTIVITY INDEX VS BRINE SATURATION. TWO-ELECTRODE METHOD. WOODBINE OUTCROP. NITROGEN PERMEABILITY 1130 md; EFFECTIVE POROSITY 38.8%.

but nevertheless different values of resistivity. Such difference will be an indication of non-homogeneity of the porous matrix. Since essentially equal values of resistivity were observed on the 60 core samples included in this investigation, it is concluded that these samples are essentially homogeneous insofar as electrical resistivity is concerned.

2. That, in determinations of the saturation exponent n , resistivity values at both equilibrium and non-equilibrium brine saturations may be used.

In all resistivity measurements it is unquestionably helpful to use both methods on the same sample, in order to check one measurement against the other. This is particularly desirable in resistivity index determinations.

ACKNOWLEDGMENT

Appreciation is expressed to the Magnolia Petroleum Co. and its management for permission to publish this paper.

REFERENCES

1. Dunlap, H. F., Bilhartz, H. L., Shuler, E., and Bailey, C. R.: "The Relation Between Electrical Resistivity and Brine Saturation in Reservoir Rocks," *Trans. AIME*, (1949) 186, 259.
2. Morgan, F., Wyllie, M. R. J., and Fulton, P. F.: Tech. Note, "A New Technique for the Measurement of the Formation Factors and Resistivity Indices of Porous Media," *Trans. AIME*, (1951) 192, 371.
3. Archie, G. E.: "The Electrical Resistivity Log as an Aid in Determining Some Reservoir Characteristics," *Trans. AIME*, (1942) 146, 54.
4. Beeson, C. M.: "The Kobe Porosimeter and the Oilwell Research Porosimeter," *Trans. AIME*, (1950) 189, 313.
5. Peters and Van Voorhis: *Statistical Procedures and Their Mathematical Bases*, 427-429.
5. Patnode, H. W., and Wyllie, M. R. J.: "The Presence of Conductive Solids in Reservoir Rocks as a Factor in Electric Log Interpretation," *Trans. AIME*, (1950) 189, 47. ★ ★ ★

Table IV — Resistivity Index as a Function of Brine Saturation, Woodbine Outcrop
Permeability 1,130 md
Effective Porosity 38.8%

		Values of Resistivity Index						
Capillary Pressure psi	Brine Saturation Per Cent of Pore Volume	Four-Electrode Measurements						Two-Electrode Measurements Position 7
		Position**	Position**	Position**	Position**	Position**	Position**	
		1	2	3	4	5	6	
	100	1.00	1.00	1.00	1.00	1.00	1.00	1.00
2	93.0	1.14	1.21	1.16	1.10	1.14	1.14	1.12
2	82.4	1.38	1.60	1.46	1.51	1.48	1.51	1.60
2	73.4	1.74	2.01	1.90	1.99	1.86	1.86	2.10
2	55.1	3.84	4.25	3.87	3.70	3.93	3.81	3.71
2	52.0	4.42	4.87	4.47	4.27	4.41	4.43	4.59
2	50.2	4.78	5.39	5.00	4.77	5.04	4.97	5.01
2*	44.9	6.60	7.60	6.96	6.63	7.09	6.92	6.69
4*	38.7	8.23	9.74	8.92	8.54	8.94	8.75	9.50
12*	34.7	13.5	10.8	13.5	12.8	14.6	13.2	14.4
20*	33.8	15.2	12.5	15.3	14.5	15.9	14.9	15.9
		$n_1 = 2.33$	$n_2 = 2.34$	$n_3 = 2.40$	$n_4 = 2.36$	$n_5 = 2.31$	$n_6 = 2.36$	$n_7 = 2.40$

*Equilibrium saturation values

**Refer to Fig. 9 for location of measurement positions along sample

USE OF ACTIVATED CHARCOAL IN CEMENT TO COMBAT EFFECTS OF CONTAMINATION BY DRILLING MUDS

B. E. MORGAN, JUNIOR MEMBER AIME, AND G. K. DUMBAULD, MEMBER AIME, HUMBLE OIL AND REFINING CO., HOUSTON, TEX.

ABSTRACT

Results of laboratory investigations of the effects of drilling muds on oil well cements are presented which show that relatively large quantities of untreated muds do not seriously interfere with the setting of cement slurries, but that relatively small quantities of treated muds seriously retard the setting of cement slurries. Laboratory results also indicate that the harmful effects of contamination with treated muds can be counteracted by the addition of activated charcoal to cements. Also described is the successful use of cement containing activated charcoal for the placement of plugs in open hole after previous attempts with ordinary cement had been unsuccessful.

INTRODUCTION

The contamination of cement slurry by dilution with drilling mud has long been considered a cause of failure in oil well cementing. The cement slurry must displace the drilling mud from the annulus between the casing and the walls of the borehole, and it is probable that some mixing of the slurry and the mud occurs even under the most nearly ideal displacement conditions. Hole enlargement, failure to center the casing in the hole, and formation of gel structure in the drilling mud increase the probability of contamination. In some cementing operations, such as the placement of a cement plug in open hole, considerable mixing of the mud and slurry is likely. Many cement failures which can be attributed logically to no cause other than contamination of the cement slurry by the mud attest the need of a better understanding of this problem.

Considerable attention was given to the problem of mud contamination of cements about 20 years ago.^{1,2,3,4} The effects of field mud upon cement slurries prepared with different amounts of mix water were investigated thoroughly, and the data obtained were invaluable in determining the causes of the high percentage of failure in oil-well cementing at that time and in bringing about improved cementing results. Since then, many aspects of the problem have changed, due primarily to advancements in cement and drilling mud technology. Today, several types of portland cement are used in well cementing and numerous chemical additives are used in drilling muds. An excellent report on the effects of drilling mud additives on oil-well cements was issued during 1951 by the American Petroleum Institute.⁵ Data in the report revealed that many mud additives, notably organic materials in relatively small amounts, produce a marked effect on the properties of cements. Prior to this time, little information has been available on the effects of chemicals commonly used in the treatment of drilling muds upon the properties of cements. Another aspect of the problem of mud contamination of cements, which has received no attention heretofore, is the possibility of producing a cement having properties unaffected by a reasonable amount of mud contamination.

In view of the need for additional information on the contamination of present-day cements by currently-used drilling

muds, the investigation described herein was initiated several years ago with a two-fold purpose: first, to determine the capacity of cement slurries to tolerate contamination by both untreated and treated muds without loss of ability to set and develop strength within a reasonable time; and, second, to investigate the possibility of enhancing the ability of cement slurries to withstand mud contamination by incorporating additives in the cement. The data for this study were obtained by mixing drilling mud with cement slurry and testing the resulting slurry-mud mixture for rate of set and development of strength. Also, several materials were tested for their possible improvement of the property of cement slurry to withstand mud contamination; these materials were tested in both contaminated and uncontaminated cement slurries.

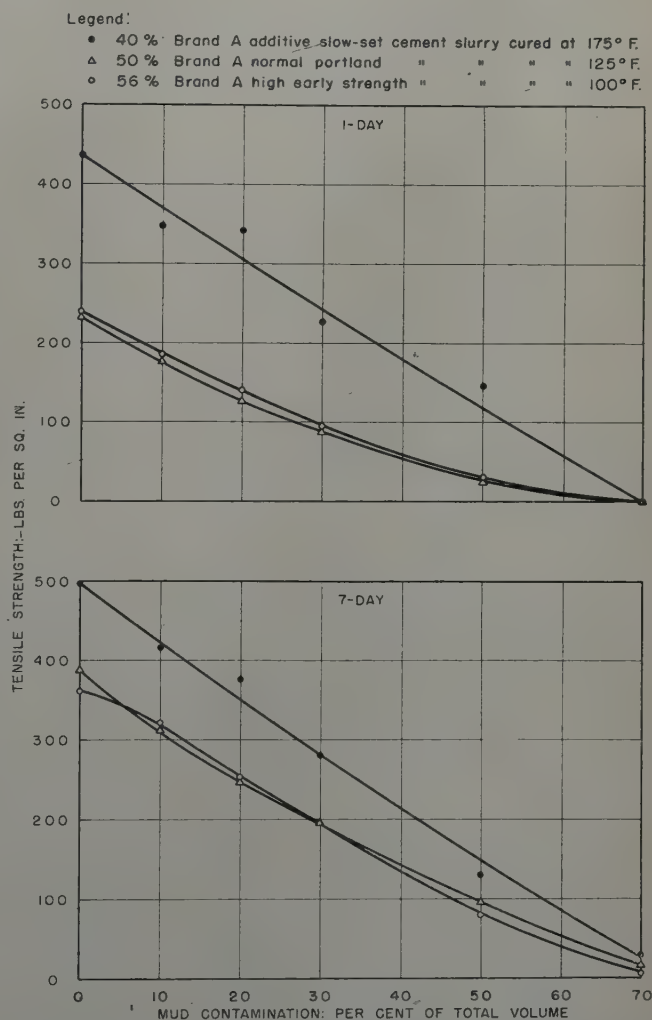


FIG. 1 — EFFECT OF MUD CONTAMINATION ON TENSILE STRENGTHS OF THREE TYPES OF OIL-WELL CEMENTS. UNTREATED FIELD MUD FROM WELL IN FORT BEND COUNTY, TEXAS.

References given at end of paper.
Manuscript received in the Petroleum Branch office June 19, 1952.
Paper presented at the Houston meeting, Oct. 1-3, 1952.

LABORATORY INVESTIGATION OF MUD
CONTAMINATION OF CEMENTSEffect of Untreated Mud on the Strength
Development of Cements

The first series of tests was performed to determine the capacity of three types of oil-well cements, *i.e.*, highly early strength, normal portland, and slow-set, to tolerate contamination by an untreated mud without loss of ability to develop strength within a reasonable time.

The effect of contamination on the tensile strength of the cements was determined by adding to the cement slurries an untreated field mud in concentrations of 10, 20, 30, 50, and 70 per cent by volume of the total slurry-mud mixture. Given volumes of cement slurry and drilling mud were mixed together by hand for one minute and the resulting mixtures were poured into briquet molds. After the briquets were aged under water for one and for seven days, respectively, tensile strength measurements were made.

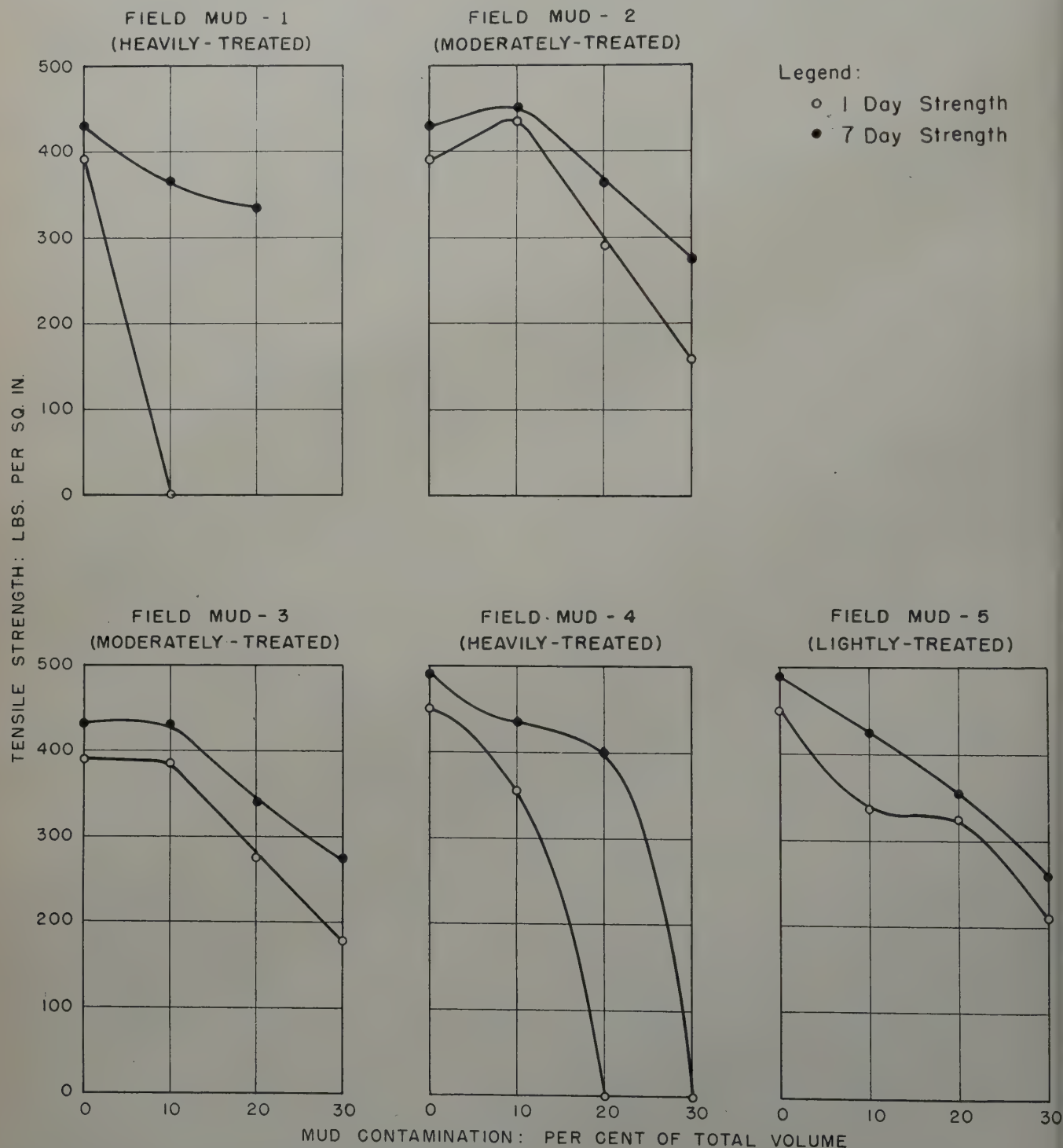


FIG. 2—EFFECT OF MUD CONTAMINATION ON TENSILE STRENGTH OF A SLOW-SET CEMENT. MUD ADDED TO 40% SLURRY OF BRAND "A" ADDITIVE SLOW-SET CEMENT. TEST TEMPERATURE: 175°F.

Table I—Treated Muds Used in Cement Contamination Tests

Mud	Chemicals in Mud						Days Drilling	Depth Ft
	NaOH	Quebracho	Lime	SAPP	Starch	Dry Tan ^a		
			Total added to mud system, lb					
Field-1	8,900	12,050	6,500	—	19,875	—	113	10,000
Field-2	1,450	3,175	500	1,225	—	—	45	10,176
Field-3	1,350	2,600	—	—	—	4,300	19	9,623
Field-4 ^c	4,375	7,150	2,890	—	—	—	79	9,931
Field-5	—	—	—	—	—	—	93.2	8,960
			Added to 7% bentonite clay suspension, lb/bbl					
Lab-1	0.1	0.1	—	—	—	—	—	—
Lab-2	1	1	—	—	—	—	—	—
Lab-3	2	2	—	—	—	—	—	—

^aDry mixture of equal portions of quebracho, lime, and sodium carbonate.

^bChemical solution of caustic-quebracho.

^cMud system changed to caustic, quebracho, lime mud 25 days prior to sampling. Workover job in cased hole.

These results, presented in Fig. 1, show the comparative effects of mud contamination on the one-day and seven-day tensile strengths of the three types of oil-well cements. The strength of the cements decreased as the mud concentration increased to 70 per cent of total volume. At 70 per cent mud concentration, all of the mixtures developed very little or no tensile strength. At mud concentrations less than 70 per cent, slurry-mud mixtures prepared with the slow-set cement developed greater one-day strengths than slurry-mud mixtures prepared with either the high early strength or the normal portland cement. For example, the slow-set cement slurry containing 50 per cent mud by total volume had a greater one-day tensile strength than did the high early strength and normal portland cement slurries contaminated with 30 per cent mud by total volume. All cements tested, however, developed sufficient one-day strength to produce a satisfactory set cement even when contaminated with as much as 30 per cent mud by total volume.

These data indicate that the contamination of cement slurries with untreated drilling mud is probably not a serious problem.

Effect of Treated Muds on the Strength Development of Cements

A second series of tests was made to determine the capacity of cement slurries to withstand contamination by treated muds. This second series of tests was divided into two groups. One group of tests was made using field muds obtained from wells drilling in the Gulf Coast area of Texas. Since it was not practical to ascertain the concentration of the chemicals in the field muds, another group of tests was made using laboratory-prepared muds treated with known concentrations of caustic-quebracho or starch. These two treating agents were selected because they are used very extensively in field operations. Pertinent data on the muds are presented in Table I. Since chemically treated muds are generally used at depths where slow-set cements are required, these tests were made using a slow-set cement.

The tests were made by mixing the muds separately in concentrations of 10, 20, and 30 per cent by total volume of cement slurry-mud mixture, and determining the strength development of the resulting mixtures. The slurry-mud mixtures were poured into briquet molds, the briquets were aged under water at 175°F for periods of one and seven days, removed, and tested for tensile strength.

Results Using Field Muds

Data obtained by use of the field muds as contaminants, presented in Fig. 2, indicated that the contamination of cement slurries with some field muds may seriously affect the cement job.

Addition of 10 per cent of Field Mud 1, which had been heavily treated with caustic, quebracho, lime, and starch, retarded set so that no strength was developed at the end of one day. Field Mud 4, which also had been heavily treated with caustic, quebracho, and lime, had less effect upon early strength development. The addition of 10 per cent of the latter mud caused some reduction in one-day tensile strength, and the addition of 20 per cent of this mud retarded set so severely that no strength was developed at the end of one day. A slurry containing 30 per cent of Field Mud 4 failed to set even after seven days. Contamination with the other field muds, which were only moderately or lightly treated, caused less pronounced retardation of the strength development of the cement.

Results Using Laboratory Muds

Data obtained by use of laboratory-prepared muds containing caustic-quebracho, presented in Fig. 3, showed that heavily treated caustic-quebracho mud seriously retarded the strength of cement, but that moderately treated caustic-quebracho muds did not seriously affect the cement. A cement slurry-mud mixture containing 20 per cent of a mud treated with two lb caustic and two lb quebracho per bbl failed to set in one day, and one containing 30 per cent of this mud failed to set after seven days. Slurry-mud mixtures containing as much as 30 per cent mud treated with smaller concentrations of these chemicals (one lb/bbl of each chemical, and 0.1 lb/bbl of each chemical, respectively), developed reasonable tensile strengths in one day.

Data obtained by use of laboratory-prepared muds containing starch, presented in Fig. 4, showed that starch muds seriously retarded the strength development of cement. Twenty to 30 per cent contamination with muds containing fresh starch produced slurry-mud mixtures which failed to set in one day. All of these mixtures, however, developed reasonable tensile strengths after aging seven days. The fermented starch muds had a more pronounced effect upon the one-day strengths than did the fresh starch muds, but the effects of the fermented starch and fresh starch muds upon the seven-day strengths were about the same.

Effect of Treated-Mud Contamination on the Strength Development of Different Slow-Set Cements

Conventional slow-set cements are of two types: the straight non-additive type, in which the slow-setting property is due principally to the adjustment of the raw components in the cement clinker, and the additive type, in which the slow-setting property is due principally to the addition of a small amount of organic material or combination of materials to the cement. These additive materials are called "retarders." The data on

Legend:

○ 1-Day Strength

● 7-Day Strength

Mud contained 7% Bentonite

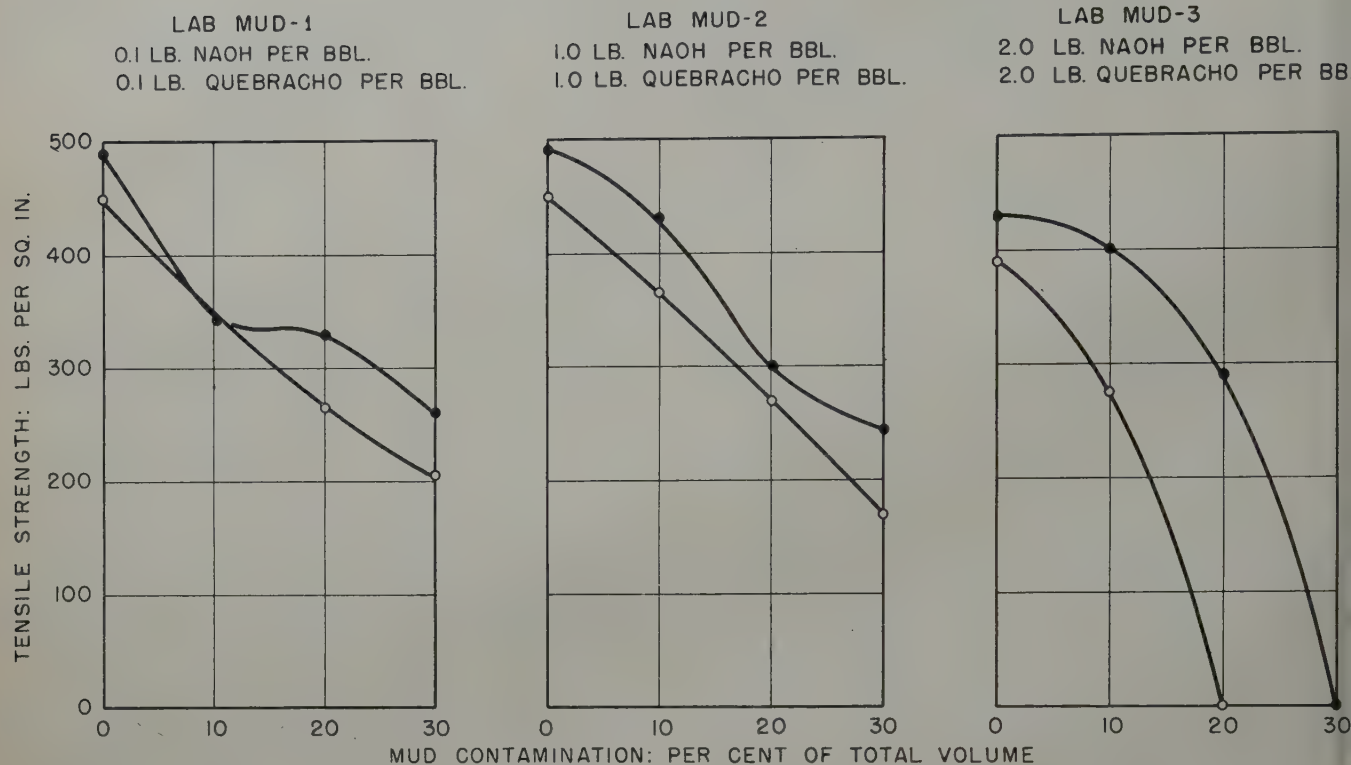


FIG. 3 — EFFECT OF MUD CONTAMINATION ON TENSILE STRENGTH OF A SLOW-SET CEMENT. MUD ADDED TO 40% SLURRY OF BRAND "A" ADDITIVE SLOW-SET CEMENT. TEST TEMPERATURE: 175°F.

slow-set cement presented heretofore in this paper were obtained using an additive-type cement. Results obtained using one slow-set cement do not necessarily indicate that similar results will be obtained using other slow-set cements, because different retarders are used in different brands of additive slow-set cements and no retarder is used in straight slow-set cements. In view of these differences in slow-set cements, it seemed advisable to investigate the effect of treated-mud contamination upon the properties of several slow-set cements. Accordingly, slurries prepared from three additive slow-set cements and one straight slow-set cement were contaminated with a mud heavily treated with both caustic-quebracho and starch. The slurry-mud mixtures, containing 16.7 per cent mud by total volume, were aged under water at 175°F and observed for setting and strength development.

The results, presented in Table II, showed that two of the additive slow-set cements failed to set at 175°F even after seven days when the slurries were contaminated with 16.7 per cent mud by total volume. Under similar curing conditions and with a like amount of contamination, the straight slow-set cement and one of the additive slow-set cements developed reasonable strength within four days. This information indicates that straight slow-set cements may be affected less severely by treated muds than some additive slow-set cements. The results suggest that the retarders used in slow-set cements may be responsible for the difference in the effect of treated-mud contamination on different additive slow-set cements.

Effect of Temperature on the Strength Development of Cement Slurries Contaminated with Treated Mud

Tests were made to determine the effect of temperature on the strength development of cement slurries contaminated with treated muds. To this end, several laboratory-prepared muds containing 1:1 caustic-quebracho in concentrations of 1.9, 2.8, 3.6, and 4.3 lb of each chemical per bbl of mud were used to contaminate slurries of two cements. These muds were added to slurries of an additive slow-set cement and a straight slow-set cement in concentration of 16.7 per cent of total volume. The results of the tensile strength measurements made on

Table II — Effect of Treated-Mud Contamination on Strength Development of Four Slow-Set Cements

Brand of Cement	Water Content of Slurry cu cm water/100 gm cement	Mud Contamination ^a Vol. Per Cent	Tensile Strength psi ^b	
			3 days	4 days
A ^c	40	16.7	0	150
B ^c	40	16.7	0	0 ^d
C ^c	40	16.7	0	0 ^d
D ^e	40	16.7	0	160

^aUntreated field mud from well in Harris County, Tex., was treated in laboratory with 3 lb quebracho, 3 lb caustic, and 10 lb pre-gelatinized starch per bbl of mud 3 days prior to start of tests. No odor of fermentation noted.

^bTest specimens cured under water at 175°F.

^cAdditive slow-set cement.

^dNot to initial set at end of 7 days.

^eStraight slow-set cement.

These slurry-mud mixtures after curing under water at temperatures of 150, 175, and 200°F are presented in Table III.

The data showed that, as the curing temperature of the slurry-mud mixtures was lowered from 200°F, the retardation effect of the caustic-quebracho mud upon the setting and strength development properties was more pronounced. The straight slow-set cement slurry contaminated with 16.7 per cent mud containing 2.8 lb caustic and 2.8 lb quebracho per bbl developed a tensile strength of 223 psi in one day when cured at 200°F. The same slurry-mud mixture failed to set in one day when cured at 175 and 150°F. With the additive slow-set cement, a like retardation was noted for a similar composition when the curing temperature was lowered.

The results showed also that increasing the amount of caustic-quebracho in the mud resulted in retardation of the strength development of the slurry-mud mixtures. This retardation effect was greater for the additive slow-set cement than for the straight slow-set cement when the mud contained more than 2.8 lb each of caustic and quebracho per bbl. For in-

stance, the slurry-mud mixture prepared with the straight slow-set cement developed a tensile strength of 140 psi in one day at a curing temperature of 200°F when contaminated with 16.7 per cent mud by volume which contained 4.3 lb caustic and 4.3 lb quebracho per bbl. Under similar test conditions, the slurry-mud mixture prepared with the additive slow-set cement did not set in one day and developed a tensile strength of only 50 psi after curing for two days. Since the additive slow-set cement used in these tests was the one least affected by treated-mud contamination in tests presented previously in Table II, it appears that a straight slow-set cement may be superior to an additive slow-set cement in its ability to withstand contamination by heavily treated muds.

It is significant to note that the cement slurry-drilling mud mixtures developed about the same strengths after aging seven days, regardless of the amount of caustic-quebracho present in the mud. This shows that the action of the caustic-quebracho in the mud is one of retardation of set of the cement rather than reduction of ultimate strength development.

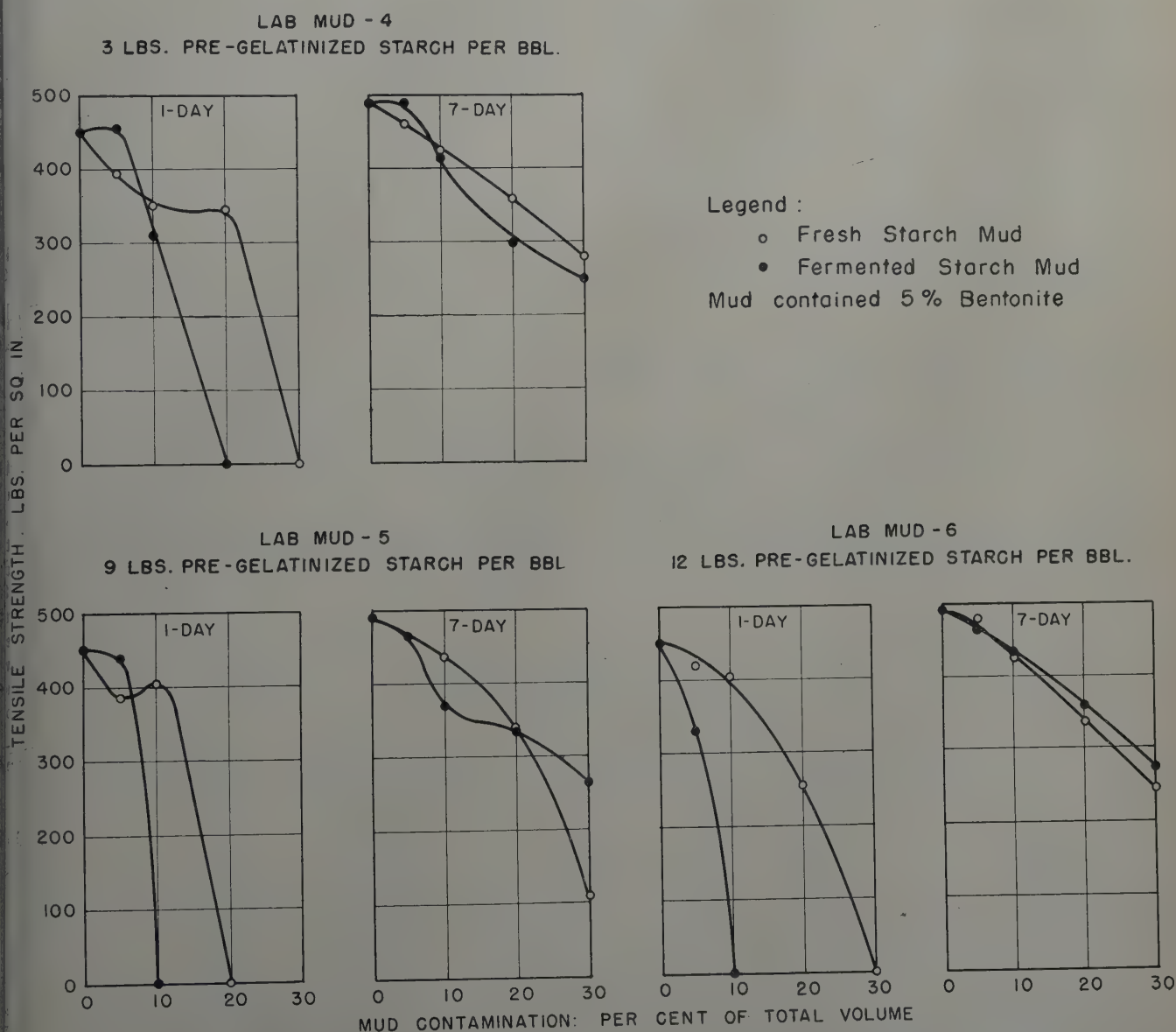


FIG. 4—EFFECT OF MUD CONTAMINATION ON TENSILE STRENGTH OF A SLOW-SET CEMENT. MUD ADDED TO 40% SLURRY OF BRAND "A" ADDITIVE SLOW-SET CEMENT. TEST TEMPERATURE: 175°F.

Table III — Effect of Temperature on Tensile Strength Development of Slow-Set Cements Contaminated with
Caustic-Quebracho Muds

Mud Contamination Vol. Per Cent	Concentration of Caustic and Quebracho ^a lb each/bbl	Tensile Strength, psi					
		150°F		175°F		200°F	
		1 day	7 days	1 day	7 days	1 day	7 days
Brand "A" Additive Slow-Set Cement (40 per cent slurry)							
16.7	1.9	173	330	150	330	No test made	No test made
16.7	2.8	0	330	0	330	223	260
16.7	3.6	No test made	No test made	0	320	0	305
16.7	4.3	No test made	No test made	0	0	0	280
Brand "D" Straight Slow-Set Cement (40 per cent slurry)							
16.7	1.9	110	283	151	342	260	345
16.7	2.8	0	358	0	325	205	310
16.7	3.6	No test made	No test made	0	313	156	263
16.7	4.3	No test made	No test made	0	330	140	301

^aIn 6 per cent bentonite clay suspension.

LABORATORY INVESTIGATION OF THE COUNTERACTION OF MUD CONTAMINATION OF CEMENTS

The second phase of the work was undertaken in an effort to enhance the ability of cement slurries to withstand mud contamination. Data presented previously have shown that cement slurries contaminated with 30 to 50 per cent untreated mud (by total volume) developed sufficient one-day tensile strengths for a good cement job, whereas cement slurries contaminated with only 10 to 20 per cent mud which was heavily treated with caustic-quebracho or starch failed to set within one day. It appeared, therefore, that the deleterious effect of treated-mud contamination might be eliminated if the treating agents in the mud were rendered inactive at the time of contamination. It was thought that this might be accomplished by either the precipitation or the adsorption of the mud treating agents by the addition of suitable materials to the cement.

Investigation of Additives to Combat Treated-Mud Contamination of Cement Slurries

Preliminary tests were made for the purpose of evaluating the usefulness of various materials as cement additives in enhancing the ability of cement slurries to withstand contamination with a mud treated with caustic-quebracho. These materials were tested by mixing each with dry cement (a straight slow-set), forming slurries by the addition of suitable amounts of water, and mixing the resulting slurries with lab-

oratory-prepared muds containing caustic-quebracho. The mixtures were then aged under water at 175°F and observed for set time or tested for strength development. To determine the effect of each additive upon the properties of the cement slurry containing no mud, similar tests were made on a neat cement slurry containing no mud, and on a cement slurry containing each test additive and no mud. The materials tested included contact clays, bentonite, Attapulgitic clays, diatomaceous earths, aluminum oxide, activated bauxites, sodium silicates, activated magnesium silicate, silica gels, synthetic resins, a variety of carbonous substances, and numerous inorganic chemicals.

These preliminary tests revealed that calcium hydroxide, activated charcoal, and several clays showed promise in accelerating the set and strength development of cement slurries containing caustic-quebracho mud without appreciably affecting the strength properties of the uncontaminated cement slurry. Therefore, more detailed laboratory information was obtained on the use of these additives. The test results are presented in Table IV. A special contact clay, which was the most promising clay tested, was used in these tests.

The results of tensile strength measurements showed that either calcium hydroxide or activated charcoal was more effective in increasing the early strength of cement slurry-drilling mud mixtures than was the contact clay. However, pumpability tests showed that the addition of calcium hydroxide in an amount sufficient to cause early strength development of the contaminated slurry reduced the thickening time of the uncontaminated cement slurry. On the other hand, the addition of sufficient activated charcoal to effect early strength develop-

Table IV — Effect of Calcium Hydroxide, Charcoal, and Clay on Tensile Strength of Cement with and without
Caustic-Quebracho Mud Added

Substance Added to Dry Cement ^a	Wt. Per Cent (Based on Cement)	Water Content of Slurry cu cm Water/100 gm Cement	Mud Contamination ^b Vol. Per Cent	Consistency RPM at 400 gm Stormer	Tensile Strength, psi ^c		
					1 day	2 days	7 days
None	0	40	0	750	331	—	525
None	0	40	16.7	1,090	0	0	313
Calcium hydroxide	2	43	0	920	301	—	393
Calcium hydroxide	2	43	16.7	1,090	0	167	325
Calcium hydroxide	5	43	0	750	341	—	425
Calcium hydroxide	5	43	16.7	950	145	—	362
Activated charcoal	5	43	0	720	363	—	520
Activated charcoal	5	43	16.7	1,090	123	—	362
None ^d	0	40	0	770	205	—	618
None ^d	0	40	16.7	920	0	—	373
Special contact clay ^d	5	43	0	380	265	—	477
Special contact clay ^d	5	43	16.7	860	0	175	423

^aBrand "D" straight slow-set cement.^bSix per cent bentonite mud containing 3.6 lb sodium hydroxide and 3.6 lb quebracho per bbl.^cTest specimens cured under water at 175°F.^dDifferent bag of cement used for these tests.

Table V—Effect of Various Concentrations of Activated Charcoal on Strength Development of Cement Slurry Contaminated with Caustic-Quebracho Mud

Charcoal Added Wt. Per Cent (Based on Cement) ^a	Water Content of Slurry cu cm Water/100 gm Cement	Mud Contamination ^b Vol. Per Cent	Tensile Strength, psi ^c	
			1 day	2 days
0.0	40	16.7	0	0 ^d
0.2	40	16.7	0	0 ^d
0.5	40	16.7	0	165
1.0	40	16.7	0	168
5.0	40	16.7	108	—
10.0	43	16.7	112	—
20.0	50	16.7	73	—

rand "D" straight slow-set cement.

Untreated field mud from well in Harris County, Tex., was treated in laboratory with 4 lb sodium hydroxide and 4 lb quebracho per bbl of mud. Test specimens cured under water at 175°F. Did not set within 4 days.

ment of the contaminated slurry did not change appreciably with the thickening time of the uncontaminated slurry. Since it may be dangerous on some jobs to add a material which reduces the thickening time of cement slurry, it appeared that activated charcoal was the most promising additive of the three for combating the deleterious effect of cement contamination by muds containing caustic-quebracho. Attempts to produce a composition containing cement and various combinations of calcium hydroxide, clay, and activated charcoal which would be superior to a composition containing cement and activated charcoal were unsuccessful.

Amount of Activated Charcoal Needed to Counteract Treated-Mud Contamination of Cement Slurries

To determine the optimum concentration of activated charcoal to counteract the deleterious effect of treated-mud contamination, slurries of a straight slow-set cement were prepared and tested which contained 0, 0.2, 0.5, 1, 5, 10, and 20 per cent charcoal by weight of dry cement. These slurries were mixed with a mud containing four lb caustic and four lb quebracho per bbl in the concentration of 16.7 per cent mud by total volume. The briquets were aged under water at 175°F and their tensile strengths measured after the mixtures had set.

The results, presented in Table V, showed that less than 5 per cent charcoal was not satisfactory in accelerating the strength development of the slurry-mud mixtures. Increase of charcoal content up to 10 per cent resulted in increase of tensile strength. From a practical standpoint, it appeared that the optimum charcoal concentration was about five per cent for this particular charcoal. Smaller concentrations of a more highly activated charcoal may be used.

Counteraction of Contamination of Cement Slurries with Muds Containing Various Treating Agents

Since it was found that the retardation of strength development caused by caustic-quebracho muds could be largely counteracted by the addition of activated charcoal to the cement, it was thought that charcoal might be effective also in counteracting the retardation effect of other mud treating agents, especially starch. Accordingly, tests were made to determine the effect of the addition of muds containing starch, calcium lignosulfonate, and sodium acid pyrophosphate on the strength development of cement slurries, and to determine if the addition of activated charcoal to the cement would counteract any deleterious effects caused by these chemicals in the mud.

For this investigation, slurries were prepared with a straight slow-set cement, both with and without the addition of activated charcoal. Tensile strength tests were made on the uncontaminated slurries and on slurries contaminated with muds which had been treated separately with starch, calcium lignosulfonate, and sodium acid pyrophosphate.

The results of these tests, presented in Table VI, indicated the following:

1. Muds treated with starch which had fermented seriously retarded the strength development of cement slurries, and the addition of activated charcoal was effective in counteracting contamination by such a mud.
2. Muds heavily treated with calcium lignosulfonate seriously retarded the set of cement slurries, and the addition of activated charcoal was effective in counteracting contamination by muds containing calcium lignosulfonate.
3. Muds heavily treated with sodium acid pyrophosphate did not cause serious retardation of the set of cement slurries.

Effect of Activated Charcoal on the Pumpability of Cements

Information presented previously has shown that the addition of activated charcoal to a straight slow-set cement accelerated the strength development of the slurry contaminated with treated muds without adversely affecting the pumpability of the uncontaminated slurry. Many of the slow-set cements on the market, however, are additive type cements; they obtain their slow-setting property by the addition of small quantities of organic substances. In order to investigate the possibility that activated charcoal might adsorb these substances in additive slow-set cements and thereby reduce their pump-

Table VI—Effect of Treated Muds on Strength Development of Cement Slurry with and without Activated Charcoal Added

Charcoal Added Wt. Per Cent (Based on Cement) ^a	Water Content of Slurry cu cm Water/100 gm Cement	Type of Treating Agent Added to Mud ^b	Concentration of Treating Agent in Mud lb/bbl	Mud Contamination Vol. Per Cent	Tensile Strength, psi ^c			
					1 day	2 days	7 days	30 days
0	40	None	0	0	195	—	—	570
5	40	None	0	0	272	—	—	573
0	40	Starch ^d	10	16.7	0	160	—	—
5	40	Starch ^d	10	16.7	103	250	—	—
0	40	SAPP ^e	5	16.7	159	—	—	—
5	40	SAPP ^e	5	16.7	157	—	—	—
0	40	SAPP ^e	10	16.7	164	—	—	—
5	40	SAPP ^e	10	16.7	181	—	—	—
0	40	Lignin ^f	12	16.7	0	0 ^g	415	—
5	40	Lignin ^f	12	16.7	0	102	425	—

rand "D" straight slow-set cement.

Untreated field mud from well in Harris County, Tex., used as base mud. Test specimens cured under water at 175°F.

^d pre-gelatinized starch. Mud was well-fermented when tested.

^e sodium acid pyrophosphate, commercial grade, obtained from field sample.

^f calcium lignosulfonate.

^g did not set within 4 days.

Table VII—Effect of Activated Charcoal on Pumpability of Cements

Cement Tested	Charcoal Added Wt. Per Cent (Based on Cement)	Water Content of Slurry cu cm Water/100 gm Cement	Thickening Time			
			Schedule 5 ^a		Schedule 8 ^b	
			hr	min	hr	min
Normal Portland—Brand "B"	0	46	1	50	—	—
Normal Portland—Brand "B"	5	53	1	47	—	—
Normal Portland—Brand "E"	0	46	2	30	—	—
Normal Portland—Brand "E"	5	53	2	30	—	—
Straight Slow-Set—Brand "D"	0	40	—	—	1	50
Straight Slow-Set—Brand "D"	5	43	—	—	1	50
Additive Slow-Set—Brand "A"	0	40	—	—	2	46
Additive Slow-Set—Brand "A"	5	43	—	—	2	32
Additive Slow-Set—Brand "B"	0	40	—	—	2	40
Additive Slow-Set—Brand "B"	5	43	—	—	1	40

^aTested according to API Code 32 for 8,000 ft well depth.^bTested according to API Code 32 for 14,000 ft well depth.

ability, pumpability tests were made on two additive slow-set cements, one straight slow-set cement, and two normal portland cements.

The results, presented in Table VII, showed that the thickening times of slurries prepared with the normal portland cements and the straight slow-set cement were not changed appreciably by the addition of activated charcoal. The thickening time of one of the additive slow-set cement slurries was reduced only slightly but the thickening time of the other additive slow-set cement slurry was reduced quite drastically. From these data, it appears that satisfactory cementing compositions containing activated charcoal may be prepared with either normal portland cements or straight slow-set cements but that activated charcoal should not be added to additive-type slow-set cements without checking its effect upon the pumpability of the particular cement prior to its use.

FIELD USE OF CEMENT CONTAINING ACTIVATED CHARCOAL

Cement containing activated charcoal has been used in two field jobs for the purpose of setting cement plugs in a well drilling in Tyler County, Tex. Attempts to recover 150 ft of drill collars and bit which had been left in the hole at a depth of 10,775 ft had been unsuccessful and it was decided to sidetrack around them. Four cement jobs using conventional slow-set cements in an effort to obtain a firm plug on which to set a whipstock to sidetrack the hole were unsuccessful, apparently due to the failure of the cement to set firmly. Soft cement was washed out after each job. It was thought that the mud in use, which was an oil-emulsion mud treated with quebracho, caustic, and sodium acid pyrophosphate, might be deleteriously affecting the cement and that the addition of activated charcoal to the cement might alleviate the trouble. The fifth cement plug was placed, therefore, with 100 sacks of straight slow-set cement containing 500 lb of activated charcoal. Twenty hours later the top of the cement plug was located and medium hard cement was drilled from 10,462 to 10,476 ft. An attempt to sidetrack at this point was unsuccessful. The hole was reamed and drilled to 10,525 ft and successfully sidetracked to 10,559 ft where a survey showed that the hole was five degrees off vertical. During subsequent drilling, however, the pipe worked back into the old hole, resulting in the necessity of setting another plug. The next plug was placed with 200 sacks of straight slow-set cement containing 500 lb of activated charcoal. The top of the cement plug was located at 10,232 ft and medium hard cement was drilled to 10,291 ft 28 hours after placement. The hole was successfully sidetracked at 10,305 ft and subsequently drilled to total depth in the new deviated hole.

These field jobs were done on short notice and time was not taken to core the set cement and to obtain other data

which would have been helpful in evaluating the effectiveness of the activated charcoal. A more detailed program to evaluate the usefulness of cements containing activated charcoal in the field is planned.

CONCLUSIONS

The conclusions reached from consideration of the information presented may be summarized as follows:

1. Contamination of cement slurries with untreated drilling mud in concentrations likely to occur in the cementing of wells does not seriously affect the properties of cements. The contamination of cement slurries with untreated field muds, therefore, is probably not a serious problem.

2. Contamination of cement slurries with treated muds may cause serious retardation of the set of cements. This retardation effect caused by the mixing of treated muds with cement slurries may result in the failure of some cement jobs.

3. Straight slow-set cement appears to be superior to additive slow-set cement in its ability to withstand contamination with treated muds.

4. The retardation effect caused by the contamination of cement slurries with treated muds is more pronounced at low temperatures than at high temperatures. Mud contamination may be more critical, therefore, in wells of moderate depth than in extremely deep wells.

5. The deleterious effects of the contamination of cement slurries with treated muds may be partially counteracted by the addition of activated charcoal to the cement.

6. Satisfactory cementing compositions containing activated charcoal may be prepared with either normal portland cement or straight slow-set cement but activated charcoal should not be added to additive slow-set cement without prior checking of its effect upon the pumpability of the particular cement.

7. Cement containing activated charcoal has been used successfully in the field for the placement of two cement plugs in open hole.

REFERENCES

1. Doherty, W. T., and Manning, M.: "Cementing Problems on Gulf Coast," *Oil and Gas Jour.*, (Sept. 11, 1930) 30, 148.
2. Wilde, H. D., Jr.: "Cementing Problem on the Gulf Coast," *Trans. AIME*, (1930) 371.
3. Reid, A.: "Oil Well Cementing," *Jour. of Inst. of Pet. Tech.*, (1932) 18, 52.
4. Doherty, W. T.: "Oil Well Cementing in the Gulf Coast Area," *API Drill. and Prod. Prac.*, (1933) Bull. 212, 60.
5. "The Effects of Drilling-Mud Additives on Oil-Well Cements," *API Bull. D-4*, (Sept., 1951).

★ ★ ★

THE SLIP VELOCITY OF GASES RISING THROUGH LIQUID COLUMNS

N. STEIN, E. B. ELFRINK, JUNIOR MEMBER AIME, L. D. WIENER AND C. R. SANDBERG, MEMBER AIME, MAGNOLIA PETROLEUM CO., DALLAS, TEX.

ABSTRACT

This paper presents the results of a study of the slip velocity of gases rising through liquids in vertical tubes, inclined tubes, and vertical annuli. The data were obtained in gas-liquid systems which included combinations of air, propane and natural gas (over 97 per cent methane) with water, lubricating oils, and crude oils. The 214 data points obtained in this study along with 11 data points reported in the literature are incorporated in an empirical correlation which relates the mean slip velocity of gases flowing through liquids with the parameters gas rate, tube size, ratio of liquid viscosity to liquid density, gas density, liquid density, and the angle of the tube from the vertical.

The average numerical deviation of the measured slip velocity data from values obtained from the correlation is 9.2 per cent. The average algebraic deviation between measured and predicted data is 0.31 per cent, an indication that the correlation is a satisfactory representation of the data.

The correlation presented in this paper will be useful primarily in the design of subsurface gas-oil separation equipment for increasing the efficiency of oil-well pumping installations, but may perhaps be extended to other situations of gases rising through liquid columns.

INTRODUCTION

The production of oil by pumping is often complicated by the presence of free and dissolved gas in the oil at bottom-hole conditions. This gas can be drawn into the pump barrel and result in "vapor locking" the pump, thus reducing the efficiency of the pumping operation. Large amounts of free gas may be excluded from the pump by the use of a gas-anchor, which is designed to allow the separation of free gas from the oil before it is drawn into the pump. The design of a suitable gas-anchor depends on a knowledge of the difference

between the velocity of the free gas and that of the oil as the oil travels down toward the pump intake. This rate of gas rise through the oil is termed "slip velocity."

As a first step toward the full understanding of this problem, the mean slip velocities of gases flowing through static

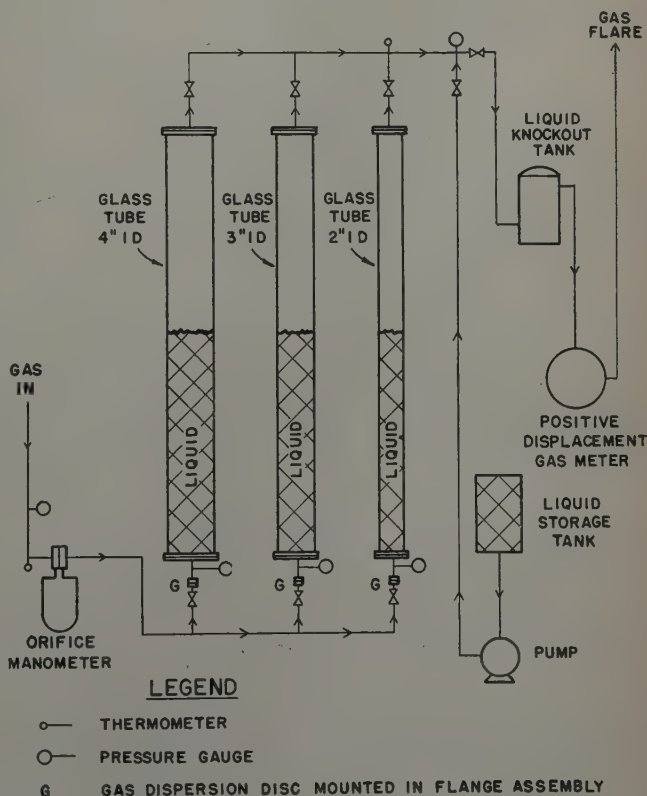


FIG. 1 — SLIP VELOCITY APPARATUS, SCHEMATIC DIAGRAM.

¹References given at end of paper.

Manuscript received in the Petroleum Branch office Aug. 7, 1950. Paper presented at the Fall Meeting of the Petroleum Branch in New Orleans, La., Oct. 4-6, 1950.

heads of liquids were measured and the data correlated. The correlation is presented in this paper.

PROCEDURE AND EQUIPMENT

In the past, a number of different techniques have been used to determine the rate at which gases rise through liquids. A dynamic method was employed by Moore and Wilde,¹ which involved the simultaneous metered circulation of both gas and liquid through vertical pipes. At an arbitrarily chosen time interval after the start of this operation, two quick-closing valves, one at the bottom and the other at the top of the pipe being tested, were closed. The volumes of gas and liquid caught in the pipe were measured, and from this information and the known rates of flow the slip velocity of the gas was calculated. In these calculations it was assumed that the relative portions of the cross-sectional area of the pipe occupied by the gas and liquid streams were directly related to the volume ratio of gas and liquid caught in the pipe.

A semi-static method was employed by Gosline² to measure slip velocity. In this procedure gas was bubbled through a static column of liquid, and the slip velocity calculated from

the rise in the level of the liquid in the column. This method is based on an analysis of the mean specific weight of the mixture of gas and liquid during a gas-lift operation. The mean specific weight in such an operation is dependent on the specific weights of the gas and liquid used at the conditions of the experiment as well as the relative quantities of gas and liquid present. This mean specific weight can be expressed in terms of the gas rate, the gas velocity, the specific weight of the liquid, the specific weight of the gas, and the cross-sectional area of the pipe. It can also be expressed in terms of the initial height of the liquid in the pipe, the increased height of liquid in the pipe due to injection of gas, the area of the pipe, and the specific weight of the liquid. By equating these relationships the following mathematical expression for slip velocity is derived:*

$$V_s = \frac{H + \Delta H}{D_1 \Delta H} \left[\frac{W_g R D_1}{2A} \left(\frac{T_1}{P_1} - \frac{T_2}{P_2} \right) - \frac{W_g}{A} \right] \quad (1)$$

This expression represents the mean slip velocity of the gas rising in a static fluid column. All of the variables in this equation can be easily determined experimentally.

The studies of Wilde and Moore¹ and of Gosline² provided considerable data for use in gas lift operations. Their studies covered a reasonable variety of tube sizes and liquids but did not provide a great deal of information in the range of low gas rates normally encountered in subsurface gas-oil separation equipment. The present investigation was conducted because of this lack of data. In addition to the extension of slip velocity data into the region of lower gas rates, data were obtained to better define the effects of gas and liquid properties on slip velocity.

In this investigation, the experimental techniques employed by Gosline² were used to determine gas slippage. The experimental determination of gas slippage was investigated in 15-ft vertical glass columns, having reasonably uniform inside diameters of two, three and four in. Auxiliary equipment was provided for the measurement of gas rates into and out of the columns and for the measurement of temperatures and pressures at the bottom and top of the columns. Gas-permeable porous discs were installed at the bottom of the columns to disperse the inlet gas. The four-in. column was installed so that it could be tilted from the vertical in order to study the effect of inclination from the vertical on gas slippage. Solid rods of various diameters were provided for insertion in the glass columns to study slip velocity in annuli. A schematic diagram of the experimental equipment described herein is shown in Fig. 1.

In the operation of the equipment, the liquid to be studied was first pumped into the column of interest. Gas was then bubbled through the liquid until it was saturated with the gas. At the start of an experiment the liquid height in the column was measured. The desired gas rate was then established and this rate was maintained constant into and out of the column. During the operation the liquid rise in the column was measured and the temperatures and pressures at the bottom and top of the column noted. Using these measured quantities, the mean slip velocity was calculated from Equation (1).

During the slip velocity measurements visual observations were made of the type and character of gas bubbles formed in the column. A description of the flow of methane through the three-in. tube filled with the heavy refined oil is typical of the phenomena observed. In this case, at low gas rates (0.09 Mcf/D) bubbles of varying size rose slowly as flattened

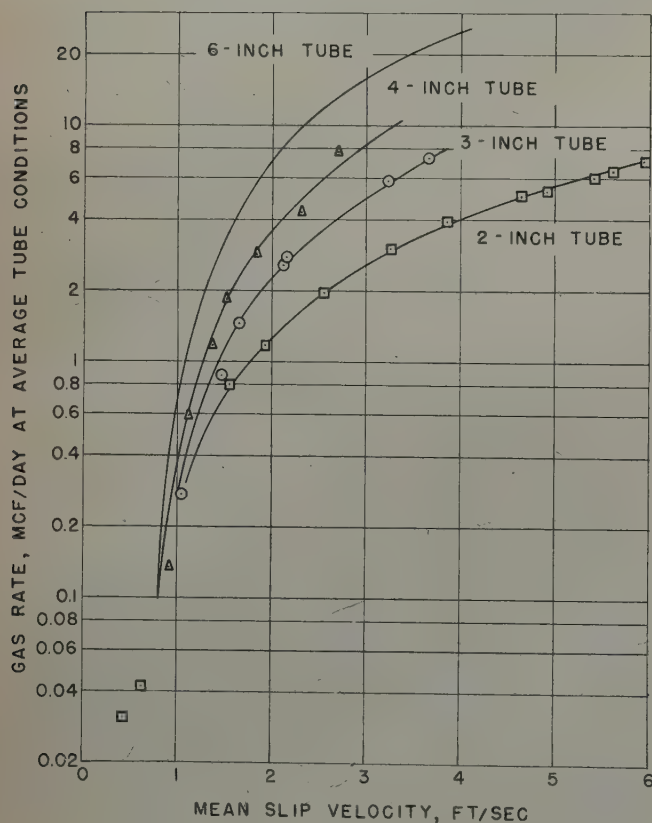


FIG. 2—MEAN SLIP VELOCITY OF NATURAL GAS THROUGH LIGHT REFINED OIL IN VERTICAL TUBES.

Average Conditions: Gas density—0.050 lb/cu ft; Liquid density—53.4 lb/cu ft; Liquid viscosity—0.536 cp

*Nomenclature at the end of paper.

Table I — Properties of Liquids Used in Slip Velocity Study

Liquid	Density at 60°F, lb/cu ft	Viscosity at 80°F cp
Water	62.4	0.87
Light refined oil	53.9	33.1
Heavy refined oil	56.4	159
Light crude oil	58.5	924
Heavy crude oil	62.1	16,000

spheres. At higher gas rates (0.37 Mcf/D) some of the larger bubbles became umbrella-shaped. The umbrella spread to the diameter of the tube and developed a tail to give a bullet shaped appearance when the gas rate was increased to 1.12 Mcf/D. At still higher gas rates (around 11.15 Mcf/D) alternate slugs of gas and liquid occupied the tube. In the course of the foregoing observations, it was also estimated by a semi-quantitative material-balance technique that the mean slip velocities measured represented the slip velocity of over 99 volume per cent of the gas present. The remaining one per cent, or less, of the total gas was in the form of smaller bubbles which had no measurable slip velocity.

SCOPE OF WORK

A total of 214 data points giving the rate at which gases slip through liquids was obtained. These data were determined in vertical tubes, in inclined tubes, and in vertical annuli.

Three gases were utilized in this investigation:

1. Natural gas (over 97 per cent methane)
2. Air
3. Propane (Phillips Technical Grade)

The liquids employed in conjunction with the various gases are listed together with other pertinent data in Table I.

In the course of this investigation, the following process variables were studied: gas rate, gas density, tube diameter, liquid density, liquid viscosity, gas dispersion, disc permeability, inclination of tube from the vertical, average tube temperature, and average tube pressure. The effects of all of

Table II — Ranges of the Experimental Data

Variable	Range	
	Minimum	Maximum
Gas rate, Mcf/D at average tube conditions	0.0187	39.366
Gas density, lb/cu ft at average tube conditions	0.0426	0.7066
Tube diameter, in.		
Open tube	2	4
Annuli on equivalent tube basis*	2.79	3.97
Liquid density, lb/cu ft at average tube conditions	53.9	62.4
Liquid viscosity to density ratio, cp		
at average tube conditions	0.0103	181.9
Gas dispersion disc permeability, md	58	2,000
Inclination from vertical, degrees	0	45
Temperature at average tube conditions, °F	60	104
Pressure at average tube conditions, psia	15	83

* $D_a = \sqrt{D_o^2 - D_i^2}$

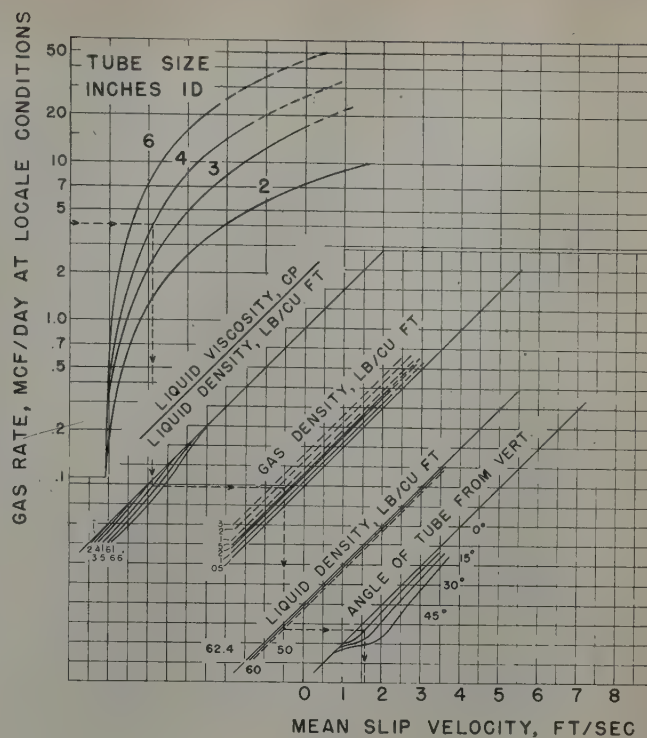


FIG. 3 — MEAN SLIP VELOCITY OF GASES THROUGH LIQUIDS.

these variables were investigated over the ranges summarized in Table II. These data are tabulated in detail in Tables III and IV.

CORRELATIONS

In the correlation of the data over the operating ranges investigated, it was found that the gas rate and the tube or pipe size had the greatest effect on the gas slip velocity. The effects of such other variables as liquid viscosity, liquid density, gas density, and angle of tube from the vertical were relatively minor in comparison. The effects of temperature and pressure on the system were exhibited as changes in the physical properties of the gas and liquid used so it was not necessary to consider temperature or pressure in the correlation as specific physical properties. Gas dispersion disc permeability had no measurable effect on slip velocity over the range of permeabilities from 58 to 2,000 md, so it was not utilized in the correlation of data.

Fig. 2 presents a correlation of slip velocity with tube size and gas rate. For the data plotted all other variables were constant. An excellent correlation is shown. This graph includes, in addition to the data obtained from Table II for two, three, and four-in. tubes, a plot for a six-in. tube calculated from data obtained by Gosline.² Similar plots were also made relating gas rate to slip velocity using angle of inclination, gas density, liquid density and liquid viscosity-to-density ratio as correlating parameters. As in Fig. 2, all other variables except those correlated were held constant. None of these variables affected slip velocity as significantly as tube size. All of these individual plots were then combined to produce the final correlations shown in Figs. 3 and 4. In the correlation,

Table III — Open Tube Gas Slippage Experiments and Results

Liquid	Gas	Tube Size, Tube Tilt		Gas Rate Mcf/D**	Temperature °F	Average Pres- sure, psia	Density, lb/cu ft**		Liquid Vis- cosity, cp**	Slip Velocity ft/sec
		In.	From Vertical				Gas	Liquid		
Water	Natural Gas*	4.0	0°	0.0818	76	16.5	0.0485	62.3	0.92	0.92
Water	Natural Gas*	4.0	0°	1.9062	82	16.4	0.0475	62.2	0.84	1.44
Water	Natural Gas*	4.0	0°	5.1112	82	16.4	0.0475	62.2	0.84	2.29
Water	Natural Gas*	4.0	0°	9.4335	82	16.9	0.0490	62.2	0.84	2.96
Water	Natural Gas*	4.0	0°	12.6029	76	24.7	0.0726	62.3	0.92	4.08
Water	Natural Gas*	4.0	20.5°	0.0298	88	15.6	0.0449	62.2	0.78	0.79
Water	Natural Gas*	4.0	20.5°	0.5518	90	16.2	0.0465	62.2	0.76	1.58
Water	Natural Gas*	4.0	20.5°	2.5507	90	16.0	0.0460	62.1	0.76	2.06
Water	Natural Gas*	4.0	20.5°	3.7548	91	16.8	0.0480	62.1	0.75	2.52
Water	Natural Gas*	4.0	20.5°	6.5591	92	20.8	0.0595	62.1	0.74	3.00
Water	Natural Gas*	4.0	35.5°	0.0377	91	16.2	0.0463	62.1	0.75	0.92
Water	Natural Gas*	4.0	35.5°	0.5080	92	15.7	0.0449	62.1	0.74	1.61
Water	Natural Gas*	4.0	35.5°	1.9125	92	16.1	0.0459	62.1	0.74	2.02
Water	Natural Gas*	4.0	35.5°	3.2537	93	16.6	0.0474	62.1	0.73	2.35
Water	Natural Gas*	4.0	35.5°	6.3000	93	20.2	0.0576	62.1	0.73	3.03
Water	Natural Gas*	4.0	45°	0.0222	93	15.3	0.0435	62.1	0.73	1.10
Water	Natural Gas*	4.0	45°	0.6668	81	15.8	0.0460	62.2	0.86	2.18
Water	Natural Gas*	4.0	45°	1.6104	81	15.4	0.0448	62.2	0.86	2.26
Water	Natural Gas*	4.0	45°	2.1485	81	15.5	0.0452	62.2	0.86	2.38
Water	Natural Gas*	4.0	45°	2.9507	81	15.8	0.0460	62.2	0.86	2.55
Water	Natural Gas*	4.0	45°	5.8192	82	18.6	0.0540	62.2	0.85	3.20
Water	Natural Gas*	4.0	45°	7.1392	82	21.2	0.0616	62.2	0.85	3.33
Water	Natural Gas*	3.0	0°	0.0173	74	16.3	0.0430	62.3	0.95	0.67
Water	Natural Gas*	3.0	0°	0.0412	90	15.8	0.0453	62.2	0.76	0.90
Water	Natural Gas*	3.0	0°	0.0429	93	15.7	0.0449	62.1	0.73	0.90
Water	Natural Gas*	3.0	0°	0.0704	94	15.7	0.0448	62.1	0.72	0.94
Water	Natural Gas*	3.0	0°	0.1015	90	15.8	0.0453	62.2	0.76	0.96
Water	Natural Gas*	3.0	0°	0.1553	74	17.2	0.0508	62.3	0.95	0.94
Water	Natural Gas*	3.0	0°	0.2055	90	15.8	0.0454	62.2	0.76	1.05
Water	Natural Gas*	3.0	0°	0.2624	94	15.8	0.0451	62.1	0.72	1.09
Water	Natural Gas*	3.0	0°	0.4051	94	16.9	0.0482	62.1	0.72	0.60
Water	Natural Gas*	3.0	0°	0.4155	90	16.5	0.0472	62.2	0.76	0.80
Water	Natural Gas*	3.0	0°	1.2207	91	16.3	0.0465	62.1	0.75	1.57
Water	Natural Gas*	3.0	0°	1.7953	97	15.8	0.0449	62.1	0.70	1.79
Water	Natural Gas*	3.0	0°	2.3237	91	16.3	0.0467	62.1	0.75	1.98
Water	Natural Gas*	3.0	0°	2.8945	97	16.1	0.0457	62.1	0.70	2.17
Water	Natural Gas*	3.0	0°	3.1379	97	16.2	0.0459	62.1	0.70	2.22
Water	Natural Gas*	3.0	0°	4.0147	91	16.3	0.0467	62.1	0.75	2.53
Water	Natural Gas*	3.0	0°	16.0050	74	23.6	0.0698	62.3	0.95	6.25
Water	Natural Gas*	2.0	0°	0.0130	94	83.2	0.2368	62.1	0.72	0.90
Water	Natural Gas*	2.0	0°	0.0133	103	45.8	0.1284	62.0	0.65	0.57
Water	Natural Gas*	2.0	0°	0.0279	102	32.8	0.0922	62.0	0.66	0.88
Water	Natural Gas*	2.0	0°	0.0320	70	15.6	0.0465	62.4	1.02	0.88
Water	Natural Gas*	2.0	0°	0.0796	103	45.3	0.1270	62.0	0.65	0.70
Water	Natural Gas*	2.0	0°	0.1192	102	34.3	0.0964	62.0	0.66	1.01
Water	Natural Gas*	2.0	0°	0.1970	91	63.4	0.1816	62.1	0.75	0.93
Water	Natural Gas*	2.0	0°	0.2692	102	33.8	0.0950	62.0	0.66	1.02
Water	Natural Gas*	2.0	0°	0.3785	103	46.1	0.1292	62.0	0.65	1.09
Water	Natural Gas*	2.0	0°	0.4696	102	34.4	0.0966	62.0	0.66	1.14
Water	Natural Gas*	2.0	0°	0.5457	96	83.2	0.2359	62.1	0.70	1.16
Water	Natural Gas*	2.0	0°	0.5554	72	15.6	0.0462	62.3	0.98	1.46
Water	Natural Gas*	2.0	0°	0.5934	94	63.8	0.1817	62.1	0.72	1.22
Water	Natural Gas*	2.0	0°	0.7688	73	15.6	0.0463	62.3	0.96	1.29
Water	Natural Gas*	2.0	0°	0.8674	103	45.8	0.1284	62.0	0.65	1.45
Water	Natural Gas*	2.0	0°	0.9397	97	83.8	0.2374	62.1	0.70	1.44
Water	Natural Gas*	2.0	0°	0.9804	102	33.8	0.0950	62.0	0.66	1.55
Water	Natural Gas*	2.0	0°	1.1018	94	63.9	0.1820	62.1	0.72	1.56
Water	Natural Gas*	2.0	0°	1.2339	97	83.2	0.2357	62.1	0.70	1.61
Water	Natural Gas*	2.0	0°	1.4322	94	63.7	0.1814	62.1	0.72	1.77
Water	Natural Gas*	2.0	0°	1.4444	102	34.6	0.0972	62.0	0.66	1.83
Water	Natural Gas*	2.0	0°	1.7486	74	15.6	0.0462	62.3	0.95	2.17
Water	Natural Gas*	2.0	0°	1.8811	90	46.4	0.1332	62.2	0.76	2.30
Water	Natural Gas*	2.0	0°	4.4634	75	15.1	0.0446	62.3	0.94	3.72
Lt. Ref. Oil	Nat. Gas*	4.0	0°	0.1361	90	16.0	0.0458	53.2	24	0.92
Lt. Ref. Oil	Nat. Gas*	4.0	0°	0.5952	80	16.0	0.0466	53.4	33	1.12
Lt. Ref. Oil	Nat. Gas*	4.0	0°	1.1827	80	19.0	0.0553	53.4	33	1.39
Lt. Ref. Oil	Nat. Gas*	4.0	0°	1.8452	80	16.4	0.0479	53.4	33	1.52
Lt. Ref. Oil	Nat. Gas*	4.0	0°	2.8660	82	16.9	0.0492	53.4	32	1.84
Lt. Ref. Oil	Nat. Gas*	4.0	0°	3.7503	83	17.4	0.0505	53.4	30	2.05
Lt. Ref. Oil	Nat. Gas*	4.0	0°	4.3333	83	17.9	0.0520	53.4	30	2.31
Lt. Ref. Oil	Nat. Gas*	4.0	0°	7.8713	80	19.2	0.0562	53.4	33	2.70
Lt. Ref. Oil	Nat. Gas*	3.0	0°	0.2785	92	16.0	0.0456	53.2	22	1.05
Lt. Ref. Oil	Nat. Gas*	3.0	0°	0.5187	62	16.5	0.0498	53.8	86	1.15
Lt. Ref. Oil	Nat. Gas*	3.0	0°	0.8712	92	16.9	0.0483	53.2	22	1.49
Lt. Ref. Oil	Nat. Gas*	3.0	0°	1.0162	63	17.5	0.0528	53.8	81	1.47
Lt. Ref. Oil	Nat. Gas*	3.0	0°	1.2975	63	18.6	0.0562	53.8	81	1.63

Table III — (Continued)

Fluid	Gas	Tube Size, Tube Tilt		Gas Rate Mcf/D**	Temperature °F	Average Pres- sure, psia	Density, lb/cu ft**		Liquid Vis- cosity, cp**	Slip Velocity ft/sec
		In.	From Vertical				Gas	Liquid		
Ref. Oil	Nat. Gas*	3.0	0°	1.4229	92	16.0	0.0456	53.2	22	1.67
Ref. Oil	Nat. Gas*	3.0	0°	1.5993	64	20.3	0.0611	53.8	78	1.75
Ref. Oil	Nat. Gas*	3.0	0°	2.5152	92	16.1	0.0461	53.2	22	2.12
Ref. Oil	Nat. Gas*	3.0	0°	2.7167	92	16.5	0.0471	53.2	22	2.17
Ref. Oil	Nat. Gas*	3.0	0°	5.8028	76	17.6	0.0518	53.5	41	3.22
Ref. Oil	Nat. Gas*	3.0	0°	7.2325	76	19.0	0.0558	53.5	41	3.67
Ref. Oil	Nat. Gas*	2.0	0°	0.0310	78	16.8	0.0468	53.5	38	0.43
Ref. Oil	Nat. Gas*	2.0	0°	0.0419	82	16.0	0.0466	53.4	32	0.62
Ref. Oil	Nat. Gas*	2.0	0°	0.7981	82	16.7	0.0485	53.4	32	1.56
Ref. Oil	Nat. Gas*	2.0	0°	1.1799	83	16.0	0.0465	53.4	30	1.91
Ref. Oil	Nat. Gas*	2.0	0°	1.9175	83	16.0	0.0465	53.4	30	2.56
Ref. Oil	Nat. Gas*	2.0	0°	2.9940	100	15.1	0.0426	53.0	20	3.28
Ref. Oil	Nat. Gas*	2.0	0°	3.9510	100	15.5	0.0437	53.0	21	3.87
Ref. Oil	Nat. Gas*	2.0	0°	4.9689	80	17.0	0.0498	53.4	33	4.66
Ref. Oil	Nat. Gas*	2.0	0°	5.3572	78	16.4	0.0479	53.5	38	4.92
Ref. Oil	Nat. Gas*	2.0	0°	6.1310	100	16.4	0.0469	53.0	21	5.36
Ref. Oil	Nat. Gas*	2.0	0°	6.5650	78	17.3	0.0508	53.5	38	5.61
Ref. Oil	Nat. Gas*	2.0	0°	7.1776	79	17.6	0.0514	53.5	38	5.97
Ref. Oil	Nat. Gas*	2.0	0°	7.8880	100	17.7	0.0499	53.0	21	6.32
Ref. Oil	Nat. Gas*	2.0	0°	10.9190	100	22.4	0.0631	53.0	21	8.12
Ref. Oil	Nat. Gas*	2.0	0°	29.8850	95	19.8	0.0563	53.1	23	19.66
Ref. Oil	Nat. Gas*	2.0	0°	39.3660	96	24.6	0.0698	53.1	22	24.02
Ref. Oil	Nat. Gas*	4.0	0°	0.1513	70	16.1	0.0478	56.2	257	0.74
Ref. Oil	Nat. Gas*	4.0	0°	0.1588	79	16.0	0.0469	56.0	180	0.52
Ref. Oil	Nat. Gas*	4.0	0°	0.4421	70	16.1	0.0512	56.2	257	0.58
Ref. Oil	Nat. Gas*	4.0	0°	1.7420	70	16.1	0.0494	56.2	257	1.49
Ref. Oil	Nat. Gas*	4.0	0°	1.8934	80	16.1	0.0470	55.9	159	1.55
Ref. Oil	Nat. Gas*	4.0	0°	2.2776	70	16.2	0.0481	56.2	249	1.58
Ref. Oil	Nat. Gas*	4.0	0°	2.8250	80	16.1	0.0471	55.9	159	1.90
Ref. Oil	Nat. Gas*	4.0	0°	5.9005	70	17.9	0.0533	56.2	249	2.56
Ref. Oil	Nat. Gas*	4.0	0°	7.6235	69	19.4	0.0578	56.2	249	2.93
Ref. Oil	Nat. Gas*	3.0	0°	0.0335	73	16.0	0.0474	56.1	217	0.43
Ref. Oil	Nat. Gas*	3.0	0°	0.1553	73	16.0	0.0474	56.1	217	0.62
Ref. Oil	Nat. Gas*	3.0	0°	0.4194	69	16.2	0.0482	56.2	249	0.82
Ref. Oil	Nat. Gas*	3.0	0°	0.4385	69	17.8	0.0532	56.2	249	1.38
Ref. Oil	Nat. Gas*	3.0	0°	1.3199	72	15.9	0.0470	56.1	222	1.14
Ref. Oil	Nat. Gas*	3.0	0°	1.6786	69	20.5	0.0612	56.2	249	1.66
Ref. Oil	Nat. Gas*	3.0	0°	2.3346	72	15.9	0.0470	56.1	222	1.64
Ref. Oil	Nat. Gas*	3.0	0°	2.9222	73	15.9	0.0471	56.1	217	2.01
Ref. Oil	Nat. Gas*	3.0	0°	5.2590	73	17.1	0.0507	56.1	217	3.07
Ref. Oil	Nat. Gas*	3.0	0°	6.8819	67	17.3	0.0518	56.2	281	3.58
Ref. Oil	Nat. Gas*	2.0	0°	0.0446	68	16.0	0.0479	56.2	263	0.61
Ref. Oil	Nat. Gas*	2.0	0°	0.0837	68	16.0	0.0479	56.2	263	0.62
Ref. Oil	Nat. Gas*	2.0	0°	0.3163	69	16.0	0.0478	56.2	249	0.85
Ref. Oil	Nat. Gas*	2.0	0°	1.4912	69	16.0	0.0478	56.2	249	1.96
Ref. Oil	Nat. Gas*	2.0	0°	4.5597	76	15.8	0.0465	56.0	190	4.68
Ref. Oil	Nat. Gas*	2.0	0°	6.8953	76	17.6	0.0517	56.0	190	6.38
Crude Oil	Nat. Gas*	4.0	0°	0.0255	89	16.2	0.0464	57.8	384	0.17
Crude Oil	Nat. Gas*	4.0	0°	0.2077	89	16.2	0.0466	57.8	384	0.33
Crude Oil	Nat. Gas*	4.0	0°	1.0964	89	18.4	0.0528	57.8	384	0.88
Crude Oil	Nat. Gas*	4.0	0°	2.2587	89	16.2	0.0464	57.8	384	1.01
Crude Oil	Nat. Gas*	4.0	0°	3.3586	89	16.4	0.0470	57.8	384	1.30
Cr. Oil	Nat. Gas*	4.0	0°	0.0437	86	16.1	0.0465	61.5	8,860	0.20
Cr. Oil	Nat. Gas*	4.0	0°	0.4039	89	16.1	0.0462	61.5	7,070	0.49
Cr. Oil	Nat. Gas*	4.0	0°	0.9201	90	16.1	0.0462	61.4	6,680	0.69
Cr. Oil	Nat. Gas*	4.0	0°	1.4600	91	16.1	0.0461	61.4	6,280	0.85
Cr. Oil	Nat. Gas*	4.0	0°	1.8404	91	16.1	0.0461	61.4	6,280	0.96
Cr. Oil	Nat. Gas*	4.0	0°	2.0586	92	16.1	0.0460	61.4	5,690	1.03
Cr. Oil	Nat. Gas*	4.0	0°	4.8847	83	17.6	0.0511	61.6	11,300	1.78
Cr. Oil	Nat. Gas*	4.0	0°	8.6519	86	22.6	0.0652	61.5	8,860	2.81
Cr. Oil	Nat. Gas*	4.0	0°	9.8006	87	27.2	0.0804	61.5	8,460	3.18
er	Air	4.0	0°	0.3122	71	16.6	0.0844	62.3	0.99	0.83
er	Air	4.0	0°	3.6123	77	17.7	0.0890	62.3	0.91	1.62
er	Air	4.0	0°	4.5410	77	18.9	0.0950	62.3	0.91	1.86
Ref. Oil	Air	4.0	0°	0.1585	86	15.9	0.0785	53.3	27	0.57
Ref. Oil	Air	4.0	0°	1.7225	87	16.0	0.0789	53.3	25	1.50
Ref. Oil	Air	4.0	0°	2.6763	83	16.5	0.0820	53.4	30	1.68
Ref. Oil	Air	4.0	0°	0.0295	73	16.2	0.0819	56.1	217	0.68
Ref. Oil	Air	4.0	0°	0.1380	76	16.3	0.0820	56.0	190	0.55
Ref. Oil	Air	4.0	0°	1.2096	76	16.3	0.0820	56.0	190	1.26
Ref. Oil	Air	4.0	0°	1.6820	76	16.4	0.0827	56.0	190	1.29
Ref. Oil	Air	4.0	0°	3.8836	79	17.7	0.0885	56.0	180	2.11
Ref. Oil	Air	4.0	0°	6.3202	80	21.1	0.1054	55.9	159	2.57
er	Propane	4.0	0°	0.0756	78	16.6	0.1268	62.3	0.89	0.84
er	Propane	4.0	0°	2.7218	79	17.9	0.1365	62.3	0.88	1.51
er	Propane	4.0	0°	3.4777	80	18.8	0.1431	62.2	0.87	1.65

Table III — (Continued)

Liquid	Gas	Tube Size, Tube Tilt		Gas Rate Mcf/D**	Temperature °F	Average Pres- sure, psia	Density, lb/cu ft**		Liquid Vis- cosity, cp**	Slip Velocity ft/sec
		In.	From Vertical				Gas	Liquid		
Water	Propane	4.0	0°	3.6331	79	18.8	0.1434	62.3	0.88	1.75
Water	Propane	2.0	0°	0.0080	103	84.9	0.6741	62.0	0.65	0.55
Water	Propane	2.0	0°	0.0585	89	83.6	0.6828	62.2	0.77	0.57
Water	Propane	2.0	0°	0.0702	103	82.8	0.6575	62.0	0.65	0.52
Water	Propane	2.0	0°	0.1968	89	83.6	0.6878	62.2	0.77	0.81
Water	Propane	2.0	0°	0.2973	103	83.8	0.6654	62.0	0.65	0.86
Water	Propane	2.0	0°	0.3249	90	83.6	0.6872	62.2	0.76	0.88
Water	Propane	2.0	0°	0.3774	90	83.3	0.6847	62.2	0.76	0.87
Water	Propane	2.0	0°	0.4292	103	83.1	0.6598	62.0	0.65	0.94
Water	Propane	2.0	0°	0.5212	103	83.1	0.6598	62.0	0.65	1.05
Water	Propane	2.0	0°	0.5355	103	82.7	0.6567	62.0	0.65	1.04
Lt. Ref. Oil	Propane	4.0	0°	0.3319	88	16.3	0.1221	53.3	24	0.50
Lt. Ref. Oil	Propane	4.0	0°	0.6878	75	16.0	0.1226	53.6	45	1.04
Lt. Ref. Oil	Propane	4.0	0°	1.3167	75	16.0	0.1233	53.6	45	1.12
Lt. Ref. Oil	Propane	4.0	0°	4.5151	75	19.1	0.1470	53.6	45	2.02
Hvy. Ref. Oil	Propane	4.0	0°	0.0303	79	16.1	0.1236	56.0	180	0.64
Hvy. Ref. Oil	Propane	4.0	0°	0.1478	83	16.2	0.1228	55.9	141	0.85
Hvy. Ref. Oil	Propane	4.0	0°	1.3167	85	16.3	0.1231	55.8	128	1.48
Hvy. Ref. Oil	Propane	4.0	0°	1.4607	85	16.4	0.1238	55.8	128	1.24
Hvy. Ref. Oil	Propane	4.0	0°	3.4625	86	17.7	0.1334	55.8	125	1.87
Hvy. Ref. Oil	Propane	4.0	0°	5.5106	86	21.7	0.1635	55.8	125	2.41
Hvy. Ref. Oil	Propane	2.0	0°	0.1997	96	82.7	0.1997	55.6	42	0.57
Hvy. Ref. Oil	Propane	2.0	0°	0.3814	96	83.1	0.3814	55.6	42	0.78
Hvy. Ref. Oil	Propane	2.0	0°	0.4461	96	83.1	0.4461	55.6	42	0.85
Hvy. Ref. Oil	Propane	2.0	0°	0.5121	96	83.1	0.5121	55.6	42	0.91

*Over 97% Methane.

**Measured at conditions of temperature and pressure specified in the table.

Table IV — Annuli Gas Slippage Experiments and Results

Liquid	Gas	Annuli Dimensions*		Equivalent Open Tube Size, In.	Tube Tilt From Vertical	Gas Rate Mcf/D***	Tempera- ture, °F	Pressure, psia	Density, lb/cu ft***		Liquid Viscosity cp***	Slip Velocity, ft/sec
		OD, In.	ID, In.						Gas	Liquid		
Water	Natural Gas**	4.0	0.50	3.9	0°	0.0279	91	16.1	0.0461	62.1	0.75	0.78
Water	Natural Gas**	4.0	0.50	3.9	0°	0.2551	92	16.2	0.0464	62.1	0.74	1.02
Water	Natural Gas**	4.0	0.50	3.9	0°	0.8197	93	17.1	0.0488	62.1	0.73	1.24
Water	Natural Gas**	4.0	0.50	3.9	0°	1.7861	103	16.5	0.0461	62.0	0.65	1.40
Water	Natural Gas**	4.0	0.50	3.9	0°	2.2252	103	16.6	0.0464	62.0	0.65	1.56
Water	Natural Gas**	4.0	0.50	3.9	0°	2.6382	104	16.7	0.0468	62.0	0.64	1.67
Water	Natural Gas**	4.0	0.50	3.9	0°	2.6561	93	16.5	0.0472	62.1	0.73	1.78
Water	Natural Gas**	4.0	1.1	3.8	0°	0.0425	90	15.6	0.0447	62.2	0.76	0.94
Water	Natural Gas**	4.0	1.1	3.8	0°	0.1150	90	15.6	0.0447	62.2	0.76	1.01
Water	Natural Gas**	4.0	1.1	3.8	0°	0.3302	90	15.7	0.0450	62.2	0.76	1.08
Water	Natural Gas**	4.0	1.1	3.8	0°	1.1327	90	15.6	0.0447	62.2	0.76	1.33
Water	Natural Gas**	4.0	1.1	3.8	0°	1.7875	90	15.7	0.0450	62.2	0.76	1.57
Water	Natural Gas**	4.0	1.1	3.8	0°	2.4034	90	16.0	0.0458	62.2	0.76	1.75
Water	Natural Gas**	4.0	1.1	3.8	0°	2.8750	90	16.0	0.0458	62.2	0.76	1.92
Water	Natural Gas**	4.0	1.1	3.8	0°	4.4800	90	16.9	0.0486	62.2	0.76	2.30
Water	Natural Gas**	4.0	1.1	3.8	0°	6.5864	90	19.0	0.0544	62.2	0.76	2.73
Water	Natural Gas**	4.0	1.1	3.8	0°	7.9794	90	21.6	0.0620	62.2	0.76	2.99
Water	Natural Gas**	4.0	2.0	3.5	0°	0.0280	99	16.3	0.0460	62.0	0.68	1.08
Water	Natural Gas**	4.0	2.0	3.5	0°	0.0289	95	16.4	0.0467	62.1	0.71	0.92
Water	Natural Gas**	4.0	2.0	3.5	0°	0.1756	99	16.4	0.0464	62.0	0.68	1.06
Water	Natural Gas**	4.0	2.0	3.5	0°	0.3460	96	16.6	0.0472	62.1	0.70	0.99
Water	Natural Gas**	4.0	2.0	3.5	0°	0.6135	101	16.9	0.0476	62.0	0.67	1.21
Water	Natural Gas**	4.0	2.0	3.5	0°	0.7529	97	17.3	0.0490	62.1	0.70	1.30
Water	Natural Gas**	4.0	2.0	3.5	0°	0.8827	102	16.4	0.0461	62.0	0.66	1.28
Water	Natural Gas**	4.0	2.0	3.5	0°	1.5212	97	16.5	0.0468	62.1	0.70	1.68
Water	Natural Gas**	4.0	2.0	3.5	0°	1.5889	101	16.6	0.0466	62.0	0.67	1.62
Water	Natural Gas**	4.0	2.0	3.5	0°	2.1307	97	16.7	0.0472	62.1	0.70	1.89
Water	Natural Gas**	4.0	2.0	3.5	0°	2.1434	102	16.7	0.0468	62.0	0.66	1.84
Water	Natural Gas**	4.0	2.0	3.5	0°	2.7911	102	16.8	0.0473	62.0	0.66	2.00
Water	Natural Gas**	4.0	2.0	3.5	0°	2.9434	98	16.9	0.0477	62.0	0.69	2.15
Water	Natural Gas**	3.0	1.1	2.8	0°	0.5422	87	16.1	0.0465	62.2	0.79	1.42
Water	Natural Gas**	3.0	1.1	2.8	0°	1.0601	85	16.3	0.0470	62.2	0.81	1.58
Water	Natural Gas**	3.0	1.1	2.8	0°	1.4839	85	16.3	0.0470	62.2	0.81	1.82
Water	Natural Gas**	3.0	1.1	2.8	0°	1.5847	90	16.2	0.0465	62.2	0.76	1.75
Water	Natural Gas**	3.0	1.1	2.8	0°	1.9768	86	16.6	0.0480	62.2	0.80	2.00
Water	Natural Gas**	3.0	1.1	2.8	0°	2.0670	89	16.3	0.0469	62.2	0.77	1.94
Water	Natural Gas**	3.0	1.1	2.8	0°	2.8481	84	16.7	0.0480	62.2	0.82	2.32

*Equivalent Open Tube Size = $\sqrt{(OD)^2 - (ID)^2}$

**Over 97% Methane

***Measured at conditions of temperature and pressure specified in the table.

most of the data were found easily resolvable to correlations of the type shown in Fig. 2, so no mathematical analysis of the data was attempted. Extrapolated portions of data are represented by dotted lines.

Fig. 4 is an expansion of that portion of Fig. 3 used to determine the slip velocity in the range below 7.5 ft/sec. Consequently, the effects of the different variables in this region, corresponding to low gas rates, may be presented in greater detail. The emphasis on this region of the chart by means of the expansion is reasonable since 208 of the 214 experimental data points used for correlating purposes are included in Fig. 4.

Fig. 3 presents slip velocity values as high as 24.0 ft/sec. However, these high values are based on a limited amount of experimental evidence. This chart is useful primarily for systems having relatively high slip velocities and to obtain rough estimates of systems having low slip velocities. In both Figs. 3 and 4, the data for the six-in. columns were taken from the investigation reported by Gosline.²

Temperature and pressure changes affect the measured physical properties of gases and liquids. As presented in this paper, the slip velocity of gases through liquids has been related with the various parameters at the temperature and pressure of measurement. Since the effects of temperature and pressure on slip velocity are included in the changes in physical properties exhibited by the gases and liquids, the correlations in Figs. 3 and 4 are deemed usable at temperatures and pressures outside the ranges given in Table I, provided that the physical properties of the gas and liquid involved at the temperatures and pressures in question fall within the limits covered for these variables in this investigation. From the data in Table IV it was found that slip

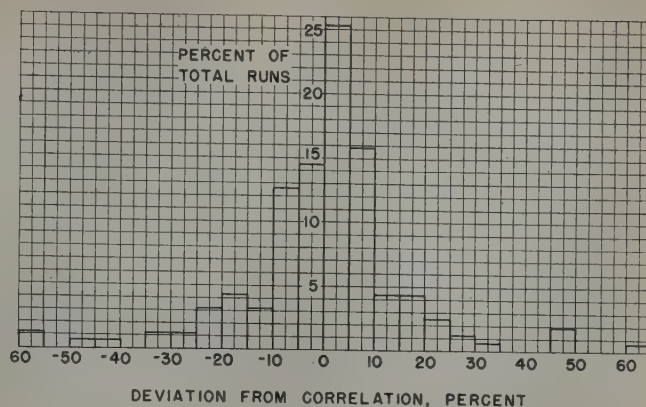


FIG. 5—DEVIATION OF DATA FROM THE CORRELATION.

velocities in annuli were related to slip velocities in tubes by the tube equivalent diameter. This diameter is defined as the diameter of an open tube of cross-sectional area equal to the annulus cross-sectional area, or

$$D_a = \sqrt{D_o^2 - D_i^2} \quad (2)$$

Slip velocities in annuli can thus be obtained by using the correlation in Figs. 3 and 4 along with the relationship shown in Equation (2). The equivalent tube diameter is calculated from Equation (2) and this tube diameter is then used in Figs. 3 and 4 for the prediction of slip velocity.

The overall accuracy of the correlation representing the experimental data from this investigation is demonstrated by a value of 9.2 per cent for the average numerical deviation between measured slip velocities and those predicted from the correlation obtained from these same measured values. The average algebraic deviation between measured and predicted slip velocities of +0.31 per cent indicates that the correlation is a reasonable representation of the data obtained. A further evaluation of the correlation accuracy is demonstrated by the error distribution chart presented in Fig. 5. This chart shows that 71.2 per cent of the measured slip velocities fall within a ± 10 per cent deviation from values predicted by the chart and that the errors fall approximately on a normal distribution curve.

APPLICATIONS

In the use of the correlation presented in Figs. 3 and 4, it should be emphasized that the numerical values of the variables used in the correlation must correspond to the conditions actually existing at the locale where the slip velocity is to be determined. Where the properties of the gas and oil of interest are known only at well-head conditions, these properties must be corrected to those existing at bottom-hole conditions in order to predict slip velocity at the bottom of a well.

The procedure which should be used to determine the mean slip velocity from the correlation in Figs. 3 and 4 is illustrated

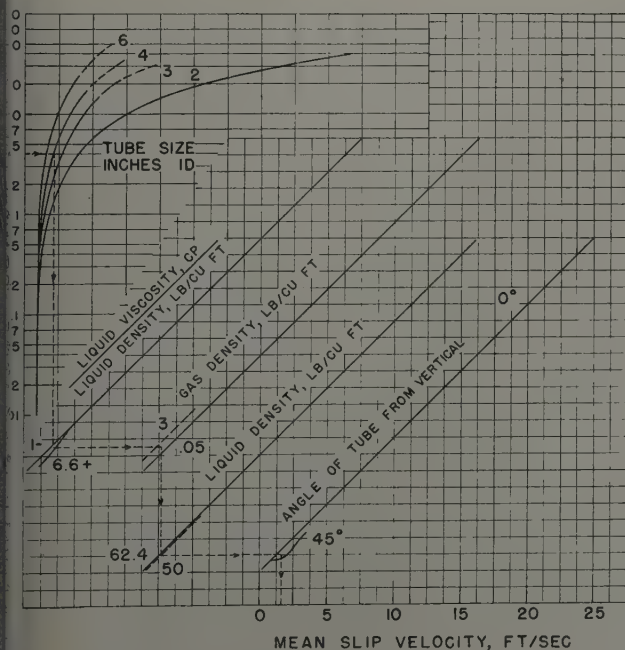


FIG. 4—MEAN SLIP VELOCITY OF GASES THROUGH LIQUIDS.

by the following example. Let us assume that calculated conditions, at some depth, x , in a well, result in the following values:

Gas rate = 4 Mcf/D under conditions at level x
 Tubing size = 4 in.

Viscosity-density ratio $\left(\frac{cp}{lb/cu\ ft} \right) = 5$

Gas density = 1 lb/cu ft

Liquid density = 50 lb/cu ft

Inclination of tube from vertical = 15°

The determination of the mean slip velocity from Fig. 3 using the parameters given above can be accomplished by following the directionally indicated dashed line on Fig. 3. This produces a mean slip velocity of 1.5 ft/sec. By following the same procedure on Fig. 4 a somewhat more accurate slip velocity of 1.58 ft/sec is obtained.

ACKNOWLEDGMENTS

The authors wish to express their appreciation to the Magnolia Petroleum Co. for permission to publish this paper, and to operating department personnel of Magnolia and its affiliates, Socony-Vacuum Oil Co. and General Petroleum Corp., for their suggestions and comments. Credit is also due to T. A. Pollard of the Magnolia Petroleum Co. Field Research Laboratories, who made many helpful suggestions during the course of the work.

NOMENCLATURE

A	= Cross sectional area of the tube, sq ft
cp	= Viscosity in centipoise
D_a	= Equivalent tube diameter, in.
D_i	= Inside diameter of annulus, in.
D_l	= Density of liquid, lb/cu ft
D_o	= Outside diameter of annulus, in.
H	= Static liquid level, ft
ΔH	= Increment in liquid level due to the presence of flowing gas, ft
P	= Pressure in the tube, psia
R	= Perfect gas law constant, $\frac{10.72}{\text{molecular wt}}$
T	= Temperature in the tube, $^\circ R$
V_g	= Average slip velocity, ft/sec
W_g	= Mass rate of gas flow, lb/sec
Subscript 1	= Bottom of tube
Subscript 2	= Top of tube

REFERENCES

1. Moore, T. V., and Wilde, H. D., Jr.: "Measurement of Slippage in Flow Through Vertical Pipes," *Trans. Pet. D. AIME*, (1931) **92**, 296.
2. Gosline, J. E.: "Experiments in the Vertical Flow of Gas-Liquid Mixtures in Glass Pipe," *Trans. AIME*, (1931) **118**, 56. ★ ★

NATURAL GAS IN THE PROVINCE OF ALBERTA, CANADA

F. DOUGHERTY, EMPIRE TRUST CO., NEW YORK, N. Y., MEMBER AIME; ANTHONY FOLGER, DeGOLYER AND MacNAUGHTON, DALLAS, TEX.; HOWARD R. LOWE, DELHI OIL CORP., DALLAS, TEX.; JOFFRE MEYER AND E. G. TROSTEL, DeGOLYER AND MacNAUGHTON, DALLAS, TEX., MEMBERS AIME

ABSTRACT

The status of the natural gas industry in Alberta, Canada, is described with particular reference to the current extent of natural gas reserves and possibilities for additional development. Certain major fields are discussed as representative of the types of gas accumulations within various broad geographical divisions of the province. The estimation of the future performance of a gas reservoir is discussed as the basis for the estimate of the future availability of natural gas from presently known reserves. The future availability of the provincial reserves and the estimated future demand for gas within the province are described.

INTRODUCTION

This paper is a condensation of a detailed study of the natural gas reserves and the future availability of pipeline gas in the province of Alberta as prepared for Trans-Canada Pipe Lines Limited and presented in public hearings at Edmonton and Calgary before the Petroleum and Natural Gas Conservation Board of the Province of Alberta. The study was completed in October, 1950, and resulted in the preparation of a report containing volumes of data at the expenditure of more than 20,000 man-hours. This paper is designed to afford a broad picture of the natural gas situation in detail limited to a type example of both natural gas accumulations and future availability of gas supply.

The province of Alberta has an area of 255,285 square miles which, for sake of comparison, is 8,359 square miles smaller than the state of Texas. Natural gas was first discovered in 1883 at the now abandoned Alderson well located some 15 miles southeast of the town of Princess. The first gas in commercial quantities was found at Medicine Hat in 1890. During the last 68 years, 187 localities have been discovered which are capable of gas production, and 73 per cent of these

have been found since 1945. Sixty fields currently are producing gas, including 22 non-associated gas accumulations.

Location of the oil and gas fields and prospects in the province of Alberta is shown in Fig. 1, together with a list of the localities of measurable gas, Fig. 1A.

The estimated total provincial gas reserve as of Jan. 1, 1952, for the 104 fields estimated, is 11.7 trillion cu ft proved and probable, and for the 187 known areas capable of production is in excess of 16 trillion cu ft on a total proved, probable, and possible basis. Five fields (Pincher Creek, Leduc-Woodbend, Viking-Kinsella, Cessford and Medicine Hat) are estimated to have recoverable reserves of more than one trillion cu ft each. A sixth field, Turner Valley, was initially in this group, but its reserves have been depleted substantially. Twenty-four fields, of which the above mentioned six fields are a part, have estimated gas reserves (including the possible category) in excess of 100 billion cu ft. These 24 fields account for 79 per cent of the total provincial reserves.

Comparative systemic analyses reflect that 56 per cent of Alberta's gas reserves are contained in sediments of Cretaceous age; 30 per cent in sediments of Mississippian age; 10 per cent in sediments of Devonian age; three per cent in sediments of Triassic age; and the remaining one per cent in Jurassic and Permo-Pennsylvanian sediments. It is expected that the relative importance of the Mississippian, Devonian, and Triassic sediments will be increased as exploration progresses.

GENERAL GEOLOGY

The western Canada basin comprises the sedimentary area between the Canadian Shield and the Rocky Mountain Front Range, the Arctic Ocean, and the International Boundary. The basin has an approximate area of 765,000 square miles and embraces parts of the provinces of Manitoba, Saskatchewan, Alberta, British Columbia and the Northwest Territories.

Generalized columnar sections for the Province of Alberta are shown in Fig. 2. Substantially all of Alberta, except its northeast corner, has sedimentary cover. Sediments of all the geologic systems are represented, except those of Silurian age.

References given at end of paper.

Manuscript received in the Petroleum Branch office Feb. 1, 1952.
Presented at the Annual Meeting of the AIME in New York City, 18-21, 1952.

Ordovician sediments are present only in the Rocky Mountain belt of Alberta and in the southeastern corner of the province. Great thicknesses of Tertiary sediments occupy parts of the Alberta syncline, but this interval represents a small portion of Tertiary time. Throughout about one-half of the province, in the north and east parts, Cretaceous sediments rest directly on Devonian rocks.^{1,2} The two principal overlapping rock units are of Cretaceous and Upper Devonian age. In a northeast-southwest line (normal to the regional strike) between the Foothills Belt and the Canadian Shield, Cretaceous sediments overlap progressively the stratigraphic section from Jurassic to pre-Cambrian. East of the Alberta syncline, the sediments of Jurassic through Mississippian thin to zero forming several wedge-out belts many hundreds of miles in length. Throughout some 20,000 square miles of the Peace River Ridge, Devonian rocks rest on the pre-Cambrian. Over the apical area of this ridge, high Upper Devonian sediments rest on pre-Cambrian, with successively older Devonian rocks developing flankward.

GEOLOGIC HISTORY

The sedimentary history of the Western Canada Basin has been discussed in considerable detail in a recent paper by J. B. Webb.³

The major portion of the clastic sediments composing the sedimentary section of the province of Alberta was derived from the west. During certain depositional periods these sediments were deposited relatively close to the present Rocky Mountains, while at other times the seas extended into Saskatchewan or beyond. A relatively small thickness of clastics present in eastern and central Alberta were derived from the Canadian Shield.

Lower and Middle Cambrian sediments accumulated in the Cordilleran geosyncline which later became the site of the present Rocky Mountains. Upper Cambrian time witnessed general submergence of the province and the usual succession of Upper Cambrian sediments, so characteristic of central North America, were deposited. From the end of the Cambrian to the beginning of the upper Devonian, Alberta was mostly emergent except for local deposits of Ordovician and the development of a deep Middle Devonian evaporite basin in the eastern portion of the province. During Upper Devonian time the presence of shallow seas over most of the central region of Alberta made possible the widespread growth of reefs.

Between the beginning of Upper Devonian and the beginning of Cretaceous time, the province of Alberta east of the Rocky Mountain Front Range was generally an area of subsidence in the Foothills Belt and was emergent throughout most of the rest of the province. Important exceptions were the accumulation of Devonian and Mississippian sediments in the southeastern portion and parts of the central portion of the province. Although sediments of Triassic age are present generally throughout the Foothills Belt, it is significant that in the isolated Peace River Basin great thicknesses of marine Triassic accumulated.

During all Cretaceous time, thick sediments were deposited in Alberta. Much of this was due to marine transgression but occasional continental deposits are in evidence, especially in the upper portion of the Blairmore. Climate favorable to deposition of coal and conditions favoring the presence of volcanic ash were widespread.

Thick Tertiary sediments accumulated in the Alberta syncline. These, however, represent only a small portion of Ter-

tiary time, and most of Alberta was emergent during the Cenozoic and continued erosion developed the physiographic features which characterize the present topography of the province.

The principal periods of orogeny were the Nevadan Revolution at the close of the Jurassic and the Laramide Revolution at the close of the Cretaceous which culminated in the development of the Rocky Mountains and the deepening of the Alberta syncline.

STRUCTURAL CHARACTER OF THE PROVINCE

The principal structural alignment of Alberta is northwest and southeast. Many of the local producing structures are superimposed on these regional folds and have a more north-south trend. The chief structural features are the Rocky Mountains, the folded and faulted Foothills Belt,^{4,5,6} the Alberta syncline, the Sweetgrass arch, the Alberta shelf, the Moose Jaw-Mackenzie syncline, and the Peace River Ridge.

The Alberta shelf, instead of being a single homocline appears to consist of a series of semi-parallel northwest-southeast regional anticlines and synclines of low relief which persist for long distances and develop shallow local closures. Some of the Devonian reefs are associated with these axes, and their orientation generally follows a structural pattern.

While many of the known tectonic features of Alberta have Paleozoic counterparts and result from several periods of recurrent movement, the principal orogeny took place in Nevadan and Laramide time. The Alberta shelf area is characterized by gentle folding, and no great subsurface structural features are known which are similar to those prevalent in the Mid-Continent area of the United States. The closest approach to such a feature is the Peace River Ridge.

RELATIVE IMPORTANCE OF RESERVOIR TYPES AND THEIR STRATIGRAPHIC DISTRIBUTION

Most of Alberta's oil and gas fields have been discovered so recently that it is still too early to name the controlling factor in reservoir traps and recovery mechanisms. Despite incomplete data, certain generalized trends suggest the relative importance of structural *vs* stratigraphic traps and depletion *vs* waterdrive recovery mechanisms of these gas accumulations.

Structurally controlled accumulations relatively uncomplicated by elements of stratigraphic trapping, are limited in number and distribution. The Madison reservoirs of the Foothills Belt are structurally controlled. The oil reservoirs in the Joseph Lake and Excelsior fields are localized by structural closure. A few of the basal Cretaceous and Viking gas-reservoirs of the Central and Southeastern Alberta Plains are structurally controlled.

Stratigraphically controlled reservoirs and composite reservoirs (both stratigraphically and structurally controlled) dominate the Central and Southeastern Alberta Plains. Typical examples of stratigraphic reservoirs are those in the Viking-Kinsella, Medicine Hat, and Pendant d'Oreille Fields, and

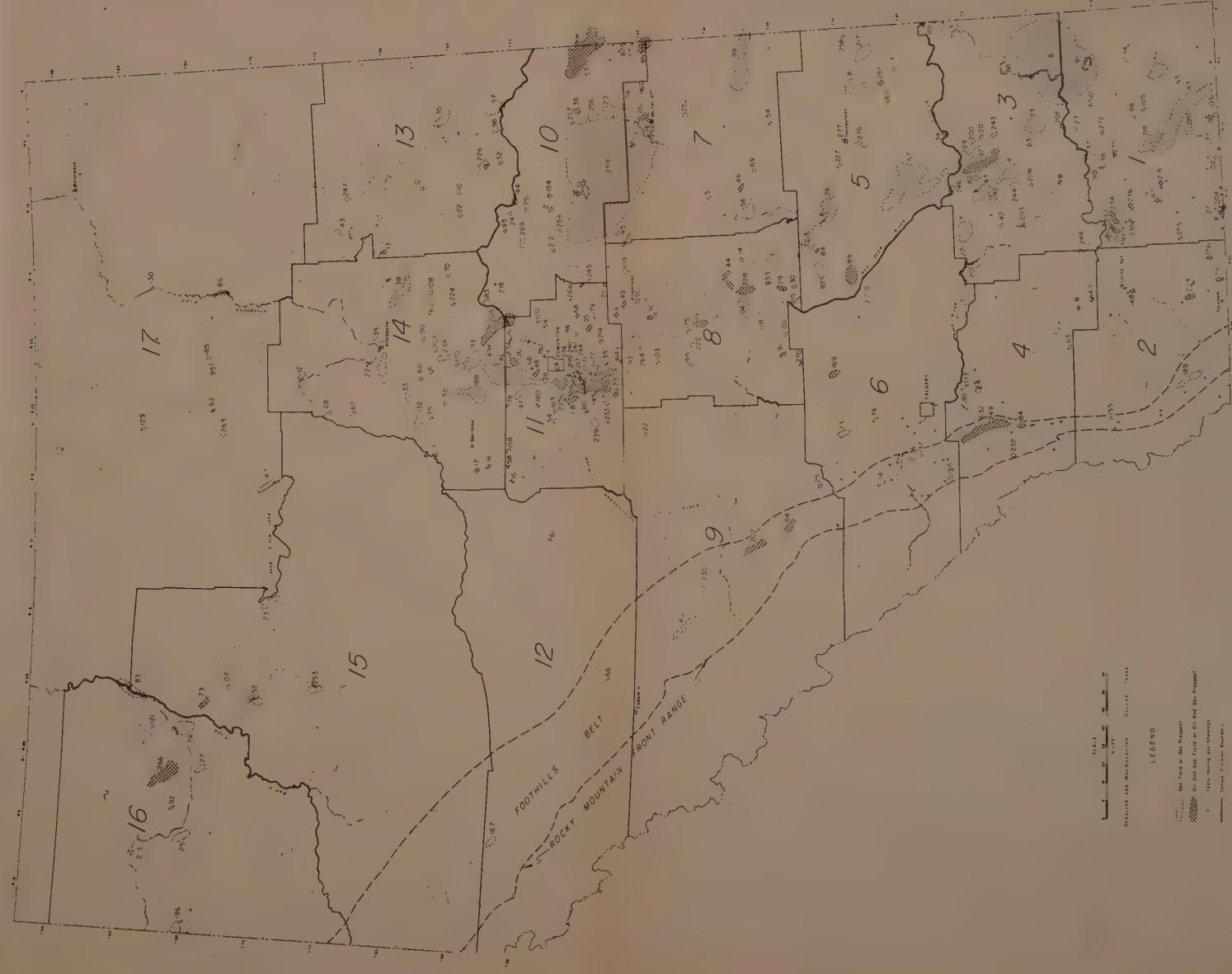


FIG. 1—MAP OF GAS AND OIL FIELDS AND PROSPECTS, PROVINCE OF ALBERTA, CANADA.

No.	County	Discovery Date	Field or Prospect Name	No. Drilling	Current Inventory	Field or Prospect Name	No. Drilling	Current Inventory	Field or Prospect Name
1	1930	1930	Albion	82	10	1930	1930	1930	1930
2	1930	1930	Albion	82	10	1930	1930	1930	1930
3	1930	1930	Albion	82	10	1930	1930	1930	1930
4	1930	1930	Albion	82	10	1930	1930	1930	1930
5	1930	1930	Albion	82	10	1930	1930	1930	1930
6	1930	1930	Albion	82	10	1930	1930	1930	1930
7	1930	1930	Albion	82	10	1930	1930	1930	1930
8	1930	1930	Albion	82	10	1930	1930	1930	1930
9	1930	1930	Albion	82	10	1930	1930	1930	1930
10	1930	1930	Albion	82	10	1930	1930	1930	1930
11	1930	1930	Albion	82	10	1930	1930	1930	1930
12	1930	1930	Albion	82	10	1930	1930	1930	1930
13	1930	1930	Albion	82	10	1930	1930	1930	1930
14	1930	1930	Albion	82	10	1930	1930	1930	1930
15	1930	1930	Albion	82	10	1930	1930	1930	1930
16	1930	1930	Albion	82	10	1930	1930	1930	1930
17	1930	1930	Albion	82	10	1930	1930	1930	1930
18	1930	1930	Albion	82	10	1930	1930	1930	1930
19	1930	1930	Albion	82	10	1930	1930	1930	1930
20	1930	1930	Albion	82	10	1930	1930	1930	1930
21	1930	1930	Albion	82	10	1930	1930	1930	1930
22	1930	1930	Albion	82	10	1930	1930	1930	1930
23	1930	1930	Albion	82	10	1930	1930	1930	1930
24	1930	1930	Albion	82	10	1930	1930	1930	1930
25	1930	1930	Albion	82	10	1930	1930	1930	1930
26	1930	1930	Albion	82	10	1930	1930	1930	1930
27	1930	1930	Albion	82	10	1930	1930	1930	1930
28	1930	1930	Albion	82	10	1930	1930	1930	1930
29	1930	1930	Albion	82	10	1930	1930	1930	1930
30	1930	1930	Albion	82	10	1930	1930	1930	1930
31	1930	1930	Albion	82	10	1930	1930	1930	1930
32	1930	1930	Albion	82	10	1930	1930	1930	1930
33	1930	1930	Albion	82	10	1930	1930	1930	1930
34	1930	1930	Albion	82	10	1930	1930	1930	1930
35	1930	1930	Albion	82	10	1930	1930	1930	1930
36	1930	1930	Albion	82	10	1930	1930	1930	1930
37	1930	1930	Albion	82	10	1930	1930	1930	1930
38	1930	1930	Albion	82	10	1930	1930	1930	1930
39	1930	1930	Albion	82	10	1930	1930	1930	1930
40	1930	1930	Albion	82	10	1930	1930	1930	1930
41	1930	1930	Albion	82	10	1930	1930	1930	1930
42	1930	1930	Albion	82	10	1930	1930	1930	1930
43	1930	1930	Albion	82	10	1930	1930	1930	1930
44	1930	1930	Albion	82	10	1930	1930	1930	1930
45	1930	1930	Albion	82	10	1930	1930	1930	1930
46	1930	1930	Albion	82	10	1930	1930	1930	1930
47	1930	1930	Albion	82	10	1930	1930	1930	1930
48	1930	1930	Albion	82	10	1930	1930	1930	1930
49	1930	1930	Albion	82	10	1930	1930	1930	1930
50	1930	1930	Albion	82	10	1930	1930	1930	1930
51	1930	1930	Albion	82	10	1930	1930	1930	1930
52	1930	1930	Albion	82	10	1930	1930	1930	1930
53	1930	1930	Albion	82	10	1930	1930	1930	1930
54	1930	1930	Albion	82	10	1930	1930	1930	1930
55	1930	1930	Albion	82	10	1930	1930	1930	1930
56	1930	1930	Albion	82	10	1930	1930	1930	1930
57	1930	1930	Albion	82	10	1930	1930	1930	1930
58	1930	1930	Albion	82	10	1930	1930	1930	1930
59	1930	1930	Albion	82	10	1930	1930	1930	1930
60	1930	1930	Albion	82	10	1930	1930	1930	1930

FIG. 1A—LIST OF GAS AND OIL FIELDS AND PROSPECTS AS OF AUG. 1, 1951. PROVINCE OF ALBERTA, CANADA.

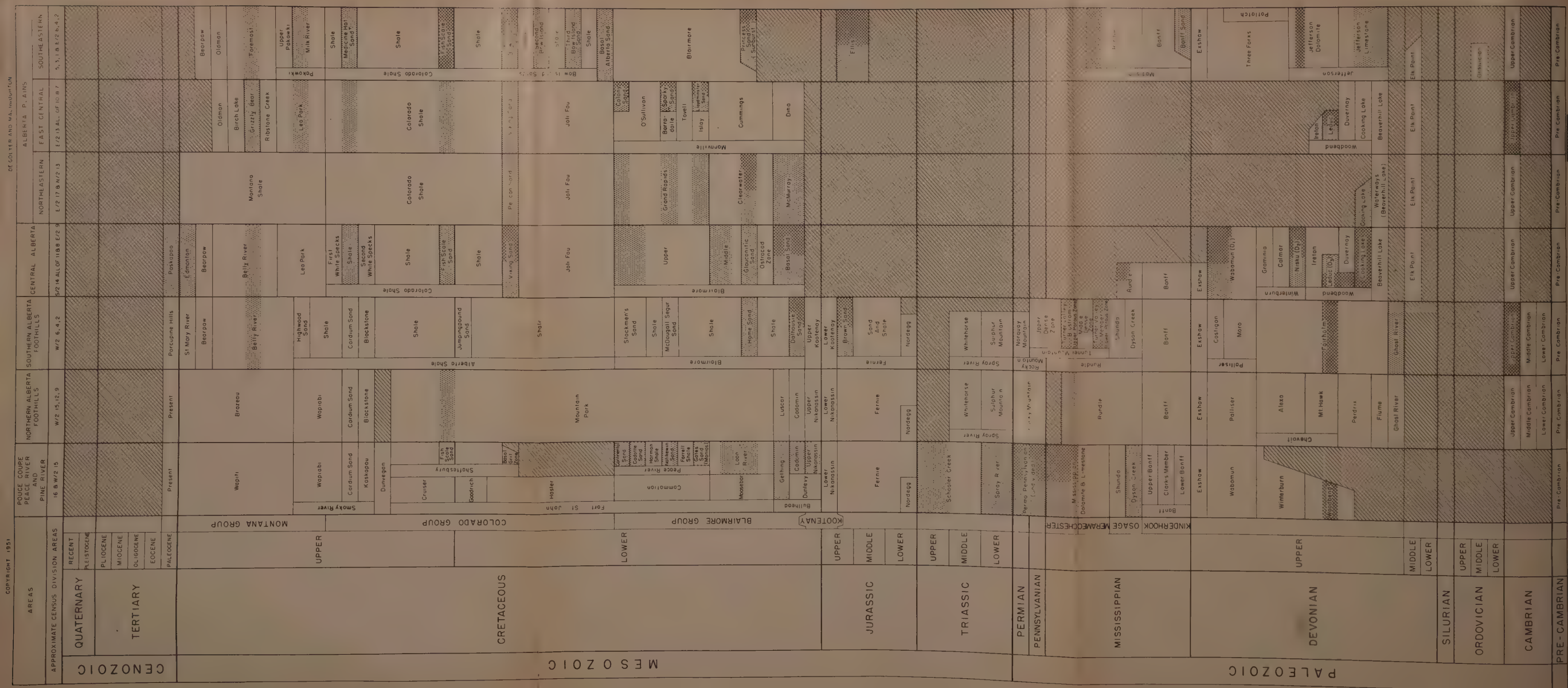


FIG. 2 - GENERALIZED COLUMNAR STRATIGRAPHY, PROVINCE OF ALBERTA

the biohermal reef oil accumulations. Type examples of composite reservoirs appear to be those in the Cessford and Legal-Morinville Fields, and the biostromal reef oil accumulations.

Available data suggest that composite reservoirs are the most numerous, but it is possible that such a conclusion is more apparent than real because of insufficient data to determine the dominant control. This is particularly true of the newly discovered gas accumulations in the Peace River area.

In a broad generalization, the Devonian Leduc (D₁) reservoirs are stratigraphically controlled and Nisku (D₂) reservoirs are composite in nature. Mississippian reservoirs are dominated by structure. The Permo-Pennsylvanian, Triassic, and Jurassic reservoirs are composite, with likelihood of dominant stratigraphic control. The Cretaceous reservoirs are composite, but most of the major gas accumulations seem to be dominated by at least some type of stratigraphic variation.

Certain broad generalizations can be made with respect to the stratigraphic distribution of the recovery mechanisms of the various major gas accumulations in Alberta. The Devonian reservoirs appear to show appreciable evidence of some degree of waterdrive, but the Mississippian reservoirs probably will not have appreciable waterdrive. The Cretaceous accumulations are dominated by the depletion type recovery mechanism borne out by experience to date.

HISTORY OF DEVELOPMENT

The initial discovery of gas in the province of Alberta was the Alderson well in 1883. The first commercial gas field was found at Medicine Hat in 1890, and the first commercial oil well was completed in Turner Valley in 1914. During the 3 years, between 1883 and 1952, drilling has developed meas-

Table I—Number of Oil and Gas Fields and Prospects Completed Annually in the Province of Alberta Between 1883 and 1952

Discovery Year	No. Completed	Name of Principal Discovery	Discovery Year	No. Completed	Name of Principal Discovery
1883	1	Alderson	1935	2	
1890	1	Medicine Hat	1936	1	
1897	1		1937	3	
1909	1	Bow Island	1938	1	
1910	1	Brooks	1939	4	Steveville
1913	4		1940	4	Princess
1914	5	Turner Valley*	1941	1	
		Viking-Kinsella	1942	4	
1916	3	Peace River	1943	2	
1917	2		1944	6	Jumping Pound
1918	1		1945	7	
1920	1		1946	14	Pendant d'Oreille
1923	3	Foremost	1947	17	Leduc-Woodbend
1924	1		1948	17	Pincher Creek
1925	2				Redwater
1926	2				
1927	3		1949	53	Cessford
1928	4				Golden Spike
1929	3		1950	57	Acheson
1930	3				Whitelaw
1932	4		1951	74	Bonnie Glen
1933	2				Hamelin Creek
1934	1	Lloydminster			Wizard Lake
TOTAL 316					

* Mesozoic oil was discovered in Turner Valley in 1914. The Turner Valley Madison gas cap was discovered in 1924, and the Madison oil band in 1936.

Table II—Classification of Fields and Prospects by Types of Gas as of Jan. 1, 1952

	Proved	Semi-Proved	Others	Total
Non-Associated				
Producing	22			
Shut-in	39			
Potential	35			
Prospect	34			
Limited Prospect		101		
Farm Wells			6	
Gas Storage			1	
Abandoned			4	
Subtotal	130	101	11	242
Associated and Dissolved				
Producing	41			
Shut-in	11			
Potential	4			
Prospect	1			
Limited Prospect		12		
Abandoned			5	
Subtotal	57	12	5	74
GRAND TOTAL	187	113	16	316

Notes:

Potential, refers to fields with gas zones cased off pending development of markets for the gas.

Prospect, refers to areas in which testing has established the presence of measurable gas in quantity, but all test wells were abandoned.

Limited Prospect, refers to an area in which testing has established some measurable gas, but the occurrence is apparently subcommercial to date.

urable gas volumes in at least 316 localities. As reflected by Table I, only 27 per cent of these localities can be credited to the first 62 years of development. With the discovery of the Leduc-Woodbend Field in the 64th year, 1947, competitive drilling was so accelerated that 70 per cent of Alberta's discoveries have been made since 1947. Even more significant, 58 per cent have been found in the last three years, and, due in part to the activity resulting from applications for permits to export gas from Alberta, 24 per cent were found during 1951.

Table II illustrates that 77 per cent of the localities showing measurable volumes of gas appear to be non-associated in character and only 23 per cent associated with oil accumulation. While Alberta has only 22 producing non-associated gas fields and 41 producing oil fields which contain associated and/or dissolved gas reserves, it is significant that 187 localities, or 60 per cent, are presently capable of gas production if a pipeline outlet were available. In addition, there are 113 limited gas prospects (*i.e.*, localities in which measurable gas has been found but the test wells have been abandoned because the small amount of gas developed has only local or farm use) which, with future drilling, might yield commercial volumes of gas.

Table III indicates that gas has been found in 29 reservoirs of different stratigraphic age. Of the presently known reservoirs in the province, 63 per cent are found in sediments of Cretaceous age, and 17 per cent in Devonian sediments. A commercially significant feature of the future of Alberta gas production is the wide distribution of its gas reservoirs throughout the geologic column.

Finally, it is important to note that the majority of these 316 localities of measurable gas have been discovered incidental to the search for oil. Since permission to remove gas from the province in long distance transmission lines has yet to be granted, there is little incentive to develop gas reserves beyond a point sufficient to serve the existing local gas demand. When, and if, permission to export gas is given, and wells are drilled in search of gas, the rate of gas discovery should accelerate, and areas where gas has been discovered will be

Table III — Summary List of Fields and Prospects in the Province of Alberta

Classified According to Their Respective Reservoirs and Arranged in Approximate Stratigraphic Order as of Jan. 1, 1952

Reservoirs	No. of Fields or Prospects Showing Measurable Gas in Each Reservoir
Cretaceous	220
Upper Cretaceous	20
1. Upper Cretaceous sand (Undivided)	1
2. Paskapoo sand	2
3. Edmonton sand	2
4. Belly River sand	10
5. Lea Park-Pakowki sand	3
6. Milk River sands	8
7. Medicine Hat sands	2
8. Colorado sands	9
9. Cardium sand	1
10. Fish Scale sand	1
Lower Cretaceous	200
11. Lower Cretaceous sands (Undivided)	22
12. Pelican-Viking-Bow Island sands	132
13. Basal Alberta sand	8
14. Blairmore-Grand Rapids sands	165
15. Nikanassin sands	13
Jurassic	14
Triassic	5
Permo-Pennsylvanian	5
Mississippian	43
19. Mississippian Dolomite (Undivided)	3
20. Chester Dolomite	2
21. Madison-Rundle Dolomite	38
Devonian	60
22. Devonian Dolomite (Undivided)	4
23. Wabamum (D ₁) Dolomite	19
24. Nisku (D ₂)-Jefferson Dolomite	31
25. Leduc (D ₃) Dolomite	17
26. Cooking Lake Dolomite	6
27. Beaverhill Lake Dolomite	1
28. Ghost River Dolomite and sand	3
Cambrian	2

re-activated. This has been the experience of the oil and gas industry in other areas which have been actively explored to meet an increasing market demand.

NATURAL GAS RESERVES

Estimation of Reserves

The reserve estimates presented were calculated using the volumetric and/or pressure decline methods, depending upon the suitability of the available data.

Wherever possible, all pertinent wells and reservoir data, including drillers' logs, sample logs, core analyses and core descriptions, electrical and gamma ray-neutron logs, drill stem tests, flow tests, pressure and production histories, and reservoir fluid analyses, were used in preparing the estimates. Structural maps, isopachous and/or isobaric maps, and cross sections were utilized in determining the areal extent and volume of the reservoirs in the great majority of the fields considered.

These basic geological and engineering data served as bases for exercising judgment in appraising both the extent of reservoirs and the economic recovery of gas from such reservoirs.

The reduction of the volumes of gas in place to recoverable reserves available for sale at the wellhead was carefully considered, both with respect to reservoir losses and to surface losses. Reference is made to "remaining gas in place at terminal pressure, or at terminal conditions" in preference to "abandonment pressure" in view of the profound effect of economic years hence, upon the actual abandonment pressure.

Considerable volumes of gas will be produced from all the reservoirs after the terminal conditions are reached, some for long distance transportation, but largely for local uses.

Surface losses, primarily field and fuel uses, including fuel for compression and shrinkage, have been deducted in arriving at the estimated recoverable gas available for sale. Actual physical waste of gas probably will become an almost negligible quantity in future years when the value of natural gas is realized fully and is reflected in adequate wellhead price.

Classification of Reserves

Reserve estimates have been classified in three categories according to the quality of the reserves, the limitations of the data, and the assumptions made from those data in arriving at the estimates. In many instances, it is not possible to segregate reserves into these classifications with equal reasoning because of the wide variations in the types of structures, reservoirs, and in the basic data. The equality with which these divisions are made, therefore becomes subject primarily to the judgment of the appraiser.

Proved Reserves—Reserves proved for oil or gas production in a given reservoir by actual well tests, either in the cased hole or by definitive open hole drill stem tests, are classified as proved reserves. These reserves are defined areally by reasonable geological interpretation of structure and known continuity of oil and/or gas-saturated reservoir material above limiting water saturation.

Probable Reserves—These reserves, considered as essentially proved or capable of being proved, are defined by less direct well control but are based again upon evidence of producible gas or oil within the limits of a structure or reservoir above inferred or known water saturation.

Possible Reserves—This category is similarly determined but may be based largely upon electrical log interpretation or widespread evidence of commercial gas saturation defined by widely spaced test wells. It may also include areas of geological physical anomaly that are immediately adjacent to proved productive areas of like geophysical character.

Tabulation of Natural Gas Reserves

There are 24 major fields in Alberta, each of which has a recoverable reserve in excess of 100 billion cu ft of gas, on a proved, probable, and possible basis. These 24 fields account for 79 per cent of the total provincial gas reserve, which means that the major reserves as now known are concentrated in seven per cent of the 316 localities of measurable gas. Only six fields had initially recoverable reserves in excess of one trillion cu ft. Pertinent data on these six fields are as follows:

Field	Discovery Date	Principal Reservoir	Approx. No. of Wells Drilled in Field	Estimated Initially Recoverable Gas to Terminal Pressure (Proved and Probable) (MMcf)
Pincher Creek	1948	Mississippian	5	2,204,729
Turner Valley	1914	Mississippian	620	2,130,055
Leduc-Woodbend	1947	Devonian	925	1,349,322
Medicine Hat	1890	Upper Cretaceous	120	1,127,477
Cessford	1949	Lower Cretaceous	25	1,092,667
Viking-Kinsella	1914	Lower Cretaceous	160	1,015,217

Table IV summarizes the natural gas reserves of the province of Alberta, Canada, as of Jan. 1, 1952, in categories of estimated recoverable gas reserves to terminal pressure and estimated gas available for sale. The estimated proved and probable recoverable reserve of the 104 fields studied is 1,687,14 million cu ft and the volume of gas available for sale from these fields is 9,440,283 million cu ft after deduction of approximately 30 per cent of the recoverable gas for surface losses and field or pipeline uses. A tentative estimate for the total provincial proved, probable, and possible recoverable gas reserve of the 187 localities capable of gas production is 5,146,835 million cu ft.

PRODUCING REGIONS

The following discussion of producing regions is grouped to four areas, namely, the Foothills Belt, the Central Alberta Plains, the Southeastern Alberta Plains, and the Peace River area. Examples of type fields are discussed for each area. Their descriptions include a short historical account, major details of structure, and type of productive reservoir.

Alberta Foothills Belt

The discovery, in 1924, of large volumes of Rundle gas in the Turner Valley Field gave rise to exploratory drilling programs in the Foothills Belt. The search for oil and gas has varied in intensity because of high exploration costs resulting from rugged terrain and depth to prospective pay zones.

Large accumulations of non-associated gas have been found in Pincher Creek and Jumping Pound. It seems reasonable that there should be other accumulations on known structures in the Foothills. Recently, a drilling program has been commenced at Winchell Coulee, and the Sullivan Creek and Brazeau prospects have been reactivated. The Brazeau structure contains a known commercial gas accumulation in Lower Cretaceous sands and in the Madison limestone, and two wells drilled over a decade ago reported flows up to 10 million cu ft of gas per day.

These folded and overthrust fault structures of the Foothills Belt are large elongated structures paralleling the Front Range of the Rocky Mountains. They represent an area in which there are possibilities of large, high pressure gas accumulations. Additional exploratory drilling should add major reserves to the province.

Pincher Creek Field

The Pincher Creek structure is a representative Foothills field since it is a strongly asymmetric fold of the Rundle formation in a complex of thrust sheets. The discovery resulted from highly competent geological and geophysical work by the staff of Canadian Gulf Oil Co. The extremities of the structure are not well defined and may extend beyond the limits as currently estimated. The eastern limit of the field is a low angle thrust fault and the western limit is a gas-water contact at an estimated subsea elevation of 8,200 ft. The estimated gas reserve recoverable to a terminal reservoir pressure of 700 psia is 2,292,465 million cu ft, representing 1,543,310 million cu ft of gas available for sale after deduction of estimated field and fuel uses and shrinkage losses.

Central Alberta Plains

Accumulations of natural gas in the Central Plains of Alberta are of the non-associated, associated, and dissolved types. Gas occurs in Lower Cretaceous sands and Devonian carbonates over a large area, ranging from Edmonton on the west to the border of Saskatchewan on the east, and from Lac la Biche on the north to the vicinity of Drumheller and Hanna on the south.

The development and growth of great coral reefs in the Upper Devonian account for a considerable number of these gas accumulations. Their development was accompanied by rapid lateral facies changes. The reefs are normally at least 1,000 ft in thickness and frequently contain water almost to their tops. Throughout the Central Plains, Upper Devonian is generally overlain by Lower Cretaceous.

Major oil discoveries in the Devonian Nisku (D_2) and Leduc (D_3) carbonates account for a large portion of the natural gas reserves in this area. Most of the Devonian and Lower Cretaceous accumulations are due to combined stratigraphic and structural conditions.

Leduc-Woodbend Field

In 1947 Imperial Oil Co. drilled a seismic anomaly at Leduc as a part of a regional stratigraphic test exploratory program. Originally scheduled as a deep pre-Cambrian test, it unexpectedly found oil in Nisku (D_2) dolomite, and it became the first commercial Devonian oil completion in the central part of the province. A second well successfully established the presence of biohermal reef oil in the subjacent Leduc (D_3) dolomite. Together these became the most important completions since the discovery of the Rundle reservoir in the Turner Valley Field in 1924, and was the beginning of Alberta's increasing importance as an oil and gas province. Their drilling initiated the development of what is now the Leduc-Woodbend Field which includes some 925 wells. The reef has been completely penetrated, and one deep test ends in Elk Point evaporites of Middle Devonian age. In addition to Devonian oil, a large Lower Cretaceous non-associated gas reserve has been established.

The Leduc-Woodbend Field is a large biohermal reef over which superjacent Devonian and Cretaceous sediments have been arched. Regional dip is to the southwest, and the apex of the structure lies almost at its northeast end. The gas-water interfaces in the Cretaceous sands rise to the northeast, while the Devonian water tables essentially are flat.

The Viking sand of Lower Cretaceous age has one producing gas well. Normally, drill stem tests are not taken in the Viking sand, but the few which do exist illustrate that this reservoir is capable of limited commercial gas production throughout the structurally higher portions of the field.

The Blairmore sands in the Leduc-Woodbend Field have multiple gas pays. More than 100 drill stem tests reflect daily gas volumes ranging from 1 to 10 million cu ft. The principal gas reservoir occurs in the Basal Cretaceous sand. One Lower Cretaceous sand in the Woodbend area of the field contains oil, but the area of oil saturation is limited.

An occasional drill stem test is taken in the Wabamun (D_1) dolomite and a few of these demonstrate appreciable volumes of oil and gas, but no test has been commercially successful. The Nisku (D_2) dolomite, primarily an oil zone, contains the major dissolved gas reserve in the province. The northeast

Table IV—Summary of Natural Gas Reserves in the Province of Alberta, Canada, as of Jan. 1, 1952
(All Gas Volumes in MMcf at Base Pressure of 14.4 psia and 60°F)

Field Name (1)	Census Division (2)	Discovery Date (3)	Reservoir (4)	Depth (5)	Type of Gas (6)	Estimated Recoverable Reserves		Est. Gas Available for Sale (9)
						Proved and Probable (7)	Proved Probable and Possible (8)	
Pincher Creek	2	1948	Rundle Limestone	11,700	Non-Associated	2,204,115	2,291,850	1,542,880
Leduc-Woodbend	11	1947	Viking Sand	3,450	Non-Associated	6,888	18,083	6,372
		1947	Upper Blairmore Sands	3,800	Non-Associated	8,828	24,758	8,153
		1948	Lower Blairmore Sands	4,000	Associated
		1948	Lower Blairmore Sands	4,000	Dissolved
		1947	Lower Blairmore (Composite Sands)	4,200	Non-Associated	333,161	391,705	305,452
		1951	Wabamun (D ₁) Dolomite	4,540	Dissolved
		1947	Nisku (D ₂) Dolomite	5,000	Dissolved	286,760	299,677	229,408
		1947	Leduc (D ₃) Dolomite	5,250	Associated	583,480	583,480	438,480
		1947	Leduc (D ₃) Dolomite	5,400	Dissolved	107,455	107,455	85,964
Total						1,326,572	1,425,158	1,073,829
Cessford	5	1949	Viking Sand	2,800	Non-Associated	128,006	222,139	118,579
		1949	Upper Blairmore Sand	3,100	Non-Associated	594,073	670,325	550,989
		1950	Second Blairmore (Stray Sand)	2,910	Non-Associated	8,928	18,026	8,267
		1949	Princess (Sunburst) Sand	3,460	Non-Associated	361,660	418,602	313,901
		1951	Princess (Sunburst) Sand	3,350	Associated
		1951	Princess (Sunburst) Sand	3,356	Dissolved
Total						1,092,667	1,329,092	991,736
Medicine Hat	3	1890	Milk River Sand	800	Non-Associated
		1908	Medicine Hat Sand	1,075	Non-Associated	1,023,167	1,179,303	818,534
		1926	Bow Islands Sands	2,350	Non-Associated
		1926	Blairmore Sand	2,700	Non-Associated
		1926	Blairmore Sand	2,925	Non-Associated
		1926	Ellis Limestone	3,075	Dissolved
Total						1,023,167	1,179,303	818,534
Viking-Kinsella	10	1914	Viking Sand	2,100	Non-Associated	844,301	1,093,363	726,099
Jumping Pound	6	1944	Rundle Limestone	10,100	Non-Associated	715,860	849,193	536,895
Whitelaw	16	1950	Upper Nikanassin Sand	2,800	Non-Associated	179,291	203,363	166,712
		1950	Upper Triassic Sand	3,300	Non-Associated	408,512	420,367	379,555
		1950	Lower Triassic Sand	3,650	Non-Associated	11,289	15,984	10,454
		1950	Permo-Pennsylvanian Dolomite	3,880	Dissolved
Total						599,092	639,714	556,721
Turner Valley	4	1914	Mesozoic Sands	2,200	Non-Associated
		1914	Mesozoic Sands	to	Associated
		1914	Mesozoic Sands	5,500	Dissolved
		1924	Rundle Limestone	3,800	Associated	325,671	325,671
		1936	Rundle Limestone	9,150	Dissolved	228,420	228,420
Total						554,091	554,091	343,536
Princess	3	1940	Bow Island Sands	2,450	Non-Associated	10,485	189,267	9,721
		1945	Basal Alberta Sand	2,850	Non-Associated	117,809	146,957	109,023
		1940	Princess (Sunburst) Sand	3,250	Non-Associated	103,682	124,639	96,100
		1947	Madison Limestone	3,300	Associated	27,770	34,253	21,383
		1940	Madison Limestone	3,330	Dissolved
		1948	Jefferson Dolomite	3,930	Associated	23,297	23,297	17,939
		1944	Jefferson Dolomite	3,960	Dissolved
		1947	Cooking Lake Dolomite	4,845	Non-Associated
		1940	Beaverhill Lake Dolomite	5,130	Non-Associated
Total						283,043	518,413	254,166
Legal-Morinville	14	1947	Viking Sand	2,700	Non-Associated	21,480	26,317	19,688
		1947	Upper Blairmore Sand	2,965	Non-Associated
		1948	Blairmore Glauconitic Sand	3,380	Non-Associated	317,863	356,836	294,411
		1947	Basal Blairmore Sands	3,500	Non-Associated
		1949	Basal Blairmore Sand	3,670	Dissolved
Total						339,343	383,153	314,099
Pendant d'Oreille	1	1946	Bow Island Sands	2,100	Non-Associated	329,746	329,746	322,600
Provost	7	1946	Viking Sand	2,350	Non-Associated	123,837	151,523	113,167
		1946	Upper Blairmore Sand	2,450	Non-Associated	14,606	87,974	13,303
Total						138,443	239,497	126,470
Golden Spike	11	1949	Viking Sand	3,560	Non-Associated	2,986	5,054	2,759
		1949	Basal Blairmore "A" Sand	4,300	Non-Associated	24,198	28,675	22,357
		1949	Basal Blairmore "B" Sand	4,400	Non-Associated	14,742	28,600	13,637
		1949	Wabamun (D ₁) Dolomite	4,500	Associated	25,048	27,005	22,293
		1951	Wabamun (D ₁) Dolomite	4,600	Dissolved
		1950	Nisku (D ₂) Dolomite	5,000	Dissolved	10,463	10,463
		1949	Leduc (D ₃) Dolomite	5,350	Dissolved	118,221	118,221
		1949	Cooking Lake	5,900	Dissolved	13,564	13,564
Total						209,222	231,582	61,046

Table IV — (Continued)

Field Name (1)	Census Division (2)	Discovery Date (3)	Reservoir (4)	Depth (5)	Type of Gas (6)	Estimated Recoverable Reserves		Est. Gas Available for Sale (9)
						Proved and Probable (7)	Proved Probable and Possible (8)	
North Tarent	16	1951	Upper Peace River Sand	1,150	Non-Associated	26,644	33,486	24,721
		1950	Upper Nikanassin Sand	2,405	Non-Associated	75,528	100,623	70,091
		1951	Triassic Sand	2,840	Non-Associated	89,686	95,791	83,248
Total						191,858	229,900	178,060
ooks Northeast	3	1948	Bow Island Sands	2,580	Non-Associated	18,560	74,815	17,261
		1948	Basal Alberta Sand	2,900	Non-Associated	67,970	90,192	63,212
		1946	Princess (Sunburst) Sand	3,265	Non-Associated	14,064	56,080	13,080
Total						100,594	221,087	93,553
anna	5	1949	Viking Sand	3,195	Non-Associated	22,054	83,069	20,391
		1949	Princess (Sunburst) Sand	3,720	Non-Associated	1,006	21,097	906
		1947	Madison Limestone	3,770	Non-Associated	19,031	57,018	17,047
Total						42,091	161,184	38,344
veville	3	1939	Bow Island Sand	2,500	Non-Associated	15,048	82,849	13,980
		1939	Basal Alberta Sand	2,750	Non-Associated	14,374	52,839	13,268
		1939	Princess (Sunburst) Sand	3,050	Non-Associated	12,573	21,907	11,620
Total						41,995	157,595	38,868
cheson	11	1950	Viking Sand	3,300	Non-Associated	17,027	20,390	15,821
		1950	Blairmore Glauconitic Sand	3,800	Non-Associated	7,965	59,229	7,363
		1950	Basal Blairmore Sand	4,000	Non-Associated	30,266	54,292	28,102
		1950	Basal Blairmore Sand	3,960	Dissolved
		1951	Wabamun (D ₁) Dolomite	4,320	Non-Associated
		1950	Nisku (D ₂) Dolomite	4,700	Dissolved	1,322	1,322	925
		1950	Leduc (D ₃) Dolomite	5,000	Dissolved	12,171	12,171	8,520
Total						68,751	147,404	60,731
yle-Mustang- Amisk Lake	14	1949	Pelican Sand	1,385	Non-Associated
		1949	Upper Grand Rapids Sand	1,610	Non-Associated	25,812	65,092	23,945
		1951	Middle Grand Rapids Sand	1,810	Non-Associated	8,256	15,151	7,626
		1951	Lower Grand Rapids Sand	1,890	Non-Associated	20,692	38,413	18,934
		1949	McMurray Sand	1,940	Non-Associated	7,500	10,744	6,960
		1949	Nisku (D ₂) Dolomite	2,040	Non-Associated	11,626	16,171	10,716
Total						73,886	145,571	68,181
bbald	5	1950	Viking Sand	2,580	Non-Associated	54,808	138,693	50,759
		1950	Banff Sand	3,000	Non-Associated
Total						54,808	138,693	50,759
stor	7	1914	Belly River Sand	1,430	Non-Associated
		1949	Viking Sand	3,140	Non-Associated	55,792	61,074	51,547
		1949	Lower Blairmore Sand	3,470	Non-Associated	63,014	73,161	58,371
		1950	Basal Blairmore Sand	3,550	Non-Associated	1,116	1,503	1,015
Total						119,922	135,738	110,933
untess	3	1950	Bow Island Sand	2,950	Non-Associated	77,599	87,130	72,022
		1950	Bow Island Sands	3,050	Non-Associated	25,369	28,380	23,503
Total						102,968	115,510	95,525
dwater	14	1949	Viking Sand	1,950	Non-Associated	15,943	17,755	15,315
		1948	Upper Blairmore Sand	2,100	Non-Associated
		1949	Middle Blairmore Sand	2,250	Non-Associated
		1948	Blairmore Glauconitic Sand	2,400	Non-Associated	2,615	4,149	2,463
		1948	Basal Blairmore Sand	2,550	Non-Associated
		1948	Leduc (D ₃) Limestone	3,100	Dissolved	84,735	84,735	4,237
Total						103,293	106,639	22,015
nyberries	1	1947	Bow Island Sands	2,600	Non-Associated	107,443	107,443	105,176
TOTAL RESERVE ESTIMATE FOR 24 MAJOR FIELDS						10,667,271	12,730,919	8,530,756
TOTAL RESERVE ESTIMATE FOR 80 MINOR FIELDS AND PROSPECTS						1,019,843	1,715,916	909,527
TOTAL — (104 Fields and Prospects)						11,687,114	14,446,835	9,440,283
NTANTATIVE RESERVE ESTIMATE FOR 83 ADDITIONAL LOCALITIES						1,700,000
RAND TOTAL EST. PROVINCIAL RESERVES (187 Localities Capable of Gas Production)						11,687,114	16,146,835	9,440,283
SUBDIVISION OF RESERVES BY TYPE OF GAS (24 MAJOR FIELDS)								
ON-ASSOCIATED GAS RESERVES						8,818,894	10,861,185	7,358,071
SOCIATED GAS RESERVES						985,266	993,706	702,011
SSOLVED GAS RESERVES						863,111	876,028	470,674
TOTAL GAS RESERVES						10,667,271	12,730,919	8,530,756

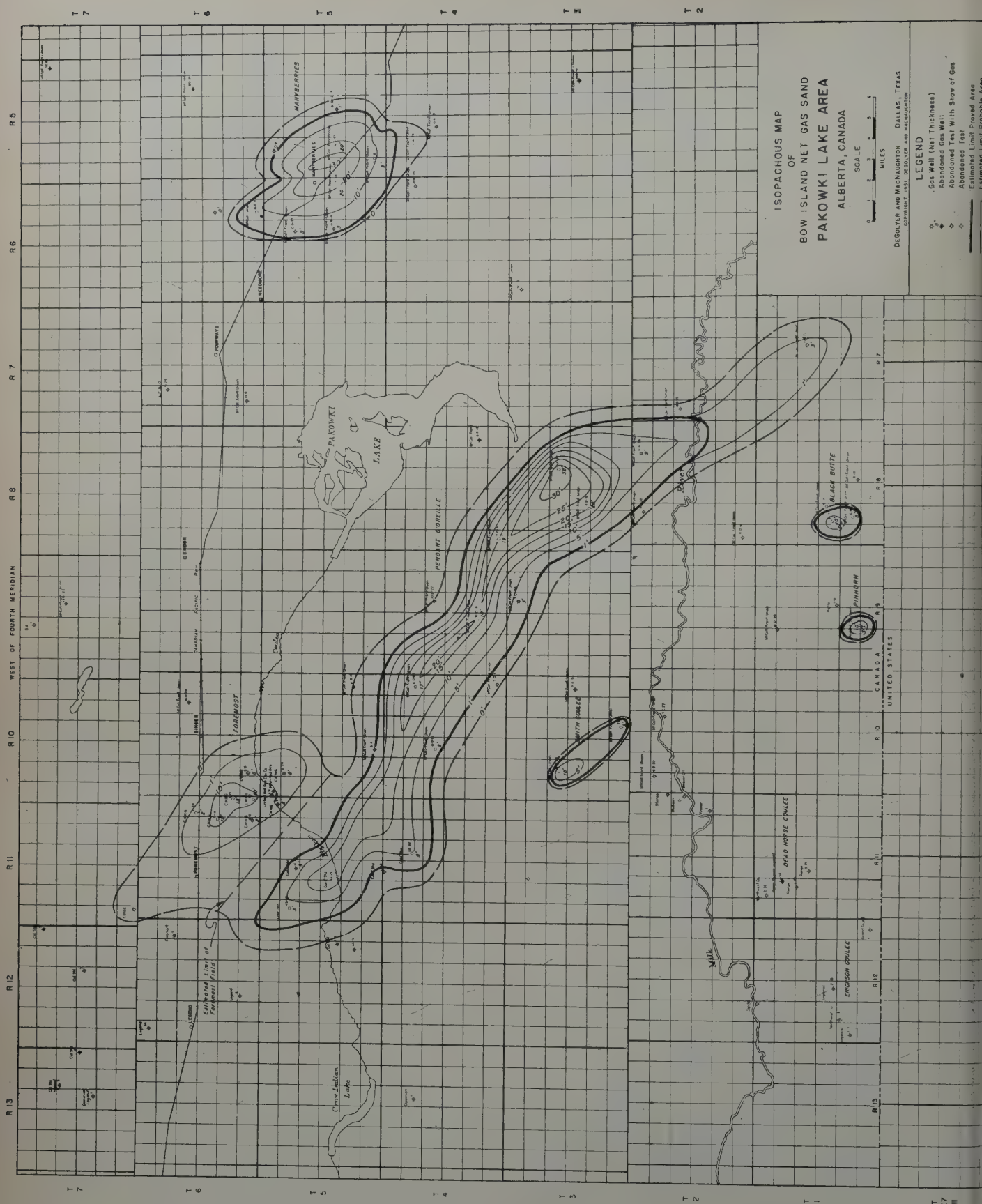


FIG. 3 — ISOPACHOUS MAP OF BOW ISLAND NET GAS SAND, PAKOWKI LAKE AREA, ALBERTA, CANADA.

productive limit of the Nisku (D_2) reservoir is defined by a permeability pinchout caused by a change of facies from dolomite to anhydrite. The largest accumulation of Devonian gas discovered in the province occurs in the Leduc (D_3) dolomite. Its gas cap has an approximate area of 14,000 acres and an average gross thickness of 65 ft. An additional large reserve of dissolved gas is contained in the oil accumulation.

Viking-Kinsella Field

The Viking-Kinsella Field is located about 80 miles east and slightly south of the city of Edmonton. This field was discovered in 1914 and produces non-associated gas from the Viking sand of Lower Cretaceous age found at an average depth of 2,100 ft. The Viking is a blanket sand, containing approximately 497,000 acres within the proved limits. Lack of permeability and/or local pinching out of the sand updip, to the east of the proved limits, results in a stratigraphic trap. The Viking-Kinsella Field is the principal gas supply field of Northwest Utilities Limited. This company furnishes gas to the Edmonton area.

Southeastern Alberta Plains

The majority of the natural gas accumulations in the Southeastern Plains occur in Lower Cretaceous sands. The area included extends from north of the Cessford Field south to the international border, and from the Foothills Belt eastward to the Alberta-Saskatchewan boundary.

In the Southeastern Plains Lower Cretaceous rocks lie unconformably on Mississippian beds which are in turn conformable on Upper Devonian. Severe eastward truncation of Mississippian beds caused an irregular topography, and this relief is commonly several hundred feet. Deposition of Lower Cretaceous sands on this irregular Mississippian erosional surface is at times a controlling factor in the formation of Lower Cretaceous structures, modified by gentle post-Cretaceous arching along pre-Cretaceous axes of folding. This type of deposition often results in loss of porosity and permeability.

Cessford Field

Cessford Field is the third most important non-associated gas accumulation in the province. Commercial quantities of gas in the Viking, Blairmore, and Princess (Sunburst) sands of Lower Cretaceous age have been tested over an area of some 6 miles by 15 miles.

Gas accumulations in general are associated with structural closure but the dominating control is stratigraphic. Three regional northwest southeast parallel anticlinal axes, plunging northwestward, pass through the field. Local closures are separated by saddles.

The discovery well was drilled in 1949 in the Sunnynook portion of the field by Amerada Petroleum Corp. and Stanolind Oil and Gas Co. In the fall of 1950 Canadian Delhi Oil Limited and Hudson's Bay Oil Co. Limited began a drilling program south of this discovery. Subsequent development has lined these two areas of gas production and some 25 wells have been drilled, of which 15 produce gas.

The Sunnynook area offers the more favorable possibilities for commercial accumulations of gas in the Viking sand. While a few measurable flows of Viking gas have been found in the

southern portion of the field, no wells have been completed, presumably due to high connate water content and low permeability. A deep structural saddle separates the Sunnynook area from the remaining portion of the field and this may have contributed to a difference in sand quality and hence a lack of commercial gas saturation in the southern portion of the field.

The principal gas reserve occurs in the Blairmore sand. Porosity pinch-outs to the east and to the west, limit the productive area. The gas-water interface is tilted upward to the southeast, in the direction of the major axis, and also rises slightly toward the porosity pinch-out at the eastern limit of the field. The gas-water interface is considerably lower in the Sunnynook area. A deep and nonproductive saddle separates the Blairmore gas production of the northern and southern portions of the field.

The Princess (Sunburst) sand occurs some 40 ft above the Paleozoic erosional surface, and structural mapping indicates increased closure on this horizon. A reasonably well defined porosity pinch-out has been established at the southern limit of the field by several nonproductive Princess sand tests. In the Sunnynook portion of the field there is no appreciable variation in porosity.

Pakowki Lake Gas Area

The Pakowki Lake area lies in the extreme southeastern portion of the province of Alberta and includes the Pendant d'Oreille, Foremost, Manyberries, Smith Coulee, Black Butte, and Pinhorn Fields. Exploratory drilling which began in 1923 has proved considerable reserves of natural gas. Isopachous maps of the fields in the Pakowki Lake area are shown in Fig. 3.

The major field of the Pakowki Lake area is Pendant d'Oreille, discovered in 1946 when McColl-Frontenac Oil Co. Limited and Union Oil Co. of California completed their Bow Island gas well. The field now contains eight gas wells which produce from five Bow Island sands. The uppermost sand contains the major gas reserve due to its greater porosity, net productive thickness, and areal extent. The gas accumulation is a typical stratigraphic trap, with the sands pinching-out or becoming low in permeability updip and containing water downdip.

Medicine Hat Field

Interest was first directed to natural gas at Medicine Hat by gas seepages in the South Saskatchewan River. Early in 1890 a bore hole was sunk in search of coal which discovered gas in the Milk River sand at a depth of approximately 700 ft. In 1908 the Canadian Pacific Railway Co. drilled a well to a depth of 1,000 ft and obtained gas from the Medicine Hat sand, which later proved to be the principal gas reservoir of the field.

The accumulation of gas in the Medicine Hat Field is dependent primarily on the variation in permeability, and structure is relatively unimportant. An area of sand with low permeability surrounds the field. Shows and small measurable volumes of gas are encountered in this area of low permeability, and it is likely that a substantial volume of gas can be drained from this area by the producing wells.

More than 100 gas wells have been completed, but there were no systematic records of early drilling or production. Since 1927, accurate records have been kept only of gas

metered for domestic use. To estimate the natural gas reserves of the field by the equal pound loss method, it was necessary to use production and pressure data for the interval from 1945 to 1950. A comparative estimate also was made by the volumetric method. Although the limited data available for calculation of reserves by either method makes it difficult to state which computation provides the better estimate, it would seem that the estimate based on the equal pound loss method is probably the more reliable.

Peace River Area

The first well to indicate the possibilities of large gas reserves in this area was drilled north of Peace River Townsite in 1916 in what is now known as the Peace River Field. Large quantities of gas were found in the Lower Cretaceous sands from depths of 335 to 1,200 ft. Subsequent to this discovery, 18 wells were drilled in the immediate area. The principal gas pay occurs in Loon River sands of Lower Cretaceous age. Seven old wells still are flowing gas and water.

During the summer of 1950 a major gas discovery was completed by Shell Oil Co. and British-American Oil Co. at Whitelaw, some 35 miles southwest of the old Peace River Field. The well was significant because it discovered the first accumulation of gas in Triassic sediments in the province. Gas was also proved in Lower Cretaceous sands. The drilling and completion of six additional wells have confirmed the occurrence of both Lower Cretaceous and Triassic gas pays over a large area.

The accumulation of gas at Whitelaw occurs in a northwest-southeast trending anticline plunging to the northwest, with the possibility of a porosity pinch-out to the northeast.

A second major discovery was made in 1951, 15 miles to the southeast of the Whitelaw Field by Hudson's Bay Oil Co. Limited and the Union Oil Co. of California in Lower Cretaceous and Triassic sands. The discovery well of the North Tangent Field blew out, but was brought under control and capped for later completion as a gas well. Four additional widely separated wells have been drilled, each of which had commercial quantities of gas in both reservoirs.

Although the field is not yet defined, present available data make it reasonable to assume that the North Tangent accumulation is similar in nature to that at Whitelaw.

POSSIBILITIES OF FUTURE GAS DISCOVERIES

Exploration for natural gas reserves in the province of Alberta has been accelerating rapidly during the past two years, primarily because of the prospect of an increased market demand resulting from the possible export of gas. The scope of this paper does not allow a complete discussion of all the gas prospects in the province, and will be limited to the more favorable areas.

Eastern Flank of Alberta Syncline

While the present density of drilling precludes any definite statement of boundary, it is apparent that a place is reached on the Alberta shelf where the rate of dip steepens into the Alberta syncline. This relatively steeper flank of the shelf area parallels the Foothills Belt from the Athabaska River south to the international border, and has a width approximating 60 to 75 miles.

The few wells drilled suggest that throughout this eastern flank of the Alberta syncline, Cretaceous sands will be thicker and better developed than on the Alberta shelf. Moreover, it is likely that at several stratigraphic levels certain sediments present in the syncline will be overlapped updip by younger sediments resulting in intraformational stratigraphic traps of Devonian, Mississippian, and Cretaceous ages.

A combination of these factors leads to the possibility that along this eastern flank of the Alberta syncline continued exploration may result in important new gas reserves. Until wells are drilled, it will not be known whether porosity and permeability will be developed suitably, but this should not condemn initial exploration. Possibly the most unfavorable factor will be in greater drilling depths.

Two discoveries late in 1951 demonstrate these possibilities on this eastern synclinal flank, namely, the gas in Devonian sediments at Neapolis (T31,R27,W4) and the gas in Cretaceous sediments at Chancellor (T25,R21,W4).

Central Alberta Plains

More than 60 per cent of the localities of measurable gas which have been found in Alberta are concentrated in the Central Alberta Plains. One-half of the 24 fields reflecting recoverable reserves in excess of 100 billion cu ft are located in this area. Included are the important associated and dissolved gas reserves of Leduc-Woodbend, Golden Spike, Acheson, and Redwater Fields, and such non-associated gas fields as Viking-Kinsella, Legal-Morinville, and Provost. The Central Alberta Plains is presently the most attractive area in Alberta in which to continue exploration. Drilling depths are generally less than 6,000 ft. Most of the Devonian reefs are confined to this area. Despite the fact that the density of drilling is greatest in this area, it ranks first in current operations. Major additions to gas reserves are continuing as evidenced by the recent discovery of associated and dissolved gas at Bonnie Glen (T47,R27,W4) and non-associated gas at Hackett (T36,R18,W4).

Throughout most of the Central Alberta Plains sediments of Cretaceous age rest on Devonian. Multiple non-associated gas pays are common in the Lower Cretaceous and gas is productive from sands, both blanket and lensing in type, characterized by local pinch-outs of porosity and permeability. Multiple oil pays are common in the Devonian and these contribute important reserves of associated and dissolved gas.

The Central Alberta Plains is usually referred to as a homocline. In a stricter sense, it is composed of many semi-parallel northwest-southeast regional folds of low relief which apparently persist for long distances. Geophysical prospecting has been successful in outlining local closures, structural terraces, and areas of reef development related to those axes. Many such prospects, when drilled, have produced oil or gas. Accordingly, this high percentage of success, even where the density of dry holes has been relatively high, suggests that the Central Alberta Plains will continue to be the most favored area for exploration.

The newest area in the Central Alberta Plains to receive attention as a gas prospect is at Lac la Biche located some 200 miles northeast of Edmonton. Two years ago several wells encountered considerable volumes of non-associated gas, less than 2,000 ft in depth, in Lower Cretaceous sands and in Devonian dolomites. The principal gas occurrence was found at 800 ft in Pelican (Viking) sand. These wells were widely separated and suggest that substantial gas accumulations exist over a large area. Mechanical difficulty in completion caused

gas blowouts, together with their distance from a gas market, caused the wells to be capped as potential gas wells. A drilling program is now in progress, which if successful, may contribute major gas reserves.

southeastern Alberta Plains

Gas prospecting in this area has been extremely successful in the past several years. The discovery of Cessford, Oyen, Ribbald, Countess, and other fields, has increased substantially the gas reserves of the province.

In many fields, multiple gas pays have been encountered in the Lower Cretaceous sands. These sands are blanket over the southeastern plains but manifest local pinch-outs in porosity and permeability. A maximum drilling depth of 4,000 ft makes wildcat drilling attractive. Locations for wildcats have been made frequently on seismic highs with a satisfactory success ratio.

From the Saskatchewan border to the Alberta foothills on the west, many semi-parallel northwest-southeast regional folds apparently exist which plunge to the northwest. It is along and adjacent to the axes of these folds that the greatest accumulations of gas in Lower Cretaceous sediments have been found. While the density of drilling is not great, the majority of dry-holes record gas and/or oil shows in Cretaceous sands. Because of this fact, and due to local reversals of plunge, these regional axes afford one of the more favorable areas to explore for gas in the Cretaceous.

Peace River Area

Developments to date indicate the possibilities of large accumulations occurring over wide areas. Recently a well was completed at Hamelin Creek approximately 25 miles northwest of Whitelaw which gauged 66 million cu ft of gas per day on production tests from Cretaceous sands. Gas saturation also was proved in the Triassic by drillstem tests, but the gas obtained was not in commercial quantities.

Numerous successful tests have been made in Upper Cretaceous, Lower Cretaceous, Triassic, and Mississippian reservoirs within the general Peace River area. While Lower Cretaceous and Triassic sediments seem to offer the reservoirs of most promise, it is significant that in the eastern portion of the Peace River Area sediments of Mississippian, Pennsylvanian, Permian, Triassic, and Jurassic age all thin to zero under Cretaceous cover. Such a subsurface relationship produces stratigraphic traps many miles in length, and at relatively shallow depths, in which gas and oil could accumulate. Apparently the most suitable areas for such potential accumulations would be at the updip edge of a trap where it is crossed by existing northwest-southeast regional folds.

RATE OF GAS DISCOVERY

An interesting approach to the prediction of future gas discovery in Alberta is to examine the results of past efforts. Table V lists the initially recoverable gas reserves (proved and probable) as now estimated and credited to the year of discovery together with the cumulative total for each year listed. The same material is depicted graphically in Fig. 4.

Table V—Cumulative Initial Recoverable Gas by Years for the Province of Alberta, Canada
(All Volumes Expressed at Base Pressure of 14.4 psia and 60°F)

Year (1)	Initial Recoverable Gas Found Each Year, MMcf (2)	Cumulative MMcf (3)
1890	1,127,477	1,127,477
1897	5,000	1,132,477
1909	50,066	1,182,543
1910	5,555	1,188,098
1914	1,015,217	2,203,315
1923	95,179	2,298,494
1924	2,130,055	4,428,549
1932	1,448	4,429,997
1934	8,379	4,438,376
1937	9,875	4,448,251
1939	54,693	4,502,944
1940	326,874	4,829,818
1941	48,252	4,878,070
1942	48,144	4,926,214
1943	16,056	4,942,270
1944	786,831	5,729,101
1945	42,973	5,772,074
1946	582,849	6,354,923
1947	1,892,937	8,247,860
1948	2,328,909	10,576,769
1949	1,803,689	12,380,458
1950	990,428	13,370,886

It will be noted that during the five-year period, 1946 to 1950, inclusive, more gas reserves were discovered than during the entire preceding period of 63 years. This effect will become more pronounced as development drilling progresses, permitting a better evaluation of the reserves found in recent years, particularly in 1949 and 1950. It should be appreciated that the majority of gas reserves to date have been found incidental to the search for oil. None of the major gas reserves discovered in the last five years is being marketed in appreciable volume. Of the discoveries made in the last decade, Jumping Pound is the only field from which gas is being marketed, and this outlet was not realized until 1951, seven years after its discovery.

Any reasonable extension into the future of the reserve discovery curve of Fig. 4 indicates that large volumes of gas remain to be found in Alberta. Relative exploration of the Alberta sedimentary basin is in its infancy compared with most similar basins in the United States, even though drilling activity in 1951 reached an all-time high. When an adequate market for gas is provided, it is likely that the gas reserves of Alberta will more than double during the following decade.

FUTURE AVAILABILITY OF PIPELINE GAS

Future availability might be defined as projected possible rates of gas delivery from a property, reservoir, field, or a group of fields and deliverability as rates limited by market demand or regulatory practice.

Estimation of Projected Performance of Free Gas

Procedure for estimating projected performance of free gas reservoirs may be stated simply as the application of pressure-volume-temperature relationships and the back pressure method of rating a gas well's potentiality as presented in a publication of the Texas Railroad Commission⁷ and in the Bureau of Mines' Monograph 7.⁸

Prior to commencing the actual mechanics of a performance study, an estimate of the future availability of pipeline gas

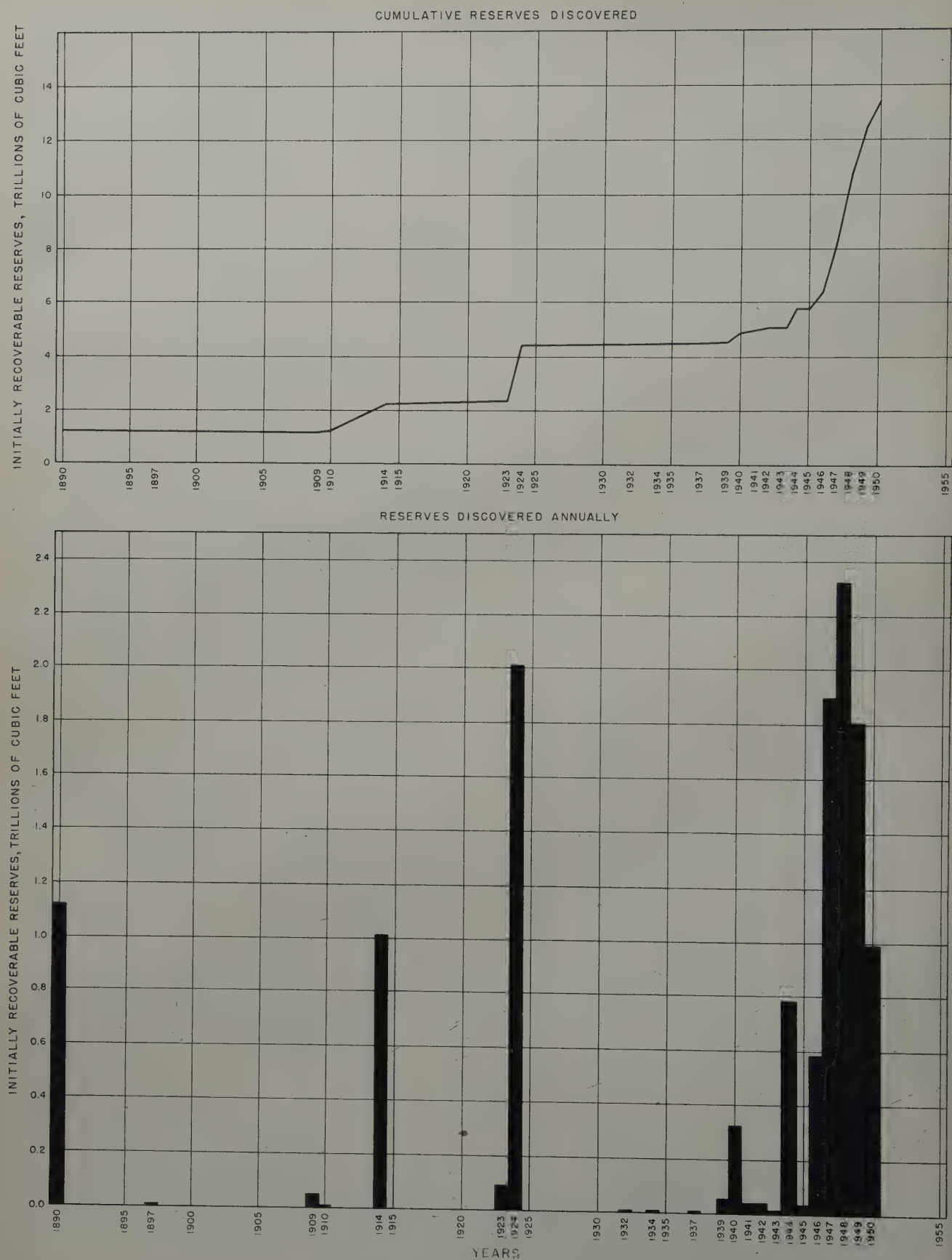


FIG. 4 — DISCOVERY RECORD OF INITIALLY RECOVERABLE GAS RESERVES (TOTAL PROVED AND PROBABLE), PROVINCE OF ALBERTA, CANADA.

from a free gas reservoir should be based on a considerable volume of detailed data including, but not limited to:

1. Initial gas in place.
2. Recoverable gas.
3. Production history, preferably at intervals to coincide with pressure determinations.
4. Initial static reservoir pressure.
5. Initial average static wellhead pressure.
6. Average static reservoir and wellhead pressures immediately prior to the date of the first projected delivery, if the reservoir has been producing.
7. An estimate of the amount of gas which will be required over the period of the study for development, field and fuel uses, shrinkage, compression fuel if required, line losses, etc.
8. An estimate as to the number of wells which will be required for final development, as well as their approximate location.
9. Limits of the reservoir and its structural configuration.
10. Open flow capacity tests, preferably back-pressure tests, on the completed wells.
11. Operating pressure of the line.
12. Term of the projection.

The expected pressure drop per unit of production must be predicted. If adequate and accurate pressure *vs* production data are available for a producing reservoir for which the productive limits are well established, these data should be used in predicting pressure drop per unit of production. In the ideal case, where instantaneous stabilization would be achieved and the pressure thereby equalized throughout the reservoir, the productive limits of the reservoir would not be necessary in determining the average pressure. Care should be exercised in evaluating the data to determine the effect, if any, of water encroachment. Extreme care also should be used in determining the average pressure of the reservoir. In this respect, perhaps the most accurate approach, knowing the limits of the reservoir, is to construct at various time intervals, isobaric maps superimposed on net pay isopachs to arrive at average static pressures weighted by reservoir volumes. This

is particularly important early in the life of the reservoir. If the reservoir has not been produced, the pressure drop per unit of production can be estimated from the average initial pressure and the initial volume of gas in place if no water drive is expected. In most cases, sufficient accuracy results from assuming a linear relationship between pressure and cumulative production. Where data permit, deviation from the perfect gas law should be considered to improve the accuracy of the estimate.⁹

The average shut-in wellhead pressures corresponding to the weighted average reservoir pressure then can be determined. Frequently, availability studies are required on reservoirs which have experienced little or no production and generally are lacking in some of the important factual data. In such instances, it is necessary to work with the available data, known theories, and judgment.

Availability forecasts based on average wellhead shut-in and working pressures interrelated with the wellhead open flow capacity curve of the average well take into consideration both well and reservoir performance characteristics, and hence, perhaps more nearly reflect the physical deliverability to be expected from a field than forecasts based entirely on bottom-hole conditions.

Projected Performance of the Manyberries Field

A projected performance study of the Manyberries Field is presented as a typical example. This field is located on the plains of southeast Alberta approximately 95 miles east and slightly south of the city of Lethbridge and approximately 35 miles northwest of the southeast corner of the province.

The gas accumulation is found in two permeable Bow Island sands of lower Cretaceous age which are limited updip to the west either by pinching out and/or lack of permeability and are defined downdip to the east by contact with water, forming a stratigraphic trap. This field was discovered on June 26, 1947, with the completion of McColl-Frontenac-Union's well No. 7 for an estimated 30 million cu ft of gas

Table VI—Manyberries Field Estimated Natural Gas Reserves, Bow Island Sands
(All Volumes Measured at Base Pressure of 14.4 psia at 60°F)

Line (1)	Item (2)	Units (3)	Proved (4)	Probable (5)	Totals (6)
			Non-Associated	Non-Associated	
1	Type of Gas		0.59		
2	Specific Gravity (Air = 1)		943		
3	Heating Value	BTU/Cu Ft			
4	Estimated Productive Area	Acres	21,019	4,800	25,819
5	Estimated Average Thickness	Feet	12.0	2.0	
6	Estimated Reservoir Volumes	Acre-Ft	251,183	9,600	260,783
7	Estimated Average Porosity	Per Cent	21.2		
8	Estimated Interstitial Water	Per Cent	25.0		
9	Estimated Initial Reservoir Pressure	Psia	870		
10	Terminal Reservoir Pressure	Psia	100		
11	Estimated Reservoir Temperature	°F	85		
12	Estimated Compressibility Factor, Initial Conditions		0.87		
13	Estimated Compressibility Factor, Terminal Conditions		0.99		
14	Initial Gas in Place per Acre-Ft	Mcf	458	458	
15	Remaining Gas in Place per Acre-Ft	Mcf	46	46	
16	Total Initial Gas in Place	MMcf	115,042	4,397	119,439
17	Total Remaining Gas in Place at Terminal Pressure	MMcf	11,554	442	11,996
18	Initial Recoverable Gas to Terminal Pressure	MMcf	103,488	3,955	107,443
19	Estimated Cumulative Production to Jan. 1, 1951	MMcf	Negligible		
20	Remaining Recoverable Gas to Terminal Pressure	MMcf	103,488	3,955	107,443
21	Estimated Field and Fuel Uses	MMcf	118		118
22	Estimated Shrinkage Losses at 2 Per Cent	MMcf	2,070	79	2,149
23	Estimated Recoverable Gas Reserves (Available for Sale)	MMcf	101,300	3,876	105,176

per day through perforations from 2,519 to 2,530 ft in a Bow Island sand.

An isopachous map of net gas sand in the Manyberries Field is shown in Fig. 3. Table VI presents pertinent data and the estimated reserves of the Manyberries Field, illustrating a typical method of procedure.

Data used and assumptions made in the availability study for the Manyberries Field follow:

1. Estimated initial gas in place, 119,439 MMcf at 14.4 psia and 60°F.
2. Estimated initial recoverable pipeline gas, 105,176 MMcf.
3. Cumulative production, negligible.
4. Initial static reservoir pressure, 870 psia.
5. Initial average static wellhead pressure, 825 psia.
6. Estimated allowance of seven per cent for field and fuel use, shrinkage, compression, etc.
7. Present number of wells, four. Estimate three additional wells to bring to final development. Therefore, the final density is 25,819 acres for seven wells, or 3,690 acres per well.
8. The four present wells have a reported total wellhead open flow capacity of 89,000 Mcf per day. The three addi-

tional completions, if well located structurally and if the sand characteristics are relatively uniform, should add approximately 80,000 Mcf per day. This would result in an overall average well equivalent to 24,000 Mcf per day at the initial static wellhead pressure of 825 psia. It is estimated that the slope of the curve will approximate 0.85. The estimated average well curve is illustrated in Fig. 5.

9. The calculated pressure drop to production ratio is:

$$\frac{\text{Initial wellhead pressure}}{\text{Initial Gas in Place}} \quad \text{or}$$

$$\frac{825 \text{ psia}}{119,439 \text{ MMcf}} \quad \text{or}$$

$$0.0069073 \text{ lb per MMcf}$$

10. Initial line pressure assumed at 600 psig (613 psia).
11. It was decided to determine the availability of gas from the field over a 25-year period under a reasonable development program and rate of production.

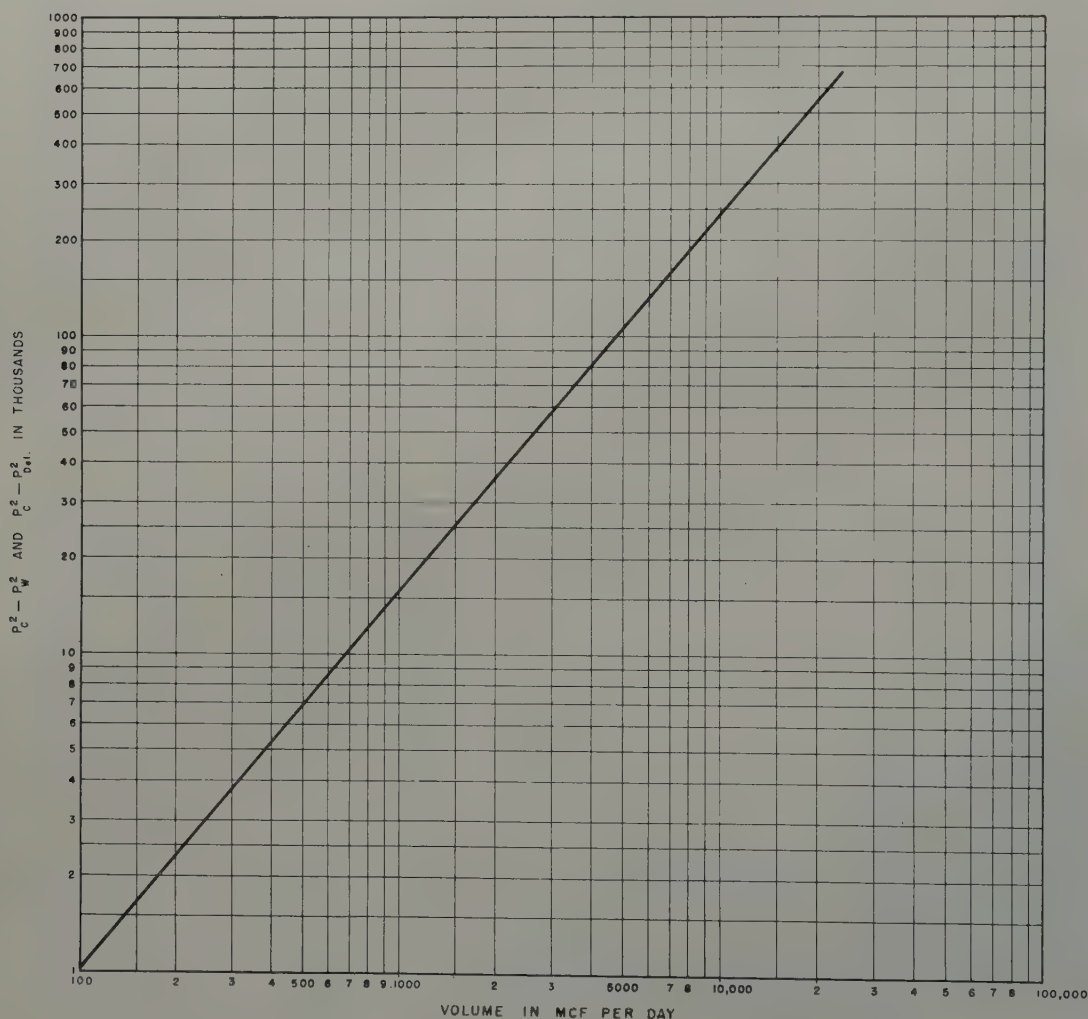


FIG. 5 — MANYBERRIES FIELD, ESTIMATED WELLHEAD OPEN FLOW CAPACITY OF AVERAGE WELL, 24,000 Mcf PER DAY AT $P_c = 825$ PSIA, SLOPE = .85.

The estimated average wellhead pressure at the end of each year is calculated by subtracting the product of the cumulative gross gas production in MMcf and the pressure drop to production ratio in lb per MMcf, from the initial static wellhead pressure.

By applying the square of the shut-in wellhead pressure at year-end to the curve, Fig. 5, the wellhead open-flow capacity of the average well can be determined. The total wellhead open-flow capacity is the product of the number of wells and the open-flow capacity of the average well.

From the same figure, by the application of the difference of the squares of the shut-in wellhead pressure and the line pressure, the volume of gas which the average well will produce against line pressure can be read. The number of wells times the volume of the average well is the total delivery capacity.

Table VII illustrates in detail the projected performance of the Bow Island sands in the Manyberries Field under the conditions and assumptions listed. Fig. 6 is a graphical presentation of certain of the pertinent data contained in Table VII.

Composite Future Availability

Approximately 50 detailed availability studies have been made on individual reservoirs and/or fields either singly or in groups. These studies were made for essentially all of the presently known non-associated gas reserves in the province of Alberta. In addition, availability studies were made on the substantial dissolved gas reserves of the Nisku (D_2) zone and the associated and dissolved gas reserves of the Leduc (D_3) zone in the Leduc-Woodbend Field, as well as the associated and dissolved gas reserves of the Rundle Limestone in the Turner Valley Field. From that number of studies, it was statistically possible to estimate the potential future availability of gas from the known gas reserves of the province of Alberta. The reserves used in the availability projections are as of Jan. 1, 1951, but reflect data available to Aug. 1, 1951.

Table VIII presents a composite future availability projection of gas from the currently known reserves of the province of Alberta. Availability data are presented graphically in Fig. 7. Although these illustrations present available productivity based on a practical development program and production at a reasonable fraction of open-flow capacity, actual

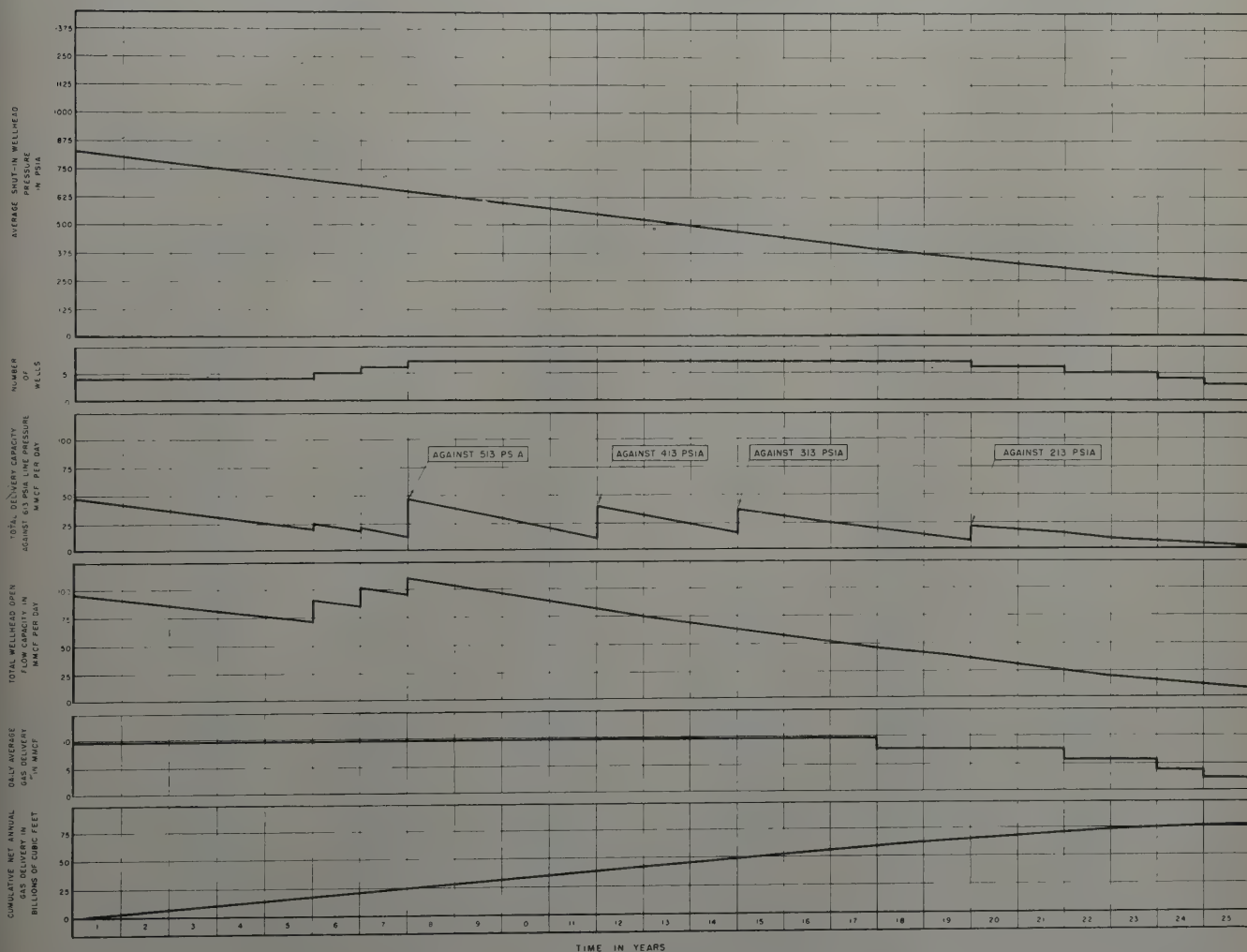


FIG. 6 — MANYBERRIES FIELD, PROJECTED PERFORMANCE — BOW ISLAND SANDS. ALL VOLUMES EXPRESSED AT BASE PRESSURE OF 14.4 PSIA AND 60°F.

deliverability will be determined by market demand, which, in turn will influence the rate of development.

It should be stressed that the composite future availability of gas which is herein presented can in no sense be viewed as a prediction of the actual amounts of natural gas which will become available from the province of Alberta during the period 1951 to 1976. The natural gas supplies in Alberta will unquestionably be increased, and substantially, by future exploration. Therefore, the volumes of gas as presented in Table VIII should be viewed as absolute minimum volumes to be expected at any certain period. In fact, recent extensions and developments since the date of the various availability studies have materially increased the supply of gas.

GAS REQUIREMENTS AND GAS SUPPLY IN ALBERTA

The natural gas requirements of the province are being served principally by two major gas utility systems: the Canadian Western Natural Gas Co., and the Northwestern Utilities Limited. The Canadian Western Natural Gas Co. supplies the Calgary area, and Northwestern Utilities Limited serves the Edmonton area. In addition, there are approximately 15 local systems furnishing gas to as many small communities.

Gas consumption in the province of Alberta has shown a substantial increase during the period from 1940 through 1950

according to The Petroleum and Natural Gas Conservation Board.¹⁰ During 1940, a total of approximately 15 billion cu ft of gas was consumed. In 1950, the annual consumption of gas had risen to approximately 48 billion cu ft. This reflects an increase of 220 per cent. The per capita rate of gas consumption was approximately 19 Mcf in 1940 and 54 Mcf in 1950, or an increase of 184 per cent during the period.

The Petroleum and Natural Gas Conservation Board has estimated the total annual gas requirements of the province at 58.6 billion cu ft for 1952, increasing to 98.9 billion cu ft in 1960, and to 131.0 billion cu ft in 1980. The estimated requirements from 1952 to 1981 total slightly more than 3.0 trillion cu ft.

Based on the assumption that a surplus gas supply exists in the province of Alberta, at least six companies have applied to The Petroleum and Natural Gas Conservation Board for permission to remove gas or cause it to be removed from the province. Following a joint hearing held in 1950, the board published its findings in an Interim Report released in January, 1951.¹⁰ After an exhaustive study of data presented to that time, the board concluded that it would not grant a permit to any of the applicants and recommended that the applications be continued.

During 1951, a series of hearings was held at which applicants presented new and more detailed estimates concerning provincial requirements, gas reserves, and gas deliverability. The conservation board, at the time of writing, is in the process of studying data presented in the 1951 hearings and should

Table VII — Manyberries Field,
(All Volumes Expressed at Base)

Year (1)	Net Annual Gas Delivery, MMcf (2)	Cumulative Net Annual Gas Delivery, MMcf (3)	Estimated Required Annual Gross Gas Pro- duction, MMcf ^a (4)	Cumulative Gross Annual Gas Production, MMcf (5)	Daily Average Net Gas Delivery, Mcf (6)	Daily Average Gross Gas Production, Mcf (7)	Estimated No. of Wells (8)
1	3,490	3,490	3,750	3,750	9,600	10,300	4
2	3,490	6,980	3,750	7,500	9,600	10,300	4
3	3,490	10,470	3,750	11,250	9,600	10,300	4
4	3,490	13,960	3,750	15,000	9,600	10,300	4
5	3,490	17,450	3,750	18,750	9,600	10,300	4
6	3,490	20,940	3,750	22,500	9,600	10,300	5
7	3,490	24,430	3,750	26,250	9,600	10,300	6
8	3,490	27,920	3,750	30,000	9,600	10,300	7
9	3,490	31,410	3,750	33,750	9,600	10,300	7
10	3,490	34,900	3,750	37,500	9,600	10,300	7
11	3,490	38,390	3,750	41,250	9,600	10,300	7
12	3,490	41,880	3,750	45,000	9,600	10,300	7
13	3,490	45,370	3,750	48,750	9,600	10,300	7
14	3,490	48,860	3,750	52,500	9,600	10,300	7
15	3,490	52,350	3,750	56,250	9,600	10,300	7
16	3,490	55,840	3,750	60,000	9,600	10,300	7
17	3,490	59,330	3,750	63,750	9,600	10,300	7
18	2,790	62,120	3,000	66,750	7,600	8,200	7
19	2,790	64,910	3,000	69,750	7,600	8,200	7
20	2,790	67,700	3,000	72,750	7,600	8,200	6
21	2,790	70,490	3,000	75,750	7,600	8,200	6
22	2,080	72,570	2,240	77,990	5,700	6,100	5
23	2,080	74,650	2,240	80,230	5,700	6,100	5
24	1,390	76,040	1,490	81,720	3,800	4,100	4
25	860	76,900	930	82,650	2,400	2,500	3
Totals (25-Year Period)	76,900		82,650				
Averages (25- Year Period)	3,076		3,306		8,400	9,100	

^aIncludes allowance of 7 per cent for field and fuel uses, shrinkage, compression, etc.

^bOriginal.

^cReduce line pressure to 513 psia.

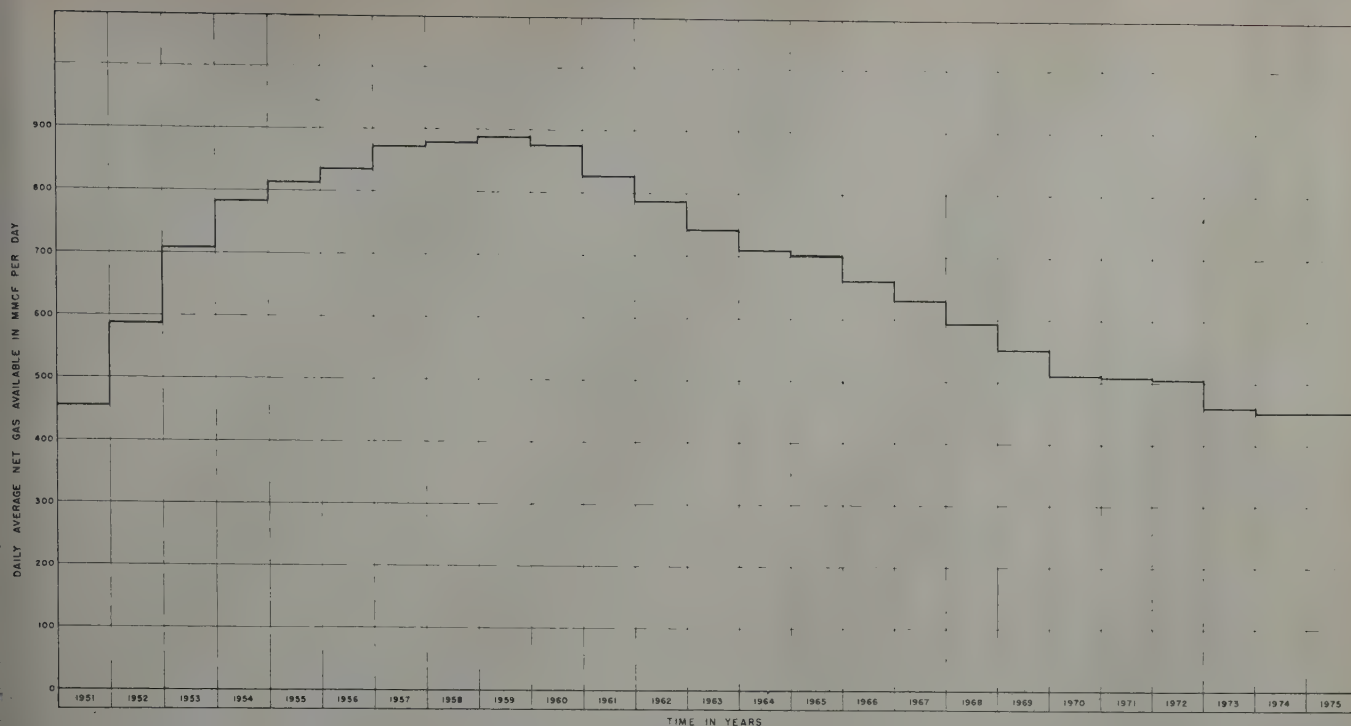


FIG. 7 — A COMPOSITE FUTURE AVAILABILITY PROJECTION FOR THE PROVINCE OF ALBERTA, CANADA. ALL VOLUMES EXPRESSED AT BASE PRESSURE OF 14.4 PSIA AND 60°F.

Projected Performance — Bow Island Sands

Pressure of 14.4 psia and 60°F)

Cumulative Pressure Drop at Year End, psi (9)	Average Shut-in Wellhead Pressure at Year End, psia (10)	Estimated Average Well Open Flow Capacity, Wellhead Conditions, at Year End, Mcf/D (11)	Estimated Total Wellhead Open Flow Capac- ity at Year End, Mcf/D (12)	Estimated Average Well Delivery Capacity Against 613 psia at Year End, Mcf/D (13)	Estimated Total Delivery Capacity Against 613 psia at Year End, Mcf/D (14)	Gross Daily Gas Production as a Per Cent of Total Estimated Wellhead Open Flow Capacity (15)	Per Cent Net Gas Delivered of Initial Pipe Line Gas (16)
0	825 ^b	24,000	96,000	12,100	48,400		
26	799	23,000	92,000	10,800	43,200	11.2	3.3
52	773	21,500	86,000	9,300	37,200	12.0	6.6
78	747	20,100	80,400	7,900	31,600	12.8	10.0
104	721	19,100	76,400	6,400	25,600	13.5	13.3
130	695	18,000	72,000	5,000	20,000	14.3	16.6
155	670	17,000	85,000	3,600	18,000	12.1	19.9
181	644	15,700	94,200	2,100	12,600	10.9	23.2
207	618	14,700	102,900	5,500 ^c	38,500	10.0	26.5
233	592	13,600	95,200	4,200	29,400	10.8	29.9
259	566	12,600	88,200	3,000	21,000	11.7	33.2
285	540	11,700	81,900	1,600	11,200	12.3	36.5
311	514	10,600	74,200	4,500 ^d	31,500	13.9	39.8
377	488	9,800	68,600	3,400	23,800	15.0	43.1
363	462	8,900	62,300	2,300	16,100	16.5	46.5
389	436	8,100	56,700	4,400 ^e	30,800	18.2	49.8
414	411	7,300	51,100	3,500	24,500	20.2	53.1
440	385	6,600	46,200	2,600	18,200	22.3	56.4
461	364	6,000	42,000	2,000	14,000	19.5	59.1
482	343	5,400	37,800	1,200	8,400	21.7	61.7
503	322	4,900	29,400	3,000 ^f	18,000	27.9	64.4
523	302	4,400	26,400	2,500	15,000	31.1	67.0
539	286	4,000	20,000	2,000	10,000	30.5	69.0
554	271	3,600	18,000	1,600	8,000	33.9	71.0
564	261	3,400	13,600	1,400	5,600	30.1	72.3
571	254	3,300	9,900	1,200	3,600	25.3	73.1

^dReduce line pressure to 413 psia.
^eReduce line pressure to 313 psia.
^fReduce line pressure to 213 psia.

Table VIII—Composite Future Availability of Gas of the Province of Alberta, Canada, from Reserves as of Jan. 1, 1951

(All Volumes Expressed at Base Pressure of 14.4 psia and 60°F)

Year (1)	Estimated Daily Average Net Gas Delivery in MMcf (2)	Year (1)	Estimated Daily Average Net Gas Delivery in MMcf (2)
1951	455	1964	711
1952	588	1965	703
1953	709	1966	662
1954	782	1967	631
1955	814	1968	594
1956	836	1969	553
1957	872	1970	510
1958	879	1971	509
1959	889	1972	505
1960	875	1973	460
1961	827	1974	453
1962	789	1975	456
1963	742		
Average (1951-1976 Period).....			672

present its recommendations in the spring of 1952. The petroleum industry may be assured that the findings of the board will be based on a conservative but sincere and thorough analysis of the voluminous data presented in the hearings. It appears from an engineering and geological standpoint that a substantial gas surplus exists beyond estimated provincial requirements through 1980. However, should the board not see fit at this time to recommend granting an export permit, continued exploration in Alberta undoubtedly will assure the development of a market outlet for gas within the next few years.

CONCLUSION

Recent drilling activity in the province of Alberta has resulted in a sharp increase in its natural gas reserves, bringing the estimated total recoverable volume on a proved and probable basis, as of Jan. 1, 1952, to 11.7 trillion cu ft. During the five-year period of 1946 to 1950, it is estimated that more gas reserves were discovered than during the entire preceding period of 63 years, and with the provision of an adequate market for the sale of gas, it is likely that provincial reserves will more than double in the decade to follow the realization of such market.

The present density of drilling in Alberta is about one well to 100 square miles. While measurable gas exists in every system present excepting Ordovician, a consideration of the localities capable of gas production indicates that Mississippian and Cretaceous reservoirs offer a better chance for the discovery of major non-associated gas reserves, and Devonian reservoirs for the discovery of associated and dissolved gas reserves. All of Alberta, between the Canadian Shield and the Rocky Mountain Front Range, has attractive gas possibilities and the choice of where to explore is largely a matter of an operator's preference and resources. The rate of development of one area over another may depend on its proximity to a gas pipeline should permission to export gas be granted.

A method was presented for estimating future availability of gas from a type field, and a composite estimate of the availability of gas from the province was developed. This composite future availability estimate cannot be viewed as a prediction of the actual amounts of gas which will become

available. The natural gas supplies in Alberta unquestionably will be increased, and substantially, by future exploration.

At the present time no market exists for the major gas reserves discovered in recent years. Applications for permits to remove gas or cause it to be removed from the province now are pending before The Petroleum and Natural Gas Conservation Board. It appears from an engineering and geological standpoint that a substantial gas surplus exists beyond estimated provincial requirements, and that continued exploration in Alberta will assure the development of a market outlet for gas within the next few years.

ACKNOWLEDGMENTS

The authors wish to acknowledge assistance from many people, too numerous to mention individually, who contributed materially to the data used in the preparation of this paper. We acknowledge the detailed geological and well data compiled by George S. Hume and A. Ignatieff in the reports of the Geological Survey of Canada, and the "Schedules of Wells Drilled for Oil and Gas" compiled by The Petroleum and Natural Gas Conservation Board of the Province of Alberta. Special acknowledgment is made of the valuable assistance rendered by Floyd K. Beach, consultant of Calgary, Alberta, Canada, in obtaining basic geological and engineering data. We express our thanks to DeGolyer and MacNaughton for permission to publish this paper, including certain copyrighted material, and to R. B. Gilmore for his helpful suggestions in reviewing this paper. And finally, we acknowledge permission given by P. T. Bee and Frank A. Schultz, Jr., of Delhi Oil Corp. to present data contained herein.

REFERENCES

1. Alberta Society of Petroleum Geologists: "Alberta Symposium," *Bull. AAPG*, (1949) 33, 4.
2. Geological Staff, Imperial Oil Ltd.: "Devonian Nomenclature in Edmonton Area, Alberta," *Bull. AAPG*, (1950) 34, 9, 1807.
3. Webb, J. B.: "Geological History of Plains of Western Canada," *Bull. AAPG*, (1951) 35, 11, 2291.
4. Link, T. A.: "Interpretations of Foothills Structures, Alberta, Canada," *Bull. AAPG*, (1949) 33, 9, 1475.
5. Scott, J. C.: "Folded Faults in Rocky Mountain Foothills of Alberta, Canada," *Bull. AAPG*, (1951) 35, 11, 2315.
6. Gallup, W. B.: "Geology of Turner Valley Oil and Gas Field, Alberta, Canada," *Bull. AAPG*, (1951) 35, 4, 797.
7. Baumel, J. K., and Smith, S.: "Back-Pressure Test for Natural Gas Wells, State of Texas," Railroad Commission of Texas, Oil and Gas Division, Austin, Tex., (1948).
8. Rawlins, E. L., and Schellhardt, M. A.: "Back-Pressure Data on Natural Gas Wells and Their Application to Production Practices," Monograph 7, U. S. Department of the Interior, Bureau of Mines, (1935).
9. Gruy, H. J., and Crichton, J. A.: "A Critical Review of Methods Used in Estimation of Natural Gas Reserves," *Trans. AIME*, (1949) 179, 249.
10. The Petroleum and Natural Gas Conservation Board, Province of Alberta: Interim Report, (January, 1951). ★

A HIGH-PRESSURE WELLHEAD LUBRICATOR

HOWARD E. MCKINNEY, SHELL OIL CO., HOUSTON, TEX.

ABSTRACT

A high-pressure wellhead lubricator has been developed to facilitate telemetering electrical measurements from subsurface reservoirs to the surface with the well under normal flowing conditions.

The field unit in use at the present time employs a 5/16-in.-diameter, single-conductor armored cable and is to be used in wells with surface pressures up to 5,000 psi. It has a pressure sealing element that maintains a continuous and absolute seal around the cable as it enters or leaves the tubing at speeds up to 175 ft per minute. A cable injecting device is used which obviates sinker bars or weight sections on the instrument.

INTRODUCTION

The development of instruments for securing physical measurements in pressure wells has been confined in the past to those instruments which would operate on a wire line and record the necessary measurements in the downhole instrument itself, or those which would operate on an electric cable in a well with the surface pressure killed by the use of weighted fluids or by the use of tubing plugs. In one case the accuracy of the measurements is questionable, and in the other the range of application is very limited.

Considerable work has been done by other interests to provide effective means to accomplish the necessary telemetering. The U. S. Bureau of Mines developed a wellhead lubricator prior to 1947 which permitted a 5/16-in.-diameter single-conductor cable to be lowered into a well with a surface pressure of approximately 500 psi. This unit was used successfully in a number of tests in Oklahoma. A company which tests wells has recently offered on a service basis a wellhead lubricator with a 3/16-in.-diameter cable that reportedly operates up to 2,500 psi surface pressures. Each of the above operates on a staging principle to effect a seal. In both of these units some leakage of well fluid occurs when the cable is moved.

SPECIFICATIONS FOR DESIGN

In order to provide the maximum flexibility in its use, the following parameters were established for the design of our high-pressure wellhead lubricator:

1. An absolute well fluid seal up to 5,000 psi surface pressures.
2. Means for raising and lowering the instrument at speeds of at least 100 ft per minute.
3. Provision for the instrument to enter and leave the well without disturbing the well flow or the reservoir conditions.
4. A cable large enough to provide suitable electrical characteristics and suitable mechanical properties.
5. A method of operation that will not damage the well in any way.

The present high-pressure wellhead lubricator field unit fulfills the above requirements.

DESCRIPTION OF THE UNIT AND ITS OPERATION

The cable selected for this use is the standard Amergraph 1H2 as manufactured by the American Steel and Wire Co. This particular cable is normally used by the Halliburton Oil Well Cementing Co. in their conventional well logging operations. Although the cable presents a noncircular cross-section (Fig. 1), its diameter is very consistent; for example, maximum diameter is 0.325 in., minimum diameter 0.314 in. This factor permits the use of the sealing element, as later described.

Early in the development of the high-pressure wellhead lubricator it was apparent that we could not effect a direct gas seal around a moving 1H2 cable. This becomes evident when an examination of the cable cross-section is made. The voids between the strands of the outer armor provide natural channels for the flow and escape in large quantities of a low-viscosity fluid such as gas. However, it is relatively simple to

Manuscript received in the Petroleum Branch office July 29, 1952. Paper presented at the Petroleum Branch Fall Meeting in Houston, Tex., Oct. 1-3, 1952.

effect a seal around the moving cable when a viscous fluid (transfer fluid) of our own choosing, rather than gas, is used in the pressure chamber. Sealing is achieved in our field unit by this indirect method. The sealing element is so designed that the cable can enter the well only through a relatively long, small-diameter tube, providing a very small cross-sectional area (annular space) for the well pressure to act upon, and sufficient length that the cylindrical shear area of the transfer fluid is large enough to permit only a very low rate of flow of the transfer fluid through the sleeve. A continuous supply of transfer fluid is injected into the sleeve a few inches downstream from the well-fluid chamber. Since the pressure of the transfer fluid is well-pressure plus 200 psi, the fluid tends to flow in both directions from its entry port; that is, towards the well fluid chamber and towards the atmosphere, thus preventing the well fluid's escape.

The cross-sectional area of the annulus between the cable and the sleeve is 0.003 sq in. There is approximately 0.016 sq in. of void area in the cable itself, giving a total well-fluid force area of only 0.019 sq in. Thus, in a well with 5,000 psi surface pressure, only 95.5 lb are actually applied to force the transfer fluid out of the sleeve. A sleeve 18 in. long provides ample cylindrical shear area so that a very low flow rate occurs at this pressure.

A sealing sleeve of the above type was constructed and subjected to rigorous bench and field testing prior to its assembly in a field unit. At the time this testing was proceeding, considerable effort was made to select a transfer fluid that had suitable rheologic properties and, at the same time, met the requirements of noncorrosiveness, proper solubility in well fluids, temperature stability, availability, and economy. The transfer fluid selected for use was Shell Indus 5169 grease.

The sealing element of the field unit offers very little drag to resist cable movement. However, when a cable with a diameter of 5/16 in. is placed in a pressure chamber, a considerable force (80 lb per thousand psi well pressure) acts to extrude the cable from the chamber. This force must be overcome with a counterforce that acts to pull the cable into the pressure chamber before entry can be made. The use of sinker bars on the bottom of the instrument is not practical with a 5/16-in.-diameter cable, since more than 66 ft of 1½-in.-diameter bars are required to lower an instrument into a 5,000-psi well with two-in. tubing. A cable cannot be pushed in from the outside, as a compression force of only 100 lb on a one-in. section of cable will cause basketing in the outer strands. Hence, it has become necessary to devise a method of pulling

the cable into the well from inside the pressure area itself. This is accomplished in the field unit by use of a grooved sheave. The groove in the sheave is essentially a half circle of slightly smaller diameter than the cable diameter. The gripping action of the groove is further increased by employing rollers that push the cable more tightly into the groove. As the cable is forced into the groove, the whole sheave is turned, thereby providing a continuous pull on the cable from the pressure chamber. As this entire cable injector assembly is operated at well pressure or greater, its design along conventional lines would result in a very heavy and cumbersome apparatus. By removing the center portion of the assembly, a modified torus ring is formed which materially decreases the wall thickness required for the pressure housing.

Details of the unit are shown in Fig. 2. The instrument, normally 1¼-in. diameter and five-ft long, is shown in the lubricator section. The cable head is designed to connect the cable mechanically and electrically to the instrument. Although the cable has a rated breaking strength of 9,200 lb, the mechanical connections to the cable head are made to provide a weak connection of 3,000 lb pullout so as to insure that the cable will pull free from an instrument stuck in the hole. The cable from the well side leaves the instrument to pass into the instrument catcher assembly. This is a safety feature to be used in case the instrument, as it is being brought up hole, is not stopped at the top of the lubricator. In this event the head of the instrument will hit a plug and shear two pins, thus allowing the spring fingers to grab the instrument as the cable is pulled from the weak link in the head. The cable goes next into the cable cutter assembly. This device can be used to cut the cable and allow it to fall clear of the master valve on the wellhead. The conditions requiring severing the cable will occur very infrequently, if ever. However, severing the cable could permit the well to be shut in at the wellhead, even though the instrument and a section of cable would remain at the bottom of the tubing.

The cable goes next through the cable brake assembly. This unit may be used to govern the uphole speed of the instrument. It is actuated by forcing high-pressure hydraulic fluid from an external source into the annulus around the rubber-like sleeve causing it to press steel brake shoes against the cable.

The next section is a cable valve, or stationary cable seal. This unit is physically the same as a cable brake except that it has no shoes. The neoprene sleeve is pressed directly into the outer strands of the stationary cable to effect a seal. Transfer fluid is injected into this seal to fill the inner voids

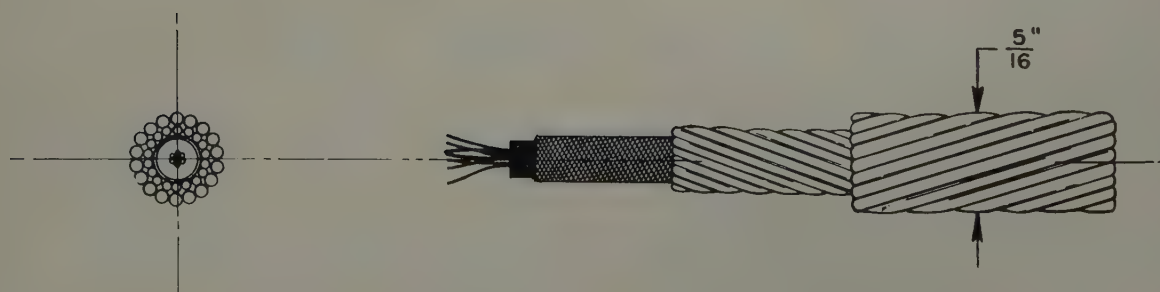


FIG. 1 — AMERGRAPH 1 H 2 SINGLE CONDUCTOR ARMORED CABLE.

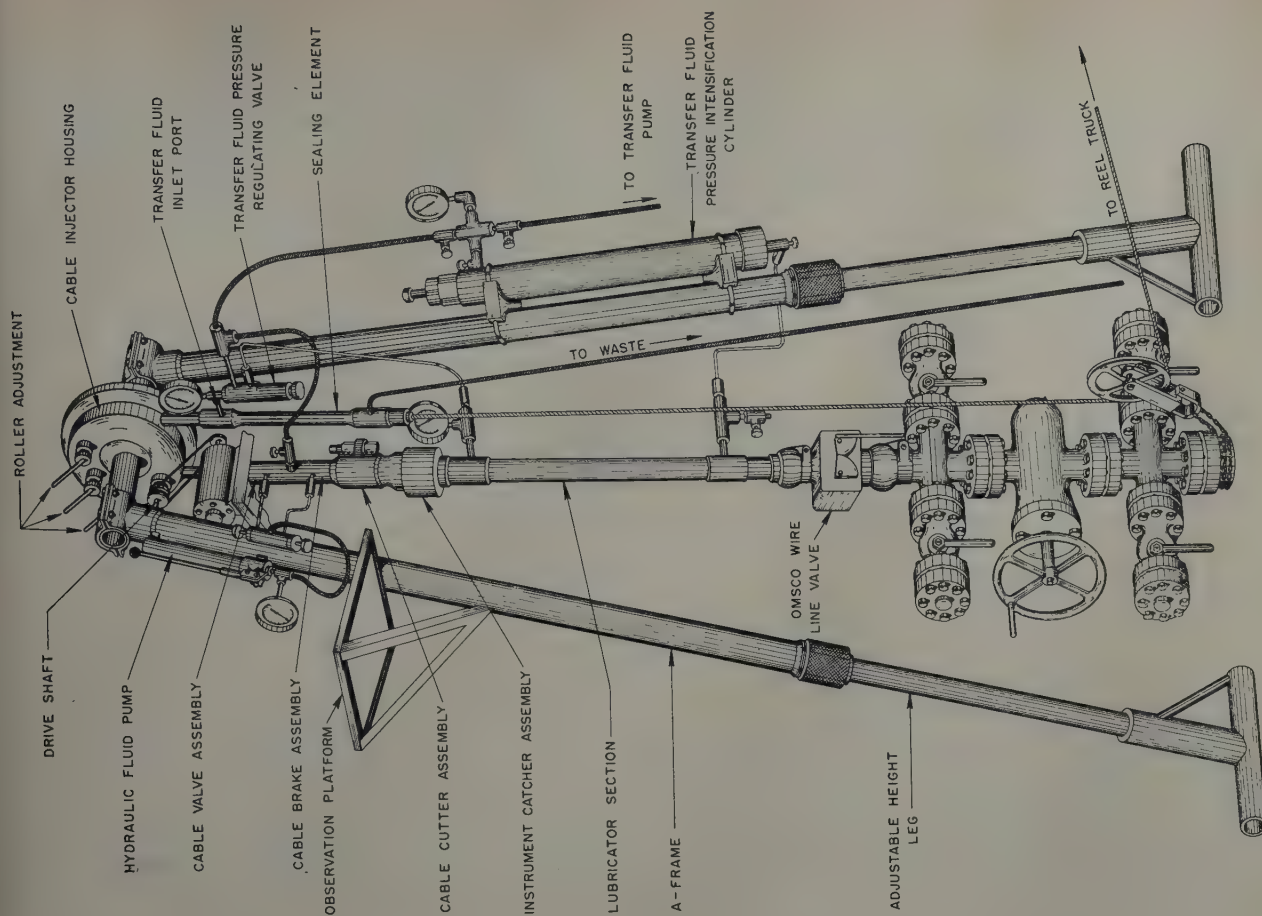


FIG. 3 — FIELD UNIT ASSEMBLY.

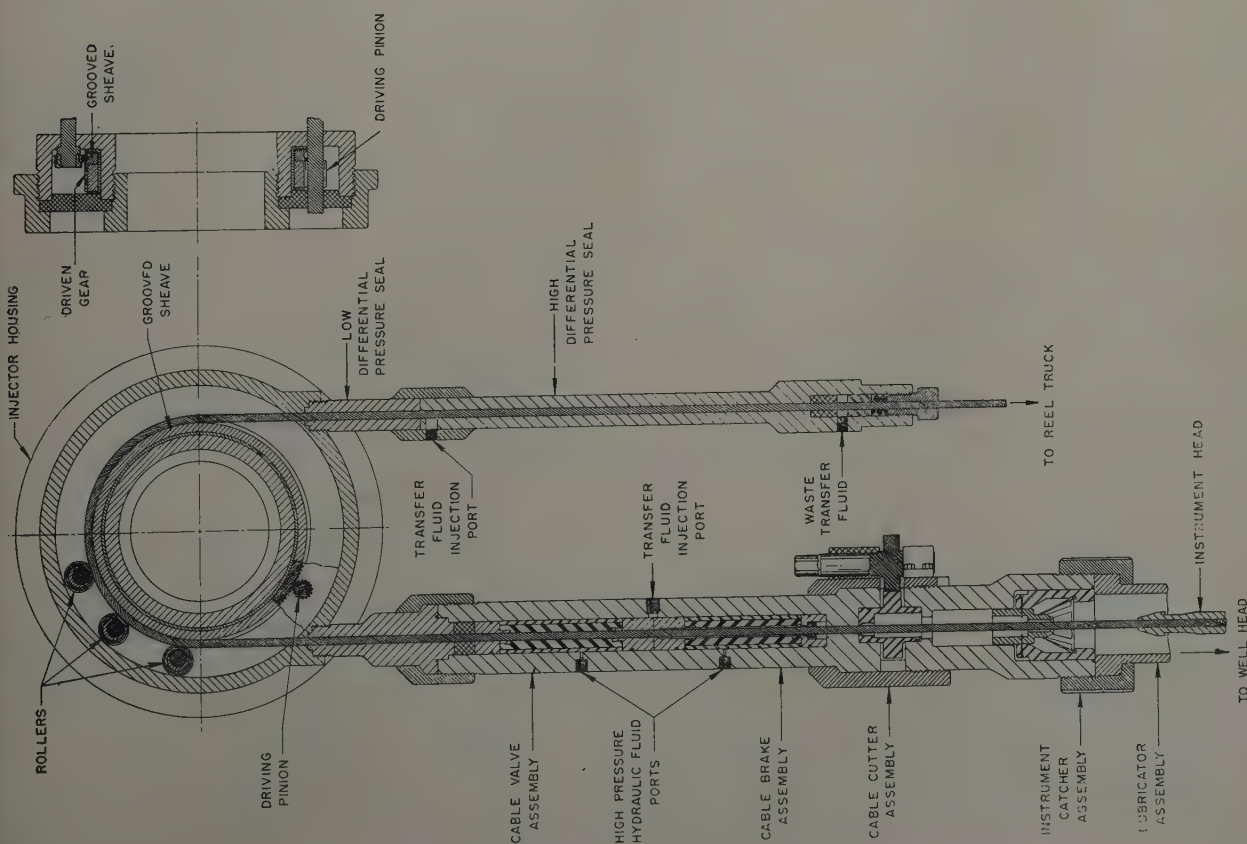


FIG. 2 — HIGH PRESSURE LUBRICATOR.

of the cable. It is used when it is necessary for the instrument to stay in one place for a long period of time, for example, in securing bottom-hole pressure-build-up data. The cable next enters the injector where it goes around the sheave and under the pressure wheels. The pressure wheels are not normally required, as the gripping action of the sheave is ample for most well pressures. The injector sheave is rotated in either direction by an externally located explosion-proof electric motor.

The cable next passes into the low differential pressure portion of the sealing element, past the transfer fluid injection port, through the high differential pressure portion of the sealing element, and then out of the sealing element to the reel truck.

Fig. 3 shows the general layout of all the components as they are assembled over a well. The wellhead equipment is mounted on and supported by an A-frame adjustable in height to facilitate connection to most Xmas trees. This frame, when connected to the Xmas tree, forms a rigid tripod with the lubricator section or instrument chamber acting as the third leg. This assembly is designed to support safely a pull in excess of the cable strength of 9,200 lb. The complete unit is designed to work at well pressures up to 5,000 psi; it incorporates a reel truck with 12,000 ft of the 5/16-in. single-conductor cable. The field unit can be assembled over a well in approximately four hours. A reduction in this time is anticipated in the future. Normally three men are required to operate the complete unit and the reel truck. Fig. 3 also shows the transfer-fluid pressure-intensification cylinder. This unit is a piston and cylinder arrangement from which a supply of transfer fluid is available for injection at a given pressure above well pressure. It takes care of sudden fluctuations in well pressure and acts as a high-pressure transfer-fluid reserve.

The amount of transfer fluid used in a normal well is approximately two lb per thousand ft of cable. The sealing element uses approximately 0.02 lb per minute per thousand psi wellhead pressure when the cable is stationary. For a moving cable the transfer-fluid requirement is almost independent of the well pressure and of the cable speed. The quantity of transfer fluid used is approximately that required to fill the voids in the cable, and since it is dissolved by the well fluid, the transfer fluid must actually fill the voids both going in and coming out of the well.

TESTS OF THE UNIT

Tests have been made where the packing element was deliberately made to fail by stopping the transfer fluid pump which allowed the well gas to enter and flow through the sealing element. At 5,750 psi wellhead gas pressure, the flow of gas was quite hard, but was easily stopped within ten seconds after the transfer fluid pump was started. Usually one stroke of the transfer fluid pump (0.016 lb of transfer fluid) is sufficient to stop the flow of gas and regain an absolute seal about the cable.

The well service unit has been bench-tested to 8,700 psi, thoroughly field-tested at well pressures up to 3,060 psi, and mock-tested at gas pressures of 5,750 psi. The unit is presently being utilized to run into pressured wells the several electrical telemetering instruments being developed at the laboratory. To date the field unit has logged an accumulated cable travel of over 115,000 ft.

The design and development of the unit will continue with the hope that the high-pressure electrical cable service can be made generally available to the field.

★ ★ ★

X-RAY SHADOWGRAPH STUDIES OF AREAL SWEEPOUT EFFICIENCIES

R. L. SLOBOD, MEMBER AIME, AND B. H. CAUDLE, JUNIOR MEMBER AIME, THE ATLANTIC REFINING CO., DALLAS, TEX.

ABSTRACT

In the past, the main emphasis in attacking the problem of the recovery of oil has been on the determination of fluid flow characteristics and residual oil saturation in the part of the reservoir which is contacted by a displacing phase. It is recognized that the determination of the fraction of the reservoir contacted in secondary recovery operations is also of great importance in predicting the ultimate recovery to be expected. A method is described in which radiographic techniques are used to determine these areal sweepout factors for any type of well spacing. Data showing the relationship of viscosity ratio and relative permeability to areal sweepout efficiency are presented for the five spot and the direct line drive well spacing patterns. Further applications of the method to studies of the displacement efficiency in the area contacted are mentioned.

tedious for systems with mobility ratio different from unity. Recently several such determinations have been reported,^{2,3} and an experimental method involving a step-wise use of potentiometric models has been described.²

A new method which has been developed for studying the areal distribution of phases in a porous medium is discussed below. This tool can be used to determine the effect of operating variables such as viscosity, relative permeability, presence of gas, mobility ratio, rate and stratification on the fraction of the reservoir contacted by the displacing medium. This development based on the use of X-rays gives a pictorial representation of the location of the phases. Further, the amount of each phase at each point of interest can be determined quantitatively.

INTRODUCTION

The problem of increasing oil recovery from typical reservoirs is generally attacked by trying to devise some means for reducing the residual oil in that part of the reservoir which is contacted. The fraction of the reservoir contacted in the displacement process, however, is also of major importance but has been given less consideration in the past. One reason for this neglect is the meager information available on the portion of the reservoir contacted and the magnitude of changes in this factor as operating conditions are varied. Until recently, the only means available for determining this quantity has involved the use of the electrolytic or potentiometric models¹ in which one is limited to working with a mobility ratio of unity. While means for calculating the volume of a reservoir contacted do exist, the calculations are very

X-RAY METHOD FOR AREAL STUDIES

In this method the location of various phases distributed over a test area are observed simultaneously by obtaining a photographic record of the transmission of X-rays through the test plate. This procedure is an adaptation of the radiographic techniques which have long been used in the medical and industrial fields. Just as the medical profession uses a chest plate to show spatial interrelationships, the location of an X-ray absorbing fluid and a nonabsorbing fluid in a porous medium can be determined by obtaining a photographic record of transmitted X-rays. Moreover, as changes occur in such a system, these changes can be observed by taking successive photographs. Previously,⁵ X-ray methods have been used in fluid flow studies to determine quantitatively the saturation at a given point in the system. The intensity of the transmitted X-rays was measured by an ionization chamber, so that a point by point survey of saturation could be made. In comparison with this earlier quantitative procedure, the photographic procedure which simultaneously observes the saturation at many

¹References given at end of paper.

Manuscript received in the Petroleum Branch office July 31, 1952. Paper presented at the Petroleum Branch Fall Meeting in Houston, Tex., Oct. 1-3, 1952.

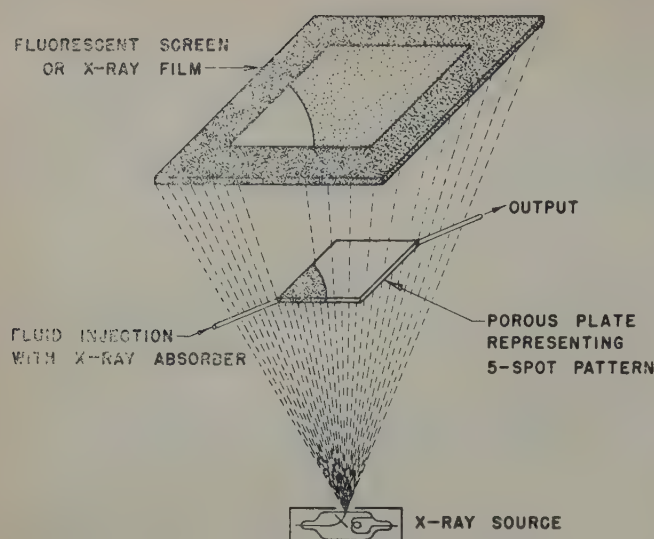


FIG. 1 — X-RAY APPARATUS FOR STUDYING AREAL SWEEPOUT PATTERN.

points obviously lends itself to studying areal effects, particularly when changes are taking place rather rapidly.

The radiographic technique is particularly applicable to the study of samples of uniform thickness. In practice, such a plate is saturated with one phase and displaced with a second — one of the two phases containing the X-ray absorbing material (iodobenzene, potassium iodide, etc.). A uniform field of X-rays is directed against one face of the plate, and a photographic film is mounted behind the plate to record the transmitted X-rays. In this manner those portions of the film directly behind a portion of the sample rich in X-ray absorbing fluid will remain essentially unexposed while the other portions of the film where X-rays have penetrated will be darkened. The developed plate, therefore, shows the relative position of the phases in the area studied. The size of the sample which may be investigated with a single exposure is limited only by the area of the uniform X-ray field and the dimensions of available film.

Quantitative Determination of Saturations From Film Density

Quantitative saturation data at any point in the porous plate being studied may be obtained by utilizing the linear relationship between the optical density of the developed radiograph and the concentration of X-ray absorbing matter in the path of the X-ray beam. This relationship can be derived from a consideration of Lambert's Law and the sensitometric characteristics of X-ray films.⁶

Thus:

$$\frac{I_t}{I_o} = e^{-kx} \text{ — Lambert's Law (1)}$$

$$\text{or } \log \frac{I_t}{I_o} = -kx \log e \text{ (2)}$$

where:

- I_o = Intensity of the incident X-ray beam
- I_t = Intensity of the transmitted X-ray beam
- k = absorption coefficient
- x = thickness of the material
- ρ = saturation of the X-ray absorbing material
- E = relative exposure of the photographic film
- D = optical density of the developed radiograph

In a porous plate of uniform thickness with an X-ray absorbing fluid in one of the fluids present, $-k \log e$ is constant and the thickness of the absorbing material is directly proportional to the saturation of the X-ray absorbing fluid in the porous medium. Therefore:

$$\log \frac{I_t}{I_o} = K\rho \text{ (3)}$$

Since $\frac{I_t}{I_o}$ is the relative exposure, E , given the radiograph:

$$\log E = K\rho \text{ (4)}$$

The relationship between the original exposure and the optical density of the developed radiograph is given by the characteristic curve for the film being used. If the film chosen exhibits a linear relationship between $\log E$ and density (as does Eastman Blue Brand X-ray film) then:

$$D = K'\rho \text{ (5)}$$

for the density interval in which the characteristic curve is a straight line.

Since small differences in either exposure or development change the exact relationship given in equation (5), the step-wedge is included in each radiograph taken. This step-wedge is constructed of aluminum to have, on one end, the same X-ray absorptive capacity as the unsaturated plate and, on the other end, the absorptive capacity of the plate fully saturated with the phase containing the tracer. By these means, the relationship between density and saturation may be determined experimentally for each radiograph taken.

Saturation values obtained by this method have been found experimentally to be accurate to well within plus or minus

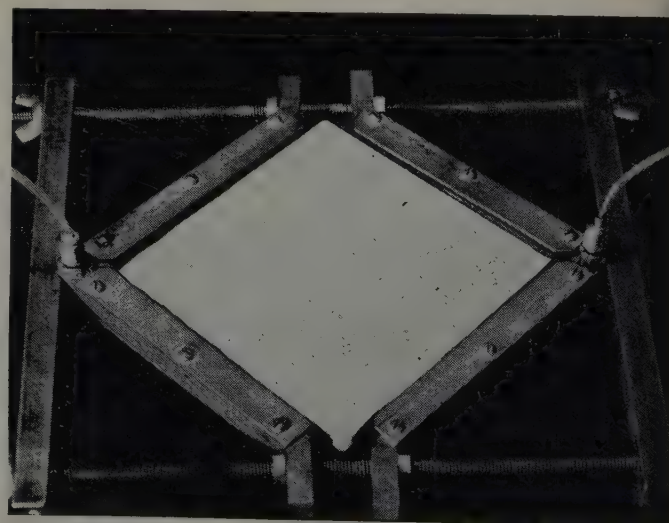


FIG. 2 — POROUS PLATE ASSEMBLY FOR STUDYING FIVE-SPOT FLOODING PATTERNS.

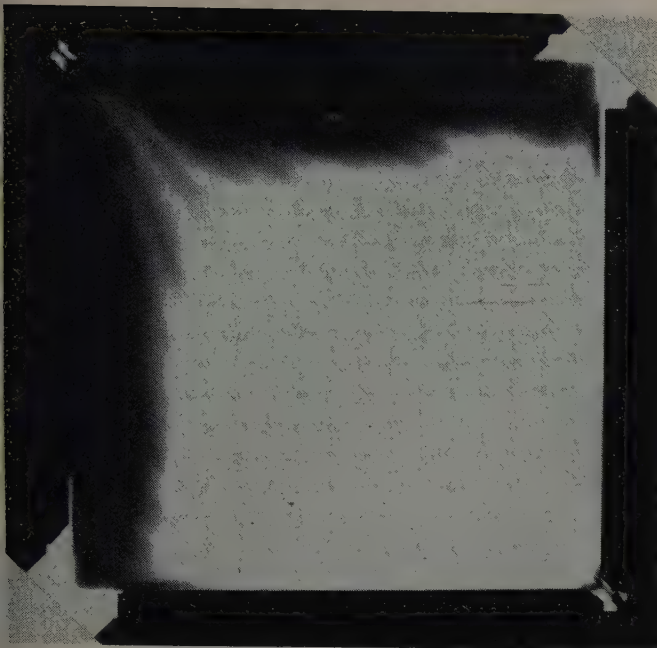


FIG. 3—TYPICAL RADIOGRAPH SHOWING AREAL SWEEPOUT EFFICIENCY FOR THE FIVE-SPOT WELL SPACING. MOBILITY RATIO = 1.

five per cent of the pore volume, and on a given photographic plate saturation differences of one per cent of the pore volume may be detected.

EQUIPMENT, MATERIALS AND PROCEDURE

The X-ray source used was a Westinghouse medical unit rated for 80 kilovolts and 30 milliamperes. The apparatus was arranged as shown in Fig. 1. The X-ray beam was directed vertically through the sample under study to the fluoroscopic screen or X-ray film, and the entire apparatus was suitably enclosed in lead shielding to protect the operator from stray radiation.

The porous media used in the study were of fused Alundum (made by the Norton Co., Worcester, Mass.) fabricated in plate form with a thickness of $\frac{1}{4}$ in. These plates, when cut to the correct dimensions for the well spacing pattern to be studied, were placed in metal holders with rubber gaskets as shown in Fig. 2. All remaining exposed surfaces had been sealed with a ceramic type glaze fused onto the Alundum surface at 2,000°F. (This is a sodium borosilicate glaze containing small amounts of potassium, calcium and aluminum.) Fluids were carried to and from wells in metal fittings which projected through the gaskets.

When the oil phase was selected to absorb X-rays, iodobenzene in concentrations up to 50 per cent by volume was added to a pure hydrocarbon to give the desired absorption of X-rays. Similarly, a solution of potassium iodide in distilled water (Sp. Gr.-1.5) was used when it was more desirable to make the water phase the X-ray absorber.

Eastman Kodak Blue Brand Medical X-ray Film, because of its favorable characteristic curve, was used with calcium tungstate intensifying screens to record the shadowgraph patterns

produced. With the X-ray source at a distance of 30 in. from the film, an exposure of $\frac{1}{2}$ second at five milliamperes and 56 kilovolts was found to produce radiographs with a satisfactory range of densities. The film was developed in accordance with the manufacturer's recommendation. With this technique radiographs such as the one shown in Fig. 3 were obtained.

AREAL SWEEPOUT EFFICIENCIES FOR A FIVE-SPOT WELL SPACING

Areal sweepout patterns which have been obtained in earlier studies have shown that the area swept at breakthrough for a five-spot well spacing is 72 per cent. A listing of both published and unpublished results of sweep efficiencies in the five-spot pattern for unit mobility ratio is as follows:

a. Muskat (early electrolytic method) ¹	75±3%
b. Muskat (early analytical solution) ⁷	72.3%
c. Hurst (analytical solution) ⁸	72.6%
d. Muskat (later analytical solution) ⁷	71.5%
e. Fay and Prats (numerical solution) ³	73 %
f. Aronofsky (unpublished potentiometric results)	70 %

Average 72.2%

These results would apply in a system in which no capillary forces are acting, the displacement efficiency of the flood is 100 per cent, and the viscosity ratio is unity. It was believed that reproducing these conditions using the X-ray shadowgraph technique should give the same areal sweepout pattern and thus serve as a calibration of the newer method.

The square plate shown in Fig. 2 which represents one section of a five-spot pattern was saturated with a non-X-ray absorbing oil which was then displaced at a constant rate with an X-ray absorbing oil of the same viscosity. The two fluids were miscible in all proportions. The X-ray shadowgraph obtained at the time of breakthrough is shown in Fig. 3. The area swept at breakthrough was 69 per cent. These results

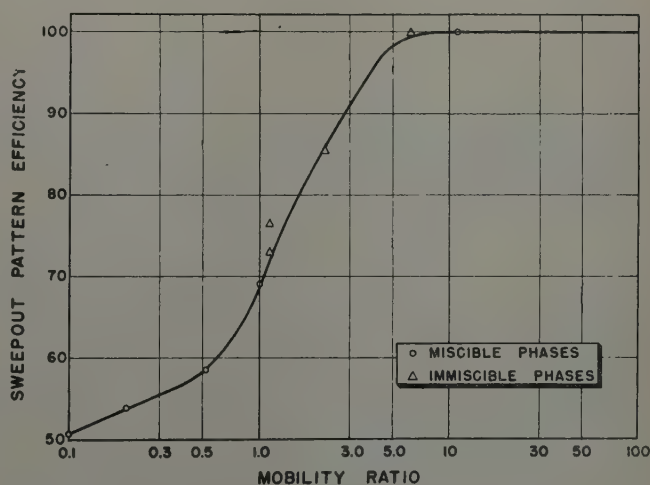


FIG. 4—SWEEPOUT PATTERN EFFICIENCY VS. MOBILITY RATIO FOR THE FIVE-SPOT WELL SPACING.

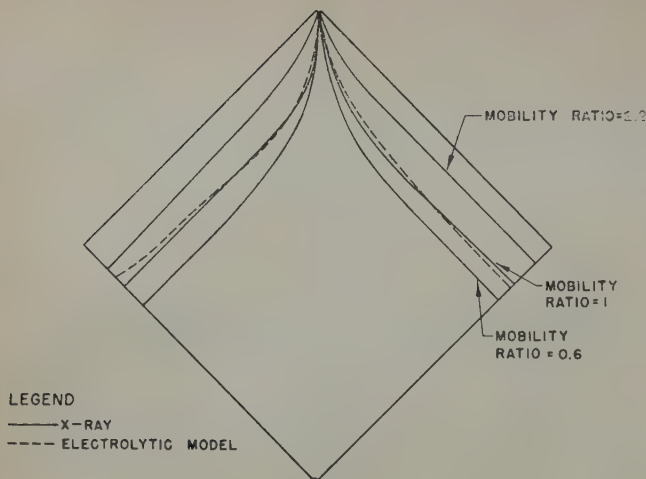


FIG. 5 — AREAL SWEEPOUT PATTERNS, FIVE-SPOT WELL SPACING

indicated that at the only checking point available the potentiometric model and the X-ray technique were in good agreement.

It has been previously established that the areal sweep efficiency is markedly dependent upon the mobility ratio

$$M = \frac{k/\mu \text{ (ahead of the front)}^2}{k/\mu \text{ (behind the front)}}$$

rather than upon the viscosity ratio alone. In the special case where the injected fluid is miscible with the produced fluid the permeabilities ahead of and behind the front are equal and

$$M = \frac{\mu \text{ (behind the front)}}{\mu \text{ (ahead of the front)}}$$

When the miscible fluids used have equal viscosities the mobility ratio is one, and by varying the viscosities of the fluids other mobility ratios may be studied.

Using miscible phases of varying viscosity ratios, areal sweepout efficiencies for the five-spot pattern were determined for mobility ratios between 0.1 and 11.0. The data obtained are shown by the circles plotted in Fig. 4. The curve drawn through these data portrays the effect of mobility ratio on the areal sweepout efficiency at breakthrough of the injected fluid. Areal sweepout efficiencies range from 50 per cent at unfavorable mobility ratios of 0.1 to 100 per cent at mobility ratios of six or better. In the range of mobility ratios between one and three—in which a large number of field water floods fall—substantial benefits in sweepout pattern efficiency can result from moderate increases in mobility ratio.

In order to verify experimentally the role of mobility ratio as determined from relative permeability measurements on the areal efficiency of the test flood, water was injected into the five-spot plate which contained oil and connate water. From the relative permeability curves for the porous material being used, and the average saturation behind the water front, the mobility ratios were determined to be 1.14, 2.15, and 6.2. Two experiments were done at 1.14 mobility ratio. Areal sweepout efficiencies observed for these calculated mobility ratios are also shown in Fig. 4. It may be seen that these data agree within experimental error with the results obtained when miscible phases were used. It should be realized that there is a possible source of error in the relative permeability data used which were determined on a core plug of similar

material. It is felt that the agreement between the two types of displacement studies offers proof of the role of permeability as a factor in determining area sweepout efficiencies. The agreement in these data has also been interpreted as providing justification for the use of miscible phase displacements to determine the effect of mobility ratio on areal sweepout efficiencies.

Typical five-spot breakthrough patterns for a range of mobility ratios are shown in Fig. 5, together with the areal sweepout efficiency for a mobility ratio of one as obtained from electrolytic model studies.¹ It may be seen that the breakthrough pattern for a mobility ratio of one, which was obtained using miscible phases, corresponds closely to that predicted by the electrolytic model.

AREAL SWEEPOUT EFFICIENCIES FOR A STRAIGHT LINE DRIVE

The technique of using miscible phases at various viscosity ratios was also used to study the effect of mobility ratio on areal sweepout efficiencies for a straight line drive type of well spacing in which the ratio of the distance from injection well to producing well to the distance between injection wells is 1.5:1. (Same ratio as used in Reference 2.) Sweepout pattern efficiencies were determined for mobility ratio values from 0.25 to 8.3. Results of these experiments are shown in Fig. 6. The value of 68 per cent areal sweepout efficiency obtained at a mobility ratio of one is considered to be experimental verification of the 71 per cent value estimated from mathematical analyses and electrolytic model studies. A listing of available data on the sweep efficiency for unit mobility ratio for the straight line drive pattern is as follows:

a. Muskat (analytical solution) ¹	70.5%
b. Aronofsky (numerical solution) ²	70.0%
c. Aronofsky (potentiometric method) ²	71.6%
Average	70.7%

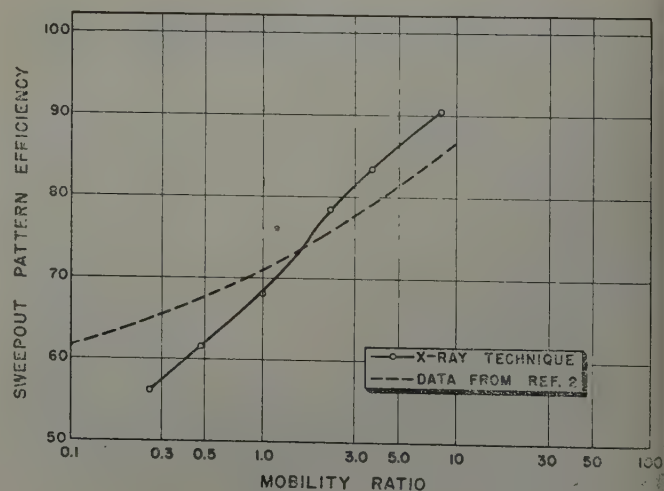


FIG. 6 — SWEEPOUT PATTERN EFFICIENCY VS. MOBILITY RATIO FOR THE DIRECT LINE DRIVE.

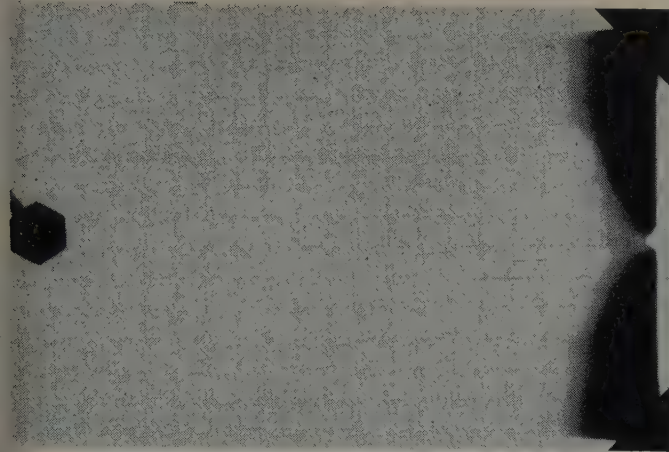


FIG. 7 — AREAL SWEEPOUT PATTERN AT INITIAL BREAKTHROUGH FOR THE STRAIGHT LINE DRIVE. MOBILITY RATIO = 8.3.

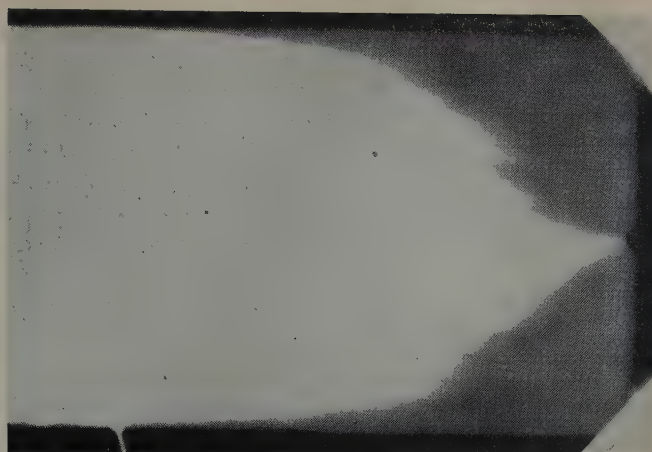


FIG. 8 — AREAL SWEEPOUT PATTERN AT INITIAL BREAKTHROUGH FOR THE STRAIGHT LINE DRIVE. MOBILITY RATIO = 1.0.

It may be noted by comparing Fig. 6 with Fig. 4 that the areal sweepout efficiency for the line drive pattern is less responsive to changes in mobility ratio than is that for the five-spot pattern.

Also shown in Fig. 6 are the sweepout pattern efficiencies obtained by a modified potentiometric model technique.² The discrepancies between these two sets of data are believed to be greater than the possible experimental error in the X-ray technique, and may be due, at least in part, to the stepwise procedures employed in the modified potentiometric model technique.

PROBABLE RELIABILITY OF AREAL SWEEP-OUT EFFICIENCIES OBTAINED BY THE X-RAY TECHNIQUE

In the study of frontal advance patterns with the X-ray technique, the small permeability variations which are usually found in both natural and synthetic porous media causes some sections of the front to advance disproportionately, the net result being the formation of fingers of the invading fluid toward the output well. As might be expected, this phenomenon is more pronounced at low mobility ratios and becomes practically non-existent at mobility ratios above one. Figs. 7, 8 and 9 show the initial breakthrough pattern on a straight line drive section for mobility ratios of 8.3, 1.0, and 0.48 respectively. By comparing these three figures it may be seen that: (1) at the higher mobility ratio (Fig. 7), there is no apparent distortion of the front that could be caused by fingers; (2) at a mobility ratio of one (Fig. 8) there are small fingers which do not influence the pattern unduly; (3) at a mobility ratio of 0.48 (Fig. 9) the fingering is of such an extent that the areal sweepout efficiency measured at this initial breakthrough may be appreciably lower than would be obtained if the frontal advance were uniform.

It would thus appear that the values of areal sweepout efficiency shown in Figs. 4 and 6 are substantially correct for mobility ratios above one, but that the use of the initial breakthrough of the invading phase as the criterion for determining

areal sweepout efficiencies may result in erroneous values for the lower mobility ratios. Errors thus incurred would cause the measured areal sweepout efficiencies to be low and the percentage error would increase (as the amount of fingering increases) with decreasing mobility ratios.

FURTHER APPLICATIONS OF THE RADIOGRAPHIC TECHNIQUE TO FLUID FLOW STUDIES

By the use of specially constructed porous plates, factors which affect areal sweepout patterns other than mobility ratio may be studied such as:

1. The effect of barriers (either natural or artificially formed in the reservoir) upon the area swept at breakthrough.

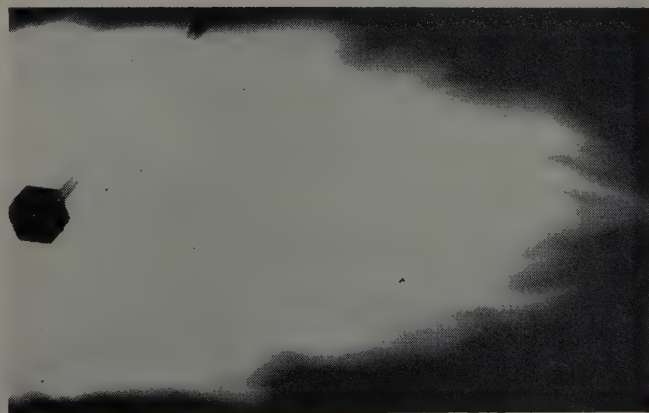


FIG. 9 — AREAL SWEEPOUT PATTERN AT INITIAL BREAKTHROUGH FOR THE STRAIGHT LINE DRIVE. MOBILITY RATIO = 0.48.

2. The effect of horizontal strata of different permeabilities covering all or a part of the reservoir.
3. The effect of permeability variations leading to channeling or by-passing in the reservoir.
4. The effect of fractures and fracture system either surrounding the wells or extending throughout the reservoir.
5. The effect of free gas in the reservoir when an oil bank build-up ahead of the water flood creates a constantly changing mobility ratio during the progress of the flood.

The displacement efficiencies within the area swept can also be studied by the use of the X-ray technique and the method of obtaining saturation data as outlined above. The effect of factors such as viscosity, rate and relative permeability on the displacement efficiency within the area contacted by the flooding fluid may be studied.

CONCLUSIONS

1. A technique using the principles of radiography has been developed which may be used to study the effect of factors which influence the areal sweep efficiency in secondary recovery practices.
2. The extension of this technique to include the determination of the fluid saturation by means of the optical density of the radiographic plate makes possible quantitative studies of displacement efficiencies within the area swept.

3. Studies on five-spot and straight line drive well spacing patterns have shown that areal sweepout efficiencies may vary by as much as 50 per cent of the reservoir area between mobility ratios of 0.1 to 10.0.

REFERENCES

1. Muskat, M.: *The Flow of Homogeneous Fluids Through Porous Media*, McGraw-Hill Book Co., Inc., (1937) Chapter 9.
2. Aronofsky, J. S.: "Mobility Ratio — Its Influence on Flood Patterns During Water Encroachment," *Trans. AIME*, (1952) 195, 15.
3. Fay, C. H., and Prats, M.: "The Application of Numerical Methods to Cycling and Flooding Problems," *Proc. Third World Petroleum Congress*, Section II, (1951), 555.
4. Dyes, A. B.: "Discussion on T.P. 3221," *Trans. AIME*, (1952) 195, 22.
5. Boyer, R. L., Morgan, F., and Muskat, M.: "A New Method for Measurement of Oil Saturation in Cores," *Trans. AIME*, (1947) 170, 15.
6. *Radiography in Modern Industry*, Eastman Kodak Co., X-ray Division.
7. Muskat, M.: *Physical Principles of Oil Production*, McGraw-Hill Book Co., (1949), 659.
8. Hurst, W.: "The Determination of Performance Curve in Five-Spot Water Flood," presented at Oklahoma City Meeting of Petroleum Branch, AIME, October, 1951. ★ ★ ★

BUBBLE FORMATION IN SUPERSATURATED HYDRO-CARBON MIXTURES

HARVEY T. KENNEDY, A AND M COLLEGE OF TEXAS, COLLEGE STATION, TEX., MEMBER AIME, AND CHARLES R. OLSON, OHIO OIL CO., SHREVEPORT, LA., JUNIOR MEMBER AIME

ABSTRACT

In many investigations of the performance of petroleum reservoirs the assumption is made that the liquid, if below its bubble-point pressure, is at all times in equilibrium with gas. On the other hand, observations by numerous investigators have indicated that gas-liquid systems including hydrocarbon systems, may exhibit supersaturation to the extent of many hundred psi in the laboratory. Up to the present, there has been no reliable data on which to judge the actual extent of supersaturation under conditions approaching those existing in petroleum reservoirs.

The work reported here deals with observations and measurements on mixtures of methane and kerosene in the presence of silica and calcite crystals. Bubbles were observed to form on crystal-hydrocarbon surfaces in preference to the glass-hydrocarbon interface or to the body of the liquid. Statistically, it was found that the number of bubbles formed per second per square centimeter of crystal surface was a function of the supersaturation only, and the function was evaluated graphically.

Supersaturations were observed up to 770 psi, under which condition bubbles formed quickly and with considerable violence. With decreasing degrees of supersaturation, the frequency of bubble formation became less, until at 30 psi supersaturation and lower, no bubbles were observed to form, even though the observation at 30 psi was continued for 138 hours. It was found that silica and calcite crystals had identical effects, within experimental error, in accelerating the formation of bubbles, and that small amounts of water and crude oil had no effect on the results.

It is shown that the maximum supersaturation that can exist in a reservoir may be calculated from the data presented and from the area of the rock surface. It is also shown that the number of bubbles formed in the reservoir, in order of magni-

tude, may be calculated for any rate of pressure decline imposed on the reservoir by production. The bearing of the number and distribution of bubbles on reservoir performance is discussed.

INTRODUCTION

A liquid system is supersaturated with gas when the amount of gas dissolved exceeds that corresponding to equilibrium at the existing pressure and temperature. The degree of supersaturation may be conveniently expressed as the difference between the bubble-point of the mixture and the prevailing pressure. Thus, if a mixture having a bubble-point of 1,000 psi at a given temperature exists in single liquid phase at 700 psi at the same temperature, it is supersaturated to the extent of 300 psi.

There are many examples of high supersaturations, mostly in aqueous solutions, reported in the literature. Thus, Kenrick, Wismer and Wyatt¹ showed that water may be saturated with oxygen, nitrogen or carbon dioxide at 100 atmospheres, and the pressure reduced to one atmosphere without producing bubbles immediately. When liquids are in a state of tension, they may be considered as supersaturated at least to the extent of the tension. The tensile strength of water has been reported as 30 atmospheres by Meyer,² 60 atmospheres by Budgett,³ 30 to 50 atmospheres by Temperley and Chambers,^{4,5} 200 atmospheres by Dixon,⁶ and 223 atmospheres by Briggs.⁷

Vincent^{8,9} determined the tensile strength of a mineral oil as 45 psi. Gardescu¹⁰ maintained pressures for short times in a model reservoir at 115 psi below the bubble-point.

It should be noted that the high supersaturations observed were obtained on systems carefully purified to remove particles or surfaces which might promote the formation of bubbles. These "nuclei" were considered as contaminants which interfered with the determination of a property of the liquid. In

¹References given at end of paper.

Manuscript received in the Petroleum Branch office June 10, 1952.
Paper presented at the Petroleum Branch Fall Meeting in Houston, Tex., Oct. 1-3, 1952.

petroleum reservoirs, the mineral and water surfaces with which oil is in contact must be accepted as essential parts of the system under investigation. Further, the data, to be of greatest utility for engineering purposes, should deal quantitatively with the number of bubbles formed in the reservoir under prevailing conditions. It is clear that observations of the maximum supersaturations that can be maintained for unspecified short periods, cannot yield this type of information.

In the direction of developing a quantitative approach to the phenomenon of supersaturation, it was noted that bubbles are always formed on a solid surface rather than in the liquid phase. Their formation appears to be distributed at random both as regards time and location on the solid surface. It would therefore be expected that a sufficiently large number of observations would give, at a fixed supersaturation, a constant average number of bubbles formed per square centimeter of surface per second. This theory of random formation of bubbles is in accord with the wide variation of supersaturations reported in the literature on apparently identical systems, and is supported by the data obtained in this investigation.

EXPERIMENTAL METHOD

Methane used in this investigation was the commercial material, obtained in 1,500 psi cylinders and rated as 96 per cent pure, the impurities being ethane, propane, nitrogen and oxygen. The kerosene had an API gravity of 46.3°, with an average boiling point (10 per cent intervals) of 344°F. The quartz and calcite minerals used were accurately cut from large natural crystals. The crude oil used was from the East Texas Field.

The choice of test methods was complicated by the fact that at high supersaturations, glass was the only solid found which did not accelerate bubble formation. In a steel observation cell, bubbles were observed to form repeatedly at certain points on the steel surface and on the exposed surfaces of the gaskets. The slightest scum on a mercury surface would promote bubble formation at high supersaturations, although no trouble from this source was observed in the lower range of values. However, at low supersaturations, due to the longer periods of observation required, the greater effect of diffusion of gas across gas-liquid boundaries eliminated the possibility of employing such surfaces.

Two methods were therefore employed. In the first method, used at high supersaturations, the system was confined in a glass tube with a gas-liquid contact as an upper boundary. For lower supersaturations, the system was confined above carefully purified mercury. As will be shown later, diffusion was not a factor for the periods of observation required in the first method, while no bubbles were observed to form on the mercury surface in the low supersaturation tests for which the second method was used.

In both methods, filtered kerosene and methane were agitated together in an Aminco mixing bomb for several hours, at 500 psi or 1,000 psi and room temperature. An amount of gas was released that would cause a slight drop in pressure, and shaking continued. A rise in pressure to the original value indicated that saturation was complete. The gas phase was bled off from the mixture at constant pressure, and the pressure then raised to 2,000 psi, to give an unsaturated solution of accurately known bubble-point.

In the first test method, used for high supersaturation values, quartz or calcite crystals were stacked in a test tube within a Penberthy visual cell as shown in Fig. 1. The crystals had rectangular faces of accurately known areas, the total area

for each crystal averaging about 4.5 sq cm. Sufficient kerosene containing no dissolved gas was introduced into the tube to cover the bottom and one-half of the sides of the lowest crystal. The pressure in the cell was then raised to the test pressure, usually 1,000 psi, by introducing methane, and enough saturated kerosene was added to raise the liquid level to the center of the next higher crystal, holding the pressure constant.

A valve, connecting the cell to a fixed and calibrated orifice, was then opened, and the pressure allowed to fall. An electric timer was started when the valve was opened, and the time at which the first bubble appeared was noted. In conjunction with the calibration curve, the time indicated the pressure, and thus the supersaturation pressure, at which the bubble formed. A typical calibration curve is shown in Fig. 2. Where warranted by temperature fluctuations, corrections based on several calibration curves made at different room temperatures, were applied.

The appearance of a bubble terminated a run, since considerable mixing and evolution of gas generally accompanied its formation. To prepare for the next run, the cell was then allowed to fall to atmospheric pressure to desaturate its contents. It was then again brought to the test pressure by the induction of gas, and live kerosene was added until the liquid level rose to the center of the next higher crystal. The pressure was allowed to fall by opening the valve to the calibrated orifice, and the observation repeated. After the glass tube containing the crystals was filled above the top crystal, the tube was emptied, and another set made. Normally, 85 observations constituted a series, which could be analyzed

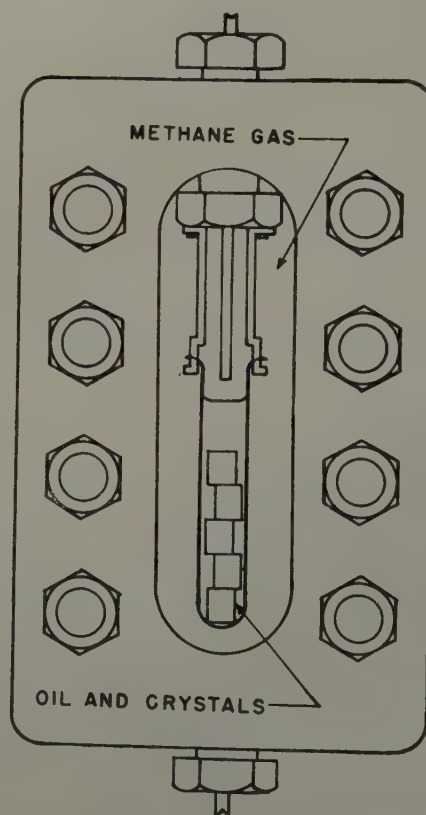


FIG. 1 — WINDOWED CELL FOR HIGH SUPERSATURATION TESTS.

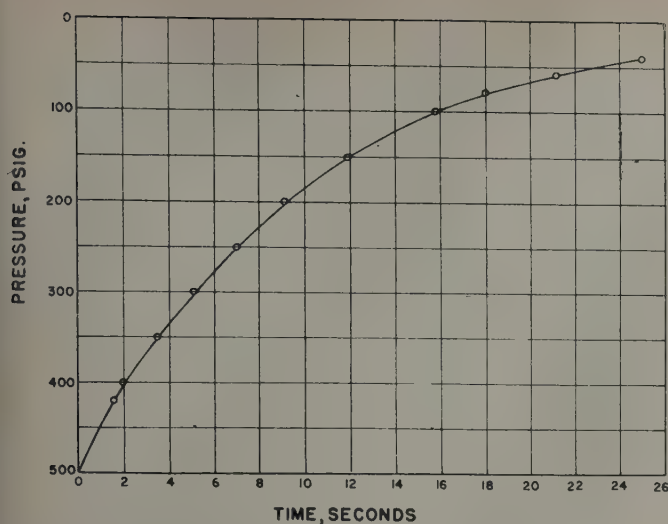


FIG. 2 — TYPICAL ORIFICE CALIBRATION CURVE.

statistically. On one series (Series E), in which the crystal area was twice the usual area, 170 observations were made to provide more points in the high supersaturation range.

The data desired from this method were (1) the number of bubbles formed in a definite narrow range of supersaturation values, (2) the total number of seconds during which the system was in this range, and (3) the area of crystal-oil interface involved. To obtain (1), the supersaturation ranges were selected to correspond to two-second intervals on the orifice calibration curve, and the number of bubbles observed in each of these intervals totaled. To obtain (2) for a given interval, two seconds for each test that went through the interval were added to the time spent in the interval by those tests terminating in the interval; (3) was determined as the average crystal-oil area for the tests terminating in the interval involved.

An example of the calculation of the number of bubbles formed per second per square centimeter (termed the frequency) by this method follows. In the interval zero to two seconds, corresponding to the supersaturation range of 0-95 psi supersaturation, no bubbles were formed and the frequency is zero. In the interval two to four seconds, corresponding to 95-165 psi supersaturation, nine bubbles were formed, and 76 tests passed through the interval without forming bubbles. The actual time spent in the interval in those tests terminated by bubble formation in the interval is shown in the first nine terms in the first bracket of the denominator below.

$$F = \frac{9}{[1.1+1.2+0.9+1.5+0.3+1.4+0.7+1.5+0.6 + (76) 2] [4.47]} = 0.0125$$

The term 4.47 represents an average of the crystal areas exposed to live oil. The frequency, thus determined, represents the probability that a bubble will form in one second on one square centimeter of crystal surface, at the average supersaturation in the interval.

In the second method, employed where the degree of supersaturation was so low that long times of standing were required, mixtures were confined above mercury as shown in Fig. 3. In order that no reaction products between kerosene

and mercury could be formed and act as nuclei, the kerosene was distilled over sodium. After this precaution was taken no bubbles formed on the mercury surface.

In determining the frequency of bubble formation by this method the cell was assembled as shown in Fig. 3 with a single crystal inside the glass tube. The cell was then evacuated to less than 1 mm mercury pressure and purified mercury was drawn into the cell through the bottom connection until the inverted test tube was completely immersed in and filled with mercury. Water was then pumped into the top of the cell, with mercury being withdrawn from the bottom, until the test tube could be observed to a position well below the crystal, which had floated to the top of the test tube. The pressure in the cell was then adjusted to 1,000 psi which was 500 psi above the bubble-point of the mixture. A sample of kerosene-methane mixture was then introduced into the open lower end of the test tube, and then collected above the mercury.

Then the pressure on the system was lowered by bleeding off water from the top of the cell until the desired supersaturation was reached. The system was then allowed to stand until a bubble was observed to form, or in one case, until 138 hours had elapsed without bubble formation. After a bubble had been observed, the pressure was quickly raised to 1,700 psi, so as to redissolve the bubble before appreciable diffusion had taken place. One filling could thus be used for a number of tests without refilling the tube.

To correct for small variations of bubble-point with temperature, which could not be considered as negligible in this method, the magnitude of the bubble-point variation was

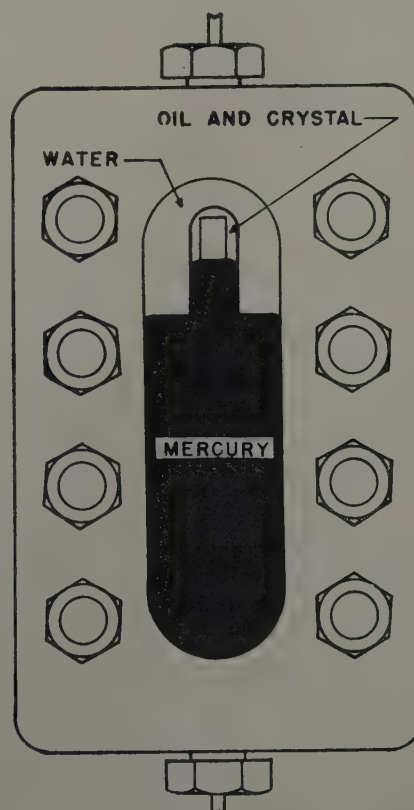


FIG. 3 — WINDOWED CELL FOR LOW SUPERSATURATION TESTS.

estimated by using available *K*-value charts for methane in a 200 molecular weight solvent. Correction was then applied by raising or lowering the pressure in the cell to keep the supersaturation of the liquid constant.

The frequency, as measured by this method, was simply the reciprocal the time which elapsed at a given supersaturation before a bubble was observed, divided by the crystal area.

DISCUSSION OF RESULTS

At any vapor-liquid interface in a supersaturated system vaporization is taking place. In the first method employed, such an interface existed and it was necessary to determine what influence, if any, this process exerted on the measured frequencies. To this end, two series of tests, "A" and "B," were run, the first involving an initial rate of pressure decline of 55 psi per second, while the initial pressure decline rate for Series "B" was 30 psi per second. If the loss of gas at the interface were effective in lowering the supersaturation, it should be more pronounced in the second series, and the frequency of bubble formation should be lower. Reference to Tables I and II, and to Fig. 4, in which the average frequencies for all series are plotted against the supersaturation, shows no effect in this direction. All subsequent runs by Method 1 were made with pressure decline rates higher than those used in Series "B," so as to eliminate the possibility of this source of error.

Both Series "A" and "B" were made with kerosene saturated with methane at 500 psi in the presence of quartz crystals. The temperature of saturation and testing ranged from 84°F to 86°F. As in the other series investigated, the errors introduced by this variation did not exceed others inherent in the method and no correction for temperature was applied.

Series "C" was made with a mixture of kerosene and methane with a bubble-point of 1,000 psi, to determine the effect of absolute saturation pressure on bubble frequency. The data are contained in Table III and are plotted in Fig. 4. It is seen that, within the error involved in statistical observations of this type, there is no difference between liquids of different bubble-point at the same supersaturation. The crystals used in this series were quartz, as in the two previous series.

Series "D" was made with 1,000 psi bubble-point oil, and in all respects was similar to Series "C" except that calcite crystals were substituted for quartz. The data are shown in Table IV and are plotted on Fig. 4. It is seen that the composite curve drawn fits the data of this series as well as the previous data, and that calcite must be considered as equivalent to quartz as an accelerator of bubble formation.

In Series "E," a volume of saturated oil sufficient to cover twice the area of crystal as in previous tests was introduced. In other respects the runs were identical with those of Series "D." An examination of Table V, and the points for this series plotted on Fig. 4, indicates that the frequency of bubble formation, in terms of bubbles formed per second per square centimeter of crystal surface, is comparable to that obtained in the other runs. In order that sufficient data for statistical purposes should be available, twice as many runs as usual were made under the conditions of this series.

Undiluted crude oil could not be used in the tests described, because its dark color interfered with the observation of bubbles. However, it was thought possible that nuclei might be present in crude oil and might influence the frequency

Table I—Summary of Test Data for Series "A"

Time Interval Sec.	Average Supersaturation psi	No. Bubbles Observed	Bubble Frequency Bubbles/cm ² /sec x 100
0-2	48	0	0
2-4	130	9	1.25
4-6	194	13	2.08
6-8	249	16	3.34
8-10	295	14	3.50
10-12	333	9	3.44
12-14	364	7	3.79
14-16	391	6	4.96
16-18	412	4	5.14
18-20	427	3	6.04
20-22	439	2	6.21
22-24	449	0	0
24-26	458	1	10.15

Table II—Summary of Test Data for Series "B"

Time Interval Sec.	Average Supersaturation psi	No. Bubbles Observed	Bubble Frequency Bubbles/cm ² /sec x 100
0-2	32	0	0
2-4	86	0	0
4-6	129	7	.962
6-8	166	10	1.52
8-10	197	9	1.55
10-12	227	11	2.26
12-14	254	11	2.86
14-16	278	8	2.68
16-18	301	8	3.52
18-20	321	7	4.30
20-22	338	5	4.76
22-24	354	3	5.20
24-26	369	3	7.89
26-28	382	1	3.99
28-30	394	1	6.38
30-32	405	1	44.7

Table III—Summary of Test Data for Series "C"

Time Interval Sec.	Average Supersaturation psi	No. Bubbles Observed	Bubble Frequency Bubbles/cm ² /sec x 100
0-2	80	0	0
2-4	216	10	1.39
4-6	318	21	3.68
6-8	406	22	5.22
8-10	484	15	7.26
10-12	550	9	7.51
12-14	609	5	12.85
14-16	663	2	15.96
16-18	709	0	0
18-20	747	1	18.61

data obtained. In Series "F," therefore, the maximum amount of East Texas crude oil which would still allow visibility, 1.6 per cent, was added to the system. Other conditions were the same as in Series "E," i.e., 1,000 psi bubble-point oil in contact with calcite. As shown in Table VI and Fig. 4, there is no discernible effect of the addition of crude oil to the system.

Data on frequencies at supersaturations below 50 psi, where effects of diffusion at the gas-liquid interface were considered to render results by the first method of investigating unreliable, are shown in Table VII. The frequencies are also

Table IV—Summary of Test Data for Series "D"

Time Interval Sec.	Average Supersaturation psi	No. Bubbles Observed	Bubble Frequency Bubbles/cm ² /sec x 100
0- 2	80	0	0
2- 4	216	14	2.01
4- 6	318	17	3.08
6- 8	406	18	4.71
8-10	484	16	6.63
10-12	550	12	9.95
12-14	609	5	10.25
14-16	663	2	12.09
16-18	709	0	0
18-20	747	0	0
20-22	778	1	76.5

Table V—Summary of Test Data for Series "E"

Time Interval Sec.	Average Supersaturation psi	No. Bubbles Observed	Bubble Frequency Bubbles/cm ² /sec x 100
0- 2	81	0	0
2- 4	220	43	1.69
4- 6	322	51	2.98
6- 8	406	42	4.68
8-10	481	21	6.15
10-12	548	8	7.68
12-14	605	4	11.13
14-16	656	1	16.46

Table VI—Summary of Test Data for Series "F"

Time Interval Sec.	Average Supersaturation psi	No. Bubbles Observed	Bubble Frequency Bubbles/cm ² /sec x 100
0- 2	81	0	0
2- 4	220	12	1.71
4- 6	322	18	3.13
6- 8	406	20	4.98
8-10	481	17	7.71
10-12	548	9	8.49
12-14	605	4	7.85
14-16	656	4	14.2
16-18	700	1	17.2

Table VII—Summary of Low Supersaturation Tests by Second Method

Supersaturation psi	Dry Quartz Crystal				Water-Wet Crystal			
	No. Bubbles Observed	Time Before First Bubble, Sec.			No. Bubbles Observed	Time Before First Bubble, Sec.		
50	10	36.3-87.2	56.7		10	39.1-77.2	58.1	
40	4	104-600	287.4		6	102-343	236.5	
30	None in 138 hours				None in 27 hours			

plotted on Fig. 4. As indicated in the table, 14 observations on dry quartz crystals were made and 16 on quartz crystals which had been wet with water. It is seen that the presence of water has no discernible effect. It should also be noted that the data obtained by this method fit very well on the composite curve obtained by the method employed for investigation systems of high supersaturation. The conformity of the data by the two methods in the region of low supersaturation is further evidence that the error due to diffusion in the first method is not appreciable under the conditions employed.

The composite curve shown in Fig. 4 was drawn as the best curve to fit all of the data obtained. It is of interest to note, however, that this curve fits the points for each series almost as well as any that could be drawn.

SIGNIFICANCE OF DATA IN PETROLEUM RESERVOIR STUDIES

In the work described, an effort was made to duplicate the essential conditions which affect the formation of bubbles in petroleum reservoirs, insofar as these conditions are known. It is appropriate, therefore, to discuss some of the implications of the results in regard to a reservoir to which they may apply.

When oil is produced from a reservoir, the pressure normally declines, even if an effective water-drive is present. Some reservoirs, such as the East Texas reservoir, are so undersaturated, that substantially their entire recoverable contents may be produced at restricted rates without the pressure falling below the bubble-point of the oil. More commonly, however, the oil becomes supersaturated in the early stages of production, even though it may have been highly undersaturated initially.

On the basis of data presented here, bubbles would be expected to form only after the supersaturation exceeds 30 psi. Supersaturation in excess of this figure and bubbles will naturally occur first in the low-pressure regions in the immediate vicinity of the producing wells. Because of the comparatively high velocities and intimate contact between gas and oil, substantial equilibrium should exist between the two phases at this location under normal flowing conditions.

As the reservoir pressure declines, and the isobar corresponding to 30 psi supersaturation moves outward from the wells, bubble formation will follow it. If the reservoir oil is uniform in composition and subject to normal gravitational pressure distribution, the surfaces connecting the bubbles farthest from the wells will be an inverted and truncated cone, with sides of constant slope. The expanding cone will follow the isobar to the limit of the reservoir or to the region of interference with another well.

When a bubble is formed, diffusion of gas from the surrounding oil begins, decreasing the supersaturation in its immediate vicinity and expanding the bubble. Surface forces, tending to compress the bubble, become negligible when its radius exceeds about .01 mm. (If the surface tension is taken as five dynes per centimeter, and bubble radius, or the radius of the pore through which the bubbles are expanding, is .01 mm the excess pressure in the bubble is only .15 psi.) Due to the phenomenon of supersaturation, the equilibrium pressure of the gas dissolved in the oil is at least 30 psi higher than the pressure inside the bubble initially, and rapid evolution of gas occurs. This situation accounts for the observation that bubbles expand to about 1 mm in radius almost instantly after they are formed on crystal surfaces.

Aspects of reservoir behavior on which the data presented may shed some light may be listed as follows:

1. The extent to which reservoir fluids may be considered to be truly at equilibrium. This is a function of the number of bubbles formed and the rate of diffusion from the oil into the gas phase as well as the rate of pressure decline imposed by production from the reservoir.

2. The order of magnitude of the number, size and distribution of bubbles formed in reservoirs.

As a first step in estimating the departure from equilibrium, the maximum supersaturation possible in the reservoir may

be estimated. It is evident that this maximum will occur in the early life of the reservoir as bubbles are forming, rather than at a later date when concentration gradients have been lowered by diffusion. As an example, consider a reservoir rock with a surface area of 450 sq cm per cu cm. (The unit area assumed corresponds to a rock made up of spheres .01 cm in diameter with rhombohedral packing.) From the slope of the frequency curve, Fig. 4, we may estimate the bubble frequency, as the curve approaches its intercept, as 10^{-4} bubbles per second per square centimeter per psi supersaturation. Thus, if a supersaturation of only 31 psi could persist for one day, more than four thousand bubbles would be formed in each cubic centimeter of rock. The aggregate volume of gas, if each bubble were the equivalent of one mm in diameter, would be more than twice the entire rock volume. It is clear, therefore, that the maximum supersaturation is less than one psi in excess of the intercept value on Fig. 4, and differs from this value by less than the uncertainty in our measurement of the intercept. The intercept value of 30 psi will therefore be taken as the maximum value of supersaturation that can exist more than momentarily in a reservoir.

It should be noted that while 30 psi represents the maximum supersaturation in a reservoir, the reservoir as a whole will

never have an average supersaturation approaching this figure. While bubbles are forming in one position, oil in contact with bubbles already formed in another position will be substantially at equilibrium with them. If the reservoir pressure remains constant for a time, the oil and gas phases will approach complete equilibrium due to diffusion. If the pressure is declining at a uniform rate, supersaturation in excess of 30 psi and bubble formation will occur only if the diffusion rate into bubbles already formed is insufficient to prevent such supersaturations at all points. We thus have a criterion and a means of determining the number of bubbles that is necessary and sufficient to provide the amount of diffusion required for a given rate of pressure decline. This requirement may be expressed

$$\frac{dp}{dt} = \frac{dp_s}{dt} = \frac{Q}{V_o} \cdot \frac{dp_s}{ds} \quad \dots \dots \dots (1)$$

where $\frac{dp}{dt}$ is the rate of pressure decline imposed by production from the reservoir;

$\frac{dp_s}{dt}$ is the rate of decline of saturation pressure due to

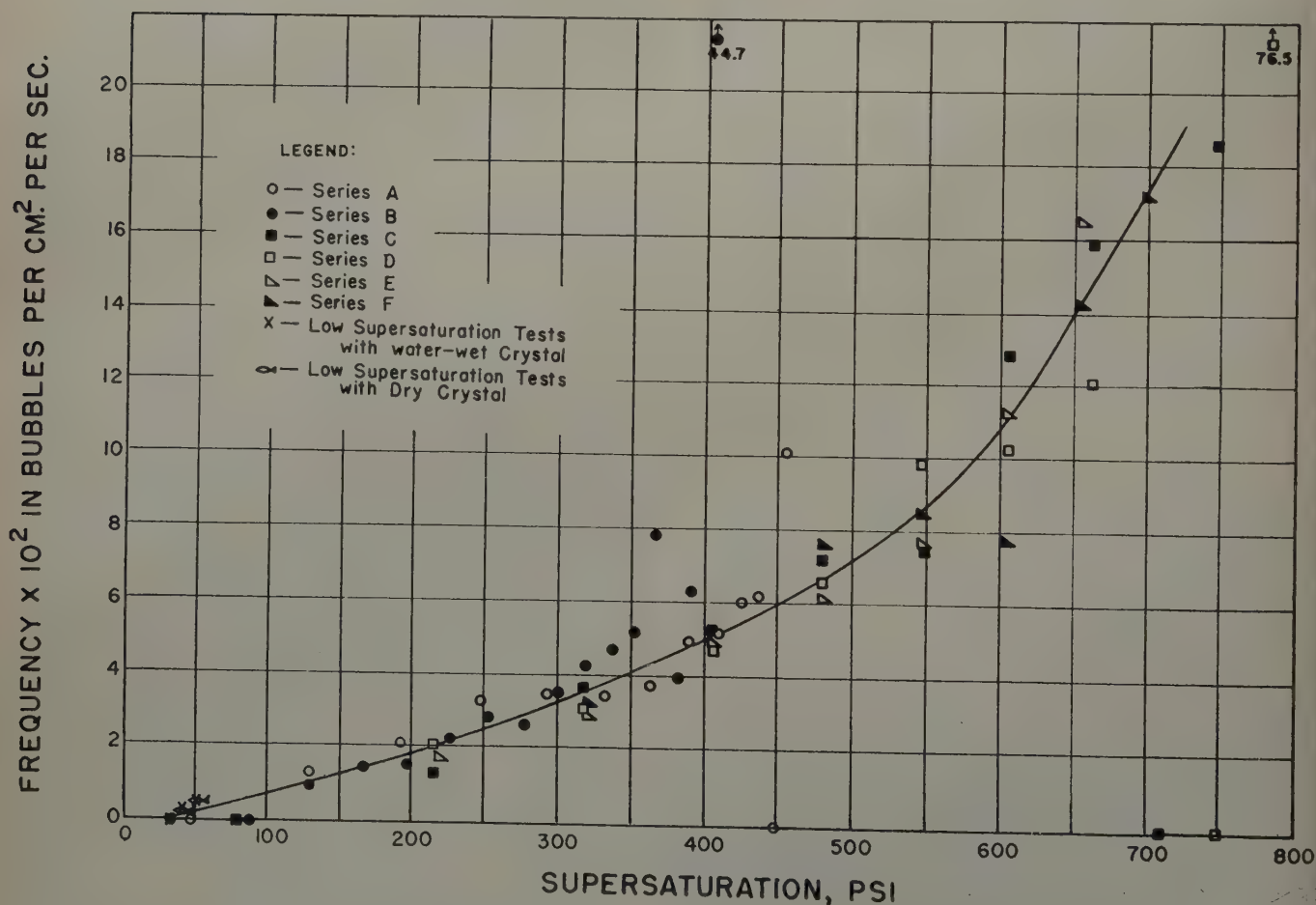


FIG. 4 — COMPOSITE BUBBLE FREQUENCY CURVE.

PETROLEUM TRANSACTIONS, AIME

diffusion at the point in the region of influence of a bubble farthest removed from the bubble;

Q is the volume of gas, in surface measure, which diffuses through the volume V_o of oil in unit time;

$\frac{dp_s}{ds}$ is the decrease in equilibrium pressure due to the evolution of unit volume, in surface measure, of dissolved gas.

In determining the number of bubbles required to reduce the maximum saturation pressure at a rate equal to the reservoir pressure decline, steady state spherical flow is assumed. As shown by Bertram and Lacey,¹¹ the entire effect of the reservoir rock on diffusion may be expressed as a factor of about 0.8, representing the increased length of path attributable to the presence of the aggregate. (The truth of this statement is evident when it is remembered that both the amount of diffusible gas and the cross section available for diffusion are decreased by a factor representing the fractional porosity. Except for the above correction, therefore, the presence of the reservoir rock will be ignored.)

We may write, for each bubble in the reservoir,

$$Q = 0.8 \frac{4\pi D (S_o - S_b)}{\frac{1}{r_b} - \frac{1}{r_o}} \quad (2)$$

where D is the diffusion constant, and r_b and r_o are respectively the radius of the bubble and of the region of influence of the bubble, and S_b and S_o are the concentrations of gas at r_b and r_o , respectively. Each cubic foot of the reservoir may be assumed to contain N bubbles, each of which has a region of influence comprising $\frac{1}{N}$ cu ft. r_o may be expressed in terms of N as

$$r_o = \sqrt{\frac{3}{4\pi N}} \quad (3)$$

V_o in equation (1) is simply $\frac{1}{N} = \frac{4}{3} \pi r_o^3$.

Equations (1), (2) and (3) may then be combined to give

$$\frac{dp}{dt} = \frac{dp_s}{dt} = \frac{3.2\pi ND(S_o - S_b)}{\frac{1}{r_b} - \sqrt{\frac{4\pi N}{3}}} \frac{dp_s}{ds} \quad (4)$$

If the relation between the saturation pressure, p_s , and the gas dissolved at this pressure S , be linear, then $\frac{S}{p_s} = K_s$, and

$$S_o - S_b = K_s(p_{se} - p_{sb})$$

where K_s is the slope of the pressure-solubility curve, and p_{se} and p_{sb} are respectively, the equilibrium pressures at r_o and r_b . Further, $\frac{dp_s}{ds}$, for a linear solubility relation, may be

represented by $\frac{1}{K_s}$. For a reservoir in which the maximum supersaturation is 30 psi, the maximum value of $K_s(p_{se} - p_{sb})$

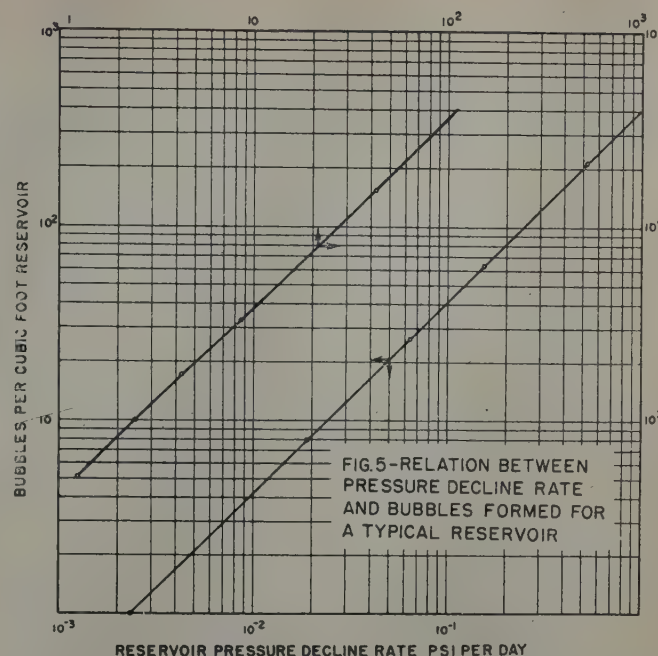


FIG. 5—RELATION BETWEEN PRESSURE DECLINE RATE AND BUBBLES FORMED FOR A TYPICAL RESERVOIR.

must equal $30 K_s$. As a final equation, relating the number of bubbles with the rate of pressure decline, we may write

$$\frac{dp}{dt} = \frac{dp_s}{dt} = \frac{96\pi ND}{\frac{1}{r_b} - \sqrt{\frac{4\pi N}{3}}} = \frac{301 ND}{\frac{1}{r_b} - \sqrt{4.2N}} \quad (5)$$

If, in accordance with our observation that bubbles almost instantly reach the radius of 1 mm we assign this value to r_b , and let D equal 10^{-4} sq ft per hour as an average value,¹² we may calculate the number N for a typical reservoir, for any value of $\frac{dp}{dt}$. Fig. 5 shows a plot of N against the right-hand term of Equation (5). For reservoir pressure declines of 0.1, 1 and 10 psi per day, we may read corresponding numbers of bubbles per cu ft of reservoir satisfying the imposed conditions 40, 400 and 4,000. Due to the assumptions made in determining the diffusion rate, particularly the assumption of the value of r_b , the calculation must be considered correct only as to order of magnitude.

For a rock consisting of grains averaging 0.1 mm in diameter, there are about 10^9 pores per centimeter cube, or some $3 \cdot 10^{10}$ pores per cu ft. It is clear that even at the most rapid reservoir pressure decline rates, only about one pore in a million will have a bubble originating in it. Where unaffected by flow, the gas will be present as a continuous enlarged bubble, encompassing many pores, surrounded by oil which is free of gas. When gradients are applied, the gas inside the continuous bubble will flow with a relative permeability characteristic of a much higher gas saturation than corresponds to the overall reservoir content, while the oil will be characterized by a relative permeability equal to the homogeneous fluid permeability of the rock. Equilibrium gas saturations,

at which gas exhibits zero relative permeability, should not exist in a reservoir with gas distributed in this manner. It is noteworthy that such behavior, although detectable by a decline in gas/oil ratio in the early life of gas-drive reservoirs and generally reported in laboratory studies, has been reported absent in all field measurements.¹³

CONCLUSIONS

The data and calculations presented support the following conclusions:

1. Supersaturations as high as 770 psi are possible for short periods in a system consisting of kerosene, methane and crystals such as silica and calcite.

2. When crystals such as silica or calcite are present, bubbles invariably form on their surfaces rather than in the oil itself.

3. The tendency of bubbles to form in systems of this kind may be measured by the frequency, *i.e.*, the number of bubbles formed per second per square centimeter of crystal surface in contact with liquid.

4. Under the conditions of the tests, the frequency varied from .22 at 800 psi to zero at 30 psi saturation. No bubbles were observed to form at 30 psi supersaturation or lower, even though the test at 30 psi supersaturation was continued for 138 hours.

5. Calcite and silica surfaces are equally effective in promoting bubble formation.

6. The presence of water or crude oil, when added to the above system, had no measurable effect on bubble frequency.

7. From the bubble frequency measured, it may be calculated that maximum supersaturations in reservoirs cannot exceed 30 psi by more than a fraction of one psi, and that average supersaturations will be substantially less than this amount.

8. It is shown that the number of bubbles formed per cu ft of reservoir depends on the rate of diffusion of gas through oil and on the pressure decline rate imposed by production. For decline rates of 0.1, 1 and 10 psi per day, the number of bubbles formed will be 40, 400 and 4,000 per cu ft respectively, in order of magnitude.

9. Even at the higher rates of pressure decline, only one bubble is formed per million pores in the rock, suggesting that the increase of gas saturation in reservoirs takes place by the enlargement of gas bubbles into gas masses encompassing many rock pores.

10. Variations in the manner in which gas is distributed in permeable media may account for different relative perme-

abilities for the same gas saturation, and may explain discrepancies between laboratory and field data on the same type of rock.

ACKNOWLEDGMENT

It is a pleasure to acknowledge the financial support of the Tennessee Gas Transmission Co., under whose fellowship this work was done, and the encouragement given by Herman A. Otto and O. H. Moore of this company. The interest taken in this project and the advice freely given by Harold Vance, head of the petroleum engineering department, A. and M. College of Texas, is also gratefully acknowledged.

REFERENCES

1. Kenrick, F. B., Wismer, K. L., and Wyatt, K. S.: "Supersaturation of Gases in Liquids," *J. Phys. Chem.*, (Dec., 1924), 28, 1308.
2. Meyer, J.: *Zeits f. Electrochemic*, (1911), 17, 743.
3. Budgett, H. M.: "The Adhesion of Flat Surfaces," *Proc. Roy. Soc.*, London, (1912), A-86, 25.
4. Temperley, H. N. V., and Chambers, L. G.: "The Behavior of Water under Hydrostatic Tension, Part I," *Proc. Phys. Soc.*, London, (July, 1946), 58, 420.
5. Temperley, H. N. V.: "The Behavior of Water under Hydrostatic Tension, Part II," *Proc. Phys. Soc.*, London, (July, 1946), 58, 436.
6. Dixon, H. H.: "On the Tensile Strength of Sap," *Proc. Roy. Soc.*, Dublin (1914), 14, 229.
7. Briggs, L. J.: "A New Method for Measuring the Limiting Negative Pressure in Liquids," *Science*, (April 29, 1949), 109, 440.
8. Vincent, R. S.: "Measurement of Tension in Liquids by Means of a Metal Bellows," *Proc. Phys. Soc.*, London, (1941), 53, 126.
9. Vincent, R. S.: "The Viscosity Tonometer—A New Method of Measuring Tension in Liquids," *Proc. Phys. Soc.*, London, (1943), 55, 41.
10. Gardescu, I. I.: "Experiments on Natural Gas in Oil Sand," *Oil and Gas Jour.*, (Feb. 25, 1932), 30, (41), 22.
11. Bertram, E. A., and Lacey, W. N.: "Rates of Solution of Gases in Oils," *Ind. and Eng. Chem.*, (March, 1936), 28, 316.
12. Hill, E. S., and Lacey, W. N.: "Rate of Solution of Propane in Quiescent Liquid Hydrocarbons," *Ind. and Eng. Chem.*, (Dec., 1934), 26, 1327.
13. Muskat, Morris: *Physical Principles of Oil Production*, McGraw-Hill Book Co., Inc., (1949), 464. ★ ★ ★

PHASE AND VOLUMETRIC BEHAVIOR OF NATURAL GASES AT LOW TEMPERATURES

T. L. GORE, STANDARD OIL CO. (INDIANA), SUGAR CREEK, MO.; P. C. DAVIS, ETHYL CORP., BATON ROUGE, LA., AND F. KURATA, UNIVERSITY OF KANSAS, LAWRENCE, KANS.

ABSTRACT

An experimental method and apparatus for the study of the low-temperature phase and volumetric behavior of volatile mixtures are described. The phase diagrams, including the critical points, and the volumetric behavior of a natural gas and a mixture of the natural gas with methane at temperatures from -40°F to -200°F and pressures to 1,200 psi are given.

INTRODUCTION

Knowledge of the phase and volumetric behavior of mixtures of the light hydrocarbons at low temperatures is becoming increasingly important as interest in low-temperature separation processes increases. Distillation at low-temperatures has been used for some time to recover ethane and ethylene from natural gas and refinery gas for petrochemical uses. Removal of excess nitrogen from natural gas by distillation has been proposed as a means of increasing the capacity of gas transmission lines and of improving the marketability of the gas.^{5,20} Evaluation of the latter process has been hampered, however, by the scarcity of data from which the phase behavior of natural gases at low temperatures might be predicted. While existing correlations of vaporization equilibrium constants may be used to predict the behavior of such mixtures

at lower pressures, high-pressure computations often require knowledge of the location of the critical point of the system involved. Although correlations have been developed^{17,22} for the prediction of the critical temperature and pressure of certain types of hydrocarbon systems, they do not apply to very volatile systems such as nitrogen-bearing natural gases. This paper describes the initial stages of an investigation of the low-temperature behavior of a number of natural gases and other gases of commercial interest. The experimental method and apparatus are described, and the phase and volumetric behavior of a natural gas and a mixture of the natural gas with methane are presented.

PREVIOUS WORK

The published low-temperature vapor-liquid equilibrium data for hydrocarbons and mixtures of hydrocarbons with nitrogen and helium are listed in Table I. Most of these data are for binary systems, and the data of Stutzman and Brown²⁴ at 100 psi are the only data on a natural gas. The data of Bloomer and Parent³ on the methane-nitrogen system, which have been published since this study was completed, are a valuable addition to the knowledge in this field. Prior to the publication of these data the only published critical point data on systems having critical temperatures below the ice point were those of Ruhemann,²¹ on the methane-

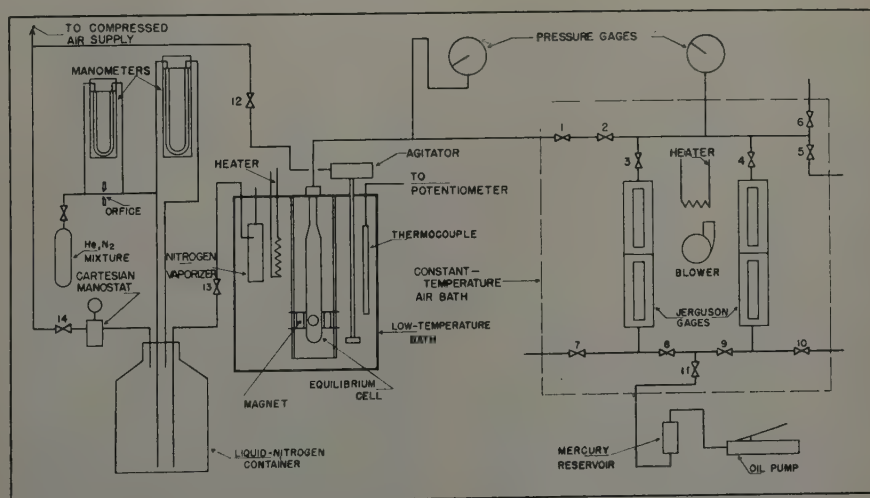


FIG. 1 — FLOW DIAGRAM OF APPARATUS

⁵References given at end of paper.
Manuscript received in the Petroleum Branch office April 29, 1952. Paper presented at the Petroleum Branch Fall Meeting in Houston, Tex., Oct. 1-3, 1952.

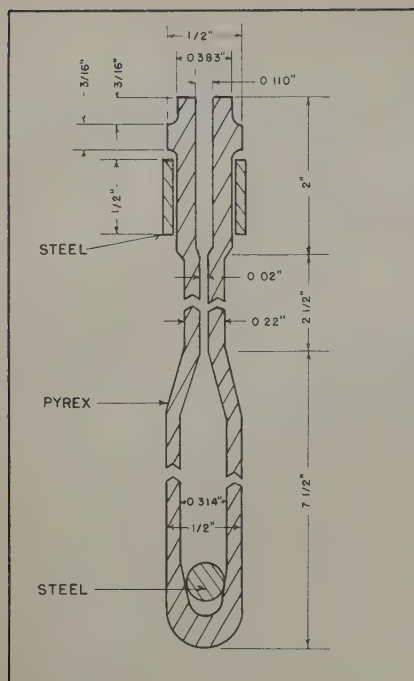


FIG. 2—CROSS-SECTION OF EQUILIBRIUM CELL

ethane system, and those of Eilerts, *et al.*,⁷ on a gas-condensate system. These data alone were not sufficient to allow accurate estimation of the critical behavior of the very volatile systems of engineering interest. While the publication of complete data on the methane-nitrogen system has done much to ease this problem, it is felt that additional data on more complex mixtures are still of considerable value.

EXPERIMENTAL METHOD

The experimental method selected for this study is a modification of the dew-point bubble-point method used previously^{13,17,7} at higher temperatures. In the usual application, a sample of the gas mixture, of known composition, is placed in a glass vessel maintained at constant temperature, and the pressure on the system is increased by introducing mercury, or an alloy of mercury and gallium, into the vessel. As the pressure is thus increased the mixture is caused to pass through its dew and bubble points, and these limits of the two-phase region are determined by visual observation. The freezing point of the mercury-gallium alloy

limits this method of pressure variation to temperatures above -70°F . In the method described here, the pressure variation is accomplished by increasing the mass of sample contained in a cell of constant volume.

The dew-point bubble-point data resulting from this method can be analyzed to yield the equilibrium constants of the components of the mixture only if the mixture is binary. The method was chosen for this study of more complex mixtures because it permits precise location of the critical point of the mixture, because it decreases the number of analyses required, and because it allows concurrent determination of the volumetric behavior of the system. The dew-point bubble-point data, while not reducible to equilibrium constants, are still of value, since they offer a means of checking equilibrium constants predicted by generalized correlations.

APPARATUS

A flow diagram of the apparatus is shown in Fig. 1. The phase separation occurs in a glass cell of about 12 ml volume which is suspended in a bath of pentane contained in a glass Dewar flask. Unsilvered strips on opposite sides of the flask allow observation of the contents of the equilibrium cell. The pentane bath is cooled by a stream of liquid nitrogen delivered from a metal Dewar flask by controlled air pressure. The temperature of the bath is held constant by manually adjusting a Variac which controls the heat input into the bath from a resistance coil. The bath is agitated by an air-driven agitator, and circulation of the bath liquid is encouraged by a draft tube mounted coaxially with the agitator. Agitation of the contents of the cell, to insure equilibrium, is obtained by moving a steel ball inside the cell with a magnet. The fitting by which the glass equilibrium cell is joined to the steel tubing which connects it with the gas reservoir was developed during this study and has been described previously.⁶

A cross-section of the glass equilibrium cell used in the majority of this study is shown in Fig. 2. It was found that such cells, made from Pyrex high-pressure gauge-glass tubing, will withstand pressures up to 1,300 psi for at least 24 hours. Though one cell burst at 800 psi after being tested to 1,250 psi and used at pressures up to 1,000 psi for two months, another cell was used for four months at pressures to

Table I—Published Phase Data on Hydrocarbon-Nitrogen-Helium Systems at Low Temperatures

System	Temperature Range $^{\circ}\text{R}$	Pressure Range psia	Ref.
He-N ₂	140-196	16-4,340	10
	123-202	5-3,675	16
	126-198	59-221	9
He-CH ₄	162-191	2,350	7
	162-229	2,645-3,380	8
N ₂ -CH ₄	152-194	14.7	19
	162-239	14.7-147	25
CH ₄ -C ₂ H ₄	180-322	40-740	3
	229-456	9-640	26
	304-492	7-588	14
CH ₄ -C ₂ H ₆	304-492	74-735	11
	321-336	441-588	18
CH ₄ -C ₂ H ₄ -C ₂ H ₆	305-492	74-735	11
C ₂ H ₄ -C ₂ H ₆	438-582	25-794	1
Natural Gas	222-330	100	24
Gas-Condensate			

1,300 psi without failure. Because of the possibility of rupture of the cell, the low-temperature bath is mounted behind a steel safety plate and is observed through a Plexiglas-covered slit.

The neck of the cell and the line which leads to the gas reservoir are made of small-diameter tubing in order to minimize the volume between the body of the cell and valve 1, which separates the cell from the reservoir. This volume was determined to be about 3.7 ml.

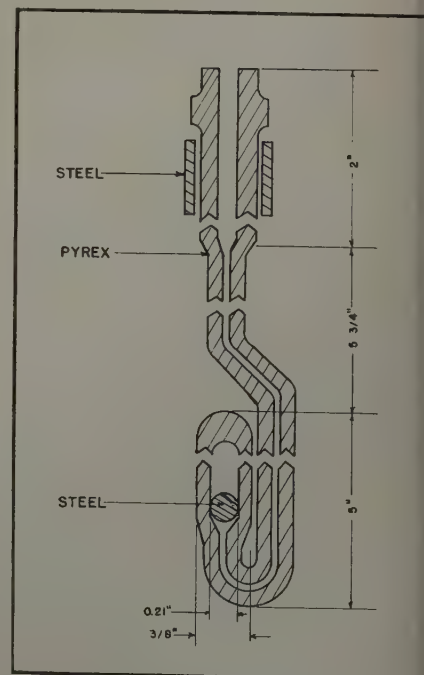


FIG. 3—CROSS-SECTION OF INVERTED CELL

The gas reservoir consists of two liquid-level gauges, one of which is calibrated for internal volume and serves as a high-pressure gas burette; the other serves as a reservoir of high-pressure gas with which to fill the burette. Manifolds and valves connect these gauges to the rest of the apparatus, and an air bath maintains the reservoir at a constant known temperature. The pressure required to force the gas from the reservoir into the equilibrium cell is developed by a manually-operated hydraulic jack which displaces mercury into the liquid-level gauges.

The pressures in the equilibrium cell and gas reservoir are measured by Bourdon gauges having ranges of 0 to 2,000 psi and 0 to 5,000 psi, respectively. Comparison of these gauges with a dead-weight tester at intervals of several months indicates them to be accurate to ± 3 psi.

The temperature of the low-temperature bath is measured by a four-junction thermocouple, the EMF of which is measured with a Leeds and Northrup Type K-2 potentiometer. The thermocouple was calibrated against a platinum resistance thermometer; accuracy of the temperature measurement is judged to be $\pm 0.5^\circ\text{F}$ or better.

PROCEDURE

The gas reservoir is brought to a constant temperature of 100°F , and the gas burettes are evacuated and then flushed with the gas to be studied by alternately charging to a high pressure and venting to the atmosphere a number of times. The equilibrium cell is similarly purged at room temperature, and then suspended in the pentane bath. The bath is cooled to the desired temperature and then maintained at that temperature by throttling the flow of nitrogen through valve 13 and adjusting the Variac which controls the power to the heater element. The thermocouple and potentiometer will indicate temperature changes on the order of 0.01°F , and by constant attention, one person can control the temperature to 0.1°F , as long as no gross heat effects occur. The condensation of a large amount of gas causes temperature increases as large as 2°F , but the temperature is always stabilized to within 0.1°F of the control point before readings are made.

Increments of gas are added to the cell through valves 1 and 2, while maintaining a constant pressure in the reservoir by raising the mercury level.

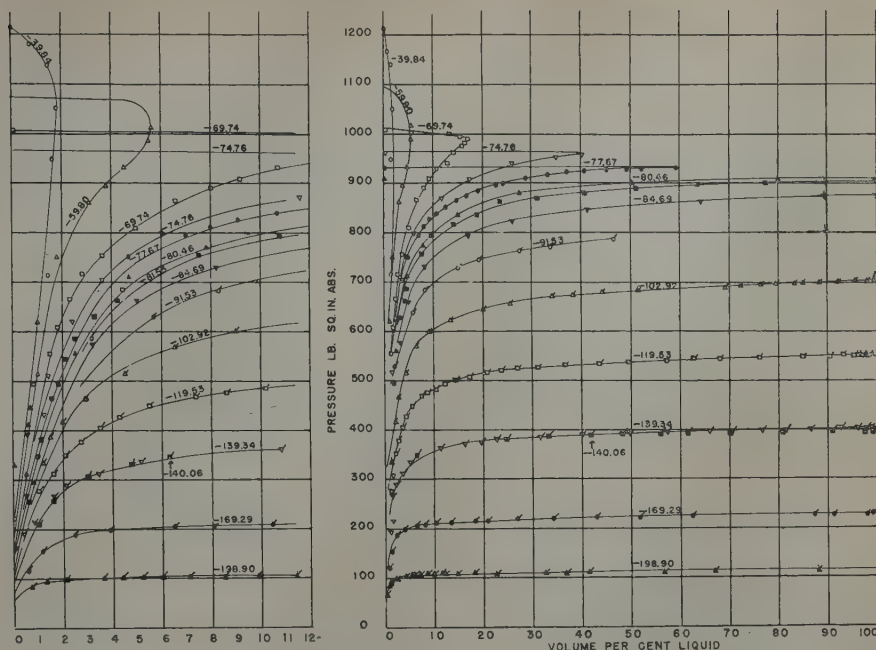


FIG. 4 — EXPERIMENTAL ISOTHERMS OF MIXTURE "A"

After each addition of gas the contents of the cell are agitated until the pressure no longer changes with time, and the cell is examined for the presence of liquid. The pressure at which dew is first apparent on the agitator ball is taken as the dew point; this pressure is usually considerably below that at which measurable liquid is formed. When liquid is present in the cell the mixture is agitated until neither pressure nor liquid level changes with time; the time required to reach this equilibrium varies from one minute at low pressures to ten minutes in the region of the critical point. The level of liquid in the cell is read against a platinum-inked scale fixed to the cell; this scale is calibrated to read in volume per cent liquid.

Successive increments of the gas are added until the level of liquid reaches the constricted neck of the cell. Since the volume of the neck of the cell is only about 0.1 per cent that of the body of the cell, the mixture in the cell is considered to be completely liquefied, i.e., at its bubble point, when the liquid enters the neck. Because this lack of an absolute boundary between the equilibrium cell and the rest of the apparatus might conceivably lead to error in the determination of the bubble point, the inverted cell shown in Fig. 3 was developed for more precise bubble point determinations. The results obtained

with this cell agree with those obtained with the upright cell shown in Fig. 2, within the accuracy of the temperature and pressure measurements, so the latter cell was used throughout most of the investigation.

RESULTS

The compositions of the two gases are given in Table II. The analysis of gas "A" was made by the Phillips Petroleum Co., which donated it, by low-

Table II — Properties of Gases Studied

	Gas "A"	Gas "AB"
Composition, Mol %		
Methane	90.89	96.68
Ethane	4.40	1.60
Propane	1.91	0.70
i-Butane	0.33	0.14
n-Butane	0.60	0.20
i-Pentane	0.21	0.07
n-Pentane	0.13	0.05
Hexanes	0.15	0.05
Heptanes-plus	0.18	0.07
Carbon Dioxide	1.20	0.44
Critical Pressure, psia	925	765
Critical Temperature, $^\circ\text{F}$	-79	-101
Critical Density, g/ml	0.230	0.183
Molecular Weight	18.40	16.90
Pseudo Critical Press., psia	676	674
Pseudo Critical Temp., $^\circ\text{F}$	-91	-90

temperature fractionation. The behavior of this gas was established by the determination of 14 isotherms between -40°F and -200°F . Gas "AB" was prepared by mixing gas "A" with Phillips "Pure" grade methane, which is stated to contain less than one per cent of ethane, nitrogen, and carbon dioxide as impurities. The composition of gas "AB" was calculated from the composition of gas "A" and the amount of methane added to this gas, and was checked by mass spectrometer analysis. The behavior of gas "AB" was determined at seven temperatures from -80° to -200°F .

PHASE BEHAVIOR

The experimental isotherms are plotted in Figs. 4 and 5. The shape of these isotherms is consistent with the composition of the gases; they are quite steep at low percentages of liquid, because of the presence of small amounts of heavy components, and much flatter at higher percentages of liquid, because of the absence of components more volatile than the major component, methane. Retrograde behavior is indicated by the higher temperature isotherms for each gas, which show double values of pressure at a single per cent of liquid.

The phase envelopes in Figs. 6 and 7 were obtained by crossplotting the data at constant percentages of liquid. The points shown in Figs. 6 and 7 are not experimental points, but are read from the curves, through the experimental points in Figs. 4 and 5.

The smoothness with which the data above about two per cent liquid crossplot, indicative of internal consistency, is regarded as favorable evidence of the reliability of the data. The steepness of the isotherms at low percentages of liquid makes accurate determination of the dew points very difficult, as is

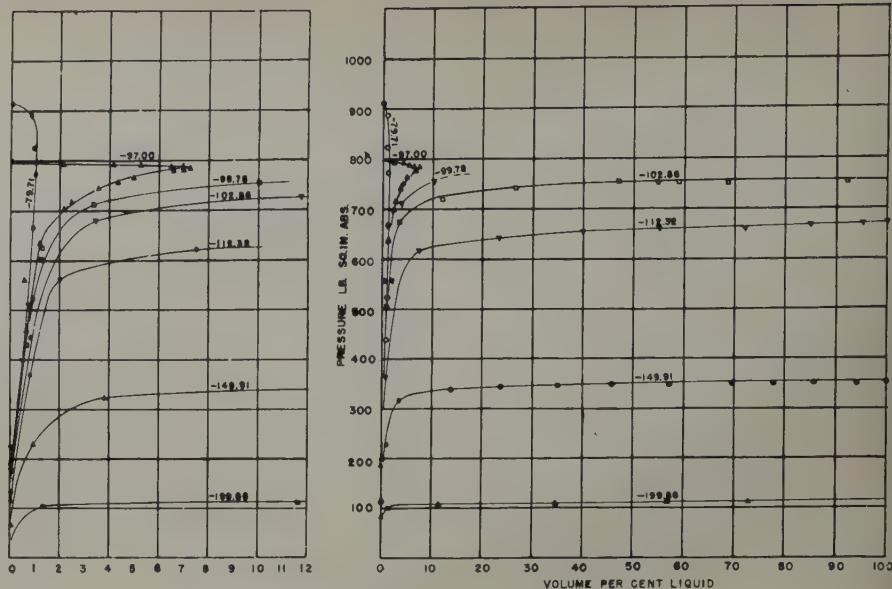


FIG. 5 — EXPERIMENTAL ISOTHERMS OF MIXTURE "AB"

shown by the considerable scatter of the data around the dew point lines in Fig. 6 and 7, and these lines are therefore considered as approximations only. Bubble points read from the smoothed curves of Figs. 6 and 7 are tabulated in Table III.

From the phase diagrams the location of the critical point, the point to which all the constant-per-cent-liquid lines converge, can be definitely determined. The critical points given in Table II are believed to be accurate to $\pm 1^{\circ}\text{F}$ and ± 10 psi.

Apart from the location of the critical point, the main utility of these phase data is their use to check vaporization equilibrium constants obtained from generalized correlations. Such a check is possible only along the boundary curves, where the composition of one of the phases is known. The inaccuracy of the dew point data given here makes such a check meaningful only along the bubble point line. In Table IV the experimental bubble point temperatures are compared with those calculated by use of the M. W. Kellogg equilibrium constants.^{2,14} In these calculations carbon dioxide was assumed to behave as ethane, and it was necessary in some cases to make slight extrapolations of the correction factors involved in the Kellogg correlation. The calculations otherwise followed the procedure described in the references cited.

Since the product of the equilibrium constant and mol fraction of each of the components except methane is quite small, even at the higher temperatures,

this comparison essentially reduces to a check of the methane constants. The agreement indicated in Table IV might be anticipated from the fact that the bubble point curve of each of the gases is not far removed from the vapor pressure curve of pure methane, since the equilibrium constants obtained from any correlation should be relatively more accurate in that region. However, it is significant that the agreement is good at the higher pressures, near the critical points of the mixtures, where the accuracy of most correlations, which do not include parameters allowing for the composition of the phases, decreases markedly. While this is not, of course, a severe test, it is felt that this agreement lends considerable support to the use of Kellogg constants for the prediction of the low-temperature behavior of methane in mixtures which, similar to these, are primarily methane.

Table III — Smoothed Bubble Point Data

Temperature, $^{\circ}\text{F}$	Bubble Point Pressure psia	
	Gas "A"	Gas "AB"
-90	830	
-100	735	
-110	645	695
-120	550	600
-130	470	505
-140	400	425
-150	330	350
-160	270	295
-170	220	235
-180	180	180
-190	145	145
-200	110	110

Table IV — Comparison of Experimental and Calculated Bubble Points

Bubble Point Pressure, psia	Bubble Point Temperature, $^{\circ}\text{F}$			
	Gas "A"		Gas "AB"	
	Experimental	Calculated	Experimental	Calculated
150	-188	-184	-189	-187
200	-175	-172	-178	-174
300	-155	-154	-158	-157
400	-140	-140	-144	-143
500	-128	-127	-131	-131
600	-115	-115	-120	-118
700	-104	-105	-109	-109
800	-93	-95		

VOLUMETRIC BEHAVIOR

In order to calculate the density of the mixture in the equilibrium cell, the density of the gas at the conditions in the gas reservoir must be known so that the mass of gas delivered to the cell can be calculated from the measured volume delivered. In the absence of actual data on the gases studied, it was assumed that they were described by generalized compressibility-factor data for natural gases²³ which are said to be accurate to within about one per cent at the conditions of the reservoir.⁴ With this assumption, the density of the total mixture in the cell can then be calculated, the volume of the cell being known. In this calculation due allowance was made for the volume between the body of the cell and the reservoir.

Check determinations of the density of propane, the actual density of which at both reservoir and cell conditions is known, indicated an error of only 0.2 per cent when the density of the fluid in the cell is as much as 0.5 grams/ml. Somewhat greater errors should be expected at lower densities because of

Table V—Smoothed Volumetric Data

Pseudo Reduced Temperature	0.70	0.75	0.80	0.85	0.90	0.95	1.00	1.05	1.10	1.15
Compressibility Factor	Pseudo Reduced Pressure									
Gas										
0.9 "A"	0.065	0.100	0.120	0.140	0.155	0.185	0.225	0.260	0.320	0.410
"AB"	0.150	0.230	0.335	0.385	0.410	0.565	0.655	0.680	0.825	
0.8 "A"	0.100	0.150	0.200	0.250	0.300	0.375	0.470	0.525	0.625	0.825
"AB"	0.285	0.410	0.565	0.655	0.680	0.775	0.930	1.170		
0.7 "A"	0.120	0.185	0.260	0.335	0.425	0.545	0.680	0.775	0.930	1.170
"AB"	0.385	0.555	0.730	0.850	0.900	1.000	1.205	1.435		
0.6 "A"	0.130	0.210	0.295	0.395	0.520	0.675	0.835	1.000	1.205	1.435
"AB"	0.465	0.655	0.845	1.010	1.100	1.200	1.425			
0.5 "A"	0.135	0.225	0.320	0.440	0.590	0.775	0.970	1.200	1.425	
"AB"	0.525	0.730	0.935	1.145	1.265	1.425				
0.4 "A"	0.140	0.225	0.335	0.470	0.640	0.850	1.085	1.350	1.600	
"AB"	0.565	0.775	1.000	1.260						
0.3 "A"	0.145	0.230	0.345	0.495	0.680	0.910	1.185	1.480		
"AB"	0.585	0.805	1.05							
0.2 "A"	0.150	0.235	0.350	0.510	0.700	0.950				
"AB"	0.600	0.825								
0.1 "A"	0.155	0.235	0.360	0.525	0.715					
"AB"	0.610									

the effect of the volume between the cell and reservoir. It is believed that the overall uncertainty in the volumetric data shown here, including that due to the use of the generalized data, is probably less than three per cent.

The volumetric behavior of gases "A" and "AB" is shown in Figs. 8 and 9,

in terms of the compressibility factor, PV/RT , and pseudo reduced temperature and pressure. The pseudo reduced temperature or pressure is the ratio of the absolute temperature or pressure to the molal average absolute critical temperature or pressure of the mixture. The original data were cross-plotted to

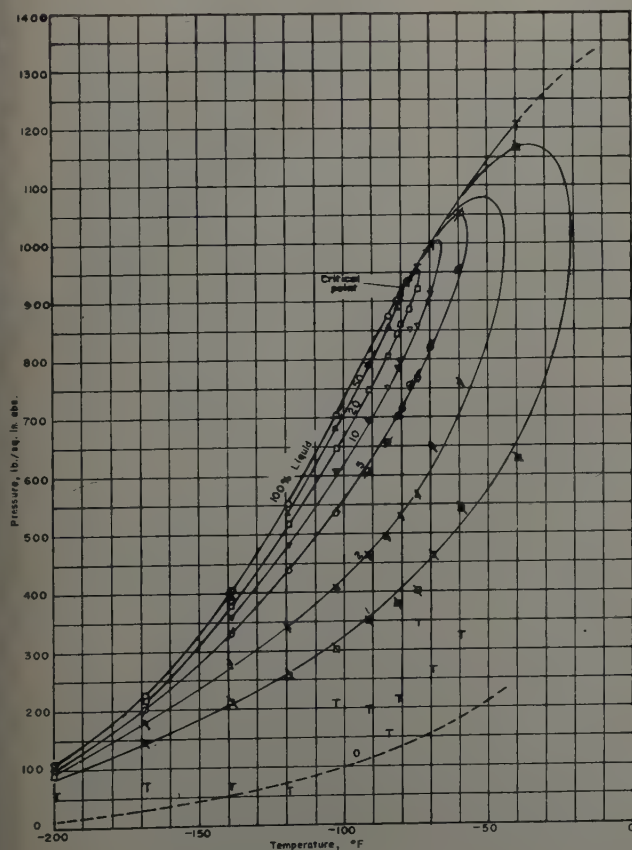


FIG. 6—PRESSURE-TEMPERATURE PHASE DIAGRAM OF GAS "A"

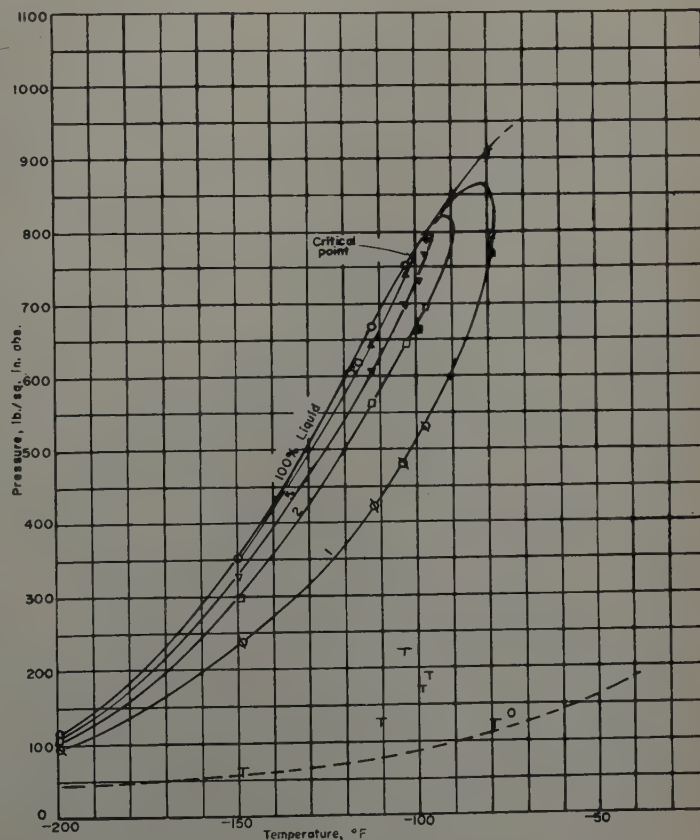


FIG. 7—PRESSURE-TEMPERATURE PHASE DIAGRAM OF GAS "AB"

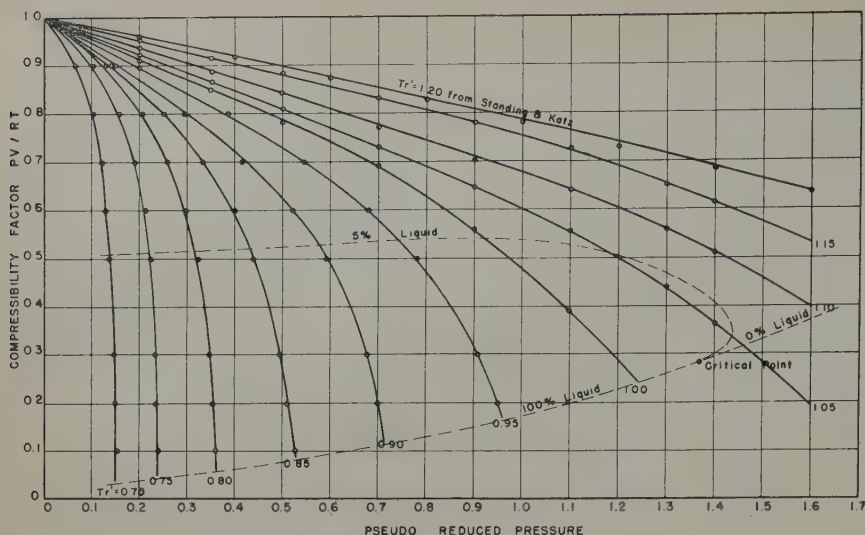


FIG. 8 — PRESSURE-VOLUME-TEMPERATURE BEHAVIOR OF MIXTURE "A"

even values of reduced temperature, and the points shown in Figs. 8 and 9 are read from the crossplotted curves. Values read from Figs. 8 and 9 are given in Table V.

The upper isotherms in Figs. 8 and 9 overlap the lower limit of the generalized correlation mentioned above, which extends to a pseudo reduced temperature of 1.05. Above a reduced temperature of 1.10 the agreement between these data and the generalized data is quite good at low reduced pressures, falling off at high reduced pressures. At the highest reduced temperature, 1.20 for gas "A" and 1.15 for gas "AB," these data and the generalized data are practically identical, as is shown by the fact that the upper line in each chart,

while taken from the generalized data, fits the points from this study very well.

ACKNOWLEDGMENT

The assistance of A. F. Bertuzzi, who aided in the computations and the experimental work, is gratefully acknowledged.

REFERENCES

1. Atack, Evans and McCormack [given by Ruhemann, M.: *The Separation of Gases*, 2nd Ed., (1949), Oxford University Press, London.]
2. Benedict, M., Webb, G. W., Rubin, L. C., and Friend, L.: *Chem. Eng. Prog.*, (1951), 47, 609.
3. Bloomer, O. T., and Parent, J. D.: "A Study of the Physical and Physico-chemical Properties of the Methane Nitrogen System," *Inst. Gas Technology Research Bulletin*, Chicago, Ill., (April, 1951).

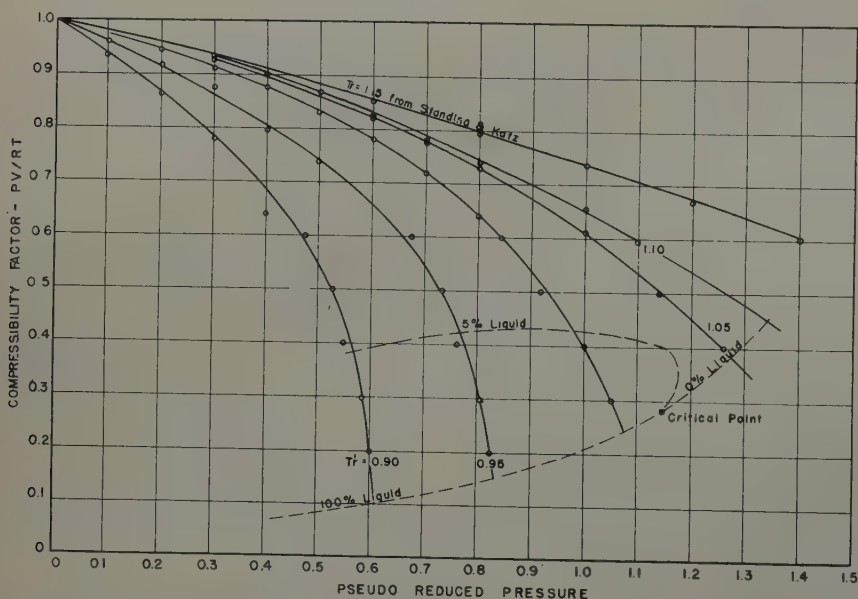


FIG. 9 — PRESSURE-VOLUME-TEMPERATURE BEHAVIOR OF MIXTURE "AB"

4. Brown, G. G., et al.: *Natural Gasoline and the Volatile Hydrocarbons*, Midwest Printing Co., Tulsa, Okla., (1948).
5. Deschner, W. W., and Bodle, W. W.: *Oil and Gas Jour.*, (1948), 46, (50), 76-79; (51), 92-98, 112.
6. Davis, P. C., Gore, T. L., and Kurata, F.: *Ind. Eng. Chem.*, (1951), 43, 1826.
7. Eilerts, C. K., Burn, V. L., Mullins, N. B., and Hanna, Betty: *The Petr. Engr.*, (1948), 20, 502-15.
8. Fastowsky, V. G., and Gonikberg, M. G.: *Acta Physicochim.* (U.R.S.S.), (1940), 12, 485-8.
9. Federotenko, A., and Ruhemann, M.: *J. Tech. Phys.*, (U.S.S.R.), (1937), 4, 36-43.
10. Gonikberg, M. G., and Fastowsky, V. G.: *Acta Physicochim.* (U.R.S.S.) (1940), 12, 67-72.
11. Guter, M., Newitt, D. M., and Ruhemann, M.: *Proc. Roy. Soc., London*, (1940), 176A, 140-6.
12. Guter, M., Newitt, D. M., and Ruhemann, M.: *Proc. Roy. Soc., London*, (1940), 176A, 146-52.
13. Kay, W. B.: *Ind. Eng. Chem.*, (1938), 30, 459-65.
14. Kellogg Equilibrium Charts: *Chem. Eng. Prog.*, (1950), 46, (3), 20.
15. Kharakhorin, F. F.: *Foreign Petr. Tech.*, (1941), 9, 411-22.
16. Kharakhorin, F. F.: *J. Tech. Phys.*, (U.S.S.R.), (1941), 11, 1133-34.
17. Kurata, F., and Katz, D. L.: *Trans. AICHE*, (1942), 38, 995-1020.
18. Levitskaja, E. P.: *J. Tech. Phys.*, (U.S.S.R.), (1941), 11, 197-204.
19. McTaggart, H. A., and Edwards, E.: *Trans. Roy. Soc. Can.*, (1919), 13, III, 57-66.
20. Mullins, P. V., and Wilson, R. W.: *Am. Gas. Assoc. Proc.*, (1948), 30, 601-8.
21. Ruhemann, M.: *Proc. Roy. Soc.*, (London), (1939), 171A, 121-36.
22. Smith, R. L., and Watson, K. M.: *Ind. Eng. Chem.*, (1937), 29, 1408-14.
23. Standing, M. B., and Katz, D. L.: "Density of Natural Gases," *Trans. AIME*, (1942), 146, 140.
24. Stutzman, L. F., and Brown, G. M.: *Chem. Eng. Prog.*, (1949), 45, 139-142.
25. Torochesnikov, N. S., and Levine, L. A.: *Chem. Ind.*, (U.S.S.R.), (1939), 16, 19-22.
26. Volova, L. M.: *J. Phys. Chem.* (U.S.S.R.), (1940), 14, 268-76. ★★

IMPROVED TECHNIQUES DEVELOPED FOR ACIDIZING GAS PRODUCING AND INJECTION WELLS

W. H. JUSTICE AND JENS P. NIELSEN, LA GLORIA CORP., CORPUS CHRISTI, TEX., MEMBERS AIME

ABSTRACT

This paper describes an improved acidizing technique which has been applied in acidizing gas wells in the La Gloria Field. Wells acidized in this manner exhibited a much greater increase in deliverability than wells acidized in the conventional manner. The acid is injected into the well in small slugs separated by a small volume of high pressure gas. The acid and gas are displaced from the tubing by high pressure gas to reduce the hydrostatic head on the well when the acid is recovered from the well. The well is opened for production as soon as the acid and gas are displaced. This procedure permits a very rapid recovery of the acid which results in large increases in the deliverability of the gas wells.

It has been found advantageous in the acidization of gas injection wells to inject the high pressure gas directly after the acid without backflowing the acid out of the well. This practice has made it possible to inject the gas in the injection wells of this field with a much lower pressure differential. This reduces the horsepower required to inject the gas and also decreases the number of injection wells required per reservoir.

INTRODUCTION

The results obtained by acidizing gas wells in the La Gloria Field have varied considerably in the past. For this reason,

a planned study of the acidizing procedure was undertaken in order to obtain more consistent results.

The Frio Sands of the La Gloria Field are rather permeable and it was not necessary to acidize many of the wells when they were originally completed. At the completion of an eight-year cycling program in several of the gas reservoirs, it became necessary to recompleteness many wells in other reservoirs. It was found that the open flow potential of the wells recompleteness in different sands was not as large as wells that were originally completed in that reservoir.

A study of the drilling records of several of these wells indicated that the sands had originally been subjected to considerable hydrostatic drilling fluid overload while the well was being drilled to the deeper sands of the field. It is indicated that during this eight-year period, the drilling mud and water that were lost into the formation when the well was being drilled had formed a relatively impermeable zone around the well bore. This impermeable zone around the well bore made it very difficult to obtain high deliverability wells when the original wells are recompleteness in other zones.

Muskat¹ has shown that in uniformly permeable and porous formations a zone of partial plugging one ft in radius around the well would drastically decrease the productivity of the well. The analysis for this problem shows that the production capacity of a well is very sensitive to the value of the permeability of the zone immediately surrounding the well bore. This is to be expected in view of the highly localized character of the pressure drop in a radial flow system about the well center. The reduction of the deliverability is not proportional to the thickness of the mud-affected zone as the major portion of the reduction in deliverability is caused by the

¹Reference given at end of paper.

Manuscript received in the office of the Petroleum Branch July 30, 1952. Paper presented at the Petroleum Branch, AIME, Fall Meeting in Houston, Tex., Oct. 1-3, 1952.

plugging of the area immediately adjacent to the well bore. Any additional increase in the thickness of the mud-affected zone causes successively smaller reductions in the well deliverability.

The major portion of the increase in production capacity from an acid treatment is due to the restoration of the permeability of the mud-affected zone to that of the main reservoir. Any increase in the permeability of the mud-affected zone or of the next few feet of the reservoir above the permeability of the rest of the reservoir, does not appreciably increase the deliverability of the well. For example, if the mud-affected zone has a radius of one ft and has a permeability of 10 per cent of permeability of the main reservoir, and this zone is restored by acid treatment so that it has the permeability of the main reservoir, the production capacity is increased 180 per cent. (See Fig. 1.) Whereas, if the permeability of this one ft zone is increased to 400 per cent more than the original reservoir permeability, the productive capacity of the well would be only 14 per cent more than the productive capacity of the well with the one ft radius zone having the same permeability as the remainder of the reservoir. (See Fig. 2.)

The object of our acidizing program was the removal of the mud and extraneous material, introduced during the drilling operation, from the well bore and the region closely adjacent to the well bore so that the original permeability of the formation could function. The need for removal of the mud and water introduced into the area closely adjacent to the well bore was more important in the case of the wells that were being worked over eight years after they were originally completed. This was evidenced by the lower open flow potential of these wells, probably due to the mud and water that was introduced into the formation having been subjected to the formation temperature for sufficient time to set up and cause the maximum reduction in the permeability of this portion of the formation.

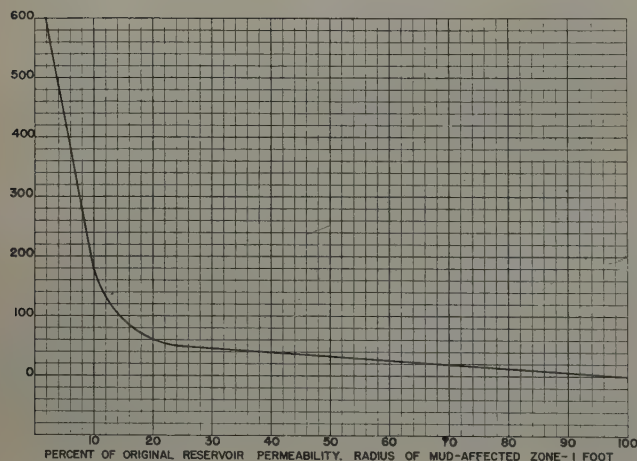


FIG. 1 — INCREASE IN THE PRODUCTION CAPACITY OF A RADIAL FLOW SYSTEM DUE TO ACID TREATMENT IF THE ACID-AFFECTED ZONE WITH A RADIUS OF ONE FT WAS PARTIALLY PLUGGED BY MUD WHICH HAD LOWERED THE PERMEABILITY BELOW THE REST OF THE RESERVOIR AND THE ACID TREATMENT RESTORES THIS ZONE SO THAT IT HAS THE PERMEABILITY OF THE ORIGINAL RESERVOIR.

It was found that acidizing these wells by conventional methods did not result in the desired increase in deliverability. The purpose of this paper is to describe the acidizing technique that was developed which has resulted in a much greater increase in deliverability than the conventional acidizing procedure.

DESCRIPTION OF THE ACIDIZATION OF A TYPICAL GAS PRODUCING WELL

This gas well was recompleted into the Frio Sand "A" after having been produced from another sand for eight years. The pertinent reservoir data for Sand "A" is shown in Table I. The well was equipped with 2½-in. tubing set on a Baker production packer in 7-in. casing. The well was jet perforated from 6,714-36 ft with six shots per ft.

On a 10-hour production test the well would only flow at a rate of 3.8 MMcf/D with a maximum flowing pressure of 800 psig. The well would not flow into the gas gathering system which is maintained at a pressure of 1,750 psig. The other wells completed in Sand "A" after acidizing were capable of producing at a rate of 8 MMcf/D into the gas gathering system. It was decided to acidize this well in an attempt to increase the productivity.

It was estimated that the total capacity of the tubing and casing below the packer to the center of the perforations was 40.5 bbl. It was also estimated that the hydrostatic head of a 6,725 ft solid column of acid would be 3,130 psig or 380 lb greater than the 2,750 psig reservoir pressure. The well, therefore, would not be capable of backflowing the acid and it would be necessary to swab the acid back if the well were acidized in the conventional manner. It was decided to inject the acid in 10 bbl slugs separated by a small volume of high pressure gas so that the well would not have to produce against the full hydrostatic head of the acid column. Each 10 bbl slug of acid would be displaced from the tubing by the expansion of the high pressure gas before the next 10 bbl slug of acid entered the tubing. This procedure would permit the rapid recovery of acid without swabbing, and would prevent the separation and deposition of mud particles around the well bore from the partially spent acid.

The acid truck and pump line were connected and tested for leaks at a pressure of 5,500 psig. The mud acid was pumped into the tubing at a rate of 2.5 bbl per minute. The initial pump pressure was 2,370 psig and the pressure decreased to 1,875 psig after 10 bbl of acid had been pumped into the tubing. In this size tubing, 10 bbl is equivalent to a column of liquid 1,700 ft long. High pressure gas was then injected into the tubing at a high rate for approximately five minutes. This cycle was repeated. After pumping a total of approximately 34 bbl of acid, the pressure built up to 2,900 psig. This indicated that the initial acid had reached the formation. A slight break in the pressure occurred and the pumping pressure decreased to 2,600 psig.

The pumping of the acid in 10 bbl slugs separated by a slug of high pressure gas was continued until a total of 96 bbl of acid had been injected into the well. The acid and gas were then rapidly displaced into the formation from the tubing with high pressure gas. The acid was then immediately backflowed from the well. Since the acid was separated into the

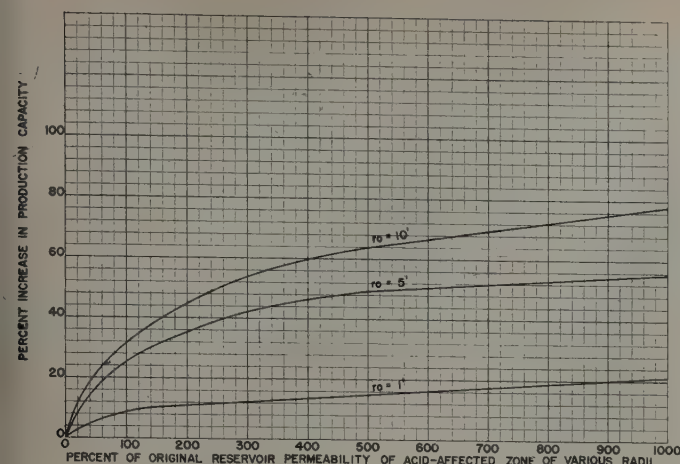


FIG. 2 — INCREASE IN THE PRODUCTION CAPACITY OF A RADIAL FLOW SYSTEM DUE TO ACID TREATMENT IF THE INITIAL PERMEABILITY IS EVERYWHERE UNIFORM AND THE PERMEABILITY OF THE ACID-AFFECTED ZONE OF VARIOUS RADII IS INCREASED ABOVE THE PERMEABILITY OF THE ORIGINAL RESERVOIR.

small slugs by the high pressure gas, each slug of acid was ejected from the tubing before the next slug of acid entered the tubing. This permitted the well quickly to clean itself of the acid without being swabbed. As the well cleaned up, the flowing pressure rapidly increased and at the end of eight hours the well was flowing at a rate of approximately 11 MMcf/D with a tubing pressure of 1,850 psig. The open flow potential of the well was estimated at 48 MMcf/D. The well is now capable of flowing into the gas gathering system at a rate in excess of the 11 MMcf/D.

DESCRIPTION OF THE ACIDIZATION OF A TYPICAL GAS INJECTION WELL

It has been found advantageous to acidize the injection wells used in the cycling program of the La Gloria Field in order to reduce the horsepower required to inject the gas and to reduce the number of wells required per reservoir. We had been acidizing these wells in the conventional manner and had obtained satisfactory increases in size of the injection wells. The end-to-end sweep plan of cycling one of the reservoirs recently included in the cycling program called for the injection of gas slightly below the original gas-water contact. The well selected for this injection was recompleted and considerable salt water was produced at a high rate in an effort to clean the well. Gas was then injected into the well, but only 3 MMcf/D could be injected at an injection pressure of 3,300 psig.

The well was then acidized with 4,000 gal of acid. (See Table I for reservoir data on Sand "B".) The acid was dis-

placed from the tubing with kerosene in an effort to increase the speed with which the acid could be recovered from the well. The acid was recovered and enough salt water was produced to clean the well. The acidization caused no increase in the volume of gas that could be injected into the well at the same injection pressure.

The decision was then made to re-acidize the well in a different manner. Two hundred gallons of wash acid were pumped into the well, followed by 3,000 gal of mud acid and 800 gal of wash acid. The acid was displaced from the tubing with the injection gas without backflowing the acid out of the well. The gas injection rate was very low for the first two hours. At the end of two hours the rate of injection increased sharply, and at the end of 12 hours the injection rate of 2,850 psig was 19 MMcf/D. The acid treatment resulted in a sixfold increase in the injection rate of the well.

In order to increase the injection rate of a well completed in a different reservoir considerably above the gas-water contact, it was decided to use the same acidizing procedure that had been used on the injection well completed below the gas-water contact. (The reservoir data for Sand "C" is shown on Table I.) Four thousand gallons of mud acid were pumped into the well. The acid was displaced from the tubing with the injection gas without backflowing the acid from the well. The gas injection rate was very low for the first two hours, but at the end of this period there was a sharp increase. At the end of 12 hours the injection rate at 2,700 psig was 36 MMcf/D, whereas, the injection rate before the well was acidized was only 9 MMcf/D with an injection pressure of 2,850 psig. The acid treatment resulted in a fourfold increase in the gas injection rate of the well with a 150 psig reduction in injection pressure.

CONCLUSIONS

Gas wells in which the permeability of the formation near the well bore has been drastically reduced by mud are the most difficult to acidize by conventional methods. It has been found that the injection of the acid in small slugs separated by a small volume of high pressure gas, reduces the hydrostatic head on the well when the acid is recovered. Each slug of acid is displaced from the tubing by the expansion of the high pressure gas before the next slug of acid enters the tubing. This procedure permits very rapid recovery of the acid which evidently restores the original formation permeability of the mud-affected zone and results in large increases in the deliverability of the gas wells. Wells that are so tight that

Table I — Reservoir Data for Various Frio Sands, La Gloria Field, Jim Wells and Brooks Counties, Texas

	Sand "A"	Sand "B"	Sand "C"
Producing Horizon	Frio	Frio	Frio
Average Porosity	22.8%	17.2%	20.8%
Average Permeability	521 md	100 md	220 md
Depth of Perforations	6,714-36'	5,724-50'	5,984-6,048'
Average Pressure, psia	2,750	2,650	2,970
Reservoir Temperature, °F	196	178	188

it would be necessary to recover the acid by swabbing can be quickly and safely acidized by this procedure without swabbing. This acidizing procedure should make it profitable to acidize many wells that are now considered too tight to acidize by the conventional method. Where high pressure gas is not available at the well, it should be profitable to use a portable gas compressor to compress and inject gas or air along with the acid, as described in this paper.

It was found to be more effective to displace the acid in a gas injection well with the injection gas without backflowing the acid out of the well. This procedure resulted in a fivefold increase in the amount of gas that could be injected into the well.

ACKNOWLEDGMENT

The authors wish to express their appreciation to the La Gloria Corp. for permission to prepare and publish this paper. We also express our appreciation to L. G. Cable, R. E. Denmead, J. Eskew and C. L. Wheless for their assistance in obtaining the data reported in this paper.

REFERENCES

1. Muskat, M.: *The Flow of Homogeneous Fluids Through Porous Media*, McGraw-Hill Book Co., (1937), 422-424. ★

SURFACE AREA MEASUREMENTS ON SEDIMENTARY ROCKS

C. S. BROOKS AND W. R. PURCELL, SHELL OIL CO., HOUSTON, TEX., MEMBERS AIME

ABSTRACT

The internal surfaces of rocks which are in contact with interstitial fluids are known to influence in some degree the recovery of hydrocarbons from pay zones. Despite the admitted importance of the influence of solid surfaces on hydrocarbon recovery, little information is available concerning the extent of surface of reservoir rocks. In this paper a description is given of the apparatus and procedure employed in the determination of the surface areas of sedimentary rocks, and values are reported for a variety of sandstone and limestone cores. In addition, consideration is given to the Kozeny equation, which relates surface area to porosity and permeability. A comparison is made between the surface areas as calculated from this equation and the geometrical areas of a series of packs of spherical glass beads. Also, for a group of sandstone cores, Kozeny areas are compared with surface areas as determined by the gas adsorption method employed in this investigation.

INTRODUCTION

It has long been recognized that many processes which are of importance to hydrocarbon production are controlled in some degree by the extent of the surface of the reservoir rock through which the hydrocarbons move. For example, the recovery efficiency that is obtained in a given reservoir is certainly determined in part by the action of interfacial forces between the reservoir fluids and rock, and this action is influenced in turn by the extent of solid surface. Despite the admitted importance of surface effects to problems of petroleum recovery, little information is available concerning the extent of surface of reservoir rocks.* It is the purpose of this paper

to describe an apparatus which has been employed for the measurement of the surface areas of rock samples and to present the values which have been obtained for a variety of sandstone and limestone cores. In addition, the relationship of surface area to permeability and porosity, as given by the Kozeny equation, will be discussed.

METHOD OF MEASURING SURFACE AREA

The method of determining surface areas as employed in this work has previously found wide use in studies of porous solids such as catalysts. The method involves the measurement of the amount of physical adsorption of an inert gas, such as nitrogen or argon, on the bare surface of the solid at reduced pressure and constant temperature near the normal liquefaction temperature of the gas. With the aid of the theory of isothermal adsorption as developed by Brunauer, Emmett, and Teller,¹ it is possible to ascertain the amount of gas (and hence the number of molecules) which is required to cover the solid surface with a single layer of molecules. From a knowledge of the covering area per molecule the total surface area of the solid can be computed.

Since the Brunauer, Emmett, Teller (BET) theory has been adequately discussed elsewhere,² it will suffice here merely to present their final equation as ordinarily employed for surface-area calculations. This equation relates the volume of gas, V , which is adsorbed at pressure, P , to the liquefaction pressure, P_0 , of the gas, and to the volume of gas, V_m , that is required to form a monomolecular layer:

$$\frac{P}{V(P_0 - P)} = \frac{1}{V_m C} + \frac{(C-1)P}{V_m C P_0} \dots \dots (1)$$

In this equation C is a quantity which is related to the heats of adsorption and liquefaction of the gas; for a particular solid-gas system at constant temperature, C is considered to have a constant value.

The basic adsorption data can be presented in the form of Equation (1) by plotting the quantity $P/V(P_0 - P)$ as a func-

*References given at end of paper.
Manuscript received in the office of the Petroleum Branch July 30, 1952. Paper presented at the Petroleum Branch Fall Meeting in Houston, Tex., Oct. 1-3, 1952.

A recent paper by Kulp and Carr [*J. Geol.*, 60, 148 (1952)] reports surface areas of deep-sea sediments. Their values are in general much higher than those reported here for reservoir rocks probably because of the high clay and silt content of the sediments.

tion of the relative pressure, P/P_0 . If the adsorption follows the BET equation (and this is generally found to be the case in the range of relative pressures from 0.05 to 0.35) then this plot yields a straight line with slope $(C-1)/V_m C$ and intercept $1/V_m C$. Thus the reciprocal of the sum of the slope and intercept of the line gives V_m .

It is customary to report the volume of gas adsorbed, V , in cubic centimeters at standard conditions of 0°C and one atmosphere pressure and, hence, V_m is referred to the same conditions. If ρ is the density of the gas at these standard conditions, in grams per cubic centimeter, then the number of molecules, n , in the volume, V_m , is given by:

$$n = \frac{V_m \rho N}{M} \quad (2)$$

where N is Avogadro's number and M is the molecular weight of the gas. The total surface area, S , is:

$$S = n \sigma = \left(\frac{V_m \rho N}{M} \right) \sigma \quad (3)$$

where σ is the effective area covered by each molecule.

The generally accepted value of σ for nitrogen is 15.4 \AA^2 and for argon 13.6 \AA^2 , and these values were employed in this work. For a detailed discussion of the methods of obtaining the covering areas of molecules adsorbed on solid surfaces, the reader is referred to a recent article by H. K. Livingston.³

APPARATUS AND PROCEDURE

The requisite data for determining the surface area of a porous solid by the BET method are the volumes of gas adsorbed, V , at various pressures, P . The apparatus employed in this work for the determination of these quantities is shown in Fig. 1.

This apparatus and the procedure employed are similar in most respects to those given by Barr, Anhorn, and Joyner,⁴ but the following modifications are worthy of note:

1. The gas burets and manometer are housed in an air thermostat wherein the temperature is maintained at $31^\circ\text{C} \pm 0.1^\circ$. The mercury levels are observed through a Thermopane window which forms the front wall of the cabinet.

2. The pressure is measured to $\pm 0.1 \text{ mm}$ by means of a cathetometer. The zero reference level in one leg of the manometer is maintained at a fixed position with the aid of a "magic-eye" indicating circuit.

3. The sample tube used in this work is considerably different in design than those customarily employed in surface-area determinations. In the study of materials of high surface area, such as catalysts, the surface created by moderate grinding is a negligible portion of the total, and hence the material can be used in powdered form. For materials such as rocks, which are found to have relatively low surface areas, there exists the possibility of introducing a measurable surface by grinding. It was deemed desirable, therefore, to study the rock samples in single large pieces rather than as a powder. Accordingly, the sample tube (Fig. 2) was designed to admit a specimen up to 1 in. in diameter by 2 in. long. To obtain the highest possible accuracy in the adsorption measurements it is necessary to keep the free gas space in the sample holder to a minimum. This is accomplished through the use of a pyrex hypodermic syringe, of internal diameter just slightly greater than 1 in., connected at one end to a capillary tube to which is affixed

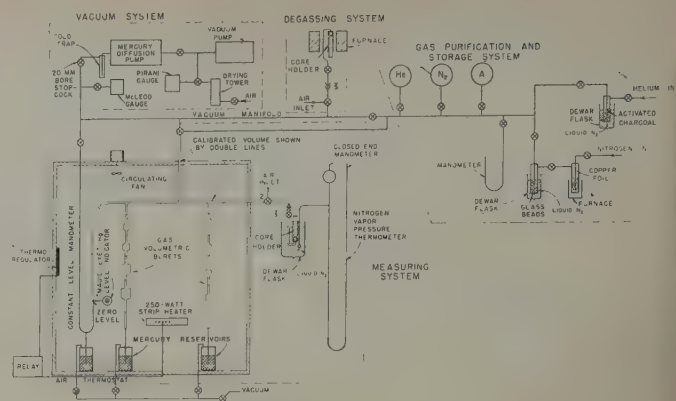


FIG. 1 — ADSORPTION APPARATUS.

a stopcock and ground glass joint. The piece to be tested is drilled to 1 in. O.D. from a larger rock sample. As long a piece as possible is used, up to 2 in. The space above the sample in the tube is completely filled by the plunger of the syringe so that the only void space remaining in the sample holder, aside from that in the pores of the rock, is the very small annular ring between the sample and the wall of the syringe. A vacuum seal is effected by lubricating the upper portion of the syringe plunger with vacuum grease. The stopcock and glass-joint arrangement, as shown in Fig. 2, enables the sample to be heated and degassed before being attached to the measuring manifold. This permits the preparation of one sample at the same time that measurements are being made on another sample.

4. In the procedure for surface area measurement as given in Reference (4), the gas in the sample tube and in the line connecting the tube to the measuring manifold is treated as though it were all at the temperature of the liquid nitrogen bath. This procedure is satisfactory for samples of high surface area, especially if the volume of the gas between the liquid nitrogen level and stopcock 2, Fig. 1, is small. This latter condition is often achieved by sealing the sample tube directly to the manifold by means of capillary tubing. In the apparatus here described the volume of gas between the liquid nitrogen level and the measuring manifold is somewhat greater than usual because of the addition of a ground glass joint and stopcock. For this reason, and because the surface areas to be measured are relatively small, it was found necessary in achieving the desired accuracy to treat our system as though it were divided into three zones. Zone A includes the gas bounded by the zero level of the manometer, stopcocks 1 and 2 (Fig. 1), and by the mercury levels in the two burets. Although stopcocks 1 and 2 are outside the air bath, they are placed as close as possible to it in order that all the gas of zone A can be treated as though it were at the constant temperature of the air bath. Zone C includes the gas which is below the liquid nitrogen level of the bath surrounding the sample tube; this volume of gas, which is at the fixed temperature of the boiling nitrogen,* is kept

*Variations in atmospheric pressure which may occur during the test are not sufficiently large to alter appreciably the boiling point of the nitrogen.

constant by periodically replacing the nitrogen that evaporates so as to maintain an essentially stationary liquid level in the bath. Zone *B* contains a small amount of gas (between stopcock 2 and the liquid nitrogen level) which varies in temperature from that of the air bath on the one side to that of boiling nitrogen on the other.

The volumes of gas contained within the three zones are determined prior to the adsorption measurements in the following manner: With the plunger of the sample holder removed, a melted wax, such as Apiezon *W*, is poured into the holder until the holder and the adjoining capillary U-tube are filled with wax up to the level at which the liquid nitrogen is to be maintained. This serves, in effect, to reduce the gas volume of zone *C* to zero. After the wax has solidified, the sample holder is attached to the measuring manifold. For these calibration tests the liquid nitrogen bath is omitted and the sample holder and adjoining tubing are at room temperature. The entire system is evacuated to a pressure of 10^{-5} mm of mercury. Helium is then admitted to zone *A* (stopcock 2 closed) and the volume of this zone, V_A , determined from pressure readings made at various settings of the mercury levels in the two burets.* Stopcock 2 is then opened, admitting gas to the previously evacuated tubing which connects the buret system to the wax-filled sample holder. Pressure readings are again made at different settings of the burets from which the volume of zone *B*, V_B , can be computed. The wax is then removed from the sample holder by heating and the tube is cleaned with a wax solvent. The core sample to be tested is placed in the sample holder which in turn is placed in the well of an electric furnace and attached to the vacuum manifold. The sample is heated and simultaneously evacuated to remove gas from the pores and from the surface of the rock. The sample tube is then closed at the stopcock, removed from the degassing furnace, and attached to the manifold of the measuring system. The volume of the gas below the reference mark of the sample holder (zone *C*) is then determined by helium expansion as in the aforementioned determination of the volume of zone *B*. Once determined for a given sample tube and adapter, V_B is constant, but V_C must be determined each time a new core sample is introduced.

To determine the average temperature of zone *B* which prevails during the adsorption measurements, the sample tube is immersed to the reference mark in the liquid nitrogen bath. The helium expansion measurements are again repeated. As before, the measuring manifold (zone *A*) is filled with gas to an initial pressure, P_1 , of about 50 mm of mercury with the mercury levels at the lowest reference marks in the two burets. The gas volume is equal to the previously determined value of V_A . The gas is then expanded into the sample holder to a pressure P_2 . The quantity ($Z_B T_B$) is calculated from the equation:

$$Z_B T_B = \frac{P_2 V_B T_A T_C Z_C}{[(P_1 - P_2) V_A Z_C T_C + P_2 (\Delta V_A T_C Z_C - V_C T_A)]} \quad (4)$$

where V_B and V_C are the previously determined values** of the volumes of zones *B* and *C*, respectively; T_A and T_C are the known absolute temperatures of the air bath and of the liquid nitrogen bath; and Z_B and Z_C are the compressibility factors for helium corresponding to the pressure and tem-

perature of zones *B* and *C*. The compressibility factor for zone *A* is considered to be unity. Duplicate determinations of ($Z_B T_B$) are made by varying P_2 through the additions of known amounts of mercury, ΔV_A , to the burets of the measuring system. The average temperature of zone *B* can then be determined from plots of (ZT) vs T which are compiled, for various helium pressures, from compressibility data obtained in the literature.⁵

Although the determination of T_B is rather time-consuming, it need be made only once for a given apparatus, for it has been found that this temperature does not depend in any large degree on the gas volumes of zones *A* and *C*, nor on the gas pressure. By accounting for this intermediate temperature, it is possible to achieve sufficient accuracy in the adsorption data that surface areas as low as 0.1 square meter per gram can be reliably measured without recourse to the more exacting procedures of Wooten and Brown⁶ or Beebe, Beckwith, and Honig⁷ which have been designed specifically for small areas. To demonstrate the marked influence on the resultant surface area value of the temperature of zone *B* used in the calculations, we cite the example of nitrogen adsorption on a sandstone sample weighing 16 grams. When the gas in zone *B* was assumed to be at the temperature of the liquid nitrogen bath, the calculated surface area was 0.53 square meter per gram. On the other hand, when the gas in zone *B* was

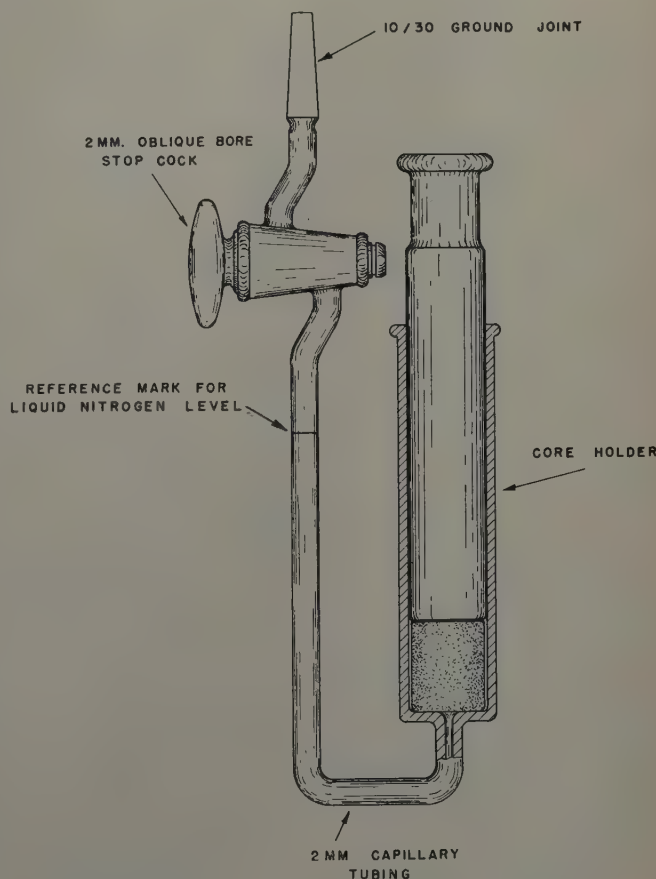


FIG. 2 — SAMPLE TUBE.

*For helium at or near 25°C and less than one atmosphere pressure, deviations from the ideal gas laws can be neglected since the compressibility factor differs from unity by less than 0.01 per cent.

**Although values for V_B and V_C were determined at room temperature, these same values may be used at temperatures down to that of liquid nitrogen, since calculations show that there is a negligible change in volume of the glass containers over this temperature range.

taken to be at 286°K, as found by the above-described procedure for the particular sample tube employed, the computed surface area was 0.71 square meter per gram. Thus, an error of about 25 per cent would have been made had not the temperature of zone B been determined.

The argon used in this work was obtained in hermetically sealed glass containers and was reported by the supplier to be spectroscopically pure. The nitrogen was purified by passing cylinder gas first over hot copper foil to remove oxygen and then through a cold trap to remove water vapor and other condensable materials. Mass spectrographic analyses of the gas before and after purification showed 98.05 mole per cent and 99.24 mole per cent nitrogen, respectively. The helium was obtained by passing "high-purity grade" tank gas over activated charcoal which was held at the temperature of liquid nitrogen.

All the core samples were prepared for the surface area measurements by extracting with a naphtha solvent (106°C B.P.), drying in an oven at 110°C and degassing for 15 hours at 110°C and 10^{-5} mm of mercury pressure. The above degassing procedure was adopted as standard sample preparation after it was demonstrated that in the case of the limestone and sandstone cores essentially constant surface area and constant weight were attained after evacuation for 15 hours at 110°C. The sample tube described above permits the weight loss of the sample to be determined after degassing, without exposure of the sample to the atmosphere, by weighing the entire sample

tube and adapter assembly. The samples ranged in weight from 15 to 60 grams. An effort was made to obtain as large a sample as possible, within the limits of size set by the dimensions of the sample tube, although it was found that consistent data were obtained provided the sample was sufficiently large to give a total adsorption of one cu cm or more at the completion of the mono-layer.

In general, about six or seven adsorption points were determined for each sample in the range of relative pressures from 0.05 to 0.35. Equilibrium conditions were usually established within 30 to 60 minutes at any given pressure within this range.

EXPERIMENTAL RESULTS

The above-described method of determining surface areas by low temperature gas adsorption has been applied to numerous samples of both sandstones and limestones. The results of these measurements are given in Table I. In column four the surface areas are expressed in square meters per gram, and it will be observed that the sandstones, for the most part, have surface areas within the range of 0.5 to 6 square meters per gram, whereas the limestones have surface areas from 0.05 to 0.5 square meter per gram. When the surface areas are referred to unit pore volume, however, as in column 5, a wider variation is encountered, with the values ranging from about

Table I-A — Surface Areas of Limestones

Sample No.	Fractional Porosity, f	Permeability, K (md)	Surface Area			Sample Description
			(sq. meters per gram)	(sq. meters per cc. pore vol.)	(sq. meters per cc. bulk vol.)	
Trenton Formation — Ordovician Age						
1	0.0102	0.34	0.38	99	1.01	dn., dk., gray, w/pyrite incl.
2	0.0136	0.03	0.13	25	0.35	hard, dk. gray, w/irr. blk. pln. and incl.
3	0.0805	0.03	0.26	8.0	0.65	gray and tan, w/dk. pln. and incl.
4	0.121	29.1	0.09	1.8	0.21	tan, visible porosity
5	0.0479	0.51	0.16	8.6	0.41	tan, w/blk. irr. plns.
6	0.0465	3.37	0.11	6.1	0.29	gray and tan, w/sec. cryst.
7	0.0378	0.79	0.12	8.2	0.31	gray and brown, fossil.
8	0.0640	0.31	0.14	5.5	0.36	lt. and dk. gray, sec. cryst.
9	0.0294	0.03	0.16	14	0.42	hard, dk. and lt. gray
10	0.0370	1.50	0.21	15	0.55	gray and tan, fossil., w/irr. sh. pln.
11	0.0432	0.04	0.17	10	0.44	gray and tan, fossil., w/irr. sh. pln.
12	0.0146	0.05	0.07	13	0.19	gray and tan, sec. cryst.
13	0.0197	0.05	0.36	49	0.95	hard, dk. gray, w/irr. blk. pln. and incl.
14	0.0085	1.56	0.17	54	0.46	gray and tan, w/dk. pln. and incl.
15	0.0080	3.87	0.23	77	0.62	gray, w/blk. incl.
16	0.0109	0.32	0.06	14	0.15	hard, fossil., w/dk. irr. incl.
17	0.0606	2.08	0.14	5.9	0.36	gray, fossil., w/sec. cryst.
18	0.0360	0.04	0.17	12	0.44	tan, w/irr. frac. filled w/sh.
19	0.0461	0.14	0.12	6.7	0.31	gray and tan, fossil., w/weathered faces.
20	0.0242	0.16	0.18	20	0.48	gray and tan, w/irr. incl.
21	0.040	*	0.13	8.4	0.35	dk. and lt. gray fossil, w/dk. sh. incl.
Caddo Formation — Pennsylvanian Age						
22	0.036	*	0.33	24	0.86	dn., w/carb. incl.
23	0.039	*	0.25	17	0.65	dn., w/sh. incl., slightly vug.
24	0.028	*	0.20	19	0.53	dn., w/carb. incl.
25	0.029	*	0.67	62	1.76	dn., carb., cryst.
26	0.023	*	0.51	59	1.35	carb., cryst.
27	0.042	*	0.01	0.6	0.03	dn., carb.
28	0.042	*	0.16	9.9	0.42	dn., carb., fossil.
29	0.035	*	0.11	8.2	0.29	dn., carb., fossil.
30	0.030	*	0.15	13	0.39	carb., cryst.
31	0.074	*	0.14	4.8	0.35	carb., cryst., slightly vug.
32	0.114	12	0.32	6.9	0.79	cryst., vug., carb.

* — permeability less than 0.1 md
 blk. — black
 carb. — carbonate (or carbonaceous)
 crs. — coarse
 cryst. — crystallization (or crystalline)
 dk. — dark

dn. — dense
 fossil. — fossiliferous
 frac. — fractures
 grn. — grained
 incl. — inclusions
 irr. — irregular

lt. — light
 pln. — planes
 sec. — secondary
 sh. — shale
 shly. — shaley
 vug. — vugular

1 to 100 square meters per cubic centimeter of pore volume for both limestones and sandstones. For a given pore volume, therefore, the limestones present surface areas of the same order of magnitude as the sandstones. The lower areas per gram and per unit bulk volume (column 6) for the limestones can possibly be attributed to the fact that their porosities are in general much lower than those of the sandstones tested.

In Table II, examples are given of the reproducibility of surface-area measurements as indicated by the values obtained in duplicate determinations. It will be seen that the precision increases somewhat with increasing surface area, but is sufficiently good at about 0.1 square meter per gram so that areas of this order of magnitude can be reproduced to within 5 per cent to 10 per cent. For areas of from 1 to 10 square meters per gram the precision is about 1 per cent to 5 per cent.

For the two samples of glass beads listed in Table II, the average bead diameters were estimated from microscopic examination to be 40 and 58 microns. The densities of the two samples were measured by water displacement and found to be 2.444 and 2.798 grams per cubic centimeter, respectively. From the average size and density, the geometrical areas were calculated to be 0.062 and 0.037 square meter per gram, with the assumption that the beads were spherical. The agreement between these values and the averages of the values obtained

by the gas adsorption method (0.070 and 0.039 square meter per gram) indicates the accuracy obtainable by the BET method.

In Table III a comparison is made of surface-area values obtained with both argon and nitrogen on the same sample. These data indicate that the two gases yield essentially the same areas and may, therefore, be used interchangeably. For samples of low surface area it is believed that, owing to the smaller effective cross-sectional area of the argon molecule, argon affords a slight advantage over nitrogen in providing a somewhat greater amount of adsorption for an equivalent area coverage.

THE KOZENY EQUATION

In recent years the Kozeny equation has attracted considerable attention as a possible aid in obtaining relationships between certain fluid and electrical flow phenomena associated with porous solids.^{8,9,10,11} This equation, which relates surface area to porosity and permeability, can be derived from a consideration of the general laws of fluid flow through capillaries of various shapes and of the surface-area - pore-volume rela-

Table I-B — Surface Areas of Sandstones

Sample No.	Fractional Porosity, ϕ	Permeability K (md)	Surface Area			Kozeny textural factor, k	Kozeny surface area (sq. m/g.)	Ratio of Adsorption Area to Kozeny Area	Sample Description
			(sq. m. per gm.)	(sq. m. per cc. pore vol.)	(sq. m. per cc. bulk vol.)				
Upper Wilcox Formation — Eocene Age									
33	0.189	0.48	4.03	45.8	8.66	18.0	0.413	9.8	hard, gray, shly.
34	0.168	0.26	3.54	46.4	7.80	11.2	0.582	6.1	hard, gray, shly.
35	0.207	1.33	3.56	36.1	7.48	25.3	0.246	14.5	hard, gray, shly., w/irr. sh. pln.
36	0.221	17.2	2.93	27.4	6.05	14.8	0.100	29.3	hard, shly.
37	0.197	9.58	2.65	28.6	5.64	15.6	0.107	24.8	hard, shly.
38	0.193	4.93	4.01	44.5	8.58	17.2	0.137	29.3	hard, shly.
39	0.183	0.34	5.10	60.3	11.0	19.6	0.445	11.5	hard, shly.
40	0.156	0.17	5.57	80.0	12.5	11.4	0.629	8.9	dk. gray, very shlv.
41	0.158	0.13	5.48	77.4	12.2	11.4	0.734	7.5	dk. gray, very shlv.
42	0.184	0.24	5.41	63.6	11.7	11.4	0.700	7.7	dk. gray, very shly.
43	0.190	0.37	6.12	69.2	13.1	12.5	0.570	10.7	gray, shly., w/irr. blk. streaks
44	0.189	571	0.79	9.0	1.70	13.5	0.0139	56.8	crs. grn., slightly shly.
45	0.213	755	1.32	12.9	2.75	11.3	0.0162	81.5	crs. grn., slightly shly.
46	0.219	217	1.17	11.1	2.44	22.2	0.0227	51.5	crs. grn., slightly shly.
47	0.193	94.8	1.59	17.6	3.40	22.5	0.0273	58.2	crs. grn., shly., w/irr. sh. pln.
48	0.223	66.7	3.08	28.4	6.34	12.2	0.0572	53.8	crs. grn., shlv.
49	0.223	275	1.36	12.6	2.80	8.3	0.0341	39.8	gray, shly., w/irr. blk. streaks
50	0.211	198	2.75	27.3	5.75	8.3	0.0364	75.5	gray, shlv., w/irr. blk. streaks
51	0.209	174	1.49	14.9	3.12	10.0	0.0347	43.0	gray, shlv., w/irr. blk. streaks
52	0.202	71.1	2.99	31.3	6.32	11.1	0.0485	61.7	gray, shly., w/irr. sh. pln.
53	0.213	137	3.91	38.3	8.15	10.5	0.0396	93.8	gray, shly., w/irr. sh. pln.
Middle Wilcox Formation — Eocene Age									
54	0.188	13.0	1.21	13.8	2.60	18.9	0.0765	15.8	tan
55	0.207	37.2	1.42	14.4	2.98	16.5	0.0575	10.0	tan
56	0.068	0.23	1.60	58.1	3.95	8.8	0.160	10.0	gray, shly., w/irr. sh. pln.
57	0.074	0.18	1.43	47.4	3.51	38.5	0.0989	14.5	gray, shlv., w/irr. blk. incl.
58	0.181	51.7	1.28	15.4	2.78	24.7	0.0316	40.5	gray, shly., w/irr. sh. pln and incl.
59	0.156	15.0	1.96	28.1	4.38	31.8	0.0400	49.0	gray, shly., w/irr. sh. pln and incl.
Catahoula Formation — Miocene Age									
60	0.234	242	0.72	6.2	1.46	18.7	0.0264	27.2	slightly shly., w/mica incl.
61	0.231	438	0.84	7.4	1.71	9.4	0.0270	31.1	slightly limey and shly., laminated
62	0.193	16.4	1.12	12.4	2.40	11.4	0.0921	12.2	tan, limey, shly.
63	0.205	23.6	1.60	16.4	3.37	11.9	0.0834	19.2	tan, limey, shly.
64	0.249	252	0.56	4.5	1.11	11.0	0.0376	14.9	tan, shly.
65	0.256	357	1.14	8.8	2.25	9.5	0.0359	31.7	tan, shly.
Chester Formation — Mississippian Age									
66	0.149	24.8	0.39	5.9	0.88	hard, gray, w/irr. sh. pln.
67	0.182	340	0.59	7.0	1.28	7.9	0.0219	27.0	hard, gray, w/irr. sh. pln.
68	0.158	278	0.06	0.8	0.13	hard, gray, w/irr. sh. pln.
69	0.161	45.5	1.38	19.1	3.07	10.5	0.0422	32.7	hard, gray, w/irr. sh. pln.

tionships of such capillaries. For a porous matrix of permeability K md and fractional porosity f , the surface area, S , in square meters per gram of solid, is given by the Kozeny equation as:

$$S = \frac{31.8 f}{\rho(1-f)} \sqrt{\frac{f}{kK}} \quad (5)$$

where ρ is the density of the solid (grain density) in grams per cubic centimeter and k is a nondimensional textural factor, the magnitude of which depends in part on the shape of the pores and on the length of the path taken by the fluid in traversing unit length of the porous solid. The utility of Equation (5) has, in the past, been somewhat limited by the fact that k could not be readily evaluated independently of the equation itself except for very simple geometrical configurations of pore space. In general k has been calculated from Equation (5) by making separate experimental measurements of S , ρ , K , and f .

A recent paper by Wyllie and Spangler¹¹ has indicated that a textural factor suitable for use in the Kozeny equation can be obtained for a given sample from its capillary pressure curve and permeability. Thus,

$$k = \frac{f(\gamma \cos \theta)^2}{9.87 \times 10^{-12} K} \int_{s=0}^{s=1} ds/P_c^2 \quad (6)$$

where P_c is the capillary pressure in dynes per square centimeter at fractional saturation s , γ is the interfacial tension in dynes per centimeter between the fluids for which the capillary pressure curve is determined and θ is the contact angle formed by the two fluids and the solid. As before, K is the permeability in millidarcys and f the fractional porosity.

Equation (6) has been applied in the determination of textural factors for a series of unconsolidated packs of glass beads. The beads used in these experiments were obtained from the Minnesota Mining and Manufacturing Co. under the trade name, "Scotch-Lite." The beads were carefully sieved and packs made up from each of the available size fractions, as indicated in Table IV. The porosity of each pack was determined from the internal dimensions of the cylindrical tube in which the beads were confined and from the weight and density of the beads. The permeability of each pack was determined by air flow. Mercury capillary pressure curves were determined for the packs, using an apparatus described previously¹² which was modified slightly to enable injection of mercury into the cylinders containing the beads. Typical curves are shown in Fig. 3.

The textural factors, calculated by means of Equation (6) from the permeability, porosity, and capillary pressure data, are given in column 7 of Table IV. These textural factors have been used to calculate the surface area of the beads by

Table II—Typical Data Showing the Reproducibility of Surface Area Determinations

Sample*	Surface Area (sq. meters per gram)		Per Cent Difference	Adsorbate
	Run 1	Run 2		
Sandstone (40)	5.60	5.55	0.9	Nitrogen
Sandstone (52)	2.98	3.00	0.7	
Sandstone (47)	1.55	1.63	5.0	Nitrogen
Limestone (10)	0.20	0.22	10.5	
Limestone (21)	0.13	0.14	7.4	Argon
Limestone (4)	0.091	0.086	5.6	
Glass Beads				
40 microns	0.068	0.072	5.7	Nitrogen
Glass Beads (K)				
58 microns	0.037	0.041	10.3	Nitrogen

*Numbers and letters in parentheses refer to Tables I and IV, respectively.

Table III—Comparison of Nitrogen and Argon Surface Areas

Sample*	Surface Area (sq. meters per gram)	
	Nitrogen	Argon
Sandstone	4.5	4.3
Limestone (13)	0.36	0.36
Glass Beads (K)	{ 0.037 0.041	0.039

*Numbers and letters in parentheses refer to Tables I and IV, respectively.

the Kozeny Equation (5), and the results are shown in column 8 of Table IV. In addition, the geometrical surface areas of the various packs have been computed from the average bead size (taken as the arithmetical average of the sieve openings) and the glass density, with the results shown in column 9.

A comparison of the Kozeny area with the geometrical area for the various packs indicates the former to be slightly, but consistently, higher than the latter. These differences can be explained in at least two ways: (1) The geometrical areas are based on the assumption that the particles are spherical and although a microscopic examination of the beads indicated this to be a good assumption, it is possible that minor imperfections in the beads cause the true surface area to be somewhat greater than the geometrical area. However, for the one pack (K) where the surface area was sufficiently large to make possible a determination by the gas adsorption method, the average value of the surface area so determined (0.039 sq. m/g) agreed more closely with the geometrical area than with the Kozeny area. (2) In computing the textural factors by means of Equation (6), a value of 140° was assumed for the contact angle of mercury against the glass. If this value is in reality too low, then the reported textural factors are likewise too low and the calculated Kozeny surface areas too high. If a value of 148° had been assumed for θ , then the textural factors would have been 23 per cent greater than those reported in Table IV, and the Kozeny areas would have been 10 per cent less, bringing them into closer agreement with the geometrical areas. It is quite probable that a combination of the two effects discussed above account for the differences between the Kozeny and geometrical areas of the bead packs although, because of the agreement cited above between the geometrical and gas adsorption areas, it is believed that the second of the factors is the more significant. In any event it is believed that the experiments here reported for the bead packs indicate that Equation (6) provides a reliable method for evaluating the textural factor. Although the absolute values of the factors so determined may be open to question because of uncertainties in the value of the contact angle, nevertheless the method should provide very good relative values.

The data presented in Table IV confirm the observations of other workers who have shown that for unconsolidated packs of fairly uniform particle and pore size the Kozeny equation provides a convenient means of obtaining a measure of the surface area. We turn now to a consideration of the applicability of the Kozeny equation to consolidated porous solids as represented by reservoir rocks.

For the sandstone samples listed in Table I-B, textural factors have been determined by means of Equation (6) from permeability, porosity, and capillary pressure data in the same manner as described above for the bead packs. The values of k so obtained have been employed in Equation (5) to calculate surface areas according to the Kozeny formulation. The permeabilities of the core plugs were determined by air flow at several mean pressures between about 1.5 and 7 atmospheres, appropriate corrections being made for gas slippage by the

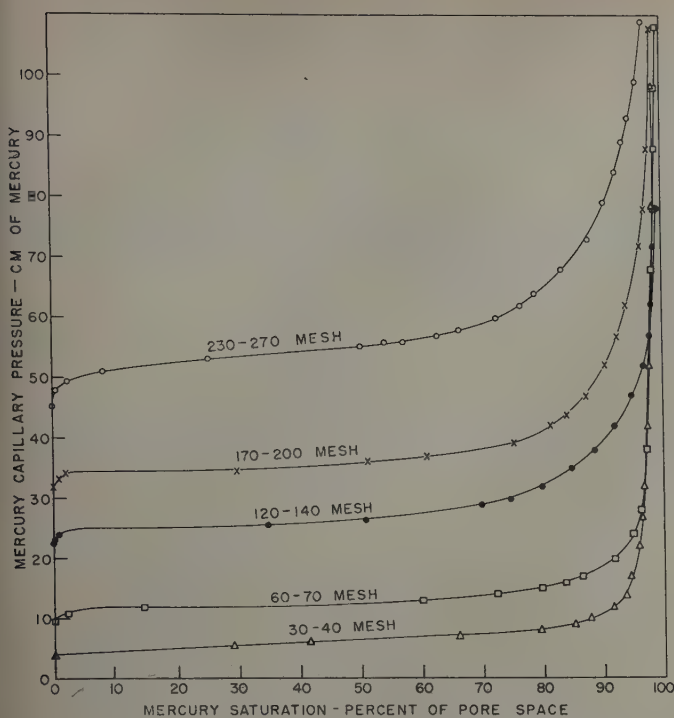


FIG. 3 — CAPILLARY PRESSURE CURVES FOR PACKS OF GLASS BEADS.

method of Klinkenberg.¹³ Porosities were determined by saturation of the plugs with an organic liquid.

Two conclusions are immediately apparent from an inspection of the values of the textural factor and of the Kozeny surface area as given in Table I-B. First, the values of the textural factor, which range from about 8 to 40, are considerably higher than the values of 3 to 4 which were found for the glass beads and the value of about 5 previously reported for unconsolidated packs of sorted sand grains.¹⁴ These higher values of k for consolidated sands appear reasonable since it may be expected that compaction and cementation will increase the tortuosity of the porous matrix.

Secondly, it will be observed that the surface areas, as determined by gas adsorption, are from about 5 to 100 times larger

than the areas calculated from the Kozeny equation. In considering in detail the gas adsorption and Kozeny methods of determining the surface areas of consolidated porous media, such as reservoir rocks, several reasons are indicated for the divergence of values obtained by the two methods. The Kozeny method can be expected to provide a measure of only the external surface of the solid particles which is contacted by a fluid in moving through the porous solid; whereas, the gas adsorption method should yield a measure of this external area plus any "internal" surface possessed by the solid particles and any surface contributed by "dead-end" pores that hold, but do not transmit, fluid. This difference is well recognized and has indeed already been pointed out by Lea and Nurse¹⁵ and others. In addition to the above, it is believed that lack of uniform pore size may play a considerable part in contributing to the divergent results obtained by the two methods. Carman¹⁶ has listed uniform pore size, together with several other factors, as a condition which must be fulfilled if the Kozeny equation is to yield a significant value of surface area for consolidated media. Intuitively, one can recognize the influence of nonuniformity of pore size in the following way: Consider first a porous solid of uniform pore size that contains no "dead-end" pores and whose surface is entirely available to a fluid which flows through the solid. Secondly, let us alter this system, insofar as the size distribution only is concerned, maintaining the same porosity and textural factor. This could be accomplished, for example, by subdividing just one of the many channels to form several smaller channels with the same shape and length as the original. This would serve to reduce the permeability by only a very small amount* but the surface area of the system could be increased without limit by continuing the subdivision of the one pore indefinitely. In other words the surface area could be altered practically independently of the permeability, whereas the Kozeny equation demands that for a given porosity and textural factor the surface area be inversely proportional to the square root of the permeability. This same point can be illustrated more rigorously by considering the following equation given by Calhoun, Lewis and Newman:¹⁷

$$S = \frac{10^{-4} f}{\rho(1-f)(\gamma \cos \theta)} \int_{s=0}^{s=1} P_c ds \quad (7)$$

*If n is the original number of pores and K_0 the original permeability, then the new permeability, K , approaches $\left(\frac{n-1}{n}\right) K_0$ as m , the number of new pores formed from the single original pore, approaches infinity.

Table IV — Surface Areas of Bead Packs

Pack	Sieve Size		Average Bead Diam. (cm.)	Fractional Porosity, f	Permeability K (darcys)	Kozeny Textural Factor, k^*	Kozeny Surface Area (sq. m/g.)	Geometrical Surface Area (sq. m/g.)	Ratio: Kozeny Area Geom. Area
	Thru	Onto							
A	30	40	0.0505	0.369	218	3.27	0.00548	0.00485	1.13
B	40	50	0.0360	0.361	99.7	3.44	0.00754	0.00682	1.11
C	50	60	0.0275	0.359	41.5	3.16	0.0121	0.00893	1.35
D	60	70	0.0230	0.359	37.9	4.00	0.0112	0.0107	1.05
E	70	80	0.0193	0.349	26.8	3.52	0.0134	0.0127	1.06
F	120	140	0.0115	0.377	11.4	3.39	0.0246	0.0213	1.15
G	140	170	0.00965	0.366	8.90	3.12	0.0273	0.0254	1.07
H	170	200	0.00810	0.394	6.41	3.38	0.0361	0.0303	1.19
I	200	230	0.00680	0.385	4.72	3.30	0.0405	0.0361	1.12
J	200	230	0.00680	0.375	4.12	3.36	0.0406	0.0361	1.12
K	230	270	0.00575	0.379	2.51	3.59	0.0450	0.0373	1.21

*Based on a measured surface tension, γ , of 480 dynes/cm and on an assumed contact angle of 140° .

Density of beads: Packs A thru J — 2.444 g/cm³
Pack K — 2.798 g/cm³

where the symbols have the same definition and units as given previously. Equation (7) accounts for variations in pore size within the porous solid and hence is not limited to systems of uniform pore size. Likewise Equation (6) should be generally valid as a means of determining k for systems of nonuniform, as well as uniform, pore size. By combining Equations (6) and (7) in such a manner as to eliminate the $(\gamma \cos \theta)$ term we find that:

$$S = \frac{31.8 f}{\rho(1-f)} \sqrt{\frac{f}{kK}} \left(\int_{s=0}^{s=1} P_c ds \sqrt{\int_{s=0}^{s=1} ds/P_c^2} \right) \quad (8)$$

The general Equation (8) reduces to the Kozeny Equation (5) only if

$$\int_{s=0}^{s=1} P_c ds = \frac{1}{\sqrt{\int_{s=0}^{s=1} ds/P_c^2}} \quad (9)$$

and Equation (9) holds only if the capillary pressure, P_c , has the same value for all values of the saturation, s (i.e., if the pores are all of the same size), a condition that is seldom encountered in reservoir rocks.

Attempts to determine quantitatively the effect of size distribution on the Kozeny equation or to introduce a measure of this property in the equation have so far met with little success. Hence, at the present time the physical significance of the surface area obtained by the Kozeny equation appears somewhat obscure when applied to porous media exhibiting nonuniform pore sizes.

SUMMARY

Results of surface-area measurements on sedimentary rocks utilizing the low-temperature gas adsorption method have shown that for the numerous samples tested the surface areas of the sandstones ranged from 0.5 to 6 square meters per gram whereas the areas of the limestones ranged from 0.05 to 0.5 square meter per gram. The porosities of the limestones tested were in general lower than those of the sandstones, and when the surface areas were compared on the basis of unit pore volume, rather than unit weight, no significant differences were observed between sandstones and limestones.

Mercury capillary pressure tests on the sandstone samples provided information from which rock textural factors were calculated. These factors were found to range from 8 to 40 as compared to the values of 3 to 4 which were obtained in the same manner for unconsolidated packs of spherical glass beads.

The textural factors have been employed in the Kozeny equation to calculate surface areas from porosity and permeability data. For the bead packs the surface areas so calculated were found to be very nearly equal to the geometrical area of the beads and, in the one instance where a gas adsorption measurement was possible, the Kozeny area agreed fairly well with the BET area. For the sandstones, the Kozeny areas were found to be much smaller than the areas determined by the gas adsorption method.

It is postulated that the lack of uniform pore size in naturally occurring rocks may limit the applicability of the Kozeny equation to such porous solids and may contribute, in

part, to the observed differences between the Kozeny and the gas adsorption surface areas.

ACKNOWLEDGMENT

The authors acknowledge with appreciation the assistance of M. I. Palmer, Jr., who carried out the measurements of permeability, porosity, and capillary pressures reported in this paper.

REFERENCES

1. Brunauer, S.; Emmett, P. H.; and Teller, E.: "Adsorption of Gases in Multimolecular Layers," *J.A.C.S.*, (1938), **60**, 309.
2. Brunauer, S.: *The Adsorption of Gases and Vapors*, Princeton University Press, Princeton, N. J., (1945), **1**, Chapter 6.
3. Livingston, H. K.: "The Cross-Sectional Areas of Molecules Adsorbed on Solid Surfaces," *J. Colloid Science*, (1949), **4**, 447.
4. Barr, W. E.; Anhorn, V. J.; and Joyner, L. G.: "Gas Adsorption Apparatus for Measuring Surface Areas," *Instruments*, (1947), **20**, 454 and 542.
5. International Critical Tables, (1938), 1st Ed., **3**, 6.
6. Wooten, L. A.; and Brown, C.: "Surface Area of Oxide Coated Cathodes by Adsorption of Gas at Low Pressure," *J.A.C.S.*, (1943), **65**, 113.
7. Beebe, R. A.; Beckwith, J. B.; and Honig, J. M.: "The Determination of Small Surface Areas by Krypton Adsorption at Low Temperatures," *J.A.C.S.*, (1945), **67**, 1554.
8. Rose, Walter: "Theoretical Generalizations Leading to the Evaluation of Relative Permeability," *Trans. AIME*, (1949), **186**, 111.
9. Wyllie, M. R. J.; and Rose, Walter: "Some Theoretical Considerations Related to the Quantitative Evaluation of the Physical Characteristics of Reservoir Rock from Electrical Log Data," *Trans. AIME*, (1950), **189**, 105.
10. Rapoport, L. A.; and Leas, W. J.: "Relative Permeability to Liquid in Liquid-Gas Systems," *Trans. AIME*, (1951), **192**, 83.
11. Wyllie, M. R. J.; and Spangler, M. B.: "Application of Electrical Resistivity Measurements to Problem of Fluid Flow in Porous Media," *Bull. AAPG*, (1952), **36**, 359.
12. Purcell, W. R.: "Capillary Pressures—Their Measurement Using Mercury and the Calculation of Permeability Therefrom," *Trans. AIME*, (1949), **186**, 39.
13. Klinkenberg, L. J.: "The Permeability of Porous Media to Liquids and Gases," *API Drill. and Prod. Prac.*, (1941), **200**.
14. Carman, P. C.: "The Determination of the Specific Surface of Powders," *J. Soc. Chem. Ind.*, (1938), **57**, 225.
15. Lea, F. M.; and Nurse, R. W.: "Permeability Methods of Fineness Measurement," Symposium on Particle Size Analysis, Institution of Chemical Engineers and Society of Chemical Industry, Feb. 4, 1947; Supplement to *Trans. Inst. of Chemical Engineers*, (1947), **25**, 54.
16. Carman, P. C.: "Some Physical Aspects of Water Flow in Porous Media," *Discussion of the Faraday Society*, (1948), No. 3, 72.
17. Calhoun, J. C.; Lewis, M.; and Newman, R. C.: "Experiments on the Capillary Properties of Porous Solids," *Trans. AIME*, (1949), **186**, 189.

★ ★ ★

THE PRESSURE PERFORMANCE OF FIVE FIELDS COMPLETED IN A COMMON AQUIFER

W. D. MOORE, HUMBLE OIL AND REFINING CO., MIDLAND, TEX., AND L. G. TRUBY, JR., HUMBLE OIL AND REFINING CO., CORPUS CHRISTI, TEX., JUNIOR MEMBERS AIME

ABSTRACT

This paper presents the results obtained after calculating matches of the observed pressure performance of five fields completed in a common aquifer. A general description of the Central Basin Platform area in West Texas in which the five fields, Andector, Embar, Martin, TXL, and Wheeler, are located is contained in the paper. The method of utilizing the electric analyzer to calculate simultaneously matches of the observed pressure performance of the five fields is outlined. The determination of boundaries of pressure communication is discussed and the extent of pressure interference between fields consistent with the configuration of the area aquifer is shown graphically.

INTRODUCTION

Anomalies in the pressure performance of the Andector Ellenburger Field resulted in an investigation of pressure interference between several Ellenburger fields located on the Central Basin Platform in West Texas. Four fields, Embar, Martin, TXL, and Wheeler, were found to contribute significantly to the pressure drawdown at Andector.

An initial investigation of the pressure performance of the Andector Ellenburger Field revealed that the reservoir pressure could not be matched by the calculation technique usually applied to water drive reservoirs. In the past, many have advanced the opinion that fracturing in the Ellenburger was a local condition restricted to the immediate uplifted area

around the field, in which case each field would in all probability be surrounded by its own relatively small aquifer. Following several unsuccessful attempts to account for the pressure performance at Andector, a system assuming a common aquifer involving several fields in the immediate vicinity of Andector was placed on the electric analyzer and the effect of interfield interference was noted. A refinement of the initial analyzer calculations involved the determination of the approximate boundaries of the aquifer, the calculation of detailed matches of the pressure performance of the interfering fields, and an evaluation of the degree of communication between fields.

DISCUSSION

Geology and Development

The fields considered in this work are located in the Central Basin Platform, a north-south trending structural feature in West Texas lying between the Delaware Basin to the west and the Midland Basin to the east. The locations of various individual Ellenburger fields in this general are shown in Fig. 1 with the five major fields which appear to be definitely intercommunicating colored in black and located in the circled portion of the figure.

Production from the five fields was first obtained from the Embar Field discovered in July 1942, followed by the Wheeler Field in 1943, the TXL Field in 1945, and the Martin and Andector Fields in 1946. The total reservoir fluid production from these fields is indicated in Fig. 2. As illustrated in this figure, very little production was taken from these fields prior

¹References given at end of paper.

Manuscript received in the Petroleum Branch office July 31, 1952. Paper presented at the Petroleum Branch Fall Meeting in Houston, Tex., Oct. 1-3, 1952.

to 1946, when the total withdrawals began to climb rapidly, reaching a peak of approximately 120,000 reservoir bbl of fluid per day in December 1948.

The Ellenburger formation on the Central Basin Platform in the area under consideration is a dense dolomite approximately 1,000 ft thick. Oil production in the Ellenburger is found on local structural highs generally characterized by a high degree of fracturing. Although some vugs and solution channels are present, the dolomite matrix is dense with a very low porosity and a low permeability on the order of 0.1 md. Several fracture systems are present in the Ellenburger, as indicated by the observation of fresh fractures cutting across secondary deposits in older fracture systems. The fracture observed in the Ellenburger cores are primarily of the jointing type in which there has been little or no displacement parallel to the plane of the break. Pressure communication within fields is generally good and well productivities are high, indicating a relatively high permeability in the fracture system.

It has been previously supposed by many that the fracturing observed in the Ellenburger fields was of a local nature, being confined primarily to the local structural features. This condition, if present, would result in a series of fields surrounded by individual aquifers of limited extent. In such a case, there

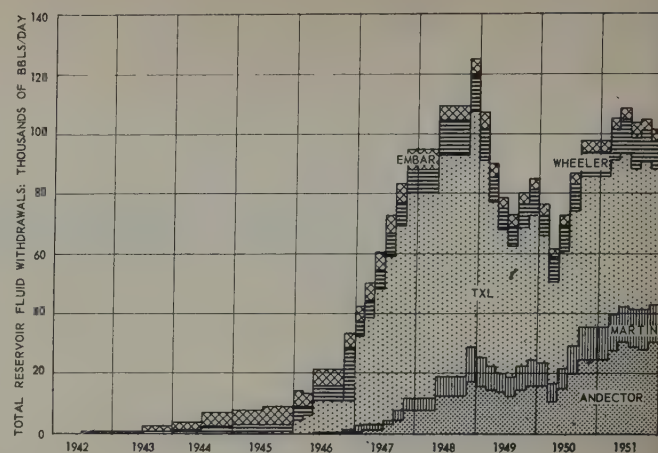


FIG. 2 — DISTRIBUTION OF FLUID WITHDRAWALS FROM FIVE FIELDS IN THE ELLENBURGER AQUIFER.

would probably be no effective pressure communication between fields during their productive history. A survey of available geologic information on the Ellenburger was made in order to determine if any of the available data would actually preclude consideration of continuous permeability and communication between fields. No data of this type were found. On the contrary, an examination of available drill-stem test data on wildcat wells on the central Basin Platform area indicated the presence of appreciable permeability in wells between producing fields. Since very little matrix permeability is present in the Ellenburger, the permeability encountered on the wildcat tests is indicative of an extension of the fracture system away from the producing areas.

Calculation Technique

The utility of the electric analyzer for appraising the pressure performance of water drive reservoirs has been discussed.¹ The electric analyzer is particularly well suited for evaluating reservoir pressure performance where more than one reservoir is producing from a common aquifer in that it provides a method for simultaneously calculating the magnitude of the pressure drawdown in reservoirs where interference is taking place.

Attempts were made to match the pressure performance of the five major fields on the electric analyzer water drive unit by considering each field individually and withdrawing production from all of the fields at the appropriate location on the water drive network. A discussion of this water drive network and pool unit network calculation technique on the electric analyzer as applied to an aquifer in which more than one field was producing has been published in the literature.² Fair pressure performance matches were obtained for Andector,



FIG. 1—ELLENBURGER FIELDS IN THE CENTRAL BASIN PLATFORM AREA.

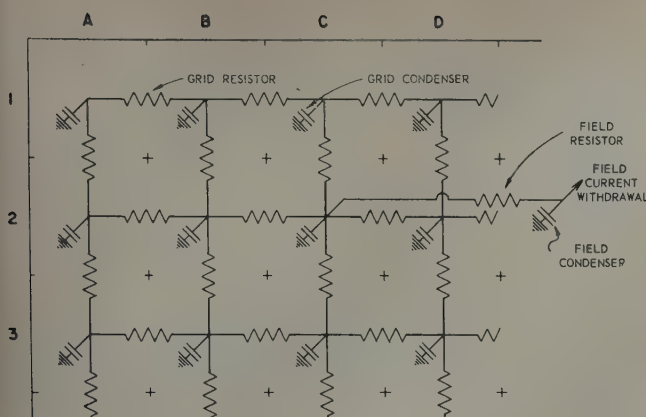


FIG. 3 — ELECTRIC ANALYZER POOL UNIT CIRCUIT DIAGRAM.

Fig. 4 illustrates the grid system on the analyzer as it was superimposed on the area being studied. The electric network was then developed to correspond with the location of the fields on the grid. The electrical analogy of the TXL Field, which occupies portions of two grid squares, 6-C and 7-C, was developed by having no resistance between the two grids in which the field falls and withdrawing the field production from a field condenser and field resistor wired to the two grid condensers.

Boundaries of Pressure Communication

The location of the boundaries of pressure communication in the aquifer is important to the calculated pressure behavior of the five fields considered in that they control the agreement between calculated and observed pressure behavior and also the relative magnitude of the pressure interference between

Embar, and Martin in this manner, but attempts to obtain pressure matches for the TXL and Wheeler Fields with an electrical representation of the aquifer configuration that appeared to be consistent with that used for the northern three fields were unsuccessful. It was thought that the relative position or porosity pinchouts, could account for the fact that the pressure performance of all the five fields was not matched on the water drive unit. In order to pursue this approach, the five fields and the surrounding areas were depicted through the use of the pool unit on the electric analyzer.

The basic electrical circuit of the analyzer pool unit is shown in Fig. 3. The electric network is set up on a grid pattern so that the pressure in any grid is analogous to the voltage on the condenser. The condenser is analogous to the potential expansibility of the fluids under the grid area, the resistances are analogous to the reciprocal of the permeability, and the current withdrawals from the field condensers are analogous to the fluid withdrawals from the reservoirs. In this study, the individual fields were investigated by separating them from the grid area in which they were located by adding a field resistor and field condenser to the grid condenser, as shown in Fig. 3. The individual reservoir fluid withdrawals were represented by the magnitude of the current withdrawn from the network at the field condenser.

The electrical analogy of the pool unit represents fluid flow in two dimensions and not three dimensions. For this reason, it was necessary to adjust the observed individual field pressures to a common datum. A pressure datum of 6,000 ft subsea was selected at which the original aquifer pressure was estimated to be 3,900 psi. All production data were converted to reservoir barrel fluid withdrawals, as is routine in an electric analyzer study. The sizes of the condensers in the grid areas were determined by assuming equal formation thickness and porosity in the five-field area. The sizes of the field condensers were calculated by taking into consideration the volume and expansibility of the oil in each field. The reservoir pressure in all five fields under consideration has not yet fallen below the saturation pressure for any field, and, for this reason, the coefficient of expansion for the oil in any individual field was held constant.

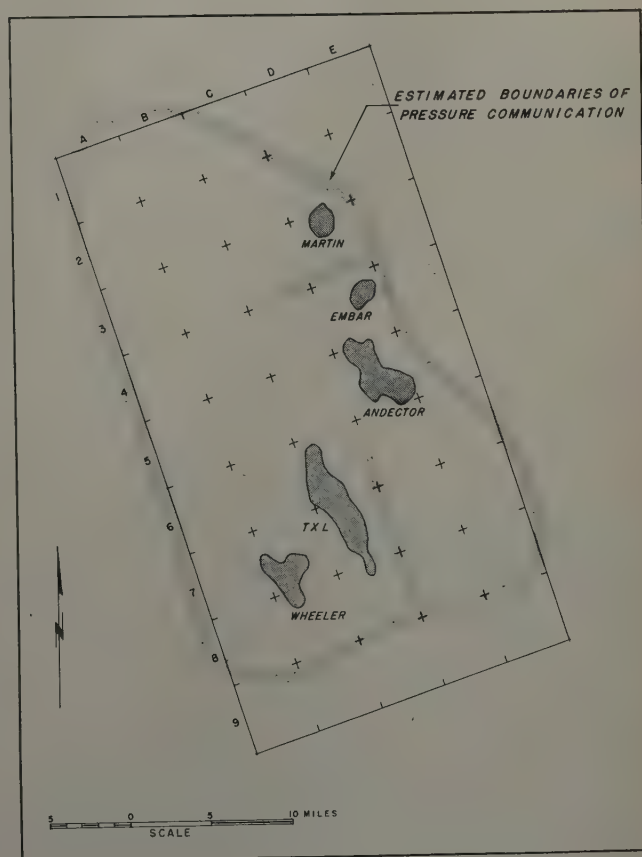


FIG. 4 — ANALYZER POOL UNIT GRID SYSTEM SUPERIMPOSED ON FIVE-FIELD AREA WITH ESTIMATED BOUNDARIES OF PRESSURE COMMUNICATION.

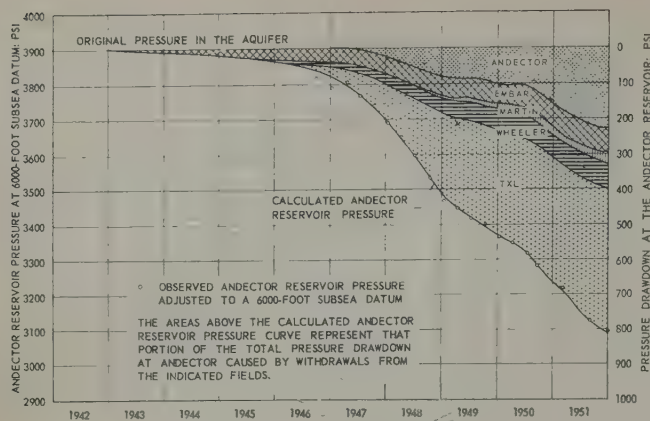


FIG. 5—ANDECTOR ELLENBURGER PRESSURE PERFORMANCE WITH INTERFIELD INTERFERENCE.

fields. The estimated boundaries of pressure communication, shown in Fig. 4, were determined after an examination of the geologic data available and after trial-and-error calculations of the pressure performance of all five fields. This trial-and-error process consisted of depicting a boundary on the analyzer that would be compatible with geologic data and would also allow the pressure performance history of all five major fields in the aquifer to be matched simultaneously on the analyzer. The boundaries shown represent barriers to pressure communication or fluid flow in the area considered and could be the result of either faulting and displacement of the Ellenburger or of a porosity or permeability pinchout in the aquifer.

The boundaries within the aquifer and in the northern portion of the aquifer are based primarily on geologic data relative to major faulting systems that actually displace the Ellenburger section. The boundaries indicated on the southern edge of the aquifer are based primarily on the pressure production performance of the fields completed in the Ellenburger. For example, it was determined that the Keystone Field, located approximately 12 miles west of the Wheeler Field, was not in communication with the five-field area as a result of the trial-and-error calculations of the field pressure performance. It was not possible to match the pressure performance of Keystone in a system where pressure communication was assumed to exist between Wheeler and Keystone; whereas, the difficulty disappeared when a boundary to flow was assumed to be located between the two areas. A boundary of this type could be due either to faulting or porosity pinchout.

Even though a complex faulting system is located to the south of the five-field area, the location of the estimated boundary of communication in this area is based primarily on pressure performance data. The pressure history of the five-field area indicates that an almost completely closed boundary exists to the south, but it is necessary to maintain a small amount of pressure support from the south or southeast. To date, there has not been sufficient production or pressure drawdown in fields to the south, such as Yarbrough and Allen or Jordan, to determine definitely whether or not they are in partial communication with the five-field area to the north.

Even though some of the boundaries or restrictions to flow are indefinite, they represent the configuration of the aquifer as reflected in the pressure performance of the five fields and are consistent with available geologic data.

Calculated Pressure Performance

The resulting matches of the calculated and observed pressure performance for the five major fields within the aquifer system described previously are illustrated in Figs. 5 through 9. Referring specifically to the Andector data in Fig. 5, excellent agreement exists between the calculated and observed pressures with a maximum deviation of 15 lb throughout the last four years of the pressure history. Matches of the calculated and observed pressures are shown for Embar, Martin, TXL, and Wheeler Fields with greater deviation in pressure noted in some instances.

After obtaining the pressure matches for the five fields, the interference effects between the fields were evaluated by selectively withdrawing production from only one field and observing the effects of the withdrawals from this one field on the pressure at each of the other fields. The interference effects of all the fields as observed at any one field are additive and the summation of the pressure drawdown caused by the withdrawals from each individual field is equal to the total drawdown observed in any field. This process of selective withdrawals was continued until the interference between all five fields was evaluated. The relative interference effects of the five fields on the Andector pressure performance are shown in Fig. 5 as component parts of the total pressure drawdown observed in Andector. It will be noted that production from the Andector Field has caused a reduction in pressure at Andector of only 230 lb as of Jan. 1, 1952, or less than 30 per cent of the total pressure decline of 810 lb observed in that field as of that date. In other words, if none of the fields except

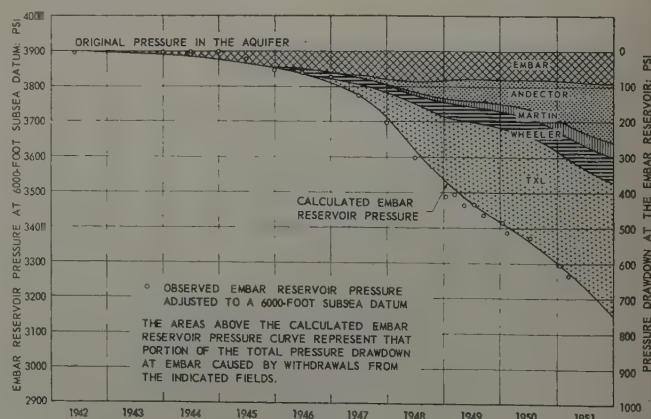


FIG. 6—EMBAR ELLENBURGER PRESSURE PERFORMANCE WITH INTERFIELD INTERFERENCE.

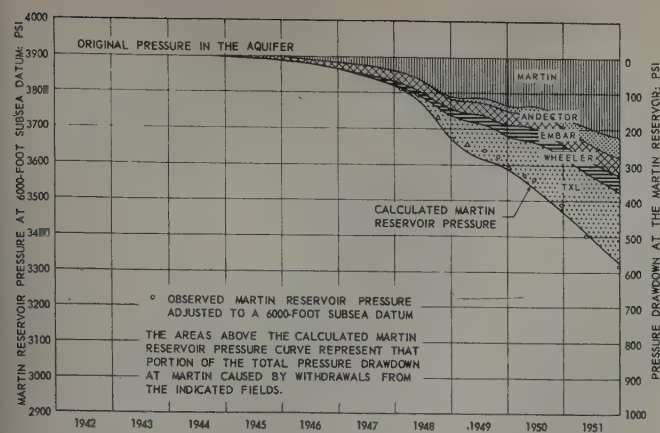


FIG. 7 — MARTIN ELLENBURGER PRESSURE PERFORMANCE WITH INTERFIELD INTERFERENCE.

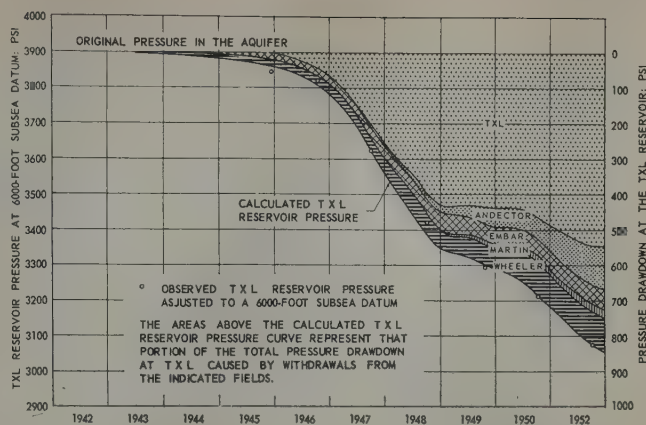


FIG. 8 — TXL ELLENBURGER PRESSURE PERFORMANCE WITH INTERFIELD INTERFERENCE.

Andector had been discovered, the pressure in Andector on Jan. 1, 1952, would have been 3,670 lb at 6,000 ft subsea, 580 lb higher than the adjusted pressure of 3,090 lb at 6,000 ft subsea. The pressure in Andector as of Jan. 1, 1952, has been reduced 80 lb by withdrawals from Embar, 30 lb by withdrawals from Martin, 75 lb. by withdrawals from Wheeler, and 405 lb by withdrawals from TXL. Thus, the withdrawals from the other four fields in the aquifer have resulted in slightly more than 70 per cent of the total pressure decline observed at Andector.

Similar interference effects on the other four fields are shown in Figs. 6 through 9. As will be noted from these illustrations, the withdrawals from the smaller fields, such as Embar, Martin, and Wheeler, have had relatively little effect on either their own pressure or on the aquifer pressure. The major portion of the pressure reduction within the aquifer has resulted from withdrawals from Andector and TXL, with TXL alone being responsible for a substantial portion of the pressure decline throughout the aquifer up to Jan. 1, 1952.

Two small Ellenburger fields, Bedford and Goldsmith, are located within the boundaries of pressure communication shown on Fig. 4. Bedford Field is located approximately 10 miles west of Embar Field and would fall in Grid 3-B. A match of the pressure performance of the Bedford Field, in conjunction with the general pattern of interfield interference, was not obtained. The pressure at Bedford is primarily the result of fluid withdrawals from the field itself and is attributed to a local permeability condition. Goldsmith Field is located approximately seven miles east of TXL and falls in Grid 7-E. A satisfactory match of the pressure in this field was obtained with the pressure drawdown attributed almost entirely to the pressure interference from nearby major fields, particularly TXL and Andector.

The calculated isobaric pattern effective Jan. 1, 1952, is shown in Fig. 10. This isobaric map was constructed by referring to the calculated pressure in the grid areas represented on the pool unit of the electric analyzer. As indicated on this illustration, the pressure profile throughout the aquifer is relatively flat with a maximum differential in pressure of 400 lb in an area approximately 35 miles in length and 20 miles in

width. This degree of pressure communication throughout an area of this magnitude is indicative of a relatively high order of permeability throughout the aquifer. The analyzer results indicate that the aquifer has a mean permeability of approximately 50 md.

The discovery well of the Block 12 Ellenburger Field, Phillips' University Well EE-1, has been drilled early in 1952 within the estimated boundaries of communication for the five-field area. A pressure of approximately 3,320 lb adjusted to a 6,000-ft subsea datum was measured in the well in April 1952. This discovery is located approximately seven miles west of Martin Field and would fall in Grid 2-B near the 3,400-lb contour on the isobaric pattern effective Jan. 1, 1952. At the rate of pressure decline in the aquifer calculated during 1951,

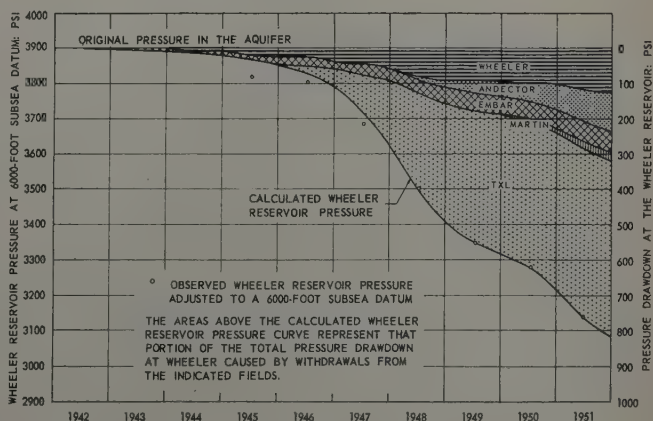


FIG. 9 — WHEELER ELLENBURGER PRESSURE PERFORMANCE WITH INTERFIELD INTERFERENCE.

the pressure in the area of this well would be approximately 3,360 lb as compared with the observed pressure of 3,320 lb. Since the observed pressure is 580 lb lower than the estimated original aquifer pressure of 3,900 lb at 6,000 ft subsea, the agreement between the observed and calculated pressure is considered good.

In summarizing the results of this study, it is pointed out that a match of the pressure performance of a water drive reservoir is only one of the several considerations involved in a complete reservoir study made for the purpose of translating an understanding of the reservoir behavior into operating recommendations. In a large majority of previous reservoir studies, apparent satisfactory matches of pressure performance have been obtained without considering the effect of pressure interference among fields producing from a common aquifer. It is realized that the interference effect in most aquifers has only an insignificant bearing on the results obtained using the simple, direct unsteady state solution of pressure performance. However, in the case of limited aquifers, such as the one discussed in this paper, pressure interference may be of such magnitude that the normal approach is entirely inadequate for calculating reasonably accurate pressure predictions. The results of this study further illustrate the utility of the electric analyzer in obtaining solutions to problems of this general type.

REFERENCES

1. Bruce, W. A.: "An Electrical Device for Analyzing Oil Reservoir Behavior," *Trans. AIME*, (1943) 151, 112.
2. Rumble, R. C., Spain, H. H., and Stamm, H. E., III: "A Reservoir Analyzer Study of the Woodbine Basin," *Trans. AIME*, (1951) 192, 331.

★ ★ ★

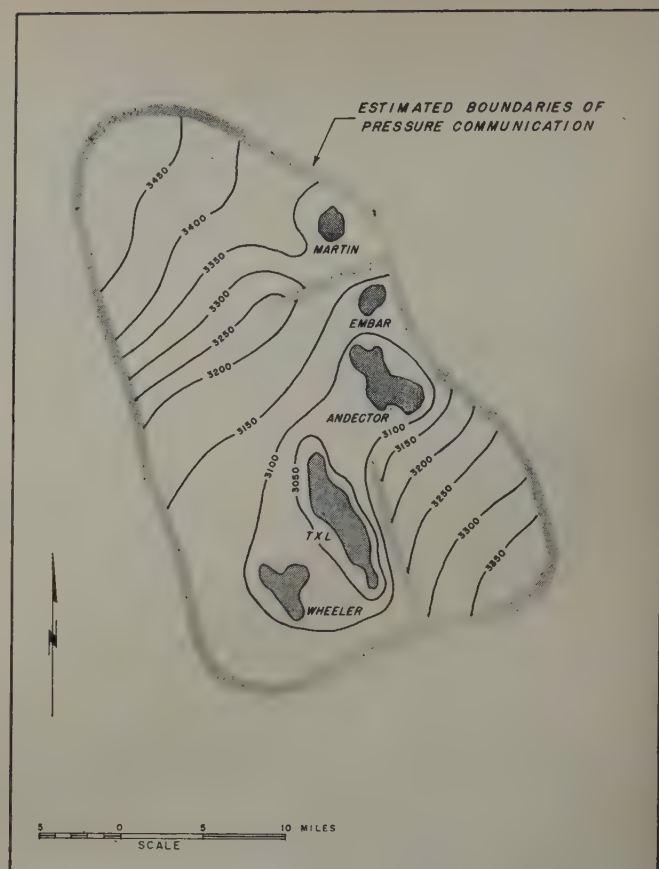


FIG. 10 — CALCULATED ISOBARIC PATTERN EFFECTIVE JAN. 1, 1952.

A METHOD OF PERFORATING CASING BELOW TUBING

M. P. LEBOURG AND G. R. HODGSON, SCHLUMBERGER WELL SURVEYING CORP., HOUSTON, TEX.

ABSTRACT

The introduction in the field of a new type well completion called for the setting of tubing open-ended in the well before perforating the casing. This paper describes a new perforating tool of the shaped charge expendable type, small enough to pass through tubing and powerful enough to perforate the casing. The perforations are produced at an angle and are large enough for optimum production. Performance of this tool in targets and under various well conditions is described.

Very often no lifting equipment will be available at the well. In some cases, pressure will exist in the well at the time of the perforating operation (workover wells or multiple trip perforation); therefore, new equipment and new technique for the perforating operation were devised. This paper describes this equipment and technique, particularly casing collar recording, sheave support, and cable pull-down device, this last item being necessary for wells under pressure. Results obtained with this tool in the field are given.

INTRODUCTION

One of the key requirements for the introduction in the field of a new method of permanent well completion was the development of a new perforating method involving the use of a perforating gun small enough to go through tubing and with enough penetrating power to perforate the casing satisfactorily.

The equipment described in this paper was basically designed to go through open-ended two-in. tubing and to perforate 5½-in. casing. The equipment is illustrated in accompanying figures.

NEW COMPLETION METHOD

With the new permanent type well completion, the production string of casing is run and cemented through the potential producing zone. Open-ended tubing is then run into the well and used to replace the drilling fluid with oil or water. The amount of the oil or water "cushion" can be varied according to the expected bottom hole pressure. Thus, if desired, the hydrostatic head can be greater, equal to, or less than the expected pressure within the zone to be perforated.

Mud having been displaced, the tubing is then positioned so that the end is above the zone to be perforated.

The Christmas tree and flow lines are installed and tested. The drilling rig can now be removed from the well since it is not necessary for the perforating operation, thus resulting in a saving in rig time. The perforating equipment is then moved to the well and the gun lowered through the tubing. After the gun passes out of the open end of the tubing, the depth measurements are correlated with casing collars and the gun placed opposite the zone to be perforated. Upon firing, the gun body is shattered and falls to the bottom of the well.

Since the lubricator has been closed before firing, it is possible to withdraw the casing collar locator and head and then open the well immediately to the tanks.

DESCRIPTION OF GUN

An investigation of two basic types of perforators, namely a bullet perforator and a shaped charge gun, was undertaken towards the development of a gun to meet the aforementioned requirements.

Preliminary tests on various bullet perforator designs within the diameter limitations did not give results encouraging enough to warrant further study.

Somewhat better results were obtained by using conventional shaped charges; but, as in the case of the bullet types, the necessarily small overall diameter proved to be a severe limitation and resulted in insufficient penetration.

A shaped charge employing a new design was developed which gave excellent penetration. These shaped charges were designed to produce a large hole directed upward at a 45° angle.

In order to obtain the maximum space possible for these charges, it was decided to use an expendable carrier made of drillable material, usually aluminum, which would shatter at the time of firing, leaving only harmless fragments at the bottom of the hole. The fixed spacing is five shots per ft. with

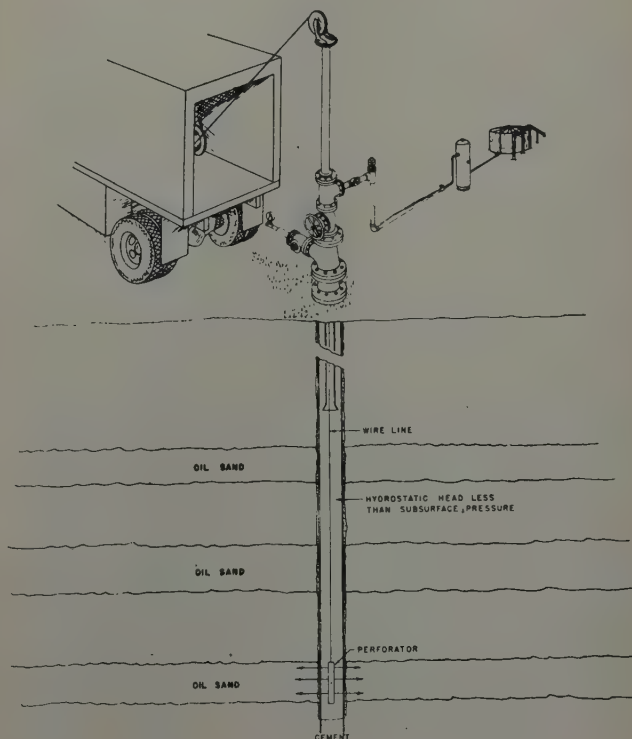


FIG. 1 — PERFORATING FOR ORIGINAL COMPLETION.

References given at end of paper.

Manuscript received in the Petroleum Branch office Aug. 21, 1952. Paper presented at the Petroleum Branch Fall Meeting in Houston, Tex., Oct. 1-3, 1952.

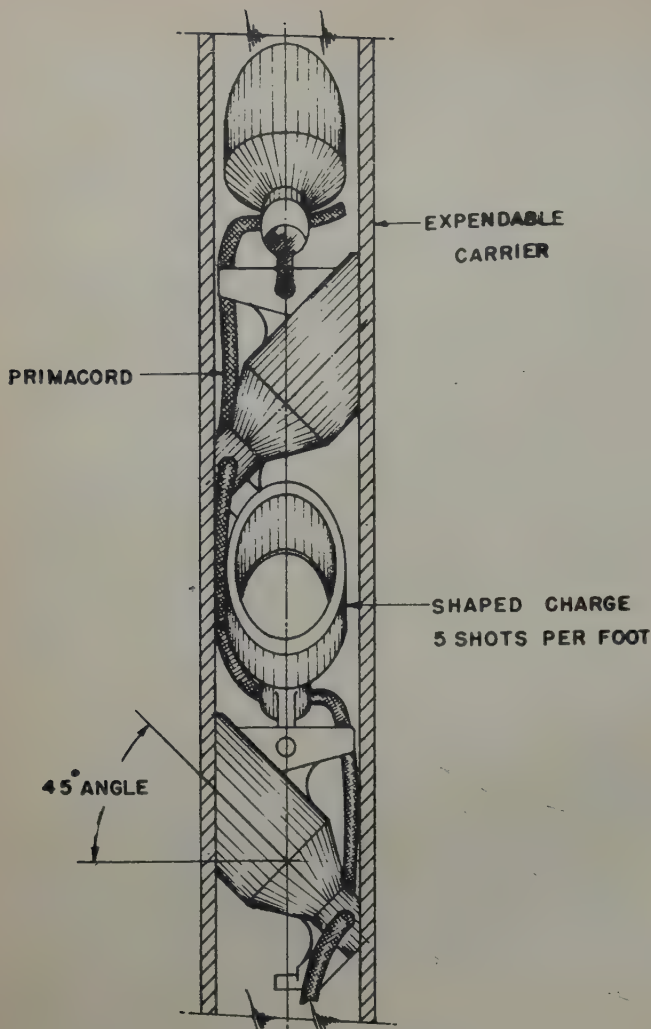


FIG. 2 — GUN CROSS SECTION.

a spiral pattern for the holes, and all charges are fired simultaneously. A sketch of the perforator is shown in Fig. 2.

The outside diameter of the aluminum carrier is $1\frac{3}{4}$ -in., which allows passage through clean 2-in. tubing. The length of the gun is determined by the interval to be perforated. The carrier will withstand a bottom hole pressure up to 4,000 psi. However, due to the low hydrostatic head pressure encountered at the time of completion, this has not been found to be a limiting factor in the use of this gun. A dimension sketch of the complete gun assembly is shown in Fig. 3.

In cases of higher bottom hole pressure, $1\frac{3}{4}$ -in. brass carriers have been used for running through 2-in. tubing, maximum pressure 7,000 psi. When $2\frac{1}{2}$ -in. tubing is used, the carrier can be made from heavy wall aluminum pipe able to withstand up to 9,000 psi.

LABORATORY TESTS VS. FIELD EXPERIENCE

Figs. 4 and 5 show the results obtained in laboratory targets by firing the angle shooting shaped charge in the carrier under water with a standoff of $\frac{1}{2}$ in. Other laboratory tests prove that when this gun is fired, no damage to casing results, even when the casing is unsupported.

It is most interesting to find, however, that field performance has proven that in many cases, penetration has exceeded that

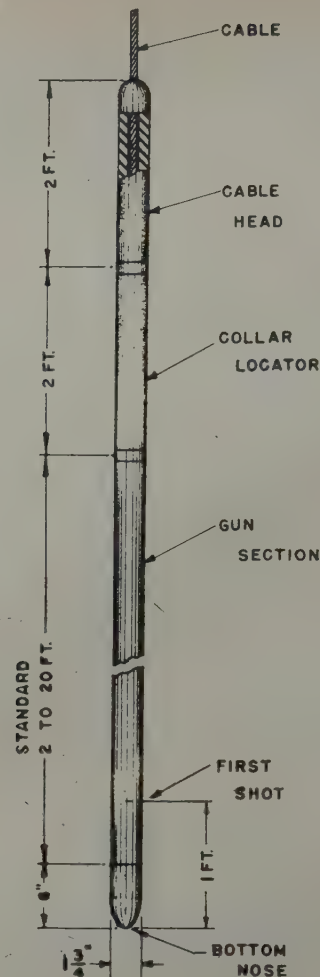


FIG. 3 — COMPLETE GUN ASSEMBLY.

anticipated from laboratory tests, for instance, perforating through 2-in. tubing and $5\frac{1}{2}$ -in. casing.

Since excellent production was recorded, a theory has been advanced that in cases of unconsolidated sand backing the cement sheaf, there is localized fracturing of the cement due to the wedge effect when shooting at an angle.

CASING COLLAR LOCATOR

In order to obtain accurate perforating depths and to give the oil company a permanent record of the tubing and casing setting, a casing collar log is essential.

A special magnetic casing collar locator was designed with a diameter of $1\frac{3}{4}$ in. to go through 2-in. tubing. This tool not only gives a clear record of the casing collars, the end of the tubing, and the tubing joints, but it also gives a clear indication of the packer back of the tubing (see Fig. 6). The collar locator comprises two magnetic circuits in opposition and a coil in between. Any unbalance in the magnetic circuits, for instance a casing collar, produces in the coil a transient voltage which is transmitted through the cable to the surface recorder.

Signals on the recorder while going down serve as a definite indication of the downward motion of the gun, eliminating the possibility of the piling up of cable in the well if the gun should be stopped by an obstruction.

PREPARATION OF THE WELL

New Wells

1. **Perforating Zone in Regard to Total Depth:** The gun is designed so that there is a distance of one ft from the bottom charge to the gun end. Therefore, this amount of clearance is necessary between the lowest perforating point and total depth. In actual field practice, it is recommended that this distance be at least two or three ft.

In the use of this perforator for the completion of new wells, certain steps must be taken.

2. **Tubing Setting with Reference to Production Zone:** The tubing should be set at least 10 ft above the zone to be perforated. Preferably enough open casing should be left for the recording of casing collars.
3. **Hydrostatic Head of Fluid:** If the pressure of the zone to be perforated is known, it is advantageous to keep the fluid level low enough so that the hydrostatic head will be smaller than the formation pressure. However, pressure should not be decreased to a point permitting violent pressure differentials at the time of shooting which could damage the reservoir.

In the case of a new sand of unknown pressure, a safe hydrostatic head can be applied within the limitation of the collapsing pressure of the gun. It should be pointed out that some method of fluid removal should be provided, such as gas lift valves, straight gas injection, or a swabbing unit to remove the excess fluid after perforation.

4. **Gauging Tubing for Gun Clearance:** A very important phase of the operation is the preparation of the tubing string. It is recommended that a gauge be run through the joints of tubing before they are run into a well. This will eliminate any crooked or "tight" joints that would give trouble in the well. It should be remembered that any gas lift valves, packer mandrels, or other devices installed in the tubing string should have a clearance equivalent to the inside diameter of 2-in. tubing.

5. **Closure of Tubing End Subsequent to Perforating:** Since some operators will have objections to leaving the tubing open-ended, a removable tubing stop can be installed. It will be necessary to provide a seating nipple for this device at the down-well tubing-end before running the tubing into the well.

A sketch of one type of landing nipple and tubing stop is shown in Fig. 7. The stop is pushed down the tubing after the perforating operation. It can be removed at any time by use of a standard wire line fitted with a standard 2-in. pulling tool.

6. **Cleaning Well Opposite Zone to be Perforated:** The cleaning of the well in preparation for the perforating operation is highly desirable in this type of completion. After cementing the casing, the tubing is installed and the displacement of the drilling fluid begun. In order to eliminate the possibility of heavy mud at the bottom, sufficient extra tubing should be placed in the string to assure a washing action below the depth to be perforated. A thorough washing of



FIG. 4 — CLOSE-UP OF TEST TARGET SHOWING JET PATH.

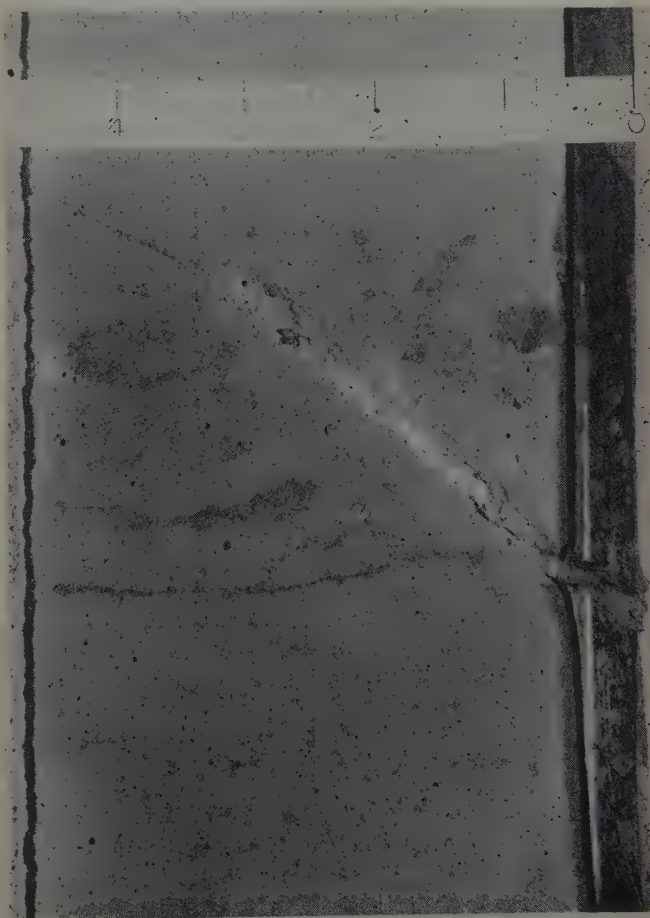


FIG. 5 — CLOSE-UP OF TARGET. STEEL: $\frac{1}{2}$ IN. N-80. CEMENT: NEAT CEMENT. BACKING: $\frac{1}{4}$ CEMENT, $\frac{3}{4}$ SAND. NOTE HAIRLINE CRACKS.

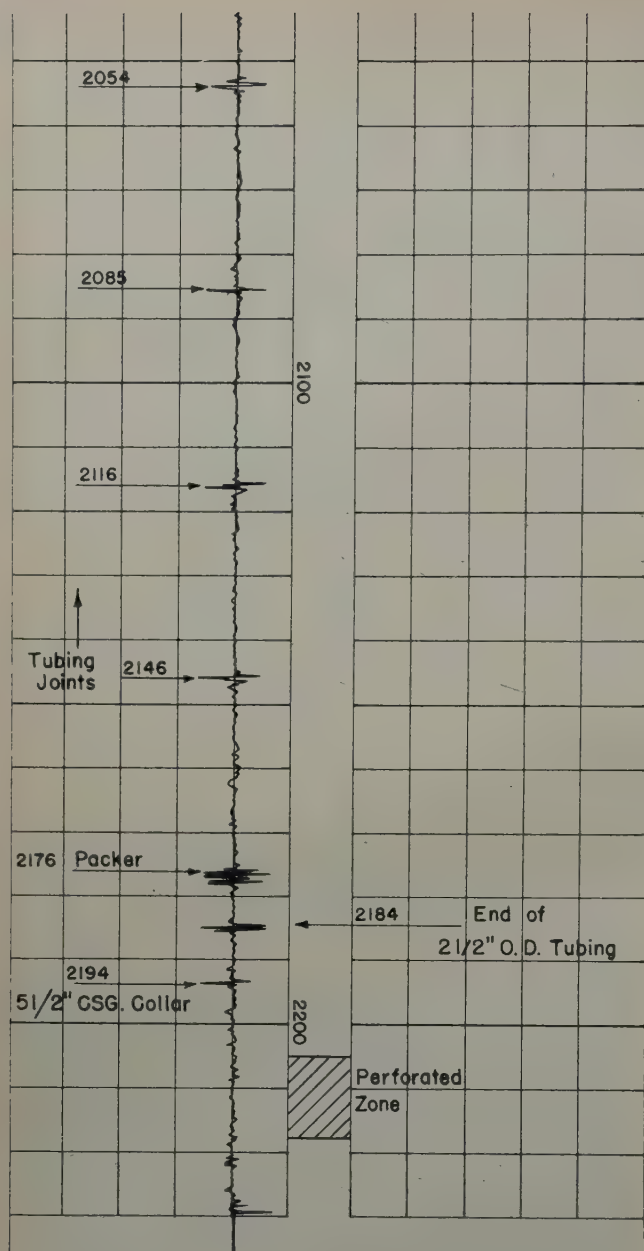


FIG. 6 — TYPICAL CASING COLLAR LOG.

After the tubing is in place, the well head can be installed and the drilling rig moved off the location if desired. In the event that a series of zones are to be shot and tested, it may be advisable to perforate with the drilling rig over the well.

Workover Wells

The preparation of a workover well for this type of perforating will differ from the procedure used on a new well.

1. Removal of Tubing End: The first consideration in this type of well is the removal of the tubing end. There are three methods for accomplishing this removal. They are (a) Withdrawal of tubing, (b) Opening tubing end by use of wire line tools and "jars," (c) Opening of tubing end by means of special explosive charge.
2. Elimination of Tubing Pressure at the Well Head: In many types of workover operations, this tubing pressure may be non-existent because the well is "dead" or because work on the well with drilling equipment has necessitated the killing of the well. In cases where the operator is unsuccessful in eliminating the pressure, a special method, described later in the paper, will have to be used.
3. Gauging for Tubing: The third factor in workover jobs is the gauging of the tubing to verify that sufficient clearance exists for the passage of the gun. This operation is especially important in wells where the tubing has not been pulled. It has been found on many occasions that the inside

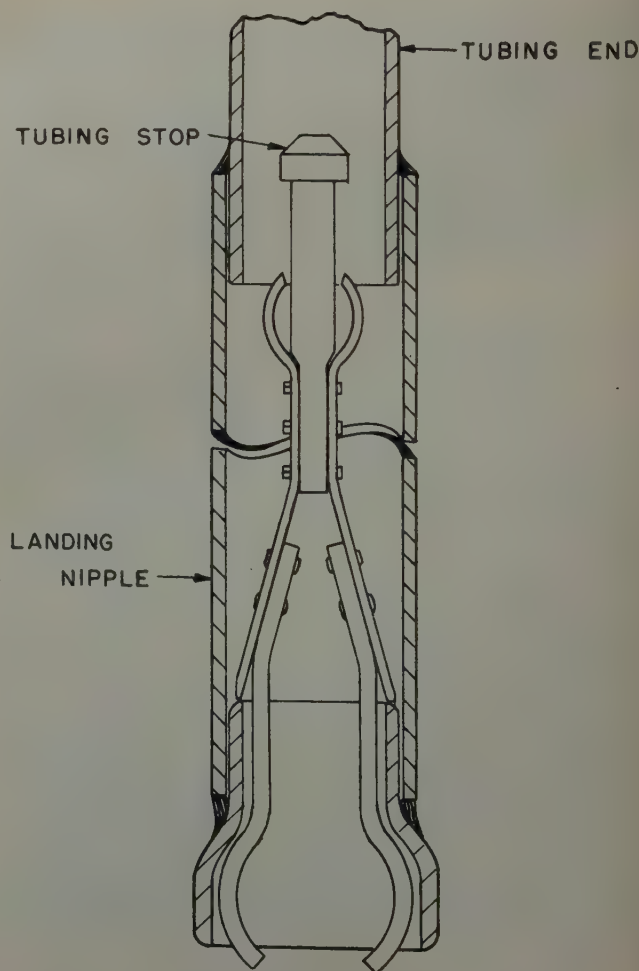


FIG. 7 — SEATING NIPPLE WITH TUBING STOP IN PLACE.

the well will eliminate any cuttings settling in the lower part of the well. It will also insure the removal of mud and other foreign particles from the inside of the tubing string.

7. Check Points in Casing Below Tubing: In setting the tubing, the uncovering of at least two check points, such as casing collars or other known points, will be an advantage in correlating depth measurements.
8. Use of Tubing Packer: If a tubing packer is used, it is an advantage to use one of the types that do not require downward weight for their operation since any bending of the tubing above the packer could prevent the passage of the gun.
9. Placement of Fluid Cushion: The fluid to be placed within the tubing can be oil, fresh water, or salt water. Salt water has been found the least desirable from the standpoint of obtaining a clean opening through the tubing consistently.



FIG. 8 — SWABBING UNIT.

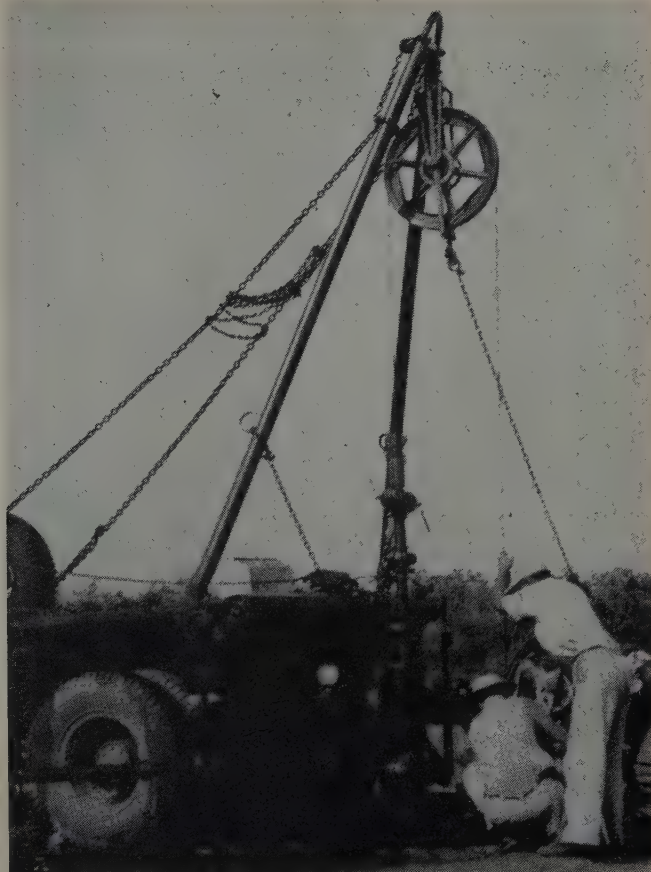


FIG. 9 — A-FRAME TRUCK.

of the tubing was coated with paraffin, scale, or salt, preventing descent of the gun to shooting depth.

The length of the wire line gauge used should be at least equal to the length of the gun and the cable head planned for perforating. In the event a wire line tool is used to remove the tubing end, then the tubing gauging can be carried on at the same time. In addition, the wire line can be used to check the casing below the tubing end for possible fill-up.

4. **Placement of Fluid Cushion:** The placing of fluid in the well is the same operation as that described previously. However, in some cases, the well itself can be allowed to "load-up" and thus produce its own hydrostatic cushion. It is recommended in all cases to keep a minimum of 40 ft of fluid above the zone to be perforated to avoid damage to the perforating equipment. In most workover wells, the pressures to be encountered are definitely known, allowing the use of a differential pressure into the well bore. When properly applied, this method will eliminate the need for swabbing or other similar operations to bring the well in.

FIELD OPERATION

Sheave Support for Shooting Line and Perforator

Auxiliary surface equipment is necessary to support the sheave for the cable, for the lifting of tools, and the erection of the lubricator. If the derrick is available at the well, it is possible to use standard perforating line and trucks. If no derrick is available, a tubing pulling unit, the mast of a swabbing unit (Fig. 8), or even an A-frame or "gin pole"

truck can be used as shown on Fig. 9. This use of a gin pole truck has proven to be very economical in workover wells on which it is unnecessary to remove the tubing.

In some cases, mostly in workover wells, such devices are not available. To provide for this type of operation, a light perforating truck equipped with a small 3/16-in. diameter armored cable has been designed. The cable and upper sheave are supported by the lubricator. The lifting equipment is carried disassembled on the truck and is used in the following manner:

1. On wells that do not have pressure on the tubing, a simple arrangement can be used, as shown in Fig. 10. Since any arrangements for sealing against pressure must be made only after the well is shot, the lubricator is made only long enough to contain the cable head and collar locator.

A light "gin pole" is mounted parallel to the lubricator and is used to lower the gun into the well.

2. In case of pressure in the tubing at the time of the first or of successive trips in the hole, a 30-ft portable derrick is erected, as shown on Fig. 11. This arrangement has been used with good results, but increases the time required for the perforating operation because of the need for erecting a derrick, and also the fact that the 16-ft maximum length of the lubricator limits the length of the gun, thus reducing the number of shots possible in one trip. When the pressure exceeds 150 psi, a special wire line stuffing box and cable feeder device are required.

Pressure Sealing Equipment

As the perforator has a small diameter, the pressure sealing equipment is also of a smaller size. A sketch of a section of



FIG. 10 — SIMPLE GIN POLE SET-UP.



FIG. 11 — PORTABLE DERRICK AND FULL RISER.

the lubricator is shown in Fig. 12. The body of the lubricator is made of $2\frac{1}{2}$ -in. tubing fitted with quick connecting 3,000 psi unions. The blowout preventer is the ram type with a full $2\frac{1}{2}$ -in. opening. The stuffing box is the split rubber packed type with design modifications for grease injection. All of the equipment is tested to 3,000 psi cold water pressure.

When perforating a well under pressure, a full lubricator must be used. In addition, the stuffing box is grease packed continuously and requires careful adjustment. A cable feeder is installed at the top of the lubricator and feeds the cable into the well until the cable weight will overcome the upward thrust due to well pressure. Because of this upward force, this operation has only been performed with the $3/16$ -in. cable. A sketch of the cable feeder is shown in Fig. 13. To date, this operation has been on a limited basis because of the many difficulties involved.

SHOOTING OPERATION

The gun is loaded five shots per ft to cover a length equivalent to the zone to be perforated. The maximum length of carrier used up to date has been 31 ft containing 155 shots.

The cable with the casing collar locator and gun attached to the head assembly are lowered into the well. The downward motion of the gun is checked by the casing collar locator readings and in addition by the weight indicator.

When total depth is reached, a casing collar log is made, recording upward until a maximum of two or three joints of tubing are located. This log is then a permanent record of the depth of perforation relative to casing collars. If other logs are available, it is possible to correlate the placement of perforations accurately within the zone to be shot with reference to depth.

The gun is then located at the shooting depth by watching both the depth indicator and casing collar recorder. The lubricator is closed and the current is applied to the gun, shooting all charges at once. Definite indication of the shooting is given by the listening circuit.

The casing collar locator and head are pulled up into the lubricator. The well valve can be closed and the cable head and lubricator removed. The well can now be opened immediately to the regular production equipment since there is no mud in the tubing.

At the time of the shooting, the carrier falls to the bottom of the well in the form of a distorted tube in one or more pieces. While the well is in production, the remnants of the carrier will be attacked by acid or salt water. This is illustrated in Fig. 14, which shows the distorted tube after two weeks in a well.

In Fig. 15, it is shown that only fragments are recovered in a well after three months. The pieces were washed out of the well by the mud circulation in a subsequent workover operation.

Table I—Summary of Work to Date

Normal Operations

Ninety-five per cent of the wells were run under the following conditions:

Formations Perforated—Gulf Coast Sands

Depth—From 2,000 to 9,000 ft; averaging 4,500 ft.

Casing—Typical 5½ in., 15.5 lb.

Tubing—50 per cent 2-in. tubing; 50 per cent 2½-in. tubing.

Hydrostatic Head Pressure—Less than formation pressure in all cases. (Under normal conditions, this operation would have required a full column of fluid.)

Number of Shots—Maximum in a well 250

Minimum in a well 20

Average 50

Type of Completion—New wells 40 per cent of the jobs

Workovers 60 per cent of the jobs

Performance—Effective penetration obtained on 99 per cent of all operations.

Outstanding Operations and Special Applications

Deepest Well—9,916 ft; 2-in. tubing; 50 shots.

Greatest Number of Shots—155 shots in one gun below 2½-in. tubing, 7,750 ft.

Toughest Penetration—5-in. liner in 9⅝-in. underreamed hole, 2-in. tubing, 50 shots.

Highest Hydrostatic Pressure—Perforating a well with 18 lb/gal mud at 8,837 ft; pressure 8,450 psi—25 shots.

Two Strings of Pipe—2-in. tubing cemented inside of 5-in. liner; 50 shots; well flowed 101 B/D.

Perforating Under Pressure—Ran into well with tubing pressure of 1,040 psi; 50 shots; increased gas production 22 per cent.

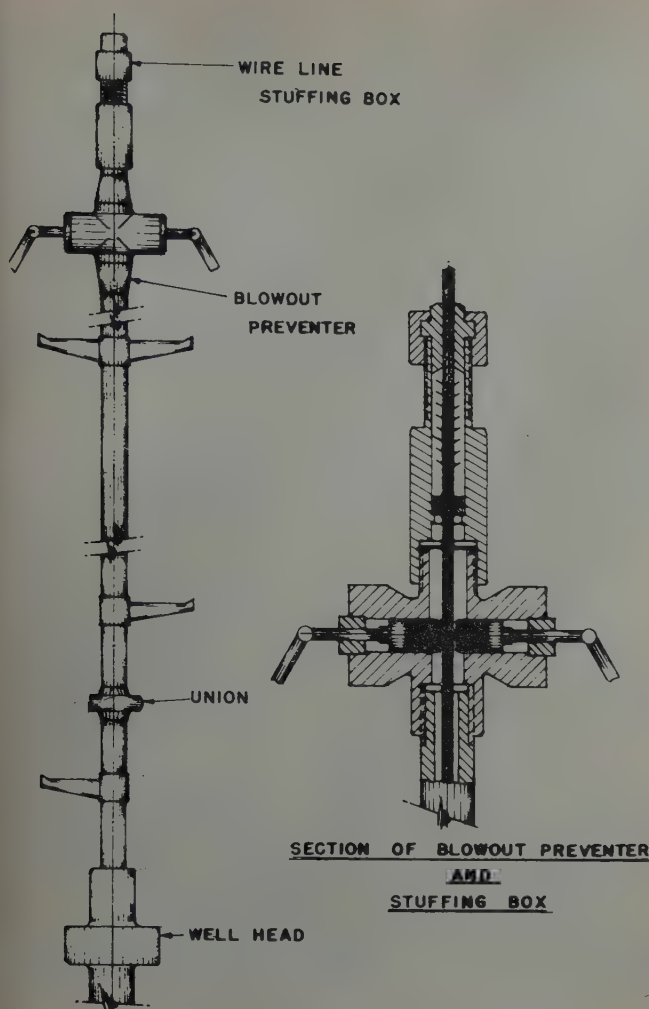


FIG. 12 — LUBRICATOR.

FIELD PERFORMANCE

During the past ten months, over 400 wells have been perforated following this procedure and successfully completed. A summary of these operations is shown in Table I.

In many cases, wells completed by this method have had a higher potential than wells completed by conventional methods. The reason for these results seem to be:

1. The penetration of the specially designed shaped charge and the employment of angle shooting.
2. Perforating and completing the well under optimum reservoir conditions. Since only a slight differential pressure exists between the formation and the bore hole at the time of shooting the formation is not contaminated by the drilling fluid. Normally, the existing differential pressure will be directed toward the bore hole, permitting an immediate flushing of the perforation and a free path for production. Moreover, no contaminating fluid need ever touch the formation subsequent to perforating because it is unnecessary to load the well with fluid at any time during the completion operation.

It is also gratifying to find that even though the tool has been used in cases where extreme penetration was required, only in very few cases has the gun failed to penetrate. The tool used in all operations to date was primarily intended for shooting 5½-in. casing; and while excellent results were obtained in larger casings, a gun specially designed to go through

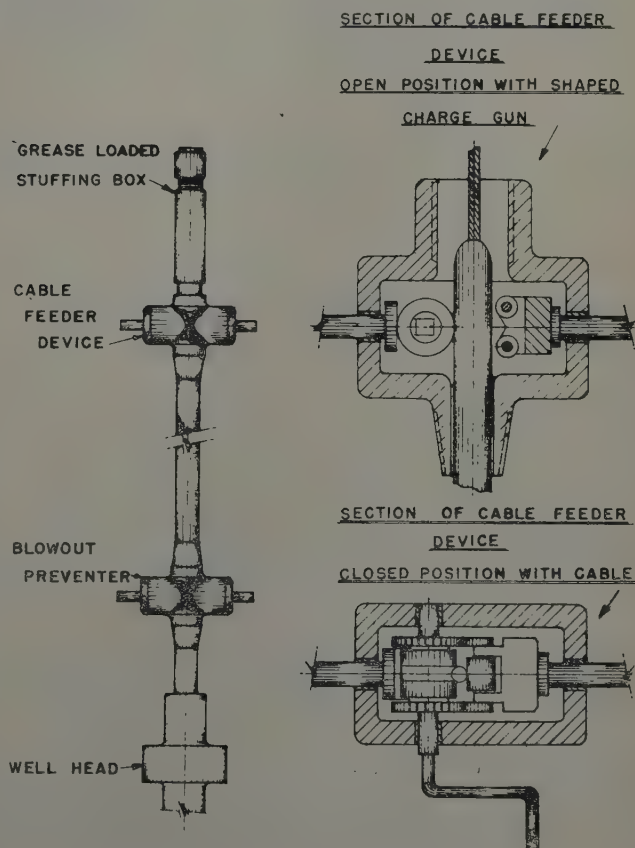


FIG. 13 — ARRANGEMENT OF CABLE FEEDER.



FIG. 14 — DISTORTED TUBE AFTER SHOOTING.

2½-in. tubing and for the shooting of 7½-in. or larger casing is presently being studied. Preliminary tests on this gun show that an increase of penetration of 50 per cent can be expected.

CONCLUSIONS

It is believed that the use of this new perforator in the permanent type completion practices has the following advantages over the present field completion and workover practice:

1. Better production can be obtained in low pressure reservoirs since no mud touches the formation after perforation. Field results confirm this.
2. The use of this tool results in substantial savings on workover jobs since there is no need to move a rig on location. There is also a substantial saving in mud costs since it is not necessary to load the well with mud before perforating.
3. On new wells, substantial saving in rig time can be effected since the rig can be moved off the location prior to perforating and completing.
4. It is possible with this gun to shoot a very large number of shots in one trip, thus eliminating time-consuming multi-run perforation.
5. By permitting the setting of the tubing prior to perforation, it eliminates some of the dangers always present when trying to complete wells for production after standard perforating procedure. All operations are conducted with pressure handling equipment in place on the well, thereby eliminating danger of blowouts or accidents.



FIG. 15 — FRAGMENTS RECOVERED THREE MONTHS AFTER SHOOTING.

6. A safer practice of reperforating workover wells results with the use of this perforator because the well does not have to be killed or the tubing removed.
7. In cases where, due to accidental setting of drill pipe or tubing in the well, conventional perforating tools cannot be used, satisfactory production can often be obtained by shooting with this new gun; whereas in the past such wells would have had to be abandoned or side tracked. This has been proven by several successful jobs in the field.

ACKNOWLEDGMENT

The authors wish to express their appreciation to the Humble Oil and Refining Co. for the use of diversified wells for initial tests and for furnishing field data necessary to the first development of the perforator. They also wish to thank other members of the Schlumberger Well Surveying Corp. for their cooperation.

REFERENCES

1. Huber, T. A., Allen, T. O., and Abendroth, G. F.: "Well Completion Practices," API Meeting, Los Angeles, Calif., Nov. 1950.
2. Kastrop, J. E.: "Completing Wells in Gulf Coast Sands," *World Oil*, (June 1952).
3. Huber, T. A., and Tausch, G. H.: "Permanent Type Well Completion," presented at AIME Meeting, Houston, Tex., Oct. 1952.

★ ★ ★

FURTHER DISCUSSION OF PAPERS PUBLISHED IN TRANSACTIONS, VOLUME 195 (1952)

ENGINEERING STUDY OF THE COOK RANCH FIELD, SHACKELFORD COUNTY, TEXAS

WALLACE W. WILSON, CONTINENTAL OIL CO., PONCA CITY, OKLA., MEMBER AIME

(Published as T.P. 3285, Page 77)

DISCUSSION

By Henry J. Welge, Carter Oil Co., Tulsa, Okla.,
Member AIME

This paper calls to attention for the first time, to the writer's knowledge, a purported recovery of oil by substantially horizontal gas cycling that is considerably in excess of 50 per cent of the oil originally in place. The average angle of dip along the path of travel of the gas is less than one degree of arc. The best recovery by gas cycling previously brought to the writer's attention¹ occurred in the case of the Mile Six Field in Peru, where about 68 per cent of the original oil in place has so far been recovered. In this case, however, the recovery was greatly aided by the high dip angle of about 17.5°. An approximate estimate of recovery was made by the method developed by the writer¹ for the case of the Cook Ranch Field, using an average relative permeability ratio function dictated by past experience with a number of good quality sandstones. A result of about 40 per cent recovery of the original oil in place was obtained after the 8.5 pore volumes of cumulative gas cycling undergone by the Cook Ranch Field.

The writer desires to emphasize what appears to him as the sound engineering practiced at Cook Ranch, and also the care attending the taking of data and the high quality of the calculations made. It is impossible to take issue on factual grounds with any of the conclusions drawn in the paper. It is, however, desired to point out the difficulty of explaining the unexpectedly favorable oil recovery on ordinary theoretical grounds. It would be of interest to know whether relative permeability ratios have been measured on the Cook sand. The operator is inclined to attribute some of the excess benefit to settling of the oil across the bedding planes into the lower part of the sand. It is difficult for the writer to appreciate the importance of such an effect, inasmuch as the concomitant opening of excessive vacated pore space in the upper part of the sand would be expected to cause excessive bypassing of the gas.

REFERENCE

1. Welge, H. J.: "A Simplified Method for Computing Oil Recovery by Gas or Water Drive," *Trans. AIME*, (1952), 195, 91.

AUTHOR'S REPLY TO MR. WELGE

Welge has pointed out clearly the difficulty of applying material-balance procedures in calculating the performance of low-pressure, dispersed gas injection operations. There can be no argument that even with the most favorable assumptions of K_r/K_o and with cumulative gas cycling in excess of normal expectations, the calculated oil recovery will be considerably less than the 72.5 per cent recovery realized from this project to Jan. 1, 1951. There probably are at least two reasons for the unusually high recovery from this reservoir, the effects of which would be difficult or impossible to calculate by known methods:

1. The operator did not use the same injection wells for the entire operation, and exercised considerable control over producing GOR by changing the locations of injection wells whenever well performance indicated excessive bypassing. Fifty-six wells were used for injection, not over 29 of which were in use simultaneously. This procedure resulted in frequent shifting of the fluid movement patterns in the reservoir and undoubtedly increased the ultimate recovery. The writer knows of no satisfactory procedure for calculating the effect of this practice.
2. Vertical movement of oil across the bedding planes of the reservoir rock by gravity drainage tended to maintain a relatively high oil saturation, and hence a favorable K_r/K_o ratio, in the lower sections of the reservoir. As pointed out by Welge, this condition has aggravated the tendency for high producing GOR, but at the same time it has resulted in increased oil recovery. As may be seen from the performance charts for the various battery areas, operating GOR's have been quite high for the last several years of reported history.

★ ★ ★

LABORATORY DETERMINATION OF RELATIVE PERMEABILITY

J. G. RICHARDSON, J. K. KERVER, JUNIOR MEMBERS AIME, J. A. HAFFORD AND J. S. OSOBA, HUMBLE OIL AND REFINING CO., HOUSTON, TEX.

(Published as T.P. 3375, Page 187)

DISCUSSION

By Forrest F. Craig, Jr., Stanolind Oil and Gas Co., Tulsa, Okla., Member AIME

The authors are to be commended for their experimental verification of the influence of boundary end effect as predicted from the equations of fluid flow. Research workers have long recognized the need for this comparison of the experimental and theoretical saturation gradients due to boundary effect. It is also satisfying to note the authors' work comparing the experimental and theoretical effects of gas expansion. Their careful and ingenious experimental work is a high point of the paper.

The comparison of the various methods of laboratory determination of relative permeabilities is most valuable. It has been found, however, in the Stanolind Oil and Gas Co. Research Laboratory, that the calculation of gas-oil relative permeability ratios from gas drives, using one-half the effluent oil rate and specifying the k_g/k_o values, thus obtained, at the average saturation can be greatly in error.¹ Gas drives on more than 20 different sandstone and limestone core samples have shown that the gas-oil relative permeability ratios, so calculated, vary from the true values, as calculated by the recently proposed method,² by from 10 to over 800 per cent. To date no rigorous method of calculating individual gas and oil relative permeabilities from external gas drive data has been devised.

REFERENCES

1. Craig, F. F., Jr.: "Errors in Calculation of Gas Injection Performance from Laboratory Data," *Trans. AIME*, (1952) 195, TN 126.

2. Welge, H.: "A Simplified Method of Computing Oil Recovery by Gas or Water Drive," *Trans. AIME*, (1952) 195, 91.

AUTHORS' REPLY TO MR. CRAIG

The comments of Craig are appreciated and his point concerning the calculation of relative permeabilities from gas-drive experimental data is well taken. The factor of one-half used in calculating the relative permeability to oil from gas-drive data is an empirical correlation number which for many samples brings the relative permeabilities to oil determined from gas-drive experiments into agreement with those determined by steady-state methods. In comparing results obtained on 60 core samples by both steady-state and gas-drive methods, this correlation factor brought gas-drive permeabilities to oil into exact agreement with those determined by the steady-state method in 60 per cent of the cases. Of those which disagreed to a varying extent, about one-half were high and the other half were low. Many of the samples on which disagreement was obtained were heterogeneous in character, for example, vugular limestones or sandstones with shale streaks.

On the other hand, for a limited number of cases, K_g/K_o saturation relations did not agree with those determined by steady-state methods. Since the Welge method involves a number of simplifying assumptions, it was felt that perhaps these assumptions were not valid for the particular runs that were made. It is to be hoped that further work will yield a better understanding of the utility or limitation of each of the calculation procedures for handling the laboratory gas-drive data.

★ ★ ★

ELECTRICAL RESISTIVITY MEASUREMENTS ON RESERVOIR ROCK SAMPLES BY THE TWO-ELECTRODE AND FOUR-ELECTRODE METHODS

C. F. RUST, MAGNOLIA PETROLEUM CO., DALLAS, TEX.

(Published as T.P. 3397, Page 217)

DISCUSSION

By H. F. Dunlap, The Atlantic Refining Co., Dallas, Tex., Member AIME

We believe that the conclusions stated in this paper are too sweeping. Our own experience indicates that (1) two-electrode resistivity measurements are in general not as reliable as four-electrode measurements, and (2) use of non-equilibrium brine saturations in determining the saturation exponent n may, in some cases, lead to quite erroneous determinations. While we do not contend that the data reported are incorrect, the conclusions drawn from them are too general.

The paper gives the impression that the two-electrode and four-electrode methods are equally reliable. Actually, the data given in Table I show significant differences between two-electrode measurements obtained using the painted end electrode technique and two-electrode measurements made without using painted ends. Table I shows that of 13 measurements using cores with painted ends, 11 showed a lower resistivity

than was recorded by the four-electrode technique on these cores, while of the 47 cores measured without painting the ends, 29 cores showed a higher resistivity using the two-electrode instead of the four-electrode method. While the differences in resistivity referred to here are in general small, the largest being about 17 per cent, these results at least suggest that (1) where painted end electrodes are not used, there is a tendency for the two-electrode method to give a value of resistivity which is somewhat too high, and (2) where painted end electrodes are used, the resistivity values obtained with the two-electrode method are somewhat too low (possibly due to penetration of the rock by the conducting paint?). While it is not our contention that careful work cannot yield reliable resistivity measurements using the two-electrode method, it has been our experience that four-electrode measurements are just as easy to make and are fundamentally much more reliable. The reliability of measurements made with a two-electrode method might be considered analogous to the reliability of voltage measurements made with a low resistance voltmeter,

while the four-electrode method might be considered analogous to voltage measurements made with a potentiometer.

We also wish to take exception to the second conclusion offered by Rust, in which he states that in determining the saturation exponent n , resistivity values at both equilibrium and non-equilibrium brine saturations may be used. Fig. A shows an experiment, given in a previous paper by Dunlap, *et al.*,¹ on the relation of resistivity to brine saturation in reservoir rocks, which demonstrates that very erroneous answers for n can be obtained if non-equilibrium values are used. We have made many other runs showing this effect, particularly on unconsolidated samples.

We are also surprised at the excellent reproducibility of the resistivity *vs* average saturation plots shown in Fig. 10 which were obtained for the three-in. long core equipped with multiple potential electrodes shown in Fig. 9. We have also performed many experiments exactly like this, and we find that, in general, when long cores are desaturated in this way, water is usually trapped in the upper sections so that resistivity measurements made in the upper section of the core are quite different from those made closer to the porous diaphragm, even after many days have elapsed since the desaturating pressure was first applied. Fig. B shows one experiment which illustrates this effect occurring in a rather permeable oolitic limestone. This core was about one-in. high and seven-eighths-in. in diameter, and after 10 days there was still a pronounced resistivity gradient, indicating that water has been trapped at the top of the core. In another experiment, a Strawn sandstone core 10-in. long, 1 in. in diameter, permeability of about 500 md, was mounted vertically on a capillary plate and desaturated for two months with a constant pressure of 10 psi of naphtha. At the end of this time the core was broken up and analyzed one section at a time. It was found that a pronounced saturation gradient existed, with the portion of the core closest to the porous disk being essentially at connate water (about 30 per cent water), while the top portion of the core still contained 50 per cent water. Resistivity measurements were not made on this last experiment, but the lower portion would undoubtedly have shown a higher resistivity than the upper portion.

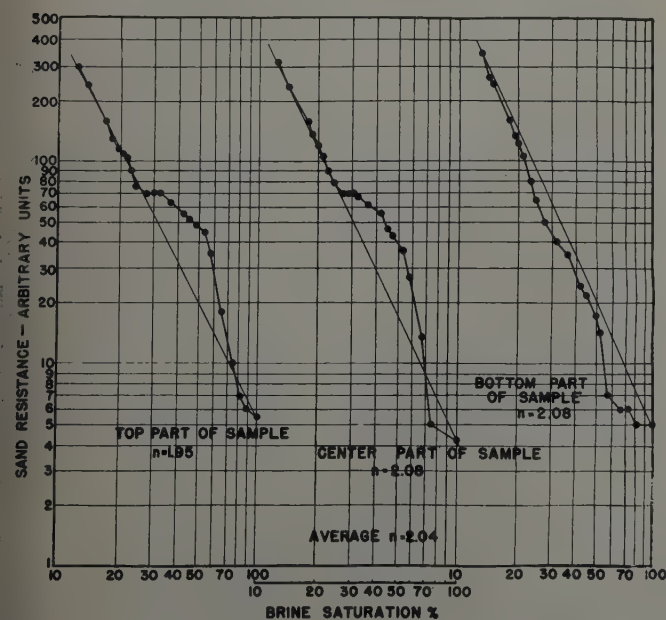


FIG. A — RESISTANCE AS A FUNCTION OF BRINE SATURATION FOR A CLEAN UNCONSOLIDATED SAND. POROSITY, 37 PER CENT; DISPLACING MEDIUM, N_2 ; CONSTANT DISPLACEMENT PRESSURE, 2 PSI.

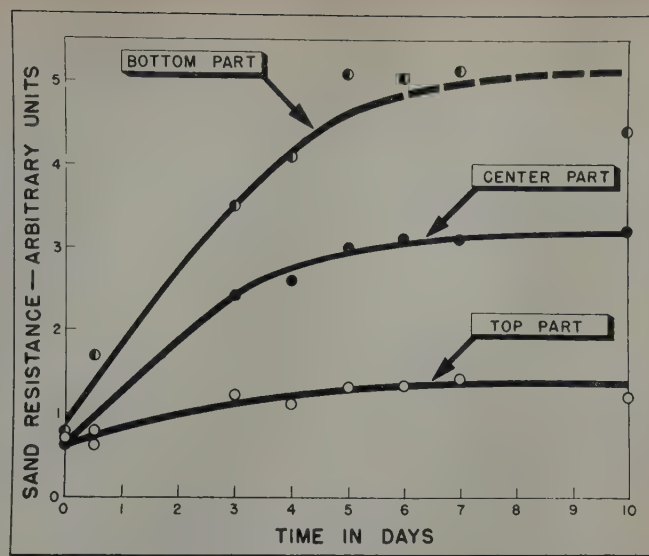


FIG. B — RESISTANCE AS A FUNCTION OF TIME. K_a , 1129 MD; P , 19.7 PER CENT.

REFERENCE

- Dunlap, H. F., Bilhartz, H. L., Shuler, E., and Bailey, C. R.: "The Relation Between Electrical Resistivity and Brine Saturation in Reservoir Rocks," *Trans. AIME*, (1949), 186, 259. ★ ★ ★

AUTHOR'S REPLY TO MR. DUNLAP

The conclusions drawn are based entirely on the results of the measurements presented in this paper. On the basis of these measurements one must conclude that, provided proper techniques are employed, either the two-electrode or four-electrode method will yield reliable resistivity values. The writer is aware of the fact that comparisons of resistivity measurements made by different laboratories on the same core samples often leaves much to be desired, not only when the comparison is made between two different methods, but between measurements utilizing the same method.

These laboratories have employed the four-electrode method in electrical resistivity measurements almost exclusively for several years. Other laboratories in the industry, particularly commercial laboratories, prefer, for reasons of their own, the two-electrode method. It was not the intent of this writer to suggest the substitution of one method for the other, but only to compare and evaluate differences between them. A comparison of the two methods seemed desirable because often the size of core samples is such that the four-electrode method cannot be applied and one is forced to employ a two-electrode system. As Dunlap admits, the differences between the two types of measurement are small. He points out that 29 of the unpainted samples show higher resistivities when the two-electrode method is used; for seventeen samples, however, the two electrode method yields lower values, while for one sample the measurements are the same. The writer does not accept the suggestion that two-electrode measurements made on painted samples are lower than four-electrode measurements. Generally, two-electrode measurements made on the same samples, with and without the use of silver paint, agree well within the experimental errors permitted in resistivity measurements. There appears to be no reason, therefore, to segregate the painted from the unpainted samples. As this writer has pointed

out, the painting technique of Morgan, Wyllie, and Fulton¹ is a novel one and most satisfactory, particularly if resistivity measurements are made over long intervals of time. However, the use of silver paint is not always desirable, particularly if the samples are to be subjected to other tests such as chemical, or X-ray analyses following the resistivity measurements.

Dunlap's analogy between the two methods of resistivity measurement to voltage measurements with a low resistance voltmeter and a potentiometer appears to be irrelevant to the problem at hand.

With regard to the use of non-equilibrium brine saturations in determining the saturation exponent n the writer again wishes to emphasize that the conclusions drawn are based on his own experimental results. He is aware of the fact that this topic has been the subject of considerable debate among workers in this field in the past and it is well to recognize the experimental difficulties associated with this problem and to be aware of erroneous results due to faulty techniques. It is apparent that there are differences between the work of Dunlap *et al*² and that of the writer. These differences pertain to both the type of sample compared as well as difference in measuring technique and procedures. For example, the results shown in Fig. A of the above discussion were obtained on an "unconsolidated" sample, while those presented in this paper are for consolidated samples only. The displacing medium for the former was nitrogen, for the results presented in this paper a liquid (isooctane) was used. It is perhaps significant, also, that in all cases the pressure was increased stepwise, while for many of the results shown by Dunlap *et al* the final desaturation pressure is applied immediately. The author has

measured saturation exponents for scores of samples, but in no case have anomalies of the type described in this discussion been observed.

Finally, Dunlap expresses surprise at the excellent reproducibility in the case of the long core sample obtained from a *homogeneous, clean* Woodbine outcrop and contrasts these results with those obtained by him on a limestone sample. At these laboratories our experience with studies of long samples is limited to this single case. The measurements have since been repeated, inverting the core sample, and finally by breaking up the sample into three samples of inch length yielding the same results. No resistivity gradient could be detected.

It is this writer's opinion that electrical resistivity measurements on reservoir rocks can be made successfully only if precautions are taken all along the line from the proper extraction of both salt and oil from the sample to the determination of its degree of saturation. These precautions coupled with those mentioned in connection of measuring techniques discussed in this paper will generally yield reliable and reproducible results.

REFERENCES

1. Morgan, F., Wyllie, M. R. J., and Fulton, P. F.: Tech. Note, "A New Technique for the Measurement of the Formation Factors and Resistivity Indices of Porous Media," *Trans. AIME*, (1951) 192, 371.
2. Dunlap, H. F., Bilhartz, H. L., Shuler, E., and Bailey, C. R.: "The Relation Between Electrical Resistivity and Brine Saturation in Reservoir Rocks," *Trans. AIME*, (1949) 186, 259. ★ ★ ★

USE OF ACTIVATED CHARCOAL IN CEMENT TO COMBAT EFFECTS OF CONTAMINATION BY DRILLING MUDS

B. E. MORGAN, JUNIOR MEMBER AIME, AND G. K. DUMBAULD, MEMBER AIME, HUMBLE OIL AND REFINING CO., HOUSTON, TEX.

(Published as T.P. 3396, Page 225)

DISCUSSION

By Francis M. Anderson, Halliburton Oil Well Cementing Co., Duncan, Okla.

The paper just presented is quite timely in this day of specialty drilling fluids containing large quantities of treating chemicals, almost all of which are highly detrimental to the setting of portland cement.

The advent of these highly treated drilling fluids has been followed by a marked increase in trouble with cement. Cement placed in these wells has taken an unusually long time to set, or reportedly has not set at all. This has been particularly true in wells where lime base mud has been used, as these muds are necessarily treated with large concentrations of quebracho or lignin compounds, or both, and in many cases contain such organic colloids as starch, sodium carboxymethyl-cellulose, natural gums, etc., all of which are known to affect cement adversely. To date, the effect of these drilling muds on cement has been combatted primarily by improving the mechanical techniques of performing the cementing job. Such devices as both bottom and top plugs used inside the casing, wall cleaning devices used in conjunction with pipe movement, and buffer washes used ahead of the cement, have been employed with more or less success in different areas.

The work of Morgan and Dumbauld appears to be the first successful use of an additive which can be blended with a cement to successfully counteract the effect of these muds.

The additive they have chosen apparently acts by adsorbing the offending treating chemical rather than counteracting it chemically, thus it has no effect on the setting of the cement itself. For this reason, it appears ideal for use in cements containing no chemical retarders. It is unfortunate that the retarders used in most slow setting oil well cements are very similar to the compounds used for treating drilling muds and are thus subject to being adsorbed by charcoal in the same manner. This is especially true since highly treated muds are used extensively in the deeper wells where slow setting cements are required.

A great amount of trouble has been encountered in obtaining successful plug back jobs in open hole, for it is on these jobs that the cement has the greatest chance of becoming contaminated with mud. The authors appear to have opened a new approach to this longstanding problem. The use of activated charcoal in this one application may well pay big dividends if it will help eliminate failures.

The use of activated charcoal could be an important factor in obtaining successful squeeze jobs when squeezing formations into which highly treated muds have been lost ahead of the cement. In fact, any cementing operation where trouble is encountered because of contamination with such drilling muds should be improved by the use of this additive.

The authors have done a creditable piece of work and are to be commended for the manner in which they have presented it.

AUTHORS' REPLY TO MR. ANDERSON

Anderson has mentioned the increase in trouble with cement since the advent of muds heavily treated with quebracho, lignin materials, starches, etc., particularly in operations such as the setting of a plug in open hole. It is felt that the use of activated charcoal in cement is a practical way of reducing the seriousness of this problem.

Anderson has pointed out that the chemicals commonly employed for mud treatment are similar in composition and behavior to the chemicals used to retard the set of many slow-set cements; therefore, activated charcoal is likely to adsorb the retarders and shorten the pumpability of slow-set cements. Data on these points which are presented and discussed in the paper may be summarized as follows:

1. Activated charcoal does shorten the pumpability of some slow-set cements containing organic-type retarders; hence, activated charcoal should not be added to slow-set cements containing retarders without first checking the effect upon the pumpability of the particular cement. This effect is apparently similar to that encountered when high percentages of bentonite are added to this type of slow-set cements.

2. Activated charcoal does not change the pumpability of normal portland cements and slow-set cements which contain no organic-type retarders; therefore, for moderate temperature jobs, satisfactory cementing compositions containing activated charcoal may be prepared by the use of any normal portland

cement. For high temperature jobs, satisfactory cementing compositions containing activated charcoal may be prepared by the selection of a straight, unretarded slow-set cement.

3. The effect of the contamination of cement slurries by treated muds is more pronounced at low temperatures than at high temperatures. Contamination may be more serious, therefore, in wells where heavily-treated muds are encountered at moderate depths rather than in deep, high temperature wells.

Appreciation is expressed to Anderson for his thoughtful discussion of our paper.

DISCUSSION

By S. H. Davis, *Atlantic Refining Co., Dallas, Tex.*

I would like to ask the author if any attempt has been made to separate the effect of the several additives, particularly the caustic and quebracho, if any setting time tests were made using only one or the other to see which is doing the major part of the damage.

AUTHORS' REPLY TO MR. DAVIS

Our laboratory investigation did not include tests of caustic and quebracho separately. Data on the specific effect of many chemicals, including caustic and quebracho, may be found in one of the references cited, "The Effects of Drilling-Mud Additives on Oil-Well Cements," *API Bulletin D-4*, (Sept. 1951). This publication may be obtained from American Petroleum Institute, Production Division, Dallas, Tex. ★ ★ ★

X-RAY SHADOWGRAPH STUDIES OF AREAL SWEEPOUT EFFICIENCIES

R. L. SLOBOD AND B. H. CAUDLE, THE ATLANTIC REFINING CO., DALLAS, TEX.

(Published as T.P. 3440, Page 265)

DISCUSSION

By T. M. Geffen and R. E. Gladfelter, *Stanolind Oil and Gas Co., Tulsa, Okla.*

We have followed the lead of The Atlantic Refining Co. in studying the areal sweepout of oil by pattern flooding using the X-ray shadowgraph technique, and have made studies on five-spot pattern flooding similar to those in this paper. We are in general agreement with their curve of mobility ratio vs areal sweepout efficiency for a five-spot pattern flood; however, there is one subject that was not fully discussed which is of considerable importance. This subject is the effect of scaling the fluid and rock characteristics and well bore when using small models to represent a large reservoir. Capillarity is one of the important characteristics to be considered in studying water flooding with small models. In the reservoir, considering the rates of advance of the water in pattern floods and the magnitude of the capillary forces, it is reasonable to expect that the portion of the reservoir in which water is advancing or being held back entirely by capillarity is small compared to the area under flood. In the model, with the same fluids and rock material, this zone, due to capillarity, can be relatively large compared to the model, resulting in a sweep efficiency different from that which would take place in the reservoir. The authors have handled this scaling problem by eliminating the effects of capillarity with the use of miscible fluids. This approach also creates a problem of a similar nature. The miscible fluids mix and form a zone that has the same detrimental effect as does capillarity. This mixing, or fingering, is most severe in the laboratory tests conducted with fluids in the low mobility ratio range. In the paper, the fingering nature of the flood patterns is attributed to rock characteristics. In addition to this, it is also due to the nature of the

fluids. As a solution to this problem of scaling, a one-quarter section of a five-spot flood pattern, as shown in Fig. A, was flooded using water to displace oil from a consolidated sandstone (Torpedo) model containing connate water at a mobility ratio of 0.24. The oil and water were stabilized with a mutually soluble alcohol to appreciably reduce the interfacial tension which in turn reduced, proportionately, the effect of capillarity. The capillarity has not been scaled precisely, but appears to approach what would happen in the reservoir because the boundary between the oil and water is comparatively sharp and smooth and the pattern at breakthrough is readily outlined. Using this same model and using miscible fluids at a mobility ratio of 0.25, a fingering pattern was obtained as

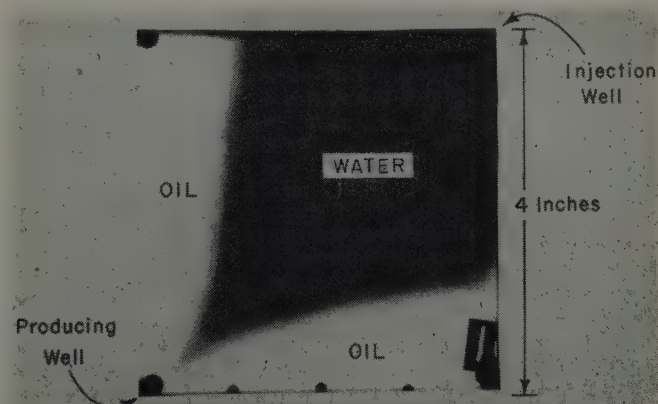


FIG. A—FIVE SPOT PATTERN FLOOD AT WATER BREAKTHROUGH FOR MOBILITY RATIO = 0.24, PATTERN EFFICIENCY = 60.7 PER CENT AND LOW INTERFACIAL TENSION.

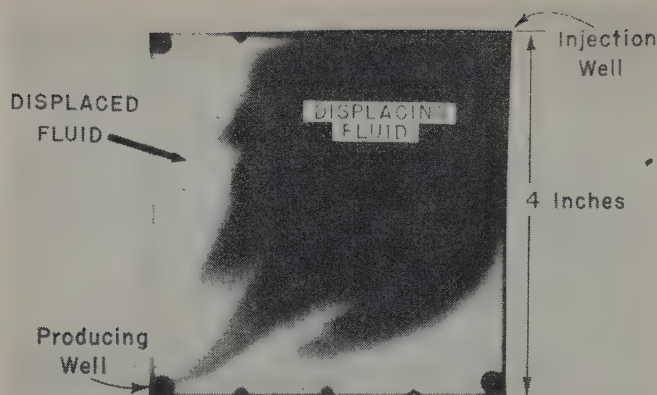


FIG. B — FIVE-SPOT PATTERN FLOOD AT BREAKTHROUGH FOR MOBILITY RATIO = 0.25, USING MISCIBLE FLUIDS.

shown by Fig. B. Fig. B is evidence of the difficulty encountered in obtaining a measure of pattern efficiency at this low mobility ratio. The use of low interfacial tension fluids may offer a better means of more precisely interpreting areal sweepout efficiency of pattern floods on models, inasmuch as the demarcation between displaced and displacing fluids is sharper.

A series of floods using the alcohol treated oil and water were made at various mobility ratios. The results are in general agreement with areal sweepout efficiency for a five-spot

given in the paper. The only significant deviation is for mobility ratios of less than one, where the results ranged up to five per cent areal sweepout efficiency above the correlation of Fig. 4 in the paper. Although Fig. 4 may not be precise over the entire range of mobility ratios, it should be satisfactory for engineering purposes for field application considering the areal variations in permeability possible in actual reservoirs.

The discrepancy between results by the potentiometric model and shadowgraph techniques for a line drive may, in addition to the author's explanation, be attributed to mixing effects and the accompanying difficulties in interpreting the results.

The effect of scaling the well bore diameter was also investigated. A 4 in. x 4 in. x $\frac{3}{4}$ in. model and a 24 in. x 24 in. x $\frac{3}{4}$ in. model were flooded corner to corner with the same fluids in the form of a quarter section of a five-spot. The well bores were $\frac{1}{8}$ -in. diameter in both models, which simulates 15.6 ft and 2.6 ft well bores, respectively, for the reservoir with the wells 500 ft apart. The area sweepout efficiency, at a mobility ratio of 0.92 was approximately 69 per cent in both cases. This agreement and the fact that the larger model was scaled to approximate field conditions, indicates that the smaller model, as well as the one the authors used, is sufficiently scaled for all practical purposes for a mobility ratio of one or greater. For mobility ratios less than 1.0, where the cusping tendency becomes greater, the scaling of the well bore may be more important when using the smaller model. ★ ★ ★

THE CALCULATION OF PRESSURE DROP IN THE FLOW OF NATURAL GAS THROUGH PIPE

FRED H. POETTMANN, PHILLIPS PETROLEUM CO., BARTLESVILLE, OKLA., JUNIOR MEMBER AIME

(Published as T.P. 3217, Page 317, Vol. 192)

DISCUSSION

By R. V. Smith, U. S. Bureau of Mines, Bartlesville, Okla.

An equation, such as Poettmann has presented,* for computing the pressure drop for the flow of natural gas through pipe, must evaluate adequately the available energy derived from the flow process and the energy used in overcoming the friction between the moving fluid and the pipe wall. The available energy is determined by the flow process that follows a path fixed by conditions of temperature, compressibility, and phase changes of the fluid during this process. The energy consumed in overcoming friction is determined by the friction coefficient, which is the dimensionless correlating function using Poettmann's nomenclature.

In a flowing gas well, the decrease in pressure as the fluid moves from the bottom to the top of the well allows the fluid to expand while the decrease in temperature usually found in gas wells allows the fluid to contract. In low-pressure gas wells with relatively low reservoir temperatures, the flow process is principally expansion; but in wells producing from high-temperature reservoirs at relatively high pressures, the temperature decrease may cause a contraction in the volume of the fluid that is greater than the expansion caused by the decrease in pressure.

In order to determine the available energy from the flow process, the integral, $\int v dp$, must be evaluated between the proper limits of pressure over the actual path of the flow

process. Poettmann has approximated this evaluation by assuming that the flow process is always an expansion at an average temperature and by assuming that compressibility of the fluid changes only with pressure. However, his treatment of compressibility is an important step toward solution of the problem of calculating subsurface pressures in flowing gas wells, and the values of $\int_{0.2}^{P_r} \frac{Z}{P_r} dP_r$, given in Table I, makes his method especially usable.

Friction coefficients, based on an absolute roughness of 0.0006 in. for the pipe used in gas wells, probably are more representative of conditions found in gas wells than are obtainable using other published values. However, it must be pointed out that an average absolute roughness value cannot apply equally to all gas wells without consideration of pipe age and corrosive conditions to which the pipe may have been exposed.

With reference to Equation (15) in the paper, the author has assumed that $[\int v dl]^2$ may be used in place of $\int v^2 dl$ or their equivalents, as is usually done in the development of flow equations. As the two expressions are not identical, the author should explore the significance of such an assumption and show the limits wherein the assumption may be used without appreciable error.

In presenting a method for calculating subsurface pressures in flowing gas wells that provides for the variation of compressibility with pressure, Poettmann has made an important contribution toward solving a complicated problem. In addition, he is to be commended for presenting his method in a convenient, usable form. ★ ★ ★

*This paper was published in Vol. 192 (1951) of AIME Transactions, rather than in the present volume as are the other papers here discussed.

ELECTRICAL RESISTIVITY MEASUREMENTS ON RESERVOIR ROCK SAMPLES BY THE TWO-ELECTRODE AND FOUR-ELECTRODE METHODS

C. F. RUST, MAGNOLIA PETROLEUM CO., DALLAS, TEX.

(Published as T.P. 3397, Page 217)

DISCUSSION

By M. R. J. Wyllie, Gulf Research and Development Co., Pittsburgh, Pa., Member AIME

Rust is to be congratulated for his choice of subject, since it is one of considerable practical importance. The industry is not only indebted to him for choosing so basic a study but is indebted also to Magnolia for permitting him to publish the results he obtained.

It is clear from Rust's data that if properly carried out on homogeneous cores both the two-electrode and four-electrode resistivity measuring methods give identical results. This has been the experience also of the writer. Unfortunately, not all cores are homogeneous; indeed homogeneity of natural cores is perhaps the exception rather than the rule. It follows that if a typical four-electrode measurement is made (two input electrodes, two pick-up electrodes such as, for example, 1 and 4 in Fig. 9) the resistivity is measured for a section of core for which the porosity is unknown. Only the *average porosity* of a non-homogeneous core can be measured unless the core is subsequently sectioned at the points where the pick-up electrodes made contact with it. In the writer's experience such sectioning followed by a porosity determination carried out on the cut section is rarely practiced by proponents of the four-electrode technique. For this reason, the preferred Gulf practice is to make a two-electrode measurement or a "four-electrode measurement utilizing the input electrodes as pick-up electrodes also. The latter practice is far from ideal. But for formation factor measurements in particular, it seems eminently desirable to find the formation factor of a section of core for which the porosity is known and not assumed. The same argument applies to resistivity index measurements. Only the *average saturation* in the core is known. If the core is non-homogeneous, at any capillary pressure the saturation distribution will not be uniform. Thus, the saturation within the core interval between the pick-up electrodes is indeterminate. Again the advantages of a properly performed two-electrode measurement are manifest.

The fact that Rust found the relationship between log (resistivity index) and log (saturation) to be linear irrespective of whether a partially saturated core was or was not at equilibrium with an applied capillary pressure is not in accordance with similar data presented elsewhere.¹ On page 223 in discussing this point, Rust qualifies his remarks with the statement "for the samples investigated." On the other hand, in the same paragraph he states that linearity "is consistent with numerous results obtained during routine measurements but not reported." It has been the experience in these laboratories that linearity is sometimes observed (generally for exceptionally homogeneous cores) but in general is not unless capillary equilibrium is reached. It would be interesting to learn whether Rust has ever obtained any data comparable to those published by Wyllie and Spangler.¹

Fig. 8 is qualitatively similar to curves obtained in these laboratories. It differs from them by the fact that curvature occurs abruptly at low saturations instead of increasing steadily

as saturation diminishes (*cf.* Fig. 10 of Wyllie and Morgan²) Theoretically, if a core possesses a resistivity component which is not saturation dependent, a gradual curving of the resistivity index-saturation plot is to be expected. The plot shown in Fig. 8 would indicate that the "conductive solids" resistivity was saturation dependent. If Fig. 8 exemplifies earth resistivity phenomena, more should be known of these phenomena since they will profoundly affect log interpretation procedures for "dirty" sands. Can Rust expand his views on this problem, particularly whether he considers Fig. 8 to be typical or atypical of dirty sands?

Finally, the values of n shown in Fig. 10 are of interest because in the writer's experience they are somewhat higher than is usual for natural porous media. Would Rust care to say whether he accepts the view that the best average value for n in sandstones is about 1.8, or would he incline to a higher value?

REFERENCES

1. Wyllie, M. R. J., and Spangler, M. B.: "Application of Electrical Resistivity Measurements to Problem of Fluid Flow in Porous Media," *Bull. AAPG*, (1952), 36, 359.
2. Wyllie, M. R. J., and Morgan, F.: "Comparison of Electric Log and Core Analysis Data for Gulf's Frank No. 1, Velma Pool, Stephens County, Oklahoma," Fifteenth Conf. on Pet. Prod. Min. Ind. Exp. Stn., *Bull. No. 59*, Penn. State Coll., (1951), 111.

AUTHOR'S REPLY TO MR. WYLLIE

The discussions of the subject paper imply that only homogeneous samples were selected for this study, and that the conclusions reached are therefore of limited applicability. This is not the case. The samples on which data are reported represent an entirely random group from unselected sources, which were run over a period of time as a part of routine laboratory operations. The comparison between the two methods of resistivity measurement was made as a result of necessity. Many samples received from the field during the course of these routine operations were of insufficient length to be measured satisfactorily with the four electrode system. As a consequence it became necessary to obtain quantitative comparisons between the two methods of measurement so the accuracy of data obtained on samples so small that only the two-electrode method could be employed, could be estimated. Similar comparisons on samples from other sands have been made since the paper was written. These additional results further support this writer's conclusions in the original paper.

Wyllie's contention that the porosity and saturation of core samples whose resistivity has been measured, by the four-electrode method, should be determined on the sectioned portions of the samples between the potential probes is fundamentally correct. The writer has been forced to conclude, however, as a result of this work that in practice, it is not necessary to utilize this technique when small samples are involved. For such small samples, which are the only size commonly avail-

able for routine work, it must be concluded from the resistivity data obtained that differences in the two porosity and saturation values must be negligibly small. This view is supported by the data presented in Fig. 6 of the original paper, where formation resistivity factors are plotted *vs* porosity fractions measured only on the gross sample for samples from the Annona chalk, measured by both the two- and four-electrode methods. While this writer is fully aware of problems arising from the heterogeneity of cores it would seem that such effects influence the measurement of physical parameters to a lesser degree in small samples from larger cores.

With regard to the relationship between resistivity index and saturation for equilibrium and non-equilibrium capillary desaturation, data comparable to those of Wyllie and Spangler* have not been observed during this work. It should be noted, however, that the non-equilibrium points obtained by Wyllie and Spangler correspond to saturation values intermediate to two equilibrium saturations differing in capillary pressure by 28 psi. In the technique used by this writer, the pressure is increased stepwise, six pressure points being taken at 2, 4, 8, 12, 16, and 20 psi, the greatest pressure increment therefore being only 4 psi. The non-equilibrium points shown

*Reference (1) of the above discussion.

in this paper represent measurements made between successive equilibrium saturations in these six capillary pressure values.

The writer agrees with Wyllie's qualitative interpretation of curved resistivity-saturation relationships. The writer has observed two different types of curves: first, cases in which a linear relationship is observed to some low brine saturation at which curvature occurs abruptly (Fig. 8 of original paper); second, cases where curvature is gradual, commencing at 100 per cent brine saturation (Fig. 10, Wyllie and Morgan**). The writer wishes to exercise restraint in speculating on the causes for such differences in behavior of rocks but there is strong evidence that both the type and amount of interstitial clay are responsible.

The values of *n* for the Woodbine outcrop sample, shown in Fig. 10 of the original paper, are higher than those measured for subsurface samples of the Woodbine formation. They are higher also than the average value of *n* = 1.92 obtained by the writer for a large number of samples representing 20 formations. The individual values range from 1.4 to 2.8 for sandstones, the extremes being the rare exception rather than the rule.

★ ★ ★

**Reference (2) of the above discussion.

SURFACE AREA MEASUREMENTS ON SEDIMENTARY ROCKS

C. S. BROOKS AND W. R. PURCELL, SHELL OIL CO., HOUSTON, TEX.

(Published as T.P. 3458, Page 289)

DISCUSSION

By M. R. J. Wyllie, Gulf Research and Development Co., Pittsburgh, Pa., Member AIME

The paper is most stimulating. Quite apart from its important theoretical implications, it described apparatus which should prove of value to all who are concerned with the problem of determining relatively small gas adsorption surface areas.

The data for unconsolidated packings of spheres, given in Table IV, tend to confirm the accuracy of Equation (6) if, as hazarded by the writers, the contact angle of mercury against glass was closer to 148° than the assumed 140°. It is of interest, however, to compute Kozeny constants for the packings of spheres in the manner outlined by Wyllie and Spangler (authors' reference 11). For this purpose, it is necessary to know the electrical tortuosities of packings of spheres. These tortuosities may be obtained from the experimental data of Wyllie and Gregory.¹ If a constant shape factor of 2.5 is assumed, Kozeny textural factors are obtained as shown in Table A. In Table A is also shown the ratio of the electrical and geometrical surface areas. The electrical surface areas were found from the Kozeny equation using the electrical Kozeny textural factor. Also given in Table A is the theoretical Kozeny textural factor, *i.e.*, the textural factor which is found when the geometrical surface area is equated in the Kozeny equation. A final column gives the shape factor. The shape factor is the theoretical Kozeny textural factor divided by the electrical tortuosity.

It will be observed that the average electrical area is 8 per cent less than the geometrical area, that the average theoretical Kozeny textural factor is 4.44 and the average shape factor 2.13. While the value of the average electrical surface area is perhaps suggestive of the usefulness of the electrical method

of determining Kozeny textural factors, the rather wide variations in the theoretical Kozeny textural factors render suspect the accuracy of the basic experimental data; as a corollary, any detailed deductions from those data. For example, a Kozeny textural factor of 3.57 is considerably below those previously observed for packings of spheres by other workers (see, for example, the data in Reference 11). It is also difficult to believe that the Kozeny textural factor could vary from 4.21 to 5.25 as porosity changes from 0.375 to 0.379 (packs J and K).

In discussing the data of Table I-B, the writers attribute the very wide divergence between the Kozeny and gas adsorption surface areas to (1) the fundamentally different nature of the two surface areas measured and (2) to non-uniformity of pore-size distribution. It is certainly true that both these factors are important but, of the two, the first seems here to be dominant. The fact that so many of the cores tested are shaly would alone contribute to very high gas adsorption surface

Table A

Pack	Electrical Kozeny Textural Factor	Ratio Kozeny Electrical Area Geometrical Area	Theoretical Kozeny Textural Factor	Shape Factor
A	5.2	0.885	4.17	1.99
B	5.25	0.896	4.17	1.98
C	5.25	1.045	5.75	2.72
D	5.25	0.913	4.41	2.08
E	5.33	0.860	3.95	1.84
F	5.16	0.927	4.49	2.16
G	5.25	0.823	3.57	1.70
H	5.07	0.970	4.78	2.36
I	5.12	0.895	4.13	2.00
J	5.17	0.900	4.21	2.03
K	5.15	1.006	5.25	2.54
		Average: 0.92	Average: 4.44	Average: 2.13

areas. This phenomenon is probably enhanced by the effect on the cores of the degassing procedure used (*cf.*, for example, reference 15). That the gas adsorption surface areas tend to give rise to rather unrealistic average spherical grain sizes may be seen from the data presented in Table I-B. For example, Sample No. 46, an average case, shows an average spherical grain size of 0.0193 mm. This is certainly an unexpectedly small value for a core with a permeability of 217 md.

While it is agreed that surface area is of great importance in petroleum recovery, it would seem, at least for water-wet rocks, that the Kozeny surface area is a more realistic one than one derived from gas adsorption data. The surface between the oil and water phases would seem to be the operative area, not the "absolute" surface area.

Equations (7), (8) and (9) presented by the writers are unquestionably of great theoretical and practical interest. These equations represent the outstanding problem which must be resolved before the Kozeny equation can finally be accepted or rejected as a valid tool for the investigation of consolidated porous media. There is no doubt that if there are large pores and small pores continuously in parallel throughout a porous medium the Kozeny equation breaks down. But, what if there is merely a wide spectrum of pore sizes, but with no interconnected paths in the medium which involve only large pores or small pores? In other words, if there is a random distribution of pore sizes? There is certainly evidence to show (Reference 11) that for consolidated rocks which may have pores which approximate to such an ideal distribution of sizes, the Kozeny equation gives surface areas in good agreement with similar areas determined by an entirely independent procedure.

The writers appear to attribute Equation (7) to Calhoun, Lewis and Newman. In fact, at least in the petroleum literature, it originated with Leverett.² It is instructive to consider Leverett's derivation of Equation (7) and particularly the caveat he sounds regarding its indiscriminate application. Leverett points out that the equation definitely does not hold when the pendular saturation range is approached. Application throughout the pendular range is implicit in Equation (7), where the integration is carried out between the saturation limits of zero and unity. Thus, the equality shown by the writers in Equation (9) is a false one and conclusions stemming from the assumed equality may be void.

This must not be held to imply that the Kozeny equation is necessarily valid for all systems which have a random distribution of pore sizes. Such validity is still unproven. The validity or otherwise of the Kozeny equation when applied to such systems may, perhaps, best be tested by application and improvement of methods suggested in Reference 11.

REFERENCES

1. Wyllie, M. R. J., and Gregory, A. R.: "Formation Factors of Unconsolidated Porous Media: Influence of Particle Shape and Effect of Cementation," presented at Petroleum Branch, AIME, Fall Meeting, Houston, Tex., Oct. 1-3, 1952.
2. Leverett, M. C.: "Capillary Behavior in Porous Solids," *Trans. AIME*, (1941), 142, 152. ★ ★ ★

AUTHORS' REPLY TO MR. WYLLIE

We shall comment first on Wyllie's computation of the Kozeny textural factor using electrical resistivity measurements. This factor, which we have designated by the symbol, k , is the product of two other factors which characterize the void structure of the porous matrix; namely, the pore shape factor, k_o , and the tortuosity factor, T ,

$$k = k_o T \quad (A)$$

While we have evaluated k directly by means of Equation (6), Wyllie has evaluated k by assuming a value for k_o and deriving T from the formation resistivity factor, F . It should be pointed out that, except for very simple geometrical shapes for which the value of k_o can be rigorously computed from the laws of hydrodynamics and viscosity, the shape factor cannot be directly determined. Since computed values of k_o do not vary widely when the shape of the pore opening is changed from an equilateral triangle ($k_o = 1.67$) through a circle ($k_o = 2$) to a long, narrow slit ($k_o = 3.0$), we can consider the influence on the textural factor of variation in pore shape to be of secondary importance. We do not, therefore, take issue with Wyllie's assumed value of 2.5 for k_o . His method of calculating T from the formation resistivity factor, F , and the porosity, f , is, however, open to serious question. He has used the following equation:

$$T = (fF)^2 \quad (B)$$

which was presented in the paper of Wyllie and Rose (Reference 9 of our paper). In the work of Winsauer, *et al.*,¹ however, this relationship is derived as:

$$T = fF^* \quad (C)$$

We are confronted, therefore, after having taken into account differences in definition and nomenclature, with two equations for computing tortuosity from formation factor and porosity data. After examining the derivations of these two conflicting equations it is our opinion that the one given by Winsauer is the more plausible. Furthermore, Winsauer has tested the relationship experimentally and while for natural cores he found that the equation

$$T = (fF)^{1.2} \quad (D)$$

fit the experimental data better than Equation (C), unconsolidated Ottawa sand followed Equation (C) almost exactly. We feel justified, therefore, on both theoretical and experimental grounds, in applying Equation (C) to our bead packs and, as a consequence, we obtain quite different values for the electrical Kozeny textural factor than does Wyllie by the use of Equation (B). Our values are given in Table 1. It will be noted that the values obtained by Equation (C) agree quite well with the values obtained by Equation (6) of our paper. This means that the two independent methods of measuring the textural factor, one based on fluid flow and pore size

*Winsauer has defined tortuosity as a length ratio and designated it by the symbol τ . In the nomenclature used by Wyllie, and in this discussion, the tortuosity is defined as the square of this same length ratio. Therefore, $T = \tau^2$, and Equation (C) actually appears as follows in Winsauer's paper:

$$F = \frac{\tau^2}{p}$$

where p is the fractional porosity here designated by the symbol f .

Table 1

Pack	Electrical Kozeny Textural Factor		Kozeny Textural Factor From Eq. (6)**	Surface Area (sq. m/g)	
	From Wyllie's Eq. (B)*	From Winsauer's Eq. (C)*		From Eq. (7)	Geometrical
A	5.2	3.62	3.27	0.0065	0.00485
B	5.25	3.64	3.44	0.0092	0.00682
C	5.25	3.64	3.16	0.014	0.00893
D	5.25	3.64	4.00	0.012	0.0107
E	5.33	3.65	3.52	0.015	0.0127
F	5.16	3.60	3.39	0.026	0.0213
G	5.25	3.64	3.12	0.028	0.0254
H	5.07	3.56	3.38	0.040	0.0303
I	5.12	3.60	3.30	0.046	0.0361
J	5.17	3.60	3.36	0.048	0.0361
K	5.15	3.59	3.59	—	0.0373

*Based on an assumed shape factor of 2.5.

**Based on an assumed contact angle of 140°.

characteristics, the other on electrical flow parameters, yield the same values to within 10 to 15 per cent, provided the correct equation is employed in utilizing the electrical measurements.

Wyllie's charge that our basic experimental data are inaccurate is one for which it is difficult to provide an adequate rebuttal. We did not make a detailed statistical analysis of the precision of our data, but we have reason to believe that our measurements of porosity and permeability were accurate to within the customary one or two per cent. The surface areas of the bead packs were calculated from the size of the sieve openings with the assumption that the beads were spherical, but here again we have no reason to believe that this geometrical area is seriously in error.

While we agree with Wyllie that the surface between the oil and water phases in a rock may be of greater importance to petroleum recovery than the "absolute" area as measured by gas adsorption, we are not prepared to accept the Kozeny equation as a means of deriving this oil/water interfacial area for the reason already cited in the paper that lack of uniform pore size may invalidate the equation.

In regard to Wyllie's claim that our Equations (7), (8) and (9) are false, we believe that he has clearly misinterpreted the Leverett article which is cited in his discussion. The equation for which Leverett has pointed out the limitations mentioned in Wyllie's discussion is *not* the same equation as our (7) which we correctly attribute to Calhoun and co-workers. Leverett derived the following basic equation:

$$\Delta F = - \int_{s_1}^{s_2} P_c ds \quad (E)$$

where ΔF is the free energy change in going from saturation state 1 to state 2. Leverett's use of this equation was in determining the *interfacial area between the two fluids* present within the solid and *not* in determining the *surface area of the solid*. This latter application of Equation (E) was made by Calhoun. In determining the interfacial area between the two fluids Leverett had to assume, as he clearly states, that in changing the saturation of the fluids from state 1 to state 2, he did not appreciably alter the areas of contact between the solid and each of the phases, and it was this assumption that necessitated his statement that the method broke down as the pendular saturation range was approached. In Calhoun's application of Equation (E) to the determination of the solid surface area, however, it is not necessary to make the assump-

tion which Leverett had to make in dealing with the fluid/fluid interface, since the total change in free energy results from a replacement of one solid/fluid interface by another. Hence, the free energy change is given exactly by

$$\Delta F = (\gamma_1 - \gamma_2) A$$

where A is the solid surface area and γ_1 and γ_2 are the interfacial tensions between the solid and fluids 1 and 2, respectively. Since for a finite angle of contact, θ , between the two fluids and the solid,

$$(\gamma_1 - \gamma_2) = \gamma \cos \theta$$

where γ is the interfacial tension between the two fluids, Equation (7) follows as an exact solution. Equation (7) would provide a convenient means of determining the surface area of the solid if it were not for the fact that the capillary pressure curve is generally difficult to define as the wetting phase saturation approaches zero; hence, the integral $\int_{s=0}^1 P_c ds$ cannot be reliably determined. The data for the glass bead packs present unusually favorable circumstances for estimating this integral, and, while the areas under the capillary pressure curves are probably accurate to no better than 10 per cent, the values of the surface areas calculated from the integrals are given in the accompanying table to show that they are not grossly in error.

Finally, it should be stated that we not only believe Equations (7), (8) and (9) to be correct, but also feel that such conclusions as were drawn from these equations are valid. As stated in the paper, we do not purport to show the magnitude of the error involved in the application of the Kozeny equation to systems of nonuniform pore size; we merely show, from what we consider sound theoretical reasoning, that the Kozeny equation does not completely describe such systems. While Wyllie is entitled to his opinion that the methods which he has previously proposed provide the best means of testing the validity of the Kozeny equation, we shall subscribe to the hope that the methods here presented may also be of some value in this connection, and that better methods of attack may soon be developed.

REFERENCES

1. Winsauer, W. O., Shearin, H. M., Masson, P. H., and Williams, M.: "Resistivity of Brine-Saturated Sands in Relation to Pore Geometry," *Bull. AAPG*, (1952), 36, 253.

Technical Note Section

Technical Note 108—

A STUDY OF THE PERMANENCE OF PRODUCTION INCREASES DUE TO HYDRAULIC FRACTURE TREATMENTS

C. R. FAST, STANOLIND OIL AND GAS CO., TULSA, OKLA.

In order to evaluate the ability of a Hydrafrac treatment to effect a sustained increase in well production, data were accumulated on the first 65 wells in 26 fields treated by Stanolind. Since these data were obtained from such a large number of fields, it is felt that individual well or reservoir characteristics do not affect the overall picture, as might be the case if the study were made in one field or one group of wells in a field. These data are tabulated in Table I and plotted on Figs. 1 and 2.

An analysis of Fig. 1 shows that at the end of six months, 75 per cent, or 45, of 60 wells on which data were available

Manuscript received in the Petroleum Branch office Nov. 26, 1951.

Table I

	Time after treatment, years					
	0.5	1.0	1.5	2.0	2.5	3.0
Wells on which data available	60	44	35	25	22	18
Wells showing sustained production increase	45	31	24	15	15	10
Wells showing no sustained production increase	15	13	11	10	7	8
Per cent of reported wells showing sustained production increase	75	70.5	68.6	60	68.2	55.5
Per cent of pre-Hydrafrac production for wells showing sustained increase	210	223	257	203	162	184
Per cent of pre-Hydrafrac production for all wells reported	175	163	161	153	118	83

showed a sustained production increase. At the end of two years, data were available on 25 wells. Of these, 15 wells, or 60 per cent, showed a sustained production increase. At the end of three years, 55 per cent, or 10, of 18 wells had a production rate greater at that time than before Hydrafrac treatment. The lack of information on additional wells at the end of the third year is primarily a result of the small number of treatments conducted in the early stages of field application

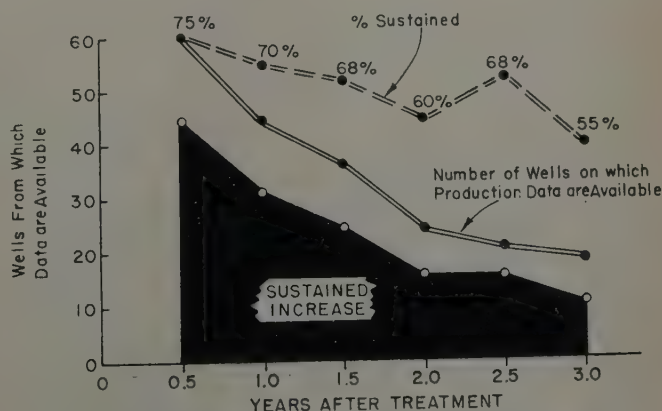


FIG. 1 — PRODUCTION SUSTAINED AFTER HYDRAFRAC.

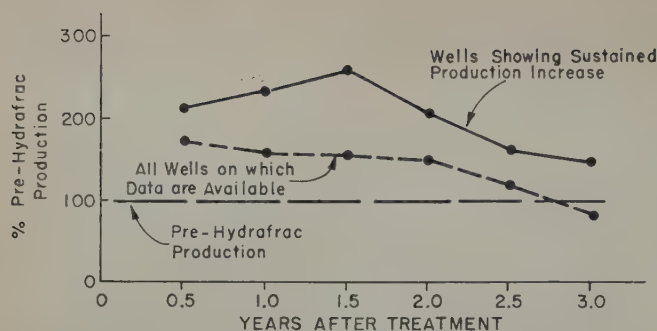


FIG. 2 — PRODUCTION DECLINE AFTER HYDRAFRAC.

of this process. Production data on wells treated more than three years ago are limited to so few wells that they were not considered.

Fig. 2 contains two plots of the production data from the wells surveyed, expressed as per cent of pretreatment production plotted against time in years after treatment. Only the

wells showing a sustained increase in production were considered in the upper plot, while all wells on which data were available were considered in the lower plot. The upper curve shows that two years after treatment, the production from these wells was 200 per cent greater than before treatment. Even after three years, these wells were producing at a rate that was 134 per cent of the pre-Hydraulic production rate. When considering all of the wells treated from which data were available, it may be seen from the lower curve that after two years over 150 per cent of pre-Hydraulic production was being maintained. The production from these wells did not decline to the pretreatment level until approximately two and three-fourths years after treatment.

The increased production shown on Fig. 2 is all net increased production, since the cost of Hydraulic treatment of all wells was paid out during the first six months of production not shown on this graph.

An analysis of these data indicates that Hydraulic treatment is capable of effecting a sustained increase in production. As additional data become available, this study will be continued to determine the duration of the production increase. ★ ★ ★

Technical Note 110—

A NOTE ON THE X-RAY ABSORPTION METHOD OF DETERMINING FLUID SATURATION IN CORES

T. M. GEFFEN AND R. E. GLADFELTER, STANOLIND OIL AND GAS CO., TULSA, OKLA., JUNIOR MEMBERS AIME

Lipson¹ has recently presented a technical note wherein theoretical considerations were used to demonstrate "... that the adsorption *vs* saturation relation for a linear absorption method is not necessarily a single valued function of saturation." It was concluded that the absorption *vs* saturation relationship is subject to the same hysteretic effect as is the flow behavior between the drainage and imbibition systems. It is the purpose of this note to show, by experimental results, that for the manner in which fluids are distributed in porous materials during fluid flow, the relative X-ray absorption *vs* saturation relationship is single-valued regardless of the saturation history.

The design of the apparatus used to measure relative X-ray absorption of cores undergoing fluid flow tests is similar to that described by Morgan, McDowell and Doty.² A few modifications have been incorporated in the design to increase sensitivity and simplicity of measurement. The sensitivity is such that for usual types of cores a

recording pen movement of approximately 12 linear in. is occasioned between the recording of the core dry and when it is completely full of an absorbing liquid, a solution of approximately five per cent by volume of iodobenzene in a close-cut hydrocarbon fraction, or a solution of 50,000 ppm sodium iodide in water.

Two types of experiments were conducted, one in which the liquid was inside the core, and the other with the liquid outside the core. Tests with the liquid inside the core were run to cover the saturation range encountered in both the drainage (gas drive) and imbibition (liquid flood) flow systems. It is pointed out that the same core was used, but the tests were conducted at different times with the recording mechanism balanced at a different position. Therefore, the absolute values of relative X-ray intensity at any saturation are not the same in each test.

In the second type of test the same core was used, but this time its pore space contained only gas, and various thicknesses of oil contained in plastic cells were placed in front of the dry core. As before, the relative X-ray ab-

sorption was measured and compared to the quantity of oil in front of the core. The arrangement of the fluids with respect to the path of X-rays in these two types of tests represent fluid distributions of a wider difference than can be expected between that established in a core just due to imbibition and drainage saturation flow histories. Thus any deviation from a straight line relationship of the log of the relative X-ray intensity *vs* saturation calibration should be readily apparent.

Results of the laboratory tests are given in Fig. 1. A schematic diagram showing the position of the fluids with respect to the path of the X-ray beam is given for the two cases investigated. In the case where the oil existed outside the core (Case B), the log of the X-ray intensity ($\log_e I/I_0$) is related directly to the cell thickness (amount of oil in X-ray beam path). This correlation is in full agreement with X-ray theory. In the case where the oil or water existed inside the core (Case A) which covers both drainage and imbibition types of flow processes, again the relationship between absorption and saturation (amount of oil in X-ray beam path

Manuscript received in the Petroleum Branch office Jan. 18, 1952.

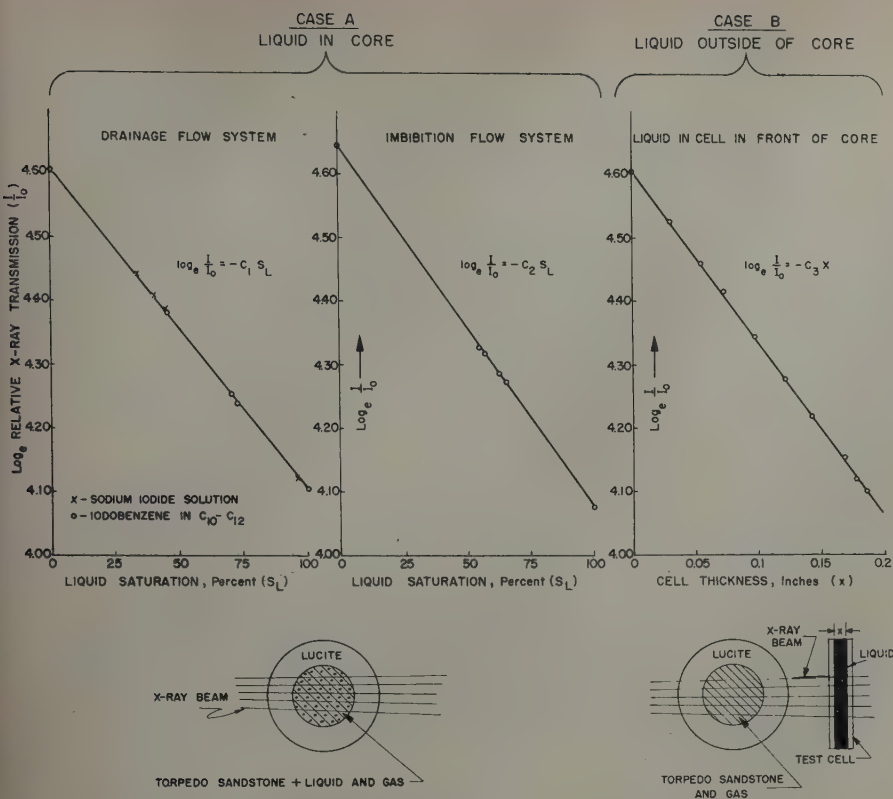


FIG. 1 — EFFECTS OF FLUID DISTRIBUTION ON X-RAY ABSORPTION.

measured by weighing the core) agrees with X-ray theory for uniform distribution of fluids. This particular porous material does show considerable hysteresis effect in flow behavior and therefore can be considered as suitable for these evaluation tests. The fact that

this experimental evidence, does not conform to the expectations of Lipson can be explained on the basis of the models used. Lipson's fluid distribution models are applicable to conditions of saturation distribution for a very small group of pores. In practice, a large

number of pores influence the absorption of the X-ray beam (approximately 10^6 pores in a $\frac{3}{4}$ -in. diameter core plug and an X-ray beam $\frac{1}{8}$ in. x $\frac{5}{16}$ in.). The cumulative effect of the multitude of pores involved in the measurement produces essentially a uniform distribution of the fluids as far as the X-ray beam is concerned. Therefore, a direct application of Lipson's theoretical consideration does not describe the relation of fluid saturation and relative X-ray absorption for the case of fluid flow in porous materials. Experimental evidence shows that for the manner in which it is used, relative absorption is uniquely related to fluid saturation in cores.

ACKNOWLEDGMENT

The authors wish to thank the management of Stanolind Oil and Gas Co. for permission to publish this technical note, and to D. R. Parrish for his assistance in making some of the measurements.

REFERENCES

1. Lipson, L. B.: "Theoretical Note on Linear Absorption Methods of Determination of Fluid Saturation in Porous Media," *Trans. AIME*, (1951) 192, 375. (*Jour. Pet. Tech.*, Aug. 1951, 19.)
2. Morgan, F., McDowell, J. M., and Doty, E. C.: "Improvements in the X-Ray Saturation Technique of Studying Fluid Flow," *Trans. AIME*, (1950) 189, 183. ★ ★ ★

Technical Note 120—

MEASUREMENT OF THE PERMEABILITY OF SET CEMENT

B. E. MORGAN, JUNIOR MEMBER AIME AND G. K. DUMBAULD, MEMBER AIME, HUMBLE OIL AND REFINING CO., HOUSTON, TEX.

INTRODUCTION

A satisfactory well-cementing composition must retain its fluidity long enough to be pumped into place; then it must develop within a reasonable length of time sufficient strength and impermeability to anchor the casing in position and to form an effective seal between the casing and the formations. These properties may be evaluated by pumpability, strength (compressive or tensile), and permeability tests. Laboratory

test procedures for the determination of pumpability time and strength development have been outlined previously and are readily available,¹ but a satisfactory and convenient laboratory procedure for the measurement of the permeability of set cement has not been developed heretofore.

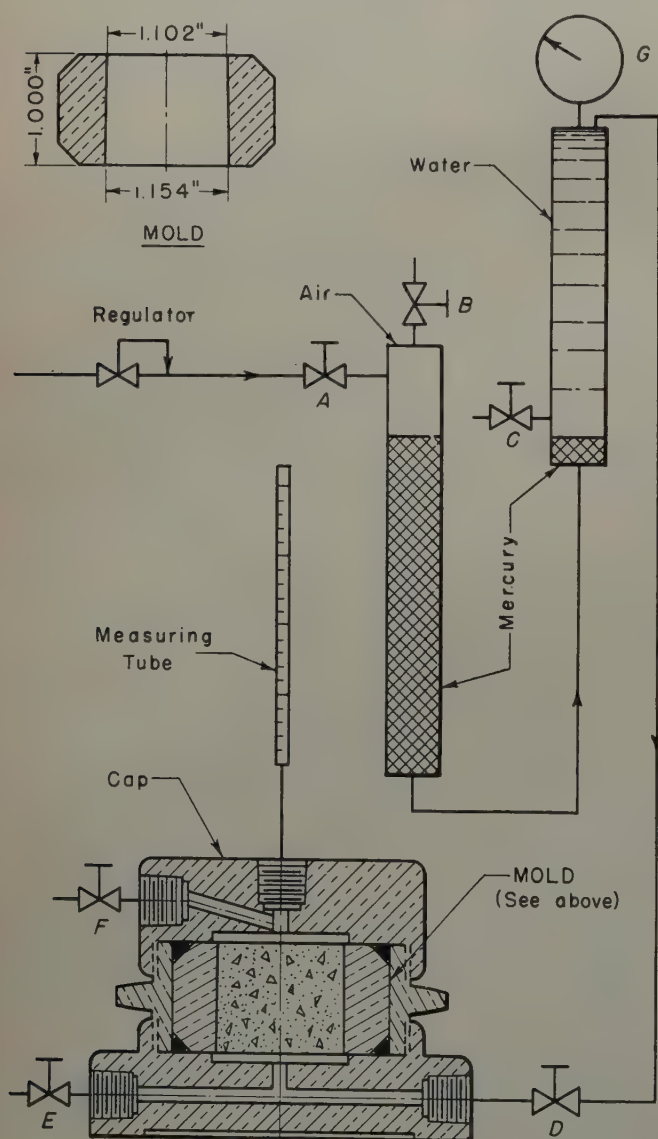
Some permeability data have been obtained previously by passing air through dried cement specimens.² Such a procedure is unsatisfactory because the drying of set cement alters its physical and chemical properties and subjects it to conditions dissimilar to well conditions. A more realistic method would be one wherein the cement remains water-saturated during

¹References given at end of paper.

Manuscript received in the Petroleum Branch office April 23, 1952.

designed cylinder by means of O-rings as shown in Fig. 1. To prevent the collection of any air in the water and under the specimen, the following procedure is followed:

The brass mold, shown in the upper left-hand corner of Fig. 1, is cleansed with emery polishing paper and placed on a flat plate and the test slurry is poured into the mold. The slurry is puddled several times with a stirring rod and levelled off with a spatula. Another flat plate is placed on top of the mold to complete the enclosure before the mold is placed under water at the desired curing temperature. After the cement slurry has aged for the desired length of time, the mold containing the set cement is taken from the water bath, the cover plates are removed, and the specimen is cooled under water to room temperature. The faces of the set cement (in the mold) are brushed under a stream of water to remove the glazed surface and foreign matter. The mold is then sealed, with its larger face downward, into the specially



1. With mercury in the system as shown, valve *A* closed, valves *B*, *C*, and *D* opened, connect an aspirator bottle containing distilled water, recently boiled, to valve *C* by means of a rubber tubing and fill chamber until water overflows through valve *D*.

2. With valves *B*, *C*, and *D* closed and valve *A* opened, adjust air regulator to obtain the desired pressure drop across the cement specimen by observing the pressure gauge *G* (25-100 psi, generally).

3. Connect aspirator bottle to valve *E*.

4. With aspirator bottle positioned 12-24 in. higher than valve *E*, open valves *D* and *E* slightly to allow a small flow of water past the mold containing the set cement as the cap is screwed into place.

5. Close valve *E* and open valve *D* fully.

6. Attach measuring tube (a one-ml pipette with tip removed) as shown in Fig. 1.

7. Connect aspirator bottle to valve *F* and bring water level into measuring tube, then close valve *F*.

8. Observe rate of flow and calculate permeability using Darcy's Law.

9. To replace water in the system, close valve *A*, open valve *B*, connect aspirator bottle to valve *C*, then open valve *C*.

In making exploratory tests, several variations in test procedure were tried. In some cases, the mold was greased with a light, water-insoluble grease prior to placement of the cement slurry into the mold. In other cases, the mold was cleansed with emery polishing paper, but no grease was applied to the mold. Permeability tests were first run on the set cement in the mold; the specimen was then removed from the mold with the aid of a hydraulic punch, placed in a rubber holder which was tightly fitted into a steel cylinder, and its permeability to water again determined. Several set cement plugs were dried at 105°C for 24 hours; then their permeability to air was measured.

Substantially the same values for water permeability were obtained with the cement specimen in the ungreased mold as were obtained with the cement specimen placed in the rubber holder. These results indicated that the permeability values obtained by casting cement specimens in ungreased molds were reproducible, that there was no leakage of water around the cement specimen under the conditions used, and that the result represented the true wet permeability of the set cement. Higher and inconsistent values were obtained when the mold was greased. Values obtained for air permeability were much higher than those for water permeability, no doubt due to the alteration of the set cement by drying.

1. API Code 32: *For Testing Cements Used in Wells* (Tentative), 2nd Edition, (June, 1950), American Petroleum Institute, New York, N. Y.
2. Coleman, J. R., and Corrigan, G. L.: "Fineness and Water-Cement Ratio in Relation to Volume and Permeability of Cement," *Trans. AIME*, (1941), 142, 205. ★ ★ ★

ERRORS IN CALCULATION OF GAS INJECTION PERFORMANCE FROM LABORATORY DATA

FORREST F. CRAIG, JR., STANOLIND OIL AND GAS CO., TULSA, OKLA., JUNIOR MEMBER AIME

Both early and more recent¹ laboratory measurements of gas-oil relative permeabilities were made by subjecting oil-saturated cores to external gas drives. In these runs* it was generally assumed that the flowing gas/oil ratio was constant at every point throughout the core. Using this assumption, the resulting equation for the gas-oil relative permeability ratio becomes

$$\frac{k_g}{k_o} = \frac{Q_g}{Q_o} \frac{\mu_g}{\mu_o} \quad (1)$$

where Q is the flow rate at the producing end of the system. This relative permeability was then specified for the average saturation of the core. The assumption and resulting equation fail to recognize that in an external drive, the oil flow rate varies from zero at the injection end to a maximum at the producing end. The assumption also fails to consider the existence of a saturation gradient during an external drive. This saturation gradient is due solely to non-steady-state flow.

Some authors^{2,3,4} have used this erroneous method of calculating relative permeability ratios from external drives. Other authors^{5,6,7} have used relative permeability ratios in calculating expected field performance by external drive, using Equation (1) and making the incorrect assumption that the saturation is uniform within the driven portion of the reservoir.

To find the correct relation between the relative permeability ratio at the average saturation and the produced gas/oil ratio, the insertion in Equation (1) of a factor, F , to adjust it for oil velocity gradient has been considered. The equation then takes the form

$$\frac{k_g}{k_o} = F \frac{Q_g}{Q_o} \frac{\mu_g}{\mu_o} \quad (2)$$

Assuming that the oil velocity is directly proportional to the distance from the injection point leads to the conclusion that, for a linear system, the average oil velocity is one-half that at the producing end. Thus, the average gas/oil ratio is twice the produced gas/oil ratio, and Equation (2) is transformed into

$$\frac{k_g}{k_o} = 2 \frac{Q_g}{Q_o} \frac{\mu_g}{\mu_o} \quad (2a)$$

However, here again the existence of a saturation gradient is not recognized.

The produced gas/oil ratio is related to the relative permeability ratio at the saturation of the outlet end of the system. It can be shown quite readily that, if the true $\log k_g/k_o$ - saturation relationship is linear over small ranges of saturation, then

$$F = (\sigma_{avg} - \sigma_2) \frac{d \log k_g/k_o}{d\sigma} \quad (3)$$

where σ_{avg} and σ_2 are the average and outlet saturations, respectively. Examination of Equation (3) shows that the factor F cannot have a single value over the whole saturation range.

Another method of dealing with external drives is that of Buckley and Leverett.⁸ Their method, which assumes no gas expansion and outlet end effects, considers fully the saturation gradient present due solely to the displacement mechanism

during an external drive, and applies Equation (1) to each point along this gradient. The calculation of production history using relative permeability ratio is straightforward. However, the calculation of relative permeability ratios from production history by this method is impractical. In a recent paper, Welge,⁹ using an approach similar to that of Buckley and Leverett, presents a simplified method for determining the saturation at the producing end of the system. At this saturation, the relative permeability ratio calculated by Equation (1) applies exactly, after breakthrough of the stabilized front. By this method, relative permeability ratios or production history may be calculated with equal ease. Use of this method as a laboratory tool in determination of relative permeability ratios by external drive requires the knowledge of the total injected fluid volume, in addition to the average saturation and producing ratio.

As a preliminary test of this method of calculation, laboratory external gas drives were run on a 3½ in. diameter, 11 in. long sample of Nellie Bly consolidated sandstone. This core sample had a permeability of 824 md and a porosity of 28.1 per cent. The driving fluid was air. Three different oils were used, having viscosities of 1.4, 9.8, and 125 cp, respectively. The runs were made under identical pressure differentials,

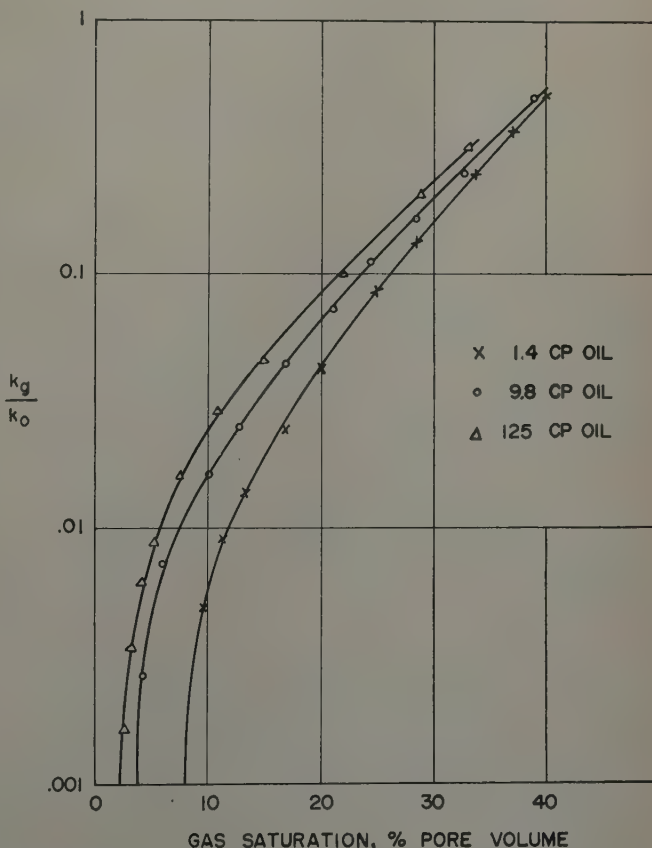


FIG. 1 — NELLIE BLY RELATIVE PERMEABILITY RATIOS, CALCULATED BY EQUATION (1).

¹References given at end of paper.

Manuscript received in the Petroleum Branch office July 14, 1952.

*These comments on external gas drives apply also to water drives.

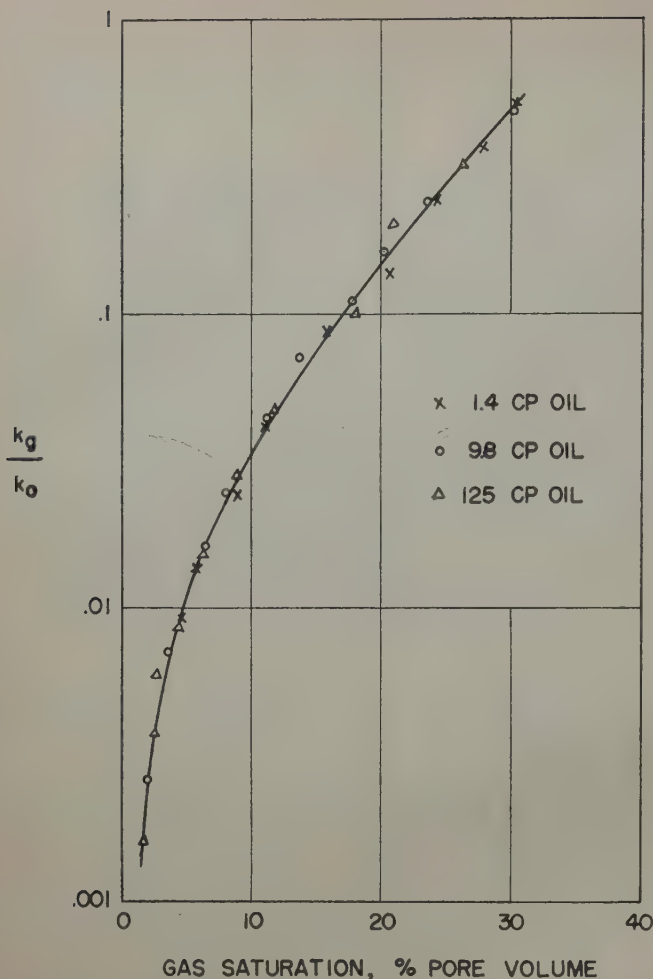


FIG. 2 — NELLIE BLY RELATIVE PERMEABILITY RATIOS, CALCULATED BY WELGE'S METHOD.

which were sufficient to reduce both gas expansion and outlet boundary effects to a negligible amount.

The relative permeability ratios for the laboratory runs, as calculated by Equation (1), are shown in Fig. 1. This method of calculation fails to recognize the existence of oil velocity and saturation gradients. The saturation gradients are markedly affected by the oil viscosity, and hence the relative permeability ratios calculated at any given saturation vary widely between the various drives.

Relative permeability ratios for the same laboratory runs were calculated using the recently proposed method.⁹ The results are shown in Fig. 2. This method of calculation, which considers oil velocity and saturation gradients, yields relative permeability ratios correctly dependent only upon gas saturation.

As a test of the magnitude of errors to be made by some methods of external drive calculation, field performance was calculated by the previously discussed methods, for a reservoir containing fluids of typical viscosities. The results of these calculations are shown in Fig. 3. These calculations apply for both linear and radial drives, for, in external drives on either of these systems, both the average saturation and outflow face saturation are dependent only on the pore volumes of fluid injected.

In Case I, the relative permeabilities were calculated from laboratory external drive data by Welge's method. Correct

relative permeabilities can also be measured in the laboratory by any method which eliminates saturation gradients, such as the various steady state methods. It may be noted that the method commonly used by reservoir engineers to obtain relative permeability ratio information from field solution gas drive data involves no calculation error. However, this method cannot be applied to obtaining relative permeability ratios from field external drive performance for the reasons cited above. The field performance calculations were based upon the assumption that every portion of the reservoir was at the same average saturation. The produced gas/oil ratio was obtained by Equation (1), using the relative permeability at the average saturation. In this case, although the correct relative permeabilities were calculated from the laboratory data, the field calculations took no cognizance of saturation gradients in the reservoir, and so yielded incorrect gas/oil ratios, much higher than the correct ones.

In Case II, the relative permeabilities again were correct. The produced gas/oil ratios were calculated for the field by the method^{8,9} which considers the effects of saturation gradients. The results are correct, because, in both the relative permeability determinations and the field performance calculations, saturation gradients were taken into account.

In Case III, the relative permeabilities were calculated from laboratory external drive data using Equation (1). The field performance was calculated by the proper method.^{8,9} In this case, although the method of calculating field performance was

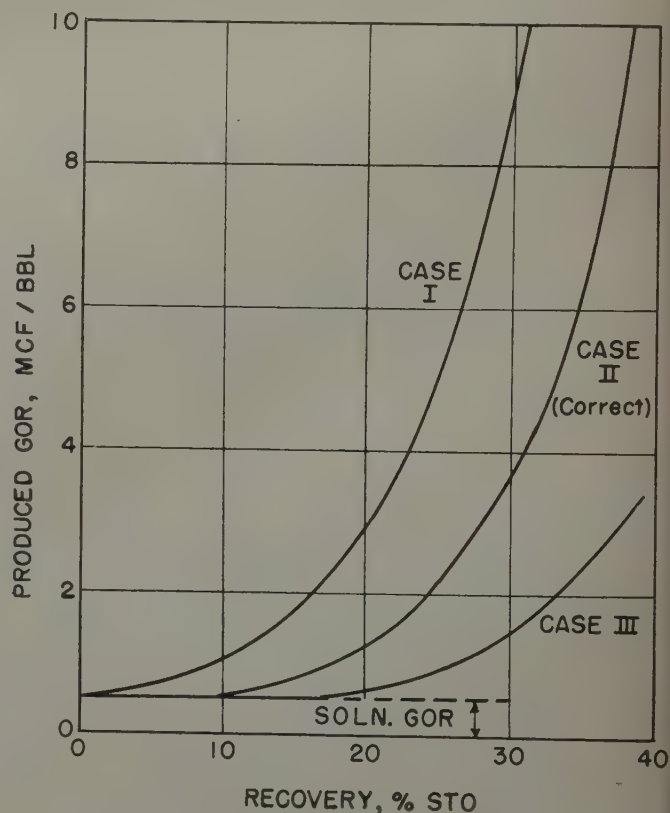


FIG. 3 — EFFECT OF METHOD ON FIELD PERFORMANCE CALCULATIONS.

Case I: Use of correct relative permeabilities in a method assuming an "average" saturation.

Case II: Use of correct relative permeabilities in a method which considers the effect of saturation gradients.

Case III: Use of relative permeabilities as calculated by Equation (1) in a method which considers the effect of saturation gradient.

correct, the relative permeabilities used were incorrectly determined, yielding produced gas/oil ratios much lower than the correct ones.

Relative permeabilities determined in Equation (1), used in connection with reservoir calculations, which assume a uniform saturation for the field, may also yield approximately correct results, provided laboratory and field gas/oil viscosity ratios are identical.

Fig. 3 shows that differences in predicted field performance can extend over a range of seven to one, depending on the method used.

Future reservoir calculations for external drive should be examined closely to make sure that the correctly determined relative permeability ratios and the correct method of field calculations are used. Use of the two incorrect combinations of methods cited may account in some measure for the many cases in which calculated and actual external drive field performance were widely divergent.

ACKNOWLEDGMENTS

The author is indebted to Charles R. Stewart and Joseph B. Egbert for their invaluable assistance in the experimental work. Thanks are also due to Richard A. Morse for his con-

structive aid in this study. Appreciation is expressed to the Stanolind Oil and Gas Co. for permission to present this technical note.

REFERENCES

1. Osoba, J. S., Richardson, J. G., Kerver, J. K., Hafford, J. A., and Blair, P. M.: "Laboratory Measurements of Relative Permeability," *Trans. AIME*, (1951) **192**, 47.
2. Krutter, H., and Day, R. J.: "Air Drive Experiments on Long Horizontal Consolidated Cores," *Petr. Tech.*, (Nov., 1943) **6**, TP 1627.
3. Nielsen, R. F.: "Prediction of Production Behavior in Air-Gas Drive," *Prod. Monthly*, (Dec., 1949) **14**, 29.
4. Muskat, M.: "A Note on Gas Repressuring," *Prod. Monthly*, (Feb., 1946) **10**, 23.
5. Patton, E. C.: "Evaluation of Pressure Maintenance by Internal Gas Injection in Volumetrically Controlled Reservoirs," *Trans. AIME*, (1947) **170**, 112.
6. Muskat, M.: *Physical Principles of Oil Production*, First Ed., New York, McGraw-Hill Book Co., (1949).
7. Pirson, S. J.: *Elements of Oil Reservoir Engineering*, First Ed., New York, McGraw-Hill Book Co., (1950).
8. Buckley, S. E., and Leverett, M. C.: "Mechanism of Fluid Displacement in Sands," *Trans. AIME*, (1942) **146**, 107.
9. Welge, H.: "A Simplified Method for Computing Oil Recovery by Gas or Water Drive," *Trans. AIME*, (1952) **195**, 91, (*J. Petr. Tech.*, April, 1952, 91). ★ ★ ★

Technical Note 136—

PROCEDURE FOR USE OF ELECTRONIC DIGITAL COMPUTERS IN CALCULATING FLASH VAPORIZATION HYDROCARBON EQUILIBRIUM

H. H. RACHFORD, JR., JUNIOR MEMBER AIME, AND J. D. RICE, HUMBLE OIL AND REFINING CO., HOUSTON, TEX.

ABSTRACT

The effectiveness of digital computing machines in making technical calculations depends on how well the work is arranged to utilize the capability of the machines. This note presents a particularly useful way of calculating hydrocarbon vapor-liquid equilibrium in the flash vaporization (or condensation) system. The method is well suited to sequence-controlled computing equipment. It is not limited to equilibrium calculations and may be used for solution of most implicit equations in one variable.

INTRODUCTION

There is increasing interest in the use of electronic digital computers in research and engineering calculations. This is a fortunate and inevitable trend in view of both the increasingly extensive numerical work which is becoming a routine part of many daily production operations and growing demand for the overwhelming amounts of calculations required by newly developed numerical methods for solving heretofore unsolved problems.

Machines are in many ways ideally suited to the task but of necessity present certain difficulties, for a particular prob-

lem to be solved must often be formulated quite differently from the way it would be arranged for manual solution. This is done in order to take advantage of the inherent speed and precision of electronic computers and at the same time to limit the need for number storage to the capacity of the machine. Therefore, this note is submitted to present a general and quite powerful method of finding solutions of the frequently encountered implicit equation:

$$F(x, y_1, y_2, \dots, y_n) = 0 \quad (1)$$

where the root, x_0 , is to be found for a given set of $y_1 \dots y_n$. The procedure is well suited for use with computing machines, for it usually requires but little storage or programming beyond that necessary to evaluate F .

HYDROCARBON EQUILIBRIUM

The method is described in terms of the problem it was designed to solve, i.e., the calculation of hydrocarbon vapor-liquid equilibrium in flash vaporization. Given the composition of a hydrocarbon mixture and appropriate values of the equilibrium ratios K , to find the phase ratio and compositions in a closed system: let z_i be the mol fraction of the i -th component in the mixture. If K_i is the ratio y_i/x_i , where y_i and x_i

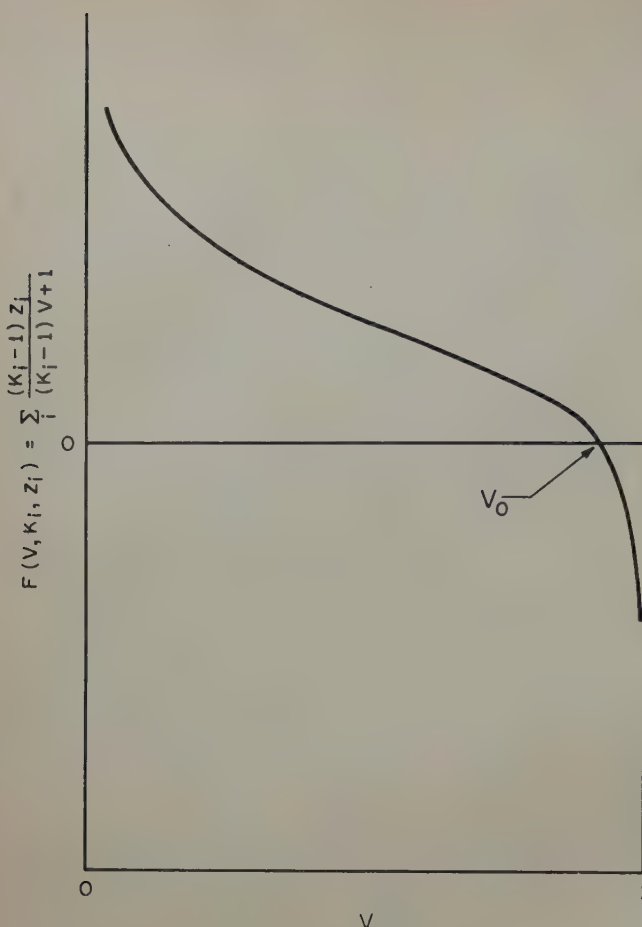


FIG. 1 — FUNCTION DEFINED BY EQUATION 6.

are the mol fractions of the i -th component in the vapor and liquid phases, respectively, then by material balance

$$z_i = Lx_i + VK_i x_i \quad \dots \quad (2)$$

where L and V are the mol fractions of the components in the liquid and vapor, respectively. Since $L = 1 - V$, the relations follow

$$y_i = \frac{K_i z_i}{(K_i - 1)V + 1} \quad \dots \quad (3)$$

$$x_i = \frac{z_i}{(K_i - 1)V + 1} \quad \dots \quad (4)$$

By a total material balance for an S -component system

$$\sum_{i=1}^S y_i = \sum_{i=1}^S x_i = 1 \quad \dots \quad (5)$$

or

$$\sum_i (y_i - x_i) = \sum_i \frac{(K_i - 1) z_i}{(K_i - 1)V + 1} = 0 \quad (6)$$

Equation (6) is of the form of (1)

$$F(V, K_1, K_2, \dots, K_S, z_1, z_2, \dots, z_S) = 0 \quad (1')$$

and for any set of K_i and z_i must be solved for root V_0 .

From physical considerations it is necessary to study only the region $0 < V < 1$, and it is known that only one, if any, root exists within these limits. Further, differentiating (6) with respect to V yields

$$\sum_i \frac{-(K_i - 1)^2 z_i}{[(K_i - 1)V + 1]^2} = \frac{dF}{dV} \quad \dots \quad (7)$$

which shows $\frac{dF}{dV}$ to be everywhere negative. Therefore, if a root exists, F must lie above the axis to the left of the root, and below the axis to the right, as shown in the figure.

When the function F has a root near either zero or one, the derivatives of F with respect to V may be high near the root. This seriously interferes with customary interpolation and extrapolation procedures; thus, it is desirable to locate the root by a method which does not depend on derivatives of the function.

PROCEDURE

Consider the V -axis from zero to one to be divided into 2^n equal segments, $(k-1)2^{-n} \leq V < k \cdot 2^{-n}$, $k = 1, 2, \dots, 2^n$. The single root must lie within one of these segments. The sign of $F(0.5, K_i, z_i)$ is negative if the root $V_0 < 0.5$, positive if $V_0 > 0.5$. There are then only 2^{n-1} segments on either side of 0.5 in which V_0 may lie. If W_1 is the set of segments which contains V_0 , and T_1 is the mid-point of W_1 , and $F(T_1, K_i, z_i)$ is evaluated, the sign of F at T_1 determines which of the two sets of 2^{n-2} segments of W_1 contains V_0 . This is defined as W_2 , F is again evaluated and the sign examined as before. The process is continued for $n-1$ cycles. The value of T_{n-1} is within 2^{-n} of V_0 .

This sequence of operations is easy to perform on any computer which has the capacity to evaluate the terms of Equation (6), and may conditionally alter its program as a result of a test for sign. The first trial $T_0 = 0.5$ is used to evaluate the sum of Equation (6). The sign is sensed to control the operation which gives $T_1 = T_0 \pm 2^{-2}$, the plus sign being used if F is positive. The function F is then computed from Equation (6) at T_1 , from which $T_2 = T_1 \pm 2^{-3}$, \dots , $T_{n-1} = T_{n-2} \pm 2^{-n}$. The value T_{n-1} is then equal to V_0 within 2^{-n} . This procedure has been used for computing V_0 for several hundred systems with values for V_0 ranging from 0.000001 to 0.999999 with good results. The work was done on an IBM 604 Electronic Calculator, which is a popular computer for accounting work and therefore, has widespread availability in the petroleum industry. The procedure is very readily programmed for this machine, and the solution is rapid. A 12-component flash may be computed to six significant figures and the results x_i , y_i , and V_0 punched onto tabulating cards in 2.4 minutes. In general, for an S -component system calculated to m significant digits in V_0 , the time, θ , in minutes for the punched answers is given approximately by

$$\theta = mS/30$$

The method is quite powerful for other types of function F . The only requirements are that in the region studied the function have no discontinuities across the axis and have only one root, and that the sign of the derivative be known at the root sought. The wide latitude in permissible behavior of F , the ease of programming the iterative procedure, and the small storage requirement provide a good general-purpose method that has been found to be quite convenient in a number of practical computing applications. ★ ★ ★

REDUCTION IN PERMEABILITY WITH OVERBURDEN PRESSURE

I. FATT, MEMBER AIME, AND D. H. DAVIS, CALIFORNIA RESEARCH CORP., LA HABRA, CALIF.

Oil bearing rocks, usually found at depths of 2,000 to 10,000 ft, are elastically deformed by overburden pressure. Although the change in porosity with pressure in a number of example rocks has been shown to be small,¹ it was thought that overburden pressure might have a significant effect on permeability. This note presents results of an investigation to determine

the magnitude of the change in permeability with pressure.

In routine core analysis, permeabilities are measured on rock samples which are not under overburden pressure. If permeability measured in this way differs from permeabilities measured under overburden pressure, a systematic error is introduced into well productivity calculations. The experiments described in this report were made to determine the magnitude of the change and thus to give an estimate of the error introduced into the calculations. The error introduced by the neglect of the change in permeability when overburden pressure is removed may account for part of the difference between well productivity calculated from core analysis and the actual well productivity.

The results obtained in this investigation have only qualitative significance because of the difficulty in reproducing in the laboratory the stress conditions on the rock buried in the earth. The assumption which is usually made is that the rocks in the earth are under a uniform pressure equal to the weight per unit area of the vertical overburden column from the rock in question to the surface of the earth less the pressure of the liquid in the pores of the rock. For an overburden consisting of sandstones and shales (of assumed average specific gravity of 2.3) and for a liquid pressure equal to the pressure in a salt water column (of specific gravity 1.0) reaching from the rock to the surface, the resulting net pressure on the rock is approximately 0.56 psi per ft of depth.

EXPERIMENTAL METHOD

Clean, dry sandstone core plugs one in. in diameter and about three in. long were mounted in a copper foil jacket as shown in Fig. 3 or molded in a Lucite jacket as shown in Fig. 4. All cores except those labeled "2" in Fig. 1 and "8" in Fig. 2 were measured in the copper foil jacket. Cores "2" and "8" were measured in the Lucite jacket.

The jacketed core was placed in a high pressure hydraulic bomb in which the liquid pressure outside the jacket could be raised to 15,000 psi. Flow lines from the core were brought out of the bomb through special fittings in the bomb head and connected to a laboratory type gas permeameter. Measurements were made with nitrogen gas; the maximum mean gas pressure in the core was 16.1 psia.

RESULTS

The specific permeability of sandstone decreases with increase in overburden pressure. Most of the decrease takes place over the range of zero to 3,000 psi overburden pressure. If the net pressure on the rock is assumed to be 0.56 psi per ft of depth as discussed above, 3,000 psi of overburden pressure is equivalent to about 5,000 ft of overburden. At 3,000 psi overburden pressure, the permeability of the eight sandstone core samples tested ranged from 59 to 89 per cent of the permeability without overburden pressure. Figs. 1 and 2 show the permeability reduction as a function of overburden pressure. The permeability of the eight cores without overburden pressure ranged from 4.35 md to 632 md; these permeabilities are listed in Figs. 1 and 2.

REFERENCES

1. Carpenter and Spencer: "Measurements of Compressibility of Consolidated Oil Bearing Sands," U. S. Bureau of Mines, R.I. 3450, (1940). ★ ★ ★

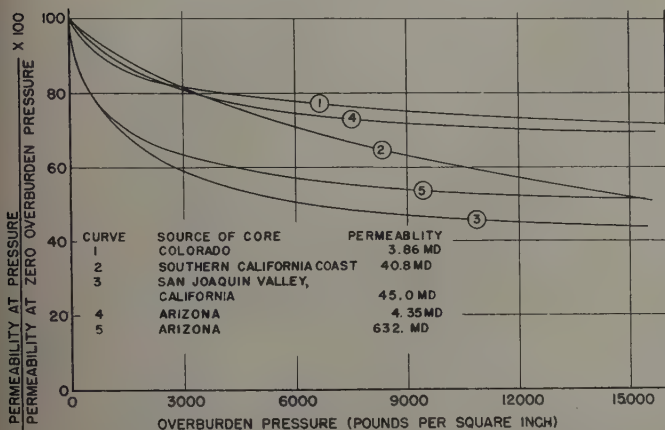


FIG. 1 — CHANGE IN PERMEABILITY WITH OVERBURDEN PRESSURE.

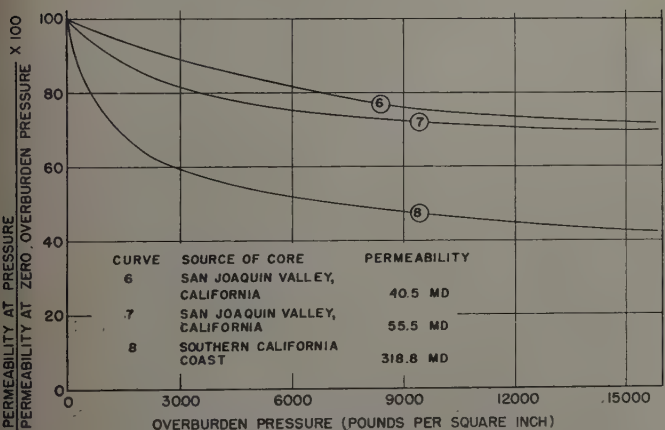


FIG. 2 — CHANGE IN PERMEABILITY WITH OVERBURDEN PRESSURE.

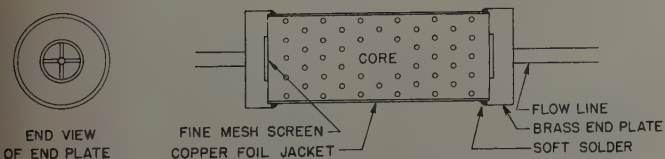


FIG. 3 — DETAILS OF CORE MOUNTED IN COPPER FOIL JACKET.

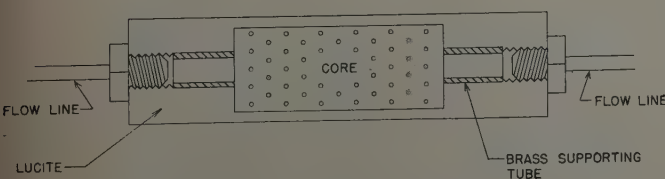
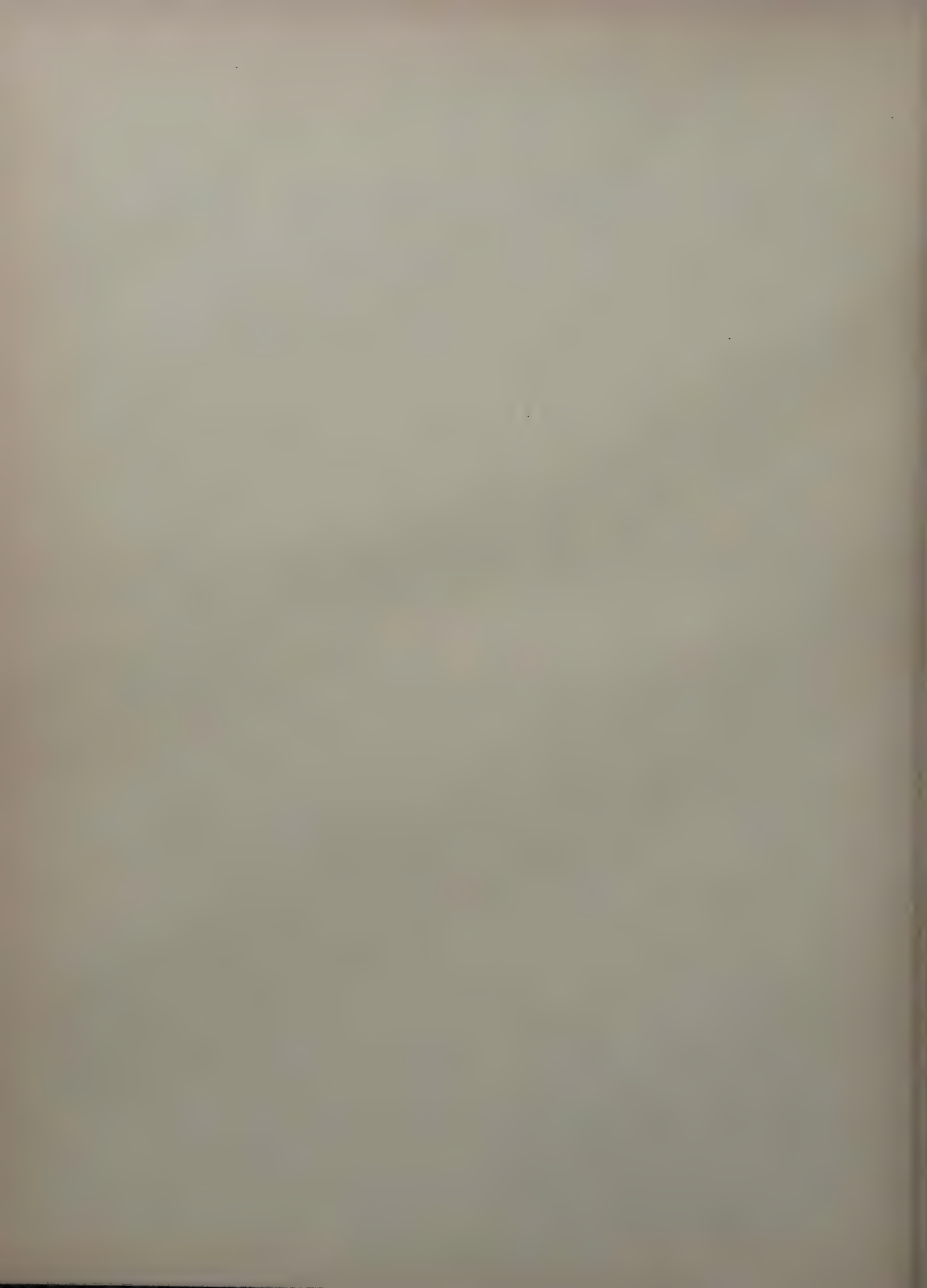


FIG. 4 — DETAILS OF CORE MOUNTED IN LUCITE, TYPE B.



INDEX TO TRANSACTIONS, VOLUME 195

(Plus Reference to Articles and Technical Notes Published in *Journal of Petroleum Technology* in 1952)

A

- ALFORD, J. B.: *The Professional Concept*, (Ed.), Sept. JPT.
ARONOFKY, J. S.: *Mobility Ratio—Its Influence on Flood Patterns During Water Encroachment*, 15
AULICK, B., et al.: *Improved Production by Chemical Treatment in Gulf Coast Areas*, (Art.), Sept. JPT.

B

- BASHAM, R. B., et al.: *The Delta-Log, A Differential Temperature Surveying Method*, 123
BERNARD, G. G., et al.: *Behavior of Dissolved Oxygen in Oil Field Brine*, 119
Bits: The effect of circulating media and nozzle design on rock bit performance, (Art.), Jan. JPT.
BLUM, H. A., et al.: *Method for Determining Wettability of Reservoir Rocks*, 1
BOTSET, H. G.: *Evaluating a Petroleum Engineering Curriculum*, (Art.), May JPT.
BRADFIELD, S. A.: *Gas Supply and Requirements in California*, (Art.), Jan. JPT.
BROOKS, C. S., et al.: *Surface Area Measurements on Sedimentary Rocks*, 289
BROWN, C. H.: *Opportunities in Engineering and Science*, (Art.), May JPT.
BURTCHAELL, E. P., et al.: *Pressure Control by Water Injection—A Resumé of Case Histories*, (Art.), July JPT.

C

- CALHOUN, J. C., JR., et al.: *Visual Examinations of Fluid Behavior in Porous Media, Part I*, 149
CAUDLE, B. H., et al.: *X-Ray Shadowgraph Studies of Areal Sweepout Efficiencies*, 265
Cementing: Lost circulation corrective; time setting clay cement, 59.
The effect of calcium chloride on high early strength cement, (Art.), June JPT.
Measurement of the permeability of set cement, (Tech. Note), June JPT.
Use of activated charcoal in cement to combat effects of contamination by drilling muds, 225.
CHATENEVER, A., et al.: *Visual Examinations of Fluid Behavior in Porous Media—Part I*, 149
Condensate: Volumetric behavior, 11.
Prediction of saturation pressures for condensate-gas and volatile-oil mixtures, 135.

Core Analysis: A note on the X-ray absorption method of determining fluid saturation in cores, (Tech. Note), March JPT.

- CRAFT, B. C., et al.: *The Effect of Calcium Chloride on High Early Strength Cement*, (Art.), June JPT.
CRAIG, F. F., JR.: *Errors in Calculation of Gas Injection Performance from Laboratory Data*, (Tech. Note), Aug. JPT.
Cycling: Possibility of cycling deep depleted oil reservoirs after compression to a single phase, 175.

D

- DAVIS, C. A.: *The North Coles Levee Field Pressure Maintenance Project*, (Art.), Aug. JPT.
DAVIS, D. H., et al.: *Reduction in Permeability with Overburden Pressure*, (Tech. Note), Dec. JPT.
DAVIS, L. E., et al.: *A Method for Predicting the Tendency of Oil Field Waters to Deposit Calcium Sulfate*, 25
DAVIS, L. E., et al.: *A Method for Predicting the Tendency of Oil Field Waters to Deposit Calcium Carbonate*, 213
DAVIS, P. C., et al.: *Phase and Volumetric Behavior of Natural Gases at Low Temperatures*, 279
DOUGHERTY, J. F., et al.: *Natural Gas in the Province of Alberta, Canada*, 241
DUMBAULD, G. K., et al.: *Measurement of the Permeability of Set Cement*, (Tech. Note), June JPT.
DUMBAULD, G. K., et al.: *Use of Activated Charcoal in Cement to Combat Effects of Contamination by Drilling Mud*, 225

E

- EGAN, E. F., et al.: *Neutron Derived Porosity-Influence of Bore Hole Diameter*, 203
ELENBAAS, J. R., et al.: *Sample Grading Method of Estimating Gas Reserves*, 207
ELFRINK, E. B., et al.: *The Slip Velocity of Gases Rising Through Liquid Columns*, 233

F

- FATT, I., et al.: *Reduction in Permeability with Overburden Pressure*, (Tech. Note), Dec. JPT.
FAST, C. R.: *A Study of the Permanence of Production Increases Due to Hydraulic Fracture Treatments*, (Tech. Note), Feb. JPT.
FEATHERSTON, R. E.: *The Engineer and the Industry Information Program*, (Art.), June JPT.

Field Studies: Volumetric behavior of condensate and gas from a Louisiana field -- II, 11.
 Cook Ranch Field, Shackelford County, Texas, 77.
 The North Coles Levee Field pressure maintenance project, (Art.), Aug. JPT.
 Flow Studies: Improved multiphase flow studies employing radioactive tracers, 65.
 Visual examinations of fluid behavior in porous media -- part I, 149.
 The strataflow process: a recent development in locating water entry in wells, 183.
 FOLGER, A., et al.: *Natural Gas in the Province of Alberta, Canada*, 241

G

Gas: Volumetric behavior, 11.
 Gas supply and requirements in California, (Art.), Jan. JPT.
 Efficiency of gas displacement from porous media by liquid flooding, 29.
 A simplified method for computing oil recoveries by gas or water drive, 91.
 Equilibrium vaporization ratios, 99.
 Sample grading method of estimating gas reserves, 207
 Errors in calculation of gas injection performance from laboratory data, (Tech. Note), Aug. JPT.
 The slip velocity of gases rising through liquid columns, 233.
 Natural gas in the Province of Alberta, Canada, 241.
 Phase and volumetric behavior of natural gases at low temperatures, 279
 Improved techniques developed for acidizing gas producing and injection wells, 285.
 GEFFEN, T. M., et al.: *Efficiency of Gas Displacement from Porous Media by Liquid Flooding*, 29
 GEFFEN, T. M., et al.: *A Note on the X-Ray Absorption Method of Determining Fluid Saturation in Cores*, (Tech. Note), March JPT.
 GLADFELTER, R. E., et al.: *A Note on the X-Ray Absorption Method of Determining Fluid Saturation in Cores*, (Tech. Note), March JPT.
 GLENN, A. H.: *Weather and Oceanographic Problems in the Petroleum Industry*, (Art.), April JPT.
 GOLDING, B. H., et al.: *Prediction of Saturation Pressures for Condensate-Gas and Volatile-Oil Mixtures*, 135
 GORE, T. L., et al.: *Phase and Volumetric Behavior of Natural Gases at Low Temperatures*, 279
 GRIMM, R. D., et al.: *Sample Grading Method of Estimating Gas Reserves*, 207

H

HAFFORD, J. A., et al.: *Laboratory Determination of Relative Permeability*, 187
 HARTLINE, R., et al.: *The Strataflow Process: A Recent Development in Locating Water Entry in Wells*, 183
 HAYNES, G. W., et al.: *Efficiency of Gas Displacement from Porous Media by Liquid Flooding*, 29
 HODGSON, G. R., et al.: *A Method of Perforating Casing Below Tubing*, 303
 HOPKINS, H. F., et al.: *Improved Production by Chemical Treatment in Gulf Coast Areas*, (Art.), Sept. JPT.
 HOWER, W., et al.: *Improved Production by Chemical Treatment in Gulf Coast Areas*, (Art.), Sept. JPT.
 HUNTER, Z. Z., et al.: *Observations from Profile Logs of Water Injection Wells*, 129

J

JACOBY, R. H., et al.: *Equilibrium Vaporization Ratios for Nitrogen, Methane, Carbon Dioxide, Ethane, and Hydrogen Sulfide in Absorber Oil -- Natural Gas and Crude Oil -- Natural Gas Systems*, 99
 JOHNSON, V. L., et al.: *Drilling Fluid Filter Loss at High Temperatures and Pressures*, 157
 JOSENDAL, V. A., et al.: *Improved Multiphase Flow Studies Employing Radioactive Tracers*, 65
 JUSTICE, W. H., et al.: *Improved Techniques Developed for Acidizing Gas Producing and Injection Wells*, 285

K

KATZ, D. L.: *Possibility of Cycling Deep Depleted Oil Reservoirs After Compression to a Single Phase*, 175
 KATZ, D. L., et al.: *Sample Grading Method of Estimating Gas Reserves*, 207
 KAVELER, H. H., et al.: *Observations from Profile Logs of Water Injection Wells*, 129
 KENNEDY, H. T., et al.: *Bubble Formation in Supersaturated Hydrocarbon Mixtures*, 271
 KERN, L. R.: *Displacement Mechanism in Multi-Well Systems*, 39
 KERVER, J. K., et al.: *Laboratory Determination of Relative Permeability*, 187
 KURATA, F., et al.: *Phase and Volumetric Behavior of Natural Gases at Low Temperatures*, 279

L

LEBEAUX, J. M.: *Some Effects of Quick-Freezing upon the Permeability and Porosity of Oil Well Cores*, (Tech. Note), Nov. JPT.
 LEBOURG, M. P., et al.: *A Method of Perforating Casing Below Tubing*, 303
 LEVY, WALTER J.: *Perils to the Free World's Essential Oil Supplies*, (Art.), Oct. JPT.
 LEWELLING, H.: *Experimental Evaluation of Well Perforation Methods as Applied to Hard Limestone*, 163
 Logging, The quantitative aspects of electric log interpretation, 47.
 Correlation of radioactivity logs of the Lansing and Kansas City groups in central Kansas, 111.
 The Delta-Log, 123.
 Observations from profile logs of water injection wells, 129
 Neutron derived porosity-influence of bore hole diameter, 203.
 Electrical resistivity measurements on reservoir rock samples by the two-electrode and four-electrode methods, 217.
 LOVEJOY, J. M.: *Oil in a Free Economy*, (Ed.), July JPT.
 LOWE, H. R., et al.: *Natural Gas in the Province of Alberta, Canada*, 241

Mc

McKINNEY, H. E.: *A High-Pressure Wellhead Lubricator*, 261
 McNIEL, J. S., JR., et al.: *Lost Circulation Corrective: Time Setting Clay Cement*, 59

M

MACUNE, C. W., et al.: *The Delta-Log, A Differential Temperature Surveying Method*, 123.
 MARSH, G. A., et al.: *Behavior of Dissolved Oxygen in Oil Field Brine*, 119
 MESSENGER, J. U., et al.: *Lost Circulation Corrective: Time Setting Clay Cement*, 59
 MEYER, J., et al.: *Natural Gas in the Province of Alberta, Canada*, 241

MINCKLER, R. L.: *Oil Supply and Demand on the West Coast*, (Art.), Oct. JPT.
 MOORE, W. D., et al.: *The Pressure Performance of Five Fields Completed in a Common Aquifer*, 297.
 MORGAN, B. E., et al.: *Measurement of the Permeability of Set Cement*, (Tech. Note), June JPT.
 MORGAN, B. E., et al.: *Use of Activated Charcoal in Cement to Combat Effects of Contamination by Drilling Muds*, 225
 MORGAN, J. V.: *Correlation of Radioactive Logs of the Lansing and Kansas City Groups in Central Kansas*, 111
 MORSE, R. A., et al.: *Efficiency of Gas Displacement from Porous Media by Liquid Flooding*, 29
 Mud: Radial filtration, 5.
 A new additive for control of drilling mud filtration, 85.
 Drilling fluid filter loss at high temperatures and pressures, 157.
 Use of activated charcoal in cement to combat effects of contamination of drilling muds, 225.

N

NIELSEN, J. P., et al.: *Improved Techniques Developed for Acidizing Gas Producing and Injection Wells*, 285

O

Offshore operations: Weather and oceanographic problems in the petroleum industry, (Art.), April JPT.
 OLSON, C. R., et al.: *Bubble Formation in Supersaturated Hydrocarbon Mixtures*, 271
 OPPENHEIM, V.: *Petroleum Development of Colombia*, (Art.), Nov. JPT.
 ORGANICK, E. I., et al.: *Prediction of Saturation Pressures for Condensate-Gas and Volatile-Oil Mixtures*, 135.
 OSOBA, J. S., et al.: *Laboratory Determination of Relative Permeability*, 187
 OWEN, J. E.: *The Resistivity of a Fluid-Filled Porous Body*, 169.

P

PARRISH, D. R., et al.: *Efficiency of Gas Displacement from Porous Media by Liquid Flooding*, 29
 PAYNE, L. L.: *The Effect of Circulating Media and Nozzle Design on Rock Bit Performance*, (Art.), Jan. JPT.
 Perforating: Experimental evaluation of well perforation methods as applied to hard limestone, 163.
 A method of perforating casing below tubing, 303.
 PLANK, W. B.: *Now is the Time to Choose Engineering*, (Ed.), May JPT.
 Porosity: Neutron derived porosity-influence of bore hole diameter, 203.
 Some effects of quick-freezing upon the permeability and porosity of oil well cores, (Tech. Note), Nov. JPT.
 PORTER, J. L.: *Oil Development in Chile*, (Art.), Nov. JPT.
 POWER, H. H.: *Characterizing Features of the Petroleum Engineers*, (Art.), May JPT.
 POWER, H. H.: *Industry's Stake in Engineering Education*, (Ed.), Aug. JPT.
 Pressure Control: Pressure control by water injection — a resumé of case histories, (Art.), July JPT.
 The North Coles Levee Field pressure maintenance project, (Art.), Aug. JPT.
 The pressure performance of five fields completed in a common aquifer, 297.
 Production Review: Production and development in the United States during 1951, (Art.), March JPT.
 Foreign production and development during 1951, (Art.), April JPT.
 PROKOP, C. L.: *Radial Filtration of Drilling Mud*, 5

PURCELL, W. R., et al.: *Surface Area Measurements on Sedimentary Rocks*, 289

R

RACHFORD, H. H., et al.: *Procedure for Use of Electronic Digital Computers in Calculating Flash Vaporization Hydrocarbon Equilibrium*, (Tech. Note), Oct. JPT.
 REAMER, H. H., et al.: *Volumetric Behavior of Condensate and Gas from a Louisiana Field — II*, 11
 REAMER, H. H., et al.: *Some Properties of Mixed Paraffinic and Olefinic Hydrates*, 197
 REISTLE, C. E., JR.: *Management Looks at the Engineer*, (Art.), May JPT.
 Relative Permeability: Laboratory determination of relative permeability, 187.
 Some effects of quick-freezing upon the permeability and porosity of oil well cores, (Tech. Note), Nov. JPT.
 Reduction in permeability with overburden pressure, (Tech. Note), Dec. JPT.
 RICE, J. D., et al.: *Procedure for Use of Electronic Digital Computers in Calculating Flash Vaporization Hydrocarbon Equilibrium*, (Tech. Note), Oct. JPT.
 RICHARDSON, J. G., et al.: *Laboratory Determination of Relative Permeability*, 187
 Rock Characteristics: Method for determining wettability, 1.
 The resistivity of a fluid-filled porous body, 169.
 Some effects of quick-freezing upon the permeability and porosity of oil well cores, (Tech. Note), Nov. JPT.
 Rock Treatment: A study of the permanence of production increases due to hydraulic fracture treatments, (Tech. Note), Feb. JPT.
 Improved production by chemical treatment in Gulf Coast areas, (Art.), Sept. JPT.
 RUST, C. F.: *Electrical Resistivity Measurements on Reservoir Rock Samples by the Two-Electrode and Four-Electrode Methods*, 217
 RZASA, M. J., et al.: *Equilibrium Vaporization Ratios for Nitrogen, Methane, Carbon Dioxide, Ethane, and Hydrogen Sulfide in Absorber Oil — Natural Gas and Crude Oil — Natural Gas Systems*, 99

S

SAGE, B. H., et al.: *Volumetric Behavior of Condensate and Gas from a Louisiana Field — II*, 11
 SAGE, B. H., et al.: *Some Properties of Mixed Paraffinic and Olefinic Hydrates*, 197
 SALATHIEL, R. A.: *A New Additive for Control of Drilling Mud Filtration*, 85
 SANDBERG, C. R., et al.: *The Slip Velocity of Gases Rising Through Liquid Columns*, 233
 SANDIFORD, B. B., et al.: *Improved Multiphase Flow Studies Employing Radioactive Tracers*, 65
 SAYE, F., et al.: *Improved Production by Chemical Treatment in Gulf Coast Areas*, (Art.), Sept. JPT.
 SCHREMP, F. W., et al.: *Drilling Fluid Filter Loss at High Temperatures and Pressures*, 157
 SCOTTY, C. B., et al.: *Neutron Derived Porosity-Influence of Bore Hole Diameter*, 203
 SELLECK, F. T., et al.: *Some Properties of Mixed Paraffinic and Olefinic Hydrates*, 197
 SLOBOD, R. L., et al.: *Method for Determining Wettability of Reservoir Rocks*, 1
 SLOBOD, R. L., et al.: *X-ray Shadowgraph Studies of Areal Sweepout Efficiencies*, 265.
 SMITH, E. R., et al.: *Pressure Control by Water Injection — A Resumé of Case Histories*, (Art.), July JPT.

STEIN, N., et al.: *The Slip Velocity of Gases Rising Through Liquid Columns*, 233.

STEPHENSON, A. H., et al.: *The Effect of Calcium Chloride on High Early Strength Cement*, (Art.), June JPT.

STIFF, H. A., JR., et al.: *A Method for Predicting the Tendency of Oil Field Waters to Deposit Calcium Sulfate*, 25

STIFF, H. A., JR., et al.: *A Method for Predicting the Tendency of Oil Field Waters to Deposit Calcium Carbonate*, 213

T

TAGGART, A. F.: *Education for Engineering*, (Art.), May JPT.

TAPPER, W., et al.: *The Strataflow Process: A Recent Development in Locating Water Entry in Wells*, 183

TROSTEL, E. G., et al.: *Natural Gas in the Province of Alberta, Canada*, 241

TRUBY, L. G., JR., et al.: *The Pressure Performance of Five Fields Completed in a Common Aquifer*, 297

TURNER, C. E., et al.: *Sample Grading Method of Estimating Gas Reserves*, 207

V

VARY, J. A., et al.: *Sample Grading Method of Estimating Gas Reserves*, 207

W

WALSTROM, J. E.: *The Quantitative Aspects of Electric Log Interpretation*, 47

Water Drive: A simplified method for computing oil recoveries by gas or water drive, 91

Waterflood: Mobility ratio—its influence on flood patterns during water encroachment, 15.

Efficiency of gas displacement from porous media by liquid flooding, 29.

Displacement mechanism in multi-well systems, 39.

Observations from profile logs of water injection wells, 129.

A method for predicting the tendency of oil field waters to deposit calcium carbonate, 213.

WEINAUC, C. F.: *Staff Problems Relating to Engineering Education*, (Art.), May JPT.

WELGE, H. J.: *A Simplified Method for Computing Oil Recoveries by Gas or Water Drive*, 91

WIENER, L. D., et al.: *The Slip Velocity of Gases Rising Through Liquid Columns*, 233

WILSON, J. W., et al.: *Improved Multiphase Flow Studies Employing Radioactive Tracers*, 65

WILSON, W. W.: *Engineering Study of Cook Ranch Field, Shackelford County, Texas*, 77

WINGER, J. G.: *The Market for Williston Basin Oil*, (Art.), Dec. JPT.

Y

YOUNG, C. A.: *International Standardization of Oil Field Equipment*, (Art.), Feb. JPT. ★ ★ ★

